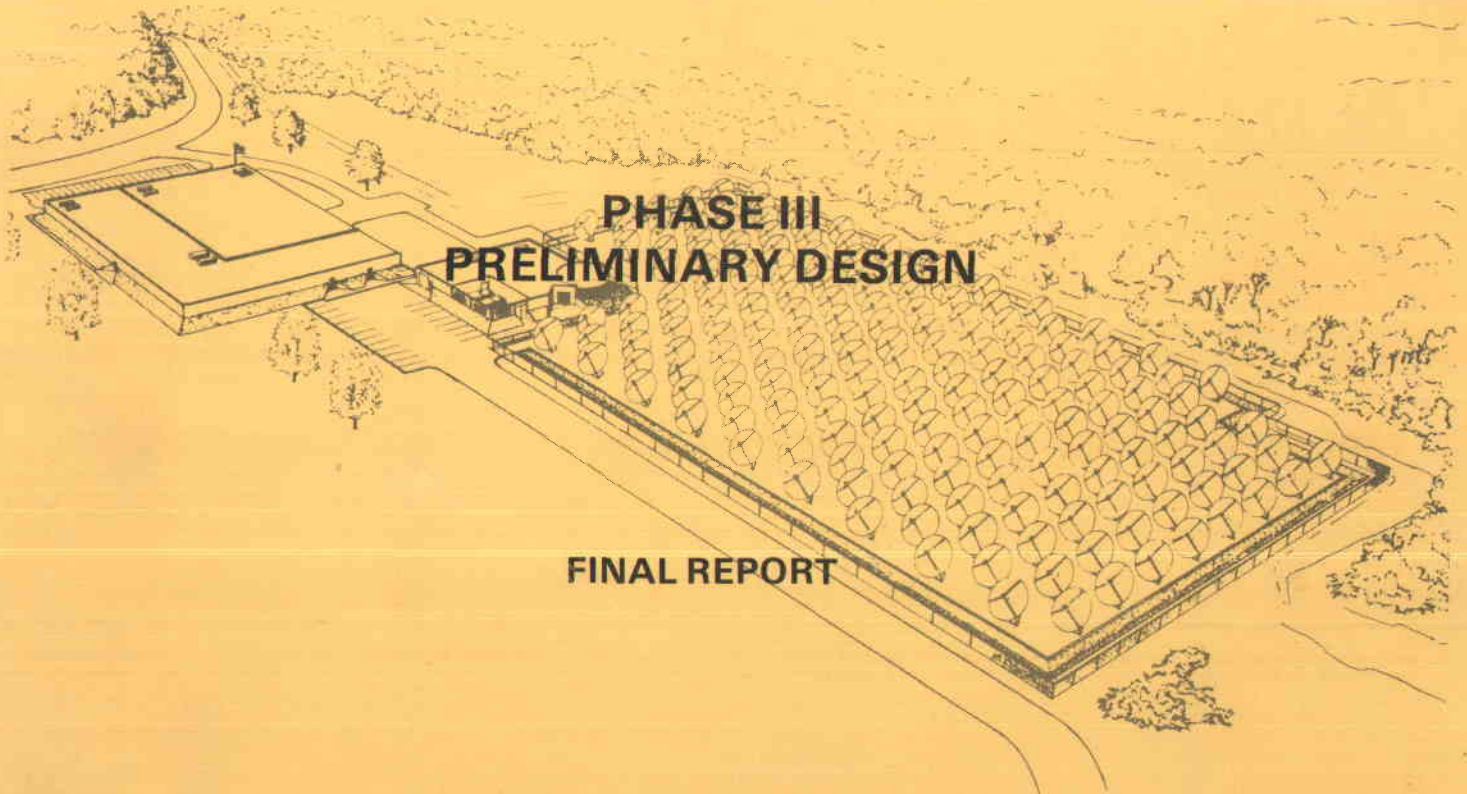


1030

*Bill M...
8453*

DOCUMENT NO. 78SD-4243
SEPTEMBER 1978

SOLAR TOTAL ENERGY — LARGE SCALE EXPERIMENT AT SHENANDOAH, GEORGIA



DEPARTMENT OF ENERGY
CONTRACT NUMBER EG77-C-04-3985

GENERAL  ELECTRIC
SPACE DIVISION

GENERAL ELECTRIC

SPACE DIVISION

GENERAL ELECTRIC COMPANY VALLEY FORGE SPACE CENTER
KING OF PRUSSIA PARK, P.O. BOX 8661, PHILADELPHIA, PENNA. 19101... TEL (215) 962-2000

SPACE SYSTEMS
OPERATIONS

In Reply Please Refer To
Reference No. 78-STE-0181

November 28, 1978

Mr. R. W. Hunke, Technical Project Manager
Dispersed Power Applications
Division 4722
Sandia Laboratories
Albuquerque, New Mexico 87115

Re: CORRECTION TO PHASE III PRELIMINARY DESIGN FINAL REPORT

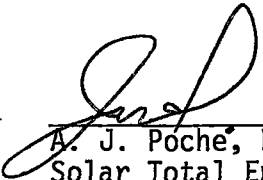
Dear Bob,

As you have indicated, on page 3-167 of the Phase III Preliminary Design Final Report for the Solar Total Energy - Large Scale Experiment at Shenandoah Figure 3.5-6 is erroneously referenced as showing the MTI steam turbine-generator set design point thermodynamic performance. The attached correction sheet will properly include the MTI Steam Turbine-Generator Thermodynamic Performance Map in the final report. The source of the Map is the approved Interface Control Document.

Please note that the (other) reference to Figure 3.5-6 which is on page 3-161, is correct in representing the 400 KW_e PCS heat/mass balance with the GE MDTD steam turbine-generator.

Copies of the attached correction sheet for the Final Report will be distributed to persons who have received copies of the Final Report, and included in copies of the Final Report distributed in the future.

Sincerely yours,



A. J. Poche, Program Manager
Solar Total Energy-Large Scale
Experiment at Shenandoah, Georgia
Room 7246, Building CC&F 7
(215) 962-4934

trm
Encls.

cc: R. Urenda, Sandia
R. Allred
S. Haas

W. Mertz
A. Schnacke

CORRECTION SHEET

PHASE III PRELIMINARY DESIGN FINAL REPORT
SOLAR TOTAL ENERGY - LARGE SCALE EXPERIMENT
AT SHENANDOAH, GEORGIA

1) Page 3-167; Last Sentence

Currently Reads: Figure 3.5-6 shows the estimated design point performance map for the MTI Turbine-Generator set.

Correct To: Table 3.5-5a shows the thermodynamic performance map for the MTI steam turbine-generator set.

2) Page 3-167

Insert attached page 3-167a

3) Page 3-161; Fifth Paragraph; Last Sentence

Correct As Is; Referencing Figure 3.5-6 as the heat/mass balance for the Power Conversion Subsystem (PCS) with GE MDTD steam turbine-generator, operating at 400 KW_e.

TABLE 3.5-5a MTI STEAM TURBINE GENERATOR THERMODYNAMIC PERFORMANCE MAP

Thermal Input Kw	2628	2110	1544	2629	2143	1569	2638	2171	1591
Electric Output Kw	400	300	200	397	300	200	391	300	200
Process Steam Flow #/hr	1380	1380	1380	1380	1380	1380	1380	1380	1380
Heat Delivered to Condenser Coolant Kw	1713	1302	846	1718	1336	871	1733	1363	893
Throttle Pressure psig	700	700	700	700	700	700	700	700	700
Throttle Temp °F	720	720	720	680	680	680	650	650	650
Pextr psig	110	110	110	110	110	110	110	110	110
Hin Btu/#	1356	1356	1356	1333	1333	1333	1313	1313	1313
Hextr Btu/#	1244	1248	1253	1225	1228	1233	1209	1212	1217
UEEP Btu/#	1152	1158	1164	1135	1143	1149	1122	1129	1135
T cond °F	230	230	230	230	230	230	230	230	230
Throttle Flow #/hr	8591	6897	5049	8789	7165	5245	8995	7402	5423
Extr. Flow to Process #/hr	1308	1304	1298	1333	1329	1323	1354	1350	1343
Extr. Flow to D/A #/hr	936	749	546	976	793	578	1014	832	607
Condenser Flow #/hr	6347	4844	3205	6480	5043	3344	6627	5220	3473

**SOLAR TOTAL ENERGY — LARGE SCALE EXPERIMENT
AT SHENANDOAH, GEORGIA**

**PHASE III
PRELIMINARY DESIGN**

FINAL REPORT

**DEPARTMENT OF ENERGY
CONTRACT NUMBER EG77-C-04-3985**

**GENERAL  ELECTRIC
SPACE DIVISION**

PREFACE

This is the final report of the General Electric Company on the Preliminary Design (Phase III) of a Solar Total Energy System - Large Scale Experiment for Shenandoah, Georgia. The work was sponsored by the Department of Energy (DOE) under Contract No. EG-77-C-04-3985. The period of performance was from October 1, 1977, to July 31, 1978.

The prime contractor for the reported work is General Electric Space Division. Supporting subcontractors included Lockwood-Greene, Architects and Engineers in the area of site requirements, definition and Preliminary System drawings, General Electric Energy Systems and Technology Division in the area of steam power conversion system definition and power conversion system trade-offs, and General Electric Ground Systems Department in the area of control system design. Through subcontracts to Scientific Atlanta, the program was supplied with data and information on paraboloidal dish design and fabrication.

The DOE Program Manager was Mr. M. Resner; the Technical Monitor was Mr. R. Hunke of Sandia Laboratories, Albuquerque, New Mexico.

LIST OF ACRONYMS

Acronym	Definition	First Section
AAC	Absorption Air Conditioner (or Conditioning)	2.3.2.5
AB	Levelized Annual Benefit	D.2
AISC	American Institute of Steel Construction	3.2.4
ANSI	American National Standards Institute	3.3.2.2.3
ASHRAE	American Society of Heating, Refrigeration, and Air Conditioning Engineers	1.2.5
ASME	American Society of Mechanical Engineers	2.1.2
ASTM	American Society of Testing Materials	3.3.2.3
BIL	Base Insulation Level	4.2.5.4.9
BTTL	Building Transient Thermal Load	2.2.1
BW	Butt Welded	3.2.7.1.2
CDR	Critical Design Review	3.8.5
CFS	Collector Field Subsystem	3.8.1.1
CIS	Control and Instrumentation Subsystem	3.8
COP	Coefficient of Performance	2.3.2.4
CRT	Cathode Ray Tube	1.3.1.4
CSIR	Capacitor Start Induction Run	3.2.7.2
DMA	Direct Memory Access	4.2.4.4.1
DOE	Department of Energy	Preface
EIA	Environmental Impact Assessment	7.5
EPC	Engineering Prototype Collector	1.3.1.1
ES	Electrical Subsystem	3.6
FFH	Fossil Fired Heater	4.2.1.3.3
FMEA	Failure Modes and Effects Analysis	2.1.2
FMEC & SA	Failure Modes Effects Criticality and Safety Analysis	7.6
GE	General Electric	2.1.1
GE/SD	General Electric/Space Division	1.2.5
GFE	Government Furnished Equipment	1.3
GPC	Georgia Power Company	2.1.1
HTS	High Temperature Storages	1.3
HUD	Housing and Urban Development	2.1.1
HVAC	Heating, Ventillating, and Air Conditioning	1.2.5
HX	Heat Exchanger	3.8.1.4
ICD	Interface Control Drawing	2.1.1
IES	Independent Energy Source	2.3.1
I/O	Input/Output	3.8.3.1
JPL	Jet Propulsion Laboratory	3.2.5
LOLP	Loss of Load Probablility	7.6
LTS	Low Temperature Storage	1.3.1.3

ACRONYMS (con't)

Acronym	Definition	First Section
MATSCO	Management and Technical Services Company	1.2.5
MDTD	Mechanical Drive Turbine Department	3.5.1
MEA	Mechanical Equipment Area	3.3.2
MOS	Metal Oxide Semiconductor	4.2.4.4.1
MTI	Mechanical Technology, Incorporated	1.3
N/A	Not Applicable or Not Available	3.2.3.3
NCC	National Climatic Center	2.1.3
NEMA	National Electrical Manufacturers Association	3.2.4
NOAA	National Oceanographic and Atmospheric Administration	2.1.3
ODT	On-line Debugging Technique	4.2.4.4.2
OSB	One Side Bright	8.1.2.4.1
OSHA	Occupational Safety and Health Administration	2.1.2
P&ID	Piping and Instrumentation Diagram	4.2.3.2
PCS	Power Conversion Subsystem	1.3
PDL	Program Design Language	3.8.5
PDR	Preliminary Design Review	3.8.5
PSW	Process Status Word	4.2.4.4.2
RAM	Remote Access Memory	3.8.2.1.2.2
RF	Radio Frequency	1.3.1.1
ROM	Read Only Memory	3.8.2.1.2.2
RMS	Root Mean Square	3.2.3.1
RTD	Resistance Temperature Detector	8.3.2.4
SA	Scientific - Atlanta	3.2.5.3
SCF	Solar Collector Field	5.4
SCS	Solar Collector Subsystem	1.3.1
SDI	Shenandoah Development, Incorporated	1.2.4
SDR	System Design Review	3.8.5
SGS	Steam Generator Supply (Subsystem)	4.2.1.2
SSMY	Shenandoah Solar Model Year	2.1.3
SLA	Sandia Laboratories - Albuquerque	2.1.1
STE-LSE	Solar Total Energy - Large Scale Experiment	1.2
STEP	Solar Total Energy Program	1.1
STES	Solar Total Energy System	1.2
STESTF	Solar Total Energy Systems Test Facility	8.3.1
TBD	To Be Determined	3.8.1.4
TG	Turbine - Generator	1.3
TRY	Test Reference Year	2.1.3
TUS	Thermal Utilization Subsystem	1.3.1
UPS	Uninterruptible Power Supply	3.6.5
WQMU	Water Quality Management Unit	F.2.11.2

TABLE OF CONTENTS

Section	Page
1 SUMMARY	1-1
1.1 Introduction	1-1
1.2 Project Overview	1-1
1.2.1 Program Objectives	1-1
1.2.2 Shenandoah System Design Objectives	1-2
1.2.3 Project Participants	1-2
1.2.4 Shenandoah Site Description	1-3
1.2.5 Bleyle Knitwear Plant Application	1-3
1.3 Preliminary Design Description Summary	1-3
1.3.1 System Description Summary	1-9
1.3.1.1 Solar Collection Subsystem	1-13
1.3.1.2 Power Conversion Subsystem	1-15
1.3.1.3 Thermal Utilization Subsystem	1-15
1.3.1.4 Control and Instrumentation Subsystem	1-15
1.3.2 Performance Summary	1-16
2 SYSTEM REQUIREMENTS	2-1
2.1 General Requirements	2-1
2.1.1 Site Description and Interface	2-1
2.1.2 Programmatic and Derived Requirements	2-5
2.1.3 Insolation and Weather Data	2-10
2.1.4 Utility Interfaces	2-12
2.2 Load Analysis	2-14
2.2.1 Bleyle Plant Load Analysis	2-16
2.2.2 System Design Loads	2-19
2.3 System Trade-Offs and Requirements Development	2-23
2.3.1 System Configuration Selection	2-23
2.3.2 System Analysis and Trade-Off Studies	2-33
2.3.2.1 Heat Transfer Fluid and System Operating Temperature Selection	2-33
2.3.2.2 Solar Collection Subsystem Trade-Offs	2-36
2.3.2.3 Turbine - Generator Efficiency Trade-Offs	2-38
2.3.2.4 Power Conversion Subsystem Condensing Temperature Trade-Off	2-40
2.3.2.5 Thermal Utilization Subsystem Trade-Offs	2-42
2.4 System Requirements Summary	2-46
3 SYSTEM ANALYSIS AND DESIGN	3-1
3.1 Site Development	3-1
3.2 Solar Collector	3-5
3.2.1 Design Goals and Approach	3-5
3.2.2 Collector and Component Design Requirements	3-7
3.2.3 Collector Concept Selection	3-13
3.2.3.1 Reflector	3-13
3.2.3.2 Mount and Drive	3-15
3.2.3.3 Receiver	3-15
3.2.3.4 Controls	3-23
3.2.4 Collector Diameter Optimization	3-27
3.2.4.1 Collector Field Parametric Relationships	3-27
3.2.4.2 Optimum Diameter Selection	3-28

Contents (con't)

Section	Page
3.2.5 Collector Preliminary Design Description	3-33
3.2.6 Reflector Design	3-35
3.2.7 Mount and Drive	3-41
3.2.7.1 Mount Structure	3-41
3.2.7.2 Drives	3-61
3.2.8 Receiver Assembly	3-69
3.2.8.1 Receiver	3-69
3.2.8.2 Receiver Support Structure	3-78
3.2.8.3 Up/Down Collector Fluid Piping	3-84
3.2.9 Collector Control	3-8
3.2.9.1 Control Selection	3-85
3.2.9.2 Control Preliminary Design	3-91
3.3 Collector Field Subsystem	3-94
3.3.1 Field Shadowing and Spacing	3-94
3.3.2 Pipe Field Design	3-96
3.3.2.2 Thermal Design	3-100
3.3.2.3 Materials	3-114
3.3.2.4 Insulation	3-115
3.3.2.5 Valves and Pumps	3-115
3.3.2.6 Hydraulic Analysis	3-117
3.3.2.7 Controls	3-124
3.4 High Temperature Thermal Energy Storage (HTS)	3-130
3.4.1 Subsystem Description	3-130
3.4.2 Syltherm 800 and Storage Media Compatibility	3-136
3.4.3 Tradeoff Analysis	3-136
3.4.4 Performance Analysis	3-138
3.4.4.1 Trickle Oil	3-138
3.4.4.2 Dual Media Mode	3-143
3.4.4.3 Holding Period Heat Losses	3-146
3.4.4.4 Structural Design Analysis	3-150
3.5 Power Conversion System (PCS)	3-157
3.5.1 Subsystem Concept Trade-Offs	3-157
3.5.2 Mechanical Component Evaluations	3-168
3.5.2.1 Steam Generator	3-168
3.5.2.2 Demineralizer Equipment	3-169
3.5.2.3 Condensate Pump	3-170
3.5.2.4 Boiler Feed Pump	3-171
3.5.2.5 Deaerating Heater	3-171
3.5.2.6 Condenser	3-172
3.5.3 Controls	3-173
3.5.3.1 Normal Operating Mode Controls	3-173
3.5.3.2 Sequencing Controls	3-181
3.6 Electrical Subsystem (ES)	3-181
3.6.1 Introduction	3-181
3.6.2 GPC Interface	3-181
3.6.3 Transient Analysis	3-181
3.6.4 Collector Field	3-187
3.6.5 Defocus System	3-188
3.7 Thermal Utilization Subsystem (TUS)	3-189

Contents (con't)

Section	Page
3.8 Controls and Instrumentation Subsystem (CIS)	3-191
3.8.1 Subsystem Requirements	3-195
3.8.1.1 Collector Field Subsystem (CFS) Control Requirements	3-195
3.8.1.2 High Temperature Storage Subsystem (HTS) Control Requirements	3-199
3.8.1.3 Power Conversion Subsystem (PCS) Control Requirements	3-200
3.8.1.4 Thermal Utilization Subsystem (TUS) Control Requirements	3-201
3.8.1.5 Data Archiving Requirements	3-201
3.8.2 Control System Computer Architecture Trade-Off	3-202
3.8.2.1 Architecture Candidates	3-202
3.8.2.2 Distributed System	3-205
3.8.2.3 Centralized System	3-208
3.8.2.4 Architecture Trade-Offs and Selection	3-210
3.8.3 System Architectural Description	3-210
3.8.3.1 Remote Processor Basic Architecture	3-211
3.8.3.2 Second Level Block Diagrams	3-211
3.8.3.3 Preliminary Equipment List	3-217
3.8.4 Supervisory Control	3-218
3.8.4.1 Operating Mode Selection	3-218
3.8.4.2 Summary Status Feature	3-219
3.8.4.3 Energy Management Panel	3-219
3.8.5 Software	3-220
4 SYSTEM DESCRIPTION	4-1
4.1 System Definition	4-1
4.2 Subsystem Design Descriptions	4-1
4.2.1 Solar Collection Subsystem (SCS)	4-1
4.2.1.1 Function	4-1
4.2.1.2 System Configuration	4-1
4.2.1.3 Detailed Subsystem Description	4-7
4.2.1.4 Major Components	4-12
4.2.1.5 Control and Instrumentation	4-23
4.2.2 Power Conversion Subsystem	4-27
4.2.2.1 Function	4-27
4.2.2.2 Subsystem Configuration	4-28
4.2.2.3 Detailed Subsystem Description	4-28
4.2.2.4 Major Components	4-28
4.2.2.5 Controls and Instrumentation	4-32
4.2.3 Thermal Utilization Subsystem	4-34
4.2.3.1 Function	4-34
4.2.3.2 Subsystem Configuration	4-34
4.2.3.3 Detailed Subsystem Description	4-34
4.2.3.4 Major Components	4-36
4.2.3.5 Controls and Instrumentation	4-37

Contents (con't)

Section	Page
4.2.4. Controls and Instrumentation Subsystem (CIS)	4-39
4.2.4.1 Function	4-39
4.2.4.2 Subsystem Configuration	4-39
4.2.4.3 Detailed Subsystem Description	4-39
4.2.4.4 Major Components	4-40
4.2.5 Electrical Subsystem (ES)	4-44
4.2.5.1 Function	4-44
4.2.5.2 Subsystem Configuration	4-44
4.2.5.3 Detailed Subsystem Description	4-44
4.2.5.4 Major Components	4-45
 5 SYSTEM OPERATING PLAN	 5-1
5.1 Introduction	5-1
5.2 Weekday Operation	5-1
5.2.1 Solar Collection Subsystem Operation	5-1
5.2.2 Power Conversion Subsystem Operation	5-6
5.2.3 Thermal Utilization Subsystem Operation	5-7
5.3 Weekend Operation	5-7
5.4 Test and Evaluation	5-8
 6 SYSTEM PERFORMANCE	 6-1
 7 SYSTEM REQUIREMENTS ANALYSIS	 7-1
7.1 Energy Displacement Analysis	7-1
7.2 Life Cycle Cost Analysis	7-4
7.3 Laws and Ordinances	7-8
7.4 Health and Safety	7-9
7.5 Environmental Assessment	7-11
7.6 Reliability Assessment	7-12
 8 SUBSYSTEM DEVELOPMENT	 8-1
8.1 Collector Development	8-1
8.1.1 Engineering Prototype Collector	8-1
8.1.1.1 EPC Description	8-1
8.1.1.2 Test Laboratory Facility	8-9
8.1.1.3 Instrumentation	8-10
8.1.1.4 Test Program	8-10
8.1.1.5 EPC Test Results	8-13
8.1.1.6 EPC Incident	8-13
8.1.2 Reflector Development	8-15
8.1.2.1 Background and Approach	8-15
8.1.2.2 Design Requirements and Selection Criteria	8-17
8.1.2.3 Test Procedures	8-18
8.1.2.4 Screening of Candidate Materials	8-18
8.1.2.5 Environmental Testing	8-23
8.1.2.6 Selected LSE Reflector Surface	8-24
8.1.2.7 Cleanability of RTV 670	8-28
8.1.2.8 Production Process Development	8-28

Contents (con't)

Section

8.2	Thermal Energy Storage Development	8-35
8.2.1	Test Assembly Description	8-35
8.2.2	Instrumentation	8-35
8.2.3	Test Results and Conclusions	8-36
8.3	Shenandoah Dish Collector Field for Sandia Solar Total Energy System Test Facility.....	8-41
8.3.1	Introduction	8-41
8.3.2	Facility Design	8-42
8.3.2.1	Site Improvement	8-42
8.3.2.2	Bulkhead Interface	8-42
8.3.2.3	Loop Schematic	8-45
8.3.2.4	Controls and Instrumentation	8-45
8.3.3	Test Plan	8-48

APPENDICES

A.	Bleyle Plant Building Load Model	A-1
B.	Electrical Transient Analysis	B-1
C.	Solar Total Energy System (STES) Computer Code	C-1
D.	Life Cycle Cost Methodology	D-1
E.	Solar Easement Agreement	E-1
F.	Environmental Impact Assessment - Shenandoah STE-LSE	F-1
G.	Solar Collector Subsystem Failure Modes Effects Criticality and Safety Analysis	G-1
H.	Absorption Air Conditioner Failure Modes Effects Criticality and Safety Analysis	H-1
I.	High Temperature Thermal Energy Storage Failure Modes Effects Criticality and Safety Analysis	I-1
J.	System and Controls Failure Mode Effects Criticality and Safety Analysis	J-1
K.	Derivation of Garver's Equation	K-1
L.	Reflective Surface Tests	L-1

LIST OF ILLUSTRATIONS

Figure		Page
1.2-1	Aerial Photograph - Looking South	1-4
1.2-2	Solar Total Energy - Large Scale Experiment at Shenandoah, Georgia	1-5
1.3-1	STE-LSE Site Layout	1-10
1.3-2	Shenandoah LSE System Schematic	1-12
1.3-3	Engineering Prototype Collector	1-14
1.3-4	Trickle Oil HTS Tank	1-14
1.3-5	Annual Energy Balance for Preliminary Design System	1-17
1.3-6	System Performance - Electricity	1-18
1.3-7	System Performance - Process Steam	1-19
1.3-8	System Performance - Cooling	1-19
1.3-9	Average Solar Operating Hours with Solar Input	1-20
2.1-1	Location Map	2-2
2.1-2	The Plot Plan (5.72 Acre Plot)	2-3
2.1-3	Aerial Photograph - Looking South	2-4
2.1-4	Interconnection Piping and Description	2-6
2.1-5	Daily Total Direct Normal Insolation for Shenandoah	2-11
2.1-6	Georgia Power Company Demand Profiles	2-13
2.1-7	Single Line Electrical Load Interconnecting	2-15
2.2-1	Instantaneous Cooling Load Profile	2-18
2.2-2	Diurnal and Seasonal Cooling Load Variations	2-20
2.2-3	Summary of Bleyle Plant Inrush Measurements by GPC	2-21
2.2-4	Bleyle Plant Electric Loads	2-22
2.2-5	Process Steam Demand	2-22
2.3-1	STES Operating Model Alternatives	2-24
2.3-2	System Configuration Alternatives Evaluated for Shenandoah LSE	2-26
2.3-3	Annual Performance Summary for System Alternatives	2-27
2.3-4	Seasonal STES Operating Hours	2-27
2.3-5	Sensitivity of Solar Utilization to Collector Area and STES Operating Power for Bleyle Loads	2-28
2.3-6	Reference Design System Schematic	2-31
2.3-7	Shenandoah LSE Preliminary Design System Schematic	2-32
2.3-8	Sensitivity of System Performance to Collector Temperature	2-35
2.3-9	Solar Steam Generator Pinch Curve	2-36
2.3-10	Variation of System Performance with Collector Area and High Temperature Storage Capacity	2-37
2.3-11	High Temperature Thermal Storage Capacity Selection	2-38
2.3-12	Effect of Collector Reflectivity on System Performance	2-38
2.3-13	Effect of Turbine Efficiency on Required Collector Area	2-39
2.3-14	Absorption Air Conditioner Performance Variation with Entering Hot Water Temperature	2-40
2.3-15	Absorption Air Conditioner Size and Cost Variation with Hot Water Temperature	2-43
2.3-16	Effect of Condenser Temperature on Theoretical Steam Flow Rate	2-43
2.3-17	Variation in System Performance with Condenser Temperature	2-44
2.3-18	Effect of Condenser Temperature on Required Collector Area	2-44
2.3-19	Low Temperature Thermal Storage Capacity Sizing Rationale	2-45
2.4-1	System Requirements Summary	2-47

ILLUSTRATIONS (Cont'd)

Figure		Page
3.1-1	Site Interface and Control Drawing, Rough Grading Plan	3-2
3.1-2	Site Interface and Control Drawing, Miscellaneous Details	3-3
3.1-3	Site Interface and Control Drawing, Grading and Drainage Plan	3-4
3.1-4	Mechanical Equipment Area and Visitors Center	3-6
3.2-1	Collector Preliminary Design Process	3-7
3.2-2	Nominal Collector Performance and Design Parameters	3-10
3.2-3	Focal Length Optimization	3-11
3.2-4	Reflector Surface Parameter Sensitivity Analysis	3-11
3.2-5	Slope Error Sensitivity Analysis	3-12
3.2-6	Concentration Ratio Sensitivity Analysis	3-12
3.2-7	Tracking Bias Error Sensitivity Analysis	3-13
3.2-8	Candidate Mount Configurations	3-16
3.2-9	Receiver Concepts Investigated	3-18
3.2-10	Receiver Flux Profiles	3-19
3.2-11	Integrated Receiver Flux Profiles	3-19
3.2-12	Flat Plate Receiver Analysis Results	3-20
3.2-13	Coil-In-Cavity Receiver Design Concept	3-21
3.2-14	Typical Cavity Wall Flux Profile	3-22
3.2-15	Receiver Performance Comparison	3-22
3.2-16	Hydraulic Entrance Approaches (5M Dish)	3-24
3.2-17	Selected Approach vs. Cassegrain Approach for Receiver Position	3-26
3.2-18	Total Collector Weight and Cost for Constant Structure Stiffness	3-29
3.2-19	Collector Field Costs for 79,500 Ft ² Array	3-29
3.2-20	Collector Efficiency vs. Diameter for Various Insolation Levels	3-30
3.2-21	Average Shenandoah Insolation	3-30
3.2-22	Variation of Steady State Heat Loss to Collector Diameter and Piping Radius	3-31
3.2-23	Composite Steady State Heat and Pumping Power Losses vs. Tubing Size	3-31
3.2-24	Collector Field Thermal Capacity vs. Collector Diameter for Average 10 Hr Day	3-32
3.2-25	Daily Average Total Field Energy Parameters vs. Collector Diameter	3-32
3.2-26	Optimization Results - Collector Diameter vs. Cost/Btu Delivered	3-33
3.2-27	LSE 7-Meter Collector	3-34
3.2-28	7-Meter Collector Petal Configuration	3-39
3.2-29	7-Meter Collector Hub Section	3-43
3.2-30	Reflector Truss Design	3-45
3.2-31	Collector Structural Element Options	3-46
3.2-32	Collector Geometry	3-49
3.2-33	Base Assembly	3-51
3.2-34	Collector Base Frame Model	3-54
3.2-35	Yoke Support Assembly	3-57
3.2-36	Yoke Stress Model	3-61
3.2-37	Counterweight	3-63
3.2-38	On-Off Control for Polar Drive	3-66
3.2-39	Actuator and Motor Assembly	3-71
3.2-40	View of Polar Axis of Dish Drive Mechanism	3-73
3.2-41	Receiver Design Flux Levels	3-74
3.2-42	Receiver Film Coefficient Matching	3-75
3.2-43	Receiver Tube Sizing/Pressure Drop Relationship	3-76
3.2-44	Receiver Sizing for A Single Coil Configuration	3-77
3.2-45	Twin Parallel Coil Configuration	3-77
3.2-46	Channel Flow Receiver Configuration	3-78
3.2-47	Receiver Configuration Selection	3-79

ILLUSTRATIONS (Cont'd)

Figure		Page
3.2-48	Receiver Assembly	3-81
3.2-49	Receiver Support Model	3-83
3.2-50	Flex Hose Layout	3-87
3.2-51	Tracking Error Sensitivity	3-89
3.2-52	Energy Collected as a Function of Bias Error	3-90
3.2-53	Equatorial Mount Effects of Tilt Error	3-90
3.2-54	Optical Sensors Positioning	3-92
3.2-55	Collector Control Schematic	3-93
3.3-1	Alternative Parabolic Dish Field Layout Geometries	3-95
3.3-2	Typical Properties of Dow Corning Syltherm 800	3-97
3.3-3	Common Feed and Return Field Piping	3-98
3.3-4	Branched Feed and Return Field Piping	3-99
3.3-5	Alternative Pipe Field Arrangements	3-103
3.3-6	Heat Loss Coefficient vs. Pipe Diameter and Insulating Thickness	3-105
3.3-7	System Heat Loss vs. Pipe Radius and Dish Diameter	3-105
3.3-8	Effect of Reducing Piping Diameter on Field Heat Loss and Pumping Power	3-107
3.3-9	Nested Pipe Configuration	3-107
3.3-10	Parametric Analysis Summary of Nested Pipes (Tubes)	3-110
3.3-11	Parametric Analysis of Nested Pipes (Tubes)	3-110
3.3-12	Temperature Drop and Heat Loss vs. Pipe Diameter and Flow Rate	3-111
3.3-13	Branch Line and Manifold Arrangement	3-113
3.3-14	Dual Controlled - Flexing Expansion Joints for Thermal Expansion Compensation	3-113
3.3-15	Full Flow Temperature Distribution for Nested Branch and Up and Down Pipes	3-114
3.3-16	Typical Insulation Outline for Syltherm 800 Piping	3-116
3.3-17	Collector Field Interface P&ID Layout	3-119
3.3-18	Mechanical Equipment Area High Temperature Storage Piping	3-121
3.3-19	Collector Pump Characteristics for Single Field Pump	3-122
3.3-20	Collector Pump Characteristics for Parallel, 50 Percent Flow Pumps	3-123
3.3-21	Collector Field Circulating Pumps Performance Pumps	3-123
3.3-22	Solar Insulation and Pump Power vs. Solar Time	3-124
3.3-23	Collector Field Control Scheme Variations	3-125
3.3-24	Pneumatic Control Valves	3-127
3.3-25	STE-LSE Site Layout	3-128
3.3-26	STE-LSE Site Layout with Added Control Valves	3-129
3.4-1	Trickle Oil Schematic - Charging Mode	3-131
3.4-2	Trickle Oil Schematic - Discharging Mode	3-134
3.4-3	Trickle Oil Schematic Modification to Dual Media - Discharging Mode	3-135
3.4-4	Flow Rate Variation Effects on Discharge	3-139
3.4-5	Heat Transfer Parameter Effect	3-139
3.4-6	Tank Height Tradeoff Results	3-140
3.4-7	Allowable Tank Height	3-140
3.4-8	Effect of Particle Size on Heat Transfer	3-141
3.4-9	System Design Performance for Trickle Mode	3-142
3.4-10	Trickle Flow - Series Charge Performance	3-144
3.4-11	Inversion Profiles for the Large Tank Initially Charged at 62% Available Energy	3-145
3.4-12	HTS Tank Inversion Efficiency	3-146
3.4-13	Dual Media Mode Performance	3-147
3.4-14	Holding Period Temperature Profiles for the Trickle Oil System With the Tank Initially Fully Charged	3-150
3.4-15	Holding Period Temperature Profiles After 24 Hour Hold for a Tank Initially Partially Charged	3-151

ILLUSTRATIONS (Cont'd)

Figure		Page
3.4-16	Holding Period Losses After 24 Hour Hold for a Tank Initially at 500°F	3-152
3.4-17	Trickle Oil Tank Layout	3-153
3.4-18	Tank Inlet Piping Arrangement	3-155
3.4-19	Tank Outlet Piping Arrangement	3-156
3.5-1	Heat Input Sensitivity to Throttle Pressure and Temperature	3-162
3.5-2	Steam Generator ΔT Sensitivity to Throttle Pressure and Heating Fluid Inlet Temperature	3-162
3.5-3	Solar Steam Generator Pinch Curve	3-163
3.5-4	Estimated Performance Comparison Between Multi-Stage and Two Single Stage Turbines	3-163
3.5-5	Power Conversion Subsystem Requirements Summary	3-164
3.5-6	PCS Heat/Mass Balance Diagram 400 KWe Output	3-166
3.5-7	PCS Heat/Mass Balance Diagram 300 KWe Output	3-166
3.5-8	Heat Input to Power Conversion Subsystem vs. Gross Electric Output	3-167
3.5-9	Steam Generator Component Group	3-173
3.5-10	Condenser/Makeup Injection Component Group	3-174
3.5-11	Condensate Pump/Deaerator Component Group	3-174
3.5-12	Demineralizer Unit	3-175
3.5-13	Chemical Injection Unit	3-175
3.5-14	Process Steam Desuperheater	3-176
3.5-15	Boiler Feed Pump Unit	3-176
3.5-16	Steam Generator Pressure Control Loop	3-179
3.5-17	Condenser Pressure Control Loop	3-180
3.6-1	Single Line Electrical Load Interconnection	3-182
3.6-2	Transient Model Diagram	3-183
3.6-3	System Root Locus	3-184
3.6-4	Effect of Inertia and Load Step	3-184
3.6-5	25 KW Step Interconnected	3-185
3.6-6	25 KW Step Isolated	3-186
3.6-7	Field Sensor and Control Cable	3-187
3.7-1	Thermal Utilization Subsystem Reference Design Excess Energy Dissipation	3-190
3.7-2	Single Tank Thermal Utilization Subsystem Normal Operation/Storage Temperature Less Than AAC Return Temperature	3-192
3.8-1	Control and Instrumentation Subsystem Block Diagram	3-197
3.8-2	CIS Preliminary Design Requirements	3-199
3.8-3	Distributed Control System Computer Architecture	3-202
3.8-4	Centralized Control System Architecture	3-207
3.8-5	Typical Alternate Computer Architectures	3-207
3.8-6	Remote Processor Design Architecture	3-212
3.8-7	PCS Second Level Block Diagram	3-213
3.8-8	Collector Field Second Level Block Diagram	3-214
3.8-9	HTS Second Level Block Diagram	3-215
3.8-10	TUS Second Level Block Diagram	3-116
3.8-11	Summary Status Feature	3-219
3.8-12	Energy Management Panel	3-221
3.8-13	STE-LSE Operator Control Console	3-222
3.8-14	STE-LSE Control Center	3-222

ILLUSTRATIONS (Cont'd)

Figure		Page
4.1-1	Shenandoah System Schematic	4-3
4.2-1	Solar Collection Subsystem	4-5
4.2-2	Piping and Instrumentation Diagram - Solar Energy Collector Field - Syltherm 800 at 400 KW	4-6
4.2-3	Piping and Instrumentation Diagram - Syltherm 800 Oil at 400 KW	4-8
4.2-4	Nested Pipe Analysis	4-9
4.2-5	Branch Isolation and Control	4-11
4.2-6	Pneumatic Control Valves	4-11
4.2-7	Thermal Expansion Compensator Linear Type	4-11
4.2-8	Collector Geometry	4-13
4.2-9	Receiver Configuration	4-14
4.2-10	Actuator Speed Selection	4-16
4.2-11	Layout Oil/Storage Medium Tank	4-18
4.2-12	Tank Inlet Piping Arrangement	4-20
4.2-13	Tank Outlet Piping Arrangement	4-21
4.2-14	Sump Design	4-22
4.2-15	Pump Cross Section and Materials	4-24
4.2-16	Solar Insolation and Pump Power vs. Solar Time	4-25
4.2-17	CFS Pump Characteristic Curve	4-25
4.2-18	HTS and SGS Pump Characteristic Curves	4-26
4.2-19	Piping and Instrumentation Diagram - Power Conversion Subsystem	4-29
4.2-20	Power Conversion Subsystem Flow Circuit	4-30
4.2-21	Demineralizer Unit Flow Circuit	4-31
4.2-22	Boiler - Turbine Control	4-33
4.2-23	Turbine - Generator Speed/Load Governor Control	4-33
4.2-24	Piping and Instrumentation Diagram - Thermal Utilization Subsystem	4-35
4.2-25	Piping Material Specification	4-38
4.2-26	Computer Architecture	4-40
4.2-27	Electrical Subsystem	4-44
4.2-28	Defocus Circuit	4-46
4.2-29	Field Sensor and Control Cable	4-46
4.2-30	Single Line Electrical Load Interconnection	4-48
5.4-1	System Operation - Preliminary Activities Schedule	5-8
5.4-2	Subsystem/Component Tests (SCF)	5-10
5.4-3	Subsystem/Component Tests (HTS)	5-11
5.4-4	Subsystem/Component Tests (SGS)	5-12
5.4-5	Subsystem/Component Tests (PCS)	5-13
5.4-6	Subsystem/Component Tests (TUS)	5-14
5.4-7	Instrument Location and Identification	5-17
6.0-1	System Performance Model	6-1
6.0-2	System Performance-Electricity	6-2
6.0-3	System Performance-Process Steam	6-2
6.0-4	System Performance-Cooling	6-3
6.0-5	System Field Losses and Parasitic Power	6-4
6.0-6	Average Low Temperature Excess	6-4
6.0-7	System Energy Flow-Monthly Totals - MTI Turbine	6-5
6.0-8	Thermal Output Summary - Monthly Totals - MTI Turbine	6-5

ILLUSTRATIONS (Cont'd)

Figure		Page
7.1-1	Effect of Turbine Efficiency on Annual Energy Cost Savings For Natural Gas	7-5
7.1-2	Effect of Turbine Efficiency on Annual Energy Cost Savings for Fuel Oil	7-5
7.2-1	Projected Economics of Solar Total Energy	7-7
7.3-1	Solar Easement Reference Lines	7-10
7.3-2	Setback and Height Restrictions for Property Near LSE, Shenandoah	7-11
7.6-1	Reliability Block Diagram, STES-LSE	7-16
7.6-2	Solar Availability for Bleyle Plant Loads	7-17
7.6-3	Utility Demand Profiles	7-19
7.6-4	Solar Availability for Utility Peak Loads	7-20
7.6-5	Characteristic Utility System Availability	7-21
7.6-6	Effect of Size on Load Carrying Capability	7-22
8.1-1	Layout of 5-Meter Engineering Prototype Collector	8-2
8.1-2	Front View of EPC	8-3
8.1-3	Side View of EPC	8-3
8.1-4	EPC Receiver	8-4
8.1-5	Sketch of EPC Receiver	8-5
8.1-6	EPC Receiver: Coil Assembly	8-7
8.1-7	Flexible Pipe Assembly	8-8
8.1-8	EPC Control System Interface Drawing	8-8
8.1-9	Typical Flux Scan	8-14
8.1-10	Flux Profile Test Results	8-14
8.1-11	GE Parabolic Dish Receiver Thermal Loss	8-15
8.1-12	LSE Reflector Surface Development Process	8-16
8.1-13	LSE Reflector Surface Candidates	8-16
8.1-14	Reflector Surface Design Requirements	8-17
8.1-15	Reflector Surface Candidates	8-19
8.1-16	Comparison of 5457 and 5657 Specular Reflectance with ALGLAS Coating	8-26
8.1-17	Specular Reflectance Test Data for 5657 Substrate with Various Coatings	8-27
8.1-18	Photos of Contaminated and Cleaned Surfaces	8-30
8.1-19	Typical Chemical Brightening Process	8-31
8.1-20	Specular Reflectance of Treated 5052 Samples from 5-Meter Reflector Panels	8-31
8.1-21	RTV 670 Coating Process	8-32
8.1-22	Cross Section of Vacuum Bonding Rig	8-32
8.1-23	Partially Bonded Petal	8-33
8.2-1	Schematic of the Trickle Oil Column Experiment	8-36
8.2-2	Trickle Oil Test Column	8-37
8.2-3	Trickle Oil Experiment Instrumentation Layout	8-38
8.2-4	Trickle Oil Column Results	8-39
8.2-5	Column Test Results	8-40
8.3-1	Quadrant Test Site Plan Interface Drawing	8-43
8.3-2	Quadrant Test Bulkhead Interface Drawing	8-44
8.3-3	Quadrant Test Schematic	8-46
8.3-4	Quadrant Test Electrical Schematic	8-47

LIST OF TABLES

Table		Page
1.2-1	Design Electric Loads	1-6
1.2-2	Design Cooling Loads	1-6
1.3-1	Systems Evaluated for the Shenandoah LSE	1-7
1.3-2	Comparison of Steam and Organic Cycle Systems for the Shenandoah LSE	1-8
1.3-3	Specifications for Major Equipment	1-11
2.1-1	Overall Requirements Summary	2-7
2.1-2	Top Level System Requirements for the Shenandoah LSE	2-10
2.1-3	Atlanta 1975 Weather Analysis	2-12
2.1-4	Operational Modes of Electrical Supply Interface System	2-13
2.2-1	Bleyle Plant Loads for 42,000 Ft ² Expanded Plant	2-16
2.2-2	Internal Heat Gains for Plant Load Calculations	2-17
2.2-3	Bleyle Plant Electric Load Breakdown	2-17
2.2-4	Design Electric Loads	2-21
2.2-5	Design Cooling Loads	2-23
2.3-1	System Sizing/Operating Power Selection Trade-Off Summary	2-29
2.3-2	Comparison of Three Heat Transfer Fluids	2-34
2.3-3	Heat Transfer Fluid Comparison for Shenandoah LSE	2-35
2.3-4	Absorption Air Conditioner Characteristics Desired	2-41
2.3-5	Comparisons of Conditions with and Without Chilled Storage	2-46
3.2-1	Shenandoah Collector Design Requirements	2-8
3.2-2	Large Diameter Reflector Dish Construction Options	3-14
3.2-3	Hydraulic Approach Conclusions	3-25
3.2-4	Shenandoah Collector Control Options	3-27
3.2-5	LSE Collector Low Cast Design Features	3-35
3.2-6	Collector Parameters	3-35
3.2-7	Design Point Performance Parameters	3-36
3.2-8	Petal Manufacturing Option Evaluation	3-37
3.2-9	Mechanical Properties of Candidate Petal Alloys	3-41
3.2-10	Rib vs. Truss Deflection & Stress in 90 mph Head-on Wind	3-47
3.2-11	Parabolic Dish Forces/Moments in 90 mph Wind	3-48
3.2-12	Yoke Stress Analysis Summary	3-65
3.2-13	Actuator Selection	3-68
3.2-14	Hydraulic Cylinder vs. Electric Jackscrew Actuator Trade-off	3-68
3.2-15	Receiver Thermal Performance	3-83
3.2-16	Strut Location Tradeoff	3-84
3.2-17	Collector Control Features	3-91
3.2-18	Optical Sensor Fiber Bundle Specifications	3-92
3.3-1	Field Piping Configuration Trade-off	3-100
3.3-2	Insulation System Candidates	3-101
3.3-3	Steady State Heat Loss and Thermal Capacity Summary for Collector Loop Subsystem	3-102
3.3-4	Trade-off of Field Performance with Number of Dishes in Series	3-104
3.3-5	Steady-State Heat Transfer Calculations for Turbulent Flow in an Insulated Two-Pipe System/Dow Corning Silicon-B Fluid	3-108
3.3-6	Results of Pipe Nesting Analysis	3-109
3.3-7	Suggested Pipe Support Spacing	3-112
3.4-1	Description of HTS Subsystem	3-132
3.4-2	Properties of Syltherm 800	3-137
3.4-3	Taconite Chemical Composition Summary	3-137

TABLES (con't)

Table		Page
3.4-4	Trickle Flow Operation	3-143
3.4-5	Dual Media Operation	3-148
3.4-6	Hold Conditions Considered and Material Properties Used in Transient Heat Loss Analysis	3-149
3.4-7	Thermal Losses for Holding Periods	3-151
3.4-8	Summary of Tank Thermal Losses	3-154
3.5-1	1 Expander Non-Condensing Cycle	3-158
3.5-2	2 Expander Cascaded Cycle 500 psig	3-159
3.5-3	Multistage Uncontrolled Extraction Turbine Cycle	3-160
3.5-4	Summary of Rationale for Selection of Multi-Stage Extraction Cycle	3-164
3.5-5	Power Conversion Subsystem Performance Tabulation For Modified GE MDTD Multi-Stage Uncontrolled Extraction	3-165
3.5-6	Demineralizer Requirements	3-170
3.5-7	Condensate Pump Alternatives Evaluation	3-171
3.5-8	Boiler Feed Pump Characteristics	3-172
3.5-9	Steam Generator Component Group Controls Requirements	3-177
3.5-10	Condenser/Makeup Injection Component Group Controls Requirements	3-177
3.5-11	Condensate Pump/Deaerator Component Group Controls Requirements	3-177
3.5-12	Make-up Demineralizer Component Control Requirements	3-178
3.5-13	Chemical Injection Unit Component Control Requirements	3-178
3.5-14	Process Steam Desuperheater Control Requirements	3-178
3.5-15	Boiler Feed Pump Component Control Requirements	3-178
3.6-1	Defocus Power Supply	3-188
3.7-1	Single Stage Absorption Chiller Characteristics for Trane Unit	3-193
3.7-2	TUS Equipment List	3-194
3.8-1	Baseline Operational Data Set Summary	3-202
3.8-2	Operational Data Set Details	3-203
3.8-3	Central Control and Computer Complex Equipment List	3-217
3.8-4	Software Management Plan Outline	3-223
4.2-1	Suggested Pipe Support Spacing	4-7
4.2-2	Tubing Insulation Schedule	4-9
5.2-1	Weekday System Operating Modes	5-2
5.3-1	Weekend System Operating Modes	5-8
7.1-1	Bleyle Energy Consumption and Cost Projections for 42,000 Ft ² Plant	7-1
7.1-2	Summary of Energy Rate Schedules Applicable to Bleyle Plant	7-2
7.1-3	Computation of Typical Bleyle Plant Monthly Bills	7-3
7.1-4	Energy Displacement of Shenandoah STES	7-3
7.1-5	Shenandoah STES Annual Savings Potential	7-4
7.2-1	Economic Assumptions	7-6
7.2-2	Experimental System Capital Cost Summary	7-6
7.2-3	Projected System Economics	7-7
7.3-1	Site Planning Guidelines	7-9
7.6-1	FMEC and SA Data	7-12
7.6-2	STE-LSE Shenandoah FMEC and SA Identification	7-13

TABLES (Con't)

Table		Page
7.6-3	Solar Collector FMEA - Significant Design Impact Items Identified	7-13
7.6-4	Absorption Air Conditioner FMEA Summary	7-14
7.6-5	High Temperature Storage FMEA Summary	7-14
7.6-6	Total System FMEA Summary	7-15
7.6-7	System Availability for Bleyle Loads	7-17
7.6-8	Availability Prediction Worksheet - Fossil Heater	7-18
7.6-9	Availability Prediction Worksheet - Steam Generator	7-18
7.6-10	Availability Summary - Key Items	7-19
8.1-1	EPC Test Matrix	8-11
8.1-2	Reflector Surface Selection Criteria	8-18
8.1-3	Substrate Candidate Characteristics	8-19
8.1-4	Solar Reflectance Values of Typical Substrate Materials	8-20
8.1-5	Candidate Reflectance Enhancement Characteristics	8-21
8.1-6	Typical Enhanced Reflectance Test Results	8-21
8.1-7	Candidate Protective Coating Characteristics	8-22
8.1-8	Characteristics of GE RTV 670	8-23
8.1-9	Critical Environmental Test Results	8-25
8.1-10	Combined Environmental Test Results	8-26
8.1-11	LSE Reflector Petal Incremental Production Costs	8-27
8.1-12	Effect of Cleaning on Reflector Surface Performance	8-29
8.1-13	Test Data Evaluation of Bonding Materials for Reflector Sheet	8-30
8.2-1	Summary of Preliminary Trickle Oil Column Tests	8-39
8.3-1	Outline of Planned Tests for Parabolic Dish Quadrant Test	8-48

**SECTION 1
SUMMARY**

SECTION 1
PROGRAM SUMMARY

1.1 INTRODUCTION

The Solar Total Energy Program (STEP) is a separate activity of the National Solar Electric Applications Program and is supported by the U.S. Department of Energy (DOE). During the program, a series of solar total energy systems is planned which will be designed, constructed, and operated to provide electricity and thermal energy to localized users such as Government and institutional facilities, apartment houses, shopping centers, and industrial and commercial plants, buildings, and complexes. The overall purpose of these energy systems is to demonstrate the high potential that solar energy offers for total energy systems, to develop a solar-oriented technology compatible with the high temperature demands of electric power conversion via thermodynamic cycles, and to provide the stimulus required so that private industry will aggressively participate, both as manufacturers and users.

1.2 PROJECT OVERVIEW

The first industrial application of the solar total energy concept has been initiated as a cooperative venture of the U.S. Department of Energy and the Georgia Power Company. The Solar Total Energy-Large Scale Experiment (STE-LSE) project consists of the design, construction, operation, and technical evaluation of a solar total energy system providing power to a knitwear factory operated by Bleyle of America, Inc. The preliminary design phase of the project has been completed with the publication of this final report. The definitive or Final Design Phase (Phase IV) will extend over a fourteen (14) month period that will be completed in October, 1979. During this phase the design definition will be completed, and fabrication of hardware for the Solar Total Energy System (STES) will be initiated. Phase V, Site Construction and Installation, will extend over the 18 month period after completion of Phase IV and will terminate with the STES being in a ready status for operational testing. Phase VI Operation will extend over a minimum period of 24 months. During this phase, the preliminary period of operation will provide verification checkout of the system control and other subsystems in order to finalize modes, sequencing, and setpoints. A period of normal operation for collection of system data will be followed by system experimental operation to determine the effect of variations in the electric utility interface and the thermal input to the Bleyle plant from the STES as related to the solar insolation availability.

1.2.1 PROGRAM OBJECTIVES

The U.S. Department of Energy (DOE) objectives for the Solar Total Energy - Large Scale Experiment at Shenandoah are to design, construct, test, evaluate, and operate a Solar Total Energy System (STES) in conjunction with an apparel manufacturing plant at Shenandoah, Georgia. An important feature of the site specific design is that it retains flexibility for experimental modes of operation relevant to other site applications. Meaningful performance analysis for the Shenandoah site and performance evaluation for broader applications are desired project results. Specifically stated, the program objectives are to:

1. Develop within industry the engineering and development experience on large scale solar total energy systems for subsequent demonstration projects.
2. Assess the interaction of solar energy technology with the application environment.
3. Narrow the prediction uncertainty of the cost and performance of solar total energy systems.
4. Expand solar engineering capability and experience with large-scale hardware systems.
5. Disseminate information on solar total energy.

1.2.2 SHENANDOAH SYSTEM DESIGN OBJECTIVES

The primary objective of the current program phase has been to develop and define the Preliminary Design based on an extension of the previous Conceptual Design. The design has been aimed at satisfying two major objectives:

1. The design must reflect a system size large enough to encounter problems typical of full-scale demonstration and commercial applications.
2. The design must utilize all collected energy in the most cost-effective manner consistent with overall experiment objectives.

The first objective has led to component sizes and hardware selections compatible with normal on-site cogeneration requirements for typical light industrial applications. These requirements are typified by the Bleyle knitwear plant, which requires electrical power output in the range of 200-500 kWe and accompanying thermal output greater than 1 MWt. Within the context of the total energy concept of maintaining energy rejected from a power cycle at a high enough temperature level to enable its use to satisfy thermal needs, the second objective provided guidance in the selection of the solar plant size relative to system output balance with on-site plant loads. The achievement of these objectives will provide a solar total energy system design which will lead to a system experiment to evaluate the effectiveness and efficiency of using solar energy to provide electrical power, process steam, and thermal energy for space heating and cooling.

1 2.3 PROJECT PARTICIPANTS

The first industrial application of the solar total energy concept has been initiated as a cooperative venture of the United States Department of Energy (DOE) and the Georgia Power Company. Under terms of the cooperative agreement, the Georgia Power Company and DOE share site costs on a 50-50 basis for those activities of common interest. Additional services are provided to DOE by Georgia Power and their participants on a reimbursable basis. Member organizations of the Georgia Power team and their activities include:

1. Shenandoah Development, Inc. Developer and factory building owner.
2. Georgia Institute of Technology. Solar consultation to Georgia Power.
3. Heery and Heery, Inc. Site architectural and engineering liaison services.
4. Owens - Corning Fiberglas. Energy conservation services.
5. Westinghouse Electric Corp. Site liaison.

The General Electric Company, Space Division (GE-SD) was selected by DOE following a competitive conceptual design phase as the subcontractor to design, fabricate, install and operate the DOE funded and owned STES for the Shenandoah Large Scale Experiment. GE-SD has engaged the following organizations as members of the STES team:

1. GE Energy Systems Technology Division. Steam system analysis and component selection.
2. GE Management and Technical Services Company (MATSCO). Hardware procurement and site construction management.
3. GE Ground Systems Department. Control system design and analysis.
4. Lockwood-Greene. Engineering and architectural design.

Sandia Laboratories, Albuquerque, N.M., is DOE's technical manager for the STE-LSE. This large scale experiment is an outgrowth of research started in 1972 by Sandia.

1.2.4 SHENANDOAH SITE DESCRIPTION

The site for the STE-LSE is located in the industrial park of Shenandoah, Georgia, which is about 40 kilometers (25 miles) south of the Atlanta airport on U.S. highway I-85. Shenandoah is a new town near Newnan, Georgia being developed by Shenandoah Development Incorporated (SDI). The site that was made available by SDI for the total energy facility consists of approximately 23,000 square meters (5.72 acres) of land. As shown on Figure 1.2-1, the site is near the intersections of Interstate 85 and Georgia Highway 34, connecting the site to Atlanta and Newnan, respectively. The Bleyle Knitwear Plant is located along the west property line of the development. Access to the Bleyle facilities is via Amlajack Boulevard and St. Johns Circle.

1.2.5 BLEYLE KNITWEAR PLANT APPLICATION

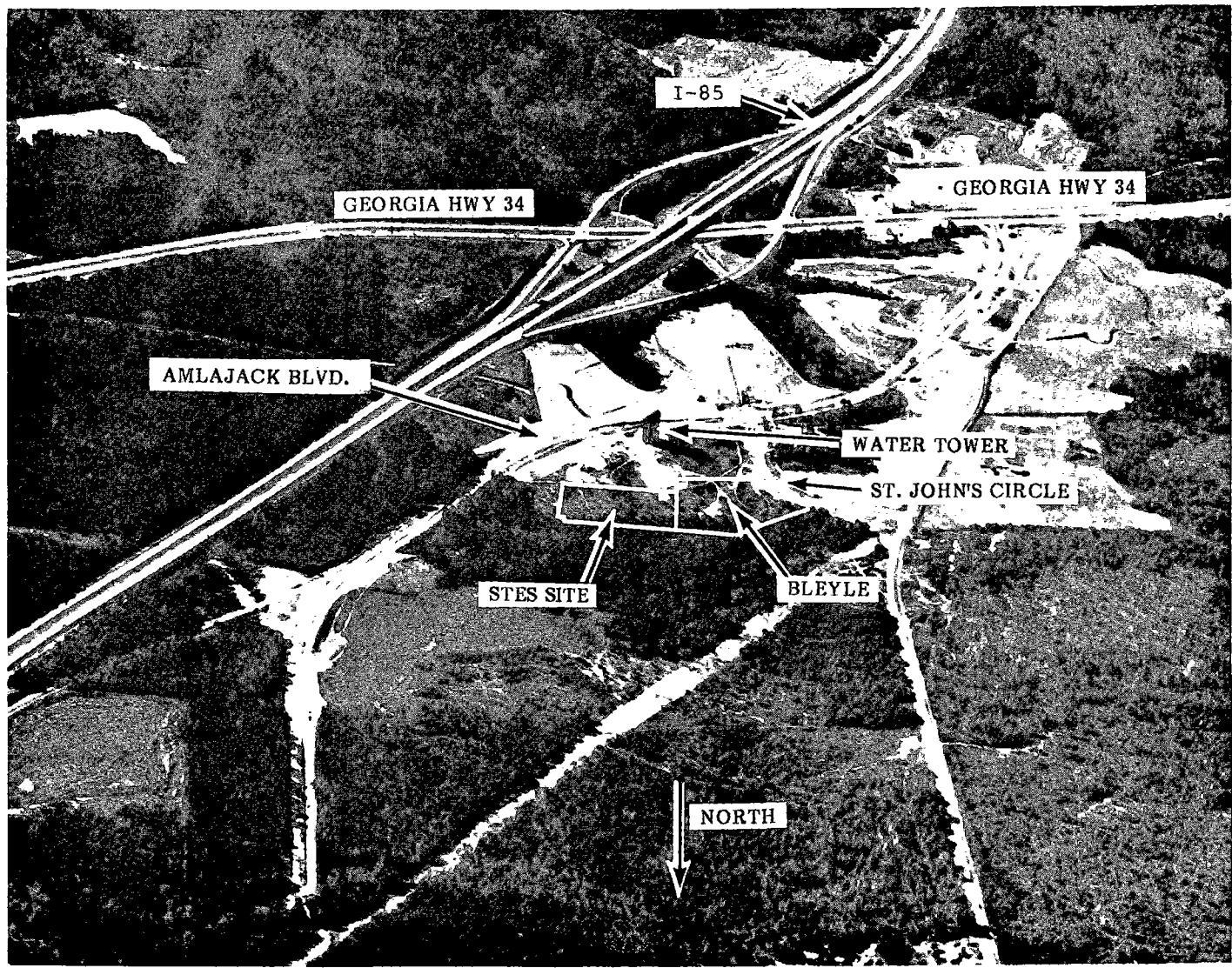
The basic function of the STES at Shenandoah is to supply the electric power, process steam, and space heating and cooling demands of the expanded 3900 square meters (42,000 ft²) Bleyle Plant and for the STES Mechanical Building. The Bleyle factory, initially equipped with its own independent (conventional) energy source, will derive at least 60 percent of its annual energy needs from the sun when the solar energy system becomes operational in the first quarter of 1981. Figure 1.2-2 is an artist's concept of the STE-LSE at the Shenandoah site showing the STES in relation to the Bleyle Plant which is located in the upper left of the figure.

The design electric loads used to size the STES generator are summarized in Table 1.2-1. The plant loads have been estimated by Heery and Heery, Architects. In normal operation, the site electric load will not exceed 400kW. To accommodate load fluctuations and to provide a better match with the site thermal loads, the STES normally operates with a 100kW base load from the utility and electric load follows between 200-300kW in normal operation. Except for the lunch and shift breaks, the plant electric load profile is relatively constant over the two shift operation.

The plant's process steam demand is currently supplied by a natural gas fired boiler. Process steam at saturated conditions which is used to press fabric is required during all working hours. The design cooling loads, based on ASHRAE design conditions, are summarized for the Bleyle Plant and STES mechanical building in Table 1.2-2. The cooling loads consist primarily of internal heat generated by the process and building lighting and are relatively constant during plant operating hours. However, the plant Heating, Ventilating and Air Conditioning (HVAC) system incorporates an economizer cycle which supplies a major portion of the internally generated cooling load from December to February. To provide a more optimum site thermal to electric load ratio for the STES, the cooling loads are served by a chilled water system supplied by an absorption chiller.

1.3 PRELIMINARY DESIGN DESCRIPTION SUMMARY

The preliminary design of the Shenandoah LSE System has evolved during the Conceptual and Preliminary Design phases as a result of extensive system and subsystem evaluations. The initial phase of the Program included a study to identify the best overall experimental system by which to achieve the program objectives and to supply the electric power, process steam, and heating and cooling demands of the Bleyle Plant. Basic systems evaluated for the Shanandoah LSE are shown in Table 1.3-1. Eleven different configurations were evaluated, including seven distributed collection/central generation systems employing both steam and organic Rankine power conversion systems, two small-scale central receiver systems, one distributed collection/distributed generation system, and one photovoltaic/solar total energy system. All of the candidate systems were carefully screened with respect to specific performance and cost, hardware maturity, and projected adaptability to larger, commercial size installations.



1-4

Figure 1.2-1. Aerial Photograph - Looking South

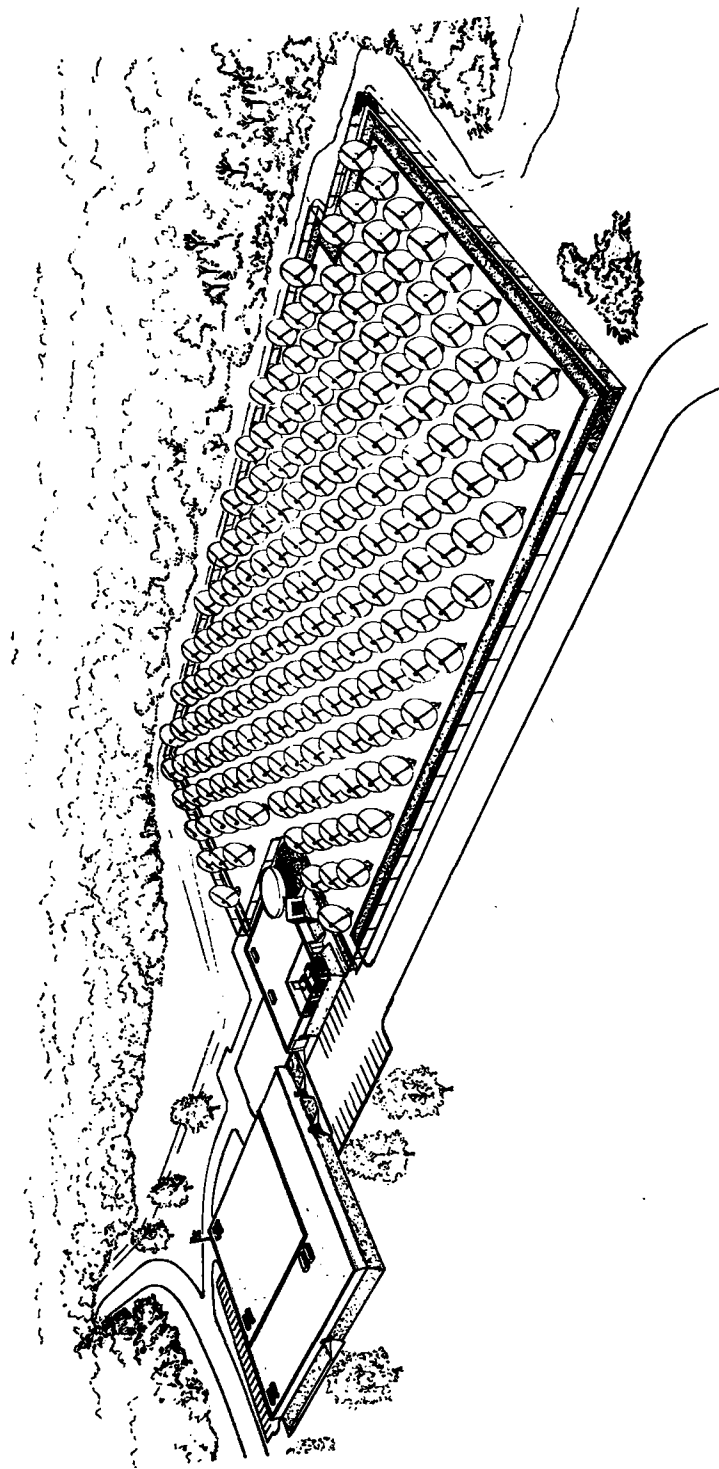


Figure 1.2-2. Solar Total Energy-Large Scale Experiment at Shenandoah, Georgia (Artist's Concept)

Table 1.2-1. Design Electric Loads

Bleyle Plant		STES Operation	
Process Machinery	83	Collection Subsystem	38
Lighting	80	Power Conversion Subsystem	20
Air Handling Equipment	59	Thermal Utilization Subsystem	66
Process Equipment	32	STES Mechanical Bldg.	10
Miscellaneous	16		
Total	270 kW	Total	134 kW

Table 1.2-2. Design Cooling Loads

Load Source	Load (Tons)
Bleyle Plant	143
Loading/Storage Area	20
STES Mechanical Building	10
Total	173

Table 1.3-1. Systems Evaluated For The Shenandoah LSE

Candidate System Concept	Overall Evaluation
Distributed Array/Steam PCS*	Minimum Hardware Development Large Size Hardware Availability Good Load Match Cascaded Total Energy Configurations
Distributed Array/Organic PCS*	Hardware Adaptable to LSE Non-Cascaded Process Steam High Electrical Efficiency
Small Scale Central Receiver	Field Shape/Size Mismatch Diseconomies Of Small Scale
Distributed Collection/ Distributed Generation	Good Performance Hardware Development Schedule Incompatible
Photovoltaic/Hybrid STES	Separate Process Steam System Required.
*Power Conversion Subsystem	

Energy cascading, using collected energy at a high temperature to generate electricity and then again at reduced temperature to supply thermal loads, was a primary consideration. Candidate configurations were required to provide exhaust heat and extraction steam from the electrical generating equipment to match site thermal load pressures, temperatures, and flow rates in order to maximize energy utilization. Leading system configurations that survived the evaluations screening were determined to be those which included steam and organic Rankine power conversion systems.

Four steam and three organic configurations were evaluated. Candidate hardware was restricted to systems requiring minimum development consistent with the LSE schedule. Steam systems included dual turbines, small extraction turbines, and steam engines. Both back pressure and condensing organic turbine configurations were evaluated.

The two most promising generic systems resulting from the previous comparisons included (1) a fully cascaded steam system providing process steam from an intermediate extraction stage and heating and cooling from a back pressure condenser and (2) a back pressure organic system that would provide process steam through direct heat exchange with collector fluid in a series boiler arrangement with the organic cycle boiler. The results of additional trade-offs to compare these two systems specifically for the STE-LSE Shenandoah application are summarized in Table 1.3-2. The organic Rankine system showed better electric power generation efficiency (13%) at the STE-LSE power level than the steam Rankine system. However, the other selection factors, including availability of large scale hardware with minimum development requirements and ready acceptance by public utilities and users for commercial applications, led to the selection of the steam Rankine system.

Of particular concern with organic systems are their toxic and flammable organic working fluids and the limited experience related to actual performance, reliability, and maintainability of large organic power conversion systems. In addition, organic systems available for the Shenandoah LSE cannot provide cascaded process steam without significant modifications. Therefore, the steam system was selected as the best system for meeting the Bleyle requirements with the most potential for widespread commercial application.

Table 1.3-2. Comparison of Steam and Organic Cycle Systems for the Shenandoah LSE

Major Criteria	Selector Factor	Steam	Organic	Selection
Performance	Annual Energy Savings Design Point Electric Power Generation Efficiency Parasitic Power	2.6 X 10 ⁶ kWh 10.3%	3.1 X 10 ⁶ kWh 13.0%	Organic
Design	Boiler ΔT Operating Pressure Physical Size Start-Up Safety	250 ^o F 500 PSIA 17' LG X 5'W X 10' H 30 Min Higher Pressure	160 ^o F 200 PSIA 30' LG X 15'W X 10' H 15-20 Min Toxic Fluid And Flammable	Steam
Maintainability- Reliability	Hardware With Field Experience	Understood And Accepted	Limited Experience	Steam
Cost/Availability	PCS Cost for LSE Cost Benefit Factor Availability Risk	\$400k 1.14 Low	\$600k 1.00 Moderate	Steam
Development	PCS Development Required	None (Application Engineering)	Hardware Development	Steam
System	Ability To Serve Various And Changing Loads	Wide Steam Range W/Auto Extraction	No Process Steam	Steam
Growth	Large Scale Hardware Performance	Available Significantly Better Performance	Potentially Available Small Improvement Only	Steam
Commercial	Rapidity Of Acceptance	Accepted Acceptance Environmental Issues	Delays In User Acceptance Environmental Issues	Steam

Ten different solar collectors potentially capable of efficient operation at a temperature of 589°K (600°F) and higher, were evaluated for performance under Shenandoah direct insolation and climatic conditions. The types of collectors investigated included parabolic dish, fixed mirror, tilting mirror, Fresnel lens, and parabolic trough. Design specifications, performance data, and cost data for each of the collectors evaluated were obtained directly from manufacturers and developers, and comparisons were made using GE-developed computer programs with representative collector models.

A parabolic dish solar collector was selected because it collects substantially more energy per square meter of collector aperture area and collector field area than any of the other collector types considered. The Shenandoah site collector field area is limited to five acres and is located in a solar region of only moderate direct insolation availability. The dish field is the only collector which collects enough energy on the available field area to serve design loads throughout the Georgia Power system peak demand period.

Numerous thermal energy storage and heat transfer fluid candidates compatible with operation at 589°K (600°F) and above were also evaluated during the screening activity. Choice of sensible heat storage from the broad range of thermal storage technology options was based on its state-of-the-art readiness for incorporation into near term plants. The High Temperature Storage (HTS) subsystem selected is a trickle oil/dual media concept which uses a relatively low cost, solid storage medium for essentially all storage and uses the collector heat transfer fluids in a trickle or dual media mode to provide heat transfer, thereby minimizing the overall inventory of high-cost transfer oil. The use of this cost-effective storage approach led to the selection of a high temperature silicone oil, Syltherm 800*, as the heat transfer fluid for both the collector and high

* Dow Corning Trade Name

temperature storage loops. This allows the system to operate at 672°K(750°F), which enables maximized turbine performance on superheated steam up to 655°K(720°F).

The system configuration developed during the preliminary design effort reflects increased knowledge in terms of site loads definition and hardware requirements and capabilities resulting from system analysis and laboratory and field testing. The design also reflects the incorporation of a GFE (Government Furnished Equipment) steam Turbine-Generator(TG) to be supplied by Mechanical Technology, Inc. (MTI).

1.3.1 SYSTEM DESCRIPTION SUMMARY

General features of the Shenandoah STE-LSE are shown in the site layout of Figure 1.3-1. Dominating the layout and setting the land use requirement of approximately 20235m² (5 acres) are 192 7-meter diameter, parabolic dish, solar collector modules. The collectors are arranged on the field in a repeating diamond pattern. The spacing has been optimized to provide maximum annual field energy output. The piping arrangement places all collectors in parallel and consists of a main supply/return line and 20 branch lines as shown in the layout. This design minimizes piping length and allows individual collectors or branches to be removed from service without degrading field outlet temperature. The modularity associated with both the collector itself and the piping arrangement provides versatility of design and flexibility in operational deployment in that site variations and sizing variations over broad ranges can be accommodated by this basic design.

The site also includes a mechanical area which incorporates an STES mechanical building and visitor center and all other plant components. The control room and console, turbine-generator set, absorption chiller, and condenser, deaerator, and demineralizer units for the Power Conversion Subsystem are all located in the building. The four high temperature storage tanks, the single low temperature storage tank, fossil heater, solar steam generator, and cooling towers are positioned as shown in the layout in the mechanical area surrounding the STES building. Appropriate weatherproofing will be provided for all externally located components, and the site will make provisions for oil spill containment and management. Access to the site is provided by means of a road from Amlajack Blvd. which passes along the south boundary of the collector field, and visitor and employee parking areas are provided. Access to the site is controlled by means of a fence which surrounds the entire field and mechanical areas.

Table 1.3-3 lists values of major parameters of the Shenandoah LSE system design. The design conditions have been optimized to meet performance requirements within the framework of optimum economics. The limited available collector field area led to the selection of a dish collector in a system providing the maximum practical temperature to the turbine-generator. The higher throttle temperature and pressure conditions allow supply of the 442°K(337°F) process steam requirement by means of an extraction steam turbine which is commonly available and used in industrial and power generation applications. The high temperature storage system allows maximum utilization of collected energy by having sufficient capacity for weekend collection. The system also incorporates a low temperature thermal storage unit. The sensible heat storage unit uses water as the storage media and allows use of cascaded thermal energy to supply plant space heating and cooling requirements during times when the turbine-generator is not operating, such as during the third shift and on weekends.

The system design selected for the Shenandoah LSE is essentially composed of three hydraulic loops or subsystems which transfer the collected solar energy into the appropriate energy forms required by the Bleyle plant and a central control subsystem which monitors and controls the overall system operation. The design, shown in schematic form in Figure 1.3-2, is a fully cascaded total energy system. The figure shows the three major subsystems. The Solar Collection Subsystem (SCS) utilizes a series of hydraulic circuits which transport the collected solar energy from the collector field to the high temperature storage and then through the steam generator to the Power Conversion Subsystem (PCS). In the PCS, electrical power is produced by a dual steam turbine-generator, while steam for process use is extracted from the rear of the first turbine to simulate operation of an extraction turbine likely to be used

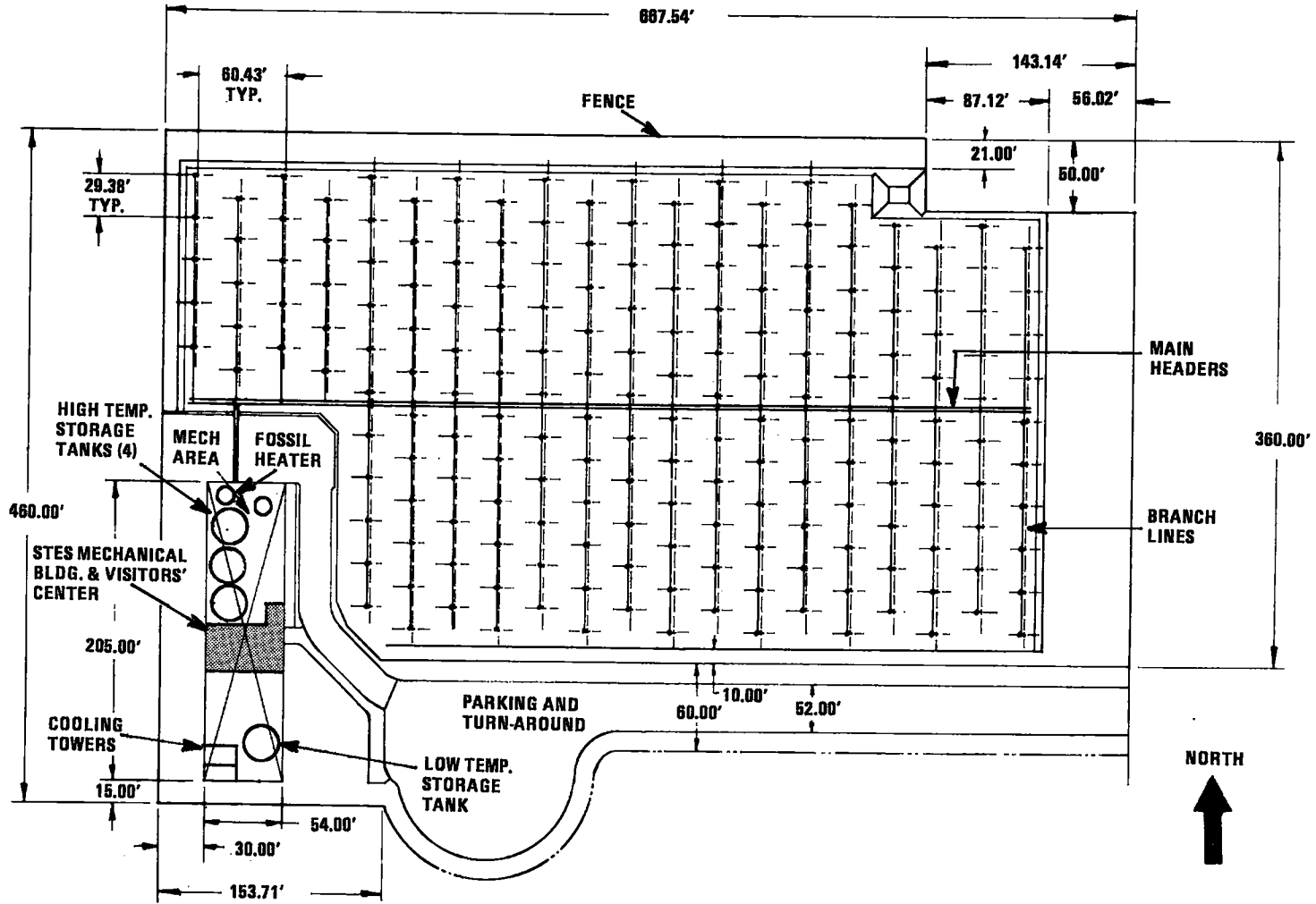
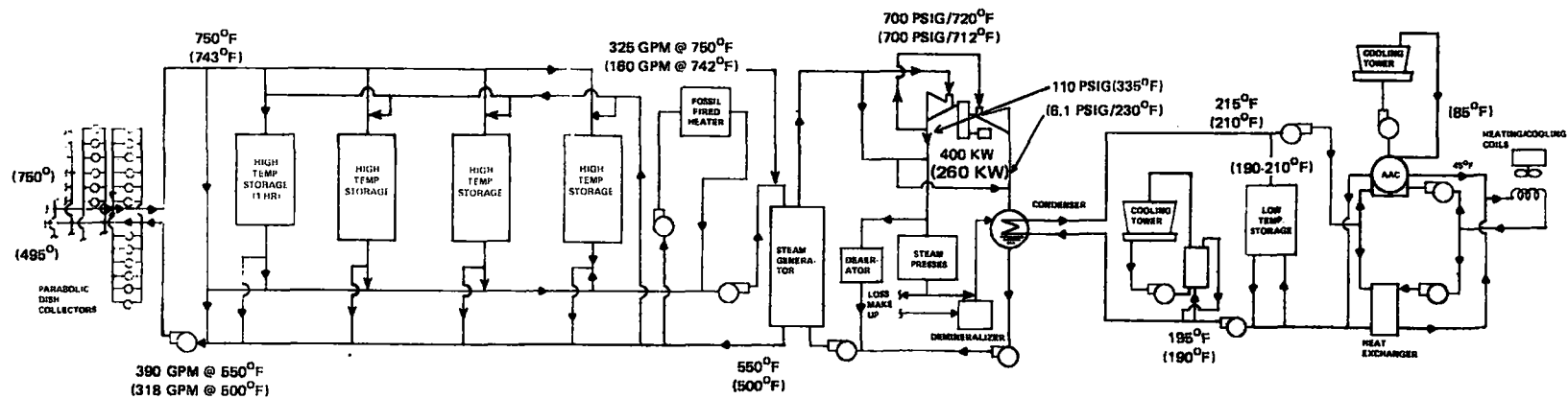


Figure 1.3-1. STE-LSE Site Layout

Table 1.3-3. Specifications For Major Equipment

Collector Field		High-Temperature Thermal Storage	
Type	Paraboloidal Dish Cavity Receiver	Type	Trickle Oil/Dual Media
Size	7m Diameter	Volume	17,600 ft ³
Area	79,500 ft ² (192 Dishes)	Size	13 ft dia, 12 ft ht (1 Tank) 20.6 ft dia, 16 ft ht (3 Tanks)
Fluid	Dow Corning Syltherm 800	Storage Medium	Taconite
Outlet Temperature Collector	750 ^o F	Void Fraction	45%
Min. Inlet Temperature Collector	500 ^o F	Temperature Change	250 ^o F
Maximum Fluid Flow Rate	390 gpm	Capacity	100 MBtu
Design Collector Output At 200 Btu/hr-ft ² (630 W/m ²) (Each)	54,440 Btu/hr	Max. Charge/Discharge Rate	16/8.2 MBtu/hr
		Insulation Thickness	14 in
		Oil Inventory (Trickle Oil)	8,700 gal @ 77 ^o F
		(Dual Media)	30,590 gal @ 77 ^o F
Turbine Generator Set		Low-Temperature Thermal Storage	
Cycle	Rankine MTI Turbine	Type	Water
Working Fluid	Steam	Volume	120,000 gal
Admission	Variable	Size	30 ft dia, 23 ft Height
Stages	Two	Storage Medium	Water
Pressure Ratio	140	Temperature Range	210 ^o F - 190 ^o F
Design Inlet Condition	720 ^o F/700 psig	Capacity	20 MBtu
Extraction Port Condition	110 psig	Insulation Thickness	4 in
Condensing Condition	6.1 psig		
Maximum Rating	400 kW _e		



NOTE:

DESIGN MAXIMUM	-	I_{DN}	=	300 BTU/HR-FT ²
		Q_{ELEC}	=	400 KW
NOMINAL	-	I_{DN}	=	270 BTU/HR-FT ²
		Q_{ELEC}	=	260 KW

Figure 1.3-2. Shenandoah LSE System Schematic

in larger commercial-size applications. The Thermal Utilization Subsystem (TUS) utilizes another series of hydraulic circuits to transport the heat rejection energy from the PCS to the low temperature storage or directly to the space heating and cooling units.

The figure also shows the major subsystem interface design conditions and normal operating conditions. In normal operation, the steam turbine generator heat is supplied from the Solar Collection Subsystem either directly from the collectors or through the High Temperature Storage (HTS) at a slightly reduced temperature. When there is no longer sufficient solar energy, the system is transferred to a fossil fired heater heat source in the syltherm loop, and operation in a total energy mode continues at the identical conditions as for solar operation. This approach simplifies control requirements and is compatible with plant requirements which include simultaneous need for electricity, process steam, and space cooling within relatively narrow load ranges.

The system has the capability to operate at rated electrical output of up to 400 kWe to serve the total site electrical loads or, as will be the case in normal operation, to operate in conjunction with a base load from the utility at a lower STES electrical output. In both operating modes, the STES generator will electric load follow to supply electric load peaks.

The following paragraphs summarize the major features of the subsystems making up the Shenandoah LSE design.

1.3.1.1 Solar Collection Subsystem

The Solar Collection Subsystem consists of an array of 192 seven meter diameter, parabolic dish collectors, which provide a 139°K (250°F) temperature rise to a flow of Syltherm 800 fluid through each collector in a parallel closed, hydraulic circuit. The design collector output temperature is 672°K (750°F). The receiver is a cavity type with the incident concentrated solar flux impinging upon an absorptive surface enclosed within an insulated cylindrical shell. The LSE parabolic dish design is based on a low-cost five meter radio frequency (RF) antenna which Scientific-Atlanta supplies for communication/Earth station applications. The LSE dish is made up of individual petals which are die-stamped aluminum, and the entire assembly is field assembled. The aluminum is chemically brightened, and a weather surface is applied to allow maintenance of reflectance in the range of 0.88. The unit tracks individually in polar and declination axes. To gain experience with fabrication and operation, petals of the 5-meter diameter Scientific Atlanta RF antenna design were used to build the Engineering Prototype Collector (EPC), Figure 1.3-3, which was tested at Sandia Laboratories, Albuquerque, NM.

The trickle oil/dual media concept was selected for the high temperature storage system. This concept offers a low-cost solid storage medium for heat storage, thus reducing the required inventory of high cost heat transfer oil. Figure 13.-4 presents a schematic diagram that shows the major components of a large trickle oil storage tank. The system includes manifolds for the back-up dual-media approach.

Storage is either charged or discharged by trickling oil over a cold or hot storage bed, and the heat is transferred by a thin film of oil trickling over the taconite solid medium. A drain plate is used to collect the oil into a sump area at the bottom of the tank. The preliminary design for the STE-LSE at Shenandoah has a 1.0×10^5 joule (100 MBtu) capacity stored in four tanks, one to provide one hour of system operation at full load, 4 meters in diameter and 3.7 meters high (13 feet in diameter, 12 feet high) and the remaining three together to provide a storage capacity adequate for holding the energy collected over an average summer weekend, 6.3 meters in diameter and 4.9 meters high (20.5 feet in diameter, 16 feet high). In the dual media approach, the storage capacity increases by the amount of energy contained in the quantity of fluid greater than that in the trickle oil mode.

During operation of the trickle oil system, flow is always into the top of each compartment, whether charging or discharging. A series of flow control valves and thermal switches direct the flow to the desired tanks.

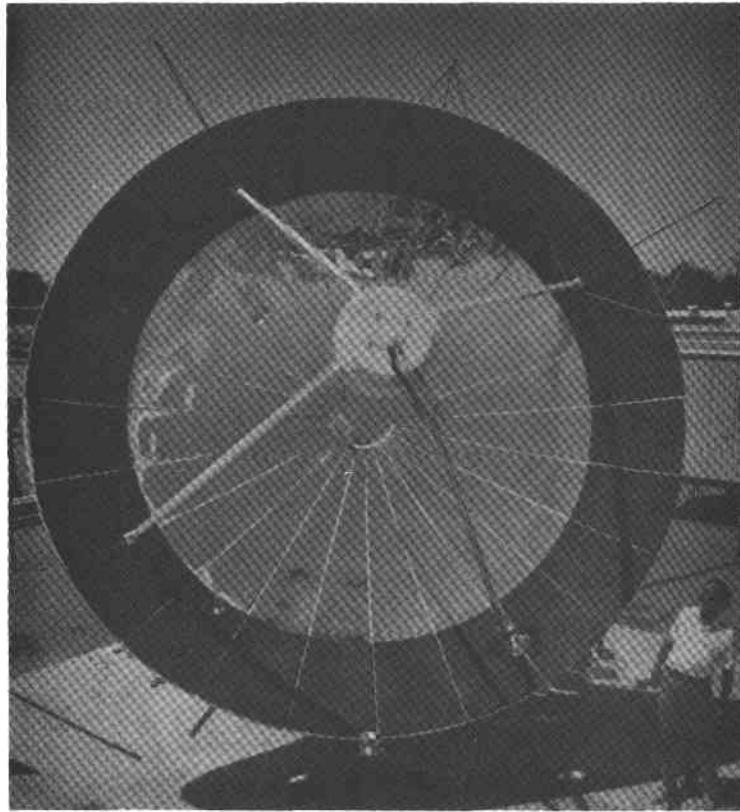
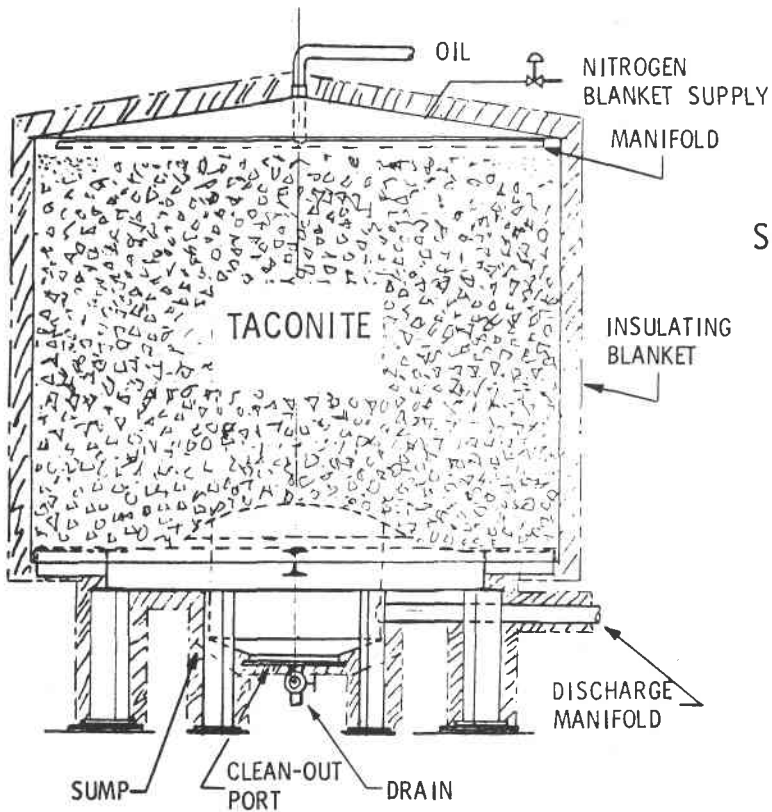


Figure 1.3-3. Engineering Prototype Collector



SIZE: LARGE TANK -
 20'6" DIA X 16' HIGH
 (LESS COVER)
 (40,065 GAL/348 TONS TACONITE)

SMALL TANK -
 13' DIA X 12' HIGH
 (LESS COVER)
 (11,860 GAL/103 TONS TACONITE)

Figure 1.3-4. Trickle Oil TES Tank

The trickle oil concept was verified by means of a scaled down column test performed at the GE Evendale facility. In the dual media mode, charging flow is into the top of the tank, and discharging flow is out of the top of the tank. The dual media concept has been shown to be feasible by Rocketdyne. The Solar Collection Subsystem also includes a fossil fired heater capable of supplying the full PCS heat input requirement when HTS is depleted.

1.3.1.2 Power Conversion Subsystem

The Power Conversion Subsystem consists of a three piece pool-type boiler with preheater, boiler, and superheater, a GFE steam turbine-generator set rated at 400kWe supplied by Mechanical Technology, Inc., a condenser and condensate storage tank, make-up demineralizer, deaerating heater, and boiler feed pump. In normal operation, steam at 655°K (720°F) and 4.8×10^6 N/m² (700 psig) is generated in the boiler-superheater, heated by Syltherm 800, and delivered to the turbine inlet. The turbine generator set consists of a multistage high speed (11,000 rpm) turbines coupled to a gear box, which reduces the speed to the 30 rev/s (1800 rpm), 60 Hz alternator. The back of the first turbine has a take-off for process steam and steam for regenerative feed water heating. The second turbine operates at a condenser temperature of 383°K (230°F) to provide 372°K (210°F) water to the Thermal Utilization Subsystem. Steam make-up is preheated to 383°K (230°F) by being introduced as a spray into the condenser.

1.3.1.3 Thermal Utilization Subsystem

The Thermal Utilization Subsystem major components include a 2.1×10^{10} Joule (20 MBtu) capacity, sensible heat water, low temperature storage (LTS) subsystem, a 1.25×10^6 Joules/second (354 ton) absorption chiller derated to provide 6.09×10^5 Joules/second (173 tons) with inlet hot water at 372°K (210°F), and two separate cooling towers for heat rejection from both the absorption chiller and the PCS condenser. The storage system is available to supply heating or cooling loads when the PCS is not operating such as at night or on weekends. The full system capacity, sized for 11°K (20°F) temperature range, is contained in a single tank 9.8 meter (32 feet) in diameter by 6.1 meter (20 feet) high. The absorption chiller and cooling towers are standard off-the-shelf items which will not require design modifications. The absorption chiller has self contained controls to sense load variations and will supply chilled water directly to the Bleyle Plant Piping System. The system will have the capability to supply heating to the office areas and cooling to the plant process areas simultaneously.

1.3.1.4 Control and Instrumentation Subsystem

The Control and Instrumentation Subsystem design allows maximum operational flexibility of the LSE system. Six modes of operation are defined:

- | | |
|-----------------|----------------|
| 1. Normal | 4. Fail Safe |
| 2. Experimental | 5. Degraded |
| 3. Diagnostic | 6. Maintenance |

In the normal mode of operation, the control system initiates collector tracking, energy storage, electrical power generation, and auxiliary air conditioning or heating. The electrical requirements of the Bleyle Plant will be monitored and sufficient power generated to supplement the base load supplied by Georgia Power Company. On weekends and during periods of lower power demand, energy will be stored for later use.

A switch to alternate modes will allow the operator to initiate solar collection experiments, monitoring, and recording experimental data as needed. The operator may initiate computer stored diagnostic routines in the event of a malfunction. The critical components of the system are fail-safed to prevent damage during power or primary control failures or over temperature conditions. Finally, the system will be operational in a degraded mode when certain components, such as a collector branch, are not available due to routine maintenance or component failures.

Control of the solar collectors will be achieved via four micro-processor control units in the collector field. Coarse solar tracking will be provided by a computer stored algorithm during start-up and coast, with fine tracking provided by an optical feedback control loop. The temperature of the fluid at each receiver will be monitored and branch fluid flow rate adjusted to achieve the desired fluid temperature. Automatic defocus will activate if the fluid in any collector receiver exceeds a safe temperature. Stowing will be initiated if necessary to protect the collectors under adverse climatic conditions.

The high temperature thermal energy storage subsystem will be monitored with level and temperature sensors to determine charge and discharge readiness. The Syltherm 800 fluid will be routed according to the HTS status. Additionally, if the system is fully charged and no additional energy can be handled, collector stowage will automatically occur to prevent fluid over-temperature. A micro-processor control unit will be dedicated to the HTS to interface with the central control console.

The power conversion subsystem incorporates the steam generation plant (boiler) and the steam turbine/generator. This subsystem is also under control of a dedicated micro-processor. Automatic start-up/shut-down sequences as well as built-in protection functions are an inherent part of this equipment. The electrical requirements of the knitwear factory will be monitored and generator output moderated according to need.

Heat to the thermal utilization subsystem will be provided by means of a fluid coolant loop from the PCS condenser. The control system will provide coolant flow and temperature control to maintain the PCS condenser pressure and temperature. The absorption air conditioning and hot water heating system will respond to the requirements of the Bleyle Plant as well as the STE mechanical building. A micro-processor control unit will provide control and monitor functions for this system.

The Control and Instrumentation Subsystem is comprised of a central control console, the central mini-computer, and seven micro-processor control units. The operator will have the capability to monitor and control basic system functions from the control panel. All other detailed monitored and controlled functions will be via the computer keyboard and CRT (cathode ray tube) interface. Monitored data will be recorded from experiments, alarms, and normal operation on magnetic tape storage and in hard copy form on the computer line printer. Signal conditioning circuitry will be provided as needed in the remote control units. The remote micro-processor will be programmable from the central mini-computer to allow a high degree of system control and monitor flexibility.

1.3.2 PERFORMANCE SUMMARY

Overall performance of the system, including both electrical and thermal output delivered to the Bleyle plant loads referenced to the collected solar energy, determines the Solar Total Energy System size necessary to meet its total requirements. The annual energy balance for energy and power accounting shown in Figure 1.3-5 has been used for system level design control. Individual subsystem performance contributions to the overall system performance are evident from the figure. Collector losses including reflector reflectivity; slope error; specularity; tracking errors; shadowing; and radiation, convection, and conduction receiver losses yield an overall annual collector efficiency of 0.53. This includes an average receiver subsystem efficiency of 0.82. Collector field piping losses, startup losses associated with warmup of the pipefield thermal mass, and thermal energy storage conduction losses are 6.3 percent, 9.9 percent, and 3.0 percent of the collected energy, respectively. Gross electrical generating efficiency is 14.3 percent, with the thermal energy available to meet process steam and absorption cooling loads as shown in the figure. End-to-end system efficiency from incident direct normal solar radiation to usable energy is 0.313. Because of the relationship between PCS thermal output and site thermal loads, on an annual basis the system provides an excess of cascaded energy as noted in Figure 1.3-5. This excess energy has been minimized by incorporating a high efficiency turbine-generator into the system. If this energy could be fully utilized either by the Bleyle Plant or by another nearby plant application, overall system efficiency would increase to 0.42.

1-17

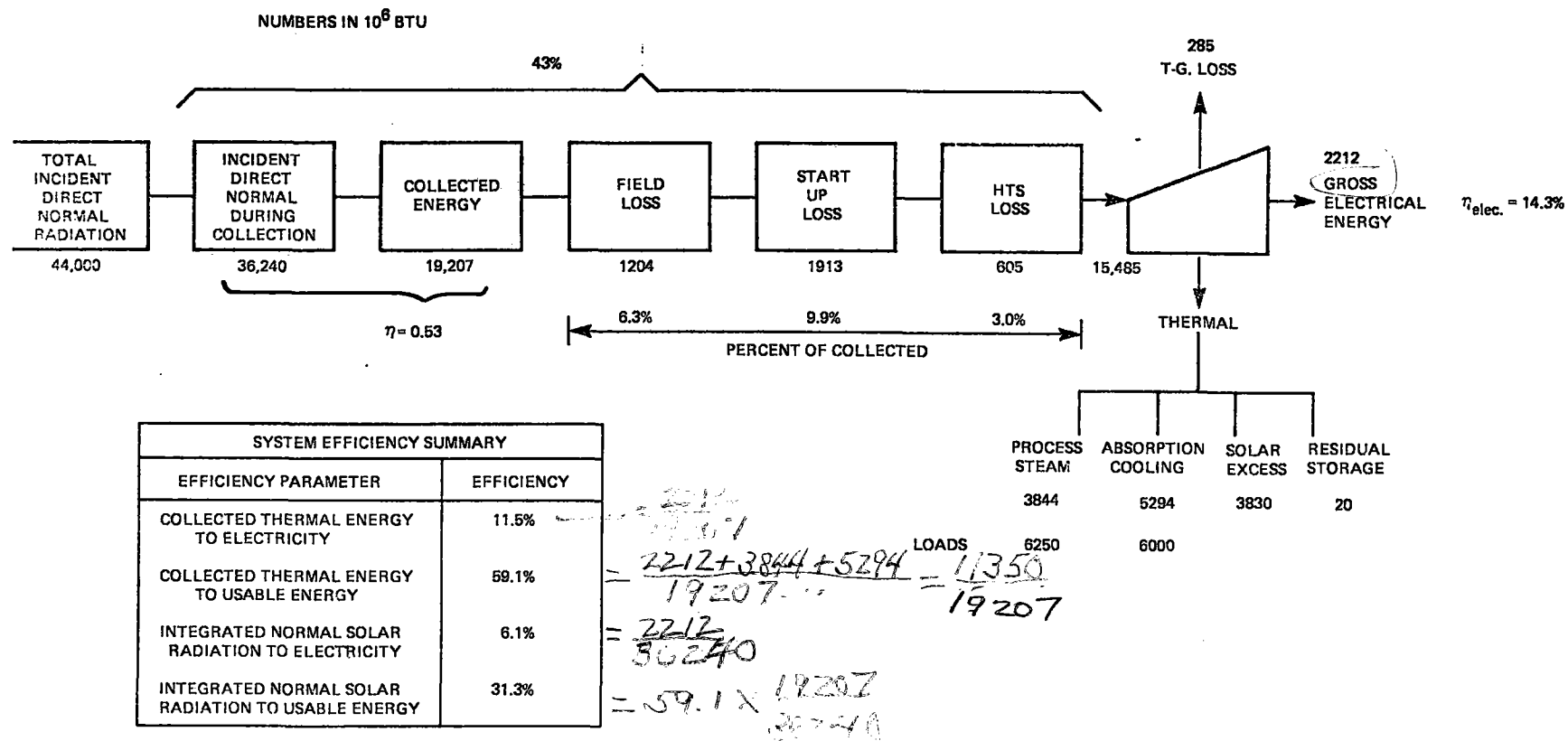


Figure 1.3-5. Annual Energy Balance for Preliminary Design System

For the system design of 192 seven-meter diameter dishes and 1.0×10^5 joule (100 MBtu) of high temperature storage capacity, direct solar contribution to the plant loads includes an estimated 33 percent of the annual electrical energy requirements, 62 percent of the process steam required, and 89 percent of the energy required to drive the absorption air conditioning system. This results in an annual solar replacement of 65 percent. The loads and solar contribution on a monthly basis are summarized in Figures 1.3-6, 1.3-7 and 1.3-8 for electricity, process steam, and absorption cooling, respectively. The figures clearly indicate the summer electric peaking reduction capability of the STES as it supplies both electricity and plant cooling loads.

In assessing STES ability to act as peak shaving capacity for the utility, the collector field will allow solar operating time sufficient to span Georgin Power Company peaks. Figure 1.3-9 summarizes calculated average operating hours on a monthly basis and indicates that the system will operate for at least one eight hour shift over the year. In addition, summer peaks can easily be spanned on solar operation during the critical summer months when the solar system operates for an average 12-14 hours.

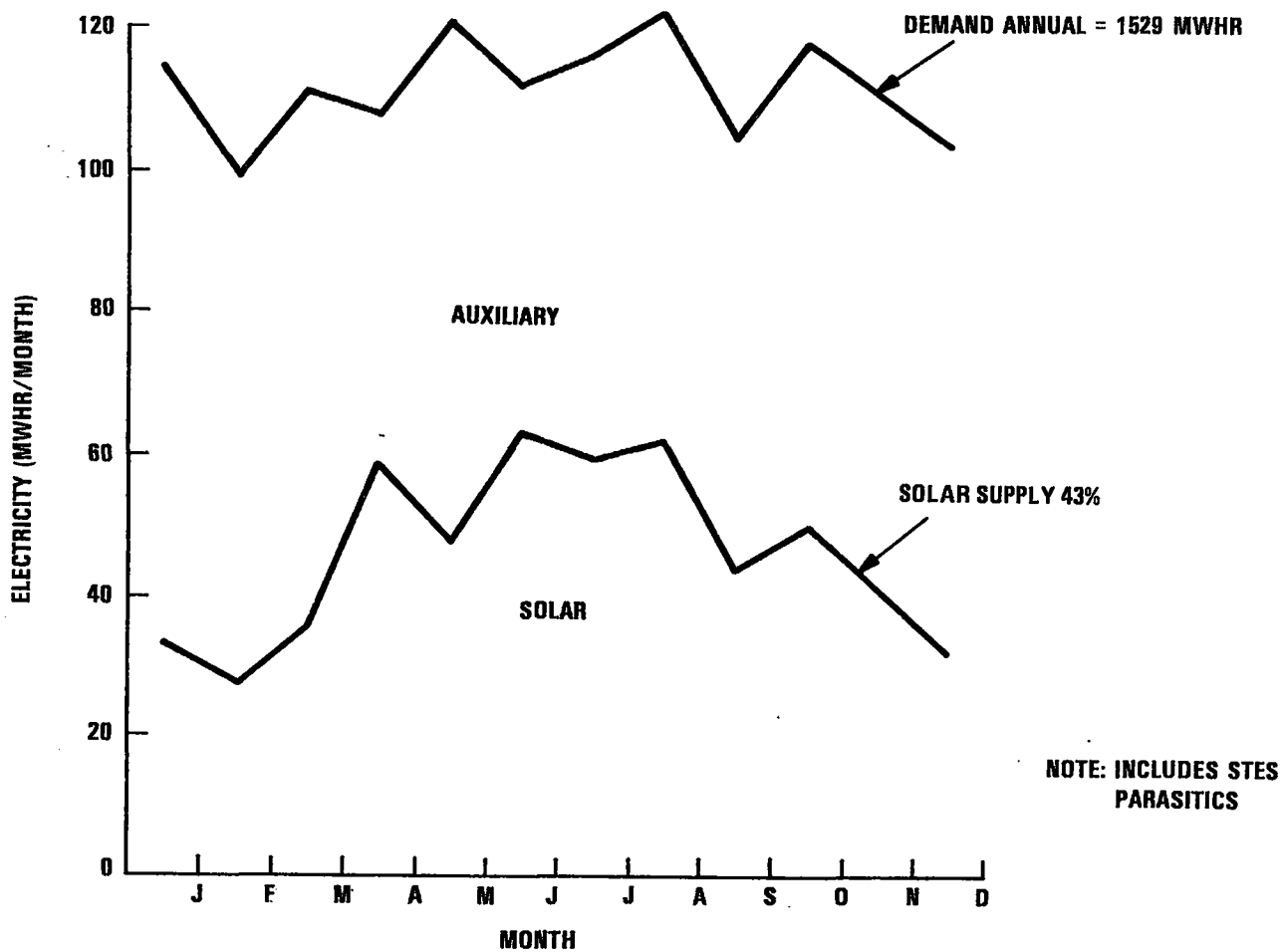


Figure 1.3-6. System Performance Electricity

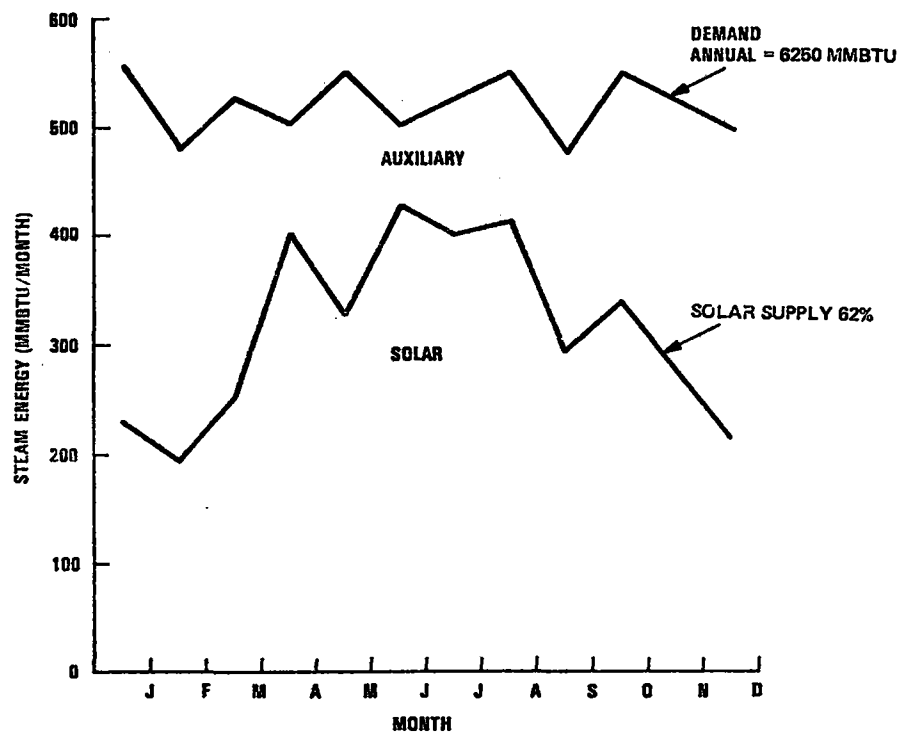


Figure 1.3-7. System Performance - Process Steam

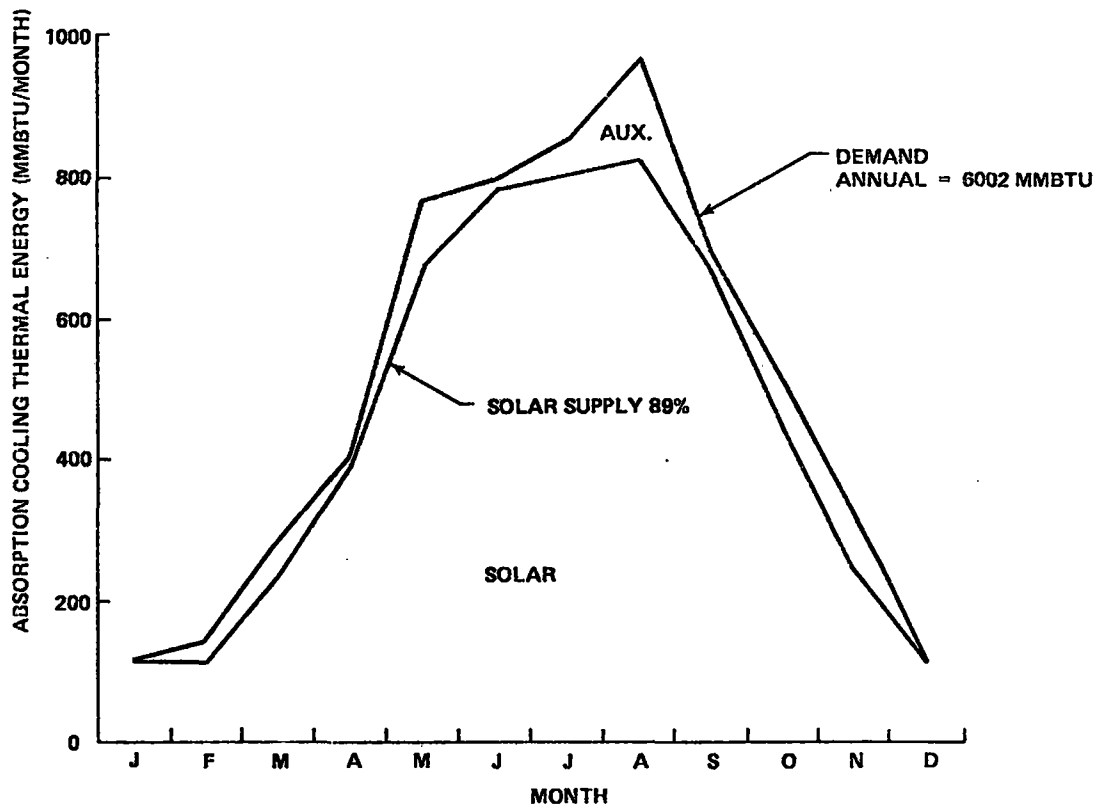


Figure 1.3-8. System Performance - Cooling

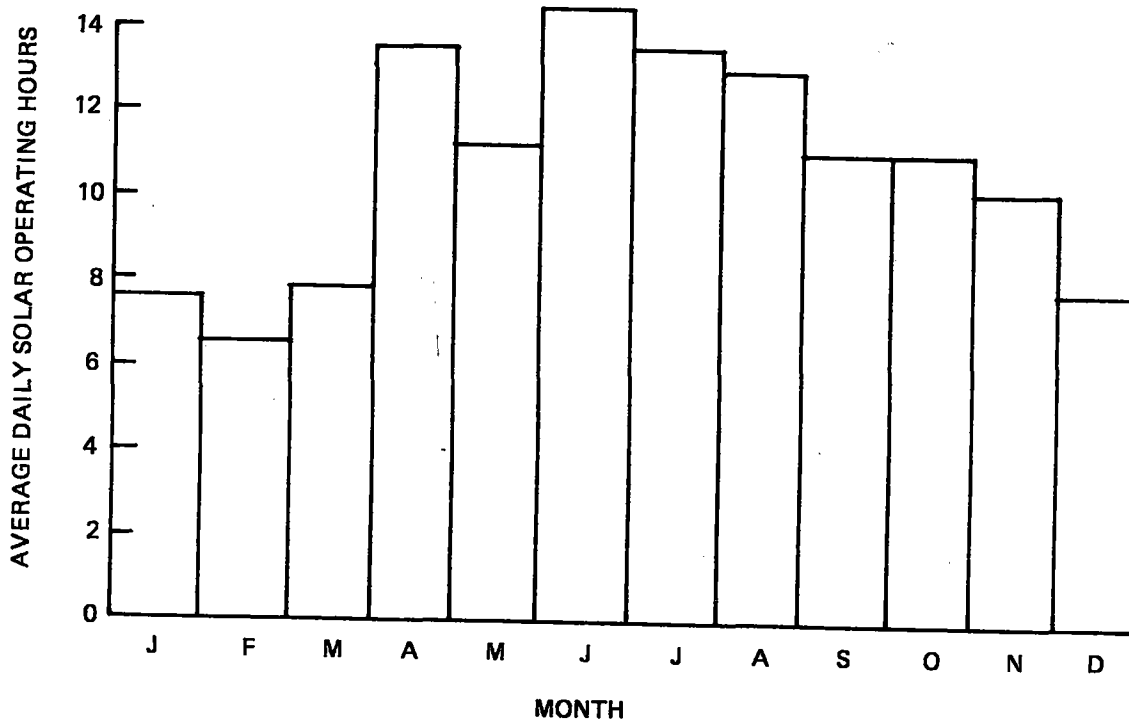


Figure 1.3-9. Average System Operating Hours with Solar Input

SECTION 2
SYSTEM REQUIREMENTS

SECTION 2

SYSTEM REQUIREMENTS

2.1 GENERAL REQUIREMENTS

The STES will be located at the Shenandoah site adjacent to the Bleyle Plant. The design must be tailored to be compatible with the site as well as the plant thermal and electrical load characteristics. General requirements include those related to the site and application, those programmatic requirements derived from overall experiment objectives developed by DOE, and derived requirements resulting from system design and analysis. A significant effort during the Preliminary Design phase has led to a definitive set of requirements which have guided the design to ensure that it meets all program objectives. The following subsections present the major system requirements and their interaction with LSE design.

2.1.1 SITE DESCRIPTION AND INTERFACE

The Solar Total Energy System - Large Scale Experiment will be located in Shenandoah, Georgia. Shenandoah is a new town near Newnan, Georgia about 40 kilometers (25 miles) southwest of Atlanta as shown in Figure 2.1-1. This new community is being developed by Shenandoah Development Incorporated (SDI) which was established in 1969 by Unioamerica-Incorporated. Approximately 30 square kilometers (7,400 acres) are currently being improved by SDI.

The site that was made available by SDI for the proposed total energy facility is defined in Figure 2.1-2 (Plat I). It consists of approximately 23,000 square meters (5.72 acres) of land. As depicted in Figure 2.1-3, the site is near the intersections of Interstate 85 and Georgia Highway 34. The site is connected to Newnan by Georgia Highway 34 and Atlanta by Interstate 85. The Bleyle Knitwear Plant is located along the west property line of the development

Access to the Bleyle facilities will be via Amlajack Boulevard. The property adjacent to the north boundaries of the Bleyle facility/STES site is neither owned nor controlled by SDI. Located near the northeast corner of the collector tract is a parcel of land measuring 15 meters by 44 meters (50 feet x 143 feet). This property is owned by the Housing and Urban Development Administration (HUD) and is designated as a green area. Green areas are intended to be land which will never be developed. However, the HUD property can be modified to control erosion at the STES site, if required.

Positioned directly south of the site, on a parcel of land with a peak elevation of 296 meters (970 feet), is a 3785 cubic meter (1,000,000 gallon) water tower. The height of the water tower is approximately 51 meters (166 feet). SDI owns and operates the water facility.

Located on the STES site itself are two man made structures. The first is a meteorological station on a 6 meter by 6 meter (20 feet by 20 feet) concrete pad. This station will eventually be dismantled and repositioned on top of the STE-LSE mechanical building to record data in conjunction with STE-LSE operations. The second structure is a 0.2 meter (8 inch) concrete sanitary sewer line. The concrete pipe is located approximately 2.7 meters (9 feet) below the existing grade elevation. Service to the sewer is via two manholes. The sanitary sewer has a three meter (10 feet) easement; manhole elevations will need to be adjusted to any changes in surrounding ground elevations.

All other lands that adjoin the collector boundary line are owned by SDI. SDI has plans to install a road southeast of the site to provide access to Amlajack Boulevard. Since the region between the collector field and Amlajack Boulevard has not been assigned to a third party by SDI, the exact position of the road is not final. The land in this area will be graded in conjunction with STE-LSE site preparation to provide fill to level the STES site. Additional site details are documented in Reference 2.1-1.

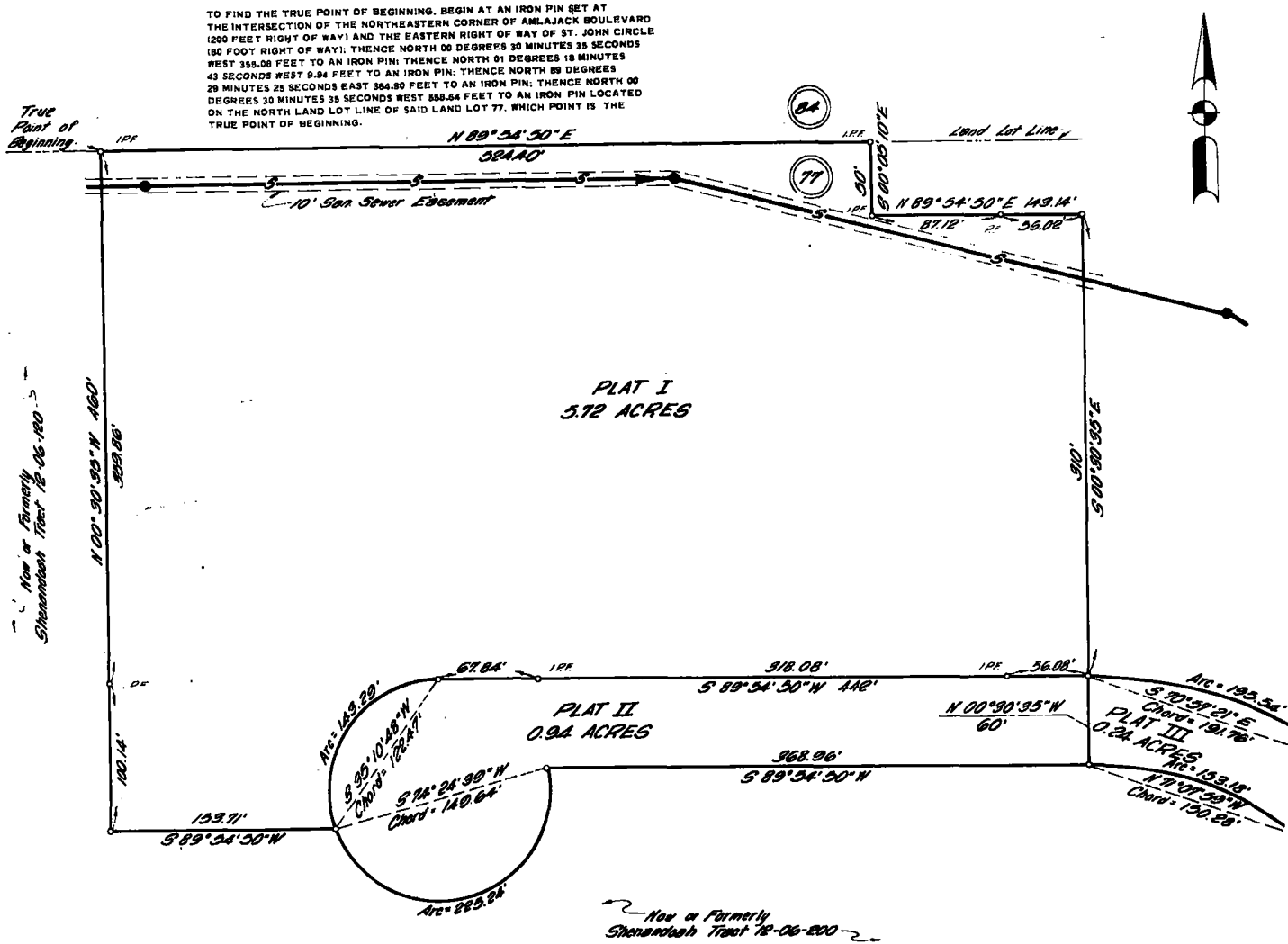


Figure 2.1-2. The Plot Plan (5.72 Acre Plot)

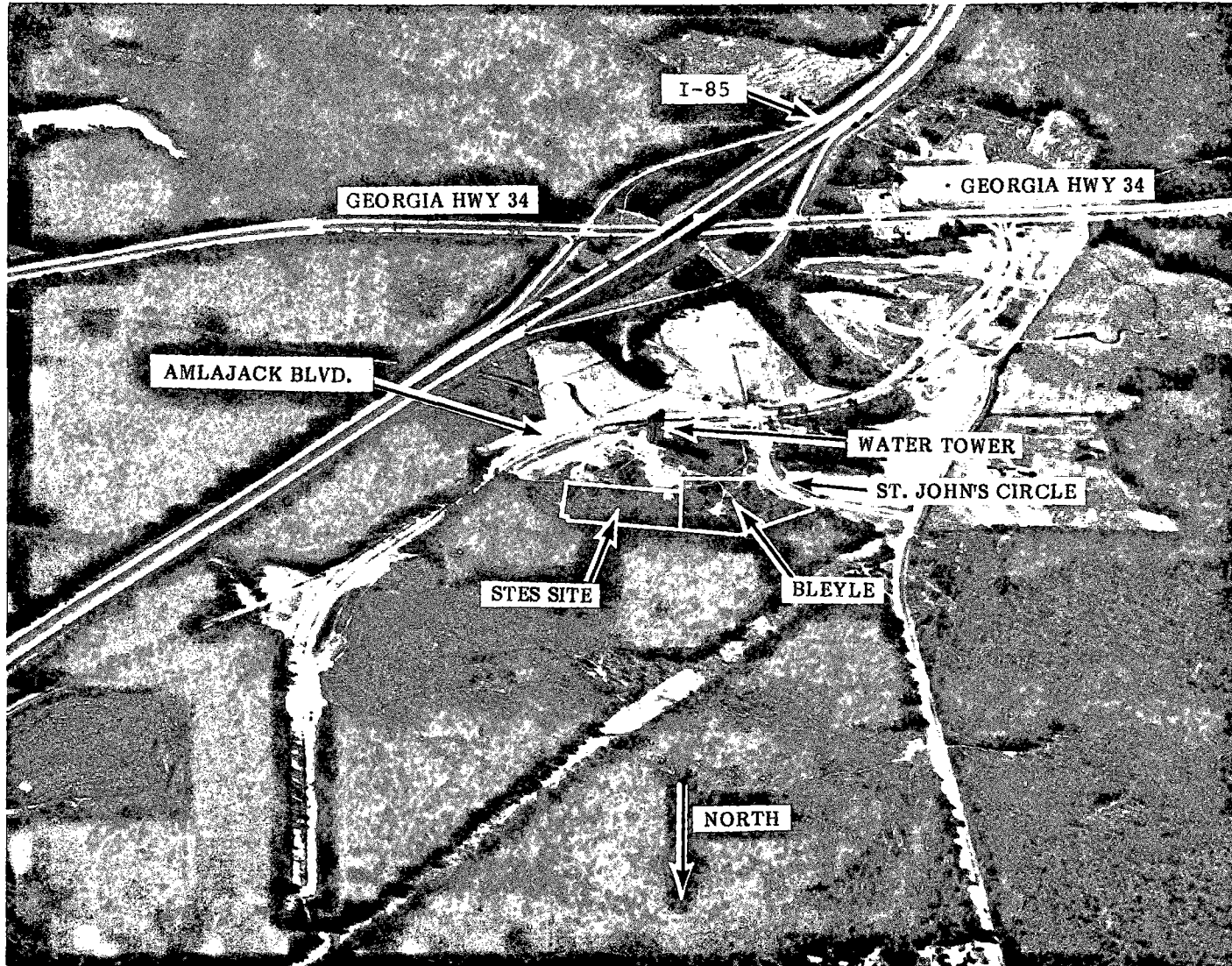


Figure 2.1-3. Aerial Photograph - Looking South

The detailed interfaces with the Bleyle plant are defined on the site Interface Control Drawings (ICD) developed and maintained by Heery and Heery, Inc. for the Georgia Power Company site team. These drawings depict physical and interface engineering requirements. Currently the interface drawing categories include site, architectural, meteorology station, mechanical, load, thermal, electrical, and instrumentation. Interface control drawings are between Sandia Laboratories-Albuquerque (SLA), General Electric (GE), and Georgia Power Company (GPC). Formal sign-off and change procedures have been instituted consistent with requirements set forth in Reference 2.1-2. A complete set of the interface drawings is included in Reference 2.1-1. The knitwear plant includes a mechanical room located in the northeast corner. All STES interface piping and wiring must be routed to this area of the plant as shown in Figure 2.1-4 for central connection to plant loads.

2.1.2 PROGRAMMATIC AND DERIVED REQUIREMENTS

The objective of the system requirements analysis was to gather, analyze, and integrate the system requirements into a consistent set of design constraints and considerations. This objective was met by:

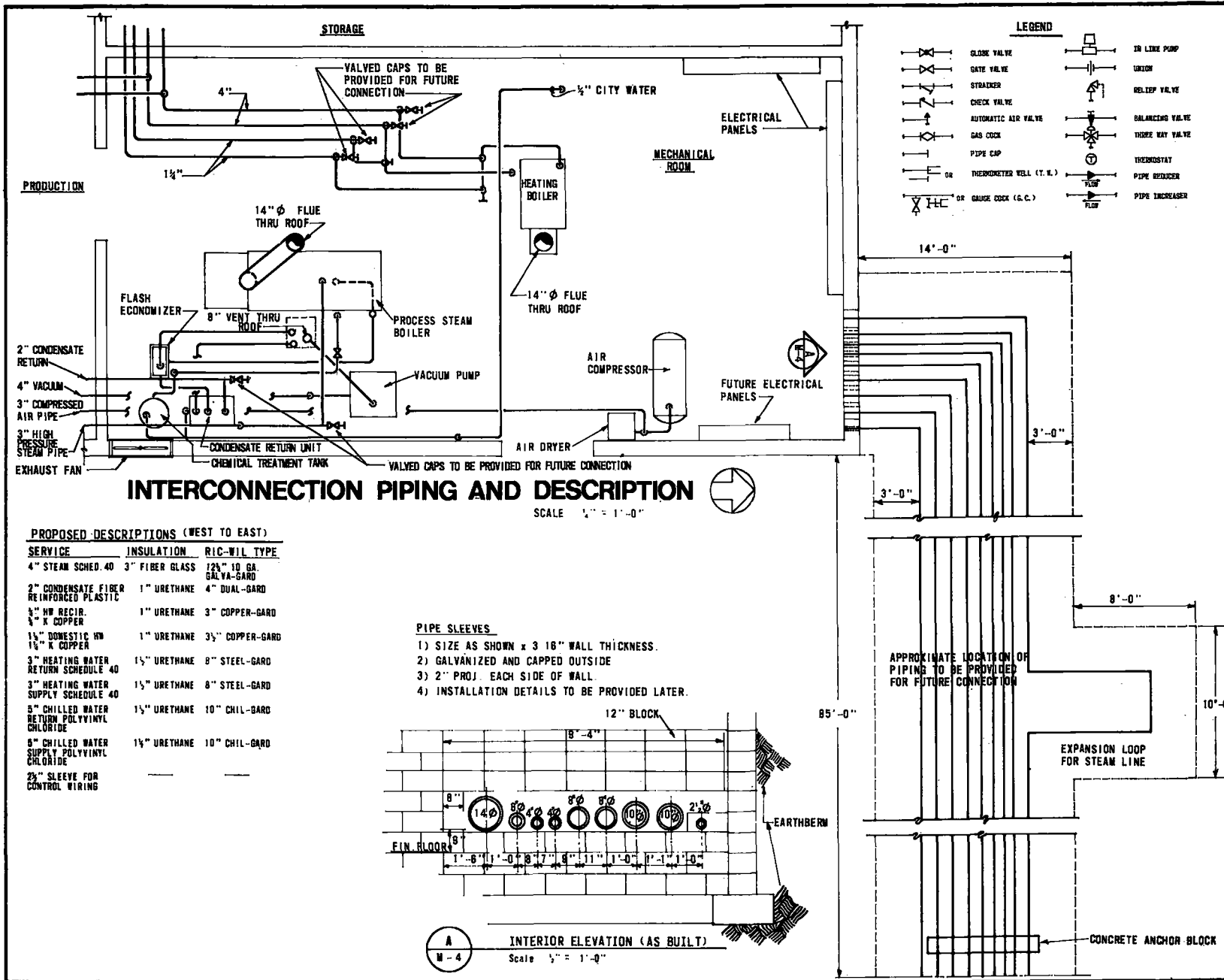
1. Reviewing applicable documents including the contract Statement of Work; GPC site interface drawings and documentation; local, state, and federal laws and ordinances; and Shenandoah Development Guidelines.
2. Interacting with DOE/Sandia and GPC.
3. Performing independent analyses.

Details of the system requirements analyses are presented in Section 6 for all areas except load analysis, which is included in Section 2.2. The resulting requirements are summarized in Table 2.1-1 and are broken down into eight categories: performance, load, design, environmental conditions, laws and ordinances, codes and standards, operational, and site requirements. These requirements were developed early in the preliminary design and were concurred with by all parties on the program including DOE, Sandia, GE, and GPC to serve as the basis for the Shenandoah LSE system design. From among those requirements in Table 2.1-1, certain top level requirements have driven the design. These top level design criteria and requirements are shown in Table 2.1-2. The design is to be optimized from the standpoint of performance and cost-effectiveness to provide a minimum of 60 percent of the site loads while operating with solar heat input. The system is to have operational flexibility to operate with the utility as peaking equipment and thus incorporates a fossil heat back-up to allow operation as a conventional on-site total energy system when solar heat is not available. The power quality from the STES must meet the GPC service quality to the Bleyle plant at all times.

The system is being designed to be compatible with future potential commercial applications, but because it will be the first industrial solar total energy system, a great degree of experimental flexibility must, of necessity, be incorporated into the design. The system must include supervisory control to accommodate that flexibility. In addition, the system will have the experimental capability to operate in a stand-alone mode to:

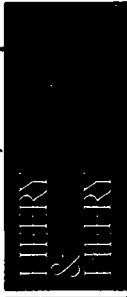
1. Demonstrate the capability of the STES to provide all site loads independently to allow evaluation of the STES as utility peaking capacity.
2. Evaluate the capabilities of STES for remote site applications.
3. Demonstrate the electric load following capabilities of the STES.

While in the stand alone mode, the system will be required to continue to meet GPC power quality requirements.



BLEYLE MANUFACTURING PLANT, SHENANDOAH, GEORGIA
STES INTERFACE DEFINITION AND CONTROL DRAWINGS
INTERCONNECTION PIPING AND DESCRIPTION

DATE	10/20/77	
DESIGNED BY		
CHECKED BY		
APPROVED BY		
REVISIONS		
NO.	DATE	DESCRIPTION
1	1/10/78	
2	2/8/78	
3	4/7/78	
4	8/1/78	



M-4

Figure 2.1-4. Interconnection Piping and Description

Table 2.1-1. Overall Requirements Summary

Requirement Category	Requirement	Major System Impact
Performance	<ul style="list-style-type: none"> ● Overall Energy Supply: Minimum of 60% of Annual Energy Requirements of LSE From Solar (Combined Thermal & Electric) ● Electric Power Quality: Voltage: 480 V \pm 5% Frequency: 60 Hz \pm 1/2% Maximum Voltage Waveform Distortion: 5% ● Steam Quality: (at Bleyle Plant) @ Min. Rate of 230 Lbs/Hr. - 115 Psia/338^oF @ Max. Rate of 1380 Lbs/Hr. - 115 Psia/379^oF 	<ul style="list-style-type: none"> ● STES Power Level ● Operating Temps. ● Collector Field Perf. ● Storage Capacity ● Desired T/G Set Eff. Range ● None for Interconnected Operation ● STES Must Meet Frequency Requirement for Standalone Operation up to 25 kW Max. Step ● No Specified Requirement From Bleyle ● Design of STES Desuperheater
Site Loads	<ul style="list-style-type: none"> ● Power Conversion Subsystem: Electric Power Range 200-400 KW Process Steam Flow Range 0-1380 Lbs/Hr. ● Thermal Utilization Subsystem Heating Load 0-559 X10³ Btu/Hr Cooling Load 0-174 Tons 	<ul style="list-style-type: none"> ● Utility Base Load and PCS Capacity ● Equipment Operating Range ● Absorption Chiller and Heating Coil Capacities
System Design	<ul style="list-style-type: none"> ● High Temperature Thermal Storage Stores Excess Energy Collected Sized for Weekend Energy Collection ● Standby Fossil Fueled Heater Sized to Supply Energy Equivalent of Collected Solar Energy ● Emergency Shutdown Capability Loss of Electrical Power Component Malfunctions ● Personnel Safety Precautions Fire Hazards Burn Hazards Exposure to High Voltage High Noise Levels Glare Hazards ● Environmental Impact ● Availability 95% 	<ul style="list-style-type: none"> ● Include in Design ● Include in Design ● Secondary Power Source ● Provide Protection ● Minimize Adverse Effects ● FMEA to Determine Redundancy Requirements

Table 2.1-1. Overall Requirements Summary (Continued)

Requirement Category	Requirement	Major System Impact
Environmental Conditions	<ul style="list-style-type: none"> ● Ambient Temperature Maximum: 104°F Minimum: -3°F ● Wind Speeds Design Operating: 30 mph Design Survival: 70 mph (Sustained) 90 mph (Gusts) ● Hail Maximum Diameter: 0.6 Inch (for Design) ● Lightning Peak Discharge Current: 100,000 amps Rise Time: 1μsec 	<ul style="list-style-type: none"> ● Minimum System Operating Range ● Design of Collector Support Structure & Tracking Drive ● Assess Implication on Collector Field ● Provide Grounding System
Laws and Ordinances	Federal <ul style="list-style-type: none"> ● Clean Air Act ● Noise Control Act ● National Environmental Policy Act ● Federal Water Pollution Control Act ● Solid Waste Disposal & Resource Recovery Act ● Toxic Substance Control Act 	<ul style="list-style-type: none"> ● Clean-Up or Containment of Oil Spills
Laws and Ordinances	State & Local <ul style="list-style-type: none"> ● Georgia Water Quality Control Act ● Georgia Erosion & Sedimentation Control Act ● Georgia Dept. of Natural Resources, Environmental Protection Division, <ul style="list-style-type: none"> a) Air Quality Control b) Solid Waste Management ● Southern Standard Building Code ● Coweta County Building Codes ● Shenandoah Development Corporation <ul style="list-style-type: none"> a) Development Guidelines b) Technical Specifications 	<ul style="list-style-type: none"> ● 20% Green Area ● Building Setbacks ● Access Road Right of Way ● Site Grading Plan ● All Site Construction
Codes & Standards	<ul style="list-style-type: none"> ● OSHA <ul style="list-style-type: none"> a) Occupational Safety & Health Standards b) Safety & Health Regulations ● NFPA <ul style="list-style-type: none"> a) National Electrical Code b) Life Safety Code c) Other National Fire Codes as Applicable 	<ul style="list-style-type: none"> ● Standard Practices ● Fire Protection in STES Bldg. ● Fossil Heater

Table 2.1-1. Overall Requirements Summary (Continued)

Requirement Category	Requirement	Major System Impact
	<ul style="list-style-type: none"> ● ANSI <ul style="list-style-type: none"> a) National Electrical Safety Code b) Other ANSI Standards as Applicable ● ASME Boiler & Pressure Vessel Code ● NEMA Standards ● AISC Steel Construction Manual 	<ul style="list-style-type: none"> ● Power Piping <ul style="list-style-type: none"> - Materials - Wall Thickness - Allowable Stresses ● PCS Vessel Design ● Standard Practice ● Field Fabricated Tanks
Operational Requirements	<ul style="list-style-type: none"> ● "Peak Shaving System" Supplies Peak Electric Loads While Utility Supplies a Base Load ● Stand Alone Operation Supplies all the Bleyle Plant Energy Requirements During Selected Periods ● Supervisory Control Mode Operator Assumes Direct Control Over System or Selected Components ● Experimental Operational Flexibility 	<ul style="list-style-type: none"> ● Electric Load Following ● PCS Control ● Experimental Mode ● STES Max. Power Level ● Include Protective Circuitry ● Sequenced Start-Up ● Flexible Computer Architecture ● Additional Components and Controls
Site Requirements	<ul style="list-style-type: none"> ● STES Constructed Within Site Boundaries ● Mechanical Building to Satisfy Minimum Setback Requirements for Shadowing ● Total Bleyle Plant Disconnect Capability ● Interface Control Drawing Compatibility 	<ul style="list-style-type: none"> ● Larger Site Required to meet Green Area Requirement ● Building and Equipment Sizes and Locations ● Isolation Valves ● Control Design ● Electrical Design ● Design

Table 2.1-2. Top Level System Requirements For The Shenandoah LSE

System Design Criteria	
<ul style="list-style-type: none"> ● Minimum 60% Annual Load ● Peak Electric Load Shaving ● Provide High Temp. TES ● Plant Disconnect Capability ● Stand-By Fossil ● Supervisory Control ● Stand Alone Experiment 	<ul style="list-style-type: none"> ● Shenandoah Environment ● Site Compatibility ● Provide Mech. Bldg & Visitor's Ctr. ● Min. 2 Yr. Operation, 20 Yr. Life Goal ● Experimental Flexibility ● Health, Safety & Code Req'mts.
↓	
System Design Requirements	
<ul style="list-style-type: none"> ● Electric Power Quality <ul style="list-style-type: none"> Voltage: 480V ±5% Frequency: 60Hz ±1/2% ● Steam Quality <ul style="list-style-type: none"> At Min. Flow Rate - 115 PSIA/338° F ● Secondary Power Source ● Redundancy Req'mts. Per FMEA ● Utility Base Load - 100 kW 	<ul style="list-style-type: none"> ● Ambient Temperatures <ul style="list-style-type: none"> Max. 104° F Min. -3° F ● Wind Speeds <ul style="list-style-type: none"> Operate - 30 MPH Survive - 90 MPH Gust ● Hail - Max. Diameter: 0.6 Inch ● Lightning Strike <ul style="list-style-type: none"> Peak Current - 100,000 Amps Rise Time - 1μSec

The system is being designed for environmental conditions specific to the Shenandoah site. However, in cases where these conditions could be extended to make the design applicable to a wider range of geographical regions without significant impact, a more restrictive environment was selected. This philosophy is consistent with the ultimate commercialization objectives of the program.

2.1.3 INSOLATION AND WEATHER DATA

During the conceptual design phase of the program, Sandia specified a solar year model for use in performance analysis. The model was based on 1975 National Oceanographic and Atmospheric Administration (NOAA) Test Reference Year (TRY) data for Atlanta, Georgia. An Aerospace Corporation magnetic tape was obtained which contained the actual measured surface observations and estimated insolation values based on cloud cover values. The insolation data included values for both total hemispherical and direct-normal insolation. This same tape has been used during the preliminary design.

Under a separate contract to Sandia, Georgia Institute of Technology has developed a Shenandoah Solar Model Year (SSMY) of data by examining hourly total hemispherical insolation values for Atlanta for the 22 year period from 1952 to 1974. From this data a composite year of typical months based on means and standard deviations from the mean has been developed, and associated surface weather observations have been compiled. The resulting composite year of data was sent to Aerospace Corporation who estimated direct-normal insolation based on an adaptation of the procedure used to estimate hourly insolation for the rehabilitated historical data archived at the National Climatic Center (NCC) in Asheville, NC. The procedure is documented in Reference 2.1-3. The data was then processed in the SOLMET format on 15 minute time intervals for use during the definitive design.

The daily total direct-normal (D-N) solar data, averaged by month, is shown on Figure 2.1-5 for the TRY and the SSMY. As seen from the figure, the TRY data shows significant fluctuations compared to the time-averaged data, particularly during the summer months. On an annual average basis, the SSMY is about 4 percent lower than the TRY. From this comparison, it is concluded that the TRY provides sufficiently accurate estimated insolation availability for the preliminary design for determination of overall system sizing and performance analysis. During the definitive design phase, the SSMY data will be supplemented with data from the meteorological station at the Shenandoah site to assure that the system design can adequately respond to site insolation conditions.

In addition to the insolation comparison, several other weather conditions were compared for 1975 and long term normals. These results are summarized in Table 2.1-3. A slightly warmer winter and cooler summer is noted along with higher humidity, precipitation and clouds as compared to the normals.

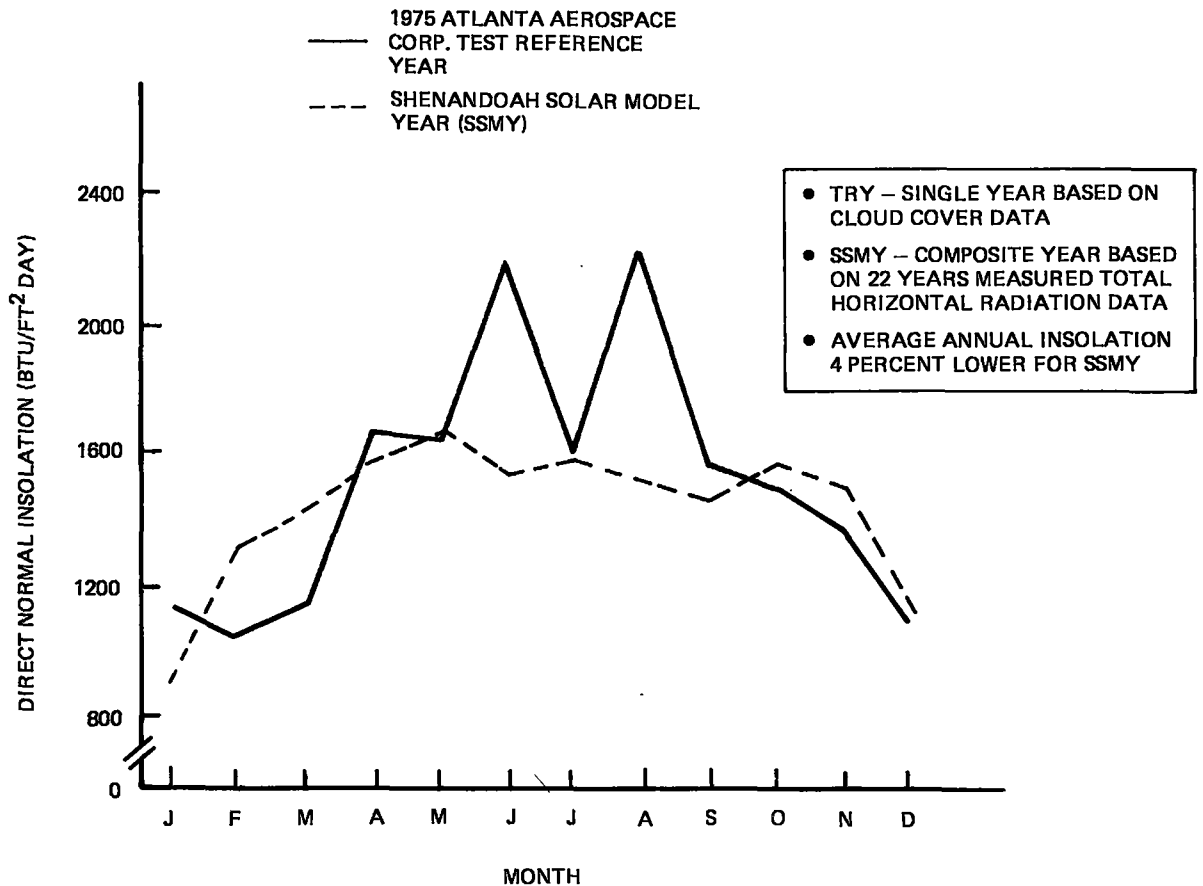


Figure 2.1-5. Daily Total Direct Normal Insolation For Shenandoah

Table 2.1-3. Atlanta 1975 Weather Analysis

Deviations (Percent) From Long Term Normals						
	Temp.	Poss. Sun	Rel. Hum.	Precip.	Sunrise To Sunset Days	
					Clear	Cloud
Jan.	+11.3	+17	0	+29	0	-6
Apr.	-2.1	0	-8	+5	0	+8
July	-2.1	-36	+8	+77	-60	+92
Oct.	-2.8	-6	+17	+104	-7	+33
Annual	+0.1	-20	+7	+36	-9	+24

2.1.4 UTILITY INTERFACES

The design, operation, and economics of an on-site system to provide electricity is dependent upon the relationship and interconnection with the local utility. During the preliminary design of the Shenandoah LSE, close coordination was maintained between GPC and the design activity to develop a workable interface relationship incorporating enough flexibility to evaluate several alternate modes of operation.

For normal operation, the STES electrical generation system will be interconnected with the GPC grid. This approach insures maximum reliability of Bleyle plant service and will provide the ability to gain field experience for a situation which might exist under utility ownership of the STES. The STES will operate to supply site load peaks, with the utility required to supply only a base load. During the experimental operation of the system, utility interactions, including scheduling of STES operation and base load requirements and variations, will be investigated, and alternative rate structures developed consistent with potential and demonstrated value to the utility.

Figure 2.1-6 shows representative Georgia Power Company daily peaking profiles for summer and winter days. The winter day shows a fairly flat profile coincident with the Bleyle plant operating day with some load reduction during the middle of the day. The summer profile shows a more distinct peak during the afternoon and indicates typically characteristic summer peaking. The profiles suggest that, from the standpoint of serving the utility as peak shaving capacity, long STES operating times are desired for all seasons. The profiles also suggest that there are two ways in which the STES system may operate to provide utility peak shaving. The first approach involves GPC supplying a constant base load to the site during all plant operating hours, with the remainder of the electrical requirements including peaks supplied by the STES in an electric load following mode. Under current rate structures this would be the most attractive to the industrial user since demand charges are kept to a minimum. However, during early morning and late evening hours when the solar energy is depleted, fossil energy must be used to supply the needed electricity above the base load. An alternative would be to operate with the base load only during utility peak periods. During off-peak periods, when the utility has excess capacity and solar energy to drive the turbine-generator is depleted, the utility would supply all electric power. Site thermal loads could then be supplied with stored low-grade solar energy. This operating approach would maximize solar utilization and utility capacity and would appear to be more desirable from the viewpoint of the utility. The constant base load has been selected as the normal operating mode, but both modes will be evaluated during the operational phase.

All of the operational modes of the electrical supply interface system between GPC and the STES are shown in Table 2.1-4. Three major modes are possible: GPC alone, GPC and STES combined, and STES alone. In order to effect these various modes, the single line electrical load interconnection design shown in

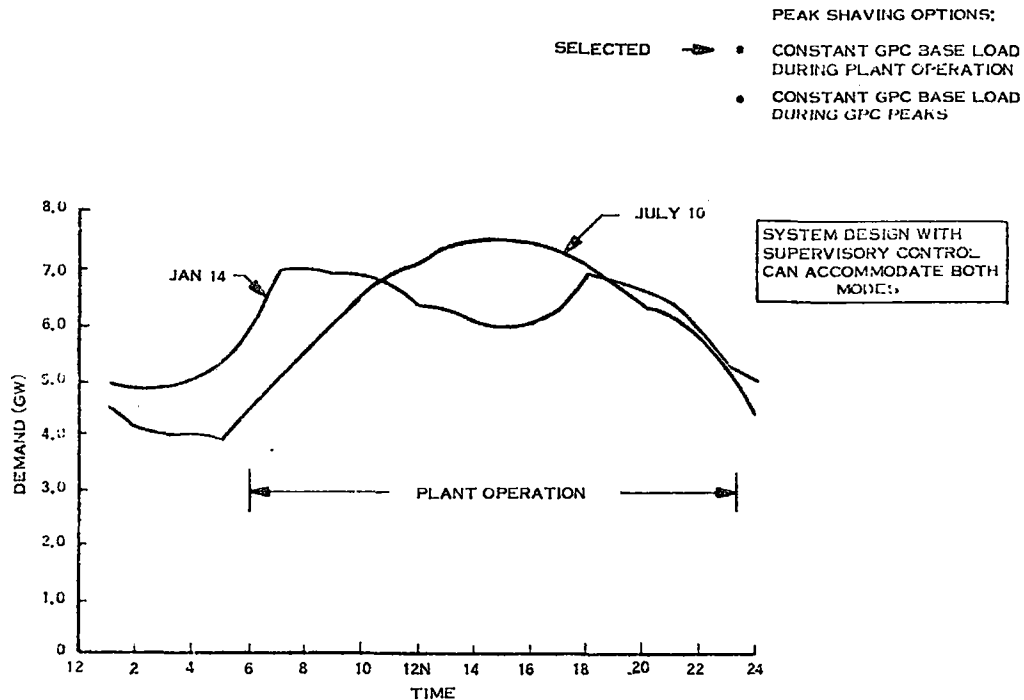


Table 2.1-4. Operational Modes Of Electrical Supply Interface System

- GPC Alone (Nighttime, Etc. Operation) Supplies Bleyle's Electrical Load, Contribution From STES.
 1. Power Supplied To Stepdown Transformer From GPC 25kV UD Line Via 25kV Circuit Breaker.
 2. The Voltage Of The Power From GPC Is Transformed From 25kV To 277/480 Volts (Grounded Wye) And Fed At This Voltage To Bleyle's Plant And To The STES Station Service.
- GPC And STES Combined (Normal Operation) Supply Bleyle's Electric Load.
 1. GPC Contributes A Portion Of Bleyle's Electric Power The Same As In 1. And 2. Above Except It Does Not Supply The STES Station Service.
 2. STES Contributes A Portion Of Bleyle's Electric Power And Supplies All Of The STES Station Service Load.
- GPC Supplies None Of Bleyle's Load, Entire Bleyle Electric Load Is Carried By STES.
 1. Power Flow From GPC To Bleyle Is "Zeroed" Out By The Throttle Setting On The STES Turbine So That The STES Generator Is Supplying All Of Its Own Parasitics And All Of Bleyle's Load. The GPC Station Remains Connected To The Bleyle Load And Energized From The GPC System Thus Serving To Help Stabilize The Frequency And Voltage Of The Power To Bleyle.
 2. Same As In III 1. Above Except Excess Power From STES Is Available And Is "Pumped" Into The GPC System Via The GPC Station And 25kV UD Line.
 3. 480 Volt Breaker Between Stepdown Transformer And The 480 Volt Bus Is Opened After Power Flow Is "Zeroed" Using The STES Throttle. STES Is Then Carrying The Entire Bleyle Load As Well As The STES Parasitics. This Is The STES "Stand Alone" Mode Of Operation.

Figure 2.1-7 has been developed and mutually agreed to by Sandia, GPC, and General Electric. Metering is provided to assess power supplied to the site by GPC and the STES generator. In addition, adequate protection is provided to insure that service to Bleyle will not be affected by any malfunction of the STES.

2.2 LOAD ANALYSIS

This section describes the assumptions and results of analysis to determine the Bleyle plant loads and the total site loads to be served by the STES. The results of the analysis are load profiles used as input to system performance and energy savings analyses. The three major loads associated with the Bleyle plant are process steam, electricity, and space conditioning. Peak demands for each of these load elements were developed by Heery and Heery, Inc., and are documented in the site interface control drawing set as Drawing L-1. These design load calculations were used to size actual equipment capacities installed in the plant and provided the basis for the more detailed hourly load histories required for the STES system simulation and design analysis.

The Bleyer plant is a typical light industrial plant in basic construction and size. However, as a requirement of the DOE in the site Cooperative Agreement (Reference 2.1-4), several energy conservation features were incorporated into the original building design to reduce the annual energy consumption of approximately 46 percent. The majority of these savings resulted from thermal load reductions. The specific features, which were incorporated into the actual building, include:

- Air conditioner economizer cycle
- Four foot earth berm around the building
- Reduced building height
- Extra wall and roof insulation ($U_{\text{wall}} = 0.27 \text{ J/s-m}^2\text{-}^\circ\text{K}$ or $0.05 \text{ Btu/hr-ft}^2\text{-}^\circ\text{F}$,
 $U_{\text{roof}} = 0.17 \text{ J/s-m}^2\text{-}^\circ\text{K}$ or $0.03 \text{ Btu/hr-ft}^2\text{-}^\circ\text{F}$)
- Reduced window area and double glazed windows
- Selected fluorescent lighting and reduced lighting levels
- Decreased lighting and motor voltages
- Rotated building to east-west orientation
- Incorporated central hot water heating - also facilitated later tie-in with solar system
- Reflective aluminum roof
- Process system refinements

All of these conservation features were incorporated into the loads analysis to determine the total loads to be served by the STES.

The plant includes lighting of about 2.1 W/ft^2 of floor area, and all motors and process equipment are located in cooled areas, increasing internal heat generation loads. The inside design temperatures assumed were 299°K (78°F) in the summer and 291°K (65°F) in the winter. During the heating season, a night-time setback to 286°K (55°F) was assumed when the building is unoccupied. Also during unoccupied periods the building ventilation was assumed to be 25 percent of the normal operating level.

The load schedule for the plant is of particular importance to the solar system design and operation. The plant operates in 2 shifts from 6:00 AM to 2:30 PM and 2:45 PM to 11:15 PM five days a week, 52 weeks per year. The schedule also includes meal breaks between 11:15 and 11:45 AM and 8:15 and 8:45 PM and

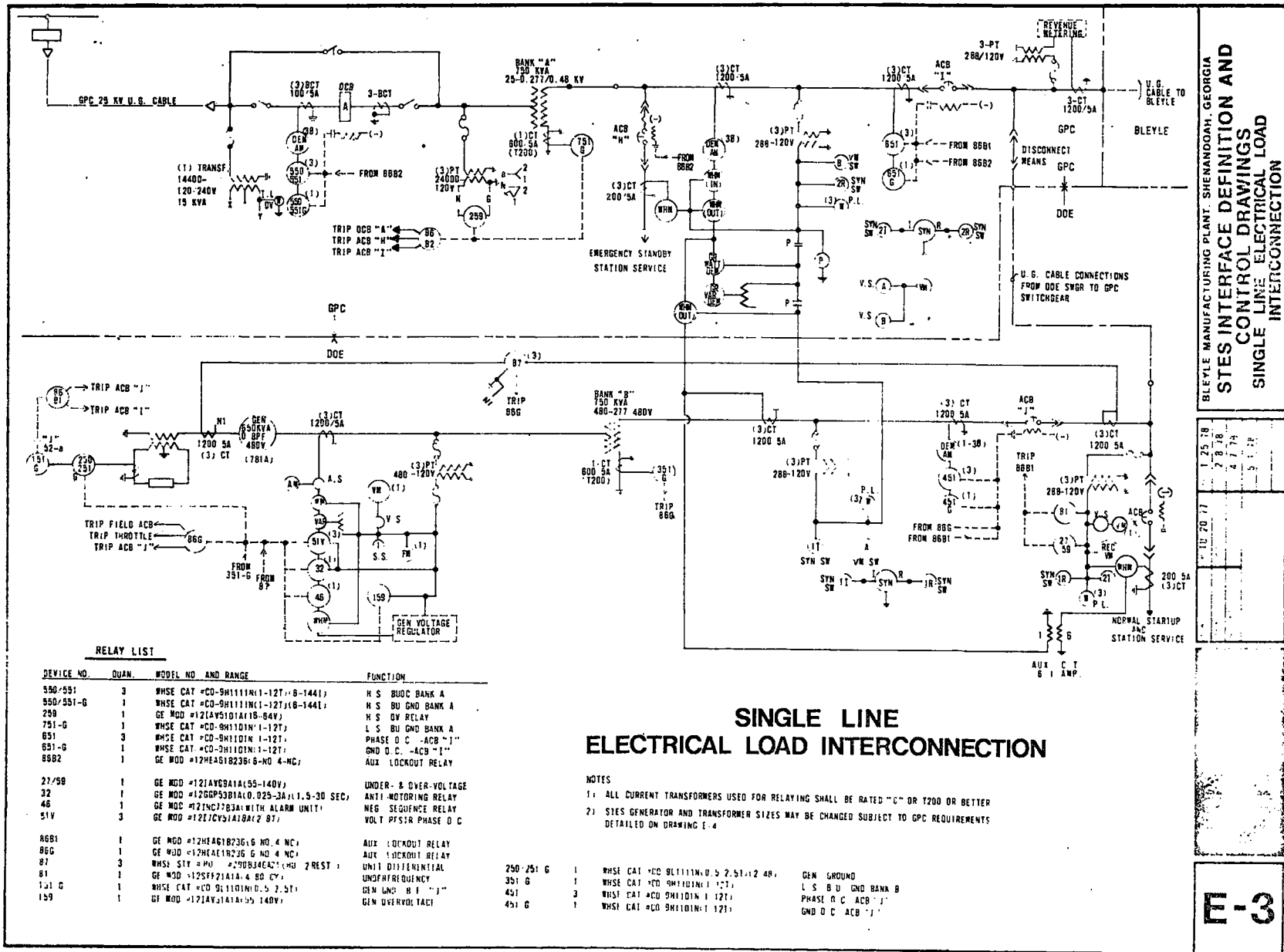


Figure 2.1-7. Single Line Electrical Load Interconnection

an additional break for each shift between 8:30 - 8:45 AM and 5:15 - 5:30 PM. During breaks, the process machinery is shut off with associated load drop on process equipment; however, steam pressure is maintained. The process steam conditions are as follows:

At Boiler	442°K	$7.8 \times 10^5 \text{ N/m}^2$	(337°F, 113.6 psia)
Piping	442°K	$7.8 \times 10^5 \text{ N/m}^2$	(337°F, 113.6 psia)
Press Faces	423°K	$4.8 \times 10^5 \text{ N/m}^2$	(302°F, 70.0 psia)

At full operation, the 3900m² (42,000 ft²) plant will employ 150 production workers on each shift, with an average of 14 office workers and visitors per day expected.

Table 2.2-1 presents a summary of the 3900m² plant loads including peaks and annual summaries. The plant has a relatively high electric load and a thermal to electric load ratio of only 4.6. To achieve the optimum total energy system/load balance, a high electrical generating efficiency is desired.

Table 2.2-1. Bleyle Plant Loads for 42,000 ft² Expanded Plant

Load	Peak (kW)	Annual Total (kWhr)
Electric	270	1.2×10^6
Process Steam	416	1.83×10^6
Cooling*	820	1.66×10^6
Heating	154	3.8×10^4

*Thermal energy input to absorption chiller (COP = 0.7) to supply plant cooling load

The following paragraphs describe the detailed development of the plant loads and the system design loads.

2.2.1 BLEYLE PLANT LOAD ANALYSIS

Based on data from the interface package (Reference 2.1-1), load profiles have been developed for electric demands, process steam demands, and space conditioning requirements for the 3900m² (42,000 ft²) Bleyle Plant. A transient thermal model was developed for the plant which incorporated both internal heat generated within the building and environmental loads. The analysis was performed on 30 minute time steps using the Building Transient Thermal Load (BTTL) computer program. The program requires two categories of inputs:

1. Actual measured weather data on magnetic tape (1975 Atlanta Test Reference Year).
2. Inputs describing building characteristics and location including zoning within the building.

The modeling inputs and characteristics are described in Appendix A. The building was divided into four zones - office, production, storage, and mechanical areas. The four zones each have unique design set temperatures, heating and cooling equipment capacities, hours of usage, number of people, and electrical, evaporation, and infiltration loads. With these inputs, the program was used to calculate various load elements including exterior heat gain or loss through conduction, convection, and radiation; ventilation heat gain; heat gain from people; electrical heat gain; and process steam heat gain. Through the use of building and equipment capacitance terms, the program then computes an instantaneous building load from the instantaneous heat gains for each zone.

The internal loads included in the total cooling or heating load calculations are summarized in Table 2.2-2. The process steam heat gains are estimated by Heery and Heery and assume that ten percent of the total

process steam flow is released and contributes to the latent load. This will be verified by the plant energy measurement program being conducted by GPC. When full plant production is reached, the data will allow performance of a complete energy balance on the steam/condensate system to confirm load estimates. The electrical loads in the plant which were used in all load analyses are summarized in Table 2.2-3.

Table 2.2-2. Internal Heat Gains for Plant Load Calculations

Item	Heat Gain (Btu/hr)		
	Sensible	Latent	Total
Process Machinery (Production)	276,794		276,794
Lighting	295,696		295,696
Air Handling Equipment	176,111		176,111
Process Equipment (Equip. Area)	110,240		110,240
Heating/Cooling System Pumps	5,461		5,461
Water Heater	1,090		1,090
Pipe Gains	59,124		59,124
Presses	151,892	164,220	316,112
People	44,750	74,050	118,800

Table 2.2-3. Bleyle Plant Electric Load Breakdown

Use	Demand (kW)
Process Machinery	83
Lighting	80
Air Handling Equipment	59
Process Equipment	32
Misc. (Receptacles, Vending Machines, Etc.)	16
Total Electric Load	270

Figure 2.2-1 shows a typical cooling load profile for the plant, calculated for a design day ambient temperature condition. The peak total building load is approximately 4.9×10^5 Joules/second (140 tons), with about 80 percent of the load occurring in the high internal heat production area. Because of this high internal heat and as a result of nighttime ventilation setback, the cooling load drops significantly when plant operations shut down. However, some cooling is maintained in the plant during the third shift and on weekends to protect the knitwear fabric. This non-operating cooling load has been confirmed by the Bleyle plant measured data.

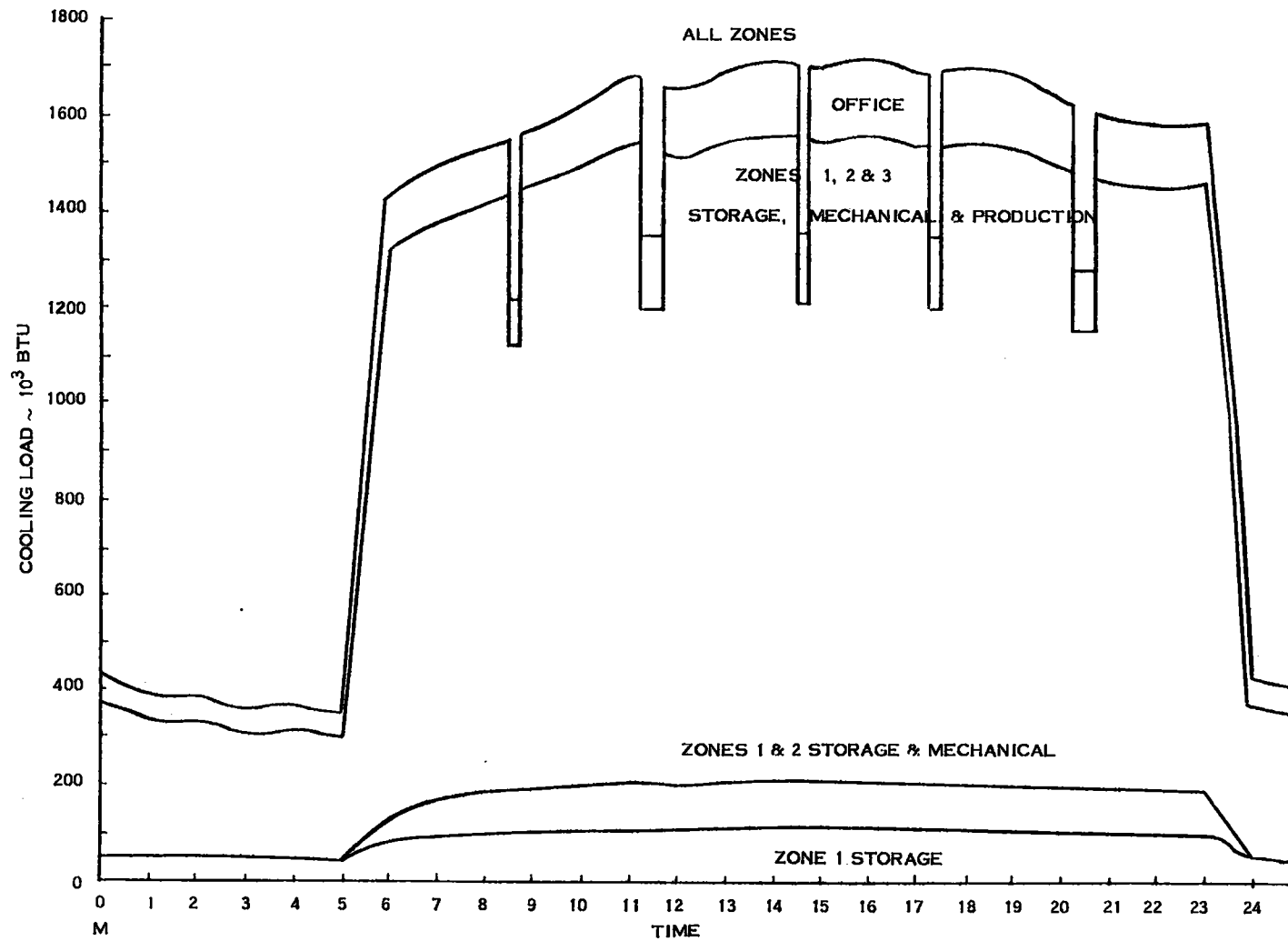


Figure 2.2-1. Instantaneous Cooling Load Profile

Diurnal profiles resulting from the transient analysis for summer and winter conditions are shown in Figure 2.2-2. The space conditioning system in the Bleyle plant incorporates an economizer cycle which operates to bring in outside air to reduce cooling loads when the ambient temperature is below 286°K (55° F). The economizer reduces the winter cooling load shown in Figure 2.2-2 to zero and minimizes fall and spring loads.

The plant loads and load profiles presented here have been estimated by Heery and Heery and derived by General Electric for the preliminary design. The plant has been in operation on a partial production basis since February, 1978, and since that time, actual plant measurements have been taken by GPC to supplement estimates and establish preliminary load step and transient requirements which impact the STES design. From these operating data, more detailed profiles, including short term fluctuations and alternative plant operating scenarios, will be developed during the definitive design phase.

The Georgia Power Company measured transient data on current and voltage in the Bleyle plant in March, 1978. The voltage was essentially constant from a transient effect viewpoint. Current records were typically as shown in Figure 2.2-3. Inrush measurements show 3-4 times full load current on air conditioning which will not be in operation with the STES. The air compressor inrush is 6 times running current which will be seen by STES, and the vacuum pump draws 8 times running current as inrush but could be started before normal STES operation or sequenced with other loads since subsequent measurements indicate that the vacuum pump operates continuously after morning start-up. The measurements do not reflect full Bleyle operation but do indicate the expected variation for transient analysis purposes. These measurements, in addition to examination of all plant motor characteristics and operation, were used to establish a 25 kW step as the preliminary requirement for the STES power conversion system.

2.2.2 SYSTEM DESIGN LOADS

As a total energy system, the STES has been designed to serve all of the loads on the site and sized to supply at least 60 percent of the expanded 3900m² (42,000 ft²) Bleyle Plant loads with solar energy consistent with the overall experiment objectives stated in Section 2.1. The site loads include the Bleyle Plant electric loads and STES operating power and power for the STES mechanical building, process steam to the Bleyle Plant used for pressing fabric, and heating and cooling for both the Bleyle Plant and the STES mechanical building. The design electric loads used to size the STES generator are summarized in Table 2.2-4. The plant loads have been estimated by Heery and Heery, Architects. In normal operation, the site electric load will not exceed 400 kW. To accommodate load fluctuations and to provide a better match with the site thermal loads, the STES operates with a 100 kW base load from the utility, and electric load follows between 200-300 kW in normal operation (see Section 2.3). Except for lunch and shift breaks, the plant electric load profile is relatively constant over the two shift operation as shown in Figure 2.2-4.

The plant's process steam demand is currently supplied by a natural gas fired boiler. Process steam at saturated conditions is required during all working hours, with the design profile shown in Figure 2.2-5.

The design cooling loads, based on ASHRAE design conditions, are summarized for the Bleyle plant and STES mechanical building in Table 2.2-5. The cooling loads consist primarily of internal heat generated by the process and building lighting and are relatively constant during plant operating hours. However, the plant HVAC system incorporates an economizer cycle which supplies a major portion of the internally generated cooling load from December to February. To provide a more optimum site thermal-to-electric load ratio for the STES, the cooling loads are served by a chilled water system supplied by an absorption chiller. The maximum site heating load is 1.64×10^5 Joules/second (559×10^3 Btu/hr), which would occur if the design outdoor ambient temperature occurred when the plant was not in operation with the system supplying maximum ventilation to the Bleyle plant.

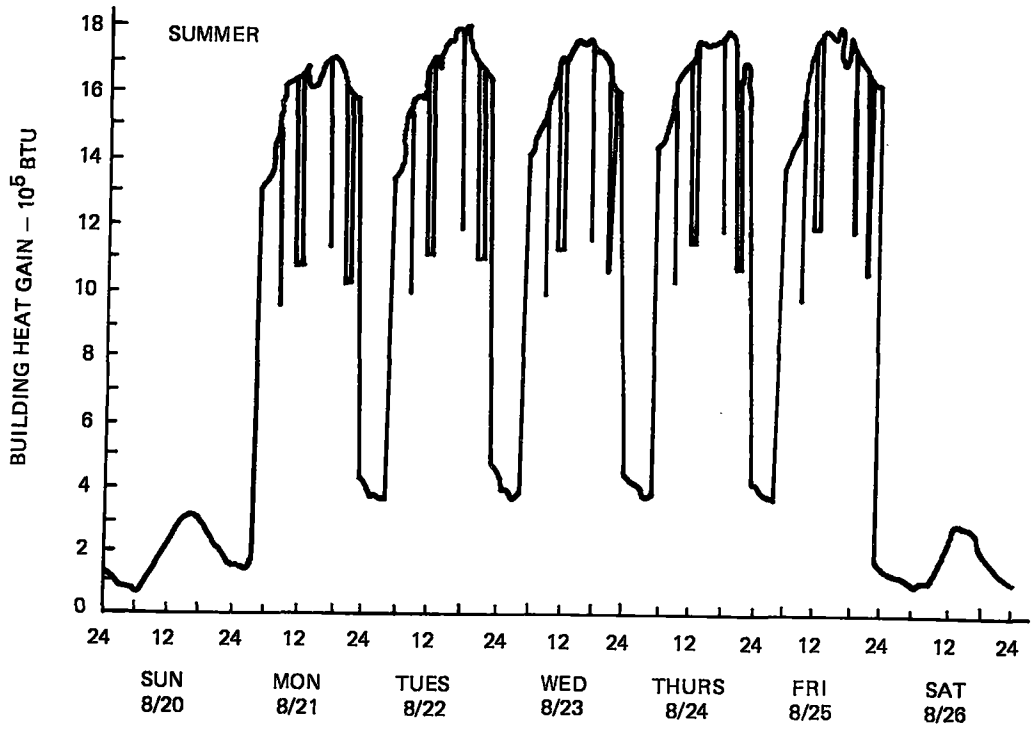
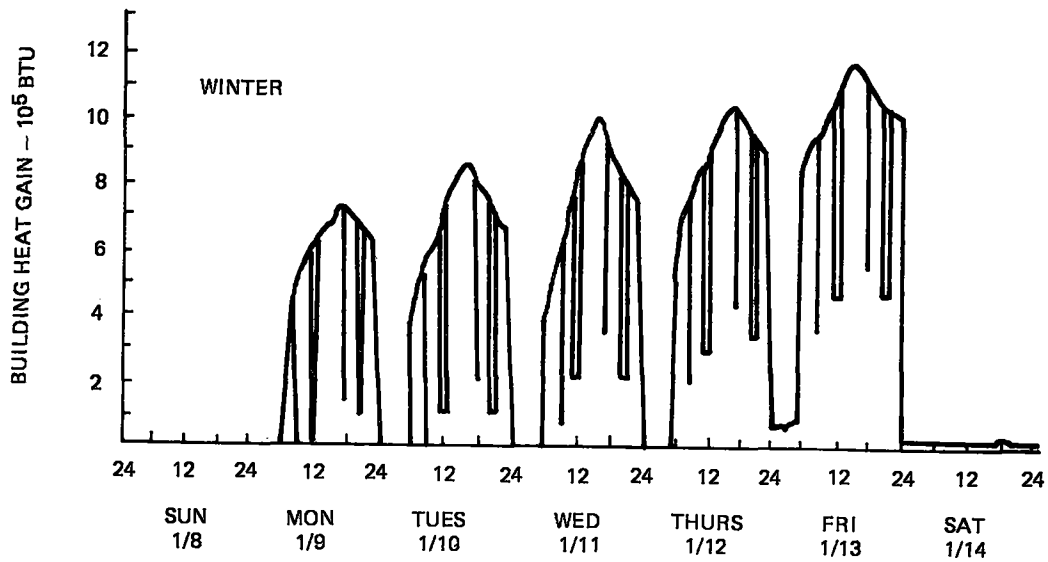


Figure 2.2-2. Diurnal and Seasonal Cooling Load Variations

<u>LOAD</u>	<u>PEAK</u>	<u>-AMPS-</u>	<u>LOAD</u>
BASE			20
AIR COMPRESSOR	66		11
LIGHTS	32		30
AIR CONDITIONER -FAN	32		8
-COMPRESSOR	46		36
VACUUM PUMP	152		18

NOTE: 1.0 amp at 480 volts, 3 phase = 0.83 KVA

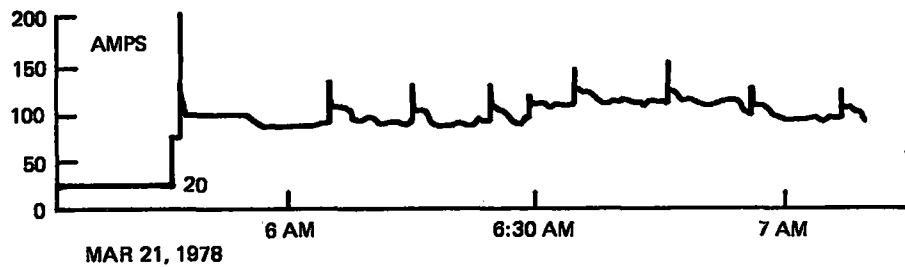


Figure 2.2-3. Summary of Bleyle Plant Inrush Measurements by GPC

Table 2.2-4. Design Electric Loads

Bleyle Plant		STES Operation	
Process Machinery	83	Collection Subsystem	38
Lighting	80	Power Conversion Subsystem	20
Air Handling Equipment	59	Thermal Utilization Subsystem	66
Process Equipment	32	STES Mechanical Building	10
Miscellaneous	16		
Total	270 kW	Total	134 kW

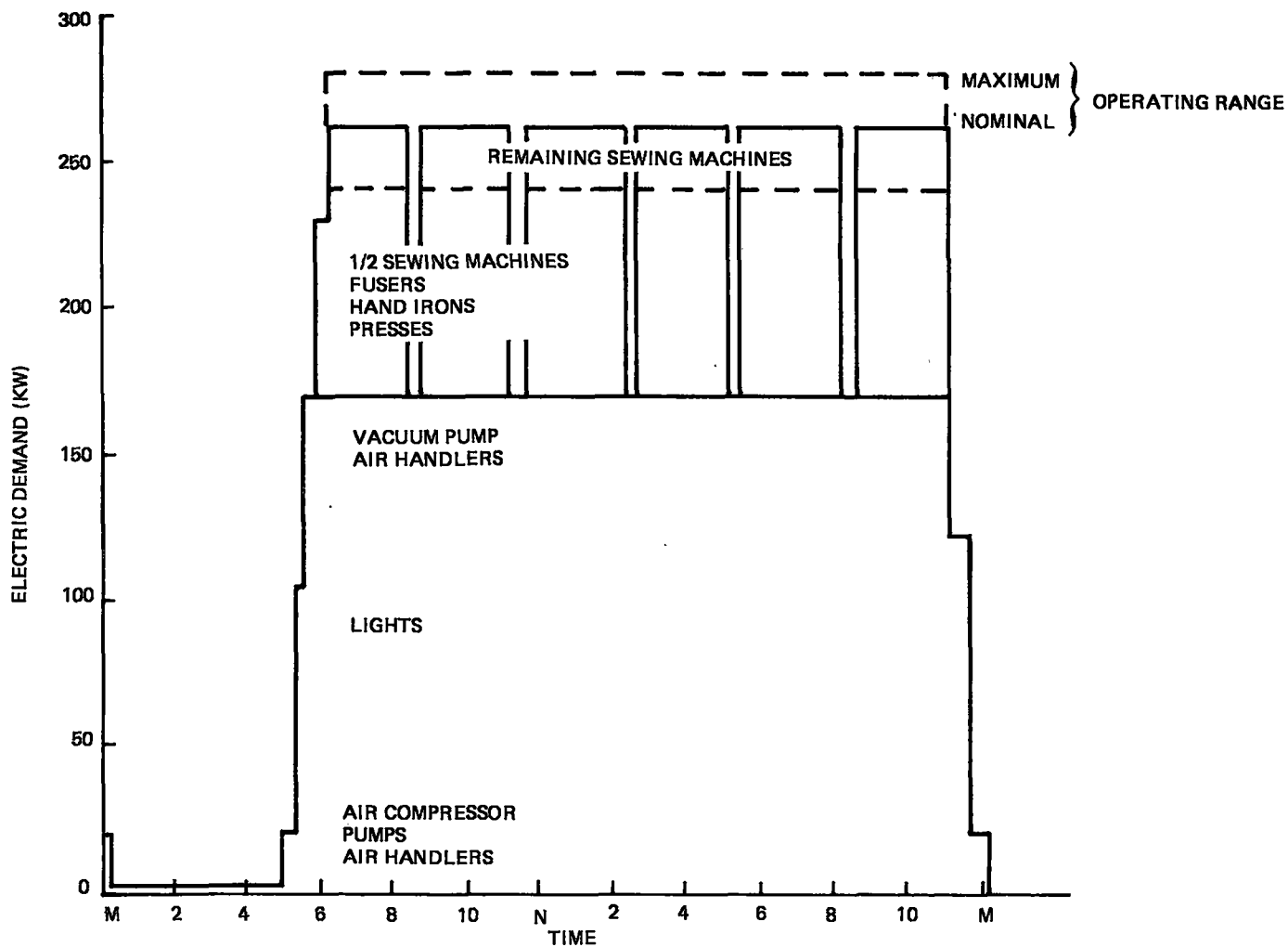


Figure 2.2-4. Bleyle Plant Electric Loads

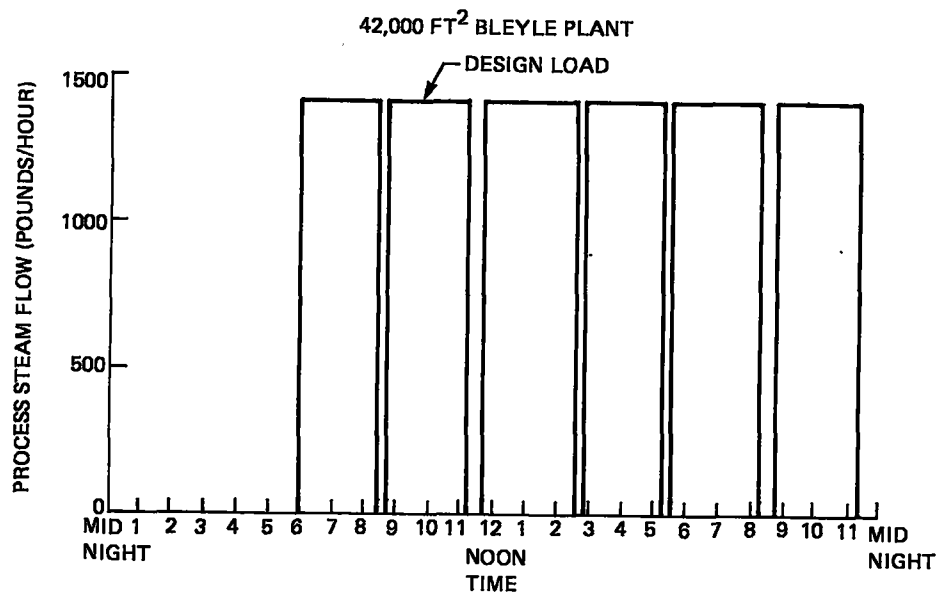


Figure 2.2-5. Process Steam Demand

Table 2.2-5. Design Cooling Loads

Load Source	Load (Tons)
Bleyle Plant	143
Loading/Storage Area	20
STES Mechanical Building	10
Total	173

2.3 SYSTEM TRADE-OFFS AND REQUIREMENTS DEVELOPMENT

The basic technical approach taken for the preliminary design was to utilize the conceptual design developed during Phase II as a reference design. All basic features of the reference design were then re-examined and optimized analytically in a trade-off phase which iterated with the development of a set of derived design requirements based on updated site loads and more definitive hardware descriptions. This effort culminated in the baseline design which defined all major component requirements and descriptions. A finalization design period included a further re-examination of more detailed design features and included the incorporation of a GFE steam turbine-generator set. This portion of the design activity led to the preliminary design system and a finalized set of overall system design requirements. The following subsections describe the major system level trade-offs and the resulting design requirements for the Shenandoah LSE.

2.3.1 SYSTEM CONFIGURATION SELECTION

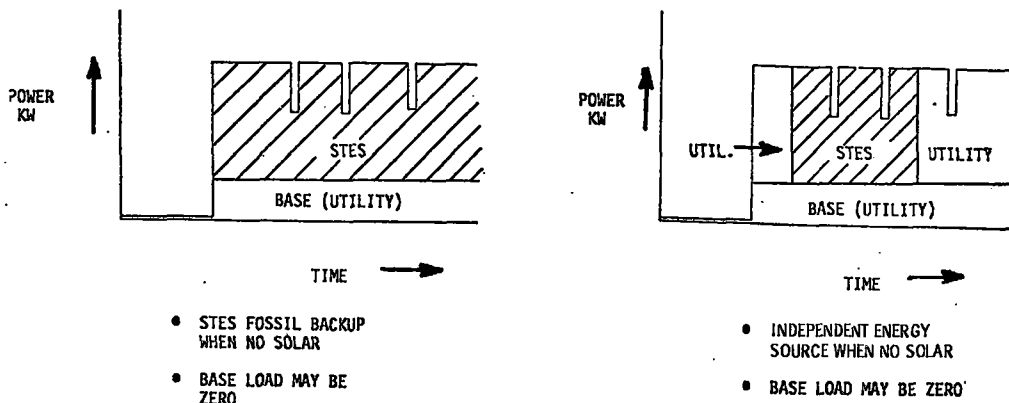
One of the major criteria applied to the selection of both the Solar Total Energy System configuration and its size was to maximize its cost effectiveness within the constraints set by the overall experiment objectives presented in the previous section. Cost effectiveness as applied to solar total energy systems implies maximizing the value of the displaced electrical and thermal energy with the minimum possible system size. The STES designer has several design variables which can be used to optimize cost effectiveness relative to a given set of site loads. Primary among these variables are system configuration, system sizing criteria, component selections and efficiencies, and system operating philosophy with the utility grid.

System studies performed by GE during the Conceptual Design as well as previous studies by Sandia have concluded that the most cost effective solar total energy system should be designed to provide maximum possible utilization of cascaded thermal energy. This conclusion results from the fact that the majority of the solar total energy plant levelized annual benefits result from credit for thermal energy savings. Also, thermal energy revenues are more sensitive to escalation in fossil fuel prices than electric energy costs, which reflect approximately 80 percent capital equipment.

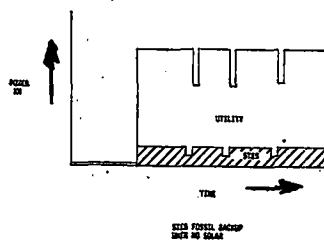
Ideally, maximum thermal utilization would occur when the thermal/electric load ratio matches the system thermal/electric output when operating on solar heat input or, for a total energy system with fossil backup, when the site thermal/electric load ratio is matched with equipment output and is constant over the year. For the Shenandoah Bleyle Plant application and for most other potential industrial applications of STES, loads are not in the exact appropriate ratios, and some compromises occur either in terms of excess thermal energy availability and/or the system being undersized for site electricity production because of the use of a utility base load to adjust the thermal/electric load ratio to minimize thermal excess.

During the early portion of the Preliminary Design Phase, system studies were performed to select the baseline system configuration and operating mode from which the system size was derived. There are three major modes of operation possible for an on-site solar total energy system. Shown graphically in Figure 2.3-1, these include electric load following, thermal load following, and constant electric output.

Electric Load Following



Thermal Load Following



Constant Electric Output

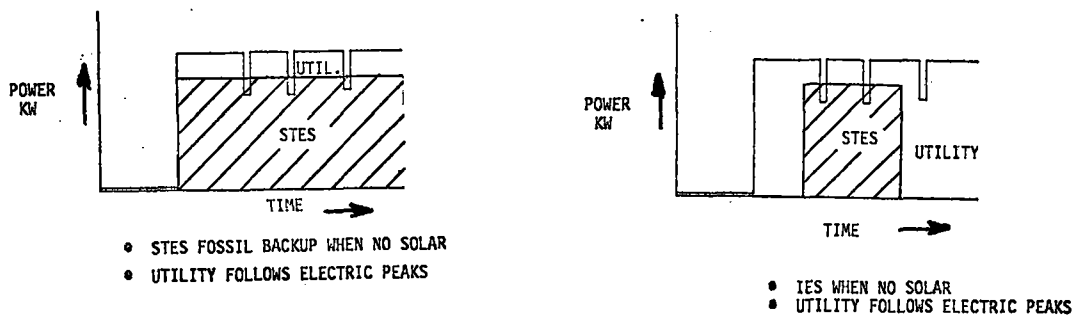


Figure 2.3-1. STES Operating Mode Alternatives

Each mode has distinct advantages and disadvantages, and for most solar total energy applications, the mode selected will have a significant effect on the size of the solar collection system and the site loads supplied by solar.

Electric load following, which has been selected as the baseline operating mode for the Shenandoah LSE, offers maximum flexibility in operating with the utility as peak shaving capacity. In this mode the PCS follows the site electric load peaks while a base load is supplied by the utility. In the case of a single system with a local owner such as the Shenandoah system, the baseload is selected to match the site loads with minimum excess thermal energy. For many utility owned STES sites in a grid, it would be possible to adjust base loads provided to individual sites to allow the aggregate of STES produced electrical power to serve as a supplement to fossil supplied grid peaking capacity.

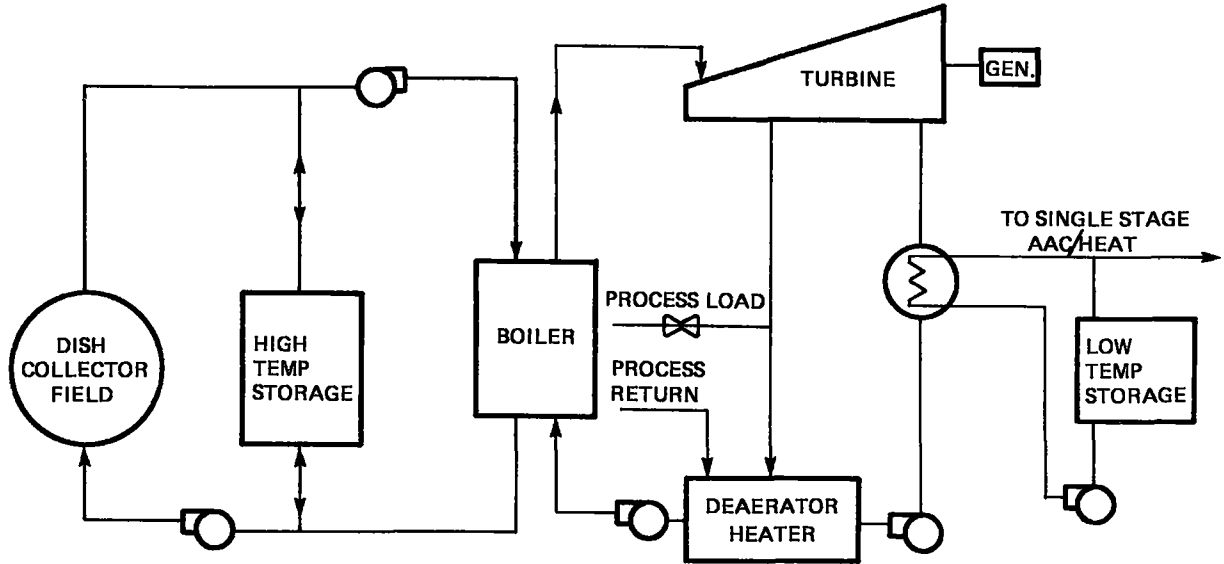
The thermal-load-following, system operation mode would result in the smallest size STES and the most economical from the standpoint of the fact that no excess low-temperature thermal energy would result from system operation. This operating philosophy would be ideal for a site having a very high thermal/electric load ratio. However, for the more typical thermal/electric load ratios represented by the Bleyle site, a thermal-load-following system results in the generation of very small amounts of electrical power and as such would not be capable of serving effectively as peak shaving capacity for the utility. For solar applications under these conditions, it is more cost effective to supply the thermal energy directly at the required temperature than to provide cascaded energy through electrical generation.

The third mode, constant electric output, has the advantage of allowing the PCS to operate at its maximum efficiency design point. However, the STES does not follow electric peaks and would have to have greater storage capacity to insure that electricity could be supplied to the grid during peaking periods. However, even though electric load following was selected as the baseline system operating mode and used to size the system, the constant electric output mode will be evaluated on an experimental basis during the system operational testing phase.

Figure 2.3-2 shows the two basic system configurations investigated to evaluate the electric and thermal load following options. Both systems represent fully cascaded, total energy designs. The electric load following system incorporates the Conceptual Design extraction turbine with backpressure condenser. The extraction provides process steam. The condenser heat is directed to a low temperature storage unit or to a single stage absorption unit. The thermal load following system uses a single stage turbine operating at backpressure to supply both the process steam load and the absorption air conditioning. However, since the plant requires $7.9 \times 10^5 \text{ N/m}^2$ (114 psia) steam for the process which establishes the backpressure, this high pressure steam can be used to drive a dual stage absorption unit with a COP of approximately 1.0. This has the effect of reducing the overall thermal load compared to the less efficient single stage machine which results in less heat input required.

The two system configurations were evaluated against the Bleyle load on an annual basis. The major performance factors considered were the base load and power level required for the electric load following system and the system size required to supply a minimum of 60 percent of the annual Bleyle demand. Figure 2.3-3 summarizes the annual system performance. The shape of the curves is highly site load dependent. As seen, the thermal load following system supplies only 10 percent of the site electrical loads while operating at a peak electrical output of only 65 kW. In the electric load following mode, increasing the electrical power level and simultaneously decreasing the utility base load results in greater electrical contribution for a given collector area; however, thermal output is decreased because of reduced STES operating time during which energy is cascaded as seen in Figure 2.3-4. Also, for collector areas above 3720 m^2 (40 kft²), some excess thermal energy results as shown on the plot of solar utilization in Figure 2.3-5. The thermal utilization can be improved by increasing both high and low temperature storage sizes, but the curves in Figure 2.3-5 have been based on practical TES sizes based on both economics and site integration considerations. Figure 2.3-3 also shows the combinations of design electric power level

Extraction or Dual Single Stage Turbine System Schematic



Single Stage Turbine Schematic

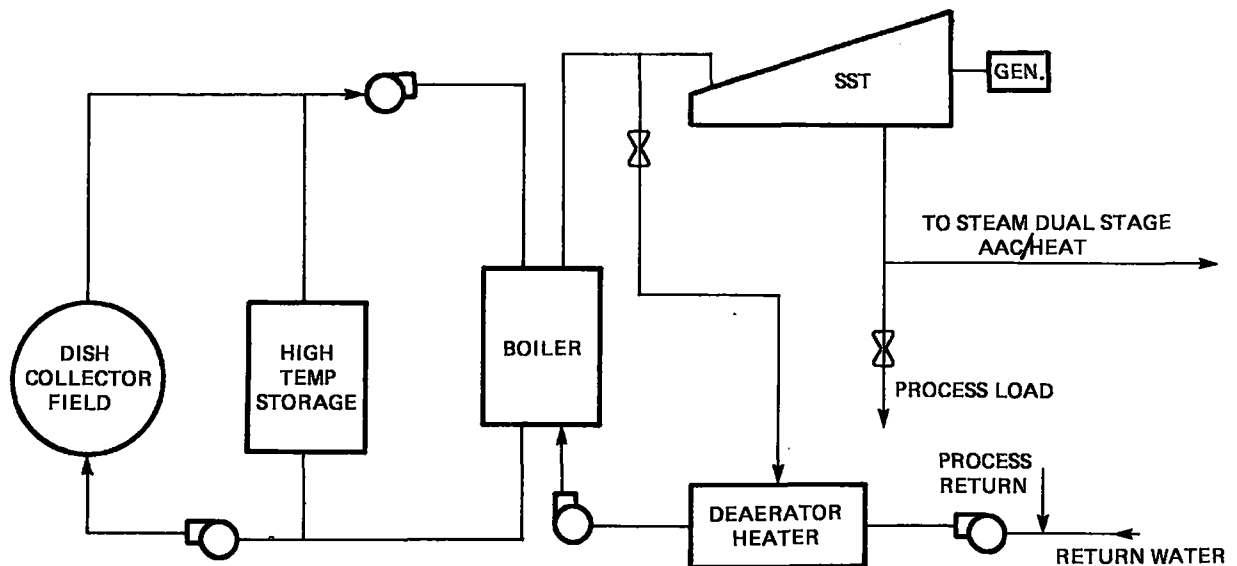


Figure 2.3-2. System Configuration Alternatives Evaluated for Shenandoah LSE

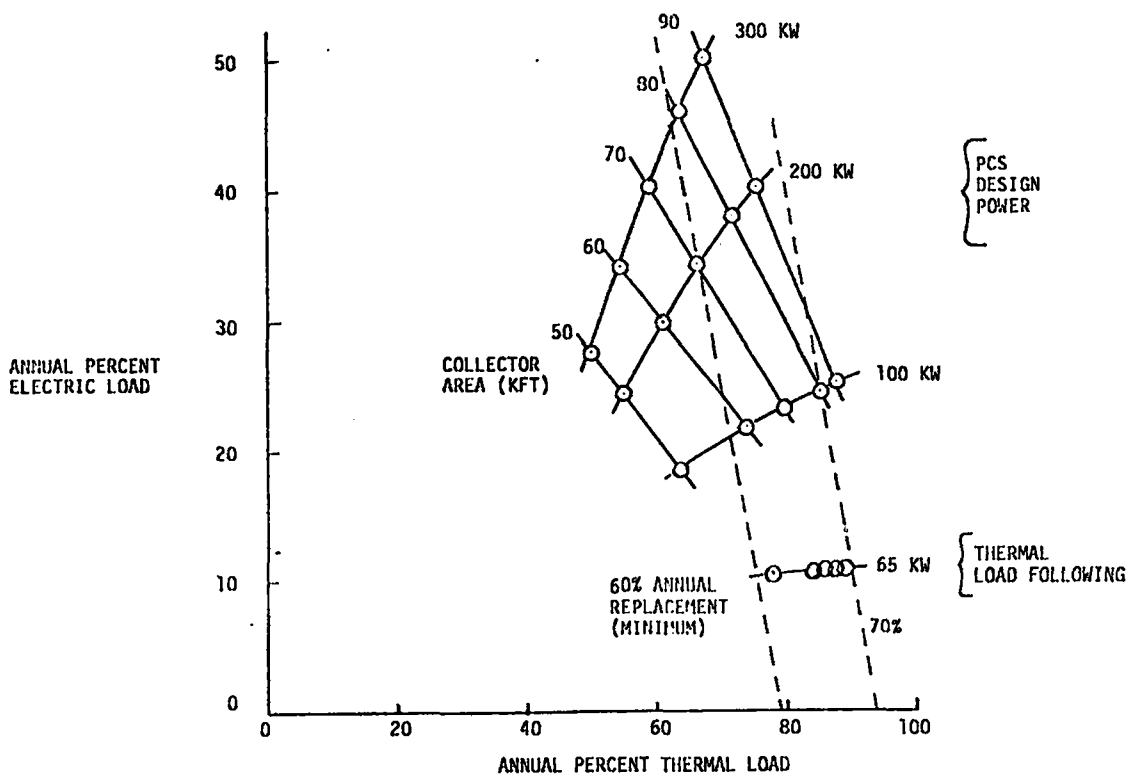


Figure 2.3-3. Annual Performance Summary for System Alternatives

$$A_c = 79,500 \text{ FT}^2$$

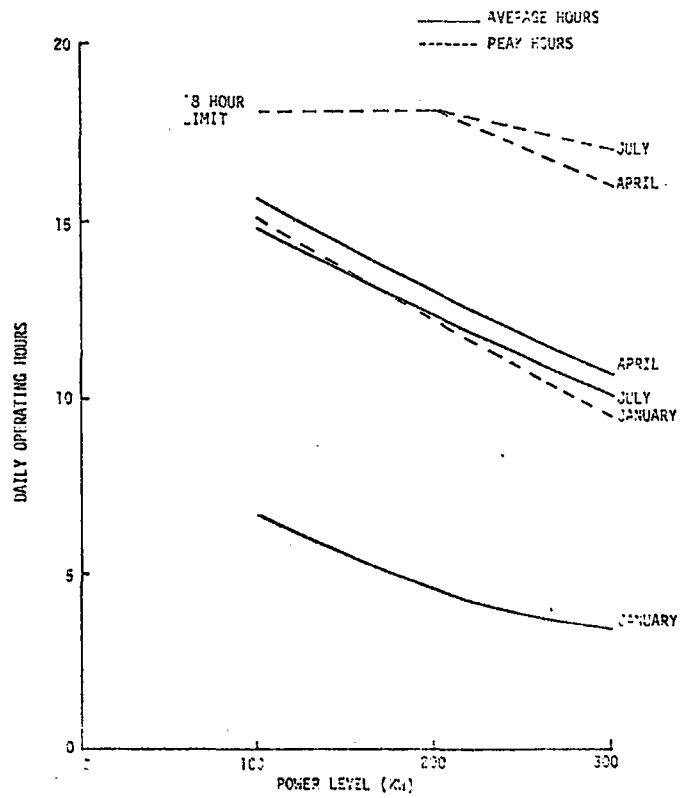


Figure 2.3-4. Seasonal STES Operating Hours

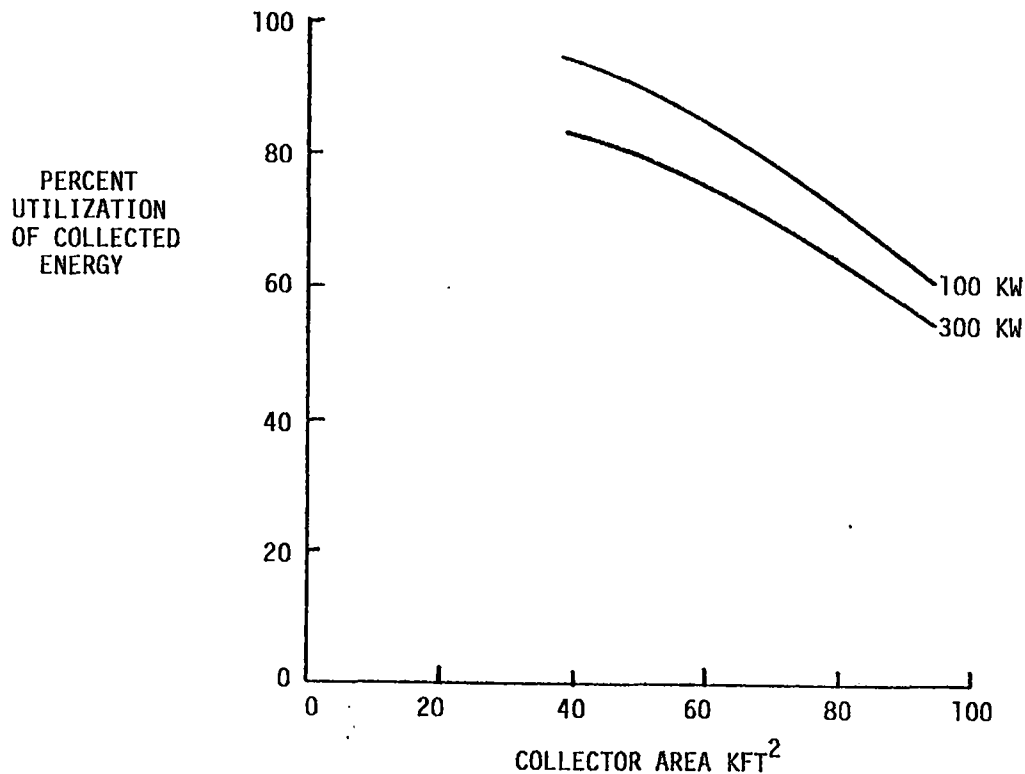


Figure 2.3-5. Sensitivity of Solar Utilization to Collector Area and STES Operating Power for Bleyle Loads

(or utility base load) and collector area required to provide the 60 percent minimum annual solar replacement. As the design electric power level increases, the electric load contribution increases; however, a larger collector area is required to meet a fixed percentage of the total site loads. At the higher power levels, the performance in terms of percentage of site loads saturates at collector areas of 7430–9290m² (80 - 100kft²), which provides a maximum collector area for consideration.

One of the program experimental requirements is the demonstration of standalone system operation. This requirement dictates the STES generator capacity and, based on the load analysis of Section 2.2, indicates a rated power of 400 kW for the turbine generator. This requirement in concert with the other selections criteria listed in Table 2.3-1 led to the selection of the 192 dish, 300 kW nominal operating power (100 kW base load) design for the Shenandoah LSE.

Performance evaluations led to the conclusion that 300 kW is the maximum operating power level desired without resulting in unacceptable thermal excess. This power level also provides for the minimum turn-down from the 400 kW rating and supplies a significant electrical contribution to the site electric loads. The thermal load following system does not produce enough electrical output to supply the STES parasitics for the Bleyle loads even though all of the collected energy is utilized.

Table 2.3-1 also shows a collector area range from 120 to 240 dishes based on a 7-meter diameter (see Paragraph 3.2.4 for dish diameter optimization). The selection of 192, 7-meter diameter dishes 7293m² or 78,500 ft²) allows all experimental objectives to be met. The major factors upon which the selection was based include:

1. Studies (summarized in Paragraph 3.3.1) showed 192 dishes provided maximum constrained field output on an annual basis.
2. The system has enough experimental flexibility to operate through GPC peaks for much of the year.

Table 2.3-1. System Sizing/Operating Power Selection Trade-Off Summary

Trade-Off Factor	Electric Operating Power Number of 7m Dia. Collectors	Thermal Load Following (65kW/20kW)				STES = 100 kW Base = 300 kW			STES = 200 kW Base = 200 kW			STES = 300 kW Base = 100 kW		
		120-240	120	192	240	120	192	240	120	192	240			
Percent Annual Electric Requirements		3	3	3	3	3	2	1	3	1	1			
Percent Annual Thermal Requirements		1	1	1	1	3	1	1	3	1	1			
Operating Hours		2	2	1	2	2	1	1	2	1	1			
Utilization of Collected Energy		1-3	1	2	3	2	2	3	2	2	3			
Bleyle Plant Stand Alone Capability		3	3	3	3	2	1	1	2	1	1			
Experiment Flexibility Over Operating Range		3	3	3	3	3	3	3	1	1	1			
Projected Economics		1-2	2	2	3	2	2	2	2	2	2			
Scalability		3	3	3	3	1	1	1	1	1	1			

- 1 Good
- 2 Acceptable
- 3 Unacceptable

↑
SELECTED SYSTEM

3. The system provides a significant annual site electrical replacement.
4. The system has projected economics potential for applications involving full utilization of collected energy.

These trade-offs led to the selection of a fully cascaded system using a steam extraction turbine in the electric load following mode as the concept for the LSE design able to satisfy both performance requirements and experiment objectives. The Reference Design system schematic is shown in Figure 2.3-6. The system incorporates a multi-stage turbine with an extraction for the process steam. The system has the capability to operate with full process steam extraction between 200 and 400 kW with a nominal design operating point of 300 kW.

During the course of the Preliminary Design, system optimization studies resulted in modifications to the reference design, with the resulting Preliminary Design shown in the Figure 2.3-7 schematic. The major design changes are summarized below:

1. Fossil backup heat for the system is provided by a Syltherm 800 heater located in the collector loop rather than by a fossil steam boiler as previously specified. The Syltherm 800 heater is a standard unit using low pressure parts and would be less expensive than the pressurized steam boiler. The piping arrangement has also been modified to allow series flow of solar heated oil through the boiler so that solar to fossil switchover can be accomplished in a very short time with minimum impact on turbine inlet conditions.
2. The overtemperature heat exchanger and associated large cooling tower for use as a heat dump for excess high temperature energy was eliminated and replaced with a collector defocus mode.
3. The buffer tank, included in the Reference Design collector field to control field inlet transients, was eliminated. Its function is served by the one-hour trickle oil tank. In addition, the void space within the trickle oil tanks provides the necessary expansion for the solar collection subsystem inventory of Syltherm 800.
4. The high temperature thermal storage system design was modified to allow operation with both dual media and trickle oil approaches.
5. The design also incorporates the GFE turbine generator set to be supplied by MTI. The turbine-generator consists of dual, high speed, turbines with a gearbox to reduce the speed to the 1800 rpm alternator. The system operates at backpressure only. The solar boiler design has been modified from the previous once-through concept to a three-piece pool type boiler with a flash economizer and blow down to eliminate impurities. This boiler is commercially available and allows elimination of the polishing demineralizer. In addition, the system configuration was modified to eliminate the requirement for redundant pumps, where possible, by maintaining a stock of spare parts, thereby minimizing installed piping and valving costs.
6. Rather than directly piping process condensate and make-up water into the PCS boiler feed, the make-up will be preheated to approximately 383^oK (230^oF) by circulating it directly into the PCS condensate tank.
7. The piping design has been modified to allow full thermal storage by-pass to supply loads directly from both HTS and LTS to maintain fully charged tanks.
8. The two-tank LTS system was replaced by a simpler, single mixed tank. Studies show that sufficient temperatures for both the absorption air conditioner inlet and the PCS condenser can be maintained, and the second 454m³ (120,000 gallon) tank can be eliminated.

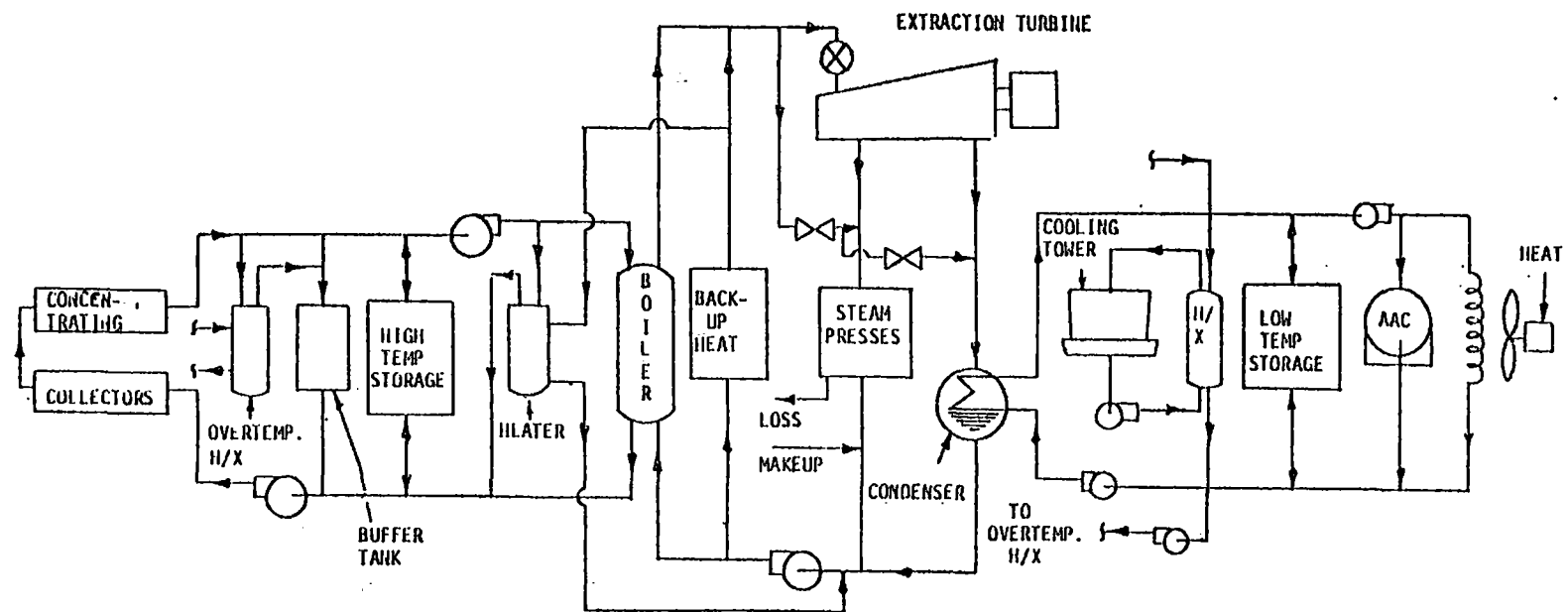


Figure 2.3-6. Reference Design System Schematic

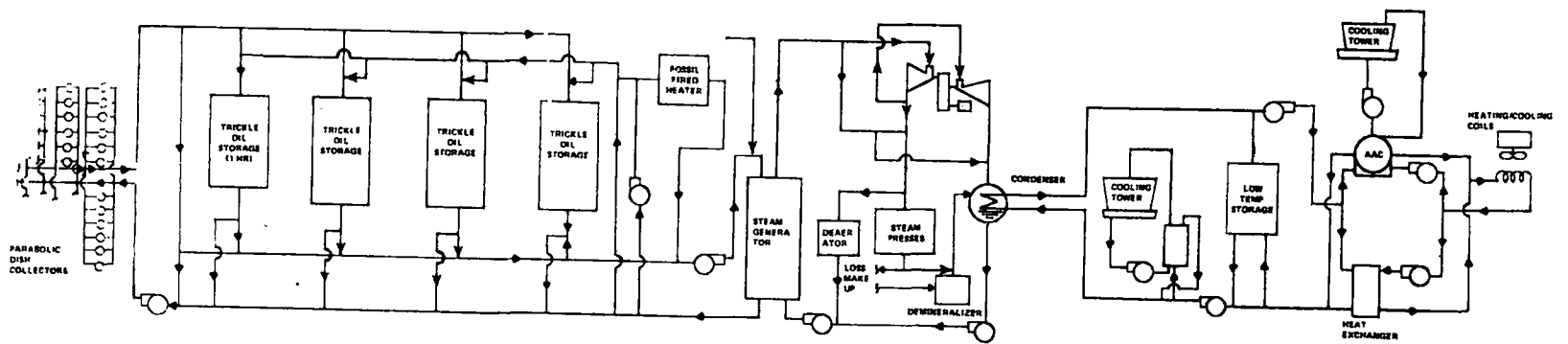


Figure 2.3-7. Shenandoah LSE Preliminary Design System Schematic

2.3.2 SYSTEM ANALYSIS AND TRADE-OFF STUDIES

During the Preliminary Design, a significant effort was devoted to performing system analyses and trade-off studies to optimize the system design and cost-effectiveness. Major studies were performed to select the collector and TES heat transfer fluid and associated system operating temperature, to determine high temperature thermal energy storage capacity; to define system performance and cost sensitivity to collector and collector field parameters, to evaluate performance sensitivity to turbine efficiency and condenser temperature/pressure, and to optimize the low temperature storage system in the thermal utilization subsystem. Through these studies, system level design requirements were derived as discussed in the following subsections.

2.3.2.1 Heat Transfer Fluid and System Operating Temperature Selection

The system operating temperature is a highly significant design parameter because it affects both the solar collector efficiency and the heat engine efficiency. In general, collector efficiency decreases and heat cycle efficiency increases with increasing operating temperature. In addition, the desired operating temperature dictates the heat transfer fluids which can be used in the system.

For the point source collector selected for the Shenandoah system and site, sensitivity of efficiency to temperature is not as severe as for the less efficient line source concentrating collector. In addition, the commercial type steam turbine generator systems compatible with on-site size installations experience relative low prime mover efficiency. These systems can have significantly higher electrical generation efficiency for higher temperatures. These considerations, along with the fact that higher cycle efficiency results in a better STES output balance with the Bleyle plant loads, suggests selection of the highest possible operating temperature consistent with standard components and field costs.

Three heat transfer fluids were considered for the system: Exxon's Caloria HT 43 and Monsanto's Therminol 66 for operation up to bulk temperatures of 589°K (600°F) and Dow Corning's Syltherm 800 for operation up to bulk temperatures of 672°K (750°F). These were considered to be the maximum practical operating temperatures for these fluids based on currently available data. Caloria HT 43 at 589°K (600°F) was considered based on recent degradation experiments run at Sandia Laboratories, Livermore; however, the data still is limited. Therminol 66 can operate at bulk temperatures up to 616°K (650°F); however, severe degradation rates result, and 589°K (600°F) appears to be the practical upper temperature. Although there is limited data for Syltherm 800 at 672°K (750°F), Dow Corning indicates that operation at 750°F can be achieved with reasonable fluid stability. Table 2.3-2 compares the three fluids on a relative advantage/disadvantage basis, considering only basic property characteristics available from direct contacts with manufacturers and published literature. As noted, specific data is required to verify the performance of each fluid at the temperatures and conditions required for LSE application. During the Preliminary Design, significant basic materials and material compatibility testing was performed both at Dow Corning and at Sandia's Livermore Laboratories on Syltherm 800 to support selection of TES media and system materials. Characterization testing is planned to continue during the Definitive Design. However, the temperature advantage of Syltherm 800 and the cost advantage of Caloria HT 43 are obvious from the table.

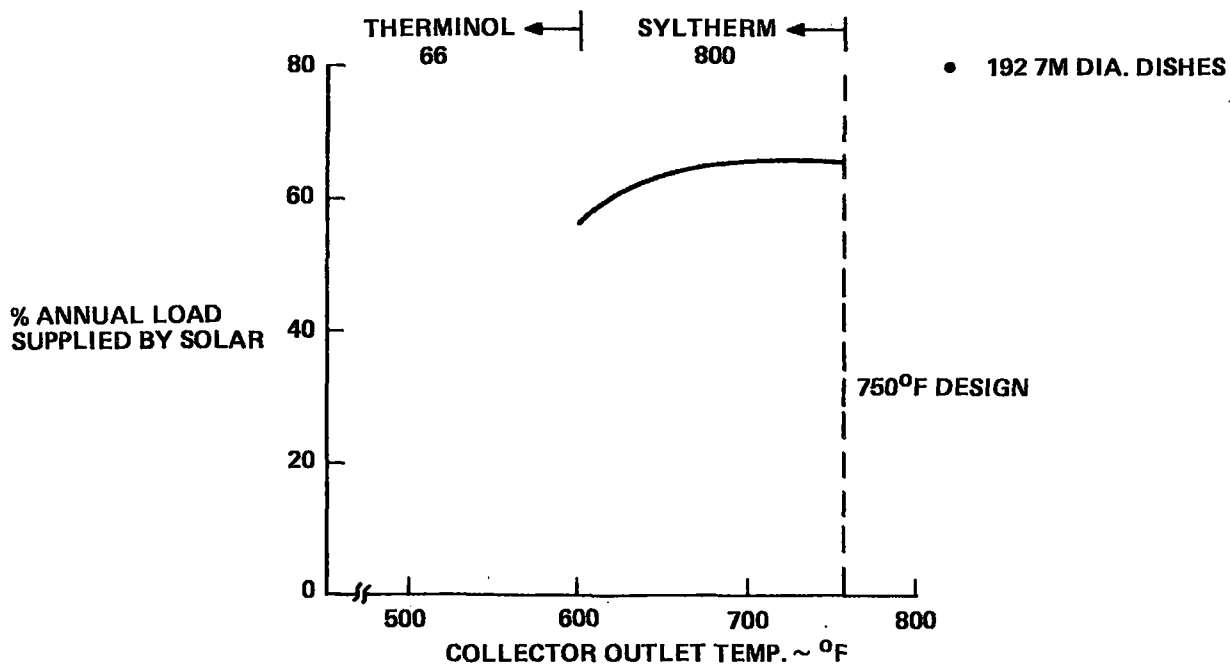
A study was performed to assess the impact of fluid and temperature selection on system performance and application for LSE, assuming Syltherm 800 system operation at 672°K (750°F) and Therminol 66 at 589°K (600°F) operation. Caloria HT 43 was eliminated from consideration because of uncertainty in its thermal stability at 600°F. A comparison between Syltherm 800 and Therminol 66 is shown in Table 2.3-3 for the most significant parameters. As seen, the most significant advantage of the Syltherm 800 higher temperature operation is a 15-20 percent increase in system electrical output for the same heat input. As shown in Figure 2.3-8, in terms of annual system performance, the use of Therminol 66 at 589°K (600°F) results in less than the minimum 60 percent solar replacement for the 192 dish system. This performance result indicates that the decreased PCS efficiency resulting from reducing the throttle temperature and pressure conditions more than offsets the reduced collector and field losses associated with lower operating temperature. The higher temperature operation also allows for the maximum heat transfer ΔT for the system as

Table 2.3-2. Comparison of Three Heat Transfer Fluids

Fluid	Advantages	Disadvantages/Limitations	Conclusions
Caloria HT 43	<ul style="list-style-type: none"> - Highest flash pt. = 400°F - Low cost - \$1.50/gal. 	<ul style="list-style-type: none"> - Pour point +15°F - Highest viscosity - Catalytic effect with copper 	<ul style="list-style-type: none"> - Possible candidate for 600°F operations - Stability data required, tests underway at Sandia - Most economical fluid
Syltherm 800	<ul style="list-style-type: none"> - Good long term stability @ 700°F - Low viscosity - Materials compatibility good - Low freezing point 	<ul style="list-style-type: none"> - Lowest flash point, 310°F - Very high cost - Some ill effects from leakage vapors reported 	<ul style="list-style-type: none"> - Good stability to 700°F - Potentially hazardous - High initial and replenishment cost - Compatibility data with metals/rocks needed
Therminol 66	<ul style="list-style-type: none"> - Lower viscosity than Caloria HT 43 - High operating bulk temp., 650°F - Low freezing point 	<ul style="list-style-type: none"> - High cost - Less stable than Syltherm 800 - Moderate flash point, not fire resistant - Catalytic effect on contact with rock 	<ul style="list-style-type: none"> - Long term stability data lacking - Significant initial and replenishment cost - Potential leakage hazard problems

Table 2.3-3. Heat Transfer Fluid Comparison for Shenandoah LSE

Factor	Therminol 66 600°F	Syltherm 800 750°F
Cycle Electrical Output	Base	Increase 15-20%
Collector/HTS ΔT	125°F	250°F
Initial Cost	\$7/gal	\$16-24/gal
Operating Cost		
Fluid Replacement	Base	Increase 20-50%
Pumping Power	Base	Decrease 50%
Degradation	Solids	Non-volatiles only



- ALTERNATE FLUIDS RESULT IN LESS THAN 60% SOLAR REPLACEMENT
- TEMPERATURE BELOW 700°F PENALIZES PCS PERFORMANCE – LOWER TURBINE INLET PRESSURE
- 750°F DESIGN GIVES SYSTEM PERFORMANCE MARGIN

Figure 2.3-8. Sensitivity of System Performance to Collector Temperature

shown in the boiler pinch curve in Figure 2.3-9. The increased ΔT increases the operating range for the HTS which allows the same stored energy in a system containing only half the mass of a Therminol 66 system. Finally, system flow rates for both the collector field and the boiler are reduced as the ΔT is increased, resulting in reduced parasitic pump power.

Syltherm 800 has potentially low degradation rates with non-volatile products at operating temperatures. However, complete testing in a dynamic loop with the Shenandoah LSE materials has not been performed to confirm actual behaviour. Such testing is being planned to support the Definitive Design activity. However, because of the inherent system advantage and potential life cycle cost savings if a system using Therminol 66 at 589°K (600°F) had to be periodically flushed, Syltherm 800 has been selected for the preliminary design system.

2.3.2.2 Solar Collection Subsystem Trade-Offs

Major solar collection subsystem trade-offs include determination of sensitivity of system performance to collector area and high temperature thermal storage capacity and impact of collector reflectivity on system performance. The study to evaluate the impact of high temperature storage capacity on system performance was performed for the following set of conditions and assumptions:

1. Weekend collection
2. 300 kW turbine/generator design ($\eta_{\text{turb}} = 50\%$)
3. Electric load following operation
4. 7-meter diameter dish
5. Low Temperature Storage of 2.1×10^{10} Joules (20 MBtu)

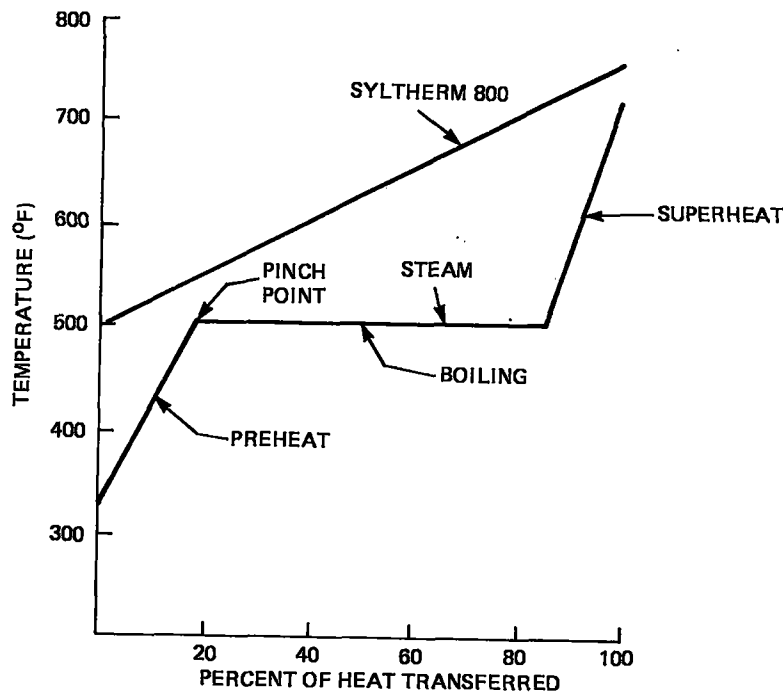


Figure 2.3-9. Solar Steam Generator Pinch Curve

Figure 2.3-10 summarizes the variation of system performance with collector area and high temperature storage capacity. The figure shows that a fixed system performance can be achieved by combinations of collector areas and HTS size, and in particular, 60 percent of the annual energy of the Bleyle Plant plus STES parasitics can be supplied by combinations ranging from 192 dishes and 4.2×10^{10} Joules (40 MBtu) to 150 dishes and 2.1×10^{11} Joules (200 MBtu). An economic study based on the relative collector and storage costs and considerations of the practical limitations of large storage systems dictates the most cost effective design. The selected 192 dish design point is shown.

Figure 2.3-11 shows the impact of HTES capacity for a fixed collector field of 192 dishes. Significant performance improvements result up to about 1.6×10^{11} Joules (150 MBtu). Beyond that point, virtually no system benefits result.

Figure 2.3-11 also shows the effect of collector field availability on the required HTS size to meet a fixed 60 percent solar replacement factor with a 192 dish collector system. The curve shows a range based on possible system efficiency variations. It should be noted that even with reasonable allowances for efficiency, uncertainties for field losses, HTS losses, and 5 percent of the dishes unavailable, a 1.1×10^{11} Joules (100 MBtu) HTS capacity is sufficient to assure satisfaction of the 60 percent annual energy displacement requirement. Hence a 100 MBtu HTS was selected for the baseline design.

To guide the requirement for the reflector surface reflectivity, system performance sensitivity was calculated on an annual basis. Figure 2.3-12 summarizes the calculations, which show a potential performance improvement of 5 percentage points resulting from increasing the reflectance from the nominal 0.88 up to 0.98. The figure also shows that the average reflectivity must be maintained above 0.77 to assure meeting the annual system performance requirements.

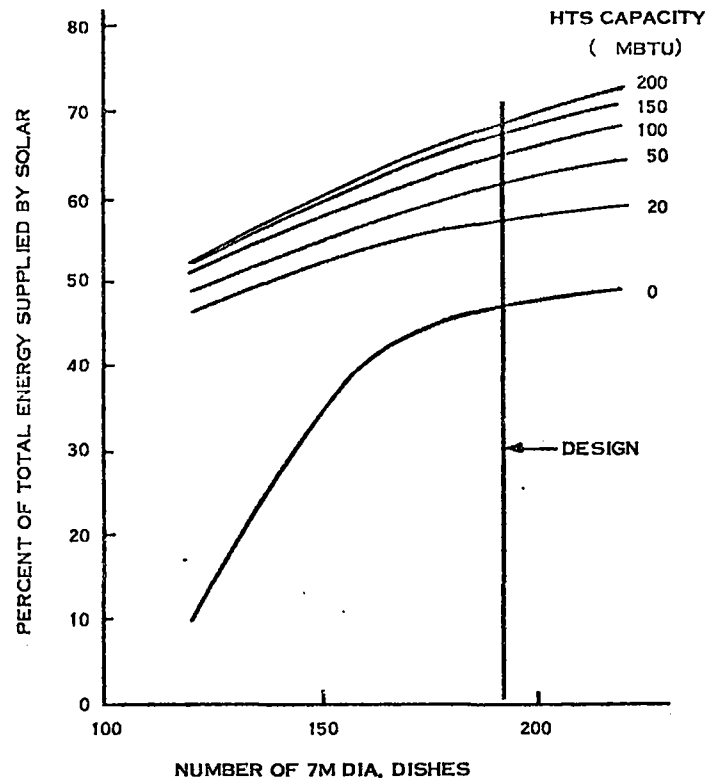
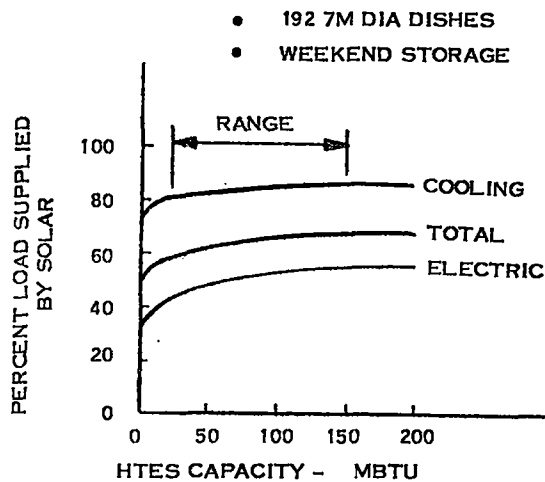


Figure 2.3-10. Variation of System Performance with Collector Area and High Temperature Storage Capacity



100 MMBTU TES PROVIDES:

- AVERAGE WEEKEND STORAGE CAPACITY
- 11 HOURS SYSTEM OPERATION
- 95 PERCENT FIELD AVAILABILITY FOR NOMINAL SYSTEM EFFICIENCY

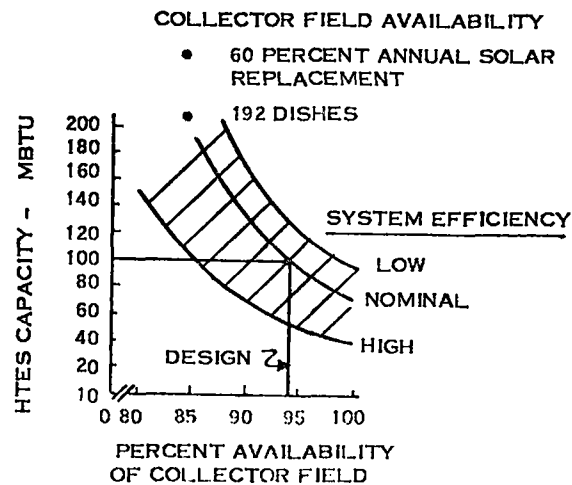
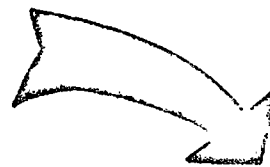


Figure 2.3-11. High Temperature Thermal Storage Capacity Selection

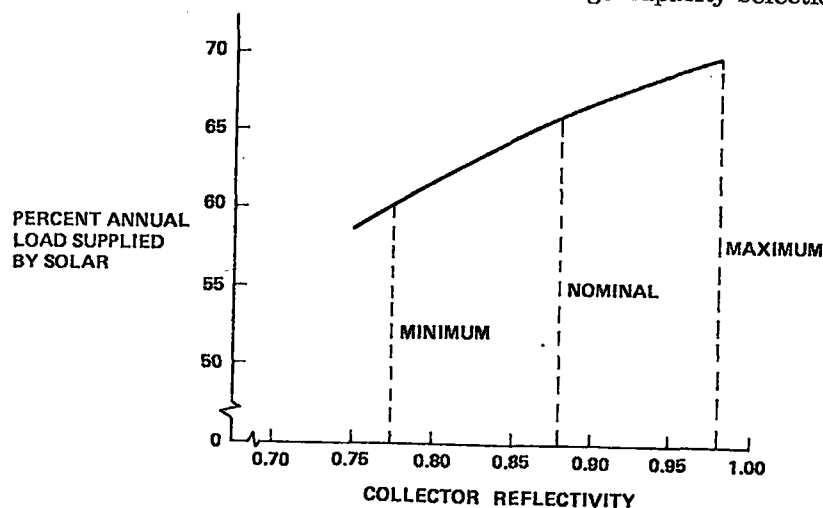


Figure 2.3-12. Effect of Collector Reflectivity on System Performance

2.3.2.3 Turbine - Generator Efficiency Trade-Offs

The LSE Reference Design incorporated a GE marine turbine with a turbine efficiency of 50 percent when operating at throttle conditions of 672°K (750°F) and 4.8×10^6 N/m² (700 psig). An analysis was performed to determine the effect of increasing turbine performance on total energy system performance for the Shenandoah site loads.

In the most general case, a solar total energy system would be sized to match the site thermal loads and generate electricity as a system operation by-product. In an ideal case, all of the energy would be used, and system performance and economics would not be particularly sensitive to the electrical conversion efficiency. Thus, increased Power Conversion Subsystem (PCS) efficiency is of major interest in applications having site thermal/electric load ratios such that sizing a total energy system to match the thermal load would result in an electrical output which is not sufficient to justify economically including the PCS in the system. In these cases, increasing PCS efficiency improves the output distribution for matching the thermal loads giving more electric output benefit.

The Shenandoah system was sized to supply more electrical output than that which would match the thermal loads. This system, which resulted in excess thermal energy being generated, was selected to allow experimental flexibility while demonstrating the capability of a solar total energy system to supply significant electrical output.

Increasing the electrical generating efficiency for a fixed heat input (collector area) does increase the overall system performance somewhat. This results from the fact that, for a fixed collector area and electric load, a higher electrical efficiency results in a lower heat input rate to meet that load. This means that more energy is available for high temperature storage which provides longer system operating times. The longer operating time increases both the electrical and cascaded thermal energy supplied to the load. Since the system has excess thermal energy, even at higher turbine efficiency, the major improvement associated with the increased running time is in a higher percentage of the electrical load supplied. However, since the electrical load is only about one-fourth of the thermal load for Shenandoah, the resulting annual performance improvement is not significant.

The more significant impact of increased PCS efficiency is that it allows a given percentage of the annual load to be met with fewer collectors. The collector area can be reduced because, for an electric load following system, less heat input is needed to supply the required electric output. Based on the Shenandoah site loads, excess cascaded thermal energy is available from the PCS. Thus, the reduced collector area in conjunction with a higher PCS efficiency would provide a better load match without sacrificing thermal energy supplied. This may not always be true for solar total energy systems if the application was a higher thermal/electric load ratio than Shenandoah. In the case of higher T/E ratio applications, increasing PCS efficiency will reduce thermal output and may require more collector area to match site loads.

The results of the analysis to investigate improved efficiency T-G units are summarized in Figure 2.3-13. As shown, an increase in efficiency from 50 to 80 percent, although unlikely to be achieved for a 300 kW power level, would result in a 22 percent decrease in collector area required to supply 60 percent of the

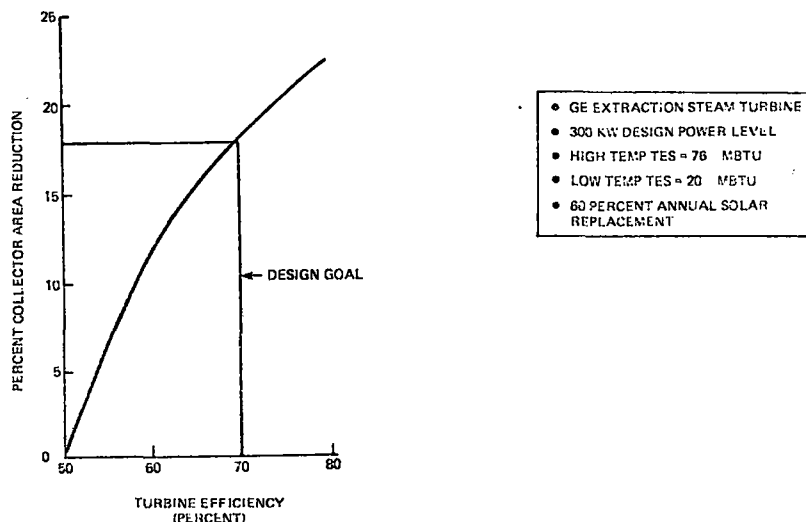


Figure 2.3-13. Effect of Turbine Efficiency on Required Collector Area

annual LSE energy requirements. For the 4:1 thermal to electric load ratio existing at Shenandoah, the curve has a decreasing slope as the turbine efficiency increases above 60 percent indicating decreasing benefit. However, an increase of 10 percentage points to 60 percent appears to offer significant economic advantage, resulting in a 10-15 percent decrease in collector area. Particularly, if the Bleyle plant load ratio is common for potential solar total energy applications, an extraction steam turbine with an efficiency of 60-70 percent could significantly enhance solar system economic attractiveness. A design goal of 70 percent for Shenandoah led to the selection of a high performance, high speed T-G set manufactured by MTI Inc. for the Preliminary Design. This unit potentially provides a better site load match and gives the system a performance margin for meeting the required 60 percent minimum solar replacement.

2.3.2.4 Power Conversion Subsystem Condensing Temperature Trade-Off

Because of the Shenandoah thermal to electric design load mix, the net effect of increasing power conversion system efficiency is to improve the percentage of loads supplied by solar for a fixed collector area or to reduce the collector area required to provide a fixed load percentage. Reducing the PCS condensing temperature increases cycle efficiency but at the same time reduces the cooling output from the absorption air conditioner. For the Shenandoah total energy system, the most cost effective system results from balancing these two effects within the constraints of practical limitations such as thermal utilization loop component sizes and operation parasitics.

Figure 2.3-14 shows the effect of entering hot water temperature on single stage absorption air conditioner coefficient of performance (COP) and fraction of rated capacity. The data was taken from a Trane catalogue, Reference 2.3-1. The curves show that COP is relatively constant from 394°K (250°F) down to 372°K (210°F) and then begins to drop steeply. As indicated, the COP actually increases somewhat as the unit is derated. Full capacity for the unit is about 400°K (260°F), and lowering the hot water temperature to 361°K (190°F) reduces the output to 30 percent of the rated value. The associated machine capacity required to meet the Shenandoah design cooling loads and incremental cost as a function of entering hot water

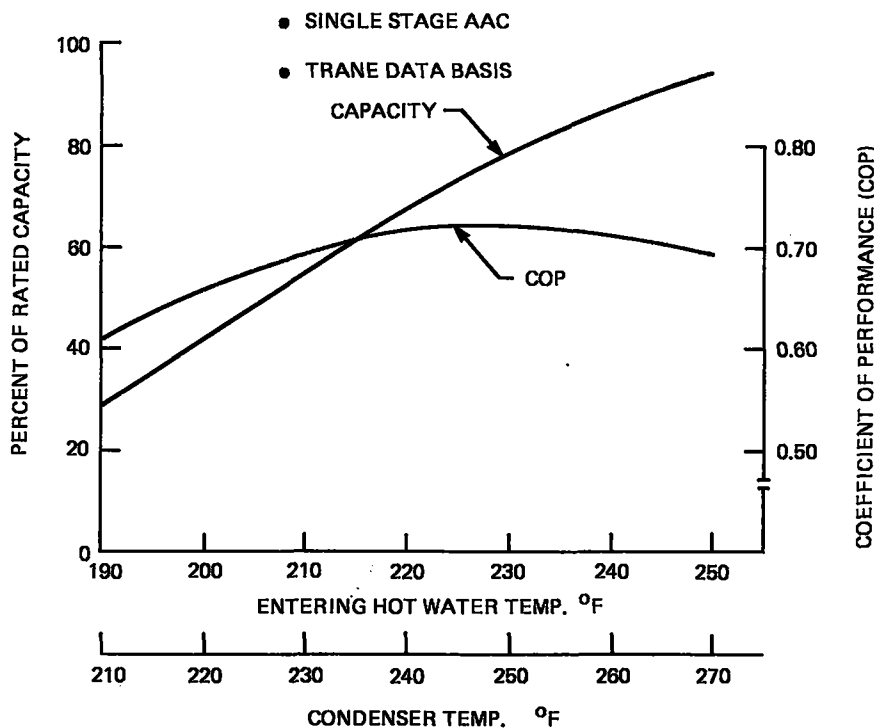


Figure 2.3-14. Absorption Air Conditioner Performance Variation with Entering Hot Water Temperature

temperature are shown on Figure 2.3-15. For 394°K (250°F) hot water temperature 405°K or (270°F condenser), a 6.1×10^5 Joules/second (175 ton) unit would be required. Lowering the hot water temperature to 361°K (190°F) would result in a 2.34×10^6 Joules/second (665 ton) unit to meet the 6.1×10^5 Joules/second (173 ton) load.

Table 2.3-4 shows the operating conditions, machine capacities, unit pump powers, heat inputs, and unit sizes required to supply a 6.1×10^5 Joules/second (174 ton) design load as the inlet temperature is reduced. In all cases, a 11°K (20°F) generator temperature drop is assumed to allow a constant low temperature TES volume. Reducing the temperature from the reference 383°K (230°F) to 372°K (210°F) requires about a 30 percent increase in parasitics. However, going below 372°K (210°F) results in significant increases in both system parasitics and size and does not appear to be practical or warranted in light of the fact that the COP also decreases as the temperature drops below 372°K (210°F).

Table 2.3-4. Absorption Air Conditioner Characteristics Desired (Max. Capacity = 173 Tons)

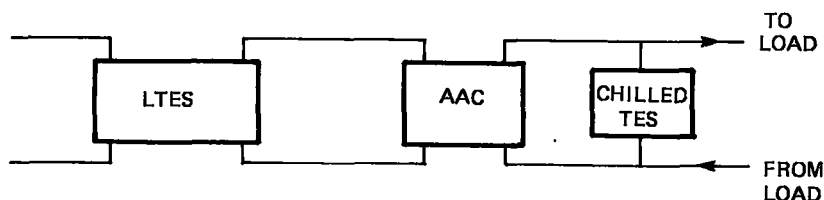
Hot Water to Generator (°F)				
Inlet	250	230	210	190
Outlet	230	210	190	170
Number of Generator Passes	2	3	4	5
Heat Source Correction Factor	.95	.79	.55	.29
Selected Machine Capacity (tons)	174	228	354	665
Avail. Cap. at Given Conds. (tons)	174	180	195	193
Heat Input to Generator				
-Btuh ton	17,400	17,000	16,400	17,200
-Total (10^6 Btu)	3.03	2.94	2.84	3.00
Unit Pump Power (kW _e)	5.1	5.8	7.5	10.2
Size	12-1/2'L x 5-1/2'W x 8'H	16'L x 5-1/2'W x 8'H	19'L x 6'W x 8'H	22'L x 7'W x 10'H
Hot Water Flow (gpm)	200	238	250	296
Condenser Water Flow (gpm)	500	600	900	1700
Evap. ΔP (ft. H ₂ O)	25	30	48	45

Figure 2.3-16 shows the effect of condenser temperature on the theoretical steam flow rate for an extraction turbine meeting the Bleyle process steam requirement designed for 200, 300, and 400 kW power levels. A common inlet condition of 655°K (720°F) and 4.8×10^6 N/m² (700 psig) was used in the calculations. Condenser temperature is seen to have a much more significant effect for the lower power level. However, even for the planned operating level of 300 kW, reducing the condenser temperature from 394°K (250°F) to 383°K (230°F) provides a 16 percent reduction in turbine input. Figure 2.3-17 shows the effect of reducing condenser temperature on annual system performance. Reducing the temperature from 394°K (250°F) to 383°K (230°F) results in about a 5 percent improvement in annual performance whereas further reducing the temperature to 372°K (210°F) provides only an additional 2-1/2 percent improvement in addition to resulting in significant absorption air conditioner size and operational penalties. Figure 2.3-18 expresses the sensitivity of condenser temperature in terms of collector area required to meet a fixed 60 percent saving associated with reduction to 383°K (230°F). At that point the curve changes slope, and it becomes significantly less cost effective to reduce the temperature further. Thus, for the preliminary design, a condenser temperature of 383°K (230°F) has been selected. This results in a requirement for a 1.25×10^5 Joules/second (354 ton) single stage absorption unit which operates in a nominal derated condition to supply the 6.1×10^5 Joules/second (173 ton) peak cooling load.

2.3.2.5 Thermal Utilization Subsystem Trade-Offs

The major trade-off within the Thermal Utilization Subsystem involved selection of the low temperature storage capacity. The water, sensible heat, low temperature storage subsystem has been included in the design to supply site thermal loads when the PCS is not operating to maintain relatively stable inlet conditions to the absorption air conditioner and to provide system experimental flexibility. The rationale used for sizing the low temperature TES (LTES) system is summarized in Figure 2.3-19. During weekends and third shift, when the PCS is not operating, the TES system must have sufficient capacity to provide cooling for the Bleyle plant and the STES mechanical building and to offset thermal losses. For design load conditions for third shift and weekend operation, this results in a TES capacity requirement of 6.1×10^9 Joules (5.8 MBtu) and 2.1×10^{10} Joules (20 MBtu), respectively. To assure capability to serve the weekend load, a 2.1×10^{10} Joule (20 MBtu) capacity was selected for the Preliminary Design. For the 11°K (20°F) temperature saving for the absorption air conditioner as discussed in the previous section, this results in a TES tank capacity of 454m³ (120,000 gallons).

An evaluation was made of the use of chilled storage to reduce the capacity of the absorption air conditioner (AAC) and the LTES capacity in the thermal utilization loop. A schematic of the system is shown below:



The design approach taken was to size the absorption air conditioner for the average cooling load occurring over a complete 24 hour period rather than to size for the peak load which occurs during the day. Thus, during daytime operation, the load is met by the AAC output supplemented by chilled water from the appropriately sized chilled TES. During night-time hours when the plant is not operating and the load is low, the AAC operates from an appropriately sized LTES to charge the chilled TES for use during the next day.

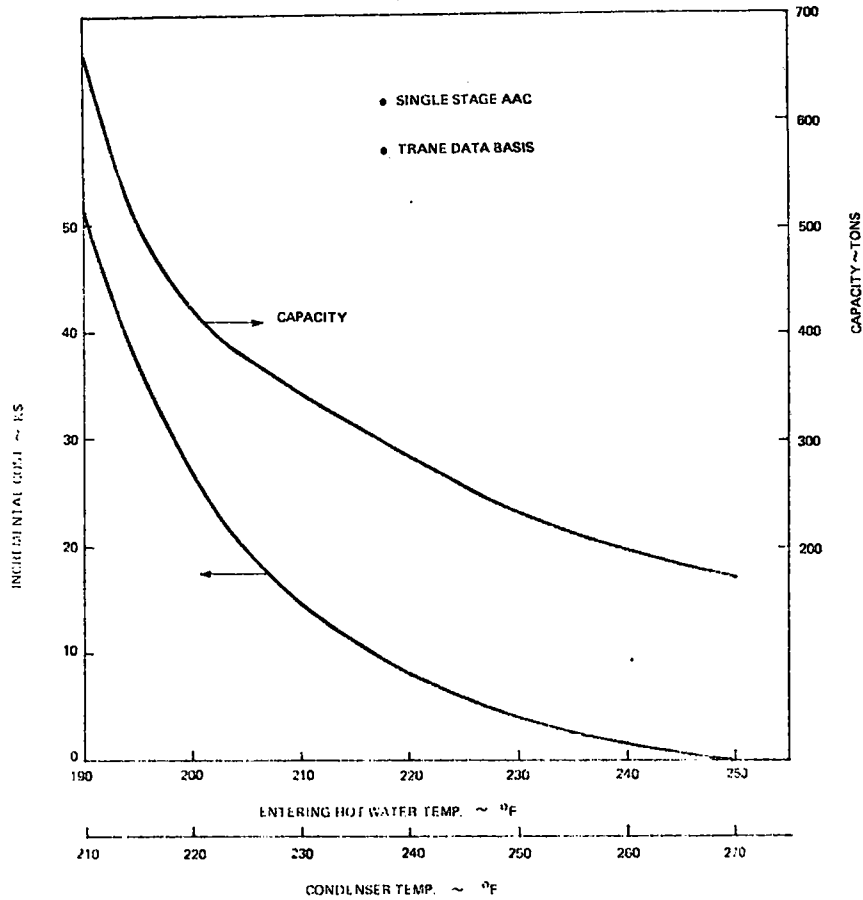


Figure 2.3-15. Absorption Air Conditioner Size and Cost Variation with Hot Water Temperature

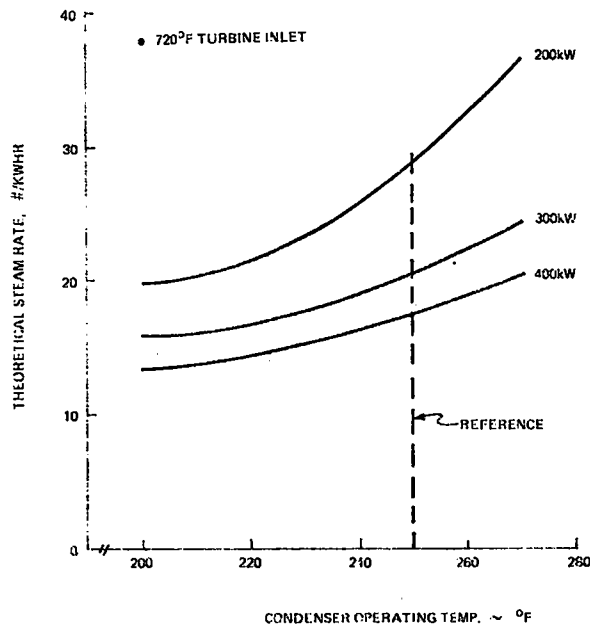


Figure 2.3-16. Effect of Condenser Temperature on Theoretical Steam Flow Rate

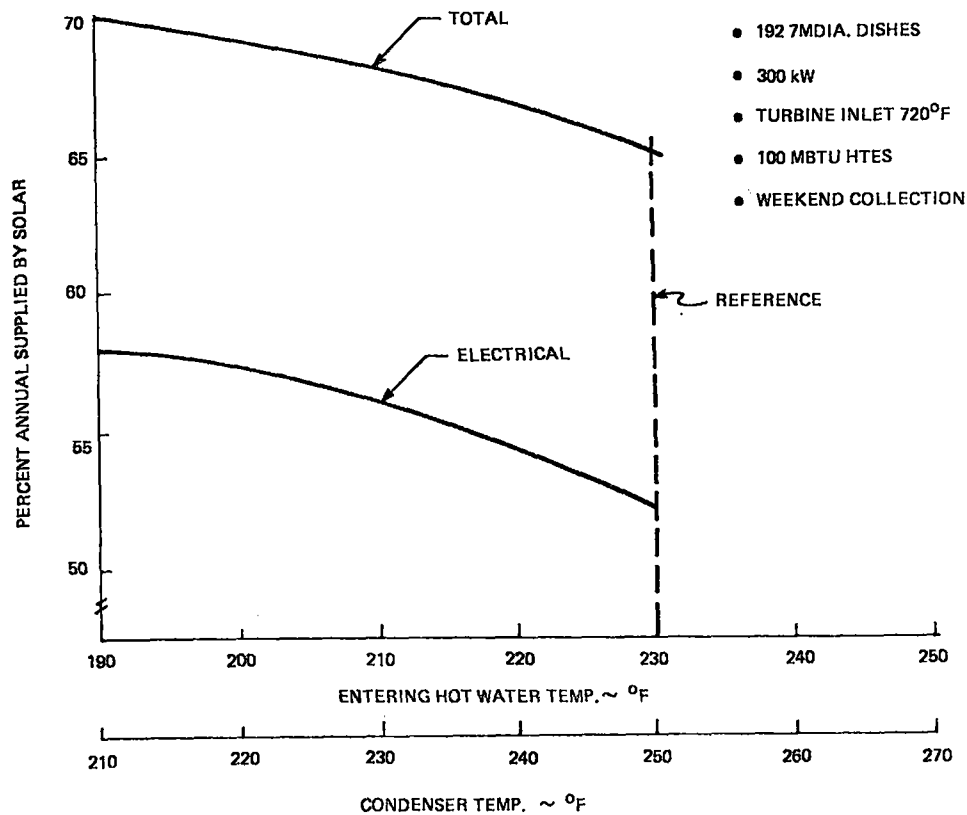


Figure 2.3-17. Variation in System Performance with Condenser Temperature

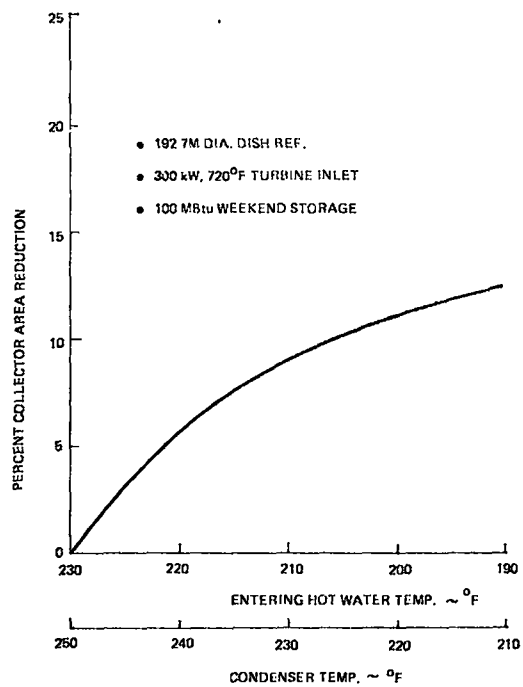


Figure 2.3-18. Effect of Condenser Temperature on Required Collector Area

REQUIRED TO SUPPLY THERMAL LOADS WHEN PCS NOT OPERATING:

- WEEKEND
- NIGHT
- EXPERIMENTAL

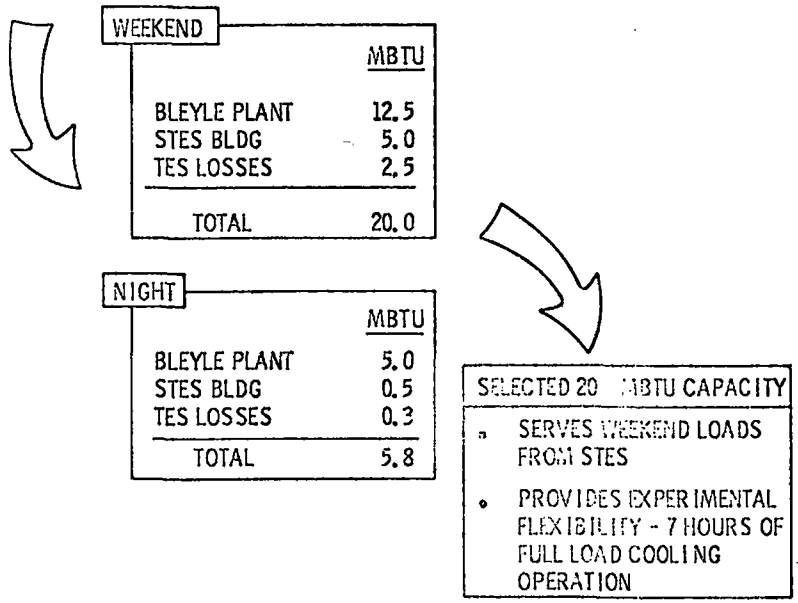


Figure 2.3-19. Low Temperature Thermal Storage Capacity Sizing Rationale

The following design cooling loads are to be served by the LSE:

Bleyle Plant	143 tons
Loading/Storage Area	20 tons
STES Mechanical Bldg.	10 tons
Total	173 tons

The constant internal portion of the load which will exist during plant operating hours will be about 4.75×10^5 Joules/second (135 tons). For sizing the chilled TES, an annual average of 5.3×10^5 Joules/second (150 tons) was assumed for the 16 hour work day which results in an average daily cooling load of 3.0×10^{10} Joules (28.8 MBtu). To distribute this 16 hour load over 24 hours with a chilled TES, the following average load is determined.

$$\text{LOAD} = \frac{28.8 \times 10^6 \text{ Btu}}{24 \text{ hrs}} \times \frac{1 \text{ ton}}{12,000 \text{ Btu}} = 120 \text{ tons or } 4.2 \times 10^5 \text{ Joules/second}$$

To define cooling capacities and LTES and chilled TES sizes to meet this load, the following assumptions were made:

- Trane data for AAC
- A water ΔT of 11°K (20°F) on the hot side of the AAC
- Chilled water ΔT of 8.3°K (15°F)
- A chilled storage tank capacity corresponding to seven hours of operation from midnight to 7:00 A. M.

The comparison of systems with and without chilled storage is shown in Table 2.3-5 with hot water inlet temperature to the AAC a variable parameter. The reduction in machine capacity is relatively constant on a percentage basis as a function of inlet water temperature. A significant factor is the large tank volume needed to store the 7-hour overnight output of the AAC for subsequent use the next day. The LTES capacity for the reference case (2.1×10^{10} Joules or 20 MBtu) without chilled storage is 454m^3 (120,000 gallons). The combined capacity of the LTES and the chilled TES tanks would increase to 636m^3 (168,000 gallons) for a thermocline chilled TES tank. In actual operation, the chilled TES system will more likely require two tanks: one chilled water supply storage tank, and one chilled water return storage tank. This would increase total TUS tankage capacity requirements to 939m^3 (248,000 gallons), or double that required without chilled storage.

At the bottom of Table 2.3-5, the tradeoff of AAC capital cost savings against LTES and chilled storage tank costs are shown for both two tank and thermocline systems. As indicated, there is a capital cost penalty associated with the application of chilled storage for all conditions investigated except 361°K (190°F) AAC entering hot water. However, reducing the hot water temperature to 361°K (190°F) would result in a 1.5×10^6 Joules/second, (420 ton) AAC unit which is impractically large for the 4.2×10^5 Joules/second (120 ton) load. Thus, on the basis of capital costs, site integration, and system complexity, a chilled water storage system was not incorporated into the preliminary design.

2.4 SYSTEM REQUIREMENTS SUMMARY

A summary of the system design requirements resulting from overall system analysis described in the previous subsections is shown in Figure 2.4-1. The requirements are site and system specific and have resulted from iterations with the subsystem designs during the preliminary design activity to assure that system cost and performance goals will be met. From these top level system requirements, more detailed requirements on a subsystem and component level have been developed and are discussed with each individual subsystem in the following report sections.

Table 2.3-5. Comparison of Conditions With and Without Chilled Storage

AAC Conditions	175 Ton Output				120 Ton Output with Chilled TES			
	250	230	210	190	250	230	210	190
Hot Water Temp ($^\circ\text{F}$)	250	230	210	190	250	230	210	190
Machine Cap (Tons)	200	228	354	665	129	152	228	420
Cost (K\$)	35	39	54	86.5	28	30	39	62
Cost Savings (K\$)	-	-	-	-	7	9	15	24.5
<u>Cold Side</u>								
Chilled Water $\Delta(T^\circ\text{F})$	← 15 →				← 15 →			
Storage Tank (10^3 Gal)	← 80 →				← 80 →			
Tank Costs (k\$)								
• Thermocline	← 36 →				← 36 →			
• 2 Tank	← 72 →				← 72 →			
<u>Hot Side</u>								
Storage Capacity (MBtu)	← 20 (REF) →				← 14.7 →			
Storage Tank Cost Savings (k\$)					← 15 →			
<u>Net Savings (AAC + Tanks) k\$</u>								
• Thermocline					-14	-12	-6	+3.5
• 2 Tank					-50	-48	-42	-32.5

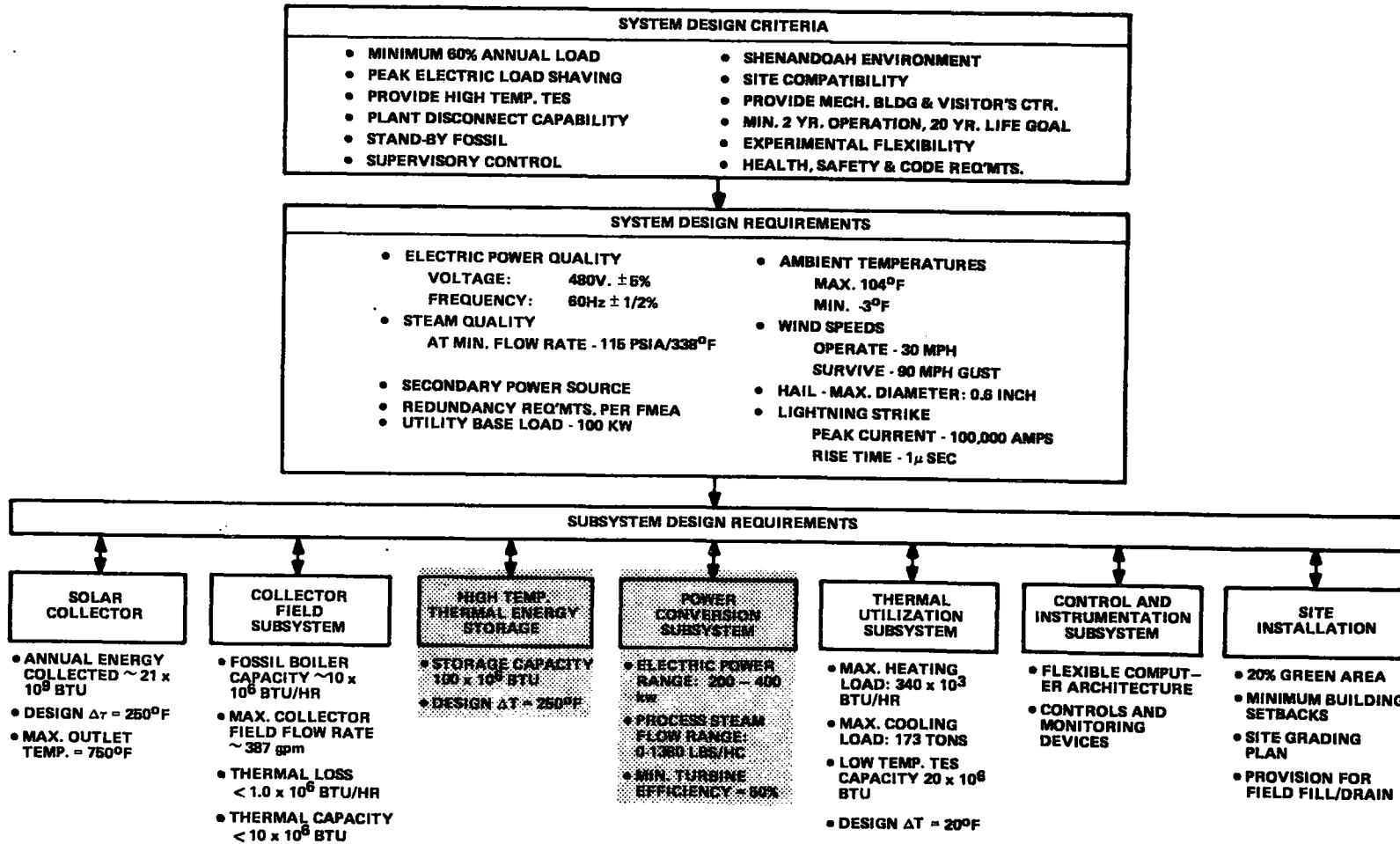


Figure 2.4-1. System Requirements Summary

SECTION 3
SYSTEM ANALYSIS AND DESIGN

SECTION 3
SYSTEM ANALYSIS AND DESIGN

3.1 SITE DEVELOPMENT

In conjunction and cooperation with Shenandoah Development, Incorporated, a site design for the solar experiment site and adjacent sites is being developed in parallel with the Solar Total Energy System design. During the conceptual design phase, a preliminary site plan was developed. This plan was reviewed with DOE, Sandia, and SDI early in the Preliminary Design Phase and modified to include not only the site of the STES but also land parcels to the south and east of the STES site. During the Preliminary Design, the following site design activities were completed:

1. Enlarged the total STES site from 20,016m² (4.946 acres) to 23,149m² (5.72 acres) to meet SDI green space requirements.
2. Performed total site topographical survey from Amlajack Blvd. to northern site line.
3. Performed total boundary survey of the STES site.
4. Developed a grading plan and construction specification package for the total site grading to be initiated during Phase IV.
5. Developed Preliminary Design update of the STES Mechanical Building and Visitors Center.

The plot plan (Figure 2.1-2) shows the 23,149m² (5.72 acre) plot located northeast of the knitwear factory site in the Shenandoah industrial development. It defines the boundaries for the Large Scale Experiment-Solar Total Energy system. During Phase III of the program, the land designated as Plat I was transferred from Shenandoah to HUD. The site will be regraded to allow for a continuous two degree slope to the northeast corner of the property. In the northeast corner a drainage system will be installed for collection and discharge of rain water into a drainage runoff area located at the property corner. Site soil samples have been obtained in the collector field and mechanical building areas so that detailed designs can be completed for collector supports, building foundations, and equipment supports.

An access road on the south side of the property, shown as Plats II and III in Figure 2.1-2 will be installed and built to Coweta County specifications. This access road will allow access to Amlajack Boulevard, the main road in the industrial park. This road will be used as the access during the construction phase for personnel and construction equipment. During Phase IV the road will not have its finished top coat of asphalt applied. The road will be constructed to meet the technical specifications of Shenandoah Development, Incorporated. The collector field will be secured by a fence during the construction phase. This fence will be left in place at the completion of construction. The fence will be constructed and located to prevent any person from entering into the sun hazard area inadvertently.

Figure 3.1-1 shows the site grading plan for the entire site. Grading will begin at Amlajack Blvd. where the cut to the south of Plat I will be used to fill the northern portion of the site to provide the continuous two degree slope. Grading the entire site to approximately the same elevation has the advantage of allowing more flexibility in the type and height of building or structure which can be placed to the south of the collector field while still meeting shadowing restrictions. Figure 3.1-2 shows site design details. As noted, the design requires a sediment control dike along the northern boundary as a transition between the raised field level and the lower adjacent property. The overall grading and drainage plan for the site is shown in Figure 3.1-3. The collector field will be completely covered by bituminous paving. To avoid filling the utility trench with runoff water, a slot drain is included to direct field runoff to the drainage system in the northeast corner of the field.

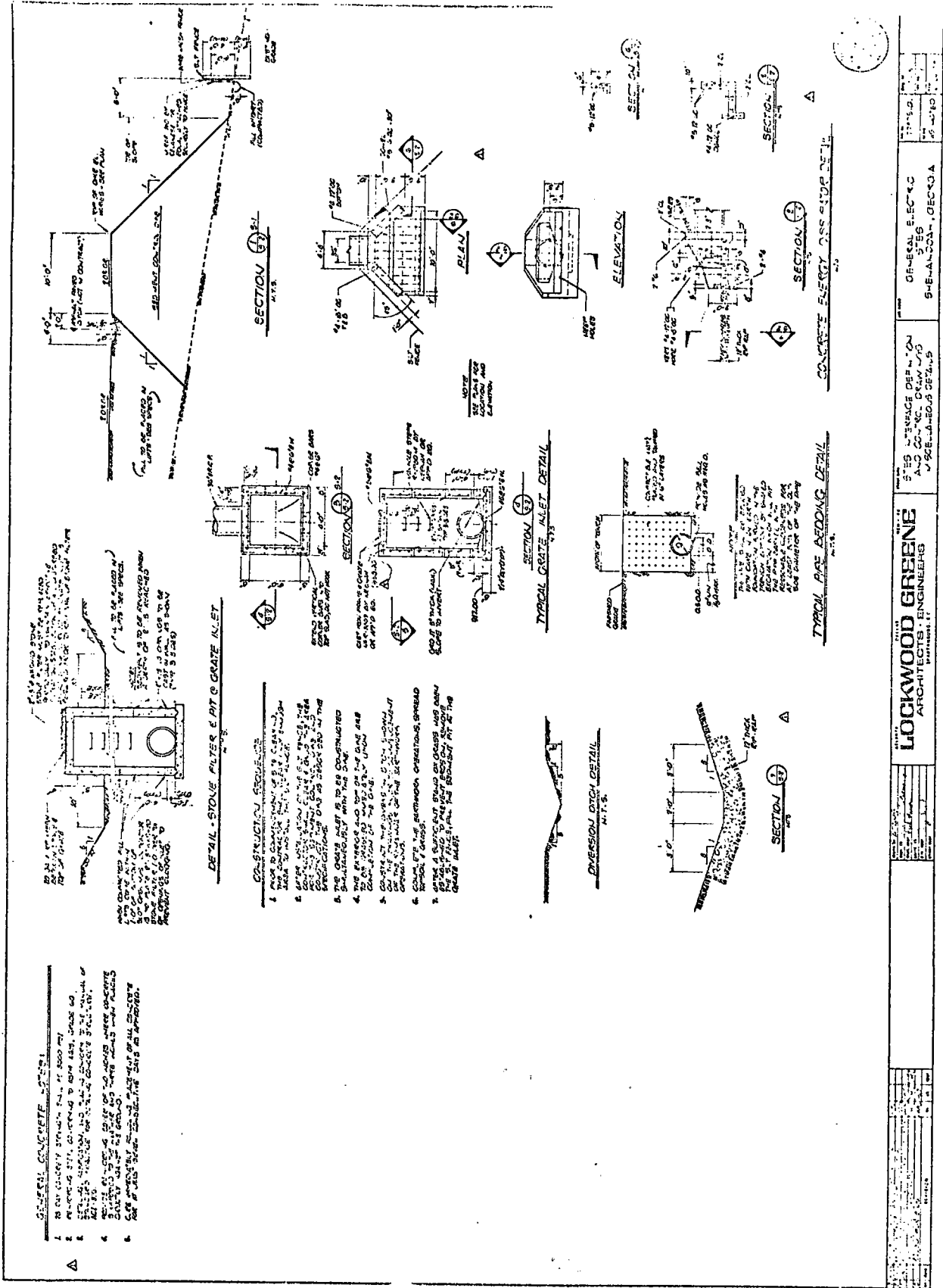


Figure 3.1-2. Site Interface and Control Drawing, Miscellaneous Details

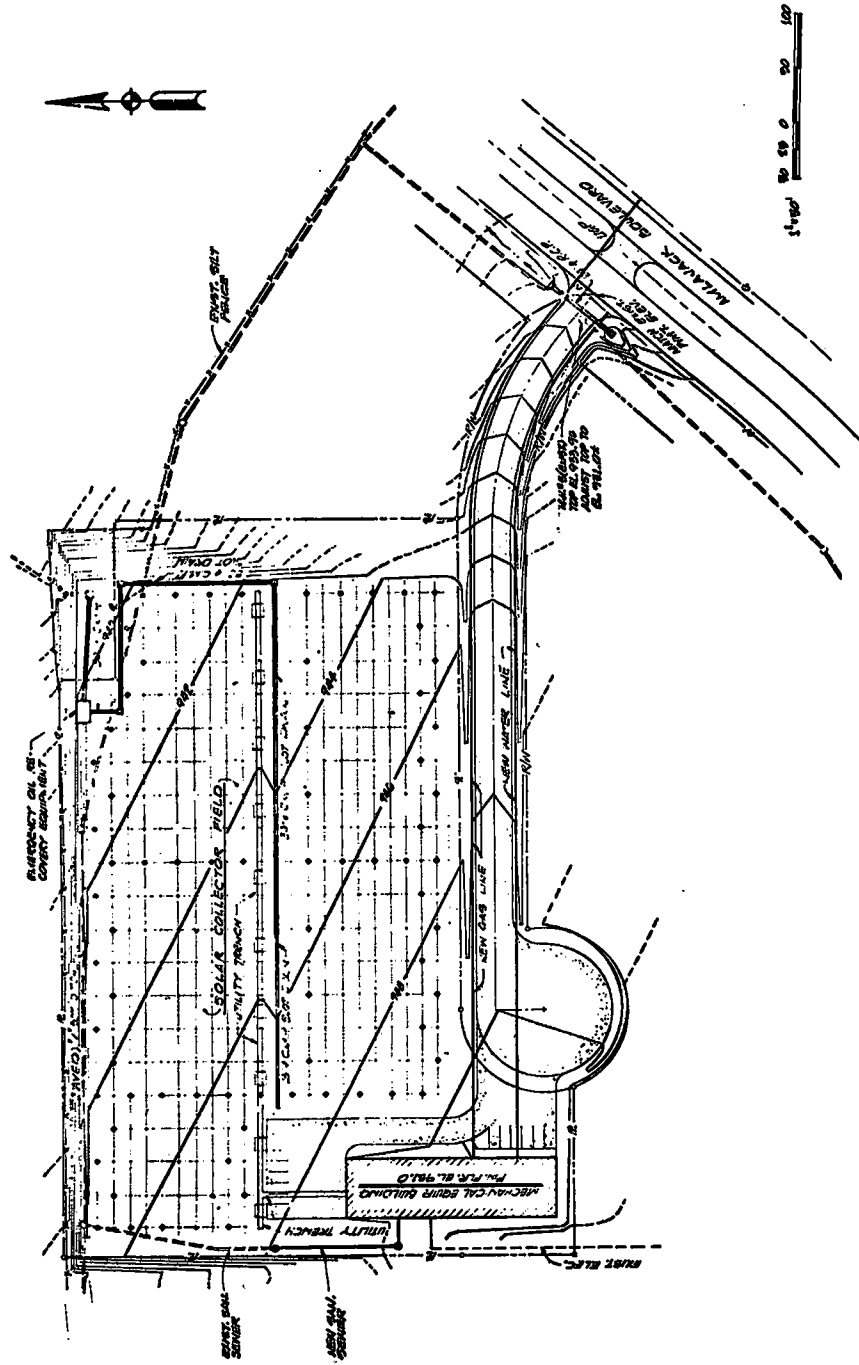


Figure 3.1-3. Site Interface and Control Drawing, Grading and Drainage Plan

The STES mechanical building and visitors center and equipment area will be located in the southwest corner of the STE-LSE property as shown in Figure 3.1-3. The location selection was based on a study of alternative locations performed during the Conceptual Design which considered Bleyle plant and STES building shadowing, utility and services interfaces, cooling tower drift, drainage, road and parking availability, and impacts on existing features. The preliminary layout of the STES Mechanical Building and visitors center and mechanical equipment area is shown in Figure 3.1-4. The building area will contain the control room, office and visitors area, maintenance area, storage area, motor control center, absorption air conditioning unit, and turbine. Located north of the building will be the Syltherm 800 equipment, the three large storage tanks, and one small storage tank, the Syltherm 800 fossil fuel heater, and the collector array and boiler pumps. The hardware will be installed on a concrete pad with provisions for containing spills of Syltherm 800. Also contained in this area will be the solar steam generator and its ancillary equipment. All of this equipment will be insulated and sealed for outdoor application.

Equipment located on the south side of the building will include the low temperature storage tank, air conditioner cooling tower, condenser cooling tower, condensate storage tank, and ancillary equipment. The low temperature storage tank will contain an expansion tank and will be insulated for outdoor application.

The meteorology station will remain in its present location during the site preparation work and later will be installed on the roof of the Mechanical Building. The Mechanical Building will be designed to allow for visitor access to the building to observe the operation in the control room and visual access to the mechanical equipment. Parking will be provided at the end of the access road for visitors and plant operational personnel.

3.2 SOLAR COLLECTOR

3.2.1 DESIGN GOALS AND APPROACH

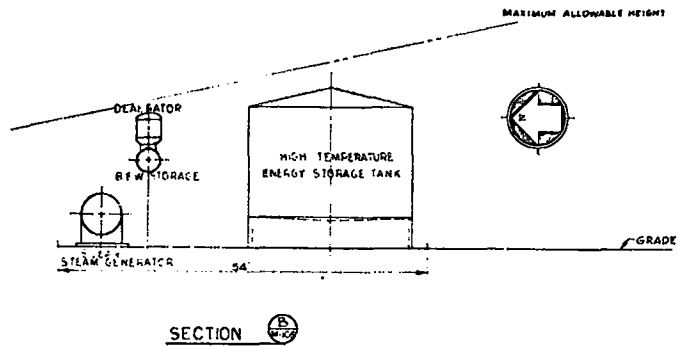
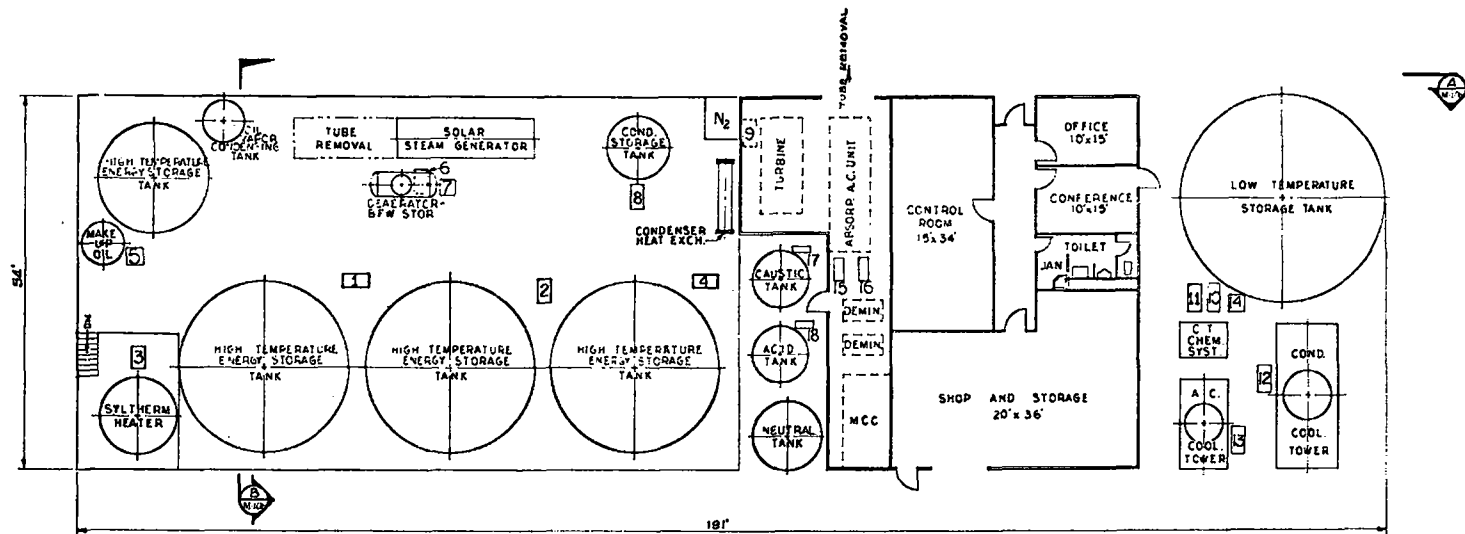
The collector is the most cost and performance critical component of the LSE Shenandoah system. It also represents the greatest technical challenge of the LSE Shenandoah program; to meet its performance and reliability requirements with acceptable costs, the technology developed for the collector must be a blend of commercially available materials and fabrication processes cast into a high performance configuration.

To accomplish these goals, the process summarized in Figure 3.2-1 was followed to develop the preliminary design. Starting with the basic paraboloidal dish collector concept, overall collector configuration options and component concepts were screened to determine those options which were:

1. Inherently low in fabrication costs.
2. Capable of meeting performance requirements.
3. Feasible to develop, construct, and install within the LSE Shenandoah schedule.

These three guidelines were followed throughout the preliminary design but were especially emphasized at the outset. The approach taken was to pursue only those configurations and component concepts that either were already being produced in similar forms for other applications or were composed of standard production elements. Such options were then compared on their cost and performance differences and on their technical, cost, and schedule risks.

As an iterative part of the screening process, a reference collector configuration was established. The reference collector embodied the selected component concepts and overall configuration of the LSE collector. Tradeoff studies and optimization analyses then established specific design requirements, component approaches, and sizing leading to a baseline design.



PLAN

PUMPS

- 1 COLL. FIELD OIL CIRCULATION PUMPS- 100% & 50%
- 2 HIGH TEMP. OIL CIRCULATION PUMP
- 3 SYL THERM HEATER OIL CIRCULATION PUMP
- 4 ENERGY STORAGE CIRCULATION PUMP
- 5 OIL FILL PUMP
- 6 BFW PUMP
- 7 BFW CHEM. INJ. PUMP
- 8 CONDENSATE STORAGE PUMP
- 9 CONDENSATE PUMP
- 10 HOT WATER PUMP
- 11 LOW TEMP. STORAGE PUMP
- 12 CONDENSER COOLING TOWER PUMP
- 13 ABSORPTION AIR COND. LOADING TWR PUMP
- 14 HOT WATER SYST. CHEM. INJ. PUMP
- 15 CHILLED WATER PUMP
- 16 HEATING WATER PUMP
- 17 CAUSTIC PUMP
- 18 ACID PUMP
- 19
- 20

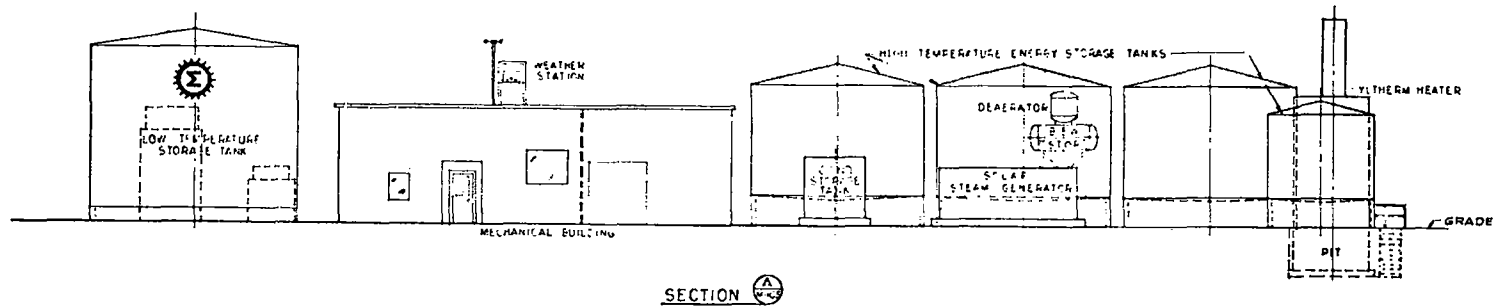


Figure 3.1-4. Mechanical Equipment Area and Visitors Center

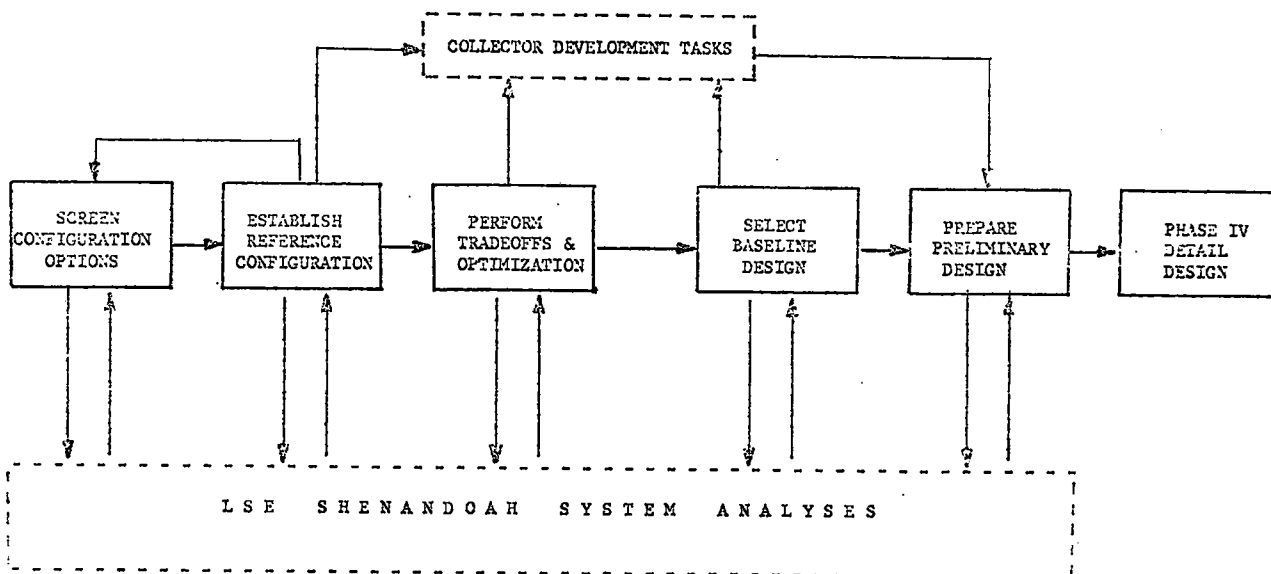


Figure 3.2-1. Collector Preliminary Design Process

The preparation of the preliminary design layouts and supporting analyses started with the baseline design and evolved a specific configuration. Since the collector has several long lead time components, the preliminary design of some of the collector components progressed directly into detailed designs. As a result, the component descriptions given in subsequent sections often provide detailed design data.

Throughout the preliminary design phase, system analyses provided system level cost and performance trade-off data upon which collector design decisions were based. In addition, concurrent collector development tasks addressed critical technology issues related to the collector design. An Engineering Prototype Collector (EPC) was designed, fabricated, and tested to verify component concept selections and to validate design tools used to prepare the LSE Shenandoah collector design. Testing of the EPC was still underway at the end of the preliminary design phase and will continue into the definitive design phase. A reflector surface materials development task was also carried out in support of the preliminary design. This task established the critical reflector substrate, reflectance enhancement, and protective coating to support the design effort. Both the EPC and reflector surface development tasks are detailed in Section 8.1.

3.2.2 COLLECTOR AND COMPONENT DESIGN REQUIREMENTS

The LSE collector requirements are summarized in Table 3.2-1. These requirements were derived through an iterative process with the overall system requirements and collector field requirements providing the primary inputs. With the minimum system requirements to be met having been established, individual collector component requirements were developed by trading off candidate component capabilities. This was accomplished by using the reference design configuration and apportioning the total system errors to achieve the collector efficiency required by the Shenandoah system.

Table 3.2-1. Shenandoah Collector Design Requirements

Type:	Concentrating, Two-Axis Tracking, Parabolic Dish		
Coolant Fluid:	Syltherm 800		
Output:	1.09 x 10 ⁸ Btu/Yr		
Operating Conditions:	● Ambient Temperature Range	:	17°F - 95°F
	Fluid ΔT	:	250°F
	● Max. Working Fluid Bulk Temperature	:	750°F
	● Wind Loads	:	30 mph
	● Tracking Range: Polar Axis	:	180-210°
		Declination Axis	:
	● Insolation Levels	:	Design - 200 Btu/ft ² -hr
			Min. - 50-75 Btu/ft ² -hr
Non-Operating Survival Conditions:	● Ambient Temperature Range	:	-3°F to 104°F
	● Wind Loads	:	90 mph
	● Hail Impact	:	0.6 inch diameter
	● Lightning strike	:	100 kA peak current
Maintenance, Routine:	● Reflective Surface Washable	}	Design Provisions
	● Receiver Cleanable without removal		
	● Control Calibration		
Maintenance, Unscheduled:	● Disk petals replaceable	}	Design provisions
	● Receiver replaceable		
	● Receiver/dish alignment		
	● Controls removable		
Hazard Shutdown:	● Defocus time	:	2°/sec minimum
	● Over temperature	:	Automatic
	● Loss of fluid flow	:	Automatic
	● Power loss	:	Stand-by-power
	● Environmental	:	Manual override

To establish the major collector component design requirements, collector optical and receiver thermal models were derived and incorporated into a collector system analysis model. This model described the collector performance in terms of the following key variables:

1. Concentration Ratio. The ratio of receiver aperture area to dish aperture area.
2. Dish Surface Reflectivity. The total hemispherical reflectance and the specular distribution.
3. Slope Error. The statistical deviation of the surface from a true paraboloid.
4. Tracking Error. The displacement of the receiver relative to the flux profile at the image plane.
5. f/D . The focal length to diameter ratio of the dish.

For the requirements analysis, simplifying assumptions were made. The source (sun), slope and specular error distributions were assumed to be normally distributed, the tracking error was treated as a bias error rather than a random error, and the convection losses were calculated based on a constant wind speed of 10 mph and an orientation midway between the horizon and noon time positions at an average declination. With this model being used, nominal design point and off-design point performance was calculated. Figure 3.2-2 presents the nominal values of the key trade-off parameters, the design point performance predictions, and the off-design performance characteristics. The values selected as nominal for the key design variables were the result of a sensitivity analysis conducted on these parameters. The final values for these parameters varied from their nominal values due to refinements in the preliminary design effort that followed the optimization analysis.

The first variable selected was the f/D ratio. This variable is descriptive of the dish configuration. For each f/D , an optimum concentration ratio was calculated balancing greater acceptance ratios versus larger receiver heat losses. Figure 3.2-3 presents the results of the analysis. Based on this analysis, an optimum f/D ratio was chosen at $f/D = 0.5$.

Major parameters to be specified are those associated with the reflective surface: the total reflectance and the specularity. By calculating the collector performance at the nominal value and then varying only the parameter of interest, a measure of the performance sensitivity was established. Figure 3.2-4 presents the results of this analysis for the reflector parameters. In this figure, the performance as well as the parameter has been normalized. As would be expected, the collector performance is very sensitive to total reflectance. A total reflectance of 88 percent is required to achieve the overall collector efficiency goal of 67 percent. However, the sensitivity of the performance to reflector specularity is weak below about 8 mrad. This is largely due to the moderate concentration ratios (for a parabolic dish) that are being specified. This established the specular reflectance level at 8 mrad RMS.

A major parameter which influences the construction technique and manufacturing tolerances is the surface slope error. Figure 3.2-5 presents the performance sensitivity to RMS slope error. As can be seen, although this is a very important parameter, below one-half degree slope error, collector performance is less sensitive. Based on this analysis, a slope error of one-half degree rms was specified.

The parameter which determines the size of the receiver is the concentration ratio. With the performance and concentration ratio normalized, the sensitivity of this parameter is plotted in Figure 3.2-6. As shown, concentration ratios in the 200-275 range are acceptable with 250 selected as optimum for design purposes.

The final major design parameter specified through the use of the model was the tracking bias error. This bias is relative to the position of the receiver over the flux distribution at the focal plane. The bias error is caused by alignment tolerances, tracking sensor accuracies, and position indicator accuracies. Figure 3.2-7 presents the results of tracking bias error sensitivity calculations. As bias error is introduced, the energy that is not intercepted by the receiver does not become significant until about one-quarter degree bias. Based on these results, the tracking bias error was set at one-quarter degree maximum.

COLLECTOR PARAMETERS

PARAMETER	NOMINAL VALUE
D_{DISH}	7 METERS
CR	250
F/D	0.50
REFL	88%
σ_{SPEC}	8 MRADS
σ_{SLOPE}	8.7 MRADS ($1/2^\circ$)
σ_{TRACK}	4.4 MRADS ($1/4^\circ$)
INSOLATION	200 BTU/HR-FT ²
T_{IN}	500°F
T_{OUT}	750°F
$T_{AMBIENT}$	50°F

NOMINAL DESIGN POINT PERFORMANCE

% CAPTURED BY RECEIVER	= 96%
$Q_{RADIATION LOSS}$	= 7410 BTUH
$Q_{CONVECTION LOSS}$	= 3890 BTUH
$Q_{CONDUCTION LOSS}$	= 930 BTUH
$Q_{INTO FLUID}$	= 55,500 BTUH
COLLECTOR EFFICIENCY	= 67%

OFF-DESIGN PERFORMANCE

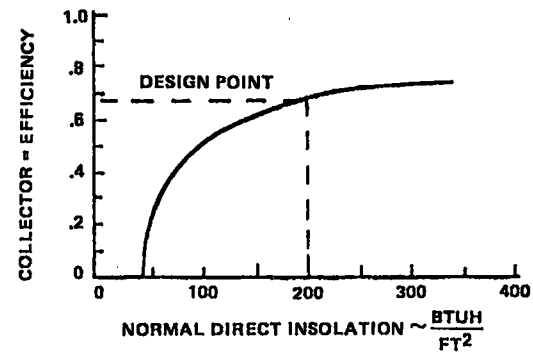
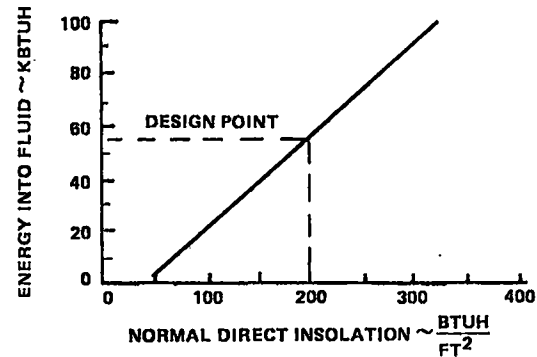


Figure 3.2-2. Nominal Collector Performance and Design Parameters

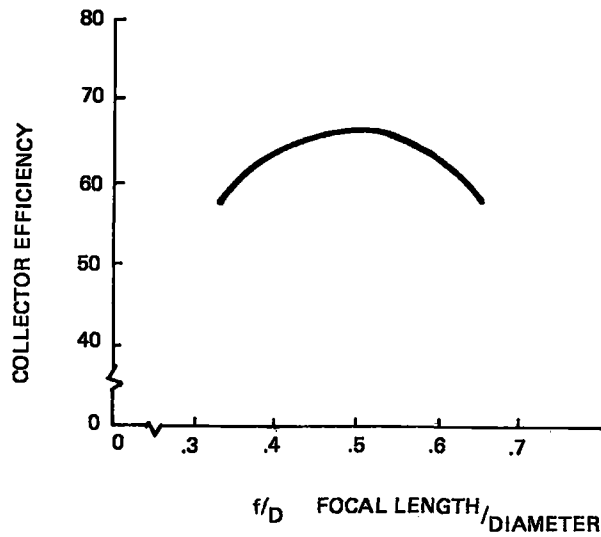


Figure 3.2-3. Focal Length Optimization

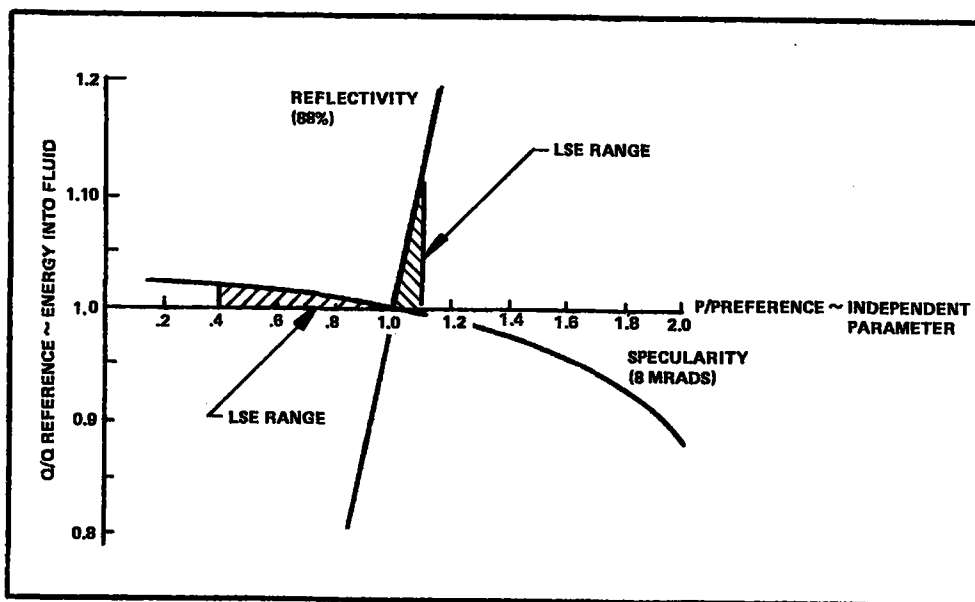


Figure 3.2-4. Reflector Surface Parameter Sensitivity Analysis

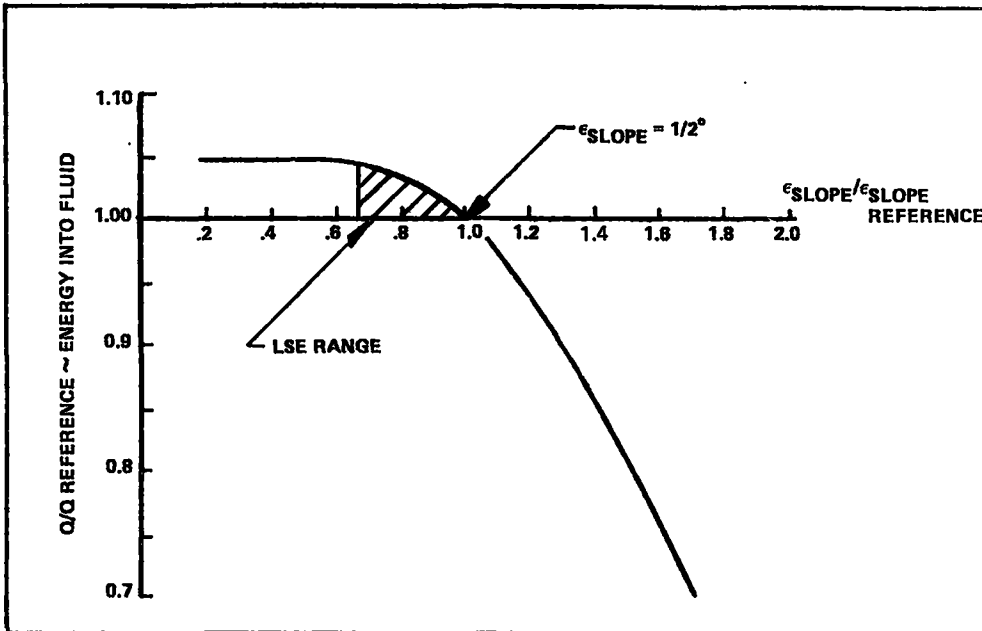


Figure 3.2-5. Slope Error Sensitivity Analysis

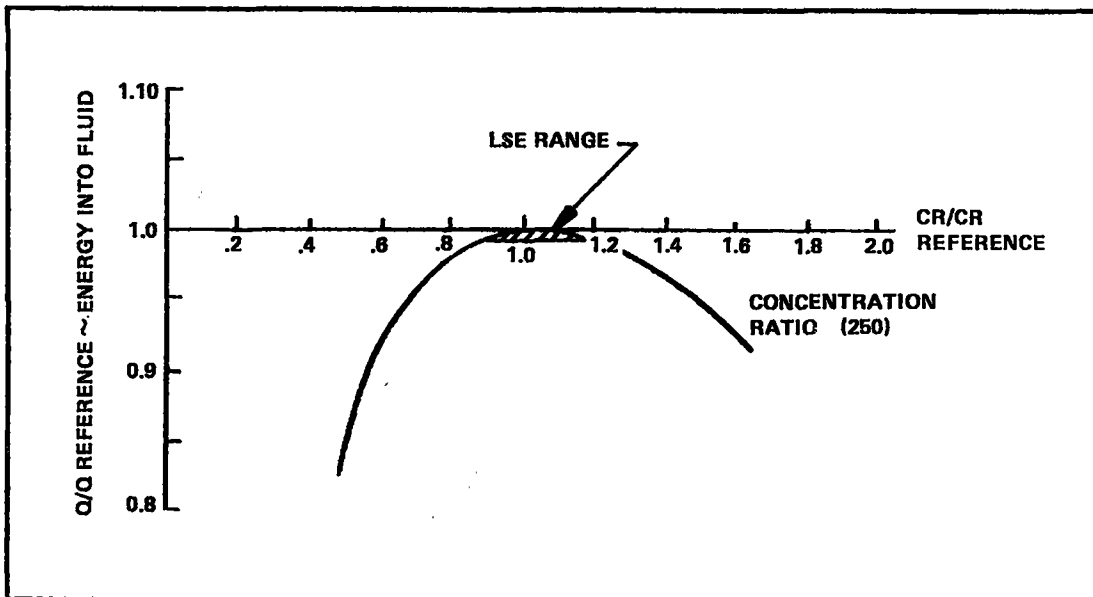


Figure 3.2-6. Concentration Ratio Sensitivity Analysis

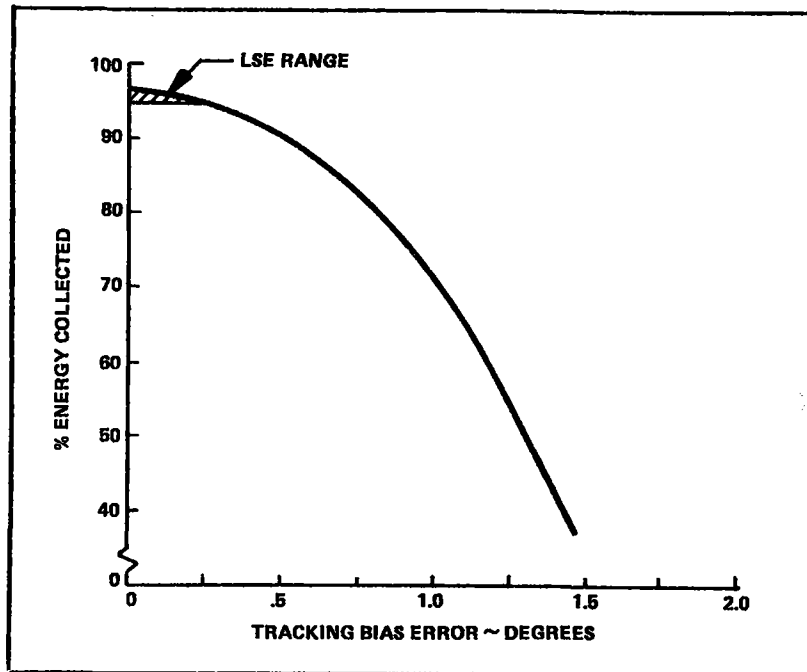


Figure 3.2-7. Tracking Bias Error Sensitivity Analysis

3.2.3 COLLECTOR CONCEPT SELECTION

Selection of the basic LSE collector concept established the reference design used to develop component requirements and to optimize the collector configuration. Hence, this was an important step in the preliminary design phase and one that also affected the fabrication and testing of the EPC.

3.2.3.1 Reflector

The advantages offered by the paraboloidal dish type of collector had been evaluated in the conceptual design phase of the LSE Shenandoah program, and this type of collector had been selected for the Shenandoah application. The reflector itself can be fabricated in a number of ways using techniques currently employed in the large antenna industry. Varying degrees of surface accuracy (slope accuracy and surface finish) can be obtained with a rough correlation of surface accuracy to cost.

Based on system requirements for a 672°K (750°F) coolant temperature and on receiver concept evaluations, a slope error requirement of one-half degree rms permitted consideration of almost all currently employed fabrication techniques. However, the materials options for fabrication were quickly reduced to aluminum or steel.

The weight and cost advantages offered by plastics and composites could not be realized within the LSE Shenandoah time frame due to the development status of these types of reflector structures. In addition, complex types of high accuracy reflectors, such as those used for radio telescopes, are not required due to the relatively low slope accuracy requirement. Costs for these types of reflectors are very high; the surface panels alone are projected to cost about $\$15/\text{ft}^2$ in volume production.

Thus, the fabrication options for the reflector were narrowed to conventional sheet forming techniques using aluminum alloy, common structural steel, or stainless steel. Selection of aluminum as the reflector material was based on both structural and fabrication characteristics and on results obtained in the reflector surface development effort being conducted in parallel with the collector design activity (see Paragraph 8.1.2). These evaluations indicated that:

1. Although stainless steel offers an excellent specular surface for the reflector, the weight and cost of the stainless steel reflector substrate and the cost of depositing a reflectance enhancing layer of aluminum or silver on the reflector surface cannot be justified from a system cost viewpoint.
2. The higher weight of a structural steel reflector would offset the lower cost potential of steel so that the net cost saving for the reflector substrate would only amount to approximately fifteen percent. However, the added cost of applying a reflective coating to the steel substrate would eliminate any cost savings realized for the substrate itself.

Several fabrication techniques for forming the reflector were compared for performance (slope error) and cost. (Since all of the fabrication options would utilize comparable aluminum alloys, no reflectance differences from one type of fabrication process to another was anticipated.) Table 3.2-2 summarizes the evaluation of four common sheet forming techniques used by the antenna industry.

Table 3.2-2. Large Diameter Reflector Dish Construction Options

Petal Options	Typical Accuracy	Cost	Experience
Hand Built to Jig	0.5° rms	Highest	Excellent
Stretch forming	0.1° rms	Average	Limited
Die stamping	1° rms	Low	Excellent
Spinning	2° rms	Low	Excellent
<u>Support Structure</u>			
Rear	Good	Higher	Excellent
Front	Good	Lower	None

Both the hand built (piece construction) and spinning techniques were eliminated from further consideration for the LSE application. The high cost of hand built reflectors ruled out this approach, and the poor accuracy achievable with spinning for large reflectors (5-10 m) was unacceptable. (For small reflectors, however, or as a center annulus in a large reflector, spun dishes offer acceptable accuracies at low cost.)

The choice between stretch forming and die stamping required a more detailed evaluation (given in Paragraph 3.2.6). Both techniques offer low costs, although die stamping reflector sections in large quantities becomes very inexpensive, amounting to only 10 to 20 cents per square foot over basic material costs. In addition, laser ray trace tests conducted by Sandia Laboratories indicated that current die-stamped 5-meter reflector petals have slope errors of 0.6-0.7 degrees rms approaching the one-half degree requirement.

Conventional rear mounted support members for the reflector were also selected in this evaluation. As indicated in Table 3.2-2, reflector petal support members mounted on the reflecting side of the petals could offer some cost advantages. Unlike conventional antennas, support struts on the reflecting side of the reflector would be technically acceptable, but lack of experience with this type of support structure would increase technical and schedule risks which did not appear to be worth the slight cost savings.

Thus, the LSE reflector concept selected and used in the reference design consisted of either die-stamped or stretch-formed aluminum petals supported by conventional struts or ribs on the reverse side of the reflecting surface. For the reflecting surface itself, parallel effort in the reflector surface development task (Paragraph 8.1.2) identified several compatible reflectance enhancement and protective coatings that could meet the LSE requirements.

3.2.3.2 Mount and Drive

Since a functional requirement of a dish type collector is two-axis tracking, the structural support of the reflector assembly and the mechanism for providing tracking become basic configuration choices. Three primary configurations for the structure and actuation techniques were evaluated. The first is an adaptation of a sophisticated pedestal type tracking antenna with high slew rates and pointing accuracy. Another approach is a modified synchronous satellite antenna where standard, low cost structural members are used. This type of approach requires the addition of a drive mechanism to track the sun. A third approach is to suspend the reflector in a cradle structure and drive the reflector through gearing on the suspension shafting. The three types are sketched in Figure 3.2-8.

Since the LSE collector tracking rate and azimuth and elevation tracking limits are much lower than for a conventional tracking antenna, the high cost of a pedestal type mount and associated gearing drives was found to have poor cost effectiveness for the Shenandoah application. The cradle support configuration, while offering low tracking drive power requirements and simple geometry, presented a substantial design challenge to overcome high support member bending moments and potential reflector/support member interference problems. In addition, the cradle configuration did not offer any cost advantages (except potentially in drive actuators or gearing) over the modified synchronous satellite antenna configuration. This evaluation led to the selection of the structural member type of mount.

For the tracking drive approach, conventional linear actuators and gear drives were examined for the selected mount configuration. Either electric or hydraulic drives appeared suitable; the final choice of power source was made in a subsequent tradeoff study. The use of linear actuators offered lower costs than a gear type drive since standard screwjack actuators are commercially available in a variety of ratings and extensions.

The principal drawback to linear drives is the complexity of the actuator assembly if it must provide azimuth travel ranges over 180 degrees. Use of a polar axis mount configuration reduced this requirement slightly (232 degrees for a polar axis mount versus 240 degrees for an azimuth mount) but still required a 40-degree travel in excess of the 180-190 degrees achievable with a simple two-actuator drive assembly. However, an analysis of the performance penalty associated with a 180-degree polar axis limit showed that the annual energy loss to the system would be approximately 0.85 percent, well worth the cost savings to the collector for the simpler drive assembly.

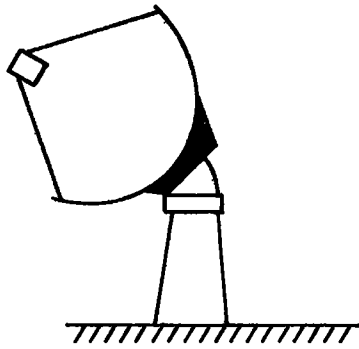
Results of the evaluations, therefore, led to the selection of the modified synchronous satellite antenna type mount utilizing linear actuators to drive the reflector through equatorial tracking axes. This concept was then incorporated into the collector reference design.

3.2.3.3 Receiver

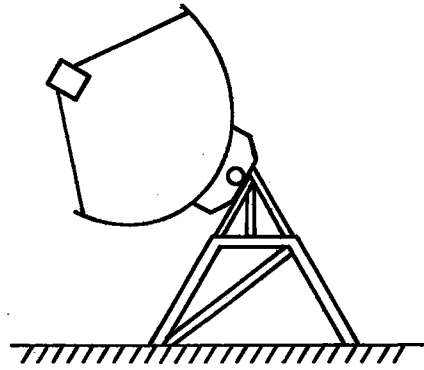
Selection of the receiver concept for the LSE collector received special emphasis for several reasons:

1. Receiver performance and cost are important factors in determining the cost/effectiveness of the LSE collector.

CONVENTIONAL
TRACKING ANTENNA
PEDESTAL MOUNT



MODIFIED LOW
COST SYNCHRONOUS
SATELLITE ANTENNA
MOUNT



CRADLE MOUNT
(POLAR AXIS)

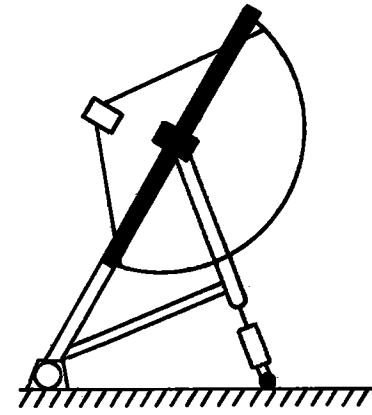


Figure 3.2-8. Candidate Mount Configurations

2. Unlike the reflector and mount/drive components, no existing industry (like the antenna industry) provided a number of well-developed technologies to draw on.
3. The Engineering Prototype Collector task required establishing the receiver concept in time to design, fabricate, and install the receiver to meet the EPC test schedule.

Many receiver configurations were analyzed and designed for a wide variety of point focus collector configurations. Figure 3.2-9 shows four receiver configurations initially examined for their potential to meet LSE performance and cost requirements. Preliminary analyses concluded that the simple flat plate and simple cavity type receivers offered the highest performance to-cost values for LSE Shenandoah.

The flat plate, direct impingement type receiver intercepts and absorbs the energy directly at the focal plane of the collector and then transfers the energy into the cooling fluid. Since the heated surface is directly exposed to the environment, radiation and convection heat losses can be high. Also, the performance is dependent on a good absorptive coating on the impingement surface. Major advantages of the flat plate receiver are its simplicity, small size, and light weight, all of which contribute to low cost.

The cavity receiver intercepts the concentrated energy at the focal plane and then absorbs and transfers the energy in a plane perpendicular to the focal plane. The radiative losses from the absorbing surface have a view factor to other regions of the cavity, and thus radiative losses are lower than in the direct impingement type. Also, convection losses are generally lower in an enclosed cavity receiver. The disadvantages of the cavity type is its size and cost.

In order to select the LSE receiver concept, a detailed analysis was conducted on both the flat plate and cavity configurations. One of the major requirements for an analysis of the receiver/collector subsystem is the generation of flux intensity profiles at the focal plane of the dish. These profiles were generated for varying focal length-to-diameter (f/D) ratios and different slope errors. A representative total error was chosen for this screening analysis of one degree rms. This error consists of manufacturing tolerances, surface specularly, deflection errors due to wind loading, weight distribution, drive forces, and control system inaccuracies. In general, lower errors yield higher concentration ratios, smaller receivers (and losses), and greater difficulties in protecting the fluid from increasingly higher flux levels. The one degree error assumption was found to be consistent with reasonable receiver sizes and performance and with the low cost stamped petal dish construction technique.

Figure 3.2-10 shows flux intensity profiles depicted for a slope error of one degree and f/D (focal length to diameter) ratios of 0.4 - 0.7. Plotted are the non-dimensional flux intensities, i/q (i. e., flux intensity divided by solar intensity), versus the ratio of r/D (i. e., aperture radius divided by dish diameter). Figure 3.2-11 presents integrations of these curves and shows the percentage of the energy intercepted as a function of geometric concentration ratio (D^2/d^2).

With these reference flux profiles being used, a flat plate receiver was configured. This receiver is shown schematically in Figure 3.2-12. The design consists of a thick flat plate with an absorptive coating on the flux impingement side and insulation on the back side. Flow passages for the heat transfer fluid are imbedded in the plate. The thickness of the plate is sized to effect a more uniform temperature distribution due to the incident flux so that the working fluid does not see excessive film temperatures.

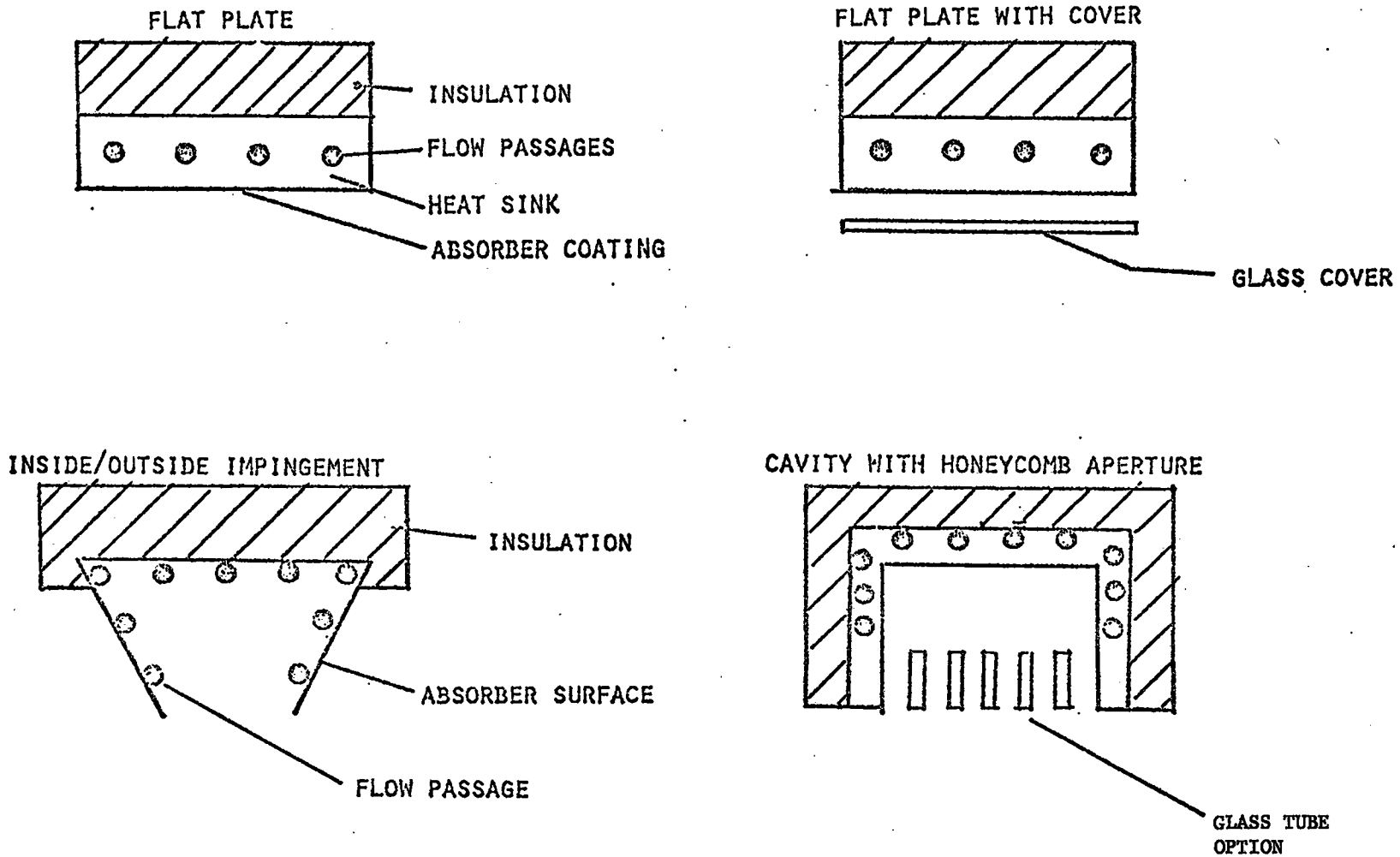


Figure 3.2-9. Receiver Concepts Investigated

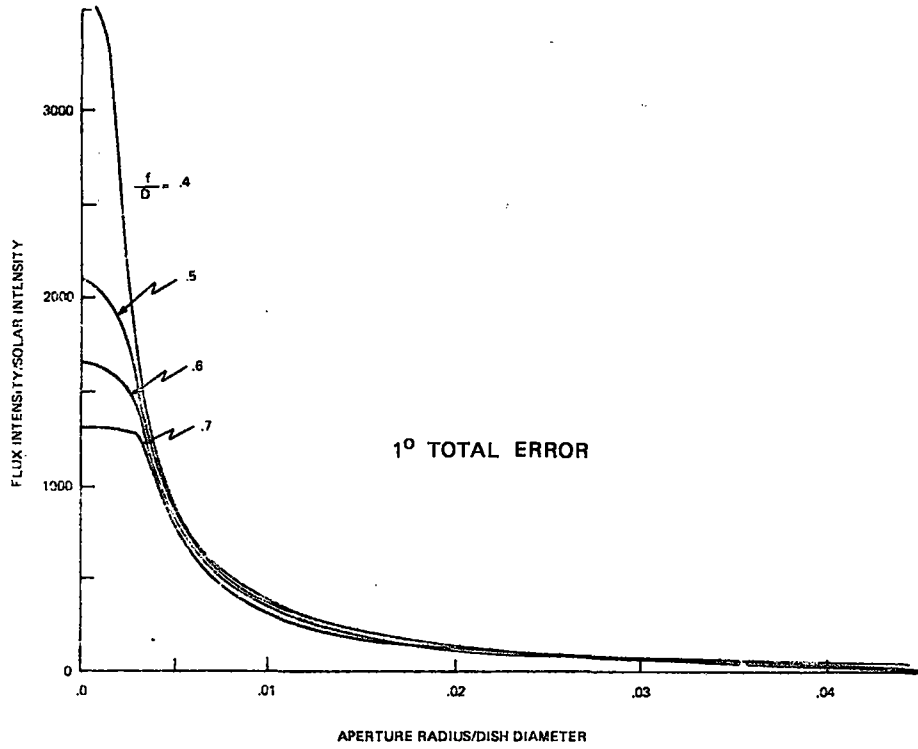


Figure 3.2-10. Receiver Flux Profiles

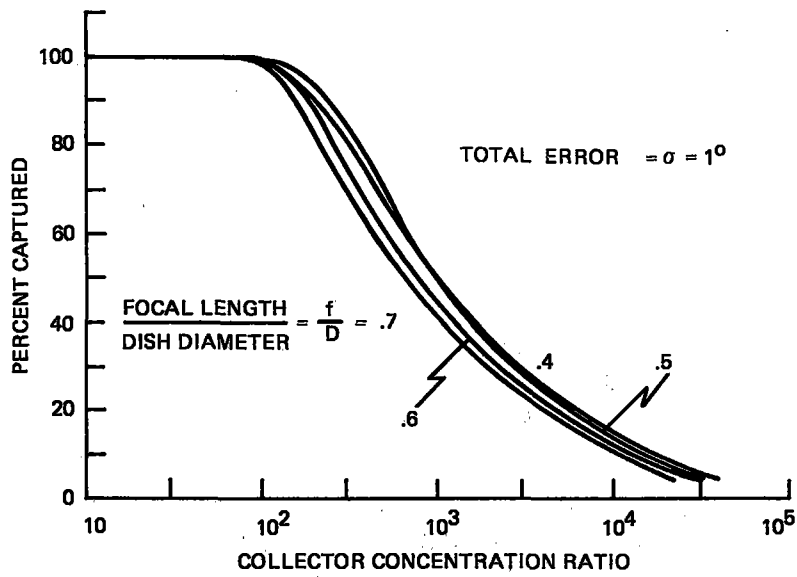


Figure 3.2-11. Integrated Receiver Flux Profiles

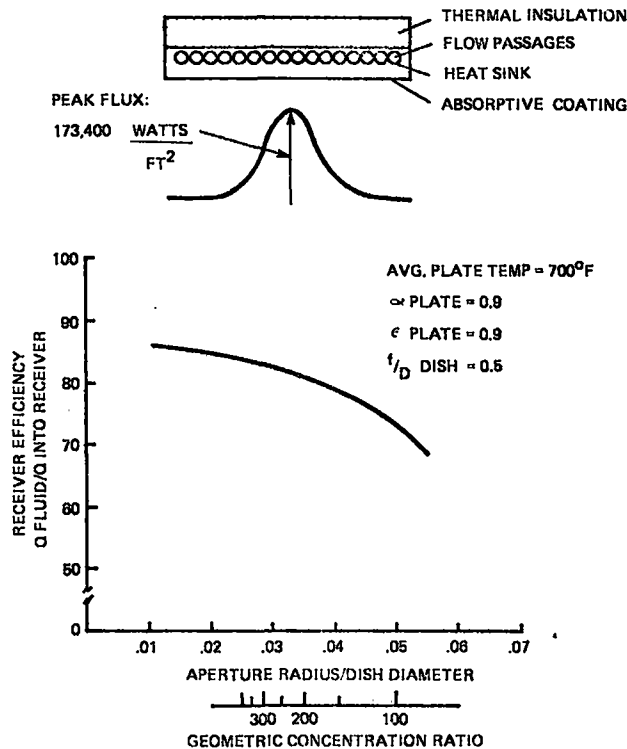


Figure 3.2-12. Flat Plate Receiver Analysis Results

The performance for the flat plate receiver is shown also in Figure 3.2-12. The following conclusions were drawn from the analysis:

1. Based on a flux profile derived for a one degree rms error, the radiative, convective, and conductive losses yield a receiver thermal efficiency of 81 percent at a concentration ratio of 200.
2. The high peak fluxes at the focal plane require thermal spreading by a high thermal conductivity material. Even the use of pure copper would result in significant temperature gradients which would aggravate thermal stresses in the plate. The use of copper or copper alloys would also require oxidation protection coatings over the entire surface.
3. Because of the small receiver area and the high heat transfer coefficients required to protect the working fluid from excessive film temperatures, the flat plate design concept inherently has higher fluid pressure losses. The fluid pressure drop calculated for the concept analysis was 3.4×10^5 N/m² (50 psi) per receiver.
4. The long-term integrity of the absorptive coating subject to thermal stress cycling is a potential problem area. Cracking or degradation of the coating will directly influence performance as well as increase the potential for hot spots within the receiver.

The second type of receiver that was evaluated in detail was the cavity type. This receiver is shown schematically in Figure 3.2-13. The basic concept of the cavity receiver is to intercept the incident flux perpendicular to the focal plane thereby diluting the flux intensity at the absorbing surface. Flux levels along the walls of the cavity located behind the focal plane of the dish are reduced considerably below those at the focal plane. In addition, the cavity performance is not as sensitive as the flat plate receiver to surface absorptivity. A fluid tube with a solar absorptivity as low as 0.6 has an effective absorptivity of 0.94 after three reflections within the cavity.

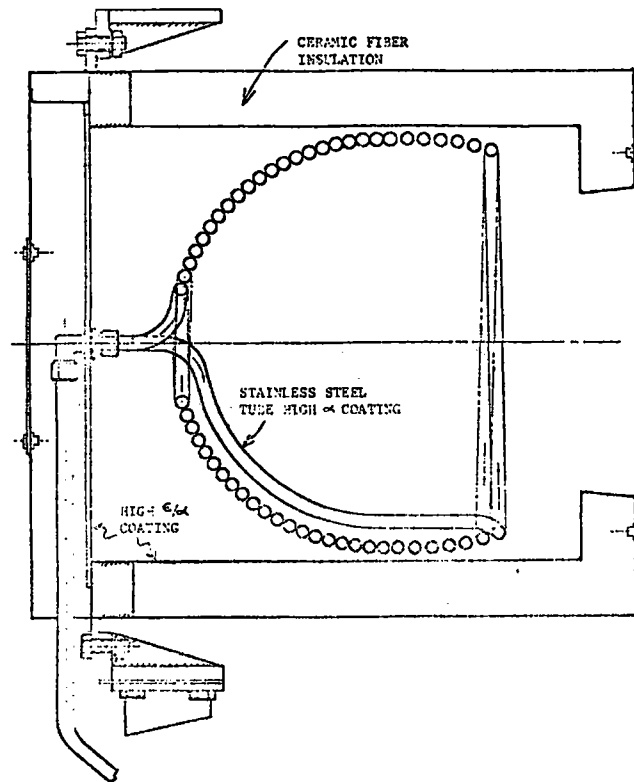


Figure 3.2-13. Coil-In-Cavity Receiver Design Concept

Figure 3.2-14 presents a calculated flux profile on the wall of a cavity cylinder for a typical cavity configuration. As can be seen, peak flux levels for this case are on the order of $26,910 \text{ watts/m}^2$ (2500 watts/ft^2), substantially lower than the focal plane peak level of $1.8 \times 10^6 \text{ watts/m}^2$ ($170,000 \text{ watts/ft}^2$). Since the flux levels are lower, lower fluid velocities are required to keep the film temperature drop down, and hence the fluid pressure drop is significantly lower in the cavity design than in the flat plate design. Typical ΔP 's are on the order of $34,475 \text{ N/m}^2$ (5 psi), an order of magnitude lower than the flat plate configuration. Finally, the cavity receiver can be designed to minimize the thermal stresses associated with the repeated cycling and the operating temperature gradients around the cavity.

Results of a comparative performance analysis conducted on the cavity and flat plate receivers are shown in Figure 3.2-15. As can be seen, the cavity has a higher performance than the flat plate when the aperture radius-to-dish diameter ratio is less than .04 (i.e., a geometric concentration ratio greater than 150). Since the range of concentration ratios for the LSE dish were expected to exceed 150 the cavity receiver offered a performance advantage over the flat plate concept. Hence, the cavity type receiver was chosen for the LSE collector due to the following factors:

1. The cavity receiver offered a performance advantage over the flat plate for the LSE concentration ratios range.
2. The cavity receiver design is less sensitive in both performance and reliability to absorptive coatings on the impingement surface.
3. Significantly lower flux levels on the impingement surface afford greater fluid protection from overheating.
4. Pressure drop of the cavity receiver can be as much as an order of magnitude lower than a flat plate type.
5. A cavity receiver can be designed to be less sensitive to thermal stresses than a flat plate design.

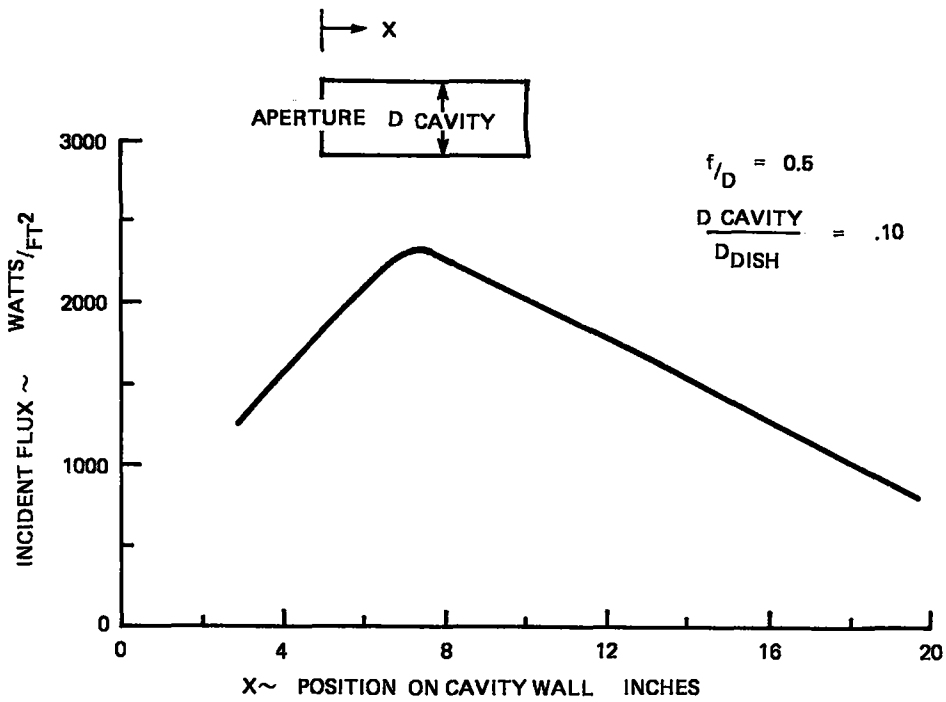


Figure 3.2-14. Typical Cavity Wall Flux Profile

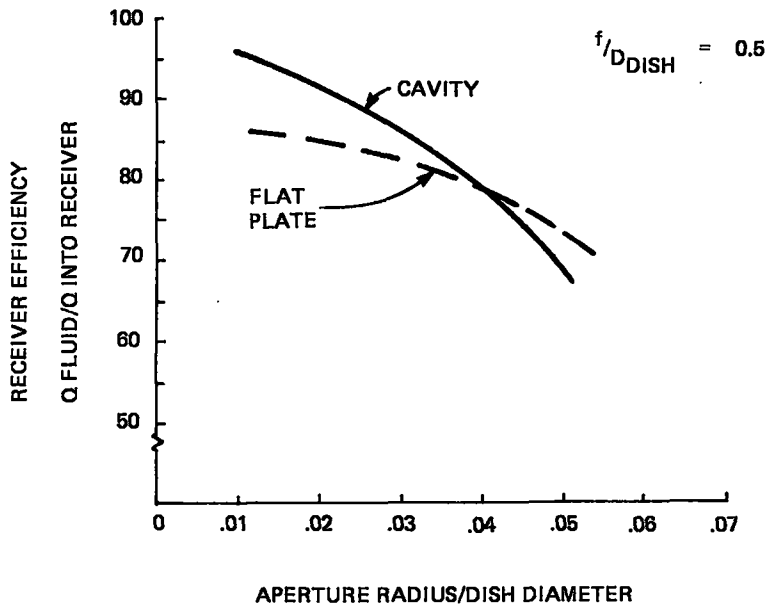


Figure 3.2-15. Receiver Performance Comparison

In addition to selecting the type of receiver, evaluations were conducted to examine the advantages and disadvantages of a Cassegrain reflector/subreflector/receiver configuration and to select the method of structurally supporting the receiver and routing the cooling fluid piping.

Three design configurations were investigated to determine the performance and cost advantages of each fluid piping configuration. These concepts were evaluated for the 5-meter Engineering Prototype Collector; however, the relative comparisons are valid for the full-scale 7-meter collector.

Figure 3.2-16 presents a schematic of the three concepts evaluated. Case I, strut mounted configuration, requires the longest up-down piping run. However, it is the least sensitive to solar and ambient conditions since the lines are fully insulated over the entire run. In Case II, central direct, the hydraulic lines are run through a receiver support from the dish vertex. This configuration requires the removal of insulation in the vicinity of the receiver aperture to avoid shadowing of the aperture. To avoid creating local hot spots on the bare tubes in the high flux region near the aperture, a reflective coating is required on the tube walls. Maintenance of this coating becomes crucial to protecting this region of the collector. Case III, a central loop configuration, avoids the excess heating problem of the central direct approach by routing the fluid lines around the high flux region and into the side of the receiver. This tubing could then be coated with an absorptive coating to pick up some of the incident flux.

The performance was calculated for each case accounting for the length of insulated tubing, uninsulated tubing, uninsulated reflective tubing, and uninsulated absorptive tubing and the conduction, convection, and re-radiation losses associated with each case. The results are shown in Table 3.2-3. The major problem encountered with Case II is the receiver aperture blockage and with Case III, the losses of the posed tubing. Thus, the configuration of Case I was selected as the approach for the collector pipe routing due to its significantly higher collector efficiency.

For the Cassagrain configuration, a secondary reflector is placed at the focal plane of the dish, and the energy is reflected into a receiver at the vertex of the dish. The advantages of this approach are elimination of considerable piping and a receiver position that reduces the stiffness requirements on the dish and the wind effects on receiver thermal performance. The disadvantages are the requirements for the secondary reflector and its optical and shadowing losses and the upward facing receiver cavity mouth. This latter disadvantage requires the use of a transparent cover for the receiver aperture to control convection and rain and dirt accumulation in the receiver cavity.

An analysis was conducted to compare the performance of the Cassegrain approach to the selected receiver position approach. The results of this study are presented in Figure 3.2-17. As can be seen in this figure, the additional reflection, shadowing, and convection losses are greater than the piping losses of the selected configuration. Therefore, the Cassegrain system was eliminated from further consideration, and direct placement of the receiver at the reflector focal plane was selected for the LSE collector concept.

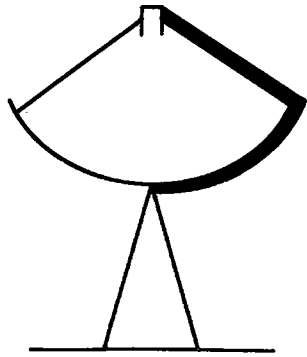
3.2.3.4 Tracking

Control concepts for the LSE collector were evaluated in three categories:

1. Direct closed-loop tracking control where the sun's image position error relative to the collector is used to actuate the control drives.
2. Computer control where the sun's position is calculated compared to an absolute position measurement of the collector and the error used to actuate the control drives.
3. A hybrid control combining both control techniques.

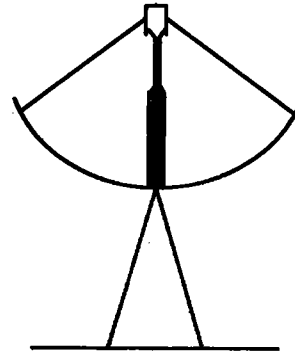
A preliminary evaluation of these options, summarized in Table 3.2-4, indicated that the open-loop computer drive would have the lowest cost and highest reliability. Since computer signal lines are to be installed for each collector in the Shenandoah LSE to serve flow control, emergency shutdown, experimental data gathering, and maintenance functions, little cost over the basic system control hardware would be required for tracking in this control approach.

CASE I
ENTRANCE ALONG SUPPORT MEMBER



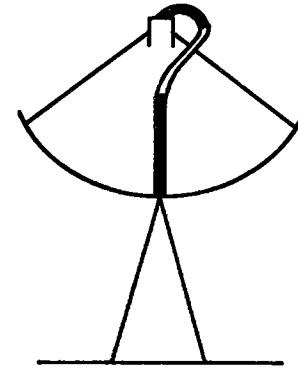
17.7' INSULATED PIPE

CASE II
CENTRAL DIRECT APPROACH



6.2' PIPE < INSULATED
EXPOSED

CASE III
CENTRAL LOOP APPROACH



7.7' PIPE < INSULATED
EXPOSED

Figure 3.2-16. Hydraulic Entrance Approaches (5M Dish)

Table 3.2-3. Hydraulic Approach Conclusions (5-meter dish)

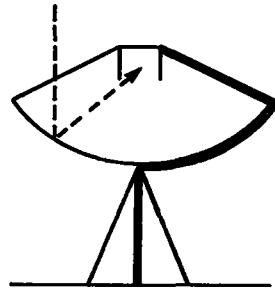
ASSUMPTIONS

- Noontime Flux Level ~ 200 Btu/Hr. Ft²
- Entrance & Exit Tubing Share Common Insulation
- 1/2" OD Tubing for Hydraulic Lines
- Application To 5M. Dish
- 8" Dia. OD Insulated Tubing

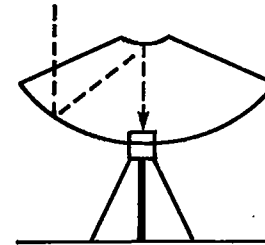
SELECTED APPROACH

	<u>Case I</u>	<u>Case II</u>	<u>Case III</u>
Approach	Along Strut	Central Direct	Central Loop
Major Problem	Length of External Tubing	Heating Rate in the Vicinity of Focus	Tradeoff to I & II
Solution Methodology	Insulate	Improve Bare Tube Reflectivity to just Counter Thermal	Remove Exposed Tube to Region of Lower Flux Where Thermal Loss is just compensated
Blockage by Insulation (% Reflected Energy)	2.1	10.8	8.5
Exposed Tube Flux Interception (% Reflected Energy)	NA	18	1.4
Bare Tube Constraint to Match Avg. Thermal Loss 850 Btu/Hr. Lft.	NA	.85 Specular Reflectivity L=3"	$\alpha = .9$ Takeoff 1' From Focus
Net Efficiency at Vertex of Paraboloid	.67	.61	.62

SELECTED APPROACH



CASSEGRAIN APPROACH



ADVANTAGES:

- ONE REFLECTIVE SURFACE
- LOWER CONVECTION LOSSES

- MINIMIZES PIPING & INSULATION LOSSES

DISADVANTAGES:

- PIPING LOSSES
- PIPING & INSULATION COSTS

- SUBREFLECTOR
- HIGHER SHADOWING LOSSES
- RAIN, DIRT ACCUMULATION

EFFICIENCIES:

REFLECTOR(S):	87%
PIPING:	92%
RECEIVER:	84%
	<hr/>
	67%

SUBREFLECTOR	87%
	95%
	97%
	84%
ADDITIONAL CONVECTION	95%
ADDITIONAL SHADOWING	96%
	<hr/>
	61%

Figure 3.2-17. Selected Approach Vs. Cassegrain Approach for Receiver Position (5-meter dish)

Although costs for this approach were judged low, error estimates for the computer drive indicated that the fiducial alignment requirements placed on the collectors were impractical to achieve in practice without incurring excessive installation and maintenance costs. In addition, precision fabrication of the reflector polar and declination axis assemblies would be required. Using commercial low-cost production assembly accuracies and field alignment procedures would result in excess energy losses due to control errors significantly higher than the LSE collector requirement.

It was therefore concluded that a closed loop tracker capability was more cost effective than a computer drive. The additional cost of tracking sensors and signal conditioning equipment was judged far lower than the cost of precision polar and declination axis assemblies and the associated installation and maintenance costs of precise fiducial alignment. However, since control logic to provide tracking under cloud cover conditions, initial positioning, emergency shutdown, and similar functions are required for any control approach and the incremental cost of a collector computer drive is very low, the hybrid control concept was selected for the Shenandoah application.

Table 3.2-4. Shenandoah Collector Control Options

Type	Closed Loop Tracker	Computer Drive	Hybrid
Cost	\$400-600/Collector	Lower	Higher
Performance	Lowest	Moderate	Highest
Reliability	Adequate	High	Adequate
Maintenance	Moderate	Low	Moderate
Accuracy	Adequate	Adequate	Highest

3.2.4 COLLECTOR DIAMETER OPTIMIZATION

One of the most important collector design parameters is the reflector diameter since it has a major effect on both collector and collector field costs and performance. After the collector concept was selected and the reference design established, the collector diameter was optimized. This then permitted tradeoff and optimization analyses to be performed on the collector components and the collector pipefield leading to the baseline design.

The parameters which were used to select the collector diameter considered both delivered energy per day for Shenandoah and the estimated cost of the entire collector field system. It was initially suspected that, as the number of dishes for a given field size was increased (i.e., smaller diameters), the costs of the collectors would decrease and the necessary pipe field cost increase would eventually provide an optimal cost point. In fact, however, for the range of collector diameters examined, the pipe field costs were an order of magnitude lower than the collector costs and did not significantly affect the variation of costs with diameter.

The optimization study did reveal that the driving parameter is pipe field losses. Even modest improvements in thermal loss reduction had a dramatic effect on total energy collected and a significant effect on the optimum collector diameter. This conclusion also indicated that significant effort should be directed to the reduction of thermal loss from the pipe field to improve overall LSE performance

3.2.4.1 Collector Field Parametric Relationships

Several parametric relationships were developed to optimize the LSE collector diameter. One of the most important is the variation of collector costs with diameter. Structural analyses of collector dish and mounts under wind and gravity loadings yielded the parametric weight versus diameter data shown in Figure 3.2-18. For high production volumes, reflector and mount costs can be related to weight resulting in the cost

trends shown in the figure. The prominent feature of the data in Figure 3.2-18 is the rapid increase in collector weight and, hence, cost with collector diameter. When the cost of the receiver, piping, controls, and reflector surface were added to the costs in Figure 3.2-18, total collector costs were estimated in the \$30-40/ft² region depending on the specific design. With these cost trends for the collector being used, the cost versus diameter relationships for the entire collector field were generated. These are given in Figure 3.2-19 and illustrate the dominating effect that collector costs have on overall field costs.

Scale effects on collector performance are largely determined by receiver performance. Figure 3.2-20 shows this variation as a function of insolation level. To relate costs to performance, an insolation model was assumed. The average insolation conditions were assumed to be a more reasonable assumption than peak conditions (which would tend to emphasize the smaller dishes). The Liu Jordan 10-year average solar insolation as a function of time of day for the four seasons is shown in Figure 3.2-21. Integrating the curve and averaging over a day shows that the average day has a direct normal of 158 W/m² (50 Btu/hr-ft²). To account for some self shadowing, a 10-hour average day was assumed.

Pipefield losses were a major consideration in the optimization study. These losses were broken into three categories: (1) steady state thermal losses, (2) pumping power losses, and (3) thermal capacity. Similar geometries of pipe field layout assuming two collectors in series to provide the necessary temperature rise of 139°K (250°F) were used for all diameters as a common basis for comparison. Pipes were sized for constant flow velocity independent of dish diameter. Insulation thicknesses were chosen from standard guide tables based on economical thickness for pipe size and temperature.

The resulting heat losses are shown in Figure 3.2-22. Initial analyses indicated very high losses for the reference system. Two approaches were taken to reduce these losses. The first was to increase the thickness of insulation. This approach quickly led to very large insulation thickness to achieve significant reductions in heat loss. The second method was to reduce the diameter of the smaller pipe along with nesting of the up-down feed and return lines to the receiver. This resulted in the reduced losses shown in Figure 3.2-22. However, the significant heat loss savings were realized at the expense of pumping power.

Pumping power was treated as a chargeable parasitic loss to the collector system. In order to express this loss in thermal units, an overall conversion efficiency of 33 percent (thermal to electrical) was utilized. The curve of pumping power required for various pipe size reductions from the reference size at a typical collector diameter is shown in Figure 3.2-23 along with the associated heat losses. Combining the two relations yields the optimum pipe size for minimum losses.

Thermal capacity of the field system consisting of pipe, Syltherm 800, and insulation is shown in Figure 3.2-24. Most of the thermal capacity results from the small pipe (62 percent) which cools to ambient temperature each night. Each day it must again be warmed and is, therefore, charged as a loss to the system. The curves are expressed in Btu/hr based on the 10-hour average useful energy period. The data shown assume CertainTeed 850 insulation and full nesting of all feed tubes.

3.2.4.2 Optimum Diameter Selection

The parametric data described previously was combined to yield data relating the optimizing parameter, collector field cost per unit of energy delivered, to collector diameter. As indicated before, several sub-optimizations were conducted during the analysis, the most important being the selection of insulation and nested piping to reduce the excessive thermal losses of the reference collector field design. Using the low loss configuration, field energy parameters versus collector diameter are shown in Figure 3.2-25. When combined with the cost data of Figure 3.2-19, the cost/diameter relationship for the collector field is obtained. The data in Figure 3.2-26 are presented as a function of collector production cost, the dominant parameter. At the projected collector cost of \$30/ft², the optimum collector diameter is approximately seven meters. As the cost of the collector is reduced, other collector field component costs increase in importance, and the trend is to optimize at larger diameters.

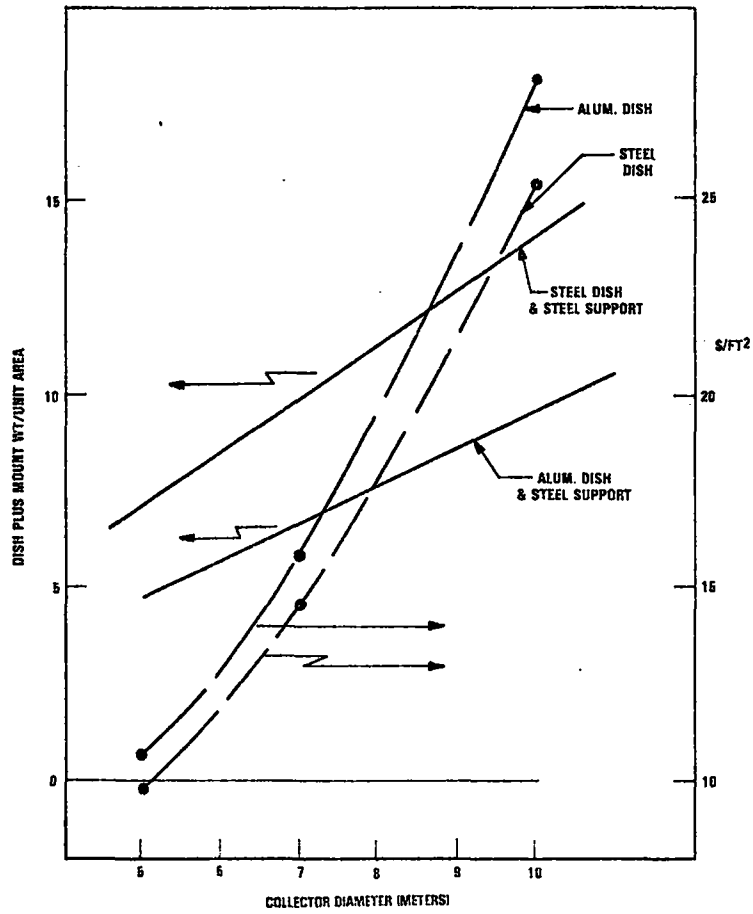


Figure 3.2-18. Total Collector Weight and Cost for Constant Structure Stiffness

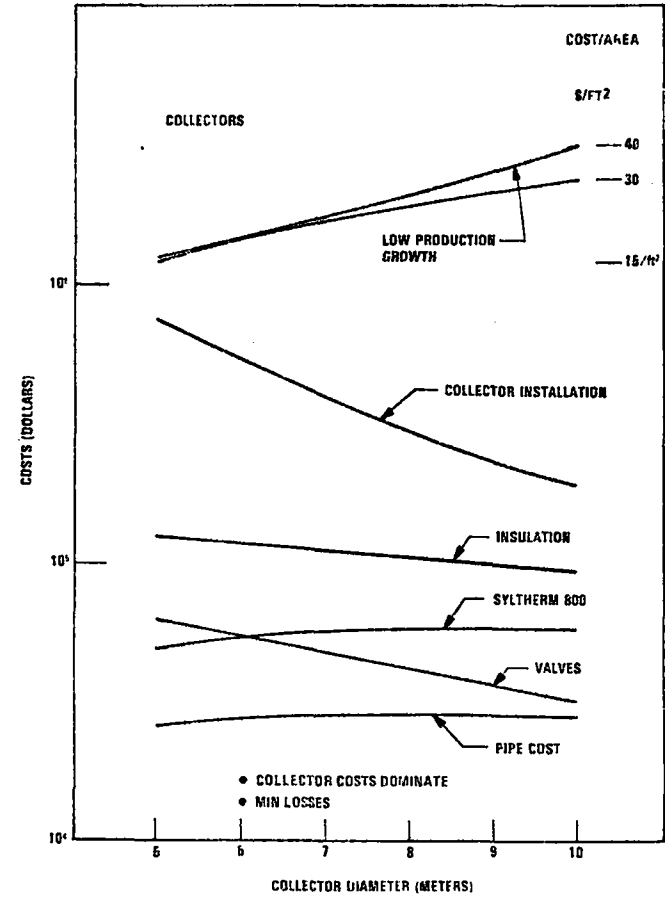


Figure 3.2-19. Collector Field Costs for 79,500 ft² Array

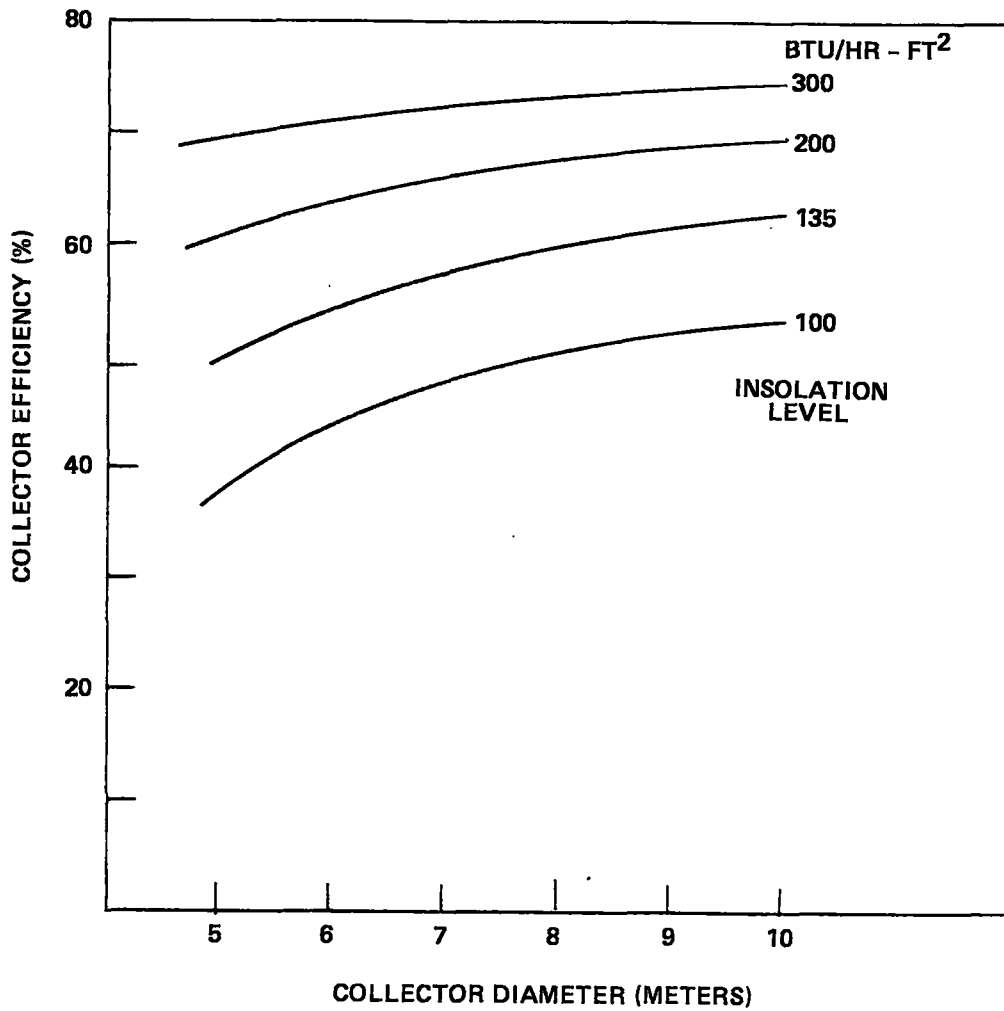


Figure 3.2-20. Collector Efficiency Vs. Diameter for Various Insolation Levels

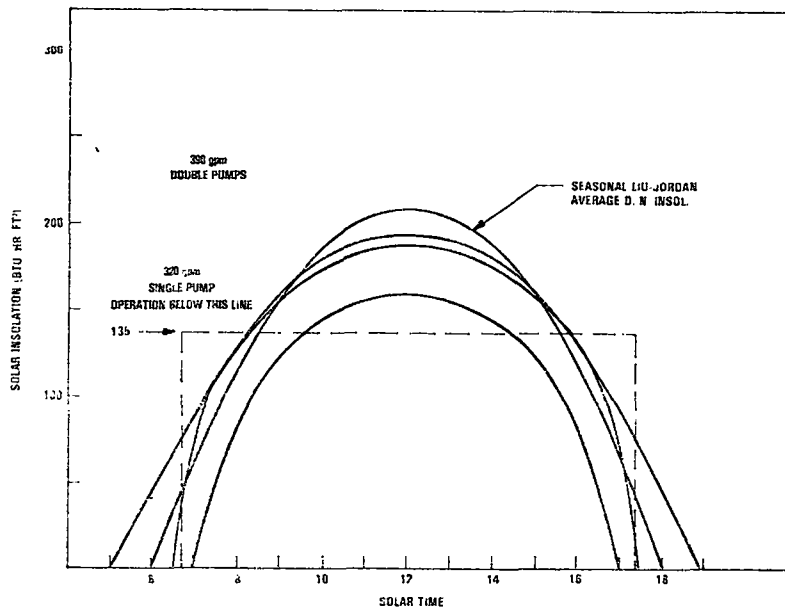


Figure 3.2-21. Average Shenandoah Insolation

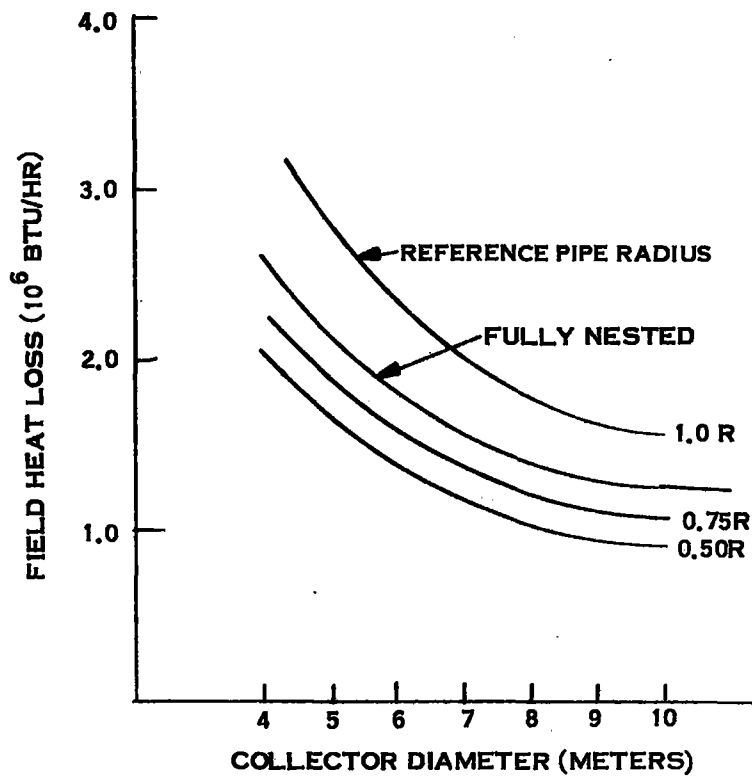


Figure 3.2-22. Variation of Steady State Heat Loss to Collector Diameter and Piping Radius

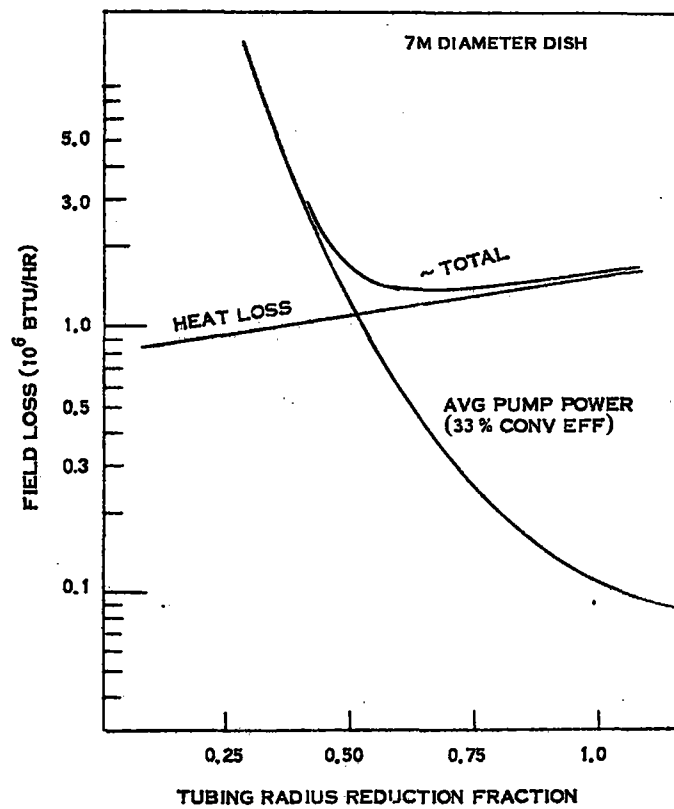


Figure 3.2-23. Composite Steady State Heat and Pumping Power Losses vs. Tubing Size

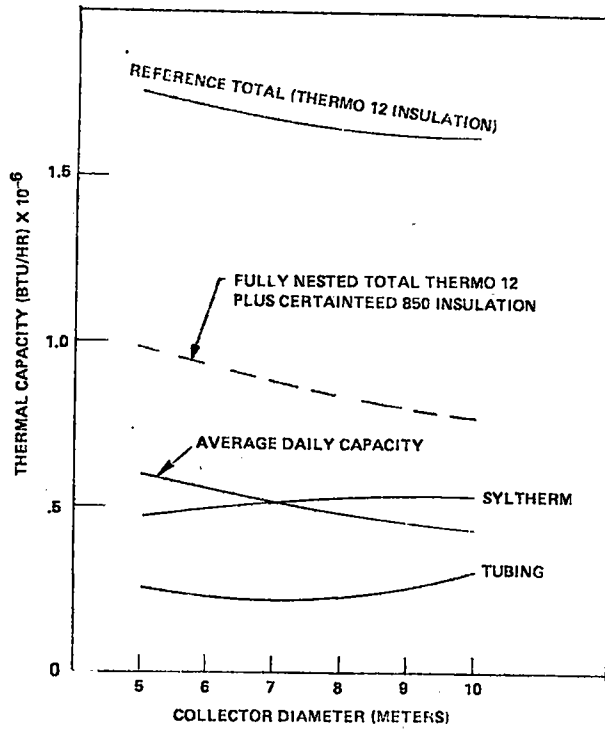


Figure 3.2-24. Collector Field Thermal Capacity vs. Collector Diameter for Average 10-Hour Day

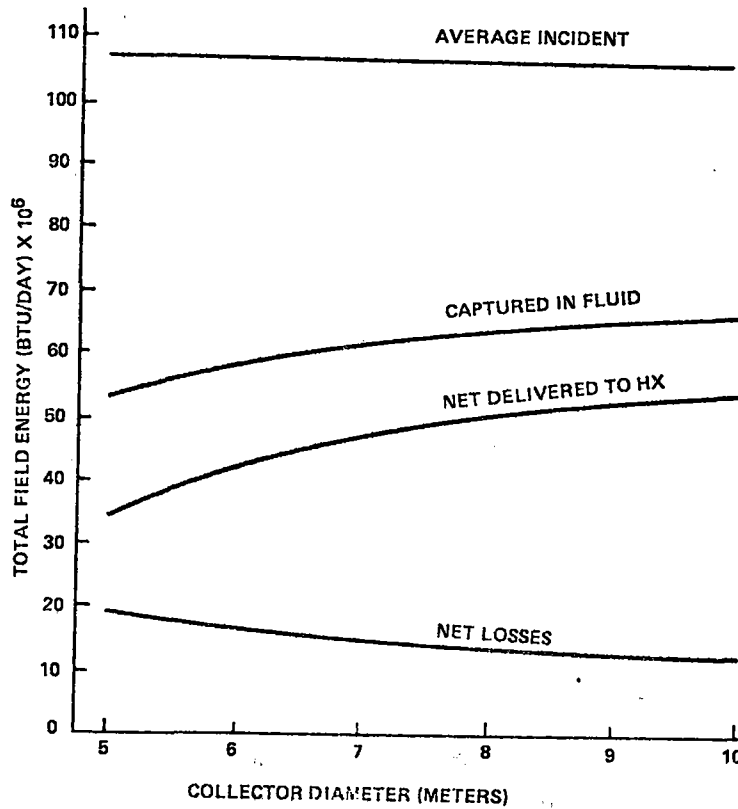


Figure 3.2-25. Daily Average Total Field Energy Parameter vs. Collector Diameter

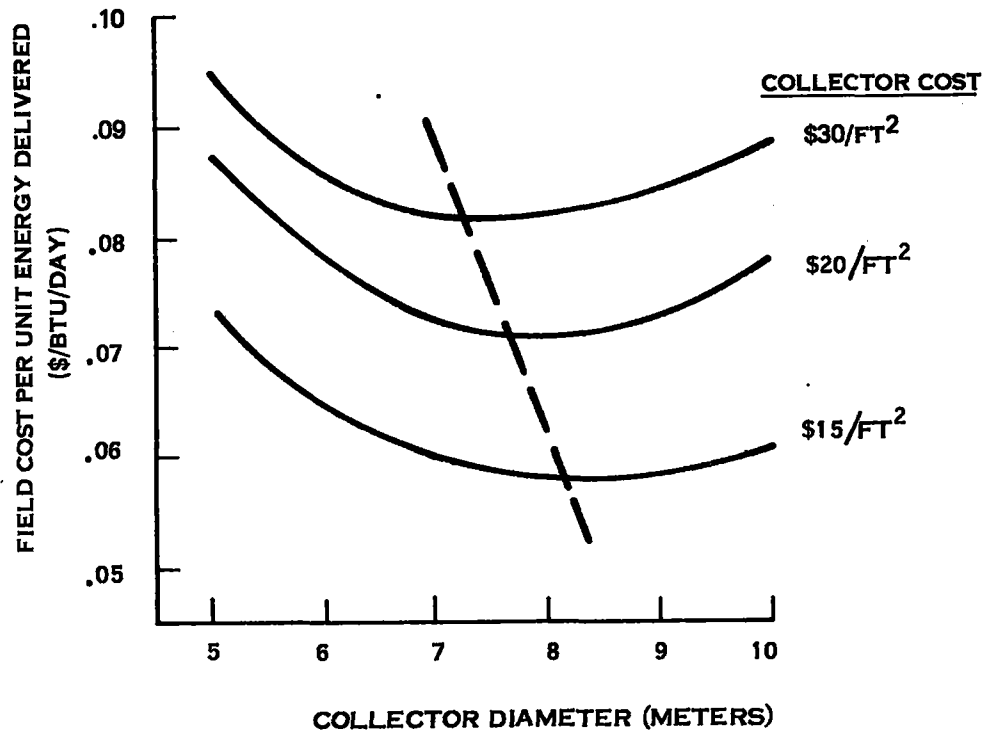


Figure 3.2-26. Optimization results - Collector Diameter vs. Cost/Btu Delivered

For the projected level of collector costs for LSE Shenandoah, the optimum collector diameter is in the seven to eight-meter region. However, reductions in pipefield losses tends to reduce the optimum collector diameter. Since such loss reductions had been identified as a major area of activity, it was anticipated that the optimum collector diameter would be reduced somewhat when the preliminary design was completed. Hence, the LSE collector diameter was selected at seven meters.

3.2.5 COLLECTOR PRELIMINARY DESIGN DESCRIPTION

The preliminary design of the LSE collector is described in Paragraphs 3.2.5 through 3.2.9. Detailed tradeoff and optimization studies for each component are described in the section describing the preliminary design of the component.

The overall configuration of the LSE collector is shown in Figure 3.2-27. The collector consists of:

1. A 7-meter aluminum reflector assembly composed of a center annulus and 21 petals on the periphery of the annulus. The reflector petals and annulus are chemically brightened to achieve the required reflectance and protected with a thin coat of a silicone material, RTV-670. The reflector petals are supported by aluminum ribs tied into a center hub which attaches to the mount.
2. A mount and drive assembly consisting of a steel yoke and base structure and electric jackscrew actuators. Two ac jackscrews provide the polar axis drive and a single ac jackscrew provides the declination axis drive. A battery powered dc motor on the polar axis provides a high speed drive for emergency defocus. A concrete counterweight is provided on the yoke to reduce drive torque requirements.

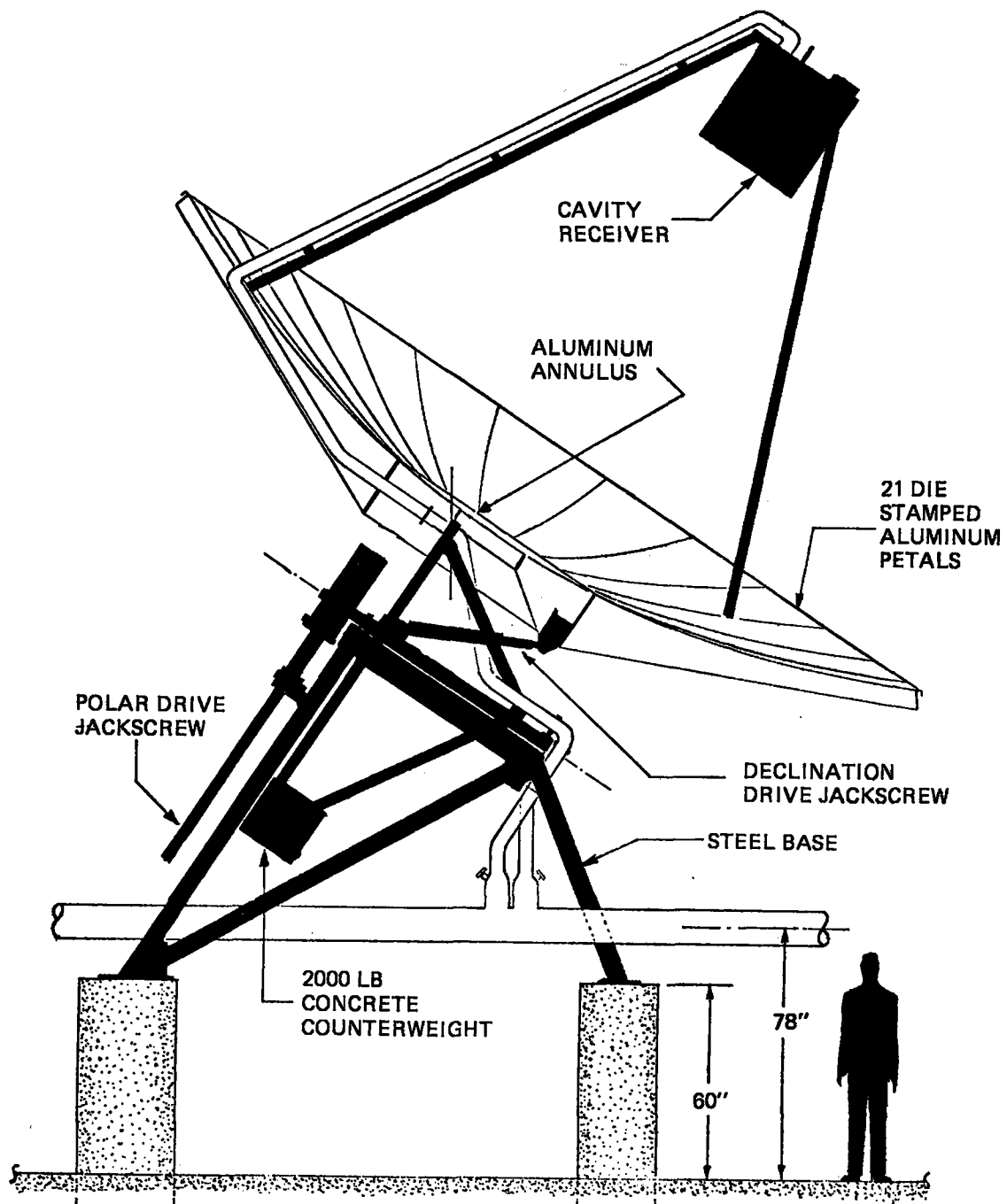


Figure 3.2-27. LSE 7 Meter Collector

3. A cavity receiver consisting of a double tube, hemispherical coil as the absorbing/heat transfer mechanism packaged in an insulated housing. Insulated piping from the receiver to the branch piping includes insulated flexible piping sections permitting motion about the polar and declination axes.
4. A control system consisting of fiber optic bundles mounted in the aperture plate of the receiver to provide direct tracking of the receiver focal plane image. Control logic and commands are provided through the system's collector field microprocessors.

Several of the low cost features of the collectors are given in Table 3.2-5 and indicate the approaches used to meet overall collector production cost goals. The principal collector parameters are given in Table 3.2-6, and its design point performance parameters are given in Table 3.2-7.

3.2.6 REFLECTOR DESIGN

The function of the parabolic dish and its reflective surface is to reflect as much of the normal solar incident energy as possible into the receiver aperture. Obviously, a highly reflective surface is desirable, and the development of this surface is presented in Paragraph 8.1.2, Reflector Development. Results of this task indicated that chemical brightening of bright rolled aluminum alloys in the 5000 series would meet specular reflectance requirements when coated with a protective film of RTV-670 but that the total reflectance requirement of 0.88 could not be met using standard mill produced, low cost aluminum sheet. The total reflectance requirement was therefore revised to a realistic 0.86 value, lowering design point collector efficiency approximately two percent. This decreases overall annual LSE output by only one percent which is well within the overall powerplant output requirement.

- Standard Steel Sections for Base
- Automotive Type Starter Motor for Defocus Drive
- Concrete Counterweight
- Chemically Brightened Mill Rolled Stock for Petals
- Low Cost Protective Silicone Coating for Reflection Surface
- Standard Fittings and Fasteners
- Carbon Steel Piping and Receiver Coil

Table 3.2-6. Collector Parameters

Parameter	Design Value
Diameter	7 Meters
Area	417 Ft ²
Concentration Ratio	250
F/D	0.5
Total Reflectivity	0.86
σ Slope Error	8.7 Mrads (1/2 ^o)
σ Specularity	8 Mrads*
σ Tracking	4.4 Mrads (1/4 ^o)
Coolant Inlet Temp	500 ^o F
Coolant Outlet Temp	750 ^o F.

*Equivalent Receiver Acceptance Ratio Value

Table 3.2-7. Design Point Performance Parameters

Parameter	Design Value
Insolation	200 Btu/hr-ft ²
Ambient Temperature	50°F
Q into Receiver	66,670 Btu *
Q Losses	12,230 Btu
Radiation	(7,410 Btu)
Convection	(3,890 Btu)
Conduction	(930 Btu)
Q into Fluid	54,440 Btu *
Collector Efficiency	65.3% *

* Based on revised total reflectance of 0.86

The design of the dish itself must provide enough stiffness to hold the reflective surface in the parabolic shape during operation under required wind loading conditions. Many methods of constructing the dish were reviewed in conjunction with Scientific Atlanta, a leading manufacturer of parabolic dishes used for communications applications in the concept selection task (Paragraph 3.2.3). More detailed evaluations were conducted in the preliminary design task. The main dish types investigated were spun dishes, stretch formed petals, and die stamped petals, all of which are used in various sizes for parabolic antennas. Results of the evaluation are presented in Table 3.2-8. This study, prepared with fabrication vendor inputs, confirmed the concept selection study results indicating die stamped petals as the preferred reflector fabrication technique for LSE Shenandoah.

The dish design shown in Figure 3.2-28 consists of stamped petals of 2.44 meters (8 ft) length with a 2.28 meter (90 in) idiameter center annulus made from a spinning. The spinning, or more properly called flow turning in the large sizes, is a familiar process with many vendors in the smaller diameters. As the size increases, tooling cost increases substantially and the number of vendors available is reduced. A simple spun 7-meter dish is feasible, but it would entail severe transportation problems. Stretch forming once widely used in aircraft industry can be performed by fewer vendors today. Because the process yields a sheet of material over a pattern, usually wood, tooling costs are moderate and accuracies good if the sheet is flat. However, flanges of some sort need to be attached to provide rigidity and attachment points. If done integrally, the flanges would be smaller than desired to prevent tearing.

A more severe problem is the predicted accuracy; slope error would be larger than in a process where the flanges are separately formed and attached in a second operation. While the latter was predicted to obtain the accuracy required, the cost was forecast to be substantially higher. The die stamping of petals was best understood since Scientific Atlanta has considerable experience using the process to produce about 100 5-meter microwave antennas a year.

The LSE petals will be very similar to those used in the EPC which contain die-stamped petals made by Scientific-Atlanta. Thus, there will be reduced development risk and costs. Compared to the EPC design, there are 21 instead of 24 petals, and the petal thickness has been reduced from 0.00396 to 0.00254 meter (0.156 to 0.100 in.) to minimize costs. After a vendor survey on the petal and annulus fabrication requirements, 5657 aluminum alloy in an H241 temper was selected for the reflector material. Reflector surface development data indicated the superiority of the 5657 from an optical properties viewpoint, but selection of the proper temper required balancing the optical advantages of a high temper versus the fabrication advantages of a low temper. Data from aluminum vendors suggested use of the H241 temper due to its high elongation, similar to that of the proven 5052 aluminum alloy used in the 5-meter reflector produced by Scientific-Atlanta (see Table 3.2-9). The 5657 H241 temper alloy was therefore selected.

Table 3.2-8. Petal Manufacturing Option Evaluation

Option	Size	Accuracy	Tooling Cost	Prod. Cost	Vendor Experience		
					Excellent	Moderate	Limited
Spinning/ Flow Turn	M	0.1° - 0.5°	\$5,000	\$300	>100		
	L	0.1 - 0.5°	\$100,000	\$2,000			>10
Stretch Form Integral Flange	M	1.0° - 2.0°	\$5,000	\$70		>50	
	L	1.0° - 2.0°	\$8,000	\$90			>10
Stretch Form Separate Flanges	M	0.1° - 0.5°	\$20,000	\$250		>50	
	L	0.1° - 0.5°	\$25,000	\$300		>50	
Die Stamp	M	0.1° - 0.5°	\$50,000	\$80	>50		
	L	0.1° - 0.5°	\$70,000	\$100			>10

Size = Petal Length
or Spinning Dia, 50">M>100", L>100".

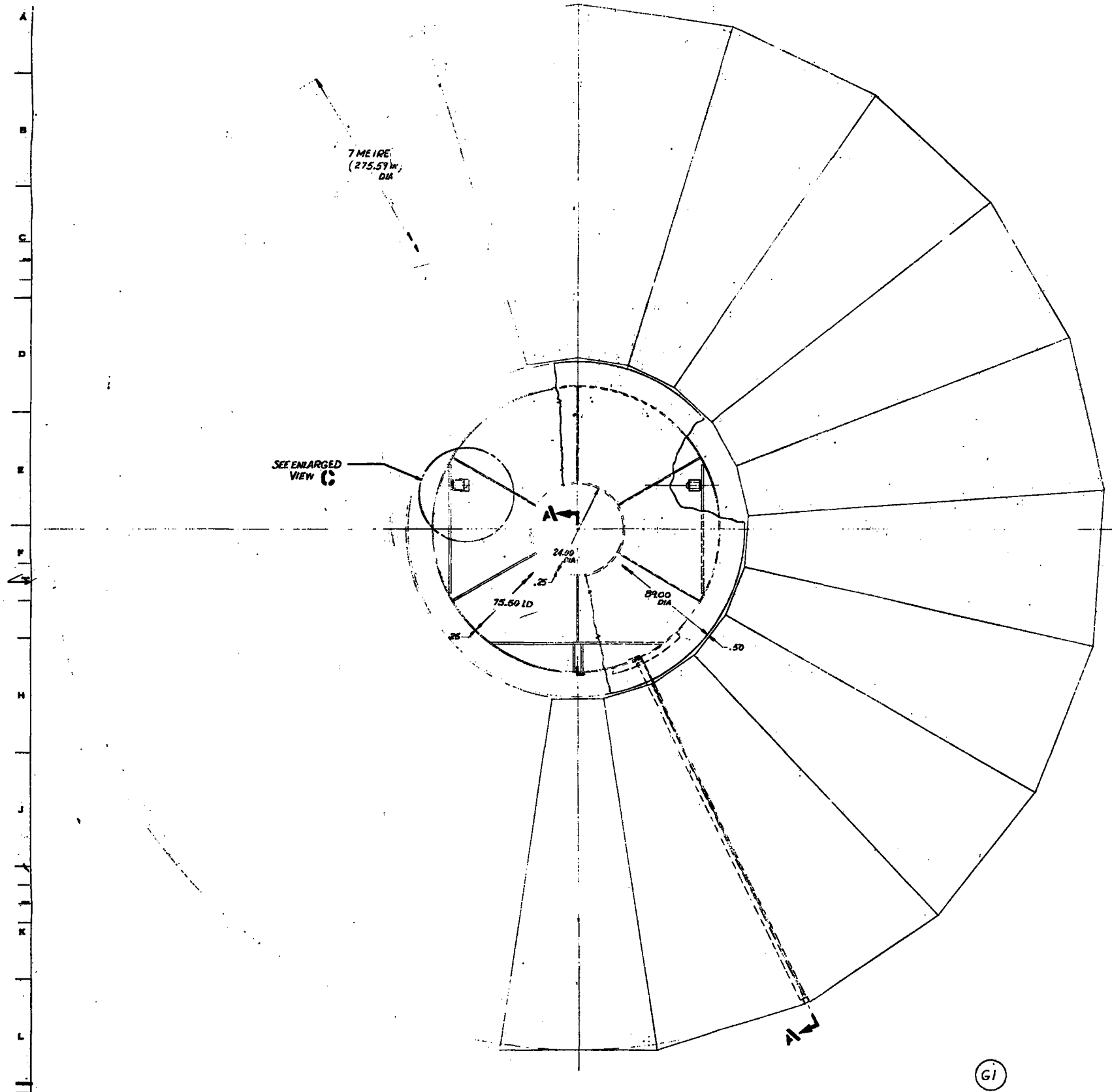
Table 3.2-9. Mechanical Properties of Candidate Petal Alloys

Material Type Al Alloy	Hardness BHN	Room Temperature Mechanical Properties			Thickness (in.)
		Ult. Str (KSI)	Yield Str. (KSI)	Uniform % Elongation	
5052-0*	47	28	13	25	0.156
5657-H241	36	25	16	19	0.100
5657-H25	40	26	23	12	0.100
5457-H25	48	26	23	12	0.100

*Material already formed (acceptably) into required petal configuration by DeKalb Tool & Die Co. Base metal prevents production of required surface finish.

The reflector petals and annulus require an accurate positioning support structure to meet overall reflector slope error requirements. To meet this requirement, the reflector hub section was made large (see Figure 3.2-29), and two techniques for supporting the petals outboard of the hub were analyzed: truss sections and ribs.

Conventional parabolic antenna designs use trusses to support the dish surface rather than the use of ribs. However, for the production quantity required for the LSE (about 4,000 units), ribs could be substantially less expensive to produce than truss sections and would provide a more uniform support for the reflector surface. The truss design is shown in Figure 3.2-30. The truss is made up of aluminum tubing 0.032 meter (1.25 in.) in diameter with 0.0032 meter (1/8 in.) walls. The stress and deflection analysis assumes that the petals' turned down edge and a portion of the surface act as a top member. The deflection of a point on the rim was calculated by taking the deflection at node 4 and adding the product of the slope between nodes 3 and 4 and the distance to the rim from node 4.



SCALE $\frac{1}{10} = 1$ #AS NOTED

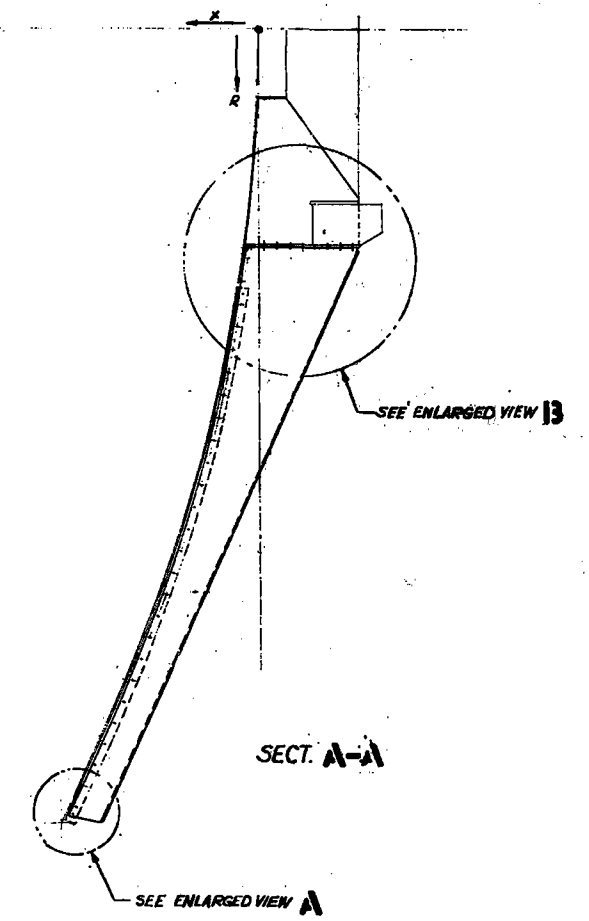


Figure 3.2-28. Seven Meter Collector Petal Configuration

The rib deflection analysis used the same assumption of the petal flange and width acting as a top flange for the rib. The deflections were computed by graphical integration of the M/EI curve since the section properties varied considerably along the length of the rib. The conclusion of the trade-off analysis summarized in Table 3.2-10 was that the rib gave superior deflection properties for the same amount of material, and since less joints and joint fittings were needed, the rib would be preferred from a cost standpoint.

Table 3.2-10. Rib vs. Truss Deflection and Stress in 90 mph Head-on Wind

	Tip Deflection	Total Applied Load	Structural Weight	Max. Stress
Truss	0.235 inch	592 lb	13.5 lb	5,232 psi
Rib	0.106 inch	600 lb	13.7 lb	3,075 psi

The stress analysis of the dish is based on a worst case of the 40 meters/second (90 mph) wind heading directly at the dish. The ribs are assumed to take the entire load; i.e., the dish membrane stresses do not aid the ribs. The stresses in the rib in this case are still at a low enough level (2.12×10^7 N/m² or 3,075 psi) to avoid local crippling of the lower flange of the rib.

Of interest in the dish design are the petal deflections under the 13.4 meters/second (30 mph) operating wind. The complicated stress analysis was simplified by assuming the petal acted as 0.025 meter (1 in.) wide strips between the two flanges. Stiffening of the beam due to the plate effect was estimated by increasing the EI divided by $(1-\nu^2)$ and assuming fixed ends. The deflection curve was differentiated to obtain the slope, and the maximum and average slope change were computed. Since the petal span varies, the beam length was adjusted to calculate slope changes at various points on the petal. Thus, a weighted average slope error was computed. For the 0.0025 meter (0.100 in.) thick petal in a 13.4 meters/second (30 mph) wind, the average slope change was 0.12 degree, and the maximum slope change was 0.43 degree near the rim. Thus, the highest operating wind condition of 13.4 meters/second (30 mph) will have an effect on reflector performance, but the performance will be dominated by the inherent slope error rms (0.5 degree) of the fabricated reflector.

3.2.7 MOUNT AND DRIVE

3.2.7.1 Mount Structure

The function of the mount structure is to hold the reflector dish and receiver assembly in the proper position as the dish tracks the sun in its daily and seasonal variations. There are two basic elements of the mount structure: (1) the base frame which does not move, and (2) the yoke structure which rotates about a polar axis holding the dish and a counterweight.

Preliminary design of the mount structure began with the selected polar axis/declination axis configuration driven by linear actuators. The general approach taken was to utilize a concrete foundation and standard steel structural elements for lowest material costs. Two basic configurations were considered: (1) a preformed large central concrete post which also acted as a foundation, and (2) a tripod steel base framework sitting on three concrete pillars. Sketches of these configurations are shown in Figure 3.2-31. The tripod was selected over the central post based on uncertainty of the soil conditions and hence the size and cost of the central post; cost estimates for the remainder of the collector were virtually the same for both configurations. For the tripod, the height above grade for the pillars was based on preliminary trades at a height of 1.52 meters (5 ft).

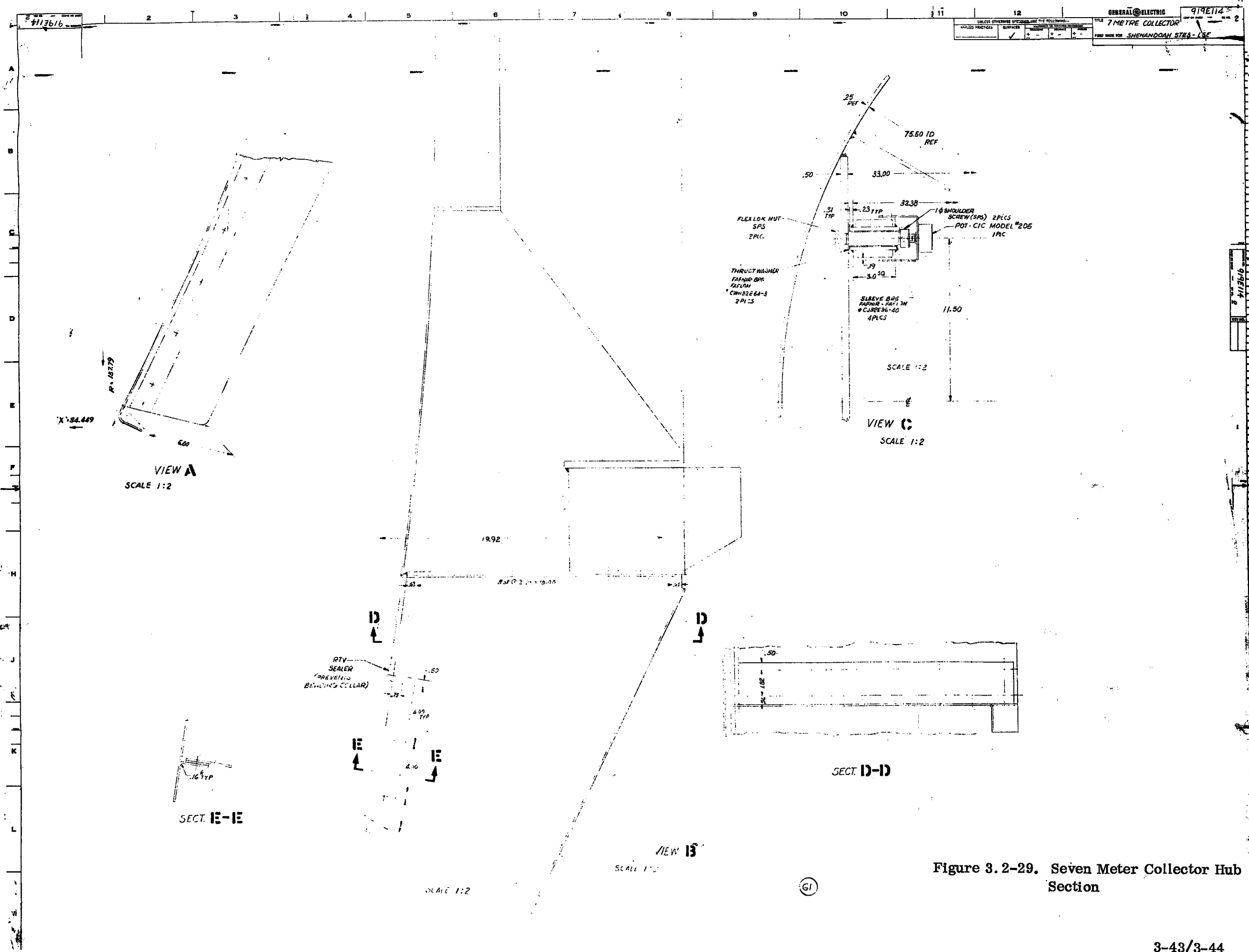


Figure 3.2-29. Seven Meter Collector Hub Section

@ 180° INCLINATION, MUST WITHSTAND 948 LBS NEGATIVE DRAG
 = 45.6 LBS/PANEL

DIAMETER = 22.97 FT AREA = 414.4 FT² (20.7 FT²/PANEL)

DYNAMIC PRESSURE = 20.4 LB/FT²

$$\frac{1}{2} C_D A \rho V^2 \quad C_D = 1.50$$

3-45

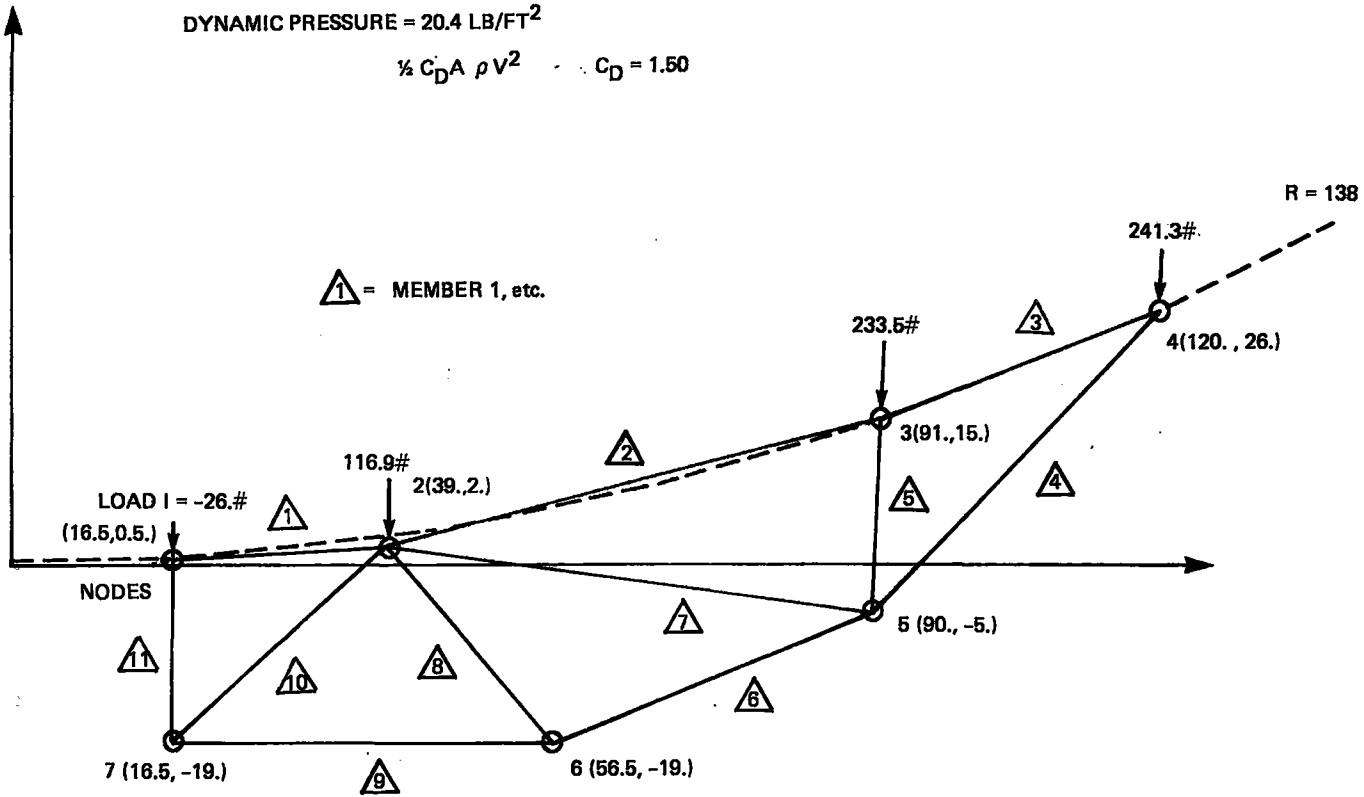


Figure 3.2-30. Reflector Truss Design

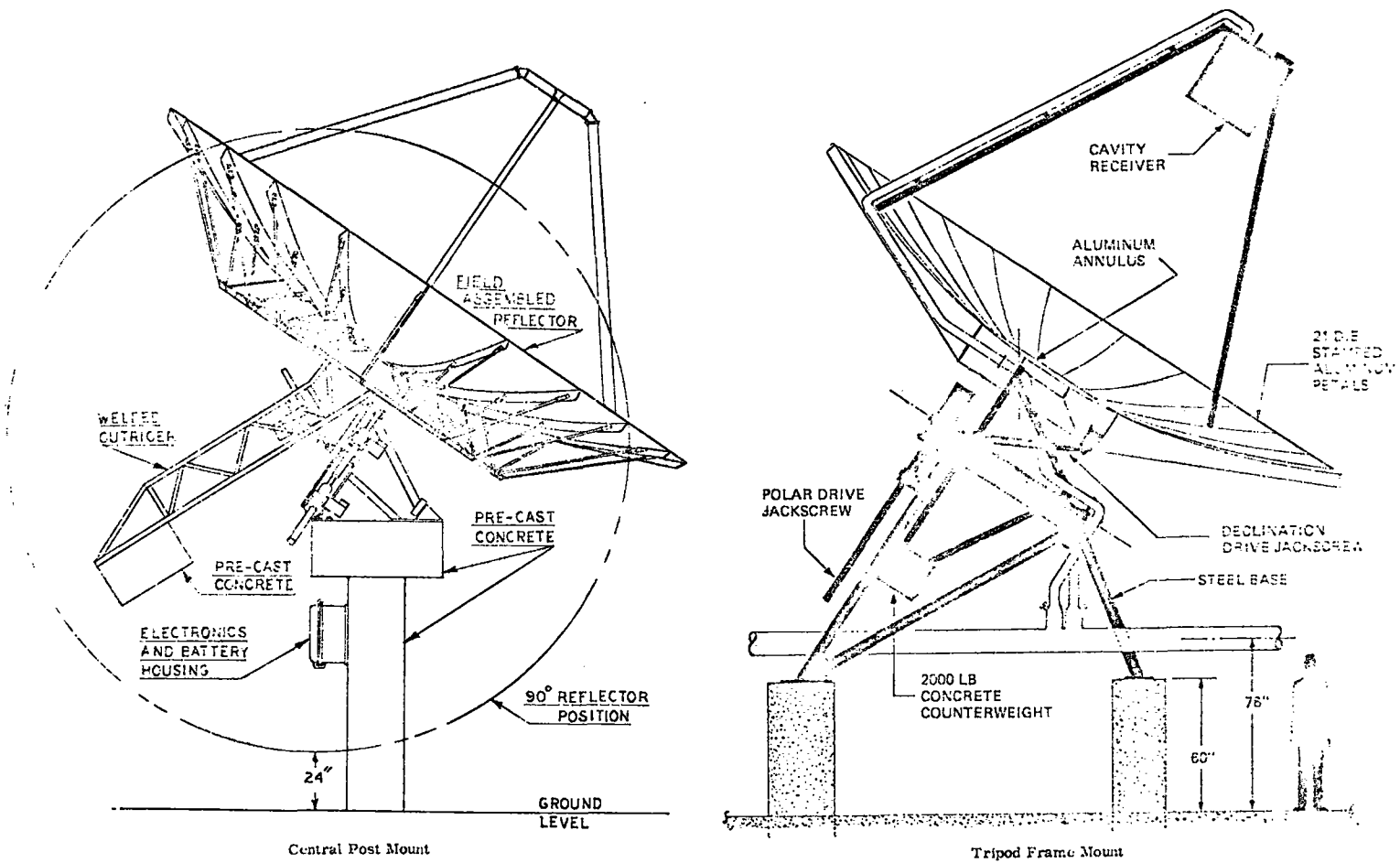


Figure 3.2-31. Collector Structural Element Options

Since the collector structure is largely steel construction and the Shenandoah site is governed by local or state codes, American Institute of Steel Construction (AISC) specifications were used as design criteria. Aluminum portions were designed with the same factors of safety as was considered good practice where fatigue was not a factor. AISC specifications are for the design of non-moving structures; since the collector has moving parts, maximum loadings were predicated on worst case conditions. The maximum design loading condition occurs for 40 meters/second (90 mph) hurricane winds with the wind blowing in any direction and the dish being in any position. Normally the dish is stowed with the polar axis at -90 degrees and declination at -23.5 degrees (toward the east and down) under adverse wind conditions. This points the dish almost 15 degrees below the horizon which also protects the reflective surface from hail damage. The worst case assumes a failure that does not allow the dish to be stowed prior to the storm.

Although there is a large variation in wind angle and dish positions, two positions are of prime concern. These positions are (1) the due east position and (2) the noon-winter position.

The loading is mainly due to the drag, lift, and moments on the reflector dish. Static weight loads are secondary. Drag forces on the non-dish portions of the structure are small and can be neglected. Table 3.2-11 gives the dish loadings. The data was generated by a Scientific-Atlanta computer program based on JPL wind tunnel data as reported in JPL-CP-3 "Preliminary Report on Parabolic Reflector Antenna Wind Tunnel Tests" February 28, 1962. The drag, lift, and torque data for the 7-meter dish given in the table were reduced to reactions at the dish supports for the various wind angles. These were then used as input loads on the yoke structural analysis computer program for a fixed yoke support bearing. The bearing reactions were then used to define the loading on the base frame structure. The base frame reactions in turn defined the foundation loads.

In addition to surviving 40 meters/second (90 mph) winds with no structural damage, another design requirement is to have as stiff a structural support as possible within acceptable costs. This is necessary because the on-off tracking control (described in Paragraph 3.2.7.2) is turned off for almost one minute during which time the wind can easily vary in magnitude. Of the 1/4 degree tracking error requirement, 1/8 degree is budgeted for structural deflection. This includes deformation of the receiver and its support, dish support structure, the yoke structure, polar and declination axis drives, and the base frame and foundation. For the 3.5-meter focal length, the 1/8 degree translates into 0.015 meter (0.60 in.) receiver deflection.

3.2.7.1.1 Base Framework

As can be seen in Figure 3.2-32 and 3.2-33, the base framework rests on three elevated concrete columns or pedestals 1.52 meters (60 in.) high. The frame consists of a backbone parallel to the polar axis supported by two legs at the rear, a single front leg, and two cross braces going from the rear pedestal to the front of the backbone. Additionally, the two rear legs are tied together near the top to provide support structure to which the rear mounted polar drive is attached. The side view shows an area through which the counterweight passes. The need for the counterweight is discussed later. The polar axis drives are mounted behind the base frame. The backbone is made from a 0.16 x 0.32 meter (4 x 8 in.) rectangular structural steel tube. To this backbone are mounted the front and rear bearing blocks for the polar axis shaft.

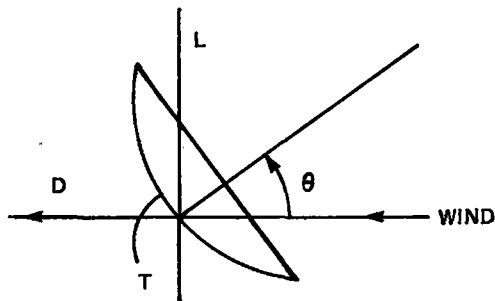
The design of the base frame work was developed to meet a sequence of design or operational requirements. First, with the dish in the due east position, a minimum ground clearance of 0.61 meter (2 feet) was established to minimize reflector surface degradation due to wind borne dirt and debris. Ground clearance in the fully stowed position is approximately one foot to allow for variations in ground level without reflector impact in the extreme stowed position. The polar axis was then set at the Shenandoah latitude (33-1/2 degrees) and the boresight line perpendicular to the polar axis established for the noon equinox position. The declination axis and support structure was oriented for the noon position above the polar axis to provide clearance from the base frame in the 6 AM and 6 PM positions and to allow the -23.5 degrees declination axis motion. The dimensions shown in Figure 3.2-32 were derived keeping the dish as low as possible (to minimize polar axis

Table 3.2-11. Parabolic Dish Forces/Moments in 90 MPH Wind

Wind Force on solid surface paraboloid reflector based on JPL wind tunnel tests. (Program revised 2/2/77)

Model Number	GE Solar Pedestal
Reflector Diameter	22.97 Feet
Reflector F/D Ratio	-500
Vertex Axial Offset	.0 Feet
Vertex Radial Offset	.0 Feet
Pivot Axis to Ref Plane	.0 Feet
Ambient Temperature	68 Degrees
Wind Velocity	90 MPH
Dynamic Pressure	20.4 Lbs/Sq-ft.

<u>O</u>	<u>T</u>	<u>D</u>	<u>L</u>
Reflector Axis From wind Degrees	Torque about Pivot axis Lb-ft	Drag Lbs	Lift/or Side Force Lbs
0	0	12664	0
10	-2230	12411	-2111
20	-4945	11486	-4390
30	-6981	10730	-6585
40	-9696	9361	-8443
50	-12314	8089	-10384
60	-24090	6060	-12073
70	-7692	4047	-10131
80	12196	2133	-4643
90	20136	1492	0
100	19533	2080	3208
110	17916	1980	422
120	19080	2421	422
130	18660	3264	1351
140	15040	4779	2026
150	11161	6020	2111
160	8834	7340	1773
170	5667	8817	1098
180	0	9118	0



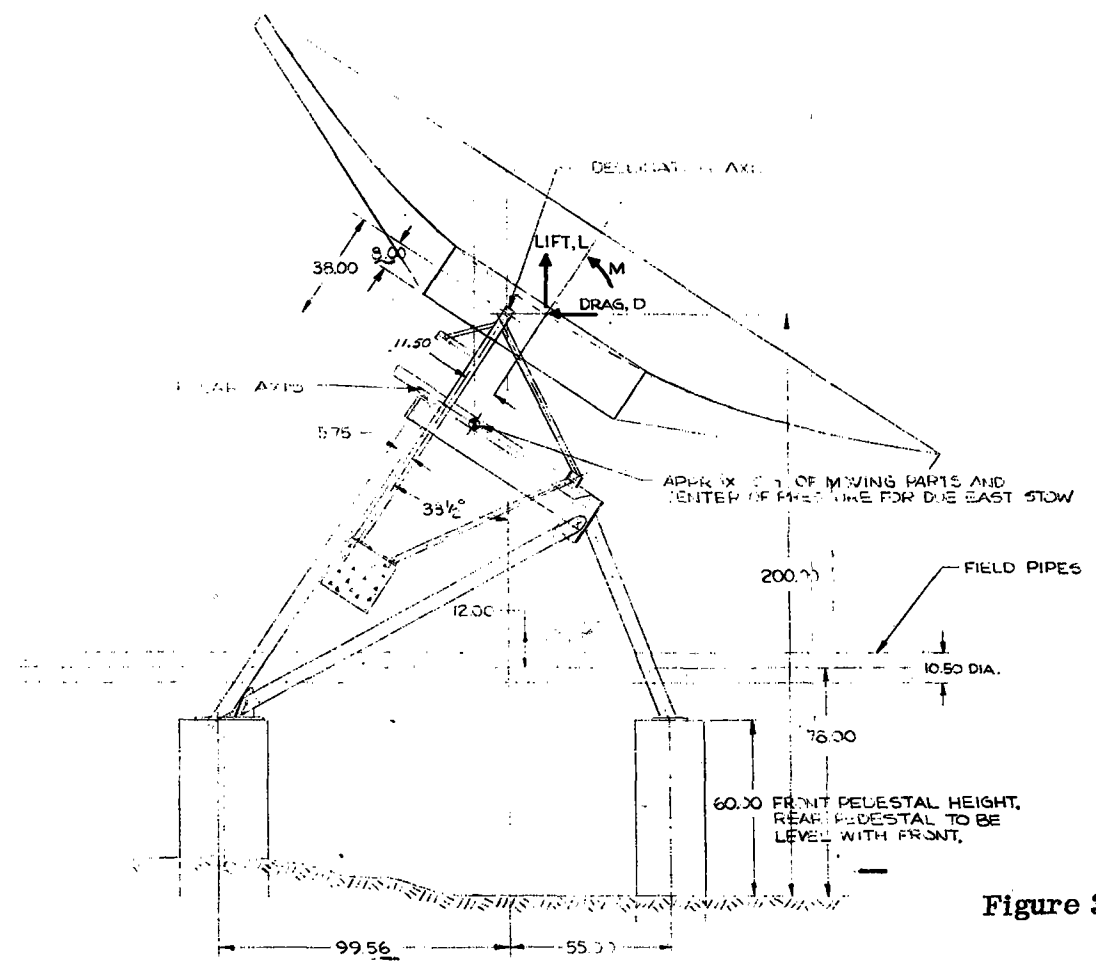
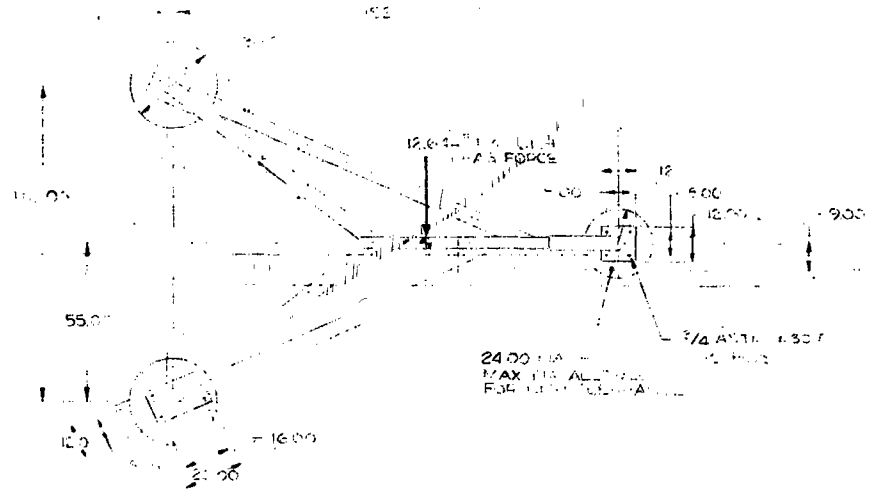


Figure 3.2-32. Collector Geometry

B
C
D
E
F
G
H
I
J
K
L
M

1 2 3 4 5 6 7 8 9 10

wind torque) and the declination axis as near as possible to the boresight axis (to minimize declination axis torque). Dimensions for the rear legs of the base frame were then established to minimize the clearance with the counterweight. In general, the design was configured to keep the plane of action of the polar actuators as close as possible to the yoke structure to minimize offset torques and to spread the base rear legs as much as possible to maximize the foundation footprint (within dish clearance allowances).

The base frame sits on three concrete cylindrical pedestals 1.5 meters (5 ft) high. The 1.5 meter height was chosen to be as high as possible without causing interference with the dish. Available clearances were checked by descriptive geometry layouts and finalized by use of the Applicon, a computer aided design technique. Clearances are more fully discussed in a later section. The concrete pedestals approach provides a large total structural stiffness and minimizes material costs. The estimated cost for the 1.5 meter (5 ft) high pedestals (two 26 in. diameter and one 20 in.) at the Shenandoah site is:

Concrete	1.77 yd ³ @ \$43/yd ³	=	\$76.11
Steel	300 lb @ \$0.22/lb	=	66.00
Forms	2 x 26 in. x 5 ft @ \$3.84/ft	=	38.40
	1 x 20 in. x 5 ft @ \$2.79/ft	=	13.95
Labor	\$14/pedestal	=	42.00
			<u>\$236.46</u>

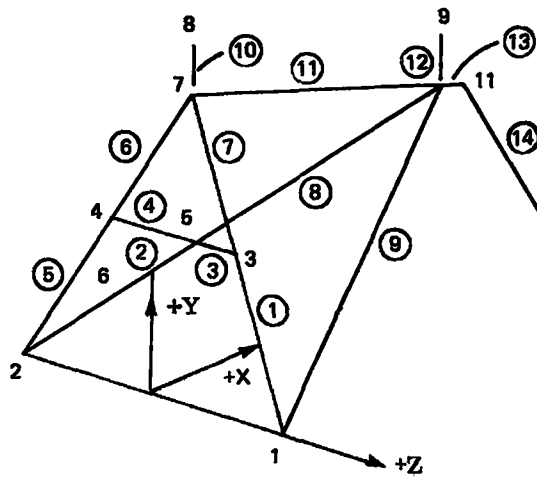
If the base frame is attached to the foundation at ground height, the pipe size would have to be increased to accommodate the AISC code condition for long slender members. A comparison of weights and cost for the baseline design yielded the following results:

Pedestal Height	5 ft	0 ft
Pipe Size	4 in. sch 40	5 in. sch 40
Length	57.83 ft	91.25 ft
lb/ft	10.8	14.6
Total wt.	524	1334
Cost @ 36¢/lb	\$224.64	-
Cost @ 60\$/lb	-	800.40
		$\Delta = \$575.76$

The 0.13 meter (5 in.) pipe is not available in the ASTM-537 Grade B BW (butt welded) as is the 0.10 meter (4 in.) pipe, and the price of the 0.13 meter (5 in.) pipe is over 60¢/pound. The saving for the baseline design is therefore \$ 800.40 - (\$ 224.64 + 236.46) = \$339.30. Subsequent evolution of the design resulted in a change to square tubing. The cost saving becomes only \$ 480.24 - (\$ 224.64 + 236.46) = \$19.14. However, to this material cost must be added other considerations such as the more difficult job of transporting, handling, fabricating, and welding the longer steel sections of the base frame without the pedestals. Therefore, the five foot pedestal configuration was selected for the foundation design.

The structural stress analysis for the base frame was done using a GE computer program. Inputs to the program include the structure dimensions, properties, type of joints (pinned, welded etc.), and applied loads. Output includes reactions on each member from which a free body diagram can be drawn and member distortion and deflection of the frame can be obtained.

The collector base frame is modeled as shown in Figure 3.2-34. The model includes the frame on the 1.5 meter (5 ft) high pedestals and incorporates the loadings from the computer model of the yoke frame structure discussed in the next section. The member weights were neglected, and the input included forces at points 8 and 9, the bearing blocks, and point 6, the polar axis actuator attachment point.



COLLECTOR FRAME

MEMBER	DESCRIPTION	SECTION	CRITICAL MEMBER JOINT		LOAD CONDITION	FS
① ② ⑤ ⑥	AFT LEGS	4 x 4 x 1/4 (TUBE)	⑥	7	90 MPH EAST	1.54
③	ACTUATOR ATTACH	6 x 2 x 3/8 (TUBE)	③	5	90 MPH SOUTH	1.33
② ④	CROSS BRACE	8 x 4 x 1/4	④	4	90 MPH SOUTH	3.3
⑪ ⑬	BEAM	8 x 4 x 33 (TUBE)	⑪	7	90 MPH SOUTH	7.3
⑧ ⑨	DIAGONAL BRACE	4 x 4 x 1/4 (TUBE)	⑨	10	90 MPH EAST	1.88
⑭	FWD LEG	4 x 4 x 1/4	⑭	11	90 MPH EAST	6.7

Figure 3.2-34. Collector Base Frame Model

3.2.7.1.2 Yoke Structure

Figure 3.2-35 shows the design layout of the yoke structure. The main component of the yoke structure is the polar axis shaft which is held by two bearing blocks at the front and rear of the base frame backbone. The polar axis shaft extends beyond the rear bearing to provide a pivot support for the polar axis swing arm assembly described below. The second polar axis actuator pushes or pulls on the yoke frame to provide the proper torques about the polar axis. The yoke structure extends upward from the shaft to support the declination axis pivot shaft bearings and downward to support the counterweight. The shaft was designed to spread the bearing supports as much as possible to reduce reactions and also to provide a space framework rather than having all the members in a single plane from the declination axis to the counterweight.

The yoke structure is composed of rectangular or square structural steel shapes which are lower in cost than pipe or tubing in these sizes and easier to fabricate. The yoke stress analysis computer model is shown in Figure 3.2-36. Load inputs are at nodes 10 and 11 which is the declination axis location and at node 4 where the declination actuator attaches. Supports at nodes 2 and 8 model the bearing block in a manner such that moments about the shaft are released. Members 19 and 20 are the polar axis jack screws which were modeled as being pin-ended but not with spherical sockets.

The minimum factors of safety calculated for the yoke members are summarized in Table 3.2-12. All members meet the code design requirements. For the jackscrew at joint 13, the computer model did not release forces parallel to the end pin's axis; thus the structural deflection caused a large side moment to be imposed on the jackscrew. In actuality, the pin hole will have sufficient clearance to avoid side loads on the jacks.

3.2.7.1.3 Counterweight

The counterweight is designed (Figure 3.2-37) to balance the dish approximately about the polar axis only. The counterweight reduces the size of the motors needed to drive the polar actuators, thus reducing the collector field parasitic electrical load. Although parasitic load reduction is essential to reduce peak electrical demand, the counterweight is cost effective under normal operation.

The 910 kilogram (2,000 lb) counterweight cost is estimated (based on 192 units) at:

Concrete	1/2 yd ³ @ \$43	21.50
Steel (Yoke frame + bolts)	126 lbs. @ .24¢/lb	30.24
Forms (4 forms @ \$500 each)		10.42
Labor - Pour concrete		28.00
Weld Yoke support - CWT portion		60.00
Install CWT. (12 bolts)		45.00
		<u>\$195.16</u>

Without the counterweight, the motor ratings for the polar and defocus drives would have to be increased, heavier electrical lines and relays would be required, and additional parasitic power costs would be incurred. The cost differences are:

	<u>Cost Difference</u>
Polar Drive Motors (2)	\$134.10 (1/10 HP vs 1/2 HP)
Defocus Motor (1)	145.48 (1-1/2 HP vs 5 HP)
20 year Power Cost (at 5¢/kw-hr)	<u>92.15</u>
	<u>\$371.73</u>

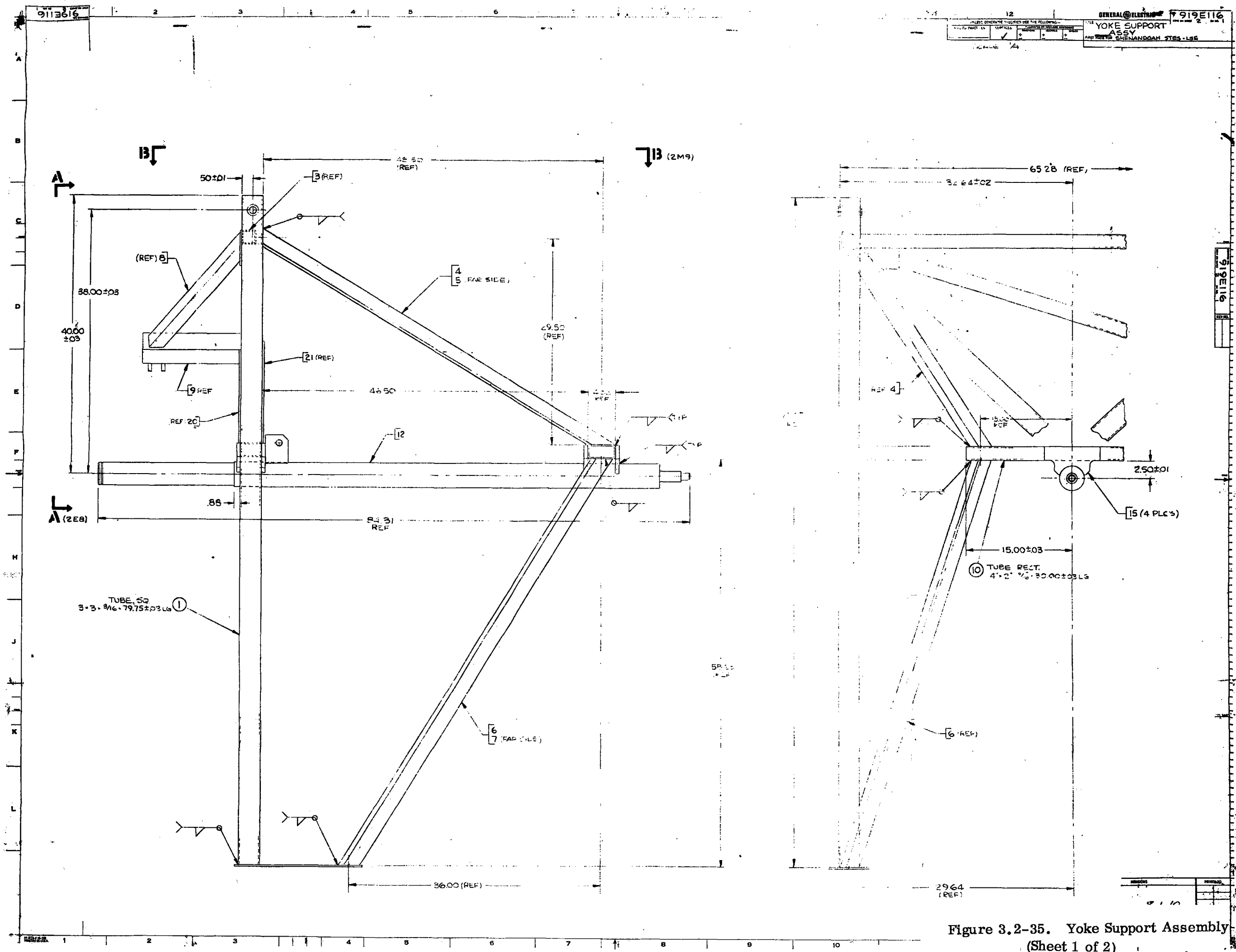


Figure 3.2-35. Yoke Support Assembly
 (Sheet 1 of 2)
 3-57/3-58

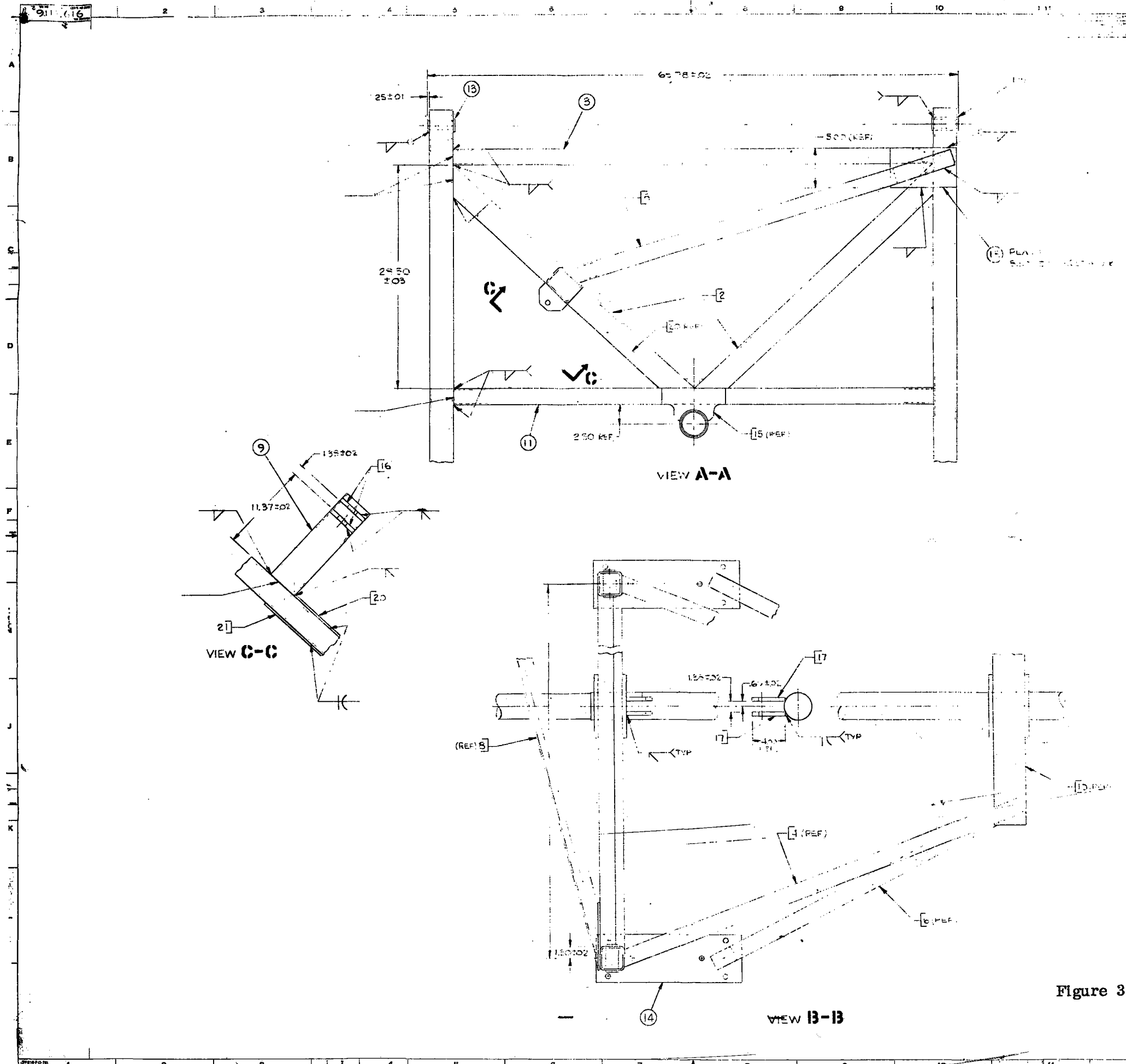


Figure 3.2-35. Yoke Support Assembly
 (Sheet 2 of 2)

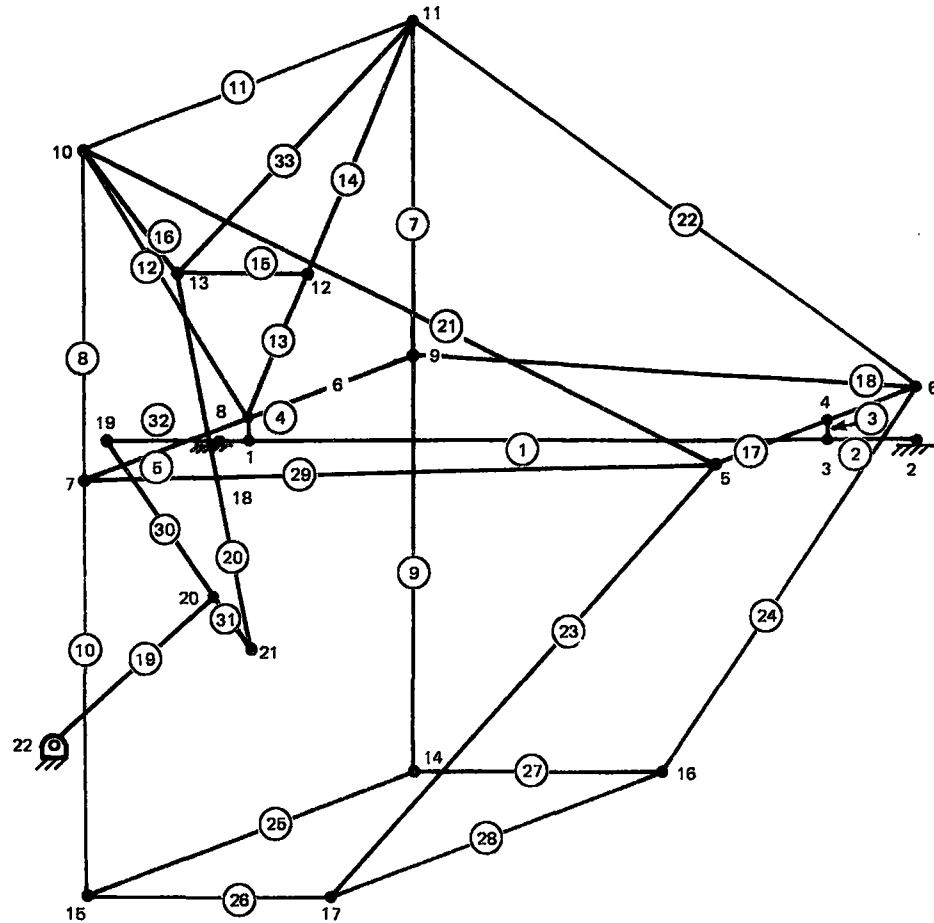


Figure 3.2-36. Yoke Stress Model

This a \$ 177 savings per collector is realized with the counterweight (without accounting for the savings accrued by using lighter relays and wiring in the drive unit power circuits).

3.2.7.2 Drives

The drive mechanism provides controlled motion of the reflector about the polar and declination axes. Although there is a wide variety of off-the-shelf commercial hardware that can perform this function, candidate hardware must satisfy both high stiffness and low cost requirements. This limits the available hardware and control approaches to a narrow set of options.

To minimize costs, immediate consideration was given to the simplest type of actuation control: an on-off system. With this scheme there are no requirements for control-type actuators or servo-amplifiers. With polar/declination axes, the only control normally used will be a polar axis drive with an essentially constant $15^\circ/\text{hour}$ rate.

The drive mount and tracking system accuracy requirement is ± 0.25 degree rms from the true boresight line to the sun. The approach selected to accomplish this with an on-off system is shown in Figure 3.2-38. The polar drive is off for approximately 57.5 seconds while the sun moves about 0.25 degree. In the middle of this time period, the sun spot will center on the receiver aperture. At the end of the time period, the drive is turned on for about 2.5 seconds moving the reflector at a rate of 0.1degree/sec and repositioning the sun image on the receiver back to the starting position. This technique is one of many where the reflector speed and allowable error band can be changed within limits. In this case the 1/8 degree error band allows the structure and drive stiffness to be such that the wind (up to 13.4 meters/second or 30 mph) can, during the 57.5 second rest period, move the dish a maximum. The 13.4 meters/second (30 mph) wind was characterized as having a mean of 10 meters/second (22.5 mph) with a varying component

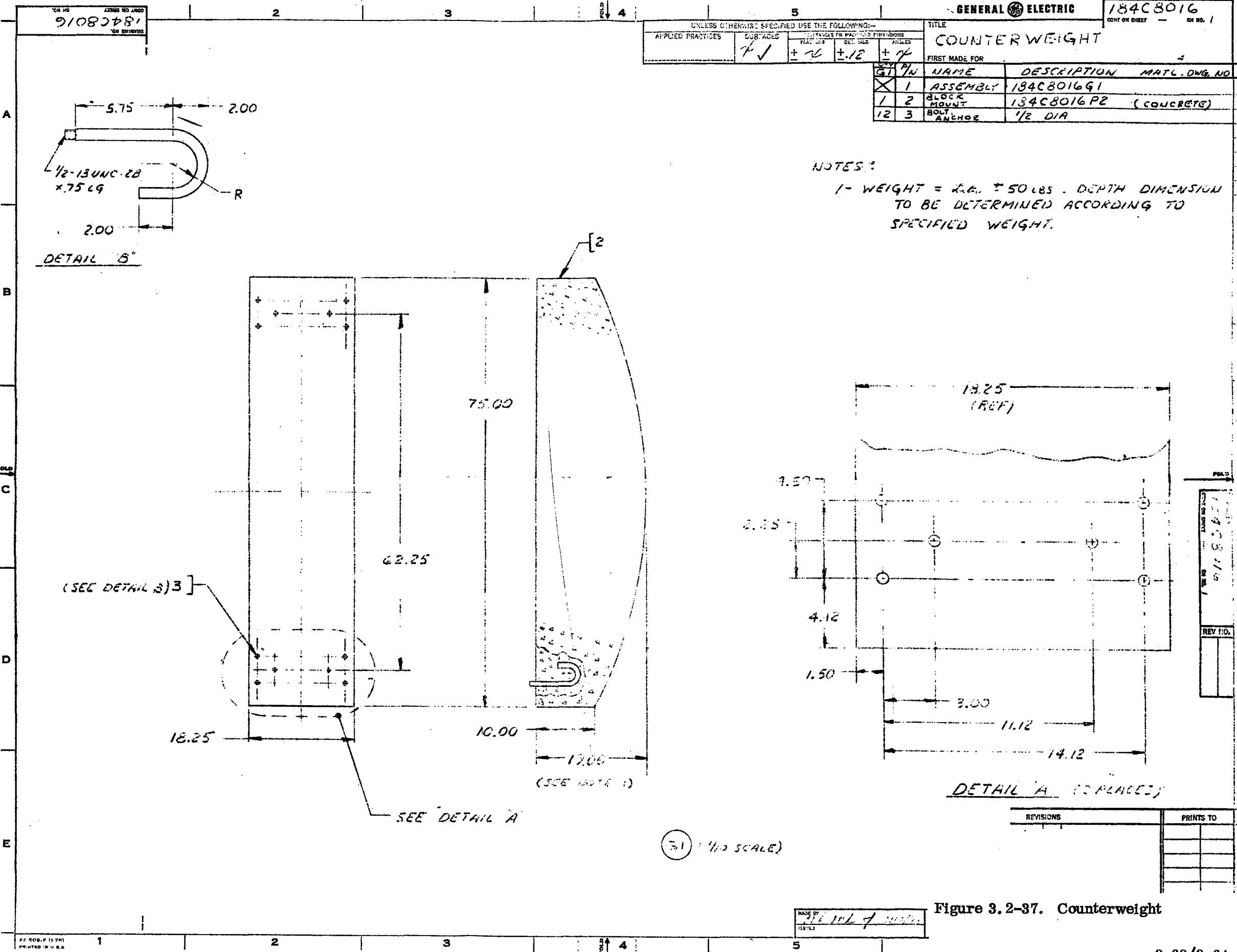


Figure 3.2-37. Counterweight

Table 3.2-12. Yoke Stress Analysis Summary

Member	No.	Critical Joint	Factor of Safety	Critical Load Condition
Shaft	1, 2, 29	18	1.48	Noon, E. Wind
	32	18	1.08	Noon, E. Wind
Plates	3, 4		1.48	Noon, E. Wind
Cross Pieces	5, 6	8	2.8	Noon, E. Wind
	17, 18	4	1.18	Noon, E. Wind
Uprights	7, 8, 9, 10	14	1.6	6 AM, E. Wind
Back Frame	11	11	5.4	6 AM, S. Wind
	12	8	1.29	Noon, E. Wind
	13	12	1.01	Noon, E. Wind
	14	12	1.40	Noon, E. Wind
	16	10	1.80	Noon, E. Wind
	33			
	15	12	2.41	Noon, E. Wind
	35	13	1.58	Noon, E. Wind
Jacks	19, 20	13	0.37	Noon, E. Wind
Braces	21, 22	11	2.63	Noon, E. Wind
	23, 24	5	2.70	6 AM, S. Wind
Swing Arm	30	20	2/73	Noon, E. Wind
	31			

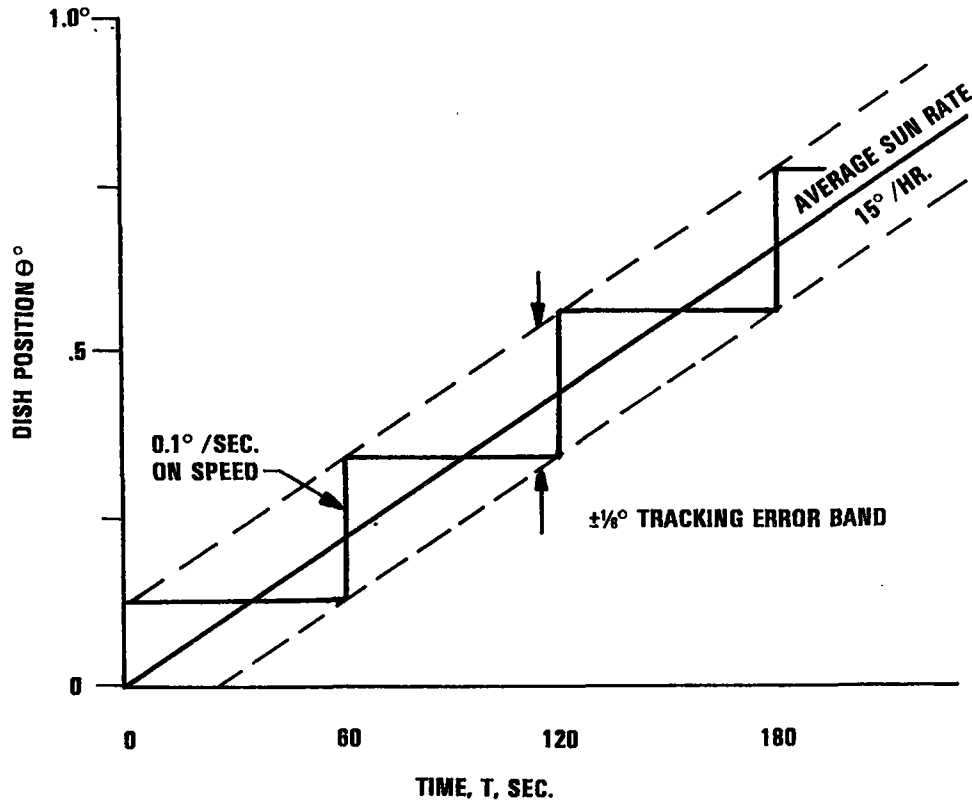


Figure 3.2-38. On-Off Control for Polar Drive

of 3.4 meters/second (7.5 mph). Thus, a 6.8 meters/second (15 mph) change in wind speed is possible during the rest period. The control approach (discussed later) compensates for the steady wind components, but the structure should not deflect more than 1/8 degree during wind gusts.

Selection of the tracking drive approach led to the derivation of a design requirement for stiffness about the polar axis. With the data from Table 3.2-11 for the reflector drag and with the known distance from the polar axis to the dish vertex, the polar axis torque can be calculated as a function of the polar axis angle. It was found that the maximum torque does not occur exactly at the noon position ($\theta = 90^\circ$) but closer to $\theta = 100^\circ$. For a 6.8 meters/second (15 mph) wind variation, the torque variation is about 4068m-N (3000 ft-lb). $K_0 = 1.86 \times 10^6 \text{ m-N/rad}$ ($1.375 \times 10^6 \frac{\text{ft-lb}}{\text{rad}}$), where K_0 is the total stiffness of the foundation, base

frame, polar axis drive, yoke, dish, and receiver support structure. Since these elements act as springs in series, each element must have considerably higher stiffness.

The speed required by the polar axis drive is based on consideration of both the normal tracking mode and other drive requirements. It is necessary to have a full-on speed sufficiently fast so that maintenance defocus or emergency stow procedures would not have to wait long periods of time to return the dish. These off-normal drive requirements led to the drive speed requirements selected. A 0.1 degree/second speed means the dish can move through a full 180 degree arc in 30 minutes, and if both polar axis drives are used, the time can be reduced to 15 minutes. On the other hand, speeds much faster than that selected would mean very short motor turn-on times causing control queing problems and, because of higher acceleration, the possibility of less smooth operation.

Another consideration related to wind loading is the desirability of low backlash and high resistance in the drives to being driven mechanically in the reverse direction. Some backlash is allowable to avoid the expense of backlash controls, but a drive system with inherently low backlash is advantageous. The resistance

to mechanical drive is related to the stiffness since, during the rest period, a variable wind must not cause a locked or braked actuator to move causing activation of the control.

Based on these design criteria, a tradeoff matrix considering both rotary and linear actuators was derived as shown in Table 3.2-13. The table indicates the two major candidates: hydraulic cylinders with simple solenoid valve control and mechanical jackscrews driven by electric motors controlled by relays. A further trade-off between these two candidates is given in Table 3.2-14. From these analyses the jackscrew was selected for the collector drive. The two main considerations that eliminated the hydraulic drives were the stiffness and power supply considerations. To achieve the required stiffness, the hydraulic cylinders were larger and longer than would be ordinarily required and hence costlier. In addition, an individual power supply for the collector was impractical since at the full 4068m-N (3,000 ft-lb) torque requirement the delivered actuator power is only 7.5 watts (0.01 hp). Hence, the hydraulic power supply would have to be centrally located with fluid piped to each collector. The cost of the tubing material and its installation was a factor that added appreciably to the cost.

The jackscrew is widely used in solar collector applications. The actuator is available in several configurations including choice of a ball-screw with a high efficiency or with a standard machine or ACME thread screw. The latter was chosen since it is inherently self-locking; thus the stiffness is very high. The typical commercially available jackscrew has a worm gear input drive, the worm gear driving the nut and the screw linearly extending without rotation. If the ball screw is used, the load drives back into the worm, and the stiffness is less because of the compliance of the worm gear set.

The ball screw drive costs more than the self-locking machine screw, and the power savings can be estimated to determine if the extra cost is warranted. The jackscrew motor runs 30 minutes/day which, for everyday over a 20 year period, is 3,650 hours. The motor is sized at 7.5 watts (0.1 hp) for the machine screw, and, assuming an average power of half peak, the total energy requirement is 7.5×10^7 Joules (220 kW-hr). At 5¢/kW-hr the power cost is \$11. Assuming the ball-screw would cut the power by the ratio of the manufacturers published efficiency, the cost for the ball-screw would have to be $\frac{22}{70} \times \$11 =$

\$3.50 or a net savings of only \$7.50. The extra cost of the brake and ball-screw exceed this savings considerably.

The jackscrew has been sized to withstand the worst case loadings of a 40 meters/second (90 mph) wind for any position of the reflector. Under worst conditions the jacks could be extended and subjected to high column loadings. Considering the actuator design and the type and location of the end supports, designing it as a column per the AISC code required a 10 ton model jack.

After the jackscrew was sized, the motor requirements were determined from screw jack manufacturer data. For the 10 ton jack, a motor speed of 40 rpm is required to produce a maximum dish speed of 0.14 degree/second and a minimum of 0.1 degree/second. The variation in speed is due to the change in effective radius of the crank arm. A 30 rpm input will produce a maximum speed of .105 degree/second and minimum of .075 degree/second. The torque requirements are 15.8m-N (140 in-lb). The drive motor was selected on the basis of torque, speed, and service life requirements. It was previously shown that motor life could be less than 4,000 hours under the assumption of full travel each day of the 20 year life. With the relatively low life and low power requirements (0.088 hp), selection of a normal industrial gear motor is not cost effective. There are several manufacturers of low cost ac gear motors used typically for vending machines, hospital beds, office machines, and other light industrial uses. The ac motor is least costly and will meet the start and pull up characteristics desired if a Capacitor Start Induction Run (CSIR) winding is used rather than a shaded pole configuration.

Because of the low motor power, the control can employ relays rather than magnetic starters. Although the dish inertia is very large, about 6100m-N-sec² (4,500 ft-lb sec²), the ratio between dish speed and motor speed is very large, about 100,000:1. Hence the reflected inertia, I/n^2 , is very small (less than 1.6×10^{-8} m-N-sec² or 10^{-4} in-oz-sec²). Thus, as start-up, the motor will essentially see only the frictional torque of the drive system (besides its own inertia). Frictional torque was estimated at

Table 3.2-13. Actuator Selection

<u>Selection Criteria</u>	
1. Meet or Exceed Required Stiffness	
2. Provide Variable Speed Requirement	
3. Reasonable Backlash	
4. Non-Back Drivable	
5. Low Cost, Including:	
- Capital	
- Installation	
- Maintenance	
<u>Candidate Actuators</u>	<u>Reason for Rejection</u>
Rotary	
● Pneumatic Motor + Gear Box	Maintenance and Stiffness
● Hydraulic Motor + Gear Box	Costs
● Electric Motor + Gear Box	Stiffness
Linear	
● Hydraulic Cylinder	Acceptable
● Pneumatic Cylinder	Stiffness
● Jack Screw	
- Pneumatic Motor	Maintenance
- Hydraulic Motor	Costs
- Electric Motor	Acceptable

Table 3.2-14. Hydraulic Cylinder vs. Electric Jackscrew Actuator Tradeoff

Actuator Type	Advantages	Disadvantages
Screwjack	<ul style="list-style-type: none"> ● Stiffer ● Simpler Power Supply ● Less Maintenance ● Long Life 	<ul style="list-style-type: none"> ● Speed Control
Hydraulic Cylinder	<ul style="list-style-type: none"> ● Performance 	<ul style="list-style-type: none"> ● Leaks ● Adds Another Subsystem

Cost Comparisons (Polar Drive)

<u>Screwjack</u>		<u>Hydraulics</u>	
Jack Screw (2)	\$ 600	Cylinders (2)	\$ 700
Gear Motors (3)	280	Valves (2)	300
Controls (Relay Box)	200	Hyd. Power Supply and Accumulator	150
Installation (3 Motors)	60	Installation	160
	<u>\$1140</u>		<u>\$1310</u>

about 165m-N (122 ft-lb) which is less than five percent of the rated output torque. Hence, the motor will start and accelerate in a few milliseconds to its operating speed.

A defocus requirement was established for the collector in the event of a flow stoppage to prevent the Syltherm 800 fluid from overheating. The requirement was established for a 2 degree/second dish defocus speed. For the maximum torque design requirement, this speed requires a 1.12 to 1.3 kW (1-1/2 to 1-3/4 HP) rated motor. Since the defocus could be required during a power outage, a back-up power source is also required. The cost of distributing emergency power from a central backup was considered but a lower cost approach was developed using 12 Vdc batteries at each collector to drive automotive type starter motors for defocus. The individual batteries also avoid the problem that single point failures in an emergency power distribution system can cause overtemperature in a large portion of the collector field.

To meet the defocus torque/speed requirements, a 12V dc motor used typically for winch operation was chosen. This motor is reversible and requires less modification to mount to the screw jack than a starter motor but costs \$122 rather than \$50. The price is still well below that of a standard NEMA frame dc motor and was considered to be cost effective for the Shenandoah application. The jack/motor assembly is shown in Figure 3.2-39.

The defocus motor is mounted in parallel with the AC motor on one of the polar axis screw jacks. A single defocus motor is sufficient since only ten degrees is needed to defocus the collector. The standard screw jack includes a worm shaft extending in two directions. The AC motor drives the screwjack and defocus through an electromagnetic clutch/coupling which is engaged to close when power is on. With ac power off, the defocus motor cannot mechanically drive the AC motor in the reverse direction (which would damage the ac motor because of the high speed defocus drive speed).

The polar axis drive mechanism uses an intermediate swing arm assembly as shown in Figure 3.2-40. The first jackscrew is pin jointed to the base frame and pushes on the swing arm which pivots freely about the polar axis. The second jackscrew is mounted on the swing arm and pushes on the yoke frame supporting the dish. The screw jacks are separately driven and are normally driven alternately to provide nearly equal extension. Both can be run simultaneously, however, which doubles the speed during refocus to prevent excessive heating of the receiver aperture ring and the receiver support struts.

3.2.8 RECEIVER ASSEMBLY

3.2.8.1 Receiver

The function of the receiver is to transfer the energy at the focal plane of the dish into the heat transfer fluid. The requirements established for the collector that directly influence the receiver design include:

1. A dish slope error $\leq 1/2$ degree rms which determines flux levels impinging on the receiver heat transfer area.
2. A concentration ratio of approximately 250 which sets the aperture size of the cavity receiver and is a measure of energy intensity.
3. A pressure drop of 34,500 N/m² (5 psi) and a fluid film to bulk temperature drop less than 56°K (100°F). These last two requirements cause design conflicts since lower ΔT 's require higher heat transfer film coefficients, higher fluid velocities, and thus higher ΔP 's.

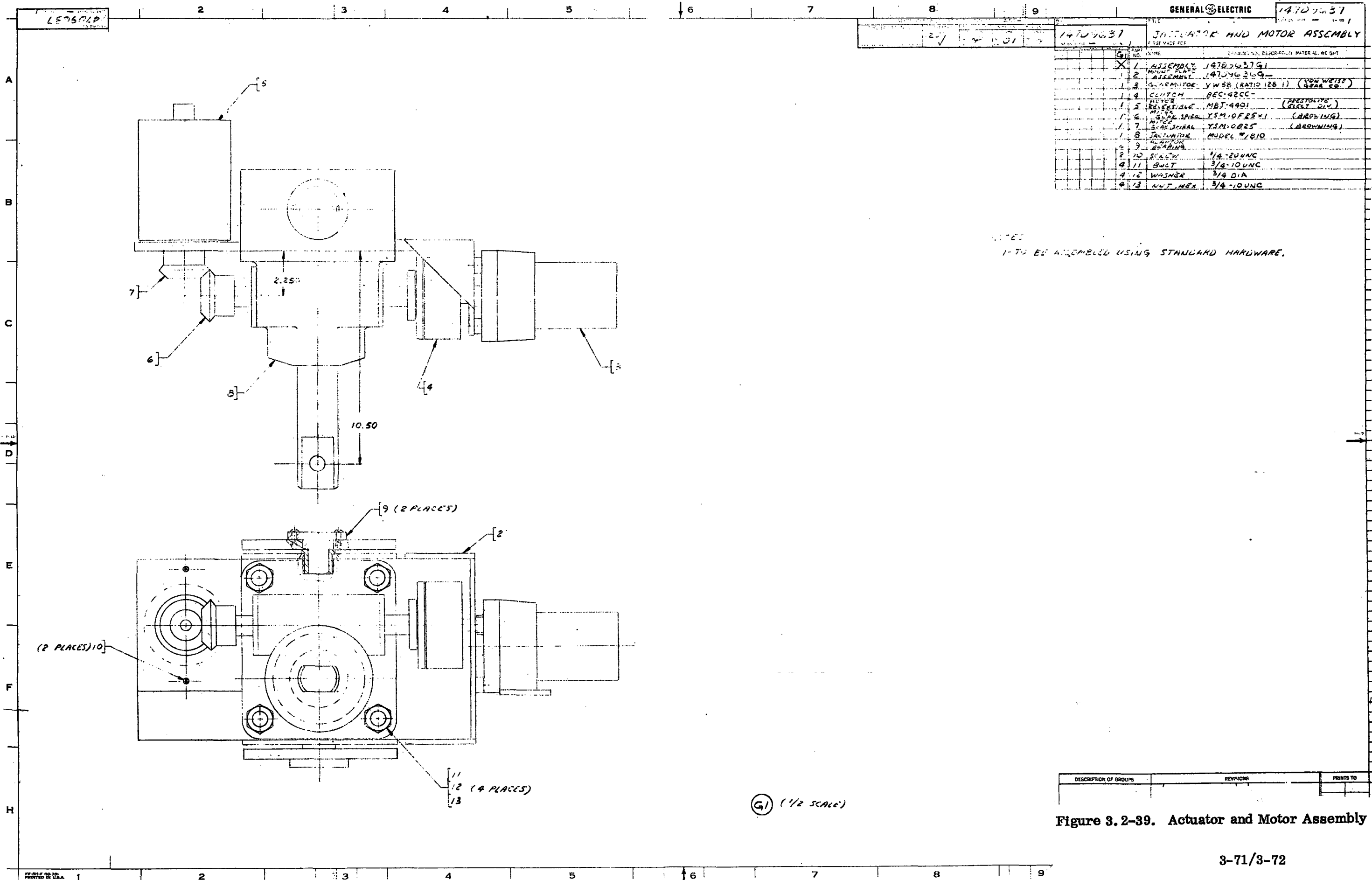


Figure 3.2-39. Actuator and Motor Assembly

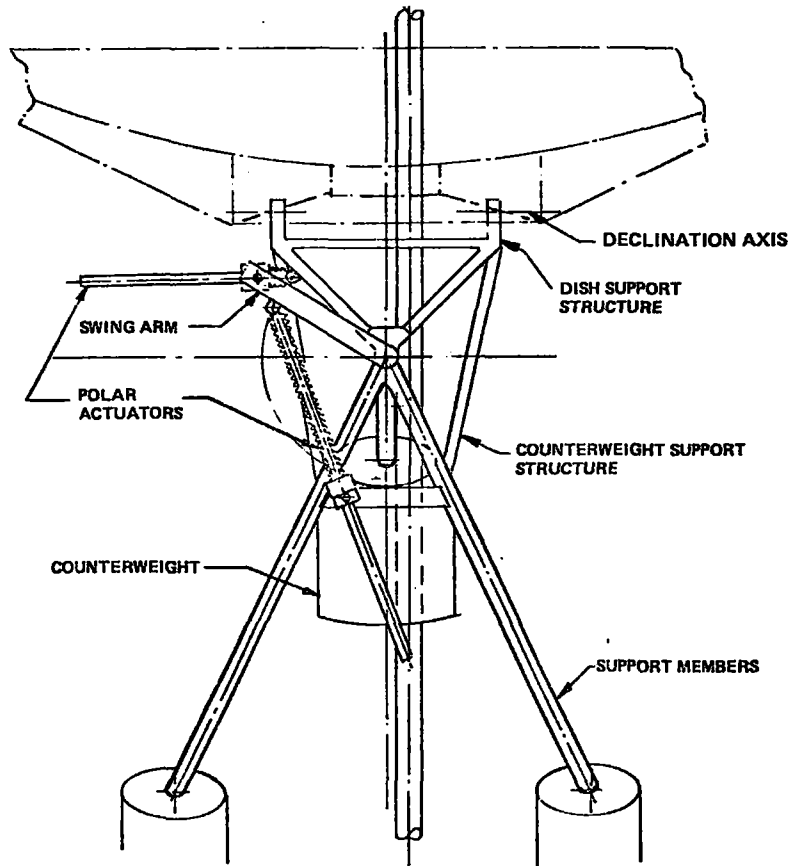


Figure 3.2-40. View of Polar Axis of Dish Drive Mechanism

The first step in sizing the receiver was to define the energy environment in which the receiver must operate. Figure 3.2-41 presents the peak flux level on the cavity wall as a function of the coil diameter for slope errors in the regime for which the collector was designed. These flux levels are for a peak solar insolation of 946 W/m^2 (300 Btu/hr-ft^2). As can be seen the larger the coil diameter, the lower the peak flux will be. The peak flux was chosen as the pertinent parameter since this would be the region of maximum fluid film-to-bulk temperature difference.

The required average film coefficient can be determined knowing the peak flux levels, the relationship of film coefficient from the front side to the back side of the coil tube, and a film-to-bulk temperature drop of 56°K (100°F). The required film coefficient is given in Figure 3.2-42 as a function of coil diameter: the larger the coil the lower the peak flux level and the lower the required film coefficient. Also plotted in the figure is the delivered fluid film coefficient as a function of the coil tube inside diameter. Since the flow rate is fixed for the specified design ΔT , higher velocities and delivered film coefficients require smaller tube inside diameters. By comparing the required to the actual film coefficients (i.e., film coefficient matching), the required tube inside diameter can be specified as a function of coil diameter. This is plotted in Figure 3.2-43 as a function of dish slope error. The aperture size of the receiver for the design concentration ratio of 250 is also indicated. The difference between the aperture size and the coil diameter is the coil set-back.

Figure 3.2-43 also shows the fluid pressure drop per 30 meters (100 feet) of tubing length as a function of tube inside diameter. With the higher velocities associated with smaller tube diameters, the pressure drop per unit length increases. Combining the characteristics depicted in this figure and calculating the length of tubing required to fill up the cavity space as a function of tube diameter and coil diameter, pressure drop as a function of coil diameter can be determined. This is shown in Figure 3.2-44 for a single spiral coil configuration. As can be seen, to maintain the system pressure drop requirement of $34,500 \text{ N/m}^2$ (5psi), a

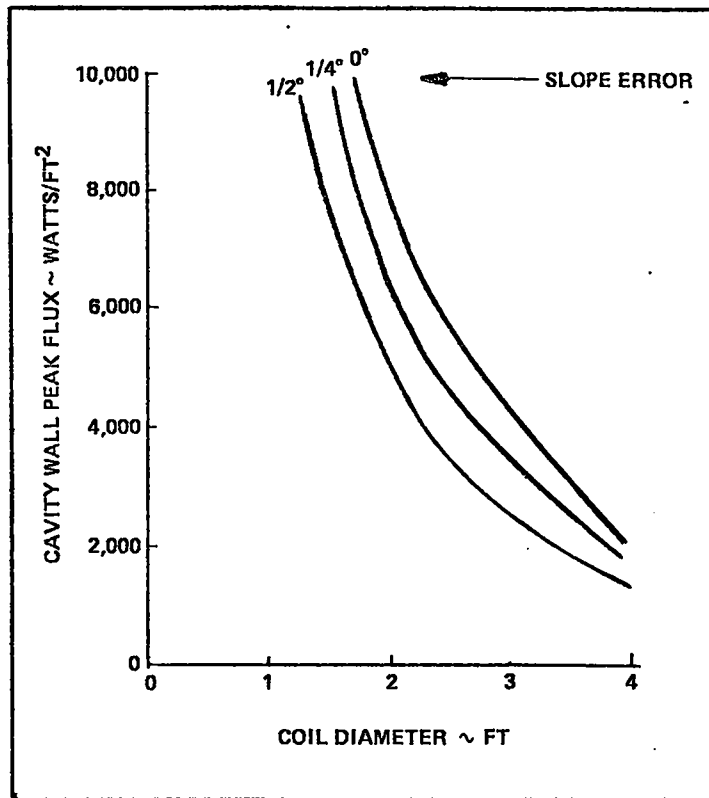


Figure 3.2-41. Receiver Design Flux Levels

coil diameter of 0.92 meter (3.0 feet) is necessary for the slope error range of the collector. Since the aperture size for the concentration ratio of 250 is much smaller than this, there is a large coil setback required. This adds bulk, weight, and cost to the receiver.

The procedure described above was repeated for a twin parallel tube coil configuration. In this configuration, the flow is split within the receiver, and parallel flow paths are established. The results of this approach are shown in Figure 3.2-45. With the parallel tube configuration, the coil diameter can be decreased to 0.69 meter (2.25 ft) 34,500 N/m² psi pressure drop, and the resulting coil set back is much less. This yields a smaller, lighter weight, and lower cost receiver configuration.

A third receiver configuration was investigated to determine the feasibility of alternate construction techniques. This configuration utilizing a flow channel offered no significant performance advantages over the twin parallel tube design as shown in Figure 3.2-46.

A summary of the receiver design analyses is shown in Figure 3.2-47. Based on these results, the double circuit coil configuration was selected for the collector. Significant advantages are substantial size and weight reductions over the single coil configuration, low fluid residence time (an advantage in minimizing overtemperature during emergency defocus), and a design configuration that can minimize thermal stresses.

The receiver preliminary design is shown in Figure 3.2-48. The concentration ratio is 235, and 96 percent of the incident flux is intercepted. Although the requirements for the receiver specified a nominal concentration ratio of 250, to use standard parts in the receiver construction, an 0.46 meter (18 in.) aperture was chosen. The receiver sensitivity analysis showed minimum decrease in performance for this slight decrease in concentration ratio; thus the 18-inch aperture was selected for the design.

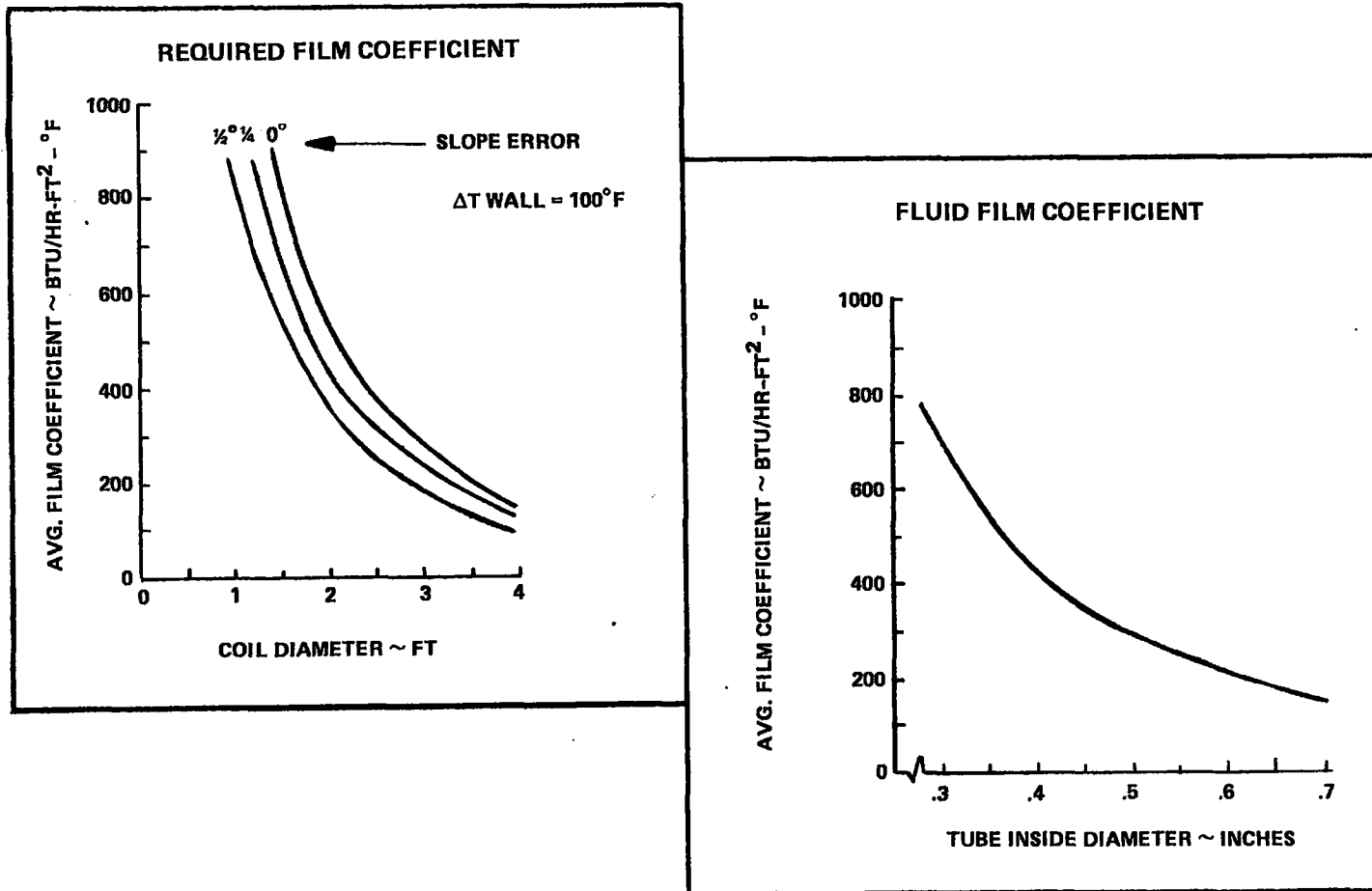


Figure 3.2-42. Receiver Film Coefficient Matching

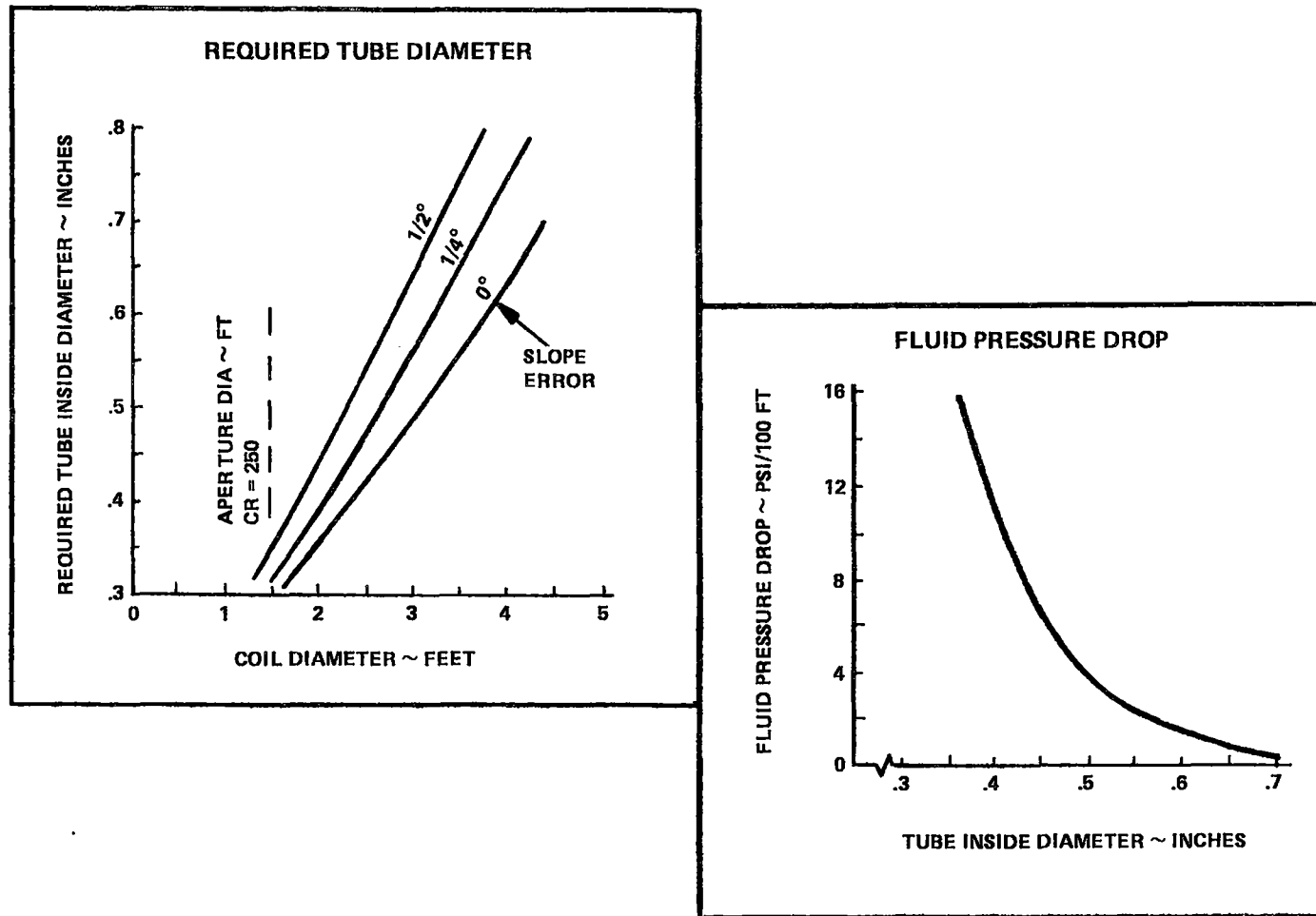


Figure 3.2-43. Receiver Tube Sizing/Pressure Drop Relationship

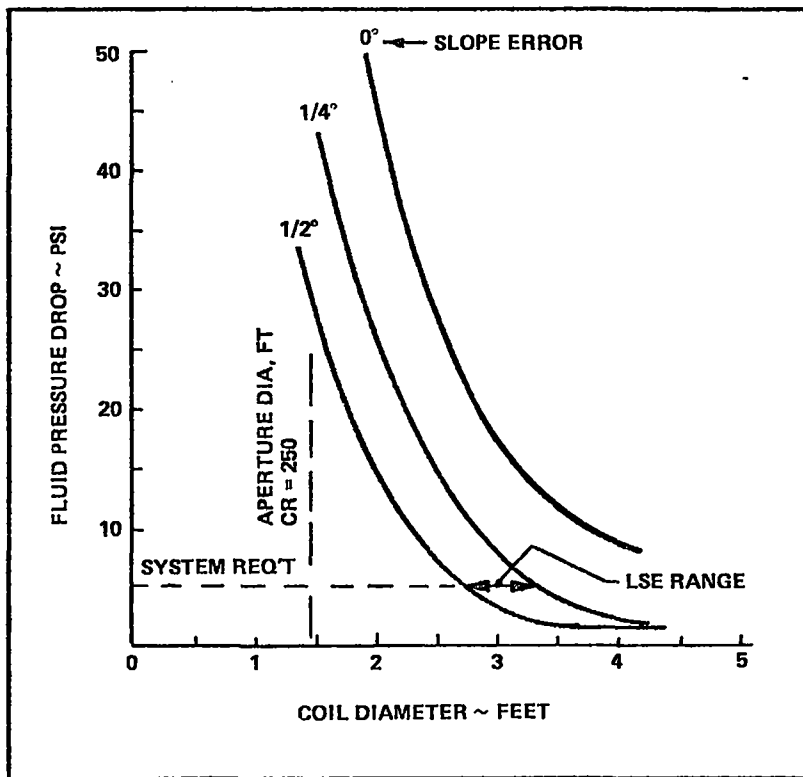


Figure 3.2-44. Receiver Sizing for a Single Coil Configuration

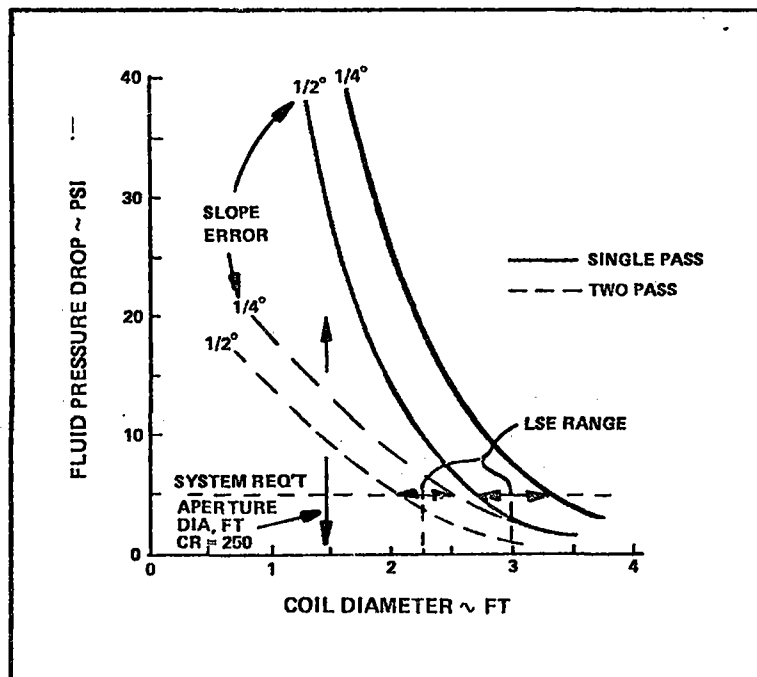


Figure 3.2-45. Twin Parallel Coil Configuration

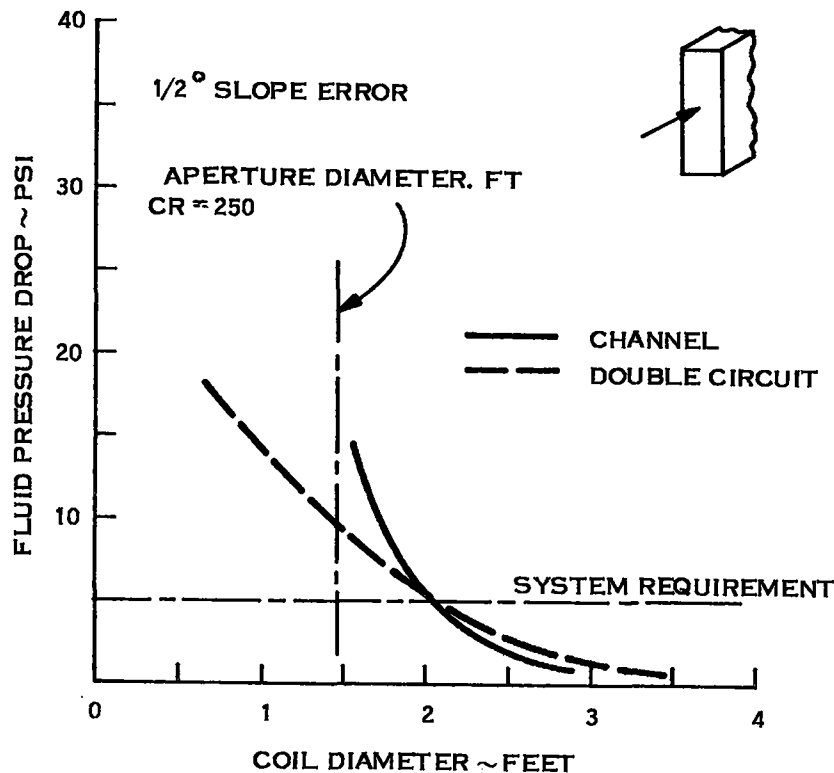


Figure 3.2-46. Channel Flow Receiver Configuration



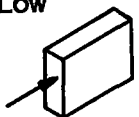
The cylindrical insulation shell has an outside diameter of 0.85 meter (33.5 in.) and a height of 0.89 meter (35 in.) with 0.051 meter (2 in.) of high temperature insulation. The inner wall of the shell is 0.75 meter (29.5 in.) in diameter. The shell outer wall is constructed of a thin wall, low carbon, steel sheet wrapped around a rigid frame and coated on both sides with a high temperature paint. The shell inner wall is constructed of low carbon steel sheet and is porcelainized with a base coat on both sides and a prime diffusely reflective coat on the cavity side. The top plate of the cavity and the face plate of the receiver also have the diffusely reflective coating. The porcelain coating has a reflectance of 0.9 and an emissivity of 0.8.

The heat transfer coil is wrapped into a cylinder with a domed top. The coil is 0.69 meter (27 in.) in diameter and is constructed of two parallel wound, low carbon steel tubes with an outside diameter of 0.013 meter (0.5 in.) and a wall thickness of 0.0015 meter (.058 in.). The total length of tubing is 64 meters (210 ft), 32 meters (105 ft) for each tube. The cold feed tube and hot exit tube are joined to the coil with a header fitting. The tubing is treated to give a high absorptivity of 0.90. Four shaped supports hold the coil in position with the legs being guided into slots in the bottom of the receiver shell. The estimated overall dry weight of the receiver is 75 kilograms (165 lb). The thermal losses for the receiver are a function of the outlet temperature and are tabulated in Table 3.2-15.

3.2.8.2 Receiver Support Structure

The receiver support must be rigid, block out a minimum amount of direct and reflected insolation, provide support for the up/down insulated Syltherm 800 tubing, and affect the dish design as little as possible. Both a four legged strut and a three legged support were examined.

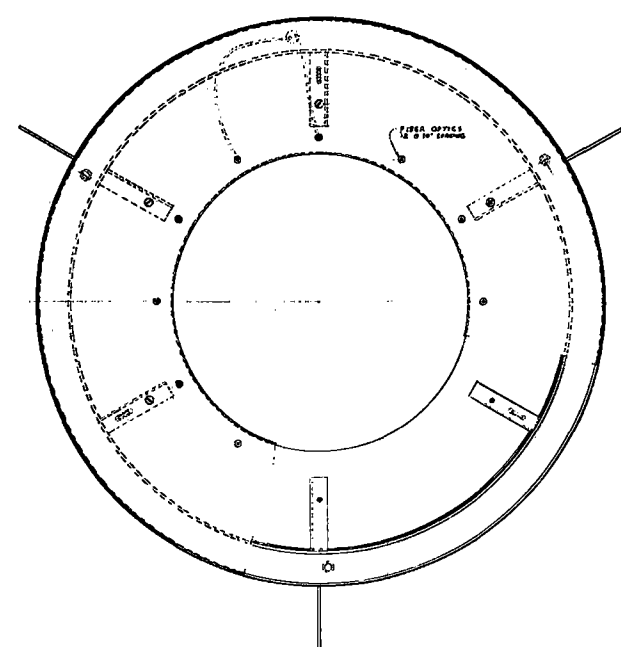
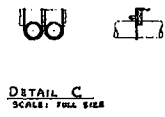
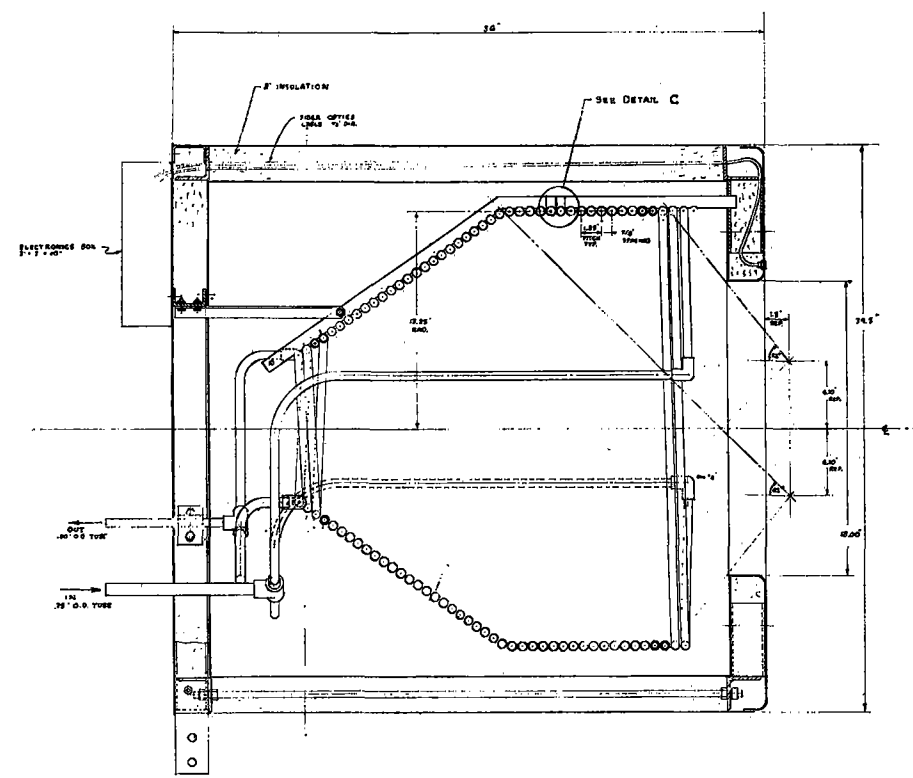
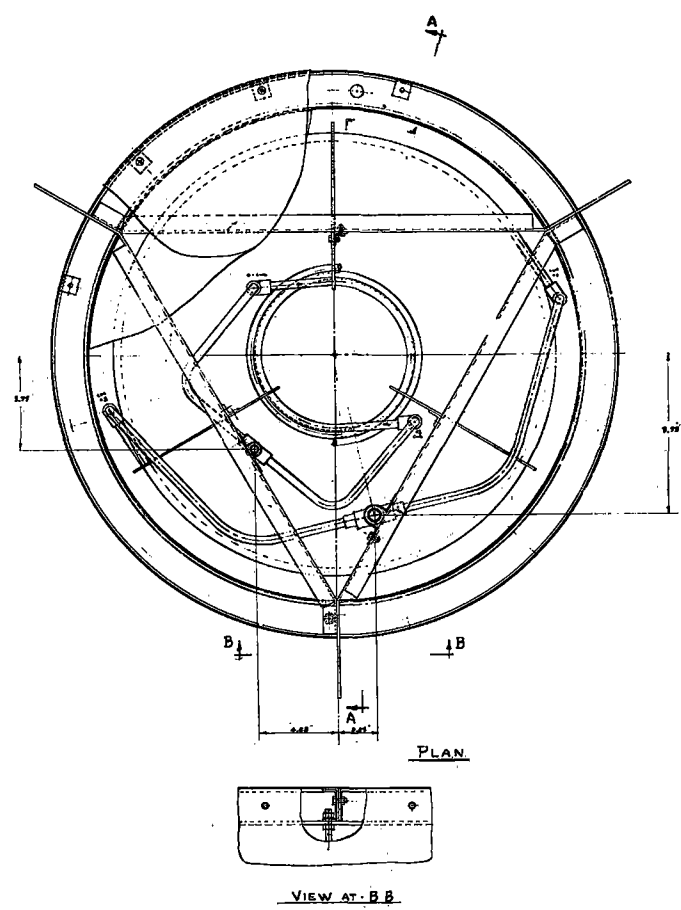
3-79/3-80

CONFIGURATION	PERFORMANCE			PHYSICAL			COMMENTS
	DESIGN POINT THERMAL EFFICIENCY	TURN DOWN RATIO $\frac{M_{MAX}}{M_{LAMINAR}}$	FLUID RESIDENCE TIME SEC.	ENVELOPE DIAMETER X HEIGHT	TUBE SIZE	DRY WEIGHT LBS	
SINGLE CIRCUIT FLOW 	67.5 %	4.5	155	40.5" X 45"	5/8 X 035" 350 FT	315	<ul style="list-style-type: none"> • LARGE COIL SETBACK TO HANDLE PEAK FLUX LEVELS • LONG RESIDENCE TIME • SLIGHT PERFORMANCE ADVANTAGE
DOUBLE CIRCUIT FLOW 	67.0 %	4.0	24	33.5" X 35"	7/16" X 035" 2 X 80 FT	165	<ul style="list-style-type: none"> • SUBSTANTIAL SIZE/WEIGHT REDUCTION • SUBSTANTIAL REDUCTION IN FLUID RESIDENCE TIME
CHANNEL FLOW 	67.0 %	3.8	63	29.5" X 33"	<u>CHANNEL GEOMETRY</u> 0.25" WIDE X 1.0" HIGH	150	<ul style="list-style-type: none"> • SMALLEST, LOWEST WEIGHT DESIGN • POTENTIAL COST REDUCTIONS • THERMAL STRESS AND INTERNAL LEAKAGE MUST BE ASSESSED

SELECTION

- DOUBLE CIRCUIT FLOW SELECTED FOR LSE
- WEIGHT/COST REDUCTION WILL BE EMPHASIZED

Figure 3.2-47. Receiver Configuration Selection



DESIGNED BY	DATE	REVISIONS	GENERAL ELECTRIC
CHECKED BY	12-1-42	1	A. S. D.
APPROVED BY			GENERAL ELECTRIC
			15E LAYOUT # 2
			8-1/16
			17237 221 R 9 4 9

Figure 3,2-48. Receiver Assembly

Table 3.2-15. Receiver Thermal Performance

Outlet Temp ° F	Thermal Losses			Total Q_{loss} Btu
	Q_{rad} Btu	Q_{conv} Btu	Q_{cond} Btu	
775	8199	4104	963	13266
750	7410	3933	926	12269
725	6676	3762	889	11727
700	5995	3591	853	10439

The four leg strut mount has more shadowing. For the best rigidity for the receiver, a space truss computer program showed that the truss members should be large diameter, thin wall tubes. A comparison of the three to the four leg configuration showed that for the same size struts the receiver deflections were about seven percent more for the three leg support than than for the four leg support. However, shadowing was reduced from 1.2 to 1.0 square meters (12.9 to 10.8 ft²), and strut weight (hence costs) were reduced from 42 to 32 kilograms (92 to 70 lb). Hence, the three leg support was selected for the receiver support configuration.

Support strut trade-offs were performed to select both the strut mount point on the dish and the strut material. The receiver structural elements and struts were modeled in a structural analysis computer program to compare alternative strut support locations. The model is shown in Figure 3.2-49. Two locations at radial distances from the dish boresight axis of 2.54 meters (100 in.-narrow) and 3.17 meters (125 in.-wide) were evaluated. The results are compared (for the same strut size of 2 in. by 1/8 in. wall aluminum tube) in the first two columns of Table 3.2-16. The narrow base approach reduced the up/down pipe length

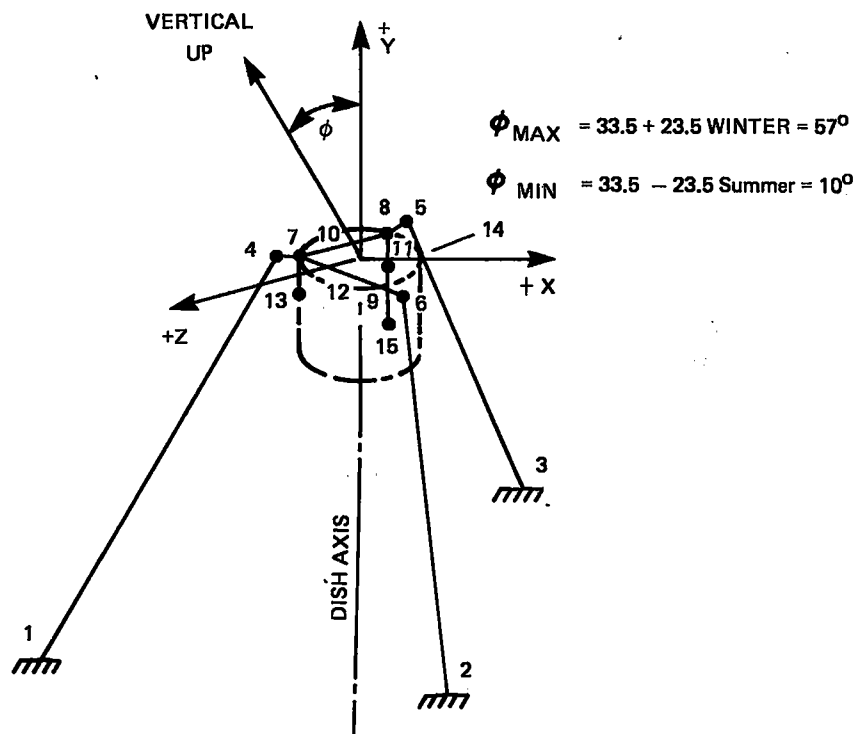


Figure 3.2-49. Receiver Support Model

Table 3.2-16. Strut Location Tradeoff

Strut Size/Material	2 Inch Square Aluminum Strut		3 Inch Square Steel Strut
	Wide	Narrow	Narrow
Radial Distance from Axis	125"	100"	100"
Pipe Length	204"	172" (32"Δ)	
Max Strut Axial Force			
6AM - 90 MPH S Wind	214 Lb.	225 Lb.	224 Lb.
Noon - 90 MPH E Wind	206	224	223
Noon - Winter	140	156	165
6AM - Wt. Only	175	178	191
Noon - Summer	115	115	116
Bending Moment @ Attach. Pt.			
Noon Sun	347 In Lb	446 In Lb	494 In Lb
Noon - Winter	1773	2259	3992
6AM	1847	1890	2119
Combined Stress			
6AM - 90 MPH S Wind	8.3 Ksi	8.9 Ksi	6.2 Ksi
Noon W 90 MPH E Wind	7.5	8.8	5.5
Deflection, Receiver			
6AM	1.69 In	1.75 In	.31 In
Noon - Winter	1.39	1.81	.44
Noon - Summer	0.12	.19	.08

of 0.81 meter (32 in.), made no significant changes in dish reactions and had only slightly reduced stresses and deflections from the wide base approach. The narrower strut base can result in a condition where the back of the struts just below the focal plane height will intercept concentrated sunlight. This area could be painted with a diffuse white paint to preclude any thermal distortion.

These results led to selection of the narrow support configuration. Further analyses were conducted to reduce deflections below the levels realized with the 0.051 meter (2 in.) aluminum struts. These analyses led to the selection of 0.076 meter (3 in.) steel struts to achieve lower deflections at minimum costs. Results of this analysis are also given in Table 3.2-16.

3.2.8.3 Up/Down Collector Fluid Piping

The up/down piping running from the branch line to each receiver is insulated nested steel tubing similar to the branch pipes (Section 3.3). At the polar and declination axis, a means must be provided to accommodate the 180 and 47 degrees polar and declination motions. Because of the type of fluid and the high temperature, the method selected was flexible metallic hose.

Three options were considered for accommodating the necessary relative motion of the piping: (1) swivel joints (2) service loops, and (3) flexible hose. Poor experience with swivel joints due to leaking of oils at high temperature led to rejection of this approach. Service loops have very high bending stresses and require longer lengths adding to thermal losses. Good experience with flexible metal bases on the Engineering Prototype Collector and cost-effective vendor cost quotes confirmed the choice of flexible metallic hose. An assembly drawing of the hose, insulation, end supports, and weatherproofing out cover is shown in

Figure 3,2-50. The base is of metallic bellows constructions with a 0.013 meter (0.5 in.) inside diameter. For economy and to keep the bending moments equal, the same hose is used for the up, 0.013 meter (0.5 in.) tube and down 0.919 meter (0.75 in.) tube with the end fittings made to match the up or down tubes. The end fittings are bulkhead fittings. The bulkhead is a ceramic material to minimize conduction heat losses and still provide the strength to accept the bending moments of the hoses.

3.2.9 COLLECTOR CONTROL

3.2.9.1 Control Selection

A preliminary evaluation of the collector control system requirements led to the selection of a closed loop, tracker/computer drive, hybrid control system. This type of control system is the most flexible and accurate and places the least demands on structural stiffness of the collector and alignment of the collector assembly. However, it also has the highest cost. To determine if the hybrid control system was the most cost effective approach for LSE, a detailed control system analysis was conducted on the collector baseline design. Three options were evaluated: the simple clock drive, a computer only drive and the closed loop, tracker/computer drive, hybrid approach.

In a clock drive type of tracking system, one axis of the collector mount is aligned parallel with the north-south pole/axis of the earth, and the declination axis is perpendicular to the polar axis. In this mode of tracking, the declination angle is set in a particular position depending on the day of the year. Rotation about the polar axis is controlled by sidereal time and the local latitude. An initialization point is necessary which could be the 90° rotation point toward the east. Depending on the exact day of the year and the time of day, a start pulse is given to the clock drive, and, from the initial reference point, the rotation proceeds at the exact rate of $\pi/12$ degrees/hour until such time that the sun is known to set. The drive system then resets itself to the reference point in time for the following day. The declination angle is indexed each day.

The main advantage to the clock drive system is the relative simplicity and the small number of components. The only requirement is the logic that determines the day of the year and the time of day. It is probably the lowest cost system available.

The disadvantage of a simple clock drive system is that it requires precise positioning of the mount and the mounted axis. To insure continued alignment requires periodic measurements of the mount position and adjustments as necessary to account for the shifting of the foundation with time. The clock-drive system cannot correct for dynamic misalignments (since it does not have any feedback) which can occur due to the overall mount sag or wind effects.

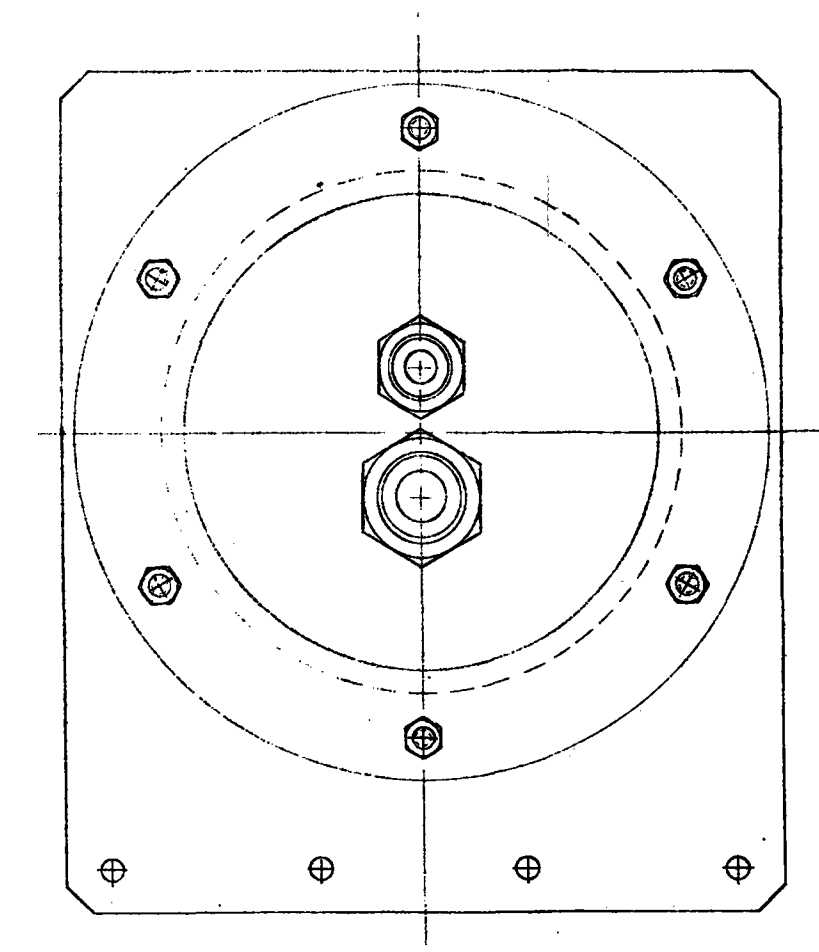
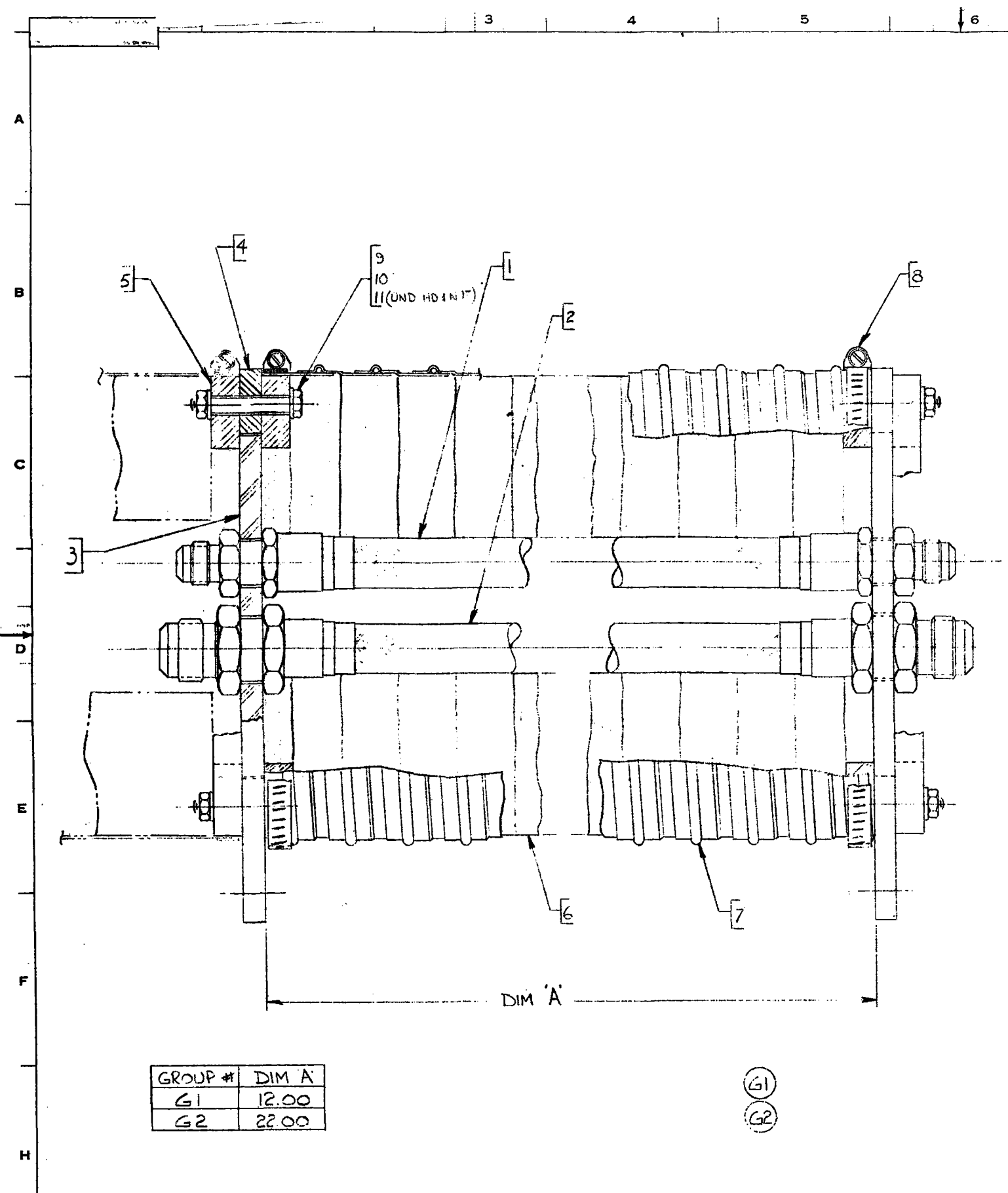
A computer tracking system incorporates a mini-computer or microprocessor to define or command mount position as a function of time at specific update rates. Feedback positioning device located on each of the two collector axes are used to sense the position or position error of the collector. Either the LSE central computer or the collector field micro-processors could be used to perform the basic calculations.

One advantage of this type of system is that the misalignments of the two axes, if known, can be compensated for through appropriate calculations. On days when the sunshine does not reach the ground until well after sunrise, there would be no need to operate the system prior to this time thereby eliminating unnecessary parasitic losses. The control system would give update commands only when an error in the position of the collector was sensed. An over-ride function which decides whether or not the sun is out would be used as a master controller. When the sun was sensed, the drive motors could be started and operated so that the correct position would be attained in a reasonable period of time.

The disadvantage of this type of system is the high precision needed for both the mount position location and the feed back system. To accomplish a 1/8 degree tracking accuracy, it would be necessary to have position accuracy approximately ten times better than the required positioning, or approximately 0.01 degree. As with the simple clock drive system, periodic measurements and adjustments of the mount would be necessary

REV.	DATE	BY	CHKD.	APP.	DESCRIPTION
1					ASSEMBLY

QTY.	PART NO.	NAME	DRAWING NO., DESCRIPTION, MATERIAL, WEIGHT
1	1	FLEX HOSE ASY	
1	2	FLEX HOSE NOZZ	
2	3	INSUL. DISK	
2	4	MIG. PLATE	
4	5	CLAMPING RING	
AR	6	INSULATION	
1	7	FLEX DUCTING	
2	8	HOSE CLAMP	
12	9	BOLT	
12	10	NUT	
24	11	WASHER	



GROUP #	DIM A
G1	12.00
G2	22.00

G1
G2

DESCRIPTION OF GROUPS	REVISIONS	PRINTS TO
	FLEX HOSE LAYOUT	

Figure 3.2-50. Flex Hose Layout

to insure that the required accuracy was maintained. Also, dynamic misalignments such as those due to sag and windloading cannot be corrected unless they are periodic in nature.

The hybrid tracking system combines a computer operating with an optical or thermal sensor which gives precise alignment. As with a computer only system, the position of the sun is determined by a calculation within the computer. The position is compared with the position feedback system on the mount axis. Unlike the computer-only system, however the computer would be required only to position within perhaps 1-4 degrees. When the mount achieves the required position to within 1 to 4 degrees, control is automatically transferred to an optical sensor whose field of view would be on the same order of accuracy (1-4 degrees). The optical sensor then provides a null indication when precise tracking is achieved.

The main advantage of this type of system is that the survey precision for locating the mount is not as critical as with a computer-only tracking system. The mount has to be positioned only within the precision of the course tracker. Periodic measurements of the mount axis are not necessary. Occasionally, however, peaking adjustments can be made to insure that energy to the receiver is maximized. This can be accomplished by sensing the fluid output temperature and adjusting a bias control in both the elevation and the polar axis to maximize the temperature. If the optical sensor is located at the receiver aperture, the potential of automatic correction of the image position even in the presence of wind or structural sag will be available. As with the computer-only system, there is no need to run the mount when the sun is not out, thereby incurring no parasitic loss penalty.

The main disadvantage of this system is that it is the most complex of the three investigated, and it has the highest initial cost. However, the higher energy collection efficiency can offset the higher cost. To evaluate the advantage of the hybrid control system in terms of collector field efficiency, an analysis of the errors for each system and the resulting collector performance degradation was conducted.

An analysis of random errors of the tracking system showed that the effect of such errors on overall collector efficiency was relatively small in the 1/8-1/4 degree range. Figure 3.2-51 shows this effect compared to the more pronounced effect of slope error changes.

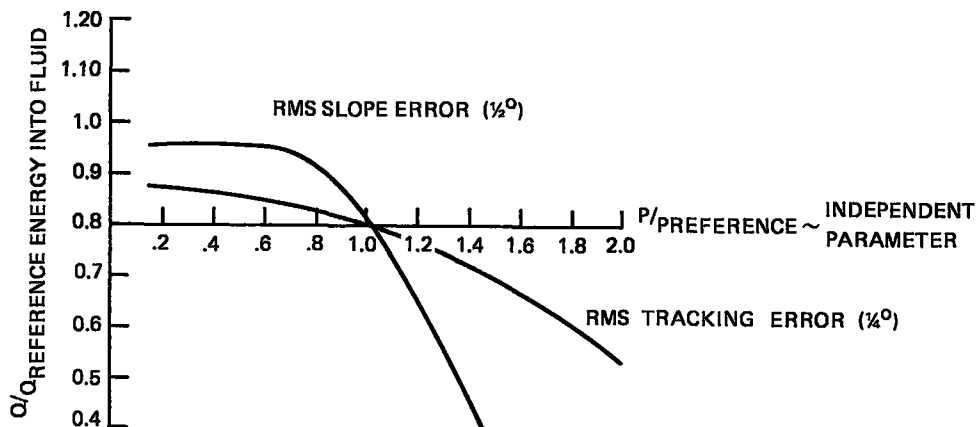


Figure 3.2-51. Tracking Error Sensitivity

A similar analyses of bias errors, however, showed a more pronounced effect. Figure 3.2-52 gives the effect of tracking bias errors. Such bias errors arise from errors in the alignment of the collector axes, structural deflection of the receiver relative to the collector, electronic and mechanical offsets of the tracking system, and natural effects such as variations in the length of the solar day and atmospheric refraction effects.

Without some means of compensating for these bias effects, severe degradation of collector performance will occur. For example, the bias error due to index-of-refraction effects and variations in the length of the solar day alone were estimated to average approximately 0.6 degrees. This would cause an eight percent penalty in delivered energy, a very high performance penalty. For this reason, the simple clock type of control was not acceptable.

Alignment precision was determined to be crucial for the computer drive option. Typical results of an analysis relating the amount of angular error introduced as a function of time for a given error in the elevation plane axis are given in Figure 3.2-53. The figure shows that a collector with an alignment error of two degrees in the elevation axis would have a 0.6 degree error in the solar image at the receiver at 8 AM (solar time) if the collector was precisely boresighted at 9:30 AM. At the 8 o'clock position, this would amount to approximately a six percent reduction in energy intercepted by the receiver. At noon the error would be 0.4 degrees with a four percent reduction in energy intercepted.

It was concluded that, when both axes were considered, alignment accuracy for the collector axes would have to approach 0.25 degrees to limit alignment error penalties on collector performance to approximately one percent. This accuracy would be for both axes relative to each other and absolute to the earth's axis. This level of fabrication and installation accuracy is impractical for the LSE application, particularly when it must be maintained over the life of the power plant. For this reason, the computer-only control system was judged impractical for the LSE application, and the hybrid system was selected.

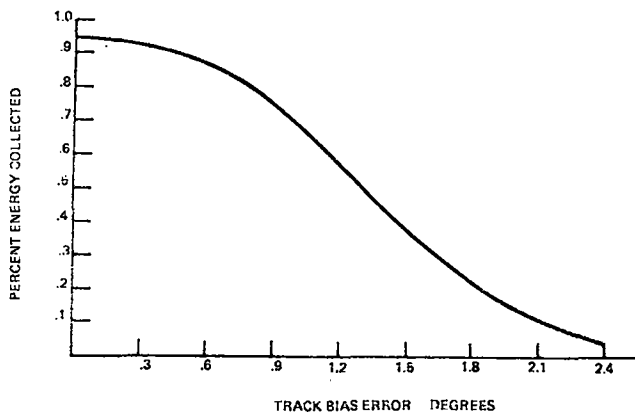


Figure 3.2-52. Energy Collected as a Function of Bias Error.

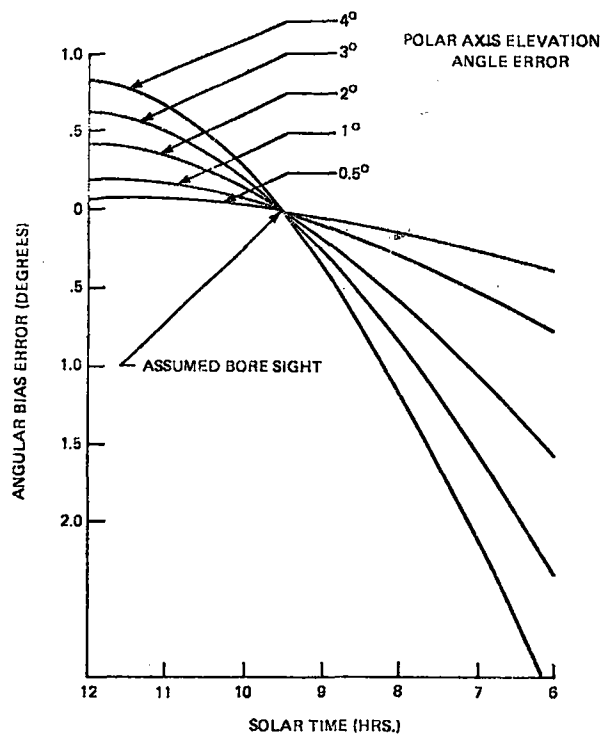


Figure 3.2-53. Equatorial Mount Effects of Tilt Error

3.2.9.2 Control Preliminary Design

The preliminary design of the hybrid control system is based on two principal elements:

1. Direct tracking of the solar image at the receiver.
2. Computer functions provided by the system control hardware.

Overall features of the collector controls are summarized in Table 3.2-17. The computer rough pointing control brings the optical image to within one degree of its correct position. The optical tracker then takes over and provides an image positioning accuracy within 6 mrad; a 3 mrad error has been budgeted for the control itself with a 3 mrad error accepted under rapid wind gusts (slowly varying forces causing structural deflection are compensated for by the direct image focusing control). Conversion from computer drive to optical tracking is automatic, but override in any operating mode is always available from the power plant control console. Control of individual collectors for maintenance, checkout, and calibration purposes is available through the collector control box attached to the mount. For this purpose, a portable control unit is plugged into the collector control box providing the required direct control.

Table 3.2-17. Collector Control Features

The optical tracker operating principal is illustrated in Figure 3.2-54. Optical sensors mounted in the receiver aperture plate (at the focal plane) directly sense the reflected energy profile at the receiver cavity face. Four sensors provide differential signals for the polar and declination controls. When a differential signal (above a threshold level) is generated as illustrated in Figure 3.2-54 the control system provides an update command to the collector drives.

To accommodate the wide span of high intensity optical signal levels encountered, fiber optic sensors have been selected. Specifications for the fiber optic bundle is given in Table 3.2-18. The control schematic is given in Figure 3.2-55.

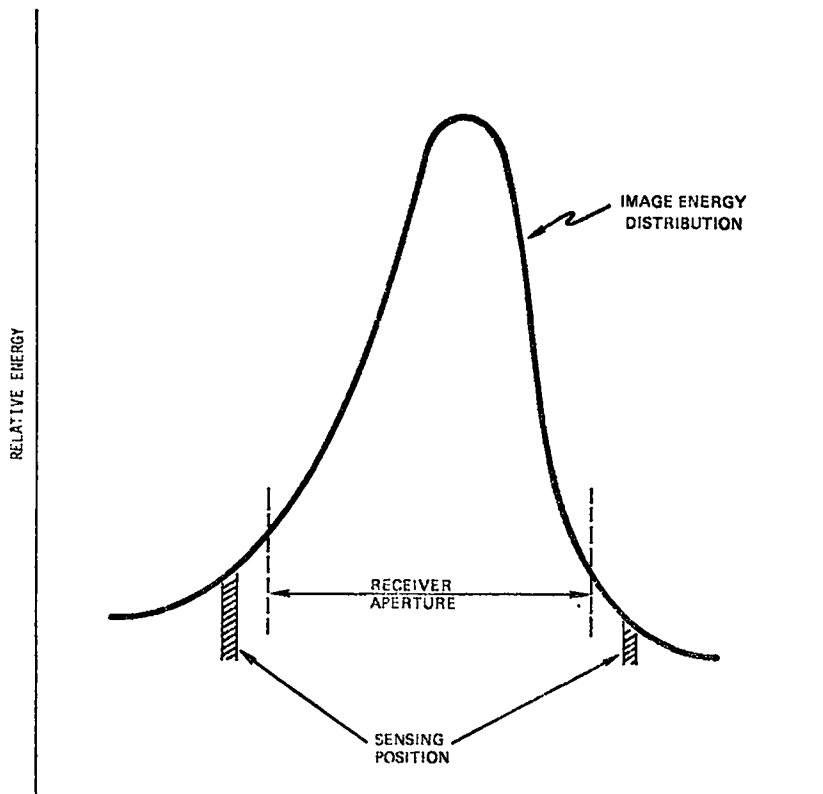


Figure 3.2-54. Optical Sensors Positioning

Table 3.2-18. Optical Sensor Specifications

Fiber Bundle	-	Glass
No. of Fibers	-	40
Size of Fiber	-	.003"
Size of Bundle	-	3/16" Diameter
Assembly	-	4 Each
Trans/ft.	-	.96
End Loss	-	8%
Length	-	8'
Temperature Limits	-	-3 to 150°F

In the computer control mode, the central control station generates command signals for all collectors. Potentiometers on the polar and declination axes provide position signals which are compared to the command signal. The resulting error for each axis and the required direction are then used to trigger an update command for the control motors by the collector field microprocessor.

Alignment in the optical tracker is accomplished by maximizing thermal output. A portable control unit with receiver thermocouple readout is plugged into the control box attached to the mount base. The optical tracking control system is then activated. With the thermocouple readout being used, the tracking bias setting is adjusted until the maximum thermocouple reading is obtained. This procedure can, in effect, update the receiver for permanent structural and alignment changes to the collector.

To align the computer drive, the collector is instructed to track on a known target (possibly a water tower at Shenandoah). The operator observes the image position on a target plane on the receiver aperture. The potentiometer positions on the polar and declination axes are adjusted until the image is on target.

3.3 COLLECTOR FIELD SUBSYSTEM

The Collector Field Subsystem includes the parabolic dish collectors, interconnecting piping with associated pumps valves, and controls, and insulation. The collector field represents the most significant cost item in the system, and consequently much effort was devoted to developing the most cost-effective design within the framework of overall system requirements. Major considerations in the collector subsystem design include the determination of the arrangement of the 192 seven-meter diameter collectors on the available field area and the manner in which the collectors are interconnected through the fluid pipefield. The overall objective of the design analysis was to maximize the annual energy output from the field. This was accomplished in two steps. First, an analysis was performed to define optimum dish spacing on the field for various alternative geometries. Once the dish locations were defined, various piping arrangements were evaluated to define a minimum cost distribution network. Further optimization of piping size and insulation within the selected network resulted in a design which minimized both thermal capacity and thermal losses. The following subsections describe the analyses and studies which led to the selected collector field design.

3.3.1 FIELD SHADOWING AND SPACING

During the conceptual design phase, a trade-off was performed between rectangular collector dish spacing and a diamond arrangement with the long dimension in the east-west direction. Figure 3.3-1 shows the two alternative array layout geometries and the definition of the parameters of interest. It should be noted that the diamond array has a higher inherent packing factor potential than that of the rectangular layout. There are three parameters which affect the field output: X and Y coordinates and packing factor. The diamond-shaped array was found to suffer less severe losses in energy with changes in X/Y ratio resulting in more flexibility in array spacing and therefore inherently allowing more collectors to be placed on a field of a definitive size.

With the use of the optimum ratio of X/Y, the shading factor and the amount of energy per square foot of field were determined on an annual basis for various packing factors. The rectangular and diamond arrays yield almost equivalent energies at equal packing factors. However, since the diamond geometry allows a higher packing factor, it can provide more energy per square foot of field, and thus was selected for the Shenandoah collector field.

During the preliminary design phase, program Dishade was developed by John Zimmerman of Sandia Laboratories to evaluate shadowing in more detail by determining the geometric overlap between adjacent collectors. This program has been coupled with the estimated annual insolation to produce the yearly output from the Shenandoah field as a function of spacing. The program is capable of accounting for the sloping field and has recently been modified to account for collectors which are not shadowed at various times of the year. It has also been incorporated into the Solar Total Energy System (STES) Program which calculates annual system performance. It was exercised for various diamond spacings consistent with 192 total collectors and the size restriction of the Shenandoah field with the resulting optimized field spacing of 8.9 meters (29.30 ft) N-S by 18.4 meters (60.63 ft) E-W.

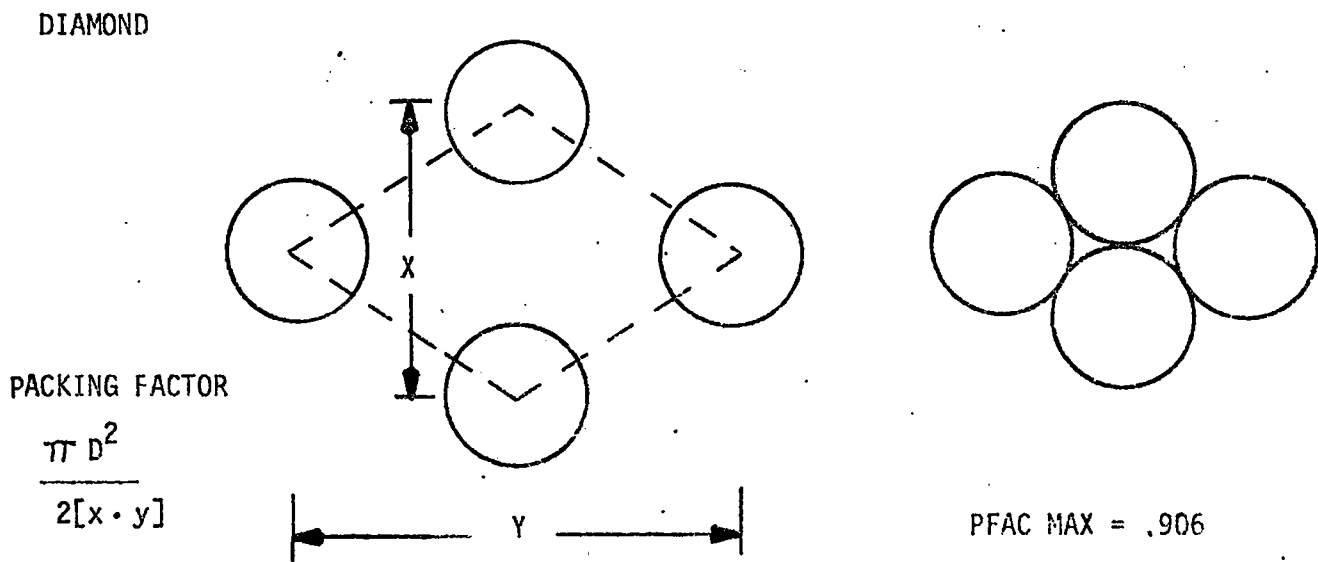
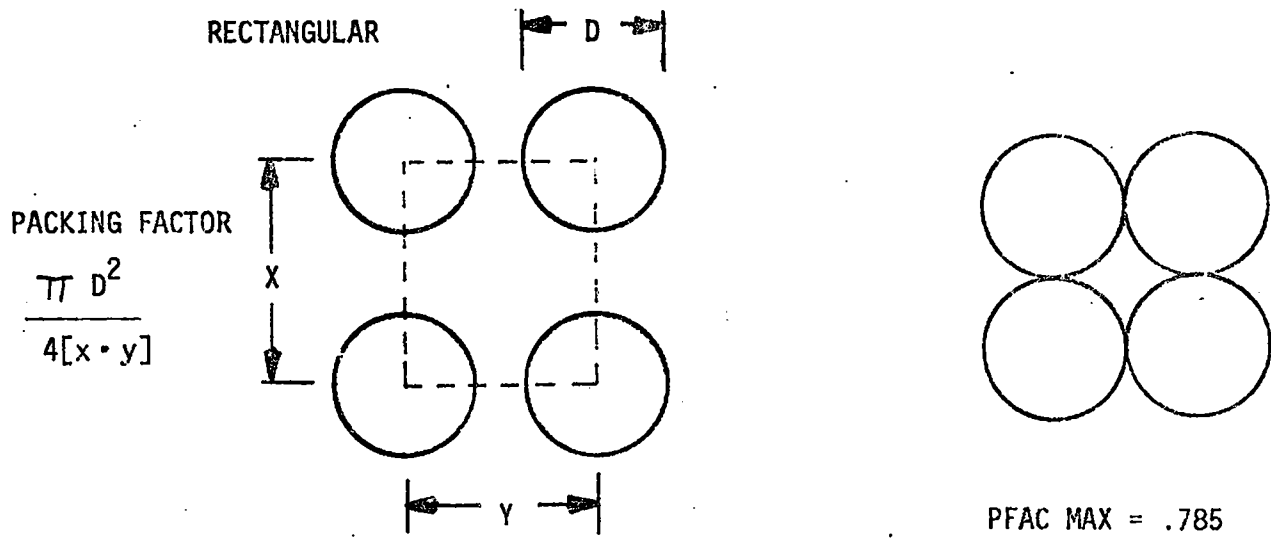


Figure 3.3-1. Alternative Parabolic Dish Field Layout Geometries

3.3.2 PIPE FIELD DESIGN

The pipefield includes the fluid transport devices either pipes or tubes, that are used to carry the working fluid from the Mechanical Equipment Area (MEA) to the solar collectors and return the heated working fluid to the MEA for use in the Power Conversion System (PCS). The field configuration selected for the Preliminary Design and the choice of fluid control elements used in the design resulted from consideration of the system design requirements stated below:

System Design Requirements

- Supply, distribute, collect, and return Syltherm 800 to and from 192 7-meter parabolic dishes, X/Y = .486.
- Maximum flow rate of 390 gpm
- Fossil boiler rated at 10×10^6 Btu/hr
- Minimum field return temperature = 725°F
- Design field supply temperature = 500°F
- Minimize heat loss and thermal capacity and parasitics
- Minimum leakage
- Individual collector isolation and trim control
- Branch isolation and control
- Provide provision for fill and drain
- Provide insulation weather protection
- Keep thermal structural loading below allowable
- Minimize safety hazards
- Meet ANSI power piping codes

Since most of the fluid control elements are standard commercially available components, the majority of the design effort centered on ways to reduce heat loss and thermal capacity while minimizing the pump power consumption. The fluid properties of the heat transfer fluid Syltherm 800 were provided by the manufacturer, Dow Corning, and are summarized in Figure 3.3-2. The following subsections of the report describe the various tradeoffs performed to select configuration and components for the Preliminary Design.

3.3.2.1 Piping Arrangement

Selection of the field piping arrangement was made from a comparison of two basic configurations. Common feed and return, Figure 3.3-3, was compared to branched feed and return, Figure 3.3-4, on the basis of thermal characteristics and potential for minimum heat loss, fluid inventory, availability, thermal stability, collector isolation, and control access and aesthetics. The results of this comparison are summarized in Table 3.3-1. Branched configurations supplying an equal number of dishes with the same X/Y spacing have a lower control valve cost, lower fluid inventory, and greater potential for lower heat loss, based on branch nesting capability, than the common feed and return configuration. In addition, the branched configuration has better maintenance access, is easier to isolate individual collectors or a branch, has greater availability for a given failure rate, and is aesthetically more acceptable. The tradeoff was conducted considering the same design criteria for both configuration and the same reference insulation system, Thermo 12 (Calcium Silicate).

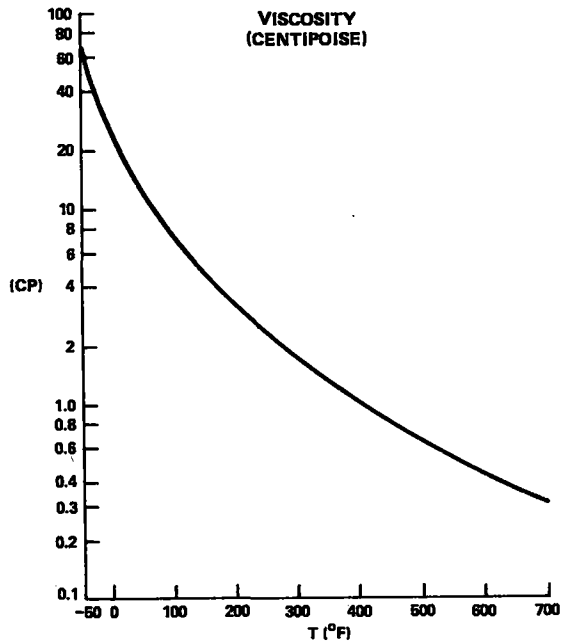
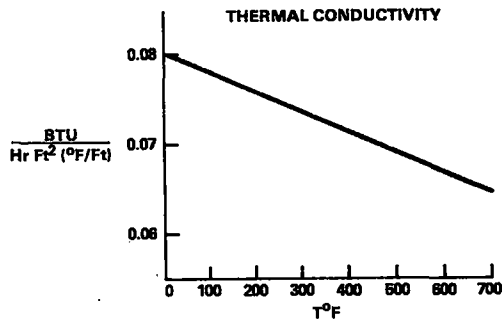
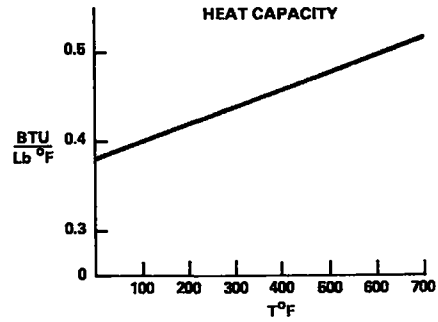
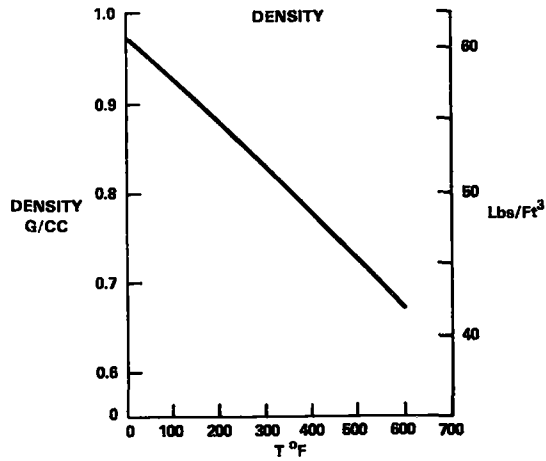
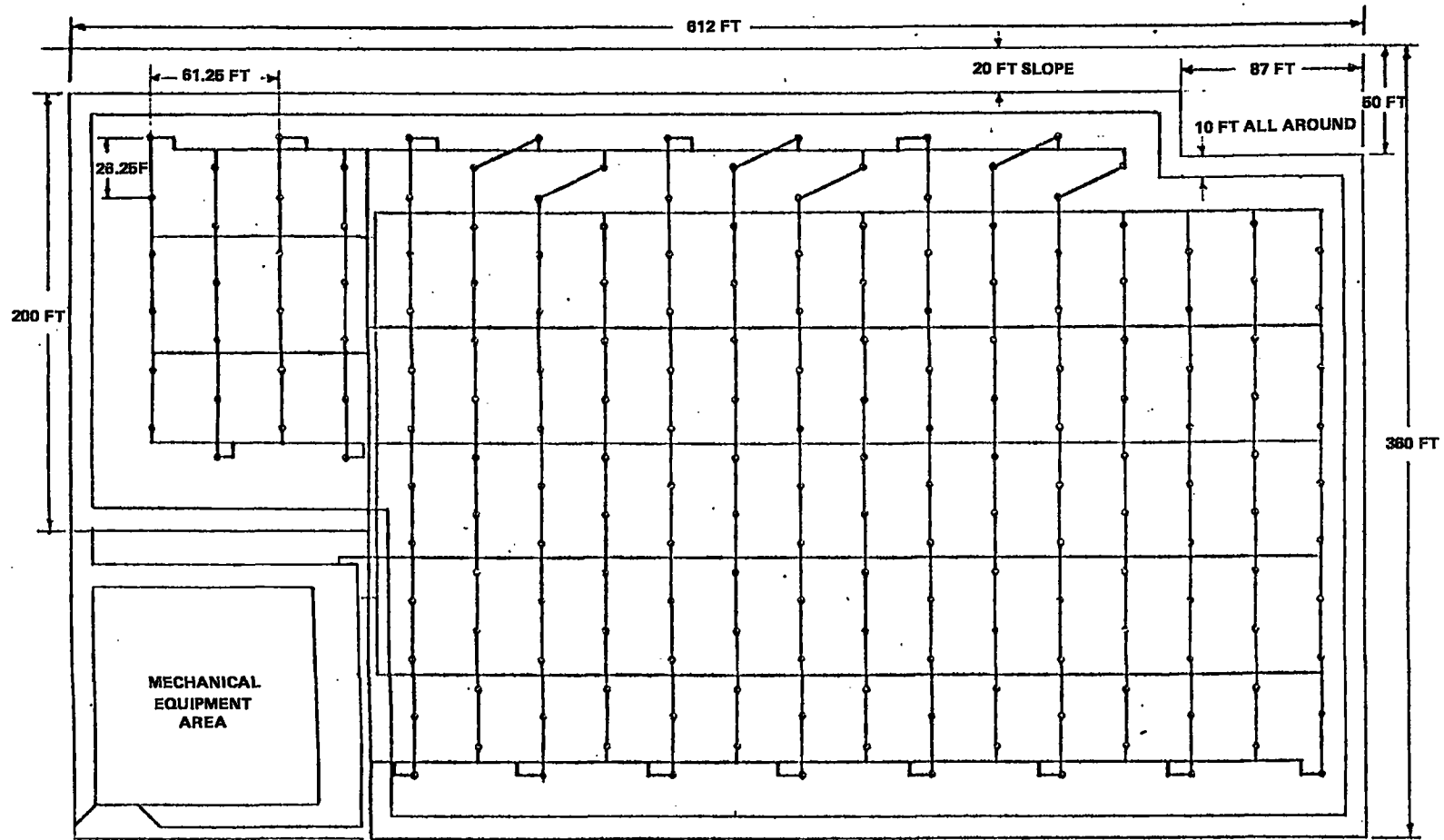


Figure 3.3-2. Typical Properties of Dow Corning Syltherm 800

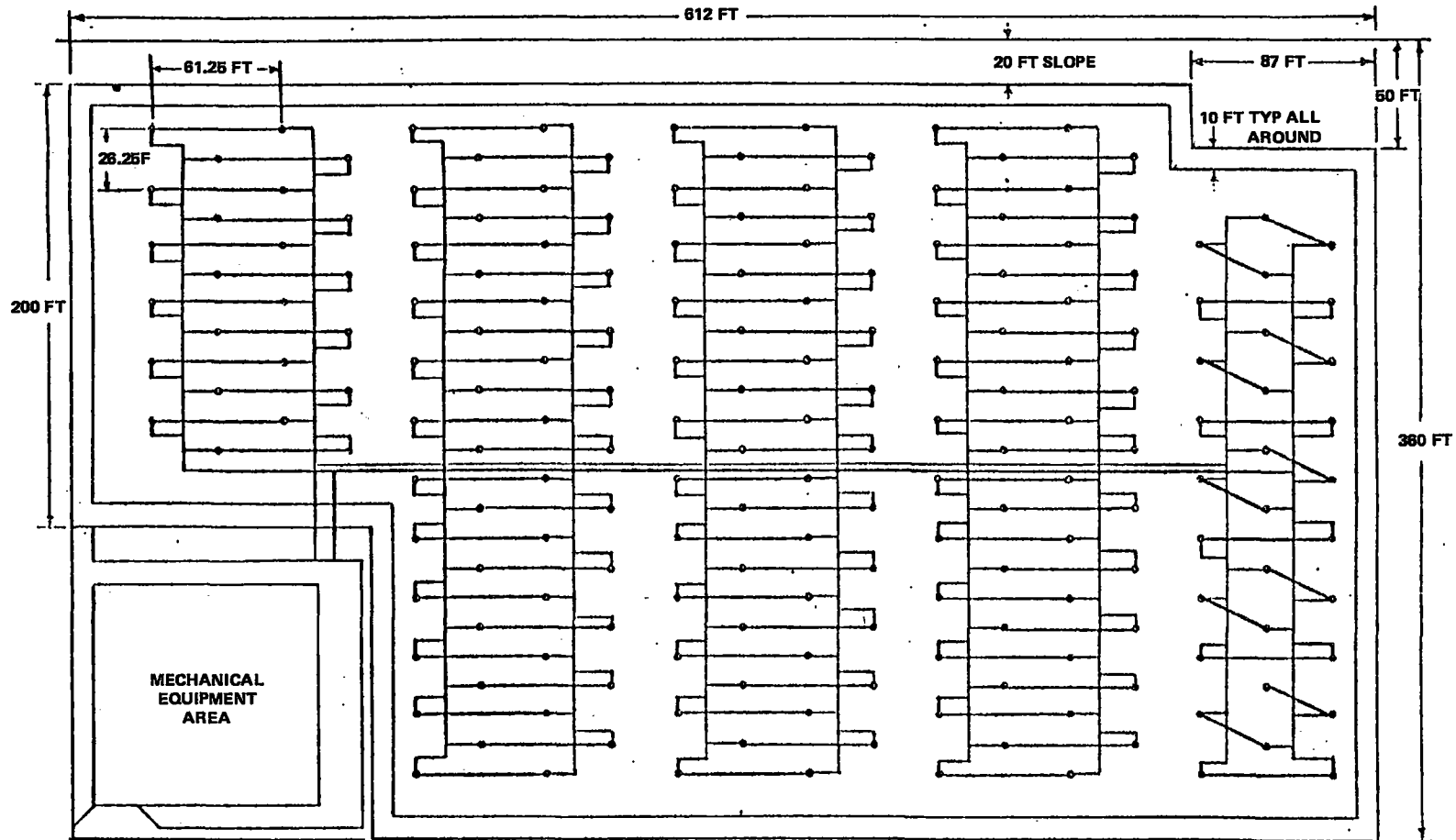
RETURN PIPING
SUPPLY PIPING
PIPING BETWEEN COLLECTORS



STE - LSE REFERENCE DESIGN: 192 COLLECTORS, 7 FEET IN DIAMETER
2 COLLECTORS IN SERIES

Figure 3.3-3. Common Feed and Return Field Piping

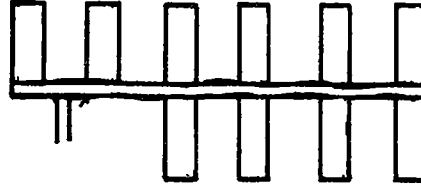
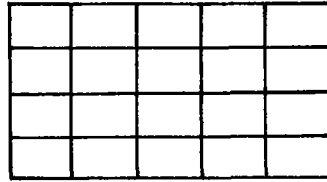
RETURN PIPING
SUPPLY PIPING
PIPING BETWEEN COLLECTORS.



STE - LSE REFERENCE DESIGN: 192 COLLECTORS, 7 METERS IN DIAMETERS
2 COLLECTORS IN SERIES

Figure 3.3-4. Branched Feed and Return Field Piping

Table 3.3-1. Field Piping Configuration Tradeoff



COMMON FEED
& RETURN

BRANCHED

Criteria	Common Feed & Return	Branched
1. Access		
2. Isolation and Control	102 x \$1000	36 x \$2000
3. Minimize Fluid Inventory	3100 Gals.	2500 Gals.
4. Ease Heat Loss	1.74×10^6	1.96×10^6
- Nesting	-21%	-41%
- Tunnel Benefit	-9.6%	-9.6%
- Small Diameter Up and Down Tubes	-	-3%
5. Maximize Availability		
- 95%		1 In Series
6. Aesthetics		

The insulation used in this comparison was selected after comparing the insulation systems shown in Table 3.3-2 against the following requirements:

1. Commercially available in pipe or tube form.
2. Operates at inner surface temperature of 672°K (750°F).
3. Chemically compatible with Syltherm 800.
4. Has a low density and conductivity.

Thermo 12 and Certainteed 850 were selected from among the insulation candidates with Certainteed 850 being the prime choice and applied in accordance with manufacturer's restrictions as noted in Table 3.3-2.

3.3.2.2 Thermal Design

The thermal design and analysis activity which led to the Shenandoah collector field design is summarized in the following subsections. A summary of the resulting field heat loss and thermal capacity at design point conditions is shown in Table 3.3-3.

The following design conditions were used to determine the data shown on Table 3.3-3.

1. One collector provides full field temperature rise
2. Ambient temperature 283°K (50°F)
3. Tube size Lockwood Greene Dwg. GE-I-100 (Refer to Figure 4.2-2)
4. Certainteed 850 the thick ≤ 0.10 meters at 672°K (≤ 4.0 in @ 750°F)
5. Thermo 12 for thick ≤ 0.10 meters @ 672°K (≤ 4.0 in @ 750°F)

Table 3.3-2. Insulation System Candidates

	Mink 1301	Thermo 12	Foam Glass	Certain Teed 850	Kaowool	Owens Corning	Micro Quartz	Cera Foam	Dyna Quartz	Fiber Flex
1. Thermal Conductivity $K = \frac{\text{Btu-in}}{\text{Hr-Ft}^2 \text{ } ^\circ\text{F}} @ 400^\circ\text{F } T_{\text{AVG}}$.22	.48	.46	.42	.40	.50	.43	.38	.44	.4
2. Density Lbs/Ft ³	20	13.0	8.5	5.25	3.00	6.00	3.00	13.0	4.5	36
3. Specific Heat CP $\frac{\text{Btu}}{\text{Lb-}^\circ\text{F}}$.23	.20	.18	.2	.244	~.2	~.2	~.22	~.2	
4. Maximum Temp ^o F	1300	1500	900	850	2300	650	2000	2100	2750	2800
5. Performed	Possible	Pipe	Pipe	Pipe	Blanket Bulk spray	Pipe	Felt (1)	Possible	Tiles, Blocks	Possible
6. Material	?	Calcium Silicate	Glass	Fiberglass with Resin	Alumina Silica	Fiberglass with Resin	Silica	?	Silica	Alumina Silica
7. Manufacturer	J-M	J-M	Pittsburg Corning	Certain Teed	Babcock & Wilcox	Owens Corning	J-M	J-M	J-M	Carborundum

Application Requirements

- C-850 ≤ 4.0 In. at 750^oF
- C-850 ≥ 4.0 In. at 500^oF
- Thermo 12 t ≥ 4.0 In. at 750^oF

Table 3.3-3. Steady State Heat Loss and Thermal Capacity Summary for Collector Loop Subsystem

Component	Heat Loss Btu/hr	Thermal Capacity Btu
Main E-W Manifolds	130 166	2,380,924
Branch Lines	261,281	2,410,696
Up & Down Lines	346,263	1,965,724
Total Field	737,704 $\frac{\text{Btu}}{\text{Hr}}$	6,757,344 Btu

6. Certaineed 850 for thick ≥ 0.10 meters at 533°K (≈ 4.0 in @ 500°F)
7. Branch lines raised to 2.0 meters (78 inches) above grade
8. Branch lines tapered (stepped) per Lockwood Greene Dwg. GE-I-100 (Refer to Figure 4.2-2)
9. Nested branch lines
10. Nested up and down lines.

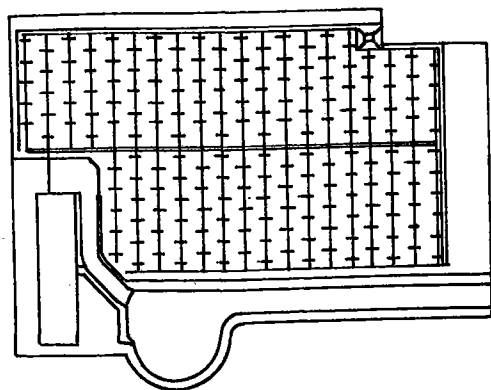
3.3.2.2.1 Number of Series Collectors

With the branched configuration having been selected, it was then necessary to select the number of collectors operating in series to provide the required 139°K (250°F) field temperature rise. The trade-offs considered configurations of 1, 2, 3, and 4 dishes in series as shown in Figure 3.3-5, the selection based on factors of collector field performance, collector design, and collector field control. The areas of major impact are thermal heat loss, thermal capacity, pumping power, and field availability.

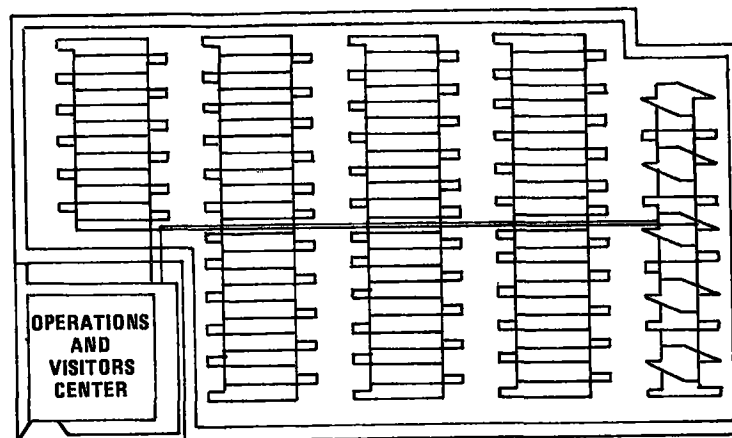
For a system designed to deliver the full field temperature increase through a single dish collector, field losses can be reduced approximately 30 percent over multiple collectors in series, thermal capacity can be reduced by 20 percent, and pumping power can be reduced up to 25 percent. In addition, if one collector is not operational, it can be individually isolated for minimum net field energy loss compared to greater losses (less field availability) for multiple series collectors. Thus, a single dish collector providing the full 139°K (250°F) field temperature rise has been selected for the Shenandoah LSE Design.

Table 3.3-4 summarizes the comparison of field performance for each of the series collector alternatives. The studies concluded that field configurations for the single dish approach will allow raising the field piping approximately 2.0 meters (6.5 ft) off the ground to minimize up and down piping and will also allow nesting of branch lines. These design approaches are not feasible with multiple series collector arrangements. The net result provides significant reductions in both thermal capacity and heat loss for a single collector approach. As shown in Table 3.3-4, steady-state heat loss for the single collector approach is approximately 2.6×10^5 Joules/second (900×10^3 Btu/hr) for the 192 dish field. Other field advantages include:

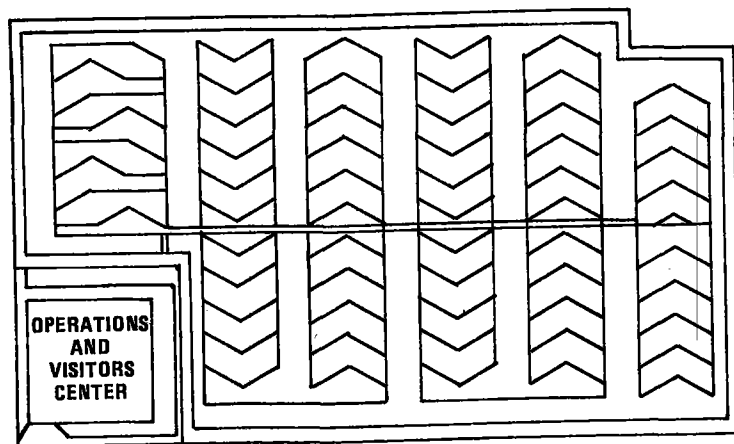
1. Lower pumping power ($\Delta p = 33785 \text{ N/M}^2$ or 4.9 psi)
2. Easier collector field maintainability.
3. Greatest potential for further field heat loss reductions.
4. Cleaner field appearance.
5. Greatest flexibility for future design applications to irregular field shapes.



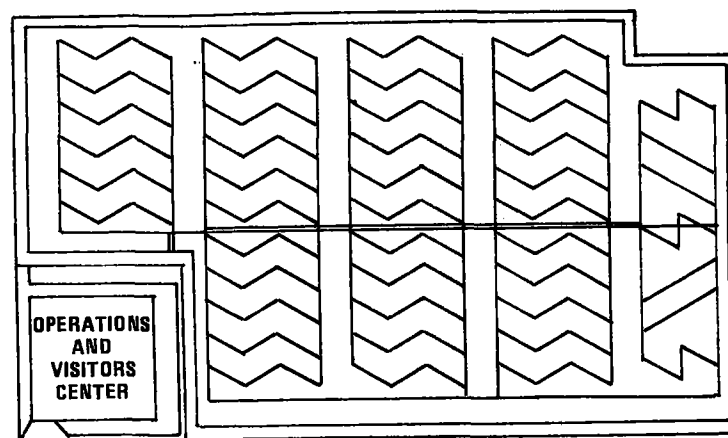
(1)
"1" IN SERIES



(2)
"2" IN SERIES



(3)
"3" IN SERIES



(4)
"4" IN SERIES

Figure 3.3-5. Alternative Pipe Field Arrangements

Table 3.3-4. Trade-Off of Field Performance with Number of Dishes in Series

Number In Series	1	2	3	4
Thermal Loss (Btu/hr)	1.493×10^6 ($.900 \times 10^6$)	1.542×10^6	1.429×10^6	1.397×10^6
Thermal Capacity (Btu)	15.93×10^6	16.84×10^6	-	-
Receiver P	4.89 PSI	5.38 PSI	6.54 PSI	6.4 PSI
Heat Loss Reduction Potential (%)	(19.6) Nested Branch (9.6) Raised Branch (20.0) Reduced Dia. (15.6) C-850 (7.0) Tapered Branches	- - Reduced Dia. C-850 Tapered	- - Reduced Dia. C-850 Tapered	- - Reduced Dia. C-850 Tapered
Note: Thermal capacity and loss for Thermo 12 insulation				

Parallel studies on the receiver design indicated that heat transfer area, film temperature margin, and receiver thermal losses were the major factors affected by the number of dishes in series. Lower receiver temperature significantly improved the average film coefficient. However, in the interest of designing a standard receiver, the heat transfer area was based on the highest temperature condition, which is the same for any number of collectors in series. Film temperature margin and receiver thermal losses were slightly improved for multiple collectors; however, the improvements were more than offset by the increased field thermal losses.

Based on a branch control philosophy for the field, fewer control valves are required for multiple collectors in series. However, the same control design approach applies. The major impact results from a single collector malfunction. For the single collector design, the malfunctioning collector can be isolated and the remaining branch collectors operated at design outlet temperature. Thus, the single isolated collector results in the smallest net field energy loss and maximum field availability.

3.3.2.2.2 Pipefield Thermal Optimization Analysis

After selection of the piping arrangement and the associated single collector in series concept, a significant effort was devoted to analyses and tradeoffs to determine the most efficient way to obtain reductions in heat loss. The methods that were identified to reduce heat loss included:

1. Lower conductivity insulation
2. Reduced pipe diameters
3. Lower density insulation
4. Greater insulation thickness
5. Nesting
6. Tapered branches
7. Reduced length of up and down pipes
8. Tube instead of pipe.

The application of lower conductivity pipe insulation, Certainteed 850*, provided about 16 percent reduction in steady state heat loss for the pipefield over the reference Thermo 12 design. The 84.1 kg/m (5.25 lb/ft³) density of this insulation greatly reduced the pipefield thermal capacity ($mc_p\Delta T$) as well.

Reducing the heat loss by increasing the insulation thickness or decreasing the pipe diameter was traded-off with the aid of Figure 3.3-6 which is a plot of the heat loss co-efficient ($q/2\pi LK\Delta T$) as a function of insulation for three different diameters. The analytical relationship between tube size, insulation thickness, conductivity, and temperature is given by the classical equation.

$$q = \frac{2\pi KL\Delta T}{\ln\left(1 + \frac{t}{r}\right) + \frac{K}{h_o r_o}}$$

where $\frac{K}{h_o r_o}$ = outer surface conductance term

Because of the low K for insulations of interest, r_o is a large number making the conductance term small compared to $\ln\left(1 + \frac{t}{r}\right)$. Therefore, in all instances the forced convection term is neglected. It was immediately apparent that reductions in diameter at the same thickness of insulation offered both lower heat loss and thermal capacity. The effect of pipe diameter reductions on the total field heat loss was estimated for the 2-in-series configuration again using Thermo 12.

From Figure 3.3-7, which shows total system heat loss as a function of dish diameter and percent reduction in pipe radius, it can be seen that a large reduction in system heat loss from the Reference Design is possible through reduction of pipe diameter. However, decreases in pipe diameter result in increased pump

*The Certainteed Corp. Technical Staff has recommended that this product not be used in thicknesses over 0.10 meter (4.0 in.) at temperatures of 672°K (750°F)

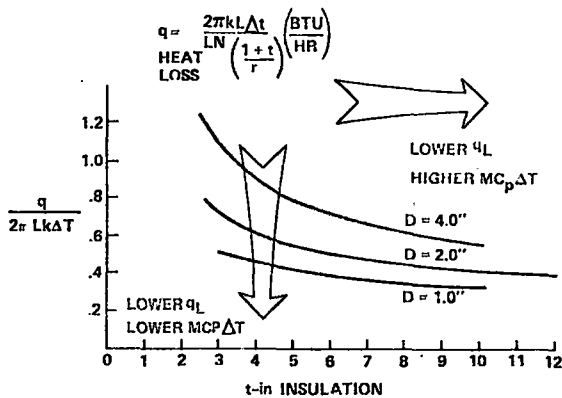


Figure 3.3-6. Heat Loss Coefficient vs Pipe Diameter and Insulating Thickness

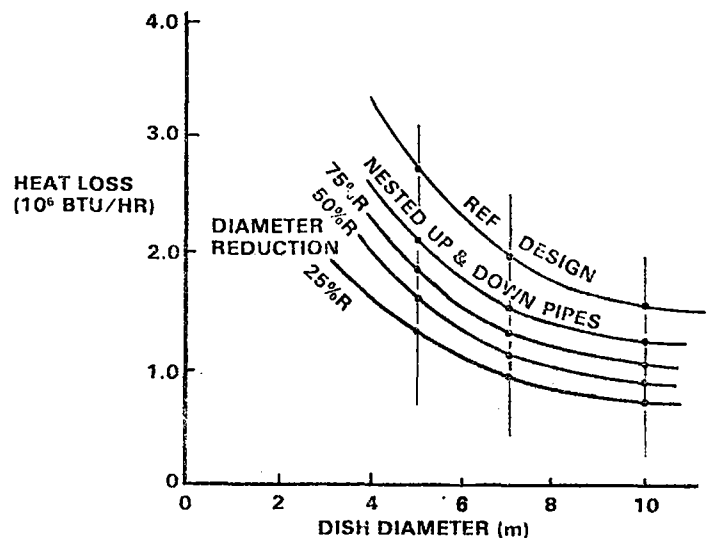


Figure 3.3-7. System Heat Loss vs. Pipe Radius and Dish Diameter

power to provide the required Syltherm 800 flow rate to the field. This suggests that a plot of the summation of heat loss and pump power should have a minimum. Figure 3.3-8 shows the results of this plot and indicates that a minimum exists at about 70 percent r_0 . Heat loss reduction associated with a 30 percent reduction in pipe diameters is about 14-16 percent. This effect, along with changes in insulation, nesting, tapered branches, and raising branch lines will be summarized in subsequent paragraphs.

Another major design contribution to reductions in heat loss is nesting. The concept of nesting and associated geometry is defined in Figure 3.3-9. This steady state heat transfer problem was modeled on a digital computer code by C. E. Sisson of Sandia Laboratories. The geometry and fluid parameters considered are given in Table 3.3-5. Typical results are shown in Table 3.3-6. Figure 3.3-10 shows plots of this data for the case of 672°K (750°F) hot tube and 533°K (500°F) cold tube for sizes of 0.0095 meter (3/8 in.) tube and 0.013 meter (1/2 in.) tube.

The curves show lowest heat loss for the 0.0095 meter (3/8 in.) tube with 0.0064 meter (0.25 in.) spacing and 0.10 meter (4 in.) of insulation at about 41 Joules/second-m (43 Btu/hr-ft). However, when temperature gradient data is plotted as a function of fractional flow rate for the same temperature and geometry, high temperature differentials result. At low flow rates, the temperature gradient of the hot tube is about 2.2 °K/m (1.2°F/ft). For 12.7 meters (41.5 ft) of hot down tube, this rate gives 28°K (50°F) temperature drop while the allowable is only 13.9 °K (25°F) maximum for the field. Figure 3.3-11 shows that the temperature gradient for .038 meter (1.5 in.) tube is lower by an order of magnitude. A crossplot of temperature gradient and heat loss versus pipe diameter and flow rate (Figure 3.3-12) confirms the indication that high gradients result from low mass flow at approximately constant heat loss rates. Analysis has shown that the maximum acceptable gradient is 0.87° K/m (.48°F/ft). The design requirement is to keep the heat loss around 48 Joules/second-m (50 Btu/hr-ft) and the $\Delta T/ft \approx 0.48$. To satisfy these requirements, the diameter of the hot tube was decreased, and the diameter of the cold tube was increased to 0.019 meter (3/4 in.) 18 ga. Thus, at the nominal low flow rate of 257 meters/second (842 ft/sec), the flow in the 0.013 meter (1/2 in.) - 18 ga tube will give $\Delta T/ft = V (.49 \text{ } ^\circ\text{F}/\text{H})$ at a $\Delta P = 28,200 \text{ N/m}^2$ (4.09 psi) while the 0.019 meter (3/4 in.) - 18 ga up tube will give $\Delta T/ft \approx 0.36 \text{ } ^\circ\text{K}/\text{m}$ (.2°F/ft) and $\Delta P = 2965 \text{ N/m}^2$ (.43 psi) for a total of 31,165 N/m^2 (4.52 psi) compared to 22,200 N/m^2 (3.22 psi) for two 0.014 meter (9/16 in.) - 20 ga tubes. In addition the use of nested tubine results in a minimum flow velocity required to maintain the minimum field outlet temperature. This velocity corresponds to a minimum solar insolation of 58-72 W/m^2 (60-75 Btu/hr-ft²) compared to 48 W/m^2 (50 Btu/hr-ft²) required if nesting is not utilized.

Finally, the percent heat loss saving of nested over singularly insulated tubes can be estimated by comprising the heat loss from the sum of a 672°K (750°F) 0.013 meter (1/2 in.) tube with 0.10 meter (4 in.) of $K = 0.061 \text{ J/s-m } ^\circ\text{K}$ $\left(.42 \frac{\text{Btu-in}}{\text{hr.-ft}^2} - ^\circ\text{F} \right)$ insulation and a 533°K (500°F) 0.013 meter (1/2 inch) tube with

0.10 meter (4 in.) of the same insulation with two nested tubes. The sandia analysis shows that, for two nested 0.013 meter (1/2 in.) tubes at 672 and 533°K (750 and 500°F), the total loss per foot is 47.2 J/s-m (49.12 Btu/hr-ft). The summed heat loss for two singly insulated tubes is 78.8 J/s-m $\left(\frac{82.02 \text{ Btu}}{\text{hr-ft}} \right)$.

The nesting saves about 40 percent in heat loss and appears to be warranted on the basis of preliminary cost studies.

Further reductions in heat loss were obtained by decreasing the length of nested up and down pipe (tube) by raising the branch lines. It was possible to raise the branch lines into the opening formed by the operating envelope of the dish rotating about the polar axis. Considering the maximum winter declination and the dish geometry, the branch lines were raised to 2.0 meters (78 inches) above grade. Branch lines were originally mounted 0.3 meters (one ft) above grade; therefore, a net savings of 1.5 meters (5ft) in 12.7 meters (41.5 ft) or about twelve percent was realized. This effect gives about six percent reduction in total heat loss.

Tapering the branch lines was also considered as another method of reducing heat loss. Comparing the branch heat loss for two 0.038 meters (1-1/2 in.) lines at 533°K (500°F) with C-850 insulation to two

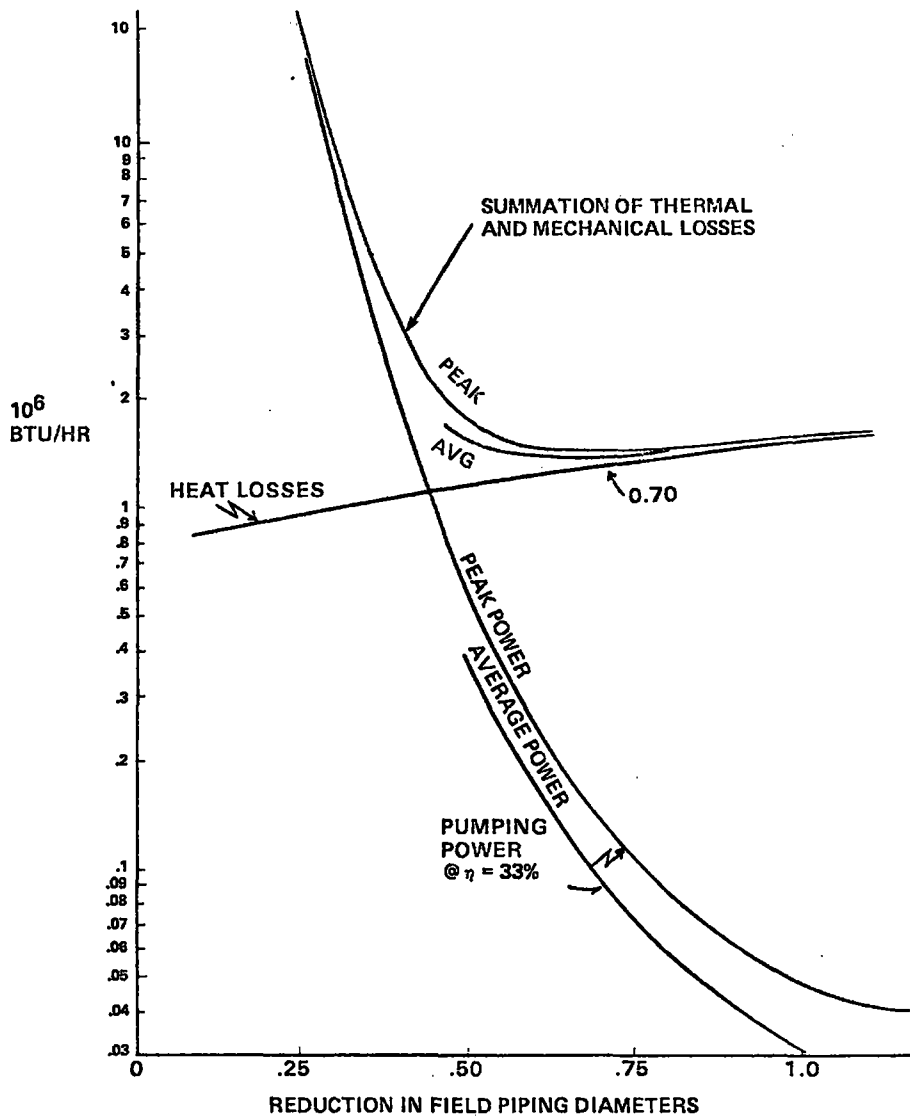


Figure 3.3-8. Effect of Reducing Piping Diameter on Field Heat Loss and Pumping Power

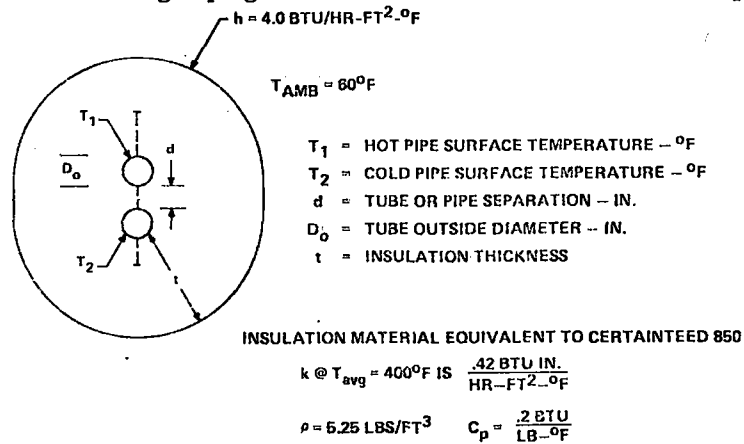


Figure 3.3-9, Nested Pipe Configuration.

Table 3.3-5. Steady-State Heat Transfer Calculations for Turbulent Flow in an Insulated Two-Pipe System/Dow Corning Silicon-B Fluid

GEOMETRY PARAMETERS

D ₀	D ₁	d _{INSUL}	d _{SPACING}
.50	.402	2.0	.25
.50	.402	3.0	.25
.50	.402	4.0	.25
.50	.402	2.0	.50
.50	.402	3.0	.50
.50	.402	4.0	.50
.75	.820	3.0	.25
.75	.820	4.0	.25
.75	.820	3.0	.50
.75	.820	4.0	.50
1.00	.870	3.0	.25
1.00	.870	4.0	.25
1.00	.870	3.0	.75
1.00	.870	4.0	.75
1.25	1.120	3.0	.50
1.25	1.120	4.0	.50
1.25	1.120	3.0	1.00
1.25	1.120	4.0	1.00
1.50	1.334	4.0	.50
1.50	1.334	5.0	.50
1.50	1.334	4.0	1.00
1.50	1.334	5.0	1.00
1.50	1.334	4.0	2.00
1.50	1.334	5.0	2.00
2.00	1.810	4.0	.50
2.00	1.810	5.0	.50
2.00	1.810	4.0	1.00
2.00	1.810	5.0	1.00
2.00	1.810	4.0	2.00
2.00	1.810	5.0	2.00
2.50	2.282	4.0	.50
2.50	2.282	5.0	.50
2.50	2.282	4.0	1.00
2.50	2.282	5.0	1.00
2.50	2.282	4.0	2.00
2.50	2.282	5.0	2.00
8.00	7.500	8.0	1.00
8.00	7.500	8.0	2.00
8.00	7.500	8.0	1.00
8.00	7.500	8.0	2.00

BY: C.E. SISSON
 FLUID MECHANICS AND HEAT TRANSFER DIV. 1262
 SANDIA LABORATORIES

h_{SURFACE} = 4.0 BTU/HR-FT²-°F
 NO RADIATION LOSSES
 FULLY DEVELOPED PIPE FLOW
 K_{INSULATION} = 0.42 BTU/HR-FT²-°F/IN
 T_{AMBIENT} = 80°F

FLUID FLOW RATE PARAMETER

VELOCITY = 0.842 FT/SEC
= 2.528
= 5.028
VELOCITIES ARE EASED ON 1/3, 1 AND 2 GPM FLOW RATES IN 1/2 IN DIAMETER PIPE!

FLUID TEMPERATURE PARAMETERS

T _{FLUID-1} (°F)	T _{FLUID-2} (°F)			
	ΔT=150	ΔT=200	ΔT=250	ΔT=300
550	400	350	300	250
650	500	450	400	350
750	600	550	500	450
850	700	650	600	550
100	100			
200	200			
300	300			
400	400			
500	500			
600	600			

TOTAL NO. OF SOLUTIONS = 2840

Table 3.3-6. Results of Pipe Nesting Analysis

$K_{INSUL} = 0.42$
(BTU/HR-FT²-°F/IN)

PIPE O.D. (INCHES)	PIPE SPACING (INCHES)	INSUL THICKNESS (INCHES)	TEMPERATURE °F FLUID-1	TEMPERATURE °F FLUID-2	FLUID VELOCITY (FT/SEC)	T FLUID-1	T FLUID-2	T ATMOSPHERE	$\left(\frac{h}{t}\right)$	BTU/HR-FT	HEAT TRANSFER COEFFICIENT (BTU/HR-FT ² -°F)		TEMPERATURE CHANGE IN FLUID (°F/FT)
											FLUID-1	FLUID-2	
.375	.25	3.	850.	400.	.842	-30.70	-5.54	38.24	83.	88.	- .948	- .184	
.375	.25	2.	850.	400.	2.529	-30.85	-5.44	38.39	294.	168.	- .318	-.094	
.375	.25	3.	850.	400.	8.096	-31.03	-5.40	38.43	368.	298.	- .189	-.027	
.375	.25	1.	850.	350.	.842	-33.78	- .28	34.06	83.	83.	-1.043	-.008	
.375	.25	2.	850.	350.	2.529	-34.10	- .10	34.20	204.	154.	- .381	-.001	
.375	.25	3.	850.	350.	8.096	-34.20	- .04	34.24	358.	271.	- .176	-.000	
.375	.25	1.	850.	300.	.842	-38.88	4.86	31.80	83.	87.	-1.138	.144	
.375	.25	2.	850.	300.	2.529	-37.25	5.23	32.01	204.	139.	- .383	.051	
.375	.25	3.	850.	300.	8.096	-37.37	5.32	32.05	358.	249.	- .182	.028	
.375	.25	1.	850.	250.	.842	-39.91	10.17	26.74	83.	81.	-1.232	.252	
.375	.25	2.	850.	250.	2.529	-40.38	10.55	26.83	204.	124.	- .418	.101	
.375	.25	3.	850.	250.	8.096	-40.53	10.67	26.88	358.	217.	- .208	.081	
.375	.25	1.	850.	200.	.842	-35.12	-8.88	34.01	84.	79.	-1.083	-.300	
.375	.25	2.	850.	200.	2.529	-35.38	-8.81	34.17	228.	162.	- .383	-.098	
.375	.25	3.	850.	200.	8.096	-35.43	-8.78	34.22	403.	339.	- .182	-.080	
.375	.25	1.	850.	150.	.842	-38.22	-4.90	42.82	84.	74.	-1.178	-.138	
.375	.25	2.	850.	150.	2.529	-38.52	-4.86	42.88	230.	181.	- .395	-.045	
.375	.25	3.	850.	150.	8.096	-38.61	-4.82	43.02	403.	318.	- .188	-.022	
.375	.25	1.	850.	100.	.842	-41.87	.88	40.58	84.	88.	-1.274	.020	
.375	.25	2.	850.	100.	2.529	-41.78	.88	40.63	230.	168.	- .428	.008	
.375	.25	3.	850.	100.	8.096	-41.70	.88	40.68	403.	283.	- .214	.005	
.375	.25	1.	850.	50.	.842	-44.40	5.82	38.80	84.	83.	-1.368	.173	
.375	.25	2.	850.	50.	2.529	-44.82	6.22	38.80	230.	154.	- .480	.061	
.375	.25	3.	850.	50.	8.096	-44.85	6.31	38.84	403.	271.	- .231	.031	
.375	.25	1.	750.	800.	.842	-39.85	-14.23	52.78	107.	87.	-1.176	-.447	
.375	.25	2.	750.	800.	2.529	-38.77	-14.18	53.95	281.	214.	- .384	-.148	
.375	.25	3.	750.	800.	8.096	-39.84	-14.17	54.80	468.	375.	- .187	-.074	
.375	.25	1.	750.	650.	.842	-42.57	-8.63	51.80	107.	85.	-1.288	-.078	
.375	.25	2.	750.	650.	2.529	-42.83	-8.63	51.78	281.	204.	- .428	-.091	
.375	.25	3.	750.	650.	8.096	-43.01	-8.60	51.81	468.	388.	- .213	-.048	
.375	.25	1.	750.	500.	.842	-48.77	-3.84	49.82	107.	78.	-1.380	-.111	
.375	.25	2.	750.	500.	2.529	-48.09	-3.48	49.87	281.	163.	- .488	-.035	
.375	.25	3.	750.	500.	8.096	-48.18	-3.43	49.82	468.	338.	- .289	-.017	
.375	.25	1.	750.	450.	.842	-48.88	1.84	47.24	107.	74.	-1.463	.048	
.375	.25	2.	750.	450.	2.529	-49.28	1.87	47.38	281.	181.	- .487	.018	
.375	.25	3.	750.	450.	8.096	-49.38	1.84	47.42	468.	318.	- .244	.010	
.375	.25	1.	850.	700.	.842	-43.97	-18.89	62.86	120.	100.	-1.282	-.062	
.375	.25	2.	850.	700.	2.529	-44.18	-18.86	62.74	283.	248.	- .422	-.187	
.375	.25	3.	850.	700.	8.096	-44.24	-18.86	62.78	468.	431.	- .211	-.094	
.375	.25	1.	850.	550.	.842	-47.10	-13.27	60.37	120.	94.	-1.352	-.408	
.375	.25	2.	850.	550.	2.529	-47.34	-13.20	60.85	283.	220.	- .482	-.138	
.375	.25	3.	850.	550.	8.096	-47.42	-13.18	60.80	468.	403.	- .227	-.088	
.375	.25	1.	850.	400.	.842	-50.22	-7.87	68.18	120.	87.	-1.441	-.280	
.375	.25	2.	850.	400.	2.529	-50.51	-7.86	68.36	283.	214.	- .483	-.082	
.375	.25	3.	850.	400.	8.096	-50.60	-7.81	68.40	468.	375.	- .242	-.041	
.375	.25	1.	850.	300.	.842	-53.33	-2.87	86.01	120.	83.	-1.530	-.083	
.375	.25	2.	850.	300.	2.529	-53.67	-2.88	86.16	283.	204.	- .513	-.028	
.375	.25	3.	850.	300.	8.096	-53.77	-2.84	86.21	468.	358.	- .287	-.013	
.375	.25	1.	100.	100.	.842	- 1.73	-1.73	2.45	28.	28.	- .048	-.048	
.375	.25	2.	100.	100.	2.529	- 1.74	-1.74	3.49	71.	71.	- .018	-.018	
.375	.25	3.	100.	100.	8.096	- 1.78	-1.75	3.80	123.	123.	- .008	-.008	
.375	.25	1.	200.	200.	.842	- 6.08	-8.08	12.16	44.	44.	- .173	-.173	
.375	.25	2.	200.	200.	2.529	- 6.12	-8.12	12.25	107.	107.	- .058	-.058	
.375	.25	3.	200.	200.	8.096	- 6.14	-8.14	12.27	188.	188.	- .028	-.028	
.375	.25	1.	300.	300.	.842	-10.48	-10.45	20.80	87.	87.	- .303	-.303	
.375	.25	2.	300.	300.	2.529	-10.51	-10.51	21.02	139.	139.	- .101	-.101	
.375	.25	3.	300.	300.	8.096	-10.53	-10.53	21.05	245.	245.	- .051	-.051	
.375	.25	1.	400.	400.	.842	-14.83	-14.83	28.88	88.	88.	- .439	-.439	
.375	.25	2.	400.	400.	2.529	-14.90	-14.80	28.80	168.	168.	- .147	-.147	
.375	.25	3.	400.	400.	8.096	-14.82	-14.82	28.84	285.	285.	- .074	-.074	
.375	.25	1.	500.	500.	.842	-18.21	-18.21	38.42	78.	78.	- .584	-.584	
.375	.25	2.	500.	500.	2.529	-18.28	-18.28	38.88	163.	163.	- .185	-.185	
.375	.25	3.	500.	500.	8.096	-18.31	-18.31	38.82	338.	338.	- .098	-.098	
.375	.25	1.	600.	600.	.842	-23.88	-23.88	47.18	87.	87.	- .741	-.741	
.375	.25	2.	600.	600.	2.529	-23.88	-23.88	47.36	214.	214.	- .249	-.249	
.375	.25	3.	600.	600.	8.096	-23.70	-23.70	47.41	375.	375.	- .124	-.124	

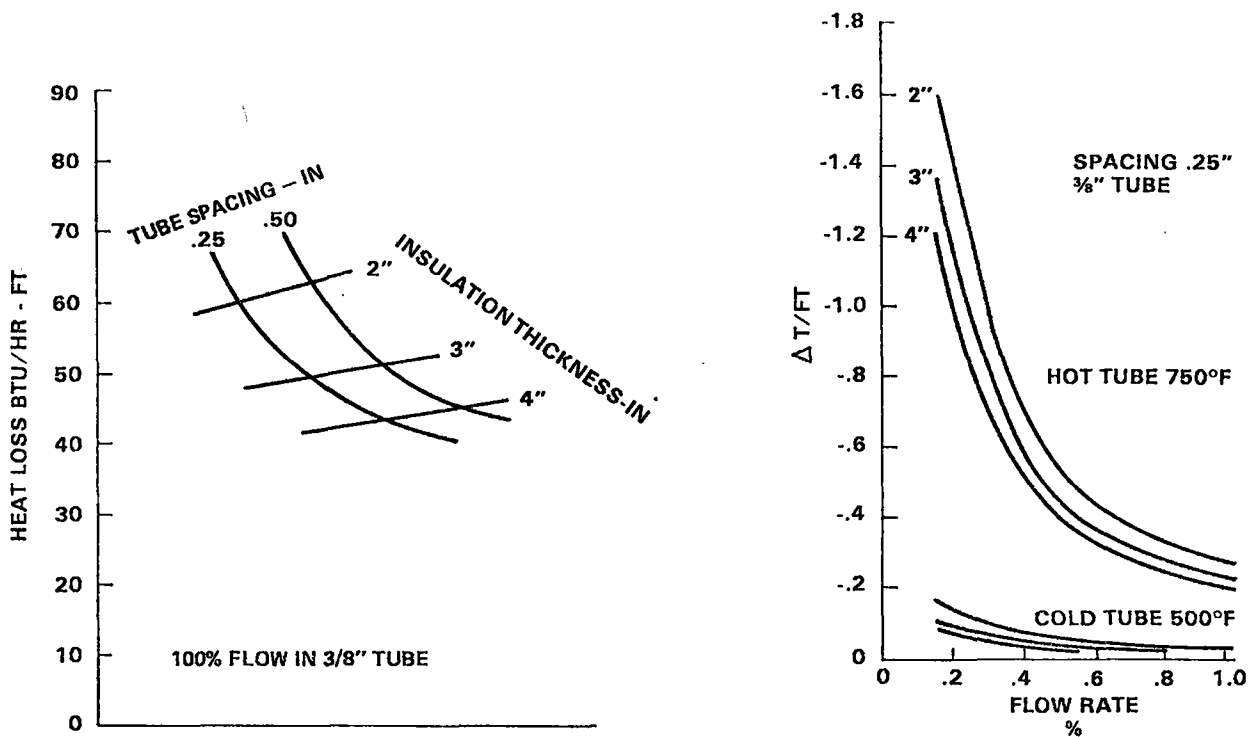


Figure 3.3-10. Parametric Analysis Summary of Nested Pipes (Tubes)

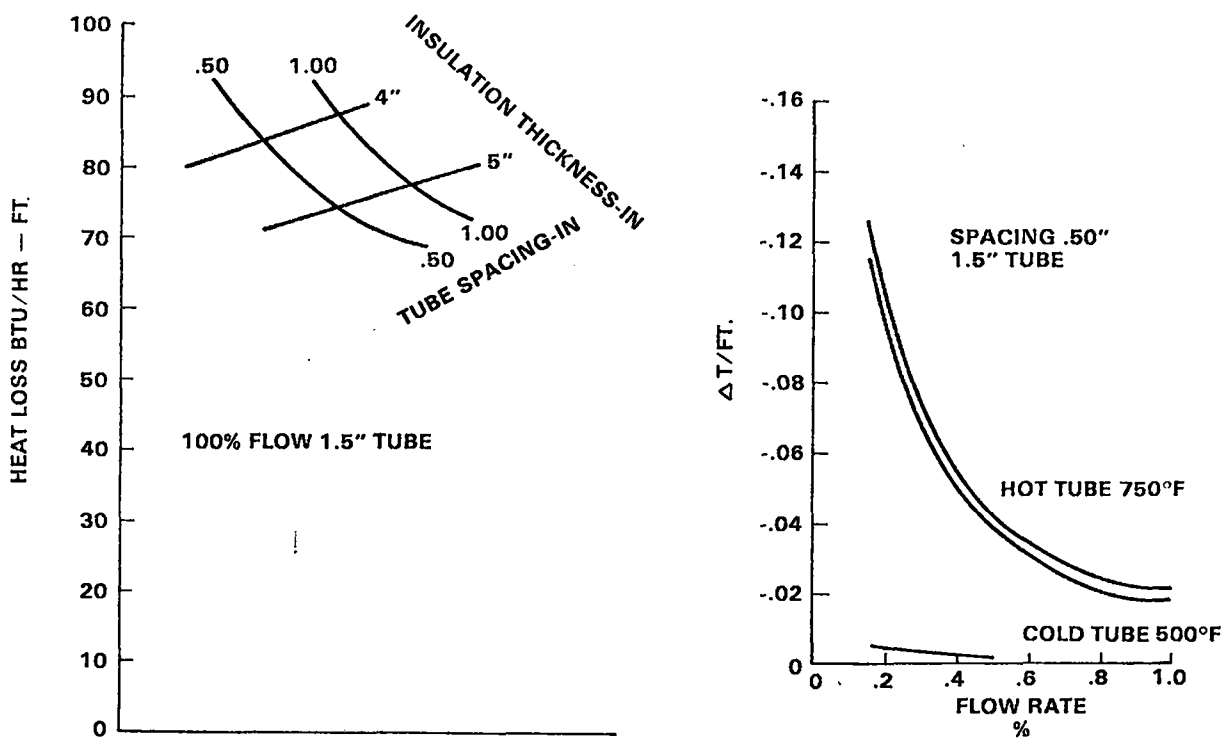


Figure 3.3-11. Parametric Analysis of Nested Pipes (Tubes)

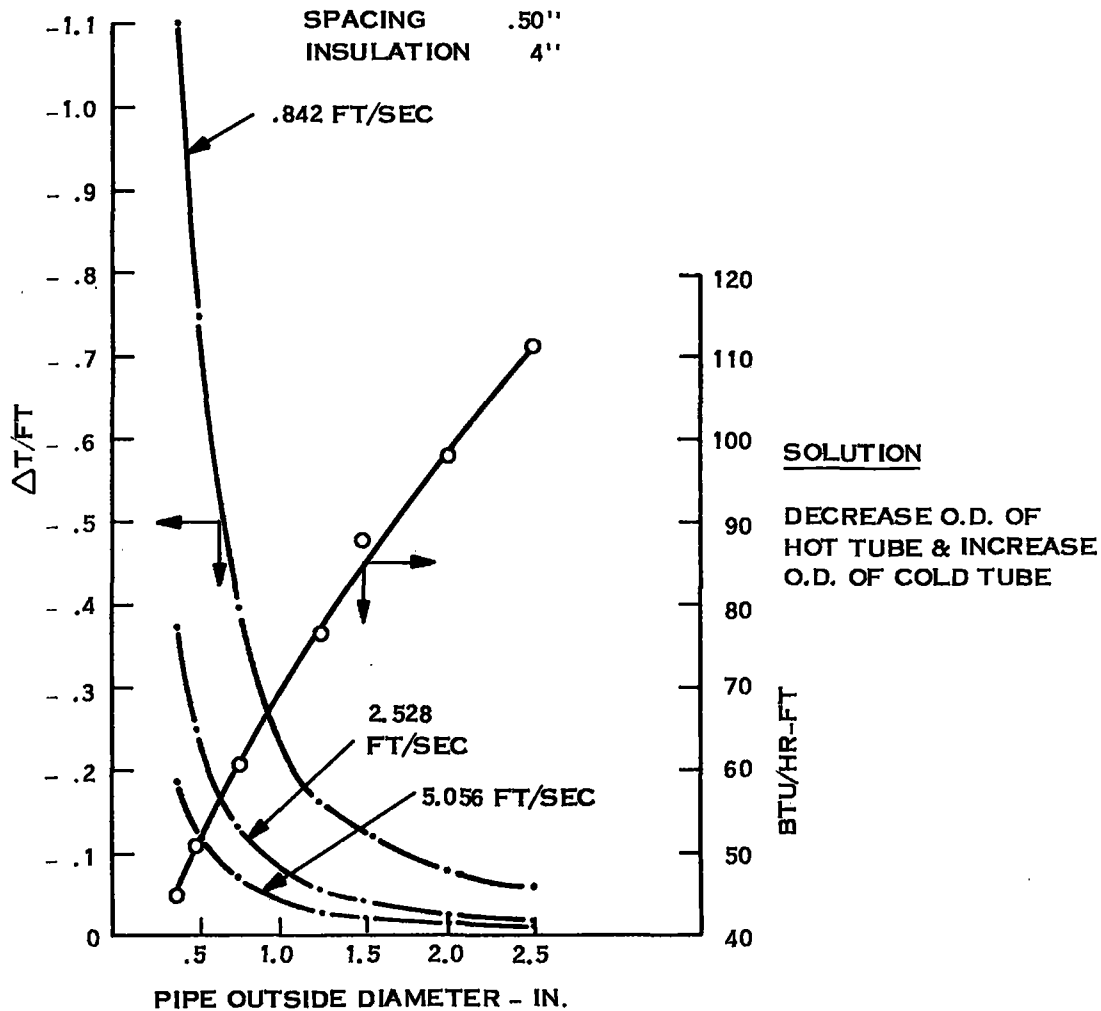


Figure 3.3-12. Temperature Drop and Heat loss vs. Pipe Diameter and Flow Rate

tapered branch (stepped) 0.038, 0.025, 0.019 meter (1-1/2, 1, 3/4 in.) tube size under the same condition indicates a heat loss reduction per branch of about seven percent or about four percent for the overall filed.

To reduce the thermal capacity of the system and thereby increase the net energy delivered to the PCS, thin walled tube has been substituted for pipe. The thinnest wall used is 18 ga. (0.0012 meter or .049 in. wall) in seamless tubing, and the savings in weight and thermal capacity is about 66 percent in sizes below 0.051 meter (2 in.) OD. For tube sizes greater than 0.051 meter (2 in.), a 0.0032 meter (0.125 in.) wall is used so that butt joints can be properly made on the tube end. Thermal capacity reduction is about 50 percent. The substitution of tube for pipe is also included in the pressure drop analysis where the friction factor for tube is about $f_T = .014$ and for pipe $f_P = .019$, or a 25 percent reduction in friction loss at the same flow rate.

3.3.2.2.3 Pipe Supports

The system design requirements specify the use of American National Standards Institute (ANSI) Power Piping Codes where applicable; pipe supports are included under the code definition. All pipe support designs will meet the code requirements specified in Section B31.1 Paragraph 121.0. The code specifies requirements for pipe or tube support spacing, and Table 3.3-7 shows the spacing requirements per the code for liquid filled tube at 672°K (750°F). The final design will concentrate on supporting the tubes per the code without excessive heat leaks.

Table 3.3-7. Suggested Pipe Support Spacing

Nominal Pipe Size Inches	Suggested Maximum Span			
	Water Service		Steam, Gas, or Air Service	
	Feet	m	Feet	m
1	7	2.1	9	2.7
2	10	3.0	13	4.0
3	12	3.7	15	4.6
4	14	4.3	17	5.2
6	17	5.2	21	6.4
8	19	5.8	24	7.3
12	23	7.0	30	9.1
16	27	8.2	35	10.7
20	30	9.1	39	11.9
24	32	9.8	42	12.8

- Note 1. Suggested maximum spacing between pipe supports for horizontal straight runs of standard and heavier pipe at maximum operating temperature of 750 F (400 C)
- Note 2. Does not apply where span calculations are made or where are concentrated loads between supports such as flanges, valves, specialties, etc.
- Note 3. The spacing is based on a maximum combined bending and shear stress of 1500 psi (10.35 MPa) and insulated pipe filled with water or the equivalent weight of steel pipe for steam, gas or air service, and the pitch of the line is such that a sag of 0.1 in. (2.5 mm) between supports is permissible.

3.3.2.2.4 Pipe Field Thermal Expansion Design

Thermal expansion in the field must be accommodated to prevent failure in the fluid lines from causing loss of fluid or failure in the insulation system from causing excess heat loss. A method developed during the preliminary design to accommodate the pipe field thermal expansion is shown in Figure 3.3-13. At every other branch line, there are two linear expansion compensators welded together, one on the hot side and one on the cold side, with an integral anchor similar to that shown in Figure 3.3-14. In addition, a fluid connection would be welded to the anchor section of pipe for the branch line connections. This method fixes the location of the nested hot and cold branch lines and prevents differential movements of the lines that would tear the insulation apart. Proper piping arrangement between the branch lines and manifolds can eliminate movement of the control valve bodies which, due to their weight, must be separately supported. Such an arrangement is shown in Figure 3.3-13. Total east-west expansion of the 1.1 meter (45 in.) manifolds is about 1.0 meter (40 in.). Placing dual compensators at every other branch in the 20 branch system requires each dual compensator to expand 0.10 meter (4 in.). This is easily accomplished with commercially available linear expansion compensators rated for 672°K (750°F) and 2.1×10^6 N/m² (300 psi) internal pressure. The unique feature of the linear compensators is that at room temperature the bellows in the compensator is fully compressed or at a maximum stress level where the bellows material has

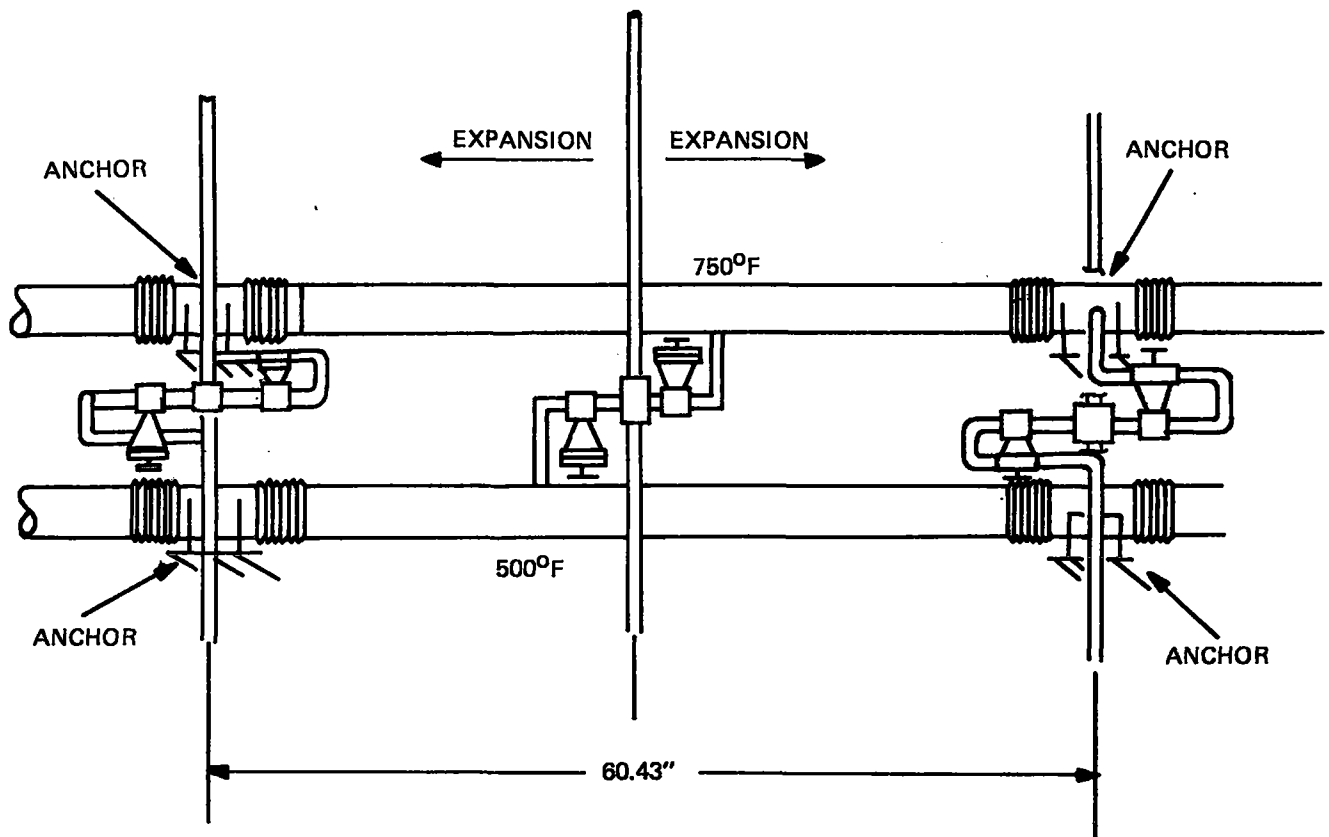
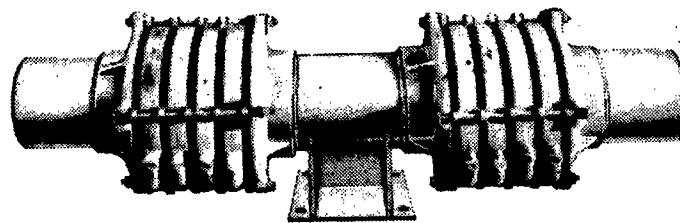


Figure 3.3-13. Branch Line and Manifold Arrangement



RATED FOR 750°F @ 300 psi

Figure 3.3-14. Dual Controlled - Flexing Expansion Joints for Thermal Expansion Compensation

maximum strength, and at 533°K (500°F) or 672°K (750°F), the bellows is in its expanded low stress state, thereby allowing the maximum use of the cycle life of the bellows material. During the next phase of the program, final design details and specifications will be developed. The same design scheme used on the manifold will be used on the nested branch line to suppress the total and differential thermal expansion of the branch lines during heatup from ambient to 533°K (500°F) and to 672°K (750°F), respectively.

3.3.2.2.5 Field Temperature Distribution

One of the system design requirements is that the field return to the TES or Mechanical Equipment Area is at a minimum temperature of 658°K (725°F). A temperature distribution was determined for the 7-meter one-in-series configuration with nested branch lines and nested up and down lines. The results of this

- Low cost, commercially available
- Material compatible with Syltherm 800 up to 672°K (750°F)
- Field assembly with conventional joining methods
- Comply with ANSI B31, 1 Power Piping Code.

The first of these requirements eliminates non metallic materials, aluminum and copper. The fourth requirement eliminates stainless steel and members of the super alloy family. This leaves carbon steel which has good strength, ductility, and low cost and is readily available. ANSI B31.1 specifies A192 or A179 seamless tubing in carbon steel for high temperature service which meets all of the collector loop piping material requirements. In addition A192 or A179 can be readily welded by Tungsten Inert Gas techniques which is necessary to meet the leak requirement.

Material for valve bodies has also been specified as carbon steel. Forged carbon steel valve bodies are preferred but may only be available in sizes less than 0.051 meter (2 in.). The control valves used in the subsystem should be made from cast carbon steel, American Society of Testing Materials (ASTM) 216WOB or equivalent. Compatibility of carbon steel and Syltherm 800 at 672°K (750°F) has been demonstrated by Dow Corning. Grafoil is an acceptable valve stem packing material, while metallic O-ring seals are recommended for flange applications.

3.3.2.4 Insulation

Figure 3.3-16 shows the insulation configuration for single and nested tubes. The configurations depicted are based on suggestions found in vendor literature. The design implies that the insulation is to be installed in layers whose 0.91 meter (3 ft) length overlap to prevent heat loss due to relative movement during heatup. In addition, the axial seam of the insulation is to be rotated 120degrees/layer to minimize heat loss during movement.

As shown the insulation is to be enclosed with an aluminum jacket to provide weather and damage protection. The jacketing is to be held in place with bands with the seam covered with a non hardening mastic. For singly insulated tubes, the insulation is readily available in layers. The 16 gage aluminum jacket and mastic are commercial items and also readily available. The insulation for the nested configuration is not a commercial item and must be fabricated per design and made up from existing configurations. (See Figure 3.3-17 for the thickness required for a given pipe or tube diameter.)

3.3.2.5 Valves and Pumps

The selection of the proper pumps and valves for handling the Syltherm 800 heat transfer fluid was based partly on the operating experience of Dow Corning, the manufacturer of Syltherm 800. For the valves the requirements are as follows:

1. Cast or forged steel meeting ANSI BB1.1
2. Globe type valve with Class IV shutoff or better
3. Grafoil packing
4. Socket or butt weld fittings
5. Bolted bonnet type for field maintenance considerations
6. Rated for 672°K (750°F) operation and 6.9×10^5 N/m² (100 psi) for 20 years.

These requirements can be met by commercially available hardware for both manual and remotely controlled valves. Valve sizes are based on minimum ΔP for manual valves and $\Delta P = 34,475$ N/m² (5 psi) for control valves.

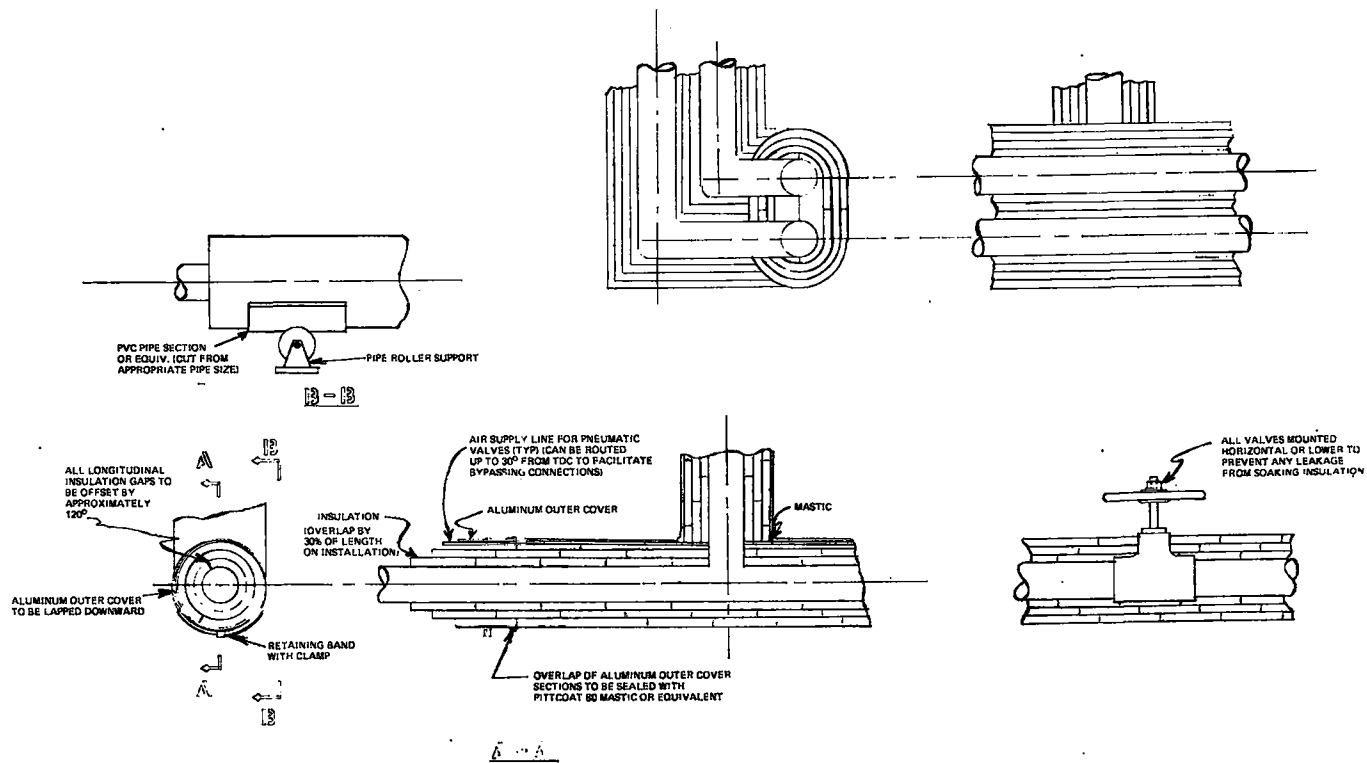


Figure 3.3-16. Typical Insulation Outline for Syltherm 800 Piping

The requirements for the selection of pumps used in the collector loop subsystem were developed based partly on inputs from Dow Corning and others developed by General Electric during the Preliminary Design phase. The pump requirements are:

1. Centrifugal type pump
2. Cast steel casing
3. Meet API 610 design specification
4. Rated for 672°K (750°F) for 20 years at working head
5. Have raised face flanges and suction and discharge ports
6. Water coolant isolated from shaft stuffing box.

Vendors manufacturing pumps meeting the above requirements are Dean Brothers, Gould, Ingersoll Rand, and Worthington. Details of the pumps selected for the preliminary design will be found in Paragraph 3.3.2.6, Hydraulic Analysis. The type of valves chosen for the preliminary design are defined in Paragraph 3.3.2.7, Controls.

3.3.2.6 Hydraulic Analysis

A hydraulic analysis of the field and Mechanical Equipment Area (MEA) was performed to determine the field and MEA ΔP and for the selection of fluid pumps. To determine the parasitic losses associated with pumping Syltherm 800 through the collector loop subsystem, it was necessary to estimate the pressure drop associated with each different flow element shown on Figure 3.3-17 for both the hot and cold sides of the loop. Pressure drops for the flow elements were estimated using the formulas given in Crane Technical Paper 410 "Flow of Fluids through Valves, Fittings, and Pipe" and the properties of Syltherm 800. Pressure drops for pipe lengths are based on relative roughness data for drawn tubing.

The pressure drop calculations were conducted for full flow, 0.025 m³/s (390 gpm), and at constant supply and return temperatures of 533°K (500°F) and 672°K (750°F), respectively. The results of this calculation are as follows:

ΔP of 500°F supply line	12.57 psi
ΔP of 500°F side of branch line	13.47 psi
ΔP of 500°F up tube	.73 psi
ΔP of receiver (maximum allowed)	5.00 psi
ΔP of 750°F down tube	3.12 psi
ΔP of 750°F return branch line	9.63 psi
ΔP of 750°F return line	9.90 psi

Total field ΔP = 54.42 psi or 3.75×10^5 N/m²

The total field ΔP at start-up with the field fluid at ambient temperature would be around 6.0 psi (4.1×10^4 N/m²) due to the low flow rate ($\sim 1/5$ full flow), even though the friction and fluid density would be somewhat higher.

The same type of analysis was performed for the lines in the high temperature thermal storage loop in the Mechanical Equipment Area (Figure 3.3-18.) The maximum pressure drop found was associated with charging the one-hour storage tank and was 2.9×10^5 N/m² (41.89 psi).

The total ΔP for the Collector Field Subsystem is therefore estimated at about 6.6×10^5 N/m² (95.5 psi) or about 67 meter (220 ft) head of water equivalent. The field pump selection was based on 0.025 m³/s (390 gpm) flow at 67 meter (220 ft) water head. Figure 3.3-19 shows a typical head-flow curve for a centrifugal pump with a 0.76 meter (3 in.) discharge line and a 0.10 meter (4 in.) suction line. The intersection of 0.025 m³/s (390 gpm) and 67 meter (220 ft) head shows a 0.076 x 0.10 meter (3 in. x 4 in.) pump

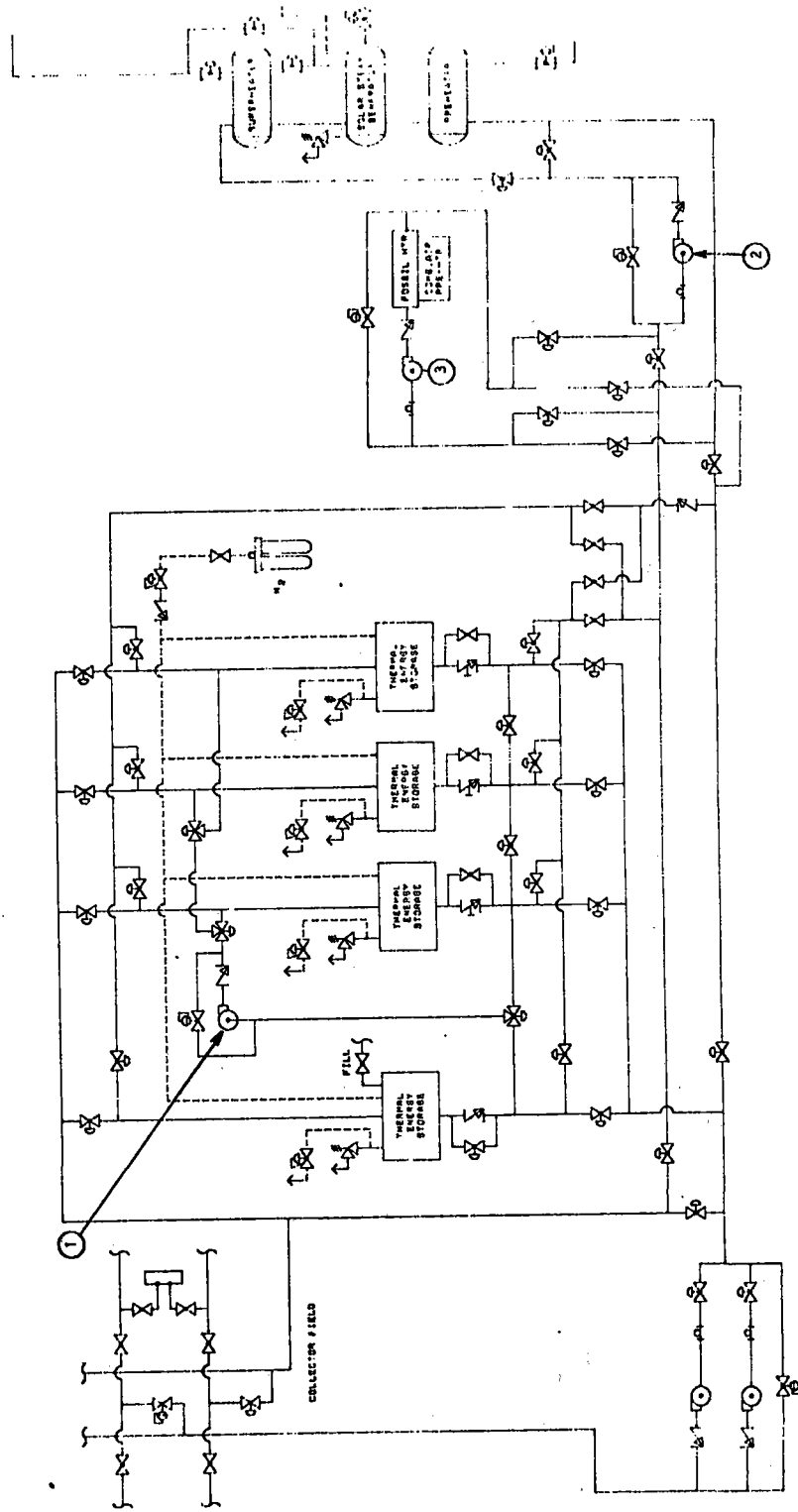


Figure 3.3-18. Mechanical Equipment Area High Temperature Storage Piping

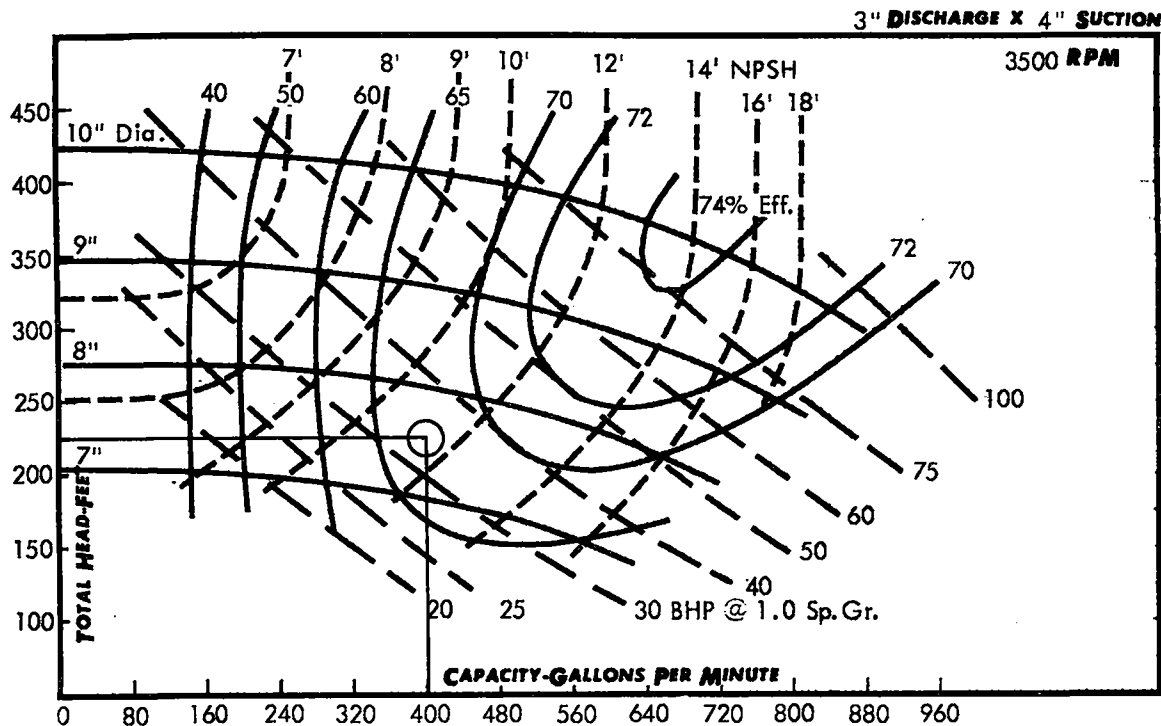


Figure 3.3-19. Collector Pump Characteristics for Single Field Pump

with an 0.20 meter (8 in.) impeller to be satisfactory. This pump, at the design point, would require about 25 kW (34 bhp) operating at 68 percent efficiency with 3.4 meters (11 ft) of net positive suction head to pump $0.025 \text{ m}^3/\text{s}$ (390 gpm) at 67 meters (220 ft) head. It is important to note that, since the pump has a bypass loop with a control valve upstream of the bypass, regardless of the field flow requirements, the pump will see a constant head which is set by the control valve. However, one of the system requirements is to keep the parasitics low and provide high reliability on the main circulating pumps. These requirements suggest the use of two pumps.

To reduce the pump parasitics, a parallel pump configuration was examined. This configuration had two full head, 50 percent flow pumps operating in parallel. Figure 3.3-20 shows that each pump would be 0.051×0.076 meter (2 in. \times 3 in.) with a 0.19 meter (7-1/2 in.) impeller operating at 64 percent efficiency and requiring about 12.7 kW (17 bhp).

Figure 3.3-21 is a plot of the system head curve with data for single and parallel pump operation shown. The operating point for a particular pump configuration is the intersection between the pump curve and the system head curve. Thus for the $0.076 \times 0.10 \times 0.25$ meter (3 \times 4 \times 10 in.) pump with a 0.20 meter (8 in.) impeller, the operating point is in excess of the $0.025 \text{ m}^3/\text{s}$ (390 gpm) requirement, and the power consumption for this single full size pump would be constant at 25.4 kW (34 bhp) for all hours of operation.

For the parallel operation of the two full head, half flow pumps, it is seen that the intersection of the pump and system curve is $0.025 \text{ m}^3/\text{s}$ (390 gpm) satisfying the flow requirement. However, when only one of these pumps is operating, the intersection of the pump and system head curve shows about $0.020 \text{ m}^3/\text{s}$ (320 gpm) or over 80 percent of the flow requirement with only 50 percent of the power consumption for that portion of the day when less than $0.020 \text{ m}^3/\text{s}$ (320 gpm) is required.

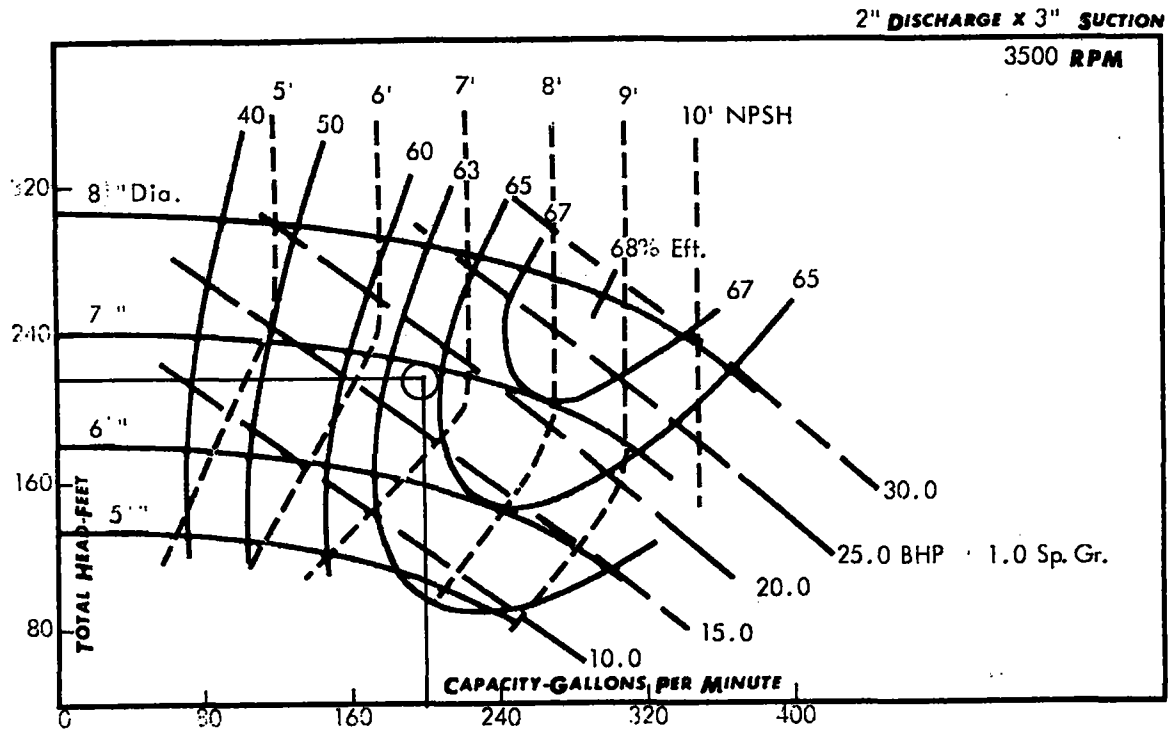


Figure 3.3-20. Collector Pump Characteristics for Parallel, 50 Percent Flow Pumps

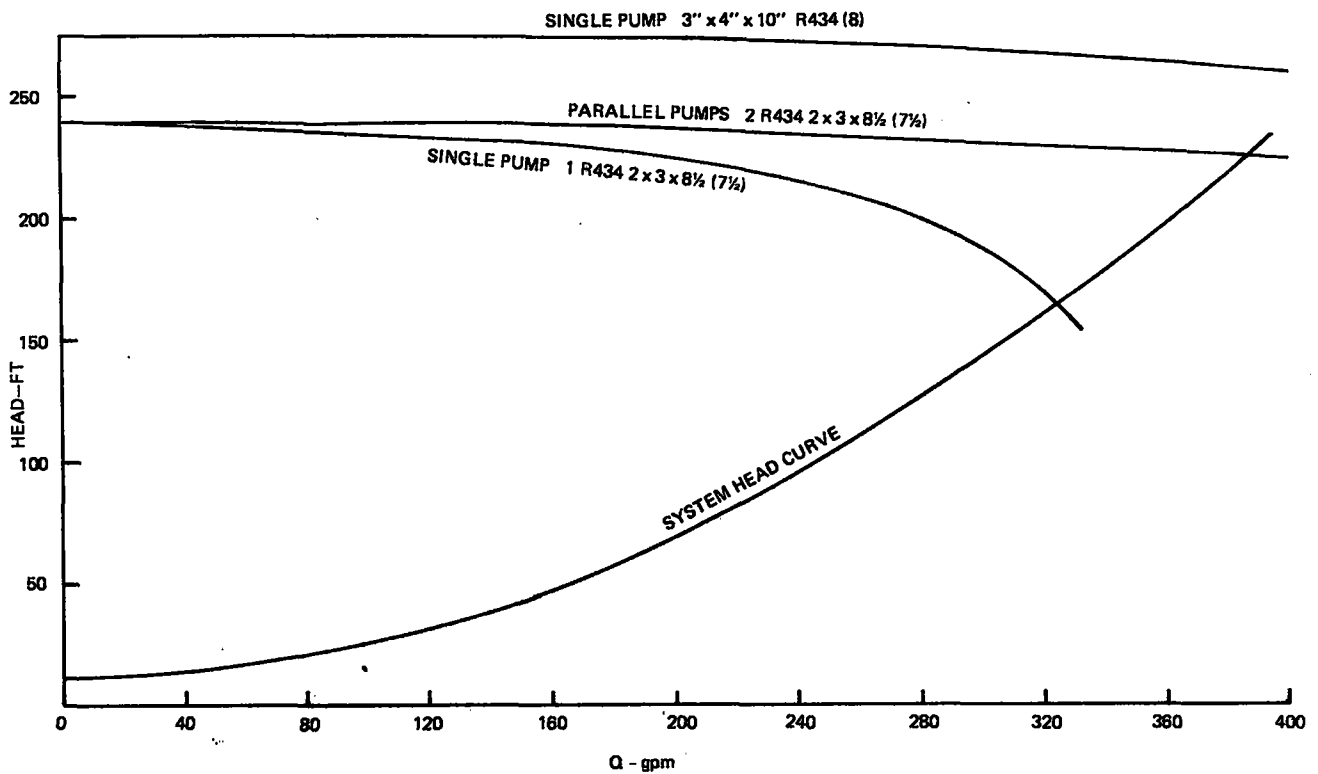


Figure 3.3-21. Collector Field Circulating Pumps Performance Curves

Figure 3.3-22 shows a relation* between solar insolation, required flow rate pump power, and solar time and indicates a major savings in energy consumption with full head, half flow pumps in parallel operation. In addition, this configuration provides the required redundancy and is also less expensive than two full size pumps.

The pumps for the Mechanical Equipment Area include the TES transfer pump 1 on Figure 3.3-18 and the Steam Generator Supply pump 2. The requirements for the TES transfer pump were 0.025 m³/s (390 gpm) at 672°K (750°F) with a 2.4 x 10⁵ N/m² (35 psi) head of 24.7 meters (81 ft) of water. The pump selected for preliminary design is 0.076 x 0.10 x 0.29 meter (3 x 4 x 11-1/2 in.) with a 0.24 meter (9-1/2 in.) impeller drawing about 8 kW. The requirements for the Steam Generator Supply Pump are 0.021 m³/s (325 gpm) at 672°K (750°F) against a 31 meter (102 ft) head. This takes a 0.76 x 0.10 x 0.29 meter (3 x 4 x 11-1/2 in.) pump with 0.27 meter (10-1/2 in.) impeller consuming about 12 kW while running. The small pump shown on Figure 3.3-18 for the Syltherm Heater 3 is to be supplied by the heater manufacturer and is estimated to be less than 373 watts (1/2 HP).

3.3.2.7 Controls

The requirements for the control elements used in the preliminary design were derived from the system requirement defined in Paragraph 3.3.2.1. The basic control requirements are to regulate the flow rate to the field and to the individual collectors in such a way that, for a supply temperature of 533°K (500°F), the minimum return temperature under a direct normal insolation is 658°K (725°F). In addition, provision for isolating the individual collectors or whole branches must be provided for maintenance. To account for variations in receiver fabrication, some means must be provided to allow all collectors in a branch to have output temperature within a range of 3°K (5°F) for the same input temperature. Several alternative field control methods were evaluated during the preliminary design as summarized in Figure 3.3-23. The first

*Note: extended from Liu and Jordan seasonal average

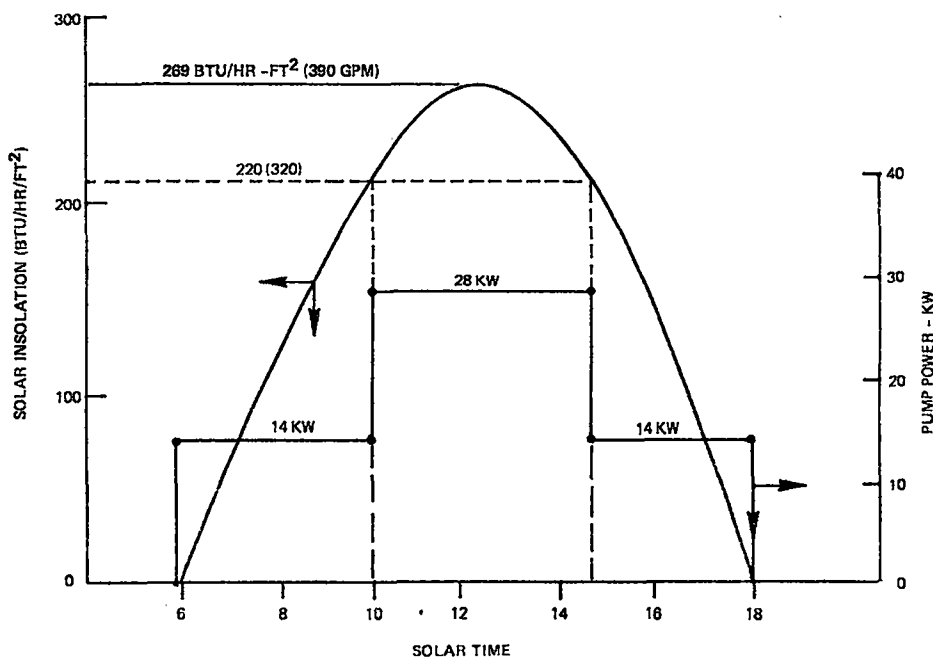
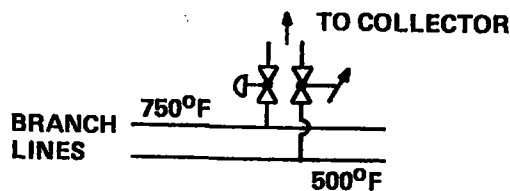


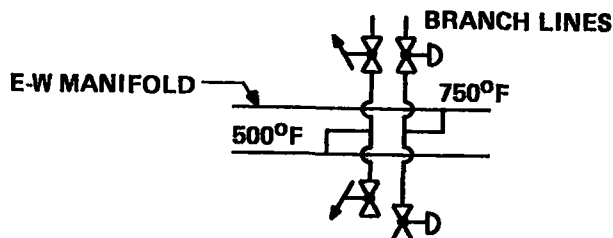
Figure 3.3-22. Solar Insolation and Pump Power Vs. Solar Time

- PNEUMATIC CONTROL VALVE AT EACH COLLECTOR



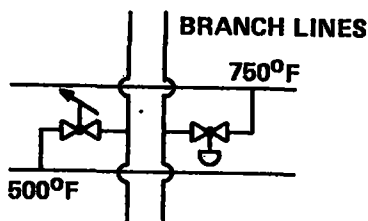
192-3/8 PNEUMATIC
CONTROL VALVES
\$ (272052) M*
(374952) R

- PNEUMATIC CONTROL VALVES ON EACH NORTH BRANCH AND EACH SOUTH BRANCH



36-1½ PNEUMATIC
(101988) M
(129960) R

- SINGLE PNEUMATIC CONTROL VALVE PER BRANCH



20-1½ PNEUMATIC
(89640) M
(113520) R

- SINGLE PNEUMATIC CONTROL VALVE PER FIELD

*DOES NOT INCLUDE
INSTALLATION COST

Figure 3.3-23. Collector Field Control Scheme Variations

scheme employs a control valve at each collector (192) with either a remote or manually operated shutoff valve on the up tube, thereby allowing maximum field temperature control under any solar input. A second possible configuration is to have control valves on each north and south branch, thereby accommodating partial field shadowing from clouds which might cover either the north or south portions of the field. This would reduce the number of required control valves to 36.

The final configuration is to provide a control valve at each north-south branch for a total of 20 valves. Assuming the use of pneumatically operated control valves, the final or third configuration is the least expensive but has the least control flexibility. Justification for using pneumatically operated control valves will be presented later in this section. Since cost is a strong design influence, the third control valve configuration was selected for the preliminary design. Modifications to this configuration were made to accommodate winter solstice and sunrise and sunset conditions to be explained later.

Two types of control valves typically used in industrial applications are electrically and pneumatically operated. Cost comparisons made in Reference 3.3-1 show the cost of electric valves to be at least twice that of pneumatic valves. In addition to cost, there is the concern for the equipment or design considerations that are required to allow valve operation under loss of electrical power conditions. With the electrically actuated valve, a battery power source with an inverter or a motor generator set would be

required. With a pneumatic system, an accumulator tank can provide compressed air for emergency operation if required. Further, with pneumatically controlled valves the valve actuator can be designed to fail open by spring actuation. For the above reasons, pneumatically operated control valves are chosen. These valves use a standard 4-20 ma signal in conjunction with a $2.1 \times 10^4 - 1.0 \times 10^5 \text{ N/m}^2$ (3-15 psig) air supply to control the globe valve position through the use of an electro-pneumatic positioner. To provide additional data on valve operation, a rotary slideware potentiometer is used for valve position feedback. A handwheel is also provided to allow the valve to be closed manually. Figure 3.3-24 depicts a typical pneumatic control valve.

Figure 3.3-17 shows one modulating control valve per branch along with a two position pneumatically operated shutoff valve. Position control of the modulating valve is based on the fluid temperature. During initial startup of the system, each branch will be operated individually under direct normal solar insolation. Manual flow trim valves on each up-line will be used to adjust each receiver output temperature to within 3°K (5°F) of 672°K (750°F). Temperatures will be read by a temperature sensing device on each receiver output tube. The temperature data will be sent to the minicomputer which will scan all collectors in a branch and change the valve position in response to the highest temperature in the branch. Should the temperature sensor fail, or if a temperature greater than 675°K (755°F) occurs, that collector(s) will be defocused.

Another field control function requirement is to regulate temperature during sunrise and sunset when some collectors are in shadow while others are in full sun. Figure 3.3-25 shows the site layout for the Preliminary Design with the branches numbered 1-20 starting with (1) on the west side. At sunrise, branch 20 receives full sun as do the northernmost collectors in branches 15, 16, 17 and 19. The temperature in branch 20 can easily be controlled with the existing control valve, but a different solution is required for temperature control in branches 15, 16, 17 and 19. The normal temperature control mode is to control from the hottest collector in the branch, but in branches 15, 16, 17 and 19, this is the northernmost collector and is the only collector in full sun. The control valve would open to allow more flow to keep the output temperature of the northernmost collector to within tolerance at 672°K (750°F). However, the other collectors in the branch are shadowed, and therefore the output temperature from these collectors would be out of tolerance. The design provides a control valve on the northernmost collector in branches 15, 16, 17, and 19 to control that valve position based on its temperature only. The other collectors in the branch would use the existing flow control valve whose position would be determined by the highest temperature read in the remaining collectors in that branch.

At sunset a similar problem occurs in branches 1, 2, 4, and 5. Temperature control of the first branch can be accomplished with the existing control valve. For branches 2 and 4, a control valve must be added to the southernmost collector. These collectors would then be able to control the fluid output temperature independently of the remaining collectors in the branch similar to the sunrise situation. The fluid temperature control solution for branch 5 is to install a control valve at the location indicated in Figure 3.3-26. During the hours of sunset, the collectors south of the control valve will receive full sun while those collectors north of the control valve will be in shadow. The flow setting of the primary control valve will be set by the highest temperature in the lower six collectors while the flow setting in the secondary valve will be determined by the highest temperature in the upper five collectors.

During winter solstice, a condition will exist where the eight southernmost dishes or collectors will be partly shadowed. The design solution is to add eight control valves to those southernmost collectors and trim the manual valves to a high pressure drop thereby forcing more flow to the southernmost collector when it is in full sun. As the shadow on the other collectors decreases, the pressure drop on the southernmost collector will be increased to provide the flow required.

In all a total of fifteen control valves have been added to the collector loop. During the definitive design, the setting of the manual valves will be determined, and an analysis will be conducted to determine the flow distribution in the field resulting from control valves operating in both parallel and series configurations.

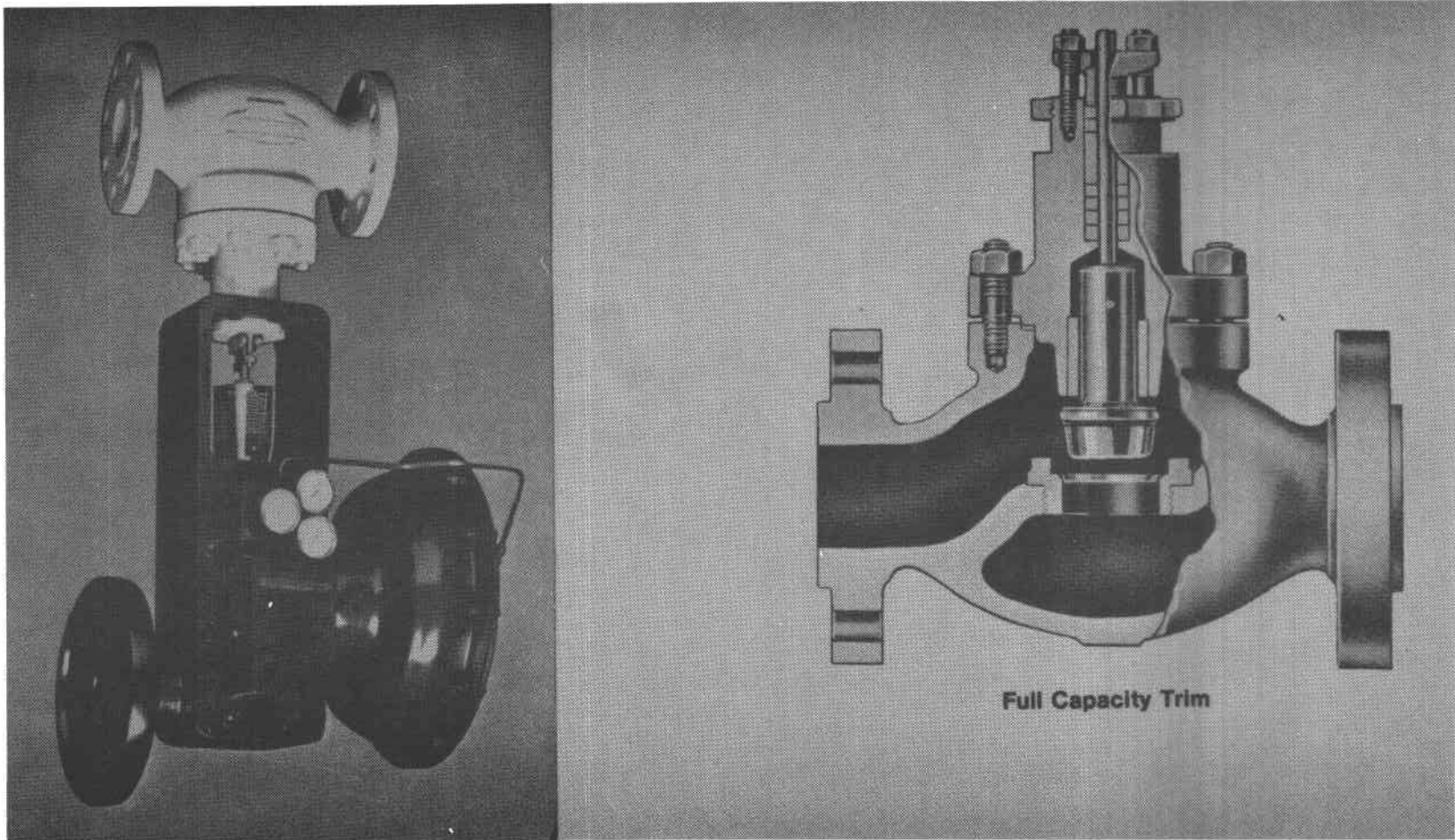


Figure 3.3-24. Pneumatic Control Valves

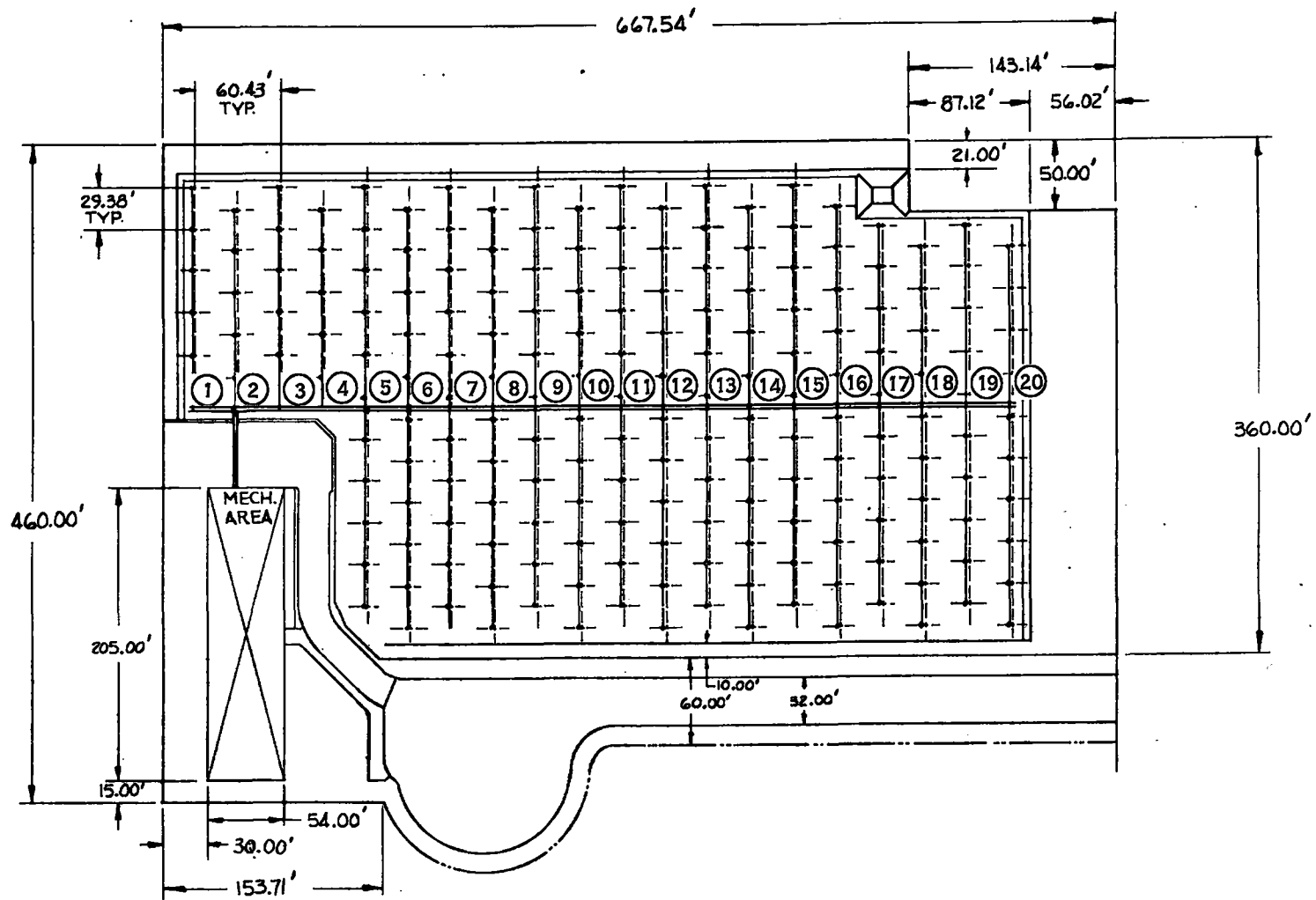


Figure 3.3-25 STE-LSE Site Layout

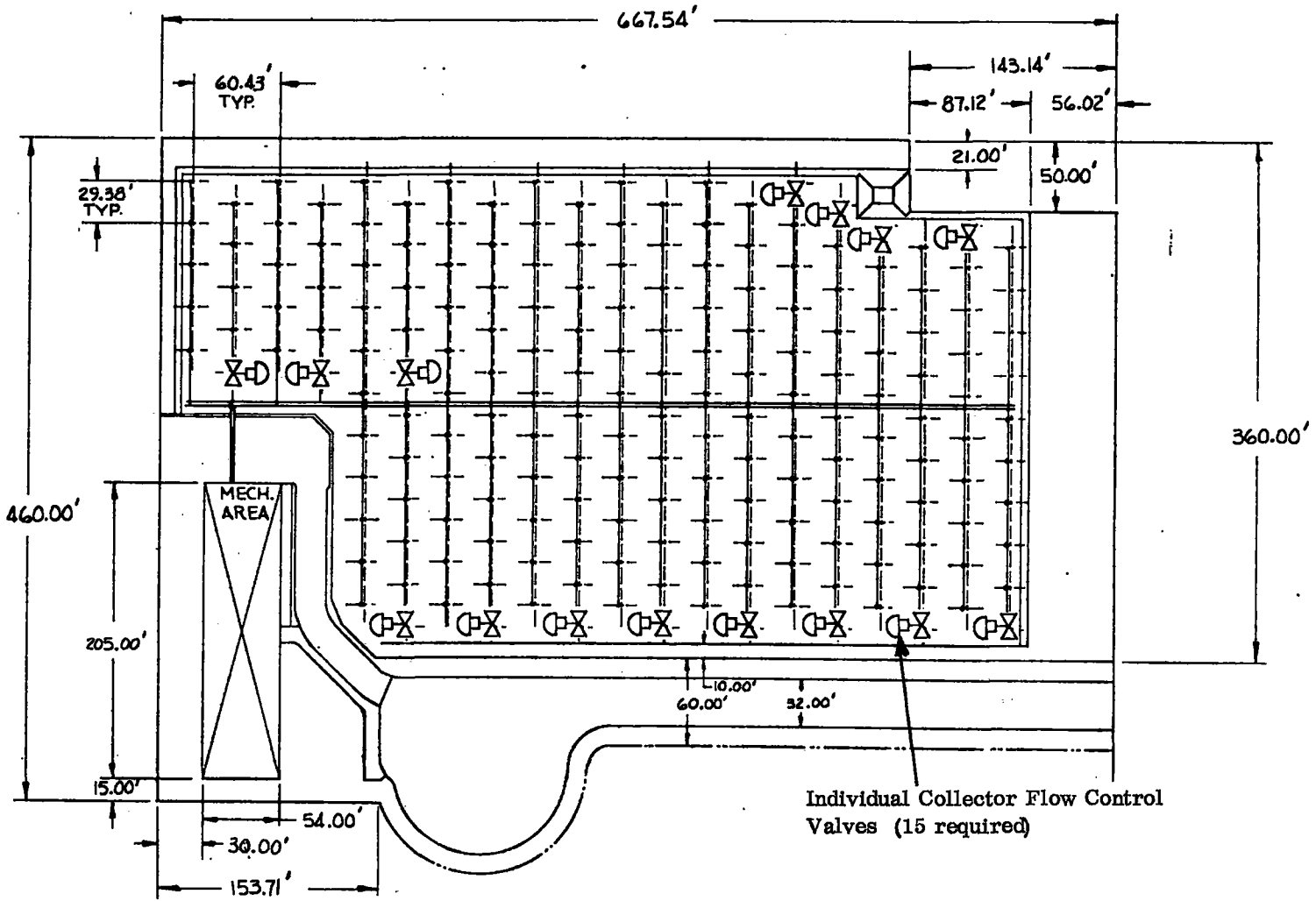


Figure 3.3-26. STE-LSE Site Layout with Control Valves

Figure 3.3-17 also shows the location of the manual isolation valves used for branch and collector isolation. In addition, the location of valves and fittings for fluid fill and drain are indicated.

3.4 HIGH TEMPERATURE THERMAL ENERGY STORAGE (HTS)

The Shenandoah LSE thermal storage subsystem has been designed to provide a low cost state-of-the-art storage system to meet the requirements of the Shenandoah STES. The subsystem requirements included the storage of excess thermal energy to provide system operation during periods of transient cloud cover and to extend system operation to meet nighttime demands. The HTS is required to deliver energy at a near constant temperature with acceptable tolerances defined by the PCS boiler design.

The specific design requirements on the subsystem include (1) a thermal capacity of 1.06×10^{11} Joules (100 Mbtu) to meet the system requirement of 60 percent of the annual load demands discussed in Section 2, (2) a storage temperature range of 533 -672°K (500-750°F), (3) maximum charge and discharge rates of 4.7×10^6 Joules/second (16 MBtu/hr) and 2.4×10^6 Joules/second (8.2 MBtu/hr), respectively, compatible with the system operating modes, (4) storage media and containment and compatibility with the Syltherm 800 collector fluid, and (5) daily thermal loss maximum of four percent of storage capacity.

Sensible heat storage was identified during the Conceptual Design, Reference 3.4-1, as the most direct state-of-the-art method of storing thermal energy. Latent heat systems offered the advantage of constant temperature delivery over a narrow temperature range with a large heat capacity per unit volume, but high temperature latent heat systems are not presently available. Sensible heat storage concepts considered for use with solar thermal systems have included thermocline with heat transfer fluid, thermocline with rocks and heat transfer fluid, and multiple tanks with heat transfer fluid. For the Shenandoah design, system studies (Section 2) indicated the desirability of operating in the 644-672°K (700-750°F) range for optimum performance. This high temperature requirement led to the selection of a silicone based oil, Syltherm 800, as the heat transfer fluid.

Since the heat transfer fluid then became a significant cost item (\$16-\$19/gallon) the design approach was to select a storage concept to minimize the fluid inventory within the TES subsystem. This was accomplished by selecting a trickle oil HTS design concept being developed by General Electric which utilizes the working fluid strictly for heat transfer. The heat transfer is accomplished by a thin film trickle fluid flow over the media bed. This approach minimizes the system fluid inventory, requiring only a filled sump beneath the tank, compared to the dual medium storage design, reference 3.4-2, which utilizes a flooded oil/bed tank.

The design approach was to identify and utilize the lowest cost acceptable solid storage media in a packed bed form that could withstand the system operating temperature. Rock was the initial choice, but subsequent test results indicating compatibility problems with the Syltherm 800 led to the tentative design selection of taconite, a pelletized iron ore. The subsystem design effort concentrated on developing a means to provide the effective heat transfer to and from the solid storage medium.

During the Preliminary Design Phase, trickle oil heat transfer capability was verified on small scale tests (Section 8.2) and additional cost tradeoffs verified the cost savings of the trickle oil system. Since large scale prototype tests of the trickle oil system were not planned, the subsystem was designed with the flexibility to operate in the dual media mode as a back-up operational mode. The following sections provide a description of the subsystem and describe the tradeoffs performed during the preliminary design effort.

3.4.1 SUBSYSTEM DESCRIPTION

The HTS subsystem consists of the four HTS tanks and the HTS transfer pump and the interconnecting piping, valves, and associated instrumentation and controls. Interconnecting flow paths throughout the HTS subsystem allow for the transfer of hot Syltherm 800 fluid from the collector field to the HTS tanks, from one HTS tank to another, and from the HTS tanks to the Steam Generator Supply subsystem. The HTS piping configuration is shown in Figure 3.4-1, and Table 3.4-1 summarizes the design characteristics.

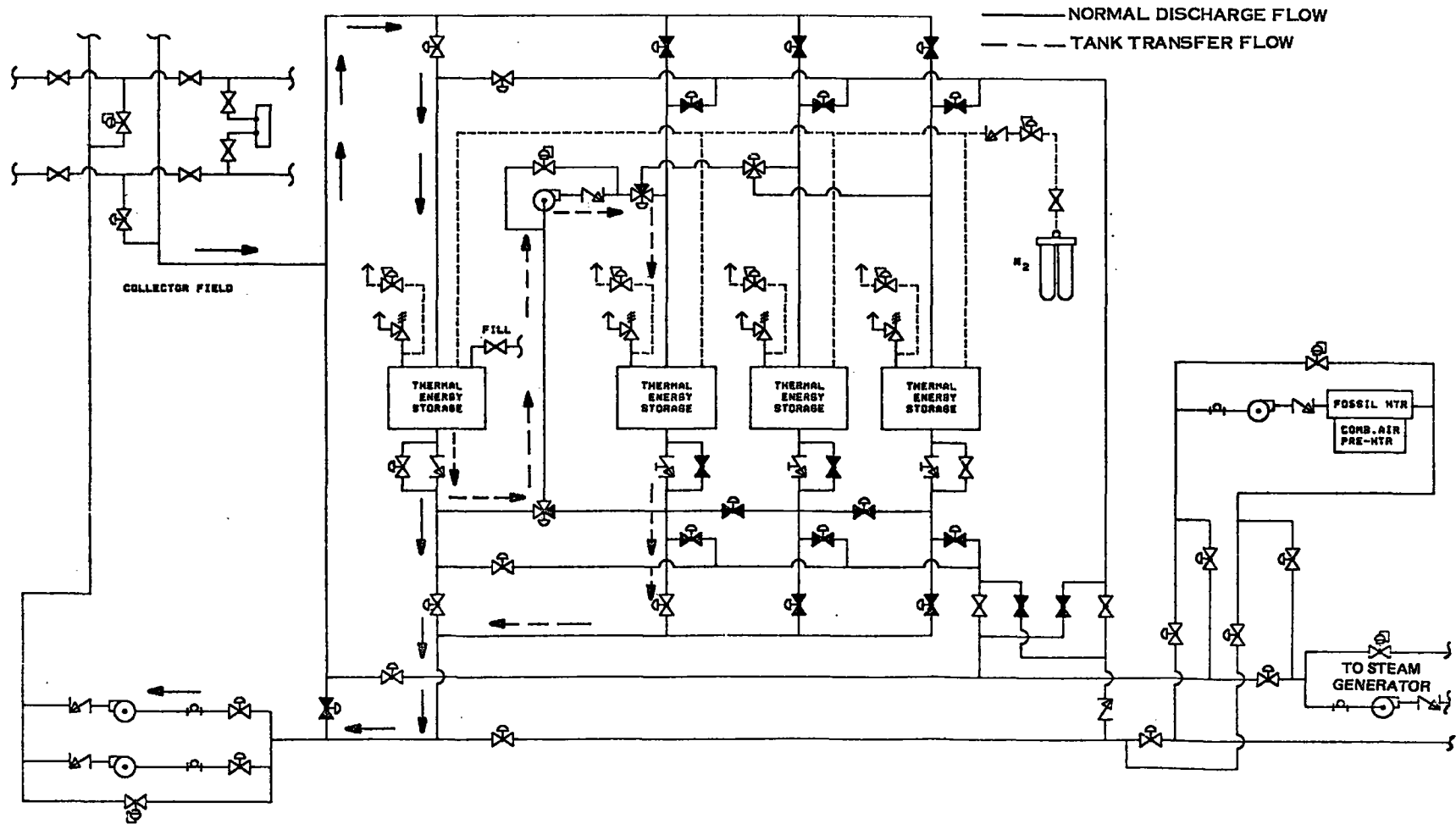


Figure 3.4-1. Trickle Oil Schematic - Charging Mode

Table 3.4-1. Description of HTS Subsystem

	One Hour Tank	Large Tank
Tankage		
Type	Cylindrical, axis vertical	Cylindrical, axis vertical
Quantity	1	3
Diameter	13 feet	20.6 feet
Height	12 feet	16 feet
Volume	11,800 gallons	40,065 gallons
Thermal Capacity		
Trickle Oil	9×10^6 BTU	30.3×10^6 BTU ³
Dual Media	11.5×10^6 BTU	38.8×10^6 BTU
Max Charge Rate	16×10^6 BTU	16×10^6 BTU
Max Discharge Rate	8.2×10^6 BTU	8.2×10^6 BTU
Storage Temperature Range (1)	500-750°F	500-750°F
Solid Media (Taconite)	103 tons	348 tons
Fluid Inventory Syltherm 800 @ 77°F		
Trickle Oil	1110 gallons	2550 gallons
Dual Media (2)	2250 gallons	7590 gallons
<p>(1) Carbon steel forms currently being considered as alternative (2) Assumes 30% voids (applies to trickle oil mode also) (3) The last tank does not get charged to this capacity since charging is terminated when the breakthrough temperature of 561°K (550°F) is reached.</p>		

Multiple tanks are required to allow discharge of a partially charged system. The first tank was sized to provide approximately one hour of energy delivery to the PCS at peak design condition. It is charged prior to system energy delivery to the PCS to provide continual system operation during intermittent energy collection. The remaining three tanks were sized equally to provide the total 1.06×10^{11} Joules (100 MBtu) capacity based on the trickle mode of operation. Four tanks were selected based on practical limitations of control complexity, interconnecting piping requirements, and physical location of the tanks within the Mechanical Building, the initial tank location. The four tanks also eliminate the need for a separate system fluid expansion tank by allowing the fluid to expand from the sump into the bottom of the tank.

In the trickle oil mode, heat transfer is accomplished by a gravity fed trickle oil flow through the bed. A fluid distribution technique is required by the trickle system, similar to the dual medium design, over the top of the rock bed to assure a uniform flow distribution and to minimize channeling effects. Both the outlet from the collectors (charge flow) and the return from the solar steam generator (discharge flow) enter the top manifold over the bed and are returned from the bottom of the bed. The gravity flow thus requires that the bed be fully charged before it can be discharged, or at least the bottom of the bed be at the delivery temperature for discharge 672° of (750°F). A sump is required beneath the tank to collect the fluid. No bottom manifold, however, is required to maintain a thermocline at the bottom of the bed.

There were several key operational considerations for the trickle storage design. These considerations include charge/discharge cycles and system lag times for fluid retention in the bed, replacement of sump capacity, and temperature inversion of a partially charged tank. With regard to the charge/discharge modes, the trickle system requirement for a fully charged tank before discharge availability required a multi-tank approach to provide partial system discharge capability. A primary design consideration was to accommodate a changing outlet fluid temperature from a tank as it attains either the fully charged or fully discharged state. For instance, in the charging mode, as the rising temperature front progresses through the rockbed and the tank approaches the 75-85 percent full capacity state, the outlet temperature leaving the tank begins to rise above the nominal 533°K (500°F) collector return fluid temperature. Similarly, during discharge, the tank outlet temperature eventually drops below the acceptable delivery tolerances to the PCS as the tank thermal capacity decreases. Two approaches, parallel and series flow to the tanks, were considered to resolve this subsystem characteristic. The series approach was selected since the parallel tank approach required monitoring of the fluid temperature at several system mixing points to determine the proper flow modulation which could have resulted in system control stability problems.

Figure 3.4-1 shows a typical charging sequence for the tanks in series. The 672°K (750°F) fluid from the collector field enters the top of the first tank and 533°K (500°F) fluid is returned to the field from the sump as indicated by the solid arrows on the figure. As the heat transfer gradient moves downward through the bed the exiting fluid from the bed, begins to rise in temperature above the allowable return temperature to the field. At this point, the bottom charge line valve is closed, and the transfer pump is activated diverting the flow to the top of the second tank allowing collector field return of 533°K (500°F) fluid from the sump of the second tank. This sequence is shown by the dashed lines in the figure and allows for the full charging of the second tank to 672°K (750°F) eliminating potential temperature degradation if a thermocline were at the bottom of the tank. When the first tank is completely charged, the transfer pump is de-activated, and all the collector field flow is through the second tank. The remaining tanks are charged sequentially.

The discharge sequence of the series configuration is shown in Figure 3.4-2. As the temperature leaving the first tank is below the acceptable delivery temperature to the PCS, P1 is turned on and the flow passed through the second tank. Thus, all the energy, including the thermocline layer, can be extracted. When the first tank is depleted, all of the flow passes through the second tank. The discharge of the last tank is performed in a similar sequential manner.

The transfer pump can also be used to complete a temperature inversion of a partially charged tank. If, at the end of a day, a tank is partially charged, (i.e., the top of the bed is hot, but the bottom of the bed is cold), the tank is not ready for discharge. The transfer pump can be turned on, and a recirculation flow initiated from the bottom of the tank to the top. This will result in movement of the hot bed layer from the top to the bottom of the tank and thus ready the tank for discharge. The performance associated with the inversion mode is discussed in Paragraph 3.4.4.1. On a system performance level, however, calculations indicated that the inversion operational mode was not required.

The trickle oil subsystem design was extended during the Preliminary Design Phase to operate also in a Dual Media mode as a back-up operational mode. This approach was taken since the trickle oil concept is a development design and no large scale prototype tests were planned within the program schedule to provide performance verification. Through minor modifications, the storage subsystem design incorporates the flexibility to operate in the dual media mode by adding fluid to fill the tanks if the trickle oil performance is inadequate. The required changes include lowering the top manifold, addition of a lower manifold, addition of four manual valves to allow discharge from the top of the tank, and additional control logic. The charging mode in the dual media operation is identical to the trickle oil operation as shown in Figure 3.4-1 except, that the switch valves are in the dual media position as shown in Figure 3.4-3. The tanks again are charged in series, eliminating any thermocline at the bottom of all except the last tank. The discharge mode is different, however, since the hot fluid is removed from the top of the tank as shown in Figure 3.4-3. The piping configuration does not allow the tanks to be discharged in series. As a result, each tank can end its discharge mode with a thermocline on top of the tank. This thermocline can be removed by continuing the discharge mode and supplementing the energy with the fossil heater, or it can be passed through the tank during the series charging sequence ending in the bottom of the last tank when the system is fully charged. The system operational mode is discussed in more detail in Section 5.

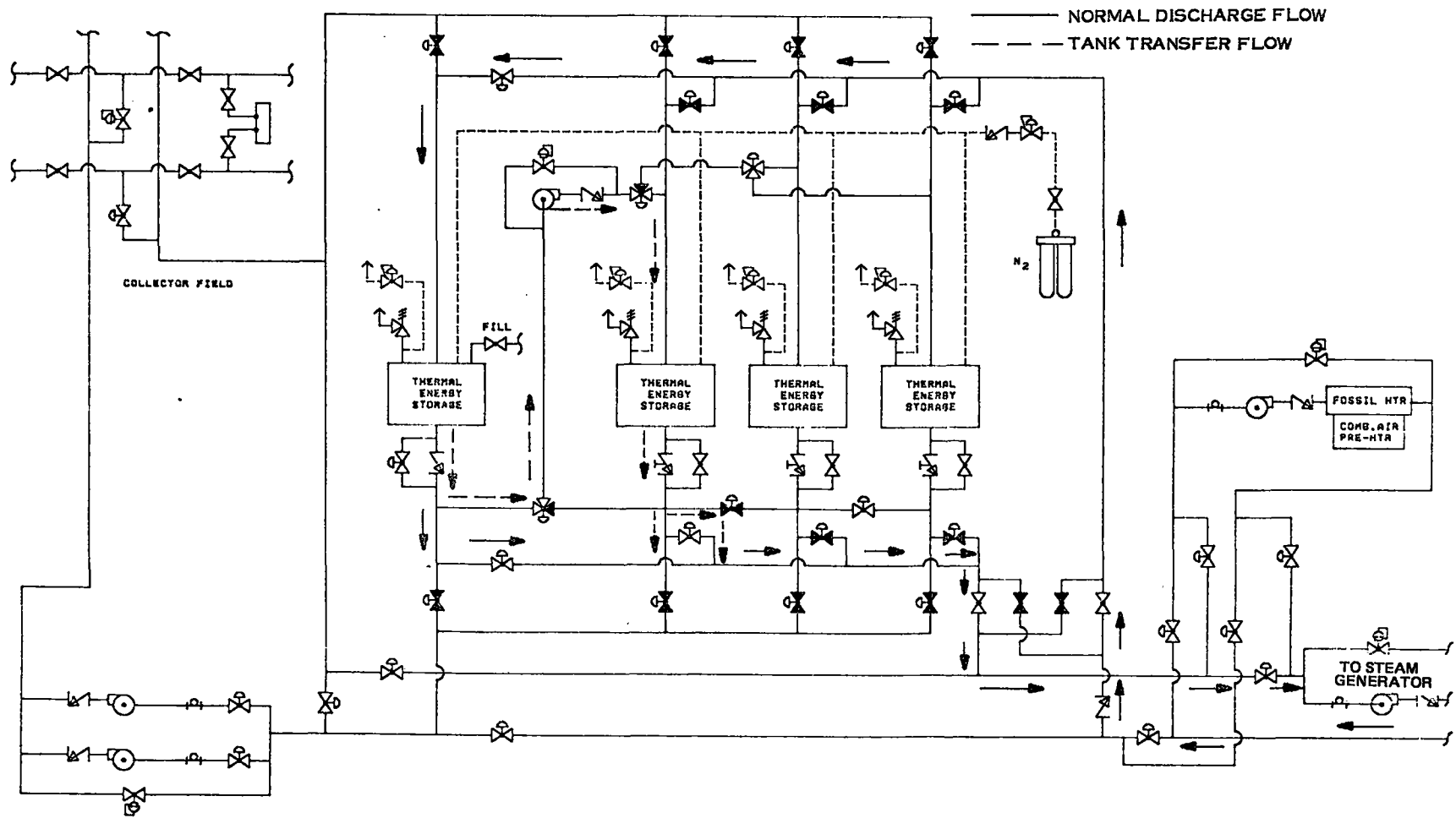


Figure 3.4-2. Trickle Oil Schematic - Discharging Mode

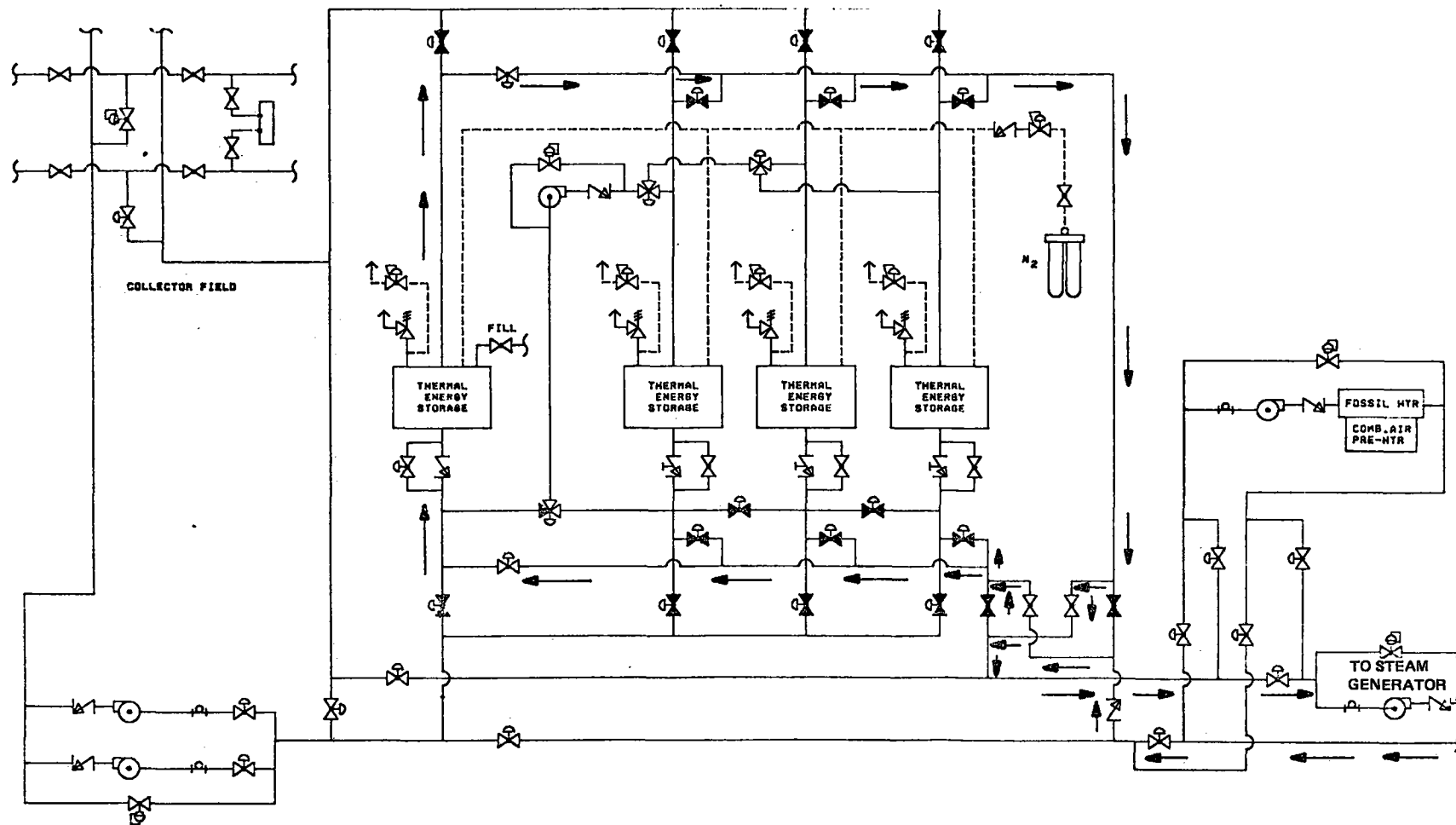


Figure 3.4-3. Trickle Oil Schematic Modification to Dual Media - Discharging Mode

3.4.2 SYLTHERM 800 AND STORAGE MEDIA COMPATIBILITY

The selection of Syltherm 800 as the collector fluid was based on the fact that it is the only heat transfer fluid for the 672°K (750°F) temperature range that can be used at atmospheric conditions which results in system performance and operation benefits (Paragraph 2.3.2.1). In addition, Syltherm 800 has a decreasing degradation rate with time (Reference 3.4-3) and therefore has the potential for much lower replacement requirements over the life of the system. Syltherm 800 is a silicone fluid marketed by Dow Corning. It degrades at high temperatures by a rearrangement of silicone molecules causing formation of low boiling volatiles in an inert atmosphere resulting in a pressure buildup. A specific break-in procedure is required initially to remove these volatiles. Subsequent removal or venting of the volatiles is then required only at periodic intervals. Table 3.4-2 lists the major fluid properties. The degradation rate, however, has been found to increase in the presence of potential storage media. Compatibility tests run by Sandia Laboratories, Livermore, between Syltherm 800 and granite, the initial storage media, shows a considerably higher degradation rate than the Syltherm alone. Subsequent tests by Dow Corning also confirmed these results. The storage media selection was then switched to taconite, an iron ore, because of its availability and reasonable cost (~\$40 per ton) and because the high iron content potentially would be more compatible with the Syltherm 800.

Crude taconite is processed by going through three or four stages of crushing of mixed iron ore, gradually reducing the size to approximately 0.019 meter (3/4 inch), and then being ball milled into a powder form. This is concentrated into pellet form and hardened at 1589°K (2400°F). This processing produces an extremely stable, very hard, sphere-like pellet composed of Fe₃O₄ (magnetic), Fe O, and iron silicates. Typical chemical composition of taconite is shown in Table 3.4-3. Many suppliers of taconite were identified across the country, and the typical composition range is shown in the table. Actual tests were performed on two samples, and the results compared with the average properties as indicated. The available data on the specific heat of taconite ranged from 585 to 794 J/kg-°K (0.14 to 0.19 Btu/lb-°F). Bulk density of the material is 2088 kg/m³ (130 lb/ft³).

Compatibility test data is just recently becoming available from Sandia, Livermore, and Dow Corning, and indications are that taconite also enhances the degradation of the Syltherm 800. The increased degradation is less than with the granite but still high enough to cause concern over the system life. The presence of the taconite does not alter the fluid composition properties but does accelerate the rate of volatile formation. The degradation rate is apparently enhanced by the trace amounts of the oxide as Al₂O₃, C₂O₃, and MgO. The use of a more controlled chemical composition carbon steel form would be expected to reduce degradation rates significantly. It is noted that the compatibility problem exists for both the trickle oil and the dual media mode of operation. In fact, the possibility exists that the rate may be higher if the system is operated in the dual media mode since more fluid would be in constant contact with the storage media.

3.4.3 TRADEOFF ANALYSIS

A transient thermal model was constructed to define analytically the performance of the trickle flow Thermal Energy Storage subsystem. The model is a one dimensional, finite difference, computer technique which is fashioned after the method of Mumma (Reference 3.4-4) and which considers fluid flow and heat transfer throughout a packed bed of solid particles. Analyses supporting concept verification and storage design were performed to determine fluid film velocity, film thickness, mass flow rate, and average surface convective conductance as a function of bed position and fluid temperature. Temperature dependent physical properties of the heat transfer fluid are incorporated into the model. The bed material is assumed to be spherical particles with the appropriate properties, and the particles are assumed to have instantaneous temperature response. Film thickness variations over the flow range for Shenandoah were predicted to be between 5.1×10^{-5} and 1.3×10^{-4} meter (.002 and .005 in.). Bed velocity variations were predicted in the 0.013 and 0.076 m/s (0.5 and 3 inch/second) range. The heat transfer coefficient was estimated according to McAdams (Reference 3.4-5), for low Reynolds numbers to be in the range of 57 to 340 J/s-m²-°K (10 to 60 Btu/hr-ft²-°F) consistent with the above values of film thickness and velocity.

Table 3.4-2. Properties of Syltherm 800

Temperature °F	Density lb/ft ³	Specific Heat Btu/lb-°F	Thermal Conductivity Btu/hr-ft ² - (°F/ft)	Viscosity Centipoise
100°F	58	.40	.078	7.5
200°F	55	.42	.076	3.2
300°F	51.7	.44	.0735	1.8
400°F	48.5	.46	.072	1.05
500°F	45.5	.48	.069	.65
600°F	42	.495	.067	.44
700°F	39	.51	.065	.31
750°F	37	.53	.064	.25

Toxicity	Excellent
Color	Water White
Odor	None
Operating Range	-40°F - 800°F
Liquid Range	-40°F - 800°F
Pressure Buildup	<1 Atm at 750°F
Corrosion/Scale	None
Flash Point	310°F
Fire Point	380°F

Table 3.4-3. Taconite Chemical Composition

Elements	% by Weight	Hanna Mining Co. (MO.)	Test	U.S. Steel	Test
Fe	62.5 - 65.1	64.7	64.7	65.1	65.8
SiO ₂	1.2 - 8.6	4.6	3.26	6.0	5.2
Al ₂ O ₃	.17 - .88	.81	.62	.17	.1
CaO	.1 - 3.4	.10	.14	.65	.32
MgO	.04 - .69	.09	.12	.53	.11
Mn	.05 - .82	.12	.09	.16	.13
P	.008 - .04	.011	.031	.014	.021
S	.002 - .08	.003	.008	.003	.007
Moisture	1.3 - 3.0	2.07	.004	-	.006

Based on system requirements involving various conditions of operation, the heat transfer fluid volumetric flow rates for the TES system are in the range of 0.0032 to 0.025 m³/s (50 gpm to 400 gpm). Accordingly, calculations were made using the TES thermal model to determine the thermocline shapes associated with these flow rates in both the charge and discharge modes. The design tradeoff analyses were performed for only a single tank and not on all of the tanks in series. A plot of discharge utilization factor (i.e., the percent of stored energy that is discharged prior to an outlet fluid temperature of 658°K or 725°F) versus fluid flow rate for the one hour tank is shown in Figure 3.4-4. As seen from the figure, energy utilization is relatively insensitive to fluid flow rate for the range of interest. The slight variation is attributed to the fact that h_c/m is sufficiently high for all cases so that the exponent in the fluid equation as shown in the Figure 3.4-5 does not produce a discernible change in the fluid exit temperature until the flow rate reaches the 0.013 m³/s (200 gpm) range, (1.5 gal./min-ft²) and greater. Figure 3.4-5 shows this effect for higher values of the heat transfer parameter.

Several discharge parametric analyses were made to assess the effect of bed height as it affected the performance of the one hour tank (9 MBtu capacity). In order to test the effect of various vessel lengths, the diameters had to be changed to keep the storage capacity constant. However, to offset the effect of diameter change, the fluid mass flow rate per unit of tank cross section was also held constant along with the taconite diameter of 0.013 meter (one-half inch). Results of the calculations are plotted in Figure 3.4-6 in terms of the utilization factor and show increased utilization and increased height.

The final selection for tank height, however, must also consider standard tank fabrication and site placement. The most cost effective tank design utilizes the full width of standard rolled steel tank sections of 1.2, 1.8, and 2.4 meters (4, 6, and 8 ft). In addition, consideration was given to the location of the tanks. Initially, the tanks were located within the Mechanical Building which imposed height limitations. Mechanical Building reconfiguration during Preliminary Design effort led to external tank location; however, shadowing and setback requirements still impose height limitations as shown in Figure 3.4-7. Finally a L/D ratio of one results in minimum surface area heat losses. All of these considerations were reviewed along with the results of Figure 3.4-6, and a 3.7 meter (12 ft) height with a 4.0 meter (13 ft) diameter was selected for the one-hour tank, and a 4.9 meter (16 ft) height and 6.3 meter (20.6 ft) diameter was selected for the larger tank. It should also be noted that since the tanks are charged and discharged in series, the effective bed height of the subsystem is 18 meters (60 ft).

Another parameter which affects the performance of the packed bed as predicted by the thermal model is the individual media particle diameter. To evaluate the bed performance sensitivity to particle diameter, parametric studies were performed with the results summarized in Figure 3.4-8. The figure shows that larger pellet diameters result in reduced heat transfer between fluid and the bed and therefore a reduced discharge utilization factor. Increasing particle diameter also increases the internal heat lag to the pellets. Since the gravity fed trickle oil system does not have pressure drop restrictions, the conclusion from the trade-offs indicate that the smallest practical pellet size should be selected. With the design extension to operate in the dual media mode as a back-up, the bed pressure drop becomes more significant. Initial results indicate particle sizes in the 0.013 meter (1/2 in.) range would be acceptable in both operational modes, and this range is the Preliminary Design selection.

3.4.4 PERFORMANCE ANALYSIS

3.4.4.1 Trickle Oil

Performance estimates were made for the design which resulted from the tradeoffs discussed in Paragraph 3.4.3. Figure 3.4-9 shows the calculated bed temperature profiles for the trickle oil mode as a function of time for the charge and discharge operation at a flow rate of 0.0032 m³/s (50 gpm) for both the small (1 hour tank, D = 13 ft, L = 12 ft) and a large tank (D = 20.6 ft, L = 16 ft). The small and large tanks have storage capacities of 9.5 x 10⁹ and 3.2 x 10¹⁰ J (9 MBtu and 30.3 MBtu), respectively. These profiles were based on the taconite properties as discussed in Paragraph 3.4.2. The profiles were generated for an initial uniform bed temperature of 533°K (500°F) for charging and 672°K (750°F) for discharging and for the Syltherm fluid inlet constant at 672°K (750°F) for charging and 533°K (500°F) for discharging.

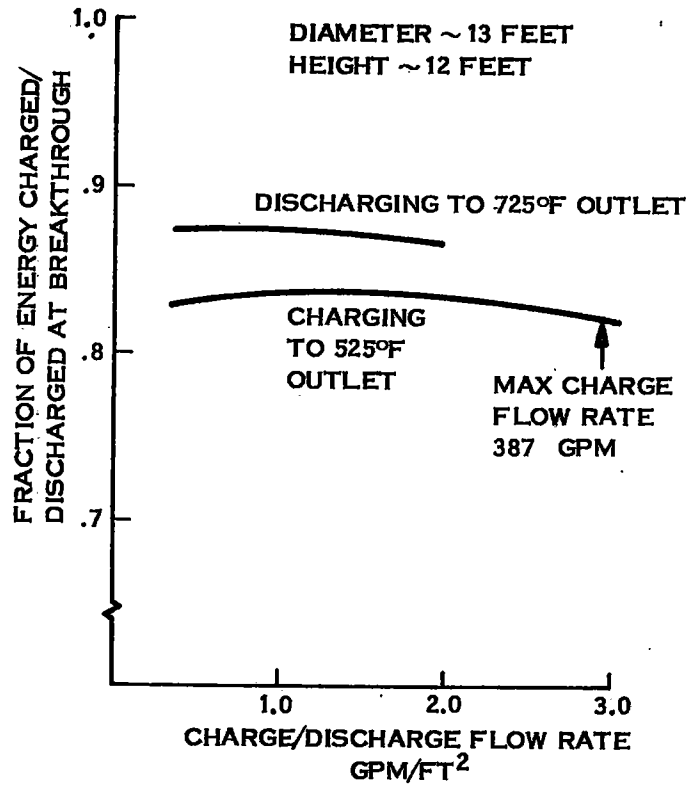


Figure 3.4-4 Flow Rate Variation Effects on Discharge

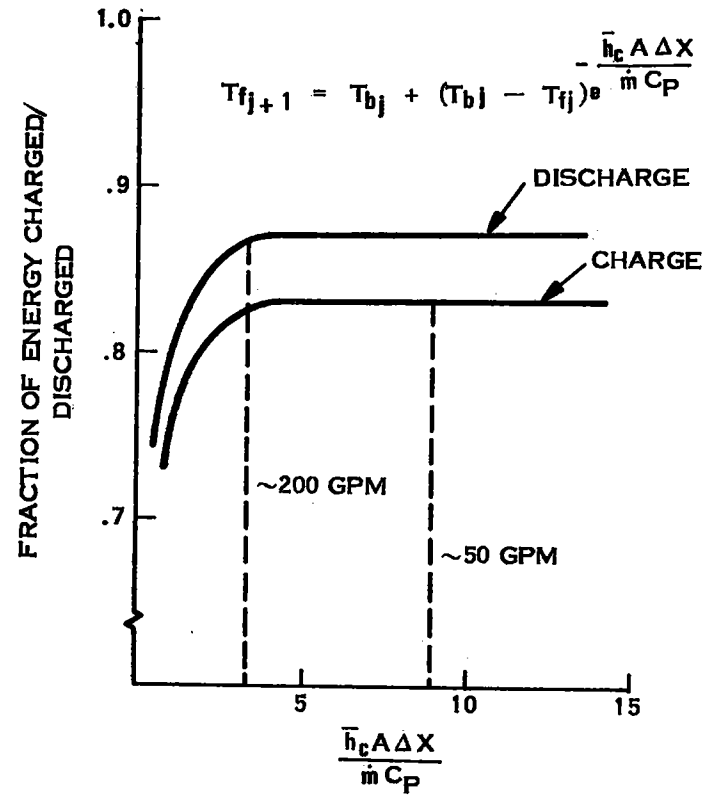


Figure 3.4-5. Heat Transfer Parameter Effect

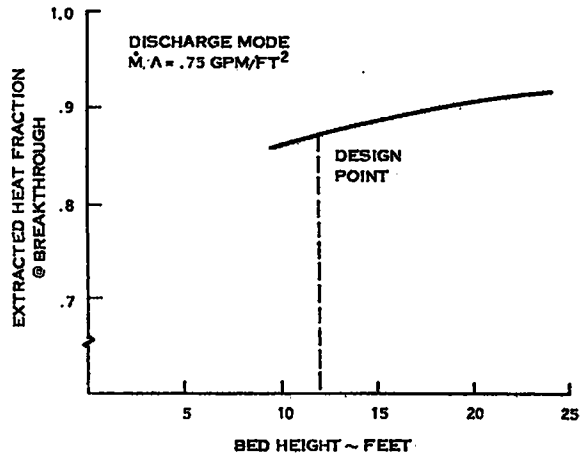


Figure 3.4-6. Tank Height Tradeoff Results

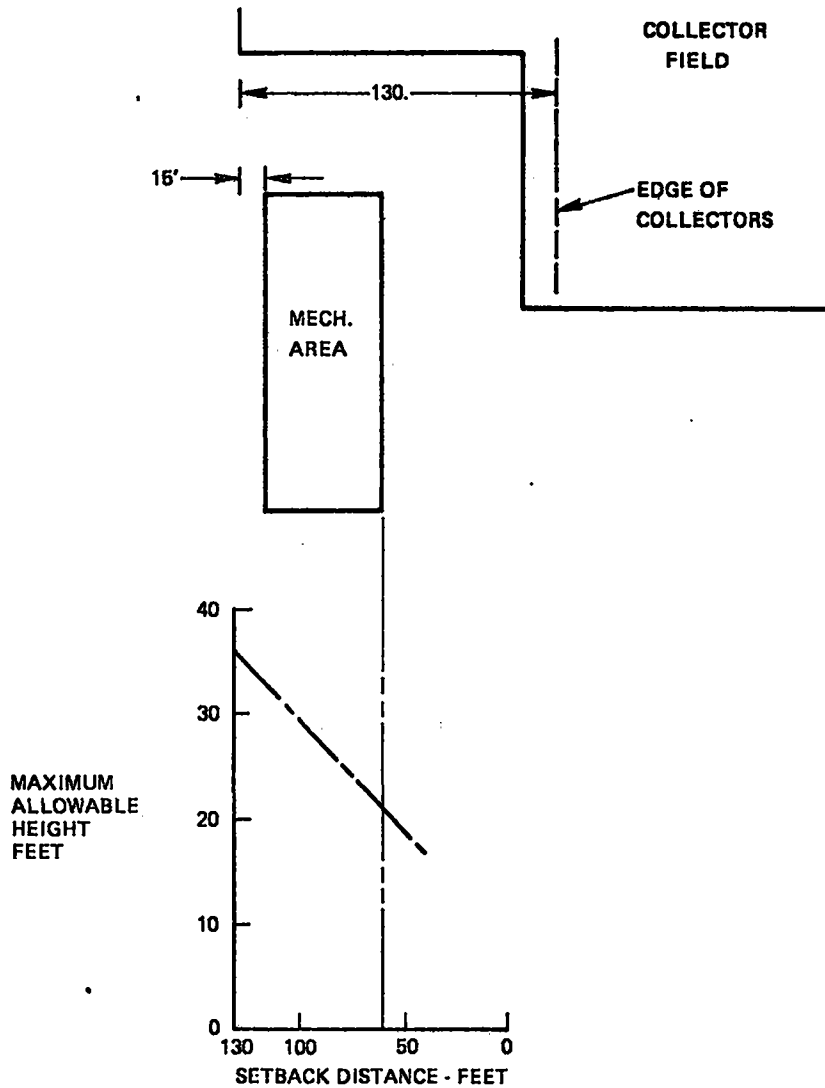


Figure 3.4-7. Allowable Tank Height

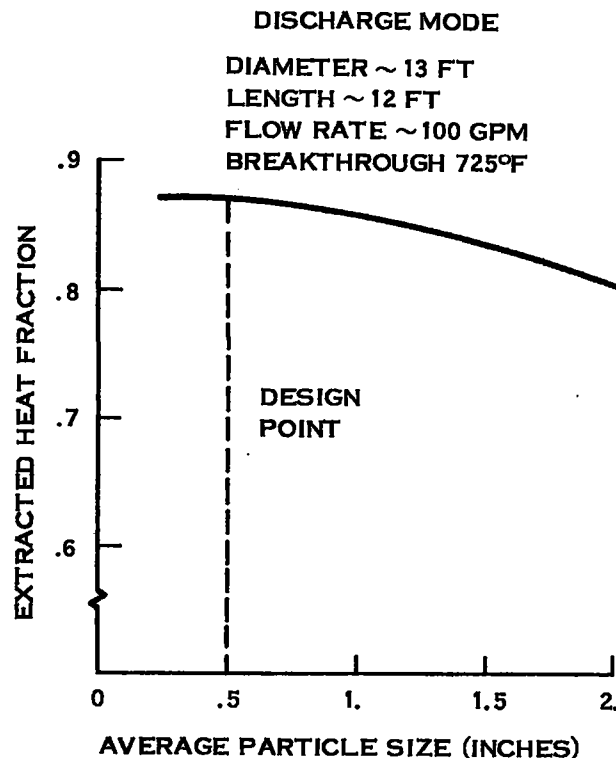


Figure 3.4-8. Effect of Particle Size on Heat Transfer

These results are based on the assumption of uniform fluid flow distribution and include surface heat loss only. Heat losses are discussed in more detail in Paragraph 3.4.4.3 and are approximately three percent of a 24 hour hold of a fully charged tank. Table 3.4-4 shows the characteristic times and charging efficiencies for a single tank at 0.0032 m³/s (50 gpm) and 0.024 m³/s (387 gpm) and discharging at 0.0032 m³/s (50 gpm) and 0.015 m³/s (230 gpm). The 0.015 m²/s (230 gpm) rate corresponds to an energy delivery rate of 2.6 x 10⁶ x 10⁶ J/s (9 MBtu/hr.)

If the tanks were charged and discharged singly, then, as shown in Table 3.4-4, the tanks can only be partially charged and discharged since a thermocline exists at the bottom of the tank when the fluid exist reaches its limit 547°K or (525°F for charge and 658°K or 725°F for discharge). To utilize storage capacity more effectively, the tanks will be charged and discharged in series as discussed in Paragraph 3.4.1. In this manner all tanks can be charged to full capacity except for the last tank which would still have a thermocline.

Figure 3.4-10 shows the bed profiles obtained at 0.0032 m³/s (50 gpm) by charging the first large tank by pumping in the effluent from the small tank as it rises above 547°K (525°F). Also shown are profiles for a constant 672°K (750°F) inlet fluid temperature. With the series charge, a slightly longer time is required to achieve a given percent charge; however, full charge can be achieved in 17 hours and 40 minutes compared to a 84.5 percent charge in 17 hours with a single tank.

Charging all tanks in series (in groups of two) results in 95 percent (95 MBtu) of maximum possible charge (100 MBtu) compared to 84 percent (84 MBtu) for single tank charging. During discharge of the four tank system which is initially fully charged (one tank has a thermocline), the directly deliverable energy above 658°K (725°F) is approximately 96 percent of the charged energy.

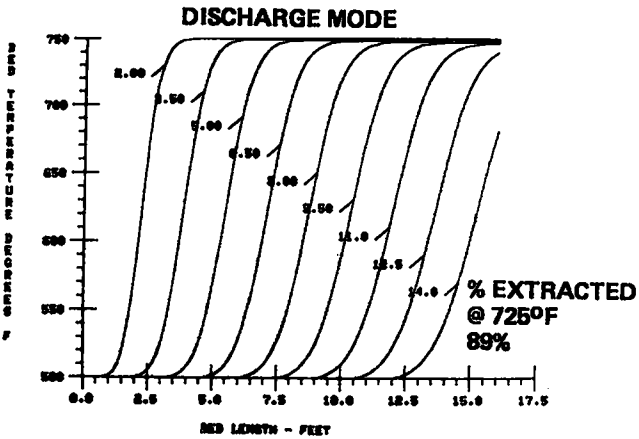
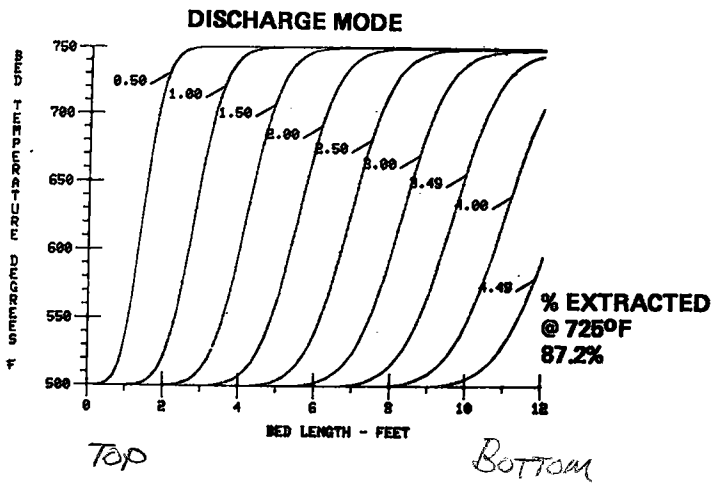
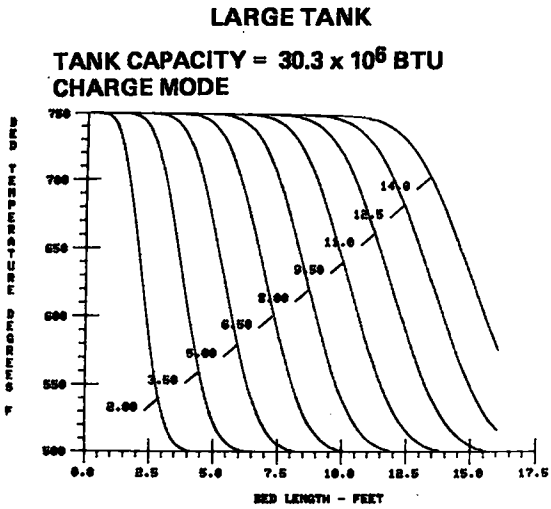
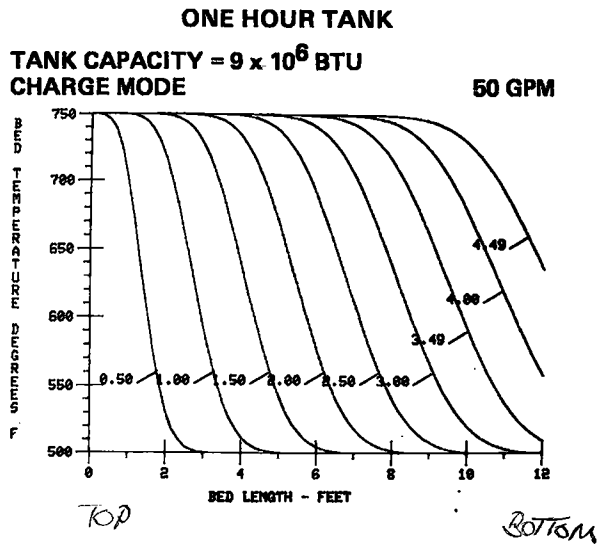


Figure 3.4-9. System Design Performance for Trickle Mode

Table 3.4-4. Trickle Flow Operation

Characteristic Times for Charge and Discharge of a Single Tank				
Charge				
Flow Rate GPM	Tank Size	Time for fluid exit to reach 525°F (hours)	% of full Charge	Time for full charge (hours)
50	Small	3.8	83	5.3
	Large	12.7	84.5	27
387	Small	.5	82	.65
	Large	1.7	83.5	2.2
Discharge				
		Time for fluid exit to reach 725°F (hours)	% Discharged	
50	Small	3.8	87%	
	Large	13.1	89%	
230	Small	.9	87%	
	Large	3	89%	

Another unique feature of the trickle oil subsystem is the thermal inversion process which brings the partially charged tank on line for discharge. Since the trickle oil system is discharged by gravity feed, at the end of a solar collection day a partially charged tank (top portion of the bed at 672°K or 750°F and bottom at 533°K or 500°F) can either be held until the next day or thermally inverted with a recirculating flow to move the hot layer to the bottom of the tank. This process results in a slight lowering of the peak temperature 1.1 to 1.7°K (2 to 3°F) and reduction of the energy available or spreading of the temperature profile. The spreading of the profile is not lost energy to the system since, under charging conditions, the bed can be brought up to 672°K (750°F) faster, and the series configuration restricts the spread profile to the last tank. The temperature profiles for inversion of a 62 percent initially charged tank at flow rates of 0.0032 m³/s (50 gpm) and 0.024 m³/s (387 gpm) are shown in Figure 3.4-11. The design inversion flow rate is 0.024 m³/s (387 gpm) to minimize the inversion time. The efficiency for a single large tank inversion is shown in Figure 3.4-12 as a function of the initial percent charged condition. The second tank must have a minimum charge of 50 percent to limit the inversion to one hour, or the third or fourth tank can be inverted with an initial charge down to 25 percent. Below an initial charge of 25 percent, inversion is not used. The annual system performance was shown to be the same with and without tank inversion. This results from the fact that only seven percent of the total energy delivered to the TES requires inversion. Therefore, the overall effect of tank thermal inversion is minimal.

3.4.4.2 Dual Media Mode

The four tank design has also been analyzed to provide performance estimates in the dual media mode. The approach taken was to utilize a computer model available at Sandia Laboratories, Albuquerque. Sandia has been developing dual media prediction capability based on their tests and the test data from Reference 3.4-2. The model is a one dimensional analytical solution to the Shumann equation (Reference 3.4-6) using average material properties. In addition, the model does not consider heat losses nor axial conduction.

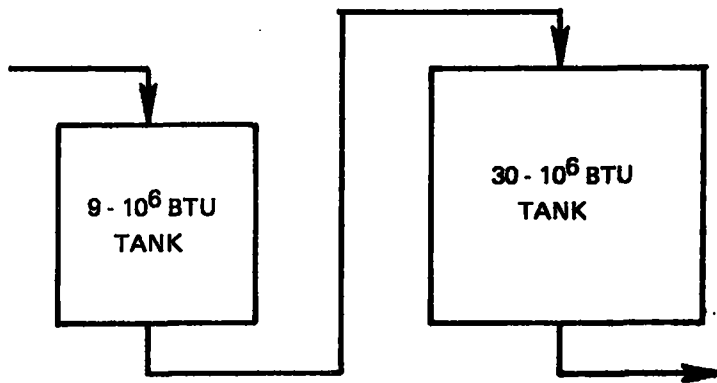
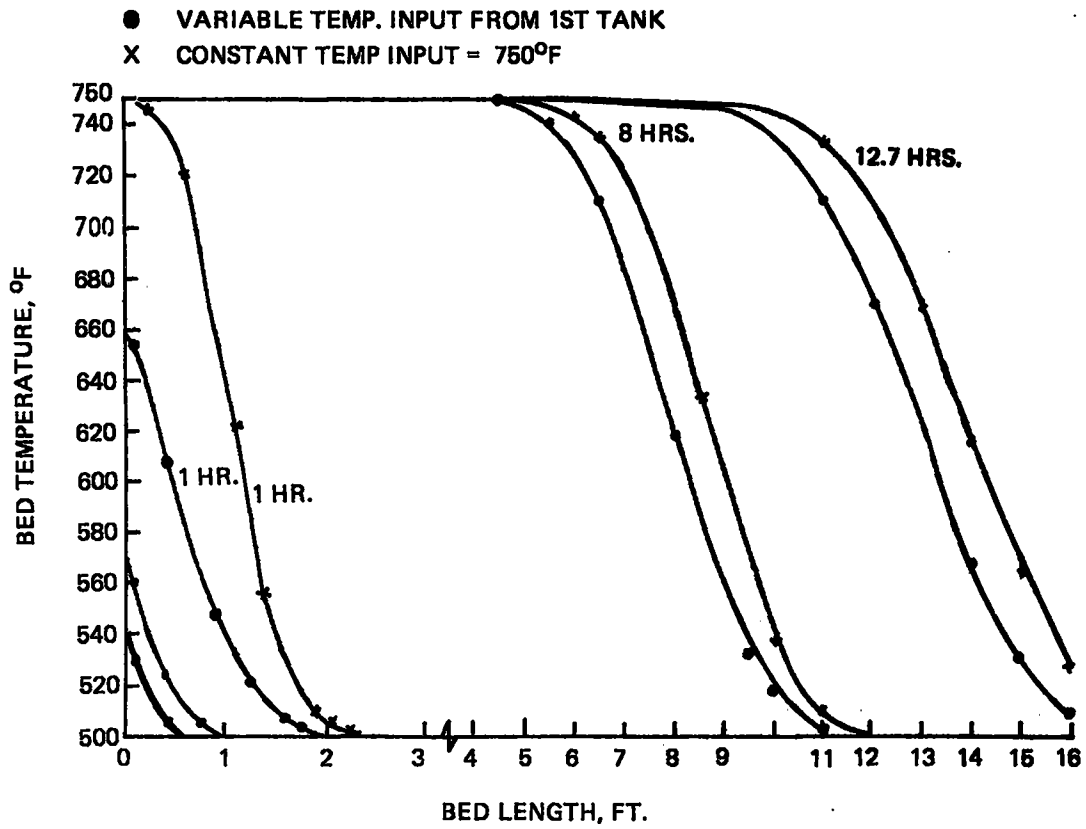


Figure 3.4-10. Trickle Flow-Series Charge Performance

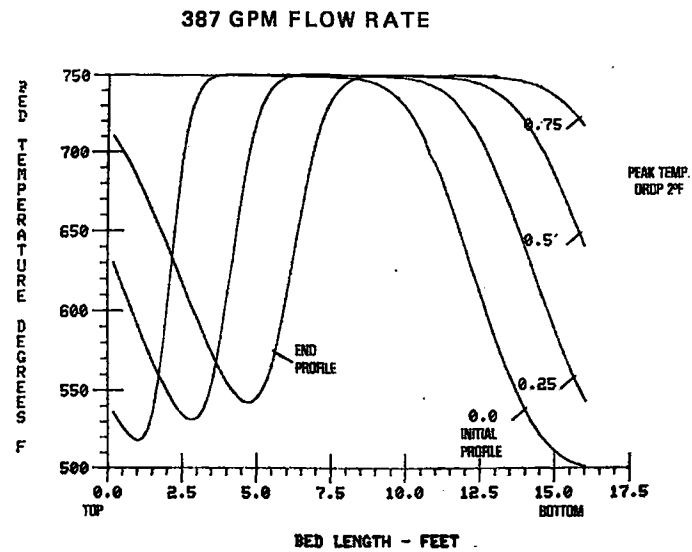
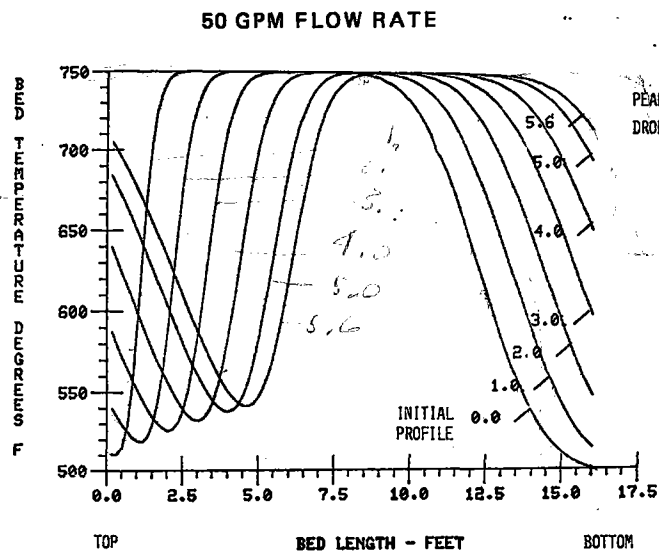


Figure 3.4-11. Inversion Profiles for the Large Tank Initially Charged at 62% Available Energy

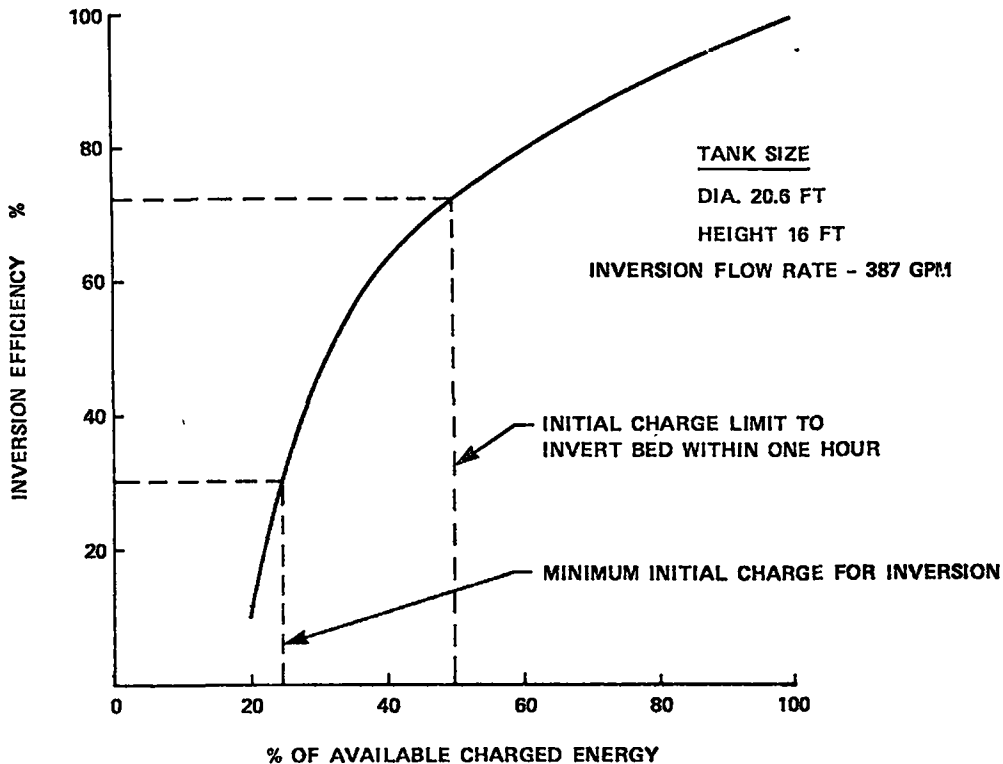


Figure 3.4-12. HTS Tank Inversion Efficiency (Variation with Initial Charged State)

These limitations, however, were acceptable for the initial performance estimates. Sandia is presently developing a finite difference model for dual media operation which will allow treatment of the additional effects.

The results are shown in Figure 3.4-13 for charge and discharge of both size tanks at $0.0032 \text{ m}^3/\text{s}$ (50 gpm). Table 3.4-5 lists the characteristic times and efficiencies for charge and discharge. Since the dual media mode utilizes the fluid also as a storage media, the capacity of the tanks is 28 percent larger than in the trickle mode, i.e., 1.2 and $4.1 \times 10^{12} \text{ J}$ (11.5 and 38.8 MBtu), respectively, for the small and large tanks. The total storage capacity of the system is $1.4 \times 10^{11} \text{ J}$ (128 MBtu).

The tanks can be charged again in series resulting in a charge of $1.3 \times 10^{11} \text{ J}$ (124 MBtu). The present plumbing arrangement does not allow series discharge in the dual media operation. For single tank discharging, the available energy is $1.2 \times 10^{11} \text{ J}$ (112 MBtu).

3.4.4.3 Holding Period Heat Losses

A heat loss analysis was performed to define the insulation thickness on the tank required to limit the daily heat losses to four percent or less of the storage capacity. A 0.36 meter (14 in.) blanket of insulation with a K value of $0.073 \text{ J/s-}^\circ\text{K-m}$ ($.042 \text{ Btu/hr-}^\circ\text{F-ft}$) limits the daily heat losses to 3.0 percent assuming a fully insulated bottom as discussed in Paragraph 3.4.4.5.

A transient analysis was also performed to determine the temperature distributions within the tank during any holding periods. A 126 node model for a large tank was developed consisting of 96 bed nodes and 30 insulation nodes. The model was two dimensional allowing determination of axial and radial gradients.

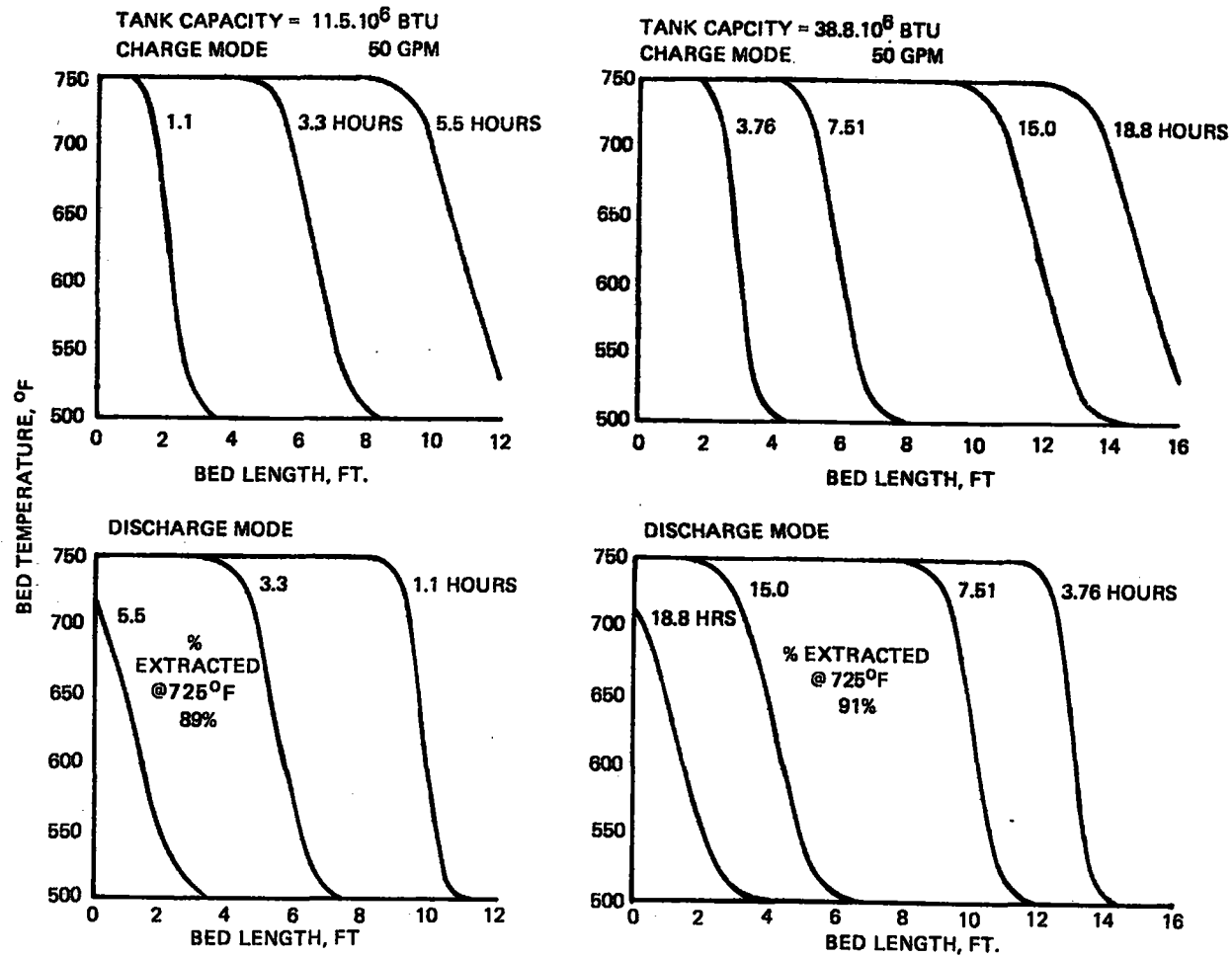


Figure 3.4-13. Dual Media Mode Performance

Table 3.4-5 Dual Media Operation

Characteristic Times for Charge and Discharge of a Single Tank				
Charge				
Flow Rate GPM	Tank Size	Times for Fluid Exit to Reach 525°F (hours)	% of Full Charge	Time for Full Charge (hours)
50	Small	5.5	88	7
	Large	18.8	90.6	23
387	Small	.7	87	1.0
	Large	2.3	89.5	2.8
Discharge				
		Times for Fluid Exit to Reach 725°F (hours)	% Discharged	
50	Small	5.4	88	
	Large	18.8	90.7	
230	Small	1.2	87	
	Large	4.0	89.5	

The selected insulation thickness of 0.36 meter (14 in.) was assumed on all surfaces of the tank. The tank is supported by twelve concrete pillars each 1.2 meters (48 in.) high and 0.093 m² (1 ft²) in cross section. To account for the heat loss through these supports, the effect conductivity of the bottom insulation nodes was increased so that the heat loss through the bottom insulation was that through the insulation plus supports. A GE transient heat transfer program was used to obtain the time temperature histories in the bed. A list of the cases studied and the properties used in the analysis is given in Table 3.4-6. The effective conductivity of the bed was calculated by the method presented in Reference 3.4-4.

The results after a 24 hour hold period are shown in Figure 3.4-14 and in Table 3.4-7. The daily head loss from a fully charged large tank to the environment is three percent of the stored capacity. On an annual basis, the losses are only two percent of the energy delivered to the storage system since the stored energy is delivered each weeknight, and more than 24 hour holds for fully charged tanks can occur only on weekends or early parts of the week. As shown in the Figure 3.4-14 profiles, the region of the bed near the walls drops below 658°K (725°F). This results in a direct deliverable energy loss of seven percent.

Losses for a partially charged tank were determined as shown in Figure 3.4-15 and Table 3.4-7. The tank was initially 50 percent charged (37 percent initial available energy is above 658°K or 725°F). After a 24 hour hold, the total energy content dropped by five percent and the direct deliverable energy by 14 percent. An analysis of the losses in a dual media storage system was made by increasing the effective bed conductivity. The results differed only slightly from the trickle charge mode as shown in Table 3.4-7 for both the fully charged and partially charged tank.

Table 3.4-6. Initial Hold Conditions Considered and Material Properties Used in Transient Heat Loss Analysis

Initial Condition	Bed Conductivity Btu/ft hr °F	Insulation Conductivity Btu/ft-hr-°F		Specific Heat, Btu/lb°F		Density, lbs/ft ²	
		Top and Sides	Bottom	Taconite	Insulation	Taconite	Insulation
750°F (1) Uniform	.46	.0417	.05	.175	.2	130 ⁽³⁾	10
Partially Charged	.46	.0417	.05	.175	.2	130	10
750°F(2) Uniform	.82	.0417	.05	.175	.2	130	10
Partially Charged	.82	.0417	.05	.175	.2	130	10
500°F(1) Uniform	.46	.032	.038	.175	.2	130	10

(1) Trickle Mode
(2) Dual Media Mode
(3) Bulk Density

For all cases - Ambient Temperature = 50°F
- Convective Heat Transfer Coefficient = $\frac{1 \text{ Btu}}{\text{ft}^2 \text{ hr } ^\circ\text{F}}$
- Bed Porosity = 30%

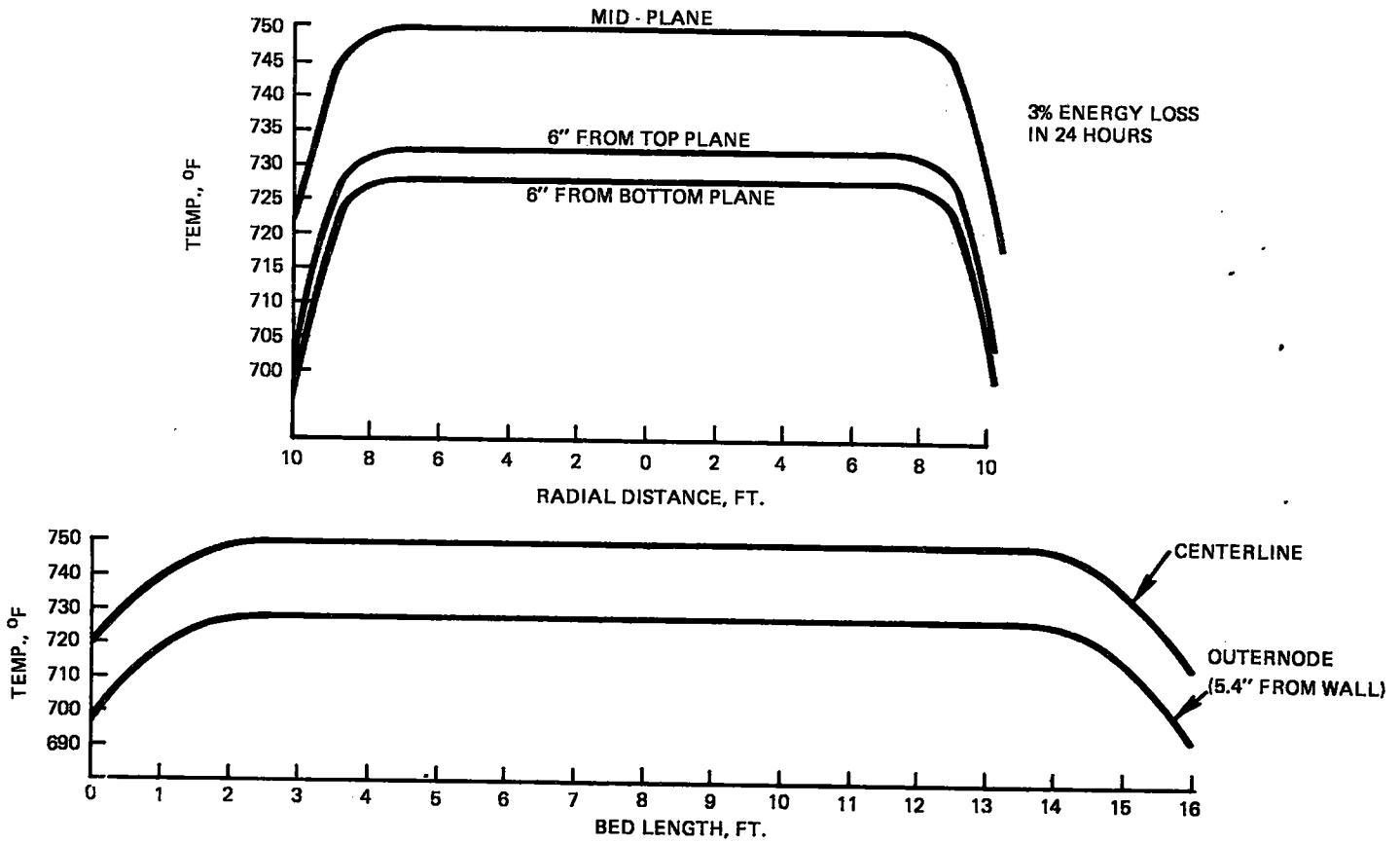


Figure 3.4-14. Holding Period Temperature Profiles for the Trickle Oil System with the Tank initially Fully Charged

In addition, the temperature profiles for a tank holding at 533°K (500°F) were defined. The average bed temperature dropped to 531°K (496.5°), with a minimum of 515°K (468°F) at the bottom of the tank as shown in Figure 3.4-16. This analysis suggests that, if a tank is not charged for several days, it may require a small amount of preheating before it is brought on-line.

3.4.4.4 Structural Design Analysis

The four high temperature storage tanks will be field fabricated using carbon steel sections and standard construction techniques. The sizes of the four tanks are listed in Table 3.4-1. Figure 3.4-17 shows the tank construction for the 6.3 meter (20.6 ft) diameter tank. The dome is conical in shape consisting of twelve flat plate (pie shaped sectors) bent to conform to the cone radius. The sections will be mutually reinforcing to provide a rigid structure. Some bracing will be required at the truncation of the sectors. The lateral wall is 0.0095 meter (3/8 in.) thick from the bottom to the top of the tank. Ratcheting in the tank, or settling of the packed bed material resulting from the differential thermal expansion of the tank wall and bed material, becomes an insignificant design problem since the storage has changed from granite to taconite and possibly carbon steel. Obviously, if a form of carbon steel is used as the medium, no significant differential expansion problem exists.

The main inlet connection to the tank is a 0.114 meter (4.5 in.) tube leading to the distribution manifold which will be an integral part of the dome as described below. The dome will also have a man-hole port for access to the tank interior. The bottom of the tank will have a 12-to-1 sloped internal base to provide good drainage to the sump. The tank will be supported on a 1.2 meter (4 ft) high structure to allow adequate bottom insulation and access to the sump. A tradeoff was performed comparing a supported bottom versus a ringwall and course gravel and sand supported tank. The latter design provides a good construction base, allows for a thinner bottom plate, and is generally more economical.

Table 3.4-7. Thermal Losses for Holding Periods

Initial Condition	Initial Charge, Btu		Charge After 24 Hours		% Charge Loss	
	Total	Above 725°F	Total	Above 725°F	Total	Above 725°F
750°F(1) Uniform	30.3 · 10 ⁶	30.3 · 10 ⁶	29.4 · 10 ⁶	28.3 · 10 ⁶	3%	6.7%
Partially Charged(1)	15.15 · 10 ⁶	11.3 · 10 ⁶	14.4 · 10 ⁶	9.7	4.9%	14%
750°F(2) Uniform	38.8 · 10 ⁶	38.8 · 10 ⁶	37.6 · 10 ⁶	36.2 · 10 ⁶	3.1%	7%
Partially Charged(2)	19.4 · 10 ⁶	14.4 · 10 ⁶	18.4 · 10 ⁶	12.3	5.2%	14.5%
500°F(1) Uniform	0	0	-.42 · 10 ⁶			

(1) Trickle Mode
(2) Dual Media Mode

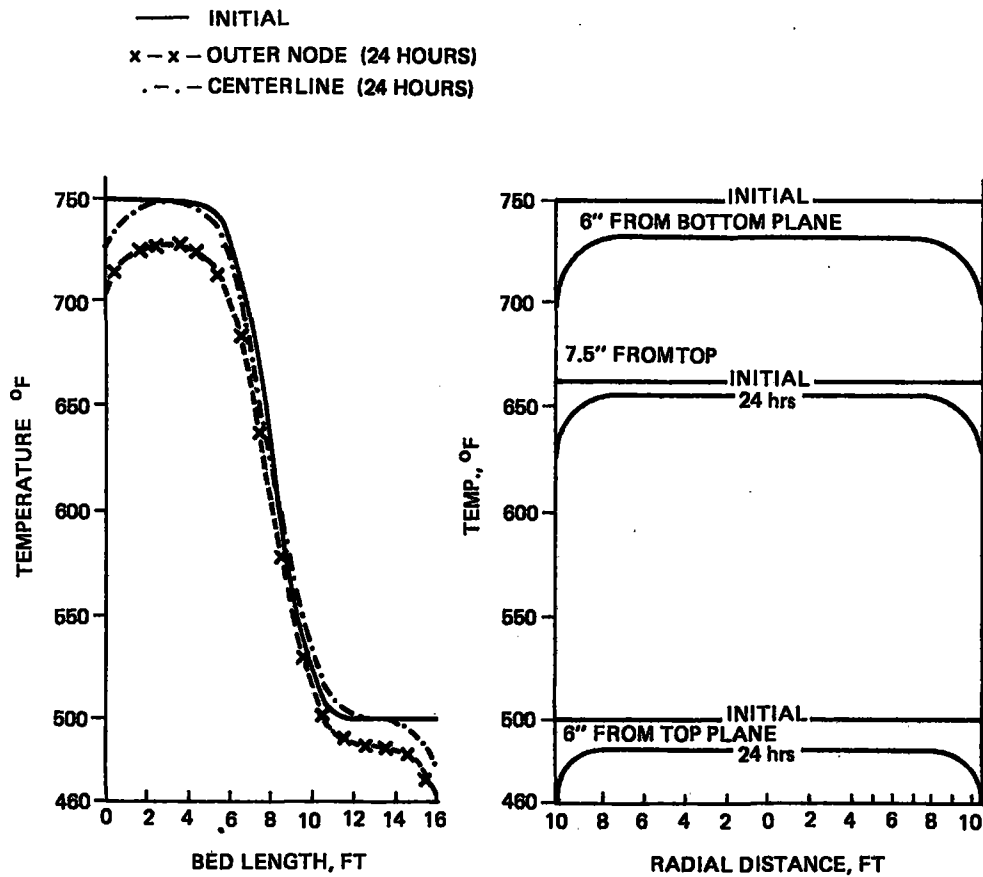


Figure 3.4-15. Holding Period Temperature Profiles After 24 Hour Hold for a Tank Initially Partially Charged

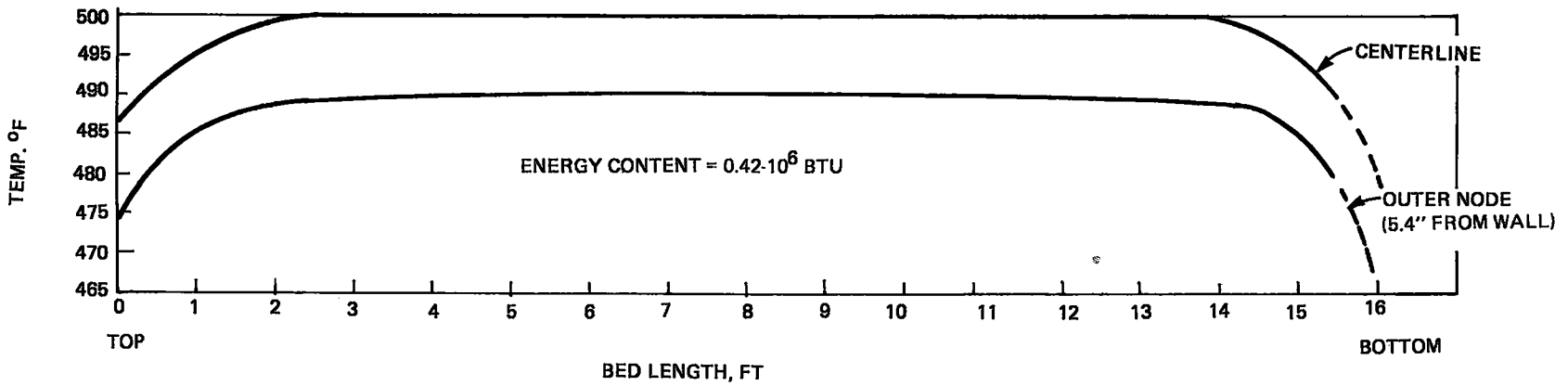
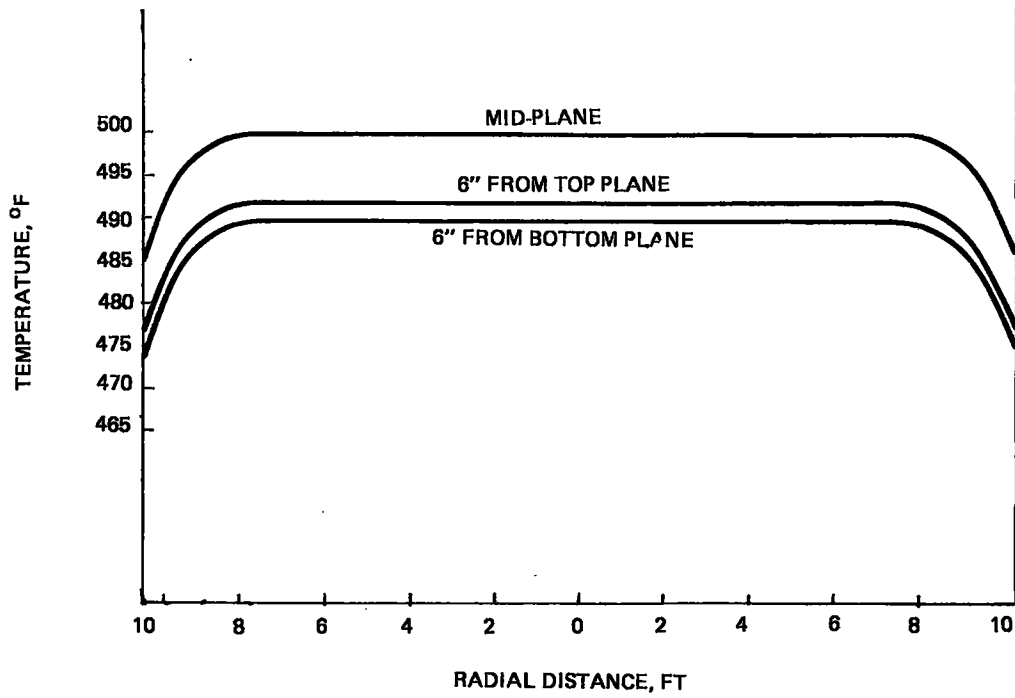


Figure 3.4-16. Holding Period Losses After 24 Hour Hold for a Tank Initially at 500°F

The disadvantages for this design, however, included the requirement for a costly sump access for cleaning and no general access to the bottom of the tank to allow full insulation. A heat loss analysis showed excessively high transient heat loss rates from the bottom of the tank. By fully insulating the bottom with 0.36 meter (14 in.) of insulation, a significant daily heat loss reduction from six to 3.7 percent is achieved as shown in Table 3.4-8. Thus, the supported tank base was selected for the LSE design.

The manifolds for each tank were designed to provide uniform flow distribution over the top of the packed bed. The trickle oil concept requires only one manifold at the top of the packed bed, but a second bottom manifold is included to accommodate the fluid filled back-up design capability. The two manifolds will be of identical construction as shown in Figure 3.4-18 and 3.4-19. The manifold design is a series of interconnecting pipes, 0.032 meter (1-1/4 in.) in diameter. There will be two holes at 0.102 meter (4 in.) intervals along the pipe length, with a hole located on both sides of the pipe at a 30° angle from the bottom or top of the pipe for the top and bottom manifolds, respectively. A total of 1424 holes each with a .00159 meter (1/16 in.) diameter gives a total flow efflux area of .0028 square meters (.0303 ft²). The top manifold will be an integral part of the dome attached by stringers at several key points, Figure 3.4-18. This design allows unit installation. The bottom manifold is located at the sump level and supported off the sloped floor as shown in Figure 3.4-19. The bottom manifold will be valved externally to the tank to allow conversion from the trickle oil sump operation to the dual medium manifold.

Each tank will have a separate sump of similar design located at the center of the tank. Each sump will be cylindrical in shape, 0.915 meter (3 ft.) in diameter and 0.915 meter (3 ft) deep with a capacity of 0.605 cubic meters (160 gallons) - see Figure 3.4-19. The fluid inventory in each tank is allowed to back up into the bottom of the bed. The sump size provides a fluid volume for the suction manifold but is sized for ease of bottom plate removal.

The bottom of the sump will be sloped toward a drain with a removable cover for sludge cleanout. The outlet pipe will enter from the side of the sump. A 0.025 meter (1 in.) grid grate is located directly above the pipe to inhibit formation of a large vortex flow which could result in pump cavitation. The outlet pipe will have a capped end with multiple holes on the bottom side also to minimize any strong vortex formation. A solid 1.52 meters (60 in.) flat plate will be mounted 0.15 meter (6 in.) above the tank floor and supported by load gussets which distribute the load directly to the support structure. Hole perforations are located around the side of the flat plate. This design prevents sludge from falling directly into the sump and allows flat layout of the bottom manifold.

Table 3.4-8. Summary of Tank Thermal Losses

Energy Losses Btu's (% of Capacity)				
	One Hour Tank Capacity - 9×10^6 Btu		Large Tank Capacity - 30.3×10^6 Btu	
Lateral Walls	$.33 \times 10^6$	(3.7%)	$.7 \times 10^6$	(2.3%)
Top Dome	$.09 \times 10^6$	(1%)	$.22 \times 10^6$	(.73%)
Base { Ringwall Sand/Stone	$.13 \times 10^6$ $.27 \times 10^6$ }	(4.3%)	$.21 \times 10^6$ $.77 \times 10^6$ }	(3.2%)
Total	$.82 \times 10^6$ Btu	(9%)	1.9×10^6	(6%)
Total with Supported Base	$.55 \times 10^6$ Btu	(6.1%)	1.12×10^6 Btu	(3.7%)
Note: Assumes 14 inches Insulation ($k = .0524$ Btu/hr - °F - ft)				

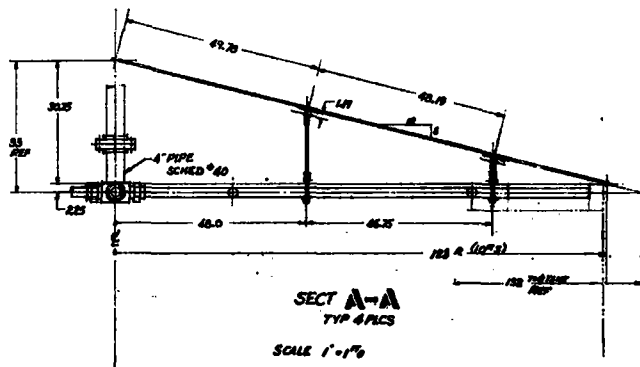
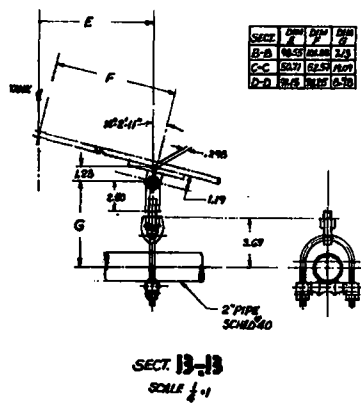
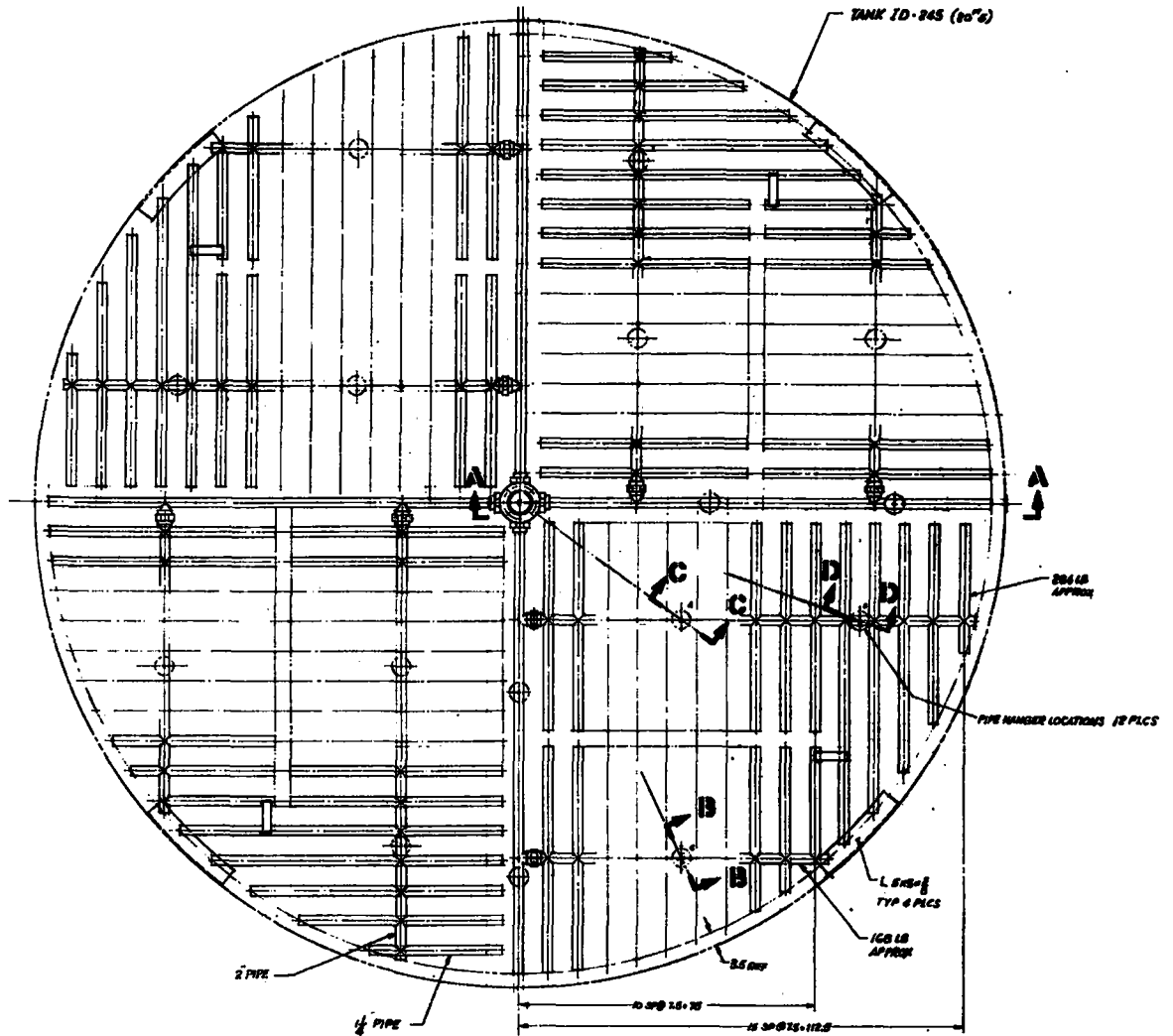


Figure 3.4-18. Tank Inlet Piping Arrangement

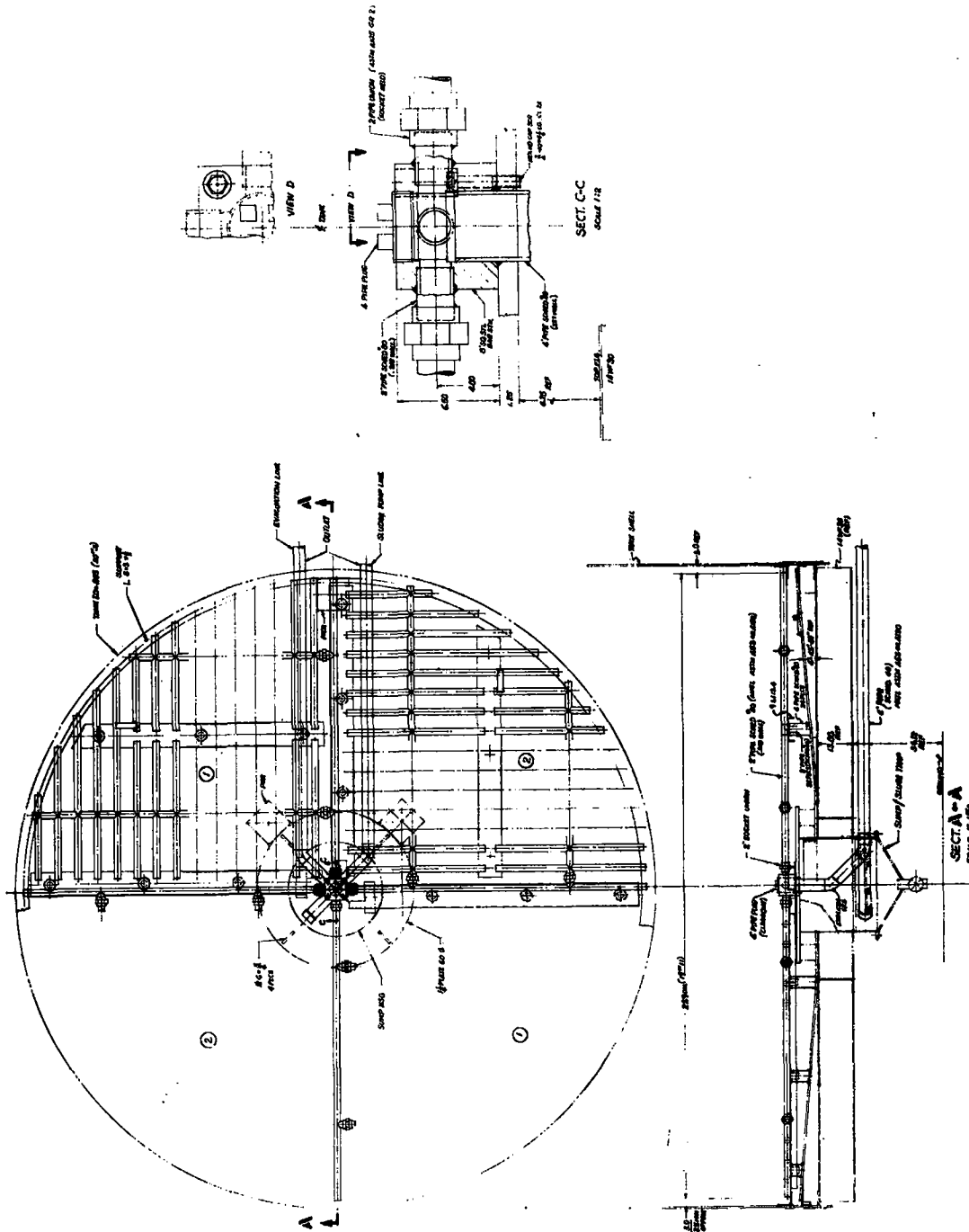


Figure 3.4-19. Tank Outlet Piping Arrangement.

3.5 POWER CONVERSION SUBSYSTEM (PCS)

3.5.1 SUBSYSTEM CONCEPT TRADE-OFFS

Initial PCS design activity centered on selection of a subsystem concept which best met the following general requirements:

1. Performance in terms of heat input to meet electrical/thermal load range when operating between specified power cycle state points.
2. Availability of hardware with minimum development required, reliability, and ease of integration into STE-LSE.
3. Compatibility with STE-LSE objectives.

Conceptual design studies concluded that steam turbine-generator systems best met these overall requirements. During the early part of the preliminary design, the steam systems selected during the conceptual design were re-evaluated to identify the most viable candidates, and then steady state thermodynamic performance analysis of the candidates was performed over a range of load conditions and power cycle state points. This information provided an input to the system design and analysis effort discussed in Section 2.

Candidate concept evaluation continued through vendor contacts to definitize the equipment associated with each concept, and finally both performance and design were evaluated in terms of STE-LSE objectives to make the final selection. Three candidate subsystem concepts were evaluated in detail. The most distinguishing feature among them is turbine type as summarized below:

1. A single/stage back pressure turbine exhausting steam at $7.2 \times 10^5 \text{ N/m}^2$ (105 psig) for use as process steam and also for absorption air conditioning. Steam flow rate is determined by thermal loads. Electric output is determined from steam flow rate, T G efficiency, and steam throttle/exhaust conditions.
2. Two single stage turbines, the first exhausting at $7.2 \times 10^5 \text{ N/m}^2$ (105 psig) at which pressure the process steam is extracted and the second exhausting at a pressure level varying between $1.0 \times 10^5 \text{ N/m}^2$ (15 psig) and $1.7 \times 10^5 \text{ N/m}^2$ (25 psig) depending upon the need for air conditioning. Electric output varied between 100 and 300 kW.
3. A multi-stage uncontrolled extraction turbine, the variable extraction pressure being maintained above $7.2 \times 10^5 \text{ N/m}^2$ (105 psig) over the load range and the exhaust being held constant at $1.0 \times 10^5 \text{ N/m}^2$ (15 psig). Electric output varied between 200 and 400 kW.

As indicated above, the extraction (or exhaust for the single stage turbine) pressure state point was maintained above $7.2 \times 10^5 \text{ N/m}^2$ (105 psig) to meet process steam requirements while the exhaust pressure state point was maintained at $1.0 \times 10^5 \text{ N/m}^2$ (15 psig) to meet a 383°K (230°F) absorption air conditioner hot water firing temperature, when applicable. The two single stage turbines were also analyzed at reduced exhaust pressure to accommodate the reduced temperature requirements of heating or at no thermal load.

Tables 3.5-1, 3.5-2 and 3.5-3 summarize the thermodynamic performance calculations for the three concepts. Consistent with the requirement for minimum PCS development, the performance for each concept was based on available hardware capabilities applied to the alternative design conditions shown in the table. Turbine efficiencies of both the single stage turbine and the dual turbine concept represent Elliot Company hardware. The multi-stage uncontrolled extraction turbine represents a modified marine turbine-generator set manufactured by GE Mechanical Drive Turbine Department (MDTD). Even though these single point data indicate relative performance among PCS alternatives for design point site loads, the final evaluation considered actual performance analyzed for a full year of operation against time-varying loads.

Table 3.5-1. One Expander Non-condensing Cycle

Inlet Pressure PSIG	Inlet Temp °F	Exhaust Pressure PSIA	Deaerator Pressure PSIA	Inlet Flow lb/HR	Process Steam Flow lb/HR	Steam Flow To Deaerator lb/HR	Tb Eff.	Alt-Gear Eff.	Tb Output kW	Alternator Output kW	Heat Input kWth	S-800 Δ Tin Boiler °F
500	570	119.7	113.7	3597	3092	505	.38	.92	49.7	45.7	1023	120
500	570	119.7	113.7	1634	1407	227	.31	.92	19.2	17.7	465	120
500	570	137.7	130.8	3458	2939	519	.38	.92	45.5	41.9	972	118
500	570	137.7	130.8	1653	1407	246	.30	.92	17.1	15.8	465	118
700	720	119.7	113.7	3566	3092	474	.38	.92	71.2	65.2	1095	250
700	720	119.7	113.7	1620	1407	213	.32	.92	27.0	24.8	498	250
700	720	137.1	130.8	3426	2939	487	.38	.92	63.3	58.2	1041	248
700	720	137.1	130.8	1638	1407	230	.31	.92	24.7	22.7	498	248
500	720	119.7	113.7	3557	3092	465	.39	.92	62.2	57.2	1104	275
500	720	119.7	113.7	1618	1407	209	.30	.92	21.7	20.0	502	275
500	720	137.7	130.8	3416	2939	477	.39	.92	54.2	49.9	1050	273
500	720	137.7	130.8	1633	1407	226	.30	.92	20.1	18.5	502	273
700	570	119.7	113.7	3613	3092	521	.38	.92	60.2	55.4	1005	80
700	570	119.7	113.7	1641	1407	234	.31	.92	22.4	20.6	456	80
700	570	137.7	130.8	3475	2939	536	.38	.92	53.3	49.0	955	78
700	570	137.7	130.8	1661	1407	254	.30	.92	20.3	18.7	456	78

Table 3.5-2. Two Expander Cascaded Cycle 500 PSIG

S-800 (Th 66) ΔT in Boiler	Inlet Pressure PSIG	Inlet Temp. °F	1st Th Exhaust Pressure PSIA	2nd Th Exhaust Pressure PSIA	Deaerator Pressure PSIA	Inlet Flow lb/HR	Process Steam Flow lb/HR	Deaerator Extraction Flow lb/HR	Condenser Flow lb/HR	1st Th EFF.	2nd Th EFF.	Alt-Gear EFF.	1st Th Output kW	2nd Th Output kW	Alternator Output kW	A/C Thermal Load kWth	Heat Input kWth	Heat Del. to Condenser Excess of A/C Load kWth
120	500	570	119.7	29.7	113.7	11144	1407	1087	8650	.46	.47	.92	194.6	131.4	300	770	3166	1635
	500	570	119.7	29.7	113.7	9097	1407	810	5889	.43	.45	.92	131.6	86.3	200	770	2300	875
	500	570	119.7	29.7	113.7	4607	1407	500	2760	.39	.43	.92	69.8	39.0	100	770	1326	7
	500	570	119.7	16.7	113.7	10268	1407	1247	7614	.45	.45	.92	175.3	150.8	300	770	2918	1385
	500	570	119.7	16.7	113.7	7421	1407	909	5105	.42	.44	.92	118.7	99.1	200	770	2109	683
	500	570	119.7	16.7	113.7	4308	1407	542	2359	.39	.43	.92	63.9	41.9	100	675	1224	0
	500	570	119.7	2.5	113.7	8532	1407	1502	5623	.43	.42	.92	139.2	186.7	300	0	2424	1661
	500	570	119.7	2.5	113.7	6334	1407	1094	3833	.41	.40	.92	98.3	119.1	200	0	1800	1143
	500	570	119.7	2.5	113.7	3846	1407	635	1804	.39	.37	.92	56.4	52.3	100	0	1093	544
	275	500	720	119.7	27.9	113.7	9546	1407	875	7203	.46	.47	.92	198.1	127.9	300	770	2962
500		720	119.7	29.7	113.7	6955	1407	655	4892	.43	.45	.92	133.7	83.7	200	770	2158	700
500		720	119.7	29.7	113.7	4050	1407	413	2231	.40	.43	.92	71.8	36.9	100	675	1257	0
500		720	119.7	16.7	113.7	8883	1407	1008	6468	.45	.45	.92	180.7	145.4	300	770	2756	1192
500		720	119.7	16.7	113.7	6445	1407	738	4300	.42	.44	.92	122.7	95.2	200	770	2090	542
500		720	119.7	16.7	113.7	3785	1407	447	1832	.39	.43	.92	66.7	42.0	100	593	1175	0
500		720	119.7	2.5	113.7	7546	1407	1234	4950	.44	.42	.92	148	178.6	300	0	2312	1546
500		720	119.7	2.5	113.7	5621	1407	899	3314	.41	.39	.92	104	113.5	200	0	1744	1055
500		720	119.7	2.5	113.7	3148	1407	525	1516	.39	.37	.92	60.2	48.6	100	0	1070	488
50		700	570	119.7	29.7	113.7	10442	1407	1057	7979	.46	.46	.92	211.3	114.8	300	770	2902
	700	570	119.7	29.7	113.7	7616	1407	790	5419	.42	.45	.92	142.3	75.7	200	770	2116	703
	700	570	119.7	29.7	113.7	4101	1407	490	2503	.39	.43	.92	75	33.8	100	686	1223	0
	700	570	119.7	16.7	113.7	9707	1407	1217	7083	.45	.45	.92	192.0	134.0	300	770	2698	1178
	700	570	119.7	16.7	113.7	7044	1407	890	4747	.42	.44	.92	129.6	88.4	200	770	1957	544
	700	570	119.7	16.7	113.7	4099	1407	532	2100	.38	.43	.92	69.2	39.5	100	602	1139	0
	700	570	119.7	2.5	113.7	8268	1407	1493	5367	.43	.42	.92	157.4	169.3	300	0	2297	1546
	700	570	119.7	2.5	113.7	6127	1407	1084	3636	.41	.39	.92	109.6	103.1	200	0	1703	1058
	700	570	119.7	2.5	113.7	3707	1407	625	1675	.38	.37	.92	62.0	46.7	100	0	1030	492
	250	700	720	119.7	29.7	113.7	8969	1407	845	6717	.46	.46	.92	215.1	111.0	300	770	2753
700		720	119.7	29.7	113.7	6553	1407	635	4511	.43	.45	.92	145	72.9	200	770	2012	562
700		720	119.7	29.7	113.7	3821	1407	401	2013	.39	.43	.92	77.0	31.7	100	599	1172	0
700		720	119.7	16.7	113.7	8397	1407	974	6016	.45	.45	.92	197.2	128.9	300	770	2578	1022
700		720	119.7	16.7	113.7	6114	1407	716	3991	.42	.44	.92	133.4	84.7	200	770	1877	427
700		720	119.7	16.7	113.7	3597	1407	434	1756	.39	.43	.92	72.0	36.7	100	530	1104	0
700		720	119.7	2.5	113.7	7273	1407	1209	4657	.44	.41	.92	165.3	161.6	300	0	2233	1446
700		720	119.7	2.5	113.7	5409	1407	878	3124	.41	.39	.92	115.0	120.7	200	0	1661	900
700		720	119.7	2.5	113.7	3308	1407	509	1392	.38	.36	.92	65.7	43.1	100	0	1016	441

Table 3.5-3. Multistage Uncontrolled Extraction Turbine Cycle

Thermal Input, kW	3311	3381	2631	2714	1899	1940
Electrical Output, kW	400	400	300	300	200	200
Throttle Pressure, psia	700	700	700	700	700	700
Throttle Temp, °F	720	680	720	680	720	680
H, Btu/lb	1356	1333	1356	1333	1356	1333
P_{extr} , psia	265	278	203	215	135	142
H_{extr} , Btu/lb	1302	1282	1291	1272	1282	1263
UEEP, Btu/lb	1198	1191	1206	1191	1215	1198
T cond., °F	250	250	250	250	250	250
H cond., Btu/lb	218	218	218	218	218	218
Throttle Flow, lb/hr	11567	12084	8899	9394	6269	6550
Extraction Flow to Process, lb/hr	1237	1261	1250	1273	1261	1284
Extraction Flow to DA, lb/hr	1750	1817	1070	1150	612	652
Process Steam Flow, lb/hr	1380	1380	1380	1380	1380	1380

As shown in the tables, independent variables of throttle temperature and pressure were analyzed. These parametric studies ultimately supported selection of the collector field fluid and operating temperature range since the collector field fluid is the heat source for the power cycle.

For concept (2), the two single stage turbines, the effect of throttle pressure/temperature on heat input is shown for 589°K (600°F) heating fluid (solar collector field fluid) and for 672°K (750°F) heating fluid in Figure 3.5-1. These temperatures correspond to the maximum operating bulk temperatures for the two prime candidate collector field fluids, Therminol-66 and Syltherm 800, respectively. As shown, increasing the throttle pressure produces a desirable reduction in heat input as does increasing the heat source temperature.

Figure 3.5-2 shows the effect on heating fluid ΔT in the steam generator versus throttle pressure for the 672°K (750°F) and 589°K (600°F) heating fluid inlet temperatures. As shown, both cases show a reduction in ΔT as throttle pressure increases, and a large reduction, approximately 139°K (250°F) versus 56°K (100°F) is seen when comparing the 672°K (750°F) to the 589°K (600°F) case. The reason for this is shown in Figure 3.5-3, the solar steam generator pinch curve for the design point (750°F heating fluid / 720°F, 700 psig steam). For the case of 589°K (600°F) maximum heat transfer fluid temperature, the margin for heat transfer between 589°K (600°F) and the 536°K (505°F) pinch point resulting from constant temperature boiling at $4.8 \times 10^6 \text{ N/m}^2$ (700 psig) is much less than the margin between 672°K (750°F) and 536°K (505°F).

Figure 3.5-4 compares heat inputs between the two single stage turbines and the multi-stage turbine, indicating the performance advantage for the multi-stage above 200 kW which, as discussed in Section 2 overall system requirements, is the minimum operating power level. This performance advantage as well as other overall conclusions summarized in Table 3.5-4 led to the selection early in the preliminary design of the GE MDTD modified multi-stage turbine. As indicated, the single stage concept did not meet the STE-LSE objectives in terms of electrical power output, while the two single stage turbines did not meet availability, reliability, and ease of integration, as well as showing a performance disadvantage.

Following selection of the GE MDTD turbine-generator, system and subsystem analysis resulted in definitized PCS requirements as summarized in Figure 3.5-5. The PCS performance shown in Table 3.5-5 is based on these definitized requirements and the GE multi-stage turbine. As noted in the table, performance up to 400 kWe is shown reflecting the requirement for stand-alone operation at full electrical output discussed in Section 2. From Figure 3.5-4, operation at the higher power level further accentuates the multi-stage turbine advantage. The PCS heat/mass for the selected configuration is shown in Figures 3.5-6 and 3.5-7 for 400 and 300 kWe operation, respectively.

Figure 3.5-8 shows the effect of steam temperature on heat input for the finalized PCS. As indicated, if the steam pressure is held constant, the steam temperature, which is actually a measure of the amount of superheat, has a minimum effect on heat input down to 616°K (650°F). This result led to the inlet temperature tolerance requirement shown in Figure 3.5-5.

As noted previously, the PCS design requirements and associated system performance were developed on the basis of the uncontrolled extraction GE MDTD turbine modified to incorporate certain non-developmental efficiency improvement features. From system analyses summarized in Section 2.0, improved turbine efficiency has a positive effect on annual system performance in terms of both solar contribution to loads as well as utilization. At the midpoint of the Preliminary Design, a search was made by means of a request-for-proposal (RFP) issued through Sandia Laboratories-Albuquerque to identify an improved efficiency turbine with a design goal efficiency of approximately 70 percent. All candidates were required to meet or exceed the requirements stated in Figure 3.5-5. In addition, in contrast to earlier hardware candidate evaluations, the RFP allowed consideration of hardware requiring some development to achieve the desired higher efficiency. However, the scope of development was required to be consistent with the overall Shenandoah LSE schedule. Several concepts capable of meeting the overall requirements were evaluated including a higher efficiency multi-stage turbine with controlled extraction. The system

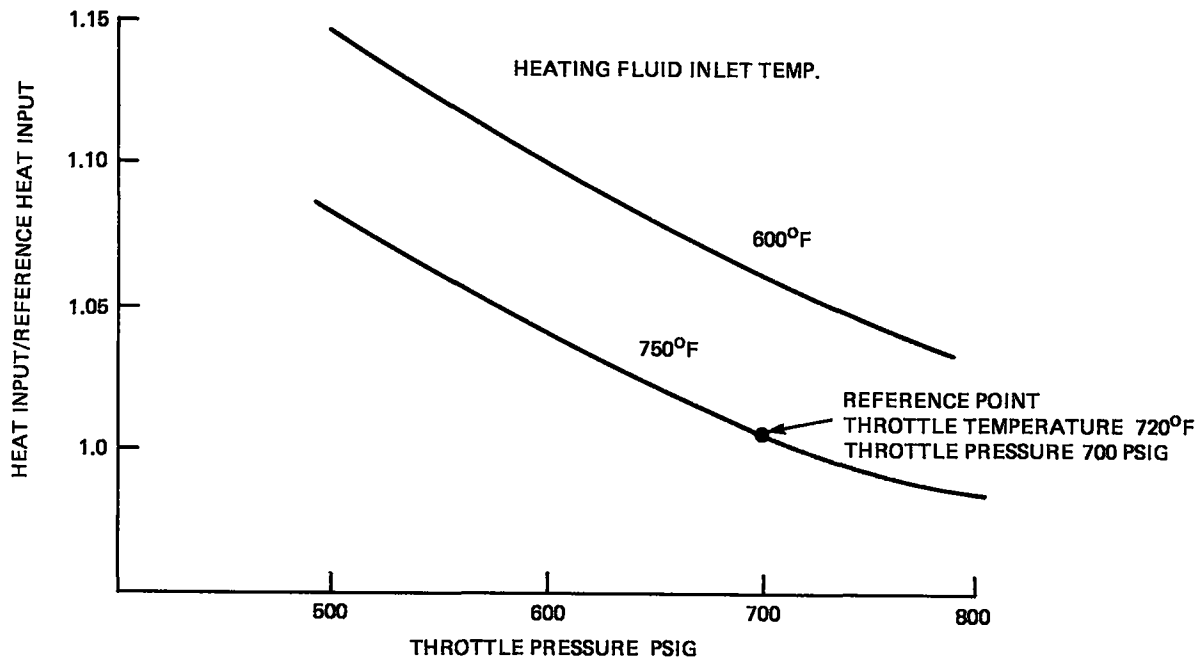


Figure 3.5-1. Heat Input Sensitivity To Throttle Pressure and Temperature

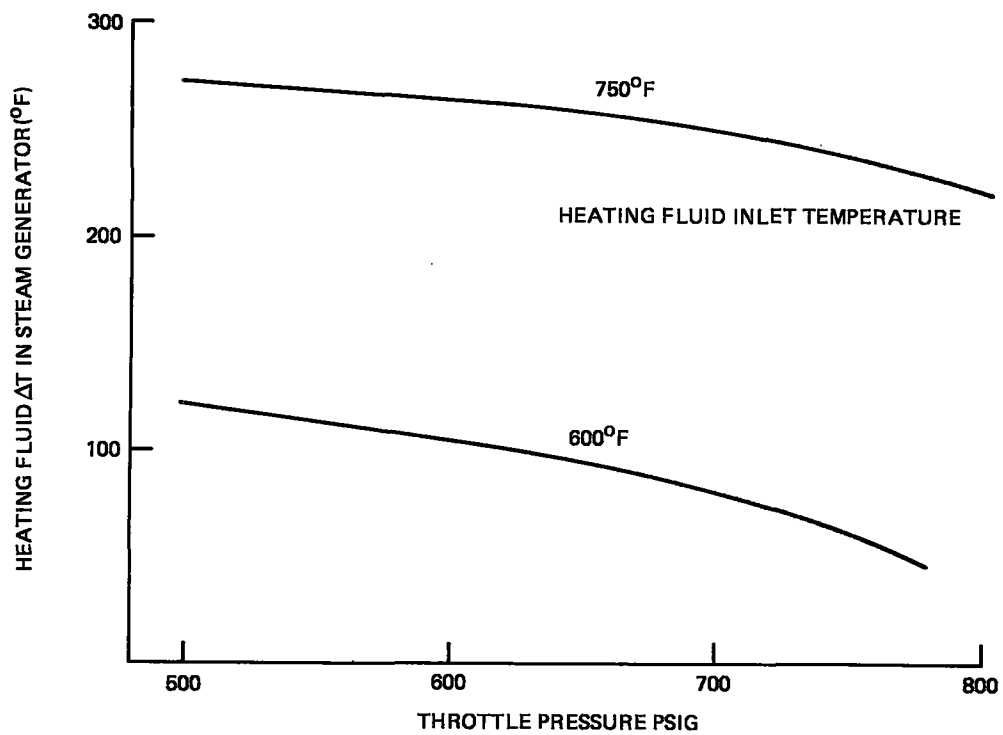


Figure 3.5-2. Steam Generator ΔT Sensitivity To Throttle Pressure And Heating Fluid Inlet Temperature

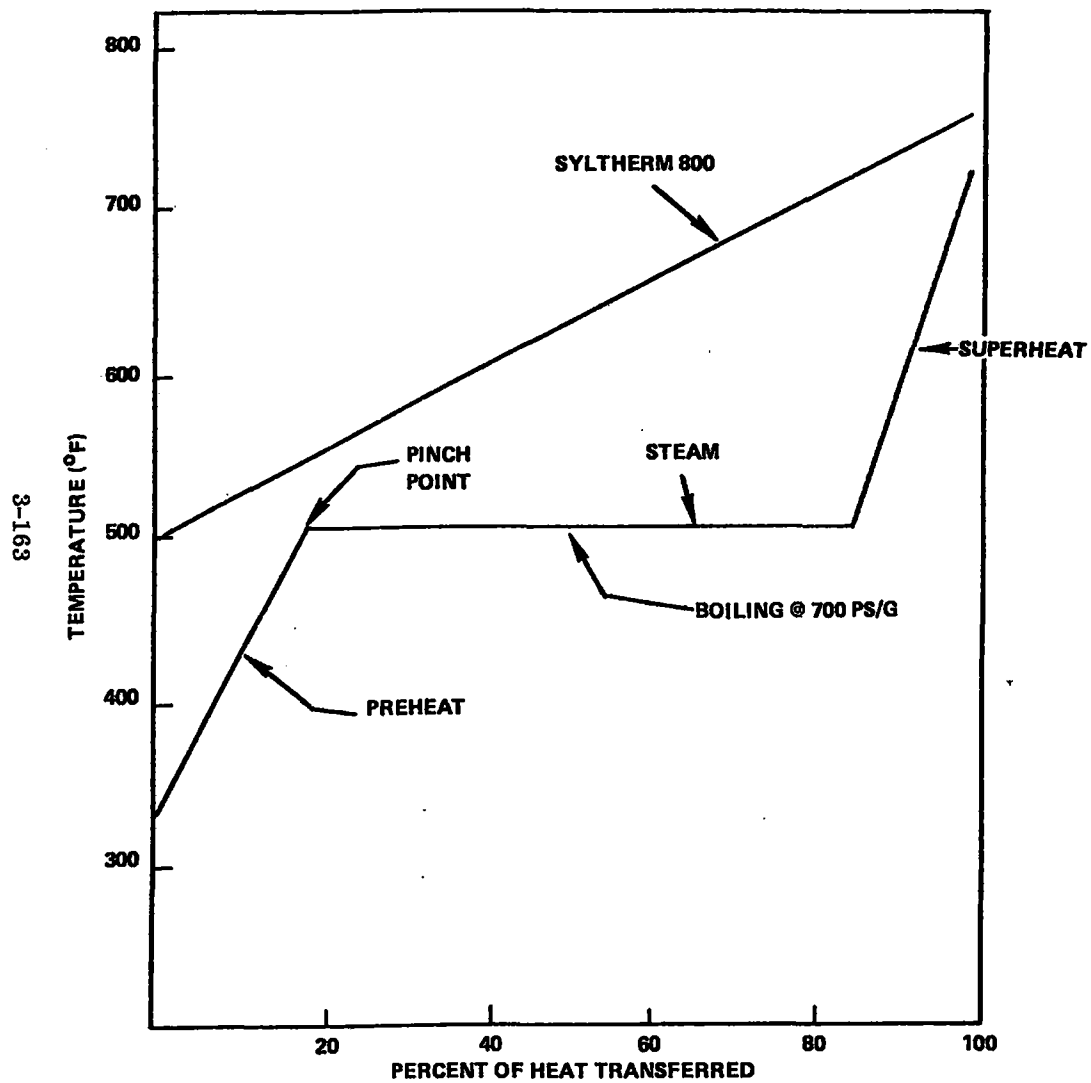


Figure 3.5-3. Solar Steam Generator Pinch Curve

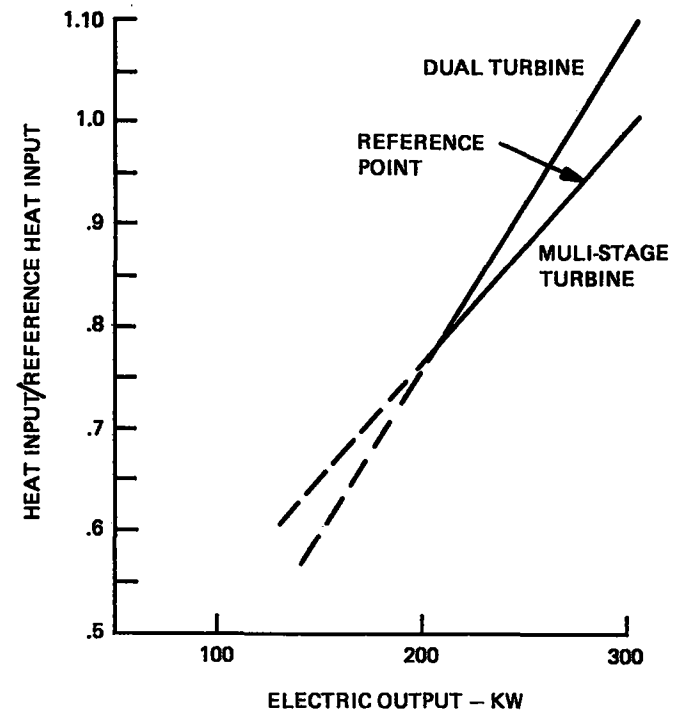


Figure 3.5-4. Estimated Performance Comparison Between Multi-Stage and Two Single Stage Turbines

Table 3.5-4. Summary of Rationale for Selection of Multi-Stage Extraction Cycle

- Modified GE MDTD Multi-Stage turbine configuration will require lower heat input than minimum development 2 single stage turbine configuration in 200-300 kW range (9 percent advantage at 300 kW).
- Pressure level at uncontrolled extraction point can be maintained above process steam pressure level throughout 200-300 kW range while realizing above performance advantage.
- GE MDTD turbine generator has significant reliability/maintainability advantages over alternate T-G assemblies.
- Program advantage of reliable single source for complete turbine generator with all necessary component controls.
- Minimum program risk for improved efficiency modifications of GE MDTD 500 kW machine.
- Single stage non extraction cycle meets thermal loads at less than half of reference design heat input but produces very small electric output.

- | | |
|---|---|
| <ul style="list-style-type: none"> • GROSS ELECTRIC POWER OUTPUT: 200-400 KW
480 V \pm 5%
60 Hz \pm 1/2% • EXTRACTION STEAM: 0-1380 LBS/HR.
105 PSIG. MINIMUM • STEAM CONDITION AT TURBINE INLET: 700 PSIG/720°F
\pm 25 PSI/\pm 25°F • CONDENSING PRESSURE: PSIG \pm 1 PSI • MAX. THERMAL INPUT AT 400 KW: 3000 KW • SYL THERM 800 TEMP. AT STEAM GEN. INLET: 700-750°F • MINIMUM ΔT: 200°F • CONDENSER COOLANT INLET TEMP: 180-195°F • CONDENSER COOLANT OUTLET TEMP: 210°F MIN. • HEAT DELIVERED TO CONDENSER COOLANT
AT 400 KW/1380 LBS/HR: 2000 KW (MIN) | <ul style="list-style-type: none"> • MAX. PARASITIC POWER: 18 KW • MAX. STEP INCREASE IN ALT. LOAD: 25 KW • MAX. RAMP INCREASE: 100 KW/MIN • MAX. STEP INCREASE IN THROTTLE
FLOW: 1000 LBS/HR. • MAX. STARTUP TIME: 30 MINUTES • AVAILABILITY OF PCS: 95% MINIMUM |
|---|---|

Figure 3.5-5. Power Conversion Subsystem Requirements Summary

Table 3.5-5. Power Conversion Subsystem Performance Tabulation for Modified GE. MDTD Multi-Stage Uncontrolled Extraction Turbine

Thermal Input, kW	2944	2403	1756	2980	2448	1798	3013	2475	1820
Electric Output, kW	400	300	200	400	300	200	400	300	200
Process Steam Flow, lb/hr	1380	1380	1380	1380	1380	1380	1380	1380	1380
Heat Delivered to Condenser Coolant, kW	2038	1607	1072	2074	1653	1114	2107	1680	1136
Throttle Pressure, Psig	700	700	700	700	700	700	700	700	700
Throttle Temp., °F	720	720	720	680	680	680	650	650	650
P exch. psia	240	188	126	248	197	131	256	203	138
H, Btu/lb	1356	1356	1356	1333	1333	1333	1313	1313	1313
H extr Btu/lb	1297	1291	1276	1277	1271	1258	1260	1253	1240
UEEP Btu/lb	1172	1185	1198	1155	1169	1182	1140	1154	1167
T cond., °F	230	230	230	230	230	230	230	230	230
Throttle Flow, lb/hr	10170	8119	5723	10540	8465	5994	10883	8735	6187
Extraction Flow To Process, lb/hr	1246	1253	1270	1269	1276	1292	1289	1298	1314
Extraction Flow To DA lb/hr	1588	1112	599	1676	1181	636	1759	1240	669
Condenser Flow, lb/hr	7336	5754	3854	7595	6008	4066	7835	6197	4204

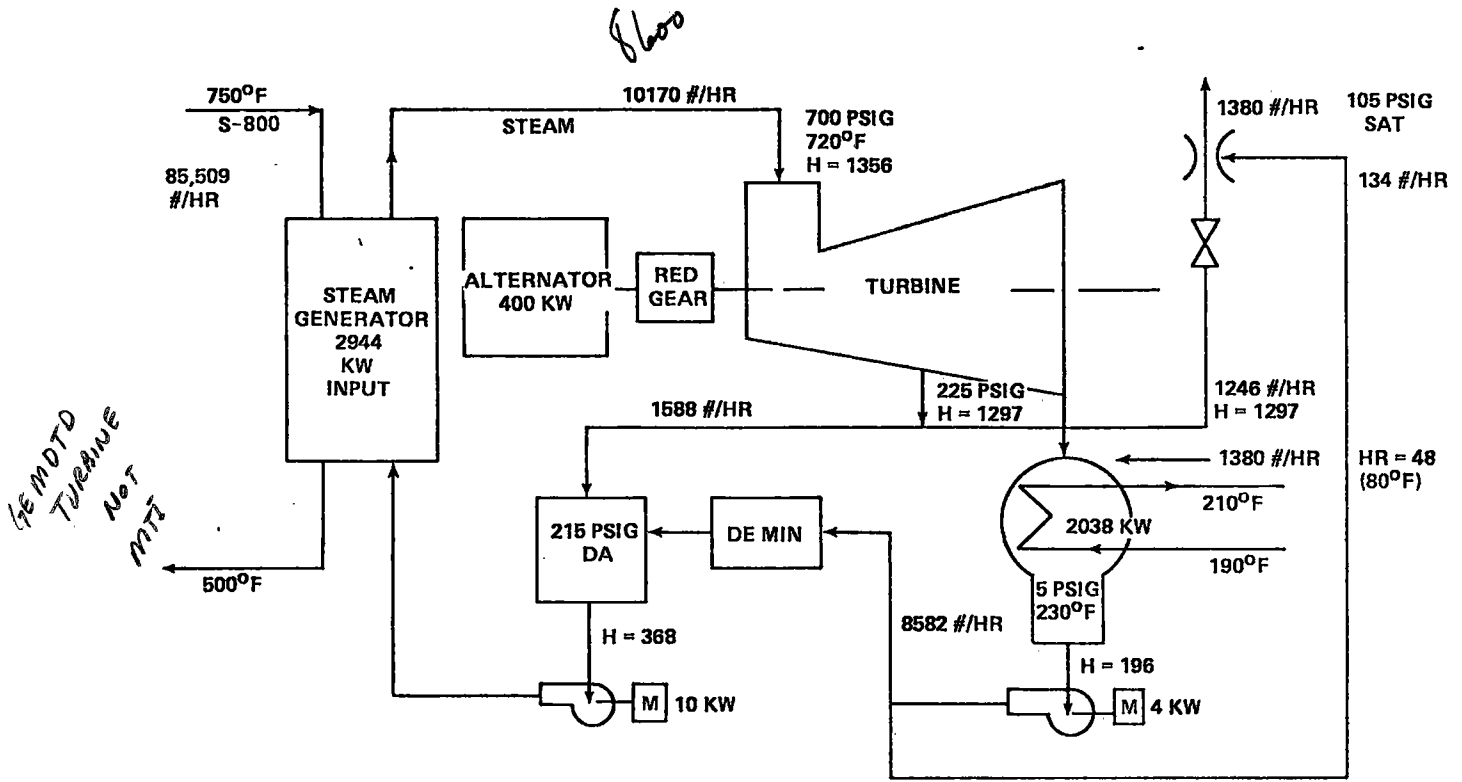


Figure 3.5-6. PCS Heat/Mass Balance Diagram 400 kW Output

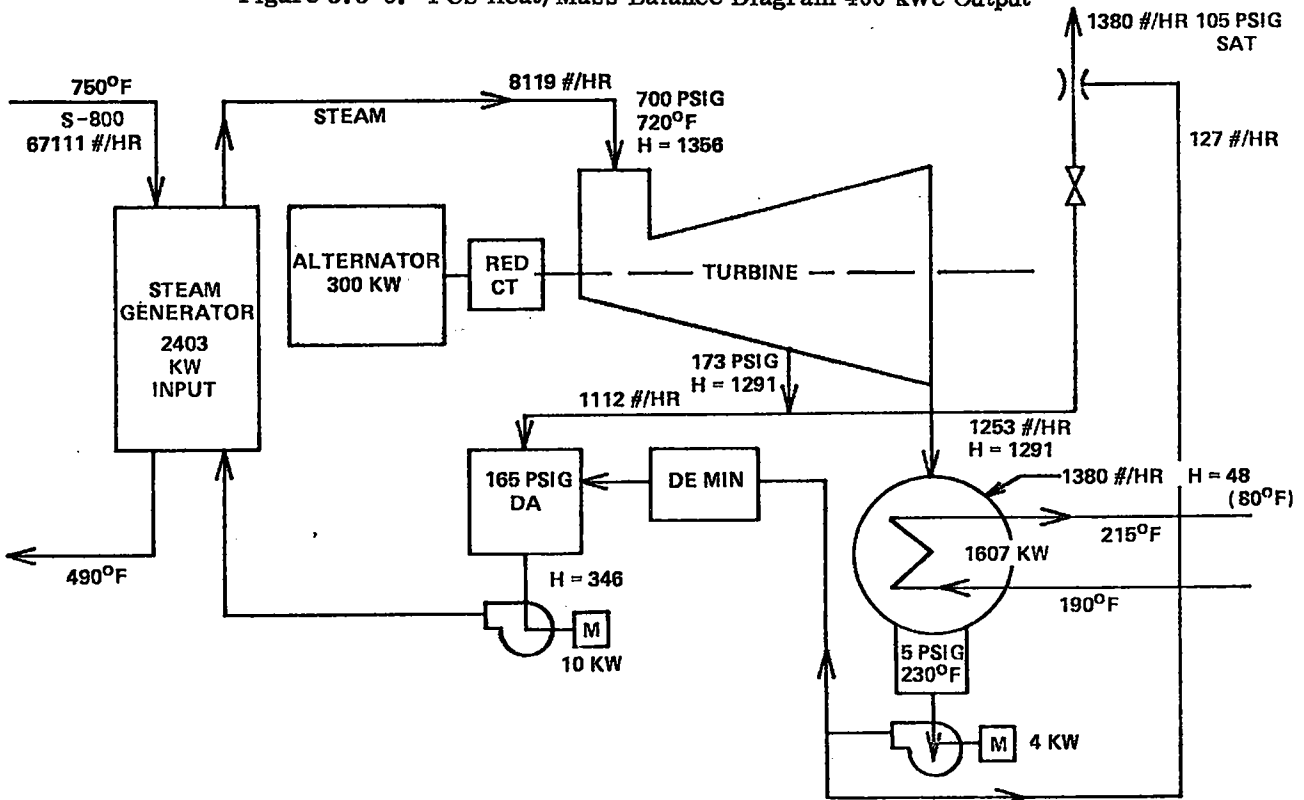


Figure 3.5-7. PCS Heat/Mass Balance Diagram 300 kW Output

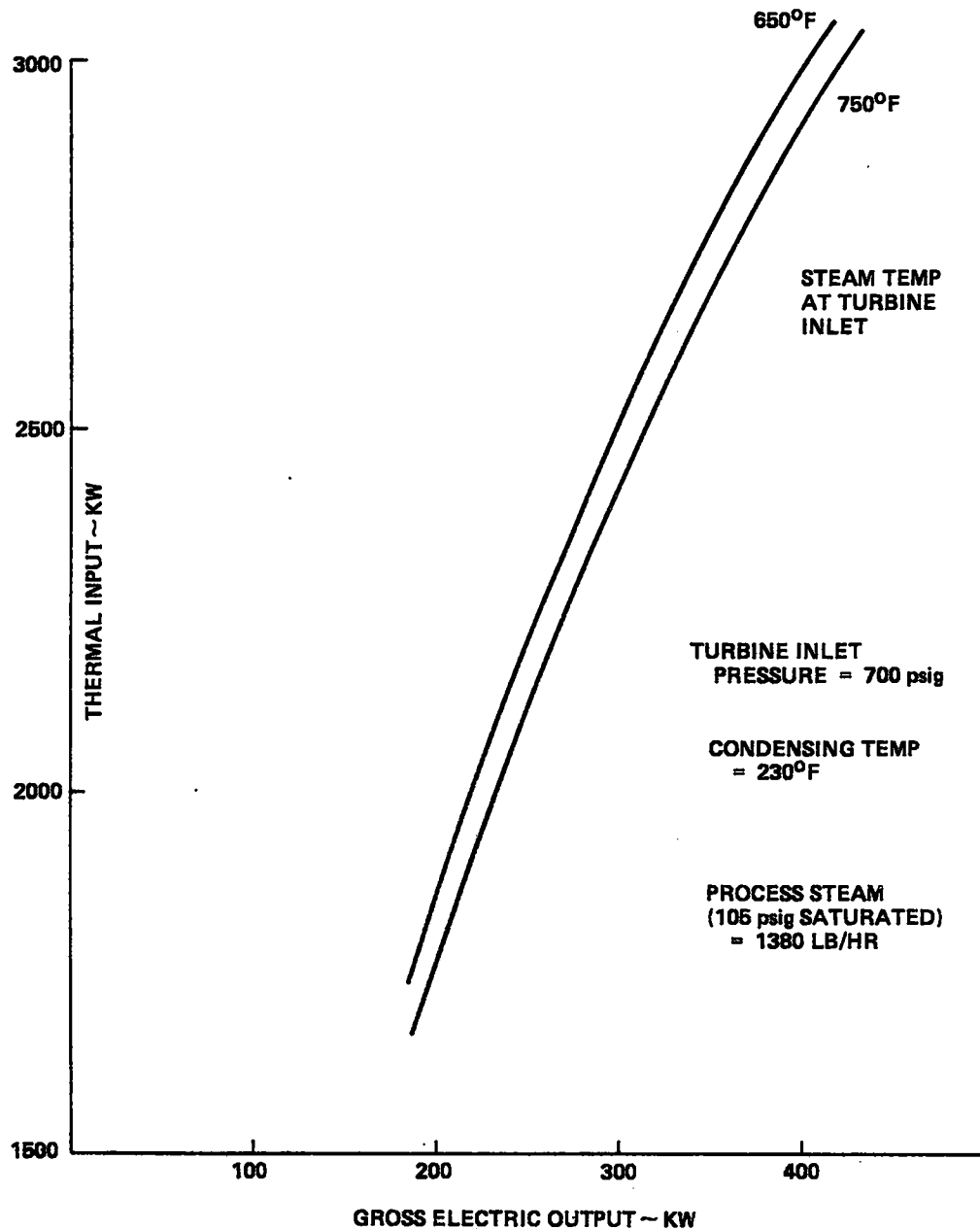


Figure 3.5-8. Heat Input to Power Conversion Subsystem vs Gross Electric Output

selected was a dual, high speed, axial flow turbine concept with controlled steam extraction between the turbines as designed and manufactured by Mechanical Technology Incorporated, (MTI). Both turbines contain two impulse type stages operating at 42,000 rpm. The two turbines operate on a single shaft through a two-stage speed reducer gearbox connected to an 1800 rpm air cooled synchronous generator. An integrated control package is also being developed for the skid mounted unit. Figure 3.5-6 shows the estimated design point performance for the MTI turbine-generator set.

3.5.2 MECHANICAL COMPONENT EVALUATIONS

In the following paragraphs, the design selection of the major components of the Power Conversion Subsystem (exclusive of the steam turbine generator, which is being supplied by MTI under an independent contract) is discussed. Alternative designs which were comparatively evaluated in making the selections and the determining considerations are indicated.

3.5.2.1 Steam Generator

Alternate steam generator designs which were evaluated for the STES are a once-through, single shell, steam generator heat exchanger and a three shell steam generator unit comprised of a counterflow preheater, a drum type pool boiler, and a counterflow superheater. Factors considered in the selection process included control and transient load response characteristics, reliability, availability of fully developed hardware on a short firm procurement schedule, component structural complexity, water quality requirements, and cost.

3.5.2.1.1 Control and Transient Load Response Characteristics

The transient load response characteristics of the once-through steam generator were analytically evaluated and were determined to be adequate for maintenance of the specified frequency variation limits during a 25 kW step function load transient under stand alone operation. However, this analysis was based on a high inertia (21 kg. m² or 500 lb. ft²) steam turbine generator rotor. Furthermore the analysis indicated a substantial drop (more than 1.7×10^5 N/m² or 25 psi) in turbine throttle pressure during the transient. For the drum type pool boiler which contains approximately 1364 kg (3000 lb) of pressurized saturated water, it may be readily calculated that, during a load transient, a 34,475 N/m² (5 psi) depression in pressure of the drum water mass will permit the spontaneous (flash) generation of approximately 1.9 kg (4 1/4 pounds) of steam. This is sufficient to carry a 25 kW load step for approximately 20 seconds without any steam generator control action at all. Twenty seconds is sufficient time for control action to increase the flow of Syltherm 800 through the steam generator. Thus, it is apparent that transient stability of throttle pressure is higher for the drum boiler than for the once through boiler. Maintenance of transient temperature stability (which is less important than pressure stability) is handled in approximately the same manner (by feed forward action) for both design options.

Steam generator control is somewhat simpler for the drum type boiler with preheater and superheater than for the once through unit. For the latter, cascaded feedback control loops are required for both temperature and pressure control, while the drum boiler unit requires only a pressure control plus a simple mechanical level control. Transient control of superheat temperature is accomplished through a short duration feed forward Syltherm 800 flow boosting/deboosting action integrated into the pressure control circuit.

3.5.2.1.2 Reliability/Complexity

Reliability and structural complexity considerations are, from a basic design standpoint, more favorable for the simpler, smaller, single shell, once-through unit. However, this is offset by the fact that the multiple shell unit is composed of proven, tested, fully developed components, whereas the once through unit is a new one-of-a-kind design.

3.5.2.1.3 Commercial Availability

Commercial availability favors the three unit option since several reliable vendors can supply this type of equipment including controls. The once through unit and its controls would have to be designed and then procured through a fabrication jobbing vendor. The schedule for delivery of fully operational hardware is somewhat unpredictable.

3.5.2.1.4 Feed Water Quality Requirements

Once through steam generator units are subject to stringent requirements on allowable feedwater solids concentrations, particularly for critical impurities such as silica. Failure to meet maximum concentration requirements will result in tube plugging. The drum type boiler permits much more relaxed water quality standards, the principal limitation being the need to limit the silica concentration in the drum water to less than 20 ppm in order to avoid carry over of silica into the turbine where it would cause fouling. This can be readily accomplished through blowdown of drum water (approximately 1% of the steam discharge flow) to a flash tank from which steam is taken to the deaerator, and the residual water containing the dissolved solids is removed through a waste water temperature control unit. This auxiliary equipment (blowdown control valve, flash tank, and waste water temperature control device) is supplied by the steam generator manufacturer.

3.5.2.1.5 Cost

Although, from a basic design comparison standpoint, the single shell once through steam generator is potentially lower in cost than the massive three unit design with its heavy steam/water drum, the two auxiliary heat exchangers, and the auxiliary blowdown equipment, cost estimates obtained for procurement of a steam generator for the STES indicated cost savings result from using the standard three unit device relative to the new design once-through unit.

3.5.2.2 Demineralizer Equipment

Selection of the STES demineralizer equipment is closely related to the steam generator selection. Comparative feed water quality standards for the once-through steam generator and for a steam generator incorporating a drum boiler with blowdown to control boiler water solids concentration are indicated in Table 3.5-6. To insure compliance with the once through steam generator water quality standards, a three bed (cation bed, anion bed, and a polishing mixed bed) demineralizer unit operating at a maximum water temperature of 300°K (80°F) is required plus a Powdex (coated resin) type of full flow polishing demineralizer, located between the condenser and the deaerator where the condensate temperature is 383°K (230°F). The latter unit serves as a partially effective, mixed resin, ion exchange type demineralizer and also as a filter for metallic oxides. Operational disadvantages of this elaborate demineralizer equipment include the following:

1. Complex regeneration cycle of the mixed bed make up demineralizer involving bed separation, acid/caustic treatment of the two resin types, back flushing, and bed remixing with compressed air.
2. Complex hydraulic back flushing/recoating cycle for Powdex polishing demineralizer which is required frequently due to rapid deterioration of the Powdex resin under thermal cycling to the 383°K (230°F) maximum temperature.
3. Reliability/availability impairment due to complexity of equipment and frequency of required regeneration.
4. Probable lengthening of subsystem start up time due to need for prestart circulation of condensate through the polishing demineralizer to establish high water quality before bringing once-thru steam generator into operation.

Substitution of the drum boiler using blowdown, with the associated lower water quality requirements (Table 3.5-6) results in elimination of the Powdex polisher and substitution of a relatively simple two bed make up demineralizer for the previously required three bed unit. Demineralizer equipment cost, maintenance cost, and reliability/availability have been improved by selection of the drum-type steam generator.

Table 3.5-6. Demineralizer Requirements

Contaminant	Raw Water (PPM)	Demin Discharge Drum Boiler w/Blowdown (PPM)	Once Through Steam Gen (PPM)
Total Solids	200	1	.03
Silica as SiO ₂	12	.3	.01
Iron	1	.16	.005
Chloride	7	.03	.001
Sodium	6	.03	.001
Calcium	17	0	0
Magnesium	2	0	0
Potassium	3	.001	.001
CO ₃	15	0	
HCO ₃	12	0	
SO ₄	14	0	
NO ₃	.2	0	
Ph	9.0	9.2	9.4

3.5.2.3 Condensate Pump

The condensate pump is required to supply a flow rate in the range of 6.3×10^{-4} to $1.0 \times 10^{-3} \text{ m}^3/\text{s}$ (10 to 16 gpm) against a head of approximately 83.8 meters (275 ft). This corresponds to an operating range of specific speed, at 1750 rpm, of 0.026 to 0.034 rev. $\frac{\text{s}^{-1} \sqrt{\text{m}^3 \cdot \text{s}^{-1}}}{\text{m}^{3/4}} \left(\frac{82 \text{ to } 104 \text{ rpm/gpm}}{\text{ft}^{3/4}} \right)$. For a

hot water pump of this capacity and operating specific speed, the commercially available pump type options are a reciprocating positive displacement pump, such as a triplex plunger type, and the turbine or regenerative type of hydrodynamic pump. The maximum temperature and pressure conditions are modest, 383°K/1.0 x 10⁶ N/m² (230°F/150 psi), and impose no limitations on the pump selection. For either type pump at this capacity level, the most practical, reliable, and economical method of operation over the required flow range is to employ a differential pressure operated bypass valve for returning to the condenser hot well the excess flow above that admitted to the deaerator by the deaerator level control. The alternative of control by discharge throttling, which could result in occasionally dead heading the pump, would lead to destructive discharge pressures in the case of the positive displacement pump and would result in very high shut off power consumption (with drive motor overloading) and also potentially destructive discharge pressure and temperature in the case of the turbine pump. The option of variable pump speed is expensive, low in reliability, and requires a D.C. motor drive. The potential power saving (1 hp or less) is not sufficient to justify this complication.

The turbine type pump has been selected for the application on the basis of the advantages indicated in Table 3.5-8. These include (1) capability for operation at a low NPSH, which is an important advantage from

Table 3.5-7. Condensate Pump Alternatives Evaluation

Pump Type	Speed (rpm)	Drive	Required Net Positive Suction Head (NPSH)	Reliability Maintainability	Power Requirement (Bhp)	Cost Range (\$)
Turbine Pump	1750	Direct Motor Drive (Induction Motor)	5-10 ft.	High	3.2	1000-3000
Triplex Plunger Pump	300	V Belt or Gear Drive (Induction Motor)	15-40 ft.	High	1.9	8000-20,000

the standpoint of required pump mounting level below the condenser hot well, (2) much lower cost, and (3) comparable reliability and maintenance characteristics. Its only disadvantage is a slightly higher power requirement.

3.5.2.4 Boiler Feed Pump

The boiler feed pump is required to supply a flow rate in the range of 7.6×10^{-4} to $1.3 \times 10^{-3} \text{ m}^3/\text{s}$ (12 to 20 gpm) against a head of approximately 549 m (1800 ft). In addition a maximum pressure/temperature requirement of $4.5 \times 10^6 \text{ N/m}^2/450^\circ\text{K}$ (800 psi/350°F) must be met. For these requirements, investigation revealed only one commercially available viable pump type - a reciprocating plunger pump. To minimize discharge flow and pressure pulsations, a triplex (three cylinder) pump was selected. The salient features/operating parameters of this pump are indicated in Table 3.5-8.

3.5.2.5 Deaerating Heater

Deaerating heater design options available for the STES application include the tray type and atomizing type units. With the tray type unit, gases dissolved in the condensate are removed through heating the water exactly to the saturated steam temperature as it is filtered through a series of heating trays in a steam atmosphere, then spreading it in thin sheets over successive layers of air separating trays, agitating it thoroughly so that the gases may be brought to the surfaces and liberated, and sweeping the liberated gases away with the steam vented to the vent condenser. Pressure drops in the condensate and steam streams which occur upon introduction to the heater are very low with this type of design.

In the atomizing type deaerator, the incoming water is first heated to almost the temperature of saturated steam by being sprayed in direct contact with steam. After this initial heating, the water contacts a high velocity steam jet which further atomizes the water droplets and scrubs away the non condensable gases.

Both types of deaerators are available at the capacity level and steam pressure level required for the STES. The atomizing type is more usual, however, at this capacity level and is less expensive.

Table 3.5-8. Boiler Feed Pump Characteristics (Ingersoll-Rand Triplex Plunger Pump)

Max Flow Rate	18 gpm
Discharge Pressure	800 psig
Suction Pressure	100 psig
Suction Temperature	328 ^o F
Net Positive Suction Head	15 ft
Pump Speed	350 rpm
Drive	V Belt
Input Power to Motor	8.6 kW
Flow Control	Differential Pressure Controlled Bypass Valve returning to the Deaerator the excess flow above that passed by boiler drum level control valve.
Number of Bearings	3 crank bearings (A); 3 sliding cross head bearings, (B); 3 conn rod bearings, (C); 2 Main Bearings (D)
Bearing Type(s)	A, B, C - Hydrodynamic, sleeve D - Tapered Roller
Lubrication	Splash/gravity
Annual maintenance Requirements	Replace plunger packing

The principal operational/performance difference between the types is that the steam pressure drop between the turbine extraction port and the discharge of the steam spray nozzle is $3.4 \times 10^4 \text{ N/m}^2$ (5 to 10 psi) greater than the extraction port-to-deaerator shell of the tray type unit. This involves a very small (virtually negligible) increase in required heat addition in the steam generator (approximately 0.3%).

Deaerator type selection will be based on evaluation of competitive vendor equipment/engineering service offerings for the condensate pump/deaerator component group. No preference can be established for either of the two available types.

3.5.2.6 Condenser

The condenser unit required to transfer heat to the TUS from the turbine discharge steam and to condense the steam operates at a temperature/pressure condition of 383^oK/ $1.4 \times 10^5 \text{ N/m}^2$ (230^oF/20.78 psia). Minimum temperature of the circulating water leaving the condenser is 372^oK (210^oF). The heat exchanger unit is enclosed in a shell approximately 0.46 meter (18 in.) in diameter and 4.6 meters (15 ft) long. The circulating water tubes are U-tubes similar to those of a closed low pressure feed water heater.

Shell and water box materials are carbon steel. Tubes are 304 stainless steel. Steam enters the shell at one end through an intersecting cylindrical passage. Within this passage is a spring loaded atomizing spray nozzle to which the makeup flow is pumped from the condensate storage tank by means of the makeup injection pump. A hot well level control valve (flow modulating type) is located between the pump discharge and the spring loaded spray valves which are designed to provide atomization over the full operating flow range.

The option of makeup spray injection into the condenser inlet steam stream as opposed to makeup injection into the hot well was selected in order to reduce the required heat input to the condensate flow stream. The result is a reduction in required heat input from the Syltherm 800 of approximately two percent for maximum load conditions.

3.5.3 CONTROLS

3.5.3.1 Normal Operating Mode Controls

Power Conversion Subsystem normal operating mode controls, with the exception of the steam turbine generator controls, are localized within component groups and will be supplied by the vendors of the group components. Interfaces between the groups are simple and involve no intergroup control action. Component groups include:

- Steam Generator
- Condenser/Make up Injection
- Condensate Pump/Deaerator
- Process Steam Desuperheater
- Chemical Injection Unit
- Demineralizer
- Boiler Feed Pump

Schematic diagrams of these component groups are shown in Figures 3.5-9 through 3.5-15, and the controls for these groups are defined in Tables 3.5-9 through 3.5-15. The steam pressure control and the condenser pressure/temperature control require control loops. These are included as Figures 3.5-16 and -17.

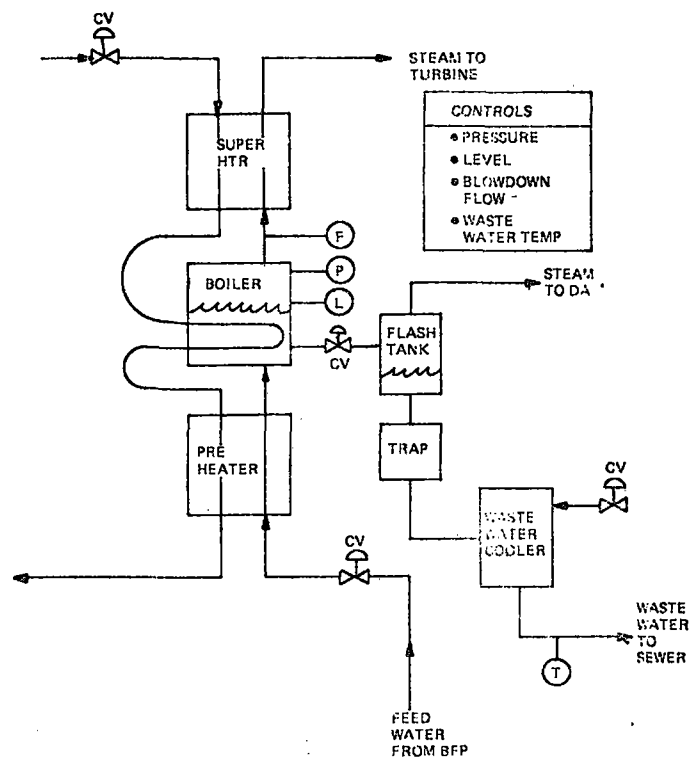


Figure 3.5-9. Steam Generator Component Group

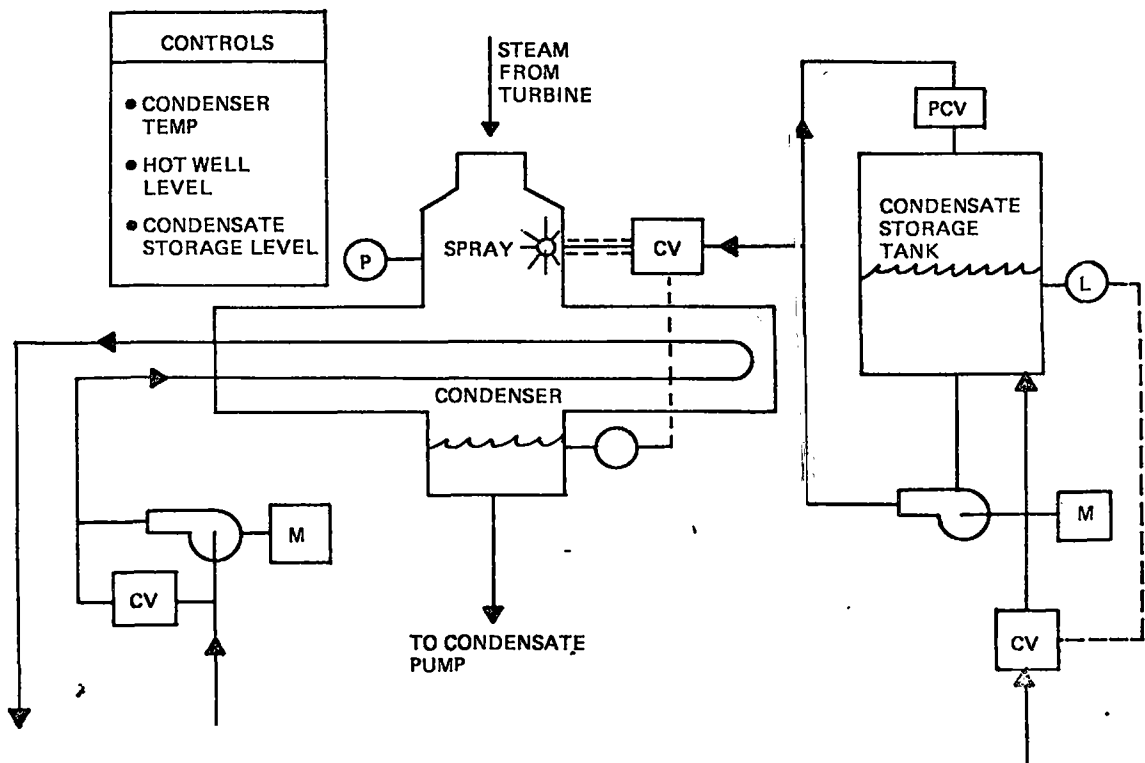


Figure 3.5-10. Condenser/Make Up Injection Component Group

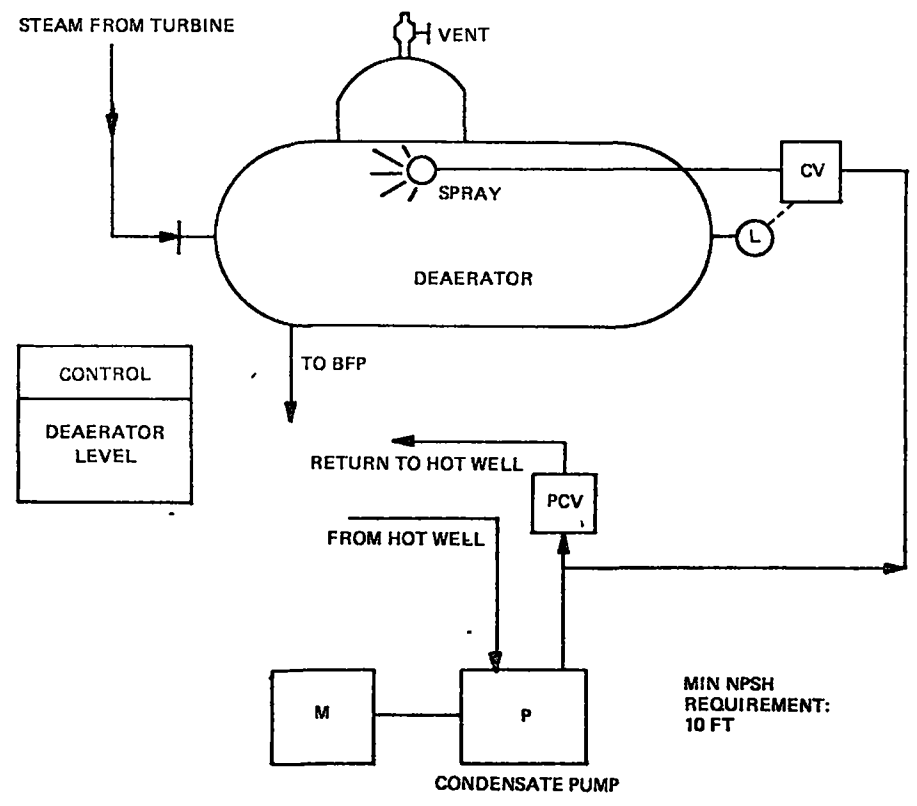


Figure 3.5-11. Condensate Pump/Deaerator Component Group

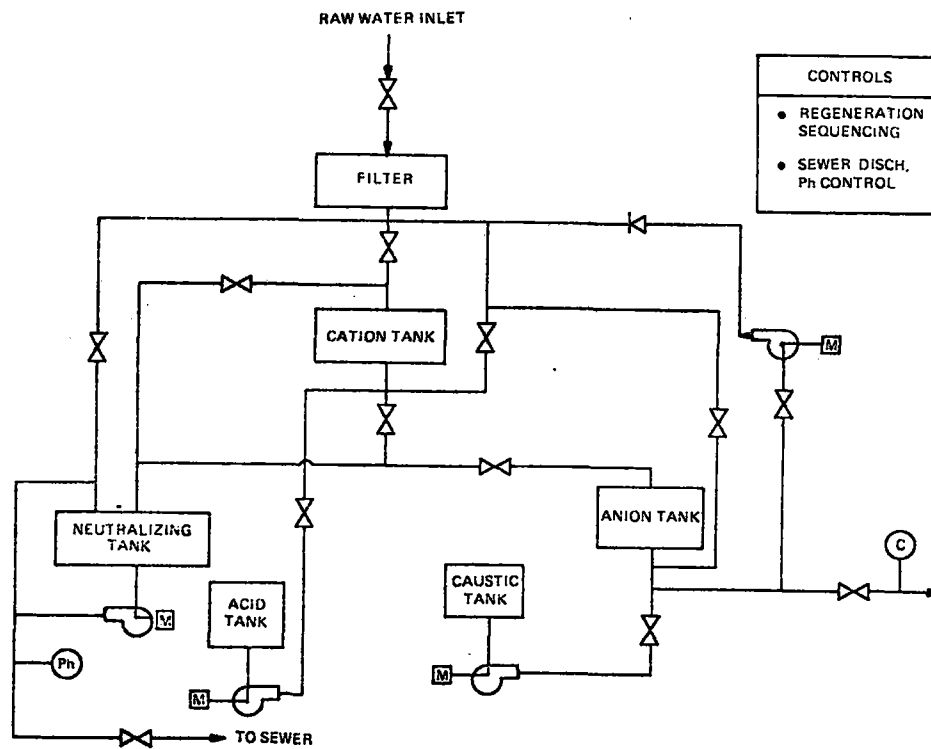


Figure 3.5-12. Demineralizer Unit

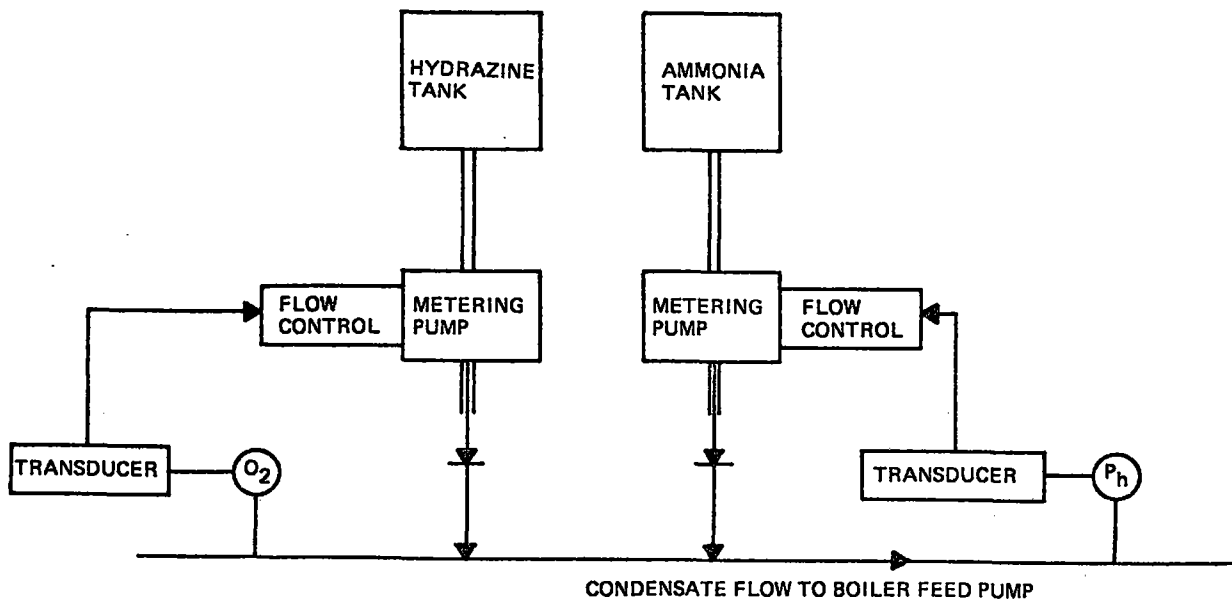


Figure 3.5-13. Chemical Injection Unit

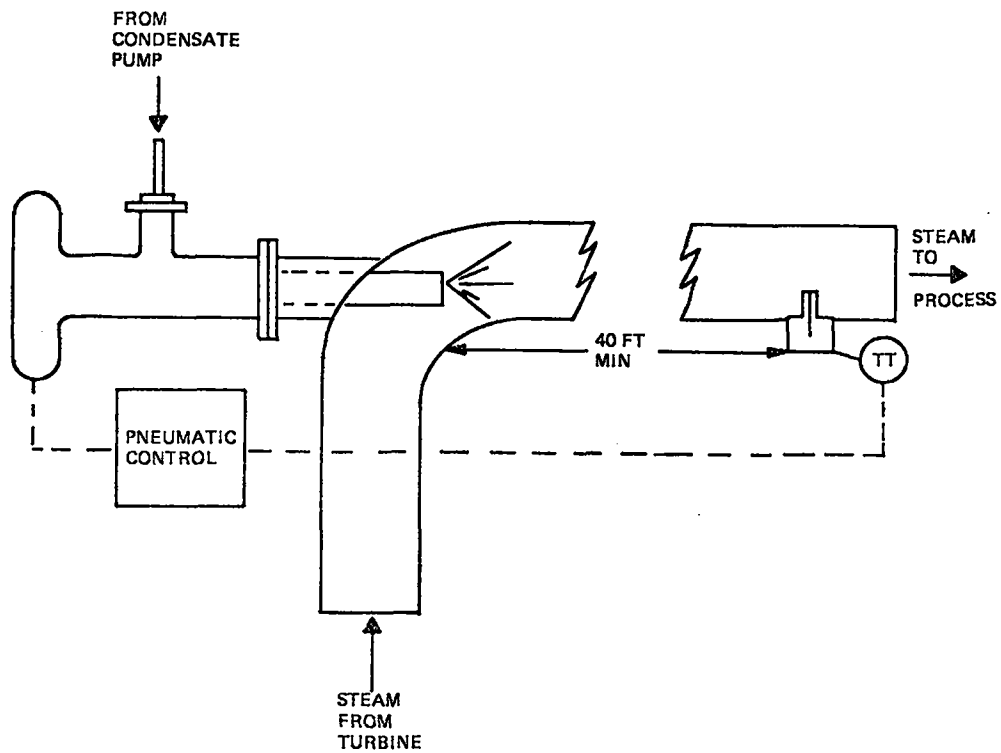


Figure 3.5-14. Process Steam Desuper Heater

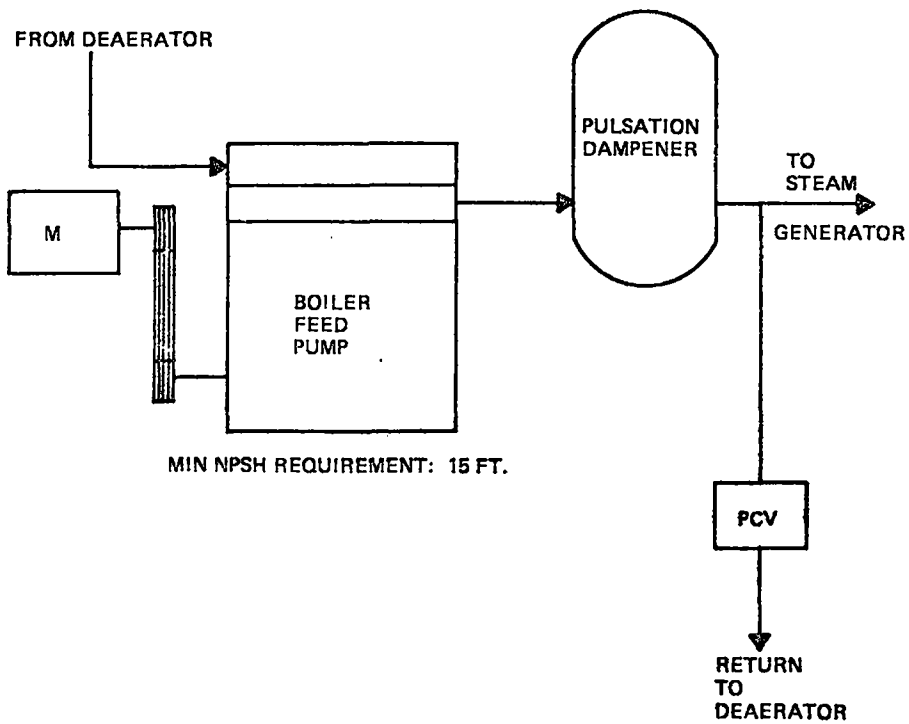


Figure 3.5-15. Boiler Feed Pump Unit

Table 3.5-9. Steam Generator Component Group Controls Requirements

Control Function	Control Components
Steam Pressure Control	Steam Pressure Controller (Electro-pneumatic) Steam Pressure Transducer Syltherm 800 Flow Regulator (Electro-pneumatic) Feed Fwd Signal Generator
Drum Level Control	Pneumatic Relay Float Type Level Transmitter Pneumatic Flow Modulating Valve
Blowdown Flow Control	Electro-pneumatic Flow Control Valve
Waste Water Temp. Control	Temperature Transducer Electro-pneumatic Flow Control Valve

Table 3.5-10. Condenser/Makeup Injection Component Group Controls Requirements

Control Function	Control Components
Condenser Pressure/Temp. Control	Pressure Transducer Pressure Controller (Electro-pneumatic) Circulating Water Flow Regulator (Electro-pneumatic)
Hot Well Level Control	Pneumatic Relay Float Type Level Transmitter Pneumatic Flow Modulating Valve
Condensate Storage Tank Level Control	Pneumatic Relay Float Type Level Transmitter
Makeup Injection Pump Disch Pressure Control	Pneumatic Flow Modulating Valve Pressure Control Valve

Table 3.5-11. Condensate Pump/Deaerator Component Group Controls Requirements

Control Function	Control Components
Condensate Pump Discharge Pressure Control	Pressure Control Valve
Deaerator Level Control	Mechanical Linkage Coupled Float Actuated Flow Modulation Valve

Table 3.5-12. Makeup Demineralizer Component Control Requirements

Control Function	Control Component
Regeneration Process Valve Sequencing Control	Mechanical Switching Type Solenoid Valve and Acid/Caustic Pump Start/Stop Sequencing Controller
Sewer Discharge ph Control	ph Transducer/Pump Start/Stop and Solenoid Valve Switching Controller

Table 3.5-13. Chemical Injection Unit Component Control Requirements

Control Function	Control Component
Feed Water Dissolved O ₂ Concentration Control	O ₂ Transducer Electronic Metering Pump Hydrazine Solution Flow Controller
Feed Water ph Control	ph Transducer Electronic Metering Pump Ammonia Solution Flow Controller

Table 3.5-14. Process Steam Desuperheater Control Requirements

Control Function	Control Components
Process Steam Temperature Control	Temperature Transmitter Pneumatic Temperature Controller Pneumatic Water Flow Control Valve

Table 3.5-15. Boiler Feed Pump Component Control Requirement

Control Function	Control Component
Pump Discharge Pressure Control	Pressure Control Valve

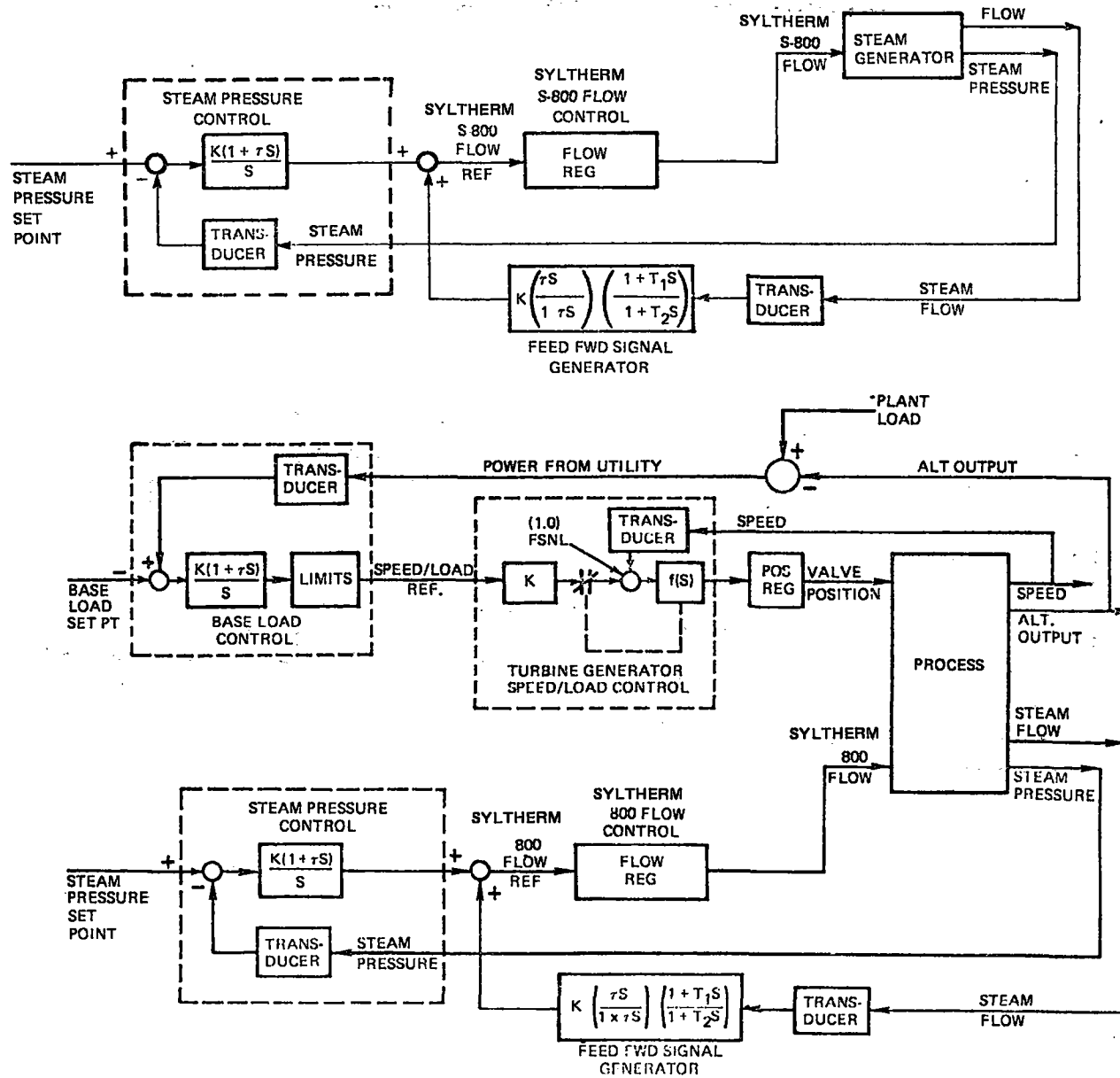


Figure 3.5-16. Steam Generator Pressure Control Loop

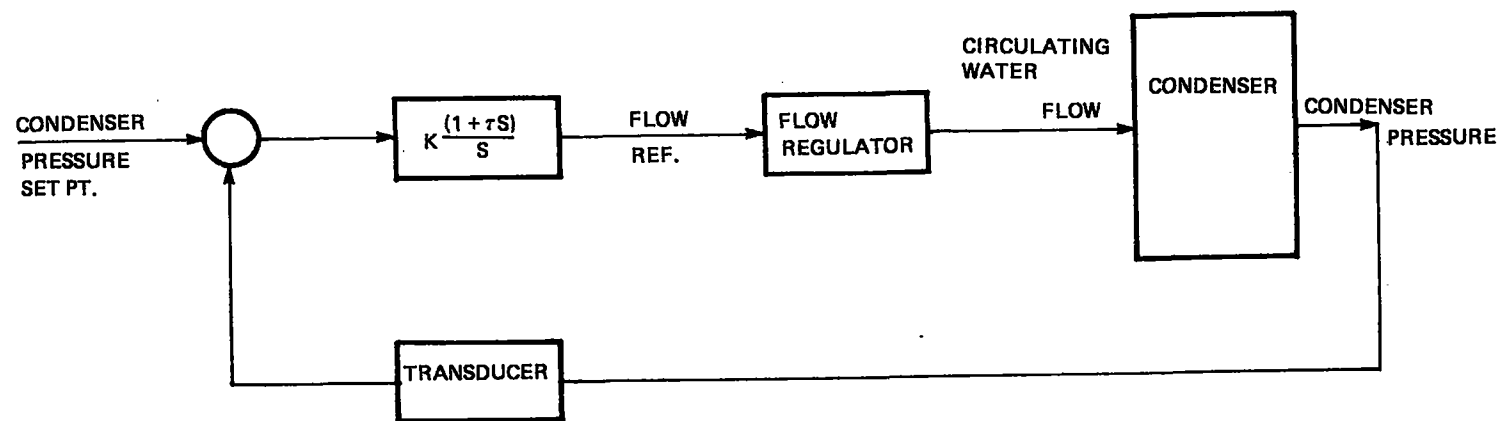


Figure 3.5-17. Condenser Pressure Control Loop

3.5.3.2 Sequencing Controls

The PCS sequencing controls initiate the actuation of valves and motor start/stop controls in proper sequence to carry out startup, normal shutdown, and emergency shutdown for the normal operating mode and also for the turbine bypass mode. These controls will be designed so that a single manual signal will be sufficient to establish operation in either the normal or turbine bypass operating mode or to effect a normal shutdown. Emergency shutdown will be initiated upon the detection by a component monitor instrument of an out of limit condition.

3.6 ELECTRICAL SUBSYSTEM (ES)

3.6.1 INTRODUCTION

Electrical System design effort has involved the following main areas:

1. Interface with Georgia Power Company (GPC) and related electrical power and relaying circuits.
2. Power Conversion System (PCS) electromechanical transient analysis.
3. Collector field lightning effects and protective methods.
4. Collector drive defocus power and control.

The system design evolution in each area is described in the following sections.

3.6.2 GPC INTERFACE

The power and protective relay circuit arrangement for the STES electrical output interconnection to the GPC-Bleyle power delivery system is shown in Figure 3.6-1. Significant changes have been included in this basic interface document (Interface Control Drawing E-3) as a result of General Electric review of the original design.

Examination of the initial version of the interface design developed by GPC led to relocation of the circuit breaker supplying the STES auxiliary loads from the generator side of the STES tie breaker to the tie line side. This permits the auxiliary breaker to operate in primarily a protective role and avoids daily switching of auxiliary service and resulting breaker mechanism wear. Elimination of several potential transformers and voltage balance relay was also accomplished which permits a less complex protective arrangement on the STES generator. The negative sequence detector relay was changed to a more sensitive solid state configuration. The resulting interface arrangement will be carried into the hardware stage with no additional changes foreseen.

The interface control and protective equipment provides cost effective STES electrical supply protection and GPC electrical supply protection to assure flexible, reliable delivery of electrical energy to the Bleyle plant from either or both sources. Experimental operating modes of the STES system are also provided for in the interface equipment such as delivery of energy from the STES generator to GPC as well as Bleyle and isolated or stand-alone operation of the STES to supply Bleyle. The primary operating mode is interconnected with GPC with load-following power delivery to Bleyle.

3.6.3 TRANSIENT ANALYSIS

A major effort was involved in modeling and analyzing the transient performance of the PCS. Initially, a model of the performance and control characteristics of the GE MDTD marine turbine with a one-pass steam generator was developed and exercised. Subsequently, the generator, excitation system, and load network were modeled and integrated with the turbine and steam generator model. Acceptable step response

performance was indicated in both interconnected and isolated operating modes. Revision of the model parameters was begun during Phase III in order to reflect the present pot-type steam generator and low-inertia MTI turbine-generator. The transient analysis work will extend into Phase IV of the program. The details of the transient analysis model development which involved analysis of mixed-phase flow and heat transfer in the steam generator are included as Appendix B of this report. Both frequency and time domain analysis techniques were utilized in determining the performance of the overall system. Figure 3.6-2 illustrates the overall model arrangement. A root-locus evaluation of the effective connection impedance is shown in Figure 3.6-3, and the effect of a limited change in inertia on step-load isolated speed response is illustrated in Figure 3.6-4, extracted from Reference 3.6-1, a portion of which is included in Appendix B. Transient response of the system to step 25 kW load changes in interconnected and isolated modes are shown in Figures 3.6-5 and 3.6-6, respectively.

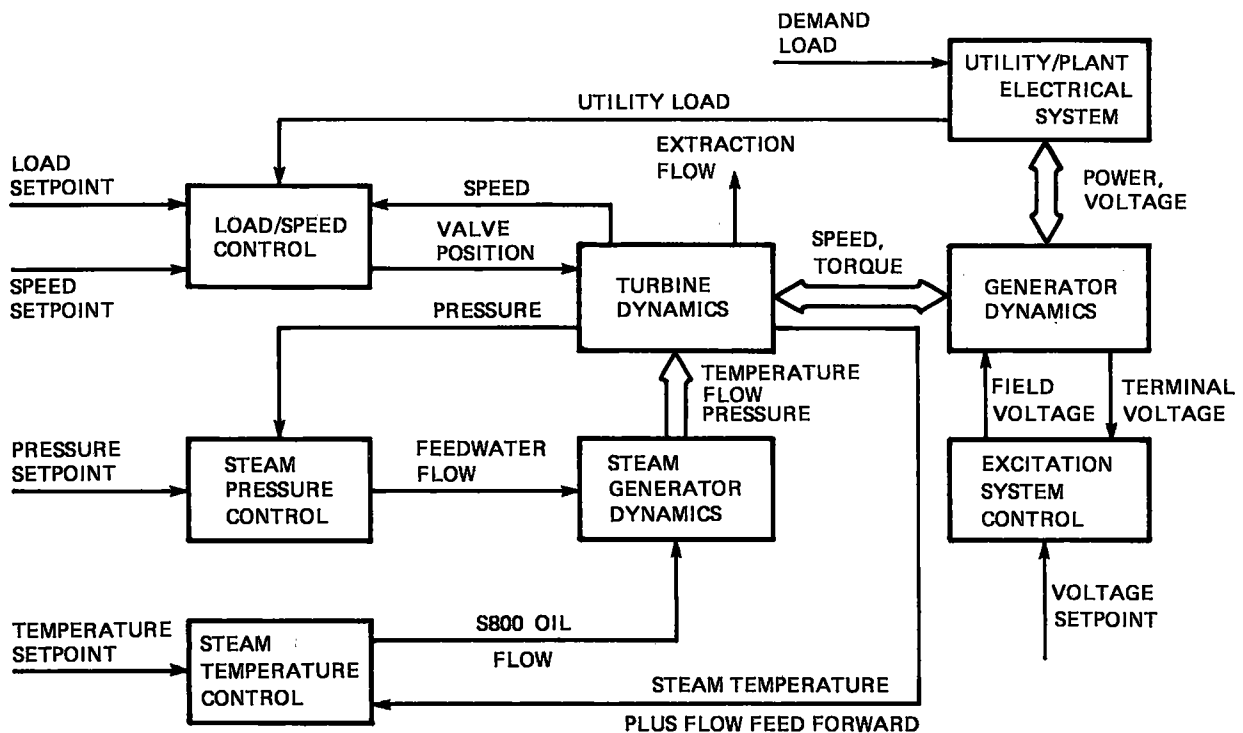


Figure 3.6-2. Transient Model Diagram

These results for the GE turbine will be utilized as a basis of comparison for the final system performance simulation incorporating the MTI turbine.

These results show satisfactory frequency and voltage control in both modes for the GE-MDTD turbine-generator. Control response requirements are not severe due to the stabilizing influence of large system inertia. Control response will probably be necessary in order to control the lower inertia MTI turbine-generator performance to meet speed control requirements in the isolated mode.

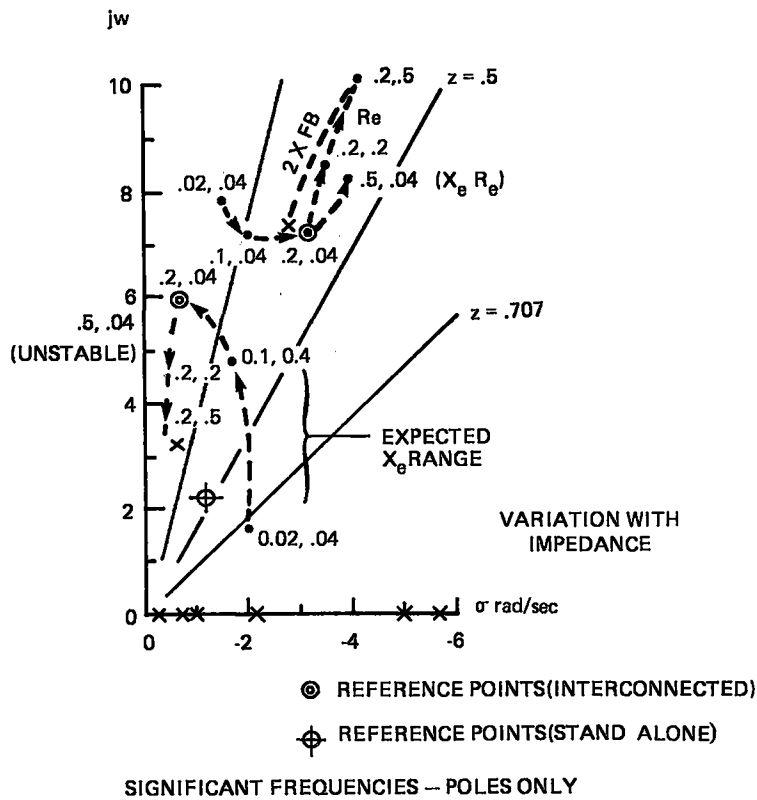


Figure 3.6-3. System Root Locus

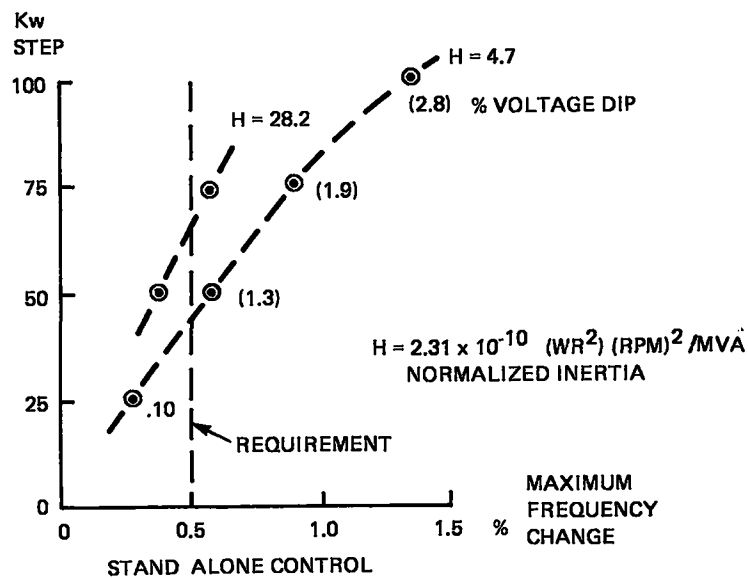


Figure 3.6-4. Effect of Inertia and Load Step

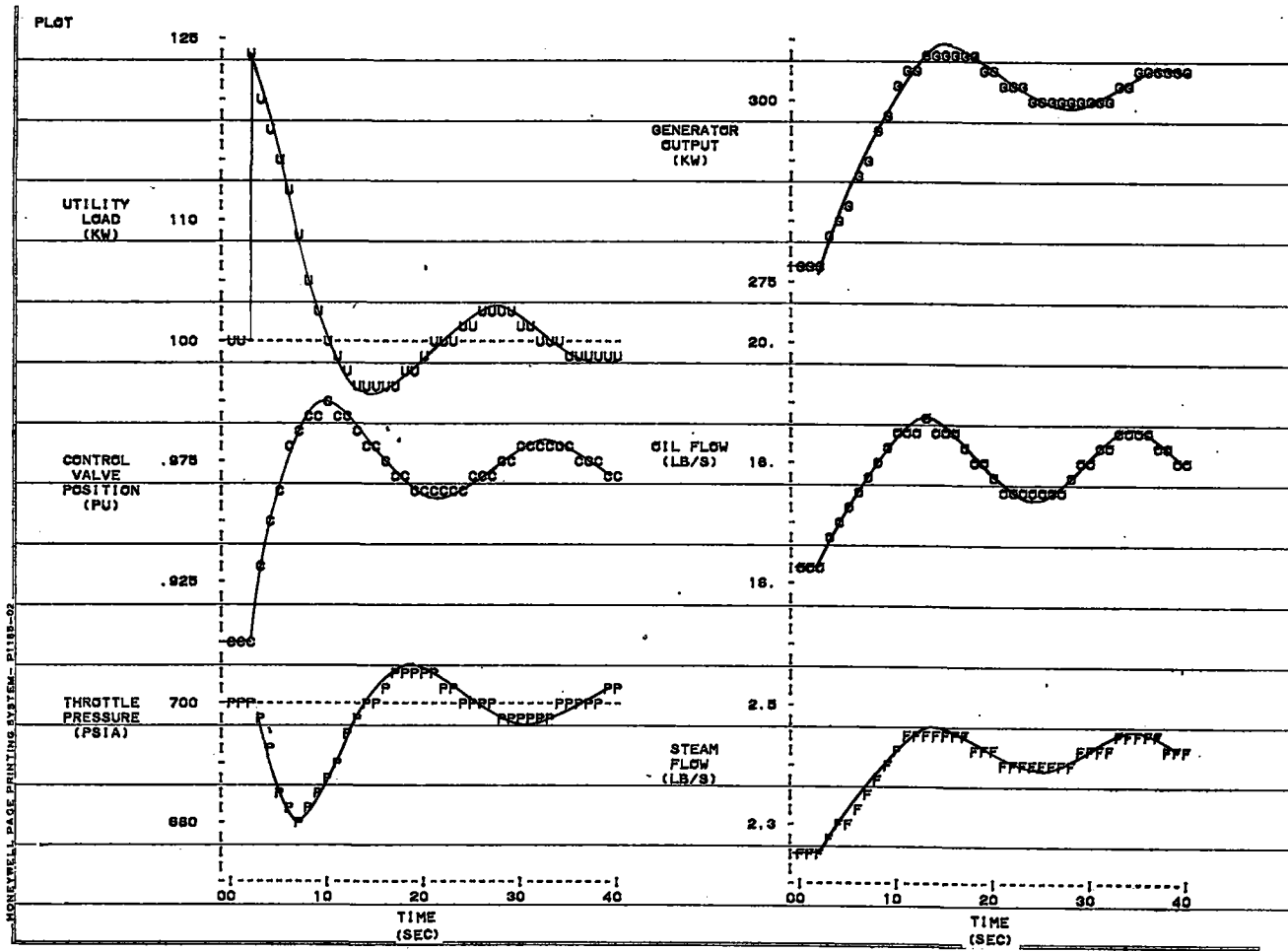


Figure 3.6-5. 25 kW Step Inter Connected

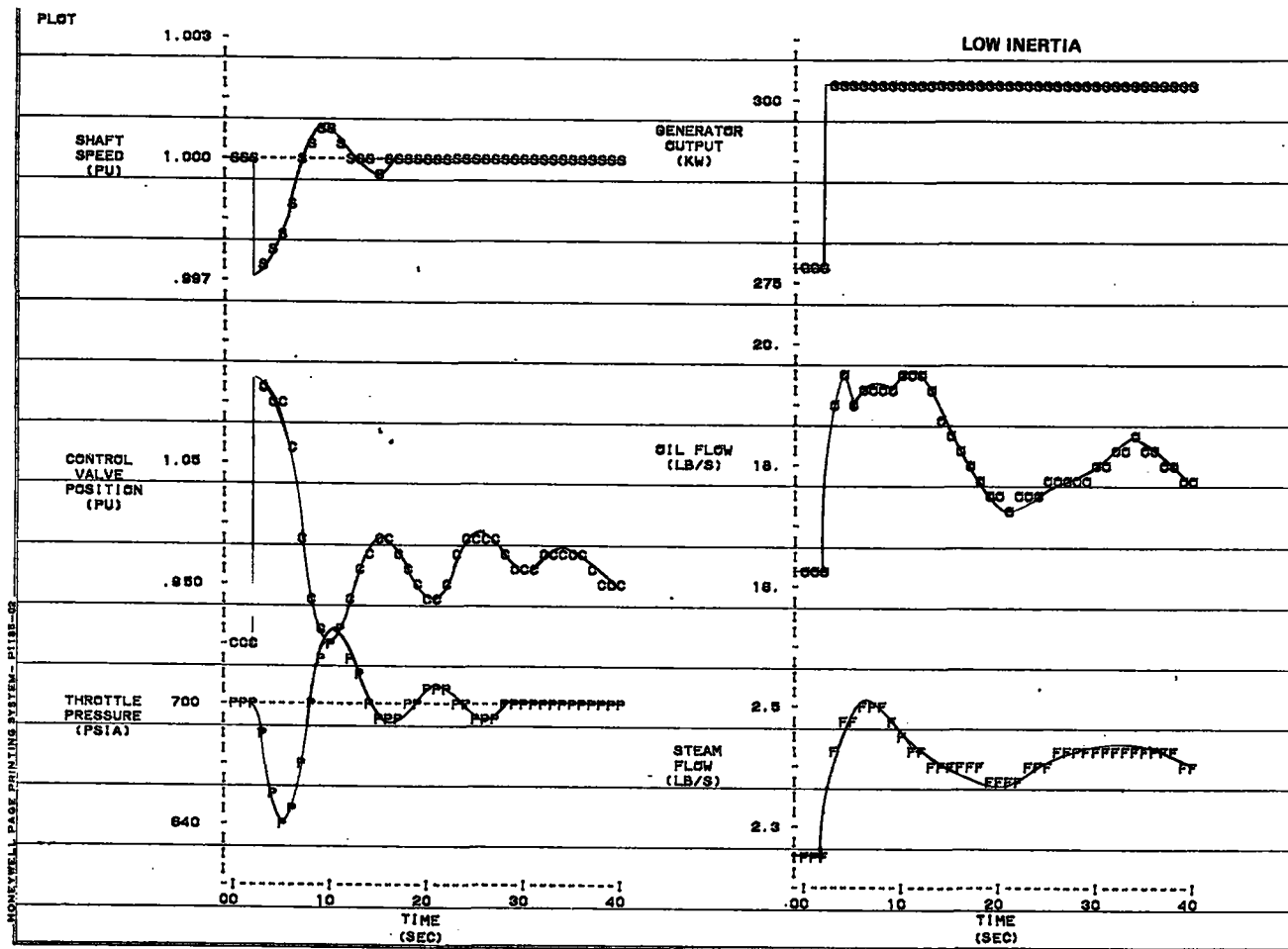


Figure 3.6-6. 25 kW Step Isolated

3.6.4 COLLECTOR FIELD

Collector field power and signal distribution arrangements and protective measures against lightning strikes on or adjacent to the field were evaluated during Phase III. A three phase 208 Y 120 volt, 60 hertz supply to the field with balanced single phase utilization at each collector was selected to reduce overall transformer and wiring costs when compared to 480 volt distribution.

Branch circuit protection and environmental protection of the field control microprocessors is provided in two field enclosures in order to minimize overall wiring and enforce modularity of design. The power and multi-conductor control wiring will be routed adjacent and parallel to the field piping in order to interconnect each collector with its zone control processor. Connection of the control wiring is illustrated in Figure 3.6-7.

Lightning is expected to strike the collector field about once every five years or less based on calculations of the field geometry and local isokeraunic activity records. The cost of an overhead ground wire arrangement prepared by GPC and GE to divert direct strikes has been judged excessive, and the possibility of collector mechanical damage due to a direct strike is accepted. After operating experience, an experimental dissipation array or conventional ground wire arrangement can be readily installed in case the history of damage is excessive with respect to predictions. Each collector will be provided with a good earth connection, and bearing-bridging braid conductors will be utilized for static and lightning current discharge paths. Surge protectors will be included on the power and control circuits to minimize induced voltage related damage from nearby lightning strikes.

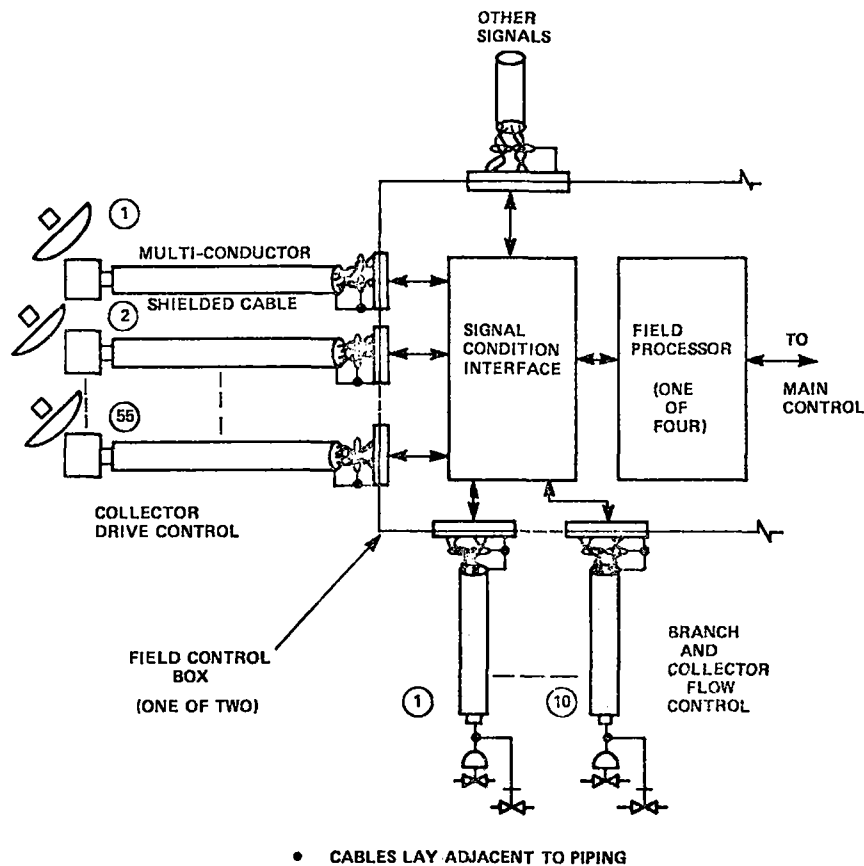


Figure 3.6-7. Field Sensor and Control Cable

3.6.5 DEFOCUS SYSTEM

A means of rapidly defocusing each collector is required in order to prevent thermal damage to the working fluid or the collector cavity in the event of loss of flow, control signal, or primary power. An immediate drive rate of 2.0 degrees per second, or 480 times sun rate, has been specified to prevent damage. An alternate, secondary power source is necessary in order to provide defocus ability with loss of primary AC power.

Several alternatives were considered as shown in Table 3.6-1. A central Uninterruptable Power Supply (UPS) must be rated for the maximum kVA demand through the inverter, and the resulting cost was found to be excessive even with minimum energy storage in batteries. A standby natural gas engine generator would require 7-10 seconds to startup and accept load and would not therefore meet the immediate drive-ability requirement. A central, high voltage dc supply at 125 or 250 volts would require a high current charger for supplying operating power at 25-50 amperes continuously and field wiring larger than the basic ac drive system due to the need to handle 2000 to 4000 amperes on a short time basis for defocus of all collectors simultaneously. The main drive and defocus motors would need to be dc rather than ac rated for optimum use of the central battery concept. Individual collector 12 volt batteries were selected as the most cost effective arrangement.

Table 3.6-1. Defocus Power Supply Alternatives

METHOD	ADVANTAGES	DISADVANTAGES
Central AC Uninterruptable Power Supply	<ul style="list-style-type: none"> ● Ease of maintenance ● Control power continuity ● Single AC System 	<ul style="list-style-type: none"> ● High capacity for short defocus time ● High capacity wiring ● Single point wiring ● High cost
Central DC Supply	<ul style="list-style-type: none"> ● Ease of maintenance ● No inverter 	<ul style="list-style-type: none"> ● Dual power system ● High capacity wiring ● Single point failure ● Battery charger capacity
Standby AC Generator	<ul style="list-style-type: none"> ● Control power restored ● Single AC system 	<ul style="list-style-type: none"> ● High capacity wiring ● High cost ● 7-10 second delay ● Single point failure ● Reliable startup requires gas.
Individual Collector Battery	<ul style="list-style-type: none"> ● Modularity ● Not subject to single point failure ● Minimum High Current wiring ● Automotive components available ● Immediate power 	<ul style="list-style-type: none"> ● Distributed maintenance ● Higher current at low voltage ● Individual battery charger required

Selection: Individual Collector Batteries

A further tradeoff between use of a long life stationary battery and an automotive type battery was performed. The automotive type battery was selected on the basis of initial cost, acceptable experiment duration life, and ready replacement availability.

The defocus power system includes a single direction, 12 volt, dc motor that draws 430 amperes at rated speed and torque which determines the battery current under cold cranking conditions and consequently the battery definition. A Delco-Remy Model 86-5 has been selected to provide 100 minutes reserve capacity and 430 amps at 255°K (0°F).

The battery charge will be maintained by a trickle charger circuit in each collector control box. A starter solenoid switch will control motor operation. The solenoid circuit will be switched by the control system on occurrence of overtemperature, loss of power, or loss of control signals. A timer circuit in the control box will disconnect the defocus control five seconds after loss of ac power to prevent motor burnout but permit continuous operation under computer control for overtemperature or manual defocus modes.

3.7 THERMAL UTILIZATION SUBSYSTEM (TUS)

The Thermal Utilization Subsystem serves as the condensing medium for the steam condenser and the heat source for the heating and cooling of the Bleyle Plant and the mechanical building. The exhaust heat from the steam turbine provides the heat input to the TUS. When the turbine is not operating, steam will be provided directly to the condenser through a bypass line to supply TUS energy needs. A large, low temperature storage tank is included in the TUS to provide operating flexibility as described in Section 2. Excess energy is dissipated through two cooling towers. Chilled and heated water are pumped to the Bleyle Plant and the mechanical building for cooling and heating purposes.

The requirements for the design of the TUS are:

1. The absorption air conditioner in the TUS shall have a maximum cooling capacity of 6.1×10^5 Joules/second (173 tons) when supplied with condenser cooling water at an outlet temperature of 372°K (210°F). This capacity is sufficient to handle the maximum combined cooling load of the Bleyle Plant and the STE-LSE Mechanical Building.
2. The hot water coil heating system in the TUS shall be capable of satisfying a maximum heat load of 1.64×10^5 J/s (559×10^3 Btu/hr) when supplied with condenser cooling water at an outlet temperature of 372°K (210°F).
3. The low temperature TES system will be sized for a maximum storage capacity of 2.1×10^{10} Joules (20×10^6 Btu).
4. The subsystem design must be compatible with the existing piping distribution system in the Bleyle Plant and be capable of supplying simultaneous heating and cooling.

These requirements were developed from the systems analysis presented in Section 2.2. The selection of the Preliminary Design configuration is discussed below.

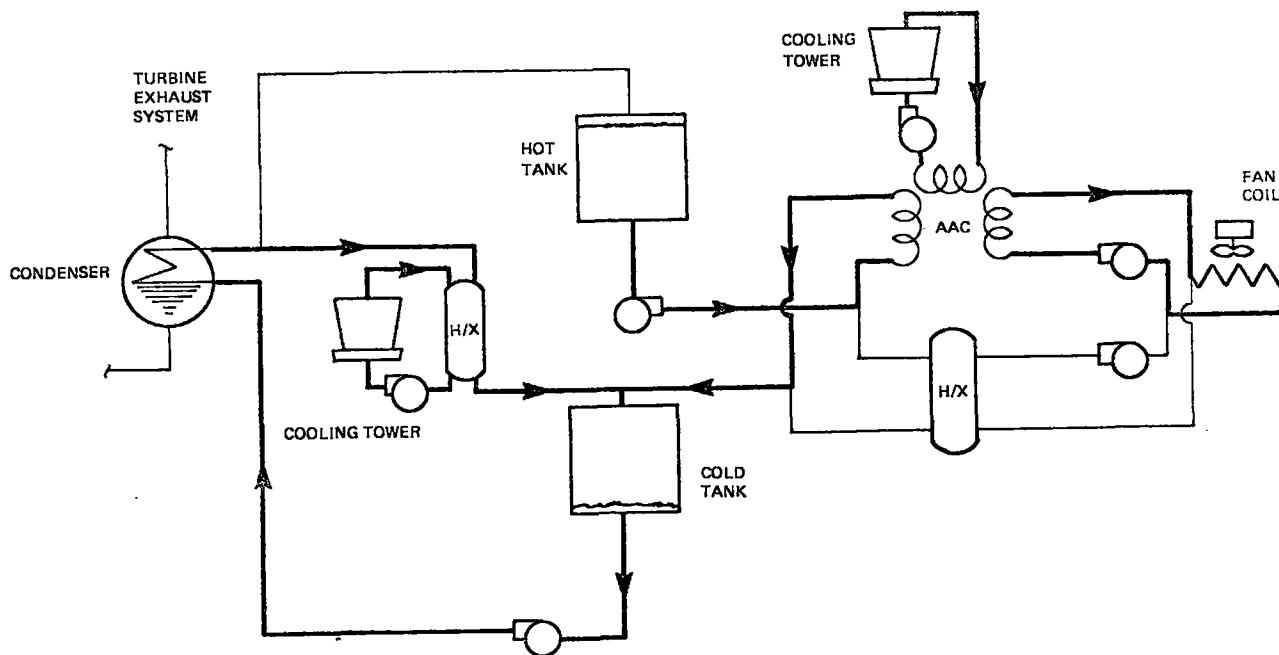
The reference design thermal utilization subsystem (TUS) included a two tank storage concept to provide constant inlet temperatures to the PCS condenser and to the absorption air conditioner. Also, the reference design TUS discharged the low temperature storage while dissipating excess energy rather than maintaining a full storage.

The following discussion shows the advantages of maintaining a full TES during excess discharge and provides a mechanical design which includes this feature for a single tank TUS. This design maintains full storage during excess discharge and also reduces by 50 percent the tank volume required by the two tank approach for equivalent storage capacity.

The reference design Thermal Utilization Subsystem shown in Figure 3.7-1 included a two tank thermal energy storage subsystem. The two tanks were employed to provide two constant temperature reservoirs: a relatively cold one which supplied 372°K (210°F) water to the PCS condenser and a relatively hot one which supplied 383°K (230°F) water to the Absorption Air Conditioner (AAC). The water levels in the two tanks varied according to the amount of energy stored with a filled hot tank indicating storage was full and a filled cold tank indicating storage was depleted. This variable level/constant temperature design required each tank to be sized to accommodate the full volume of the water storage medium. For the reference design, this resulted in an unrealistically large tankage requirement of 908 cubic meters (240,000 gallons). In addition, the design required a separate pressurization system to maintain constant pressure with fluid volume variations.

Also shown in Figure 3.7-1 is the method employed for the reference design to dissipate excess energy. All the energy transferred to the TUS at the condenser is rejected to the atmosphere via the cooling tower, and at the same time, the hot tank is supplying heat to the AAC depleting the amount of stored energy. This mode would continue until the level in the hot tank dropped to approximately 90 percent full. At this time, the cooling tower would be deactivated, and full flow from the condenser to the hot tank resumed.

An improvement in this design would result from adding a level sensor in the hot tank coupled to a modulating valve to direct only that flow in excess of AAC demands to the cooling tower. This maintains full storage during excess energy dissipation rather than allowing the level to drop, thereby providing the potential for improved thermal utilization. It also avoids cycling of cooling tower equipment and any resultant adverse affects.



DISCUSSION: When Level In Hot Tank Reaches Maximum, Cooling Tower Is Employed To Cool Full Condenser Flow While Hot Tank Continues To Supply AAC. When Level In Hot Tank Drops To Reset Level (Approximately 90% Of Maximum Level), The Cooling Tower Is Shut Off And Full Condenser Flow Is Directed To The Hot Tank To Refill It.

Figure 3.7-1. Thermal Utilization Subsystem Reference Design Excess Energy Dissipation

However, the problem of excessive tank volume is present in both designs. Figure 3.7-2 presents the selected TUS design which solves the tankage problem by utilizing a constant volume (full)/variable temperature design. The system operates by providing flow to the condenser at a variable inlet temperature of 355-372°K (180-210°F). Because the flow to the condenser is controlled to maintain 383°K (230°F) on the steam condensing side, the cooling water flow will exit from the condenser at 372°K (210°F). This results from the fact that the condenser is sized for a 11°K (20°F) approach between condensing steam and cooling water exit temperature 11°K (20°F) and for a 11°K (20°F) cooling water ΔT . The hot cooling water exiting the condenser is supplied directly to the AAC meeting its inlet temperature requirement, and flow in excess of the AAC (or heating) demand passes through the storage.

Return water from the AAC flows either directly back to the condenser or through the tank and then to the condenser as determined by a control valve. This feature combined with judicious location of the tank inlet at a midpoint in the tank and the tank outlet at the bottom to take advantage of any thermocline existing in the tank allows for selection of the coolest available water to supply to the condenser. Similarly, the hot tank outlet which supplies the AAC is located to take advantage of any thermocline in the tank although a thermocline is not a prerequisite for this design to function.

Should the inlet temperature to the condenser exceed 372°K (210°F), the cooling water is employed to bring the temperature down within the specified limits. Because the cooling tower is located at the condenser inlet, it allows all flow to pass to the storage and maintain it full before any excess is dissipated.

The absorption air conditioner was sized for a 5.3×10^{10} Joule (173 ton) cooling load and a hot water temperature of 372°K (210°F) selected from the system study summarized in Section 2. The data presented in Table 3.7-1 was generated in identifying the AAC machine rating.

The water cooling tower recommended by Marley is their Model #8808 for either of the conditions above. This tower uses a 11.2 kW (15 hp) motor and has two 0.15 meter (6 in.) diameter inlets. There is a 2.7 meter (9 ft.) static lift from the base of the tower, and they recommend a 0.61 meter (2 ft.) elevation of the base above grade.

Further definition of the TUS is presented in Section 4. A preliminary equipment list is summarized in Table 3.7-2. Detailed design calculations of pressure drop, heat loss, and thermal capacity for the TUS will be conducted during Phase IV after finalization of the equipment in the Mechanical Equipment Area.

3.8 CONTROLS AND INSTRUMENTATION SUBSYSTEM (CIS)

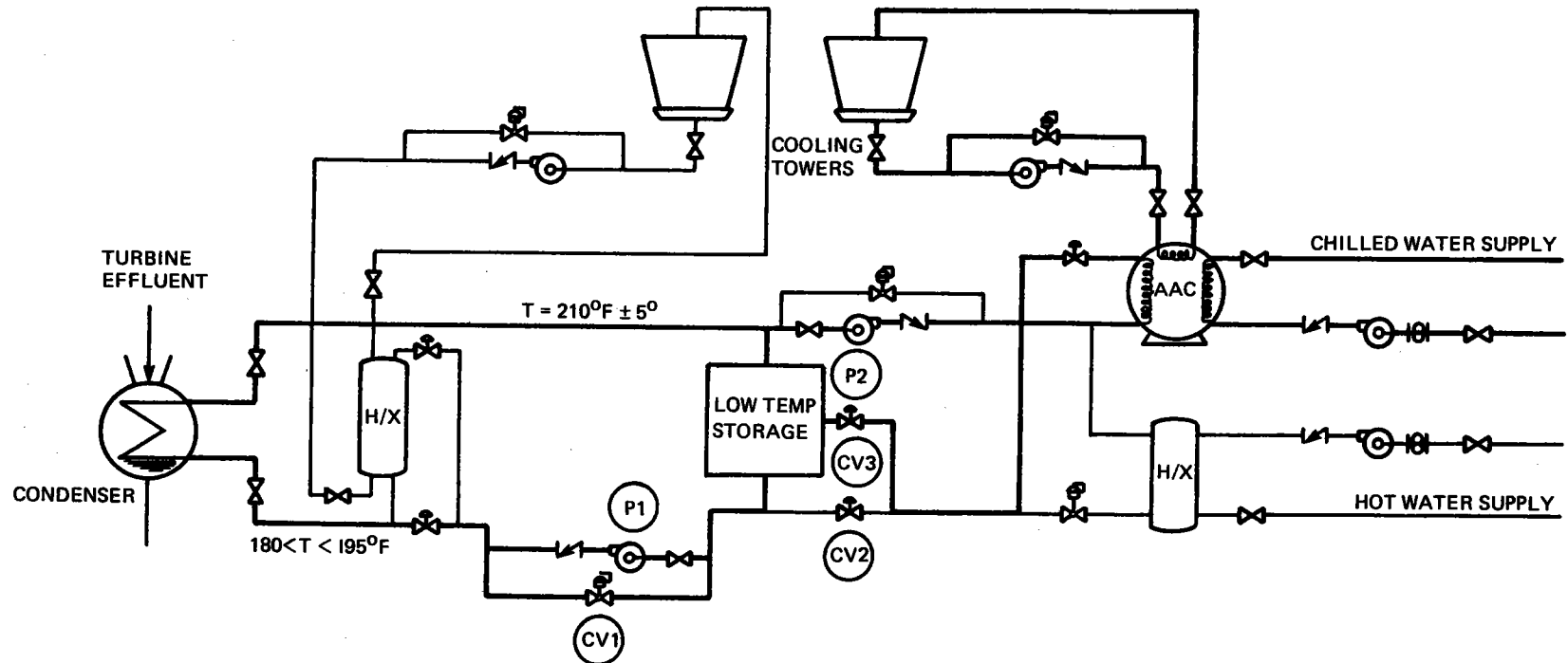
During the Preliminary Design Phase, CIS Development has been partitioned into four major areas:

1. Definition of subsystem requirements,
2. Definition of supervisory control concepts,
3. Definition of basic system architecture, and
4. Definition of software development approach.

Each of these topics is discussed in the following subsections.

The development of the CIS has had the following major design requirements:

1. Cost effectiveness
2. Incorporation of existing technology and technological implementation where feasible.
3. Reliability



NOTES: Valve CV1 controls pump P1 flow to maintain turbine exhaust pressure within setpoint limits. Pump P2 circulates hot water to the AAC; excess flow is passed through the storage tank. CV2 and CV3 are positioned to pass hot AAC return through the relatively cold tank thereby providing the condenser with the coldest available water and storing as much as possible in the tank.

Figure 3.7-2. Single Tank Thermal Utilization Subsystem Normal Operation/Storage Temperature Less Than ACC Return Temperature

Table 3.7-1. Single Stage Absorption Chiller Characteristics for Trane Unit

Characteristics Of The Concentrator and The Hot Water Circuits

Hot Water Flow

Entering Temperature	210	220	230	°F
Leaving Temperature	190	200	210	°F
Pressure drop	10.5	11.2	13.0	Ft. W.G.
Heat Source Correction Factor	.550	.680	.785	-
Load Ratio	.489	.489	.489	-
Heat Input to Concentrator	2.83	3.01	3.20	MBTU/HR

Characteristics of The Evaporator and The Chilled Water Circuit

Number of Ev. passes	5	→	-
Flow Correction Factor	1.055	→	-
Evaporator Capacity	210	→	Tons
Chilled Water Flow	407	→	GPM
Entering Temperature	55.2	→	°F
Leaving Temperature	45	→	°F

Characteristics of Condenser/Absorber and The Cooling Water Circuit

Condenser Operating Ratio	.82	→		
Cooling Water Flow Rate	900	→	GPM	
Temperature Rise Across Absorber and Condenser	10.9	11.3	11.7	°F
Pressure Drop	11.5	→	Ft. W.G.	
Total Heat Rejected to W.C.T.	4.91	5.09	5.28	MBTU/HR
Total Heat Rejected to W.C.T.	409	424	440	Tons
	327	339	352	

Overall System Characteristics

Refrigeration Load (Design Capacity)	173	→	Tons	
Trane Machine Designation	ABSC-03F	→	-	
Required Nominal Capacity	315	x	x	Tons
Nominal Rating	354	→	Tons	
Design Condition Correction Factor	1.02	→	-	
Available Capacity	199	246	283	Tons

Table 3.7-2. TUS Equipment List

HEAT EXCHANGERS	COOLING TOWERS	PUMPS
<p>Equip: A/C Cool. Tower Heat. Exch. - 1 Req'd. Equip. No.: Capacity: 238 GPM Size: 6' Dia. x 3'-0" Long Material: Vendor: American Standard #6-036 or equal</p> <p>Equip: Condenser Cool. Tower Heat Exch.: - 1 Req'd. Equip. No.: Capacity: 950 GPM Size: 1'0" dia. x 10'-0" Long Material: Vendor: American Standard #12-120 or equal</p> <p>Equip: Low Temp. Stor. Tank- 1 Req'd. Equip. No.: Capacity: 120,000 Gal. Size: 30' dia. x 23' high Material: Steel Vendor: RECO</p> <p>Equip: Absorpt. A/C Unit- 1 Req'd. Equip. No.: Capacity: 354 Tons Size: Material: Vendor: Trane or equal</p>	<p>Equip.: Condenser Cool. Tower- 1 Req'd. Equip. No.: Capacity: 600 Tons Size: 8615 Material: Vendor: Marley or Equal</p> <p>Equip.: A/C Cooling Tower - 1 Req'd. Equip. No.: Capacity: 200 Tons Size: 8603 Material: Vendor: Marley or equal</p>	<p>Pump: Low Temp. Storage Pump- 2 Req'd. Equip. No.: Capacity: 900 GPM @ 110 Ft. Head Size: 4 x 6 - 13L Material: Motor: 40 H.P. @ 1800 RPM Vendor: Gould Pump or Equal</p> <p>Pump: Condenser Cool. Tower Pump- 1 Req'd. Equip. No.: Capacity: 1700 GPM @ 40 Ft. Head Size: 6 x 8-13 Material: Motor: 25 H.P. @ 1800 RPM Vendor: Gould Pump or equal</p> <p>Pump: A/C Cool. Tower Pump- 1 Req'd. Equip. No.: Capacity: 900 GPM @ 50 Ft. Head Size: 4 x 6-10 Material: Motor: 20 H.P. @ 1800 RPM Vendor: Gould Pump or Equal</p> <p>Pump: Hot Water Pump Equip. No.: Capacity: 250 GPM Size: Material: Motor: 15 H.P. Vendor:</p>

8-194

4. Adequacy of control stability
5. Experimental flexibility
6. Maintainability

Although all decisions that have impacted the subsystem design have relied on the use of good engineering practices, past experience, proven capabilities, and consideration of the alternatives, a major subsystem tradeoff was performed and documented to define the most appropriate subsystem configuration. This tradeoff is addressed in Paragraph 3.8.2.1. The activities have been incorporated into the preliminary CIS Block Diagram (Figure 3.8-1).

3.8.1 SUBSYSTEM REQUIREMENTS

Preliminary subsystem requirements for the STE-LSE Shenandoah Control and Instrumentation Subsystem (CIS) were defined during Phase III, The Preliminary Design Phase. Based upon overall system operational requirements, CIS requirements were established for each of the major STE-LSE subsystems and for the data archiving function. Subsystem control requirements were developed according to control functions to be performed and the primary control modes under which these functions would be executed. Data archiving requirements were prepared from a preliminary sizing of the STE-LSE system in terms of parameters to be monitored and recording rate.

Figure 3.8.2 presents a summary of the CIS preliminary design requirements in block diagram form. The instrumentation and data acquisition requirement applies to all subsystems. Each subsystem is treated individually in the following sections.

3.8.1.1 Collector Field Subsystem (CFS) Control Requirements

Tracking control and field temperature control are required to provide effective control of the CIS. The CIS is responsible for providing automatic closed-loop tracking of the sun in both the polar and declination axes of each collector. The preliminary design effort summarized in Paragraph 3.2.6 resulted in definition of a tracking scheme with both coarse and fine position control. Coarse positioning is performed by the CIS central computer which is required to position each collector to within $+1^\circ$ of the sun. Fine positioning will then be achieved by the four optical tracking sensors mounted on the receiver aperture. The sensors will position each collector to within $+0.25^\circ$ of the sun. In addition to the above pointing accuracy requirements, the CIS computer will be responsible for maximizing collector performance by factoring into its positioning algorithms adjustments for cloud cover, shadowing effects, and other related conditions. The tracking control must also provide defocus and stow capabilities. The CIS will include instrumentation for monitoring all tracking control elements and making the necessary provisions for acquiring performance data from all CIS instrumentation and transferring this data to the CIS central computer.

The CIS is required to provide field temperature control by maintaining fluid temperature at 672^{+0}_{-14} °K (750^{+0}_{-25} °F). Collector overtemperature conditions must be avoided, and the alarm set point for each collector will be 675 °K (755 °F). If no other action is taken, automatic defocus will occur when a collector reaches 677 °K (760 °F). Fluid temperature will be maximized on a branch basis, with the number of collectors per branch ranging from five to eleven. Fluid temperature variations will be minimized by computer algorithm adjustments for conditions such as intrabranch shadowing or cloud cover. The CIS will also be responsible for field temperature control instrumentation and data acquisition.

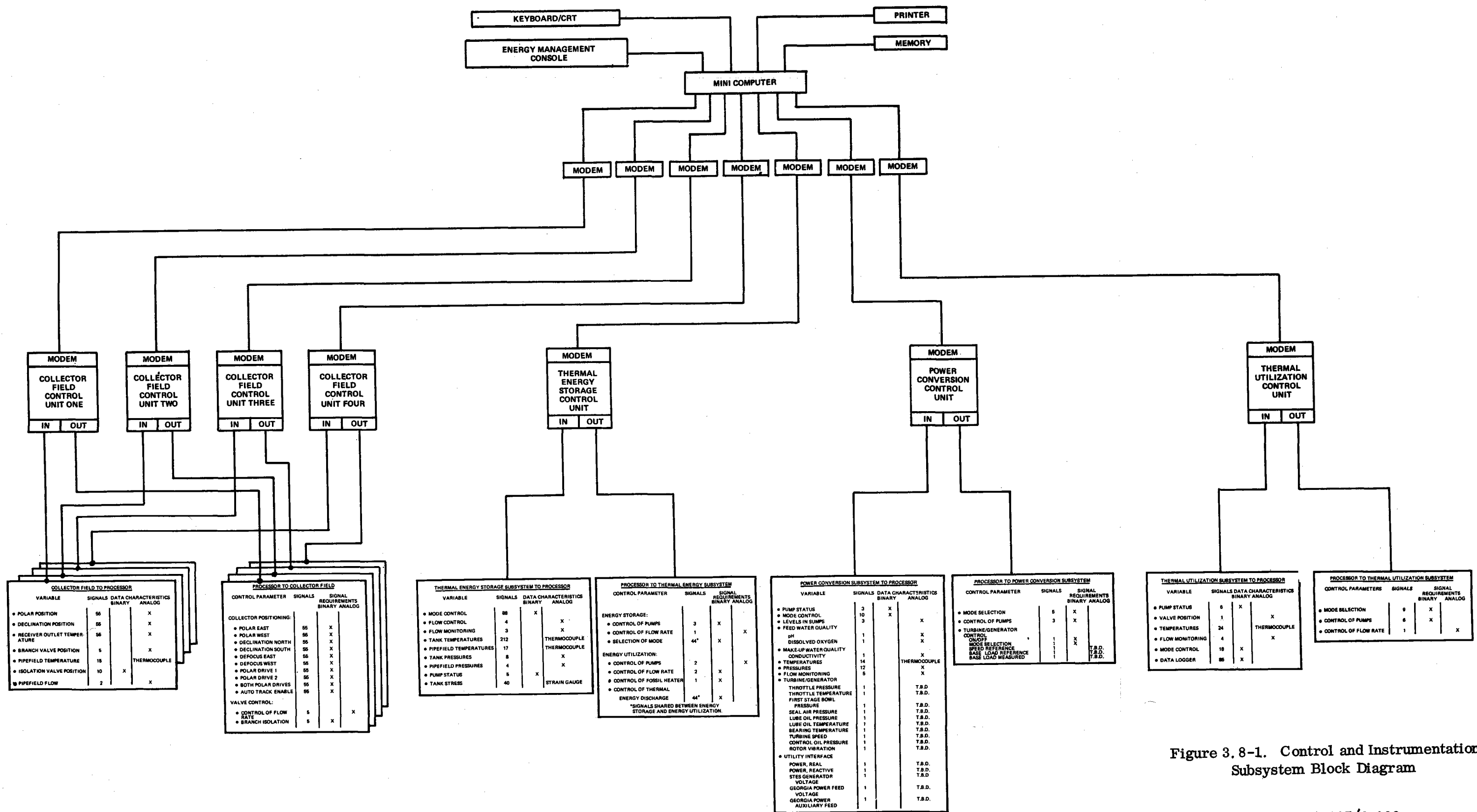


Figure 3.8-1. Control and Instrumentation Subsystem Block Diagram

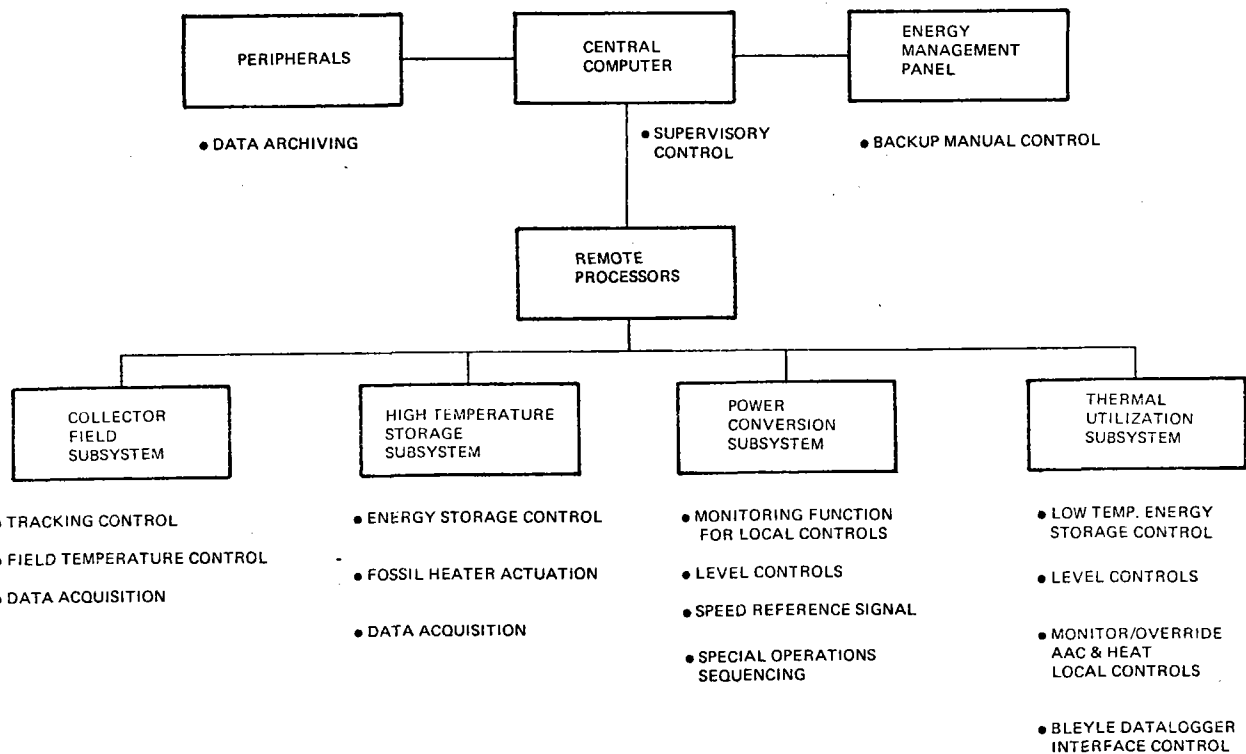


Figure 3.8-2. CIS Preliminary Design Requirements

Preliminary control modes were identified in conjunction with the above requirements to provide an indication of the various conditions under which control would be executed. They represent a preliminary estimate only, and their development will be coordinated with the development of the System Operating Plan. These CIS control modes include the following:

- Startup
- Normal
- Computer Track
- Re-start
- Shutdown
- Maintenance
- Calibration
- Degraded
- TES Charge
- Emergency

3.8.1.2 High Temperature Storage Subsystem (HTS) Control Requirements

Based upon system operational requirements, preliminary control functions were defined for CIS control of the HTS. The CIS must be capable of controlling tank charging and discharging for each of the four HTS tanks. This primarily involves valve control. The CIS will be required to determine tank status which involves monitoring tank temperatures, pressures, and levels. When necessary, the CIS will actuate the fossil-fired heater to augment or replace the solar energy supply.

Series tank transfer is another control responsibility of the CIS. This is primarily a valve control function. This task also involves portions of the tank charge/discharge and tank status functions described above.

As in all STE-LSE subsystems, the CIS will have functional control of HTS instrumentation and data acquisition. The preliminary control modes identified for CIS control of the HTS are listed below.

- Charge Tank 1 (1-hr)
- Charge Tank 2
- Charge Tank 3
- Charge Tank 4
- Discharge Tank 1
- Discharge Tank 2
- Discharge Tank 3
- Discharge Tank 4
- Trickle
- Dual Media
- Series Transfer
- Field Warmup
- Field On/Off
- Field Flow to Boiler
- Field Throttled
- Inversion
- Fossil-Fired Heater
- Fossil on Standby
- Fossil-to-Solar Transition
- Fossil Shutdown
- System Charged/Standby
- Maintenance
- Emergency

3.8.1.3 Power Conversion Subsystem (PCS) Control Requirements

Since many of the components in the PCS will have their own local automatic controls, the majority of requirements for the CIS become monitor functions rather than control functions. Two particular control functions of major significance include turbine-generator synchronization control and utility base load control. Monitoring requirements of the PCS by the CIS include:

1. Boiler-turbine control
2. Process steam temperature/pressure control
3. Condenser pressure level control
4. Condensate and deaerator storage level controls
5. Chemical injection control
6. Electrical subsystem.

In addition to the turbine-generator synchronization and base load control functions, the CIS will be responsible for sequencing PCS operations. Such sequencing will typically involve configurations of component local controls. Demineralizer regeneration is an example of a sequence to be controlled by the CIS.

PCS instrumentation and data acquisition is another functional control requirement of the CIS. Preliminary CIS control modes for PCS monitoring and control were identified and are listed as follows:

- Startup
- Turbine Bypass
- Normal
- Shutdown
- Interconnected
- Stand-Alone
- Maintenance
- Emergency

3.8.1.4 Thermal Utilization Subsystem (TUS) Control Requirements

Functional control requirements for the TUS have been divided into three segments: monitor/override functions, process control functions, and a Bleyle interface function. As in the PCS, the major components of the TUS - the absorption air conditioner and the space heating system - are characterized by automatic local controls. As a result, the CIS will primarily be responsible for monitoring the air conditioning and space heating performance. In addition, the CIS will provide override capability for both either automatically through the CIS computer keyboard or manually via the energy management panel (see Paragraph 3.8.4.3).

Process control requirements for the CIS include cooling tower and heat exchanger control. The CIS will also provide tank charge/discharge control for the Low Temperature Energy Storage (LTES) tank and determine tank status. These functions are very similar to those discussed in Paragraph 3.8.1.2 for the HTS. The preliminary CIS design is capable of interfacing with the Doric Digitrend data logger now being used in the Bleyle plant. The TUS instrumentation and data acquisition functional control requirement also applies to the CIS. Preliminary CIS control modes for the TUS include:

- Air Conditioning Demand
- Heating Demand
- LTES Tank Charge
- LTES Tank Discharge
- LTES Tank Charged/Standby
- Cooling Tower On/Off
- Heat Exchanger On/Off
- Startup
- Shutdown
- Maintenance
- Emergency

3.8.1.5 Data Archiving Requirements

The initial definition of data archiving requirements was based upon a preliminary instrumentation list that identified parameters to be measured according to subsystem. The total number of measurements based upon this estimate was 788. From these total measurements, a baseline operational data set was established. This baseline set includes all measurements which must be acquired under any system condition. These 297 measurements meet one or both of two criteria. First, they are essential to maintaining a safe operating system. Second, they are required for evaluating overall system and subsystem performance. As a result, this baseline operational data set serves as the preliminary minimum data archiving requirement. The operational data set is recorded continuously at fifteen minute intervals and has been summarized according to major subsystem and type of measurement in Table 3.8-1. A detailed listing is shown in Table 3.8-2.

In addition to data quantity and recording rate requirements, data format and data storage requirements were addressed. Several candidate format styles were identified:

1. Single total system record
2. Separate subsystem records
3. Single standard structure
4. Special structures for operations, test, experiments, etc.
5. Fixed format
6. Reprogrammable format
7. Binary form
8. ASCII form.

Table 3.8-1. Baseline Operational Data Set Summary

SCS (includes CFS, TES, SGS)	PCS (Includes ES)
4 Insolation	5 Flow
3 Flow	13 Pressure
12 Pressure	4 Level
4 Level	14 Temperature
42 Temperature	8 Valve
<u>40</u> Valve (Discrete)	<u>20</u> Electrical
105	64
TUS (Includes Bleyle)	Weather
12 Flow	6 Insolation
2 Pressure	2 Wind
72 Temperature	1 Pressure
6 Valve	1 Temperature
28 Electrical	<u>1</u> Humidity
<u>8</u> Humidity	11
117	
Total Measurements: 297	

Three data storage candidates emerged from the Preliminary Design Phase: disc, 9-track magnetic tape, and magnetic cassette tape. A specific format and storage medium will be selected based on trade studies to be performed during the next phase.

3.8.2 CONTROL SYSTEM COMPUTER ARCHITECTURE TRADE-OFF

All estimates included in this section - costs, number of signals, sampling rates - are based upon data that was available early in Phase III when this tradeoff was performed.

3.8.2.1 Architecture Candidates

Since the Solar Total Energy System is, by definition, an experimental system, it is mandatory that the control subsystem have the flexibility to handle system modifications. Typical modifications almost always result in increased demands on the control subsystem and are often implemented in the field. It is therefore necessary that the control system have reserve capacity and be easily modified. These requirements preclude the use of special analog control devices and most programmable controllers. The obvious choice for a control subsystem is digital computers which can be purchased initially with reserve capacity or easily expanded in the field and are easily modified in their operation through software changes.

Table 3.8-2. Operational Data Set Details

Subsystem	Measurement	Number of Measurements / Location		
Collector Field	Insolation	4 pyroheliometers		
	Flow	1 Collector Field Supply Line		
	Pressure	1 Collector Field Supply Pump Inlet		
		1 Collector Field Supply Pump Outlet		
	Temperature	1 Collector Field Outlet (to TES)		
		1 Collector Field Inlet		
		1 Collector Field Outlet		
		20 Branch Outlets (averages)		
		Thermal Energy Storage	Pressure	4 Tanks (top)
			Level	4 Tank Storage
Temperature	4 Tank Inlet			
	4 Tank Outlet			
Steam Generator Supply	Valve	4 Tank Pump		
		1 Return Line (to CFS)		
		1 Supply Line (to SGS)		
		40 Tank Valves (On/Off - mode determination)		
	Flow	1 Syltherm Line		
		1 Fossil Heater Natural Gas		
	Pressure	1 SGS Supply Pump Inlet		
		1 SGS Supply Pump Outlet		
		1 Fossil Heater Booster Pump Inlet		
		1 Fossil Heater Booster Pump Outlet		
Temperature	1 Steam Generator Outlet (Syltherm Side)			
	1 Fossil Heater Inlet			
	1 Fossil Heater Outlet			
	1 Steam Generator Inlet			
	1 Steam Generator Outlet			
	1 Steam Generator Intermediate			
Power Conversion	Flow	1 Steam Generator Inlet		
		1 Steam Generator Outlet		
		1 Total Extraction (Turbine)		
		1 Process Steam (to Bleyle)		
		1 Condenser (Turbine bypass)		
		Pressure	1 Steam Generator Inlet	
			1 Steam Generator Outlet	
			1 Turbine Inlet (Throttle)	
			1 Turbine Extraction	
			1 Turbine Exhaust	
	1 1st Turbine			
	1 Condenser Feed (turbine bypass)			
	1 Condenser (to condensate storage)			
	1 Deaerator Tank			
	1 Process Steam (to Bleyle)			
	1 Bleyle Steam Interface			
	Level	1 Second Turbine		
		1 Steam Generator (intermediate)		
		1 Steam Generator Boiler		
		1 Deaerator Tank		
		1 Condenser		
		1 Condensate Storage Tank		
		1 Preheater Inlet		
		1 Preheater Outlet		
		1 Superheater Outlet		
		1 Turbine Throttle		
	Temperature	1 Turbine Extraction		
		1 Turbine Exhaust		
		1 Turbine Desuperheater		
		1 Condenser (turbine bypass)		
		1 Condenser (to condensate storage)		
		1 Condensate Storage Tank		
		1 Make-Up Water		
		1 Process Steam (to Bleyle)		
		1 Bleyle Steam Interface		
8 Valve Positions				
1 Turbine Speed				
Electrical Subsystem (ES)	Frequency	1 Alternator Speed		
	Power	4 Real		
		4 Reactive		
	Voltage	1 STES Generator		
		1 GPC Feed		
		1 Aux. GPC Feed		
	Position	1 Aux. STES Feed		
		6 Discretes (TBD)		
		- mode selection		
		- breaker position		
Thermal Utilization Subsystem (TUS)	Flow	- synchronization		
		1 Chilled Water Supply		
		1 Hot Water Supply		
	Pressure	1 TUS Delivery Flow (to AAC or HX)		
		1 Condenser Return		
		1 Low Temperature Storage Tank		
		1 Condenser Inlet		
		1 Condenser Outlet		
		1 Storage Tank Inlet		
		1 Storage Tank Outlet		
		9 Storage Tank Profile		
		1 AAC Inlet		
		1 AAC Outlet		
		1 Chilled Water Inlet Interface		
		1 Chilled Water Outlet Interface		
		1 Hot Water Inlet Interface		
		1 Hot Water Outlet Interface		
		4 Bleyle Heating HX		
		4 Condenser Cooling Tower HX		
		1 AAC Condenser Inlet		
1 AAC Condenser Outlet				
1 AAC Evaporator Inlet				
1 AAC Evaporator Outlet				
Bleyle Plant	Flow	8		
	Pressure	1		
	Temperature	41		
	Humidity	8		
	Electrical	28		
Weather	Insolation	4 Pyroheliometers		
	Temperature	2 Pyranometers		
		1 (dry bulb)		
		1 (barometric)		
		1 (relative)		
		1 Velocity		
		1 Direction		

Given that digital computers are the most appropriate choice for the control system, there are many possible architectures to be considered. One such example is shown in Figure 3.8-3. This is an example of a star network consisting of a number of satellite microcomputers, each communicating only with a central minicomputer. Another example shown in Figure 3.8-4 is a centralized system consisting of only one large computer which handles all processing. Other architectures exist, e.g., rings and hierarchical trees, which are basically distributed systems allowing for increased communications between the satellite computers. These structures are shown in Figure 3.8-5.

The STES is a highly modularized system consisting of four major subsystems: solar collection, thermal energy storage, power conversion, and thermal utilization. These subsystems operate highly independently and, except for the interfaces between the subsystems, have little need to communicate with each other. Thus, the complexity of a ring or tree control system architecture is not warranted. Therefore, the trade-offs which were performed and are described in the following subsections consider only the star distributed system and the centralized system.

3.8.2.2 Distributed System

A distributed system of the type shown in Figure 3.8-3 has been proposed as the STES control system; a preliminary hardware selection (Reference 3.8-2) has resulted in a choice of the Digital Equipment Corporation (DEC) LSI-11 for the microcomputers and the PDP-11/34 for the central minicomputer. In estimating the cost for this system, certain assumptions must be made concerning processing rates and computer sizing. These assumptions are discussed below. Note that in estimating costs, only those components which differ between a distributed and centralized system are considered. Components which are common to both, such as the data input devices, storage peripherals, etc., are not considered.

3.8.2.2.1 Processing Rates

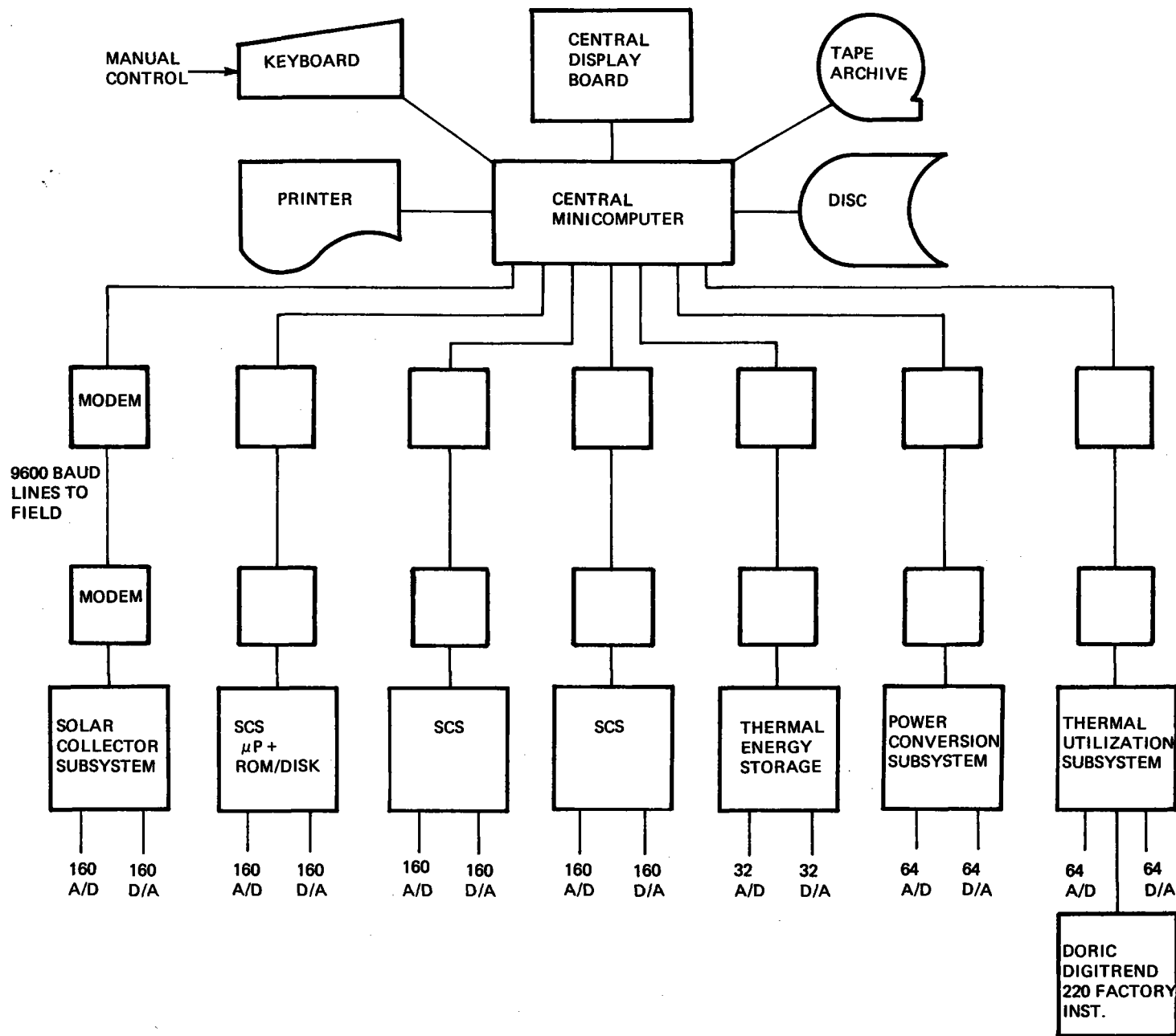
Clearly, the greatest processing load imposed on the control system is by the Collector Field Subsystem (CFS). There are 192 collectors which must be checked regularly for position and for collector temperature. To reduce the processing requirements on the CFS microcomputer and to enhance fault tolerance, this function has been distributed over four microcomputers, each one handling one fourth of the field. If the assumption is made that the tracking and field temperature control functions require about 1000 equivalent adds per collector sampled on the order of two times per second, then each CFS microcomputer will incur a processing load of

$$1000 \frac{\text{adds}}{\text{collector}} \times \frac{192}{4} \text{ collectors} \times \frac{2 \text{ samples}}{\text{second}} \approx 10^5 \frac{\text{adds}}{\text{seconds}}$$

This allows a time of 10 μsec per add which is well within the capabilities of an LSI-11. Processing rates for the remaining STE-LSE subsystems are expected to be considerably less than these and are therefore not explicitly estimated here. This is also true of the supervisory central minicomputer.

3.8.2.2.2 Computer Sizing

The LSI-11 computer is capable of supporting a maximum of 32 words of memory divided in any way between Random Access Memory (RAM) and Read Only Memory (ROM). The most appropriate operating system under which to operate these micros is the memory resident RSX-11S. This operating system in a typical configuration requires about six words of memory, leaving 26 words for user tasks. This appears to be a reasonable estimate for the sizes of the individual user tasks, keeping in mind that the maximum size for a single user task is 32 words.



8-206

Figure 3.8-3. Distributed Control System Computer Architecture

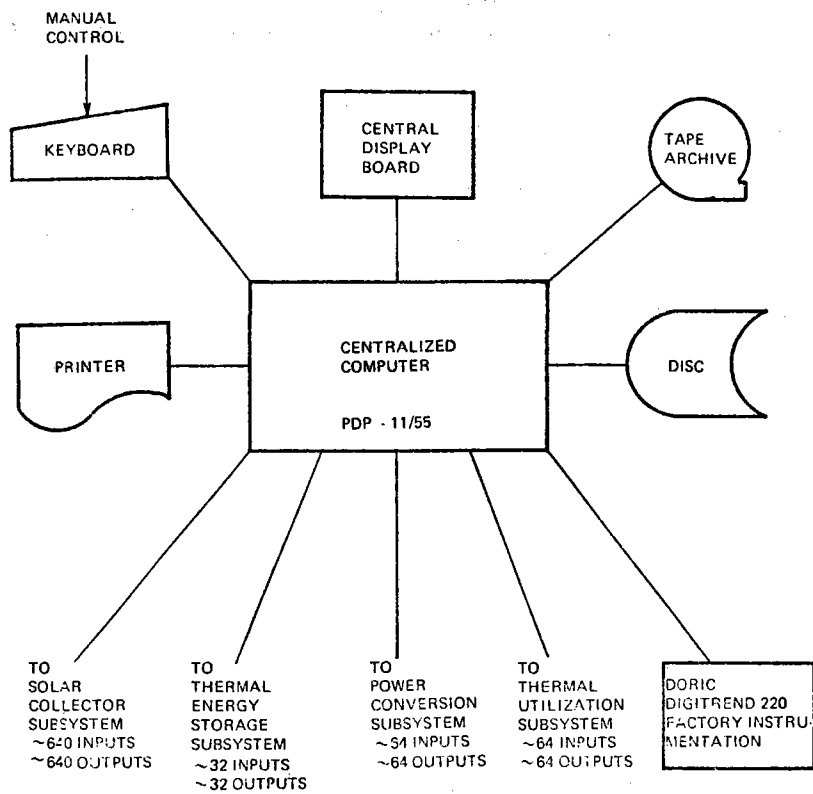


Figure 3.8-4. Centralized Control System Architecture

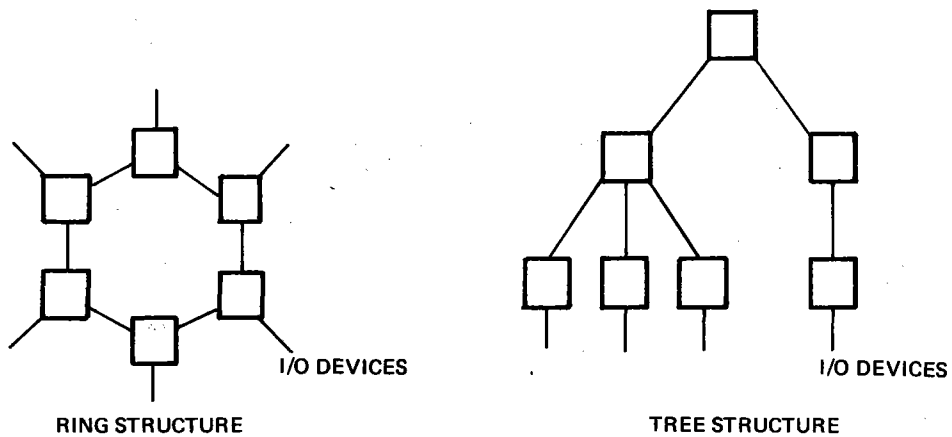


Figure 3.8-5. Typical Alternate Computer Architectures

The central minicomputer must be capable of supporting software development in addition to its processing requirements. Typical memory size for a PDP-11/34 on which development and processing is to be performed is 64 words.

3.8.2.2.3 Computer Cost

Estimated costs for the LSI-11 are derived as follows:

LSI-11 processor w/4K word RAM	990
Extended arithmetic unit	190
16K word RAM	1250
4 ea. PROM memory units	700
24 ea. EPROM memory chips (Intel chips, @ \$14/512 words)	288
2 ea. Modems	300
DL-11 communications interface	250
	<hr/>
	\$4000

Similarly, the PDP-11/34 costs are estimated as follows:

11/34 processor w/32K word RAM	10970
Floating Point Processor	4900
32K word RAM	5100
7 ea. DL-11 communications interface	5390
	<hr/>
	\$26360

The resulting total estimated cost for the distributed system is:

PDP-11/34 system	26360
7 ea. LSI-11 @ 4000	28000
	<hr/>
Total Cost - Distributed System	\$54360

3.8.2.3 Centralized System

In a centralized system, the single computer must be capable of performing all of the functions allocated to the satellite computers in the distributed system. The analysis of processing rates and size estimates are similar to those performed for the distributed system.

3.8.2.3.1 Processing Rates

As before, the maximum processing load is incurred in controlling the collector field. Using the estimate of 1000 equivalent adds per collector for tracking and field temperature control, the overall processing rate for the collector field is

$$\frac{1000 \text{ adds}}{\text{collectors}} \times 192 \text{ collectors} \times \frac{2 \text{ samples}}{\text{second}} \approx 4 \times 10^5 \frac{\text{adds}}{\text{seconds.}}$$

To this must be added the processing of all other subsystems, which is (conservatively) estimated to be an additional 10^5 adds/second, for a total of 5×10^5 adds/second. This allows a time of 2 μ sec/add which is slightly beyond the capability of an 11/34 computer (2.03 μ sec/add). Although the software might be speeded up enough to run on an 11/34, there would be essentially no capacity for expansion (and no tolerance for inaccurate estimates). It is therefore necessary to propose a somewhat faster computer. The least expensive DEC computer with the required speed is the PDP-11/55 with an add time of 0.97 μ sec using the inexpensive core memory and 0.30 μ sec using the much more expensive bipolar memory. (A DEC computer is specified for all the reasons cited in the previously referenced hardware selection Reference 3.8-2.)

3.8.2.3.2 Computer Sizing

The single computer must be capable of simultaneously storing all of the software resident in each of the micros in the distributed system, with the exception that only one copy of the CFS software is required as opposed to four in the distributed system. Memory economies could be obtained using swapping techniques, but the processing rates preclude this. The resulting memory size is therefore 4 x 28K words for the subsystem control tasks plus 64K words for the supervisory tasks and operating system for a total of 176K words. This is beyond the maximum memory limitation of the 11/55 of 128K words, but for the purpose of this tradeoff, let it be assumed that, by consolidating all of the software into one computer, sufficient economies can be realized to reduce the required memory size to the allowable 128K words (if this is not possible, then it will be necessary to propose an even more expensive system, such as the PDP-11/70).

3.8.2.3.3 Computer Cost

Estimated costs for the required 11/55 system are as follows:

11/55 processor w/16K word core and 16K word bipolar	44,100
Expander Chassis	2,420
Floating Point Processor	5,600
96K word core memory	25,300
Total Cost - Centralized System	<hr/> \$77,420
(Total Cost - Distributed System	\$54,360)

3.8.2.4 Architecture Trade-Offs And Selection

From the foregoing cost estimates, it can be seen that a savings of approximately \$23,000 can be realized from implementing a distributed control system as compared to centralized system. In addition to initial hardware costs, there are several other more qualitative advantages discussed below which led to the selection of a distributed system for the Shenandoah LSE.

3.8.2.4.1 Software Modularity

Modular, structured software has been recognized as an essential ingredient in the development of an efficient, maintainable system. A distributed system enforces this modularity while there is often a temptation in a centralized system to permit the modular structure to breakdown by merging software functions.

3.8.2.4.2 Hardware Modularity

By assigning specific functions to hardware modules, the overall system is more flexible in meeting the demands of modified systems; e.g., if more collectors are to be incorporated, an additional micro-computer can be attached. Conversely, if a future system is to use fewer collectors, one or more micros can be eliminated with a commensurate cost savings. A centralized system will have more difficulty in meeting the needs for expansion, particularly if the maximum memory limit has been reached, which appears to be the case with this system.

3.8.2.4.3 Fault Tolerance

By distributing the system control functions among a number of microcomputers, the overall STES is more immune to a failure of part of the system. For example, if one of the four CFS micros fails, the STES can continue to operate with 75 percent of the field. In a centralized system, if the one computer malfunctions, the whole system will cease to function. This also affects the spares inventory philosophy since it is economically quite reasonable to stock a complete spare microcomputer but obviously impractical to stock a spare minicomputer. This allows for more rapid repair of a malfunctioning system.

3.2.4.4 Sensor Wiring

Another cost factor in the STES control subsystem is the wiring of the various sensors (thermocouples, flow meters, etc.) to the computer. By using a distributed system, each micro can be placed closer to the sensors feeding it, greatly reducing the wiring costs. Of course, the wiring of the individual micros to the central processor must be considered, but this is only a single serial line for each micro as compared to hundreds of sensor leads.

3.8.3 SYSTEM ARCHITECTURAL DESCRIPTION

During the Preliminary Design Phase, the STE-LSE system design has matured to the point that detailed CIS requirements have been defined. Based on these functional requirements, a basic CIS architecture has evolved which provides for the control of the STE-LSE components. The top level architectural definition has been addressed in Paragraph 3.8.2. The impact of the system requirements (Paragraph 3.8.1) is reflected in the top level CIS block diagram (Figure 3.8-1). This diagram summarizes the basic system variables which are used to define the status of the STE-LSE on a subsystem basis as well as categorizes the control which is exercised over these elements, subsystem by subsystem.

In order to develop the second-level CIS Block Diagrams, a basic design philosophy has been to standardize the remote processors to as great a degree as possible. This effort has resulted in a remote processor architecture.

3.8.3.1 Remote Processor Basic Architecture

Using the system requirements (Paragraph 3.8.1) as a data base, types of transducers and controls have been defined for the CIS. The types of transducers have delineated the input requirements for all the remote processors, whereas the types of controls have provided the output requirements for all the remote processors. By reference to the computer trade-off (Paragraph 3.8.2), the communication requirement has been defined between any remote processor and the minicomputer. The input requirements, output requirements, and communication requirements describe the input/output (I/O) requirements for all of the remote processors. Based on the CIS I/O requirements, a remote processor basic architectural configuration has been designed which will meet the needs of any of the seven remote processors. The block diagram of this design is included as Figure 3.8-6.

In considering the cost impact of such an approach, it is advantageous to minimize both non-recurring (i.e., design) costs as well as recurring (hardware, etc.) costs. This leads to the approach of designing a single remote processor with capability to serve the needs of each of the seven (one design versus seven). Functional standardization and partitioning is thus addressed based on CIS requirements rather than on individual subsystem requirements as a tool to encourage the minimization of similar functional modules. Data Processing within the remote processor utilizes TTL (Transistor Transistor Logic) which is (from a reliability standpoint) one of the most fully documented logic families available.

Since a significant number of transducers and control devices have characteristics similar or identical to those which have been used in other control systems, it is possible to incorporate existing circuit boards into the STES control system. The present state of design of the CIS identifies fourteen circuit board functions, ten of which are currently available either from in-house fabrication or from commercial houses. These circuits not only reduce design and fabrication time but also are supported by performance characteristics with regard to service life and maintenance requirements.

3.8.3.2. Second Level Block Diagrams

Drawing upon the remote processor basic architecture as further defined by individual subsystem control requirements, the second level block diagrams have been generated which not only define the functional block requirements (a subset of the remote processor basic architecture) but also summarize the I/O general specifications based on the present STE-LSE design maturity. These I/O requirements are defined as to number of signals and electrical characteristics in as much detail as is presently known. These are shown in Figures 3.8-7 through 3.8-10.

The TUS second level block diagram includes the Bleyle data logger I/O interface which is preliminary and is based on a conventional parallel data transfer protocol. This same parallel data bus technique (no hand shake or communications protocols) is being utilized to service the 192 collectors in the collector field (CFS). This approach has been consistent with cost objectives as they apply to the dedicated wiring associated with collector positioning controls. Conceptually, dedicated four line parallel hexadecimal busses will be connected to each collector over which computer-generated command words will be sent to position the collector either via the suntrackers (local control with computer monitor) or by computer-generated positioning commands.

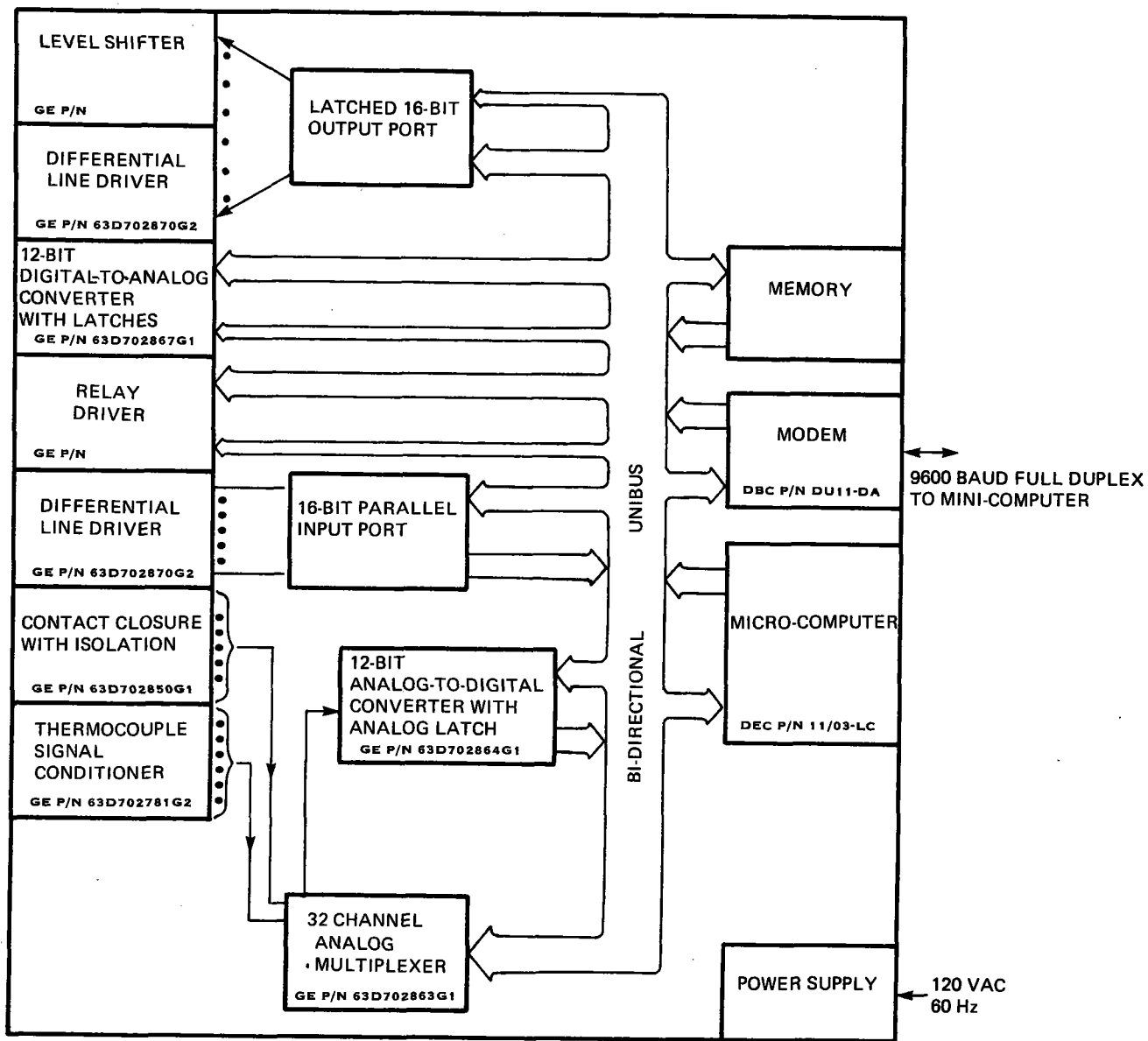


Figure 3.8-6. Remote Processor Design Architecture

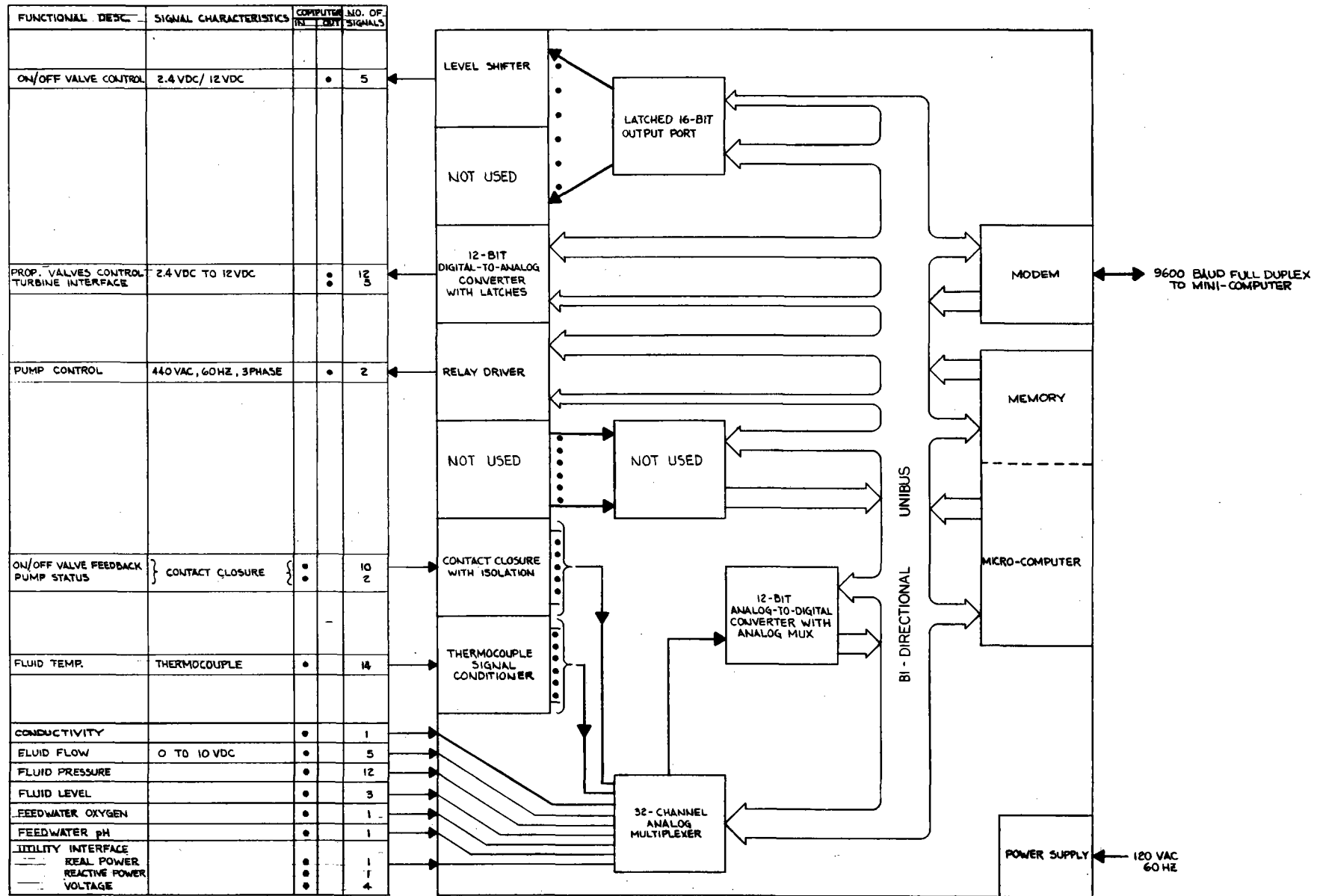


Figure 3.8-7. PCS Second Level Block Diagram

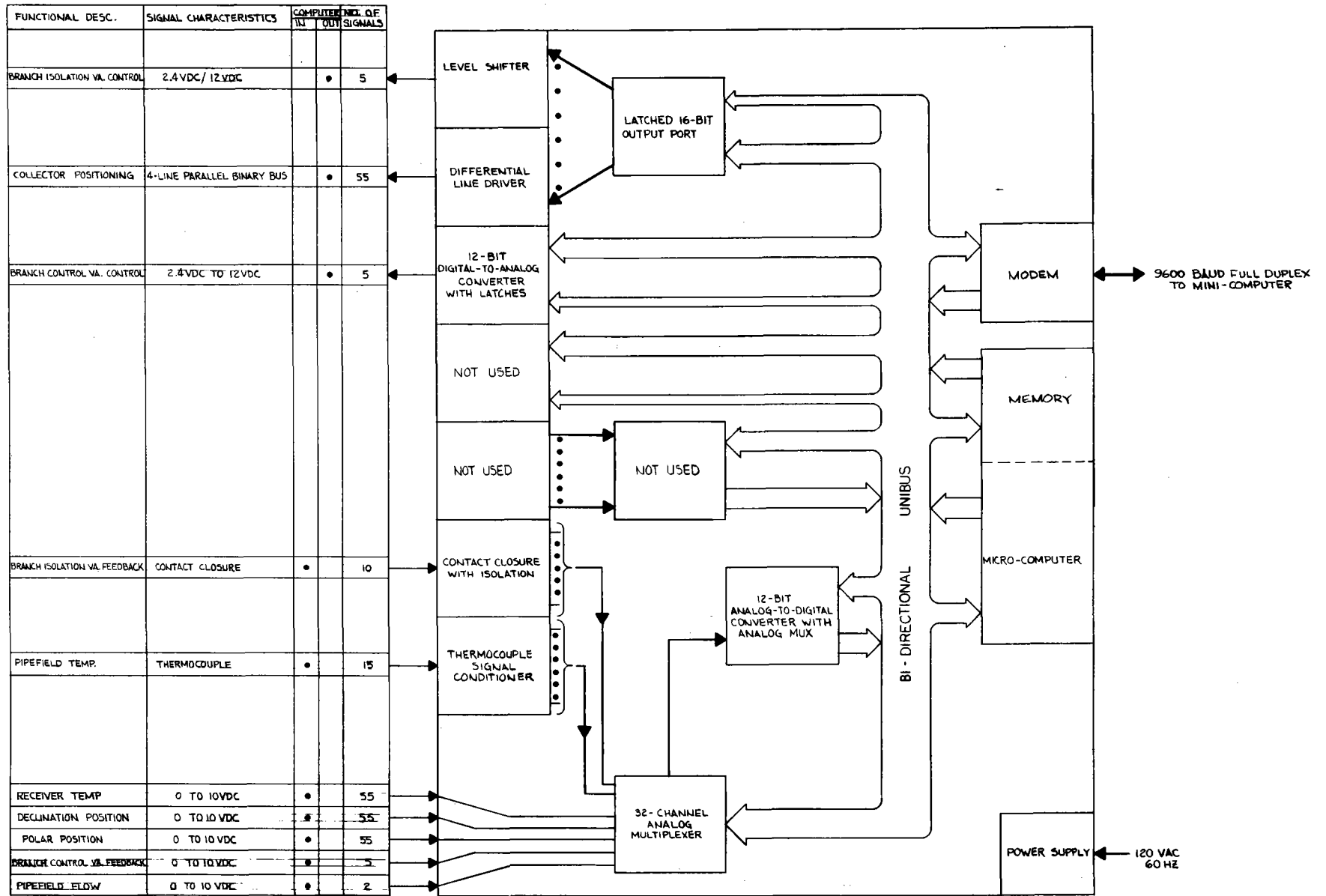


Figure 3.8-8. Collector Field Second Level Block Diagram

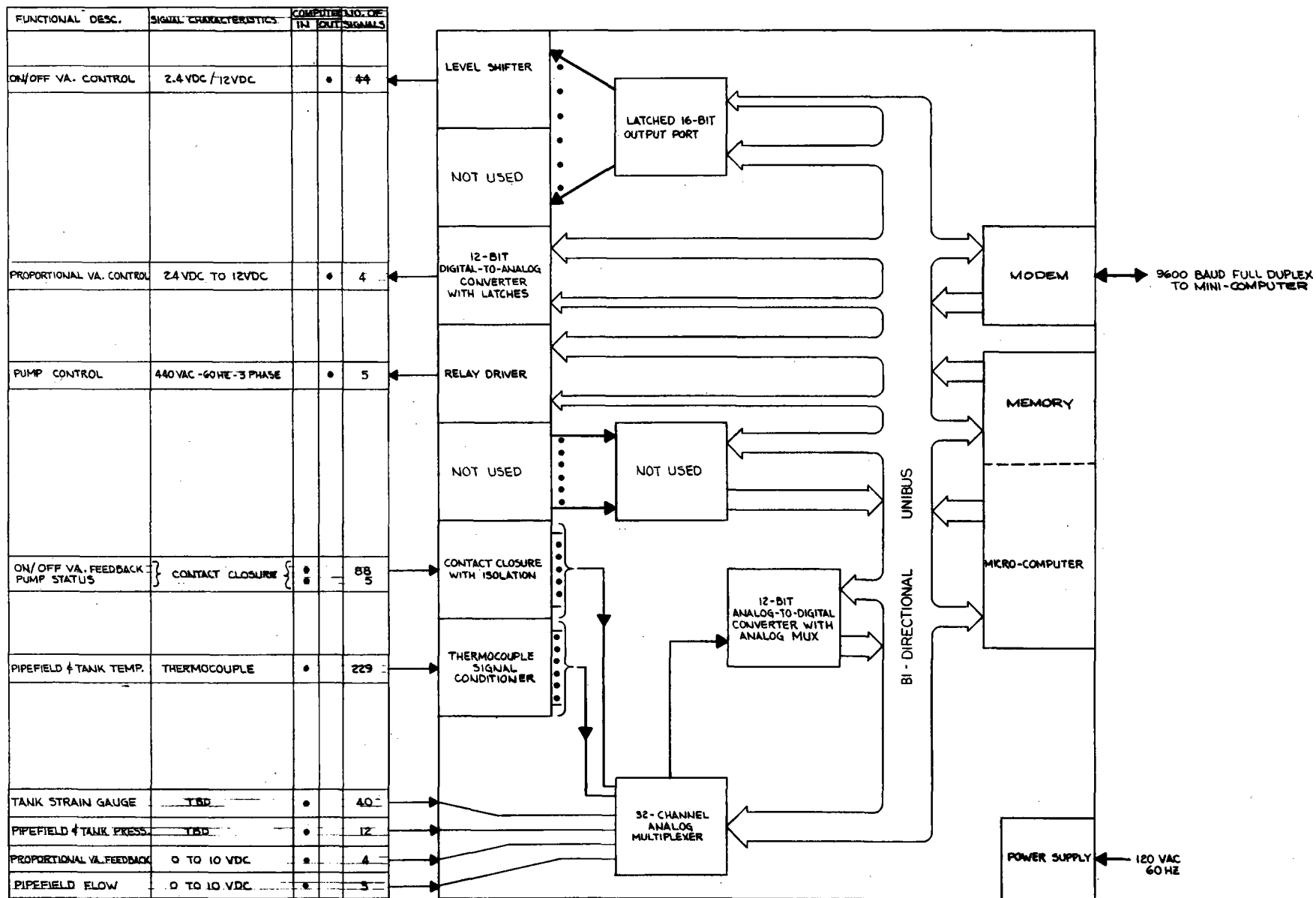


Figure 3.8-9. HTS Second Level Block Diagram

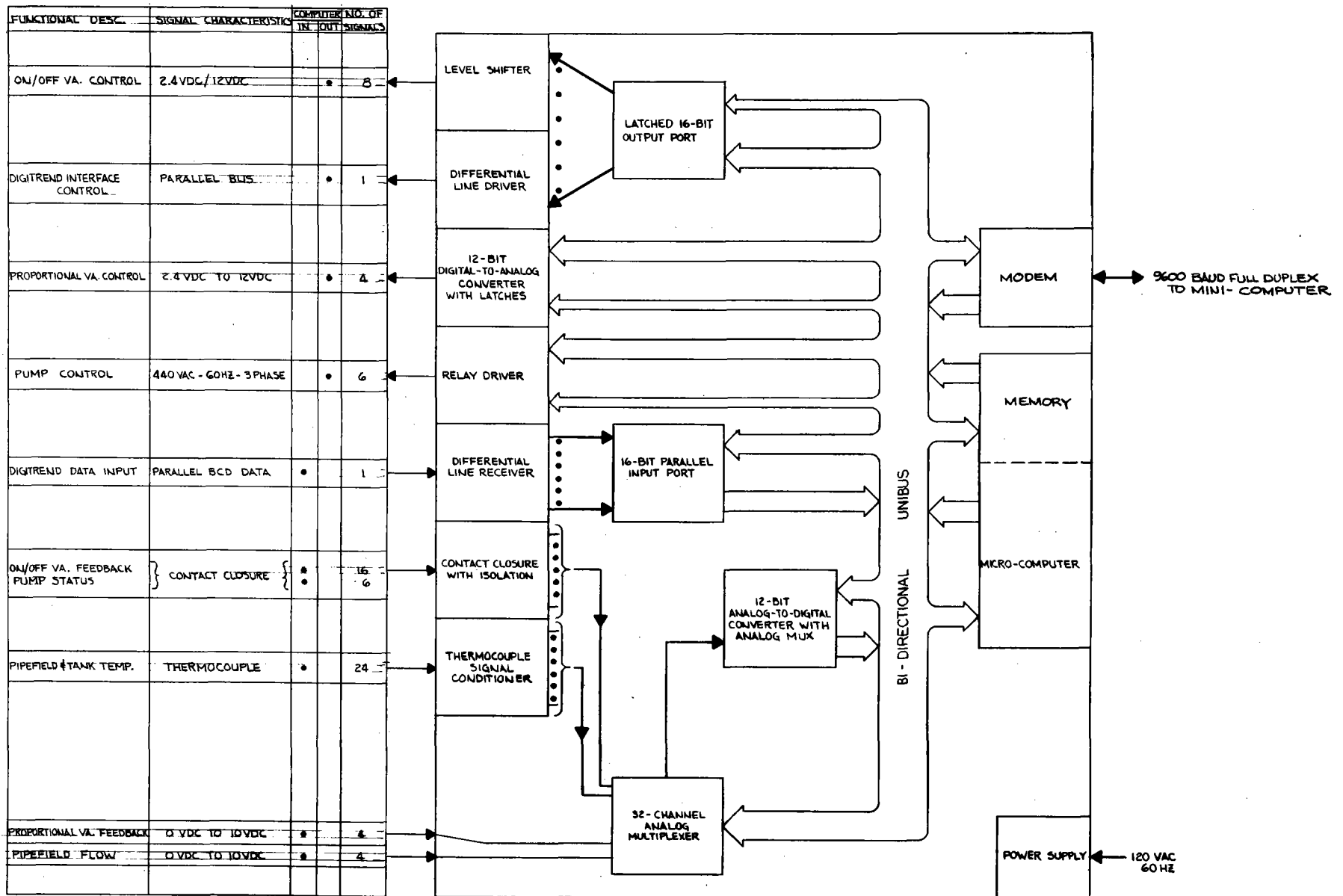


Figure 3.8-10. TUS Second Level Block Diagram

3.8.3.3 Preliminary Equipment List

The control room equipment is included in Table 3.8-3. It is anticipated that this list may be materially modified when the requirements for the energy management panel have been finalized.

The control room equipment is the hub of the CIS. Processing, formatting and maintaining the data archive, supervising the operational characteristics of the remote processors, providing human intervention, and providing data regarding performance and operating status in a real time fashion are all supported by the minicomputer and its associated peripherals.

Based on the STE-LSE design maturity in combination with the computer configuration trade-off discussed above, the majority of items in Table 3.8-3 are identified as buy items. When final requirements for the CIS have been identified, the make/buy decision will be reviewed to verify the desirability of such a decision.

Table 3.8-3. Central Control And Computer Complex Equipment List

ITEM NO.	QUANTITY	ITEM DESCRIPTION	DRAWING/PART NO.	BUY	MAKE	DESIGN STATUS
1.0	1	Mini Computer	DEC/P/N 1134A-LE	●		
2.0	1	Disk W/Controller	RL11-AK	●		
3.0	1	DMA Interface	DR11-B	●		
4.0	1	Expander Box	BA11-LE	●		
5.0	7	Modem/Terminal Interface	DL11-E	●		
6.0	1	Backplane Module	DD11-DK	●		
7.0	1	Backplane Module	DD11-CK	●		
8.0	1	System Cabinet	H960-CA	●		
9.0	1	System Software	QJ013-AQ	●		
10.0	7	Modem	DU11-DA	●		
11.0	1	Fortran IV.	QJ980-AQ	●		
12.0	1	Real Time Clock	Datum Inc. Mod 9100	●		
13.0	1	Printer (180 CPS)	DEC P/N LA11-PA	●		
13.0	1	Control & Display Console	Later		●	NEW
.1	1	KEYBOARD/CRT	VT52-AA	●		
.2	1	-Logic Ass'y	GE P/N 63E901812G1		●	
.3	1	-Logic Ass'y	63E901810G1		●	

3.8.4 SUPERVISORY CONTROL

The concept of supervisory control is a requirement for the LSE and is the primary function of the CIS central computer. It involves both executive control of the remote processor units and a group of supervisory functions which provide the STE-LSE Shenandoah system operator with automatic and manual control and display capabilities.

As central intelligence in the distributed star network of CIS processing units, the central computer is responsible for control of the remote microcomputers. In a supervisory fashion, it delegates tasks to these units as required to maintain STE-LSE system performance control.

As the interface for operator control, the central computer's supervisory control function provides the operator with the capability of executing specific control and display functions. The operator may utilize this capability either automatically through the keyboard and CRT display peripheral or manually through the energy management panel (see Paragraph 3.8.4.3).

Because of the experimental nature of the Shenandoah system, supervisory control is required to provide some degree of operator control and display capability under both normal and emergency conditions. The original concept during the early preliminary design included a control panel with dedicated hardware that could function in the event of central computer failure. Soon it was realized, however, that hardwired control features would be very expensive and difficult to implement. A decision was made to place a single AC-power breaker switch in the control center for emergency situations. It was also decided that control panel wiring would be routed only through the central computer. Based on these decisions and the CIS subsystem control requirements, a preliminary energy management panel was designed, and several supervisory control functions were identified.

The primary functions of supervisory control include operating mode selection, the summary status feature, and the energy management panel. Each of these is described in the following subsections.

3.8.4.1 Operating Mode Selection

One of the major functions of supervisory control is the selection of system operating modes. Mode selection can be achieved by normal operator-initiated control commands being entered into the central computer via the keyboards. Software development will include a program that simplifies operator/keyboard command execution procedures.

When the STE-LSE system is under operator control, the operator first selects whether the STE-LSE system is going to operate in the interconnected (with Georgia Power Company) or stand-alone configuration. He then selects either weekday or weekend system operation. This is followed by selection of one of the operating modes described in the System Operating Plan such as Series Transfer, Threshold Insolation/Activation, SCS Shutdown, etc. The selected operating mode is then executed under the supervision of the central computer. It delegates control responsibilities to the remote microcomputers as required for the particular mode selected. In this way the supervisory control concept eliminates the need for costly dedicated function switches, indicators, control panels, and bulky cabling harnesses.

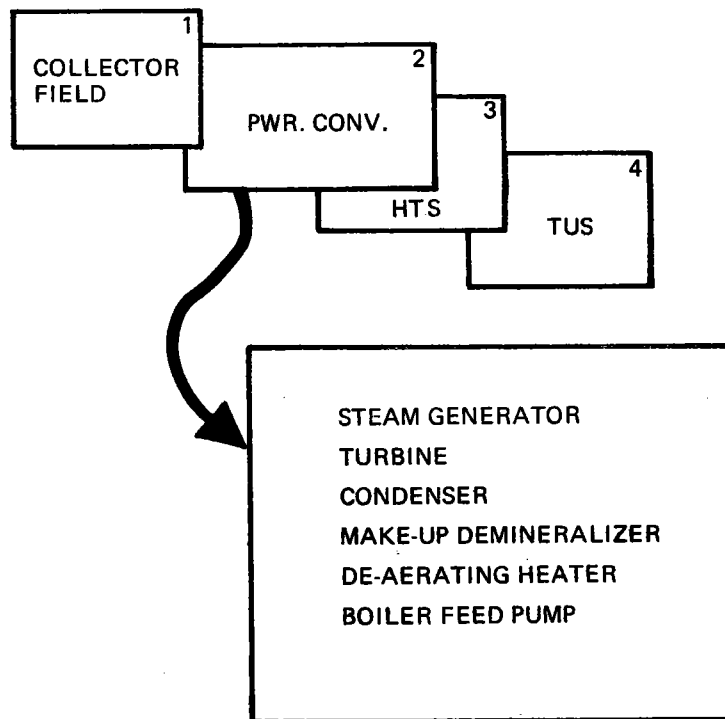
3.8.4.2 Summary Status Feature

Another implementation of the supervisory control concept, the summary status feature, allows the operator an overall top-down view of the STE-LSE system status. As described earlier, normal operator-initiated display commands will be entered into the central computer via the keyboard. Key system parameters stored in a page listing format will be displayed on the CRT. Top level status pages will list the major subsystems (SCS, PCS, etc.) and their corresponding operational status. If the operator desires, he will simply key-in that subsystem, and a detailed level status page will be displayed.

For example, if after scanning the top level status pages for the major subsystems, the operator wanted to examine the operational status of the PCS, he would call up the detailed PCS status page on the CRT and view the status of the steam generator, turbine, and other PCS components. This example is illustrated in Figure 3.8-11. If an alarm were to occur in one of the subsystems, the operator could select that subsystem via the keyboard, call up a list of its functions, and determine which function was in the alarmed state and why it was causing the alarm. In addition to the above capabilities, the operator will have the option of obtaining a printout of any summary status page displayed on the CRT by simply entering such a request on the keyboard.

3.8.4.3 Energy Management Panel

The primary control and display interface is the central computer's keyboard and CRT peripheral device. This device will be used to operate the STE-LSE system under all normal operating conditions. In case of keyboard/CRT problems or failures, however, the operator may still access the central computer via the energy management panel.



VIA KEYBOARD - OPERATOR CAN SELECT STATUS OF ANY PART OF LSE SYSTEM WHICH IS STORED FOR DISPLAY IN THIS STATUS PAGE LISTING CONCEPT.

Figure 3.8-11. Summary Status Feature

The primary function of the energy management panel is to provide a manual backup control/display capability for the keyboard/CRT device. Since it is a backup, the panel is not utilized under normal system operation conditions. If the central computer fails, the panel is no longer functional since it is wired through the computer.

As a manual backup control/display device, the energy management panel features control functions for major subsystem equipment and continuous display of key subsystem parameters. Because of these features, the panel offers the benefit of providing the operator with an instantaneous system status. In fact, as the operator becomes familiar with system operating characteristics, he will be able to determine the overall status of the system quickly at any time by simply scanning the energy management panel.

The preliminary version of the energy management panel is depicted in Figure 3.8-12. It contains control switches for the SCS and PCS; thumbwheel switches for the CFS and HTS; temperature meters for the SCS and TUS; pressure meters for the PCS; electrical meters for the ES; indicators for the SCS and PCS; status lights for the SCS, PCS, and TUS; a simplified piping layout; and a lamp test switch.

Figure 3.8-13 is an artist's preliminary concept of the operator's control console. This sketch depicts the keyboard/CRT device and the energy management panel, both of which are connected to the control computer by cabling located under the floor. Electronics associated with the keyboard/CRT and control panel are contained in the lower left portion of the operator's console.

An artist's preliminary concept of the STE-LSE control center area is illustrated in Figure 3.8-14. The central computer and its associated peripherals are depicted together with the operator's control console and devices described above.

3.8.5 SOFTWARE

Although actual software development does not begin until detailed design is underway, initial effort began during Phase III to establish a comprehensive software approach. Software techniques developed for other digital control systems by GE's Ground Systems Department in Daytona Beach were examined for possible application to the STE-LSE system. Several techniques, most notably structured programming and phased development, were selected and incorporated into a software management plan outline. This outline is shown in Table 3.8-4. The software management plan was identified as the key element in the STE-LSE software development approach. The plan outline provides the framework for the detailed CIS software design to be performed in Phase IV.

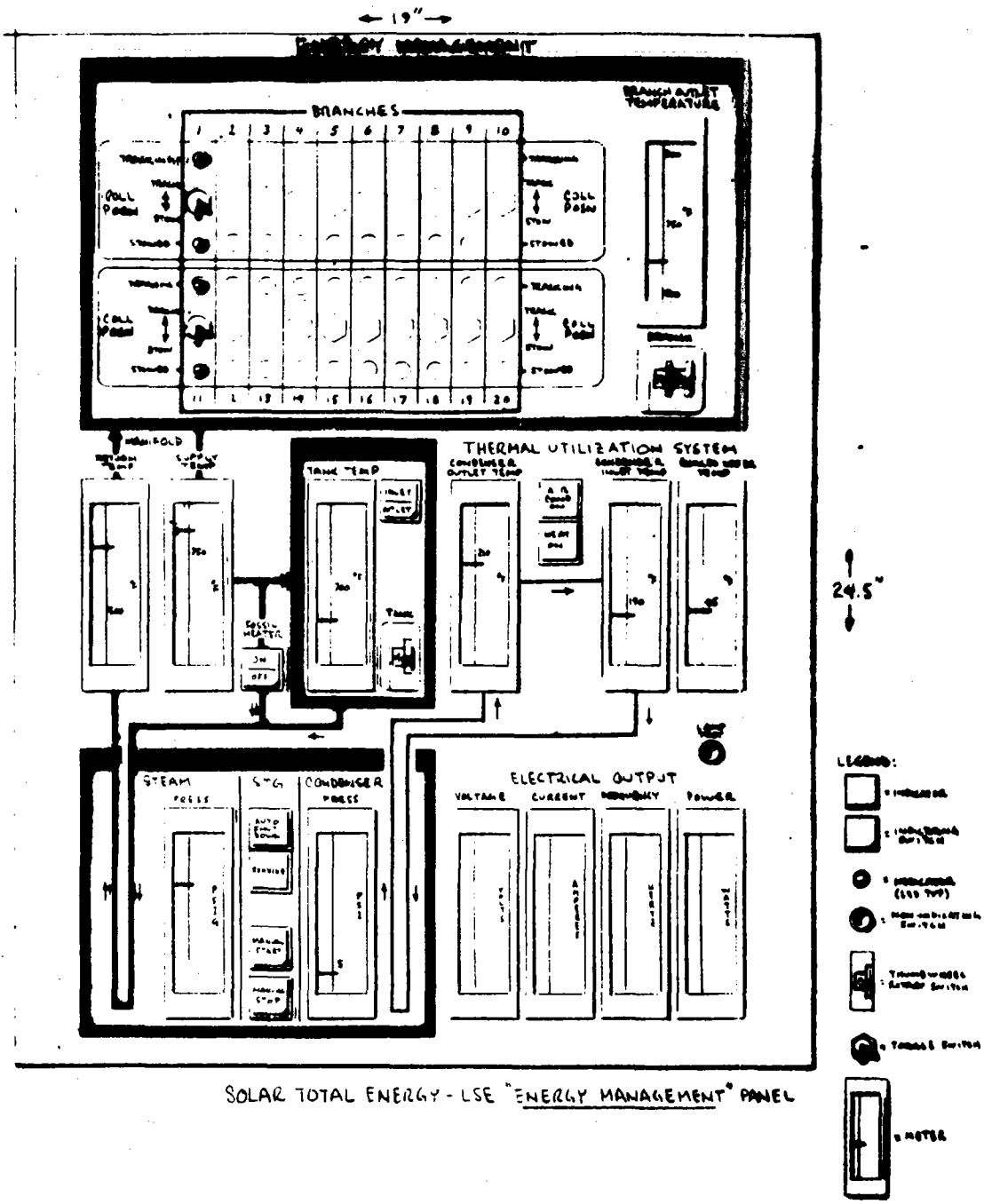


Figure 3.8-12. Energy Management Panel



Figure 3.8-13. STE-LSE Operator Control Console

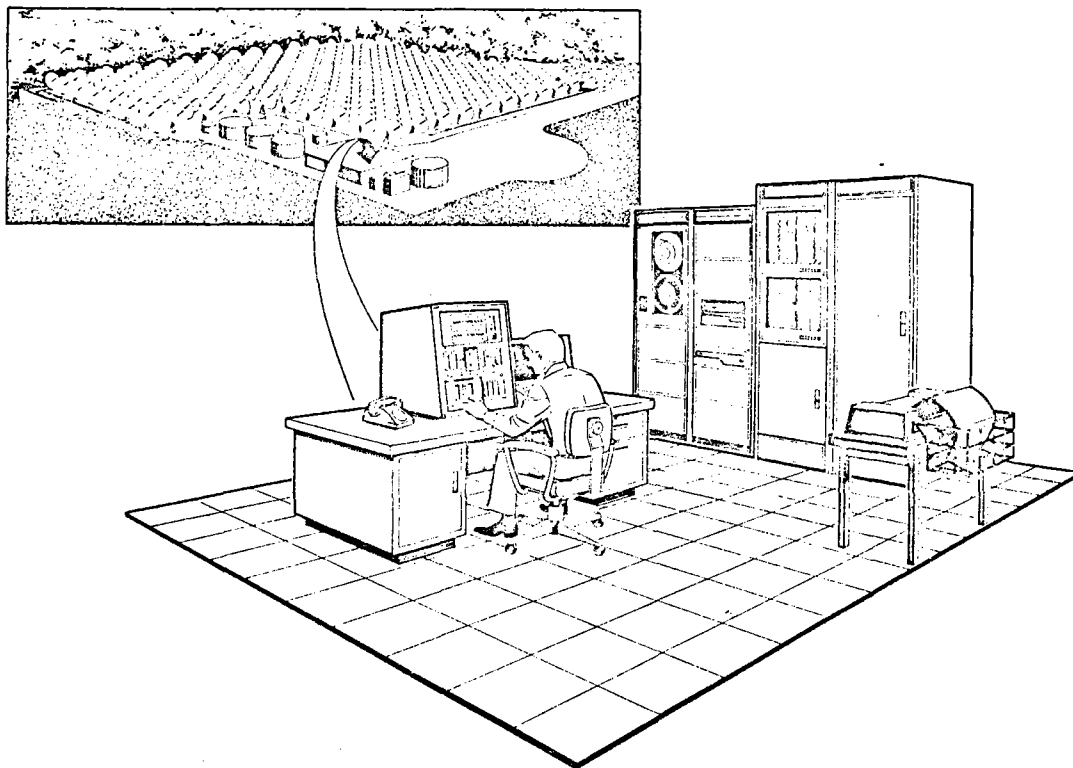


Figure 3.8-14. STE-LSE Control Center

Table 3.8-4. Software Management Plan Outline

- Management of Computer Program System Development
 - Control Systems techniques (existing)
 - Top-down Structuring
 - Computer Vendor Software
- CPS Development Organization
 - Lead Engineer
 - Lead Programmer
- Software Development Plan
 - Schedules
 - Phased development activities
 - Standards
 - Organizational control
 - Resources
 - Design (3 phases)
 - structural programming
 - Implementation
 - Verification
 - Acceptance testing
 - Integration testing
- Manning
- Reviews
- Cost, Tracking & Reporting
- Software Configuration Control
- Documentation
- Software Maintenance

SECTION 4
SYSTEM DESCRIPTION

SECTION 4

SYSTEM DESCRIPTION

This section presents the description of the preliminary design for the Solar Total Energy System (STES) to be installed at the Shenandoah, Georgia, site for utilization by the Bleye kintwear plant. It explicitly defines the requirements and the design features and characteristics of the individual subsystems and components which comprise the Solar Total Energy System for the Large Scale Experiment which have resulted from the studies described in the previous sections.

4.1 SYSTEM DEFINITION

The system is a fully cascaded total energy system design as shown in the Figure 4.1-1 schematic, featuring high temperature paraboloidal dish solar collectors with a 235 concentration ratio, a steam Rankine cycle power conversion system capable of supplying 200-400 kWe output with an intermediate process steam take-off point, and a back pressure condenser for heating and cooling. The design also includes an integrated control system employing the supervisory control concept to allow maximum experimental flexibility.

4.2 SUBSYSTEM DESIGN DESCRIPTIONS

4.2.1 SOLAR COLLECTION SUBSYSTEM (SCS)

4.2.1.1 Function

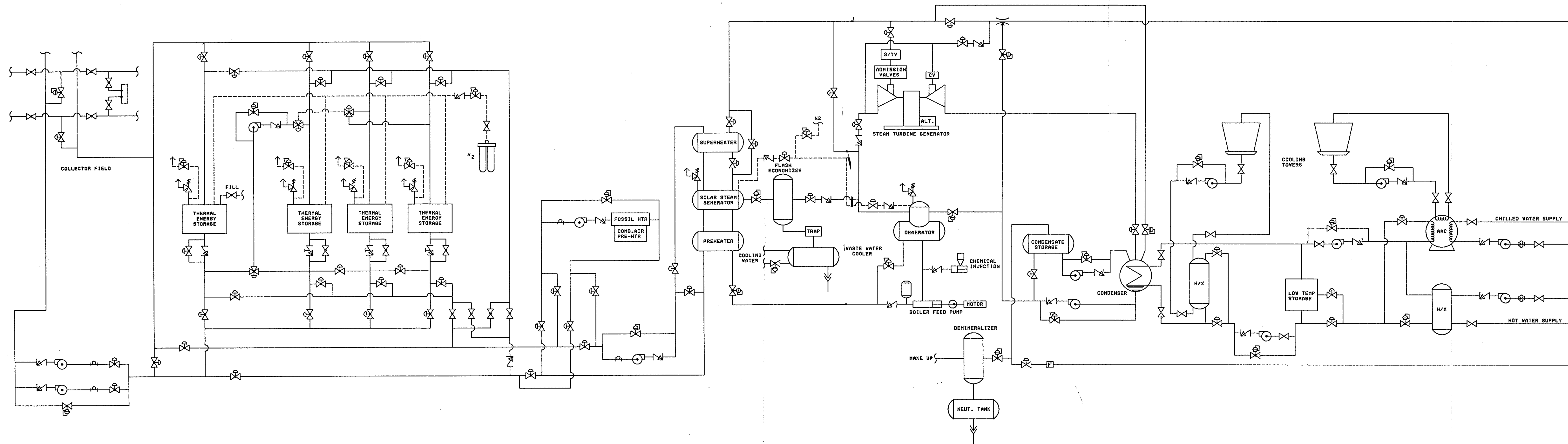
The Solar Collection Subsystem uses the sun's energy to heat the Syltherm 800 fluid flowing through the collector field. This heated fluid is then transported to the steam generator where its heat energy is used to produce steam for the Power Conversion Subsystem. A high temperature thermal energy storage subsystem is provided in the SCS to store excess solar energy. This storage subsystem supplies heated Syltherm 800 fluid to the steam generator during evening operation and periods of low solar insolation. A fossil fuel fired Syltherm 800 heater is also provided in the SCS to supply heat energy during system start-up operations and whenever the thermal energy storage is depleted.

4.2.1.2 System Configuration

The Solar Collection Subsystem is divided into three subloops (or subsystems) as shown in Figure 4.2.1. Each of these subloops is named for the function it performs within the SCS. The Collector Field Subsystem (CFS) contains the solar collectors and the collector field supply pumps. This subsystem can deliver the solar heated Syltherm 800 fluid to either the High Temperature Storage Subsystem or to the Steam Generator Supply Subsystem. The piping diagram of the CFS is shown in Figure 4.2-2.

The High Temperature Storage (HTS) Subsystem contains the storage tanks for the heated Syltherm 800 and the HTS transfer pump which is used in charging these storage tanks. The system piping diagram for the HTS subsystem is shown in Figure 4.2-3.

The Steam Generator Supply (SGS) Subsystem contains the steam generator supply pumps along with the Syltherm 800 fossil fired heater and its associated booster pump. This subsystem supplies the heated fluid from either the CFS or the HTS subsystem to the steam generator. The steam generator itself serves as the system boundary between the Solar Collection Subsystem and the Power Conversion Subsystem. The various input/output devices used throughout the SCS serve as the system interface and communication link with the Control and Instrumentation Subsystem.



LEGEND	
	GATE VALVE
	GLOBE VALVE
	CHECK VALVE
	STOP CHECK VALVE
	SAFETY RELIEF VALVE
	SELF ACTUATED PRESSURE REGULATION VALVE
	ISOLATION VALVE (ELECTRICALLY ACTUATED, DIAPHRAM OPERATED)
	THREE WAY VALVE (ELECTRICALLY ACTUATED, DIAPHRAM OPERATED)
	MODULATING VALVE (ELECTRICALLY ACTUATED, DIAPHRAM V/POSITIONER)
	DESUPERHEATER
	STRAINER
	FILTER
	DRAIN

Figure 4.1-1. Shenandoah System Schematic

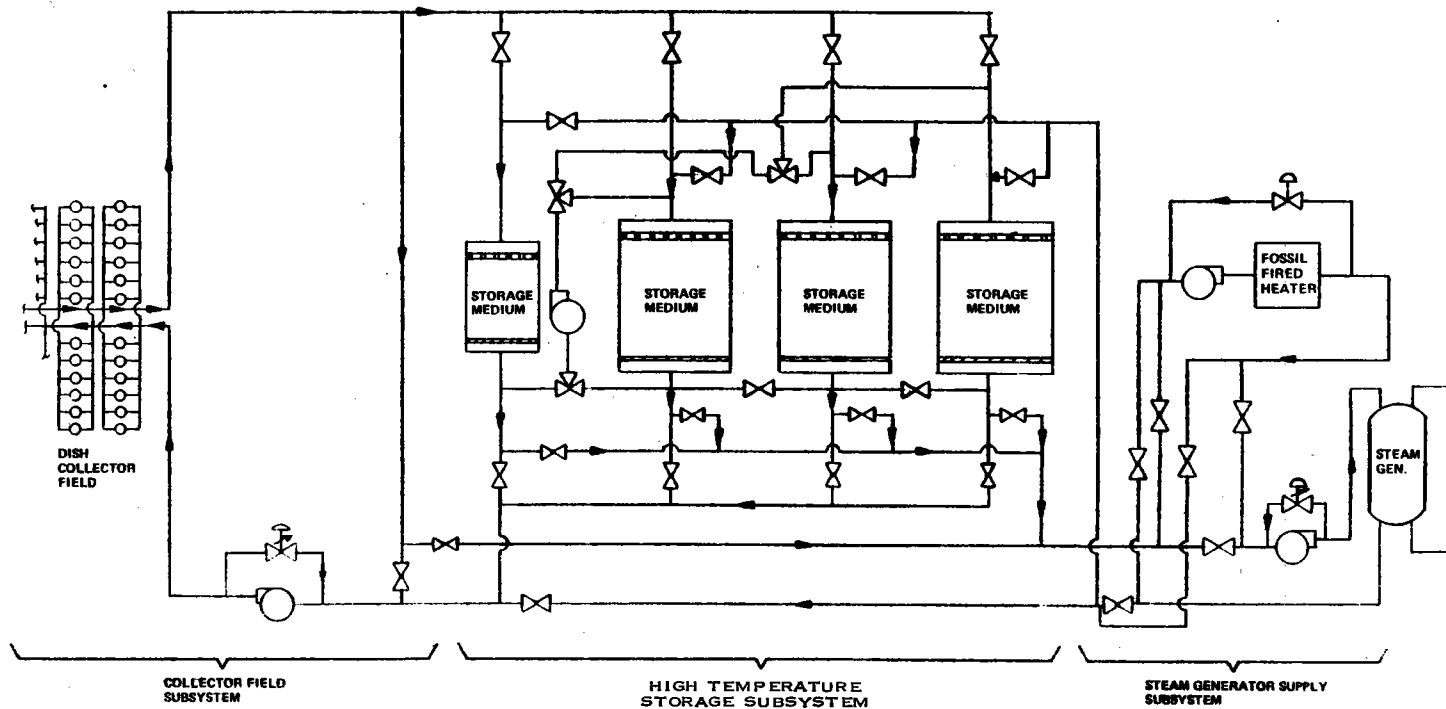


Figure 4.2-1. Solar Collection Subsystem

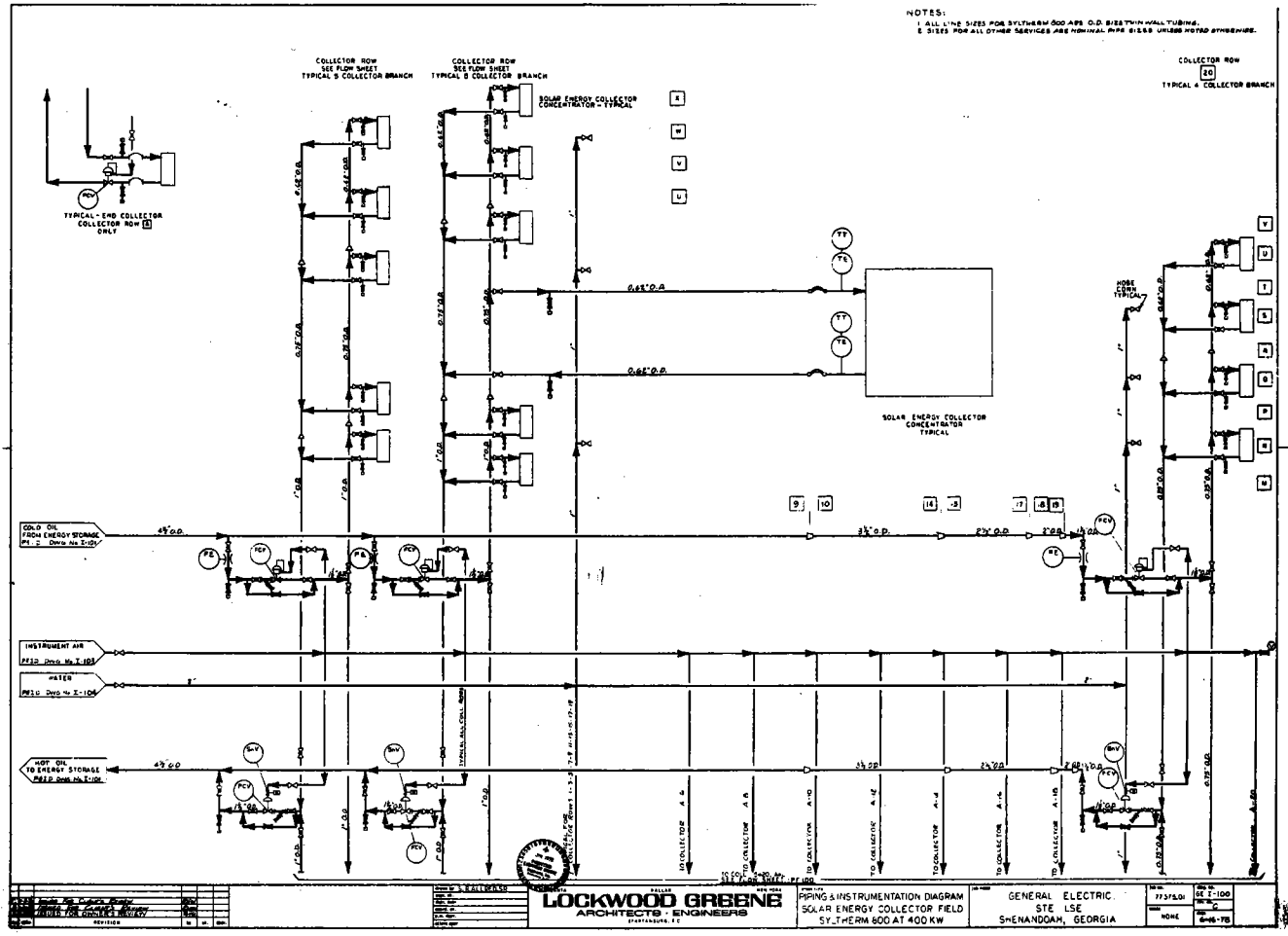


Figure 4.2-2. Piping & Instrumentation Diagram, Solar Energy Collector Field. Syltherm 800 at 400 kW.

4.2.1.3. Detailed Subsystem Description

4.2.1.3.1 Collector Field Subsystem (CFS)

The Collector Field Subsystem consists of the collector field supply pumps and the heat transfer fluid supply and return lines to the solar collectors. The main supply and return lines to the collector field run in the east-west direction, while the branch lines to and from the individual collectors run in the north-south direction. The collector field piping configuration is shown in Figure 4.2-2. These supply and return lines are constructed of seamless carbon steel tubing which complies with the requirements of ASTM A192.

The main supply and return lines consist of tubes of different diameters which have been reduced by steps to maintain a relatively constant flow velocity of approximately 2.4 m/s (8 ft/sec) throughout the collector field. The size of the lines entering and leaving the Mechanical Building are 0.114 meter (4.5 in.) O.D. with a .0032 meter (0.125 in.) wall thickness. The branch lines are also tapered to maintain a constant flow velocity. The lines running up to and down from the receiver are of different diameters. The down or hot side has a slightly smaller diameter than the cold side to decrease temperature drop during low flow conditions. Pipe supports for both the main headers and the branch lines are installed in accordance with ANSI B31.1 Power Piping Codes as shown in Table 4.2-1.

Under design conditions, Syltherm 800 is pumped to the collectors at a supply temperature of 533° K (500° F) and returns from the field at 658° K (725° F). The main supply and return lines are covered with insulation whose thickness is based upon the tube temperature (500° F or 750° F) and diameter. The recommended insulation materials and thicknesses are shown in Table 4.2-2. This insulation is covered with a 16 gage aluminum jacket which is sealed at the joints with a mastic. The branch lines are nested within a similar type of insulation jacket. This nesting of the two fluid lines with the same insulation jacket results in a net heat loss savings of between 35 to 40 percent over singly insulated tubes. A schematic representation of this nesting technique is shown in Figure 4.2-4. The individual collectors are also joined to the branch lines via nested tubing up to and down from the receiver.

Table 4.2-1. Suggested Pipe Support Spacing

Nominal Pipe Size Inches	Suggested Maximum Span			
	Water Service*		Steam, Gas, or Air Service	
	Feet	m	Feet	m
1	7	2.1	9	2.7
2	10	3.0	13	4.0
3	12	3.7	15	4.6
4	14	4.3	17	5.2
6	17	5.2	21	6.4
8	19	5.8	24	7.3
12	23	7.0	30	9.1
16	27	8.2	35	10.7
20	30	9.1	39	11.9
24	32	9.8	42	12.8

Note 1. Suggested maximum spacing between pipe supports for horizontal straight runs of standard and heavier pipe at maximum operating temperature of 672°K (730°F)

Note 2. Does not apply where span calculations are made or where there are concentrated loads between supports such as flanges, valves, specialties, etc.

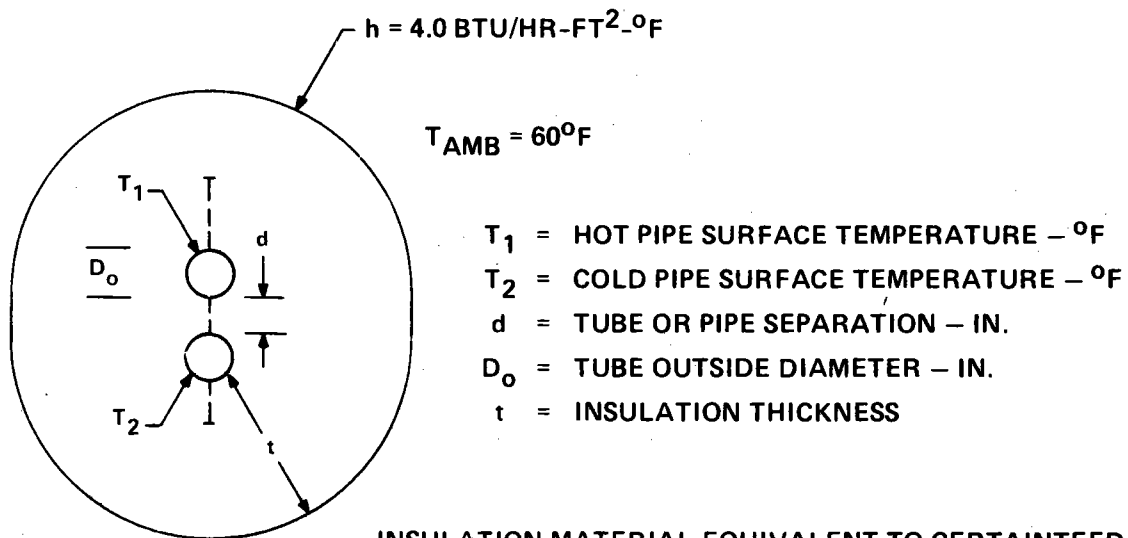
Note 3. The spacing is based on a maximum combined bending and shear stress of 1035 MPa (1500 psi) and insulated pipe filled with water or the equivalent weight of steel pipe for steam, gas or air service, and the pitch of the line is such that a sag of 0.0025m (0.1 inch) between supports is permissible.

*Applicable also to oil service pipes.

Table 4.2-2. Tubing Insulation Schedule*

Tube Outer Dia. - Inches	533°K (500° F)		672°K (750° F)	
	Thickness (inches)	Material	Thickness (inches)	Material
1/2 x 3/4 up and down nested	4.0	Certainteed 850	4.0	Certainteed 850
5/8 nested	4.0	Certainteed 850	4.0	Certainteed 850
3/4 nested	4.0	Certainteed 850	4.0	Certainteed 850
1.0 nested	4.0	Certainteed 850	4.0	Certainteed 850
1.5 single	3.0	Certainteed 850	4.0	Certainteed 850
2.0 single	3.5	Certainteed 850	4.5	Thermo 12
2.5 single	3.5	Certainteed 850	5.0	Thermo 12
3.5 single	4.0	Certainteed 850	5.5	Thermo 12
4.5 single	4.5	Certainteed 850	6.0	Thermo 12

*All Insulation multilayer



INSULATION MATERIAL EQUIVALENT TO CERTAINTEED 850

$$k @ T_{\text{avg}} = 400^\circ\text{F IS } \frac{.42 \text{ BTU IN.}}{\text{HR-FT}^2\text{-}^\circ\text{F}}$$

$$\rho = 5.25 \text{ LBS/FT}^3 \quad C_p = \frac{.2 \text{ BTU}}{\text{LB-}^\circ\text{F}}$$

Figure 4.2-4. Nested Pipe Analysis

Forged carbon steel, manually operated, Y pattern globe valves are installed in the supply and return lines of each individual collector to allow isolation for maintenance and to provide thermal trim potential. Thermal trim is accomplished only during initial system startup to give temperature balance between collectors in a branch. Fluid flow control to each branch is provided by pneumatically actuated flow control valves which operate in response to the maximum collector output temperature in the branch. A schematic representation of the branch line arrangement is shown in Figure 4.2-5. Two pneumatically operated globe valves are required; one, a modulating valve for flow control and the other, an on-off valve for branch isolation. A picture of a typical pneumatic control valve for this application is shown in Figure 4.2-6. Due to the weight of the control valve actuation mechanism, each control valve is separately supported.

Due to the low viscosity and surface tension of Syltherm 800 at operating temperatures, the entire field piping network is completely welded. Tungsten Inert Gas (TIG) welding will be used throughout. All valves and fittings in sizes 0.51 meter (2 inches) and smaller will be socket welded. Butt welds will be used for all sizes greater than two inches. Loads resulting from thermal expansion will be controlled by the use of inline, externally pressurized compensators placed in the branch lines. A typical compensator of this type is pictured in Figure 4.2-7. The external surface of the insulation will be guided to prevent lateral instabilities.

4.2.1.3.2 High Temperature Storage (HTS)

The HTS subsystem consists of the four HTS tanks and the HTS transfer pump along with the interconnecting piping and valves and associated instrumentation and controls. Interconnecting flow paths throughout the HTS subsystem allow for the transfer of hot Syltherm 800 fluid from the collector field to the HTS tanks, from one HTS tank to another, and from the HTS tanks to the Steam Generator Supply subsystem. The HTS piping configuration is shown in Figure 4.2-3.

The subsystem is designed for a trickle oil mode of operation. The design includes the capability for operation in a fluid filled or dual media storage mode. The subsystem utilizes a packed bed of taconite as the solid storage medium operating over a temperature range of 533 to 672° K (500 to 750° F).

In the trickle oil mode, heat transfer is accomplished by a gravity fed trickle oil flow through the bed. The taconite thermal capacity storage medium provides a thermal capacity of 1.06×10^{11} joules (100 MBtu) when all tanks are fully charged. Both the outlet from the collectors (charge flow) and the return from the solar steam generator (discharge flow) enter the top manifold over the bed and are returned from the bottom of the bed. The gravity flow thus requires that the bed be fully charged before it can be discharged, or at least the bottom of the bed be at the delivery temperature for discharge (672° K or 750° F). A sump is required beneath the tank to collect the fluid. No bottom manifold, however, is required to maintain a thermocline at the bottom of the bed.

In the dual media approach, the combined heat capacity of the taconite and the Syltherm 800 fluid is 1.35×10^{11} joules (128 MBtu), assuming 30 percent fluid filled voids. An additional manifold is required at the bottom of the bed to maintain thermocline stability. The dual media operation provides hot flow entering and leaving the top of the tank and cold flow entering and leaving the bottom of the tank.

The first tank is sized to provide approximately one hour of energy delivery to the solar steam generator at peak design conditions. The remaining three tanks are sized equally to provide the remaining thermal capacity.

Seamless carbon steel tubing which complies with the requirements of ASTM A192 is used throughout the HTS subsystem. The standard tube size used is 0.114 meter (4.5 in.) O.D. with a .0032 meter (0.125 in.) wall thickness. These tubes are insulated as specified in Table 4.2-2. The subsystem is completely welded except for the flanged connections to the HTS transfer pump. Thermal expansion of the piping system is controlled by inline, free flex bellows, expansion joints. Pipe supports and lateral restraints are installed in accordance with ANSI B31.1 Power Piping Codes.

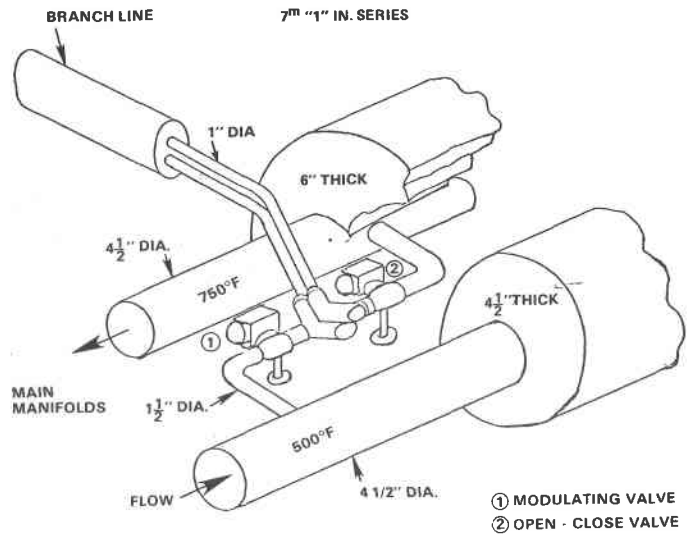


Figure 4.2-5. Branch Isolation and Control

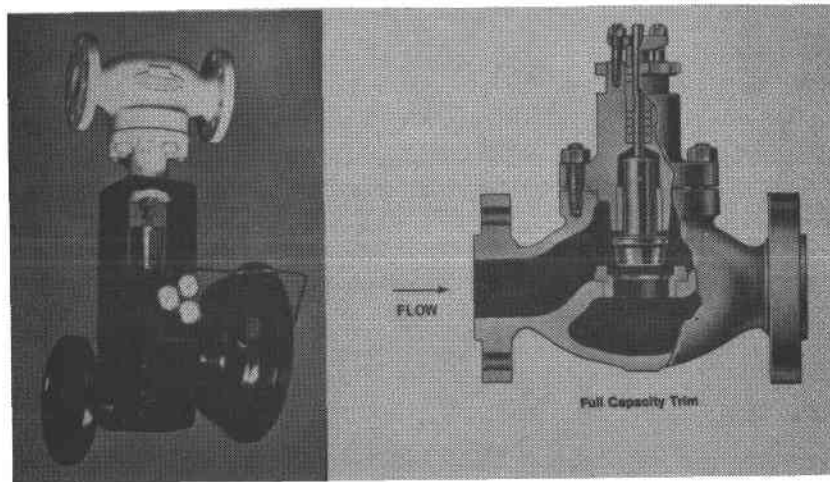


Figure 4.2-6. Pneumatic Control Valves

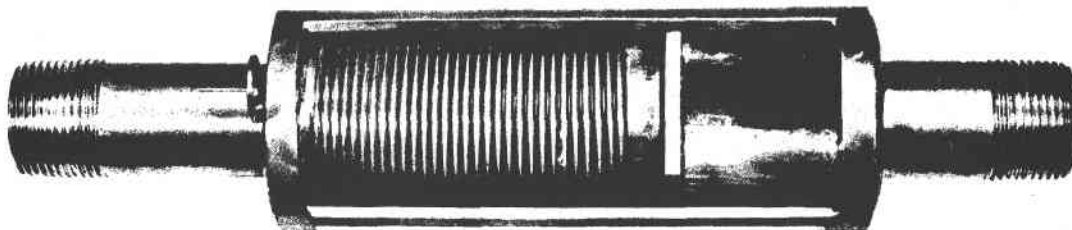


Figure 4.2-7. Thermal Expansion Compensator Linear Type

4.2.1.3.3 Steam Generator Supply (SGS)

The Steam Generator Supply Subsystem consists of the steam generator supply pump, the Syltherm 800 fossil fired heater (FFH) and the fossil heater booster pump. The steam generator supply pump delivers heated Syltherm 800 fluid to the steam generator at a rate controlled by the steam demand of the PCS. This 672° K (750° F) fluid is supplied either directly from the collector field or from the HTS tanks during normal operations. During startup and when solar insolation levels are below minimum requirements, the fossil fired heater is used to provide the heated Syltherm 800 to the steam generator.

The fluid lines in the SGS subsystem are constructed of seamless carbon steel tubing which complies with the requirements of ASTM A192. All joints are TIG welded except for flanged connections to the system pumps. Tubes having a 0.114 meter (4.5 inch) O.D. with a .0032 meter (0.125 inch) wall thickness are used throughout the subsystem. The tubing is covered with insulation per Table 4.2-2, and 16 gauge aluminum jacketing covers the insulation. Free flex expansion joints are installed to compensate for thermal expansion. The SGS piping configuration appears on Figure 4.2-3.

The stop valves used throughout the SGS subsystem are pneumatically operated globe valves rated for 672° K (750° F) operation. These valves are butt welded in place and covered by an insulation jacket. Valve stems will be mounted horizontally or below horizontal to prevent insulation contamination in the event of a seal leak. This mounting configuration is identical to that used in the collector field and high temperature storage subsystem.

4.2.1.4 Major Components

4.2.1.4.1 Solar Collectors

Figure 4.2-8 shows an overall geometry drawing of the collector and defines graphically the major components to be discussed below. The solar collectors receive the direct radiation of the sun and concentrate it to heat the Syltherm 800 fluid to a high temperature. In order to satisfy the energy requirements of the STES, the collectors must be capable of converting at least 65 percent of the direct normal insolation incident upon the collector surface into heat supplied to the heated oil. A two-axis tracking, paraboloidal dish was selected for maximum collection efficiency for insolation greater than 630 W/m² (200 Btu/hr-ft²). The mount and drive portions of the collector elevate the dish from the ground and point it at the sun. The dish retains its paraboloidal shape regardless of the changes in weight loadings or wind loadings below 13.4 m/s (30 mph). The reflective surface of the collector reflects 86 percent of the incident radiation with a specular dispersion equivalent to eight mrad RMS value. The reflected energy is concentrated in a receiver that converts 82 percent of the energy into useful heat at a design insolation rate of 630 W/m² (200 Btu/hr-ft²) and 87 percent of the maximum insolation rate of 977 W/m² (310 Btu/hr-ft²) by minimizing convection and radiation losses. The heated oil is transported up to and down from the receiver through insulated, nested piping which traverses the two axes of motion through flexible joints.

4.2.1.4.1.1 Receiver. The function of the receiver is to transfer the concentrated solar energy at the focal plane of the collector into the working fluid. The receiver is a cavity type with the incident concentrated solar flux impinging upon an absorptive surface enclosed within an insulated cylindrical shell. The aperture of the receiver is positioned in the focal plane of the dish and is 0.475 meter (18 inches) in diameter. The corresponding concentration ratio is 235, and 96 percent of the incident flux is intercepted. Figure 4.2-9 shows the design layout of the receiver.

The cylindrical insulation shell has an outside diameter of 0.85 meter (33.5 in.) and a height of 0.89 meter (35 inches) with a .051 meter (2 in.) of high temperature insulation. The inner wall of the shell is 0.75 meter (29.5 in.) in diameter. The shell outer wall is constructed of a thin wall, low carbon steel sheet wrapped around a rigid frame and coated on both sides with a high temperature paint. The shell inner wall is constructed of low carbon steel sheet and is porcelainized with a base coat on both sides and a prime, diffusely reflective coat on the cavity side. The topplate of the cavity and the face plate of the receiver shell also have the procelain diffusely reflective coating. The porcelain coating has a reflectance of 0.9 and an emmissivity of 0.8.

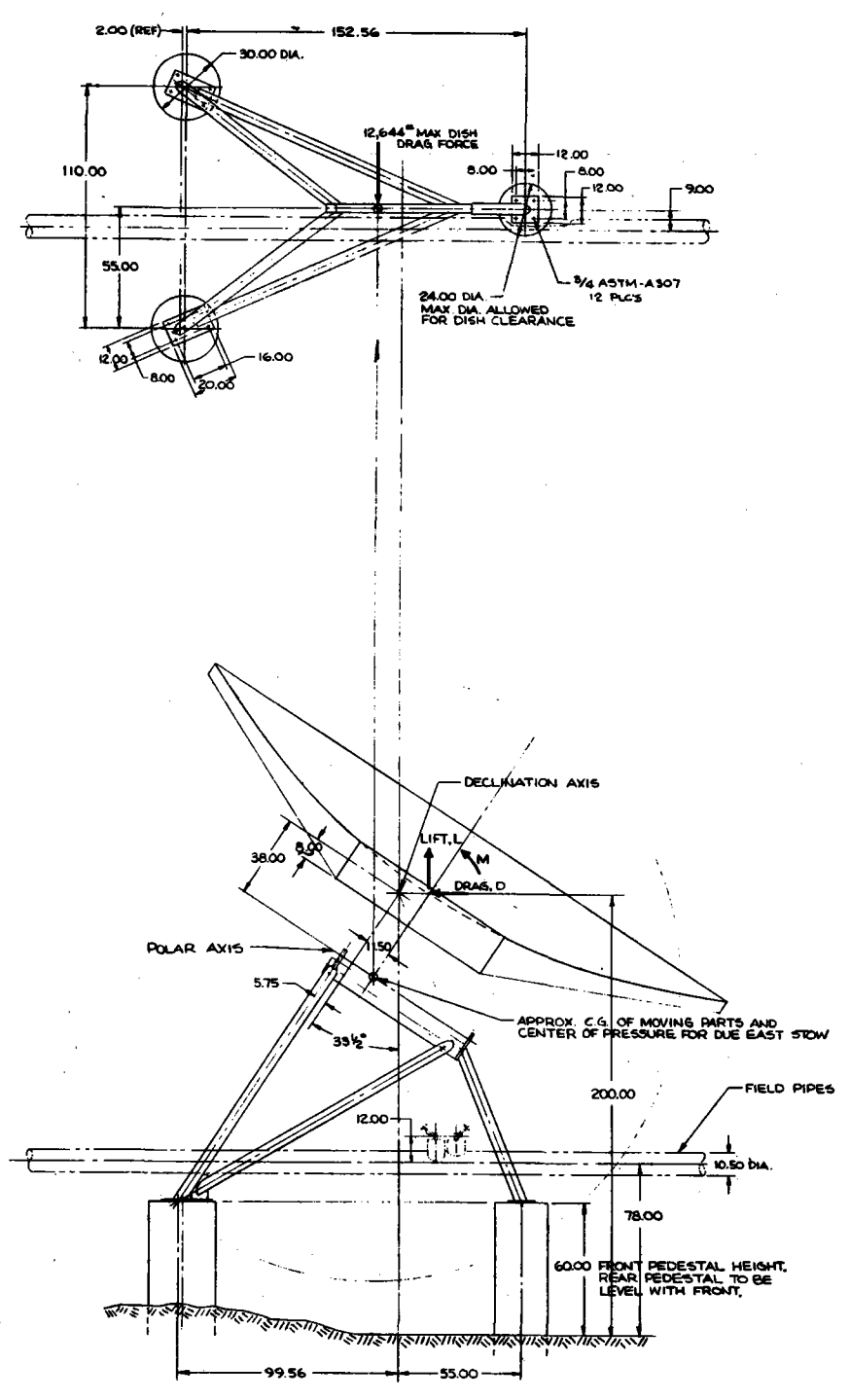


Figure 4.2-8. Collector Geometry

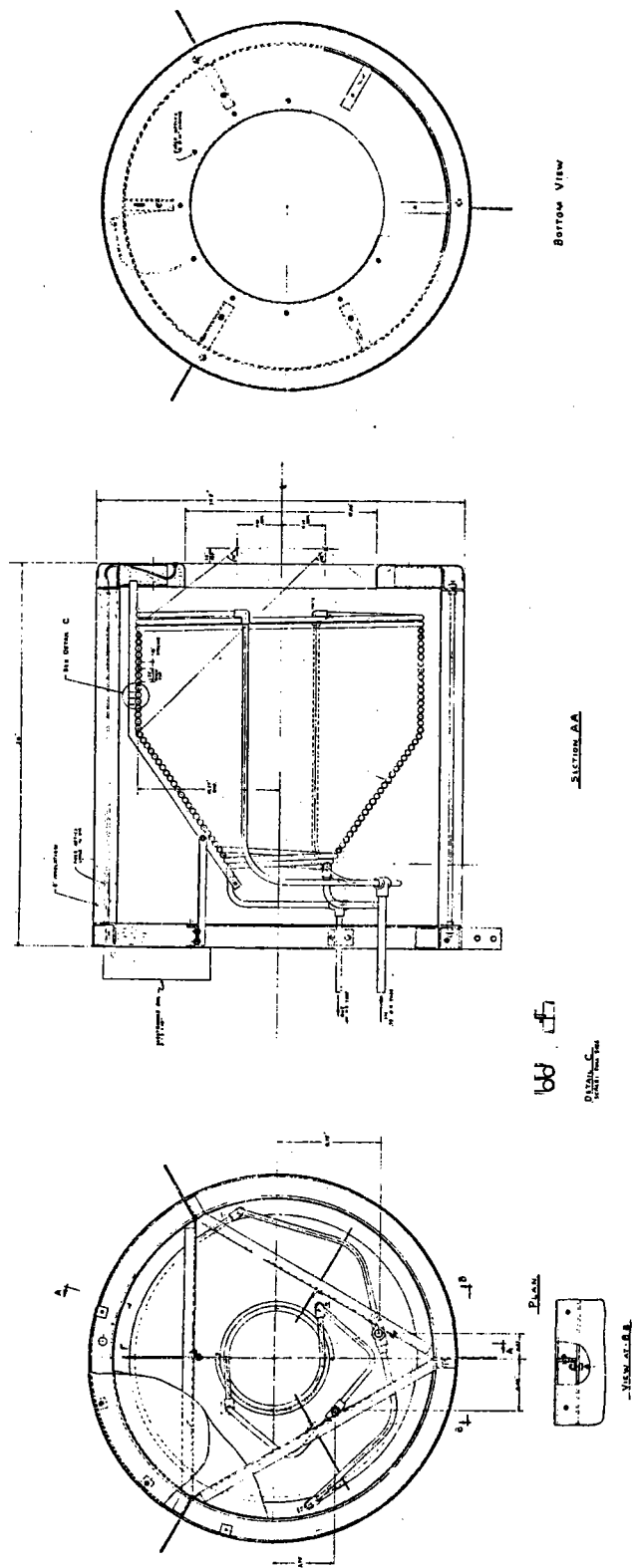


Figure 4.2-9. Receiver Configuration

The heat transfer surface is a coil wrapped into a cylinder with a domed top. This coil is 0.685 meter (27 in.) in diameter and is constructed of two parallel wound, low carbon steel tubes with an O. D. of 0.013 meter (1/2 in.) and a wall thickness of 0.0015 meter (0.058 in.). The total length of tubing is 64 meter (210ft.), 32 meters (105 ft.) for each tube. The cold feed tube and hot exit tube are joined to the coil with a header fitting. The tubing is treated to give a high absorptivity of 0.90. Four shaped supports hold the coil in position with the legs being guided into slots in the bottom of the receiver shell. The top of the supports are rigidly attached to the top of the shell. The coil is fastened to the support with clips. The overall dry weight of the receiver is 75 kg (165 lb.)

4.2.1.4.1.2 Collector Dish. The collector dish with its reflective surface concentrates the incoming solar radiation at the dish's focal point and hence can be thought of as an optical component. The dish must provide a true parabolic surface for the reflective material and hold this shape under various types of loadings such as gravity and wind forces. Typical antenna dishes measure the deviation from the true parabolic surface as an RMS value of the distances measured from a number of points on the dish. For optical reflective error calculations, the surface error is best measured as a slope error. Thus, for a given slope error distribution, the flux profile at the focal plane can be computed rather than assuming that the flux is all located at the theoretical focal point of the dish. This flux profile directly reflects the design of the receiver as discussed above, and thus, the required dish slope error distribution is defined by the receiver design. In this case, the dish slope error of one-half degree RMS or less is required.

The diameter of the dish is seven meters. To provide the stiffness required to hold the parabolic shape, the dish is made from stamped aluminum petals which are bolted together. The petals require structural backing to prevent excessive deflections under various loads. Aluminum ribs bolted to the petals are used for this purpose. The dish reflective surfaces and ribs are supported at the center by a support ring to which the declination axis pivot supports and one end of the declination actuator is attached for a three-point suspension. To expedite the manufacturing process and reduce the costs involved, the aluminum petals are not full sized, being 2.44 meters (8 feet) in length. A center dish of approximately 2.29 meters (90 inches) in diameter, which is made from a spinning, is used to complete the reflective surface in the center of the dish.

The reflective surface should reflect the sun's rays to the focal plane with minimal losses. These reflective losses are determined by measuring the total reflectance and the specular reflectance of the surface. The total reflectance refers to that portion of the solar radiation which is reflected and not absorbed. For this application, its required value is 0.86. The specular reflectance refers to how much a single ray would be dispersed after being reflected. Its required value must be equivalent to an 8 mrad RMS normally distributed specular distribution.

The reflective surface should withstand all expected adverse environmental conditions without serious degradation for the duration of the 20 years design life goal of the collector. Testing requirements for the reflective surface include:

- a) Weathering due to wind, rain and humidity
- b) Salt spray
- c) Ultraviolet degradation
- d) Thermal cycling, both daily and seasonal
- e) Cleanability requirements including resistance to abrasive scratches

The reflective surface that best meets the design requirements is chemically brightened 5657 aluminum alloy coated with RTV 670.

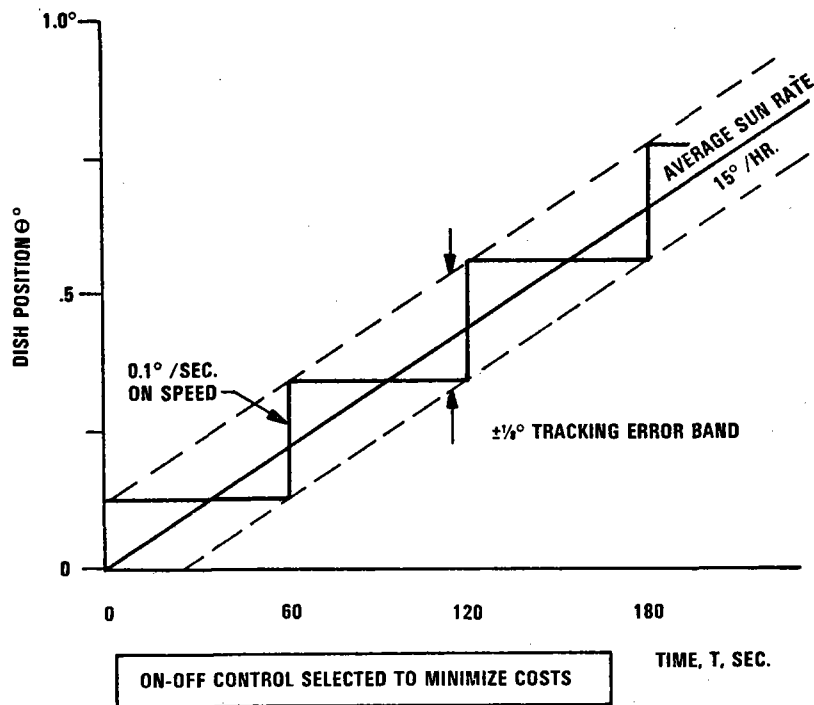


Figure 4.2-10. Actuator Speed Selection

4.2.1.4.1.3 Dish Mount and Drives. The parabolic surface of the collectors must be pointed at the sun in a semi-continuous manner to maximize the amount of heat collected. The tracking need not be continuous since up to $1/4^\circ$ tracking and bias errors are allowed. This results in the reflected sun image at the receiver not being exactly centered in the cavity at all times, which is acceptable within the angular error prescribed above. This allows the drive system to be under an on-off control. Since the sun's motion is $0.00416^\circ/\text{s}$ ($360^\circ/\text{day}$) or $1/4^\circ$ per minute, the average tracking error must match this, but need not do so continuously. With one half of the $1/4^\circ$ RMS error allowed for the tracking error, the nominal position versus time is described in Figure 4.2-10. This shows the stepwise responses about the polar axis.

Since, at the time of stepping, the dish trails or leads the sun by $1/8^\circ$ by design, $1/8^\circ$ is allowed for other errors, e.g., by the wind loading deflecting the structure or by sun sensor errors. The wind deflection is expected to be the largest contributor to the error. The system is required to operate in maximum winds of 13.4 m/s (30 mph). The 13.4 m/s wind is not steady but is characterized as having a 10 m/s (22.5 mph) mean with a 3.4 m/s (7.5 mph) varying component. A total 6.8 m/s (15 mph) change in wind speed used as the worst case to produce the $1/8^\circ$ error. (Note: the steady wind component is compensated for by the sun sensor tracking unit.)

The required system stiffness limits the types of drive system components that can be used. In general, pneumatics or inexpensive gearing cannot be used because of being too compliant. Electric screw jack actuators have been selected to provide the required stiffness and strength of minimum cost.

The mount is required to provide ground clearance of the collector dish of about 0.61 meter (2 feet). This minimizes degradation of the reflector surface due to wind-borne heavy particles. The mount should also provide protection to the reflector surface from hail and also minimize dew collection. The polar/declination axis gimbal drive was chosen over the more conventional azimuth/elevation drive for two reasons. First, angular excursion requirements are smaller to point the dish at the sun during the most useful times, and secondly, the polar drive basically uses only one motion to track, i. e. it does not require the coordination of motions the azimuth/elevation needs.

The design of the mount structure not only requires the stiffest design for the least amount of material (cost) but also must not interfere with the dish motion. The polar axis provides 180° motion and the declination axis $\pm 23 \frac{1}{2}^\circ$. Hence, as the dish sweeps out these motions, the structure must not interfere. The mount must sit on a foundation that also does not interfere.

The foundation provides the initial alignment and must support the dish without excessive settling. It, along with the rest of the mount and drive, must be able to withstand the 40.2 m/s (90 mph) maximum wind condition. The mount, drive and foundation must meet the local building codes.

The outdoor environment requires the components selected to be either inherently weather proof or housed in weather proof containers. Maintenance should be minimized, and replacement of active parts should be made easy.

To provide for certain emergency conditions, the drive should be able to defocus the collector at a rate of $2^\circ/\text{sec}$. This requirement is met by providing a higher horsepower drive on one of the polar drive actuators. Since it should operate with possible field power loss, its own emergency battery is provided. Also to focus the collector during the day, the collector should catch up to the sun by at least an order of magnitude faster than the $1/240^\circ/\text{sec}$ ($1/4^\circ/\text{min}$) sun rate. The rate used is about $1/10^\circ/\text{sec}$ ($6^\circ/\text{min}$) which is provided by turning on continuously both polar axis drives. This minimizes the heating up of the receiver aperture as the sun's image wipes across the receiver face. The $1/10^\circ/\text{sec}$ ($6^\circ/\text{min}$) rate can also be used to position the dish for maintenance purposes.

4.2.1.4.2 High Temperature Storage Tanks

4.2.1.4.2.1 Tanks. The four high temperature storage tanks will be of similar carbon steel construction. The smaller, one hour tank is 3.96 meter (13 feet) in diameter and 3.66 meter (12 ft) high with a capacity of 44.9 cubic meters (11,860 gallons). The three larger tanks each are 6.28 meters (20.6 ft) in diameter and 4.87 meter (16 ft) high with a capacity of 152 cubic meters (40,065 gallons). Figure 4.2-11 shows the tank construction for the 6.28 meter (20.5 ft) diameter tank. The dome will be conical in shape consisting of 12 flat plate (pie-shaped sectors) bent to conform to the cone radius. The sections will mutually reinforce each other to provide a rigid structure. Some bracing will be required at the truncation of the sectors. The lateral wall is 0.0096 meter (3/8 in) thick from the bottom to the top of the tank. The main inlet connection is a 0.114 meter (4.5 in) tube leading to the distribution manifold which will be an integral part of the dome as described in paragraph 4.2.1.4.2.2. The dome will also have a man-hole port for access to the tank interior. The bottom of the tank will have a 12 to 1 sloped internal base to provide good drainage to the sump described in paragraph 4.2.1.4.2.3. The tank will be supported on a 1.2 meter (4 ft) high structure to allow adequate bottom insulation and access to the sump.

4.2.1.4.2.2 Distribution Manifold. The trickle oil concept requires only one manifold at the top of the packed bed, but a second bottom manifold is included to accommodate the fluid filled back-up design capability. The two manifolds will be of identical construction as shown in Figures 4.2-12 and 4.2-13. The manifold is a series of interconnecting pipes, .032 meter (1-1/4 in) in diameter, providing a uniform flow distribution over the packed bed. There will be two holes at 0.102 meter (4 inch) intervals along the pipe length, with a hole located on both sides of the pipe at a 30° angle from the bottom or top of the pipe for the top and bottom manifolds respectively. There will be a total of 1424 holes each with a .00159 meter (1/16 in) diameter for a total flow efflux area of .0028 square meters (.0303 ft²). The top manifold will be an integral part of the dome attached by stringers at several key points, Figure 4.2-12. This design allows unit installation. The bottom manifold is located at the sump level and supported off the sloped floor as shown in Figure 4.2-13. The bottom manifold will be valved externally to the tank to allow conversion from the trickle oil sump operation to the dual medium manifold.

4.2.1.4.2.3 Sumps. Each tank will have a separate sump of similar design located at the center of the tank. Each sump will be cylindrical in shape, 0.915 meter (3 ft) in diameter and 0.915 meter (3 ft) deep with a capacity of 0.605 cubic meters (160 gallons) - see Figure 4.2-14.

The bottom of the sump will be sloped toward a drain with a removable cover for sludge cleanout. The outlet pipe will enter from the side of the sump. A .025 meter (1 in) grid grate is located directly above the pipe to inhibit formation of a large vortex flow which could result in pump cavitation. The outlet pipe will have a capped end with multiple holes on the bottom side also to minimize any strong vortex formation. A solid 1.52 meters (60 in) flat head will be mounted 0.15 meter (6 in) above the tank floor and supported by load carrying gussets which distribute the load directly to the support structure. Hole perforations are located around the side of the flat head. This design prevents sludge from falling directly into the sump and allows flat layout of the bottom manifold.

4.2.1.4.2.4 Taconite Storage Medium. Taconite is the packed bed storage medium. The taconite pellets are sphere-like pellets with a nominal size range of .00952 - .0175 meter (3/8 - 11/16 in) in diameter. The bulk density is 1760-2030 kg/m³ (110-130 lb/ft³) and its average specific heat from 273-644°K (0 to 700° F) is 793J/kg-°K (0.19 Btu/lb - ° F). Typical composition of taconite is:

Fe	62-65%
SiO ₂	5-6%
P	.01-.04%
M	.1-.3%
Al ₂ O ₃	.22-.88%
CaO	.20-.43%
MgO	.04-.66%
S	.002%
H ₂ O	1-3%
O ₂	Remainder

Approximately 9.36×10^4 kg (103 tons) of taconite will be packed into the one hour tank and 3.16×10^5 kg (348 tons) in each of the three larger tanks for a total taconite weight of 1.04×10^6 kg (1147 tons). Larger sized pellets will be screened and used as bottom layers in each of the tanks to provide adequate drainage to the sump.

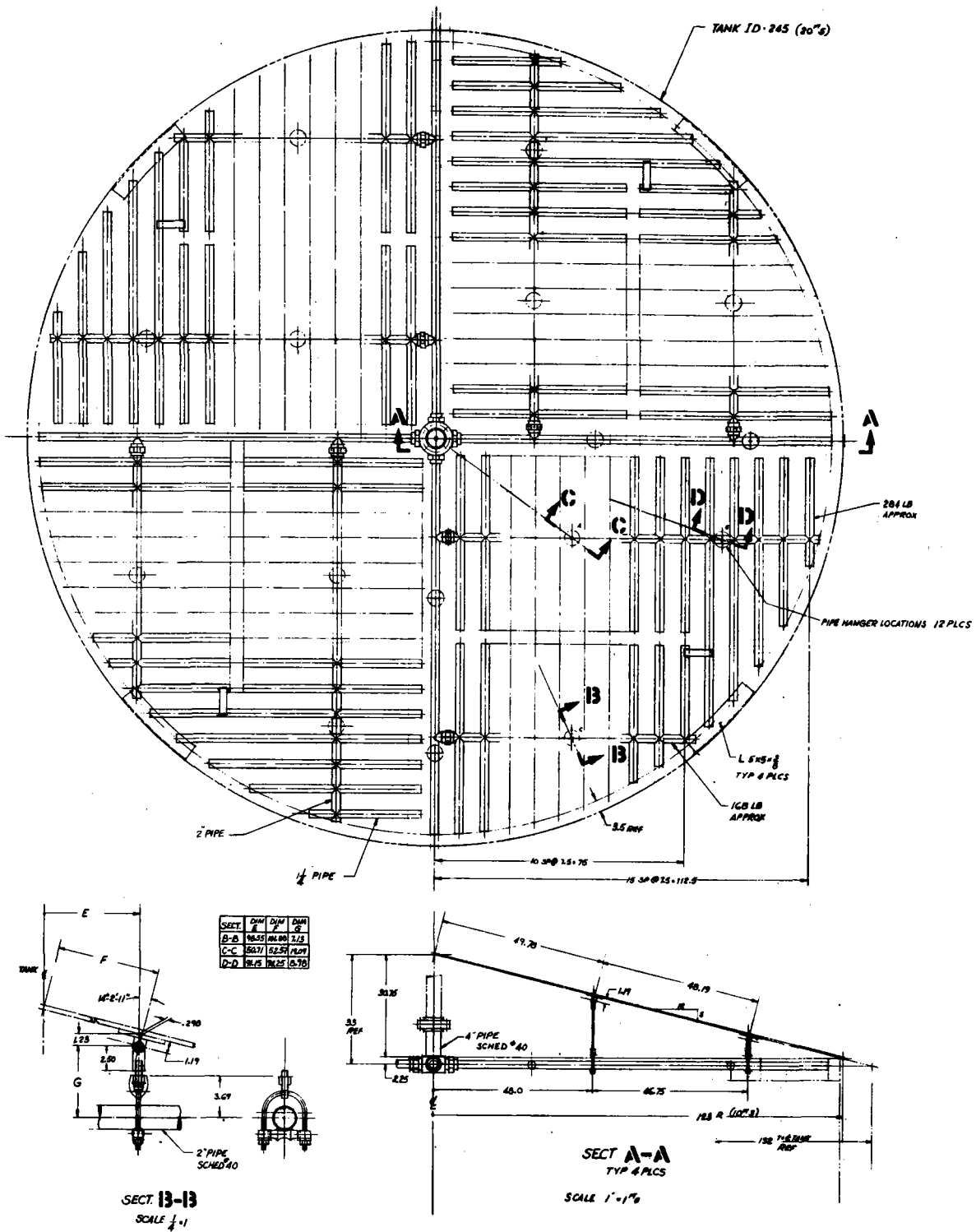


Figure 4.2-12. Tank Inlet Piping Arrangement

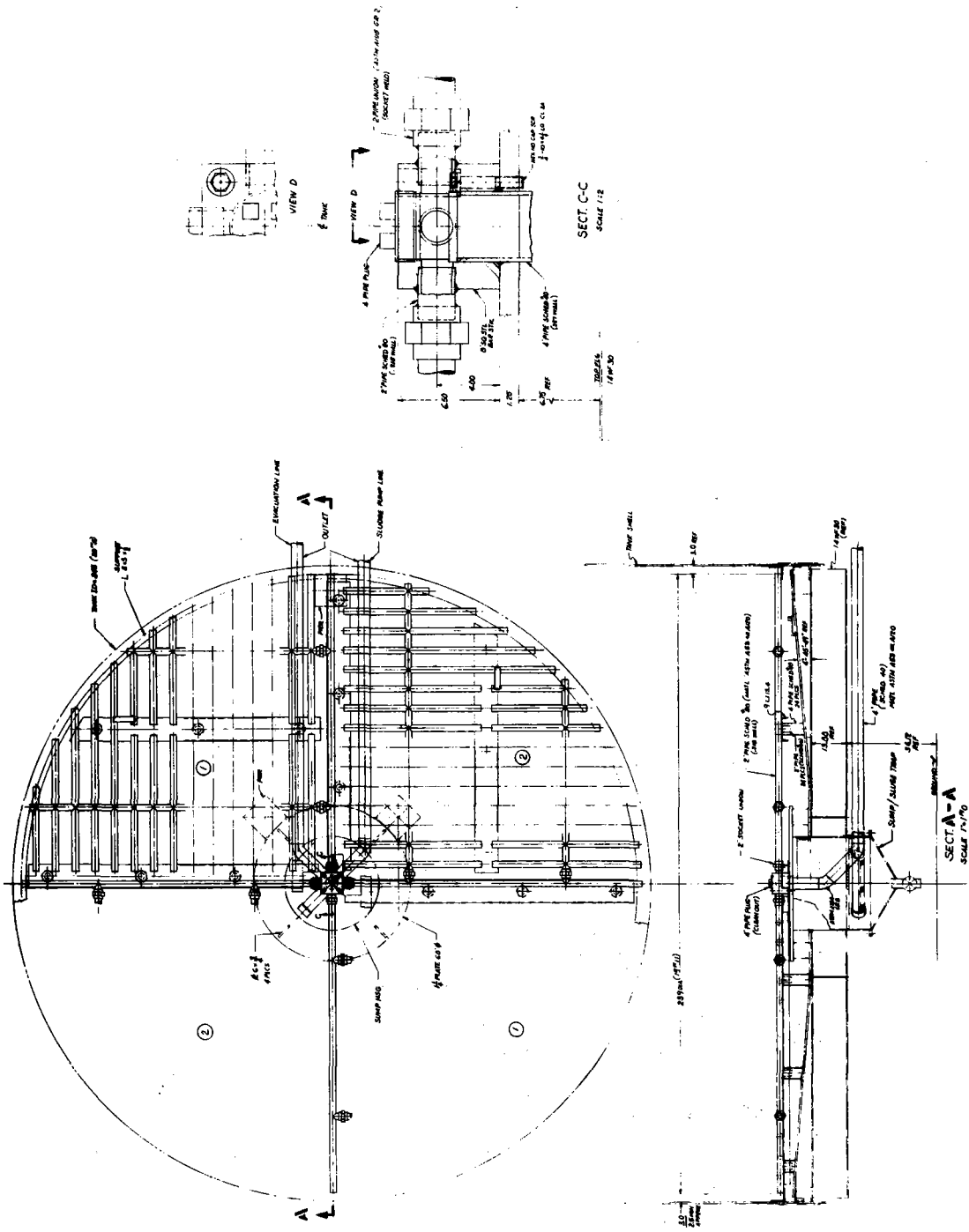
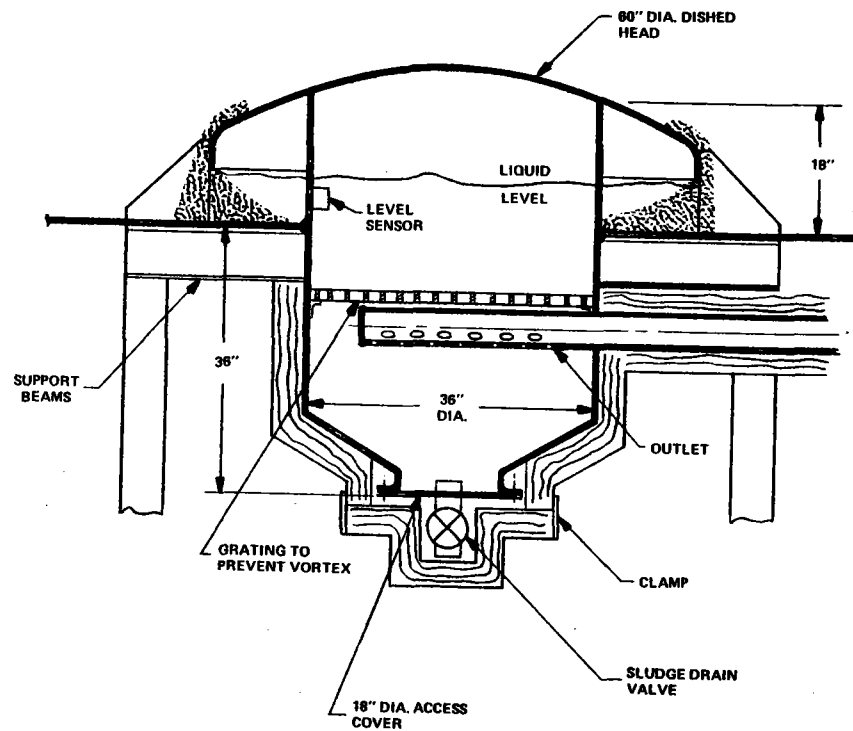


Figure 4.2-13. Tank Outlet Piping Arrangement



DESIGN CHARACTERISTICS

- SUMP LOCATED IN CENTER OF TANK WITH SLOPED BASE
- COARSE MEDIA LAYER ON BOTTOM
- SUMP VOLUME ~ 160 GALLONS
- VORTEX PREVENTION DESIGN
- GUSSET SUPPORT TO DISTRIBUTE LOAD TO BASE LEGS

Figure 4.2-14. Sump Design

4.2.1.4.3 SCS Pumps

Pumping Power for the entire Solar Collection Subsystem is supplied by high temperature centrifugal pumps which are located in the Mechanical Building. These pumps are designed to operate at 672°K (750° F) and have water cooled stuffing boxes and bearing frames. Totally enclosed, fan cooled, 3 phase motors drive the pumps. The casing of each pump in the SCS is flange connected to the tubing through free flexing expansion joints to minimize axial and lateral displacement loadings during thermal expansion. The pump casing is also insulated. Each pump has isolation valves for maintenance and a pump casing drain. A cross-sectional view of a typical pump along with a list of materials of construction is shown in Figure 4.2-15.

4.2.1.4.3.1 Collector Field Pumps. A set of two centrifugal pumps supply the pumping needs of the Collector Field Subsystem. Each pump is rated for 0.020 m³/sec (320 gpm) at 49 m (160 ft) of head, and when operated together, in parallel, they can provide the maximum collector field flow requirements of 0.025 m³/sec (390 gpm) at 67 m (220 ft) of head. This parallel pump design provides greater system reliability and reduced power consumption. As indicated on Figure 4.2-16, single pump operation can provide sufficient flow to the collector field for 2/3 of the time during the average day. The second pump is needed only during the peak insolation period each day. With this parallel operation, peak power consumption is less than 30 kW. A characteristic pump curve for the CFS pumps is shown in Figure 4.2-17.

4.2.1.4.3.2 HTS Transfer Pumps. A single centrifugal pump supplies the pumping power required to transfer the heated Syltherm 800 fluid from one HTS tank to another. This pump is rated at 0.25 m³/sec (390 gpm) at a head of 25 m (81 ft). The installation of this pump is similar to that of the CFS pumps except that there is no bypass or redundancy. A characteristic pump curve is shown in Figure 4.2-18.

4.2.1.4.3.3 Steam Generator Supply Pump. The steam generator supply pump delivers the heated Syltherm 800 fluid to the steam generator. This pump is rated for 0.021 m³/sec (325 gpm) at 31 meters (102 ft) and is capable of providing the maximum flow rate required by the steam generator during all modes of operation. This pump has a modulated bypass to provide flow adjustments to compensate for the pressure drop across the steam generator. A characteristic pump curve for the steam generator supply pump is shown on Figure 4.2-18.

4.2.1.4.3.4 Fossil Heater Booster Pump. The fossil fuel fired Syltherm 800 Heater has a single centrifugal pump rated for 0.021 m³/sec (325 gpm) at 31 meters (102 ft) of head. This pump is part of the Syltherm 800 heater package, and it can be used to supply heated fluid to the collector field, to the HTS tanks, or to the steam generator.

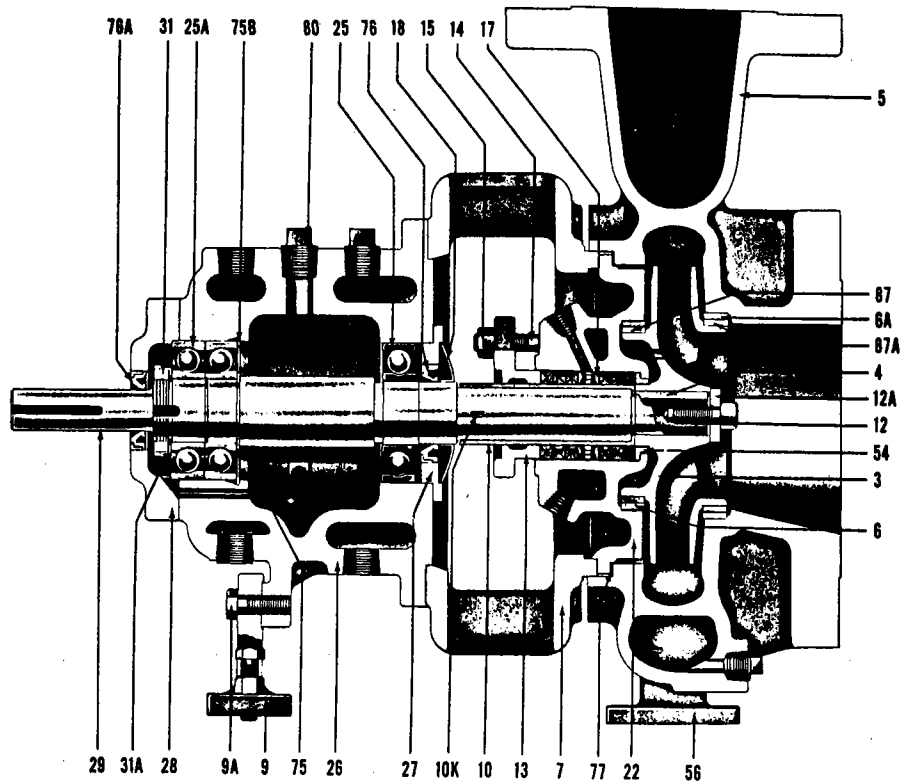
4.2.1.5 Control and Instrumentation

4.2.1.5.1 Tracking Control

When in the tracking mode, each axis of the collector will operate in one of two modes depending upon the level of solar insolation. During intermittent cloudy periods, pointing angles for each axis are calculated in the computer and provide command angles for closed loop position control. At insolation levels above threshold, sun tracker operation takes over, and each axis is operated by sun tracker developed errors. In this mode, position errors are limited by monitoring the computed positions to establish sun tracker position error thresholds.

After morning start-up, each of the polar axis motors are operated alternately. Further, within a group of collectors, motors are operated sequentially to minimize power surges on the motor supply system.

The tracking control has the capability to return to the morning start-up position after evening shutdown. The polar motors are operated sequentially as are the collectors within the group. Each collector also has the capability to be programmed to a stow position and a maintenance position if different from stow.



STANDARD MATERIALS OF CONSTRUCTION—LISTED BY MATERIAL CLASS							
PART #	PART NAME	CLASS 40	CLASS 50	PART #	PART NAME	CLASS 40	CLASS 50
3	Impeller	C.I. (1)	316 (3)	25	Shaft Bearing—Radial	Stl.	Stl.
4	Impeller Key	Stl. (2)	316 (8)	25A	Shaft Bearing—Thrust	Stl.	Stl.
5	Casing	Stl. (6)	316 (3)	26*	Bearing Housing	C.I. (1)	C.I. (1)
6*	Backhead Ring	Iron (7)	316 (3)	27*	Seal Ring	C.I. (1)	C.I. (1)
6A	Casing Ring	Iron (7)	316 (3)	28	Bearing End Cover	C.I. (1)	C.I. (1)
7	Cradle Spacer	C.I. (1)	C.I. (1)	29*	Pump Shaft	Stl. (10)	316 (8)
9	Bearing Housing Foot	C.I. (1)	C.I. (1)	31	Bearing Lock Nut	Stl.	Stl.
9A*	Brg. Hsg. Ft. Capscrew	Stl. (2)	Stl. (2)	31A	Bearing Lock Nut Washer	Stl.	Stl.
9F*	Brg. Hsg. Ft. Jack Bolt	Stl. (2)	Stl. (2)	54*	Throat Bushing	C.I. (1)	316 (8)
9G*	Brg. Hsg. Ft. Jack Bolt Nut	Stl. (2)	Stl. (2)	56	Casing Foot	C.I. (1)	C.I. (1)
10*	Shaft Sleeve	316 (8)	316 (8)	75	Snap Ring—Inner Shaft	Stl.	Stl.
10K*	Shaft Sleeve Key	304 (9)	304 (9)	75B	Snap Ring—Inner Housing	Stl.	Stl.
12*	Impeller Bolt	Stl. (2)	316 (8)	76	Oil Seal	Buna	Buna
12A*	Impeller Washer	Stl. (2)	316 (8)	76A	Oil Seal	Buna	Buna
13*	Stuffing Box Gland	Stl. (6)	316 (3)	77	Casing Gasket	Asbestos (11)	Asbestos (11)
14*	Stuffing Box Gland Stud	Stl. (4)	304 (9)	77B*	Bearing End Cover Gasket	Paper (12)	Paper (12)
15*	Stuffing Box Gland Stud Nut	Stl. (5)	304 (9)	80	Oil Vent Plug	C.I.	C.I.
17*	Lantern Gland	C.I. (1)	316 (3)	87*	Impeller Ring—Back (Optional)	C.I. (1)	316 (3)
18*	Splash Collar	Stl. (13)	Stl. (13)	87A	Impeller Ring—Front (Optional)	C.I. (1)	316 (3)
22	Backhead	Stl. (6)	316 (3)				

*Denotes parts interchangeable in all pump sizes of same type.

Figure 4.2-15. Pump Cross Section and Materials

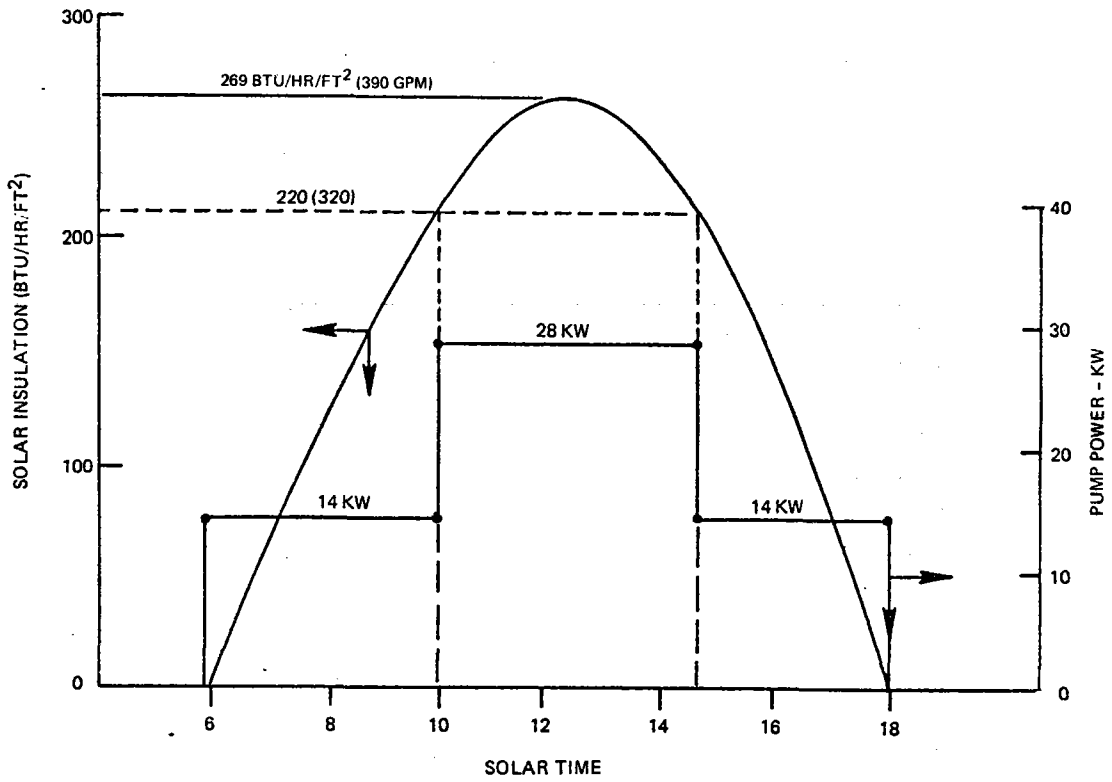


Figure 4.2-16. Solar Insolation and Pump Power VS Solar Time

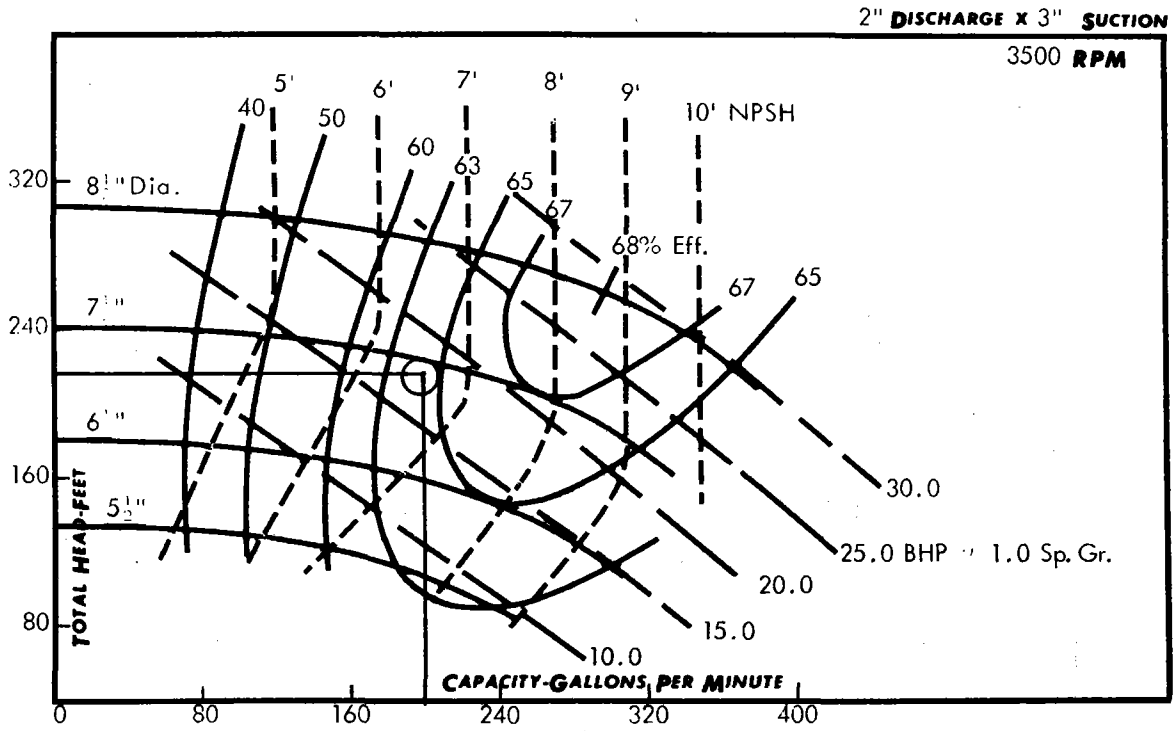


Figure 4.2-17. CFS Pump Characteristic Curve

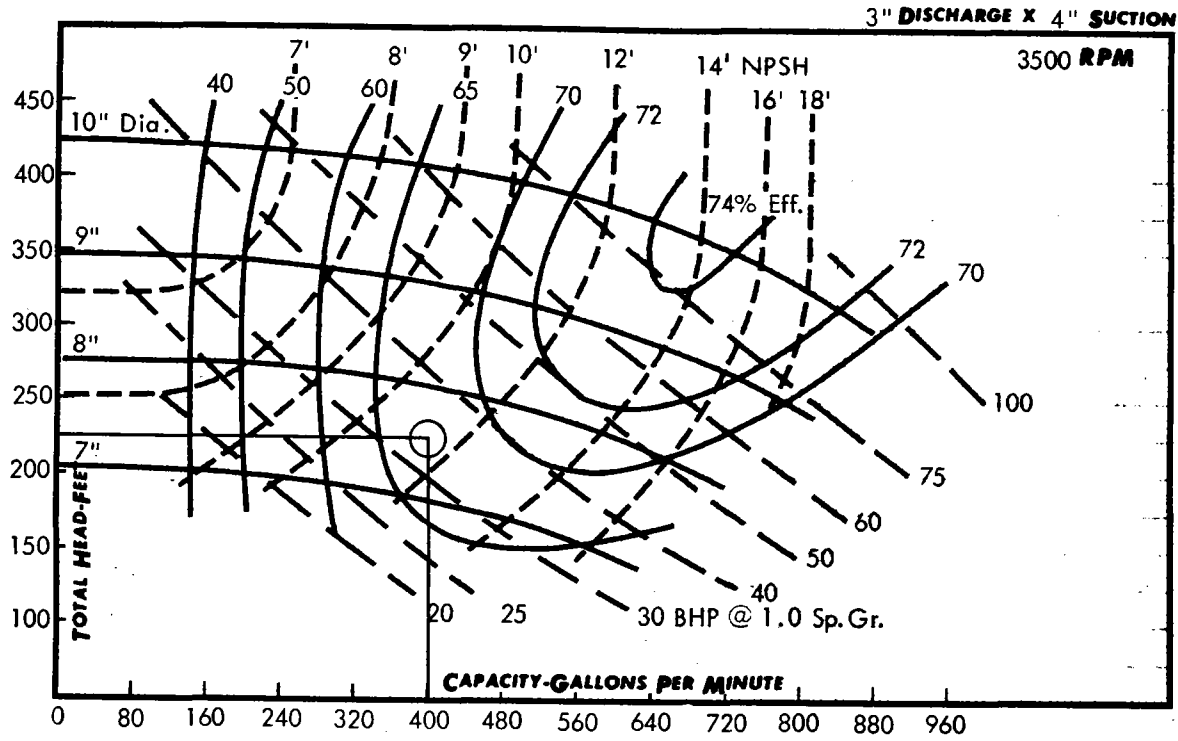


Figure 4.2-18. HTS and SGS Pump Characteristic Curves

Each receiver is provided with an overtemperature sensor and controller. In the event of an overtemperature, this controller is actuated and the collector defocused by operation of the polar dc motor. Rotation will be toward the morning position. An alarm is provided with an emergency power supply. Upon the loss of the ac bus, the dc motor will defocus the collector on emergency power. Also the controls prevent focusing of the collectors until fluid flow has been established in the receivers.

Collector tracking operation will be tested by operator command at the micro-processor or central computer level. Operation will be monitored at these locations using standard readout equipment.

4.2.1.5.2 Field Temperature Control

The required collector field flow is calculated from solar insolation, shading factor, and other pertinent parameters. The calculated value is then used to adjust the centrifugal pump bypass flow so as to provide the correct flow to the collector field. In this way, operation of the pump is held near a fixed point for maximizing its efficiency.

The collector flow paths are paralleled in groups to a branch per design field layout. The flow in each receiver is manually adjusted during initial startup with trim flow valves so that all receivers in a branch will have equal flow at maximum insolation condition. The inlet flow to the branch is controlled by a flow control valve operated by a temperature controller. The discharge temperature of all receivers is instrumented and the highest used for operating the temperature controller so long as it is below the trip out (defocus) temperature for the receiver. If the receiver discharge temperature exceeds the alarm (defocus) temperature, the collector is defocused to reduce the receiver temperature. An audible/visible alarm is provided and manual reset required.

4.2.1.5.3 Thermal Energy Storage Controls

The bottom and top tank temperatures are used to establish the status of each storage tank along with its most recent history of operation. For the trickle oil mode, a tank is charged with hot fluid in the top and discharged with hot fluid exiting the bottom. In the thermocline mode, hot fluid enters and leaves the top of the tank for charge and discharge respectively.

The control processor will determine when to charge or discharge the tank based on the energy available from the collector field and the energy requirements of the system. The various on/off valves in the system will be operated by the logic to accomplish this.

The processor will determine if sufficient energy can be obtained from the collector field to charge the tanks or operate the system. It will also determine when to discontinue field operation due to low solar insolation or a fully charged TES.

The processor will also determine the status of all tanks and the system energy requirements. The fossil heater will be actuated if the stored energy level drops below a preselected threshold value.

4.2.2 Power Conversion Subsystem (PCS)

4.2.2.1 Function

The Power Conversion Subsystem uses the steam generated in the solar steam generator to drive the turbine generator set. A portion of this steam is extracted at a mid-point in the turbine expansion to provide steam for process use in the Bleyle Plant. At the turbine discharge, steam flows to the condenser which provides the source of heat for the Thermal Utilization Subsystem. The turbine driven generator provides the electrical power required for the operation of the STES and the Bleyle Plant.

4.2.2.2 Subsystem Configuration

The Power Conversion Subsystem piping and instrumentation diagram is shown in Figure 4.2-19. As can be seen from this diagram, the PCS has direct interface connections with various other subsystems. The steam generator serves as the boundary between the PCS and the Solar Collection Subsystem. The condenser forms the boundary between the PCS and the Thermal Utilization Subsystem. The turbine generator set links the PCS with the Electrical Subsystem, and the process steam lines of the PCS connect with the Bleyle Plant steam distribution system. The various input/output devices used throughout the PCS serve as the interface and communications link with the Control and Instrumentation Subsystem.

4.2.2.3 Detailed Subsystem Description

The flow circuitry of the Power Conversion Subsystem is illustrated by Figure 4.2-20. Detailed circuitry of the make-up demineralizer unit is indicated in Figure 4.2-21.

Heat energy input to the PCS is supplied through a flow of liquid Syltherm 800 at a temperature of 672°K (750°F) from the Solar Collection Subsystem. This flow passes through the tube sides of the steam generator heat exchanger units in which superheated steam at $4.83 \times 10^6 \text{ N/m}^2$ (700 psig), 655°K (720°F) is produced. The steam pressure is controlled by variation of the Syltherm 800 flow rate. A small variation of superheat temperature ($\pm 10^\circ \text{ F}$) occurs over the full range of discharge steam flow. During normal operation, steam is admitted to the turbine through the control valves. Combined function stop valve/throttle valves are located upstream of the control valves for start-up/shutdown and emergency shutdown. The turbine drives a synchronous generator through a reduction gear. At a mid point in the turbine expansion, steam is extracted for process use and also for feedwater deaeration/heating. The extraction port pressure is maintained at or above the required process steam delivery pressure throughout the kWe/process steam load range. The extracted steam, which has a substantial superheat, is conditioned to the process requirement of $7.24 \times 10^5 \text{ N/m}^2$ (105 psig), saturated, through controlled throttling and desuperheating by spray injection of condensate out of the condenser hot well. At the turbine discharge steam flows to the condenser through a gate valve and a short make up water preheating passage into which the make up water from the condensate storage tank is sprayed. The major portion of the condenser thermal load is delivered to the Thermal Utilization Subsystem through a flow of circulating water. This flow is controlled so as to maintain a constant condenser pressure. The design provides for minimum hot well condensate subcooling in order to minimize heat input requirement. Hot well level is controlled by a float actuated valve in the make-up injection line. There is also an on-off valve through which condensate can be delivered to the condensate storage tank from the condensate pump discharge. The hot well storage capacity is sufficient for four minutes operation at full load. Make-up water needed to replace the process steam flow is admitted to the makeup demineralizer from the plant water supply at a rate controlled by the condensate storage tank level control.

From the condenser hot well, condensate is pumped by the condensate pump to the deaerator. The deaerator has a storage capacity sufficient for six minutes of operation at full load. The deaerator incorporates a storage level control which regulates condensate in-flow. In the deaerator, entering condensate leaves in a saturated condition at deaerator pressure. From the deaerator the heated condensate passes to the boiler feed pump. Near the suction of this pump, hydrazine and ammonia are injected into the feed water by means of metering pumps from which flow is controlled in response to inputs from sensors of dissolved O₂ (hydrazine control) and pH (ammonia control). The boiler feedwater pump discharge pressure is controlled by a recirculation valve which maintains a constant pressure at the steam generator control valve inlet.

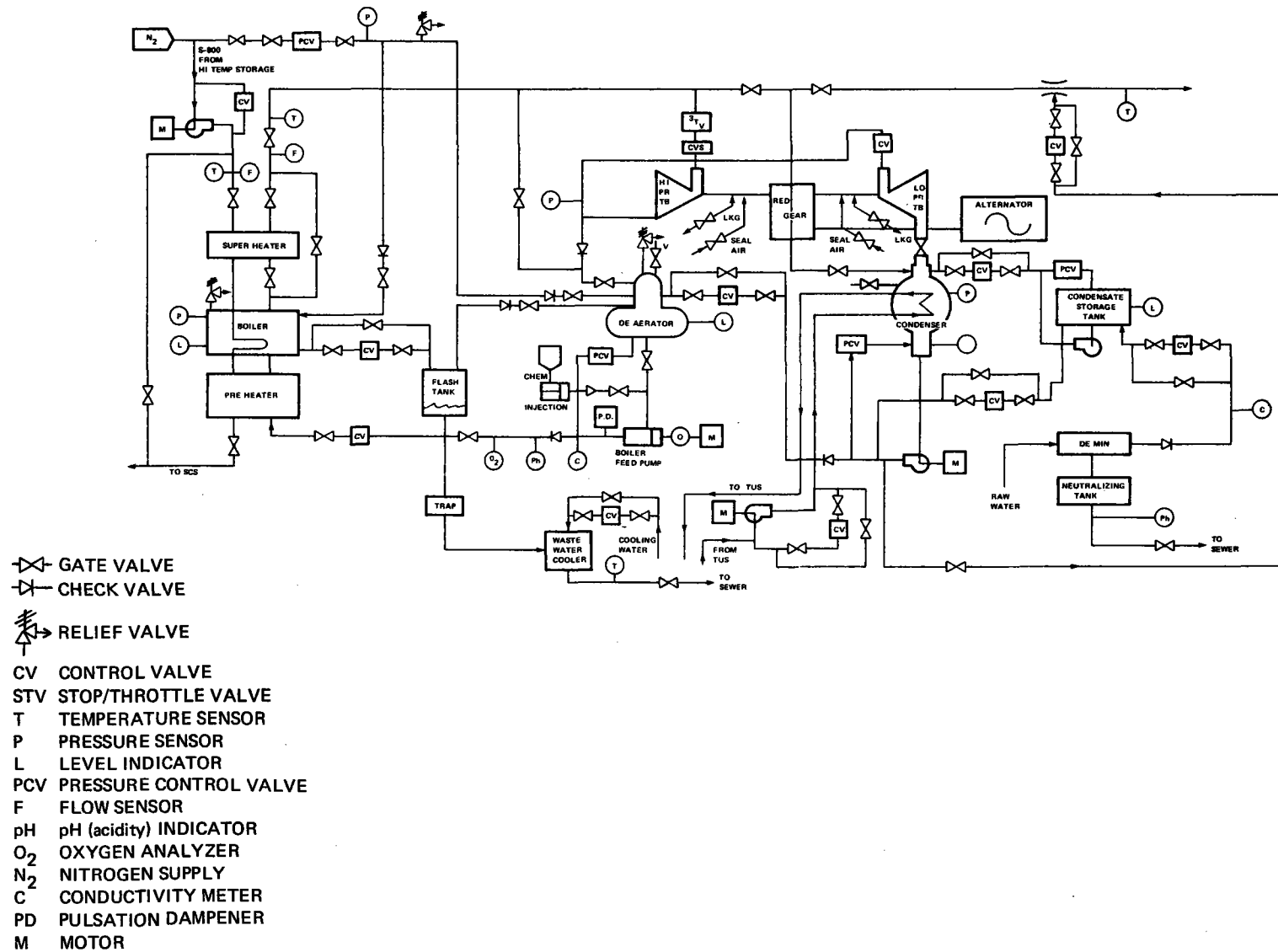


Figure 4.2-20. Power Conversion Subsystem Flow Circuit

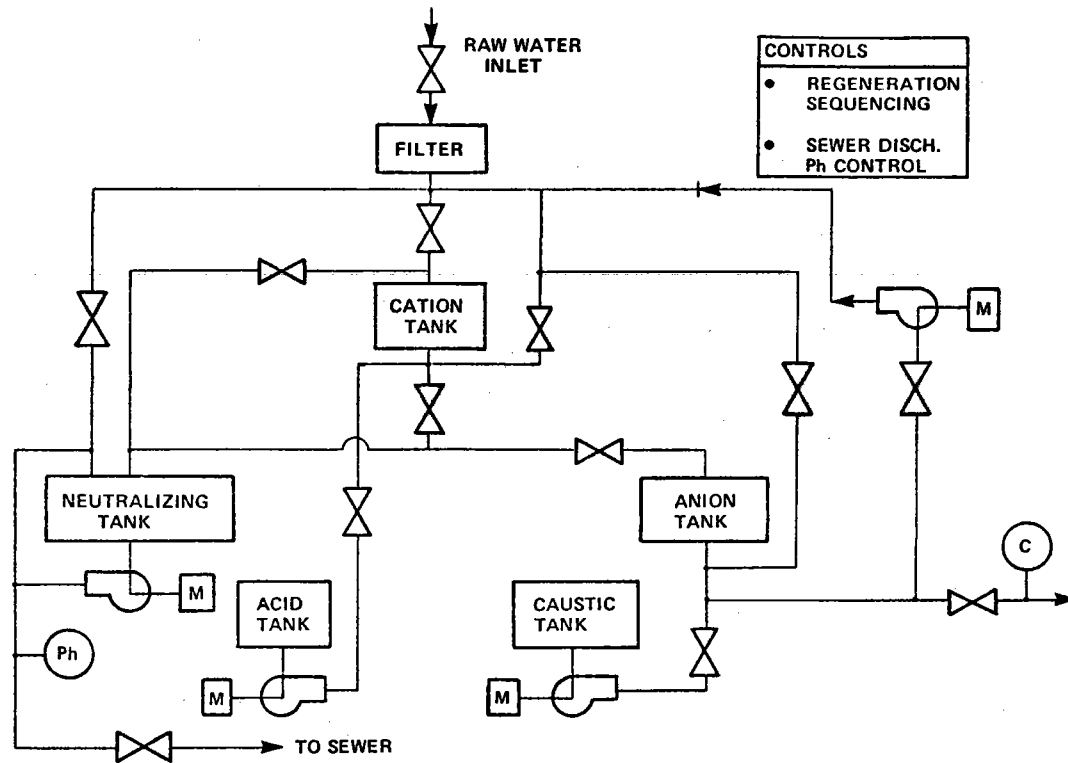


Figure 4.2-21. Demineralizer Unit Flow Circuit

4.2.2.4 Major Components

4.2.2.4.1 Steam Generator

The steam generator is a skid mounted assemblage of three heat exchangers: a counterflow preheater, a drum-type pool boiler with immersed heater tubes, and a counterflow superheater. The Syltherm 800 flow is on the tube side in all heat exchangers. Feedwater is admitted to the preheater through a control valve which operates to maintain the boiler drum level. The preheater discharges water into the boiler drum. Immersed in this drum are Syltherm 800 tubes which enter and leave at one end. Saturated steam leaves the drum and passes to the superheater from which it flows to the turbine. Approximate dimensions of the heat exchanger shells are: preheater, 0.30 meter dia. x 3.66 meter long (1 ft dia. x 12 ft long); boiler, 0.61 meter dia. x 4.57 meter long (2 ft dia. x 15 ft long); superheater, 0.30 meter dia. x 3.05 meter long (1 ft dia. x 10 ft long).

Water is continually bled from the boiler drum through a blowdown valve from which it is passed to a flash tank operating at deaerator pressure. Steam formed in the flash tank is passed to the deaerator, and the water is passed through a trap to a second (atmospheric pressure) flash tank in which both water and steam are cooled and condensed to a maximum temperature of 300° K (80° F) by a controlled flow of cooling water for discharge to the sewer.

4.2.2.4.2 Turbine Generator

The turbine-generator unit consists of two high speed axial flow turbines coupled through reduction gearing to 30 rev/s (1800 rpm) synchronous alternator. The unit is being supplied to the program GFE and is manufactured by Mechanical Technology Incorporated (MTI). An extraction port is provided after the first turbine for removal of steam for process use and for supply to a deaerating feedwater heater. The pressure level at this port is above the required process steam pressure level of $7.24 \times 10^5 \text{ N/m}^2$ (105 psig) throughout the operating range of 200-400 kW electrical load.

4.2.2.4.3 Condenser

The condenser unit comprises a two pass heat exchanger contained in a 0.61 meter (2 ft) diameter cylindrical shell. Water coolant tubes extend 4.88 meters (16 ft) between tube sheets, supported by two intermediate support plates. Tubes are expanded into the tube sheets and are slightly bowed upward for drainage and accommodation of differential expansion between the shell and the tubes. Dished heads enclose water boxes at both ends of the shell. The condenser is joined to the turbine discharge valve flange through a make up inlet spray passage discharging into the shell at an upper location. A bellows joint is employed at the turbine discharge valve connection. The shell is suspended from the turbine skid. Opposite the desuperheating passage at the bottom of the shell is the hot well. At each side of the shell near the bottom, a small group of tubes is shrouded from the main stream flow in order to subcool uncondensed vapor containing concentrated air which is vented from the shell. Air vents guarded by thermostatic valves are located at each side of the shell.

The hot well level is controlled during normal operation by variation of the rate of make-up water injection. For reduction of PCS water inventory during startup and establishment of normal steam generator operation, condensate is pumped back to the condensate tank.

4.2.2.4.4 Make-Up Demineralizer

The make-up demineralizer is a skid mounted unit including cation and anion resin tanks, caustic and acid regeneration tanks with pumps, and a neutralizing tank. An activated carbon inlet filter is also included to insure uniform discharge water quality under non constant flow. A recirculation pump is provided.

4.2.2.4.5 Condensate Pump

The condensate pump is a regenerative (turbine) type pump. This pump receives flow from the condenser hot well and discharges to the deaerator and to the process steam desuperheater. There is also a discharge connection to the condensate storage tank. Discharge pressure is controlled by a pressure control valve through which water recirculates to the hot well. The pump is directly driven by a 29.2 rev/sec (1750 rpm) induction motor.

4.2.2.4.6 Deaerating Heater

The deaerator is an open feedwater heater in which condensate is spread in thin sheets over successive layers of air separating trays where it is raised to saturation temperature through contact with injected steam. In this process, the steam is desuperheated and condensed, adding to the quantity of saturated deaerated water which is delivered to the storage volume in the lower part of the shell. Residual steam and entrained air are passed from the shell to the vent condenser which is cooled by the incoming condensate before being vented to the atmosphere.

4.2.2.4.7 Boiler Feed Pump

The boiler feed pump is a three cylinder, horizontal plunger pump driven from a crankshaft through a connecting rod-cross head mechanism. Main bearings at the ends of the crankshaft are tapered roller type. Valves are mounted in replaceable bushings. The plungers are externally sealed with packing. The pump is driven at 6.67 rev/s (400 rpm) through a V belt drive from a 29.2 rev/s (1750 rpm) induction motor.

4.2.2.5 Controls and Instrumentation

A block diagram of the boiler-turbine control is shown in Figure 4.2-22. The turbine speed/load control is indicated in further detail in Figure 4.2-23. As indicated by these diagrams, the turbine load is controlled by regulation of the utility load to a constant value for interconnected operation, and for

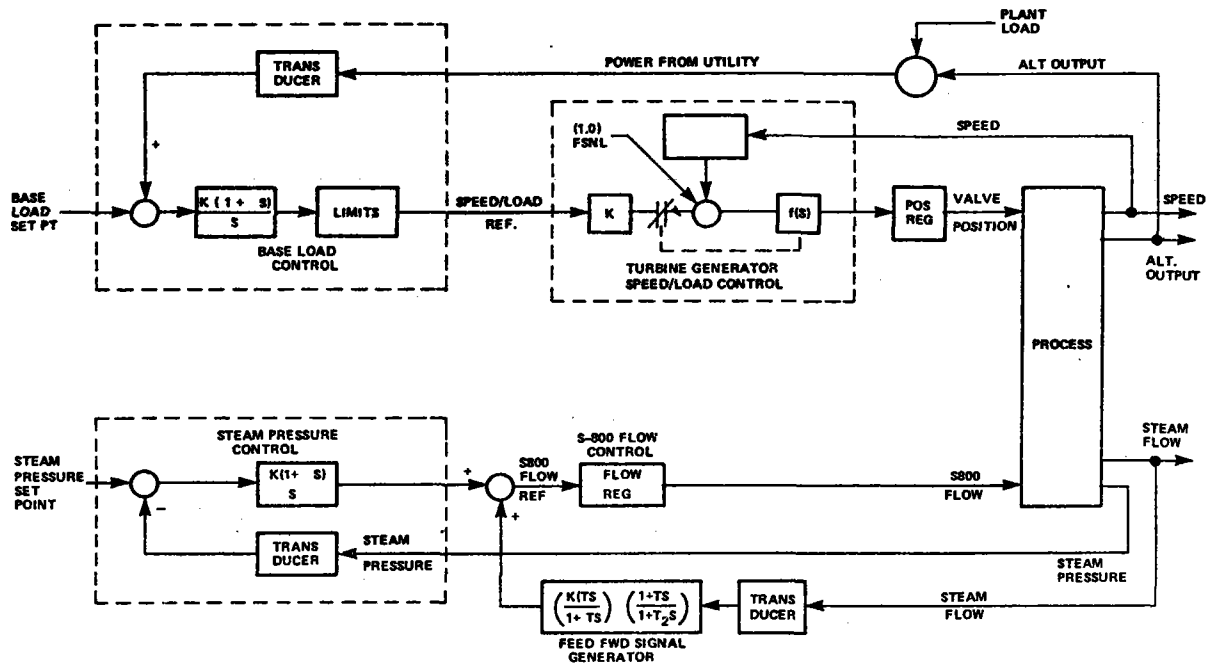


Figure 4.2-22. Boiler-Turbine Control

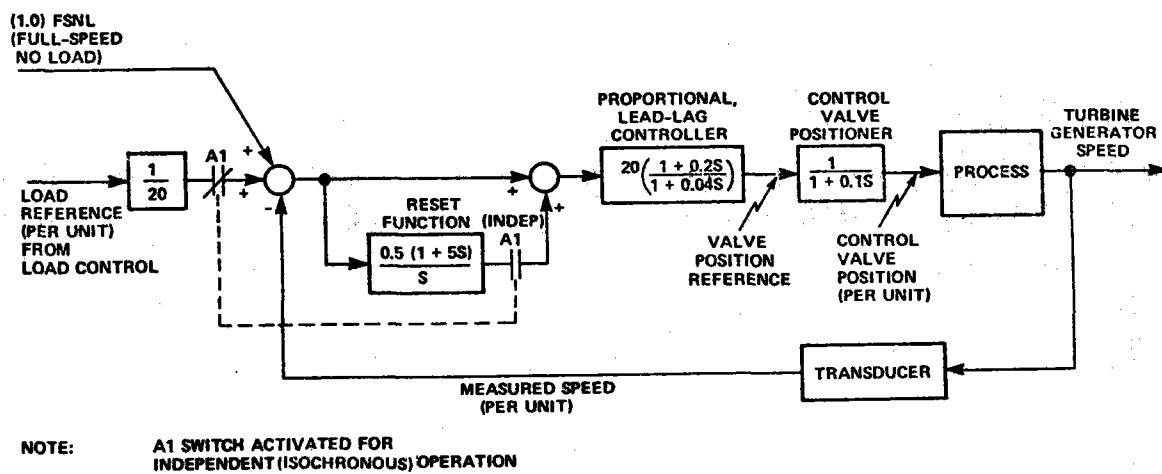


Figure 4.2-23. Turbine Generator Speed/Load Governor Control (For Both Interconnected and Independent Operation)

independent operation, the speed is regulated to a constant value as load varies. Steam pressure is controlled by variation of feedwater flow as the turbine valve position is varied, and steam temperature is controlled by variation of Syltherm 800 flow rate. The temperature control loop utilizes a feed forward signal from turbine throttle flow as indicated by first stage shell pressure as well as a feedback signal from throttle temperature. In addition to the operational controls described by the block diagrams, the turbine is subject to trip-out controls initiated by contingency events:

1. Loss of electrical load
2. Equipment malfunction as indicated by out of limit signals from monitored parameters:
 - Bearing Temperatures
 - Rotor Vibrations
 - Water quality
 - Frequency
 - Voltage

4.2.3 Thermal Utilization Subsystem (TUS)

4.2.3.1 Function

The Thermal Utilization Subsystem serves as the condensing medium for the steam condenser and the heat source for the heating and cooling of the Bleyle Plant and the Mechanical Building. The exhaust heat from the steam turbine provides the heat input to the TUS. When the turbine is out of service, steam will be provided directly to the condenser. A large, Low Temperature Storage (LTS) tank is included in the TUS for the storage of thermal energy. Excess energy is dissipated through two cooling towers. Chilled and heated water are pumped to the Bleyle Plant and the Mechanical Building for cooling and heating purposes.

4.2.3.2 Subsystem Configuration

The Thermal Utilization Subsystem Piping and Instrumentation Drawing (P & ID) is shown in Figure 4.2-24. The steam condenser acts as the system boundary between the TUS and the Power Conversion Subsystem. The chilled and heated water lines of the TUS connect with the HVAC distribution system in the Bleyle Plant.

4.2.3.3 Detailed Subsystem Description

The Thermal Utilization Subsystem is shown on the piping and instrument drawing, Figure 4.2-24. The flows shown are at 400 kW(e). Using this figure as a guide, water is circulated through the condenser by using the discharge of the low temperature storage pump. The heated water from the condenser may then be placed in the low temperature storage tank. The hot water will enter in the top of the low temperature storage tank, and relatively cold water will be removed from the bottom of the tank to the suction of the low temperature storage pump. In the event of excess thermal energy (low temperature storage tank too hot), the condenser cooling tower may be used to cool the condenser circulating water discharging from the low temperature storage tank. Water is routed from the cooling tower by the condenser cooling tower pumps to the heat exchanger and then back to the cooling tower.

A hot water pump is provided. It takes suction from the hot water line leaving the steam condenser. The pump discharges either to the heat exchanger supplying Bleyle heating or to the absorption air conditioner. The heat exchanger is used to extract the heat from the hot water pump discharge and to transfer this to the water supply for heating the Bleyle plant.

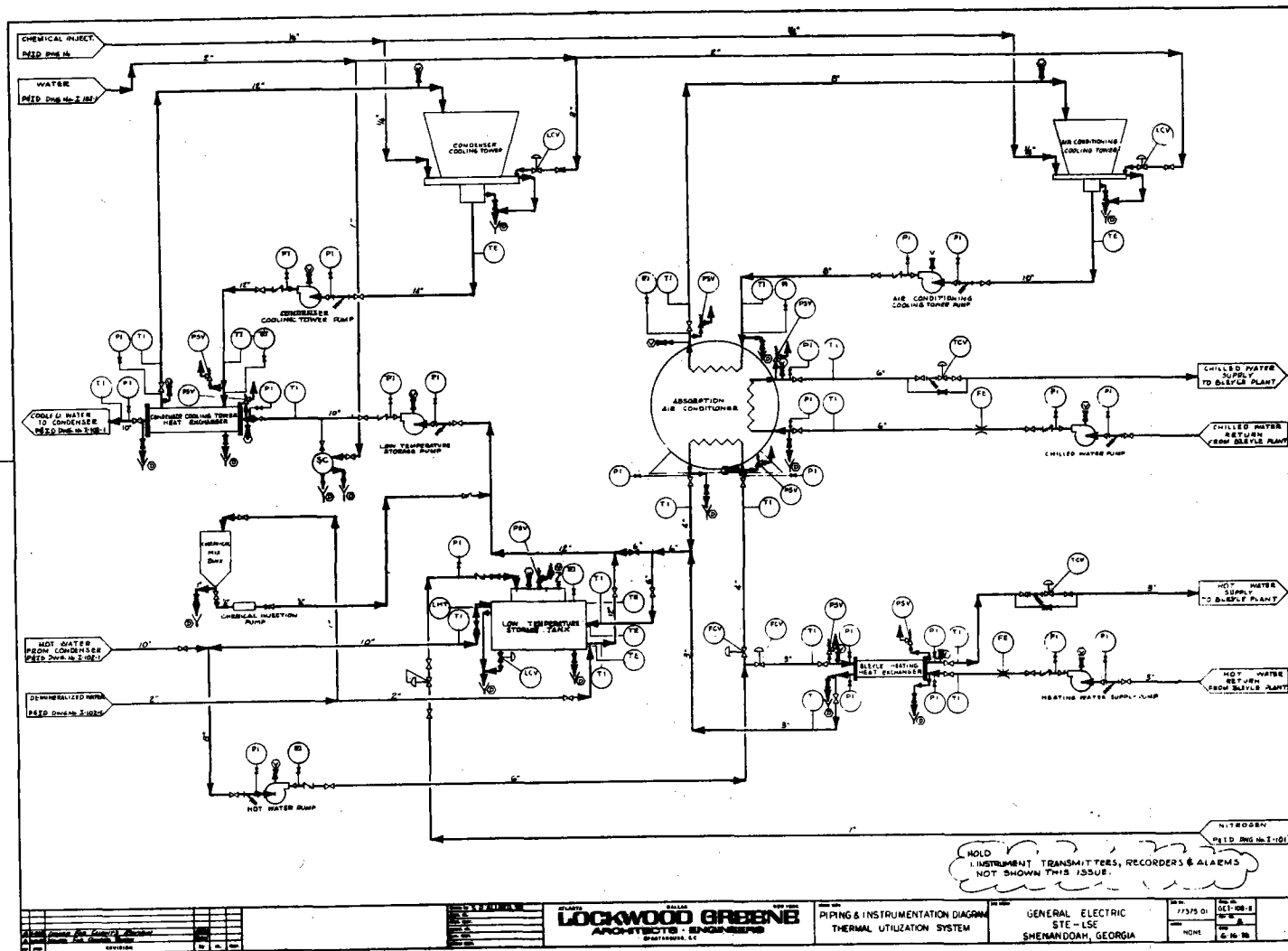


Figure 4.2-24. Piping & Instrumentation Diagram - Thermal Utilization Subsystem

The hot water from the discharge of the hot water pumps is routed through the absorption air conditioner. The heat from the water is used as the heating source in the absorption air conditioner. The expanded gas is used to cool the cooling water supply to the Bleyle Plant. The water pumped by the hot water pump leaves the absorption air conditioner and then may go to the middle of the low temperature storage tank, if heat is still available in the water, or may flow to the suction of the low temperature storage pump.

4.2.3.4 Major Components

4.2.3.4.1 Low Temperature Storage Tank

A 458 cubic meter (121,000 gallon) storage tank is provided for stratified storage of thermal energy. The storage tank is used to store heated water in the top and cool water in the bottom. There are three water connections on the tank:

1. Top connection - Hot water can enter the tank from the condenser or can be drawn from the tank with the hot water pump.
2. Middle connection - Cooled water can enter the middle connection from the Bleyle heating heat exchanger or from the absorption air conditioner.
3. Bottom connection - Provides suction (cool water) to the low temperature storage pump.

The tank is provided with a make-up water supply, relief valve, a vacuum breaker, and a nitrogen supply. The tank is sized to accommodate thermal expansion for the system. Drains and overflow controls are provided. The tank is located south of the Mechanical Building. It will be 9.1 meters (30 ft) in diameter and 7 meters (23 ft) high and insulated.

4.2.3.4.2 Absorption Air Conditioning Unit

A 1.25×10^6 J/s (354 ton) Absorption Air Conditioner (AAC) is provided inside the Mechanical Building. The packaged absorption air conditioner will consist of a 5.6 kW (7-1/2 hp) sealed pump, a 190 watt (1/4 hp) purge pump, an absorber, evaporator, concentrator, condenser and a heat exchanger. Thermal energy is provided to the AAC by $0.018 \text{ m}^3/\text{s}$ (285 gpm) water at a nominal temperature of 372°K (210°F).

Cooling tower water is provided to the AAC at 302°K (85°F) and $0.057 \text{ m}^3/\text{s}$ (900 gpm). The water leaves the AAC at 309°K (96°F). Chilled water at 280°K (45°F) will be supplied to Bleyle at a flow rate of $0.026 \text{ m}^3/\text{s}$ (407 gpm). The water will be returned from Bleyle at 286°K (55°F).

The AAC utilizes the proven lithium bromide-water, absorption refrigeration cycle. This cycle takes place in a sealed hermetic shell from which essentially all air has been removed. Consequently, the pressures within the shell are the vapor pressures of the liquids used in the cycle at their respective temperatures. In operation, the pressure in the absorber and the evaporator section is about 1000 N/m^2 (1/100th of an atmosphere). Pressure in the concentrator and condenser sections is about $1 \times 10^4 \text{ N/m}^2$ (1/10th of an atmosphere). In the operating cycle, distilled water is used as the refrigerant and lithium bromide as the absorbent.

4.2.3.4.3 Cooling Towers

Two cooling towers are being provided. The AAC cooling tower is a nominal $7.0 \times 10^5 \text{ J/s}$ (200 ton) double flow unit. It will be provided with a 7.5 kW (10 hp) fan driven through a gear reducer. The tower is capable of operating through a range of 0.012 to $0.071 \text{ m}^3/\text{s}$ (190 to 1125 gpm) of cooling tower water flow. It will be provided with an overflow, make-up system and chemical treatment system. Construction of baffles for water droplet dispersion will be PVC. Casing and louvers will be corrugated asbestos. An access ladder will be provided to the fan.

The condenser cooling tower is a 2.1×10^6 J/s (600 nominal ton) double flow unit. It will be provided with a 30 kW (40 hp) fan driven through a gear reducer. The tower is capable of operating through a range of 0.038 to 0.0151 m³/s (600 to 2400 gpm) cooling water flow. Construction materials will be similar to the AAC cooling tower.

4.2.3.4.4 Condenser Cooling Tower Heat Exchanger

The condenser cooling tower heat exchanger shall be capable of cooling 0.060 m³/s (950 gpm) of water at 375°K to 364°K (215°F to 195°F). It will give up its heat to the condenser cooling tower water that will flow at 0.011 m³/s (696 gpm) at 302°K (85°F) and return at 308°K (95°F). The hot water will flow through the shell. The cool water will be on the tube side.

4.2.3.4.5 Pumps

The following pumps will be used in the Thermal Utilization Subsystem. All pumps will be driven by 480V, 3 phase motors with local and remote start-stop controls.

1. The low temperature storage pump will be capable of pumping .057 m³/s (900 gpm) @ 34 meter (110 ft) head
2. The condenser cooling tower pump will be capable of pumping 0.107 m³/s (1700 gpm) @ 12 meter (40 ft) head.
3. The air conditioning cooling tower pump will be capable of pumping 0.057 m³/s (900 gpm) @ 15 meter (50 ft) head.
4. The hot water pump will be capable of pumping .016 m³/s (250 gpm) @ 12 meter (40 ft) head.
5. The chilled water pump will be capable of pumping 0.026 m³/s (407 gpm) @ 12 meter (40 ft) head.
6. The heating water supply pump will be capable of pumping .0063 m³/s (100 gpm) @ 12 meter (40 ft) head.

4.2.3.4.6 Piping Valves and Insulation

The piping and valve material specifications for the Thermal Utilization Subsystem are shown on Figure 4.2-25. ASTM A-53 Grade A Schedule 40 welded or seamless pipe will be used. Pipe connections will be welded except for valves and pumps that may be flanged. Standard 57 kg (125 lb) valves will be used. Insulation will be installed on the tanks and piping to minimize heat loss and to prevent sweating when necessary.

4.2.3.5 Controls and Instrumentation

Control functions required by the Thermal Utilization Subsystem include the following:

1. Low temperature storage tank level control. This control will admit make-up water and operate the overflow valve. A vacuum breaker is provided and a relief valve for over pressure protection.
2. Cooling towers - Level controls are provided for control of make-up. Fan controls will be operated remotely by hand.

3. Heating and cooling controls - Hot water may be routed to the AAC or the Bleyle heating heat exchanger. Pneumatic valves are provided for this.
4. Chemical injection - This will be controlled manually.

4.2.4 CONTROLS and INSTRUMENTATION SUBSYSTEM (CIS)

4.2.4.1 Function

The Control and Instrumentation Subsystem (CIS) provides the controls, monitors, and interfaces for all the other subsystems of intervention, the selection of the system operational mode, provisions for controlling all factors of the various subsystems, provisions for monitoring all critical parameters of the various subsystems, protection of the subsystem components, and integration of operation of the system as a whole.

4.2.4.2 Subsystem Configuration

The control and instrumentation functions are provided via the central control console, the central mini-computer and peripheral equipment, and seven remote microprocessor control units. Individual remote control units interact directly with the individual STES subsystems. These units contain conditioning circuitry to convert the digital computer outputs to signals usable by the control actuators and to transform sensor outputs to digital format for scrutiny and recording by the micro- and, as necessary, mini-computers. Control units will act autonomously where possible and will interact with the central processor in a distributed control approach as necessary. The control console and computer terminal will provide input-output control and monitor capability to the operator.

4.2.4.3 Detailed Subsystem Description

Implementation of the various control functions of the STES has been partitioned into distinct areas of device responsibility. Architecturally, the mini-computer is the master system controlling element. Reporting to the mini-computer (Digital Equipment Corp. PDP 11/34) are the various input/output devices (used for archiving, program storage, operator displays, and operator input devices) generally termed peripherals. The mini-computer has minimal control over the operating characteristics of the peripherals.

The flexibility of the total control subsystem resides in the relationship that exists between the mini-computer master controller and the seven slaved micro-computer-driven control units which are physically resident in the collector field (four micro-computers for time-effective collector and branch flow management), the Thermal Energy Subsystem, the Power Conversion Subsystem, and the Thermal Utilization Subsystem. Whereas the mini-computer has minimal influence over the operating characteristics of the peripherals, it has highly flexible control via software reconfiguration of the techniques that the individual micro-processors use to interpret data and execute control over the various transducers and control devices that are resident in their individual domain.

The basic concept is depicted in Figure 4.2-26 and is generically called a distributed star configuration. The mini-computer, as the hub of the star, is in a position to analyze inputs from each unit reporting to it for inconsistencies that may indicate improper operation and to initiate appropriate reactions (alert operator, make ready to initiate fail-safe sequencing, etc.) depending on the failure detected.

The slave/master relationship permits (via various data communications protocols and status words in comparison with transducer signals) the slave processor to quantify the basic apparent operating capability of the master controller.

Much of the task load of the entire control subsystem is the acquisition of data from the various subsystems under its control to execute the appropriate control algorithms and to create a data base to serve as an

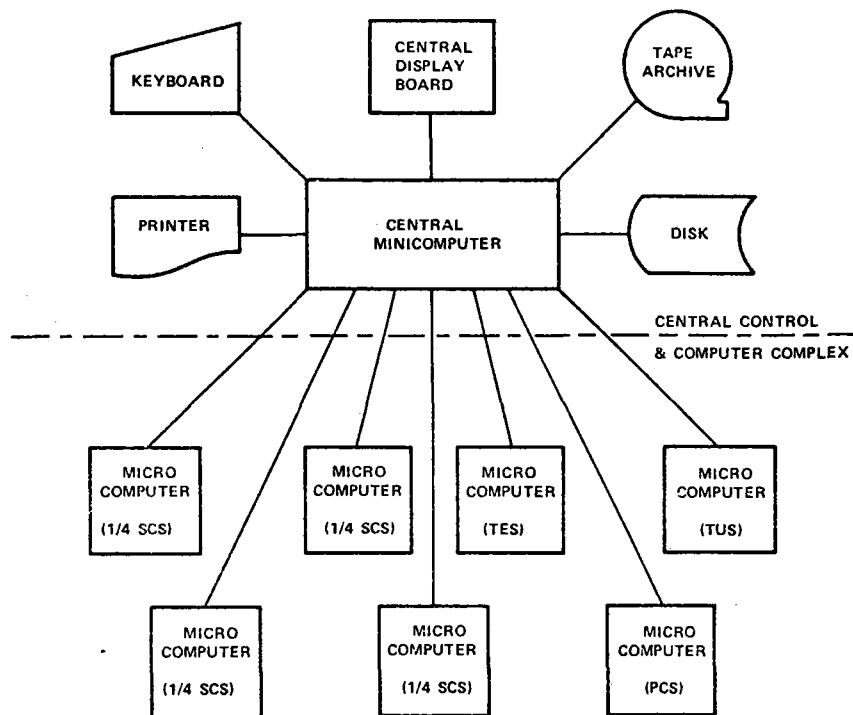


Figure 4.2-26. Computer Architecture

archive for optimization and experimentation. At the analog input interfaces of the micro-computers, the various raw transducer outputs are conditioned and presented to analog multiplexers for conversion by analog-to-digital converters into formatted digital data for linearization and incorporation into control routines and also for archiving.

Control routines may also incorporate binary status indicators to effect control and ascertain feedback stability. To execute control the micro-computer generates two types of signals:

1. Binary (on/off) for control of valves, motors, etc.
2. Analog, by means of digital-to-analog converters, for control of proportional control elements

In addition to archive control, the mini-computer supervises and checks data flow from the individual micro-computers, down loads software to effect mode changes in either a pre-programmed or an on-demand manner, serves via the keyboard or control console as the input mode for human interface, accepts software revision/update, and performs general system housekeeping tasks.

4.2.4.4 Major Components

The major components of the control system are the central control console, the central mini-computer, and the satellite micro-computers. A hardware selection analysis resulted in selection of Digital Equipment Corp. (DEC) computers. Specifically, the PDP-11/34 is selected for the central mini-computer, and the LSI-11 for the satellite micro-computers.

A distinguishing characteristic of the DEC family is its common physical architecture arising primarily from the patented DEC Unibus, a single high-speed, asynchronous, bidirectional communications path to which all system components (central processing unit - CPU, memories, and input/output I/O controllers) are connected. This common bus structure enables all functional elements to communicate with one another independently of the Central Processing Unit (CPU). This ability reduces the time spent by the CPU in supervising I/O operations and allows it to devote more time to actual data processing.

A second salient feature of the DEC family is that all models, from the smallest LSI-11 to the largest 11/70, use the same basic instruction set, thus allowing great flexibility in software development and transferability. Additional descriptions of the selected models are given below.

4.2.4.4.1 Central Minicomputer

The PDP-11/34 is a systems level computer that includes increased memory expansion to 124K words, memory relocation and protection, faster processing speeds, and hardware multiply and divide instructions. The computer system is mounted in a 0.133 meter (5 1/4 in) by 0.267 meter (10 1/2 in) chassis that mounts in a standard 0.483 meter (19 in) cabinet. The PDP-11/34 processor is prewired to accept additional memory (parity core or metal-oxide semiconductor) and standard peripheral device controllers including communications interfaces, mass storage controllers, etc. Additional mounting space is provided within the 0.267 meter (10 1/2 in) computer chassis for more complex controllers. The computer power supply within the chassis is capable of powering the optional internal devices.

The PDP-11/34 computer, as a member of the PDP-11 family, has the following features:

- Single and double operand instructions - powerful and convenient set of programming instructions
- Hardware implemented multiply and divide instructions
- 16-bit word (two 8-bit bytes) - direct addressing of 32K words or 64K bytes (K=1024)
- Parity detection on each 8-bit byte
- Hardware address expansion and protection allowing memory addressing to 124K words
- Word or byte processing - very efficient handling of 8-bit data without the need to rotate, swap, or mask
- Asynchronous operation - system components run at their highest possible speed, replacement with faster subsystems means faster operation without other hardware or software changes
- Modular component design - extreme ease and flexibility in configuring systems
- Stack processing - hardware sequential memory manipulation makes it easy to handle structured data, subroutines, and interrupts
- Direct memory access (DMA) - inherent in the architecture is direct memory access for multiple devices

- 8 internal general-purpose registers - used interchangeably for accumulators or address generation
- Automatic priority interrupt - four-line, multi-level system permits grouping of interrupt lines according to response requirements
- Vectored interrupts - fast interrupt response without device polling
- Power fail and automatic restart - hardware detection and software protection for fluctuations in the AC power

The minimum PDP-11/34 includes:

- Parity metal-oxide semiconductor (MOS) or core memory
- Memory management - program protection and relocation for memory expansion to 124K 16-bit words
- Automatic bootstrap loader - automatic starts from a variety of peripheral devices
- Self-test feature - ROM hardware automatically performs diagnostics on the CPU and memory
- Operator's front panel - allows complete control of the computer via any ACSII terminal. All front panel functions are key entries on the terminal, thereby eliminating the need and cost of a programmer's lights and switches console

The following optional equipment is available:

- Battery backup for MOS memory
- Programmer's console
- Serial communications line interface and line frequency clock
- Large variety of standard PDP-11 peripherals

4.2.4.4.2 Microcomputers

The LSI-11 is a 16-bit micro-computer with the speed and instruction set of a mini-computer.

The LSI-11 has the following features:

- 400 Plus Instruction Set. More than 400 instructions make up the LSI-11's extensive instruction set. This instruction set (also used by the PDP-11/34) permits the user to take advantage of standard PDP-11 software. The only departure from the standard software is the addition of two new instructions used to access the processor status word (PSW) explicitly. Development programs (as in the PDP-11 family) include assemblers, linkers, editors, loaders, utility packages, operating systems, and higher level languages.
- Extensive Computer Power and Small Processor Size. The processor module is built around a set of four N-channel metal oxide semiconductor (MOS) chips, which include control and data elements as well as two microcoded read-only memories (microms).

The latter are programmed to emulate the powerful PDP-11/35, 40 instruction set, along with routines for on-line debugging techniques (ODT), operator interfacing, and boot-strap loader capability. The processor also contains a 16-bit buffered parallel input/output (I/O) bus, a 4096-word MOS random-access memory (RAM), a real-time clock input, priority interrupt control logic, power-fail, auto restart, and other features to provide stand-alone operation. The entire processor plus all of the above mentioned features are contained on one 0.216 by 0.254 meter (8.5 by 10 inch) printed circuit board.

- **Modularity.** The process, memory, device interfaces, backplane, and interconnecting hardware are all modular in design. Modular selection, such as the type and size of memory and device interfaces, enables custom tailoring to meet specific application requirements.
- **Serial and Parallel I/O Modules.** Serial and parallel I/O modules are available for interfacing the processor bus with external devices. These modules simplify connection to peripherals when and if required and also facilitate assembly of prototype systems without penalizing later development of customized interfaces.
- **Choice of Memory.** Memory modules are offered for applications requiring more storage than is available with the 4096-word MOS random-access memory on the processor board. Included are a non-volatile 4096-word core memory, a 1024-word static RAM, a 4096-word dynamic RAM which can be automatically refreshed by central processor microcode, and read-only memory (PROM/ROM) with capacity to a maximum of 4096 words in 512-word increments (2048 words in 256-word increments).
- **16-Bit Word (Two 8-Bit Bytes).**
Direct addressing of 32K 16-bit words
- **Word or Byte Processing.** Very efficient handling of 8-bit characters without the need to rotate, swap, or mask
- **Asynchronous Operation.** System components run at their highest possible speed; replacement with faster devices means faster operations without other hardware or software changes
- **Stack Processing.** Hardware sequential memory manipulation makes it easy to handle structured data, subroutines, and interrupts
- **Direct Memory Access (DMA).** Inherent in the architecture is direct memory access for multiple devices
- **8 General-Purpose Registers.** For accumulators or address generation
- **Priority-Structured I/O System.** Daisy-chained grant signals provide a priority-structured I/O system
- **Vectored Interrupts.** Fast interrupt response without device polling
- **Single and Double Operation Instructions.** Powerful and convenient set of programming instructions
- **Power Fail/Auto Restart.** Whenever dc power sequencing signals indicate an impending ac power loss, microcoded power fail sequence is initiated. When power is restored,

the processor can automatically return to the run state. Four options are available for power-up sequencing

4.2.5 ELECTRICAL SUBSYSTEM (ES)

4.2.5.1 Function

The Electrical Subsystem provides for the distribution of the electrical power from the PCS generator to the components of the STES and to the parallel electrical connection with the Georgia Power Company and the Bleyle Plant. The ES also provides the backup power supply for collector defocus in the event of loss of normal electrical power. In addition, the ES contains a grounding system to prevent damage to the collector field in the event of lightning strikes.

4.2.5.2 Subsystem Configuration

The Electrical Subsystem is shown in Figure 4.2-27. The ES interfaces with all subsystems in the STES since it supplies electrical power to all electrical components and control devices. The primary ES boundary connection with the Georgia Power Company occurs at the air circuit breaker which connects the two systems in parallel. The turbine driven generator serves as the link between the ES and the PCS.

4.2.5.3 Detailed Subsystem Description

The Electrical Subsystem (ES) shown in Figure 4.2-27 consists of the electrical portions of the STES from the PCS generator through the protective relaying, transformer, and circuit breaker switchgear assemblies to the parallel electrical connection with the GPC-Bleyle 480/277 volt bus. Within the Mechanical Building, the ES also includes the auxiliary power distribution to the CIS and portions of the SCS, such as motor starter circuits.

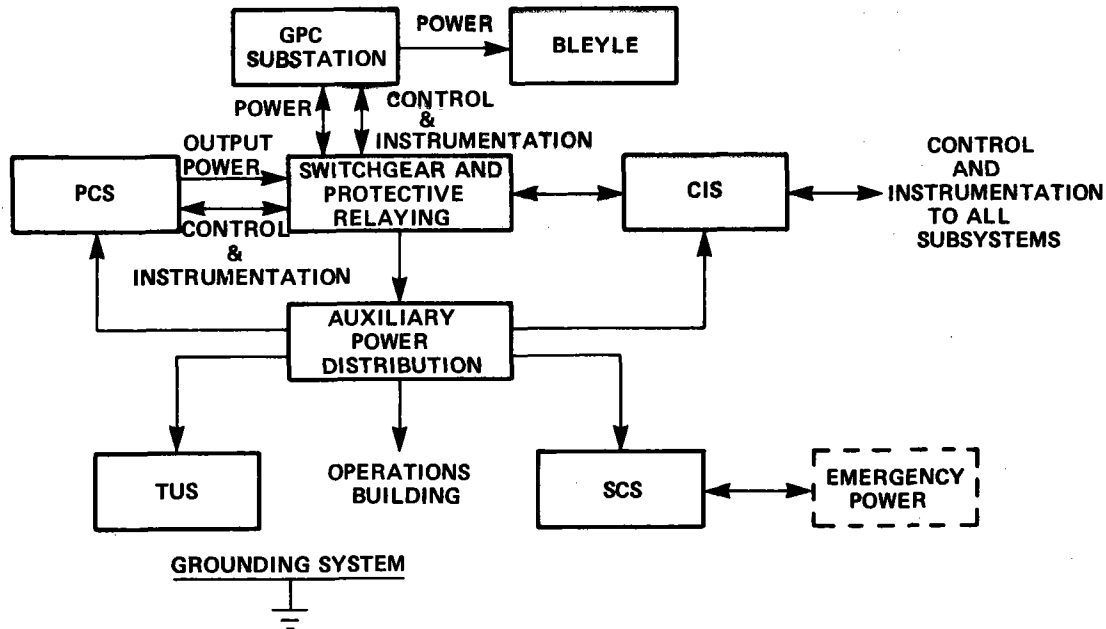


Figure 4.2-27. Electrical Subsystem

Collector field SCS power distribution consists of 208/120 volt service through panelboard circuit breakers located in the two field control enclosures which house the CIS micro-computers utilized for SCS control. Each half branch of five to six collectors has a circuit breaker, and each collector has an individually fused power circuit for maximum SCS availability. The collector field will have a ground grid installation consisting of driven rods and bonded cable.

The backup DC power supply for collector defocus consists of low maintenance batteries at each collector kept under float charge and controlled to drive an SCS motor at high rate. The system is shown in Figure 4.2-28.

Sensor and control cable to each collector and the field control valves will consist of multi-conductor shielded cable terminating at the field control boxes as shown in Figure 4.2-29.

4.2.5.4 Major Components

4.2.5.4.1 Generator and Exciter

A turbine driven generator with shaft mounted, brushless exciter is provided to generate the electrical portion of the total energy output of the STES. The generator has the following characteristics for specification purposes.

Rating	500	kVA
Power Factor	0.8	
Speed	1800	rpm
Connection	WYE	4 Leads Out
Distortion	5	Percent, Maximum
Voltage	480	Volts, Line to Line, 3 Phase
Overspeed	25	Percent, Standard
Frame	OPEN	Dripproof
Exciter	2.5	Per Unit, Forcing Capability
Shaft	Keyed	Standard Extension

Additionally, an oversized connection box will be supplied to house lightning arrestors, surge capacitors, and current transformers. The windings and bearings will have RTD detectors for operational and experimental temperature measurement.

4.2.5.4.2 Transformer

An isolation transformer will be connected in DELTA-WYE at the generator output to prevent harmonics from reaching the Bleyle Plant or Georgia Power systems. The transformer KVA rating will be the same or slightly more than that of the generator. An air insulated unit enclosed in the same metal-clad enclosure as the circuit breakers will be utilized to avoid any fire risk which could arise from the use of an oil insulated construction. The WYE connected Bleyle side will have a solidly grounded neutral with a current transformer on the neutral to detect ground fault currents.

4.2.5.4.3 Paralleling Circuit Breaker

An air circuit breaker will be used to connect the STES electrical system in parallel with the Georgia Power system to supply the Bleyle Plant load. The circuit breaker ratings will be:

Voltage	480	Volts, L-L, 3 Phase
Current	600	Amperes, continuous
Short Circuit	(TBD)	MVA, symmetrical
Operations	5000	Minimum, before major maintenance
Control	125	Volts DC, close and trip circuits
Construction	Drawout	NEMA 12 enclosure

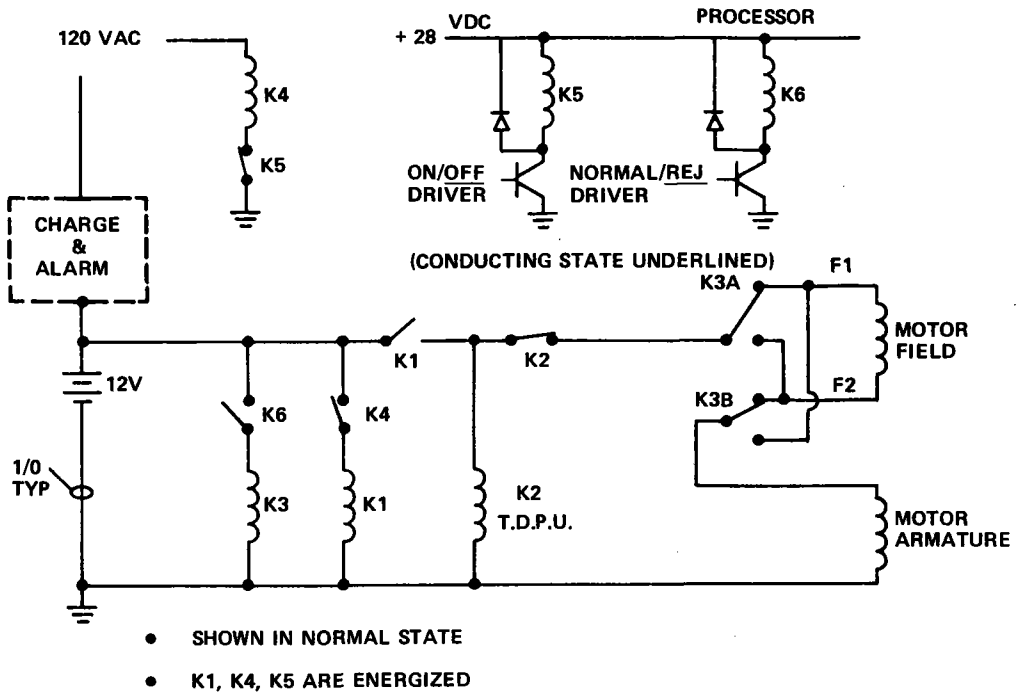


Figure 4.2-28. Defocus Circuit

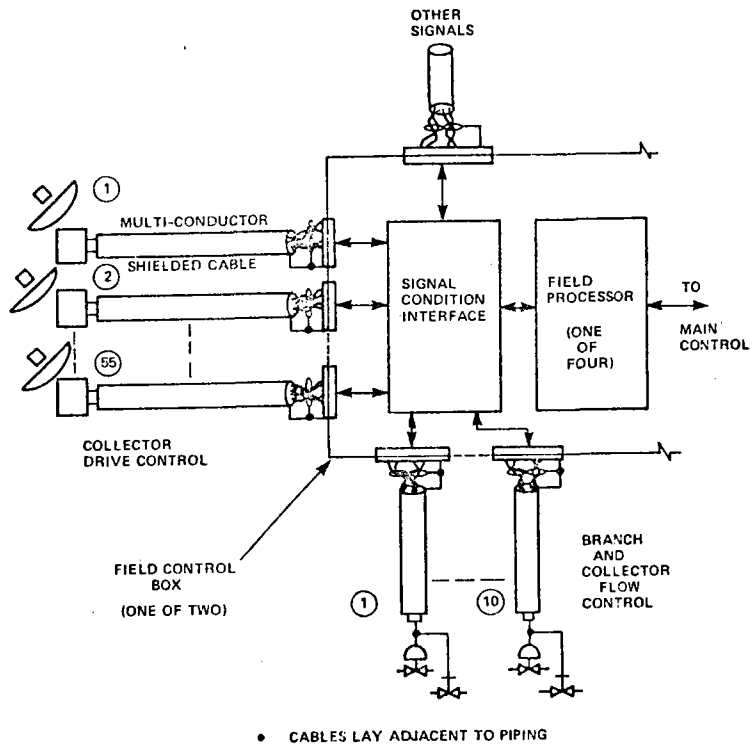


Figure 4.2-29. Field Sensor and Control Cable

Closing control of the paralleling circuit breaker will be by manual or automatic synchronizing. Tripping control will be manual, automatic, or normal shutdown and through generator or bus lockout relays in cases of protective relay operation. A cable connection serves Bleyle by paralleling with GPC at their substation through this circuit breaker.

4.2.5.4.4 Auxiliary Circuit Breaker

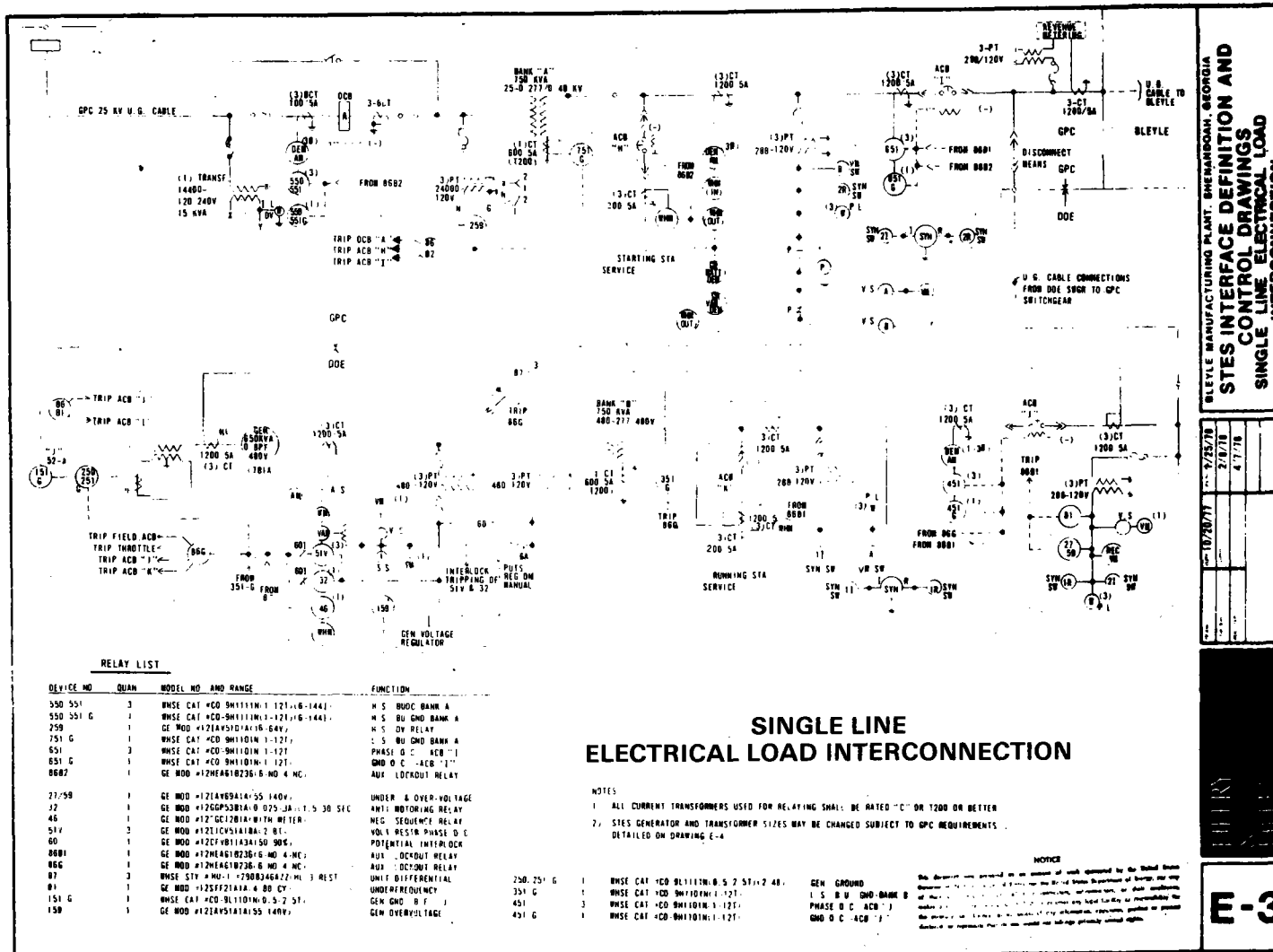
An air circuit breaker will be used to connect and provide short circuit protection to the STES station service loads. This auxiliary circuit breaker will have the same ratings as the paralleling circuit breaker and be mounted in the same enclosure structure with it and the transformer.

4.2.5.4.5 Protective Relaying

The STES output electrical system is protected from faults and some forms of equipment malfunction by a group of utility type relays. These devices operate from voltage and current signals through instrument transformers on the main 480 volt circuit. The instrument transformers will be installed in the enclosure housing the isolation transformer and circuit breakers, and the relays will be mounted in a separate, but similar and adjacent, NEMA 12 switchboard.

The relaying utilized operates as follows. Interface drawing E-3, Figure 4.2-30, has the connection points and model number of the devices.

<u>ANSI Number</u>	<u>Function</u>
27/59	Detect whether paralleling bus voltage is excessively low or high as indicative of a voltage regulator malfunction and open paralleling breaker.
32	Detect power flow towards generator or motoring as indicative of a problem with the turbine control and open breakers plus shutdown turbine.
46	Detect phase unbalance as indicative of excessive unbalanced load or loss of a phase and open breakers plus shutdown turbine.
51V	Detect phase overcurrent as indicative of a line to line fault with greater sensitivity to close voltage reducing faults and open breakers plus shutdown turbine.
86G/86B1	Lockout relays to require manual intervention after protective relay operation.
81	Detect low bus frequency as indicative of islanded system or loss of turbine control and initiate system shutdown.
87	Detect differential current across generator, transformer, and main breaker indicative of ground or phase fault and initiate system shutdown.



STES INTERFACE DEFINITION AND CONTROL DRAWINGS SINGLE LINE ELECTRICAL LOAD INTERCONNECTION

10/20/71	7/25/78
2/8/78	4/7/78

GEN GROUND
1 S B W OMO-BANK B
PHASE D C -ACB "I"
OMO D C -ACB "I"

E-3

Figure 4.2-30. Single Line Electrical Load Interconnection

151G	Backup ground fault detection in case of main breaker failure. Retrips main breaker and GPC tie breaker.
159	Detect generator terminal over voltage indicative of voltage regulator malfunction prior to synchronization plus backup on 59. Causes system shutdown on operation.
250/250G	Detect generator ground fault by level of neutral to ground current and cause system shutdown.
351G	Detect bus ground fault on Bleyle side of isolation transformer by level of neutral current and cause system shutdown. Backup 451G.
451	Detect phase overcurrent on the STES 480 volt system and cause system shutdown.
451G	Detect ground faults on bus or badly unbalanced load and cause system shutdown.

In addition to these relays, the GPC electrical system has a suitable complement of protective devices that are not part of the STES.

4.2.5.4.6 Auxiliary Power Distribution

A motor control center consisting of a factory assembled NEMA 12 enclosure with plug-in type combination motor starters and feeder circuit breakers will be utilized to distribute and control 480 volt auxiliary loads. Motors of greater than 746 watts (1.0 horsepower) rating will be run at 3 phase 480 volts, and motors of 746 watts (1.0 horsepower) or less or equivalent loads will be powered at 120 volts, single phase through a step down transducer to 208/120 volts.

At least two stepdown transformers will be required: one for Mechanical Building loads and a second, 75 kVA size for collector field supply to control boxes, convenience outlets, and collector drives. Air insulated units in stand alone enclosures or core and coil units mounted inside a throat connected compartment next to the motor control center will be used.

In the collector field, the three phase circuit will connect to panelboards at the two field control boxes. Heating and cooling requirements of the electronics in these boxes and the electronics themselves will be fed 120V, 60 hertz power through separate small circuit breakers on the panelboard. Each half branch of collectors will also be single phase circuit breaker protected in order to trip only a small section of the field for electrical shorts anywhere in the system.

From the panelboards, single phase 120 volt circuits will be laid in below-grade wireway and elevated conduit to the collectors. Convenience outlets will be provided at the collector control boxes for the use of maintenance personnel. Separate fused protection for the collector control and for the outlets is provided. Collector field area lighting will be supplied by a circuit separate from the main field circuit but running in the same wireways.

4.2.5.4.7 Backup Power Source

The preliminary requirement for the backup power source is safe shutdown of the STES system. Rapid defocus of individual collectors, or possibly the entire field in the event of an ac power outage, requires a short time, instant response capability of about 300 kVA with 1119 watts (1.5 horsepower equal to approximately 1.5 kVA) per collector ignoring inrush requirements. Remote reset of the defocus circuit is required, thereby eliminating a hydraulic dump, manually set system as utilized on the Engineering Prototype Collector.

A central, second ac or dc source was eliminated from consideration due to cost potential for single point failure, response time, and wiring sizes required to handle the simultaneous defocus of the entire field. Individual collector 12 volt batteries are provided to power the automotive type dc defocus motor drive of the collectors.

The batteries of low maintenance, lead-calcium plate, automotive construction will be float charged and power the motor through a deadman switch arrangement that requires both ac power and control circuit energization to remain open. Commanded defocus at four degrees per second of collector motion operates by control circuit de-energization. Loss of ac power has the same effect as commanded defocus but occurs automatically. After approximately five seconds or ten degrees of collector motion, the battery-motor circuit will be opened to prevent thermal damage to the motor or excessive battery discharge in the event of a sustained ac outage. Battery charging will be performed by individual collector circuits with current limited to one ampere. Battery and defocus system condition will be checked by periodic (off-operation) exercise of the defocus system manually with battery voltage drop observed with load. This check will provide the least complicated, best check of battery condition in addition to providing a beneficial low duty discharge cycle.

4.2.5.4.8 Field Control and Signal Wiring

Each collector will be connected to its field control box by a multi-conductor, shielded pair cable and thermocouple leads. The branch flow control valves will have a similar cable connection with fewer pairs. Industrial plug connectors will be used on both ends of each control cable. Cable routing is in the same wireway as, but separated from, the power cables.

The high speed serial data interface connection between the field control boxes and the main control mini-computer will utilize triaxial cable. All electronic connections will require transient protection from induced surges due to nearby lightning ground strokes.

4.2.5.4.9 Grounding and Lightning Protection

Grounding rods and interconnection to establish a field earth-to-ground resistance of less than five ohms will be provided to conduct any field lightning strikes to earth in a controlled manner. Braid jumpers across bearings will be provided for static discharge and antiweld protection.

One-kV surge arrestors will be applied on the 480 volt power circuits to limit conducted surges due to nearby power line lightning strikes to levels within the base insulation level (BIL) rating of the equipment. Power supply inputs for control circuits will have series shunt protection.

SECTION 5
SYSTEM OPERATING PLAN

SECTION 5

SYSTEM OPERATION PLAN

5.1 INTRODUCTION

The Operating Plan for the Solar Total Energy System, SD Document No. 78SDS4235 (General Electric Company, Space Division), was published in draft form at the close of the Preliminary Design Phase (Phase III) of the STE-LSE Program. The document is intended to be a technical manual that explicitly defines the operating requirements, modes, and characteristics of the individual subsystems that comprise the STES. While the first issue of the document presents the preliminary operation of the STES, the document will be updated periodically to reflect changes as the design progresses toward and includes the final system configuration.

Section 1 of the Operating Plan gives a brief introduction to the document. A generalized system description is presented in Section 2 that describes each of the three major subsystems: Solar Collection Subsystem, Power Conversion Subsystem, and Thermal Utilization Subsystem along with the major control elements and functions of each. Weekday operation and associated modes are described and defined by the use of system schematic fluid flow diagrams in Section 3 for each of the three subsystems. Section 4 provides similar information for weekend operation. Section 5 presents the preliminary test and evaluation plan. It includes the activities schedule for the two year test period, a summary of planned system and subsystem tests, and a preliminary listing of test measurements required.

5.2 WEEKDAY OPERATION

This section of the report describes the various operating modes that can occur during the normal work week. These modes are referenced by major subsystem and include those indicated in Table 5.2-1. Features of each of these modes are summarized in itemized form in the following paragraphs.

5.2.1 SOLAR COLLECTION SUBSYSTEM OPERATION

Operation of the Solar Collection Subsystem is described below:

1. Startup with Storage Depleted
 - a. Fossil Heater Steam Generator Supply and Circulation Pumps
 - FFH activated at ~5:15 A.M. by SCS controls
 - Syltherm 800 flow to steam generator controlled by signal from PCS controls to SGS valves
 - SGS isolated from CFS
 - PCS startup will be completed at ~5:45 A.M.
 - b. Threshold Insolation/Field Activation/Bypass Warmup
 - (1) Collector Tracking mechanism initiated
 - (2) Field pumps and flow control valves powered up
 - (3) If insolation signal $\geq 237 \text{ W/m}^2$ (75 Btu/hr-ft²)
 - (a) Collector field starts sun acquisition sequence
 - (b) All collectors adjusted to proper declination angle
 - (c) All collectors moved to leading position about polar axis

Table 5.2-1. Weekday System Operating Modes

Solar Collection Subsystem Operation

1. Startup with Storage Depleted
 - a. Fossil Heater Steam Generator Supply
 - b. Threshold Insolation/Field Activation/Bypass Warmup
 - c. Approach to Operating Temperature
 - d. Series Transfer to Charge Tank Fully
 - e. Fossil to Solar Transition
2. Startup with Storage Charged
 - a. Storage Steam Generator Supply
 - b. Threshold Insolation/Activation
 - c. Approach to Operating Temperature
3. Solar Power Operation
 - a. Collection/Charge Storage/PCS Direct Supply
 - b. Collection/Discharge Storage/Direct PCS Supply
 - c. Storage Operation
4. Shutdown
 - a. Solar Collector Field
 - b. Solar to Fossil Transition
 - c. Nighttime Idle/Shutdown Heating

Power Conversion System Operation

1. PCS Startup
2. Total Energy Operation with Electric Load Following
3. Shutdown

Thermal Utilization Subsystem Operation

1. Absorption Air Conditioning
2. Heating
3. Absorption Air Conditioning and Heating
4. Excess Heat Dissipation

- (d) Field pumps actuated when final lead position attained
- (e) All collectors placed in final track position on verification of stable flow within field
- (4) Field flow increased in proportion to insolation to cause a 139°K (250°F) ΔT across collectors at operating condition
- (5) Flow recirculated through collectors until outlet from field reaches 533°K (500°F)
- c. Approach to Operating Temperature
 - (1) Bypass mode discontinued when collector field outlet reaches 533°K (500°F)
 - (2) Field flow directed to one-hour tank and return
 - (3) Collector outlet temperature approaches $658 - 672^{\circ}\text{K}$ ($725 - 750^{\circ}\text{F}$) range
 - (4) Controls select hottest dish in branch and generate valve signal to control outlet to the 672°K (750°F) setpoint
 - (5) Defocus of hot dish occurs if its temperature is too high above average for branch
 - (6) Defocus of branch occurs if outlet temperature is less than 644°K (700°F) or if overall field outlet is less than 658°K (725°F) due to the branch temperature
 - (7) Field flow will be cut back to avoid excessive throttling at branch valves if a number of branches are defocused
 - (8) Field flow adjusted to allow branch valves to return to midpoint throttle
 - (9) Flow to one-hour tank continues until breakthrough temperature of 561°K (550°F) occurs
 - (10) Series Transfer to a larger HTS tank occurs to prevent the field inlet from exceeding 561°K (550°F)
- d. Series Transfer to Charge Tank Fully
 - (1) Storage Transfer pump activated
 - (2) Next available discharged tank charged with one-hour tank sump flow
 - (3) Large tank provides return flow to field
 - (4) Fossil-to-Solar mode initiated when sump temperature of one-hour tank reaches fully charged setpoint (i. e., collector field discharge temperature)
- e. Fossil to Solar Transition
 - (1) Bulk of field flow supplies steam generator load (any excess will charge large HTS tank as in d. above)
 - (2) Output from field is directed first through the FFH
 - (3) FFH operation continues until all cooler Syltherm 800 existing in pipes and steam generator exhaust is heated and pumped back through the steam generator
 - (4) FFH is then shut off and isolated
- 2. Startup with Storage Charged
 - a. Storage Steam Generator Supply
 - (1) SCS startup is same as for storage discharged
 - (2) HTS tank is placed on line to supply PCS startup and operation
 - (3) One-hour tank selected if it is fully charged; if not, next partially discharged or fully charged tank is selected

- b. Threshold Insolation/Activation
 - (1) SCS startup is same as for storage depleted
 - (2) One or more branches in the collector field may be inhibited in order to match field output to PCS demand and available storage energy
 - c. Approach to Operating Temperature
 - (1) As in startup with storage depleted, flow is directed to one-hour tank when collector field outlet reaches 533^oK (500^oF)
 - (2) When field outlet reaches normal operating temperature, flow is directed to the steam generator
 - (3) Second HTS still on line to supply steam generator as necessary
 - (4) One-hour tank still in charge mode to receive field flow if in excess of steam generator demands
3. Solar Power Operation
- a. Collection/Charge Storage/PCS Direct Supply
 - (1) SCS supplies steam generator directly
 - (2) Flow from field in excess of PCS demand goes to the HTS tanks
 - (3) Charging of tanks done in series mode until either insolation level is too low for PCS demand or charging tanks reach breakthrough
 - (4) A discharged tank is always available for charging
 - (5) If possibility exists for a discharged tank not being available, field flow is reduced by defocusing and isolation operations so that no excess exists
 - b. Collection/Discharge Storage/Direct PCS Supply
 - (1) A charged HTS tank will be discharged to supply the PCS demand if field flow is insufficient
 - (2) Discharge flow is drawn and returned to the selected HTS tank by the SGS pump
 - (3) Storage discharge logic is the same as for charging:
 - (a) One-hour tank discharged first
 - (b) Three large tanks then discharged in sequence
 - (c) Fully charged tanks only to be discharged
 - (4) When no-more extractable energy is available from the one-hour tank, the storage transfer pump is deactivated and series discharge is terminated
 - (5) The first large tank is then discharged by the SGS supply pump
 - (6) If the large tanks energy drops to a level that the PCS will consume during warmup of the FFH, the FFH is started up for the Solar-to-Fossil Transition mode
 - (7) If the insolation level drops and field shutdown occurs, the PCS is supplied by the charged tanks until necessary to change to fossil energy or until the insolation level returns for direct supply

c. Storage Operation

- (1) Collector field does not supply flow and is isolated from the HTS and the SGS
- (2) HTS supplies steam generator directly
- (3) Discharge of tanks occurs as in b above

4. Shutdown

a. Solar Collector Field

- (1) Can occur during startup or during operation
- (2) Failure-to-start signals can initiate shutdown:
 - (a) If lead tracking of field occurs for greater than six hours before threshold insolation attained
 - (b) If insolation level is less than 237 W/m^2 (75 Btu/hr-ft^2) after fine tracking and pumps are activated
 - (c) If field outlet average temperature does not exceed 658°K (725°F) with sufficient insolation level for a duration of 1 1/2 hours
- (3) During operation, if insolation drops below 237 W/m^2 (75 Btu/hr-ft^2), control system sets field flow to a minimum
- (4) When field outlet drops below 658°K (725°F), collectors are stowed and pumps shutoff
- (5) Shutdown also occurs if field outlet drops below 658°K (725°F) even if insolation level is sufficient after appropriate checks of branch defocus and isolation action and of field flow conditions by control system

b. Solar to Fossil Transition

- (1) Initiated when storage tank sensors indicate that stored energy is adequate only to meet PCS demand for time to bring FFH on line
- (2) FFH begins heatup and circulation of Syltherm 800 from hot standby to normal operating temperature in its isolated loop
- (3) When operating temperature is attained in FFH loop, flow from storage is directed through the FFH and then to the steam generator
- (4) When the storage tank sump temperature drops below the minimum supply temperature ($\sim 658^\circ \text{K}$ or 725°F), the mode is shifted to fossil

c. Nighttime Idle/Shutdown Heating

- (1) Heat input from either storage or the FFH is discontinued
- (2) System valves are set for morning startup
- (3) SGS is activated to provide shutdown heating if fluid inventory in any of the SCS subsystems cools below the allowable range
- (4) If the FFH is employed for the heat source, the steam generator supply bypass valve is opened to avoid the ΔP and heat loss in the steam generator

5.2.2 POWER CONVERSION SUBSYSTEM OPERATION

Operation of the Power Conversion Subsystem is described below:

1. PCS Startup
 - a. N_2 supply to steam generator and deaerator is shut off
 - b. Boiler drum, deaerator storage, and hot well storage are brought to full level
 - c. Syltherm-800 flow is started through the steam generator
 - d. Turbine discharge valve is opened when boiler pressure set point of $7.2 \times 10^5 \text{ N/m}^2$ (105 psig) is reached
 - e. N_2 supply to turbine is turned off
 - f. Auxiliary lube pump is turned on and cooling water flow started through the oil cooler
 - g. The turbine stop/throttle valve is partially opened and the turbine is rolled; full speed is attained over a period of 15 minutes
 - h. The synchronizer closes the generator contactor
 - i. The turbine governor is set for startup load
 - j. The steam bypass valve to the deaerator is closed
 - k. Steam generator pressure controls are set for $4.8 \times 10^6 \text{ N/m}^2$ (700 psig)
 - l. Pressure and temperature are ramped to operating levels
 - m. The turbine governor is set for normal operation
 - n. The process steam valve is opened
 - o. The auxiliary lube is turned off-startup is complete
2. Total Energy Operation with Electric Load Following
 - a. Steam extracted from the turbine generator, with substantial superheat, is conditioned to the saturated process steam at $7.2 \times 10^5 \text{ N/m}^2$ (105 psig) by controlled throttling and de-superheating by spray injection with condensate from the hot well
 - b. Steam from the turbine discharge flows through a make-up water preheating passage fed by water from the condensate storage tank and then into the condenser
 - c. Circulating water delivers the major portion of the condenser thermal load to the TUS and is controlled to maintain a constant condenser pressure
 - d. Makeup water to replace process steam flow is admitted to the makeup demineralizer from the plant water supply at a rate controlled by the condensate storage tank level control
 - e. Condensate from the condenser hot well is pumped by the condensate pump to the deaerator
 - f. Condensate and turbine extraction steam are mixed in the deaerator; saturated condensate leaves at the deaerator pressure
 - g. Heated condensate passes to the boiler feed pump
 - h. Hydrazine and ammonia are injected near the feed pump suction in response to sensors of dissolved O_2 and pH, respectively

3. Shutdown

- a. Shutdown occurs when the Bleyle plant electrical load drops to nighttime levels following second shift termination
- b. The turbine stop valve is closed
- c. The line contactor is opened
- d. The process steam is closed, and the boiler feed pump is turned off
- e. The chemical injection unit is turned off
- f. The turbine discharge valve is closed, and the turbine casing drains are opened
- g. The turbine is purged with N_2 for 15 minutes; the drains are then closed and the turbine casing pressurized to $34,475 \text{ N/m}^2$ (5 psig)

5.2.3 THERMAL UTILIZATION SUBSYSTEM OPERATION

Operation of Thermal Utilization Subsystem is described below:

1. Absorption Air Conditioning

- a. TUS cooling water is supplied to the condenser at a controlled pressure of $41,922 \text{ N/m}^2$ (6.08 psig)
- b. The thermal load supply pump provides a controlled flow of heated cooling water to the AAC
- c. If the AAC exhaust water temperature is hotter than the TES tank coldest temperature, it is directed through the tank. If colder, the exhaust water flows directly to the pump

2. Heating

- a. Operation in this mode is identical to that for the AAC except for the position of the thermal load supply valves

3. AAC and Heating

- a. Operation in this mode is identical to that for the AAC except that the thermal load supply valves are positioned to supply both heating and AAC

4. Excess Heat Dissipation

- a. If the TUS cooling water temperature entering the condenser exceeds 364°K (195°F), the excess heat cooling tower is activated
- b. Discharge water from the cooling water pump flows through the excess heat dissipation heat exchanger where it is cooled to 361°K (190°F) before entering the condenser

5.3 WEEKEND OPERATION

Table 5.3-1 presents the applicable operating modes for weekend operation. The startup sequence for the SCS is identical to that for weekday startup with the storage tanks either charged or discharged except that the PCS is not operated since the Bleyle plant is shutdown. Therefore, weekend startup does not include fossil or storage steam generator supply or fossil-to-solar transition. In the Charge Storage mode for the SCS, operation is similar to that for weekday operation except that the SGS supply and return valves are closed. Series charging is employed, and the first three tanks are fully charged if adequate insolation is present. Since there would be no additional volume available for charging once breakthrough was reached, full charging of the fourth tank is delayed until Monday morning, either before or after the one-hour tank, depending on the temperature state of the fourth tank.

Table 5.3-1. Weekend System Operating Modes

<p><u>Solar Collection Subsystem Operation</u></p> <ol style="list-style-type: none"> 1. Startup 2. Charge Storage 3. Shutdown <p><u>Power Conversion Subsystem (Non-operating)</u></p> <p><u>Thermal Utilization Subsystem Operation</u></p> <ol style="list-style-type: none"> 1. Absorption Air Conditioning 2. Heating

Since the PCS is shutdown for the weekend, the thermal load for the AAC and/or the heating modes is supplied from the low temperature storage tank. This mode applies also to early morning weekday cooling before the Bleyle Plant startup.

5.4 TEST AND EVALUATION

The preliminary activities scheduled for STES operation at Shenandoah is shown on Figure 5.4-1. The schedule begins following completion of system acceptance and pre-operational testing. Operation in the

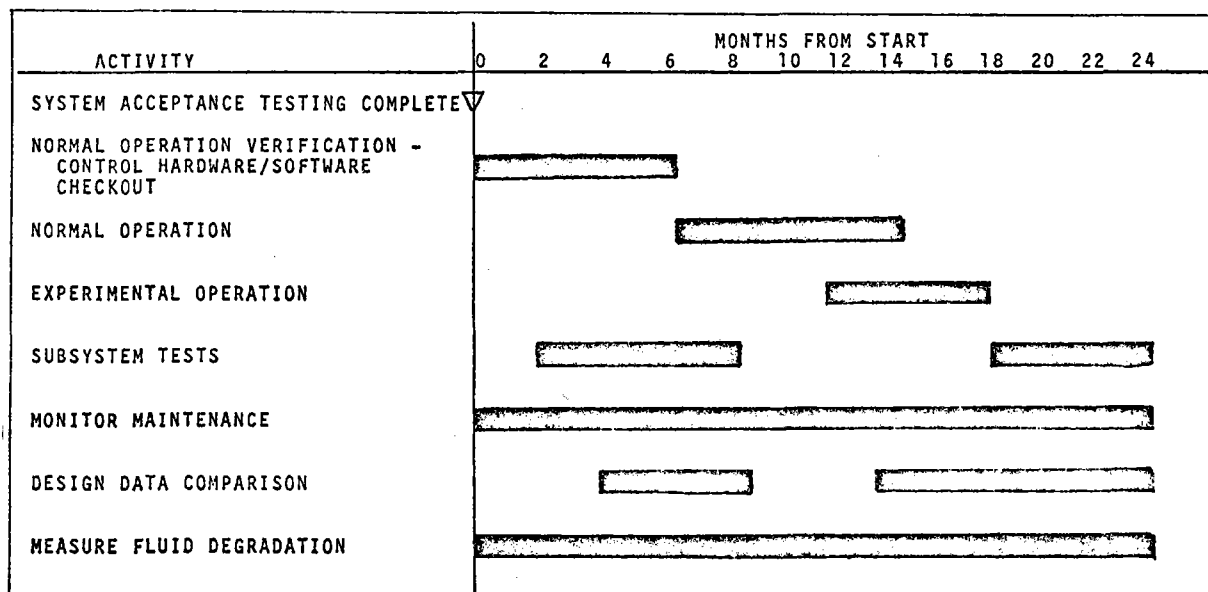


Figure 5.4-1. System Operation - Preliminary Activities Schedule

normal total energy system modes will occur during the first operating phase to provide verification checkout of the control system in order to finalize the modes, sequencing, and setpoints. Subsystem tests will be performed to support the activity, and system data collected in this verification period will be compared with design predictions. This verification operation will result in a refinement of the STES operating conditions followed by a period of six to eight months for operational performance and collection of system data for analysis. This period will span summer, winter, and spring or fall to evaluate the effects of cooling, heating, and their combination on the STES and the Bleyle plant.

System experimental operation will begin toward the completion of the normal operating period when it is determined that sufficient data has been collected to characterize normal operation. This operation will include variations in the electrical power interface with the Georgia Power Company and in the thermal input from the Collector Field Subsystem. Data will be continuously monitored and recorded at regular intervals to characterize system performance fully in terms of the Bleyle plant loads; solar, utility, and fossil contributed energy; and climatology as to its effect on system operation.

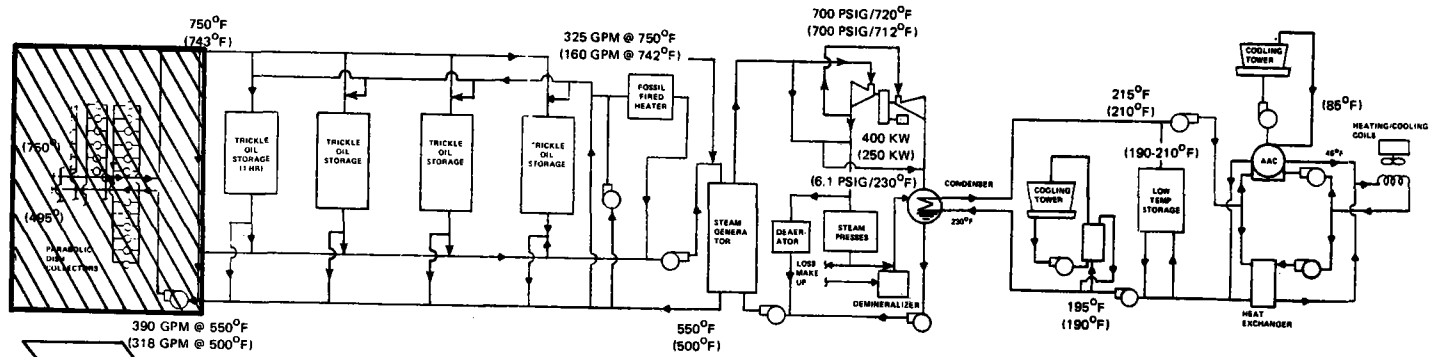
There will be three modes of testing to determine the effects of electrical power variation on system performance. Each of these three modes are briefly summarized below:

1. Stand Alone Operation. The turbine generator will not operate in parallel with the utility, but instead will operate independently to provide its own speed/load control to meet the varying Bleyle plant load. This mode will provide operational experience typical of a remote application that is isolated from the utility network.
2. Constant Power Output. The turbine generator will operate in parallel with the utility, but its output will be maintained at a constant level. The utility contribution will be variable to follow the load. This mode will allow the turbine generator to operate in the maximum efficiency range and will provide detailed characterization of its performance.
3. Variable Utility Baseload. This mode of operation is essentially the same as the normal STES operation except that the utility baseload is now allowed to vary; i. e., the STES supplies electrical power in a load following manner, but with the utility baseload not being fixed at the 100 kWe level. This operation allows the STES to operate as a peak shaving system.

In order to assess the effect of thermal power variations on STES operation, two experimental modes of operation will be employed as summarized below:

- a. Turbine Bypass. The turbine generator will be isolated, and all electrical loads will be met by the utility. Steam exiting from the steam generator will go directly to the steam presses and to the condenser for thermal utilization. The substantial reduction in steam supply pressure attendant with this operation allows the use of lower temperature solar energy and a matching supply of solar energy to the thermal load.
- b. Series Fossil Heater. Solar heated fluid from either the collector field or thermal storage is passed through the fossil fired heater before entering the steam generator. Fluid at a temperature lower than the steam generator supply can thus be used because it is boosted to the required temperature by the fossil heater. This allows the collector field to operate at a reduced temperature and also complete discharge of all four storage tanks.

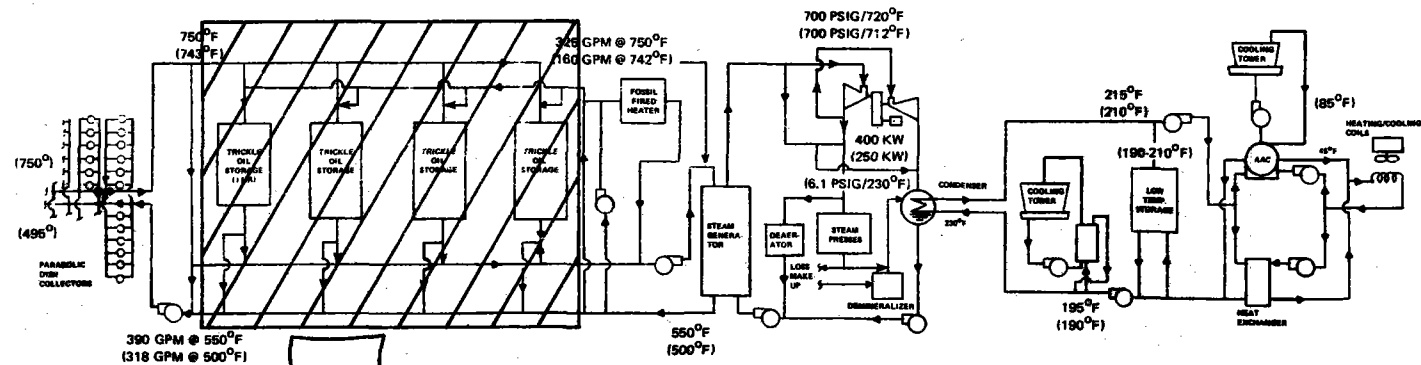
To complete the planned operation phase, detailed subsystem tests will be performed to characterize fully their operation and interaction as well as to concentrate on the major experimental components. Figures 5.4-2, 5.4-3 and 5.4-4 summarize the planned subsystem component tests and indicate data and sensor requirements for the three subsystems of the SCS. Similarly, Figures 5.4-5 and 5.4-6 summarize the tests for the PCS and the TUS, respectively.



SOLAR COLLECTOR FIELD TESTS	
• COLLECTOR EFFICIENCY	• SETPOINT VARIATIONS
• FIELD S/S HEAT LOSS	- STARTUP/SHUTDOWN INSULATION
• FIELD WARMUP	- PARTIAL FIELD STARTUP
• CLEANING CYCLE	- OPERATING TEMPERATURE
• IMAGE PROFILE	- TEMPERATURE ERROR CONTROL BAND

DATA	INSTRUMENTS	NO. SENSORS
• FLOW	FLOW METERS	3
• TEMPERATURE	THERMO COUPLES	252
• PRESSURE	TRANSDUCERS	21
• CLIMATOLOGY	WEATHER METERS	15
• CONCENTRATED SOLAR FLUX	OPTICAL SENSOR	40

Figure 5.4-2. Subsystem/Component Tests (SCF)

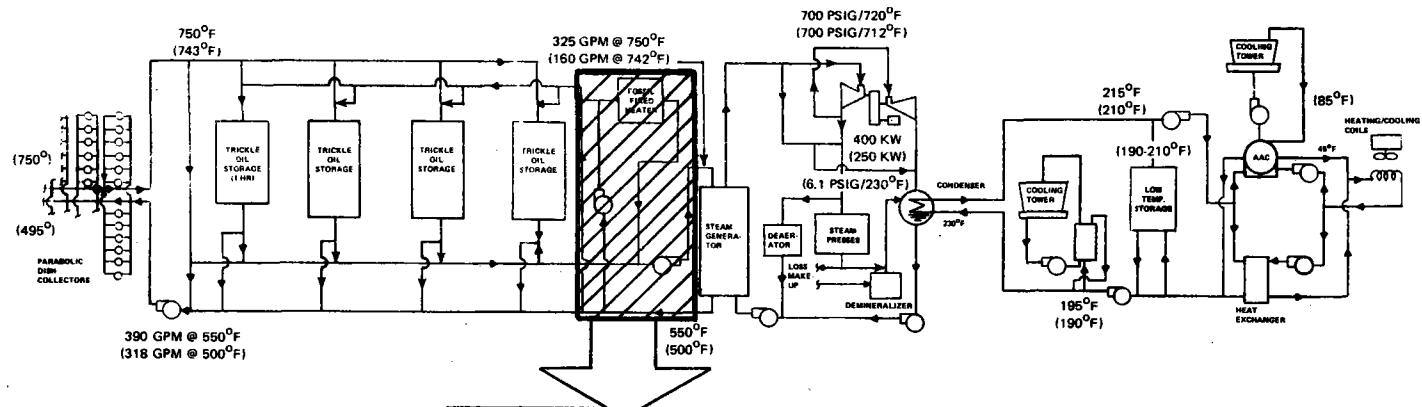


HIGH TEMPERATURE STORAGE TESTS

- EFFICIENCY
- TEMPERATURE PROFILE
- TEMPERATURE DEGRADATION
- PRESSURE GRADIENT
- THERMAL LOSSES
- STRESS/STRAIN

DATA	INSTRUMENTS	NO. SENSORS
● FLOW	FLOW METERS	2
● TEMPERATURE	THERMOCOUPLES	222
● PRESSURE	TRANSDUCER	14
● STRAIN	GAUGE	40

Figure 5.4-3. Subsystem/Component Tests (HTS)

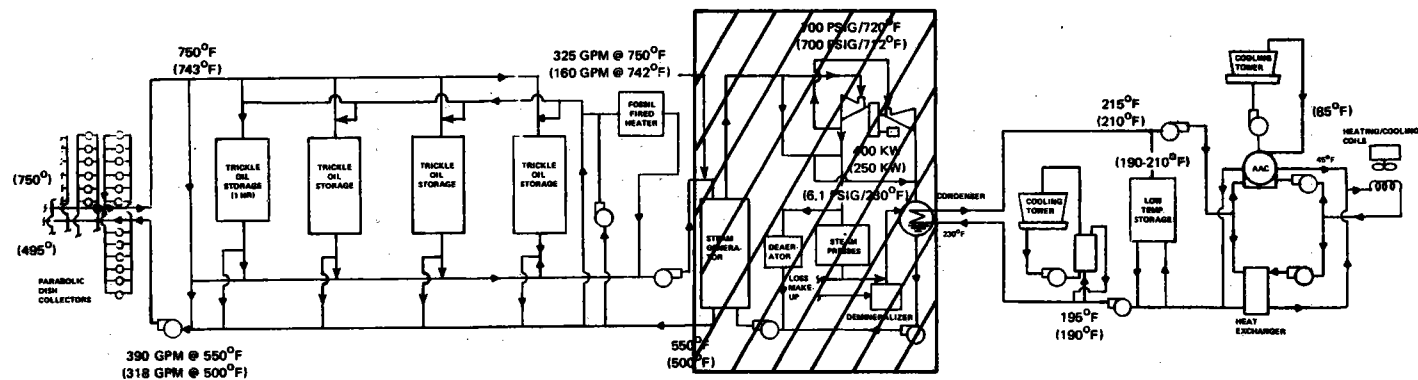


STEAM GENERATOR SUPPLY SUBSYS. TESTS

- FOSSIL FIRED HEATER EFFICIENT
- SUPPLY TEMPERATURE SETPOINT

DATA	INSTRUMENTS	NO. SENSORS
• FLOW	FLOW METERS	2
• TEMPERATURE	THERMOCOUPLE	5
• PRESSURE	TRANSDUCER	5

Figure 5.4-4. Subsystem/Component Tests (SGS)

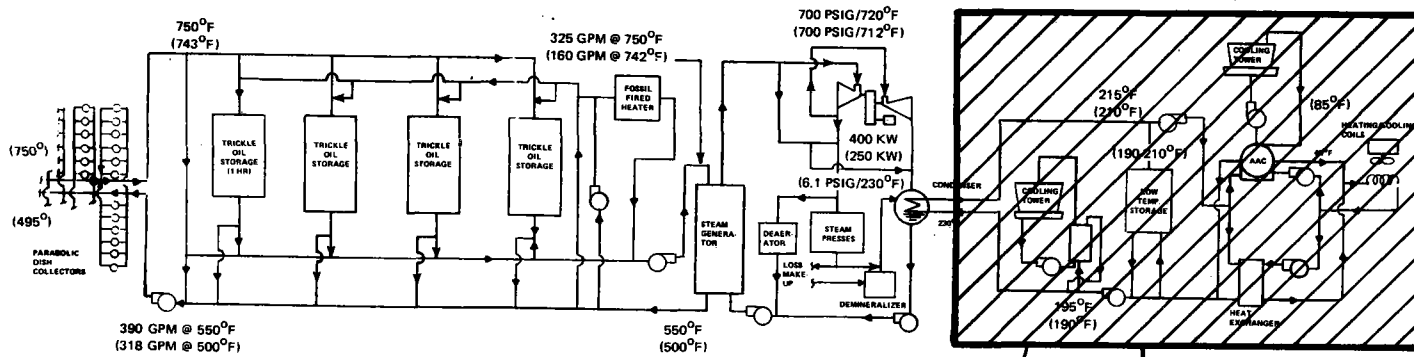


POWER CONVERSION SUBSYS. TESTS

- TURBINE EFFICIENCY
- THERMAL LOSS
- TRANSIENT RESPONSE
- SETPOINT VARIATIONS

DATA	INSTRUMENTATION	NO. SENSORS
● FLOW	FLOW METER	5
● TEMPERATURE	THERMOCOUPLE	13
● PRESSURE	TRANSDUCER	12
● LEVEL	INDICATOR	4
● POWER	TRANSDUCER	13

Figure 5.4-5. Subsystem/Component Tests (PCS)



- THERMAL UTILIZATION SUBSYS. TESTS**
- AAC PERFORMANCE
 - STORAGE EFFICIENCY
 - STORAGE TEMPERATURE PROFILE
 - SETPOINT VARIATIONS

DATA	INSTRUMENT	No. SENSORS
● FLOW	FLOW METER	4
● TEMPERATURE	THERMOCOUPLE	31

Figure 5.4-6. Subsystem/Component Tests (TUS)

The location and identification of the STES instrumentation required to provide the experimental data is shown on Figure 5.4-7. The test data management procedure will be as follows:

1. Instrument measurements will be picked up and converted to engineering units by the subsystem microprocessors.
2. The minicomputer will then scan the microprocessors for required data and store the data on magnetic tape with an intermediate disc storage.
3. The tapes containing the test data will be shipped to General Electric Valley Forge for analysis.

SECTION 6
SYSTEM PERFORMANCE

SECTION 6

SYSTEM PERFORMANCE

A generalized computer model, the Solar Total Energy System (STES) Program, was developed to allow calculation of system performance and to facilitate system trade-offs. The basic elements of the program are shown in Figure 6.0-1, and a more detailed description is provided in Appendix C. The program performs an hourly calculation using a combined weather and hourly load tape as input. In the analyses that were performed, monthly and annual solar contribution to each of the site loads; electricity, process steam, and space conditioning; were computed for the selected system size and operating characteristics. These performance summaries were then used as input to annual Bleyle energy displacement and life cycle cost analyses. The calculations were all performed with insolation and ambient conditions from the 1975 Atlanta Aerospace Test Reference Year. The annual loads correspond to the total site loads as defined in Section 2.2.

The annual system performance summaries for electricity, process steam, and cooling are shown in Figures 6.0-2 through 6.0-4, respectively. As seen from Figure 6.0-2, the 192 dish STES supplies 43 percent of the site annual electrical demands including both STES parasitics and Bleyle plant electrical load combined. While supplying its own parasitics, the STES satisfies one-third of the Bleyle annual electrical load during solar operation. This electrical system performance results from operating with a 100 kW base load from GPC. If GPC were to supply the STES parasitics in addition to the 100 kW base load, the solar contribution would increase to 55 percent. Figure 6.0-2 shows a summer peak in the solar contribution to the electrical load which roughly corresponds to the utility summer peak.

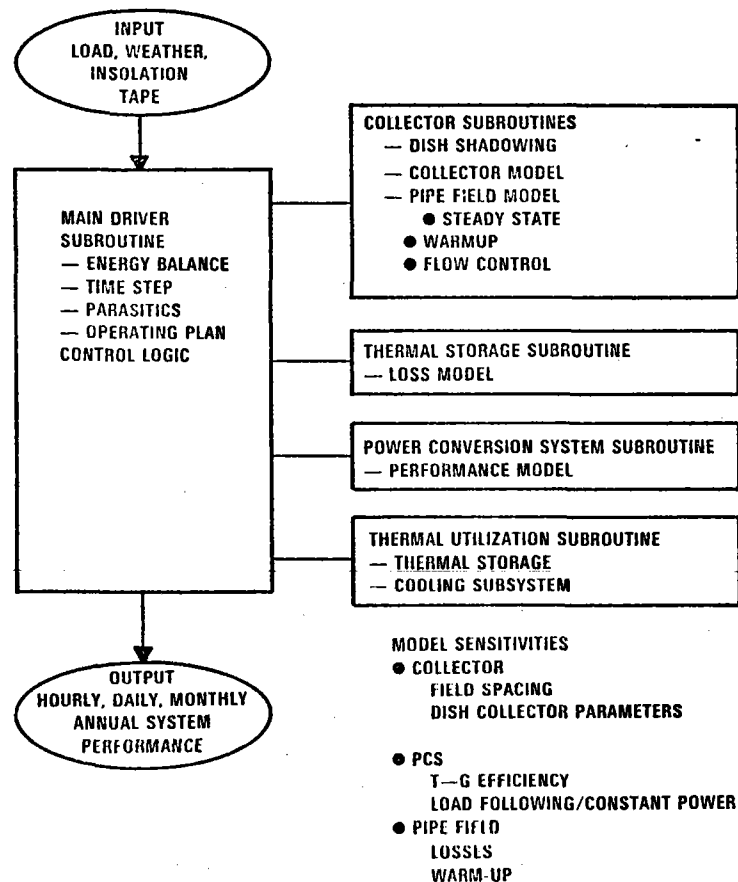


Figure 6.0-1. System Performance Model

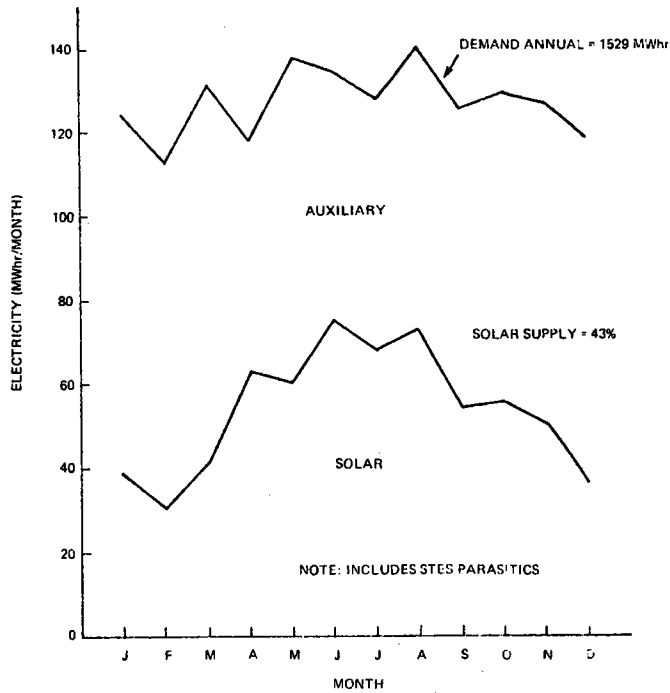


Figure 6.0-2. System Performance-Electricity

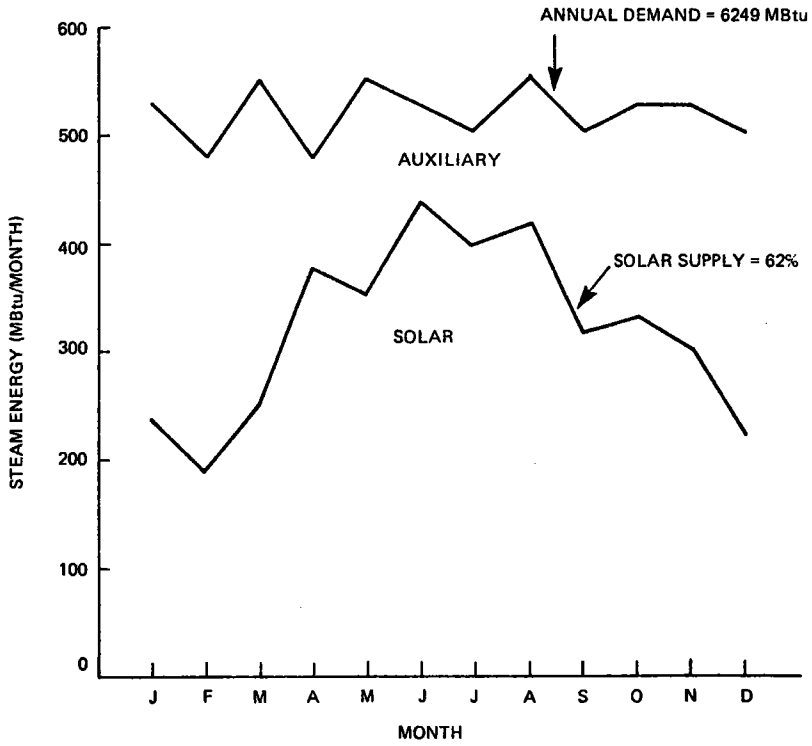


Figure 6.0-3. System Performance-Process Steam

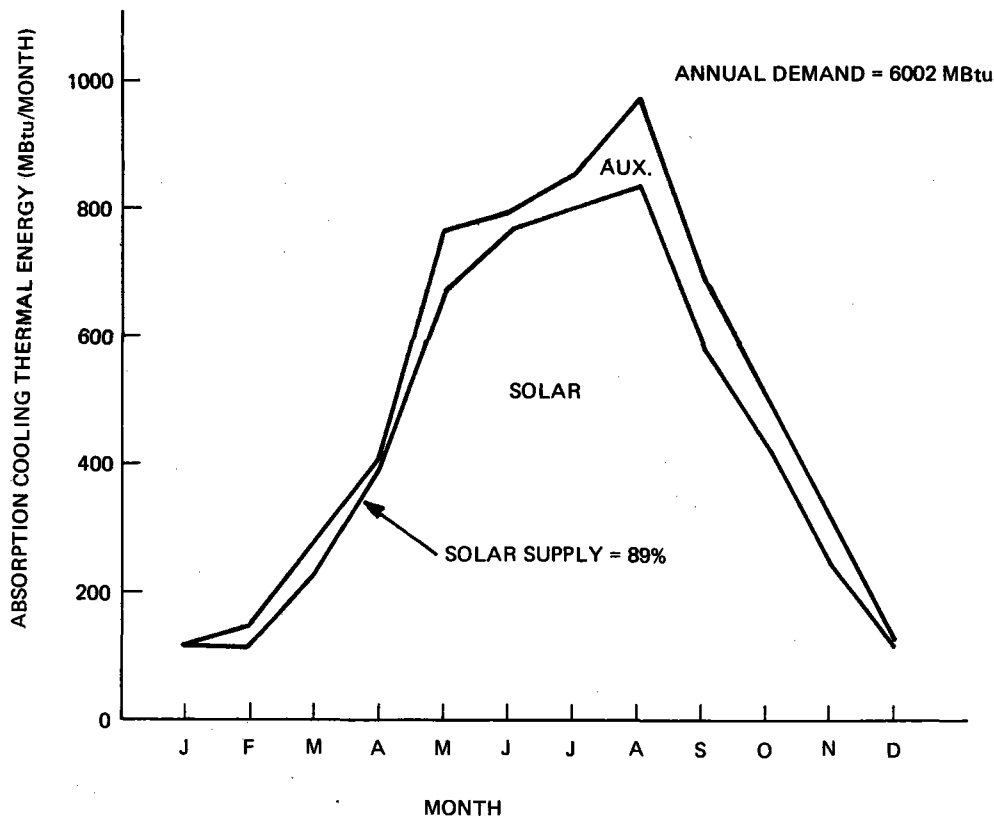


Figure 6.0-4. System Performance-Cooling

The process steam performance in Figure 6.0-3 shows an annual solar contribution of 62 percent. The process steam contribution is a direct function of solar running time since the demand is always met through the required extraction steam. Figure 6.0-4, expressed in terms of thermal energy required to drive the absorption air conditioner, demonstrates the ability of the STES to track the summer cooling load and again provide summer utility peak load shaving. By virtue of the high thermal to electric output ratio of the PCS, there is sufficient cascaded thermal energy virtually to saturate and to satisfy completely the plant cooling requirements.

Combining all of the site loads, the STES preliminary design performance analysis indicates a capability to satisfy up to 65 percent of the combined Bleyle and STES annual energy demands on solar input. The remaining site energy demands, with the exception of the electrical energy supplied by GPC as base load, are satisfied on-site through operation of the total energy system on fossil back-up heat.

Figure 6.0-5 shows annual summaries of system field losses and STES parasitic power. Field losses include both warm-up and steady state pipefield losses. Because of the significant amount of field piping required, high performance, low density insulation has been employed to reduce field operating losses to about 6 percent of the collected energy. Field warm-up losses are significant, however, giving total field losses up to 12 percent of collected energy during winter months. Operating parasitics average about 40 percent of the gross electric load.

Because of the relative mismatch between STES thermal output and site thermal loads, the system has excess thermal energy available. As seen in Figure 6.0-6, this excess energy is fairly constant over the day, averaging about 4.4×10^5 J/s (1.5 MBtu/hr) during the summer and 8.8×10^5 J/s (3.0 MBtu/hr) in winter when the economizer cycle supplies the plant cooling load. This energy, available as hot water at 372°K (210°F), is available for other nearby industrial users.

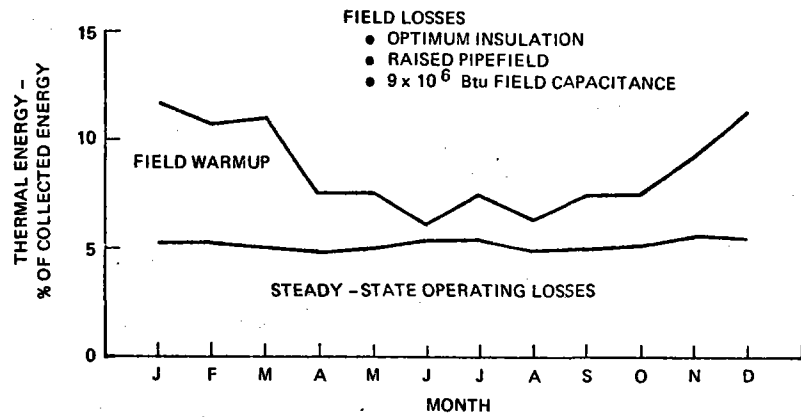
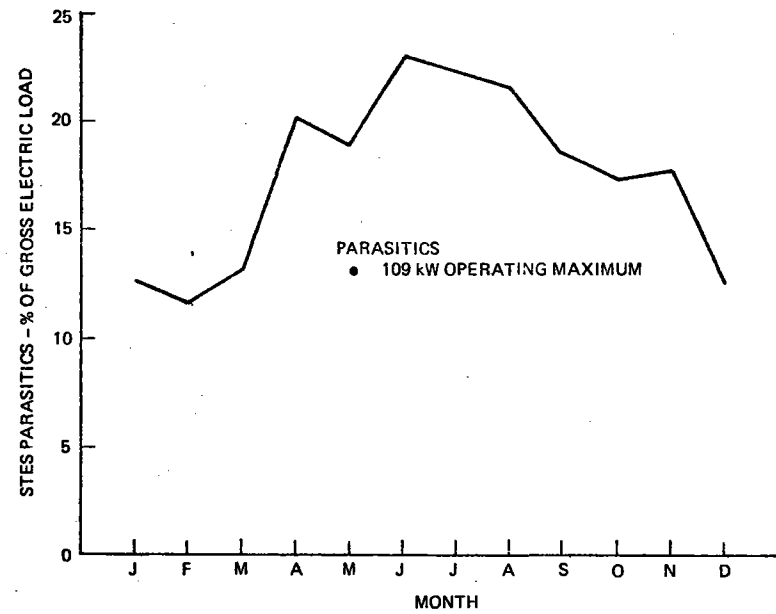


Figure 6.0-5. System Field Losses and Parasitic Power

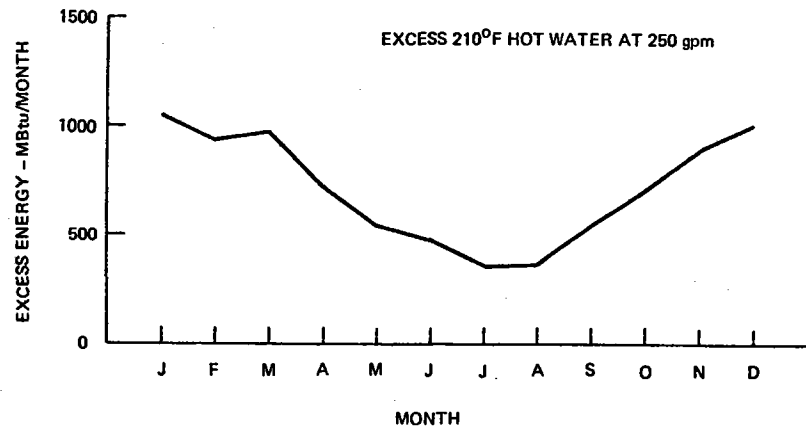
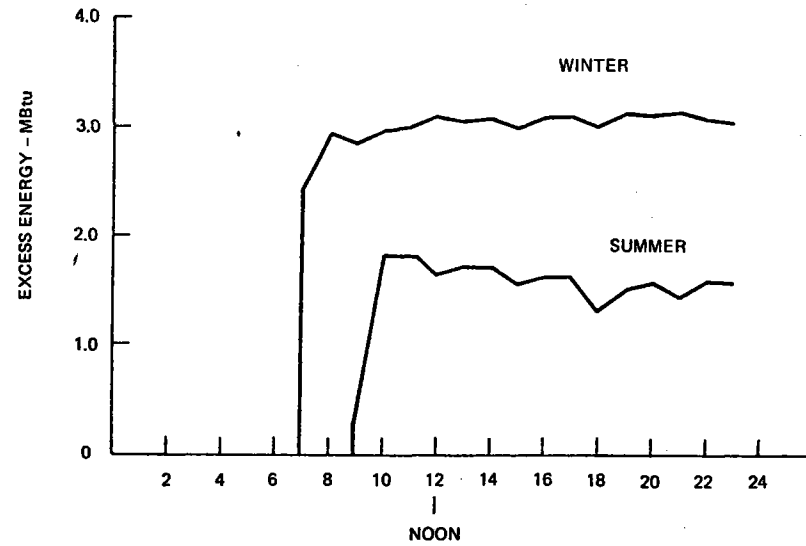


Figure 6.0-6. Average Low Temperature Excess

Overall system energy balances for winter, spring, and summer months are shown in Figures 6.0-7 and 6.0-8.

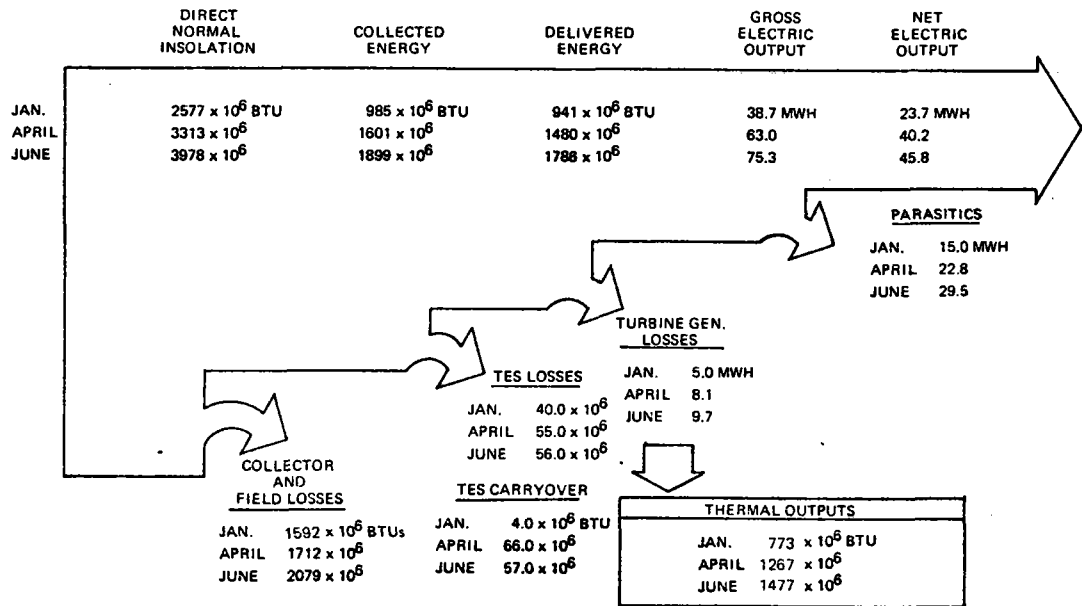


Figure 6.0-7. System Energy Flow—Monthly Totals MTI Turbine (192 Collectors)

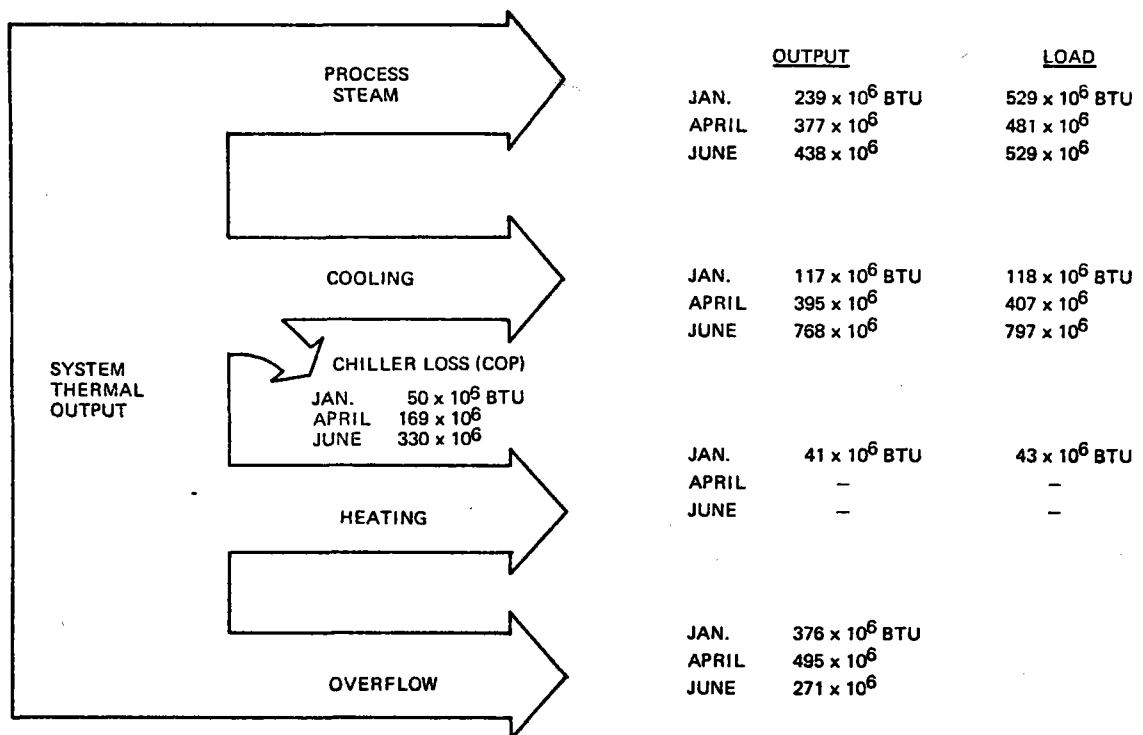


Figure 6.0-8. Thermal Output Summary Monthly Totals MTI Turbine (192 Collectors)

SECTION 7
SYSTEM REQUIREMENTS ANALYSIS

SECTION 7
SYSTEM REQUIREMENTS ANALYSIS

7.1 ENERGY DISPLACEMENT ANALYSIS

The annual electric and fossil fuel requirements of the projected 3900 square meters (42,000 ft²) Bleyle plant as determined by computer load analysis are listed in Table 7.1-1 where the electric load is broken down as shown into air conditioning and non-air conditioning loads. The corresponding plant annual electric and natural gas bills listed in Table 7.1-1 were obtained using the current Georgia Power Company and Atlanta Gas Light Company rate schedules, respectively. These schedules are summarized in Table 7.1-2. Also shown are the fuel adjustment factors applicable in June 1978 and assumed in the analysis.

The computation of typical Bleyle plant monthly gas and electric bills is illustrated in Table 7.1-3 where the appropriate rate schedules were applied to an averaged monthly energy consumption breakdown as shown. A check was made using actual monthly consumption data with no appreciable difference in annual billing.

The Solar Total Energy System (STES) energy displacement was determined from an annual system operation simulation which resulted in net STES contributions of 50 percent of the Bleyle electric load (88.2 percent air conditioning and 33.3 percent non-air conditioning) and 61.5 percent of the natural gas load. The new annual costs of energy consumed with the STES installed along with the resulting savings are listed in Table 7.1-4. The new electric bills were computed using the same procedure as described previously; i.e., applying the appropriate rate schedule of Table 7.1-2 to averaged* monthly electricity consumption with the STES included.

The 100 percent air conditioning displacement case required fossil fuel consumption which was more than offset by the increased electrical savings due primarily to reduced kilowatt demand (490kW to 270kW). Although burning fossil fuel to supply 100 percent air conditioning is cost effective, the burning of fossil fuel to supply all process steam and electrical loads (above baseload) proved to be uneconomic as shown in Table 7.1-5. If a process application could be found for the excess thermal energy generated, annual savings would be increased substantially, and full fossil fuel operation becomes cost effective. Further, it is seen that the use of oil at the current Atlanta price of 43¢/gal substantially increases savings over natural gas use at the current Atlanta price of 19.83¢/therm.

Table 7.1-1. Bleyle Energy Consumption and Cost Projections
for 3900 Square Meters (42,000 Ft²) Plant

	Annual Energy	Annual Cost
Electricity (Non A/C)	1179 MWh	\$66,000
Air Conditioning	513 MWh	
Process Steam	9.61 X 10 ⁹ Btu	\$19,300
	Total	\$85,300

*Again, a check using actual monthly electricity consumption with the STES yielded no appreciable difference in annual billing.

Table 7.1-2. Summary of Energy Rate Schedules Applicable to Bleyle Plant (June 1978)

Georgia Power Company		
Power and Light		
Schedule "PL-1"		
MONTHLY RATE — ENERGY CHARGE INCLUDING DEMAND CHARGE:		
First	50 kWh or less	@ 10.0¢ per kWh
Next	1,450 kWh	@ 6.5¢ per kWh
Next	1,500 kWh	@ 6.2¢ per kWh
Next	7,000 kWh	@ 5.5¢ per kWh
Next	190,000 kWh	@ 4.4¢ per kWh
Next	300,000 kWh	@ 3.81¢ per kWh
Over	500,000 kWh	@ 3.5¢ per kWh
All consumption (kWh) in excess of 200 hours and less than 400 hours times the billing demand		
	@	1.5¢ per kWh
All consumption (kWh) in excess of 400 hours times the billing demand		
	@	1.3¢ per kWh
(June 1978 Fuel Adjustment Rate - .2813¢ per kWh)		
Atlanta Gas Light Company		
Rate <u>N-2</u>		
<u>General Gas Service</u>		
<u>Rate:</u>		
<u>Therms</u>		<u>Net</u>
For the first 4.0 or less used per month		\$2.50
		<u>Per Therm</u>
For the next 16.0 used per month		14.6¢
For the next 580.0 used per month		10.5¢
For all over 600.0 used per month		8.7¢
(June 1978 Purchased Gas Adjustment Factor - 11.13¢ per Therm)		

Table 7.1-3. Computation of Typical Bleyle Plant Monthly Bills

Electric Bill

	Quantity	Total	Price	Cost
kWh	50	50	.10	5.00
	1,400	1,500	.065	94.25
	1,500	3,000	.062	93.00
	7,000	10,000	.055	385.00
	88,000	98,000	.044	3,872.00
	42,992	140,992	.015	644.88
	Fuel Adj.	140,992	.002813	396.61

\$5,490.74 per month
or \$65,889 annually

Natural Gas

	Quantity	Total	Price	Cost
Therms	4	4	-	2.50
	16	20	.146	2.34
	580	600	.105	60.90
	7411	8011	.087	644.62
		Fuel Adj.	8011	.1113

\$1602.12 per month
or \$19,225 annually

Table 7.1-4. Energy Displacement of Shenandoah STES

	STES% Contribution		<u>New Annual Cost</u>	
			Solar Alone	With 100% A. C.
Electricity (Non A/C)	33%	} 50%	\$41,300	\$34,400
Air Conditioning	88%			
Process Steam	62%		\$ 7,600	\$ 7,600
Fossil Fuel for AAC			-	\$ 2,200
Total Annual Costs			\$48,900	\$44,200
Net Annual Savings			\$36,300	\$41,000

Table 7.1-5. Shenandoah STES Annual Savings Potential

	Shenandoah Experiment			Full Thermal Utilization	
	NO FOSSIL	100% A/C	FULL FOSSIL	100% A/C	FULL FOSSIL
Electricity	\$24,600	\$31,500	\$48,400	\$31,500	\$48,400
Process Steam	\$11,700	\$11,700	\$19,300	\$11,700	\$19,300
Fuel Burned	—	(2200)	(28,300)	(2200)	(28,300)
Other Thermal	—	—	—	\$24,800	\$39,100
Total Annual Savings	\$36,300	\$41,000	\$39,400	\$65,800	\$78,500
Oil at 43¢/gal	\$43,000	\$46,400	\$34,300	\$85,100	\$95,400

} Natural Gas
19.83¢/Therm

The effect of turbine efficiency on annual energy cost savings is depicted graphically in Figures 7.1-1 and 7.1-2 for natural gas and oil usage, respectively. Higher efficiencies allow more running time for electrical and power steam loads thus increasing their contribution to annual savings. The potential savings with full thermal utilization vary slightly less with turbine efficiency due to reduced excess energy of the higher efficiency units.

7.2 LIFE CYCLE COST ANALYSIS

True life cycle costing must necessarily consider not only the magnitude of costs but also the timing as well due to the time value of money. This is especially critical in the analysis of alternate energy systems since almost any scenario projects steadily increasing energy costs with time and thus steadily increasing benefits from an alternate energy system such as a STES. The major element in the life cycle cost analysis is the levelized annual cost of the STES. Levelized annual cost can be compared with levelized system benefits or can be divided by annual energy production to determine the cost of delivered energy. The life cycle cost model developed for this analysis is presented in detailed form in Appendix D.

Derivation of the cost of delivered energy from the STES requires a value ratio between the electrical and thermal savings. Typical prices for electrical energy are about three times as high as thermal energy, reflecting somewhat the average power plant efficiency of 25 to 35 percent. It is shown in Appendix D that if the numerical value of the electricity cost in cents per kilowatt hour is equal to the thermal cost in dollars per million Btu, a 3:1 value ratio is closely approximated. Using this approximation, the cost of delivered energy, C_E , is related to the levelized annual cost (\overline{AC}) through the relation

$$C_E = \frac{\overline{AC}}{.01 S_{elec} + S_{thermal}}$$

where the units of C_E are both (¢/kWh) and $\frac{\$}{10^6 \text{ Btu}}$

where S_{elec} = electrical savings in kWh

and $S_{thermal}$ = thermal energy savings in 10^6 Btu

The principal assumptions used in application of the cost model are presented in Table 7.2-1. Complete assumptions specified for use in the cost model can be found in the model description - Appendix D.

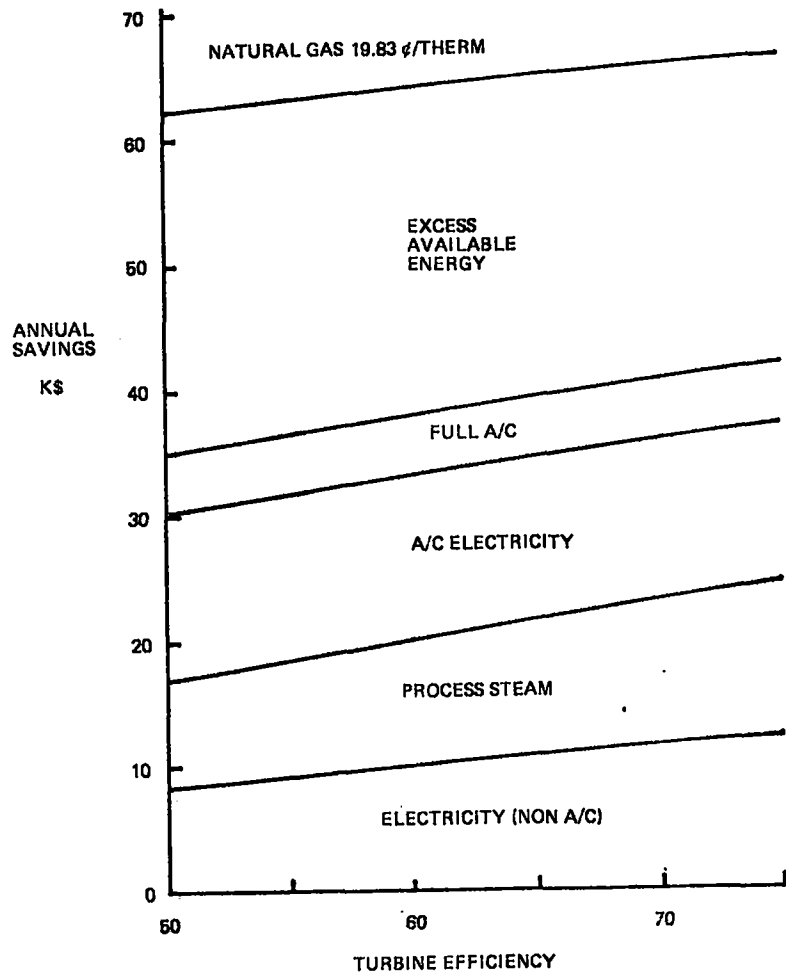


Figure 7.1-1. Effect of Turbine Efficiency on Annual Energy Cost Savings for Natural Gas

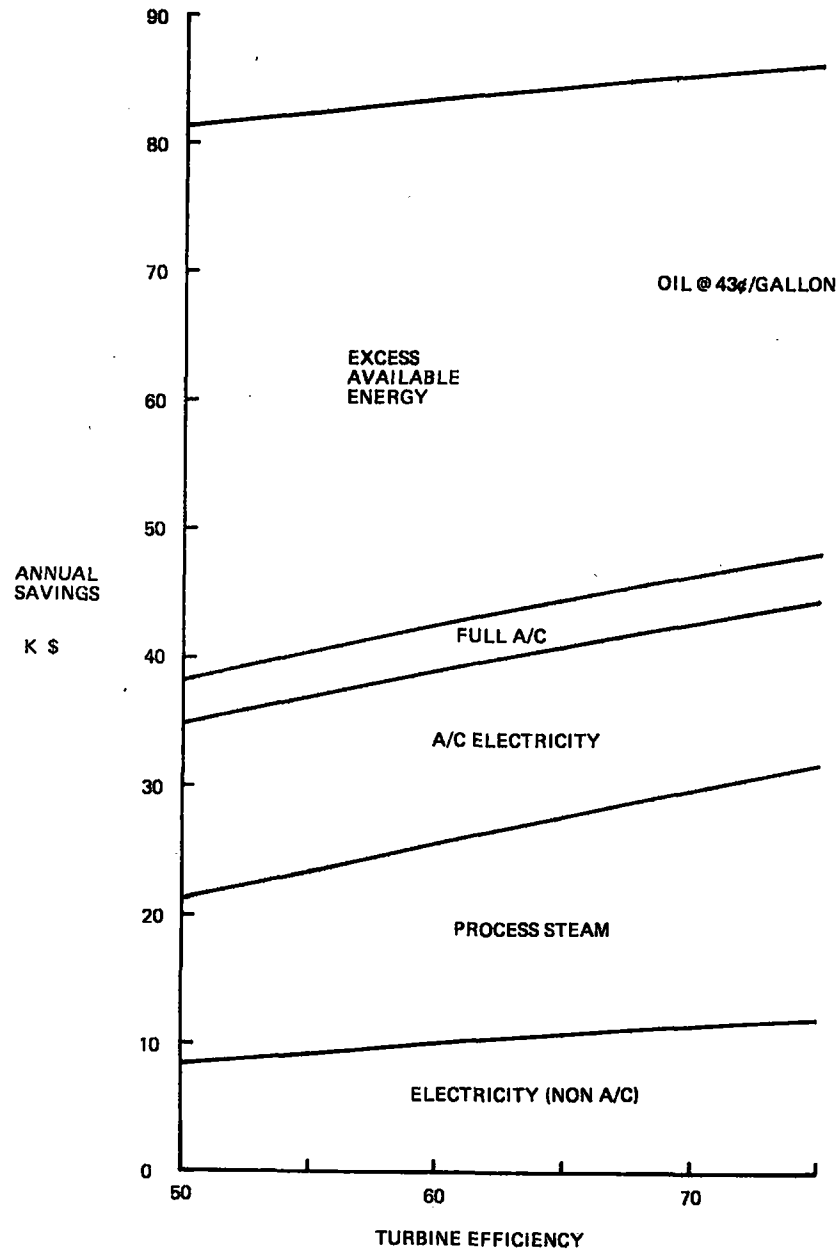


Figure 7.1-2. Effect of Turbine Efficiency on Annual Energy Cost Savings for Fuel Oil

Table 7.2-1. Economic Assumptions

System Life (years)	=	20
Discount Rate (fraction)	=	.09
Fixed Charge Rate (fraction)	=	.19
Inflation Rate (fraction)	=	.05
Energy Price Escalation Rate	=	parametic

Estimated capitol costs for the first experimental system are summarized in Table 7.2-2. Cost for the GFE turbine generator set is estimated.

Table 7.2-2. Experimental System Capital Cost Summary

Collector Field		\$4,387,950
Energy Plant		1,850,190
Turbine Generator		500,000 Est.
Control and Display		440,370
Indirect Costs		1,458,168
(1978 Dollar Value)	Total	<u>\$8,636,670</u>

The levelized annual cost of the Shenandoah experiment was determined to be \$1,122,000 using the above cost estimates and the procedure described in Appendix D. Included in the levelized annual cost are estimates for system operation and maintenance costs as well as component replacement costs (including fluid replenishment).

For annual electrical load savings of 3.06×10^{12} J (845,478 kWh) and thermal savings of 6.2×10^{12} J (5914 MBtu) for the first experiment, the cost of delivered energy (C_E) is obtained:

$$C_E = \frac{1,122,000}{.01(845,478) + (5914)} = 78.1 \frac{\text{¢}}{\text{kWh}} \cdot \frac{\$}{10^6 \text{ Btu}}$$

For full utilization of thermal energy, the thermal savings increase to 2.0×10^{13} J (18,401 MBtu) and the corresponding cost of delivered energy becomes:

$$C_E = \frac{1,122,000}{.01(845,478) + 18,401} = 41.8 \frac{\text{¢}}{\text{kWh}} \cdot \frac{\$}{10^6 \text{ Btu}}$$

Displacement of fuel burned in a furnace or boiler is generally a more cost-effective use of thermal energy than supplying it to an absorption air conditioner. If all the thermal energy supplied to the absorption air conditioner was utilized to displace fuel in thermal process, the annual electrical savings would decrease to 1.4×10^{12} J (393,100 kWh) and the annual thermal savings would increase to 2.8×10^{13} J (26,545 MBtu) yielding a new, lower cost of delivered energy:

$$C_E = \frac{1,122,000}{.01(393,100) + 26,545} = 36.8 \frac{\text{¢}}{\text{kWh}} \cdot \frac{\$}{10^6 \text{ Btu}}$$

Limiting factors in system economics are: current price of energy, full thermal utilization, and small scale of the experimental system. To attempt to show the effect of economics of scale, the system was scaled up by a factor of 10 to 1 and new costs of delivered energy computed for the 1st, 10th, and 100th units, respectively. These are summarized in Table 7.2-3. Cost reductions through learning have been estimated for all system components with varying degrees; i.e., relatively immature technologies have larger capacities for cost reduction through learning. Converting to a time frame, the same results of a 10 to 1 scale-up are graphically illustrated in Figure 7.2-1, where it is seen that economic viability occurs in a 1990 time frame at a real energy price escalation rate of six percent or about 1995 at four percent.

Table 7.2-3. Projected System Economics

Cost of Energy

- Supplying All Energy Forms
- Electricity and Process Energy Only
- Extended System Operation with No Storage or Air Conditioning

	Unit 1	Unit 10	Unit 100
	30¢/kWh	14¢/kWh	9.3¢/kWh
	26	12	8.1
	22	10	6.9

As a point of reference for the Bleyle plant, from August, 1977, to June, 1978, the effective electricity price rate (Georgia Power Co.) increased eleven percent while natural gas rates (Atlanta Gas Light Co.) increased fourteen percent, corresponding to annual price escalation rates of thirteen percent and seven-percent respectively. Assuming the general inflation rate for this period was eight percent, the real annual price escalation rates for the Bleyle plant were five percent for electricity and nine percent for natural gas over the above time period.

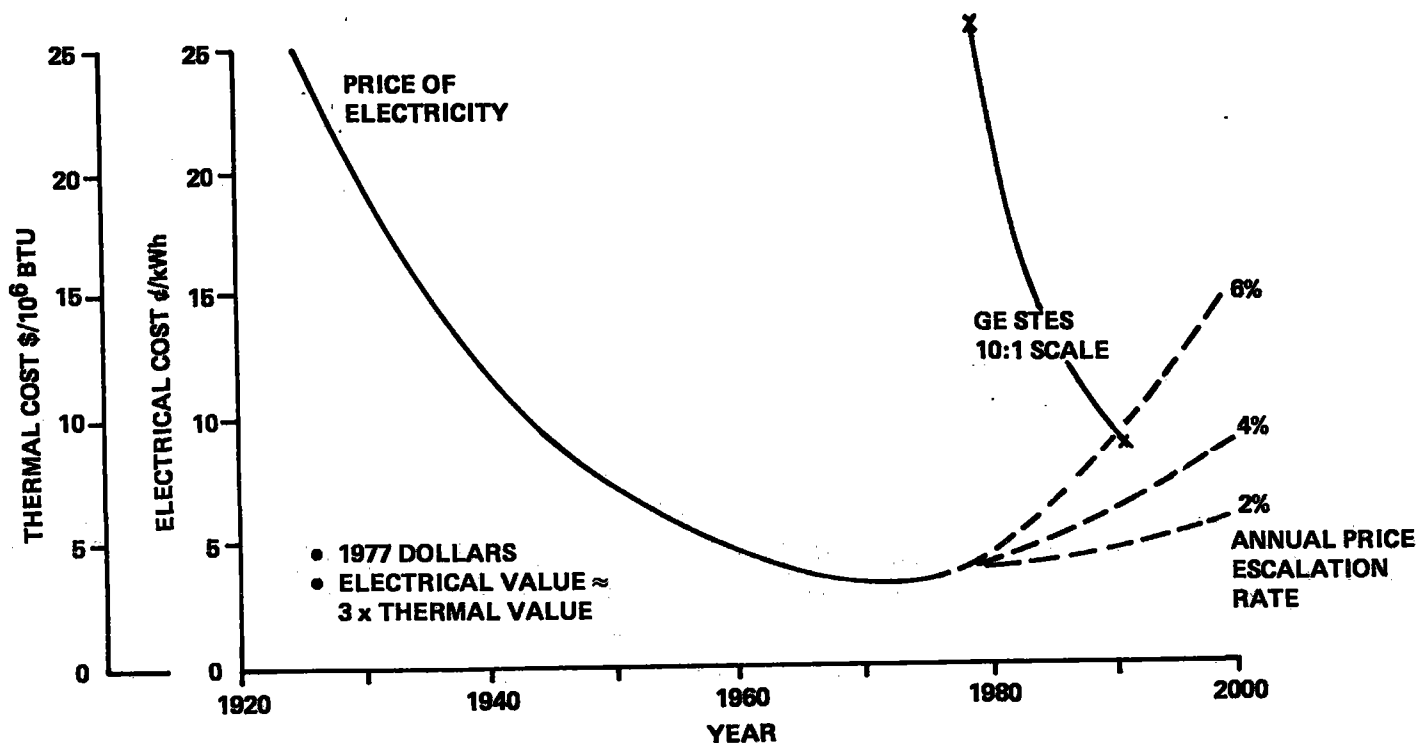


Figure 7.2-1. Projected Economics of Solar Total Energy

7.3 LAWS AND ORDINANCES

Principal laws and ordinances affecting the Shenandoah STE-LSE include:

<u>Title</u>	<u>STES Applicability</u>
● Standard Building Code (Southern)	Building Construction
● Shenandoah Development, Inc.	Site Layout
- Development Guidelines	
- Technical Specifications	
● Coweta County	Overall Construction
- Building Code	
- Plumbing Code	
- Electrical Code	

In addition, Coweta County has requirements that effect the access road planned to the south of the STE-LSE site. A 15 meter (50 ft) radius turnaround area is required at the end of any country road. Adding 7.6 meters (25 ft) of right of way on each side and the 18 meter (60 ft) right of way for the straight portion of the road results in about 4856 square meters (1.2 acres) of Shenandoah land dedicated to the access road. The STE-LSE site layout was also strongly affected by the development guidelines of Shenandoah Development Inc., which are excerpted in Table 7.3-1.

As definitive design progresses, additional portions of the development guidelines will govern such areas as landscaping, shrubbery and form and colors of structures. The objective is to ensure a design in concert with the overall Shenandoah design philosophy.

A significant achievement of the STE-LSE Shenandoah program has been the establishment of a Solar Easement Agreement protecting the solar collector field from shadowing due to future structures on adjacent land. An acceptable low level of shadowing was determined and analysis performed to determine allowable structure height as a function of distance from the collector field or set-back distance. The analysis results in quadratic forms for allowable heights as follows:

From the east and south reference lines:

$$\text{SBD} = .0665 \times (\text{H}-946)^2 + .825 \times (\text{H}-946) + 13.2$$

where SBD = Minimum set-back distance in feet

H = Allowed maximum height in feet above mean sea level

and from the west reference line:

$$\text{SBD} = .0665 \times (\text{H}-952)^2 + .825 \times (\text{H}-952) + 13.2$$

Reference lines and areas affected by solar easement are shown in Figure 7.3-1. Maximum allowed height under the above equations is shown as a function of set-back distance in Figure 7.3-2. Since the quadratic form of the equations proved difficult for legal acceptance, they were approximated by a series of three straight lines in the final Solar Easement Agreement (refer to Appendix E). It should be noted that all buildings, tanks and other structures on the STE-LSE site meet the allowable height requirements of the Solar Easement when referenced to the nearest solar collector row.

Table 7.3-1. Site Planning Guidelines

Location	<u>Shenandoah New Town, Coweta County, Georgia</u>	
Use	<u>Commercial and Industrial Sites</u>	
A. <u>Setbacks</u>		
1. Building from I-85 R-O-W	<u>100 ft.</u>	Min.
2. Building from other road R-O-W	<u>40 ft.</u>	Min.
3. Building from other property lines	<u>20 ft.</u>	Min.
4. Parking from property lines and building	<u>10 ft.</u>	Min.
5. Parking from Highway 34 R-O-W	<u>40 ft.</u>	Min.
B. <u>Lot Coverage Ratio</u>		
1. Landscaped areas and walks	<u>20%</u>	Min.
2. Building and covered structures	<u>40%</u>	Max.
3. Parking, drives, and outside storage	<u>40%</u>	Max.
C. <u>Parking Spaces</u>		
Use	Ratio	
Retail business, personal and professional services	1 space per 200 sq. ft. of floor area	
Office buildings, and retail and wholesale furniture outlets	1 space per 250 sq. ft. of floor area	
Restaurants, commercial recreation or amusement, and medical offices and clinics	1 space per 150 sq. ft. of floor area	
Places of assembly, theatres, auditoriums	1 space per 4 seats	
Manufacturing and industrial firms	1 space per 600 sq. ft. of floor area	
Warehouse or storage buildings	1 space per 1,000 sq. ft. of floor area	

7.4 HEALTH AND SAFETY

The applicable regulations pertaining to health and safety were extensively researched during the conceptual design phase of the STE-LSE Program. They include portions of:

1. OSHA Title 29 Part 1910 - Occupational Safety and Health Standards
2. OSHA Title 29 Part 1926 - Safety and Health Regulations for Construction
3. Natural Fire Protection Association - National Fire Codes - 1975
4. American National Standards Institute - Various codes and requirements
5. ASME Boiler and Pressure Vessel Code

A complete listing of applicable sections of the above documents is contained in the STE-LSE Conceptual Design Final Report, SD Document No. 78SDS4200, 12 Jan. 78.

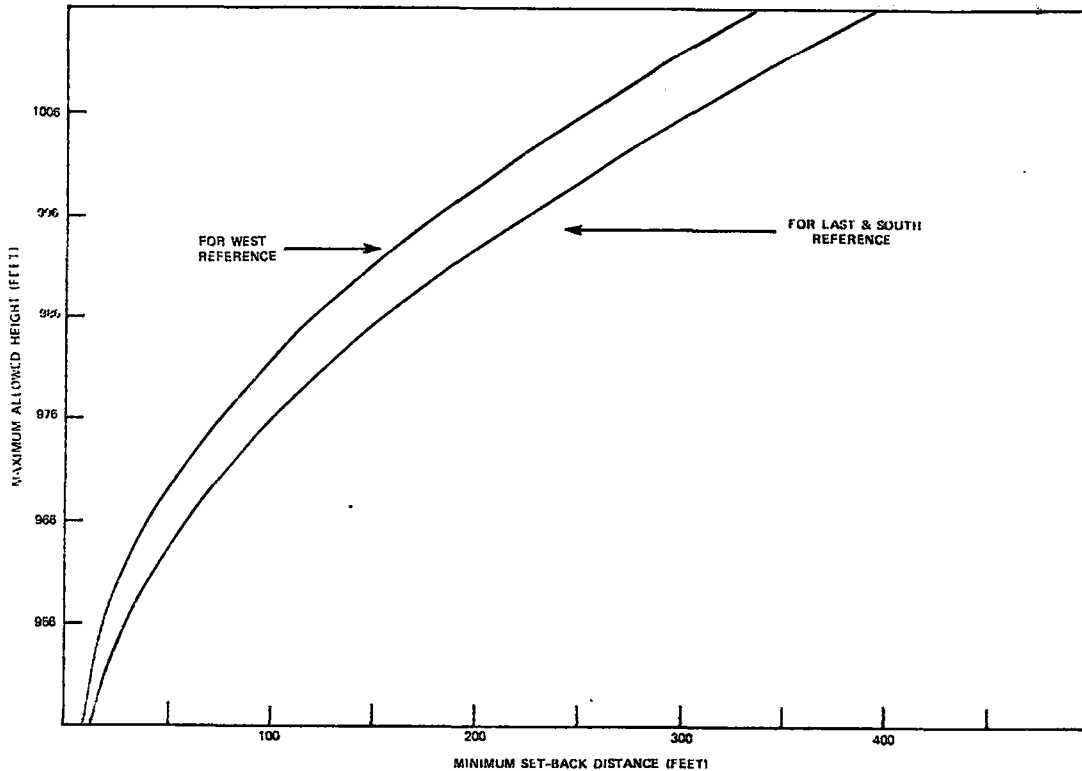


Figure 7.3-2. Setback and Height Restrictions for Property Near LSE, Shenandoah

Health and Safety of both visitors and STE-LSE personnel has been an important consideration in the preliminary design. Early indications are that no problems will be encountered in meeting regulatory requirements. Extensive thermal insulation used throughout the system to reduce energy losses provides low external surface temperature. All tanks are low pressure with the exception of the steam generator which at 700 psig, is moderate for this type of device.

Fluid lines operate at low pressure which, combined with use of welded fittings, greatly reduces leakage possibilities. Medium to low voltage electricity is used throughout, and ground grids are provided for lightning protection. Potential health and safety hazards are, with the exception of the solar collector area, similar to a conventional power plant, and thus operational procedures applicable to power plants will generally apply.

There will be certain areas of limited access, particularly in regards to visitors, and possibly some areas where protective headgear or clothing will be required. The collector field, in particular, will be completely enclosed by a high fence.

7.5 ENVIRONMENTAL ASSESSMENT

A preliminary Environmental Impact Assessment (EIA) was prepared for DOE review prior to the commencement of site preparation work on the Shenandoah STE-LSE. This will be expanded and updated prior to installation and erection of equipment on the site. The preliminary EIA is included in this report as Appendix F.

7.6 RELIABILITY ASSESSMENT

The reliability review of the STE-LSE Shenandoah system included a number of FMEC & SA's (Failure Mode Effects Criticality and Safety Analyses) on key subsystems and availability analysis of the system as well as all subsystems. The availability analysis also incorporated solar availability where the availability model was structured to address conditions for the Bleyle plant loads and for utility loads on a seasonal basis. Results of the FMEC & SA's show the STE system to be a design which is versatile and flexible with respect to providing services (electrical power, process steam, and heating/cooling) due to the use of back-up redundance for all outputs. These findings are also in support of the results which indicate a high availability index for the system equipments.

Table 7.6-1 presents the Failure Classification-Criticality Categories used in the detailed analysis. The FMEC & SA's, which were performed on a functional basis in order to be compatible with the present stage of design maturity, are listed in Table 7.6-2. This table in turn identifies the individual FMEC & SA summary tables and the appendix location for the corresponding detailed FMEC & SA worksheets.

Table 7.6-1. FMEC & SA Data

Failure Classification - Criticality Categories	
<u>Safety:</u>	
A	Hazardous to operating personnel or visitors. Critical injuries or loss of life are possible. Safety controls and warnings required. (e.g., enclosures, locks, fence, special clothing, etc.) This is coincident with the 1S Mission Critical Failure Classification. Any potential injury to a visitor, no matter how minor, will be considered in this safety category.
B	Serious, non-critical injury requiring hospitalization. A lost-time accident (e.g., 3rd degree burns). Safety instructions/warnings required.
C	Possible injury requiring medical treatment in the category of first aid (e.g., 1st and 2nd degree burns). Safety instructions/warnings required.
D	No effect.
Note:	It is assumed that personnel are in the vicinity and that proper protective measures are employed, i. e., protective clothing, shields, interlocks, sensors and remote controls as required. Instructions available and warnings prominently displayed.
<u>Mission:</u>	
1s Critical	Hazardous to visistors and/or operating personnel. Loss of life or critical injuries are possible.
1 Critical	Loss of, or severely degraded subsystem function and cessation of STES Operation to supply service(s)---must go to GPC Grid Electrical Supply, Bleyle Steam and Bleyle Air Conditioning.
2 Major	Degraded subsystem function but overall STES operational with minor time or capacity constraints. Repairs required, not necessarily immediately.
3 Minor	Negligible or no effect on subsystem or overall STES Operation.

Table 7.6-2. STE-LSE Shenandoah FMEC & SA Identification

Subsystem	Results Summary Table	Location for Detailed FMEC & SA
Solar Collectors	Table 7.6-3	Appendix G
Absorption Air Conditioner and TUS	Table 7.4-4	Appendix H
High Temperature Thermal Energy Storage	Table 7.6-5	Appendix I
System and Central Control	Table 7.6-6	Appendix J

Table 7.6-3. Solar Collector FMEA Significant Design Impact Items Identified

Unit/Assy	Function	Failure & Probable Cause	Failure Effect	Remarks
High-Speed Drive Motor - Traverse Jackuator and Piping	Provide Defocus Motion to Dish When Overtemperature is Sensed	Failure to Defocus Dish-Control Relay Contacts Inhibit Signal Due to Contamination or Aging Effects	Damaged Collector, Possible Impact on Adjacent Collectors	Low Failure Probability. Check Relay Contacts (High Speed) During Routine PM. (Drive-Motor Assumed ok - Just Used for Normal Traverse)
Overtemperature Sensor	Detect "Hot Spot" Overtemperature Condition in Receiver, Send Signal to Control Microprocessor (μ P)	Fails to Sense O. T. or to Send Signal to Central Control (μ P)	Same as Above	Low Failure Probability, Check O. T. Sensor During Routine PM

Table 7.6-4. Absorption Air Conditioner FMEA Summary

High Availability	-	Low failure expectancy Short downtime
Benign System	-	Little or no effect on other STE-LSE Subsystems
GE-RESD* Experience	-	2 machines, 600 tons total
	-	Full time operation
Machine A	1960 - 1975	4 failures - Tubing, HX
Machine B	1966 - Present	3 failures - Tubing, Pump
Machine C	1975 - Present	1 infant failure - Pump Motor

*Re-entry and Environmental Systems Division

Table 7.6-5. High Temperature Storage FMEA Summary

High Availability	-	Four tank system provides versatile solar energy storage function
	-	Almost normal operation with one tank down for repairs
	-	Low failure probability, standard tank design methods (high strength boiler plate used, low wall stresses over operating temp. Range and differential expansion compatibility between tank walls and taconite storage media)
Transfer Pump	-	Fossil heater provides energy if temperature gradient problem occurs due to pump outage
High Maintainability	-	Dome access port to reach distribution manifolds
	-	Nitrogen atmosphere to minimize oil degradation
	-	Sludge removal convenience
High Safety Index	-	Standard tank design practices followed
	-	Relief & vent valves, each tank
	-	Insulation 14 in., outside skin temp. < 120°F, enclosed area
	-	Pneumatic valves commanded to fail safe position & pneumatic supply shut down if failure condition is sensed

Table 7.6-6. Total System FMEA Summary

High Availability	-	Back-up redundancy for all services
	-	Operating flexibility
Fault Tolerant Controls Design	-	Distributed control with central minicomputer plus seven remote microprocessors
	-	Automatic remote control if central control failure occurs
High Safety Index	-	Emergency controls follow "fail-safe" principle (e.g., defocus command upon sensed overtemperature in collector receiver; TES plumbing failure occurs, controls command valves to fail-safe position & shut down pneumatic control supply)
	-	Special emphasis on safety code/practices mandatory in power conversion system (follow power plant practices)

Availability index, rather than reliability was estimated since it is more appropriate for a design which receives maintenance. Availability is also the accepted standard criteria used in electric utility reliability analysis.

The availability predictions for the STE system are based on the Availability (Reliability) Block Diagram, Figure 7.6-1. The diagram includes all functional equipment and accounts for the various system modes of operation, including backups, necessary to provide the Bleyle plant with the three basic outputs - electrical energy, process steam, and cooling/heating.

System availability predictions are summarized in Table 7.6-7 on a seasonal basis for each of the three basic energy services. Solar availability as herein defined is the fraction of the Bleyle plant loads which are met by the STES with 100 percent equipment availability and no fossil back-up. Solar availability for electricity and process steam is highest in the summer, lower in spring and fall, and lowest in winter, reflecting the seasonal insolation variations. Electric and process steam availability are approximately equal since the system operational philosophy precludes supplying un-cascaded process steam. Cooling solar availability is very high due to the large amount of low temperature (210°F) thermal energy available. The high value for winter also reflects a greatly reduced cooling load resulting from use of economizers in the Bleyle production area. Figure 7.6-2 presents solar availability on a monthly basis for the Bleyle plant loads.

Availability predictions were performed for all operational subsystems and component groups. Typical availability prediction worksheets are presented in Tables 7.6-8 and 7.6-9 for the fossil heater and steam generator, respectively. Table 7.6-10 presents an availability summary for a number of key STES subsystems.

The availability of solar total energy systems during utility peak periods is important for the case of utility STES ownership. Figure 7.6-3 presents typical summer and winter load profiles for Georgia Power Company. Assuming a typical level for peaking equipment being loads greater than 90 percent of peak, summer peaks are seen to occur in the 10 AM to 6 PM time period. Winter loads show two peaks - a morning peak from about 6 AM to noon and an evening peak from about 5 PM to 9 PM.

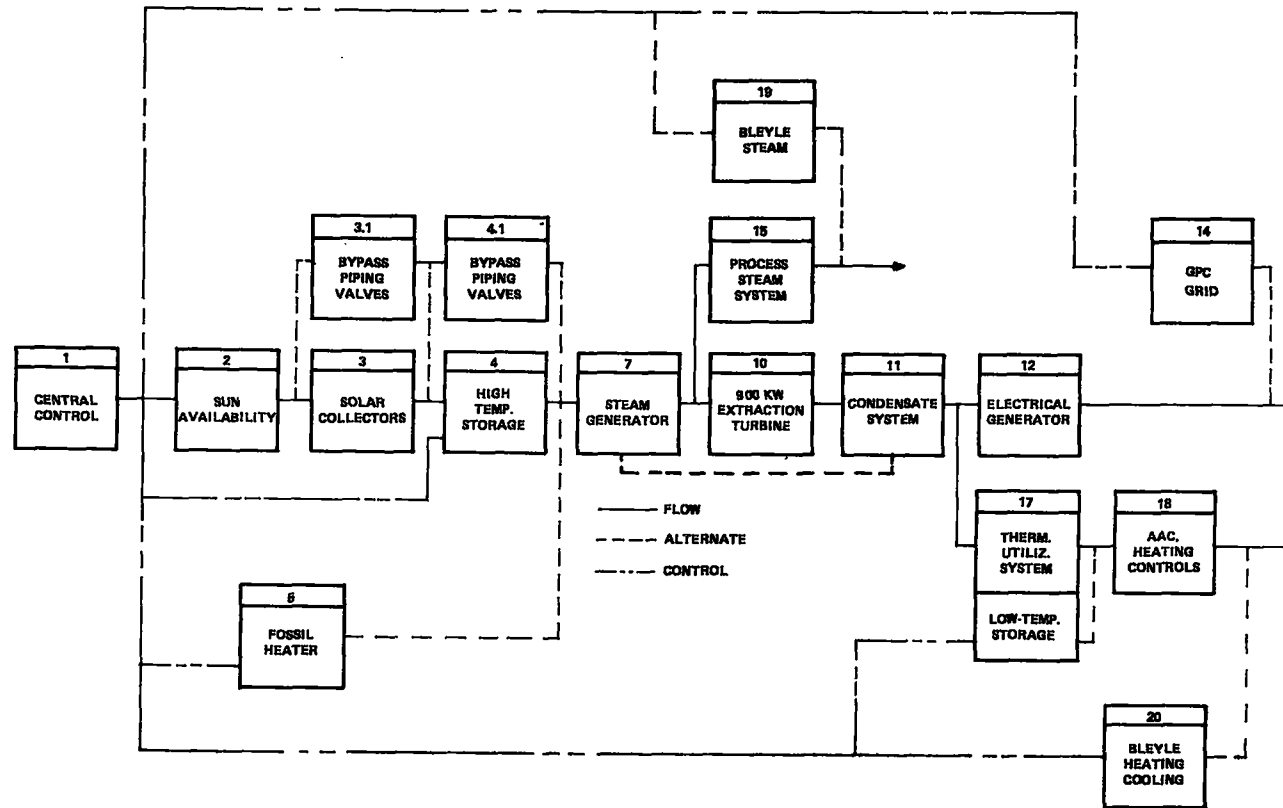


Figure 7.6-1. Reliability Block Diagram, STES-LES

Table 7.6-7. System Availability for Bleyle Loads

Load	Season	Solar Availability	Equipment Availability	Solar Plus Equipment	With Fossil Backup
Electrical	Summer	.792	.968	.766	.968
	Winter	.433		.419	.965
	Spring/Fall	.617		.597	.967
Process Steam	Summer	.790	.968	.765	.968
	Winter	.433		.419	.965
	Spring/Fall	.615		.595	.966
Cooling	Summer	.918	.965	.886	.966
	Winter	.876		.845	.965
	Spring/Fall	.852		.822	.965

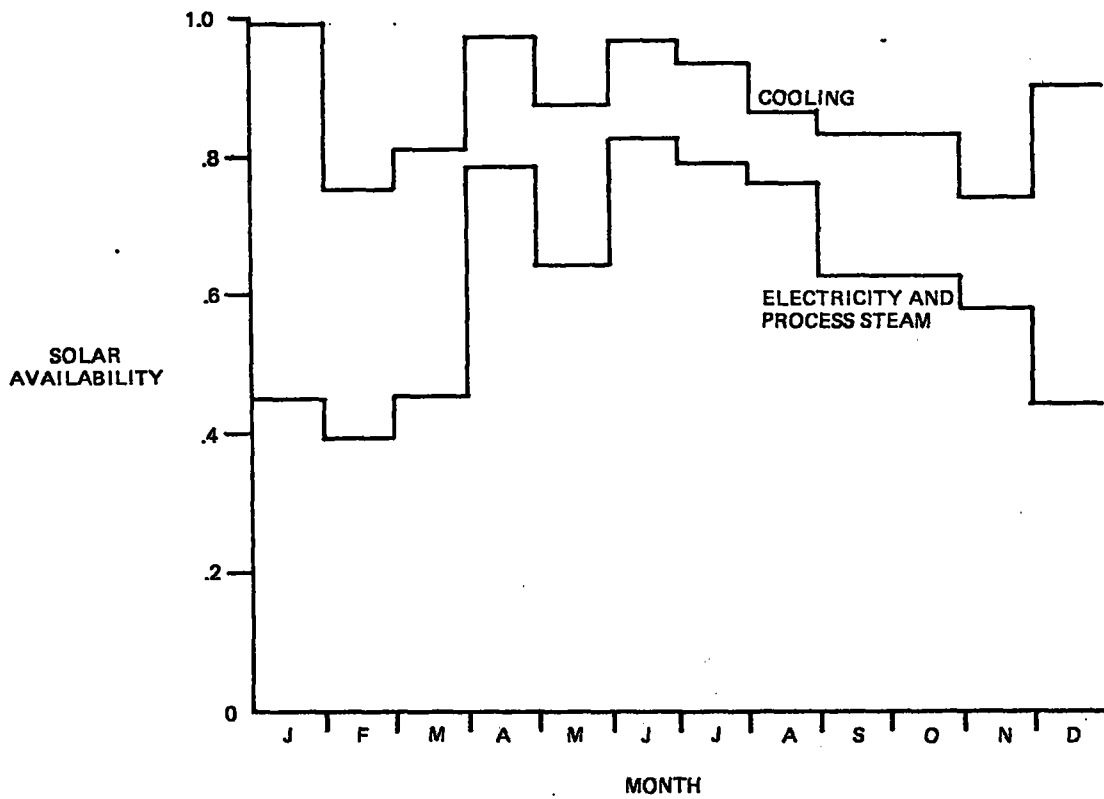


Figure 7.6-2. Solar Availability for Bleyle Plant Loads

Table 7.6-8. Availability Prediction Worksheet - Fossil Heater

HARDWARE BLOCK ASSEMBLY	FAIL. RATE λ_j (F/10 ³ HR)	MTTR \bar{M}_{ci} (HR)	EFFECTIVE MTTR \bar{M}_{ci} (HR)	EFFECTIVE $\lambda_j \bar{M}_{ci}^*$ (x 10 ⁻³)
5.0 FOSSIL FIRED HEATER				
5.1 VESSEL & SUPPORT	.005	48	32.0	.16
5.2 EXCH. TUBES & COILS	.005	80	52.0	.26
5.3 AIR SUPPLY SYSTEM	.10	8	6.25	.625
5.4 FUEL SUPPLY SYSTEM	.10	8	6.25	.625
5.5 COMBUSTION SYSTEM	1.00	8	6.25	6.25
5.6 EXHAUST SYSTEM	.01	8	6.25	.0625
5.7 PREHEATER	.10	4	3.625	.3625
	$\Sigma = 1.320$			$\Sigma = 8.3450$

$$(\text{ASSY MTTR}) \bar{M}_c = \frac{\sum (\lambda_j \bar{M}_{ci})^*}{\sum \lambda_j} = \frac{8.345}{1.320} = 6.32197$$

*EFFECTIVE VALUES BASED
UPON 16 HRS/DAY OPERATION

$$\text{UNAVAILABILITY (INHERENT)} U_I = \frac{\bar{M}_c}{\sum \lambda_j^{-1} + \bar{M}_c} = \frac{6.32197}{(.00132)^{-1} + 6.32197} = .00828$$

$$\text{AVAILABILITY (INHERENT)} A_I = 1 - U_I = 1 - .00828 = .99172$$

Table 7.6-9. Availability Prediction Worksheet - Steam Generator

HARDWARE BLOCK ASSEMBLY	FAIL RATE λ_j (F/10 ³ HR)	MTTR \bar{M}_{ci} (HR)	EFFECTIVE MTTR \bar{M}_{ci} (HR)	EFFECTIVE $\lambda_j \bar{M}_{ci}^*$ (x 10 ⁻³)
7.0 STEAM GENERATOR				
7.1 INLET & OUTLET SECT.	.005	24	16	.08
7.2 TUBES & SUPPORT	.005	80	52	.26
7.3 FEED INLET RING	.005	48	32	.16
7.4 LEVEL/FLOW CONTROL	.100	4	3.625	.3625
7.5 STEAM OUTLET SECT.	.005	24	16	.08
	$\Sigma = .120$			$\Sigma = .9425$

$$(\text{ASSY MTTR}) \bar{M}_c = \frac{\sum (\lambda_j \bar{M}_{ci})^*}{\sum \lambda_j} = \frac{.9425}{.120} = 7.8542$$

$$\text{UNAVAILABILITY (INHERENT)} U_I = \frac{\bar{M}_c}{(\sum \lambda_j)^{-1} + \bar{M}_c} = \frac{7.8542}{(.00012)^{-1} + 7.8542} = .00094$$

$$\text{AVAILABILITY (INHERENT)} A_I = 1 - U_I = 1 - .00094 = .99906$$

Table 7.6-10. Availability Summary Key Items

Steam Generator	.999
Fossil Heater	.992
Absorption Air Conditioner	.996
High Temperature Storage	.998
Condenser System	.998
Central Control	.992

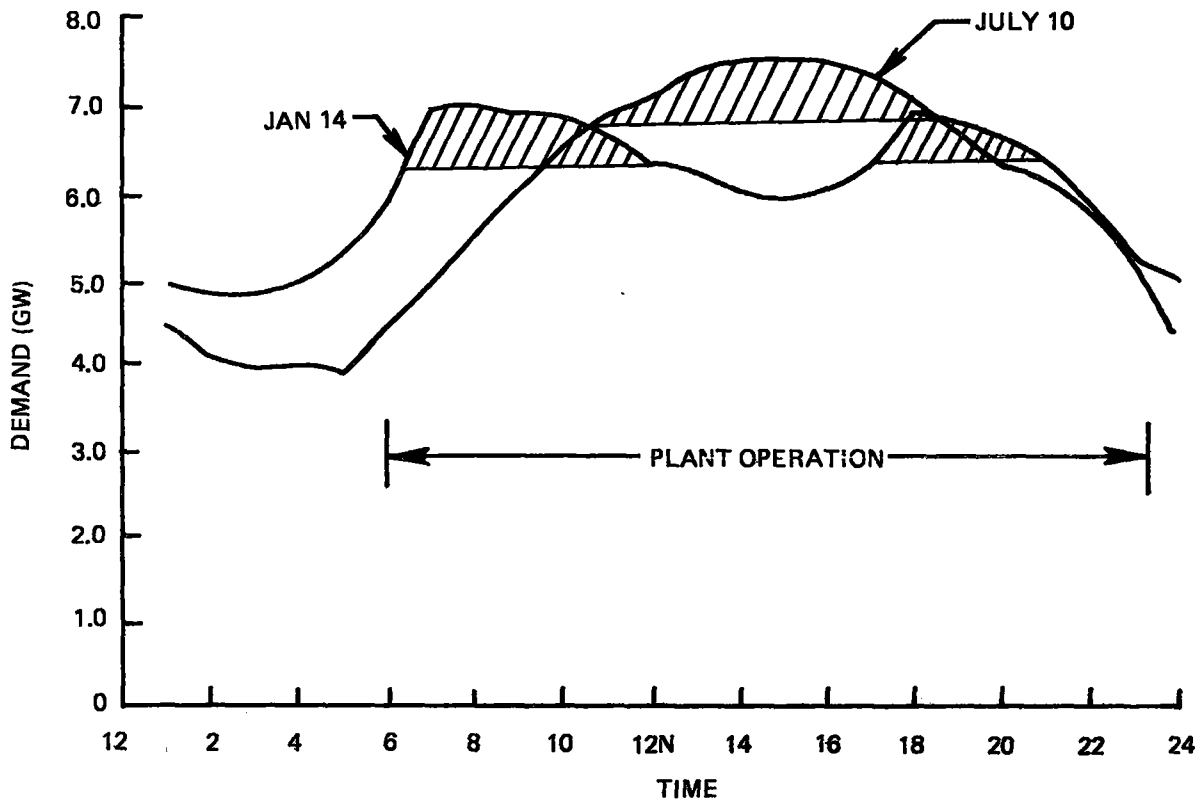


Figure 7.6-3. Utility Demand Profiles

Figure 7.6-4 shows the STES availability for electric output during the above defined peak periods. Availability ranges from a low of .374 for winter peak period to a high of .892 for summer peak periods. The actual peak load availability would be expected to be slightly higher in summer due to the general coincidence of high insolation levels and high peak loads due to air conditioning demands. In winter the situation is somewhat reversed since very high system demands due to heating requirements could appear on cloudy days with little or no STES output capability.

The addition of generation equipment to an electric utility grid will increase the reliability of the system. This is generally true regardless of the size of the generation addition or its particular reliability or availability characteristics. For a utility system designed to a specific reliability or availability

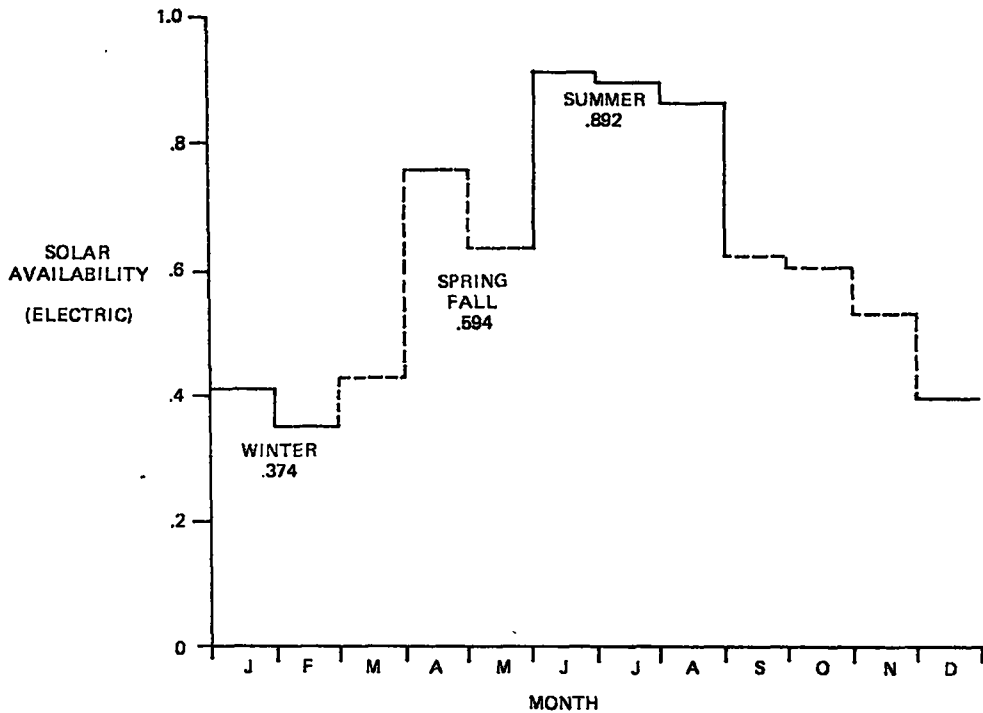


Figure 7.6-4. Solar Availability for Utility Peak Loads

requirement, the equipment addition thus allows elimination of some other equipment or extends the system load carrying ability at the required reliability. In either case, capacity is effectively displaced, and the added generation equipment gains value beyond its fuel savings.

Figure 7.6-5 shows typical availability characteristics for a utility system. The term loss-of-load probability (LOLP)* is commonly used to express system reliability, with a typical design level being 0.1 day per year at the expected system peak load. For other loads, the LOLP varies so as to approximate closely a straight line on semi-log paper as shown on Figure 7.6-5. The addition of new equipment drops the LOLP line to a lower level. The horizontal displacement of the new line from the original at the design LOLP is then the effective load carrying capability of the added equipment.

Garver (Reference 7.6-1) has analyzed LOLP characteristics and developed a relationship for load carrying capability of new equipment which is extensively used in utility system analysis. Garver's equation is:

$$C^* = C - m \ln \left[(1-r) + r e^{C/m} \right]$$

Where:

- C* = Effective Load Carrying Capability
- C = Nominal Capacity
- m = System Characteristic Slope
- r = Forced outage rate
- 1-r = Availability

*In statistical terms, loss of load probability is really not probability but expected value.

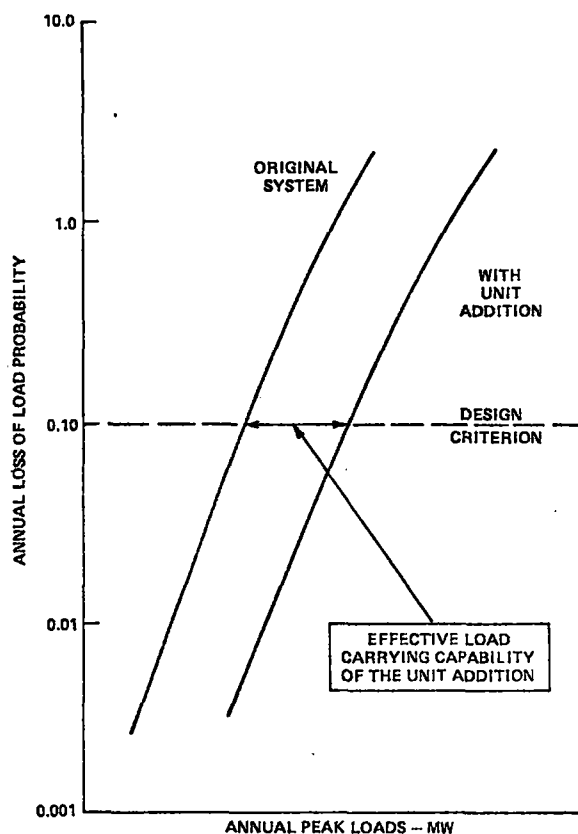


Figure 7.6-5. Characteristic Utility System Availability

Derivation of Garver's equation is shown in Appendix K. The characteristic slope m is defined as that amount of additional load which increases the LOLP by a factor of e (2.71828...). For large interconnected utility network such as the Southern system which includes Georgia Power Company, m has a value on the order of 500 to 600 megawatts.

When C , the nominal or name plate capacity of a generation addition, is very small compared to m , the effective load carrying capability is closely approximated by the unit availability times the rating as shown in Figure 7.6-6, which is a graphical presentation of Garner's equation.

Note that as the capacity of the added unit approaches and exceeds m , the load carrying capability falls off sharply. This is because availability of a large unit influences the overall system's ability to meet its load much more than the availability of a small unit. Multiple small units would thus be expected to have higher load carrying capability than a single large unit of equal capacity and availability. This is true for conventional generation equipment but generally not for solar devices since the most common cause of outage, lack of sun, will cause all units to go out. The multiple units thus perform as one large unit on an availability basis. Thus, based on the above analysis, the Shenandoah STES could displace about 89 percent of its capacity for small penetrations in a summer peaking utility system. This would be offset in the Georgia Power Company system by the very high winter demands as shown in Figure 7.6-3. Exact estimates of capacity displacement in terms of amount and types of units would require a system generation planning simulation involving not only Georgia Power Company but the system with which it is interconnected. Such an effort is beyond the scope of this program.

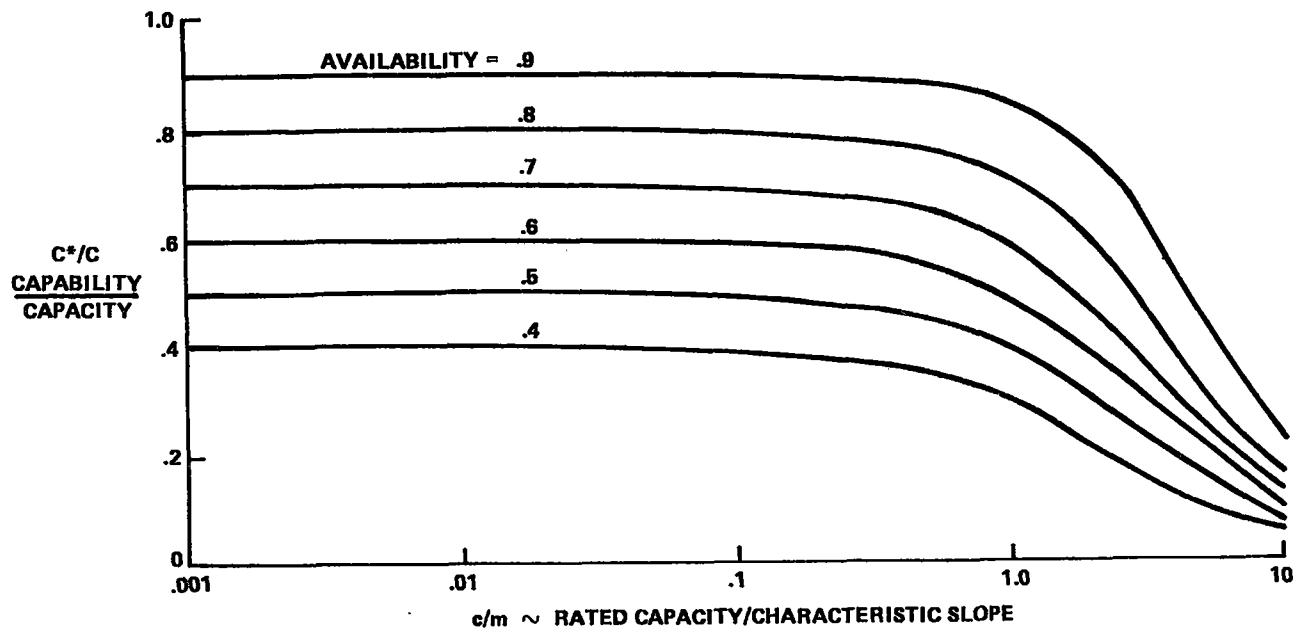


Figure 7.6-6. Effect of Size on Load Carrying Capability

The net result of the reliability/availability analysis including the FMEC & SA's shows an availability index (especially equipment availability) at a high level which is in concert with present day utility availability) at a high level which is in concert with present day utility availability expectancies for new applications. The FMEC & SA's show the system design approach to be fault tolerant and versatile, the key factor being the use of back-up redundancy for providing any service. Similarly, use of standard safety devices, practices, and design standards applicable to conventional power plants will assure that the FMEC & SA indication of a high safety index will be maintained.

SECTION 8
SUBSYSTEM DEVELOPMENT

SECTION 8

SUBSYSTEM DEVELOPMENT

8.1 COLLECTOR DEVELOPMENT

8.1.1 ENGINEERING PROTOTYPE COLLECTOR

Since the collector represents a critical cost/performance element of the Shenandoah LSE, testing of a paraboloidal collector similar to the final LSE collector design was undertaken in the LSE Shenandoah preliminary design program. The prime objectives of the test were to:

1. Measure and characterize the performance of a parabolic collector,
2. Verify and update the analytical and design tools used to design the LSE collector, and
3. Learn through representative hardware the characteristics of the mechanical and control operation of a solar tracking collector.

The collector, designated the Engineering Prototype Collector (EPC), was designed and fabricated by General Electric and its subcontractor, Scientific-Atlanta, and installed at the Sandia Laboratories solar test facility at Albuquerque, New Mexico. Testing was started during the LSE preliminary design program and is continuing into the definitive design phase.

8.1.1.1 EPC Description

The EPC is based on a modified 5-meter RF antenna supplied by Scientific-Atlanta, Inc. The modifications include the addition of a thermal receiver, the application of a reflective surface on the dish, the extension of the tracking range from that of the standard antenna, the addition of tracking drive mechanism, and the integration of an existing closed loop solar tracking unit supplied by the Mann-Russell Corp. A sketch of the assembled collector and photographs of the unit are shown in Figures 8.1-1, 8.1-2 and 8.1-3.

The collector dish provided by Scientific-Atlanta is a paraboloid of revolution 5-meters in diameter. It is constructed of 24 die stamped aluminum petals bolted together through integral flanges and a rib support structure. The reflector surface is a commercially available reflective tape, FEK 244, produced by the 3M Company.

The LSE collector optimization studies indicated that an f/d ratio of 0.5 would be optimum. Since the focal length of the 5-meter dish was fixed, it was decided to mask off an outer ring of 1.25 meters to achieve the desired f/d (Figure 8.1-2).

The receiver was designed and fabricated by GE to the same configuration as the LSE collector receiver. The receiver is of the cavity type; its geometry is similar to the full scale receiver configuration of the 7-meter dish design with modifications necessary for instrumentation testing flexibility. A photograph of the receiver mounted on the test collector is shown in Figure 8.1-4, and a schematic including instrumentation positions is shown in Figure 8.1-5.

Inside the cavity is an absorptive coil of 0.011 meter (7/16in.) diameter by .00089 meter (.035 in.) wall stainless steel tubing wound into the beehive configuration shown in Figure 8.1-6. The total length of tubing is 26.2 meters (86 ft.), and an absorptive oxidation coating has been applied to yield an absorptivity of 0.9. The wall behind the coil as well as the aperture face plate has been coated with a low α/ϵ porcelain coating. The walls of the cavity are insulated with 0.051 meter (2 in.) of a high temperature, low conductivity, ceramic insulation.

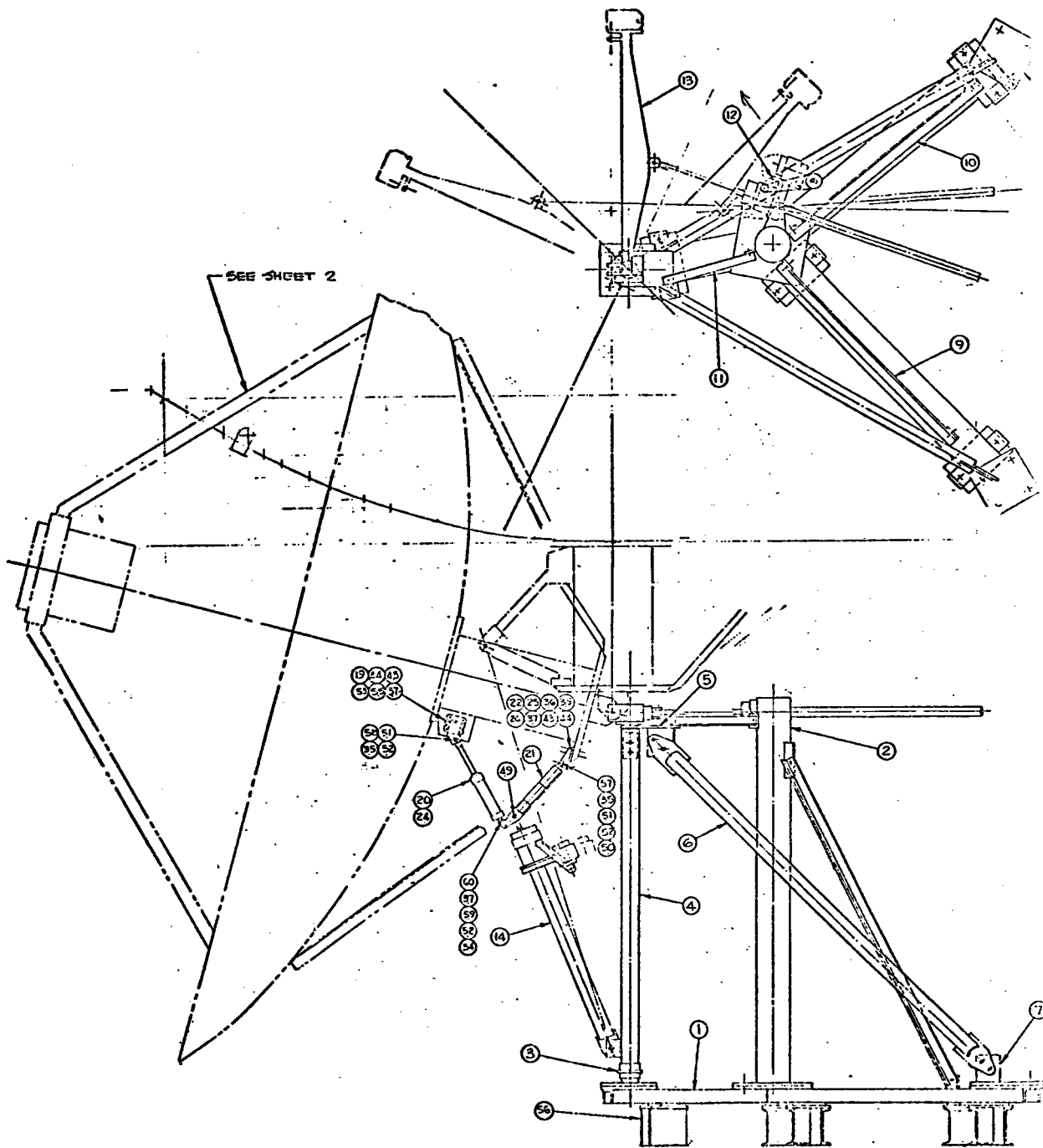


Figure 8.1-1. Layout of 5-Meter Engineering Prototype Collector

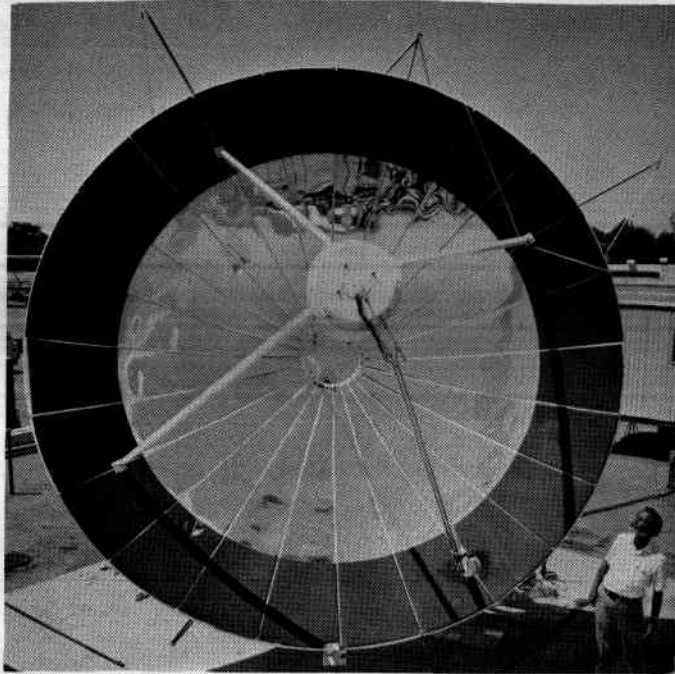


Figure 8.1-2. Front View of EPC



Figure 8.1-3. Side View of EPC

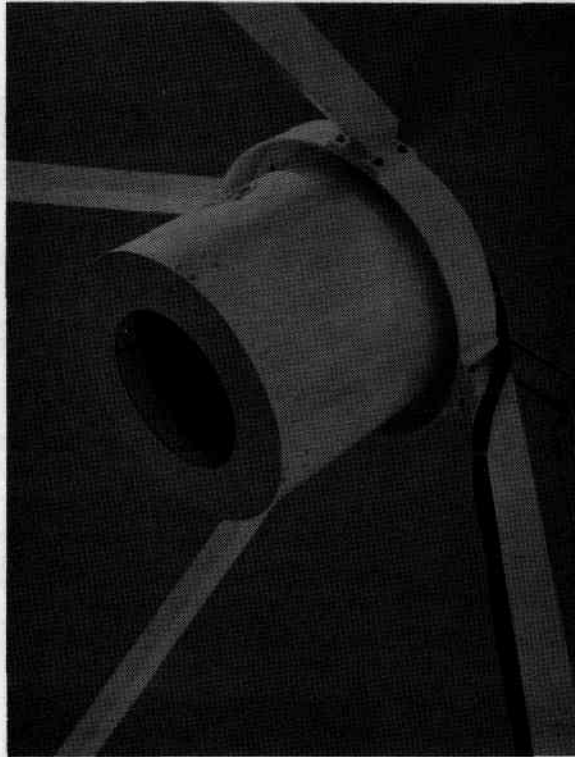


Figure 8.1-4. EPC Receiver

8.1.1.1.1 Support Stand

The collector system is supported by a structure consisting of steel channel, angle, and tubine (Figures 8.1-1 through 8.1-3). The support structure includes electric motor driven jack screws which drive the collector angularly for azimuth and elevation positioning. The angular drive rate capability is from zero to ten times the sun rate. The azimuth angular limits are from 108° east of south to 10° west of south, whereas the elevation angle limits are 15° to 90° above horizontal.

The structure is bolted to four mounting feet which, in turn, are bolted into a concrete base at the Sandia test site with anchor bolts. To compensate for a slope in the concrete base (down from east to west) of approximately 0.9° , the structure is shimmed.

Included in the support system is a hydraulic defocusing device. This hydraulic actuator has a 0.051 meter (2 in.) bore and 0.165 meter (6 1/2 in.) stroke. Upon command, a valve is opened, and the hydraulic fluid is dumped. In order to alleviate undue shock, the fluid passes through a restriction orifice. Total defocus travel is ten degrees.

All tubing carrying the heat transfer fluid, Therminol 66, is 0.013 meter (1/2 in.) diameter stainless steel tubing with 0.00089 meter (.035 in.) wall. Figure 8.1-7 shows details of the insulation for both the flexible tube and the straight runs of rigid tube. The inlet and outlet tubes are held within the insulation 0.0286 meter (1 1/8 in.) apart on centers. The flexible tube is a braided, convoluted, stainless steel hose and is required to accommodate the elevation and azimuth motions. The flexible insulation is made from 0.025 meter (1 in.) thick, 0.089 meter (3 1/2 in.) in diameter wafers of Temp Mat which is a woven fiberglass thermal insulation. The protective flexible covering is Gortiflex made from fiberglass.

T/C NO.	LOCATION	X	Y	Φ
1	COIL #23	-	-	45
2	24	-	-	45
3	24	-	-	45
4	22	-	-	45
5	20	-	-	45
6	18	-	-	45
7	17	-	-	45
8	17	-	-	45
9	1	-	-	45
10	1	-	-	45
11	25	-	-	135
12	22	-	-	135
13	12	-	-	135
14	1	-	-	135
15	25	-	-	225
16	22	-	-	225
17	12	-	-	225
18	1	-	-	225
19	25	-	-	315
20	22	-	-	315
21	12	-	-	315
22	1	-	-	315
23	INNER SHELL - OUTER SURFACE	17 IN.	-	45
24	↑	13 1/2 IN.	-	45
25	↑	5 IN.	-	45
26	↑	17 IN.	-	135
27	↑	13 1/2 IN.	-	135
28	↑	5 IN.	-	135
29	↑	17 IN.	-	225
30	↑	13 1/2 IN.	-	225
31	↑	5 IN.	-	225
32	↑	17 IN.	-	315
33	↑	13 1/2 IN.	-	315
34	↑	5 IN.	-	315
35	INNER SHELL - OUTER SURFACE	-	9 1/4 IN.	45
36	INNER SURFACE - BOTTOM ANNULUS	-	6 1/4 IN.	45
37	↑	-	9 1/4 IN.	135
38	↑	-	6 1/4 IN.	135
39	↑	-	9 1/4 IN.	225
40	↑	-	6 1/4 IN.	225
41	↑	-	9 1/4 IN.	315
42	↑	-	6 1/4 IN.	315
43	INNER SURFACE - BOTTOM ANNULUS	-	6 1/4 IN.	315
44	OUTER SHELL - INNER SURFACE	17 IN.	-	45
45	↑	13 1/2 IN.	-	45
46	OUTER SHELL - INNER SURFACE	-	5 IN.	45
47	INNER SURFACE - UPPER DISC	-	3 1/2 IN.	45
48	↑	-	3 1/2 IN.	135
49	↑	-	3 1/2 IN.	225
50	INNER SURFACE - UPPER DISC	-	3 1/2 IN.	315
51	INNER SURFACE - UPPER ANNULUS	-	4 1/2 IN.	45
52	↑	-	4 1/2 IN.	135
53	↑	-	4 1/2 IN.	225
54	FLUID INLET TUBE D=3	-	-	-
55	FLUID INLET TUBE D=4	-	-	-
56	FLUID OUTLET TUBE D=3	-	-	-
57	FLUID OUTLET TUBE D=4	-	-	-

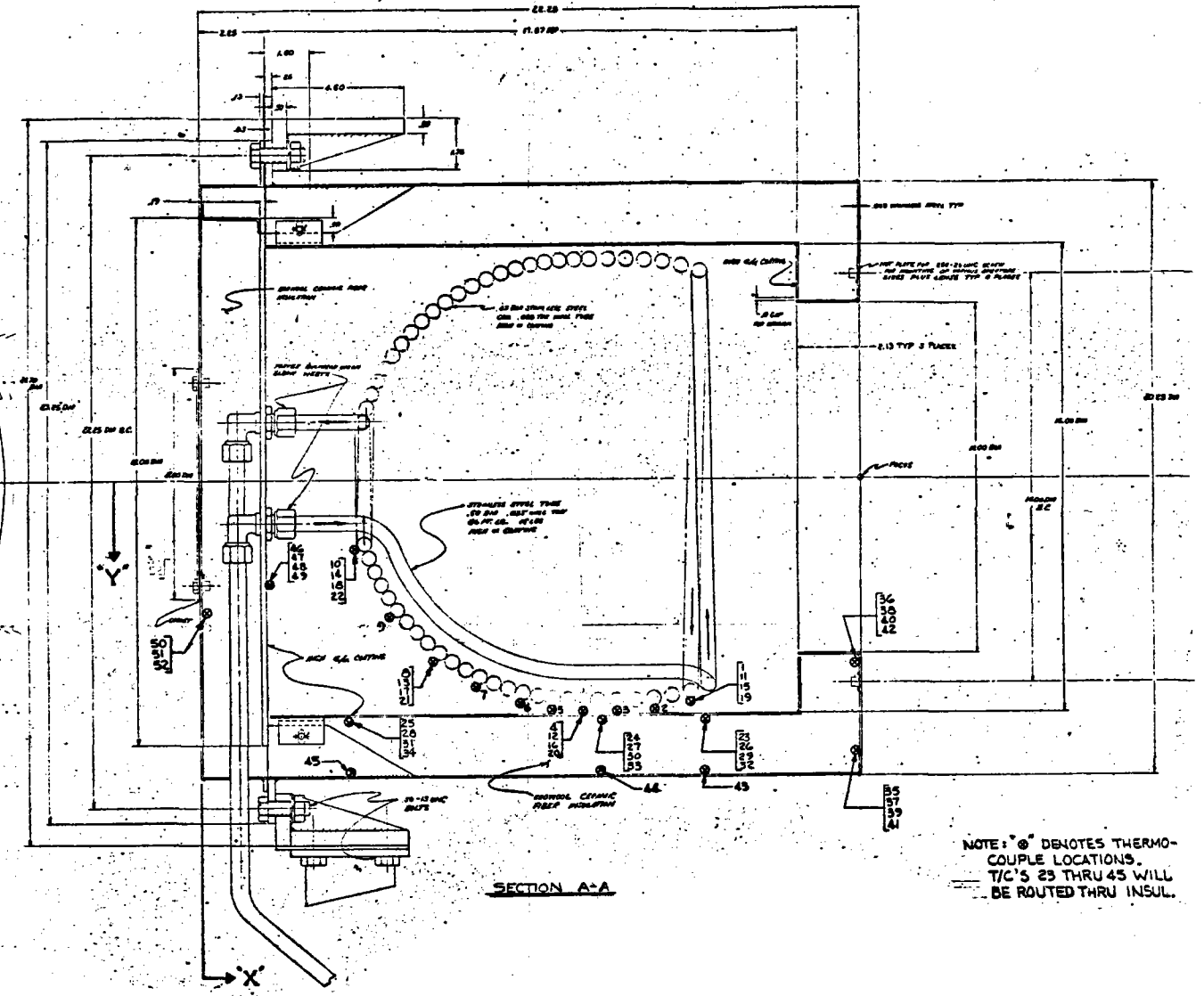
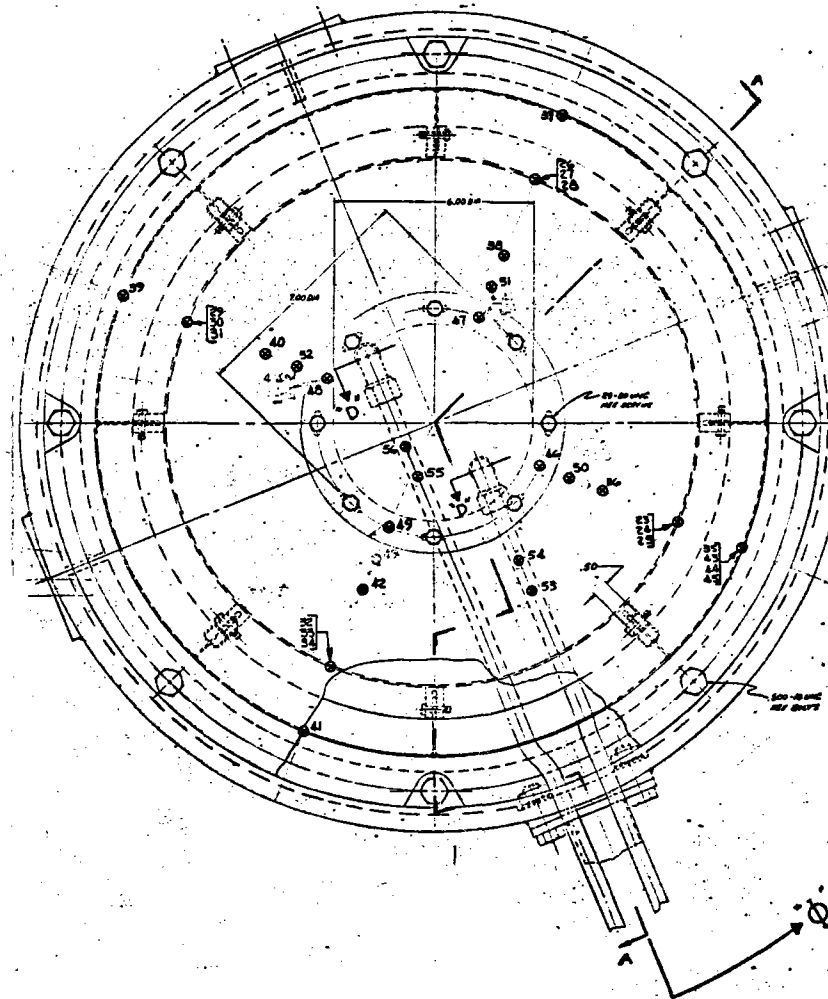


Figure 8.1-5. Sketch of EPC Receiver

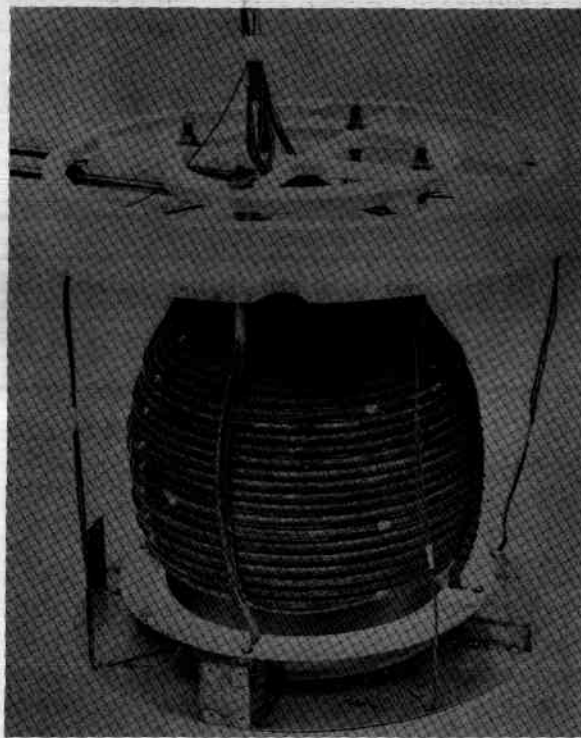


Figure 8.1-6. EPC Receiver: Coil Assembly

The fixed straight tubing is covered with a composite insulation system consisting of 0.032 meter (1 1/4 in.) thickness Temp-Mat inside 0.032 meter (1 1/4 in.) of rigid Foamglas insulation. The insulation is wrapped with a banded thin stainless steel jacket. The fixed bends are insulated in much the same manner as the flexible tubing except that the insulation is 0.127 meter (5 in.) in diameter instead of 0.089 meter (3 1/2 in.). All tube fittings are Swagelock types.

8.1.1.1.2 Control System

The control system for sun tracking and emergency shutdown consists of a sun sensor, collector drive motors, position potentiometers, a Hewlett-Packard 9825 computer, A/D counters, relays, relay actuators, timer, temperature sensors, flow rate sensor, and a solid state logic device. An interface diagram of the system is shown as Figure 8.1-8. The Hewlett Packard Model 9825 desk top calculator provided by Sandia Laboratories generates the sun azimuth and elevation angles. Position potentiometers furnished by Scientific Atlanta and mounted on the collector azimuth and elevation shafts provide collector angular position data to the analog/digital units which feed the 9820. The A/D's are HP Model 5328A counters with the digital volt meter option provided by Sandia Laboratories; two are required - one for each axis. The position error signals thresholded operate an HP Model 59306A relay actuator also furnished by Sandia Laboratories. This unit contains six relay contacts rated at 0.5 amp, 28 Vdc or 115 Vac. These contacts operate into the GE provided controller.

The controller is a solid state logic device. A mode select signal from the Sandia Laboratories control panel establishes the operating mode in the controller. Signals in the form of contact closures from the relay actuator unit are used to develop control signals for the Mann-Russell control module. A solar insolation signal from the Mann-Russell control module is required for one of the operating modes.

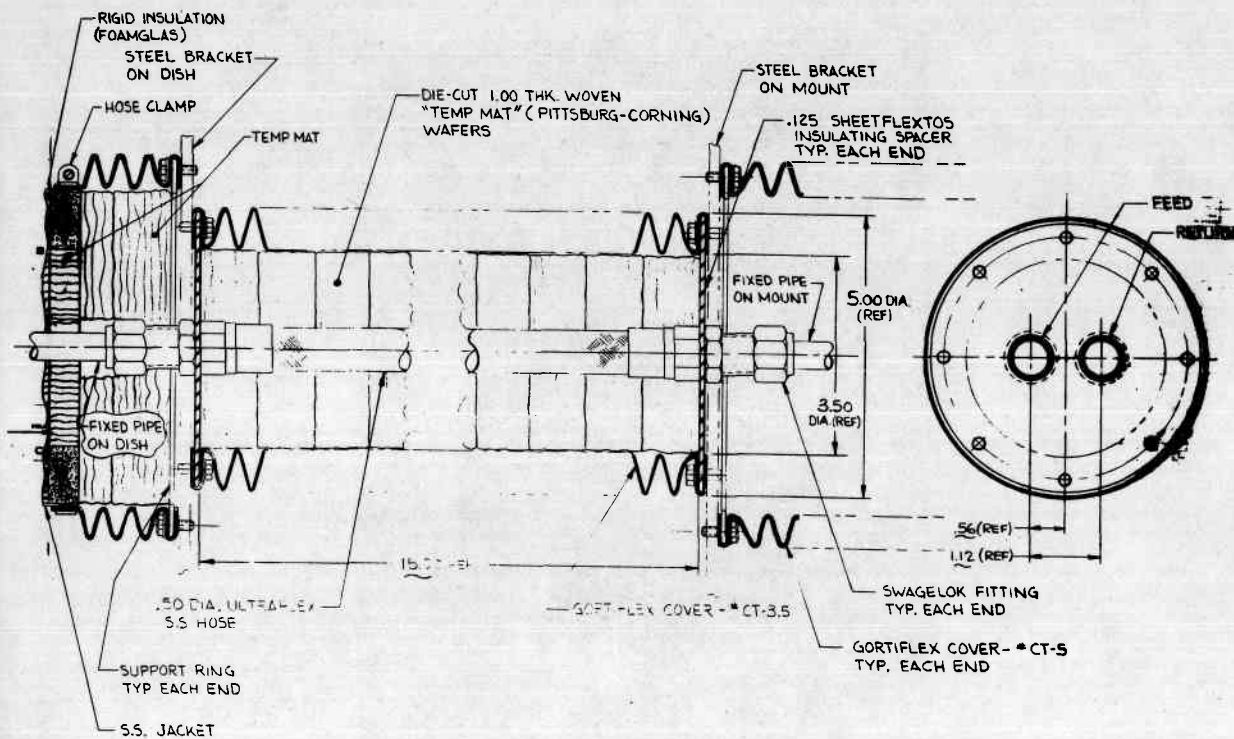


Figure 8.1-7. Flexible Pipe Assembly

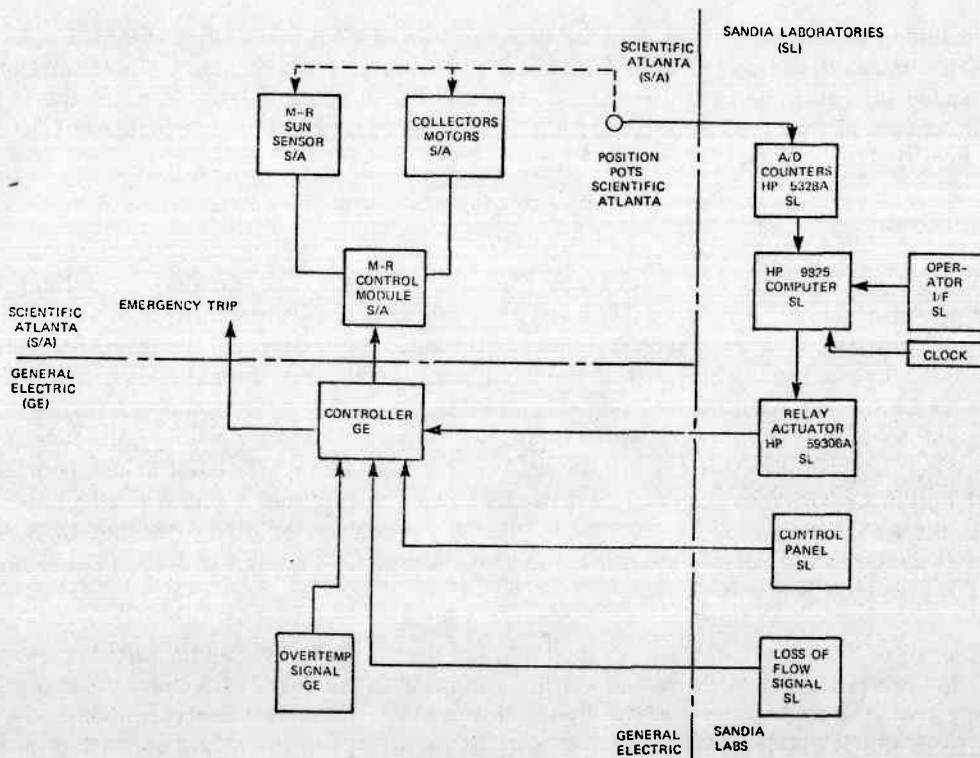


Figure 8.1-8. EPC Control System Interface Drawing

The loss of flow signal provided by Sandia Laboratories and/or an overtemp signal provided by GE energizes the emergency slew mode in the controller. This activates the emergency trip on the collector and operates the motors at slew, down in elevation and west in azimuth (10° west of south). These signals also trip the defocusing device.

The Mann Russell control module provides the timer circuitry, tracking sensor signal conditioning, control logic, and motor switching logic for the collector. Its output drives the collector motors.

The EPC tracking control system operates in three modes:

1. Computer Only Mode. In this mode the HP 9825 calculates the sun azimuth and sun elevation angles. Collector angular positions determined by the collector mounted pots and converted into digital signals are compared with the calculated positions, and the error in each axis determined. Each error is fed into an on-off motor controller for each axis to drive the collector to null.
2. Hybrid-Computer and Sun Sensor. Computer operation is identical to that described under computer only mode for computer operations. In addition, however, direct tracking by means of the sun sensor is included. When the position error in each of the axes under computer control drops below the error threshold level ($1/2$ degree) and the solar insolation level indicated by the sun sensor exceeds its minimum threshold, system operation switches to the solar array for tracking. If the insolation level drops below its threshold, operation reverts to computer command.
3. Hybrid-Timer and Sun Tracker (Mann Russell Controller). In this mode the basic Mann-Russell controller operates the tracking loop. The timer provides approximate position data for the collector when the insolation level is low due to cloud cover. The timer also resets the collector at night for morning start-up positioning. At high insolation levels, the sun tracker is operational and takes over control of the system.

In addition to these three operational modes, provision has been made to override the control system. This permits driving the collector to any elevation and azimuth angle desired by manually controlling the drive motors. This can be accomplished from the control panel or with a plug-in controller at the collector.

8.1.1-2 Test Laboratory Facility

The tests are being performed at the Solar Collector Module Test Facility, Instrumentation Fluid Loop Number One at the Sandia Laboratories in Albuquerque, New Mexico. The facility capability, a description of the equipment and operation, and requirements on contractors are described in SAND 76-0425 published by Sandia Laboratories. The system consists of a fluid loop using Therminol 66 as a heat transfer medium. The loop includes a heat exchanger wherein the fluid can be heated or cooled, circulating pumps, flow control valves, temperature sensors, flow meters, pressure gages, and the attendant valves, piping and other required plumbing and wiring.

The fluid temperature can be controlled at levels up to 589°K (600°F). Flow rates can be controlled from 6.3×10^{-6} to 6.3×10^{-4} m^3/s (0.1 to 10 gpm). The heat rejection capacity can be varied from 1000 kJ per hour to 60,000 kJ per hour. The heat exchanger contains an electrical resistance heating coil and cooling coils through which tap water is circulated.

The facility is equipped with data acquisition and processing equipment including a Doric Digitrend data logger and a HP 2116C computer. Also included is a magnetic tape system and plotter. With this system collector loop performance data can be generated. The data acquired or generated by the system are:

1. Collector identification
2. Local time
3. Solar time

4. Solar insolation, total horizontal
5. Solar insolation, direct, 5° intercept
6. Wind direction
7. Wind speed
8. Pressure drop between two points in piping
9. Mass Rate of Flow
10. 15-50 channels of thermocouple data
11. Comments affecting test result interpretation

8.1.1.3 Instrumentation

Two iron-constantan immersion thermocouples, one on each side of the flow adjustment valves are provided for inputs to the flow temperature controller. A pressure gage is included in the Therminol 66 fluid line. Two other pressure gages, one for a nitrogen pressurization line and one for the water cooling line have ranges from 0 to 4.1×10^5 N/m² (60 psi). Three flow meters are furnished in the heat transfer fluid line. Two are the strain gage type and have capacities of 6.3×10^{-6} to 6.3×10^{-5} m³/s (0.1 to 1.0 gpm) and 6.3×10^{-5} to 6.3×10^{-4} m³/s (1.0 to 10.0 gpm) capacity. The third is a turbine type meter.

For weather monitoring, wind speed and direction indicators and insolation rate sensors are furnished. The wind sensors include (1) Beckman and Whitley M-1564 wind speed indicator, (2) Beckman and Whitley M-1565 wind direction, and (3) Beckman and Whitley wind speed and direction translator. For insolation measurements, two instruments are furnished: (1) for total horizontal insolation, an Epply model PSP pyranometer and (2) for direct, 5 degree intercept insolation, an Epply model NIP pyrhelimeter.

The receiver coils are instrumented with 22 chromel-constantan thermo-couples located as shown on Figure 8.1-5. These are welded to the tubes and the leads are secured to the tubing for a distance of at least 0.051 meter (2 in.) from the bead to minimize finning effects. Thirty chromel-constantan thermo-couples are located on the receiver housing. These are also welded with a nominal length of lead wire bonded to the surface. The 52 temperatures are recorded by a Doric Digitrend digital data logger.

Two copper-constantan immersion type thermocouples are installed, one near the inlet and one near the outlet of the receiver. Also, two copper-constantan thermocouples are welded on the inlet tube wall and one on the outlet tube wall. These are connected to the test facility data system. One chromel-alumel thermocouple is welded to the outlet tube wall. It is connected to the collector control system to signal for defocusing in case of a fluid over-temperature condition. A turbine-type flow meter is located on the inlet side of the receiver tubing.

8.1.1.4 Test Program

The objectives of the testing performed during the Preliminary Design Phase were to measure the performance of a parabolic solar collector under varying environmental conditions and component configurations. The results are being used to verify and update analytical design techniques and component configurations. An outline of the test program is shown in Table 8.1-1. Several of the tests require variations in insolation and other natural conditions, and several others may be accomplished concurrently. Because of this, the order of testing is not rigid and is being arranged on site, conditions permitting.

As part of the overall performance evaluation, hardware is inspected on a regular basis throughout the test period. Structural members are checked for wear and strain. The collector coating is checked for

Table 8.1-1. EPC Test Matrix

1.0	Flux Test - Measure Concentration Distribution Without Receiver																												
2.0	Performance Testing																												
2.1	Calibration - Steady State																												
	1. Measure thermal performance at test start.																												
	2. Repeat at 1 week intervals for test duration.																												
2.2	Insolation level - vary insolation level as in following table (steady state).																												
	<table border="1"> <thead> <tr> <th>Insolation BTU/HR Ft. ²</th> <th>T-Inlet °F</th> <th>T-Outlet °F</th> <th>Estimated Flow Rate lb./hr.</th> </tr> </thead> <tbody> <tr> <td>220</td> <td>450</td> <td>600</td> <td>173.3</td> </tr> <tr> <td>300</td> <td>450</td> <td>600</td> <td>262</td> </tr> <tr> <td>220</td> <td>400</td> <td>550</td> <td>182.4</td> </tr> <tr> <td>300</td> <td>400</td> <td>550</td> <td>275.7</td> </tr> <tr> <td>220</td> <td>450</td> <td>550</td> <td>268.9</td> </tr> <tr> <td>300</td> <td>450</td> <td>550</td> <td>406.5</td> </tr> </tbody> </table>	Insolation BTU/HR Ft. ²	T-Inlet °F	T-Outlet °F	Estimated Flow Rate lb./hr.	220	450	600	173.3	300	450	600	262	220	400	550	182.4	300	400	550	275.7	220	450	550	268.9	300	450	550	406.5
Insolation BTU/HR Ft. ²	T-Inlet °F	T-Outlet °F	Estimated Flow Rate lb./hr.																										
220	450	600	173.3																										
300	450	600	262																										
220	400	550	182.4																										
300	400	550	275.7																										
220	450	550	268.9																										
300	450	550	406.5																										
2.3	Aperture - Repeat 2.2 with varying receiver apertures																												
2.4	Glass Cover - Repeat 2.2 with glass cover on receiver																												
2.5	Transient Tests																												
	1. Start up transients																												
	2. Shutdown transients																												
	3. Flow pulsations																												
2.6	Tracking Control																												
	1. Compare computer against sun tracker																												
	2. Evaluate with bias in tracker																												
2.7	Wind Effects																												
	1. Deflection of dish or other components																												
	2. Convection effects in receiver																												
2.8	Water Effects																												
	1. Test with reflector wet																												
	2. Test after having been wet																												
3.0	Flux Test - Measure Concentration Distribution Without Receiver																												
4.0	Hardware Performance																												
4.1	Collector Coating - Check after each test point.																												

signs of degradation. The receiver is examined to determine condition of the oxidized treatment on the coil. The fluid loop is checked for leaks or blockage.

8.1.1.4.1 Flux Test

The flux concentration of the collector was measured without the receiver installed. This was a base point of comparison with flux measurements to be performed at the end of testing. Analysis of these results provides indications of coating durability, collector shape and stability, and receiver positioning guidance.

8.1.1.4.2 Performance Testing

This is the major portion of the test program and determines thermal performance of the EPC parabolic collector and receiver under steady state and transient thermal conditions, varying environmental conditions, and component configuration. Basic data recorded includes the list described in Paragraph 8.1.1.2. Additional data includes the flux profiles and physical examinations of the hardware after each test point.

8.1.1.4.2.1 Calibration. One method of determining performance changes as a function of time is to establish a calibration test point at the beginning of testing and periodically repeat this point. For the EPC test, a calibration test is done on weekly intervals. Data is obtained under steady state conditions at an insolation level which will be fairly repeatable over the test span for the time of year. Results of these test points are used to help in determining the influence of time and exposure on performance.

8.1.1.4.2.2 Insolation Level. It is desired to evaluate the system under steady state conditions at various insolation levels, coolant flow rates and temperatures. The results of this test provides efficiency data. Because this test point is a function of the natural environment, the exact insolation levels or test times cannot be planned, but are obtained as they become available.

8.1.1.4.2.3 Aperture Tests. By varying apertures on the receiver, different concentration ratios can be investigated. The different sized openings will also change heat transfer characteristics both into and out of the receiver. At least two apertures are to be tested. The total number of test points obtained are a function of available time and cooperation of the elements relative to insolation levels.

8.1.1.4.2.4 Glass Cover. Installation of a glass cover over the receiver opening will affect the net exchange of energy. By installing a glass cover over the receiver and repeating (as close as possible) the previous test conditions, the effect on energy transfer can be determined.

8.1.1.4.2.5 Transient Tests. Transient measurements during start-up and shutdown are obtained while coming to conditions for the steady state tests. Flow pulsation tests simulate minor changes in flow to complete stoppage. During these tests, the defocus system can be evaluated. Measurements are made of the transient heating or cooling occurring in the system during these periods.

8.1.1.4.2.6 Tracking Control. A comparison is made of performance obtained with sun tracking relative to computer positioning. An extension to these test points determines the effect of tracking errors on performance. To accomplish this biases are set in the tracking system and steady state measurements made. The magnitude of the biases are expected to be less than $\pm 1^\circ$.

8.1.1.4.2.7 Wind Effects. Wind can affect performance of the system structurally and thermally. Structural effects would be in the form of deflections which would cause focus errors to occur. Thermal effects are in the form of convection losses in the receiver. Overall wind effect is assessed as winds up to 13.4 m/s (30 mph) become available during the test program.

8.1.1.4.2.8 Water Effects. The effects of water on collector/receiver durability and performance are also being investigated. The collector is tested while the reflector is wet to determine performance and is monitored as a function of time to determine when recovery of fully dry performance occurs. The wet condition is simulated by hosing the collector down prior to test. Pre and post-test examination of the components are performed to look for any physical degradation which may occur due to the wetting.

8.1.1.4.3 Flux Test

After the performance testing is completed, the receiver is removed and a new flux profile is taken. This is compared the pre-test profiles to determine if performance of the collector has changed during the test program.

8.1.1.5 EPC Test Results

As of the end of this reporting period, a limited portion of the EPC test schedule was executed. The collector and controls assembly and checkout was completed and initial flux scans and receiver thermal testing were conducted. The balance of the test plan, including performance mapping of the unit, model updating and hardware assessment and necessary modifications will be conducted during the next phase of the program.

8.1.1.5.1 Flux Scans

A series of energy flux scans have been made at the focal plane of the collector in two different orientations: north-south and east-west. Figure 8.1-9 presents a typical flux scan readout for a north-south or vertical scan. By averaging several scans, the flux profile of Figure 8.1-10 was constructed. Also plotted in Figure 8.1-10 is the integrated flux profile. With a maximum operative opening of 0.30 meter (12 in.), approximately 83 percent of the focal plane energy was intercepted by the receiver. This value is lower than the value predicted for a one-half degree slope error, indicating the slightly larger slope error of the 5-meter reflector and the positioning of the receiver behind the true focal plane (1-3 inches). Slope error data were confirmed by independent laser ray trace tests conducted by Sandia which indicated a basic unmounted petal slope error of 0.6-0.7 degrees. These results quantify the relationship between reflector slope error and petal die errors and are being used to establish the 7-meter LSE reflector petal die specifications.

8.1.1.5.2 Receiver Thermal Testing

Thermal loss tests were conducted on the unfocused collector/receiver. These tests circulated hot Therminol Therminol 66 into the receiver, and by measuring temperature drop and flow rate, heat losses were calculated. Figure 8.1-11 presents the results of these tests. As can be seen, measured losses are higher than predicted. Examination of detailed thermocouple data indicates that convection losses may be higher than performance models predicted. This trend is also supported by the scatter in the data at similar operating temperatures which were conducted under different wind conditions. The models are being updated to reflect the higher loss, and, in addition, the 7-meter collector receiver design is being investigated to find cost effective ways to inhibit convection losses.

8.1.1.6 EPC Incident

On July 8, 1978, the EPC collector was damaged while operating in the automatic tracking mode. The damage was caused by inadvertant startup of the tracking system driving the collector past limit switches which had been disabled to permit a laser ray trace test on the reflector. Four reflector petals, both jackscrews, one drive motor, and a structural weld were damaged. Using spare petals on site, the collector was repaired and functional by July 21. The refurbishment operation was used to replace defective petals and to install a new defocus strut mount to correct dish deformation. Checkout of the computer drive and controls was then started.

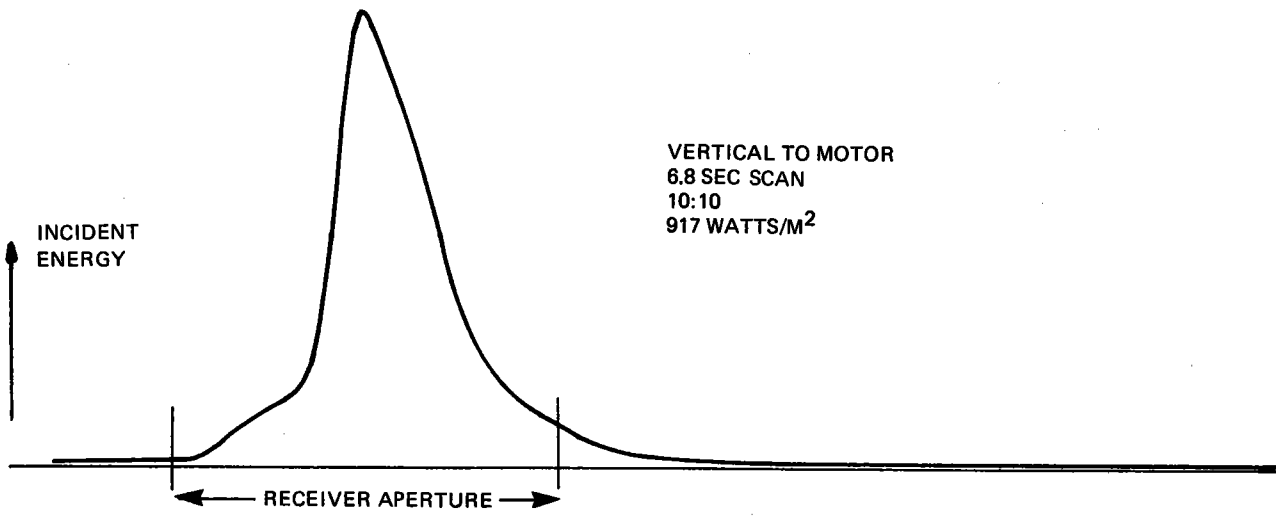


Figure 8.1-9. Typical Flux Scan

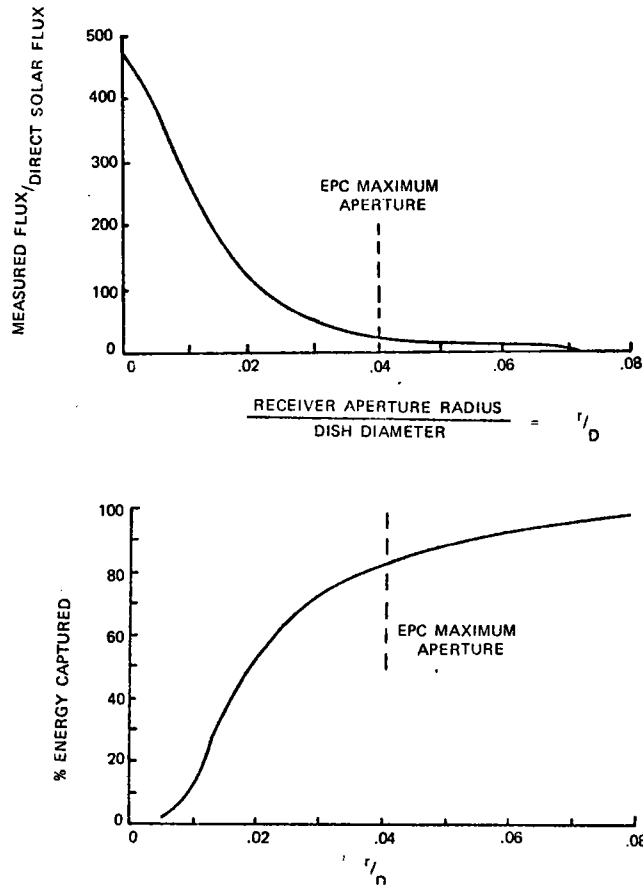


Figure 8.1-10. Flux Profile Test Results

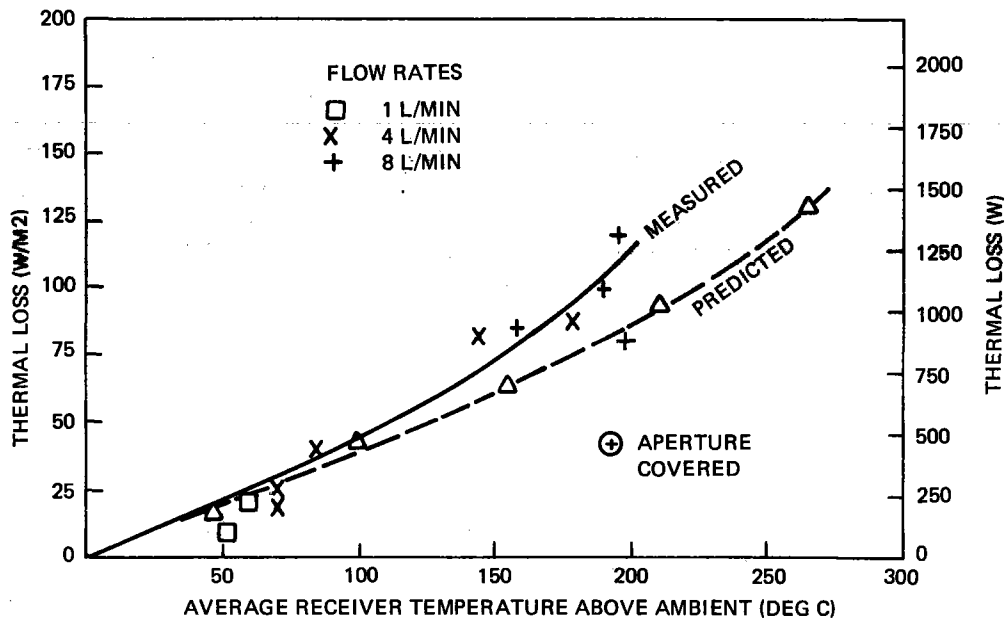


Figure 8.1-11. GE Parabolic Dish Receiver Thermal Loss

This incident, although unfortunate, illustrated the speed and the low cost with which damaged and/or defective components and parts can be refurbished and replaced in a collector designed to use commercially available parts and materials. Ready access to commercial shops for repair and maintenance of components and easily replaced parts requiring only standard tools were a major factor in the rapid repair of the EPC. This feature, which is part of the design philosophy for Shenandoah, will insure low operating costs and high availability for the LSE collectors after installation.

8.1.2 REFLECTOR DEVELOPMENT

8.1.2.1 Background and Approach

Performance of the surface of the reflector is a critical parameter affecting overall collector and hence power plant performance. As part of the Phase III program, a reflector surface development task was conducted to:

1. Identify reflector surface substrates, reflectance enhancement techniques, and protective coatings.
2. Screen and select candidate surfaces that can meet the LSE collector requirements.
3. Test the leading candidates.
4. Select the LSE reflector surface and initiate process development.

In addition to selection of the LSE reflector surface, fabrication of a set of petals for the Engineering Prototype Collector (Paragraph 8.1.1) was initiated. This activity paralleled the development of the LSE reflector surface and utilized the 5-meter EPC petals as representative proof articles for the LSE reflector petals.

The approach shown in Figure 8.1-12 was used for selecting the LSE reflector surface. The initial step was to screen acceptable candidate substrates, reflectance enhancement techniques, and protective coatings from the wide variety of potential candidates available. This was accomplished by combining available data from the literature, vendors information, and, where necessary, sample tests. After selection of prime candidates, environmental tests on candidates samples were performed using those tests most critical to each candidate. These tests led to selection of two final candidates shown in Figure 8.1-13. These candidates were then subjected to the full battery of combined environmental tests which indicated that both candidates met performance and life requirements. The final selection of the RTV 670 was based on production costs, as part of a detailed cost analysis on overall collector production costs.

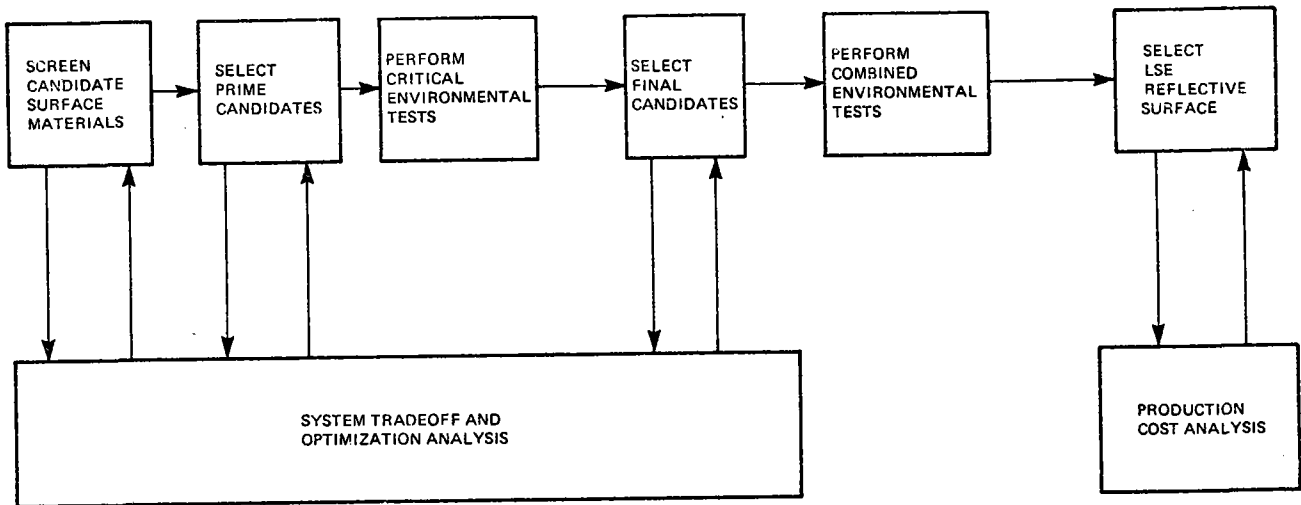


Figure 8.1-12. LSE Reflector Surface Development Process

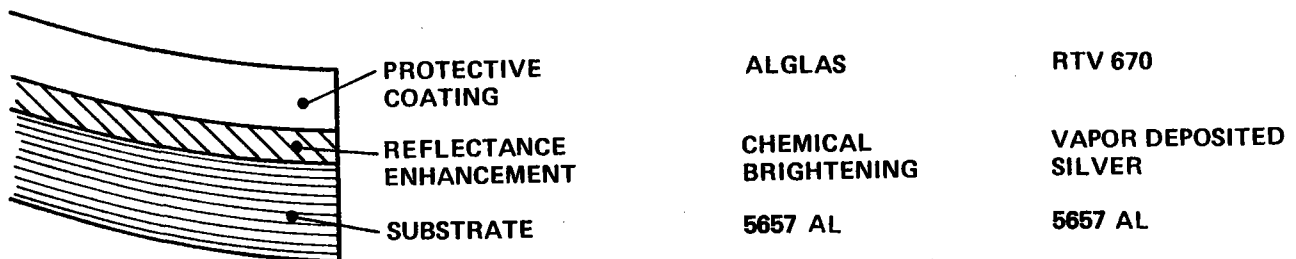


Figure 8.1-13. LSE Reflector Surface Candidates

8.1.2.2 Design Requirements and Selection Criteria

Design requirements for the reflector surface were derived as part of the development of the overall collector design requirements. The requirements are summarized in Figure 8.1-14 and emphasize long life performance under LSE environmental conditions. To simulate environmental requirements, a series of test specifications were derived to define the conditions to which candidate samples were to be subjected to meet end of life performance requirements. Paragraph 8.1.2.3 describes these in detail.

Selection criteria for the reflector surface are summarized in Table 8.1-2. As shown in Figure 8.1-12, throughout the screening and selection process, system analyses related reflector surface performance and costs to overall LSE system requirements and costs. However, in addition to reflector performance and cost data, several other criteria were used in the selection process: fabrication properties, schedule (availability), and risks.

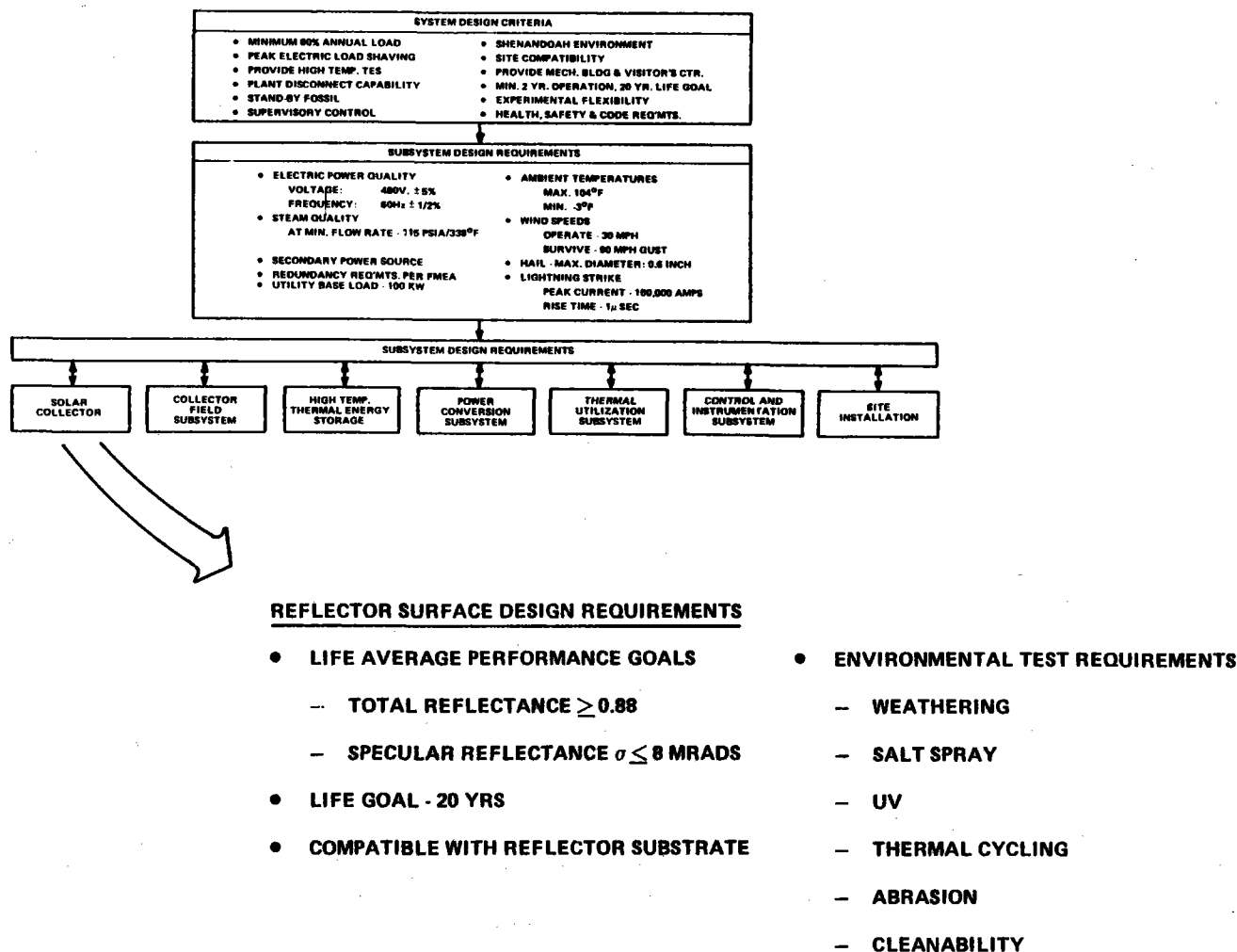


Figure 8.1-14. Reflector Surface Design Requirements

Table 8.1-2. Reflector Surface Selection Criteria

- Performance (Life Average)
 - Total Reflectance
 - Specular Reflectance
 - Slope Error Changes
- Cost
 - Initial
 - Maintenance
- Fabrication Properties
- Availability (LSE Timeframe)
- Risk
 - Cost
 - Schedule
 - Technical

Low cost, standard volume techniques for fabricating reflector-type structures were emphasized throughout the development process. Those surface candidates which required special tooling and/or processing or which were technically incompatible with standard production approaches were eliminated due to cost and schedule constraints or poor fabrication potential.

Some promising options such as advanced structural plastic reflector substrates were eliminated on the basis of lack of availability within the LSE time frame. Others, such as vapor deposited silver reflectance enhancement, represented unacceptable high cost and schedule risks; although offering the potential for very high reflectance and cost effective performance gains, the development of processing capabilities to coat reflector sized shapes and contours represented an investment risk in time and cost incompatible with the installation time frame for LSE Shanandoah.

8.1.2.3 Test Procedures

Testing of the leading candidate surface materials for LSE followed generally accepted techniques and procedures for reflective surfaces. Optical tests consisted of total hemispherical reflectance, specular reflectance, and diffuse reflectance. The diffuse reflectance measurements were primarily used for screening purposes. A detailed description of the test apparatus and test procedures for these tests are given in Appendix L along with the analytical approach used to reduce specular reflectance measurements.

Environmental testing consisted of a battery of tests designed to simulate long time exposure to the elements, industrial pollution, and periodic cleaning. Samples subjected to environmental tests were measured for optical properties before and after the tests to determine the effective degradation of the reflective surface over the simulated 20 year life. Specifications on the environmental tests are also presented in Appendix L.

8.1.2.4 Screening of Candidate Materials

Candidate substrates, reflective surfaces, and protective coatings initially considered for the LSE application are indicated in Figure 8.1-15. Each of these materials is currently employed in experimental or production solar collectors or appears capable of meeting the LSE requirement.

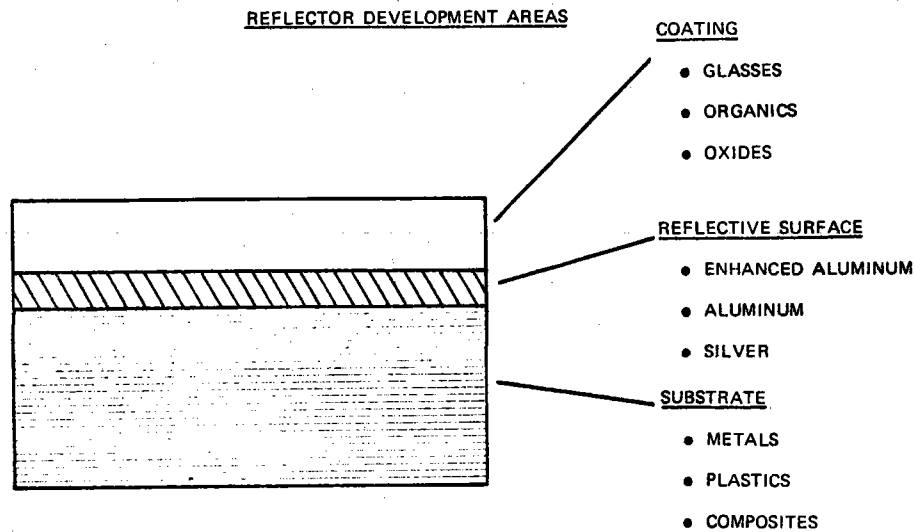


Figure 8.1-15. Reflector Surface Candidates

8.1.2.4.1 Substrate and Reflectance Enhancement

An evaluation of substrate candidates quickly led to the conclusion that plastic and composite material substrates would have very high costs if developed for the LSE application alone and that either aluminum or steel substrates were the only practical substrate choices (Table 8.1-3). The initial examination of reflector substrate materials was based upon industrial reflector materials listed in various vendors' literature. The following typical materials showed promise for the LSE reflector: aluminum alloys 5005, 5457, 5657, Alcoa No. 23 Reflector Sheet, and stainless steels of the 201, 301, and 434 types.

Table 8.1-3. Substrate Candidate Characteristics

Candidate	Properties	Comments
Aluminum	<ul style="list-style-type: none"> • High Reflectance • Moderate Strength/Weight • Inexpensive 	Current Reflector Production Technique
Steel	<ul style="list-style-type: none"> • Versatile Substrate for Depositing Enhanced Coatings • High Strength • Easily Formed 	Offers Low Cost Production Potential
Composites	<ul style="list-style-type: none"> • Light Weight • Surfaces can be Prepared with Low RMS • Thermal Stability • Corrosion Resistant 	Relatively High Costs in Limited Production

The aluminum reflector substrates were examined for their commercial availability, mill size (sheet or coil), solar reflectance, and cost. These materials typically were found to be available in mill lots from 1818 kg (4,000 lb) and up with an average cost of \$1 per pound except for the Alcoa reflector sheet, which varied in cost from \$2.25 to \$3.20 per pound. This material is currently supplied only with the Alzak process coating.

Solar reflectance tests used to screen the substrate materials were conducted on samples in the as-received and mechanically polished conditions. The test results found in Table 8.1-4 indicated that polishing of aluminum improved the diffuse reflectance but had no great effect on the total reflectance. The bright rolled, one side bright (OSB) stainless steels displayed a fairly low total solar reflectance of about 60 percent but had high specularly. The enhancement of the stainless steel surface with vapor deposited silver could produce a highly reflective and specular surface with a 96.5 percent total and a 95.9 percent specular solar reflectance. However, the high cost of a vapor deposited silver (or aluminum) stainless steel reflector appeared to be prohibitive.

Table 8.1-4. Solar Reflectance Values of Typical Substrate Materials

Material	Total Reflectance		Diffuse Reflectance	
	As Received	Polished	As Received	Polished
<u>Aluminum Alloys</u>				
5005-H25 (Alcoa-Bright Rolled)	.808	.810	.078	.028
5457-0 (Reynolds Metals-OSB*Finish)	.804	.810	.101	.062
5657-H25 (Alcoa-OSB Finish)	.796	.779	.095	.070
5657-H28 (Reynolds Metals-OSB Finish)	.718	.763	.142	.105
No. 23 Reflector Sheet (Alcoa-3003 clad with 1175)	.885	-	.029	-
<u>Stainless Steel</u>				
304 Type (Armco - Bright Annealed No. 2)	.605	-	-	-
304 Type (Cyclops-Unibrite)	.570	-	-	-
400 Series (Allegheny Ludlum)	.620	-	-	-
OSB - One Side Bright Rolled				

Based on results of these initial tests, reflectance enhancement of the substrate surface appeared mandatory to meet total reflectance requirements. To achieve a highly specular surface with high reflectance, tests on substrate materials such as those shown in Table 8.1-4 indicated that the substrate must possess a microscopically smooth surface. This led to selection of candidate substrates processed one side bright rolled on which chemical brightening or vapor deposition of aluminum or silver could be utilized (Table 8.1-5).

Table 8.1-5. Candidate Reflectance Enhancement Characteristics

Candidate	Properties	Comments
Aluminum Layer	High Reflectance (0.9) to Cost Ratio	Easily Deposited
Silver Layer	Highest Reflectance (0.95)	Easily Deposited
Chemical Brightening (Aluminum Substrate)	Low Cost	Reflectance Approaches Deposited Aluminum

A number of samples of chemically brightened aluminum and deposited layer aluminums and stainless steels were prepared to evaluate their performance. Typical results are shown in Table 8.1-6 along with two premium reflector sheet aluminum alloys.

Table 8.1-6. Typical Enhanced Reflectance Test Results

Material	As Received		Chemical Brightening		Deposited Coatings			
	Total	Diffuse	Total	Diffuse	1000 A° Aluminum		800A° Silver	
	Total	Diffuse	Total	Diffuse	Total	Diffuse	Total	Diffuse
<u>Aluminum Alloys</u>								
1. 5657-H25	.792	.072	.883	.081				
2. 5457-0	.821	.094	.886	.059	.885	.097	.919	.100
3. 5005-H25	.830	.068	-	-	.882	.039	.950	.030
4. ALCOA #23	.915	.020	-	-	.884	.029	.961	.024
5. A86BIS(French)	.907	.003	-	-	-	-	-	-
<u>Stainless Steel</u>								
6. 434	.611	.005	-	-	.895	.003	.965	.006

As shown in the table, straight chemical brightening of commercially available aluminum produces reflectivity comparable to the same substrates with deposited layers of silver. The bright reflector sheets offered by ALCOA (#23) and the imported French alloy A86BIS are superior to either chemical brightening or deposited layers of aluminum. However, use of common variety aluminum alloys chemically brightened offers very low cost compared to specialty alloys or deposited aluminum and has been evaluated to be the most cost effective approach for aluminum.

Use of a silver layer over aluminum or stainless steel does offer very high reflectance. This option appears to offer a slight cost effectiveness advantage over chemically brightened aluminum but increases investment costs and risk of degradation under environmental conditions over the life of the collector. In addition, volume quantity fabrication of large reflector sections might prove difficult to accomplish within the LSE time frame due to limited production facilities. Hence, chemically brightened aluminum has been selected for the LSE substrate and reflective enhancement approach.

8.1.2.4.2 Protective Coatings

A large number of protective coatings for the LSE reflector appear suitable. To meet cost requirements however, initial screening of protective coating materials led to the candidates listed in Table 8.1-7. Further evaluation eliminated porcelain coatings which offer low production costs but which present optical property development requirements that the other options do not require. Since no clear cost advantage existed for porcelain coatings, they were not carried beyond the screening stage.

Table 8.1-7. Candidate Protective Coating Characteristics

Candidate	Properties	Comments
Porcelain Coatings	<ul style="list-style-type: none"> • Glass like durability • Excellent weatherability • Low cost 	<ul style="list-style-type: none"> • Standard low cost production technique
Metal Oxides	<ul style="list-style-type: none"> • Can be tailored to be impervious • Can provide antistatic properties • Can enhance reflectance 	<ul style="list-style-type: none"> • Anodized type coatings can be deposited with excellent corrosion protection
Organic (Silicones)	<ul style="list-style-type: none"> • Hard silicones are commercially available • Excellent corrosion protection 	<ul style="list-style-type: none"> • Siloxanes are most promising
Glass	<ul style="list-style-type: none"> • Low cost production techniques available • Excellent Performance 	<ul style="list-style-type: none"> • Flexible, low cost glass application processes available

Of the metal oxides, organics, and glasses, only low production cost options were considered. For the metal oxides, common anodizing of the aluminum surface offers low cost, standard production technique protective coatings. ALZAK, COILZAK, and KINGSLUX samples were evaluated as readily available anodized materials with KINGSLUX carried through environmental testing.

For the organic coatings, GE RTV 670 was selected as the leading candidate. This material was designed to be used as an optical coupling material and a protective coating for photovoltaic cells and fiber optics and as a transparent encapsulation material. Its characteristics are summarized in Table 8.1-8.

For the glass coating candidate, ALGLAS[®], a proprietary General Electric process, was selected. ALGLAS is a thin, transparent, flexible coating of very high quality glass which is chemically bonded to the aluminum of a reflector. The finish is applied by dipping an aluminum reflector into an alkali silicate solution then drying and curing the finish into a thin, continuous, glass coating. The finished product combines the desirable reflectance and formability qualities of aluminum with the excellent weatherability and transparency of iron-free glass.

[®] Trademark Registered

Table 8.1-8. Characteristics of GE RTV 670

● Ozone and Sunlight Resistance	No protective coverings required.
● Moisture Resistance	Low vapor permeability onto substrate materials. Excellent corrosion protection.
● Low Dirt Retention	Because of its high durometer hardness (Shore A70), dirt will not embed in surface. Offers advantage over most silicones.
● High Thermal Conductivity	High thermal conductivity permits rapid dissipation of heat.
● High Temperature Characteristics	Demonstrated long life in high ambient temperature applications.
● Flexibility at high and low Temperatures	Will not crack at high or low temperatures. Remains flexible at -55°C.
● Reliability	Life characteristics under continuous electrical and mechanical operation over ten years at elevated temperatures.

Samples fabricated for each of these protective coatings exhibited comparable optical properties. Environmental testing conducted on anodized samples and ALGLAS in a previous effort had indicated that ALGLAS offered superior environmental performance, but testing was not conclusive nor carried out to the standards developed for LSE. RTV 670 properties also showed that environmental resistance would probably be similar to ALGLAS. Hence, all three candidate protective coatings were judged competitive in cost and performance at the conclusion of screening.

8.1.2.5 Environmental Testing

Critical environmental tests were performed on a variety of substrates to determine the environment or environments that cause surface degradation. It was determined from early studies that (thin) anodized films for reflective surfaces degraded severely under salt spray environment, whereas acrylic films degraded typically in an extended humidity test. In order to confirm these findings as well as to determine the critical environments for materials such as the RTV 670 and ALGLAS, additional tests were performed.

In addition to the prime reflector protective coatings, FEK-244 was tested as a comparative reference since this aluminum film material is widely used as a solar reflector. Kingslux samples were obtained from the manufacturer. Samples of ALGLAS were prepared using the standard production process, and RTV coated samples using bright rolled aluminum substrates were fabricated. The substrates from the RTV 670 samples were not chemically brightened since the purpose of the tests was to measure degradation due to environmental tests.

Results of the critical environmental tests are shown in Table 8.1-9. Conclusions reached as a result of these tests were:

1. FEK-244 severely degraded under weathering tests.
2. Kingslux degraded under salt spray and weathering tests most critically in its specular performance (and became pitted and difficult to clean).
3. Both ALGLAS and RTV 670 survived all individual environmental tests with minimal degradation

Hence, both RTV 670 and ALGLAS appeared technically suitable for the LSE application.

Additional samples of these materials were then fabricated and subjected to combined environmental tests to determine if the combined effects of any of the test environments would affect either candidate. For example, the slight micro-cracking of the ALGLAS surface under the weathering test, which had negligible effects on its performance, might cause significant degradation when subjected to the salt spray test. As the results in Table 8.1-10 indicate, however, negligible changes in either ALGLAS or RTV 670 protected substrates was observed under combined environmental testing.

8.1.2.6 Selected LSE Reflector Surface

After successfully completing the environmental tests, selection of the LSE protective coating was based on production costs and ability to meet required performance. To determine representative production reflector performance, a number of aluminum samples from a production coil of 5657 aluminum alloy were chemically brightened and coated with ALGLAS and RTV 670. ALGLAS samples were also prepared from some 5457 aluminum alloy. Results of optical tests on these samples are shown in Figures 8.1-16 and 8.1-17.

Final selection of the substrate alloy was narrowed to either 5457 or 5657 aluminum alloys, both widely employed as bright trim materials in the automotive and appliance industries. Both alloys offer low cost, good formability, and immediate availability from a variety of aluminum producers. Samples of both substrates with ALGLAS coating showed some variation in properties (Figure 8.1-17), but it was determined that either alloy coated with ALGLAS could meet the LSE specular requirement of 8 mrad RMS (equivalent) with proper control of the rolling and chemical brightening processes.

The data in Figure 8.1-17 shows that the total reflectance of the brightened substrate with either ALGLAS or RTV 670 was 0.86, slightly less than the 0.88 requirement, but representative of realistic production values. The additional cost of speciality aluminum or vapor deposited reflectance enhancement to achieve a two or three percent improvement in total reflectance was evaluated as not being cost effective.

The performance data shown in Figure 8.1-17 also indicates that, compared to the bare substrate, the reflector surfaces with ALGLAS, RTV670, and RTV 670 with a primer have lower specular performance at small test apertures. However, all three coating options have comparable performance in the region of interest of apertures for the LSE application, and no significant performance difference exists between surfaces coated with ALGLAS and those coated with RTV 670. (As part of the production development activity, it was determined that use of a primer with the RTV 670 would significantly increase its surface adhesion with little optical penalty.)

Final selection of RTV 670 as the protective coating over ALGLAS was made on the basis of production costs. A detailed cost comparison between the two approaches revealed a substantial cost saving of almost \$4.50/square foot of surface area. A summary of the cost analysis is given in Table 8.1-11.

Table 8.1-9. Critical Environmental Test Results

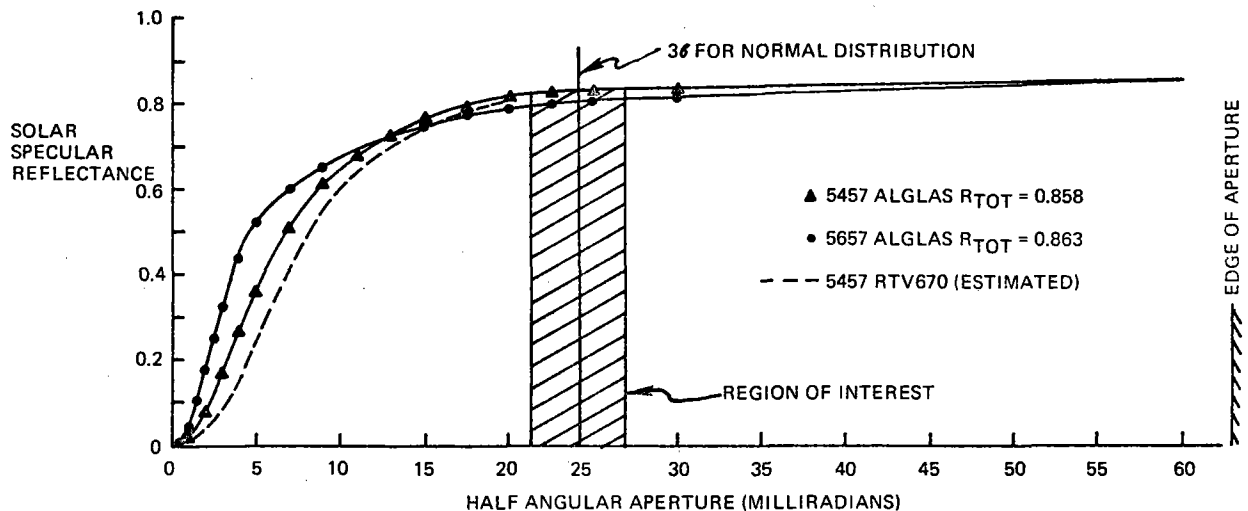
	Reflectance As Received			After Salt Spray			After Weathering			After Abrasion			Thermal Cycling			After Cleaning		
	T	D	S	T	D	S	T	D	S	T	D	S	T	D	S	T	D	S
Kingslux 012/020	.85	.076	.774	.833	.191	.642	.828	.171	.657	.850	.076	.774	.850	.076	.774	.850	.076	.774
RTV-Coated 5657 Brite-Rolled	.773	.175	.598	.773	.175	.598	.773	.175	.598	.773	.175	.598	.773	.175	.598	.773	.175	.598
FEK 244	.873	.028	.845	.873	.043	.830	.83	.18	.65	.873	.028	.845	.873	.028	.845	.873	.033	.033
Alglas-Coated 5457	.858	.028	.830	.858	.028	.830	.858	.045	.813	.858	.046	.812	.858	.028	.830	.858	.028	.830

T - Total Reflectance
D - Diffuse (3° aperture)
S - Specular Reflectance (3° aperture)

Table 8.1-10. Combined Environmental Test Results

Sample			% Change in Total Reflectance	% Change in Specular Reflectance
Substrate	Enhancement	Coating		
<u>Abrasion/Salt</u>				
5657	Chem. Brite	RTV 670	0.8	0.1
5657	Chem. Brite	ALGLAS	0.2	0
<u>Abrasion/Weathering</u>				
5657	Chem. Brite	RTV 670	0.5	2.3
5657	Chem. Brite	ALGLAS	0.4	2.3
<u>Salt/Abrasion/Weathering</u>				
5657	Chem. Brite	RTV 670	0.1	-0.6*
5657	Chem. Brite	ALGLAS	0.1	1.0
<u>Weathering/Abrasion/Salt</u>				
5657	Chem. Brite	RTV 670	-0.4*	-1.3*
5657	Chem. Brite	ALGLAS	0.4	3.1

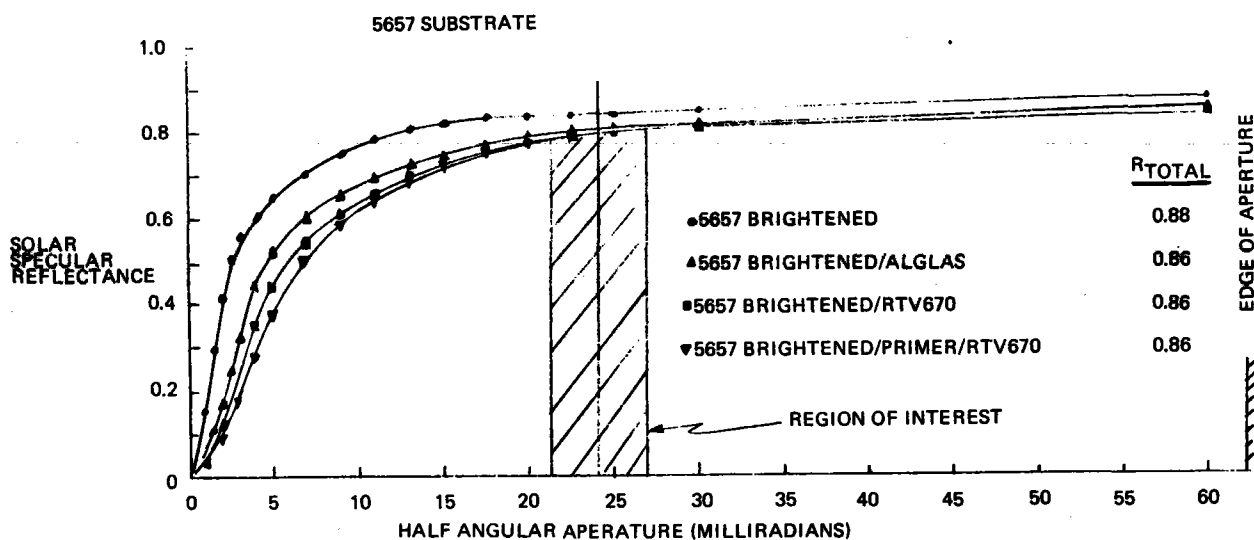
*Negative changes indicate change within experimental error limits



- 5457 SAMPLES WITH ALGLAS (RTV670) SHOW SLIGHTLY BETTER PERFORMANCE IN THE REGION OF INTEREST
- ADDITIONAL SAMPLES BEING SENT BY ALCOA

Figure 8.1-16. Comparison of 5457 and 5657 Specular Reflectance with ALGLAS Coating

SPECULAR REFLECTANCE TEST DATA



- RTV670 AND ALGLAS HAVE COMPARABLE PERFORMANCE IN THE REGION OF INTEREST WHEN PLACED ON THE SAME SUBSTRATE.
- BOTH COATINGS CAUSE $\approx 2\%$ LOSS IN TOTAL REFLECTIVITY.

Figure 8.1-17. Specular Reflectance Test Data for 5657 Substrate with Various Coatings

Table 8.1-11. LSE Reflector Petal Incremental Production Costs

	Cost, \$*	
	ALGLAS	RTV 670
Aluminum Reflective Sheet	14.14	0 (PETAL)
Chemical Brightening	0 (ALGLAS Process)	12.67*
ALGLAS Processing	20.88*	-
Adhesive	.45	-
Bonding to Petal Blank	67.88	-
RTV 670 & Primer	-	6.46
Spraying of RTV 670 & Primer	-	6.80
Total Incremental Cost	\$103.35	\$25.93
Incremental Cost Per ft²	\$5.90	\$1.48

* Cost over basic reflector dish

** Cost varies with size/shape of part $\pm 50\%$

The ALGLAS production costs are dominated by the cost to bond the ALGLAS sheet to the petal blank before stamping. Since production facilities to apply ALGLAS directly to the entire reflector petal would not be available within the LSE time frame, bonding of a thin ALGLAS sheet to the substrate sheet was selected as the most cost effective alternative. This approach also offered the advantage of decoupling the substrate material selection from the reflector sheet selection. However, overall costs favored the RTV 670 coating over the chemically brightened petal substrate, and this option was selected for the LSE reflector.

8.1.2.7 Cleanability of RTV 670

Since continually high performance is required throughout the life of the LSE reflector, some periodic cleaning will be required to remove accumulated dust, dirt and other surface contaminants. A brief investigation for cleaning of the LSE reflector was conducted as part of the reflective surface development task. The intent of the investigation was to identify an acceptable baseline cleaning technique, determine its effectiveness, and examine its effect on the RTV 670 coating. Since wiping of the LSE reflector will be impractical as a frequent cleaning procedure, effort was concentrated on spray type cleaning.

The cleaning method consisted of a relatively low pressure detergent spray and rinse. Visual appearance and reflectance measurements were taken prior to and following contaminating exposure and cleaning operation. Two cleaning systems were tested:

<u>Cleaning System</u>	<u>Supply Pressure</u> (psi)	<u>Flow Rate</u> l/min	<u>Nozzle Velocity</u> m/sec
1. Ports-Blast	75	3	31
2. Eclipse Sprayer Model A	40	1.2	21

The cleaning solution consisted of a two percent solution by volume of Hurri-Clean SH No. F1-42 biodegradable detergent and tap water. Liqui-Nox detergent was also used with identical results. The samples were contaminated with local dry dirt that was ground fine and deposited on the reflector samples with the excess removed. A fine tap water spray was allowed to fall on the dirty reflector sample after which the sample was placed in an oven and baked at 352°K (175°F) for 20 minutes.

The reflector samples tested were 5657 aluminum with RTV 670 (also primed with SS-4120), 5457 aluminum with an ALGLAS coating, and a second surface aluminized glass mirror. Each reflector sample underwent ten contamination and cleaning cycles. Results of the tests are shown in Table 8.1-12 and Figure 8.1-18.

The data in Table 8.1-12 show that commercial spray cleaning with a detergent solution can restore a reflector surface to nearly its original performance after repeated cleaning. Visual observation of the samples indicates that the RTV-670 coated surfaces seem to clean up better than the ALGLAS or glass protected surfaces. This is believed to be due to the fact that an RTV-670 surface is similar to that of Teflon in that it is a very low surface energy material (non-wettable).

8.1.2.8 Production Process Development

A reflector production process development effort was carried out concurrent with the evaluation and selection of the reflector surface substrate, reflectance enhancement, and protective coating. This task concentrated on examining the critical production techniques that would be required for the LSE reflector

Table 8.1-12. Effect of Cleaning on Reflector Surface Performance

Sample	Original	After Dirt Contamination	Difference (%)	After Cleaning	Difference (%)
Total Reflectance					
5657/RTV-670	.832	.762	-7.0	.829	-0.3
5457/Alglas	.844	.782	-6.2	.839	-0.5
Aluminized Mirror	.821	.755	-6.6	.811	-1.0
Diffuse Reflectance					
5657/RTV-670	.127	.305	+17.8	.134	+0.7
5457/Alglas	.073	.256	+18.3	.080	+0.7
Aluminized Mirror	.015	.233	+21.8	.070	+5.5

R_t is the total integrated hemispherical reflectance for an AM_2 spectrum.

R_d is the total integrated diffuse reflectance for an AM_2 spectrum.

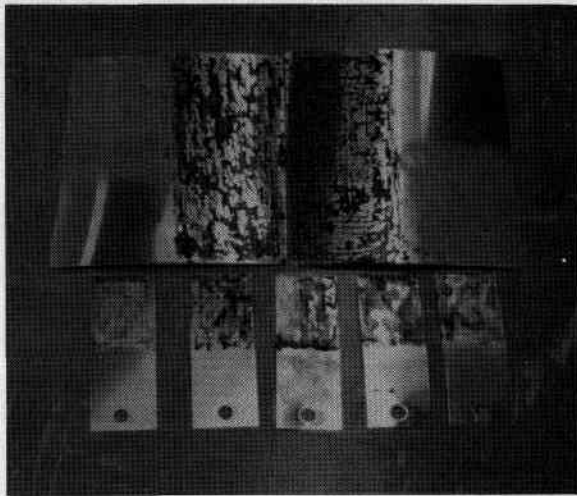
production in advance of actual production commitments. Fabrication of a prototype LSE reflector was undertaken using 5-meter reflector petals identical to those used on the Engineering Prototype Collector. The objective was to utilize existing representative hardware which could then be processed in a manner similar to the LSE reflector and, where appropriate, tested.

Brightening of the 5-meter reflector petal was attempted using the standard aluminum chemical brightening process used for the 5457 and 5657 alloys. This process, shown in Figure 8.1-19, yielded a high total reflectance but very poor specularly. It was determined that the 5-meter petal alloy, 5052, had poor brightening results due to the high content of magnesium with some chromium. As an expedient technique, mechanical polishing of the petals was utilized to improve specularly of the polished petal.

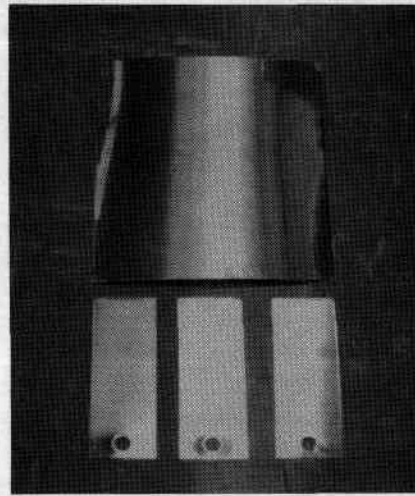
Various sequences and combinations of chemical and mechanical polishing of the petals were tried on samples of the petals. Results of optical tests presented in Figure 8.1-20 showed that mechanical polishing after chemical brightening did lower total reflectance but yielded acceptable specular reflectance. This technique was adopted for brightening of the 5-meter petals.

Application of RTV 670 and its primer (4155) followed the process outlined in Figure 8.1-21. Initial attempts to spray the RTV 670 by a vendor did not yield satisfactory results due to a lack of control on the curing process. This effort was continued into the next phase with the flow coat technique being pursued inhouse by GE and with a vendor search and qualification effort underway for spray application.

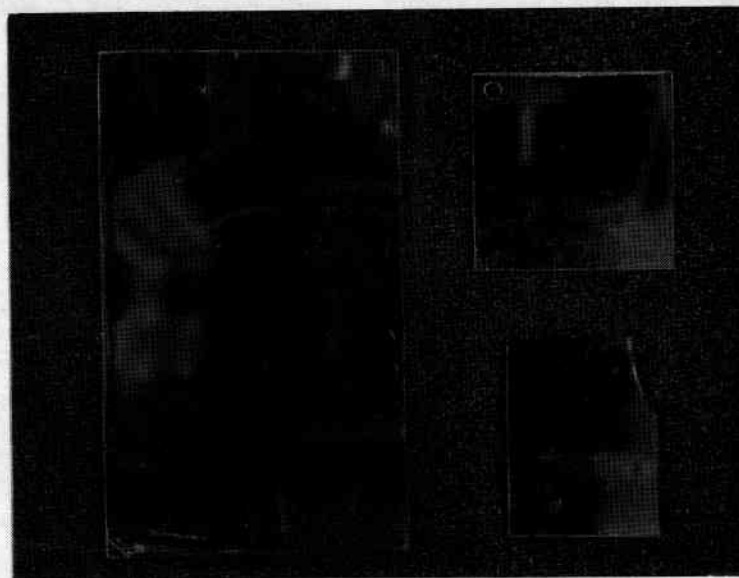
Use of ALGLAS sheet for the LSE reflector, the other promising option, required a production process evaluation to establish its technical and cost feasibility. Although the technical and cost characteristics



(a) 5657/RTV-670
CONTAMINATED



(b) 5657/RTV-670
AFTER CLEANING



5657/
RTV-670

5457/ALGLAS

2nd SURFACE
MIRROR

(c)
AFTER CLEANING

Figure 8.1-18. Photos of Contaminated and Cleaned Surfaces

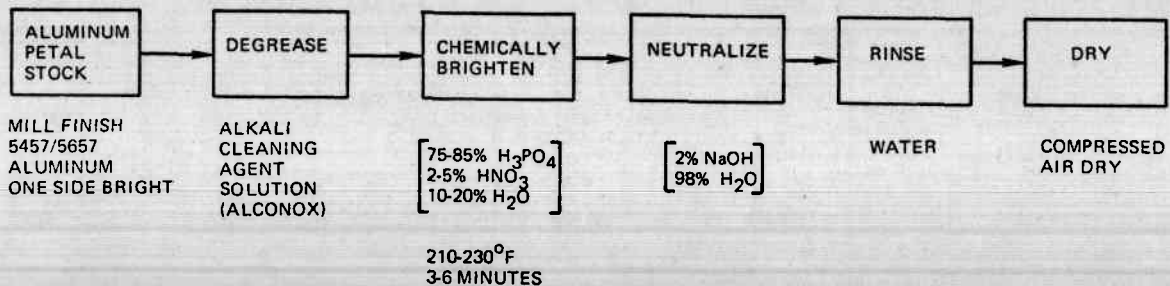


Figure 8.1-19. Typical Chemical Brightening Process

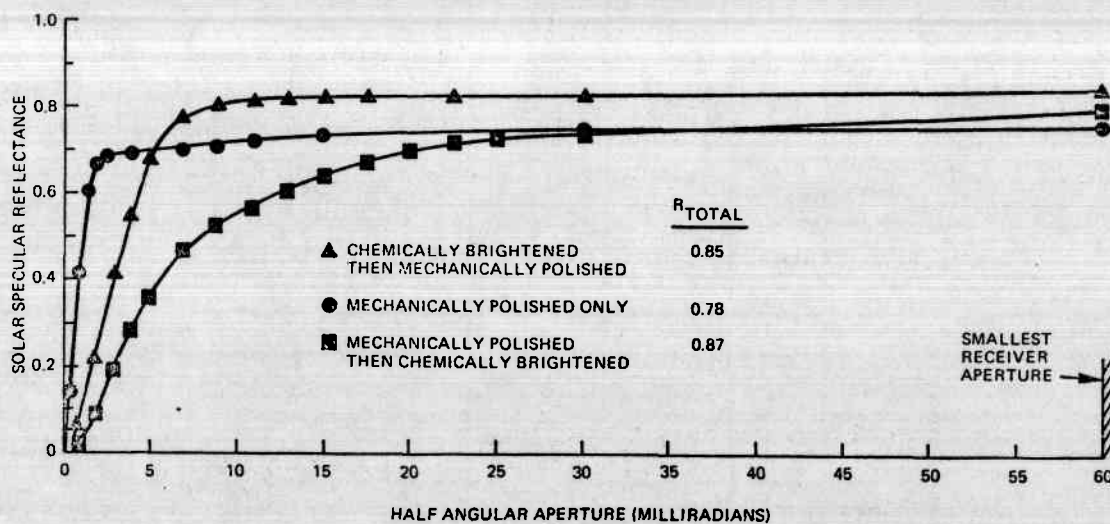


Figure 8.1-20. Specular Reflectance of Treated 5052 Samples From 5-Meter Reflector Petals

of the ALGLAS sheet were well known, the feasibility of the bonding process itself remained to be determined. This required the evaluation of adhesive materials, bonding processes, and reflector sheet configurations.

Bonding of the thin ALGLAS reflector sheet to the 5-meter reflector petal substrate was initiated with a review of several methods for bonding a conformal reflector. The bonding of a preformed conformal reflector sheet and petal was considered an attractive method, but schedule demands prevented this approach from being pursued although it would have been selected for the LSE production approach if ALGLAS was used. Bonding with the use of pressure molds was also considered, but time and availability of these molds and adequate pressing facilities precluded this approach.

The technique selected was vacuum bonding using thin (.00064 meter or 0.025 inch) 5657-H42 sheet. A sketch of the bonding rig is shown in Figure 8.1-22. Both full petal face sheets and radial strips were bonded to the petal substrate. For the purpose of fabricating a test reflector, the radial strip approach was determined to offer superior performance. This technique was therefore selected as the fabrication technique for 5-meter test reflector petals. Figure 8.1-23 shows a partially coated petal bonded by this technique.

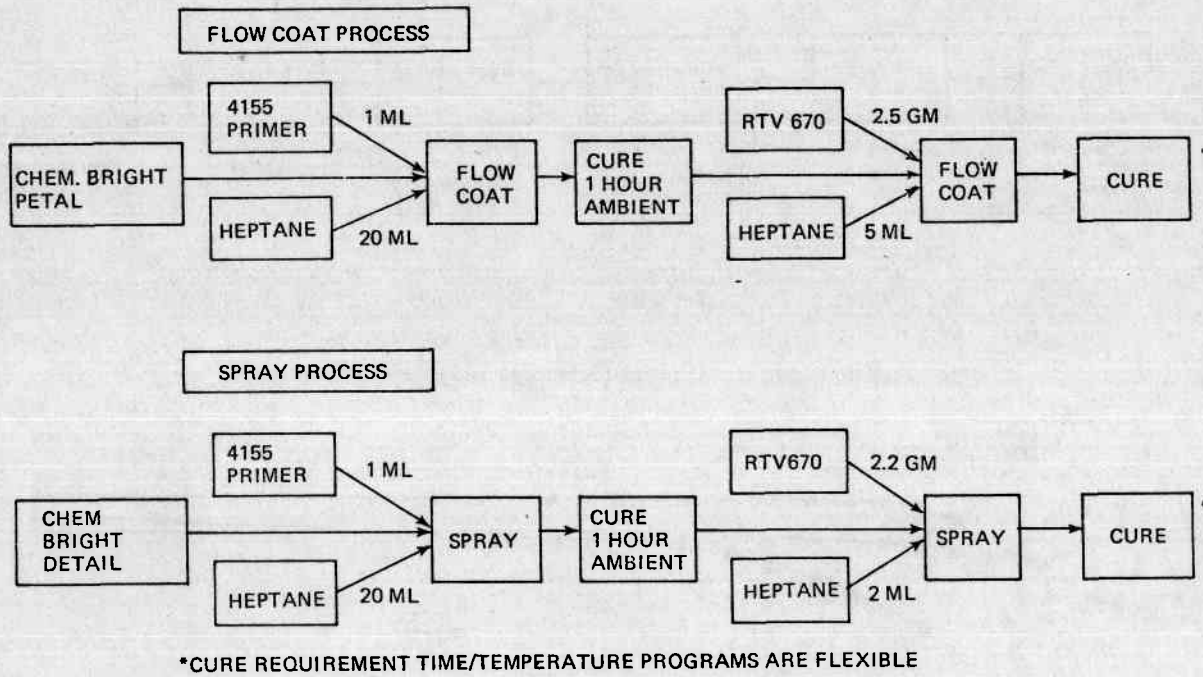


Figure 8.1-21. RTV 670 Coating Processes

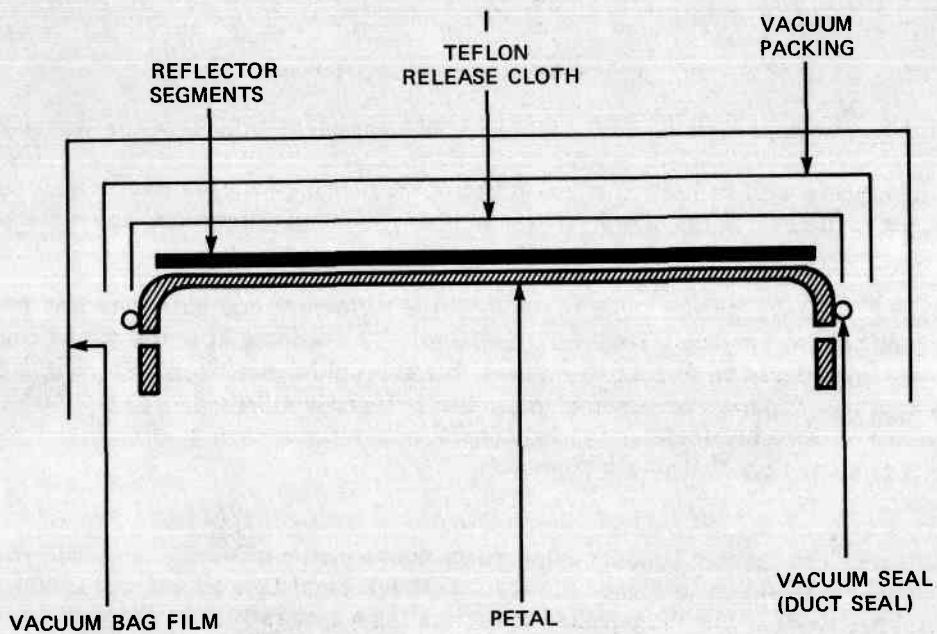


Figure 8.1-22. Cross Section Of Vacuum Bonding Rig

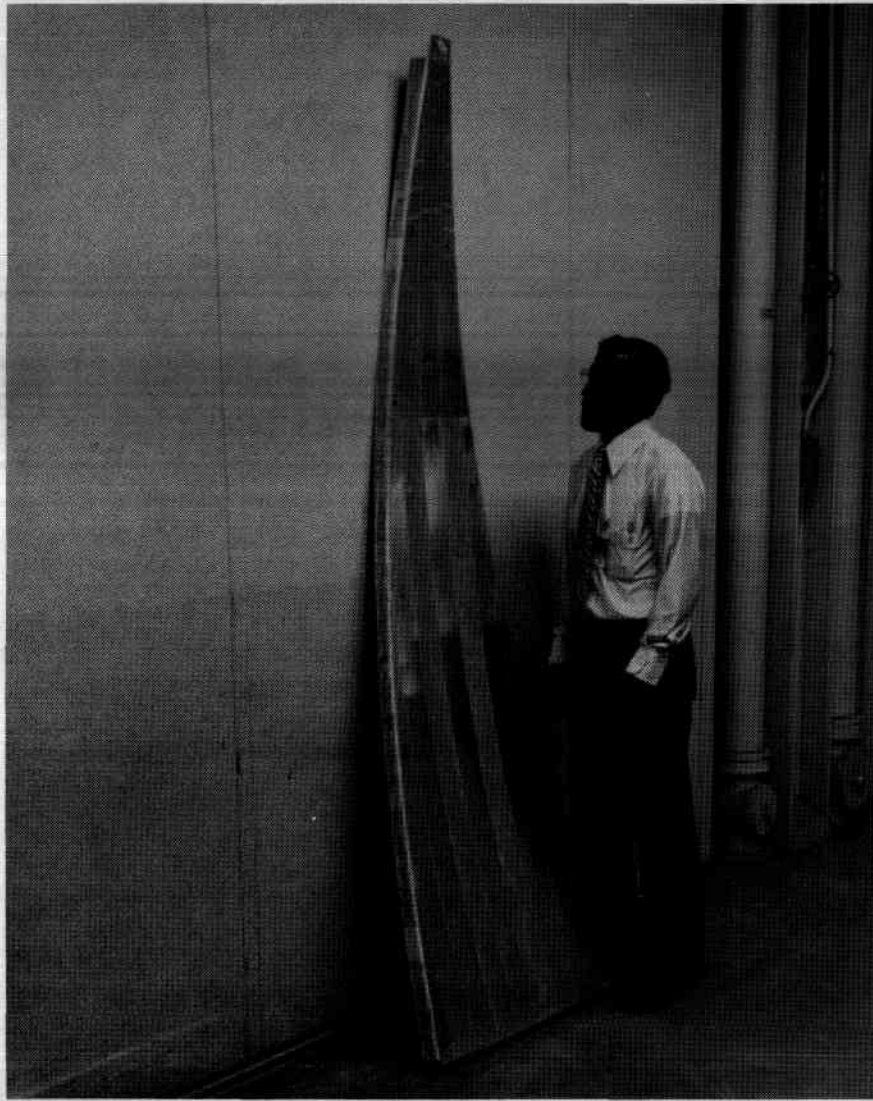


Figure 8.1-23. Partially Bonded Petal

The requirements established for bonding adhesive material were availability of adhesive, environmental stability, adequate mechanical strength, and low cost. The potential mode of failure in this application would be loss of peel strength since the edges of the reflector sheet with its exposed bond lines would be prone to environmental degradation. The total shear strength was important but not essential as there was no significant structural requirement for this application especially when preformed reflector sheets were to be used in production.

Adhesive candidates were tested to determine their characteristics after environmental exposure. The tests measured lap shear strength, peel strength, and bend strength before and after an exposure cycle of four hours of twenty suns intensity (ultraviolet light) and then twenty hours of 95-100 percent relative humidity at 336°K (145° F) for five days. Test results given in Table 8.1-13 indicated that the structural adhesives (Armstrong, 3M Hysol) exceeded the base metal strength, but the important peel strength was very low. The PRC and Emerson Cumings materials exhibited an excellent peel strength with a reasonable lap shear strength. The bend tests showed no prominent deterioration or delamination. Based on these results, the low cost Emerson Cumings adhesive was recommended for the ALGLAS bonding application.

Table 8.1-13. Test Data - Evaluation of Bonding Materials for Reflector Sheet

Environmental Test Program					
100 Hours @ 95-100% RH @ 145°F 20 Hours of 20 Suns Ultra Violet Light	PRC PR-1422-A2	Armstrong A 271	3M Co. 2216 B/A	Emerson Cumings Eccobond #45 Catalyst #15	Hysol 9309.3
1. Peel Test (lbs/in)					
a. Controls	20.1	1.0	2.0	7.0	2.5
b. Test Sample	5.0	4.0	3.0	10.0	2.0
c. Change (%)	-75.1	+300	+50	+42.3	-20
d. Type Bonding Failure					
Control	Cohesive	Adhesive	Adhesive	Adhesive	Cohesive
Test Sample	Adhesive	Cohesive	Adhesive	Adhesive	Adhesive
2. Lap Shear Strength (psi)					
a. Controls	196	338	313	214	350
b. Test Sample	130	340	294	114	346
c. Change (%)	-33.6	+0.6	-6.0	-46.7	-1.1
d. Type Bonding Failure					
Control	Cohesive	None*	Adhesive	Cohesive	None*
Test Sample	Adhesive	None*	Adhesive	Adhesive	None*
3. Bond Line Degradation					
a. Change from Control (edge) (microscopic exam @ 25X)	Slight Softening	Slightly Harder	No Significant Change	No Significant Change	Color Change
b. Change from Control (interior) (microscopic exam @ 25X)	No Deterioration	No Deterioration	No Deterioration	No Deterioration	No Deterioration
Processing Information					
1. Bend Test (125 psi @ RT)					
a. Bond Line Change (Microscopic Examination at 25X)	Uniform Bond Line No Delamination	Uniform Bond Line No Delamination	Uniform Bond Line No Delamination	Uniform Bond Line No Delamination	Uniform Bond Line No Delamination
2. Application					
a. Workability	Very Good (Brushable)	Very Good (Brushable)	Good (Thixotropic)	Very Good (Brushable)	Good (Thixotropic)
b. Pot Life (Hours)	2	1	1	3	1/2
3. Cost					
a. Dollars/Gallon	34	123	123	28	85
* The aluminum alloy elongated at this point by 0.3 inch.					
Test Methods					
1. ASTM D903 -Peel or Stripping Strength of Adhesive Bonds					
2. ASTM D1141-Effect of Moisture and Temperature on Adhesive Bonds, Test Exposure No. 9					
3. ASTM D1002-Strength Properties of Adhesives in Shear by Tension Loading					

8.2 THERMAL ENERGY STORAGE DEVELOPMENT

To support the design effort on the trickle oil High Temperature Storage Subsystem for the Shenandoah System, a small scale test program was performed at the GE Space Division facility at Evandale, Ohio. The objectives of the test program were to verify the trickle oil heat transfer capability, to obtain initial preliminary design data, and to verify computer model predictions providing a tool for the LSE design performance predictions. All of the objectives were met, and the following sections describe the test assembly and results.

8.2.1 TEST ASSEMBLY DESCRIPTION

The facility used a 0.21m^3 (55 gallon) drum, 0.57 meter (22.5 in.) in diameter and 0.71 meter (28 in.) in length, for the storage tank. To obtain data as early as possible in the Preliminary Design Phase, the system was designed to operate at a low temperature of 300 to 355°K (80 to 180°F). A 10% glycerol/water solution was used as the heat transfer fluid since it had viscosity characteristics over the test temperature range similar to Syltherm 800 over the LSE design temperature range. Thus, the flow propagation rate through the bed could be simulated to provide initial heat transfer data. The test column was filled with granite, the initial storage media selection, which was irregular in shape with characteristic dimensions from 0.0095 to 0.019 meter (3/8 to 3/4 in.) in length.

The total facility incorporates five 55-gallon stainless steel drums. Figure 8.2-1 shows a detailed schematic of the test layout. Two of the drums are equipped with commercially available, clamp-around drum heaters which were used to hold and initially heat the systems fluid inventory of approximately 0.38m^3 (100 gallons) to a uniform constant temperature. An in-line electrical calrod heater is located in the entrance line to supplement the heatup capability of the drum heaters. The heated water-glycerol solution was pumped through a bypass loop until a constant flow rate was achieved and then through the fluid distribution system providing a temperature step input to the bed. By gravity drain, the fluid passed through the bed and into a second pair of 55 gallon drums. During the next extraction from the rock tank, a source of cold fluid was pre-established by using the cooler heat exchanger to achieve the desired initial low temperature. Again, circulation through the by-pass line was utilized to achieve a uniform, well mixed, initial temperature. The cool fluid, after passage through the inlet flow sensor, was introduced to the rock tank and allowed to drain back into the hot tanks by gravity.

The rock tank itself is located on a shelf approximately 2.6 meters (8-1/2 ft.) above the floor level. This elevation insures a positive head at the inlet of the circulating pump which was located at the floor level. All tanks and pipes are insulated to reduce thermal loss. Filters are installed at appropriate locations to prevent rock lines from plugging critical flow paths, and sight glasses are used on each tank to monitor fluid levels. A shower head type of distribution is used at the top of the bed to distribute the flow over the bed uniformly. The shower head consists of 6.1×10^{-4} meter (.024 in.) diameter holes located on a .025 meter (1 inch) grid pattern. Figure 8.2-2 is a photograph of the completed assembly.

8.2.2 INSTRUMENTATION

The test set-up includes an Acurex Autodata logger to record the 64 TES rock bed temperatures, the tank inlet and outlet flow rates, and the temperature. The rock bed instrumentation points are shown in Figure 8.2-3. The centerline temperature profile was recorded from thermocouples placed at 0.025 meter (1 in.) intervals along the tank length. There were 3 planes, top, middle, and bottom, with 14 thermocouples placed radially as shown in the figure. All of the thermocouples were imbedded in the rock to assure consistency in measuring rock temperatures.

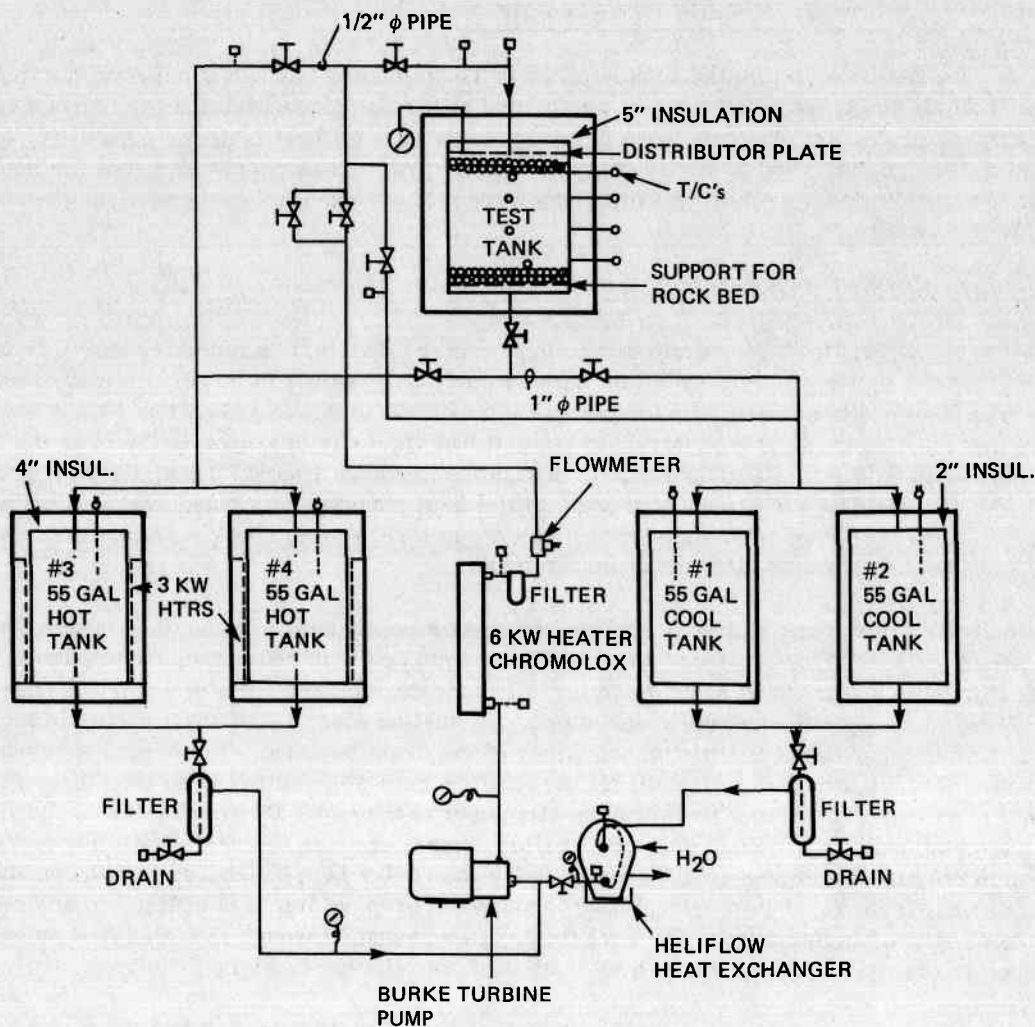


Figure 8.2-1. Schematic Of The Trickle Oil Column Experiment

8.2.3 TEST RESULTS AND CONCLUSIONS

Table 8.2-1 lists the test performed and the major objective for each. Test runs charging and discharging were made from 3.2×10^{-5} to 1.9×10^{-4} m^3/s (1/2 to 3 gpm) through the test column. This flow range simulated the m/A flow through the large tank over the LSE design range to $0.024 \text{ m}^3/\text{s}$ (387 gpm) and simulated the flow up to $0.015 \text{ m}^3/\text{s}$ (230 gpm) through the one-hour tank. Figure 8.2-4 shows the charging profiles for 6.3×10^{-5} m^3/s (1 gpm) flow. Relatively steep temperature gradients were achieved relative to the bed height verifying the heat transfer capability of the trickle oil flow. The computer model described in Paragraph 3.4.4.3 was used to compare with the measured results. The heat transfer coefficient, surface area product was varied to match the test data because the heat transfer coefficient and the actual wetted area are unknown. The model assumed full wetting of the granite surface area. Good comparison was achieved for a $h_c A$ value of ten percent of the theoretical value as shown in Figure 8.2-4. This lower than predicted value indicated that the theoretical h_c value was over estimated, and probably not all of the surface area was being wetted. The matched $h_c A$ value was used for both the charging and discharging test flow profiles, and again good comparison was obtained as shown in Figure 8.2-5. The excellent comparison between the test data and the computer model provided a tool for predictions of the LSE design.

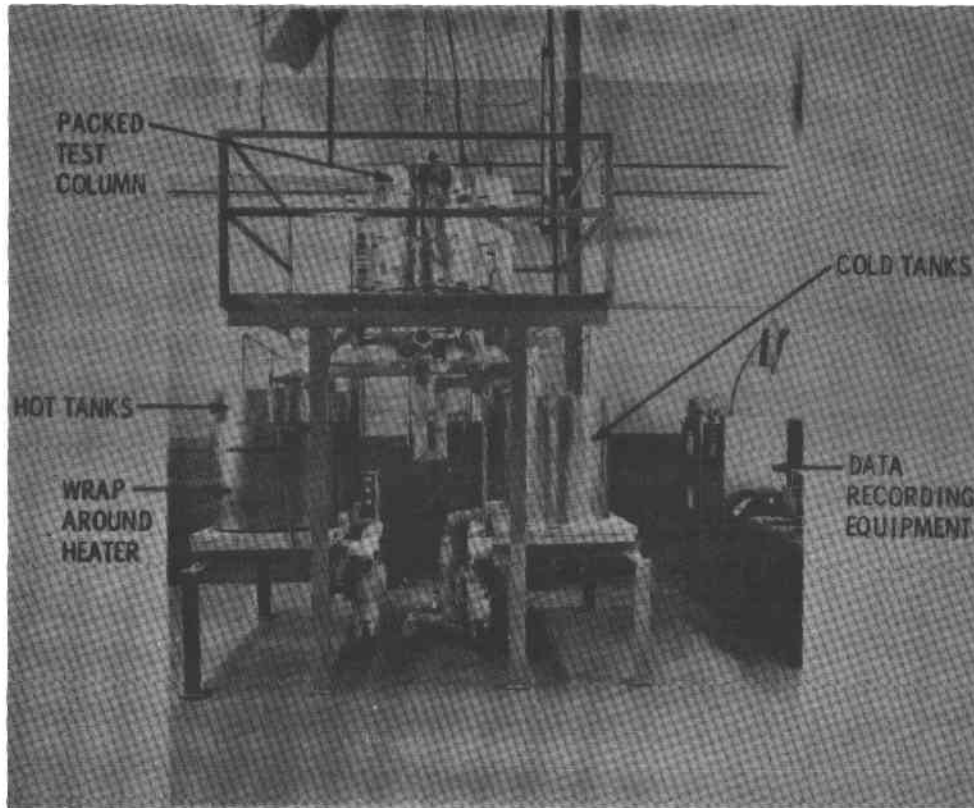


Figure 8.2-2. Trickle Oil Test Column

Some channeling effects were observed from the radial temperature measurements during the tests. These effects were expected based on the test column to particle diameter ratio of 45. As the container size increases from 50 to 100 times greater than the particle diameter, a more uniform velocity profile across the bed would be expected. Near the end of the test period, additional channeling was introduced which affected the test results, due to a partially blocked shower head plate which identifies a potential problem on the full scale system manifold design. The blockage was due to rust and scale formation since the working fluid was water. The actual system using Syltherm 800 will not be subject to this type of blockage.

Several additional tests were completed on the test assembly and on separate equipment. Holding tests of a fully charged and partially charged tank showed high heat losses to the environment especially from the bottom of the tank. Separate heat capacity tests were conducted on the granite and indicated a value of $961 \text{ J/kg} \cdot ^\circ\text{K}$ ($.23 \text{ Btu/lb} \cdot ^\circ\text{F}$) over the test temperature range. Void volume tests showed a voidage of 47 percent in the 0.21 m^3 (55 gallon) test column for the irregular shaped granite. Film thickness tests indicated films up to $2.6 \times 10^{-5} \text{ m}$ (.0067 in.) on the rock surface area. All of these data were used in analysis of the test results and provided initial preliminary data for the LSE design.

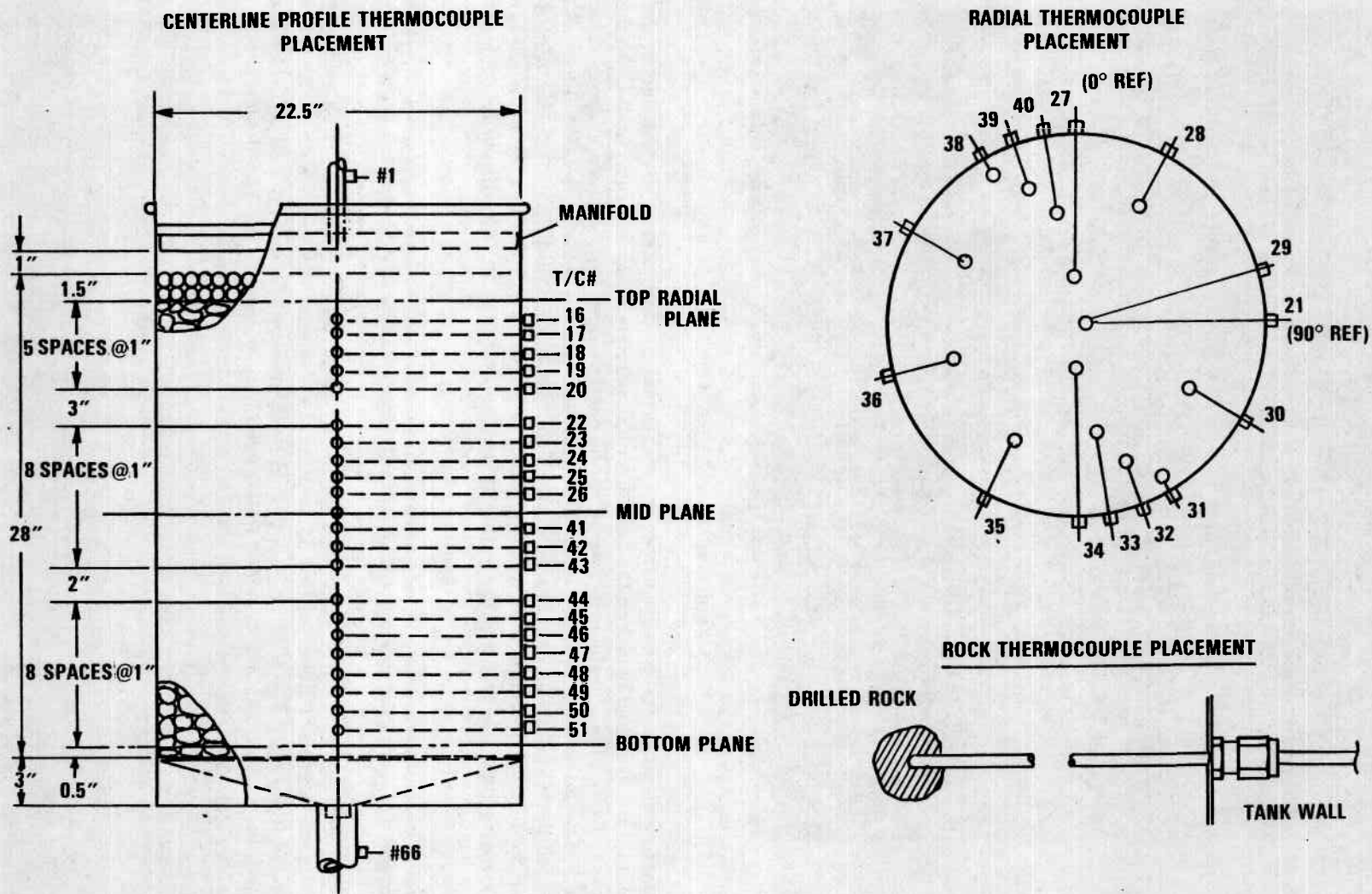


Figure 8.2-3. Trickle Oil Experiment Instrumentation Layout

Table 8.2-1. Summary Of Preliminary Trickle Oil Column Tests

Test Description	Major Objective
Charge/Discharge Flow Rate Tests (1/2, 1, 3, GPM)	Temperature Profile Sensitivity To Flow
Fully Charged Holding Test	Thermal Losses
Partially Charged Holding Test	Thermal Losses
Partially Discharged Holding Test	Thermal Losses
Inversion Profile Propagation Test	Inversion Efficiency
1 GPM Charge Test at 1. PSI Cover Gas Pressure	Temperature Profile Sensitivity To Cover Gas Pressure

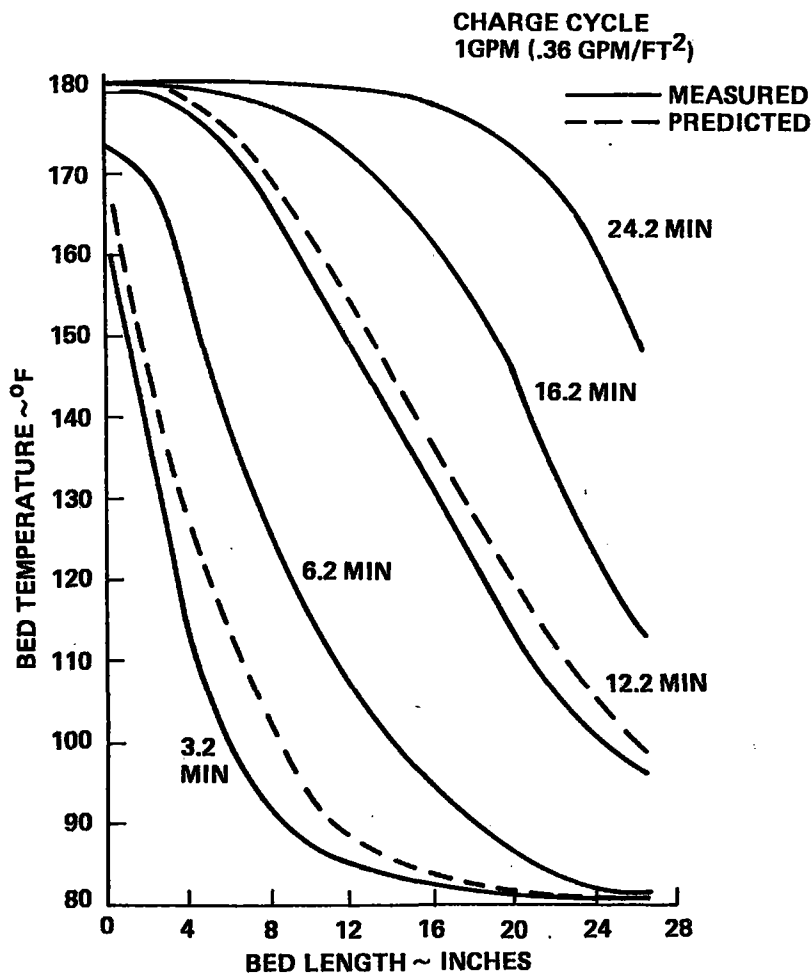
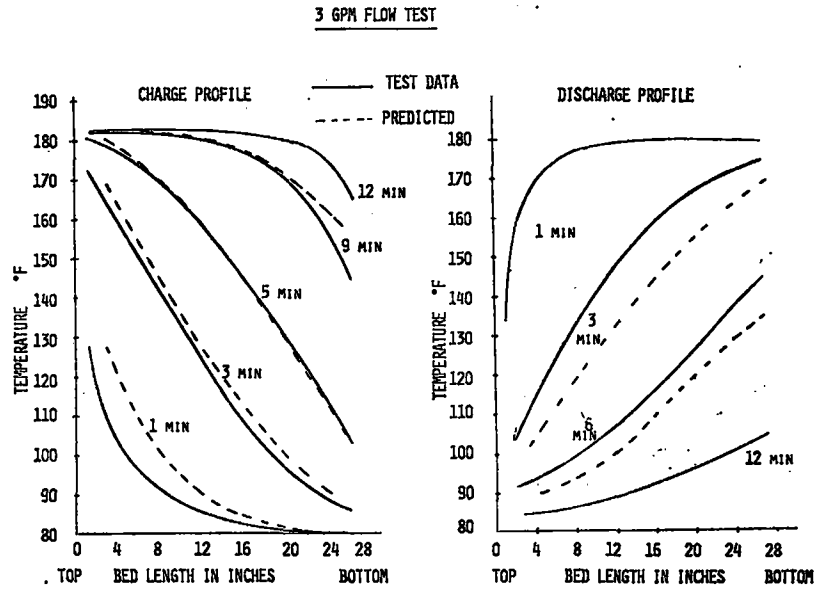
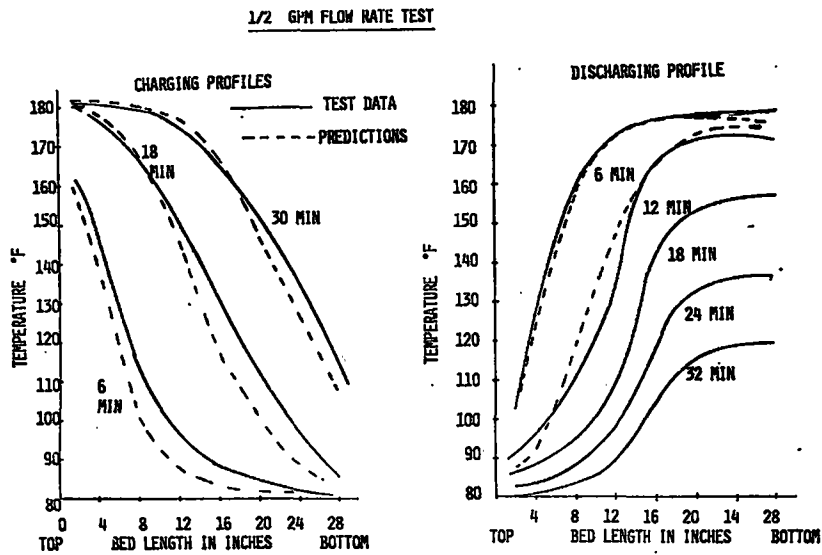


Figure 8.2-4. Trickle Oil Column Results



GOOD COMPARISONS BETWEEN DATA AND
COMPUTER PREDICTIONS

Figure 8.2-5. Column Test Results

The conclusions drawn from the trickle oil column test are:

1. Trickle oil heat transfer capability verified.
2. Flow results predictable with computer model.
3. Some channeling effects noted.
4. Heat losses from bottom of tank were high.
5. Inversion mode not fully simulated due to channeling.
6. No apparent heat transfer sensitivity to cover gas pressure.

Additional tests are planned using a 2.54 meter (100 in.) long column to allow more fully developed temperature profiles. Also the support structure is being redesigned to reduce heat losses, and the fluid distributor design is being changed to obtain a more uniform fluid distribution over the top of the bed and also to allow deliberate maldistribution.

8.3 SHENANDOAH DISH COLLECTOR FIELD FOR SANDIA SOLAR TOTAL ENERGY SYSTEM TEST FACILITY

8.3.1 INTRODUCTION

As a part of the overall collector subsystem development plan and as a logical extension of the Engineering Prototype Collector testing performed during the Preliminary Design, it was planned to incorporate a group of Shenandoah collectors into a quadrant of the Sandia Solar Total Energy Systems Test Facility (STESTF). During the Preliminary Design, program effort was initiated in several key areas to support this activity. The majority of the collector design drawings were completed as were designs for the collector foundations, the loop mechanical design and bulkhead interface, and preliminary control and instrumentation. To simulate the shadowing and control associated with the repeating diamond collector pattern for the Shenandoah field, four 7-meter diameter dishes were planned for the quadrant test.

The loop will operate with Syltherm 800 at the operating temperatures planned for Shenandoah. System operation, including the use of a hybrid tracking system with both computer and active sun sensor track, will be identical to the Shenandoah design. The quadrant test, because of its schedule relative to the LSE fabrication schedule, will serve as a proof test for many aspects of the collector and field designs. At completion of the planned test program, the facility will be used as a continuing test bed by Sandia as part of the STESTF.

Specific objectives of the facility include the following:

1. Test Prototype Of Shenandoah Collector/Pipefield
 - a. Design Verification. Tests will be designed and conducted to provide verification of the Shenandoah collector and pipefield. Test results will provide verification of design performance level of various components.
 - b. System Operation and Control Finalization. The facility will be exercised to verify system and controls operations.

2. Provide Simulation Facility

- a. Shenandoah Startup Debugging/Diagnostics. Through proper simulation of predicted Shenandoah operational procedures and potential problems, a data base will be accumulated for application to the Shenandoah System operation.
- b. New Upgraded Component Verification. As it becomes necessary or desirable to change or modify components, they may be evaluated and proved in this facility.

3. Provide Fabrication/Procurement/Installation Experience

Since the quadrant facility is to be a prototype of Shenandoah (to the extent possible), all aspects of the project will provide valuable experience. The Shenandoah architect and engineering will also design this facility and GE personnel will also be involved in both.

4. Component Development And Qualification Test Facility

Flexibility of the Quadrant Facility will allow the development of new components and evaluation of their capabilities.

8.3.2 FACILITY DESIGN

8.3.2.1 Site Improvement

Four prototype Shenandoah collectors will be installed on the Solar Total Energy Systems test facility site northeast of the existing Raytheon collector (Figure 8.3-1). The facility was located on the west side of the site to facilitate bulkhead connections and allow room to the east for future Sandia facilities.

The type of foundation planned for the quadrant test facility will differ below grade from that planned for Shenandoah. Soil loading capability at Sandia is significantly less than at Shenandoah and will necessitate a more extensive collector support. The foundation selected consists of an underground pad for each collector with three support columns for the collector legs. This approach was selected as cost effective for the soil conditions found in the Albuquerque area.

Investigation has revealed underground sanitary sewer and gas lines on the quadrant test site which may interfere with foundation installation (see Figure 8.3-1). The lines can be avoided by slight repositioning of the quadrant field which will allow work to proceed on schedule. However, if movement of the utilities is required, some schedule delay can be expected. General Electric will also install a pad on the west side of the site to house support equipment. This equipment will be detailed in following sections.

8.3.2.2 Bulkhead Interface

A bulkhead will be installed by Sandia adjacent to the west side of the field. This bulkhead will act as the interface between GE and Sandia. The interface drawing is shown in Figure 8.3-2. All interface between the quadrant test facility and Sandia will pass through the bulkhead.

Power will be contained on the west side of the bulkhead. The pumps require 480Vac and will be wired to the distribution box on the bulkhead. A transformer will accept 480Vac and convert to 220. This in turn will service the remaining power requirements in the form of 110V per leg. Control and instrumentation lines will connect to the east side of the bulkhead. From this connection they will be run to the computer, data acquisition system, and control panel.

Utilities will interface on the north side of the bulkhead. Therminol 66 heat transfer fluid will be used to carry collected heat to the Sandia storage tanks. Other utilities will include air, nitrogen and water.

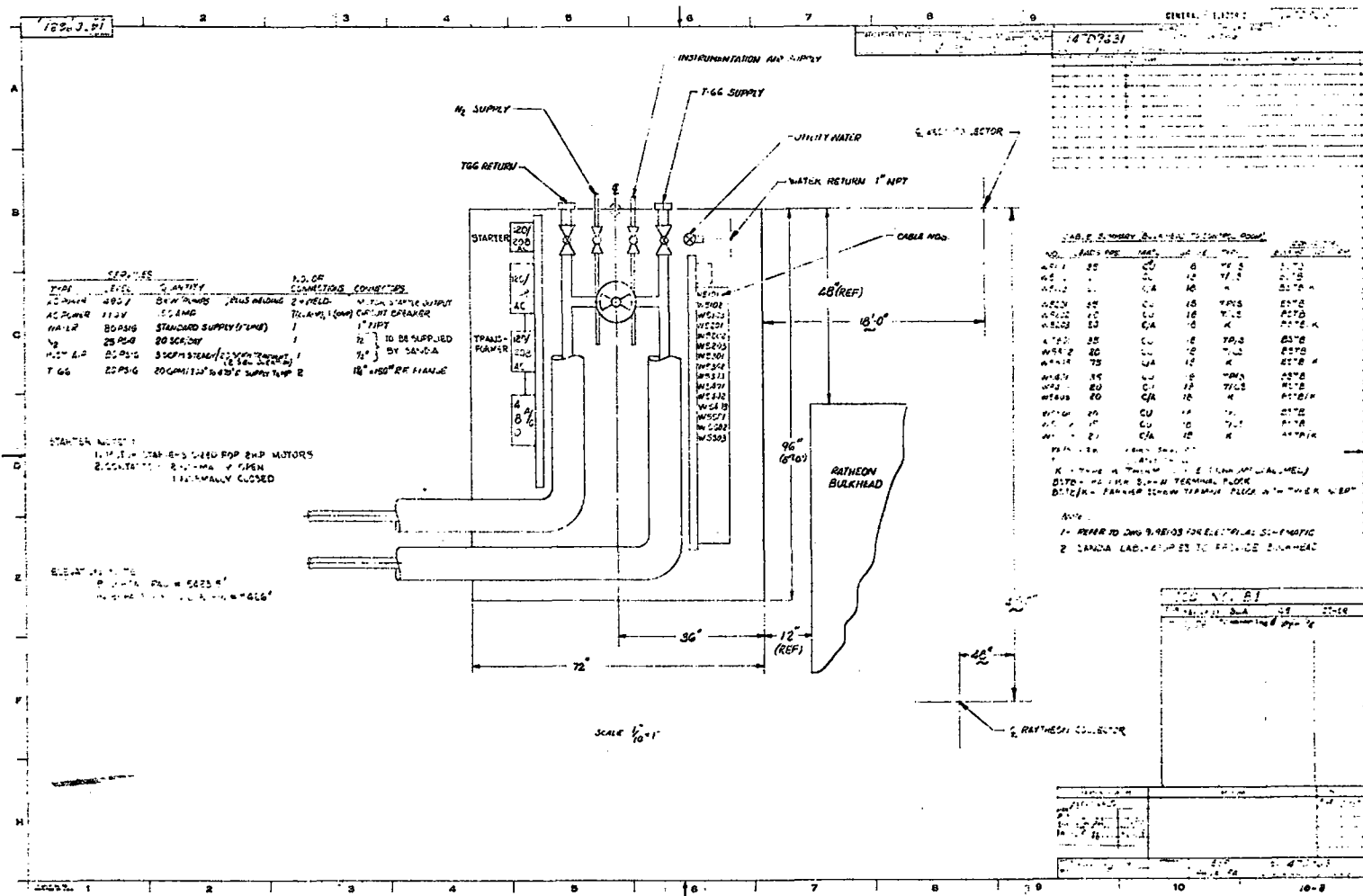


Figure 8.3-2. Quadrant Test Bulkhead Interface Drawing

8.3.2.3 Loop Schematic

A schematic of the heat transfer loop is shown in Figure 8.3-3. The loop was designed as an experimental facility. As such it will be flexible to accommodate materials, components, procedural, and other changes during the test program. There are four collectors which will collect solar energy and transfer it to Syltherm 800 heat transfer fluid. The fluid is circulated through the system and passes through a heat exchanger on the pump pad. In this unit, heat is exchanged to the Sandia Therminol 66 fluid for use in the system test facility.

Electro-pneumatic control valves are positioned in line with each collector for trim control with overall field fluid temperature controlled by a system control valve. These valves and their complementary temperature feed back controllers provide control of fluid flow in the system to maintain desired receiver and system fluid outlet temperatures. The Syltherm 800 loop design flow rate is $6.3 \times 10^{-4} \text{ m}^3/\text{s}$ (10 gpm) or $1.3 \times 10^{-4} - 3.2 \times 10^{-4} \text{ m}^3/\text{s}$ (2-5 gpm) at each collector. This represents nominal design flow through each collector with 25 percent safety margin allowance.

A centrifugal pump will circulate Syltherm 800 throughout the loop. At Shenandoah, the pump must operate at 672°K (750°F). Therefore, circuitry has been provided to transfer the pump over to the hot side for qualification during a portion of the planned test program.

An expansion tank is provided to control fluid level and provide pump (NPSH). A nitrogen inert gas blanket is provided to prevent fluid contact with air. Also included is a cold condenser tank which will collect volatiles and condense them for disposal.

All connections will be either welded or compression fittings to minimize leakage of low viscosity fluid. The one exception will be the pump which will have a raised face flanged connection. Compression fittings will be utilized on components which may require disassembly during the course of the experiment. Operating pump discharge pressure is estimated to be $2.1 \times 10^5 \text{ N/m}^2$ (30 psig). Relief valves will be set at $6.9 \times 10^5 \text{ N/m}^2$ (100 psig) with component ratings at $8.6 \times 10^5 \text{ N/m}^2$ (125 psig).

8.3.2.4 Controls and Instrumentation

Instrumentation of the quadrant facility will be extensive to support system data acquisition. Controls will be designed to simulate the Shenandoah philosophy where feasible within schedule constraints. A schematic of the controls is shown in Figure 8.3-4.

To determine system and component performance and verify design specification, measurements of temperature, flow rate, pressure, power consumption, and fluid will be made throughout the system. The prime temperature measurement device will be chromel alumel thermocouples which will be welded to various locations on the outside wall of the tubing to determine fluid temperatures. The receivers will be heavily instrumented to look at hot spots, efficiencies, and losses. Resistance Temperature Detectors (RTD) will be incorporated on the receiver to evaluate their potential for use in the Shenandoah Control Circuit. Piping losses will be determined by measuring gradients along tubes and through insulation.

Flow meters will be installed on the inlet side of each collector and at the exit of the pump circuit. These will be turbine type meters and will be operational at the high temperatures in the facility.

Pressure transducers will be installed to measure pressure levels and drops at pertinent points in the system. This data will allow verification of design calculations for Shenandoah.

Other instrumentation will include parasitic power and position indicators for valves and collectors. Valves will have potentiometer feedback devices to record position. Twelve sensors will be mounted around the receiver to sense light reflected from the collector and determine position relative to the sun. Four of these sensors will be used for control purposes.

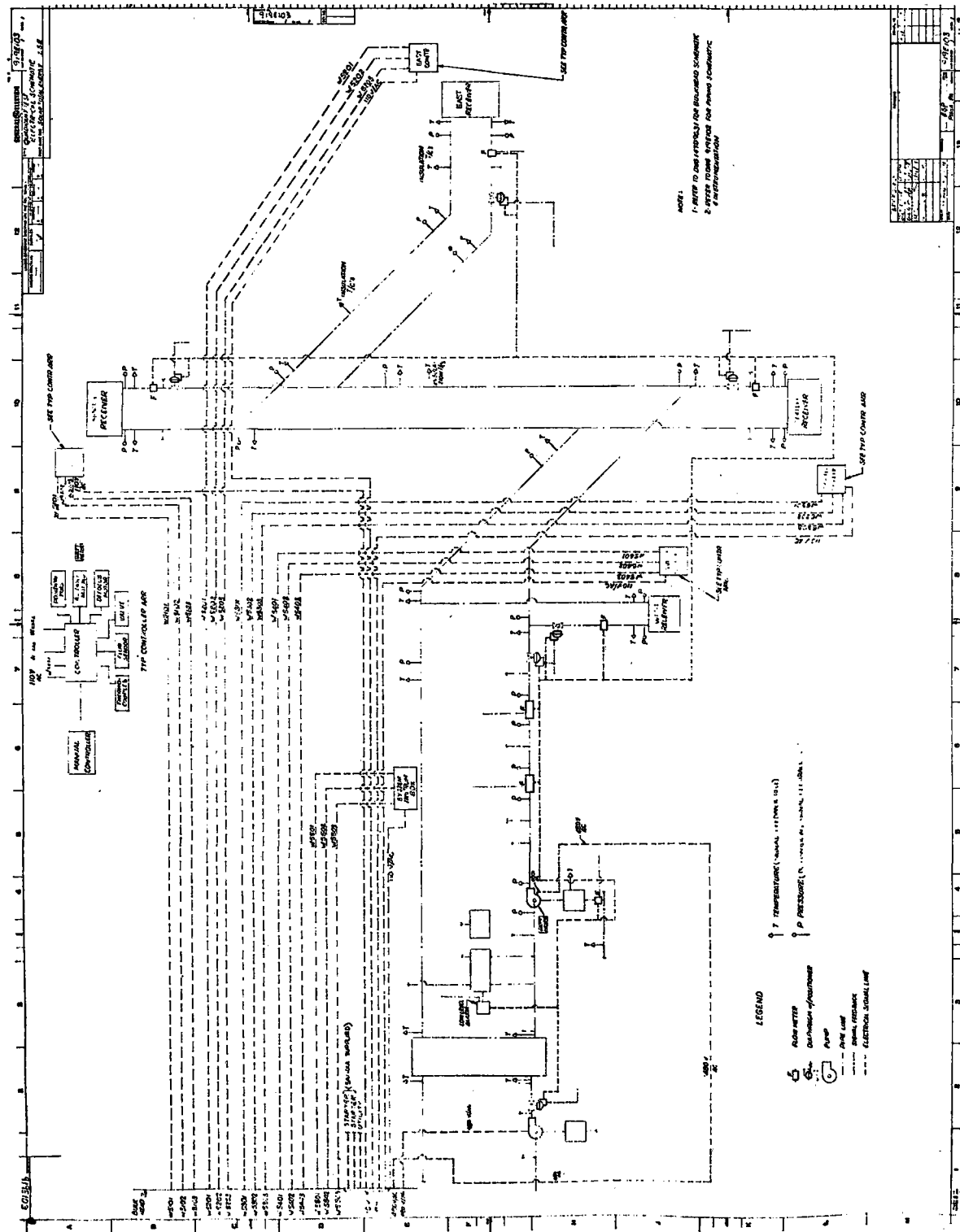


Figure 8.3-4. Quadrant Test Electrical Schematic

Many modes of control will be possible in this facility. It is planned to have one temperature controller for each collector. In this mode, flow through each collector will be independently controlled by individually set temperature levels. In a second mode, the systems controller will sample the four collector temperatures and control system flow based on the hottest collector. Other modes of control, such as manual operation, defocus, stow, etc., will also be included.

A control panel will be installed in Building 833 (Control Room) that will contain the necessary readouts and controls to operate the facility. Alarms and indicator lights will be mounted on the panel to provide continual status of the facility during operation. Several of the alarm functions will provide automatic defocus or other action based on data received from the field.

A control box will be installed on each collector to interface with facility cables and collector wiring. Each control box will contain logic, relays, and other components required to operate the collector.

The control box will be a prototype of the Shenandoah design. The Sandia HP 9825 computer will interface with the control box to provide sun position data. When close to correct orientation, sensors on the receiver will take over and provide final positioning.

8.3.3 TEST PLAN

A comprehensive test plan will be developed to insure that the Quadrant facility provides data and guidance to the Shenandoah design, installation, and operation. A preliminary test plan outline is shown in Table 8.3-1. Prior to and in conjunction with the test will be the break-in procedure at reduced temperatures for the Syltherm 800 fluid.

Table 8.3-1. Outline of Planned Tests For Parabolic Dish Quadrant Test

Checkout/Verification Tests	Operational Tests
<ul style="list-style-type: none"> ● Flux Profile Tests (1 Collector) <ul style="list-style-type: none"> - Verify Reflector Performance - Receiver Focal Plane Flux Profiles - Control System Tracking Accuracy ● Low Temperature Tests (400°F) <ul style="list-style-type: none"> - Moderate To High Insolation - Verify Receiver Thermal Performance - Identify Possible High Temperature Locations ● Moderate Temperature Tests (600°F) <ul style="list-style-type: none"> - Moderate To High Insolation - Verify Temperature Control Modes - Verify Emergency Shut-Down Modes - Verify Normal Transient Operational Modes 	<ul style="list-style-type: none"> ● Steady State Design Temperature Tests (750°F) <ul style="list-style-type: none"> - High Insolation - Exercise Temperature Control Modes - Exercise Emergency Flow Loss Failure (1 Collector) - Extended Performance Tests - Total Daily Thermal Output - Startup Time History - Piping Losses - Parasitic Power Consumption ● Transient/Stability Performance Tests (750°F) <ul style="list-style-type: none"> - Control Stability At Low Insolation Levels - Control Stability With 3 Collectors - Mid-Day Startup Thermal Transients - Intermittent Cloud Cover Transients - Control Malfunction Simulations

Testing will begin at reduced temperatures to checkout the system at levels where problems can be discovered without significant damage occurring. Receiver thermocouple data will indicate if hot spots are occurring in the tubing and show the heating distribution along the inner surface of the coil. The system will be checked for fluid leaks and component performance.

After successful performance at 477°K (400°F), the system will be stepped to 586°K (600°F) and checked again. At this level, more of the operational functions will be exercised and more detailed checks made of system performance.

After successful completion of 586°K (600°F) testing, the temperature level will be increased to the planned operational level of 672°K (750°F). At this level, substantial steady state and transient testing will take place. As outlined in the table, a full simulation of operational conditions and situations will be achieved.

Of particular importance during steady state testing will be thermal efficiency of the system. This state will provide verification of the Shenandoah design or point out areas where some modification may be needed. The transient tests are designed to evaluate system performance under conditions which are expected to occur during Shenandoah operation. These tests will confirm adequacy of the control system to accommodate variable solar conditions and startup and emergency procedures.

SECTION 9
REFERENCES

SECTION 9

REFERENCES

- 2.1-1 "Solar Total Energy - Large Scale Experiment Shenandoah, Georgia Site," Annual Report June 1977 - June 1978, Georgia Power Company, Document AL0/3394-77/3, June 1978.
- 2.1-2 "Operational Interface Control Drawing Procedure for STE-LSE, Shenandoah," George S. Kinoshita, Sandia Laboratories, SAND 78-0329, March, 1978.
- 2.1-3 C.M. Randall and M.E. Whitson, Jr. "Hourly Insolation and Meteorological Data Bases Including Improved Direct Insolation Estimates." The Aerospace Corporation, Technical Report ATR-78(7592)-1.
- 2.1-4 Hammock, R. Bruce, "A Case Study of Shenandoah Energy Conservation Features in Connection With Solar Total Energy - Large Scale Experiment", Heery and Heery, Inc., AL0/3994-78/1, Distribution Category UC-62, March, 1978.
- 2.3-1 Trane Company, Commercial Air Conditioning Division Catalogue CS-ABS2, July, 1976.
- 3.2-1 Girgoryn, R.S., Shermazlanyan, and Simouyonts. "Characteristics of an Equatorial Mounted Solar System with a Clock Control Mechanism." Geliotechknika, Vol. II, No. 5, 1975.
- 3.3-1 Poland, J. "Cost Tradeoff of Electric vs. Pneumatic Control Valves." Internal General Electric Space Division Report PIR STE-LSE-Ph. III-082, 13 Apr 1978.
- 3.4-1 "Solar Total Energy - Large Scale Experiment #2 Phase II Conceptual Design, Final Report." General Electric Space Division No. 78SDS 4200, January 12, 1978.
- 3.4-2 "Central Receiver Solar Thermal Power System - Pilot Plant Preliminary Design Report, Volume 5 Thermal Storage Subsystem", McDonnell Douglas Astronautics Company, SAN/1108-8/5, November, 1977.
- 3.4-3 Unpublished data curves from Dow Corning, July 1978.
- 3.4-4 "A Method of Simulating the Performance of a Pebble Bed Thermal Energy Storage and Recovery System", S.A. Mumma and W.C. Marvin, ASME paper 76-HT-73, August, 1976.
- 3.4-5 McAdams, W.H., Heat Transmission, McGraw Hill Co., New York, N.Y., 3rd Edition, 1954.
- 3.4-6 Schumamm, T.E., Journal of Franklin Institute, Vol. 208, PP. 405-416, 1929.
- 3.6-1 PIR U-STE-LSE-PHIII-130 "Response to A.I. DR-4. Electrical Transient Analysis (PH III)." Internal General Electric/Space Division Report, 17 July 1978.
- 3.8-1 Boerstler, L. "Response to A.I. DR 30. Investigate Interaction and Feedback of Factory Instrumentation on STES Control." Internal General Electric Space Division Report PIR STE-LSE-Ph. III-032, 24 Feb 1978.
- 3.8-2 Liebling, M. "Preliminary Control Computer Hardware." Internal General Electric Space Division Report PIR STE-LSE-Ph. III-094, 8 May 1978.
- 7.6-1 Garver, L.L. "Effective Load Carrying Capability of Generating Units." IEEE Transactions, PAS-85, No. 8, August 1966, pp. 310-319.

- 8.1-1 Saylor, W., "Environmental Exposure Tests," GE PIR U-IR30-625, 3/23/78.
- 8.1-2 Sanchez, J. "Summary of a Procedure For Making Specularity Measurements with a Laser," GE PIR U-IR30-628, 4/3/78.
- 8.1-3 Amore, L., Sanchez, J., and Saylor, W., "Initial Summary Environmental Exposure Testing Ending 15 May 1978, GE PIR U-IR30-644, 6/1/78.

APPENDIX A
BLEYLE PLANT BUILDING LOAD MODEL

APPENDIX A

BLEYLE PLANT BUILDING LOAD MODEL

This appendix contains the inputs to the Building Transient Thermal Load (BTTL) computer program load model for the 42,000 square feet Bleyle Plant. This program is used to calculate building heating/cooling loads on an hourly basis by summing conduction heat losses/gains (sensible and latent for people, electrical machinery, presses, etc.) and solar heat gains through windows. There are two types of inputs used:

- Actual measured data on magnetic tapes.
- Inputs describing building characteristics, location information, and output format directions.

The plant was sectioned into inside zones shown in Figure A-1. The four zones each have unique design set temperature, maximum air conditioning and furnace capacities, use hours, number of people, electrical loads, evaporation loads, and infiltration loads. These numbers were obtained from Reference A-2 and are listed in Tables A-1 through A-6. Night setbacks of both thermostat setting and ventilation were incorporated.

The wall conductances and capacitances (see Tables A-7 through A-15) were calculated using the information available on the present plant's building materials and information available on the enlarged plant, contained on the GPC interface control drawings. The wall area on the perimeter of the building not exposed to the sun due to the berm was considered to be floor area to simplify calculations. Other input data on materials properties are given in Tables A-16 and A-17. Table A-18 presents the node assignments, areas and shading factors for the building walls.

Solar reflectance and absorptance were taken from book estimates (see references). Wall and window shadowing factors were also estimated.

- Temperatures are calculated every half hour and can be printed out every hour "X" number of times they are calculated.
- The data is in English units.
- There are 12 discrete outside surfaces.
- There are four zones of independent temperature control.

Shenandoah, Georgia

84.7° West Longitude, 33.4 North Latitude, 5th Time Zone

Set Temperatures										
Room	Zone	Zone Node	Air Conditioning				Furnace			
			Winter Day	Winter Night	Summer Day	Summer Night	Winter Day	Winter Night	Summer Day	Summer Night
Storage	1	4	78	78	78	78	65	55	55	55
Mech. Rm.	2	5	110	110	110	110	55	55	55	55
Production	3	6	78	78	78	78	65	55	55	55
Office	4	7	78	78	78	78	65	55	55	55

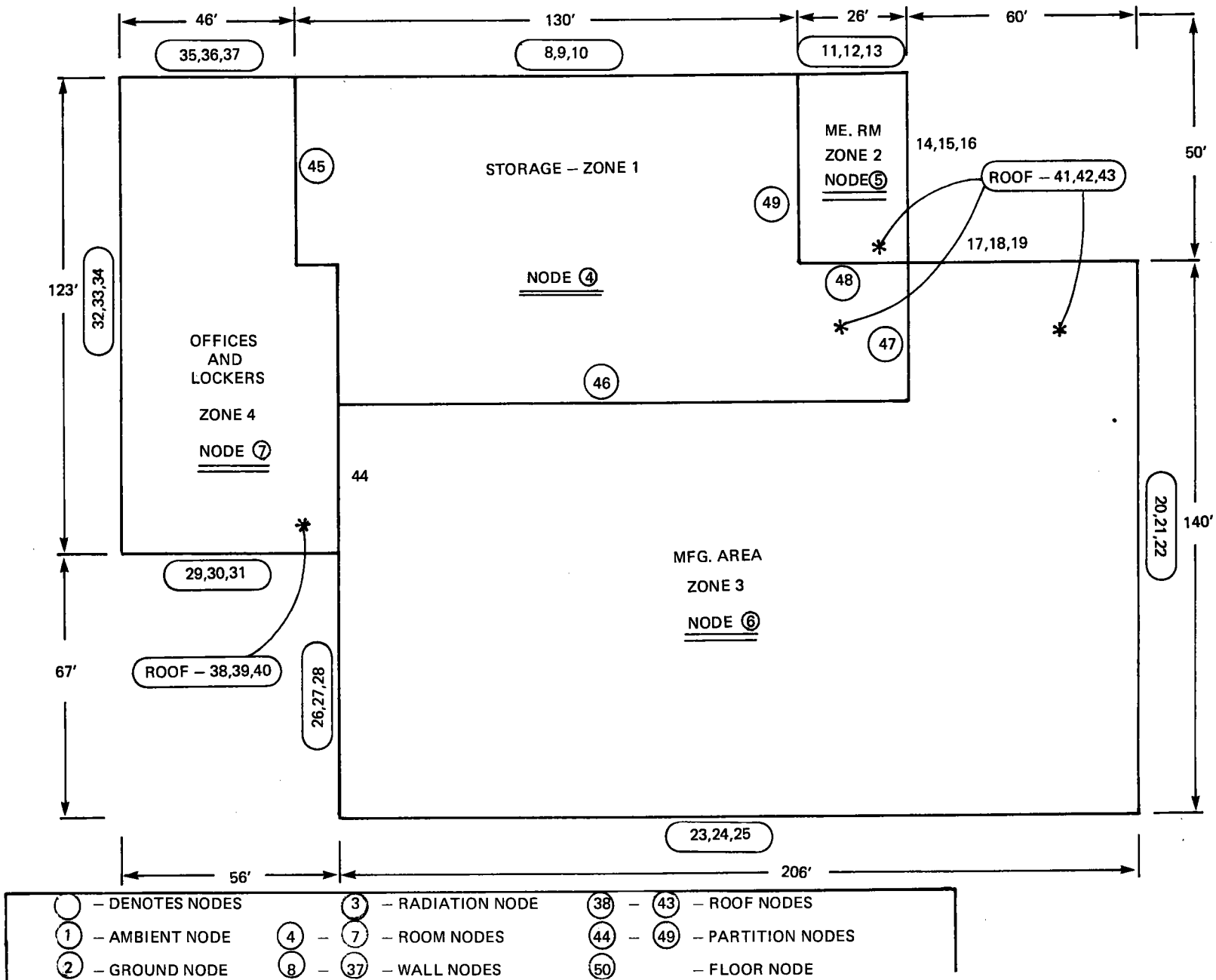


Figure A-1. Floor And Node Plan

Table A-1 Ground Temperatures

January-March

62° F

April-June

62° F

July-September

70° F

October-December

71° F

Table A-2 Peak A/C And Furnace Capacity

Zone Node	Peak Airconditioning Capacity	Peak Furnace Capacity
4	360,000	200,000
5	120,000	50,000
6	1440,000	200,000
7	240,000	300,000

Table A-3 Number of People By Zone

Zone Node	Hours			Weekends
	Midnight to 6 a. m.	6 a. m. to 3 p. m.	3 p. m. to Midnight	
4	0	0	0	0
5	0	0	0	0
6	0	150	150	0
7	0	14	2	0

Table A-4. Ventilation

Room	Zone Node	No. of Unit	Size (Tons)	Total Tons		Total CFM
Storage	4	3	10	30	$\frac{8400}{180}$ (30)	1400
Mech. Rm.	5	1	10	10	$\frac{8400}{180}$ (10)	467
Production	6	6	20	120	$\frac{8400}{180}$ (120)	5600
Office	7	1	20	20	$\frac{8400}{180}$ (20)	933
				180		

Table A-5. Ventilation

Room	Zone Node	Total Cfm	Total lbm/hr	Midnight to 6 a. m. 25% (lbm/hr)	6 a. m. - 3 p. m. 100% (lbm/hr)	3 p. m. to Midnight 100% (lbm/hr)	Weekends 25% (lbm/hr)
Storage	4	1,400	6,300	1,575	6,300	6,300	1,575
Mech. Rm.	5	467	2,100	525	2,100	2,100	525
Production	6	5,600	25,200	6,300	25,200	25,200	6,300
Office	7	933	4,200	1,050	4,200	4,200	1,050

Table A-6. Load Profiles

Zone	Area	Profile	Btu/Hr for 100% Output	Times (Week)										Time Weekend 25% off C Profile			
				C	B		D		C		B		D				
4	Storage				1	-----										24	
	Fan Coil Unit	C	16,382	16,382	-----										16,382	4095	
	Lighting	D	19,448	4,862	0	4,862	19,448	-----						19,448	0		
					21,244	16,382	21,244	35,830	35,830	35,830	35,830	35,830	35,830	4095			
Period Averages					16,000		35,800		35,800				4095				
5	Equipment																
	Miscellaneous Fan	C	5,120	5,120	-----										5,120	1280	
	H/C System Pumps	C	5,461	5,461	-----										5,461	1365	
	Process Equipment	B	110,240	0	0	0	110,240	55,120	110,240	55,120	110,240	0	0				
Lighting	D	2,161	540	0	540	2,161	-----						2,161	0			
				11,121	10,581	11,121	122,982	67,862	122,982	67,862	122,982	2545					
Period Averages					10,800		116,900		116,900				2645				
6	Production																
	Indoor Fan	C	122,322	122,322	-----										122,322	30,580	
	Pipe Gains	C	59,124	59,124	-----										59,124	0	
	Presses, Sensible	B	151,892	0	0	0	151,892	75,946	151,892	75,946	151,892	0	0				
Process Machinery	B	276,794	0	0	0	276,794	138,397	276,794	138,397	276,794	0	0					
Lighting	D	235,520	58,880	0	58,880	235,520	-----						235,500	0			
				240,326	181,446	240,326	845,652	631,309	845,652	631,309	845,652	30,580					
Period Averages					201,000		821,800		821,800				30,580				
7	Office																
	Indoor Fan	C	30,580	30,580	-----										30,580	7645	
	Miscellaneous Fan	C	1,707	1,707	-----										1,707	0	
	Water Heater	C	1,090	1,090	-----										1,090	0	
Lighting	D	38,567	9,642	0	9,642	38,567	-----						38,567	0			
				43,019	33,377	43,019	71,944	71,944	71,944	71,944	71,944	7645					
Period Averages					36,600		71,900		71,900				7645				
Profile B		Hour and Percent of Maximum															
		1-6, 0%; 7-11, 100%; 12, 50%; 13-19, 100%; 20, 50%; 21-24, 100%															
Profile C		Constant - Full Load All Hours															
Profile D		Hour and Percent of Maximum															
		1, 25%; 2-5, 0%; 6, 25%; 7-24, 100%															

Table A-7 Capacitance

Node No.	Area Ft ²	Capacitance Btu/°F-Ft ²	Capacitance *Area Btu/°F
8	1235	8.081	9980
9	1235	1.220	1507
10	1235	1.158	1430
11	247	9.5339	2355
12	247	1.3482	333
13	247	1.273	314
14	475	9.5339	4529
15	475	1.3482	640
16	475	1.273	605
17	570	9.5339	5434
18	570	1.3482	768
19	570	1.273	726
20	1330	9.5339	12680
21	1330	1.3482	1793
22	1330	1.273	1693
23	1957	9.5339	18658
24	1957	1.3482	2638
25	1957	1.273	2491
26	637	9.5339	6073
27	637	1.3482	858
28	637	1.273	811
29	532	9.5339	5072

Node No.	Area Ft ²	Capacitance Btu/°F-Ft ²	Capacitance *Area Btu/°F
30	532	1.3482	717
31	532	1.273	677
32	1109	8.791	9749
33	1109	1.254	1391
34	1109	1.186	1315
35	437	9.5339	4166
36	437	1.3482	589
37	437	1.273	556
38	6968	1.16146	8093
39	6968	1.10925	7729
40	6968	.47625	3319
41	38392	.96354	36992
42	38392	.50504	19360
43	38392	.757125	29039
44	513	2.546	1306
45	1283	2.546	3267
46	1971	2.68	7253
47	473	3.68	1741
48	351	3.68	1292
49	675	3.68	2484
50	46644	6.037	281,602

Estimated Capacitance

<u>Zone</u>	<u>Room</u>	<u>Capacitance (Btu/°F)</u>
4	Storage	10,000
5	Mech. Rm	20,000

<u>Zone</u>	<u>Room</u>	<u>Capacitance (Btu/°F)</u>
6	Storage	35,000
7	Office	15,000

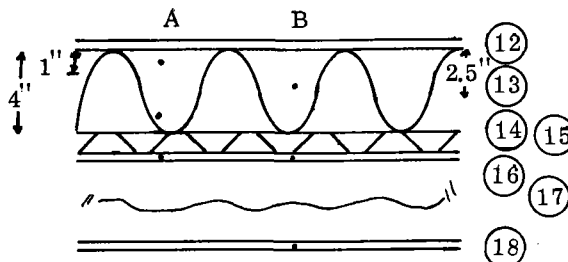
Table A-8. Conductance

Node No.	Area Ft ²	Resistance (1/Conductance) $\frac{\text{BTU}}{\text{Hr-}^\circ\text{F-ft}^2}$	A/R Btu/°F-Hr
1-8	1235	.184	6712
8-9	1235	1.379	896
9-10	1235	14.842	83
10-4	1235	.759	1627
1-11	247	.22	1123
11-12	247	1.645	150
12-13	247	17.71	14
13-5	247	.905	273
1-14	475	.22	2159
14-15	475	1.645	289
15-16	475	17.71	27
16-5	475	.905	525
1-17	570	.22	2591
17-18	570	1.645	347
18-19	570	17.71	32
19-6	570	.905	630
1-20	1330	.22	6045
20-21	1330	1.645	809
21-22	1330	17.71	75
22-6	1330	.905	1470
1-23	1957	.22	8895
23-24	1957	1.645	1190
24-25	1957	17.71	110
25-6	1957	.905	2162
1-26	637	.22	2895
26-27	637	1.645	387
27-28	637	17.71	36
28-6	637	.905	704
1-29	532	.22	2418
29-30	532	1.645	323
30-31	532	17.71	30

Node No.	Area Ft ²	Resistance (1/Conductance) $\frac{\text{BTU}}{\text{Hr-}^\circ\text{F-ft}^2}$	A/R Btu/°F-Hr
31-7	532	.905	588
1-32	1109	.226	4907
32-33	1109	1.538	721
33-34	1109	16.33	68
34-7	1109	.857	1294
1-35	437	.22	1986
35-36	437	1.645	266
36-37	437	17.71	25
37-7	437	.905	483
1-38	6968	14.58	478
38-39	6968	15.445	451
39-40	6968	2.18	3196
40-7	6968	1.55	4495
1-41	38392	6.03	6367
41-42	38392	17.1	2245
42-43	38392	6.66	5765
43-6	38392	1.08	35548
1-44	513	8.96	57
44-7	513	9.64	53
1-45	1283	8.96	143
45-7	1283	9.64	133
1-46	1971	1.515	1301
46-4	1971	2.195	898
1-47	473	1.515	312
47-4	473	2.195	215
1-48	351	1.515	232
48-4	351	2.195	160
1-49	675	1.515	446
49-4	675	2.195	308
1-50	46644	5	9329
50-2	46644	5	9329

Table A-9. Roof Capacitance

⑫	Built Up Roofing	3/8"
⑬	FURI Insulation	5"
⑭	Steel Decking	1/8"
⑮	Air	2"
⑯	Metal Lath and Plaster	3/4"
⑰	Air	5'
⑱	Acoustic Tile	3/4"



Area A (Zones 4-6) 38392 ft²
 Area B (Zone 7) 6968 ft²

(A)
 Node 1 $A \left[(\text{Th } ⑫) \left(\frac{1}{12} \right) (\rho ⑫) (\text{Cp } ⑫) + \frac{1}{2} (\text{Th } ⑬) \left(\frac{1}{12} \right) (\rho ⑬) (\text{C } ⑬) \right]$
 $A \left[\left(\frac{3}{8} \right) \left(\frac{1}{12} \right) (70) (.35) + \left(\frac{1}{2} \right) (5) \left(\frac{1}{12} \right) (2.5) (.38) \right] = A [.765625 + .1979] = \boxed{.96354(A)}$

Node 2 $A \left[\left(\frac{1}{2} \right) (\text{Th } ⑬) \left(\frac{1}{12} \right) (\rho ⑬) (\text{Cp } ⑬) + \frac{1}{2} (\text{Th } ⑭) \left(\frac{1}{12} \right) (\rho ⑭) (\text{Cp } ⑭) + \left(\frac{1}{2} \right) (\text{Th } ⑮) (\rho ⑮) (\text{Cp } ⑮) \right]$
 $A \left[\left(\frac{1}{24} \right) (5) (2.5) (.38) + \left(\frac{1}{24} \right) \left(\frac{1}{8} \right) (489) (.12) + \left(\frac{1}{24} \right) (2) (.075) (.24) \right]$
 $= A [.1979 + .305625 + .0015] = \boxed{.5054(A)}$

Node 3 $A \left[\frac{1}{2} (\text{Th } ⑭) \left(\frac{1}{12} \right) (\rho ⑭) (\text{Cp } ⑭) + \frac{1}{2} \left(\frac{1}{12} \right) (\text{Th } ⑮) (\rho ⑮) (\text{Cp } ⑮) \right]$
 $+ (\text{Th } ⑯) \left(\frac{1}{12} \right) (\rho ⑯) (\text{Cp } ⑯) \right] A \left[\left(\frac{1}{24} \right) \left(\frac{1}{8} \right) (489) (.12) + \frac{1}{24} (2) (.075) (.24) + \left(\frac{3}{4} \right) \left(\frac{1}{12} \right) (45) (.16) \right]$
 $= A [.305625 + .0015 + .45] = \boxed{.757125(A)}$

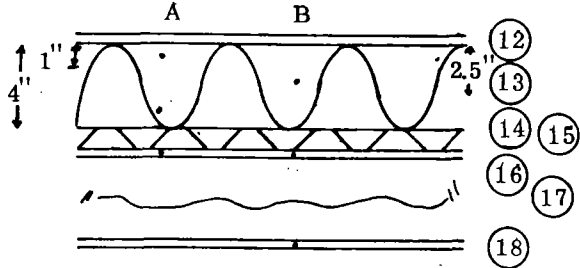
(B)
 Node 1 $A \left[(\text{Th } ⑫) \left(\frac{1}{12} \right) (\rho ⑫) (\text{Cp } ⑫) + (\text{Th } ⑬) \left(\frac{1}{12} \right) (\rho ⑬) (\text{Cp } ⑬) \right]$
 $= A \left[\left(\frac{3}{8} \right) \left(\frac{1}{12} \right) (70) (.35) + 5 \left(\frac{1}{12} \right) (2.5) (.38) \right] = A [.765625 + .39583] = \boxed{1.16146(A)}$

Node 2 $A \left[(\text{Th } ⑭) \left(\frac{1}{12} \right) (\rho ⑭) (\text{Cp } ⑭) + (\text{Th } ⑮) \left(\frac{1}{12} \right) (\rho ⑮) (\text{Cp } ⑮) + (\text{Th } ⑯) \left(\frac{1}{12} \right) (\rho ⑯) (\text{Cp } ⑯) \right]$
 $+ \frac{1}{2} (\text{Th } ⑰) (\rho ⑰) (\text{Cp } ⑰) \right] A \left[\left(\frac{1}{8} \right) \left(\frac{1}{12} \right) (489) (.12) + 2 \left(\frac{1}{12} \right) (.075) (.24) + \left(\frac{3}{4} \right) \left(\frac{1}{12} \right) (45) (.16) \right]$
 $+ \frac{1}{2} (5') (.075) (.24) \right] = A [.61125 + .003 + .45 + .045] = \boxed{1.10925(A)}$

Node 3 $A \left[\left(\frac{1}{2} \right) (\text{Th } ⑰) (\rho ⑰) (\text{Cp } ⑰) + \text{Th } ⑱ \left(\frac{1}{12} \right) (\rho ⑱) (\text{Cp } ⑱) \right] = A \left[\left(\frac{1}{2} \right) (5') (.075) (.24) \right]$
 $+ \left(\frac{3}{4} \right) \left(\frac{1}{12} \right) (23) (.3) \right] = A [.045 + .43125] = \boxed{.47625(A)}$

Table A-10. Roof Conductance

⑫	Built Up Roofing	3/8"
⑬	FURI Insulation	5"
⑭	Steel Decking	1/8"
⑮	Air	2"
⑯	Metal Lath and Plaster	3/4"
⑰	Air	5'
⑱	Acoustic Tile	3/4"



Area A (Zones 4-6) 38392 ft²
 Area B (Zone 7) 6968 ft²

Ⓐ

Node 1 $R_{⑫} + \frac{1}{5}(R_{⑬}) = .33 + \frac{1}{5}(28.5) = 6.03$ $\frac{A}{6.03}$

Node 2 $(\frac{3}{5})(R_{⑬}) = (\frac{3}{5})(28.5) = 17.1$ $\frac{A}{17.1}$

Node 3 $[\frac{1}{5}(R_{⑬}) + R_{⑭} + R_{⑮}] = [\frac{1}{5}(28.5) + 0.0 + .96] = 6.66$ $\frac{A}{6.66}$

Node 4 $[R_{⑯} + f_i \left(\begin{array}{c} \text{Film coefficient} \\ \text{Heat flow up} \\ \text{Horizontal surface} \end{array} \right)] = [.47 + .61] = 1.08$ $\frac{A}{1.08}$

Ⓑ

Node 1 $[R_{⑫} + \frac{1}{2}R_{⑬}] = [.33 + \frac{1}{2}(28.5)] = 14.58$ $\frac{A}{14.58}$

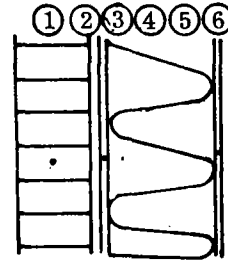
Node 2 $[\frac{1}{2}(R_{⑬}) + R_{⑭} + R_{⑮} + \frac{1}{2}(R_{⑯})] = [\frac{1}{2}(28.5) + 0.0 + .96 + \frac{1}{2}(.47)]$
 $= 15.445$ $\frac{A}{15.445}$

Node 3 $[\frac{1}{2}(R_{⑯}) + R_{⑰} + \frac{1}{2}(R_{⑱})] = [\frac{1}{2}(.47) + (1.0) + \frac{1}{2}(1.89)] = 2.18$ $\frac{A}{2.18}$

Node 4 $[\frac{1}{2}(R_{⑱}) + f_i] = [\frac{1}{2}(1.89) + .61] = 1.555$ $\frac{A}{1.555}$

Table A-11. Walls Capacitance

①	Face Brick	4"	
②	Air Space	3/4"	
③	Plywood	3/4"	
④	Insulation	6"	
⑤	Steel Studs	6"	$A = 1.3 \text{ in}^2$
⑥	Gypsum Board	1/2"	



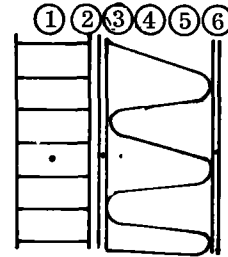
$$\begin{aligned} \text{Node 1} \quad A \left[(\text{Th } ①) \left(\frac{1}{12} \right) (\rho ①) (\text{Cp } ①) + \frac{1}{2} (\text{Th } ②) \left(\frac{1}{12} \right) (\rho ②) (\text{Cp } ②) \right] &= A \left[4'' \left(\frac{1}{12} \right) (130) (.22) \right. \\ &+ \left. \frac{1}{2} \left(\frac{3}{4} \right) \left(\frac{1}{12} \right) (.075) (.24) \right] = A [9.53 + .0005625] = \boxed{9.5339 (A)} \end{aligned}$$

$$\begin{aligned} \text{Node 2} \quad A \left[\frac{1}{2} (\text{Th } ②) \left(\frac{1}{12} \right) (\rho ②) (\text{Cp } ②) + (\text{Th } ③) \left(\frac{1}{12} \right) (\rho ③) (\text{Cp } ③) + \frac{1}{2} (\text{Th } ④) (\rho ④) (\text{Cp } ④) \left(\frac{1}{12} \right) \right. \\ &- \left. \frac{1}{2} (A ⑤) \left(\frac{1}{144} \right) \frac{1}{\frac{16'' \text{ o.c.}}{12''/\text{ft}}} (\rho ④) (\text{Cp } ④) + \frac{1}{2} (A ⑤) \left(\frac{1}{144} \right) \left(\frac{12''/\text{ft}}{16'' \text{ o.c.}} \right) (\rho ⑤) (\text{Cp } ⑤) \right] \\ &= A \left[\frac{1}{2} \left(\frac{3}{4} \right) \left(\frac{1}{12} \right) (.075) (.24) + \left(\frac{3}{4} \right) \left(\frac{1}{12} \right) (34) (.29) + \frac{1}{24} (6) (12) (.18) - \frac{1}{2} \left(\frac{1}{144} \right) \left(\frac{1.3}{1} \right) \left(\frac{12}{16} \right) (12) (.18) \right. \\ &+ \left. \left(\frac{1.3}{288} \right) \left(\frac{12}{16} \right) (489) (.12) \right] A [.0005625 + .61625 + .54 - .0073125 + .1985625] = \boxed{1.3482 (A)} \end{aligned}$$

$$\begin{aligned} \text{Node 3} \quad A \frac{1}{2} (\text{Th } ④) \left(\frac{1}{12} \right) (\rho ④) (\text{Cp } ④) - \frac{1}{2} (A ⑤) \left(\frac{1}{144} \right) \left(\frac{12}{16} \right) (\rho ④) (\text{Cp } ④) \\ &+ \frac{1}{2} (A ⑤) \left(\frac{1}{144} \right) \left(\frac{12}{16} \right) (\rho ⑤) (\text{Cp } ⑤) + (\text{Th } ⑥) \left(\frac{1}{12} \right) (\rho ⑥) (\text{Cp } ⑥) \right] = A \left[\frac{1}{2} \left(\frac{1}{12} \right) (6) (12) (.18) \right. \\ &- \left. \left(\frac{1.3}{2.88} \right) \left(\frac{12}{16} \right) (12) (.18) + \left(\frac{1.3}{288} \right) \left(\frac{12}{16} \right) (489) (.12) + \left(\frac{1}{2} \right) \left(\frac{1}{12} \right) (50) (.26) \right] \\ &= A [.54 - .0073125 + .1985625 + .5416] = \boxed{1.273 (A)} \end{aligned}$$

Table A-12. Walls

	Conductance	
①	Face Brick	4"
②	Air Space	3/4"
③	Plywood	3/4"
④	Insulation	6"
⑤	Steel Studs	6"
⑥	Gypsum Board	1/2"



Node 1 $1/2 (R_1) = 1/2 (.44) = .22$ $\frac{A}{.22}$

Node 2 $[1/2 (R_1) + R_2 + 1/2 (R_3)] = [1/2 (.44) + .96 + 1/2 (.93)]$
 $= [.22 + .96 + .465] = 1.645$ $\frac{A}{1.645}$

Node 3 $[1/2 (R_3) + R_4 + R_5 + 1/2 (R_6)] = [1/2 (.93) + 17 .016 + 1/2 (.45)]$
 $= [.465 + 17 + .016 + .225] = 17.706$ $\frac{A}{17.71}$

Node 4 $\left[1/2 (R_6) + f_1 \left(\begin{array}{l} \text{film coefficient} \\ \text{horizontal heat flow} \\ \text{vertical wall} \end{array} \right) \right] = [1/2 (.45) + .68] = .905$ $\frac{A}{.905}$

Table A-13. Glass Doors

(West Wall)

Assume $C_p = .16$

Given $U = 1.13$

$\rho = 153 \text{ \#/ft}^3$

$A = 88 \text{ ft}^2$

$Th = .25''$

Conductance $U = \frac{1}{R_T} = 1.13$ $R_T = .885$ $R_1 + R_2 + R_3 = R_T$ $R_1 = R_2 = R_3 = \frac{R_T}{3} = .295$

Area Total $1169 \text{ ft}^2 - 60 \text{ ft}^2 \text{ (windows)} - 88 \text{ ft}^2 \text{ (doors)} = 1021 \text{ ft}^2$

$\frac{88}{1109} (.295) + \frac{1021}{1109} (.22) = \boxed{.226}$

$\frac{88}{1109} (.295) + \frac{1021}{1109} (1.645) = \boxed{1.538}$

$\frac{88}{1109} (.295) + \frac{1021}{1109} (17.71) = \boxed{16.33}$

$\frac{88}{1109} (.295) + \frac{1021}{1109} (.905) = \boxed{.857}$

Capacitance $A[(1/4)(1/12)(153)(.16)] = .51(A)$ $\frac{.51(A)}{3}$

$9.5339 (1021) + \frac{.51}{3} (88) = \boxed{9749}$

$1.3482 (1021) + \frac{.51}{3} (88) = \boxed{1391}$

$1.273 (1021) + \frac{.51}{3} (88) = \boxed{1315}$

Loading Doors

(North Wall - Storage)

Assume $C_p = .11 \frac{\text{Btu}}{\text{lbm } ^\circ\text{R}}$

$A = 200 \text{ ft}^2$

$k = 31 \frac{\text{Btu}}{\text{hr - ft - } ^\circ\text{F}}$

$Th = 3/8''$

$\rho = 489 \text{ \#/ft}^3$

$A_{\text{Total}} = 1235 - 200 = \underline{1035 \text{ ft}^2}$

Conductance $R = \frac{(3/8)(1/12)}{31} = .001$ $R_1 + R_2 + R_3 = R_T = .001$ $R_1 = R_2 = R_3 = \frac{.001}{3} = .00033$

$\frac{200}{1235} (.0003) + \frac{1035}{1235} (.22) = \boxed{.1844}$

$\frac{200}{1235} (.003) + \frac{1035}{1235} (1.645) = \boxed{1.379}$

$\frac{200}{1235} (.0003) + \frac{1035}{1235} (17.71) = \boxed{14.842}$

$\frac{200}{1235} (.003) + \frac{1035}{1235} (.905) = \boxed{.759}$

Capacitance $A[(3/8)(1/12)(489)(.11)] = 1.68(A)$ $\frac{1.68(A)}{3}$

$9.5339 (1035) + \frac{1.68}{3} (200) = \boxed{9980}$

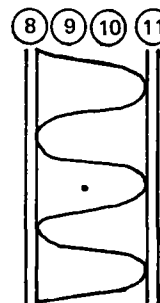
$1.3482 (1035) + \frac{1.68}{3} (200) = \boxed{1507}$

$1.273 (1035) + \frac{1.68}{3} (200) = \boxed{1430}$

Table A-14. Partition

Inside Office Walls

⑧ Gypsum Board	1/2"	
⑨ Fiberglass Battery Insulation	6"	
⑩ Steel Studs	6"	$A = 1.3 \text{ in}^2$
⑪ Gypsum Board	1/2"	



Capacitance

$$\begin{aligned}
 \text{Node 1} \quad & A \left[(\text{Th}_{\textcircled{8}}) \left(\frac{1}{12} \right) (\rho_{\textcircled{8}}) (\text{Cp}_{\textcircled{8}}) + (\text{Th}_{\textcircled{9}}) \left(\frac{1}{12} \right) (\rho_{\textcircled{9}}) (\text{Cp}_{\textcircled{9}}) - (A_{\textcircled{10}}) \left(\frac{1}{144} \right) \left(\frac{12}{16} \right) (\rho_{\textcircled{9}}) (\text{Cp}_{\textcircled{9}}) \right. \\
 & + A_{\textcircled{10}} \left(\frac{1}{44} \right) \left(\frac{12}{16} \right) (\rho_{\textcircled{10}}) (\text{Cp}_{\textcircled{10}}) + \text{Th}_{\textcircled{11}} \left(\frac{1}{12} \right) (\rho_{\textcircled{11}}) (\text{Cp}_{\textcircled{11}}) \left. \right] = A \left[2 \left(\frac{1}{2} \right) \left(\frac{1}{12} \right) (50) (.26) \right. \\
 & + 6 \left(\frac{1}{12} \right) (12) (.18) - 1.3 \left(\frac{1}{144} \right) \left(\frac{12}{16} \right) (12) (.18) + (1.3) \left(\frac{1}{144} \right) \left(\frac{12}{16} \right) (489) (.12) \left. \right] \\
 & = A \quad 2(.5416) + 1.08 - .014625 + .3973125 = \boxed{2.546(A)}
 \end{aligned}$$

Conductance

$$\text{Node 1} \quad R_{\textcircled{8}} + \frac{1}{2} R_{\textcircled{9}} + \frac{1}{2} (R_{\textcircled{10}}) = .45 + \frac{1}{2} (17) + \frac{1}{2} (.016) = \boxed{\frac{A}{8.96}}$$

$$\text{Node 2} \quad \frac{1}{2} (R_{\textcircled{9}}) + \frac{1}{2} (R_{\textcircled{10}}) + R_{\textcircled{11}} + f_1 = \frac{1}{2} (.016) + \frac{1}{2} (17) + .45 + .68 = 9.64 \quad \boxed{\frac{A}{9.64}}$$

Table A-15. Partition

Inside Walls Other Than Office Walls

Concrete blocks $U = .31$ - given
 Lightweight aggregate blocks with filled core $R \cong 3.03$ $U \approx .31$

3 core 6" 19#
 $(6'' \times 7\text{-}5/8'' \times 15\text{-}5/8'') \times \frac{1 \text{ ft}^3}{1728 \text{ in}^3} = .41368 \text{ ft}^3$

$\therefore f = \frac{19\#}{.41368 \text{ ft}^3} \cong 46 \#/\text{ft}^3$ $C_p = .16$

Capacitance $A (6'') (1/12) (46) (.16) = 3.68(A)$

Conductance $R_T \cong 3.03$

$1/2 (R_{\text{7}}) = 1/2 (3.03) = 1.515$ $\frac{A}{1.515}$

$1/2 (R_{\text{7}}) + .68 = 1/2 (3.03) + .68 = 2.195$ $\frac{A}{2.195}$

Floor

Conductance $U = .10$ (This value is given in reference 4 page 174 as representative of a slab floor)

$\therefore R_T = 10$ $R_1 + R_2 = R_T$ $R_1 = R_2 = \boxed{5}$

Capacitance

$\text{Th } (C_p) (\rho) (A) + (\text{Th}) (C_p) (\rho) (A) = 6'' (1/12) (.16) (65) (43028) + 1' (.16) (100) (3616)$

cement slab floor CMU walls

$= 223745.6 + 57856 = \boxed{281,602}$

Table A-16. Materials Properties

No.	Material	Resistance $R = \frac{1}{C} = \frac{X}{K}$ But/hr-ft ² -°F	Density ρ lbm/ft ³	Specific Heat C_p Btu/lbm-°R	Thickness Inches
1	Face Brick	.44	130.	.22	4"
2	Air	.96	.075	.24	3/4"
3	Plywood	.93	34.	.29	3/4
4	Fiberglass Batt Insulation	17.	12.	.18	6"
5	Framing (steel)	.016	489.	.12	6"
6	Gypsum Board	.45	50.	.26	1/2"
7	Concrete Blocks	3.0	45.	.16	6"
8	Gypsum Board	.45	50.	.26	1/2"
9	Fiberglass Batt Insulation	17.	12.	.18	6"
10	Steel Studs	.016	489.	.12	6"
11	Gypsum Board	.45	50.	.26	1/2"
12	Built Up Roofing	.33	70.	.35	3/8"
13	FURI Insulation	28.5	2.5	.38	5"
14	Steel Decking	0.000	489.	.12	1/8"
15	Air	.96	.075	.24	2"
16	Metal Lath and 3/4" Plaster (lt. wt. agg.)	.47	45.	.16	3/4"
17	Air		.075	.24	5'
18	Acoustical Tile	1.89	23.	.30	3/4"

Table A-17. Sensible Heat

Equipment Producing Sensible Heat	Area (Zone)	Percent of Total	Profile*	KW	Btu/hr
① Process Machinery	Production	100%	B	81.1	276,794
② Lighting	Office	Same as 25,000 ft ²	D	11.3	38,567
	Storage	(factored up according to increased area)	D	6.33(.9)	19,448
	Equipment		D	6.33(.1)	2,161
	Production		D	69.	235,520
③ Air Handling Equipment					
Fan Coil Units	Storage	100%	C	4.8	16,382
Indoor Fans	Production	80%	C	44.8(.8)	122,322
	Office	20%	C	44.8(.2)	30,580
Miscellaneous Fans	Equipment	75%	C	1.5	5,120
	Office	25%	C	.5	1,707
④ Process Equipment	Equipment	100%	B	32.3	110,240
⑤ Heating/Cooling System Pumps	Equipment	100%	C	1.6	5,461
⑥ Water Heater	Office	10%	C		1,090
⑦ Pipe Gains	Production		C		59,124
⑧ Presses, Sensible	Production		B		151,892

*Profile See Table A-6

Latent

Process steam (Latent from Presses)

1380 #/hr

Assume 10% of the total amount of steam goes into the Production Room (Zone 6).

Latent Loading 138#/hr — 6 a.m. — 3 p.m. and 3 p.m. — Midnight.

All other times and zones are 0 lbm/hr.

Table A-18. Node Assignments, Areas, and Shading Factors

Discrete Outside Surfaces	Outside Wall Node	Middle Wall Node	Inside Wall Node	Zone Node No.	Surface Azimuth Angle (degrees)	Surface Tilt Angle (degrees)	Wall Area (ft ²)	Window Area (ft ²)	Solar Absorp-tance (Outside Surface)	Wall Shading Factors			Window Shading Factors		
										Jan-Apr	May-Aug	Sept-Dec	Jan-Apr	May-Aug	Sept-Dec
1	8	9	10	4	180	90	1235		.68	0	.2	0	0	.2	0
2	11	12	13	5	180	90	247		.68	0	.2	0	0	.2	0
3	14	15	16	5	-90	90	475		.68	0	.2	0	0	.2	0
4	17	18	19	6	180	90	570		.68	0	.2	0	0	.2	0
5	20	21	22	6	-90	90	1330		.68	0	.2	0	0	.2	0
6	23	24	25	6	0	90	1957		.68	0	.2	0	0	.2	0
7	26	27	28	6	90	90	637		.68	0	.2	0	0	.2	0
8	29	30	31	7	0	90	532		.68	0	.2	0	0	.2	0
9	32	33	34	7	90	90	1109	60	.68	0	.2	0	0	.2	0
10	35	36	37	7	180	90	437		.68	0	.2	0	0	.2	0
11	38	39	40	7	0	0	6968		.75	0	.2	0	0	.2	0
12	41	42	43	6	0	0	38392		.75	0	.2	0	0	.2	0

References

- A-1. G. E. Document 76SDS4218 - Computerized Procedures For Technical and Economic Evaluation of Solar Energy Systems, General Electric, April 1976.
- A-2. GSTEP, Heery and Heery, Load Requirement and Analysis, L-2, January 10, 1978.
- A-3. ASHRAE, Handbook of Fundamentals Heating, Refrigerating, Ventilating, and Air Conditioning, George Banta Co., Inc., Menasha, Wisconsin, 1974.
- A-4. Jennings, Burgess H., Environmental Engineering Analysis and Practice, International Textbook Company, New York, 1970.
- A-5. Holman, J. P., Heat Transfer, Third Edition, McGraw-Hill Book Company, St. Louis, 1972.

APPENDIX B
ELECTRICAL TRANSIENT ANALYSIS

APPENDIX B

ELECTRICAL TRANSIENT ANALYSIS (Phase III)

B.1 INTRODUCTION AND SUMMARY

The January 1978 Design Review of the Solar Total Energy - Large Scale Experiment (STE - LSE) at Shenandoah identified a concern that transient analysis of the Power Conversion System (PCS) and electrical output were not addressed until Phase IV of the program. This appendix describes the results of a preliminary analysis of the PCS and electrical output dynamics. Appendix Section B.6 is a reproduction of the basic portion of a report describing the steam turbine and generator models used in the analysis. The work described in the following sections consists of an extension of this model to include a generator and excitation system transient model and exercise of the model in the frequency and time domains in order to evaluate more fully the transient response of the STES PCS.

B.1.1 SYSTEM REQUIREMENTS

The fundamental PCS requirements are that frequency (speed) be within ± 5.0 percent and that voltage be within ± 5.0 percent with seven percent allowed for a ten percent load step. All control loops are effective in determining the response. A step load of 25 kW is the reference transient loading on the system and is consistent with preliminary Georgia Power Company measurements at Bleyle. Both stand-alone and interconnected operating modes are analyzed.

B.1.2 RESULTS SUMMARY

The analysis has considered two representative turbine-generator inertia values. The first case analyzed corresponded to the GE marine turbine baseline design. The second case considered an inertia value of one-sixth the baseline to represent an intermediate turbine inertia. The results showed that for both cases the system is stable and response is well-behaved. Interconnected mode impedance exceeding about 0.4 pu produces instability but is well beyond the expected range at the site. Larger inertia reduces frequency deviation in the stand-alone mode, but the step amplitude in load is more important in controlling response. Interconnected load steps and process steam steps are responded to in an acceptable manner. Very low inertia turbines representative of the MTI design were not analyzed.

B.1.3 MEASURED TRANSIENTS

The Georgia Power Company measured transient data on current and voltage in the Bleyle plant in March, 1978. The voltage was essentially constant from a transient effect viewpoint. Current records were typically as shown in the plot below. Inrush measurements show three to four times full load current on air conditioning which will not be in operation with the STES. The air compressor inrush is six times running current which will be seen by STES, and the vacuum pump draws eight times running current as inrush but is started before normal STES operation. The measurements do not reflect full Bleyle operation but do indicate the expected variation for transient analysis purposes. The 25 kW step used as the transient design condition appears to be a good representation of the actual load for preliminary analysis.

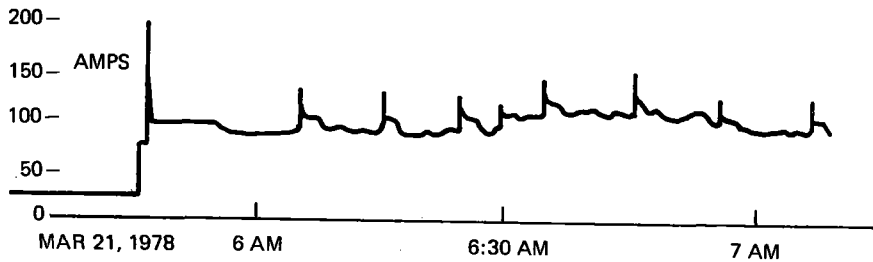
B.2 CONTROL SYSTEM DESCRIPTION

B.2.1 GENERAL

A representation of the system in block diagram format showing the formulation of the equations used in the computer model with parameter values is given in Figures B-1 through B-8.

<u>LOAD</u>	<u>PEAK</u>	<u>-AMPS-</u>	<u>LOAD</u>
BASE			20
AIR COMPRESSOR	66		11
LIGHTS	32		30
AIR CONDITIONER -FAN	32		8
-COMPRESSOR	46		36
VACUUM PUMP	152		18

NOTE: 1.0 AMP AT 480 VOLTS, 3 PHASE = 0.83 KVA



B.2.2 OPERATIONAL DESCRIPTION

B.2.2.1 Interconnected Operation

In this mode the STES electric generator is supplemented with power from the electric utility. A step increase in plant load is initially supplied by a step in the power supplied from the utility. The STES turbine-generator compensates for the unbalance by increasing its output until the power supplied from the utility falls back to its original position. Steam pressure, steam temperature, and turbine shaft speed are regulated through control subsystems by automatic adjustment of feedwater flow, Syltherm 800 flow, and steam control valve position.

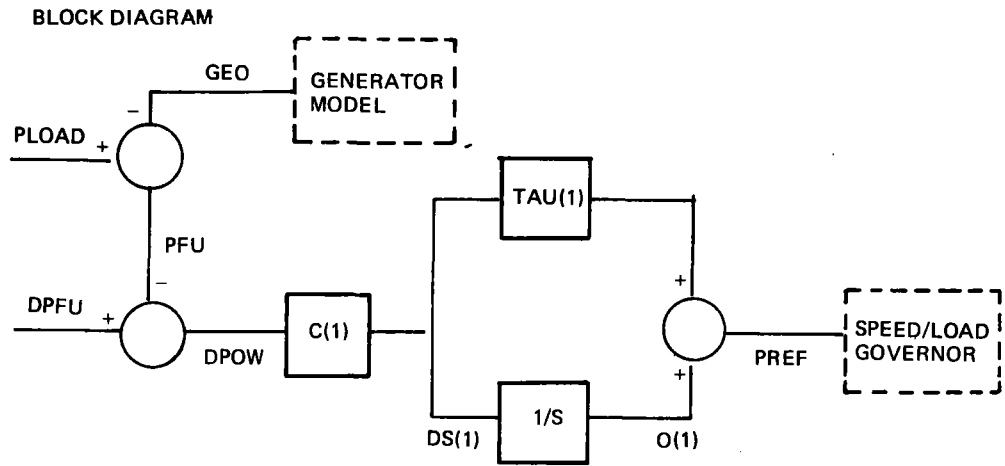
B.2.2.2 Independent Operation

In the independent or stand-alone mode, the electric generator supplies all of the electrical load for the plant. Thus, a step in the plant load causes a step in the generator electrical output. As in the interconnected mode, the feedwater flow, Syltherm 800 flow, and control valve position are adjusted by the control subsystems.

B.2.3 GENERATOR MODEL

The generator model is shown in Figure B-9. It is a typical two circuit (direct and quadrature) representation frequently used in machine and utility system studies. The regulator and exciter are shown in Figure B-10 and again are typical models described in literature and in general use for transient performance calculation for synchronous machines. Generator load modelling consisted of using typical utility system reactances and resistances to an infinite bus. Block diagrams for the generator, exciter, and voltage regulator showing equations used in the computer model and parameter values are given in Figures B-11 through B-24.

For the stand-alone mode of operation, bus voltage was set at 0.0, and the load impedance adjusted to absorb the entire output. Load changes were made by suddenly varying the values of the load impedance to reflect the increased power demand. Actual generator and excitation system data was not available for this analysis, and the time constants and other parameters utilized are approximate values for a typical GE 1200 rpm, 500 kVA 0.8 power factor, brushless, excited generator with a Basler SR-4 voltage regulator.



EQUATIONS

- PFU = PLOAD - GEO
- DPOW = DPFU - PFU
- PREF = O(1) + DS(1) * TAU(1)
- DS(1) = C(1) - DPOW

VARIABLES

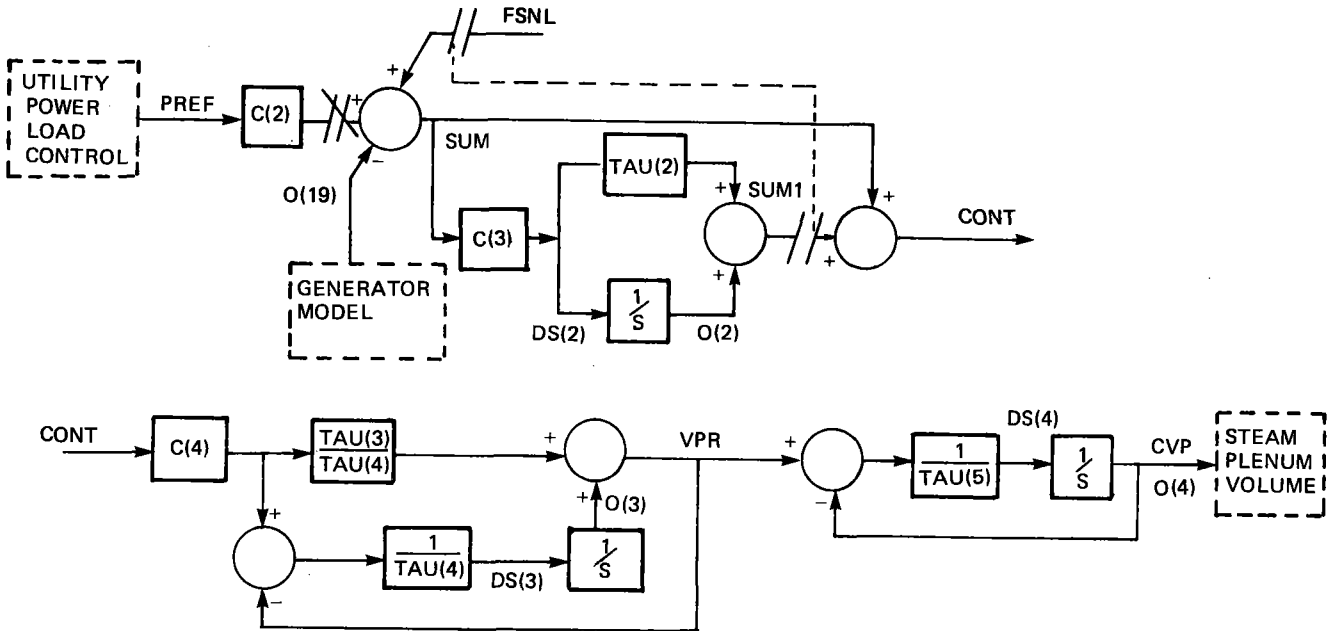
- GEO - GENERATOR ELECTRICAL OUTPUT (KW)
- PLOAD - PLANT LOAD (KW)
- PFU - POWER FROM UTILITY (KW)
- DPFU - DESIRED POWER FROM UTILITY (KW)
- DPOW - POWER CHANGE (KW)
- PREF - INTERMEDIATE VARIABLE (PU)
- C(1) - LOAD CONTROL GAIN - PU/S (KW)

PARAMETERS

PLOAD	378 KW
DPFU	100 KW
C(1)	-.001 PU/S-KW
O(1)	20 PU
TAU(1)	.5 SEC.

Figure B-1. Utility Power Load Control

BLOCK DIAGRAM



EQUATIONS

$$\begin{aligned} \text{SUM} &= \text{PREF} * \text{C}(2) + \text{FSNL} - \text{O}(19) & \text{VPR} &= \text{O}(3) + \text{CONT} * \text{TAU}(3)/\text{TAU}(4) * \text{C}(4) \\ \text{DS}(2) &= \text{SUM} * \text{C}(3) & \text{DS}(3) &= [\text{CONT} * \text{C}(4) - \text{VPR}]/\text{TAU}(4) \\ \text{SUM1} &= \text{O}(2) + \text{DS}(2) * \text{TAU}(2) & \text{DS}(4) &= [\text{VPR} - \text{O}(4)]/\text{TAU}(5) \\ \text{CONT} &= \text{SUM1} + \text{SUM} & \text{CVP} &= \text{O}(4) \end{aligned}$$

VARIABLES

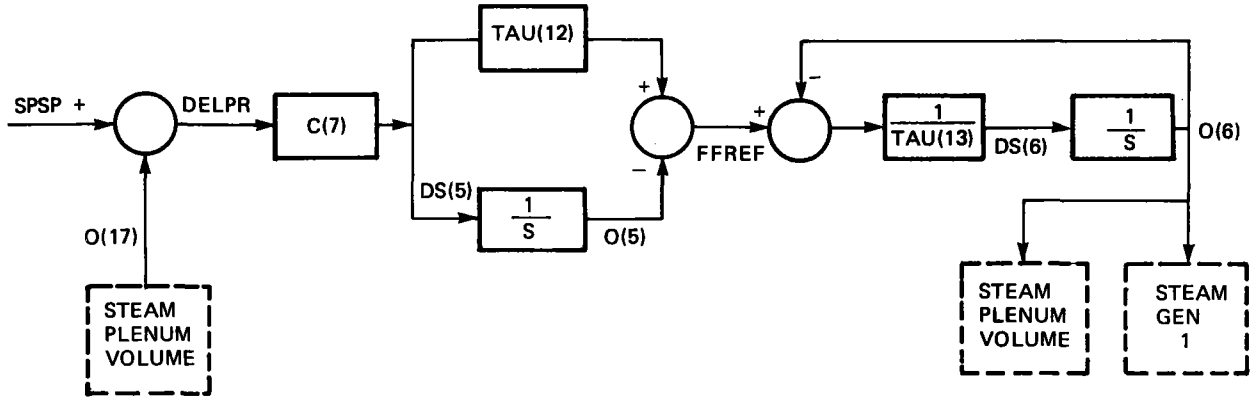
- C(2) - LOAD REFERENCE (INTERCONNECTED OPERATION ONLY) (PU/PU)
- FSNL - FULL SPEED NO LOAD REFERENCE (INDEPENDENT OPERATION ONLY) (PU)
- C(3) - RESET GAIN (INDEPENDENT OPERATION ONLY) (PU/S)
- O(19) - MEASURED SPEED (PU)
- C(4) - PROPORTIONAL LEAD-LAG CONTROLLER GAIN (PU/PU)
- VPR - VALVE POSITION REF (PU)
- CVP - CONTROL VALVE POSITION (PU)

PARAMETERS

PARAMETERS	NOMINAL	PARAMETERS	NOMINAL
C(2)	.05 PU/PU	TAU(2)	5.0 SEC
C(3)	.5 PU/S	TAU(3)	.2 SEC
C(4)	20.0 PU/PU	TAU(4)	.04 SEC
FSNL	1.0 PU	TAU(5)	.1 SEC
O(2)	.0898 PU		
O(3)	-3.592 PU		
O(4)	+898 PU		

Figure B-2. Speed/Load Governor Control

BLOCK DIAGRAM



EQUATIONS

$$\begin{aligned} \text{DELPR} &= \text{SPSP} - \text{O}(17) & \text{FFREF} &= \text{O}(5) + \text{TAU}(12) * \text{DS}(5) \\ \text{DS}(5) &= \text{C}(7) * \text{DELPR} & \text{DS}(6) &= (\text{FFREF} - \text{O}(6)) / \text{TAU}(13) \end{aligned}$$

VARIABLES

- SPSP - STEAM PRESSURE SET POINT (PSIA)
- O(17) - STEAM PRESSURE (FROM PROCESS) (PSIA)
- C(7) - CONTROLLER GAIN (LB/S - PSIA)
- FFREF - FEEDWATER FLOW REFERENCE (LB/S)
- O(6) - FEEDWATER FLOW (LB/S)

PARAMETERS

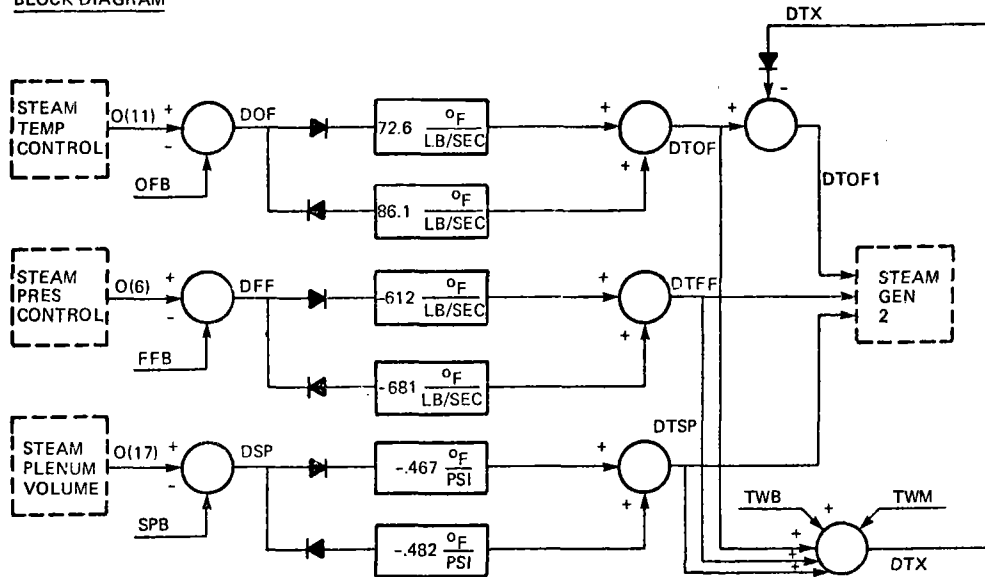
NOMINAL

PARAMETERS	NOMINAL
SPSP	700.0 PSIA
O(5)	2.243 LB/SEC
O(6)	2.243 LB/SEC
TAU(12)	1.0 SEC*
TAU(13)	.167 SEC

*TAU(12) = 2.5 SEC IN THE SPRADLIN REPORT.

Figure B-3. Steam Pressure Control

BLOCK DIAGRAM



EQUATIONS

$$\begin{aligned}
 \text{DOF} &= \text{O}(11) - \text{OFB} \\
 \text{DTOF} &= [72.6(+)\text{ OR }86.1(-)] * \text{DOF} \\
 \text{DFF} &= \text{O}(6) - \text{FFB} \\
 \text{DTFF} &= [-612(+)\text{ OR }-681(-)] * \text{DFF} \\
 \text{DSP} &= \text{O}(17) - \text{SPB} \\
 \text{DTSP} &= [-.467(+)\text{ OR }-.482(-)] * \text{DSP} \\
 \text{DTX} &= \text{TWB} + \text{DTP} + \text{DTFF} + \text{DTOF} - \text{TWM} \\
 \text{DTOF1} &= \text{DTOF} - \text{DTX} (\text{DTX} > 0.)
 \end{aligned}$$

VARIABLES

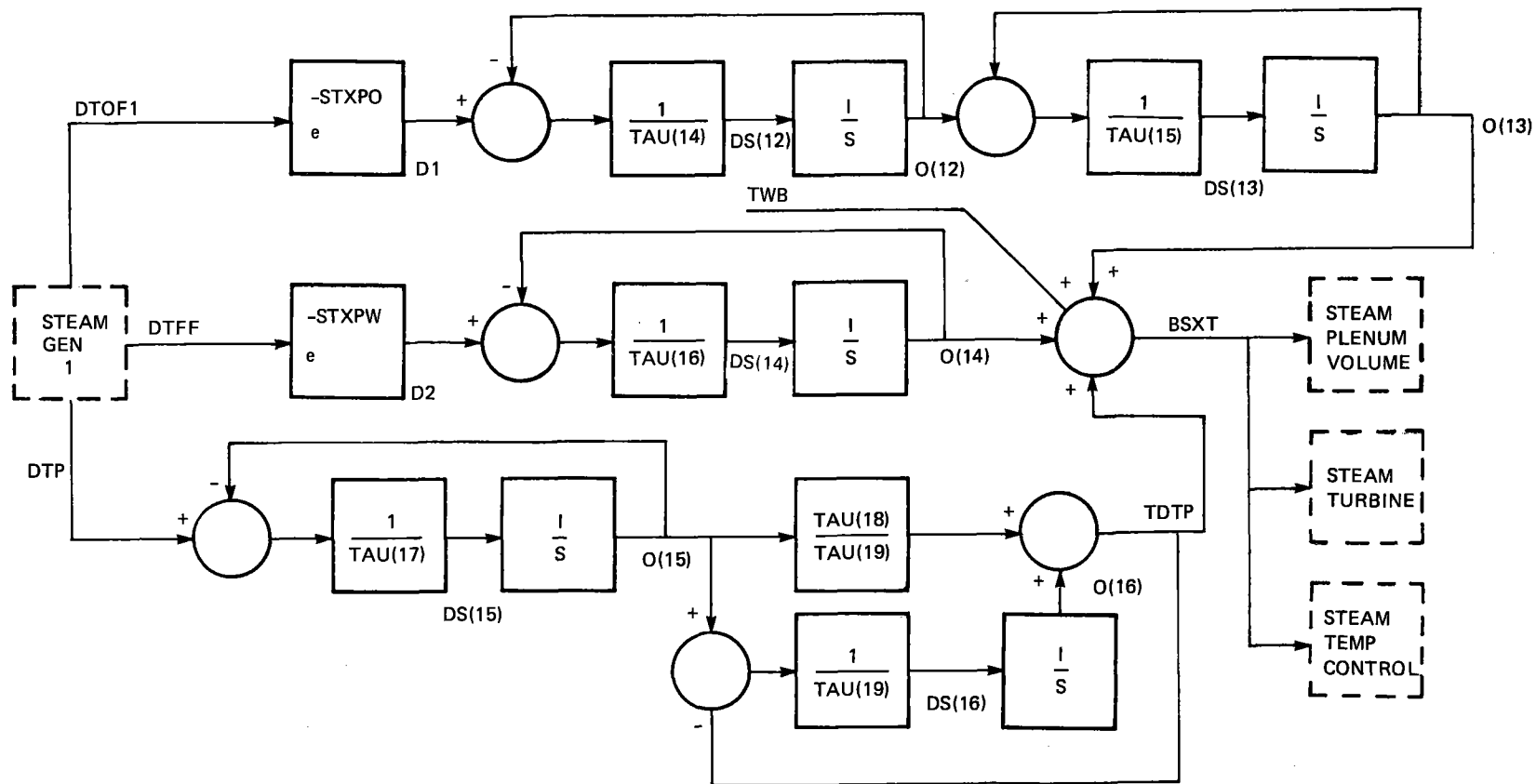
- O(11) -- OIL FLOW (LB/S)
- OFB -- BASE OIL FLOW (LB/S)
- O(6) -- FEED WATER FLOW (LB/S)
- FFB -- BASE FEEDWATER FLOW (LB/S)
- O(17) -- STEAM PRESSURE (PSIA)
- SPB -- BASE STEAM PRESSURE (PSIA)
- TWB -- BASE BOILER STEAM TEMP (°R)
- TWM -- MAX BOILER STEAM TEMP (°R)
- DTOF -- ΔT DUE TO ΔOIL FLOW (°R)
- DTFF -- ΔT DUE TO ΔFEEDWATER FLOW (°R)
- DTSP -- ΔT DUE TO ΔSTEAM PRESSURE (°R)

PARAMETERS

	<u>NOMINAL</u>		<u>NOMINAL</u>
O(11)	16.496 LB/S	O(17)	700.0 PSIA
OFB	16.496 LB/S	SPB	700.0 PSIA
O(6)	2.243 LB/S	TWB	1160.0 °R
FFB	2.243 LB/S	TWM	1189.0 °R

Figure B-5. Steam Generator 1

BLOCK DIAGRAM



B-8

EQUATIONS

- D1 = DTOF1 W/PURE DELAY
- D2 = DTFF W/PURE DELAY
- DS(12) = (D1 - O(12)) / TAU(14)
- DS(13) = (O(12) - O(13)) / TAU(15)
- DS(14) = (D2 - O(14)) / TAU(16)
- DS(15) = (DTP - O(15)) / TAU(17)
- DS(16) = (O(15) - TDTP) / TAU(19)
- TDTP = O(15) * TAU(18) / TAU(19) + O(16)
- BSXT = O(13) + TWB + O(14) + TDTP

VARIABLES

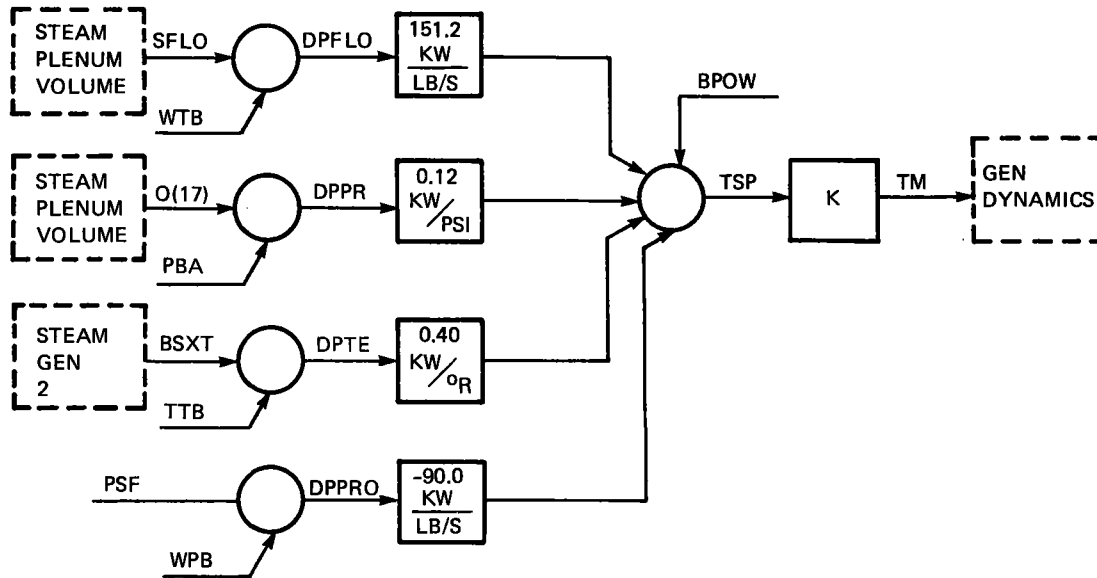
- DTOF1 - ΔT DUE TO Δ OIL FLOW
- DTFF - ΔT DUE TO Δ FEEDWATER FLOW
- DTP - ΔT DUE TO Δ STEAM PRESSURE
- D1 - DELAYED DTOF1
- D2 - DELAYED DTFF
- TWB - BASE BOILER STEAM TEMP.
- BSXT - BOILER STEAM EXIT TEMPERATURE

PARAMETERS

	NOMINAL		NOMINAL
O(12)	- 0.0 °R	TXPO	- 1.5 SEC
O(13)	- 0.0 °R	TXPW	- .2 SEC
O(14)	- 0.0 °R	TAU(14)	- 11.0 SEC
O(15)	- 0.0 °R	TAU(15)	- 1.2 SEC
O(16)	- 0.0 °R	TAU(16)	- 11.25 SEC
TWB	- 1160.0 °R	TAU(17)	- 5.0 SEC
		TAU(18)	- 33.0 SEC
		TAU(19)	- 25.0 SEC

Figure B-6. Steam Generator 2

BLOCK DIAGRAM



EQUATIONS

$$\text{DPFLO} = \text{SFLO} - \text{WTB}$$

$$\text{DPPR} = \text{O}(17) - \text{PBA}$$

$$\text{DPTE} = \text{BSXT} - \text{TTB}$$

$$\text{DPPRO} = \text{PSF} - \text{WPB}$$

$$\text{TSP} = \text{BPOW} + \text{DPFLO} * 151.2 + \text{DPPR} * .12 + \text{DPTE} * .40 + \text{DPPRO} * (-90.0)$$

$$\text{TM} = \text{K} * \text{TSP}$$

VARIABLES

- SFLO - STEAM FLOW (LB/S)
- WTB - BASE STEAM FLOW (LB/S)
- O(17) - STEAM PRESSURE (PSIA)
- PBA - BASE STEAM PRESSURE (PSIA)
- BSXT - STEAM EXIT TEMP (°R)
- TTB - BASE STEAM TEMP (°R)
- PSF - PROCESS STEAM FLOW (LB/S)
- WPB - BASE PROCESS STEAM FLOW (LB/S)
- TSP - TURBINE SHAFT POWER (KW)
- TM - MECHANICAL TORQUE (PU)
- TE - ELECTRICAL TORQUE (PU)

PARAMETERS

	NOMINAL
WTB	2.243 LB/S
PBA	700.0 PSIA
TTB	1160 °R
WPB	0.0 LB/S
BPOW	308.9 KW

$$\text{K} - \text{PER UNIT TORQUE REFERENCE FROM POWER} = \frac{1 \text{ PU}}{500}$$
 WITH SPEED ASSUMED CONSTANT.

Figure B-8. Steam Turbine

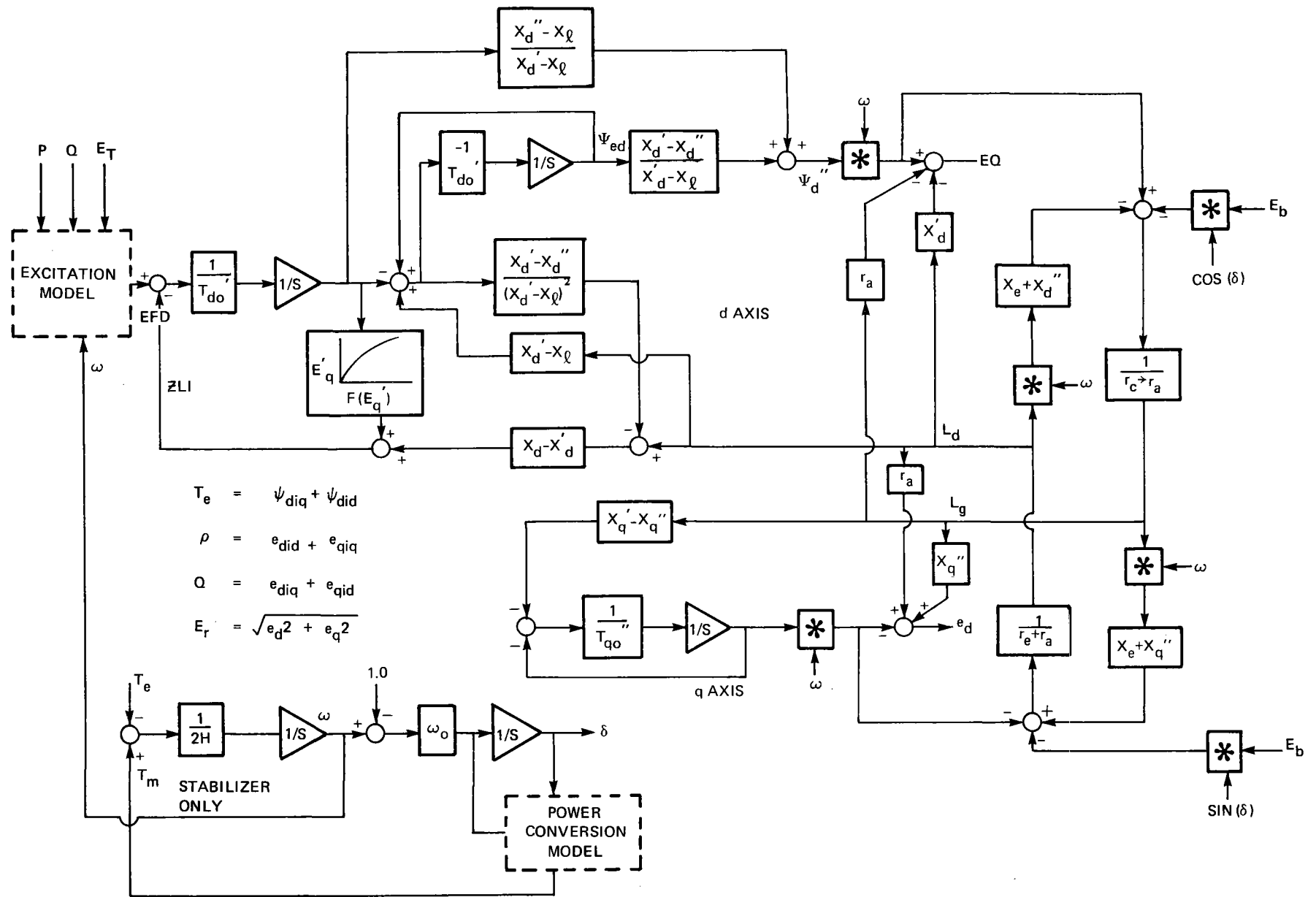


Figure B-9. Generator Model

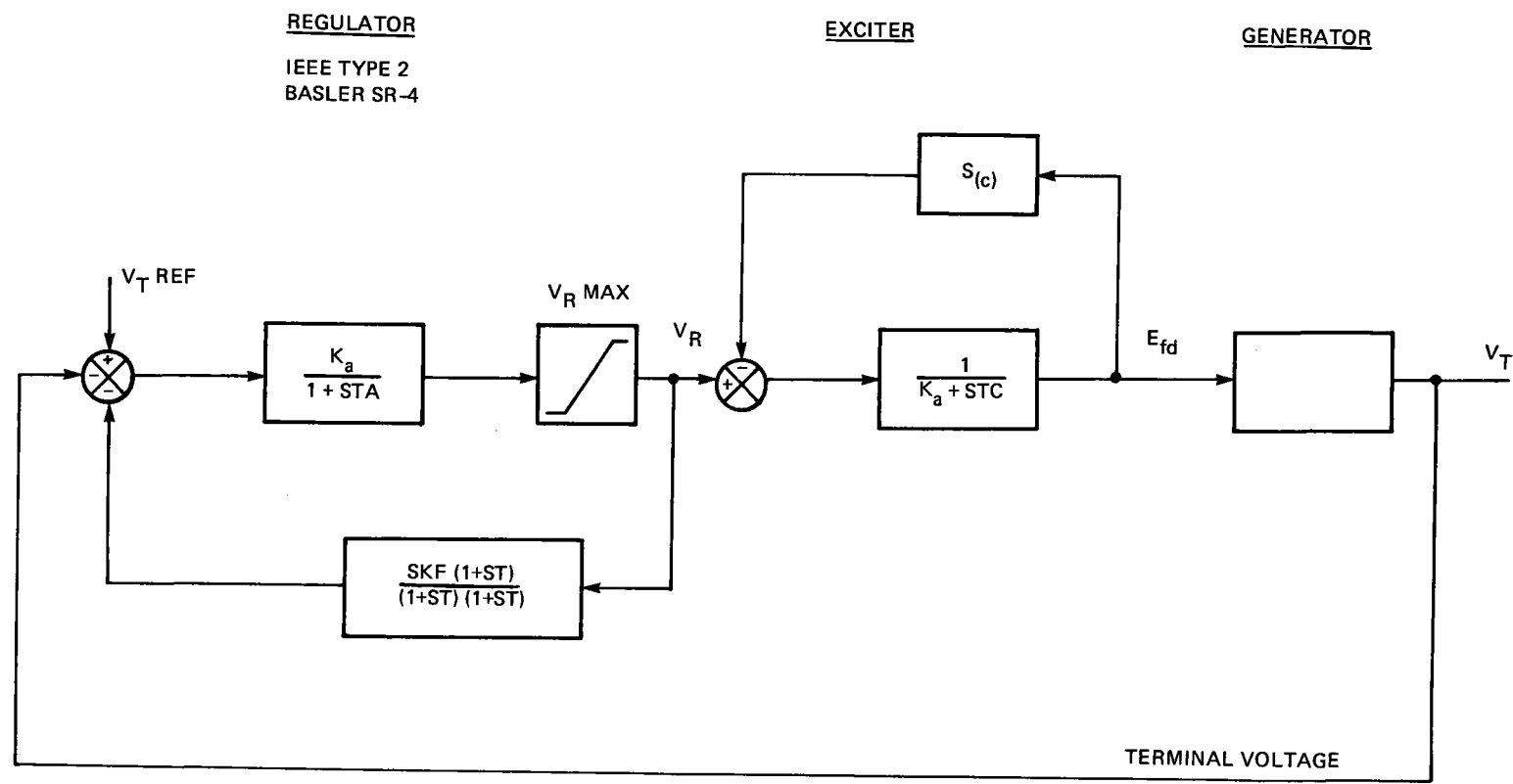
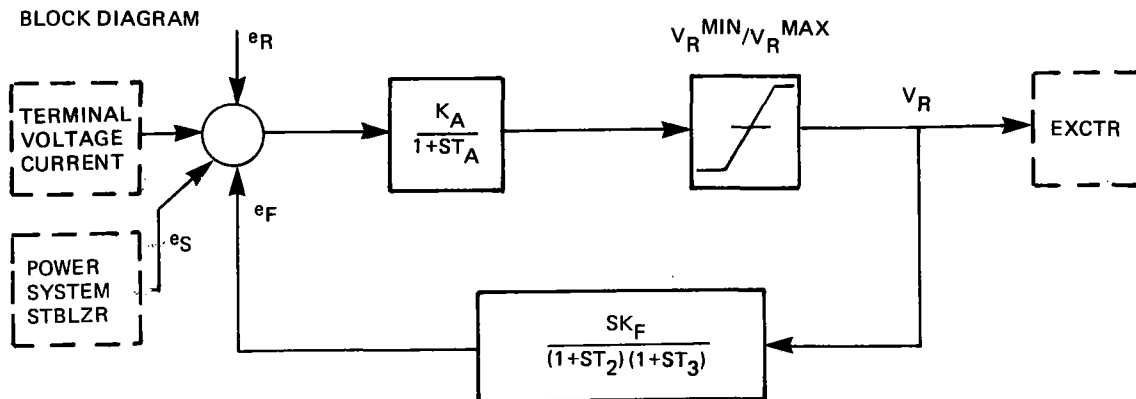


Figure B-10. Terminal Voltage Control



EQUATION

$$V_R = \frac{K_A}{1+ST_A} (e_R - e_T - e_F + e_S) V_R^{\text{MIN}} \leq V_R \leq V_R^{\text{MAX}}$$

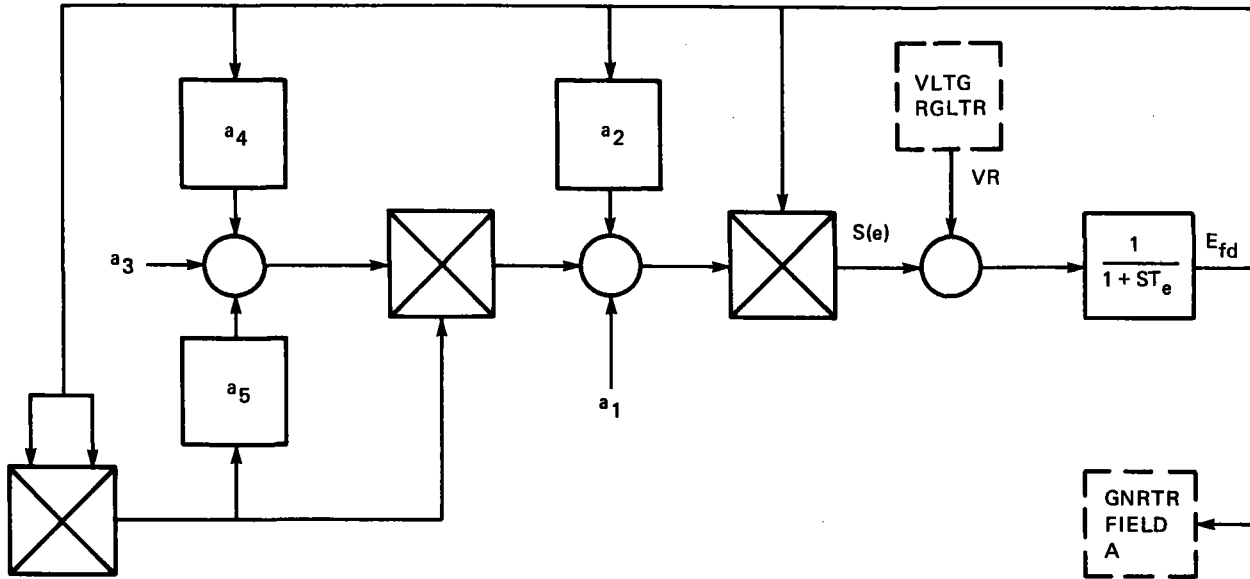
$$e_F = \frac{SK_F}{(1+ST_2)(1+ST_3)} V_R$$

NOMENCLATURE

VARIABLES		MAXIMUM
e_R	REFERENCE VOLTAGE	1.0 PU
e_T	TERMINAL VOLTAGE	2.0 PU
e_F	REGULATOR FEEDBACK SIGNAL	10.0 PU
V_R	REGULATOR OUTPUT	7.3 PU
e_S	POWER SYSTEM STABILIZER OUTPUT	
<u>PARAMETERS</u>		
K_A	FORWARD PATH AMPLIFIER GAIN	320.0
K_F	FEEDBACK GAIN	0.015
T_A	FORWARD PATH TIME CONSTANT	0.02 SEC
T_2	LAG TIME CONSTANT	0.5 SEC
T_3	LAG TIME CONSTANT	0.085 SEC
V_R^{MIN}	MINIMUM REGULATOR OUTPUT	0.0 PU
V_R^{MAX}	MAXIMUM REGULATOR OUTPUT	7.3 PU

Figure B-11. Basler Voltage Regulator

BLOCK DIAGRAM



$$S(e) = E_{fd} \left\{ a_1 - a_2 E_{fd} + (E_{fd})^2 [a_3 - a_4 E_{fd} + a_5 (E_{fd})^2] \right\}$$

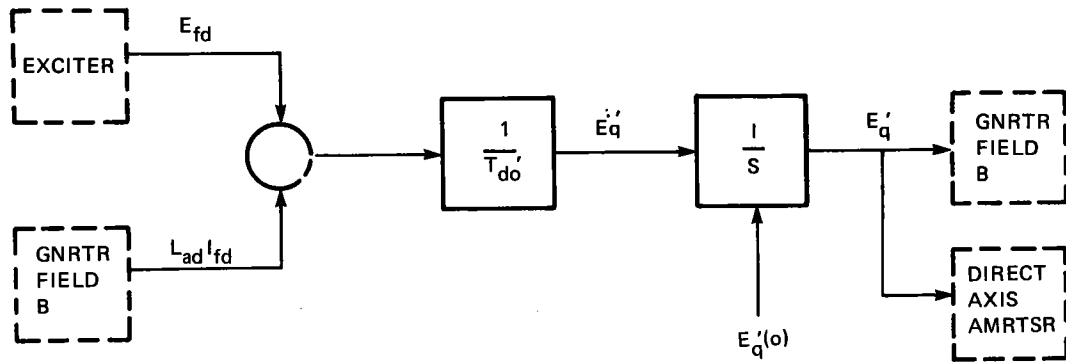
$$E_{fd} = \frac{1}{1 + ST_e} (V_R - S(e))$$

NOMENCLATURE

E_{fd}	EXCITER OUTPUT VOLTAGE	MAXIMUM	10.0 PU
V_R	REGULATOR OUTPUT		7.3 PU
$S(e)$	EXCITER SATURATION FUNCTION		10.0 PU
		NOMINAL	
a_1	EXCITER SATURATION COEFFICIENT		0.5542
a_2	EXCITER SATURATION COEFFICIENT		0.3340
a_3	EXCITER SATURATION COEFFICIENT		0.09523
a_4	EXCITER SATURATION COEFFICIENT		0.01310
a_5	EXCITER SATURATION COEFFICIENT		0.0007267
T_e	EXCITER TIME CONSTANT		0.4 SEC

Figure B-12. Exciter

BLOCK DIAGRAM



EQUATION

$$\dot{E}'_q = \frac{1}{T'_{do}} (E_{fd} - L_{ad} I'_{fd}) \quad (1)$$

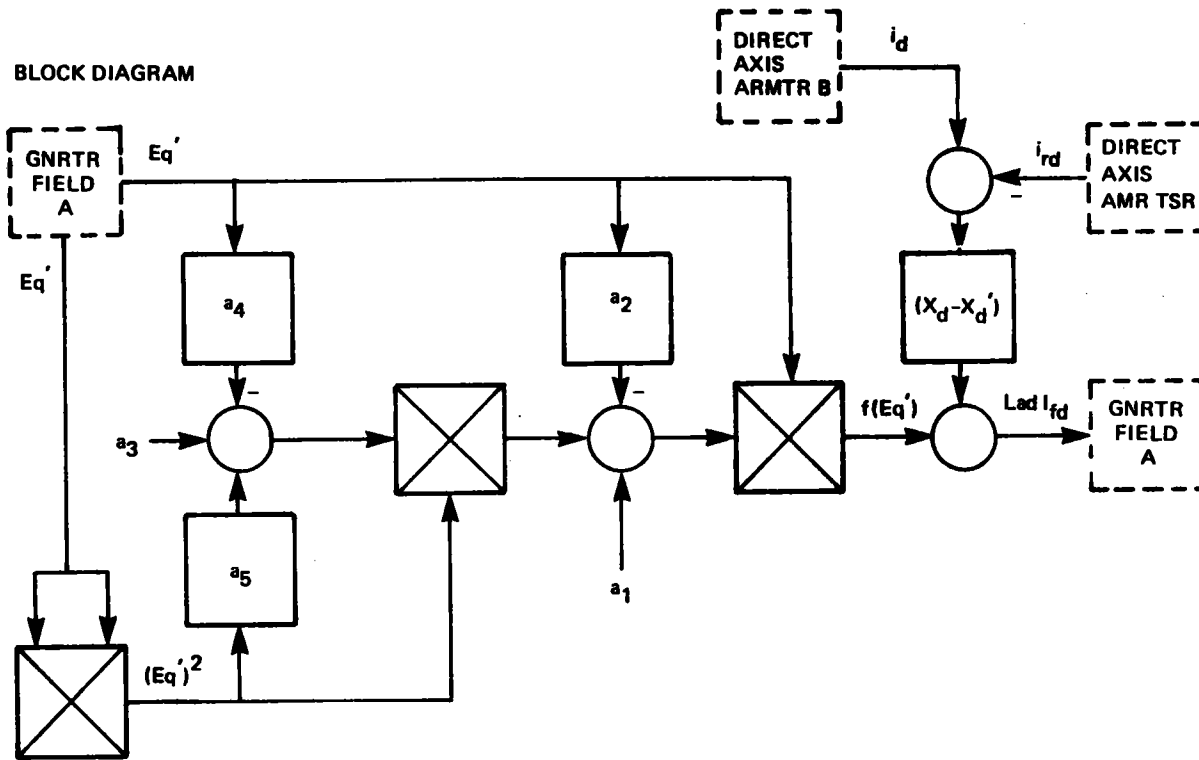
NOMENCLATURE

VARIABLES		MAXIMUM
E_{fd}	FIELD VOLTAGE	7.2 PU*
I'_{fd}	FIELD CURRENT	6.8 PU
E'_q	VOLTAGE BACK OF TRANSIENT REACTANCE	1.45 PU
PARAMETERS		NOMINAL
T'_{do}	DIRECT AXIS OPEN CIRCUIT TRANS TIME CONSTANT	1.77 SEC
L_{ad}	DIRECT AXIS MUTUAL INDUCTANCE (SEE G2)	- PU
E_{fd}^B	BASE FIELD VOLTAGE	25.0 V
I'_{fd}^B	BASE FIELD CURRENT	10.0 AMPS
$E'_{q}{}^B$	BASE VOLTAGE BACK OF TRANSIENT REACTANCE	480 VOLTS
$E'_{q}(o)$	INITIAL CONDITION	(COMPUTED) PU

* PU = PER UNIT

Figure B-13. Generator Field A

BLOCK DIAGRAM



$$f(E_q') = E_q' \left\{ a_1 - a_2 E_q' + (E_q')^2 [a_3 - a_4 E_q' + a_5 (E_q')^2] \right\}$$

$$Lad I_{fd} = f(E_q') + (X_d - X_d') (i_d - i_{Kd})$$

NOMENCLATURE

E_q' VOLTAGE BACK OF TRANSIENT REACTANCE
 I_{fd} GENERATOR FIELD CURRENT
 i_d DIRECT AXIS ARMATURE CURRENT
 i_{Kd} DIRECT AXIS AMORTISSEUR CURRENT

a_1 FIELD MAGNETIZATION COEFFICIENT
 a_2 FIELD MAGNETIZATION COEFFICIENT
 a_3 FIELD MAGNETIZATION COEFFICIENT
 a_4 FIELD MAGNETIZATION COEFFICIENT
 a_5 FIELD MAGNETIZATION COEFFICIENT

Lad DIRECT AXIS MUTUAL INDUCTANCE (EQUATION ABOVE)
 X_d DIRECT AXIS SYNCHRONOUS REACTANCE
 X_d' DIRECT AXIS TRANSIENT REACTANCE

MAXIMUM

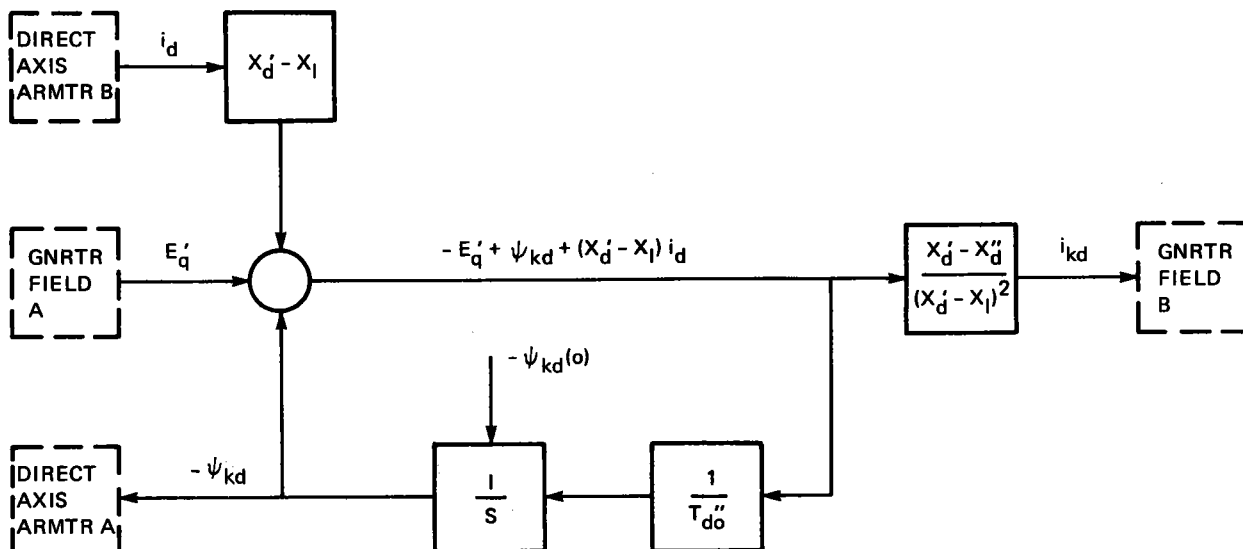
1.45 PU
 6.8 PU
 10.0 PU
 10.0 PU

NOMINAL

1.835
 5.871
 13.88
 14.26
 5.374
 PU
 1.651 PU
 0.2566 PU

Figure B-14. Generator Field B

BLOCK DIAGRAM



EQUATIONS

$$i_{kd} = \frac{X'_d - X''_d}{(X'_d - X_l)^2} [-E'_q + \psi_{kd} + (X'_d - X_l) i_d] \quad (3)$$

$$\psi_{kd} = \frac{1}{ST''_{do}} [E'_q - \psi_{kd} - (X'_d - X_o) i_d] \quad (4)$$

VARIABLES

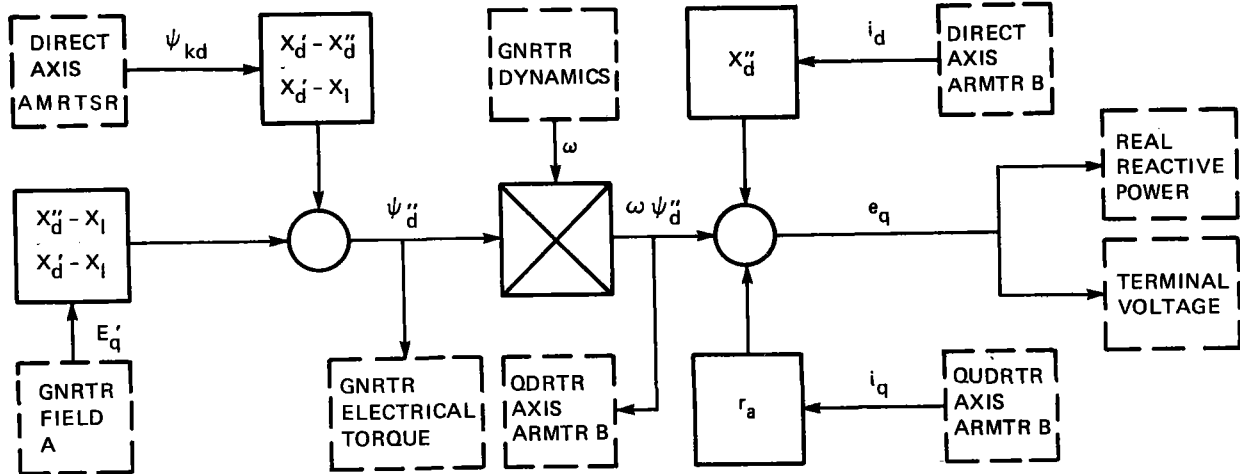
		MAXIMUM
E'_q	VOLTAGE BACK OF TRANSIENT REACTANCE	2.0 PU
i_{kd}	DIRECT AXIS AMORTISSEUR CURRENT	10. PU
ψ_{kd}	DIRECT AXIS AMORTISSEUR FLUX LINKAGE	2. PU
i_d	DIRECT AXIS ARMATURE CURRENT	10. PU

PARAMETERS

		NOMINAL (COMPUTED) PU
$\psi_{kd}(0)$	INITIAL CONDITION	
X'_d	DIRECT AXIS TRANSIENT REACTANCE	0.2566 PU
X_d	DIRECT AXIS SYNCHRONOUS REACTANCE	1.651 PU
X''_d	DIRECT AXIS SUBTRANSIENT REACTANCE	0.1622 PU
X_l	LEAKAGE REACTANCE	0.08 PU
T''_{do}	DIRECT AXIS OPEN CIRCUIT SUBTRANSIENT TIME CONSTANT	0.0118 SEC

Figure B-15. Direct Axis Amortisseur Circuit

BLOCK DIAGRAM



EQUATIONS

$$\psi''_d = \frac{X'_d - X''_d}{X'_d - X_l} \psi_{kd} + E'_q \frac{X''_d - X_l}{X'_d - X_l} \quad (5)$$

$$e_q = \omega \psi''_d - i_d X''_d - i_q r_a \quad (6)$$

NOMENCLATURE

VARIABLES

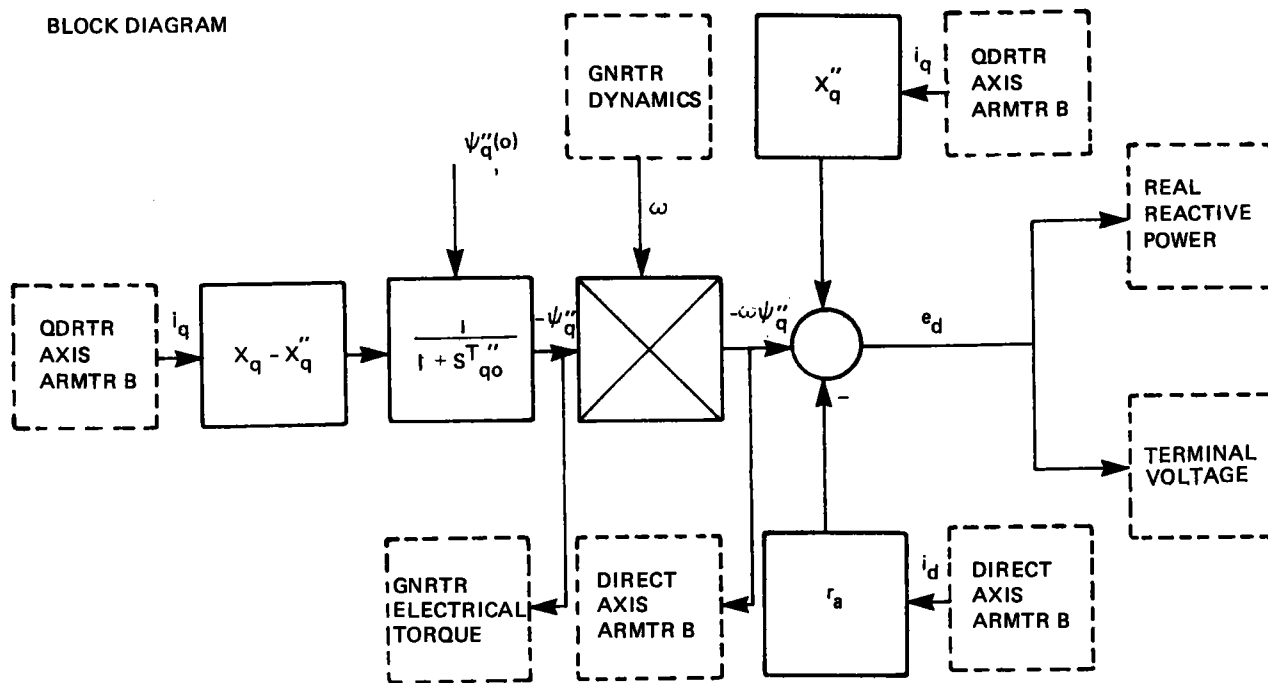
		MAXIMUM
ψ_{kd}	DIRECT AXIS AMORTISSEUR FLUX LINKAGE	2.0 PU
ψ''_d	DIRECT AXIS SUBTRANSIENT ARMATURE FLUX LINKAGE	2.0 PU
E'_q	VOLTAGE BACK OF TRANSIENT REACTANCE	1.45 PU
ω	ELECTRICAL SPEED	2.0 PU
e_q	QUADRATURE AXIS TERMINAL VOLTAGE	2.0 PU
i_d	DIRECT AXIS ARMATURE CURRENT	10. PU
i_q	QUADRATURE AXIS ARMATURE CURRENT	10. PU

PARAMETERS

		NOMINAL
X'_d	DIRECT AXIS TRANSIENT REACTANCE	0.2566 PU
X''_d	DIRECT AXIS SUBTRANSIENT REACTANCE	0.1622 PU
r_a	ARMATURE RESISTANCE	0.005 PU
X_l	LEAKAGE REACTANCE	0.08 PU

Figure B-16. Direct Axis Armature A

BLOCK DIAGRAM



EQUATIONS

$$\psi_q'' = - \frac{(X_q - X_q'') i_q}{1 + ST_{qo}''} \quad (7)$$

$$e_d = -\omega \psi_q'' + i_q X_q'' - i_d r_a \quad (8)$$

NOMENCLATURE

VARIABLES

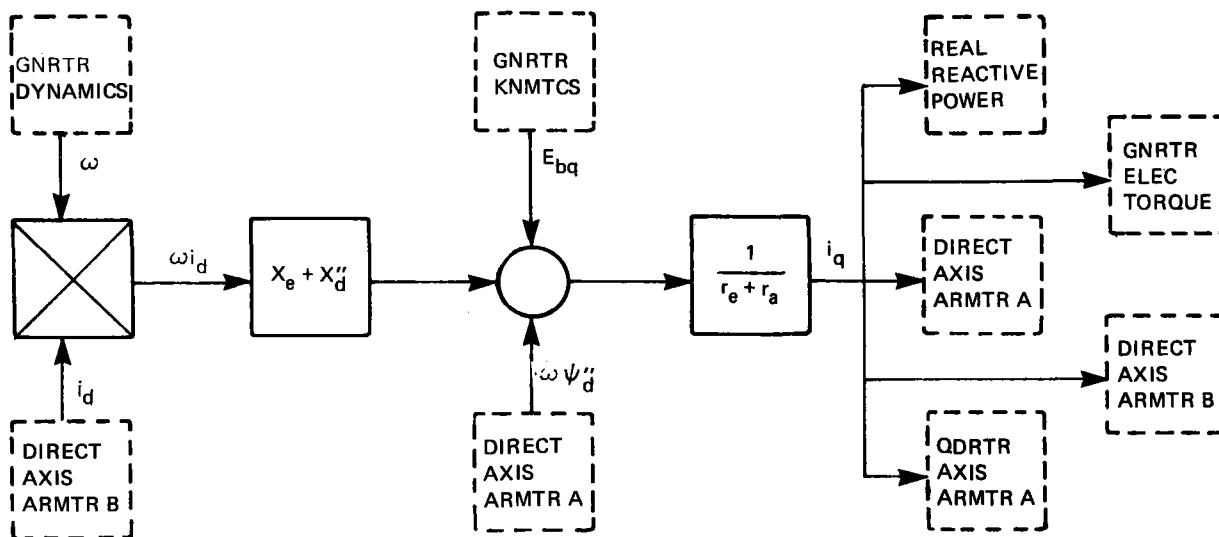
Variable	Description	MAXIMUM
i_q	QUADRATURE AXIS ARMATURE CURRENT	10. PU
i_d	DIRECT AXIS ARMATURE CURRENT	10. PU
e_d	DIRECT AXIS TERMINAL VOLTAGE	2. PU
ψ_q''	QUADRATURE AXIS SUBTRANSIENT ARMTR FLX LINKAGE	2. PU
ω	ELECTRICAL SPEED	2. PU

PARAMETERS

Parameter	Description	NOMINAL
X_q	QUADRATURE AXIS SYNCHRONOUS REACTANCE	0.9474 PU
X_q''	QUADRATURE AXIS SUBTRANSIENT REACTANCE	0.2031 PU
T_{qo}''	QUAD AXIS SUBTRANSIENT OPEN CIRC TIME CONSTANT	0.01495 SEC
r_a	ARMATURE RESISTANCE	0.005 PU
$\psi_q''(0)$	INITIAL CONDITION	

Figure B-17. Quadrature Axis Armature A

BLOCK DIAGRAM



EQUATIONS

$$i_q = \frac{1}{r_e + r_a} [\omega \psi''_d - E_{bq} - \omega i_d (X_e + X''_d)] \quad (9)$$

NOMENCLATURE

VARIABLES

i_q	QUADRATURE AXIS ARMATURE CURRENT	10. PU
E_{bq}	QUADRATURE AXIS UTILITY VOLTAGE	2. PU
ω	ELECTRICAL SPEED	2. PU
i_d	DIRECT AXIS ARMATURE CURRENT	10. PU
ψ''_d	DIRECT AXIS SUBTRANS ARMTR FLX LINKAGE	2. PU

MAXIMUM

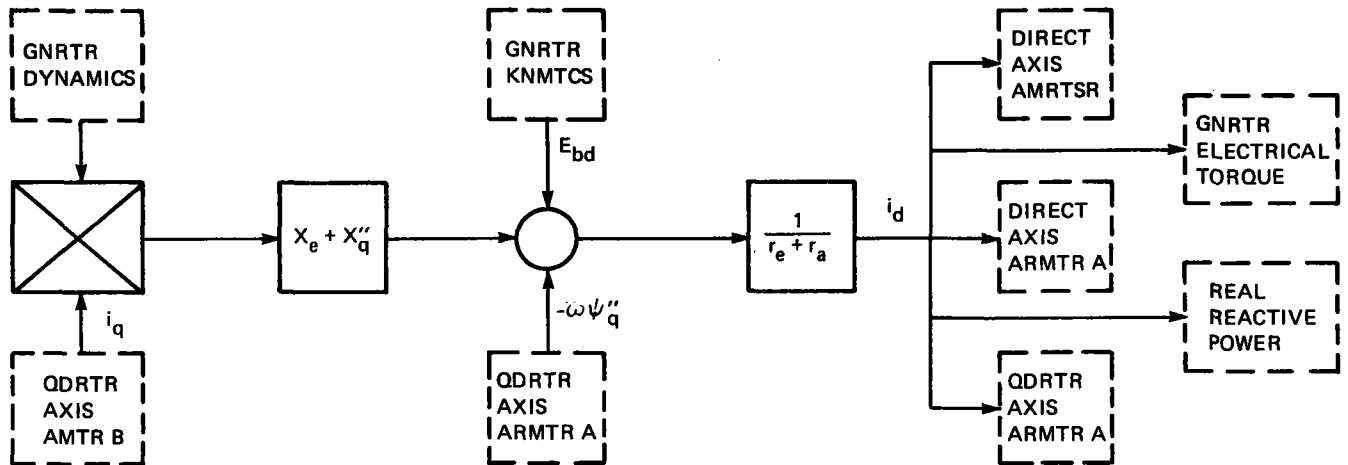
PARAMETERS

X_e	UTILITY REACTANCE	0.0 PU
X''_d	DIRECT AXIS SUBTRANSIENT REACTANCE	0.1622 PU
r_e	UTILITY RESISTANCE	1.80 PU
r_a	ARMATURE RESISTANCE	0.005 PU

NOMINAL

Figure B-18. Quadrature Axis Armature B

BLOCK DIAGRAM



EQUATIONS

$$i_d = -\frac{1}{r_e + r_a} [\omega \psi_q'' + E_{bd} - \omega i_q (X_e + X_q'')] \quad (10)$$

NOMENCLATURE

VARIABLES

i_q	QUADRATURE AXIS ARMATURE CURRENT	10. PU
i_d	DIRECT AXIS ARMATURE CURRENT	10. PU
E_{bd}	DIRECT AXIS UTILITY VOLTAGE	2. PU
ω	ELECTRICAL SPEED	2. PU
ψ_q''	QUADRATURE AXIS SUBTRANSIENT FLUX LINKAGE	2. PU

MAXIMUM

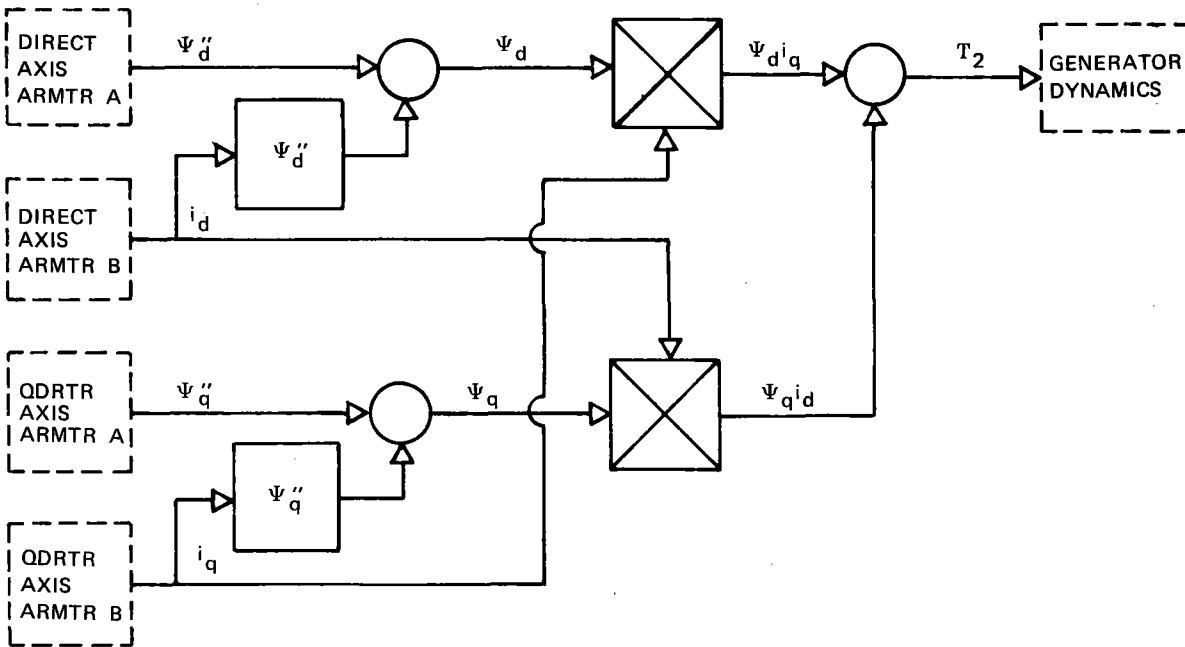
PARAMETERS

X_e	UTILITY REACTANCE	0.0 PU
X_q''	QUADRATURE AXIS SUBTRANSIENT REACTANCE	0.1622 PU
r_a	ARMATURE RESISTANCE	0.005 PU
r_e	UTILITY RESISTANCE	1.80 PU

NOMINAL

Figure B-19. Direct Axis Armature B

BLOCK DIAGRAM



EQUATIONS

$$\Psi_d = \Psi_d'' - x_d'' i_d \quad ; \quad \Psi_q = \Psi_q'' - x_q'' i_q$$

$$T_{\Sigma} = i_q \Psi_d - i_d \Psi_q$$

NOMENCLATURE

VARIABLES

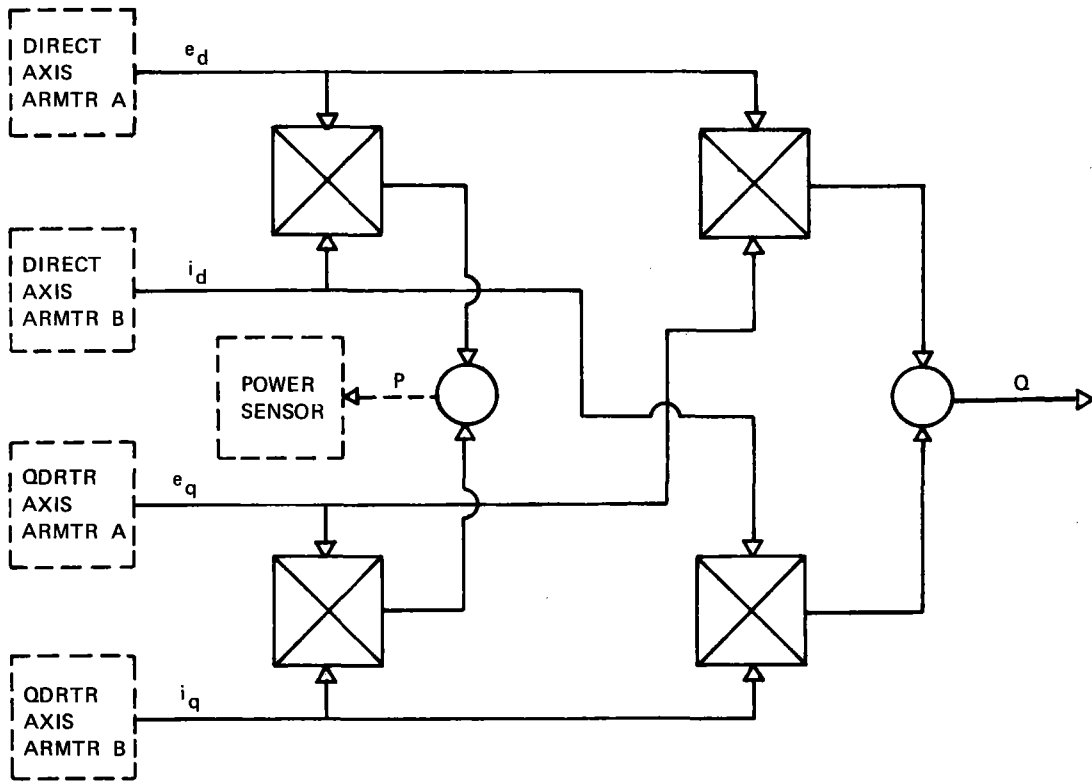
VARIABLES		MAXIMUM
Ψ_d	DIRECT AXIS ARMATURE FLUX LINKAGE	2. pu
Ψ_q	QUADRATURE AXIS ARMATURE FLUX LINKAGE	2. pu
Ψ_d''	DIRECT AXIS SUBTRANSNT ARMTR FLUX LINKAGE	2. pu
Ψ_q''	QUADRATURE AXIS SUBTRANSNT ARMTR FLUX LINKAGE	2. pu
i_d	DIRECT AXIS ARMATURE CURRENT	10. pu
i_q	QUADRATURE AXIS ARMATURE CURRENT	10. pu
T_e	ELECTRICAL TORQUE (3666.85 FT-LB)	1. pu

PARAMETERS

		NOMINAL
Ψ_q''	QUADRATURE AXIS SUBTRANS REACTANCE	0.2031 pu
Ψ_d''	DIRECT AXIS SUBTRANSIENT REACTANCE	0.1622 pu

Figure B-20. Generator Electrical Torque

BLOCK DIAGRAM



EQUATIONS

$$P = e_d i_d + e_q i_q \quad Q = e_q i_d - e_d i_q$$

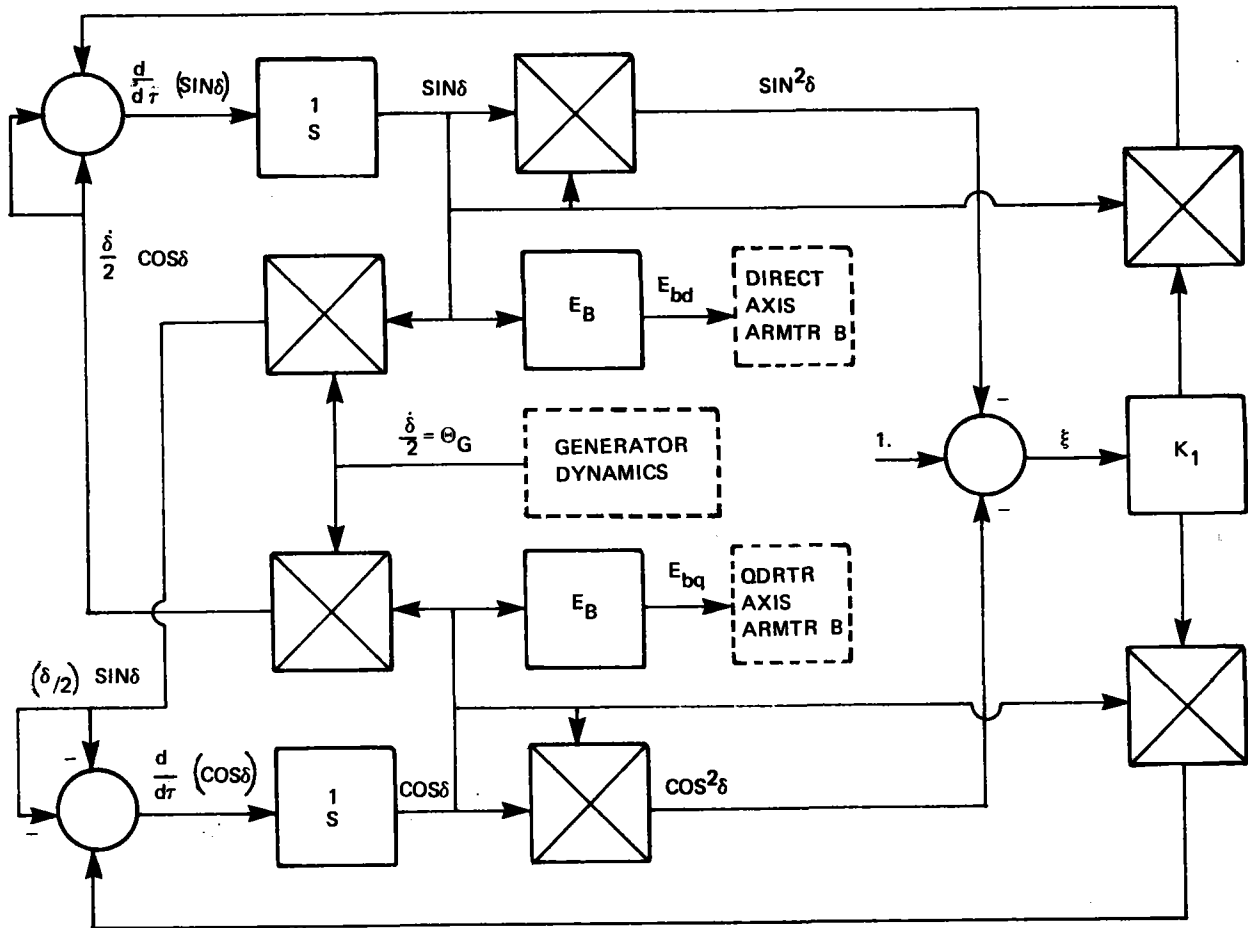
NOMENCLATURE

MAXIMUM

e_d	DIRECT AXIS COMPONENT, TERMINAL VOLTAGE	2. pu
i_d	DIRECT AXIS COMPONENT, ARMATURE CURRENT	10. pu
e_q	QUADRATURE AXIS COMPONENT, TERMINAL VOLTAGE	2. pu
i_q	QUADRATURE AXIS COMPONENT, ARMATURE CURRENT	10. pu
P	REAL POWER	10. pu
Q	REACTIVE POWER	10. pu

Figure B-21. Real and Reactive Power

BLOCK DIAGRAM



EQUATIONS

$$\frac{d}{dt} \sin\delta = \delta \cos\delta; \quad \sin^2\delta + \cos^2\delta = 1; \quad E_{bd} = E_B \sin\delta$$

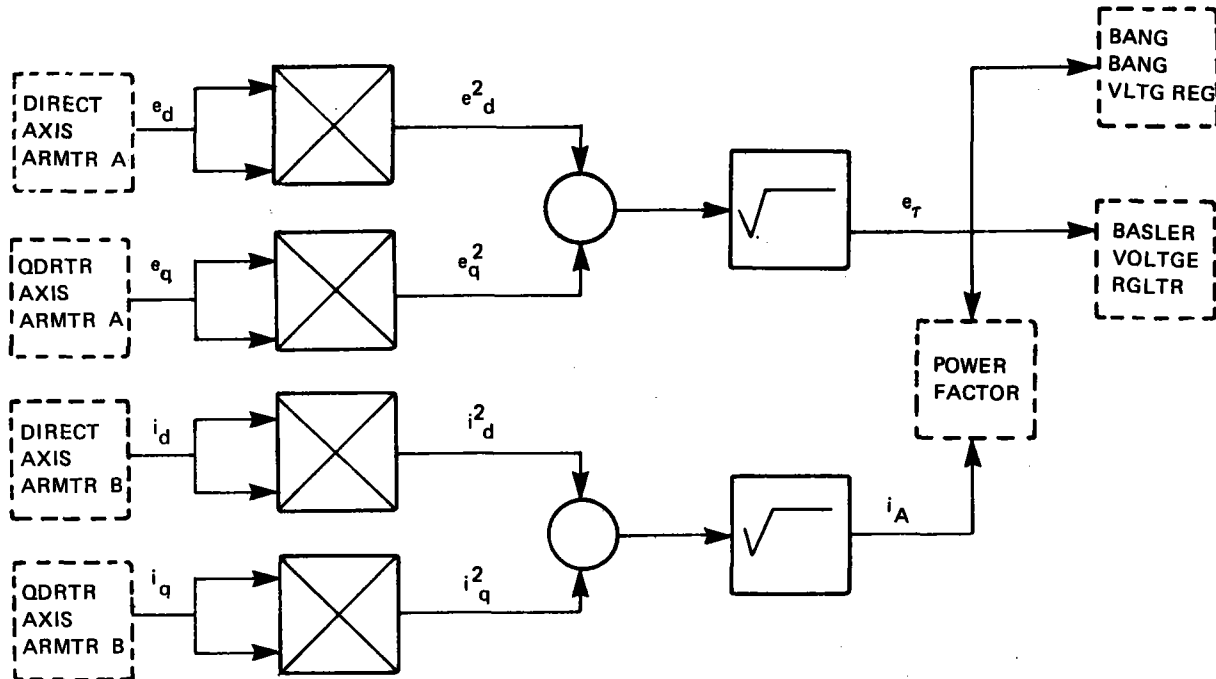
$$\frac{d}{dt} \cos\delta = -\delta \sin\delta; \quad \delta = 2\theta_G; \quad E_{bq} = E_B \cos\delta$$

NOMENCLATURE

VARIABLES		MAXIMUM
θ_G	HI SPEED SHAFT DISPLACEMENT	2π
δ	TORQUE ANGLE	2π
ξ	TRIGONOMETRIC ERROR ($1 - \cos^2\delta - \sin^2\delta$)	0.1
E_{bd}	DIRECT AXIS COMPONENT OF NETWORK VOLTAGE	2. pu
E_{bq}	QUADRATURE AXIS COMPONENT OF NETWORK VOLTAGE	2. pu
PARAMETERS		NOMINAL
K_1	ARBITRARY GAIN	100.
θ_{MH}	SCALING PARAMETER, HI SPEED SHAFT DISPLACEMENT	1. Radian

Figure B-22. Generator Kinematics

BLOCK DIAGRAM



EQUATIONS

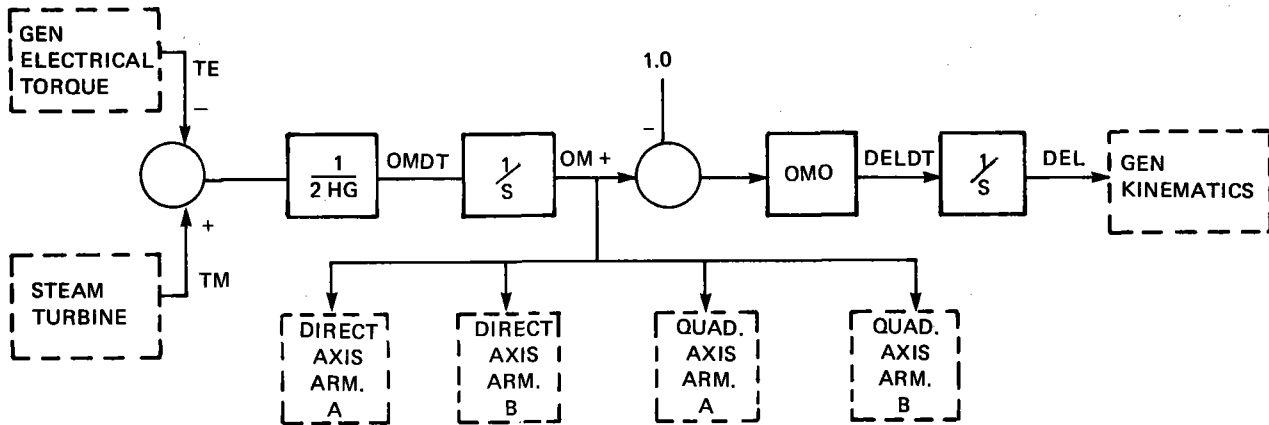
$$e_T = \sqrt{e_d^2 + e_q^2} \quad i_A = \sqrt{i_d^2 + i_q^2}$$

NOMENCLATURE

VARIABLES		MAXIMUM
e_d	DIRECT AXIS COMPONENT, TERMINAL VOLTAGE	2. pu
e_q	QUADRATURE AXIS COMPONENT, TERMINAL VOLTAGE	2. pu
i_d	DIRECT AXIS COMPONENT, ARMATURE CURRENT	10. pu
i_q	QUADRATURE AXIS COMPONENT, ARMATURE CURRENT	10. pu
e_T	TERMINAL VOLTAGE	2. pu
i_A	ARMATURE CURRENT	10. pu

Figure B-23. Terminal Voltage and Armature Current

BLOCK DIAGRAM



EQUATIONS

$$\text{OMDT} = (\text{TM} - \text{TE}) / 2\text{HG}$$

$$\text{DELDT} = \text{OMO} * (\text{OM} - 1.0)$$

VARIABLES

- TE -- ELECTRICAL TORQUE (PU)
- TM -- MECHANICAL TORQUE (PU)
- HG -- INERTIA CONSTANT (SEC-PU)
- OM -- SHAFT SPEED (PU)
- OMD -- SHAFT SPEED REF (RAD/S)
- DEL -- ANGLE OF ROTATION (RAD)
- OMDT -- SHAFT ACCELERATION (PU/S)

PARAMETERS

- HG 4.698 PU-S
- OMD 377 RAD/S

Figure B-24. Generator Dynamics

	UTILITY POWER	GEN OUTPUT	TPR	SPEED	PRESSURE	STEAM FLO	OIL FLOW	TERM VOLT	VR
1.0	100.0	278.0	0.999	1.00000	700.0	2.243	16.496	1.000	2.026
2.0	100.0	278.0	0.998	0.99999	700.0	2.243	16.495	1.000	2.026
3.0	123.0	278.0	0.998	1.00000	700.0	2.243	16.496	1.000	2.026
4.0	121.2	281.0	0.999	0.99999	696.8	2.274	16.909	1.000	2.039
5.0	116.5	284.5	0.991	1.00000	690.4	2.297	17.180	1.000	2.040
6.0	115.9	287.2	0.987	1.00001	684.5	2.320	17.335	1.000	2.042
7.0	112.3	290.2	0.979	1.00001	680.9	2.345	17.508	1.000	2.045
8.0	109.5	293.5	0.969	1.00002	679.8	2.371	17.636	1.000	2.051
9.0	106.2	296.6	0.955	1.00002	680.6	2.397	18.003	1.000	2.056
10.0	103.2	299.9	0.938	1.00002	682.7	2.421	18.312	1.000	2.062
11.0	100.0	302.4	0.918	1.00001	685.8	2.441	18.504	1.000	2.065
12.0	98.5	304.5	0.897	1.00001	689.3	2.457	18.649	1.000	2.070
13.0	97.0	306.0	0.874	1.00001	692.9	2.467	18.737	1.000	2.073
14.0	96.0	307.0	0.850	1.00000	696.4	2.472	18.797	1.000	2.075
15.0	95.4	307.8	0.825	1.00000	699.4	2.473	18.799	1.000	2.076
16.0	95.2	307.8	0.800	1.00000	703.0	2.471	18.776	1.000	2.076
17.0	95.4	307.6	0.976	1.00000	704.0	2.468	18.591	1.000	2.076
18.0	95.8	307.2	0.971	1.00000	703.4	2.457	18.378	1.000	2.076
19.0	96.4	306.6	0.953	1.00000	706.2	2.449	18.195	1.000	2.074
20.0	97.2	305.6	0.935	1.00000	709.5	2.440	18.012	1.000	2.073
21.0	98.1	304.9	0.918	1.00000	706.2	2.431	17.840	1.000	2.072
22.0	99.0	304.0	0.902	1.00000	706.5	2.423	17.694	1.000	2.070
23.0	99.9	303.1	0.882	1.00000	704.5	2.418	17.564	1.000	2.069
24.0	100.8	302.2	0.863	1.00000	703.2	2.414	17.519	1.000	2.067
25.0	101.6	301.4	0.845	1.00000	701.9	2.412	17.502	1.000	2.065
26.0	102.2	300.8	0.867	1.00000	700.3	2.412	17.535	1.000	2.064
27.0	102.7	300.3	0.970	1.00000	699.9	2.414	17.612	1.000	2.063
28.0	103.3	300.1	0.972	1.00000	697.6	2.416	17.726	1.000	2.063
29.0	102.9	300.1	0.975	1.00000	699.6	2.423	17.697	1.000	2.063
30.0	102.7	300.3	0.976	1.00000	699.9	2.429	18.000	1.000	2.063
31.0	102.2	300.8	0.960	1.00000	699.6	2.436	18.174	1.000	2.064
32.0	101.6	301.4	0.942	1.00000	699.5	2.442	18.315	1.000	2.065
33.0	100.9	302.1	0.918	1.00000	696.0	2.447	18.431	1.000	2.066
34.0	100.2	302.8	0.893	1.00000	696.7	2.451	18.515	1.000	2.067
35.0	99.4	303.6	0.862	1.00000	697.6	2.454	18.559	1.000	2.069
36.0	98.7	304.3	0.831	1.00000	699.7	2.455	18.592	1.000	2.070
37.0	98.2	304.6	0.879	1.00000	699.9	2.454	18.524	1.000	2.071
38.0	97.8	305.2	0.977	1.00000	701.1	2.452	18.450	1.000	2.072
39.0	97.5	305.5	0.974	1.00000	702.1	2.449	18.348	1.000	2.072
40.0	97.6	305.4	0.972	1.00000	702.9	2.444	18.227	1.000	2.072
41.0	97.6	305.2	0.970	1.00000	703.5	2.439	18.097	1.000	2.072

Figure B-25a. Interconnected Mode 25 kW Step in Plant Load

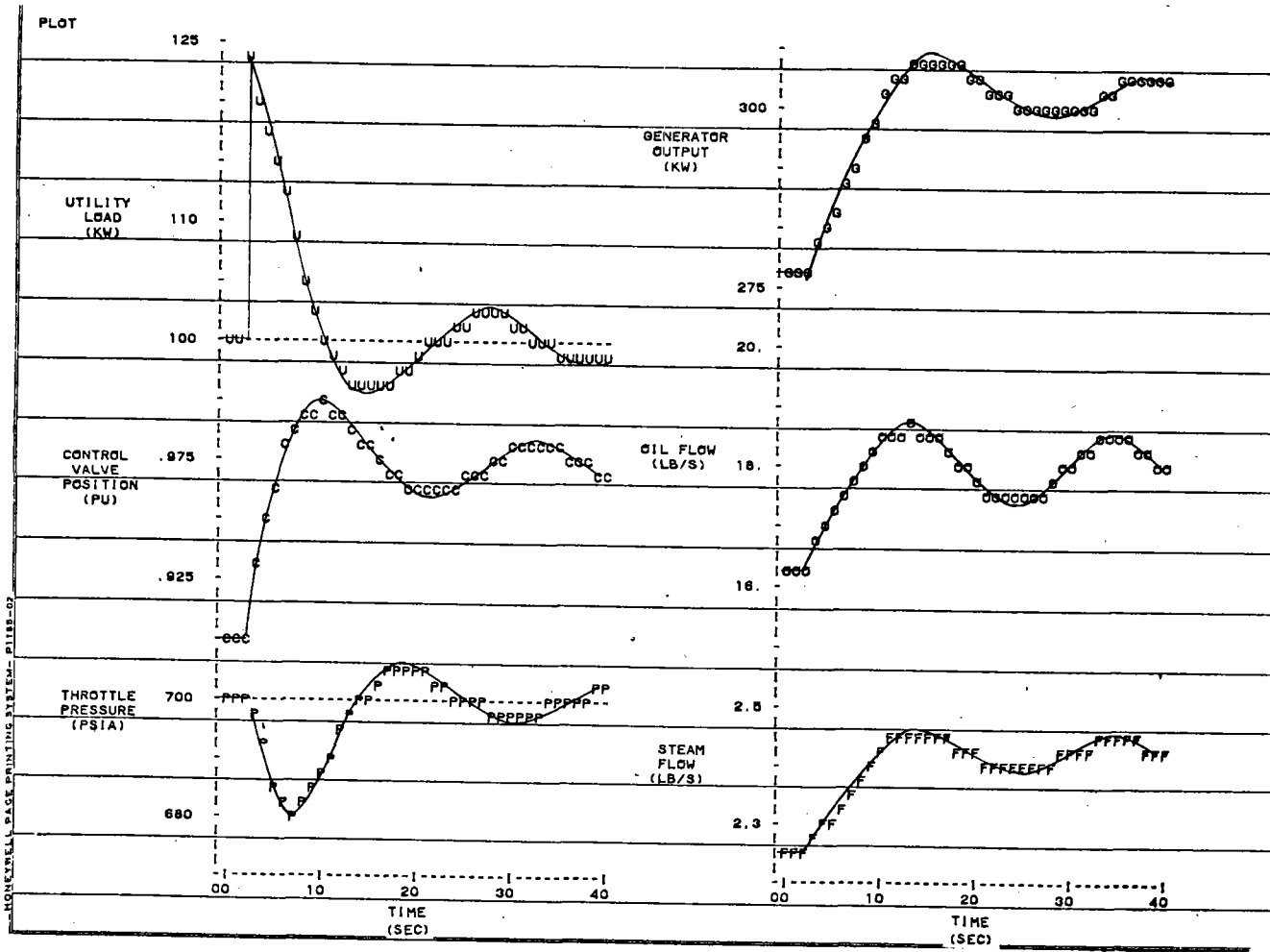


Figure B-25b. Interconnected 25 kW Step

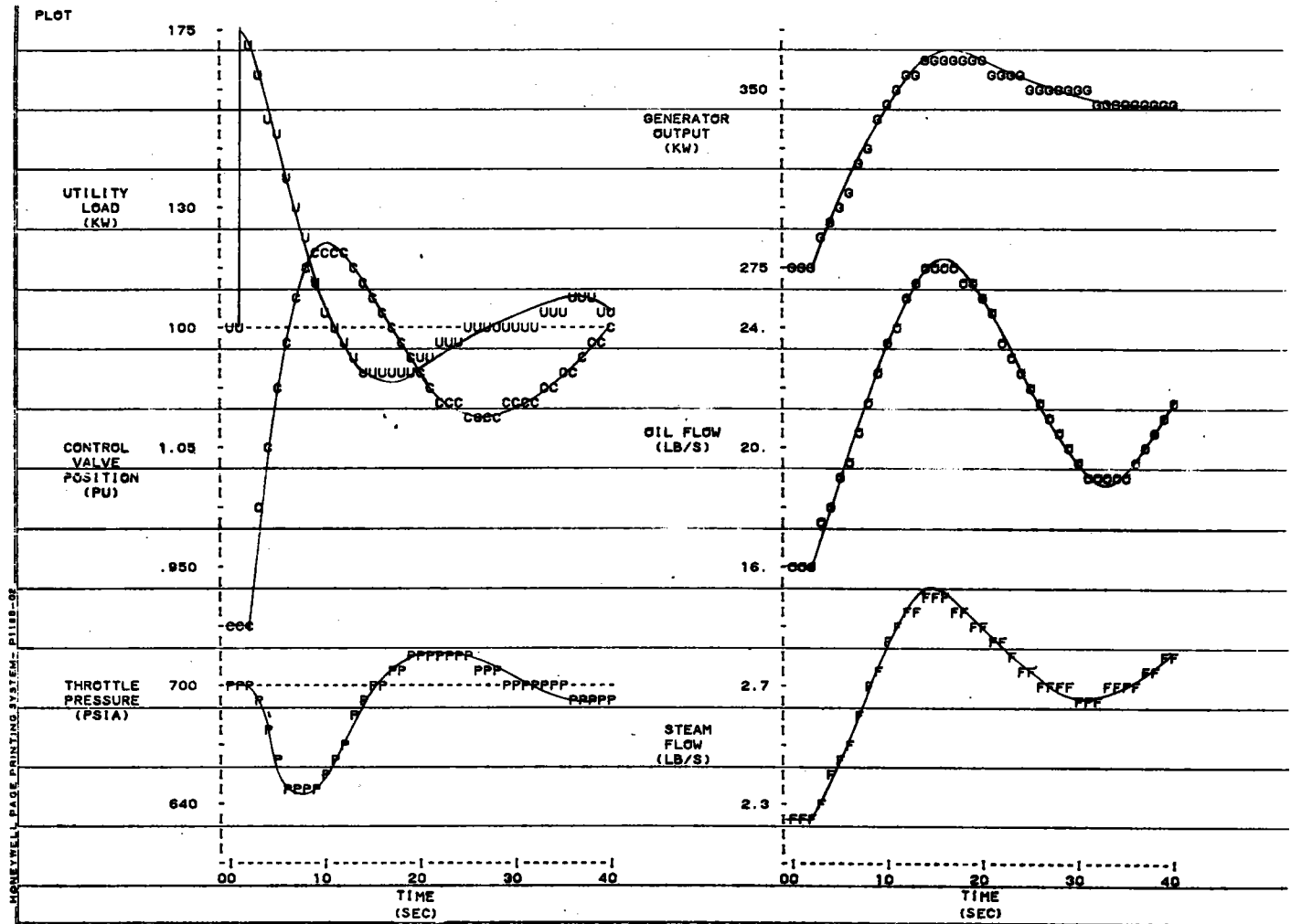


Figure B-26. Interconnected 75 kW Step

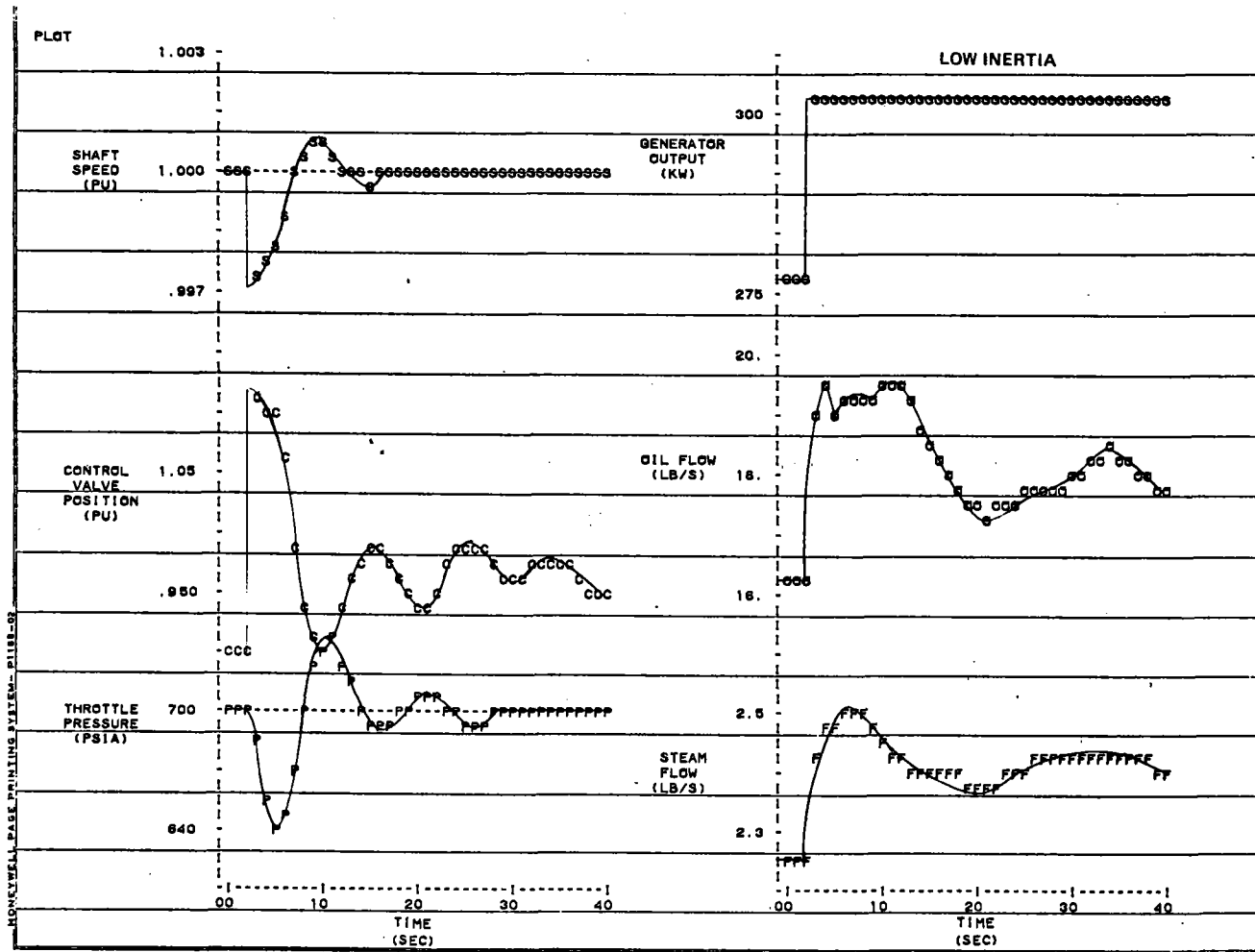


Figure B-27. Standalone 25 kW Step

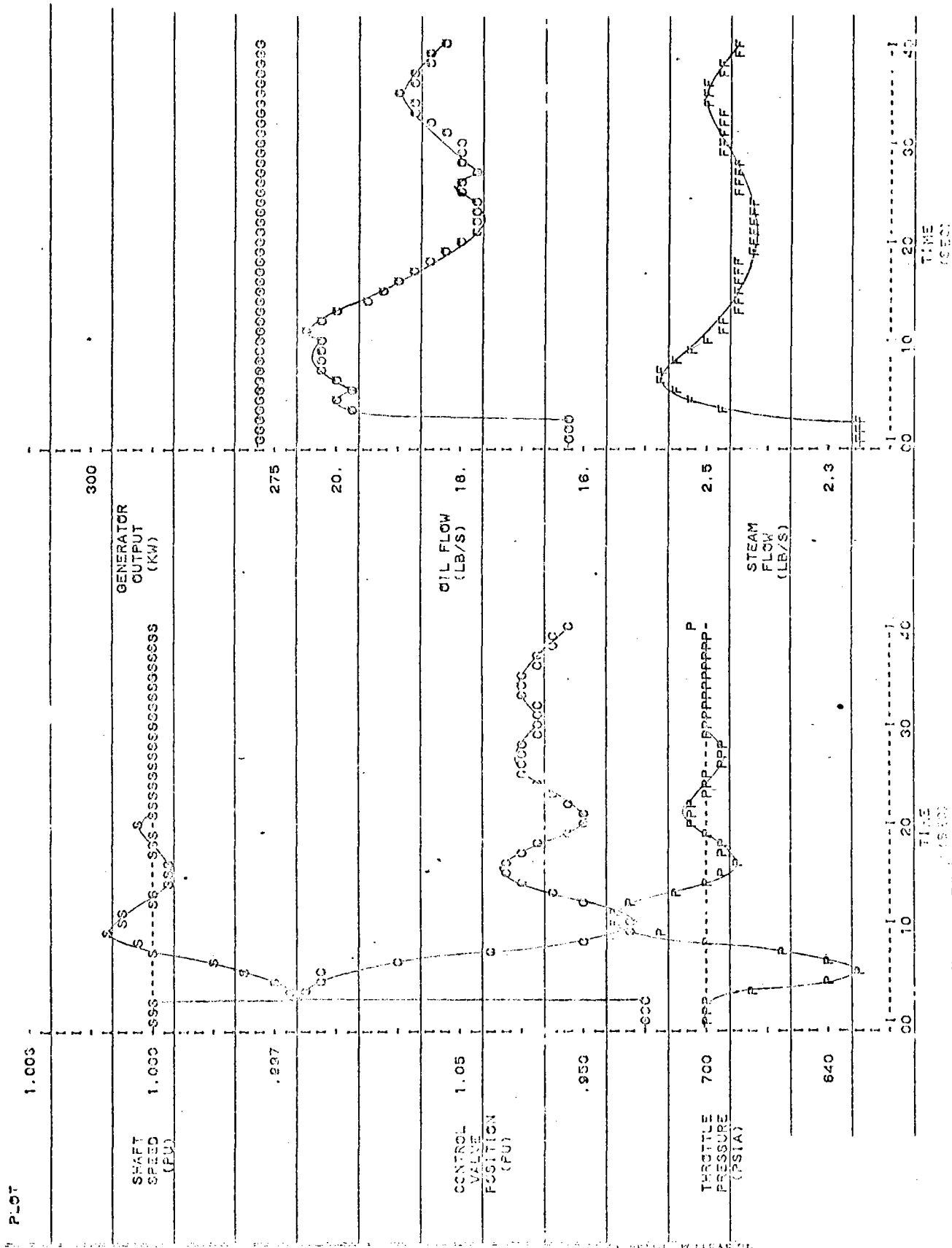


Figure B-28.

B.2 TRANSIENT SIMULATION

B.3.1 SIMULATION METHOD

The transient simulation model is coded using the FORTRAN computer language on the Honeywell 600/660 digital computer. The equation set which was formulated in Figures B-1 through B-8, and Figures B-11 through B-24 constitute the basis for the model with various subprograms included for initialization, frequency response analysis, integration, and plotting of the output.

Integration of the differential equations is achieved utilizing a modified Euler method. The Euler method was chosen because it provides the lowest computer cost for a simulation of the PCS. An integration interval of 0.005 sec was found to be the largest interval acceptable for the smallest time constants to provide accurate results.

B.3.2 RESULTS

The responses of several variables to step disturbances in the system are shown in Figures B-25 through B-28. The key control subsystem parameters are:

1. steam pressure
2. turbine shaft speed (independent mode)
3. utility load (interconnected mode)

The important adjustable parameters are:

1. control valve position
2. generator output
3. oil (Syltherm 800) flow
4. steam flow

All parameters exhibit stable response curves.

B.3.2.1 Interconnected Mode

B.3.2.1.1 25 kW step in plant load (Figure B-25 a & b)

<u>Parameter</u>	<u>Recovery Time (Sec)</u>	<u>% Overshoot</u>	<u>% Decrease</u>
Utility Load	10.	4.2	NA
Control Valve Pos	5.	2.7	NA
Throttle Pressure	14.	0.9	2.9
Generator Output	10.	1.6	NA
Oil (S800) Flow	8.	4.1	NA
Steam Flow	9.	1.6	NA

B.3.2.1.2 75 kW step in plant load (Figure B-26)

<u>Parameter</u>	<u>Recovery Time (Sec)</u>	<u>% Overshoot</u>	<u>% Decrease</u>
Utility Load	11.	14.9	NA
Control Valve Pos	6.	5.9	NA
Throttle Pressure	15.	3.1	8.4
Generator Output	11.	4.2	NA
Oil (S800) Flow	9.	16.1	NA
Steam Flow	10.	5.6	NA

B.3.2.2 Independent Mode

B.3.2.2.1 25 kW step in plant load (Figure B-27)

<u>Parameter</u>	<u>Recovery Time (Sec)</u>	<u>% Overshoot</u>	<u>% Decrease</u>
Shaft Speed	7.	0.1	.24
Control Valve Pos	8.	4.32	- 25.
Throttle Pressure	8.	5.5	8.8
Generator Output	0.0	0.2	NA
Oil (S800) Flow	17.	9.2	NA
Steam Flow	13.	4.2	NA

B.3.2.2.2 .3833 lb/sec step in process steam flow (Figure B-28)

<u>Parameter</u>	<u>Recovery Time (Sec)</u>	<u>% Overshoot</u>	<u>% Decrease</u>
Shaft Speed	8.	0.11	.355
Control Valve Pos	8.	5.5	31.
Throttle Pressure	8.	6.9	11
Generator Output	0.0	0.0	NA
Oil (S800) Flow	18.	11.	NA
Steam Flow	13.	5.1	NA

B.3.2.3 Load Step and Inertia Effect

Additional transient runs were made with the reference turbine-generator inertia value of 1/6 the GE marine turbine baseline and with the baseline inertia for load steps of 50, 75, and 100 kW in the stand-alone or independent configuration.

Results are shown in Figure B-29 with the basic control parameters held constant. The 0.5 percent frequency deviation limit is reached with about a 45 kW step for the lower inertia and a 65 kW step for the higher inertia. The frequency (speed) change is more sensitive to the step amplitude than the inertia value. Voltage dip values are well within the allowable five to seven percent but will be greater than indicated in actual practice since analytical simplifications were used and the reactive power inrush is not fully treated.

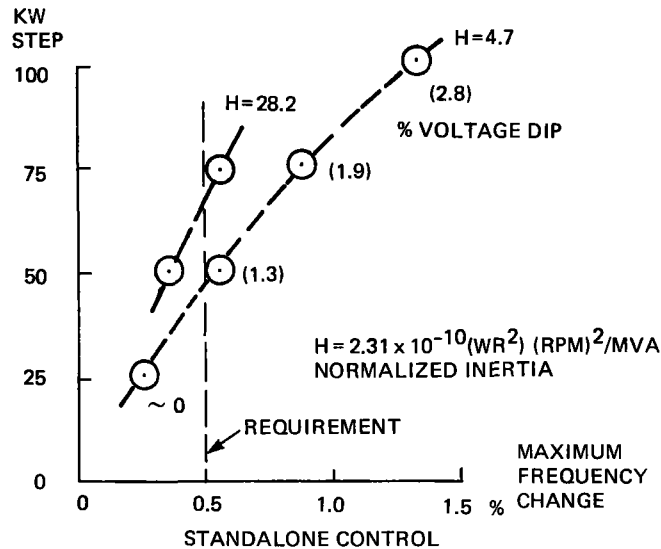


Figure B-29. Effect of Inertia and Load Step

B.4 FREQUENCY ANALYSIS

The PCS system model was analyzed in the frequency domain by determining the system eigenvalues or poles of the system transfer functions for linearized small signals around the operating point. A root locus of the poles was made for variations in connection resistance and reactance as shown in Figure B-30. Only the complex or oscillatory poles are shown. The system is well behaved for expected values of impedance; however, an external reactance of 0.5 pu caused instability of the mode near six radians/second. Adjustment of voltage regulator feedback compensates for external resistance and reactance value changes and is recommended for the final regulator hardware.

B.5 COMPUTER MODEL

The FORTRAN computer model was used for the system simulation. The model is set up either to perform a real time transient analysis or to find the poles of the system transfer functions. Either function can be performed in either the independent mode or the interconnected mode.

The main section of the program initializes most of the variables and contains the equations for the utility power load control, the turbine generator speed/load governor control, the steam pressure control, and the steam temperature control. In addition, the main program accesses the various subroutines. The following subroutines are also included in the model:

1. STEAMSYS - contains equations for the steam generator, the steam plenum control volume and control valve, and the steam turbine generator.
2. INT - Performs the integration using a modified Euler method.
3. PERT - excites each integrator variable to 101% of its steady state value and finds the system response. The results are stored in the square (27 x 27) "A" matrix.

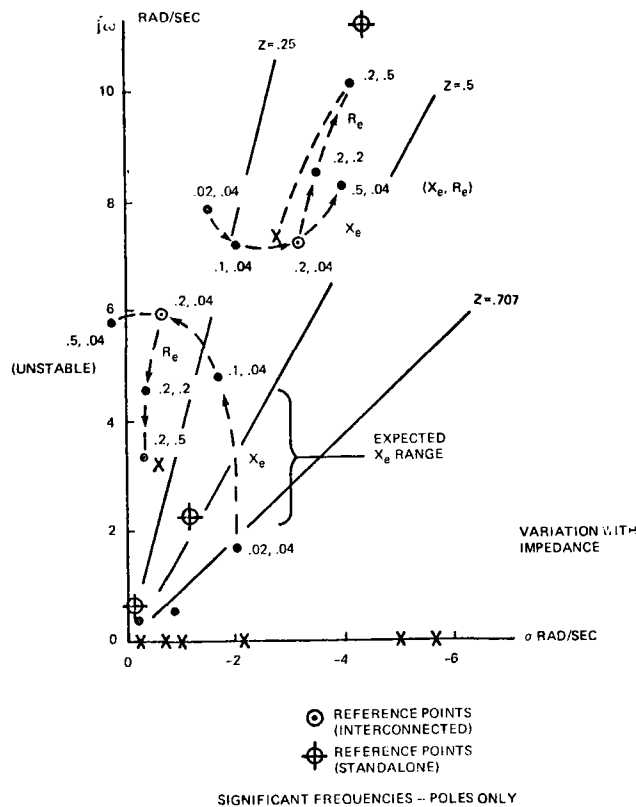


Figure B-30. System Root Locus

4. EIGVAL - finds the frequency response of the system from the "A" matrix found in PERT using a library routine called EIGRNS.
5. PLOT - documents the output of the real time transient analysis in either a tabular form or a plot. The output variables include the utility power, generator output, turbine shaft speed, control valve position, throttle pressure, oil (S800) flow rate, steam flow rate.
6. GEN - contains all of the electric generator equations, excites equations, and voltage regulator equations.
7. INIT - initializes the generator variables.

B.6 BASIC TRANSIENT MODEL

B.6.1 CONTROL SYSTEM DESCRIPTION

B.6.1.1 General

Several of the control systems associated with regulating the plant load generation and utilization will be discussed here including:

1. Utility Load Control
2. Turbine-Generator Speed/Load Control
3. Steam Pressure Control
4. Steam Temperature Control

It was concluded that a dynamic simulation of the plant and its control was required to permit the development and analysis of the control system behavior and overall performance. A more detailed discussion of the simulation itself is given in Section B.6.2.

B.6.1.2 Summary

The proposed control system configurations have been examined and adjusted to provide the required degree of regulation and response based upon the results of a transient computer simulation of the system. The response of the control system was demonstrated for step changes in plant electrical load and process steam flow for both interconnected operation with the utility system as well as stand-alone independent operation. The control systems exhibit accuracy of regulation, speed of response, and stability characteristics in keeping with the needs of the turbine-generator, steam generator, and utility interface requirements. The control systems are defined in sufficient detail to permit preliminary interface with control system vendors.

B.6.1.3 Overall Requirements

Two modes of control are available in the overall control system as indicated in Figure B-31. The first is for interconnected operation with the plant electrical system tied to the utility grid. In this mode, the utility is to supply a fixed amount of power to the plant, 100 kW, with the remainder of the load being supplied by the solar system/turbine-generator. The second mode of control is for independent system operation with no tie to the electric utility grid. In this mode, the turbine-generator is to supply all of the plant electrical load. For both modes, a portion of the process steam requirements of the plant is to be provided by extraction steam from the solar cycle.

B.6.1.3.1 Interconnected Operation

In this mode of operation, the control system adjusts the turbine generator output as required to maintain the level of power drawn from the utility grid at a value of 100 kW, with the generator supplying the remainder of the plant electrical load. The frequency is determined by the utility grid. Upon detection of a load change, the regulator acts to return the measured utility load to the desired value quickly and in a stable manner subject to the constraints associated with the steam generator, control valve, and steam turbine. Control subsystems will regulate steam pressure and temperature by automatic adjustment of feedwater flow and Syltherm 800 (oil) flow as described in Section B.6.1.4.

B.6.1.3.2 Independent Operation

In the independent mode of operation, the turbine generator supplies the entire electrical load of the plant, and the control system acts to respond as quickly as possible to load changes, to generate the required power level, and to return the frequency to the desired value (60 HZ). Since the frequency is an important parameter, particular attention is required to insure that no deviation greater than 0.3 Hz (0.5 percent) is encountered for the largest step change in plant load which might occur. Again, regulation of steam conditions, feedwater flow, and Syltherm 800 flow are accomplished by various control subsystems which will be described.

B.6.1.4 Control System Synthesis

In order to achieve the control objectives including the regulation of load, turbine-generator speed, steam temperature, steam pressure, feedwater flow, and Syltherm 800 flow, a number of control subsystems are required. These are summarized in Figure B-32. Each subsystem is briefly discussed in this section.

B.6.1.4.1 Turbine Valve Control

The steam turbine control valve is position regulated, with an assumed first-order time constant of 0.1 second, in order to provide a fast and accurate response to the valve position reference from the

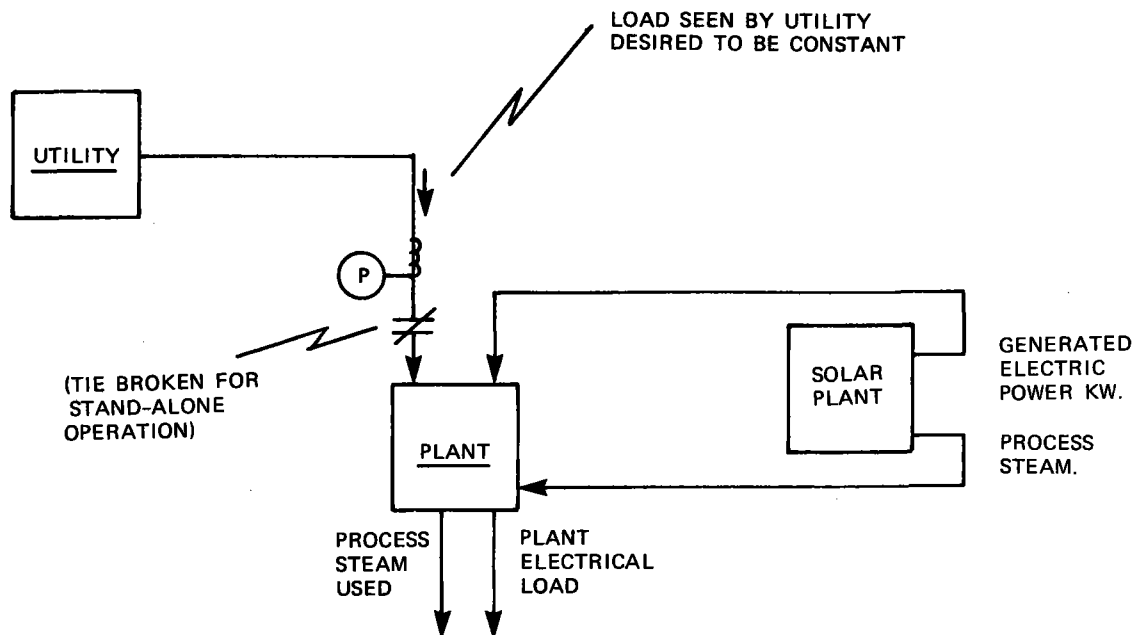


Figure B-31. Utility Interface Configuration

turbine-generator speed/load control system. The turbine control valve will have at least ten percent over-travel capability beyond the full load rated flow condition in order to provide the required degree of transient response forcing. Signals indicating valve limits are to be made available to the turbine-generator control. The valve and its position regulator are not considered in further detail in this examination of the overall system behavior but will be developed during the hardware definition phase of the project.

B.6.1.4.2 Turbine-Generator Speed/Load Control

The turbine-generator speed/load control has a dual function, providing speed governor control as well as a means of achieving the desired load output from the unit in the interconnected mode. In the independent mode, the full-speed, no-load reference is compared to the measured speed. The controller responds to the resultant error signal and provides a turbine control valve position reference. The controller is to have a reset function in this mode (only) to force the error signal to zero, providing isochronous operation (at 60 Hz). Anti-reset windup feature is required for the controller to act when turbine control valve limit conditions are encountered.

In the interconnected mode, the speed/load control is to exhibit a conventional governor characteristic with five percent droop (no reset). Figure B-33 indicates the configuration of this control subsystem with gains and stabilization networks chosen based on simulation results discussed in Section B.6.1.6.

B.6.1.4.3 Utility Power Load Control

The measured power from the utility tie is compared with the normal desired value (100 kW), and the difference acts to adjust the reference to the turbine generator speed/load control. When the measured power exceeds the reference value, the regulator increases the demand to the turbine control. As indicated in Figure B-34, the integral plus proportional controller is followed by a limiter function for minimum, maximum, and rate of change limits. The lead stabilization value is based on counteracting the dominant

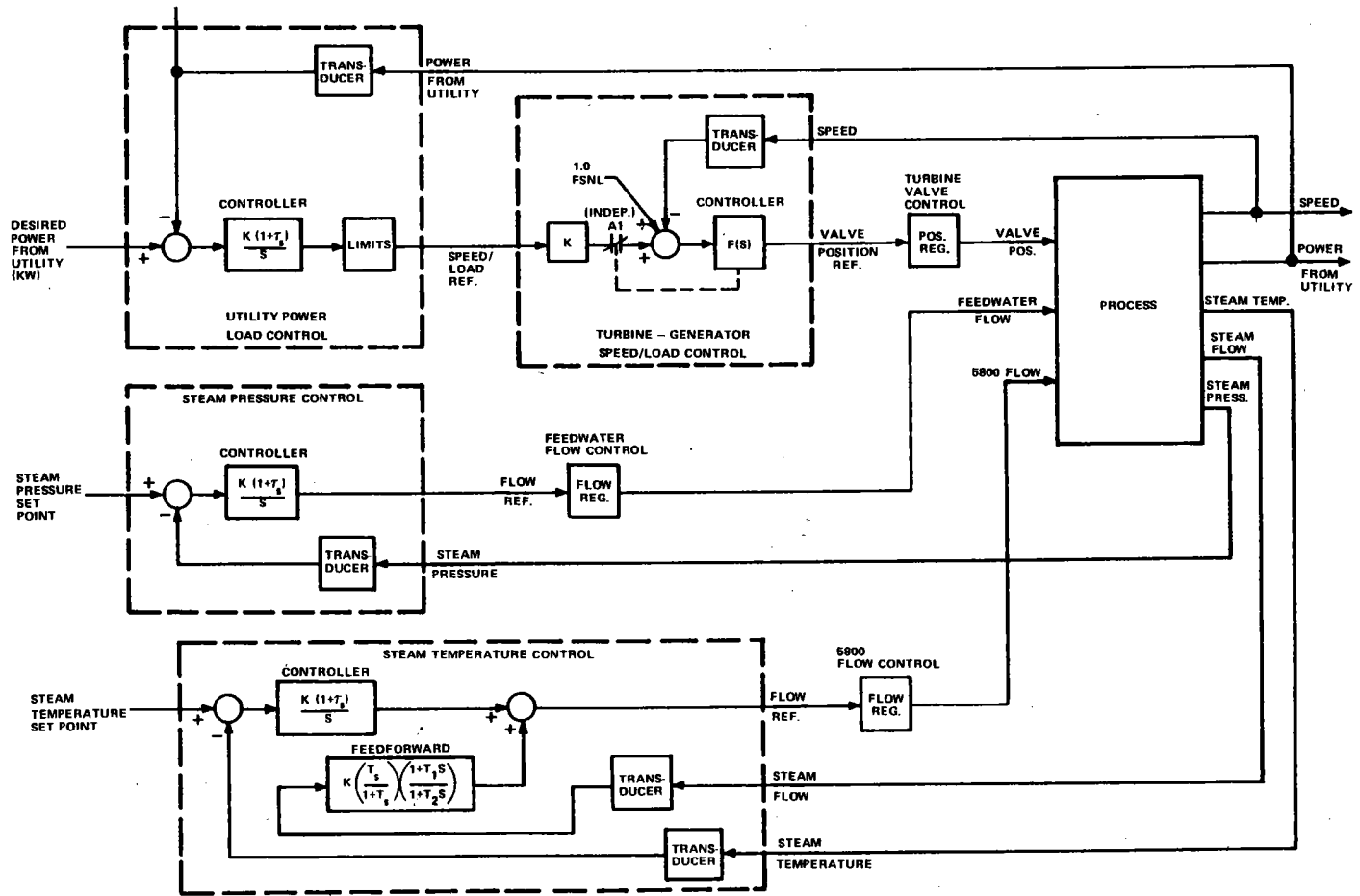
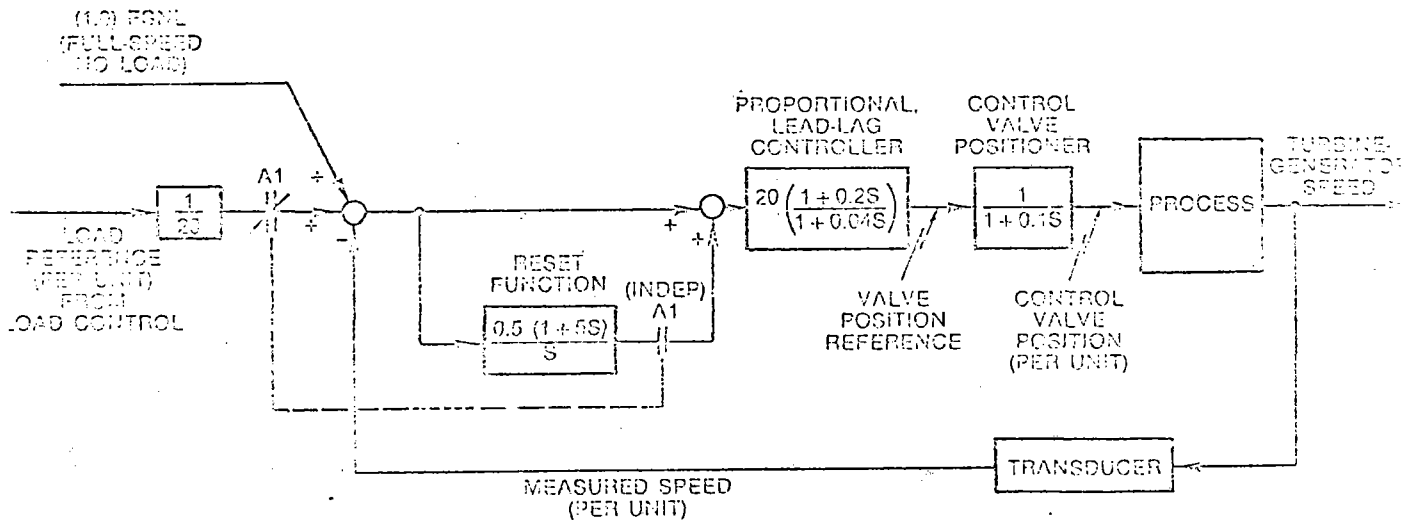


Figure B-32. Overall Control System Summary



NOTE: A1 SWITCH ACTIVATED FOR INDEPENDENT (ISOCHRONOUS) OPERATION

Figure B-33. Turbine-Generator Speed/Load Governor Control (For Both Interconnected And Independent Operation)

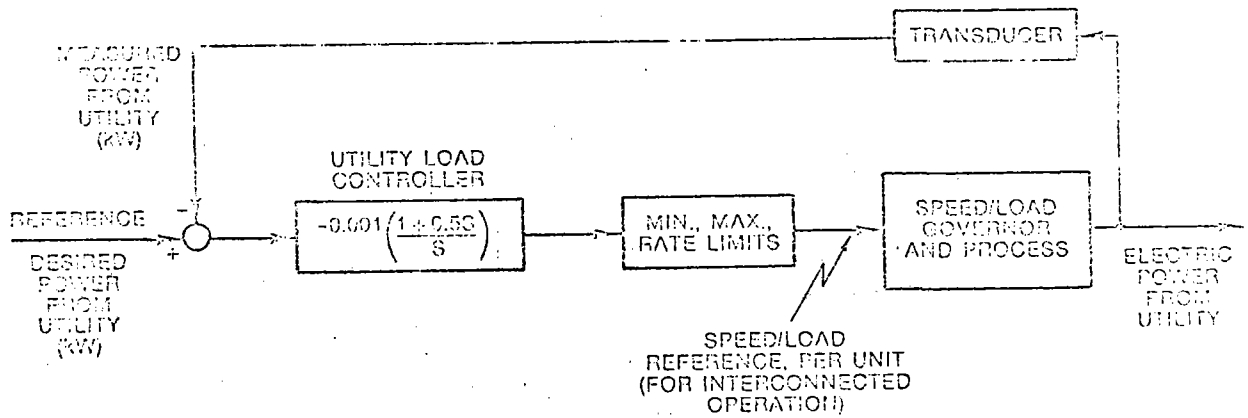


Figure B-34. Utility Power Load Control

transient characteristic of the speed/load regulator. The controller is furnished with an anti-reset windup feature to prevent regulator saturation when detected limits are encountered.

B.6.1.4.4 Feedwater Flow Control

The feedwater supplied to the steam generator is controlled to a regulated flow with the flow reference signal supplied by the steam pressure control. The flow control loop provides a faster and more consistent valve response as seen by the pressure controller and overcomes potential difficulties which might be caused by valve non-linearity, friction, sticking, and repeatability characteristics. It is assumed that the flow regulator closed-loop response is a first order lag with a one-sixth second time constant. The particulars of this regulator, including pump characteristics, bypass, valve response, etc., are not considered in further detail in this examination of the overall system behavior. It is assumed that the desired characteristics can be realized during the hardware definition phase of the project

B.6.1.4.5 Steam Pressure Control

The steam pressure control compares the pressure of the steam at the inlet of the turbine control valve to the desired reference. The controller, as indicated in Figure B-35 provides the reference signal to the feedwater flow control regulator. The integral plus proportional lead stabilization was chosen to provide an adequate phase margin for stability of response based on the examination of the simulation results. The controller is to be furnished with anti-reset windup.

B.6.1.4.6 Syltherm 800 Flow Control

The heating fluid (Syltherm 800) supplied to the steam generator is controlled to a regulated flow with the flow reference signal supplied by the steam temperature control. This regulator provides a faster and more consistent valve response than would than would an open-loop approach. It is assumed that during the hardware definition phase of the project, the desired one second time constant for the Syltherm 800 flow regulation can be achieved with appropriate design of this subsystem.

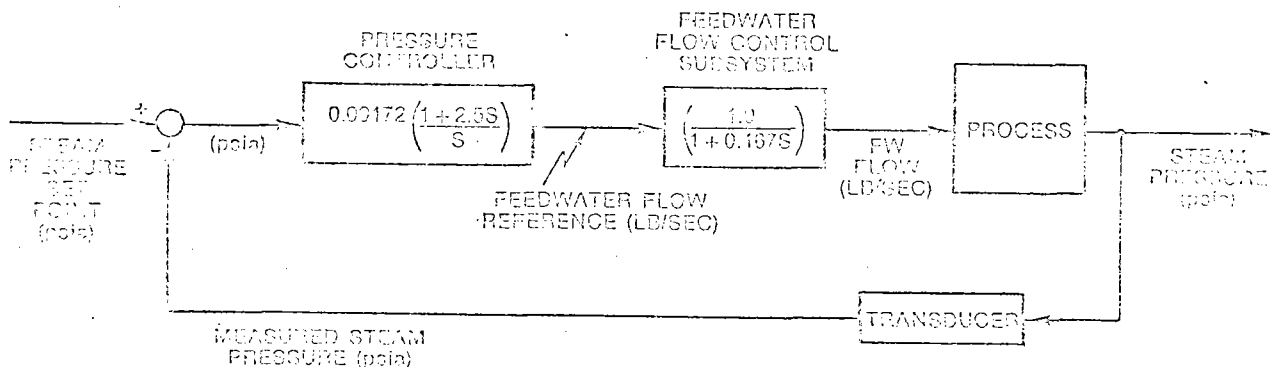


Figure B-35. Steam Pressure Control

B. 6. 1. 4. 7 Steam Temperature Control

Regulation of the temperature of the steam ahead of the turbine control valve is accomplished by adjusting the flow of heating fluid (Syltherm 800) to the steam generator. As shown in Figure B-36, the steam temperature setpoint is compared to the measured temperature, and the error acts through an integral plus proportional controller to change the reference to the Syltherm 800 flow control loop. For adequate speed of response to rapid changes in steam flow, however, an anticipatory (feed-forward) signal is also required in order to minimize the magnitude of resulting steam temperature errors. As shown, the feed-forward signal which is derived from measured steam flow utilizes a lead-lag network plus a very slow wash-out effect, $40s/(1+40s)$. In this way, rapid speed of response is achieved, and the feed-forward signal is easily kept in range, consistent with the ability of the integral plus proportional controller to provide the required reset function. The control system stabilization and gain values were chosen based on transient simulation of the system.

B. 6. 2 TRANSIENT SIMULATION DESCRIPTION

B. 6. 2. 1 General

A dynamic simulation of the process and its control was undertaken to permit the development and analysis of the control system behavior and overall performance. The simulation was implemented using digital computer programs written in FORTRAN. For simplicity, the Euler method of numerical integration' was utilized for the solution of the differential equations with the compute time interval chosen suitably small to make the solution essentially insensitive to the value chosen.

The program for transient simulation of the control system (see Section B. 6. 1, Figures B-32 through B-36) is straightforward. The representation of the dynamic elements utilizes usual techniques of derivative evaluation for each time step based on parameters calculated following the integration from preceding time increment. For example, Figure B-37 illustrates the formulation of the proportional plus integral controller for the steam pressure control. The outputs of the various control subsystems are provided as inputs to the process simulation (Figure B-38).

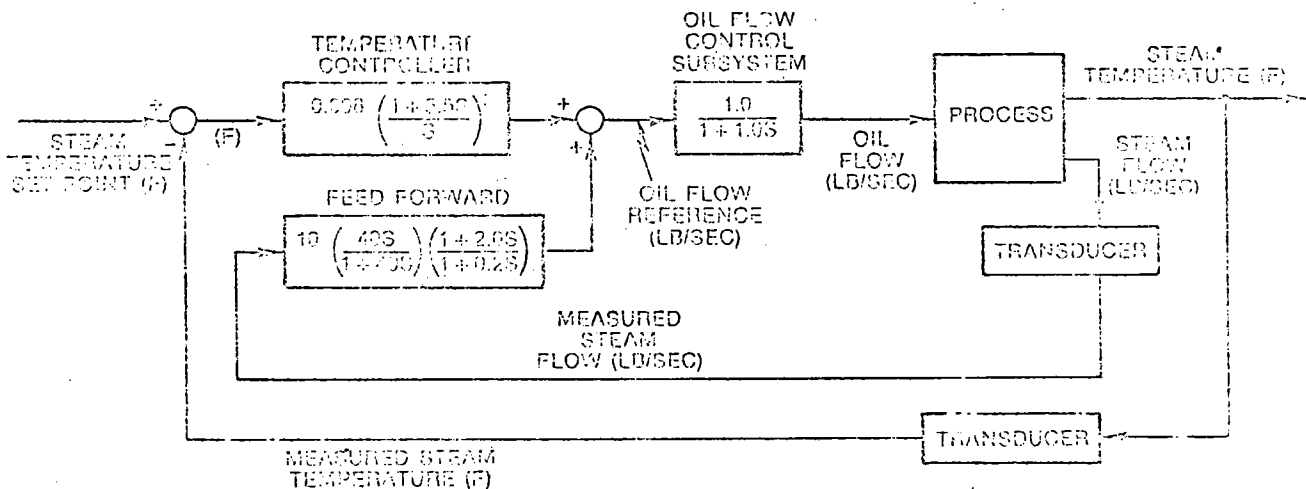
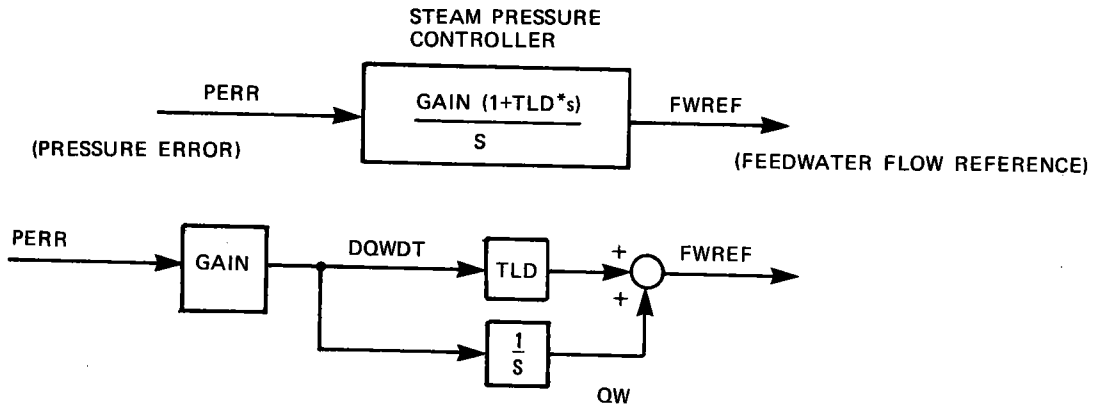


Figure B-36. Steam Temperature Control



- $DQWDT = GAIN * PERR$
- $FWREF = QW + TLD * DQWDT$
- $QW = QW + DQWDT * DT$ } INCLUDED IN INTEGRATION ROUTINE

Figure B-37. Simulation Formulation Of Proportional Plus Integral Controller

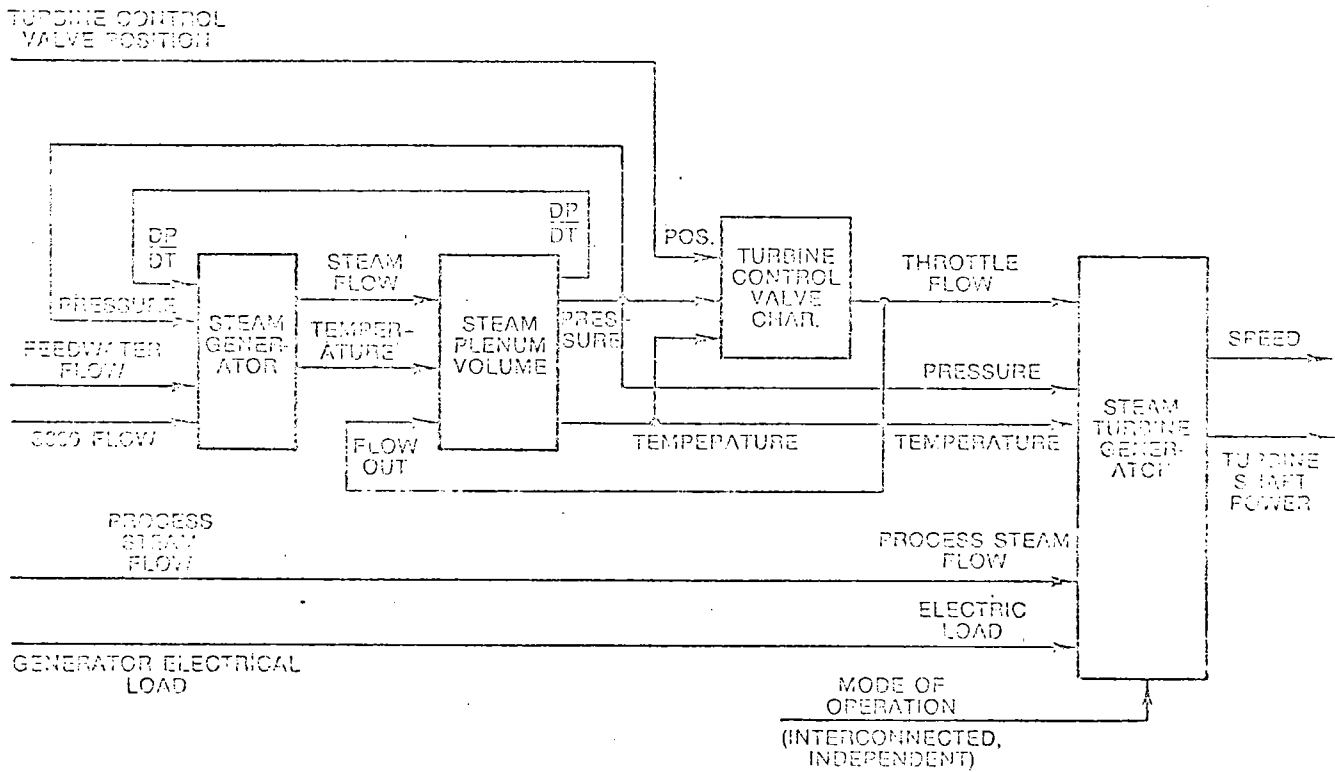


Figure B-38. Elements Of The Process Representation

The four elements of the process representation

1. Steam generator
2. Steam plenum volume
3. Turbine control valve characteristics
4. Steam turbine generator

were mentioned briefly in Section B.6.1.5. The simulation of these process elements is examined in more detail in the following sections.

B.6.2.2 Finite Slice Boiler Model

A detailed finite slice mathematical model for the steam generator was developed based on first principles. The object was to demonstrate clearly the steady state and transient characteristics of the boiler thereby permitting the overall control system to be formulated with a minimum of assumptions regarding the fundamental process behavior.

Since the detailed boiler model might be costly to run on the computer as part of the overall system response production runs, the creation of a simplified lumped parameter model of the boiler was planned which would approximate the behavior of the more detailed model. The lumped parameter model would then be used for subsequent work.

For the development of the finite slice model, a number of process behavior approximations and assumptions were made in order to simplify the analysis considering the time frame and level of effort allocated to the project. The assumptions are discussed in the descriptions to follow. Results are discussed in Section B.6.2.2.3.

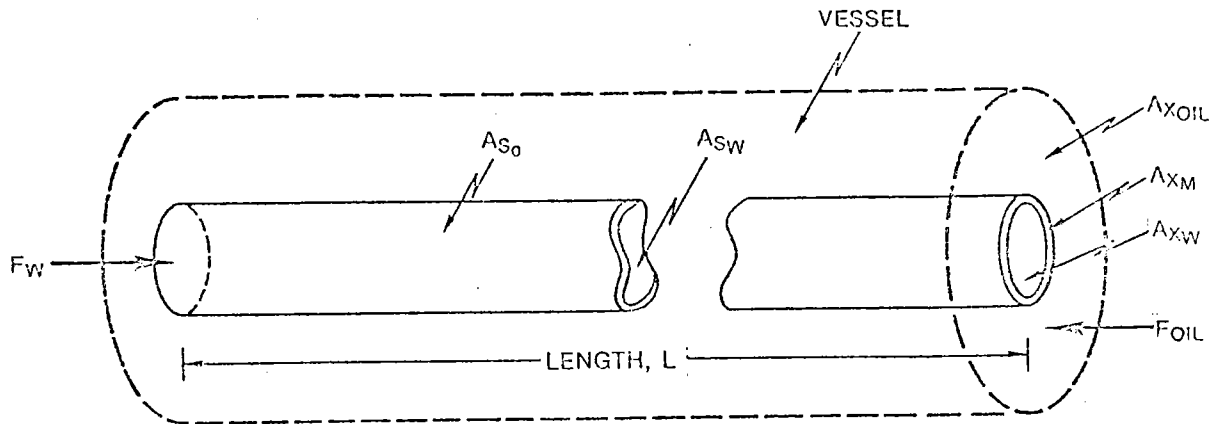
B.6.2.2.1 General Description of the Boiler

For the purpose of simulation, the boiler is assumed to consist of a single pass, tube-in-shell, counter-flow heat exchanger with water on the inside and oil on the outside as indicated in Figure B-39. It is assumed that incoming Syltherm 800 temperature is maintained constant at 672^oK, and the incoming feedwater temperature is 466^oK (380^oF). The boundary locations for the economizer, evaporator, and superheater zones will vary as a function of the flows and temperatures. The steam which exits from the steam generator tubes enters a steam plenum volume which is modeled separately.

B.6.2.2.2 Finite Slice Analytical Approach

Several fundamental simplifying assumptions are made in the derivation of the finite slice model of the steam generator. It was felt that these assumptions would enable development of the model within the project schedule constraints and available level of effort while still representing the dominant process behavior characteristics. Three of the more significant assumptions are:

1. Pressure drop along the length of the boiler tubes is ignored; at a given instant all elements are assumed to have the same water/steam pressure.
2. The water/steam mixture in the evaporator region is considered as a uniform mixture for a given element (slice) having density and enthalpy values as a function of the fluid quality.
3. Metal-to-water heat transfer coefficient value is a function of the steam quality estimated to peak (nucleate boiling) at $X = 0.3$.



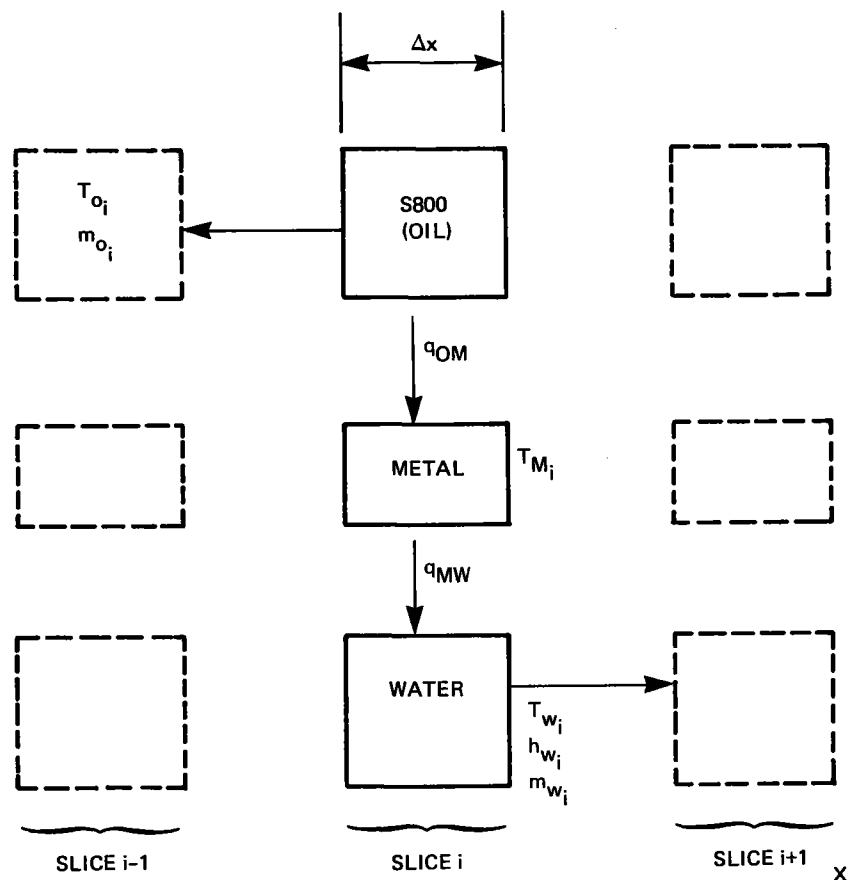
L	— 2.5 ft — Length of boiler
A_{XOIL}	— 0.5 ft ² — Flow area of oil (S800 heating fluid)
A_{XM}	— 0.1 ft ² — Cross sectional area of tube metal
A_{XW}	— 0.12 ft ² — Flow area of water
$\Delta A_{SO}/\Delta X$	— 40 ft ² /ft — Surface area per unit length, oil to metal, total
$\Delta A_{SW}/\Delta X$	— 20 ft ² /ft — Surface area per unit length, metal to water, total
Fw	— VAR. — Water flow into boiler
FOIL	— VAR. — Oil flow into boiler

Figure B-39. Boiler Parameters

The implications of these and other assumptions are discussed further in Section B.7 along with the derivation of the equations for the model.

The basic relationships for the finite slice steam generator model are indicated in Figure B-40. Nomenclature is given in Section B.7. The three differential equations for each slice are for time rates of change of oil temperature, metal temperature, and water enthalpy. The specific heat of the oil is assumed constant, and steam table properties are used for the water. The water (steam) flow from a slice is affected by rate of change of pressure which is considered to be the dominant effect. The heat transfer from oil to metal and from metal to water is considered to be a function of average temperature differences, surface area, and heat transfer coefficients. The boundary conditions are dictated by incoming feedwater conditions and incoming Syltherm 800 (oil) conditions.

A FORTRAN digital computer program, BLRSM, was written to implement the finite slice model relationships. The user furnishes initial condition values of feedwater incoming temperature, flow and pressure; incoming Syltherm 800 (oil) temperature and flow; and boiler physical parameters (lengths, areas, heat transfer coefficients, etc.). To calculate the steady state initial conditions and the transient response to a defined disturbance, the program follows the general calculation procedure summarized in Table B-1.



$$\frac{\Delta T_{O_i}}{\Delta t} = \frac{1}{\rho_{OIL} A_{X_{OIL}}} \left[-\frac{q_{OM}}{C_{P_O} \Delta X} + \dot{m}_O \frac{\Delta T_O}{\Delta x} \right] \quad (1)$$

$$\frac{\Delta T_{M_i}}{\Delta t} = \frac{1}{\rho_M A_{X_M} \Delta x C_{P_M}} [q_{OM} - q_{MW}] \quad (2)$$

$$\frac{\Delta h_{W_i}}{\Delta t} = \frac{1}{\rho_W A_{X_W}} \left[\frac{q_{MW}}{\Delta x} - \dot{m}_W \frac{\Delta h_W}{\Delta x} \right] + \frac{144}{778 \rho_W} \left(\frac{dp}{dt} \right) \quad (3)$$

$$\dot{m}_{W_i} \cong \dot{m}_{W_{i-1}} - A_{X_W} \Delta x \left. \frac{\partial \rho}{\partial p} \right|_{T=T_W} \frac{dp}{dt} \quad (4)$$

$$q_{OM} = h_{X_O} \left(\frac{\Delta A_{S_O}}{\Delta x} \right) \Delta x \left(\frac{T_{O_i} + T_{O_{i+1}}}{2} - T_{M_i} \right) \quad (5)$$

$$q_{MW} = h_{X_W} \left(\frac{\Delta A_{S_W}}{\Delta x} \right) \Delta x \left(T_{M_i} + \frac{T_{W_i} + T_{W_{i-1}}}{2} \right) \quad (6)$$

$$\dot{m}_O \left(\frac{\Delta T_O}{\Delta x} \right) = \frac{\dot{m}_O}{\Delta x} (T_{O_{i+1}} - T_{O_i}) \quad (7)$$

$$m_W \left(\frac{\Delta h_W}{\Delta x} \right) = \frac{\dot{m}_{W_i} h_{W_i} - \dot{m}_{W_{i-1}} h_{W_{i-1}}}{\Delta x} \quad (8)$$

BOUNDARY CONDITIONS

$T_{W_i=0}$ = INCOMING FEEDWATER TEMPERATURE

$T_{O_i=NSL+1}$ = INCOMING S800 (OIL) TEMPERATURE

$\dot{m}_{W_i=0}$ = FEEDWATER FLOW

Figure B-40. Finite Slice Steam Generator Model

Table B-1. Calculation Procedure

(A) STEADY STATE INITIAL CONDITION CALCULATION:

1. Assume value for outgoing oil temperature ($T_{o_i = 1}$).
2. Beginning with slice 1, calculate heat/mass balance for slice, resulting in h_{w_i} , T_{m_i} and $T_{o_i + 1}$ (assuming time-derivatives are zero).
3. Repeat for next slice. Continue until all slices are calculated.
4. Examine calculated incoming oil temperature for the last slice ($T_{ONSL + 1}$) and compare with the specified initial condition value. Based on the error, adjust the assumed value for $T_{o_i = 1}$ and repeat from step 2 until iteration convergence is achieved.
5. Print out initial condition results; temperatures, enthalpy, fluid quality, derivatives, for each slice.

(B) TRANSIENT RESPONSE CALCULATION:

1. Apply disturbance (e. g., change in flow rates, pressure, incoming temperature, etc.).
2. Calculate time derivatives for oil temperature, metal temperature and water enthalpy, for each slice.
3. Perform numerical integration of derivatives, calculating new conditions for each slice.
4. Print out the calculated conditions for selected print intervals.
5. Return to step 2 for the next time step.

B.6.2.2.3 Finite Slice Model Simulation Results

Various simulation computer runs were made not only to reveal the steam generator process behavior but also to show the sensitivity of the model to the simulation parameters (e. g., number of slices and compute time intervals). It was concluded that a twenty slice model with a 0.02 second computer interval was suitable for the boiler characteristics and process flow rates of interest.

B.6.2.3 Lumped Parameter Boiler Model

A simplified lumped parameter representation of the steam generator was formulated to approximate the process behavior exhibited by the finite slice model. A FORTRAN digital computer program, LMPSM, was written to implement the lumped parameter model relationships. This approach permits a simple process model of the boiler to be incorporated into the overall system simulation.

The lumped parameter model responds to variations in feedwater flow, Syltherm 800 (oil) flow, and water pressure and rate of change of pressure. The output is steam temperature as a function of time. The calculation procedure is given in Figure B-41. It will be noted that a steady state steam temperature is calculated

$$T_{wSS} = T_{wBASE} + \left(\frac{\partial T}{\partial F_o} \right) (F_{OIL} - F_{OIL_{BASE}}) + \left(\frac{\partial T}{\partial F_w} \right) (F_w - F_{w_{BASE}}) + \left(\frac{\partial T}{\partial P} \right) (P - P_{BASE})$$

based on partial derivative values and variations from parameter base values. The magnitude of the partial derivatives are polarity sensitive as indicated by the results of the computer runs. The calculated steady state temperature T_{wSS} is constrained to have a value no larger than the incoming oil temperature by suitable modification of the temperature contribution attributed to the oil flow as shown.

The transient characteristics for the parameter variations were chosen to provide a reasonably close match to the finite slice model results. The relationships which were implemented are polarity sensitive only in magnitude, being chosen to represent the more severe system transient of increased process flows and decreasing pressure.

8.6.2.4 Steam Plenum And Turbine Control Valve

The steam flow from the boiler enters the steam plenum, whose storage comprises a node for pressure-flow relationships. The steam which exits from the plenum then passes through the turbine control valve. The resulting throttle flow is then utilized by the plenum representation in the simulation as indicated in Figure B-38. A detailed representation of the plenum was developed as shown in Figure B-42 and Table B-2. However, for simplicity, it was decided to use a less detailed plenum model which does not use steam table relationships and considers the dynamic effects of pressure along (exit temperature is assumed equal to incoming temperature).

This representation and its derivation are given in Figures B-43 and Table B-3. The simplified approach was selected for use based on the small plenum volume and the small time constant associated with temperature differences across the plenum compared to the large temperature time constant of the boiler.

B.6.2.5 Steam Turbine Model

The linearized representation of the steam turbine characteristics is shown in Figure B-44. The input variables are throttle flow, temperature, pressure, and process steam (extraction) flow as well as generator electrical load. Variations from base values are then applied to partial derivative values to arrive at the variation from the base turbine power. The shaft acceleration is calculated based upon the available acceleration power and the machine inertia. An additional input is the mode of operation indicator. For interconnected operation (tied to utility grid), the electric load is set equal to the turbine power times generator efficiency, and the resulting acceleration will be zero.

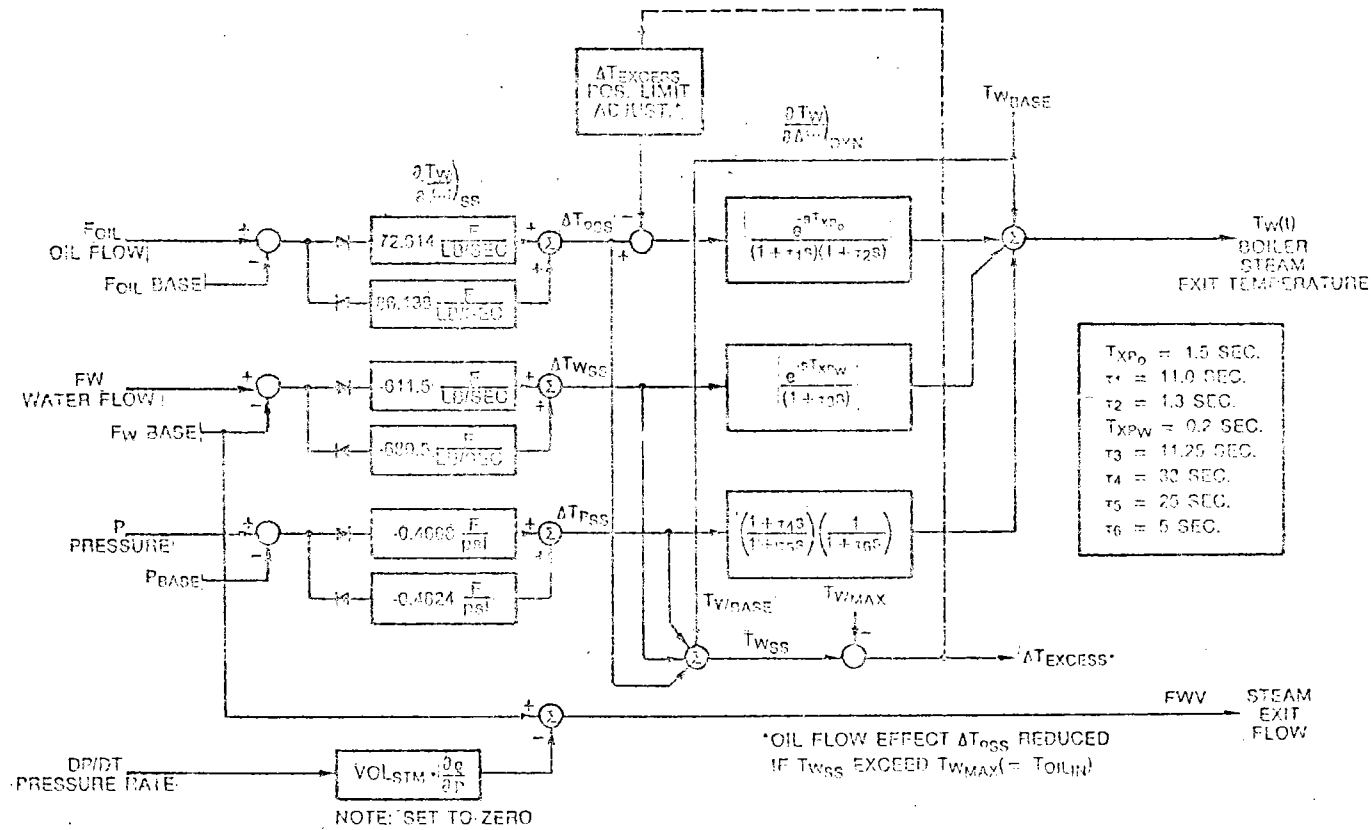
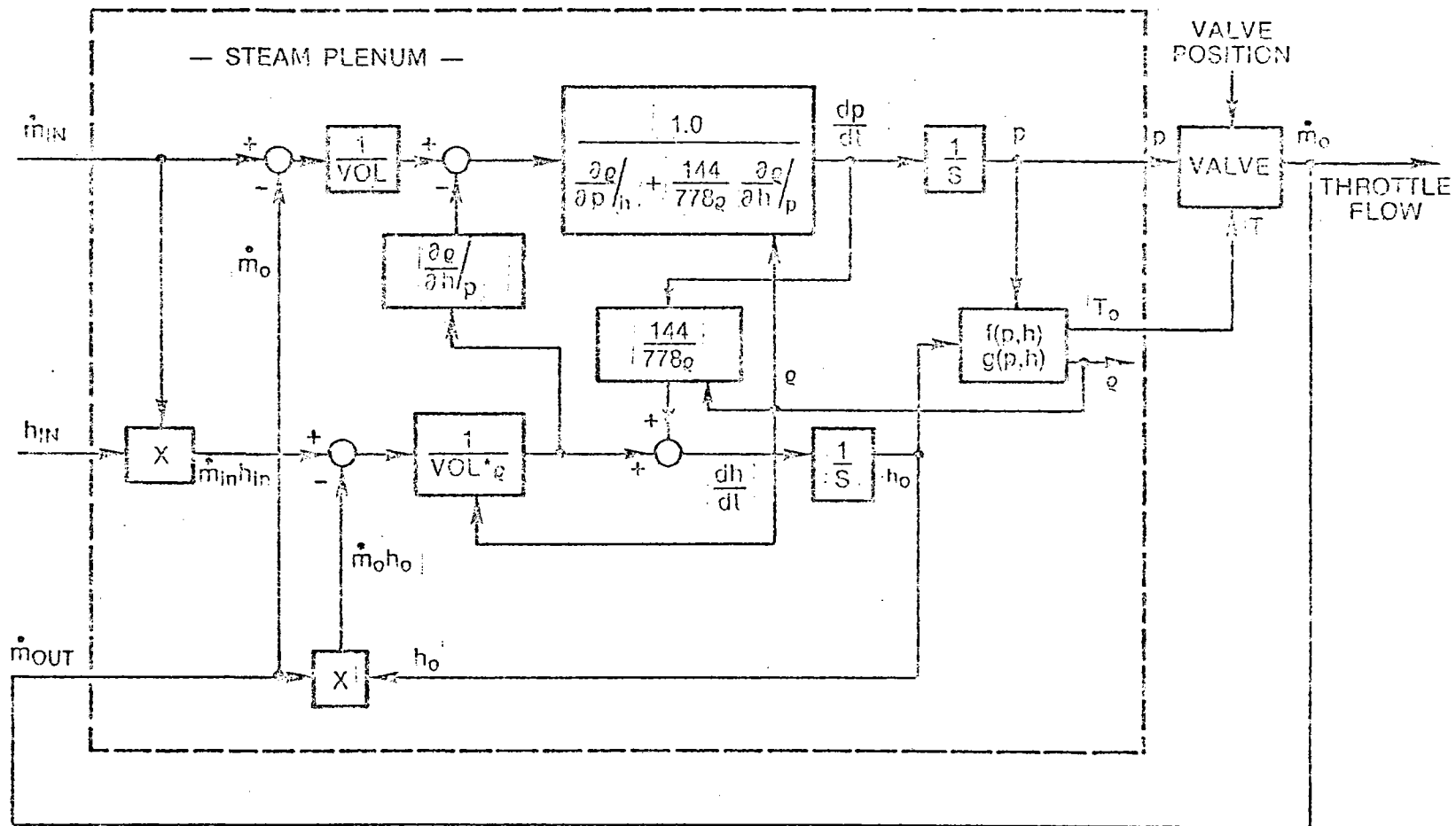


Figure B-41. Linearized Lumped Parameter Dynamic Simulation Model Of Steam Generator



NOTE: PARTIAL DERIVATIVES EVALUATED
USING STEAM TABLES

Figure B-42. Detailed Representation of Steam Plenum

Table B-2. Derivation of Detailed Representation of Steam Plenum

$$\frac{\dot{m}_{in} - \dot{m}_{out}}{VOL} = \frac{d\rho}{dt} = \left. \frac{\partial \rho}{\partial p} \right|_h \frac{dh}{dt} + \left. \frac{\partial \rho}{\partial h} \right|_p \frac{dh}{dt} \quad (1)$$

$$\text{Since } \rho = f(p, h) \quad (2)$$

Solving for the rate of change of pressure:

$$\frac{dp}{dt} = \frac{\frac{\dot{m}_{in} - \dot{m}_{out}}{VOL} - \left. \frac{\partial \rho}{\partial h} \right|_p \frac{dh}{dt}}{\left. \frac{\partial \rho}{\partial p} \right|_h} \quad (3)$$

$$\text{But } \frac{dh}{dt} = \frac{\dot{m}_{in} h_{in} - \dot{m}_o h_o}{VOL} + \frac{144}{778 \rho} \frac{dp}{dt} \quad (4)$$

Substitute (4) into (3), rearrange, and solve for $\frac{dp}{dt}$

$$\frac{dp}{dt} = \frac{\frac{\dot{m}_{in} - \dot{m}_{out}}{VOL} - \left. \frac{\partial \rho}{\partial h} \right|_p \left(\frac{\dot{m}_{in} h_{in} - \dot{m}_o h_o}{VOL} \right)}{\left. \frac{\partial \rho}{\partial p} \right|_h + \left. \frac{\partial \rho}{\partial h} \right|_p \frac{144}{778 \rho}} \quad (5)$$

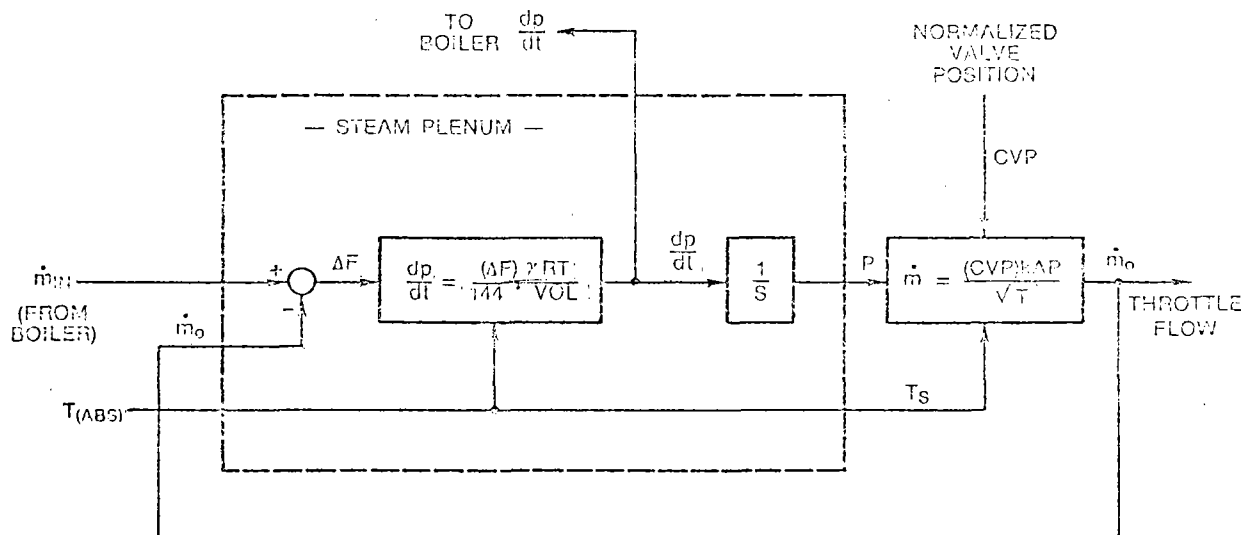


Figure B-43. Simplified Representation of Steam Plenum and Turbine Control Valve

Table B-3. Derivation of Simplified Representation of Steam Plenum

$$(\dot{m}_{in} - \dot{m}_{out}) = VOL * \frac{d\rho}{dt} \quad (1)$$

$$p\rho^{-\gamma} = \text{constant} \quad (2)$$

$$\therefore \frac{dp}{dt} = \frac{\gamma p}{\rho} \frac{d\rho}{dt} \quad (3)$$

$$\frac{p}{\rho} = RT \quad (4)$$

Substitute (4) into (3) and solve for $\frac{d\rho}{dt}$

$$\frac{d\rho}{dt} = \frac{1}{\gamma RT} \left(\frac{dp}{dt} \right) \quad (5)$$

Substitute (5) into (1) and solve for rate of change of pressure

$$\frac{dp}{dt} = \frac{(\dot{m}_{in} - \dot{m}_{out}) \gamma RT}{VOL} \quad (6)$$

The above assumes the superheated steam exhibited perfect gas behavior.

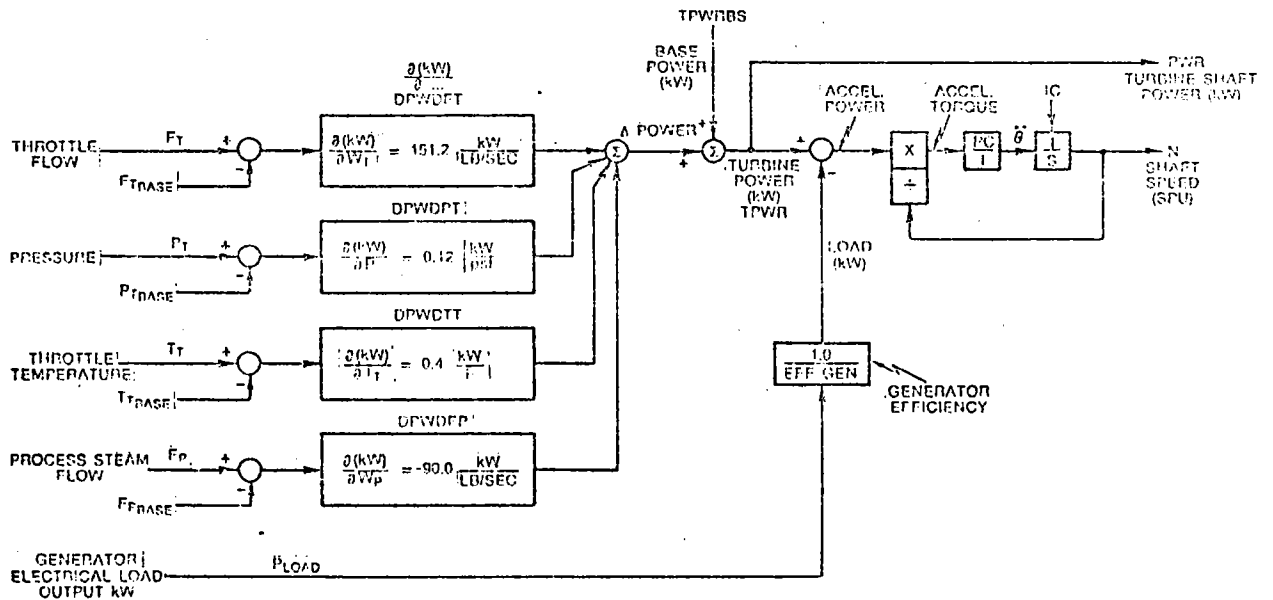
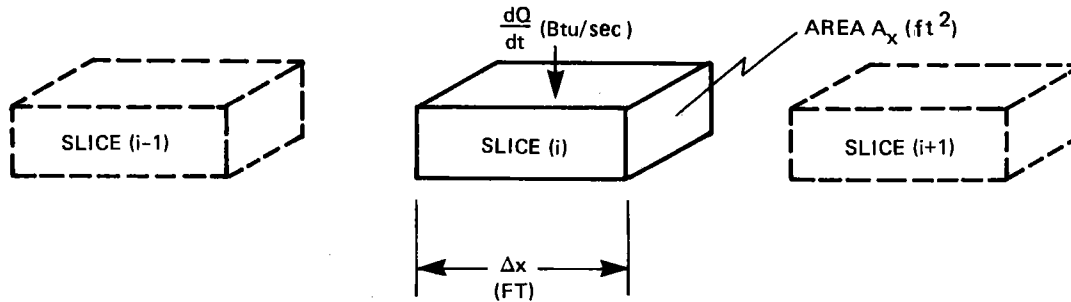


Figure B-44. Linearized Lumped-Parameter Dynamic Simulation Model of Steam Turbine

B.7 DERIVATION OF FINITE SLICE MODEL OF STEAM GENERATOR

Consider a control volume (slice) of water (Steam) experiencing a heat input rate of dQ/dt (Btu/sec).



$$\underbrace{\frac{dQ}{dt} = A_x \Delta x \frac{\partial}{\partial t} (\rho u)}_{\text{first term}} + \underbrace{A_x \Delta x \frac{\partial}{\partial x} (\rho hV)}_{\text{second term}} \quad (1)$$

for the first term, since $u = h - pv$ (2)

$$\frac{\partial (\rho u)}{\partial t} = \frac{\partial (\rho h)}{\partial t} - \frac{\partial}{\partial t} (\rho pv) \quad (3)$$

$$\frac{\partial (\rho u)}{\partial t} = \rho \frac{dh}{dt} + \frac{hd\rho}{dt} - \frac{dp}{dt} \quad (4)$$

for the second term, since $\rho A_x V = \dot{m}$ (lb/sec) (5)

$$A_x \Delta x \frac{\partial (\rho hV)}{\partial x} = \frac{\Delta x \partial (\dot{m}h)}{\partial x} \quad (6)$$

$$= \Delta x \left(\frac{\dot{m} \partial h}{\partial x} + \frac{h \partial \dot{m}}{\partial x} \right) \quad (7)$$

Assume

$$\frac{\partial h}{\partial x} = \frac{h_{\text{out}} - h_{\text{in}}}{\Delta x} \quad (8)$$

and

$$\frac{\partial \dot{m}}{\partial x} = \frac{\dot{m}_{\text{out}} - \dot{m}_{\text{in}}}{\Delta x} \quad (9)$$

Subs. (8) and (9) into (7) and rearrange

$$A_x \Delta x \frac{\partial (\rho hV)}{\partial x} = (\dot{m}_o h_o - \dot{m}_{\text{in}} h_{\text{in}}) + \underbrace{(\dot{m}_o - \dot{m}_{\text{in}}) (h_o - h_{\text{in}})}_{\text{second order effect, neglect.}} \quad (10)$$

$$\text{but } \dot{m}_o = \dot{m}_{in} - \frac{d}{dt} (\rho A_x \Delta x) \quad (11)$$

Combining (11), (10), (4) and (1)

$$\begin{aligned} \frac{dQ}{dt} = A_x \Delta x \left[\rho \frac{dh}{dt} + h \frac{d\rho}{dt} - \frac{dp}{dt} \right] \\ + \Delta x \left[\frac{\dot{m}_{in} (h_o - h_{in})}{\Delta x} - h A_x \frac{d\rho}{dt} \right] \end{aligned} \quad (12)$$

Solving (12) for (dh/dt) for slice i:

$$\frac{dh_i}{dt} = \frac{1}{\rho_{w_i} A_x \Delta x} \left[\left(\frac{dQ}{dt} \right)_i - \dot{m}_{in_w} (h_o - h_{in}) \right] + \frac{144}{778 \rho_{w_i}} \frac{dp}{dt} \quad (13)$$

For flow out of slice i

$$m = \rho A_x \Delta x \quad (14)$$

$$\frac{dm}{dt} = (\dot{m}_{in} - \dot{m}_o) = A_x \Delta x \frac{d\rho}{dt} \quad (15)$$

$$\frac{d\rho}{dt} = \left. \frac{\partial \rho}{\partial p} \right|_T \frac{dp}{dt} + \left. \frac{\partial \rho}{\partial T} \right|_p \frac{dT}{dt} \quad (16)$$

Assuming the dominant effect changing density is the rate of change of pressure, combining (14), (15) and (16) with (dT/dt ≈ 0):

$$\dot{m}_o \cong \dot{m}_{in} - A_x \Delta x \left. \frac{\partial \rho}{\partial p} \right|_T \frac{dp}{dt} \quad (17)$$

the term $\left. \frac{\partial \rho}{\partial p} \right|_T$ is evaluated from steam table data.

For the metal:

$$\frac{dT}{dt} m_i = \frac{1}{\rho_{M_i} C_{pM} A_x M} \left[\left(\frac{dQ}{dt} \right)_i \text{ OIL TO METAL} - \left(\frac{dQ}{dt} \right)_i \text{ METAL TO WATER} \right] \quad (18)$$

Similarly for the oil

$$\frac{dT_{OIL}}{dt}_i = \frac{1}{\rho_{OIL} C_{P_{OIL}} A_{x_{OIL}}} \left[- \left(\frac{dQ}{dt} \right)_i \text{ OIL TO METAL} + \dot{m}_{OIL} C_{P_{OIL}} \frac{\Delta T_{OIL}}{\Delta x} \right] \quad (19)$$

The rates of heat transfer are assumed to be proportional to the temperature differences between the metal and the oil (or water).

$$\frac{dQ}{dt} \text{ OIL TO METAL} = h_{x_o} \left(\frac{\Delta A_{S_o}}{\Delta x} \right) \Delta x (T_{o_{AVG_i}} - T_{M_i}) \quad (20)$$

$$\frac{dQ}{dt} \text{ METAL TO WATER} = h_{x_w} \left(\frac{\Delta A_{S_w}}{\Delta x} \right) \Delta x (T_{M_i} - T_{w_{AVG_i}}) \quad (21)$$

$$\text{where } T_{o_{AVG_i}} = \left(\frac{T_{o_i} + T_{o_{i+1}}}{2} \right) \quad (22)$$

$$T_{w_{AVG_i}} = \left(\frac{T_{w_i} + T_{w_{i-1}}}{2} \right) \quad (23)$$

NOMENCLATURE

- A_S - surface area for heat transfer, ft^2
 A_x - cross sectional area transverse to flow, ft^2
 C_p - specific heat, $\frac{\text{Btu}}{\text{lb.}^\circ\text{F}}$
 F - flow, lb./sec.
 h - enthalpy, Btu/lb
 h_x - heat transfer coefficient, $\text{Btu/sec. ft}^2\ ^\circ\text{F}$
 i - slice index
 m - lbs. mass, lb
 \dot{m} - flow, lb./sec
 p - pressure, psia
 Q - heat, Btu
 t - time, sec
 T - temperature, deg. F
 u - internal energy, Btu/lb
 v - specific volume, $\text{ft.}^3/\text{lb}$
 V - velocity, ft/sec
 x - slice length, ft

APPENDIX C
SOLAR TOTAL ENERGY SYSTEM (STES) COMPUTER CODE

APPENDIX C

SOLAR TOTAL ENERGY SYSTEM (STES)

COMPUTER CODE

The General Electric developed STES computer code was utilized for system performance calculations for the STE-LSE at Shenandoah. The code is structured, as is typical of annual solar system simulation codes, with a main driver program containing input and output sections and with a number of subroutines which model the performance of the components/subsystems in the system. Figure C-1 shows the top level flow chart for the code, identifying the major sections which will be covered separately below.

C.1 INPUT

System inputs include the following three categories:

1. Load profiles - Synthesized Bleyle Plant electrical and process steam demand profiles
2. Loads/weather tape - A composite hourly tape containing climatology data such as direct insolation, ambient temperature, etc., for the site and space cooling/heating loads calculated using the Building Transient Thermal Load (BTTL) computer code for the Bleyle Plant and climatology (see Appendix A).
3. System design information - Data such as number of dish collectors, storage size, etc., which defines the system being evaluated.

C.2 OUTPUT

The output section provides printout of simulation data at hourly, daily, monthly, and annual intervals. Data includes system operation information such as temperatures, flows, etc., which is more typical of hourly printout, as well as a complete energy balance identifying all electrical and thermal loads and their load supplying source.

C.3 MAIN DRIVER

The main driver routine controls the simulation to generate the desired performance evaluation output on the basis of the system inputs and component performance models. As such, it maintains the simulation hourly time step and, in doing so, updates and sums the numerous variables which reflect the system energy balance. Within each time step, the driver routine calls the various component subroutines based on the system operating plan control logic, the weather/loads tape, and the weekday/weekend Bleyle plant operation. Also, based on component operation, the routine sums up operating parasitics.

C.4 COLLECTOR SUBROUTINES

The parabolic dish solar collector field performance is modeled through use of seven collector subroutines. These subroutines are called upon by the main driver program according to the operating plan logic, the state of the collector field, and the hourly direct normal insolation after correction by a dish field shading factor. Three modes of operation are modeled for the collector field:

1. Normal operation - generating 672°K (750°F) fluid exiting from dish via flow control in proportion to the direct normal insolation

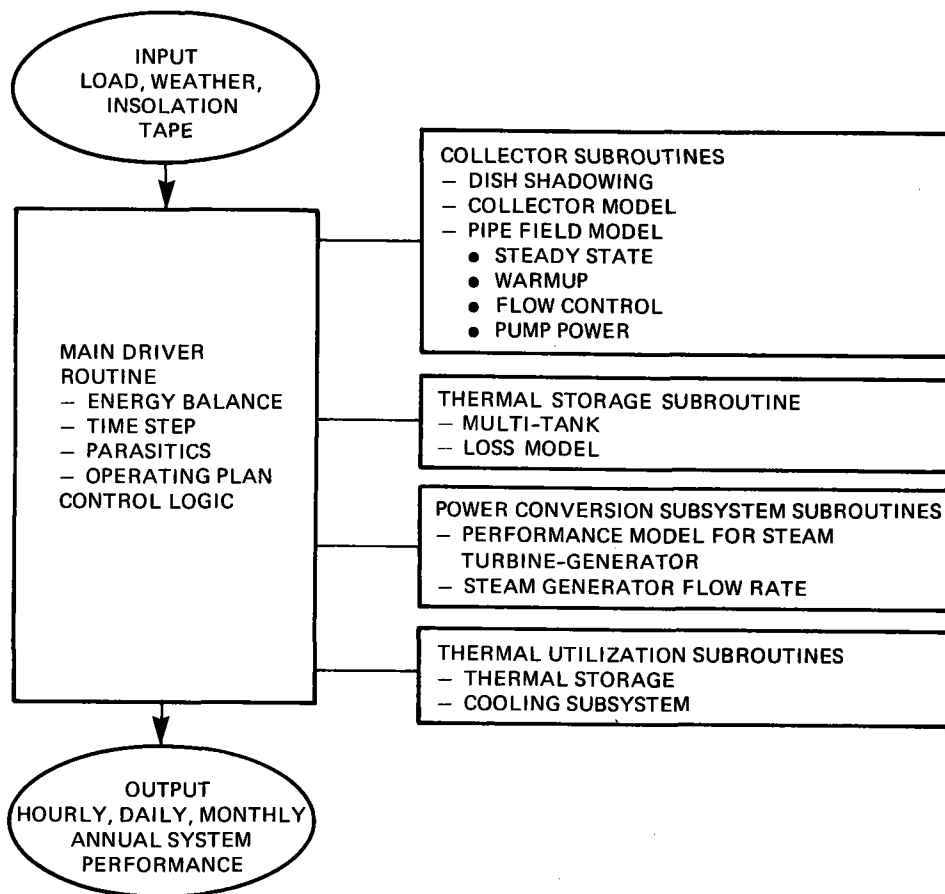


Figure C-1. STES Computer Code

2. Field warmup - Startup collection/recirculation to heat field mass to normal operating temperatures.
3. Cool down - field mass cools during shutdown when insolation is inadequate.

Figure C-2 shows the collector field subroutines flowchart identifying the subroutines utilized in each mode and the logic. A discussion of the individual subroutines follow.

C.4.1 SUBROUTINE SHADE (COLLECTOR FIELD SHADING FACTOR)

The parabolic dish solar collector field shading subroutine used in the STES code was generated at Sandia Labs. The subroutine logic is based on an eight dish repeating pattern which represents a field shading unit cell as shown in Figure C-3. The central dish in the pattern is designated the shadowing dish, and the subroutine calculates the shadow, if any, that this dish casts on the seven surrounding dishes. Recognition of the fact that all dishes in the field act as a shadowing dish, because of the choice of the eight dish repeating pattern, allows for calculation of an overall field shadowing factor neglecting edge effects. The subroutine is sensitive to all pertinent design variables including dish diameter, dish spacing (north/south and east/west), field slope (north/south and east/west), as well as latitude, time of day, etc., which define the sun position. Subroutine shade is called once a day. It calculates 48 half hour shadowing factors which are subsequently averaged to provide the hourly shadowing factors used in the remainder of the collector subroutines.

C.4.2 SUBROUTINE FIELDFLOW (COLLECTOR FIELD FLOWRATE)

This subroutine calculates the collector field Syltherm-800 flowrate which produces a 672°K (750°F) dish receiver outlet temperature based on insolation ambient temperature, field inlet temperature, and collector and pipefield performance models. The subroutine consists of two sections - initialization and calculation. The initialization section is called at the start of each yearly simulation. The first step is to make a sequence of calls to the steady state collector field piping thermal loss subroutine (see following discussion) to establish the relationship between the collector field inlet piping Δt as a function of Syltherm 800 flow rate for a constant 291°K (65°F) ambient temperature for the particular pipefield design. Next, a sequence of calls is made to the dish collector subroutine (see following discussion) to establish the relationship between receiver thermal losses and ambient temperature for the particular receiver design operating between 533°K (500°F) and 672°K (750°F). These two data sets are stored for subsequent use, completing the initialization section.

The flowrate calculation section is called each hour of the day that the collector field is in the normal operating mode. The first step is to employ a computer system software routine for polynomial interpolation to approximate the receiver thermal loss based on the stored data from the initialization section and the actual ambient temperature. Next, based on the incident insolation (provided from the collector subroutine optical section covered in following section), the approximate thermal loss, and Syltherm 800 fluid properties, an initial estimate of the Syltherm 800 flow is made. Then, based on this flowrate estimate, an approximation of the field inlet piping Δt is made using the interpolating polynomial and the other set of data from the initialization section. The flowrate is then corrected to accommodate the inlet piping Δt for subsequent use.

Typically, this approach generates a flowrate which, when used in the steady state thermal loss and dish collector subroutines, results in a receiver outlet temperature of $672 \pm 0.3^\circ\text{K}$ ($750 \pm .5^\circ\text{F}$).

C.4.3 SUBROUTINE SSDPL (STEADY STATE DISH COLLECTOR FIELD PIPING THERMAL LOSS)

This subroutine calculates the steady state pipefield thermal losses and temperature drop of the Syltherm 800 fluid for the dish collector field. It consists of two sections, field inlet piping and field outlet piping, which are appropriately called just before and just after the dish collector subroutine.

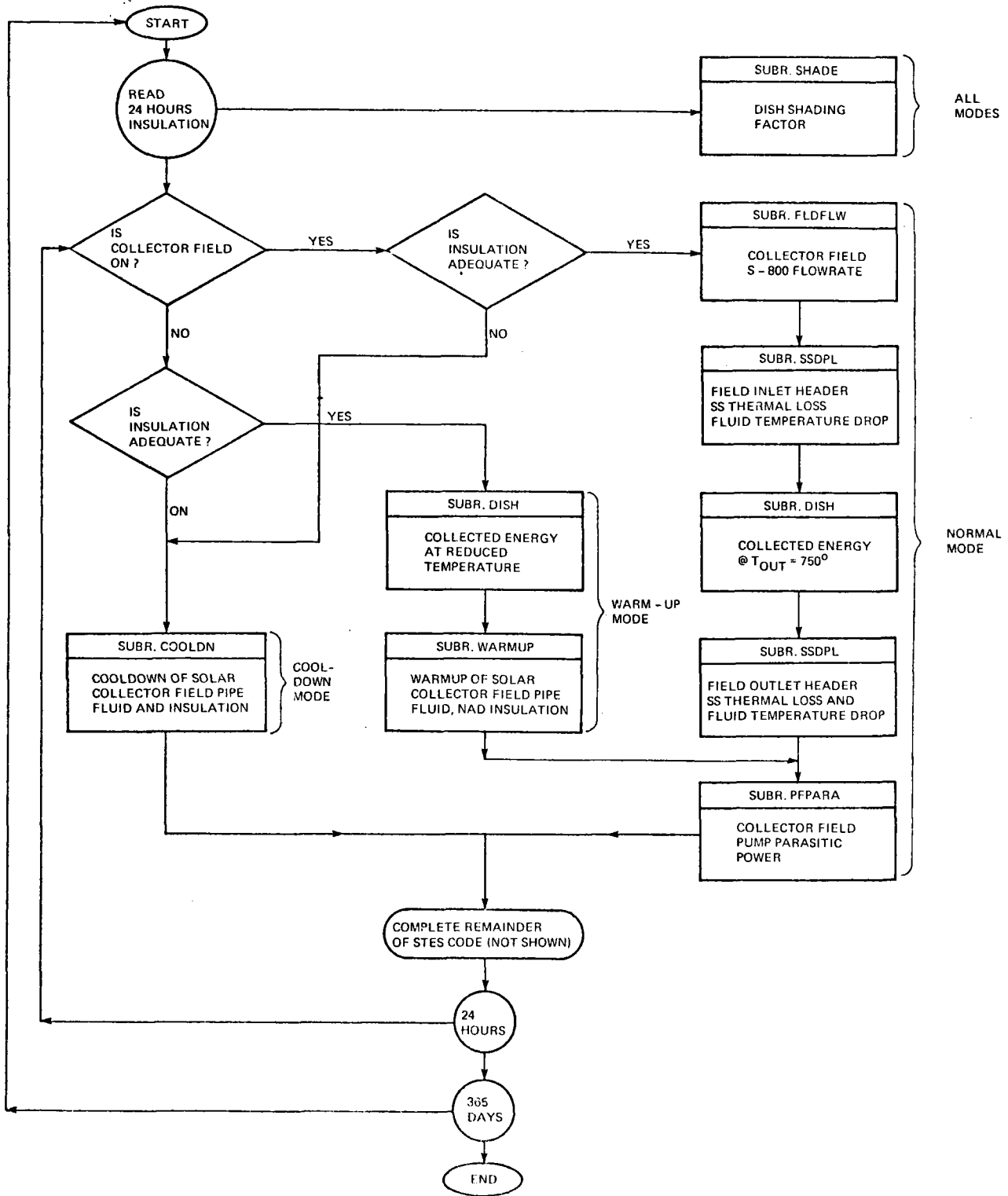


Figure C-2. Collector Field Subroutines Flowchart

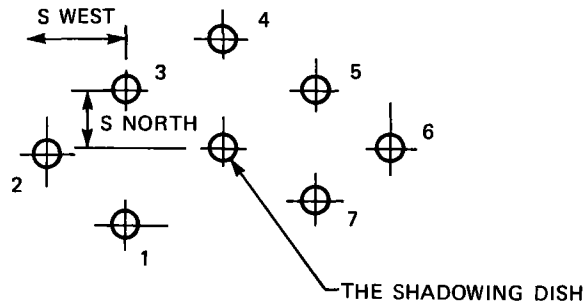


Figure C-3. Dish Shadowing Repeating Pattern

Both sections are essentially the same, with the piping being broken into three classes - large, intermediate, and small - to correspond to field headers, branches, and up and down pipe. Appropriate UA factors for each class of pipe are program inputs. The following equations are used to calculate the Syltherm 800 fluid temperature drop and thermal loss for each piping class:

$$CP = .0001875 * TIN + .38125$$

$$XMCP = XLBHR * CP$$

$$TOUT = TAMB + (TIN - TAMB) * e^{- (U/XMCP)}$$

$$QL = XMCP * (TIN - TOUT)$$

Variable	Definition
CP	S-800 heat capacity (Btu/lb ^o F)
TIN	S-800 inlet temperature to pipe class (°F)
XMCP	S-800 m c _p (Btu/hr ^o F)
XLBHR	S-800 m (lb/hr, constant for each hour)
TOUT	S-800 outlet temperature from pipe class (°F)
TAMB	Ambient temperature (°F constant for each hour)
U	Pipe class UA (Btu/hr ^o F)
QL	Pipe class thermal loss (Btu/hr)

C.4.4 SUBROUTINE DISH (PARABOLIC DISH SOLAR COLLECTOR MODEL)

This subroutine models the performance of the parabolic dish solar collector. It is a two part model containing an optical section which calculates the incident energy on the receiver based on dish/receiver design inputs and direct normal insolation and a thermal section which calculates energy delivered to the Syltherm 800 based on incident energy and receiver thermal design. The equations for each section follow.

Optical

$$DD = D^2$$

$$CDCR = DD/CR$$

$$\begin{aligned} \text{SCDRC} &= \sqrt{\text{CDCR}} \\ \text{ECS} &= (.9911 * D + 8.451 * (\text{SCDRC} + .2286)^2) / \text{ACOL} \\ \text{EBO} &= 1. - .4. / \text{CR} \\ \text{CC} &= \text{EFFREF} * \text{EFFINT} * (1. - \text{ECS}) * \text{EBO} \\ \text{QQ} &= \text{ACOL} * \text{QDN} \\ \text{QREL} &= \text{CC} * \text{SF} * \text{QQ} \end{aligned}$$

Variables

Definition

D	Dish diameter (meters, input design variables)
DD	Constant
CR	Dish concentration ratio (input design variable)
CDCR	Constant
SCDCR	Constant
ECS	Collector strut, receiver, piping, shadowing effect
ACOL	Collector area (ft ² , input design variable)
EBO	Receiver aperture energy bounce out efficiency
CC	Optical efficiency constant
QDN	Incident direct normal insolation (Btu/hr-ft ² , hourly variable)
QQ	Incident direct normal insolation (Btu/hr dish hourly variable)
SF	Field/dish shading factor (hourly variable)
QREL	Incident energy on receiver (Btu/hr hourly variable)

Thermal

$$\begin{aligned} \text{CFE} &= 6.519 / \text{RECLD} \\ \text{CQRAD} &= \text{ACOL} / \text{CR} * .1713\text{E}-8 \\ \text{A} &= 33.804 * \text{CDCR} * \text{RECLD} + 8.45 / * \text{SCDCR} / 2. \\ \text{CQCON1} &= (.015272 * (\text{RECLD} * \text{SCDCR} * 3.281 + 1/6) / \ln(1. + .2286 * \text{SCDCR})) \\ \text{CQCON2} &= 1.479 * (\text{SCDCR} + .4851) \\ \text{DTF} &= \text{THOT} - \text{TCOLD} \\ \text{CT} &= \text{THOT} - \text{DTF} * 75 \\ \text{FE} &= 1. + \text{CFE} * \text{DTE} / \text{CT} \\ \text{QRAD} &= \text{CQRAD} * \text{FE} * ((\text{CT} + 460.)^4 - (\text{TAMB} + 460)^4) \\ \text{QCONV} &= \text{A} * (\text{THOT} - \text{DTF} / 2. - \text{TAMB}) \\ \text{DELTH} &= \text{THOT} - 120 \\ \text{QCOND1} &= \text{CQCON1} * \text{DELTH} \end{aligned}$$

$$QCOND2 = CQCON2*DELTH$$

$$QABS = (QREC - QRAD - QCONV - QCOND1 - QCOND2) / A COL$$

<u>Variables</u>	<u>Definition</u>
CFE	Constant
RECLD	Receiver L/D (input design variable)
CQRAD	Constant
A	Constant
CQCON1	Constant
CQCON2	Constant
DTF	Collector fluid Δt in receiver (°F)
THOT	Collector fluid outlet temperature (°F)
TCOLD	Collector fluid inlet temperature (°F)
CT	Constant (hourly update)
FE	Constant (hourly update)
QRAD	Receiver radiation loss (Btu/hr)
QCONN	Receiver connection loss (Btu/hr)
DELTH	Constant (hourly update)
QCOND1	Receiver sidewall connection loss (Btu/hr)
QCOND2	Receiver back connection loss (Btu/hr)
QABS	Absorbed energy (Btu/ft ² of dish area)

C.4.5 SUBROUTINE PFPARA (COLLECTOR PIPEFIELD PUMP PARASITIC POWER)

This subroutine is called each hour the collector field is operational. It calculates the required pump power in kilowatts based on field flowrate and collector field pump design.

C.4.6 SUBROUTINE WARMUP (COLLECTOR PIPEFIELD WARMUP)

This subroutine models the warmup/recirculation startup mode for the solar collector pipefield during which the pipefield mass is brought from the cold temperature reached during shutdown to normal operating temperature. The subroutine consists of an initialization section and a calculating section as discussed below.

The initialization selection receives simulation input pipefield design information including heat capacity (Btu/°F), UA (Btu/hr), and a ratio

(Heat Capacity of Pipe and fluid) for each of the six classes of pipe in the field. (These (Heat Capacity of Pipe, Fluid and Insulation)

classes are header, branch, and up and down for both the field inlet and field outlet as discussed in paragraph C.4.3 Subroutine SSDPL.) The heat capacity and UA inputs are summed to provide a field heat capacity and UA. Then, a term QSTART is calculated. This term is a value for the amount of energy stored in the pipefield when it is at normal operating temperature. In calculating this term, the pipe and

Syltherm 800 fluid are assumed to be at a uniform temperature, while the insulation is at an average between the uniform temperature and ambient. QSTART is therefore calculated as follows:

$$Q_{START} = \left(\sum_{I=1}^3 CP_I * R_I \right) * 500^{\circ}F + \left(\sum_{I=1}^3 CP_I * (1-R_I) \right) * \left(\frac{500 + T_{AMB}}{2} \right) \\ + \left(\sum_{I=4}^6 CP_I * R_I \right) * 750^{\circ}F + \left(\sum_{I=4}^6 CP_I * (1-R_I) \right) * \left(\frac{750 + T_{AMB}}{2} \right)$$

<u>Variables</u>	<u>Definition</u>
I = 1-6	Corresponds to pipe classes: 1-3 are inlet, 4-6 are outlet
CP	Class heat capacity (Btu/°F)
R	Heat Capacity Ratio $\left(\frac{\text{Pipe} + \text{Fluid}}{\text{Pipe} + \text{Fluid} + \text{Insulation}} \right)$
TAMB	Ambient temperature

The calculation section, which is called each hour that the insulation is sufficient to operate the field but normal operating temperatures have not yet been reached, begins with a calculation of QFIELD. This term is calculated identically to QSTART except that the delay temperatures for each of the six pipe classes generated in the COOLDN subroutine (see following discussion) are substituted for the normal operating temperatures.

Division of QFIELD by the field heat capacity yields an average field temperature during the recirculation/warmup mode. This temperature, following update to reflect the approximate field temperature rise during warmup for the hour timestep, is used in a call of subroutine DISH to determine solar heat input.

An update of the field temperature is then made based on the solar heat input and the following equation:

$$T_{FIELD_NEW} = (T_{AMB} + S/U + C1/C2) * C2 + (T_{FIELD_OLD} - (T_{AMB} + S/U + C1/C2) * C2) * e^{-(U/CP/C2)}$$

<u>Variables</u>	<u>Definition</u>
TFIELD_NEW	Updated average field temperature
TAMB	Ambient temperature (°F)
S	Collected sun (Btu/hr)
U	Field UA (Btu/hr °F)
C1	Constant (TAMB *RRF/2)
RRF	Constant (1-RF)
RF	Heat capacity ratio $\left(\frac{\text{Field Pipe} + \text{Fluid}}{\text{Field Pipe} + \text{Field} + \text{Insulation}} \right)$
C2	Constant (RF + RRF/2)
TFIELD_OLD	Initial average field temperature
CP	Field heat capacity (Btu/°F)

Following update of the average field temperature, QFIELD is recalculated. This procedure is continued each step until either QFIELD exceeds QSTART, indicating normal operation has started, or the insolation level drops and cooldown begins.

C.4.7 SUBROUTINE COOLDN (COLLECTOR PIPEFIELD COOLDOWN)

This subroutine models the cooldown mode for the solar collector pipefield during which the pipefield cools due to heat loss to ambient. The subroutine is structured like the warmup subroutine, with an initialization section which determines the decay temperature of the six pipe classes in the field.

The subroutine is called each hourly timestep that the insolation is insufficient to operate the field. The equation used to calculate the decay temperatures for the six pipe classes are identical in form to those in the warmup subroutine.

C.4.8 HIGH TEMPERATURE THERMAL ENERGY STORAGE SUBROUTINE

The high temperature thermal energy storage subroutine is a multi-tank model which simulates a storage subsystem comprised of one tank of smaller (1 hour) capacity and multiple tanks of larger capacity. Program inputs are used to reflect the desired subsystem design. The model simulates charging and discharging of the proper tank in the storage subsystem based upon collector field and solar steam generator flowrates, subsystem control logic, and the current state of each tank. The collector field and steam generator flowrates are calculated in separate subroutines as discussed in the appropriate sections of the Appendix.

The storage subsystem control logic is comprised of four basic concepts:

1. If all the tanks are not charged, the smaller tank is charged first and energy is not supplied to the steam generator until the tank is fully charged.
2. Once the smaller tank is charged, solar energy is supplied directly to the steam generator with excess stored in the large tanks.
3. Discharge starts with the small tank and proceeds through the larger tanks. Partially charged tanks are either inverted if required, based on the inversion efficiency, or allowed to remain partially charged overnight.
4. If all four tanks are in a state other than fully discharged, the storage is considered full.

The model tracks the state of the energy in the smaller tank and in each of the larger tanks. Four states are possible: fully or partially charged and fully and partially discharged. A tank must be either fully charged or inverted before discharge, and a tank must be fully discharged before charging.

Also included in the subroutine is a thermal loss model to account for external conduction energy losses and an inversion efficiency model to accommodate tank inversion if employed. The subroutine is called each hour of the simulation by the main driver routine. Energy is subsequently added, subtracted, and stored as appropriate.

C.4.9 POWER CONVERSION SUBSYSTEM SUBROUTINE

The power conversion subsystem is modeled with two subroutines as discussed below:

C.4.9.1 Subroutine Turbine (Turbine-generator model)

This subroutine models the performance of the steam turbine-generator and is called each hour that the PCS is operating. The key to the model is the input thermodynamic performance map provided by the steam turbine-generator manufacturer. It includes state point enthalpies (inlet, extraction, and exhaust) throughout the turbine-generator operating range. This information provides the data base for interpolating polynomials which predict the turbine efficiencies for the desired electrical/steam load. From this information inlet, extraction, and exhaust steam requirements are calculated for use in the remainder of the STES code.

C.4.9.2 Subroutine STGPM (Steam Generator Flowrate)

This subroutine calculates the steam generator Syltherm 800 flowrate based on PCS energy demands, fluid properties, and steam generator statepoint temperatures.

C.4.10 THERMAL UTILIZATION SUBROUTINES

The thermal utilization subsystem is modeled with two subroutines for the major components—the low temperature storage tank and the absorption air conditioner. The storage tank subroutine considers tank storage media/capacity in support of the thermal utilization energy balance while the AAC model includes equipment design considerations such as capacity coefficient of performance (COP), and operating power as well as economizer use when feasible.

APPENDIX D
LIFE CYCLE COST METHODOLOGY

APPENDIX D
LIFE CYCLE COST METHODOLOGY

This Appendix describes the methodology employed in Life Cycle Cost analysis for the Shenandoah STE-LSE. The major element in the life cycle cost analysis is the levelized annual cost of the STES. Levelized annual cost can be compared with levelized system benefits or can be divided by annual energy production to determine the cost of delivered energy.

D.1 LEVELIZED ANNUAL COST

The levelized annual cost represents the dollar amount required to own, operate, and maintain a system during each year of the life of the system. Specifically, the levelized annual cost accounts for:

1. Paying off system capital costs
2. Paying for operating and maintenance expenses
3. Paying taxes
4. Paying a return to investors and interest to creditors
5. Building a capital fund for periodic component replacement, overhaul, and retirement of debt.

Figure D-1 schematically depicts the computation of levelized annual cost. The general expression for levelized annual cost AC is given by:

$$\overline{AC} = CRF \times PV$$

where CRF is the capital recovery factor and PV is the present value of the year-by-year cash requirements throughout the system life. The capital recovery factor is the uniform periodic payment, as a fraction of the original principal, that will fully repay a loan (including all interest) in yearly periods over the loan lifetime at a specified yearly interest rate. The interest rate used to calculate CRF is called the discount rate and is equal to the weighted average after-tax cost of capital.

The fixed charge rate (FCR) represents the yearly cost of ownership, expressed as a percentage of the initial investment, I. These costs consist of debt interest and principal payments, return on equity (where applicable), insurance, local taxes, and the net effect of Federal taxes. The concept of the fixed charge rate comes from electric utility financial analysis, but has proven to be applicable and convenient in the analysis of other sectors as well. A detailed discussion of fixed charge rate, its various components, and corporate tax effects is presented in "The Cost of Energy from Utility-Owned Solar Electric Systems" (Reference D-1). Note that the expression for FCR in Figure D-1 assumes constant or straight line depreciation. For accelerated depreciation, a year-by-year present value computation must be made.

The present value is analogous to that amount which, if deposited in an interest bearing account at the discount rate, would permit annual withdrawals to pay all system costs and diminish to zero at the end of system life. Variable system costs include operation and maintenance (OM), which would most likely tend to increase with inflation, and component replacement and overhaul which would depend on servicing schedules. Fuel costs for the back-up fossil oil heater will be included for computation of the cost of delivered energy from the STES. For a cost versus benefit comparison, the back-up fuel costs are best treated as a negative benefit or an offset to the total fuel and electricity savings. Levelized annual cost can be computed in constant or current year dollars. The former is more meaningful since comparisons with present data are easier. It is very often more representative of the actual costs; that is, they are more likely to stay constant in constant year dollars than in current year dollars. The constant dollar levelized annual cost \overline{AC} is computed from a capital recovery factor (CRF) which is based on the real, or inflation adjusted, discount rate r' , as shown in Figure D-1.

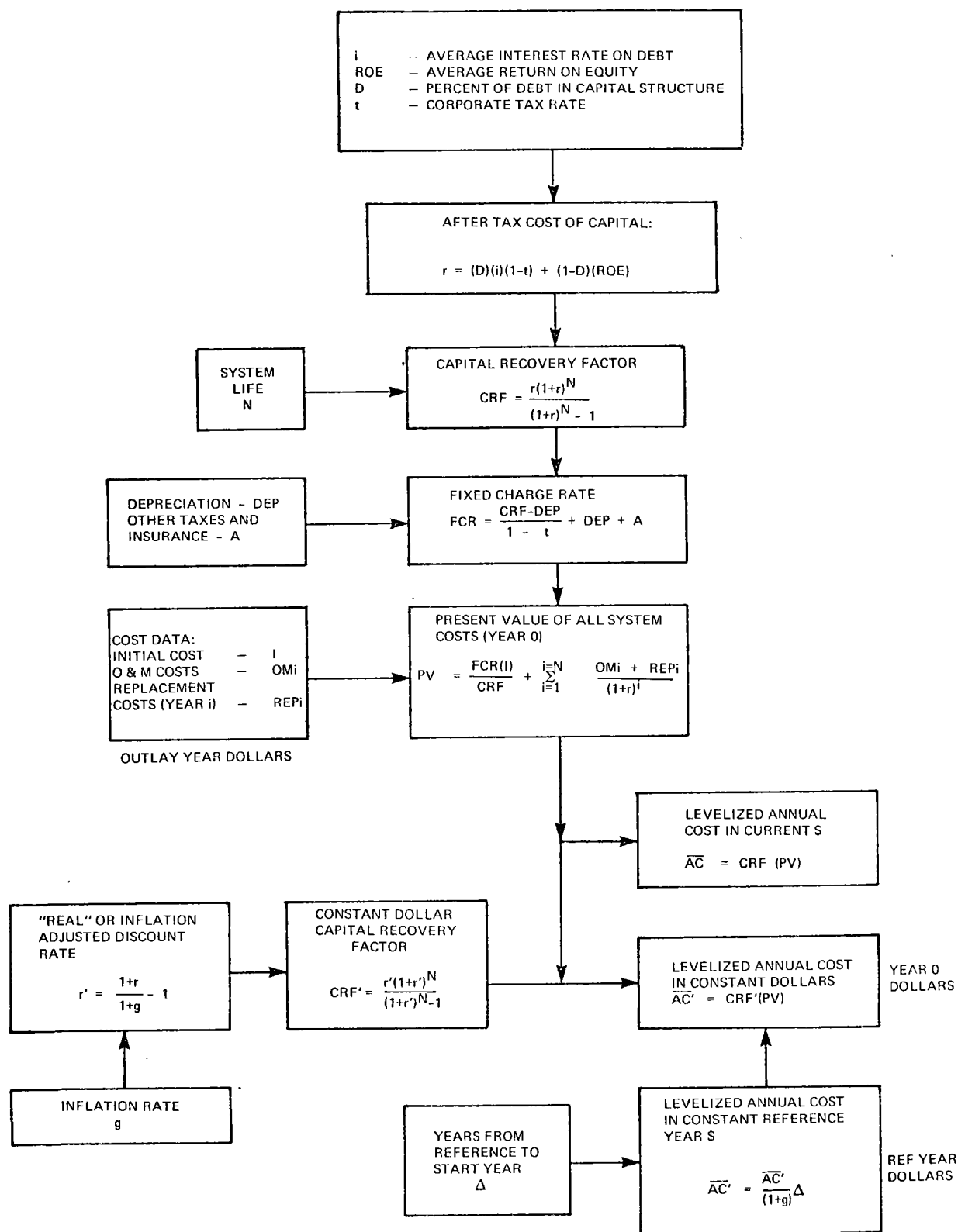


Figure D-1. Levelized Annual Cost Computation

D.2 LEVELIZED ANNUAL BENEFITS

The comparison of the energy costs savings of the STES to the levelized annual cost is accomplished by computing the levelized annual benefits (AB) for the energy savings. The procedure is identical to that for levelized annual cost with the present value of all future fuel savings computed and levelized through use of the capital recovery factor. Levelized annual benefits (AB) is obviously a function of present and projected energy prices. For a constant energy price escalation rate, f , a simple form for present value of energy savings is:

$$PV_{\text{energy}} = \frac{E_0(1+f)}{r-f} \left[1 - \left(\frac{1+f}{1+r} \right)^N \right]$$

where E_0 = energy savings in year zero
 N = system life
 r = discount rate

The levelized annual benefits become:

$$\begin{aligned} \overline{AB} &= CRF \times PV_{\text{energy}} \\ &= \frac{r(1+r)^N}{(1+r)^N - 1} \frac{E_0(1+f)}{r-f} \left[1 - \left(\frac{1+f}{1+r} \right)^N \right] \end{aligned}$$

which simplifies to

$$\begin{aligned} AB &= \frac{r(1+f)}{r-g} \left[\frac{(1+r)^N - (1+f)^N}{(1+r)^N - 1} \right] E_0 \\ &= M E_0 \end{aligned}$$

where M is a fuel savings multiplier which is a function of N , r and f . For constant dollars, the multiplier M' is employed which necessitates use of r' and f' , the inflation adjusted energy price escalation rate. Figure D-2 presents the multiplier M' plotted versus real discount rate and energy price escalation rate.

From Figure D-2 for an energy price escalation rate, f' , of .04 (4 percent over inflation) and a real discount rate of .02, the energy price or energy savings multiplier is about 1.5. Thus, for a system with estimated year zero savings of \$100,000 annually, the levelized value over the twenty year system life will be \$150,000 in year zero dollars under the above conditions.

Energy savings for the Shenandoah STES will result from:

1. Direct electricity supplied to Bleyle
2. Cooling supplied from absorption air conditioners
3. Steam supplied to process
4. Heating supplied by hot water.

The first two items above will displace purchased electricity and the last two purchased fossil fuel, natural gas for Bleyle. Electricity saved from absorption air conditioner operation will be a function of the relative coefficients of performance (COP) of the absorption cycle and vapor cycle units, while steam and heating energy savings will depend on respective boiler efficiencies.

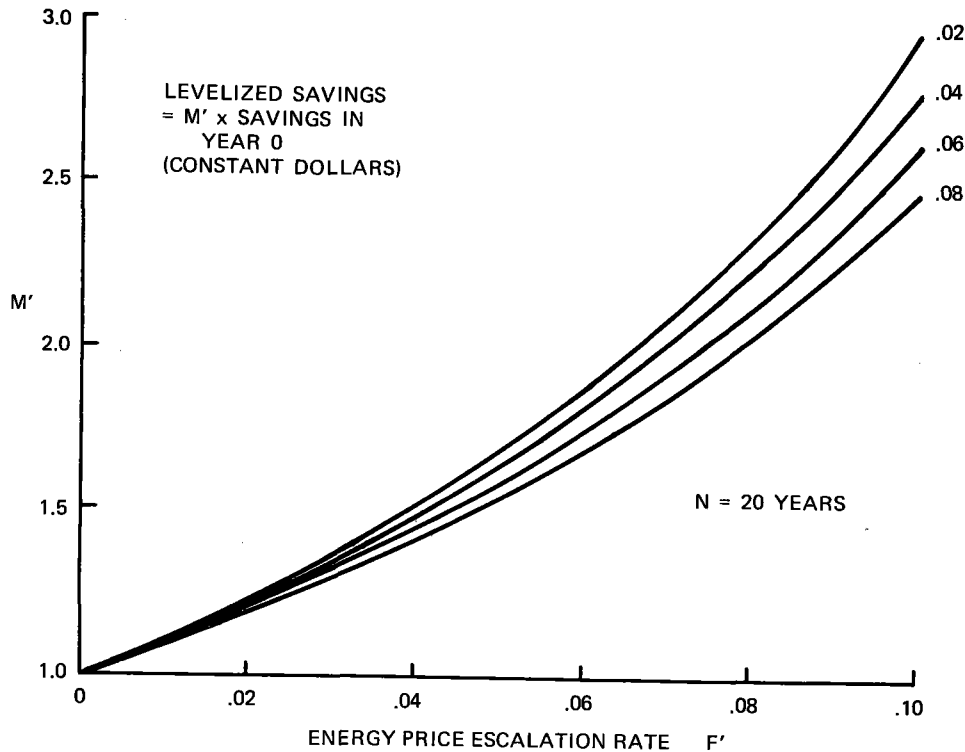


Figure D-2. Energy Price Multiplier

Energy cost savings must be computed within the context of back-up energy pricing structure, which will also contribute to system operational philosophy. For Bleyle plant estimated loads, the incremental electrical savings double for STES contributions beyond about 35 percent of the load. The linking of the electrical rate structure to peak demand makes it appear highly desirable to extend operation of the absorption air conditioner to eliminate completely the power demand of the vapor cycle units. The dollar value of the STES energy savings will be derived by computing electrical and natural gas monthly bills with and without the STES contribution. The difference then becomes the savings.

D.3 COST OF DELIVERED ENERGY

Derivation of the cost of delivered energy from the STES requires a value ratio between the electrical and thermal savings. Typical prices for electrical energy are about three times as high as thermal energy, reflecting somewhat the average power plant efficiency of 25 to 35 percent. It can be shown that if the numerical value of the electricity cost in cents per kilowatt hour is equal to the thermal cost in dollars per million Btu, a 3:1 value ratio is closely approximated.*

$$* \frac{\left(1 \frac{\text{¢}}{\text{kWh}}\right) \left(.01 \frac{\text{\$}}{\text{¢}}\right)}{\left(1 \frac{\text{\$}}{10^6 \text{ Btu}}\right) (3413) \frac{\text{Btu}}{\text{kWh}}} = 2.93 \approx 3$$

Using this approximation, the cost of delivered energy, C_E , can be derived from the levelized annual cost $\overline{AC'}$ as follows:

$$S_{\text{elec}} C_E \left(.01 \frac{\$}{\text{¢}} \right) + S_{\text{thermal}} \left(\frac{\$1}{10^6} \right) C_E = \overline{AC'}$$

where S_{elec} = electrical savings kWh

S_{thermal} = thermal energy savings Btu

thus, the cost of delivered energy is given by:

$$C_E = \frac{\overline{AC'}}{.01 S_{\text{elec}} + S_{\text{thermal}} \times 10^{-6}} \quad \frac{\text{¢}}{\text{kWh}}, \quad \frac{\$}{10^6 \text{Btu}}$$

D.4 REFERENCE

D-1. "The Cost of Energy from Utility-Owned Solar Electric Systems", Doane, J.W., et. al., June 1976, Report JPL 5040-29, Jet Propulsion Laboratory.

APPENDIX E
SOLAR EASEMENT AGREEMENT

APPENDIX E
SOLAR EASEMENT AGREEMENT

STATE OF GEORGIA
COUNTY OF FULTON

SOLAR EASEMENT AGREEMENT

THIS SOLAR EASEMENT AGREEMENT (hereinafter referred to as the "Agreement"), made and entered into as of the ____ day of _____, 1978, by and among SHENANDOAH, LTD., a Georgia Limited Partnership, acting by and through its Sole Corporate General Partner, Shenandoah Development, Inc., a Georgia corporation (herein called "Shenandoah"), DEVELOPMENT AUTHORITY OF COWETA COUNTY (Herein called "Authority"), D. SCOTT HUDGENS, JR., and HERMAN J. RUSSELL doing business as HUDGENS-RUSSELL JOINT VENTURE, NO. 1 (herein called "Hudgens-Russell No. 1"), D. SCOTT HUDGENS, JR. and HERMAN J. RUSSELL doing business as HUDGENS-RUSSELL JOINT VENTURE, NO. 4 (herein called "Bleyle"), SCOTT BUILDERS CO., a Georgia corporation (herein "Scott Builders"), and GEORGIA POWER COMPANY, a Georgia corporation (herein called "Georgia Power").

W I T N E S S E T H:

WHEREAS, Shenandoah has this date, simultaneously with the execution of this Agreement, sold to Georgia Power, and Georgia Power has purchased from Shenandoah, all that tract or parcel of land lying and being in Land Lot 77, of the 5th District, Coweta County, Georgia, being more particularly described on Exhibit "A" attached hereto and made a part hereof, and shown as "Plat I-5.72 acres" on survey prepared for Georgia Power Co. by Lowe Engineers, Inc., dated March 24, 1978, and last revised _____, 1978, said survey being attached hereto as Exhibit "B" and made a part hereof, (said land being herein called the "Georgia Power Land"); and

WHEREAS, Shenandoah is the owner of fee simple title to certain land adjacent to or near the Georgia Power Land and more particularly described on Exhibit "C" attached hereto and made a part hereof, and shown as Parcels 12-06-110, 12-06-200 (5.18 acres and 2.28 acres), 12-06-300 and 12-06-120 (Parcel 2), on Exhibit "D" hereof (said land being herein called the "Shenandoah Land"); and

WHEREAS, Scott Builders Co., a Georgia corporation, holds an option on certain of the Shenandoah Land shown on Exhibit D as Tract 12-06-120 (Parcel 2); and

WHEREAS, Hudgens-Russell No. 4, is the Purchases under a Contract for the purchase of certain of the Shenandoah Land shown on Exhibit D as Tract 12-06-110; and

WHEREAS, Authority is the owner of certain land adjacent to the Georgia Power Land and more particularly described on Exhibit "E" attached hereto and made a part hereof, and shown on Exhibit "D" hereof as "12-06-120 - Parcel 1", (said land being herein called the "Authority Land"); and

WHEREAS, Authority has leased the Authority Land to Hudgens-Russell No. 1 by Lease Agreement dated as of November 15, 1977, recorded in Deed Book 283, Page 820, Clerk's Office, Superior Court of Coweta County, Georgia; and

WHEREAS, Bleyle is a subtenant of the Authority Land by Lease dated May 17, 1977, recorded in Deed Book 280, Page 351, aforesaid records, the landlord's rights under such Lease having been assigned to the Authority; and

WHEREAS, the Authority Land and the Shenandoah Land is hereinafter referred to collectively as the "Encumbered Land"; and

WHEREAS, solar collection and energy conversion equipment is intended to be installed on the Georgia Power Land for the purpose of converting solar energy into thermal energy; and

WHEREAS, continued access to sunlight and sun rays over and across the Encumbered Land is necessary to accomplish the foregoing purpose; and

WHEREAS, Georgia Power wishes to obtain from the remaining parties hereof and such remaining parties hereof are willing to grant to Georgia Power an easement for the uninterrupted passage of sunlight and sun rays over and across the Encumbered Land to the extent and subject to the terms and conditions set forth herein.

NOW, THEREFORE, in consideration of the purchase of the Georgia Power Land by Georgia Power from Shenandoah, the mutual covenants and agreements hereinafter set forth, the sum of \$10.00 in hand paid by Georgia Power to each of the parties hereto, at and before the sealing and delivery of these presents, and for other good and valuable consideration, the receipt, adequacy and sufficiency of which are hereby expressly acknowledged by each of the parties hereto, the parties hereto mutually covenant and agree as follows:

1. DEFINITIONS

For purposes of this Agreement, the following definitions shall apply:

- A. "South Reference Line" - shall mean that certain line identified as such and depicted on Exhibit "F" attached hereto and made a part hereof.
- B. "East Reference Line" - shall mean that certain line identified as such and depicted on Exhibit "F" attached hereto and made a part hereof.
- C. "West Reference Line" - shall mean that certain line identified as such and depicted on Exhibit "F" attached hereto and made a part hereof.
- D. "Easement Areas" - "Easement Area I", "Easement Area II", and "Easement Area III" mean the areas identified as such and depicted on Exhibit "F" attached hereto and made a part hereof.
- E. "Appropriate Reference Line" - shall mean the reference line to be used in calculating the "Allowed Maximum Height" (as that term is hereinafter defined) of any building, improvement, construction, built-up ground, tree or other vegetation (herein called the "Improvement") located or to be located on the Encumbered Land. If the Improvement is to be located in Easement Area I, the Appropriate Reference Line is the East Reference Line. If the Improvement is or is to be located in Easement Area II, the Appropriate Reference Line is the South Reference Line. If the Improvement is or is to be located in Easement Area III, the Appropriate Reference Line is the West Reference Line.
- F. "Allowed Maximum Height" - shall mean the maximum height in feet above mean sea level (as defined by U. S. Geodetic Survey) of buildings, improvements, construction, built-up ground, trees and other vegetation on the Encumbered Land, which can be built or allowed to grow without violation of this Agreement. The Allowed Maximum Height for any improvement is determined in accordance with Paragraph 5 hereof, which takes into consideration certain factors including the distance of any such Improvement from the Appropriate Reference Line.
- G. "Easement Air Space" - shall mean all air space above the Allowed Maximum Height.

2. GRANT OF SOLAR EASEMENT

Shenandoah, Hudgens-Russell No. 4 and Scott Builders do hereby establish, give, grant and convey to Georgia Power, its successors, successors-in-title and assigns, an easement over, across and through the Easement Air Space and all portions thereof over and above the Shenandoah Land for the free and uninterrupted passage of direct sunlight and sun rays for the benefit of the Georgia Power Land and any improvement now or hereafter thereon. Authority, Hudgens-Russell No. 1 and Bleyle do hereby establish, give, grant and convey to Georgia Power, its successors, successors-in-title and assigns, an easement over, across and through the Easement Air Space and all portions thereof over and above the Authority Land for the free and uninterrupted passage of direct sunlight and sun rays for the benefit of the Georgia Power Land and any improvements now or hereafter thereon. For purposes of this Agreement, these easements shall herein be called the "Solar Easements".

3. PURPOSE OF SOLAR EASEMENTS

The Solar Easements granted hereunder shall be solely for the purpose of permitting the free and uninterrupted passage of sunlight and sun rays so that the energy therein may be collected on the Georgia Power Land; provided, however, that the Solar Easements granted hereunder may not be used in connection with the bio-conversion of solar energy.

4. NON-INTERFERENCE WITH SOLAR EASEMENTS

Shenandoah, Authority, Hudgens-Russell No. 1, Bleyle, Hudgens-Russell No. 4, and Scott Builders jointly and severally agree that neither they nor their assigns or successors-in-title, shall in any way cause or permit an obstruction, reduction, deflection or shading of sunlight and sun rays flowing, passing over, across or through the Easement Air Space over their respective lands except as may be caused by the following (herein called the "Permitted Exceptions"):

A. Improvements now or hereafter located on the Shenandoah Land or the Authority Land, which do not exceed the Allowed Maximum Height (except as is permitted in Paragraph 8 hereof);

B. Trees and other vegetation now or hereafter located on the Shenandoah Land or the Authority Land, which do not exceed the Allowed Maximum Height (except as is permitted in Paragraph 8 hereof); and

C. Clouds, rain, fog, haze, smoke, steam or other similar conditions over which Shenandoah, Authority, Hudgens-Russell No. 1, Hudgens-Russell No. 4, Scott Builders Co. and Bleyle and their successors and assignees have no control;

Provided, however, the Permitted Exceptions shall not include any height additions to the improvements described in subparagraph 4 A. above or any additional height growth to the trees or other vegetation described in subparagraph 4 B. above into the Easement Air Space.

5. ALLOWED MAXIMUM HEIGHT

For purposes of determining the Allowed Maximum Height, the Base Height of the East Reference Line shall be 946 feet above sea level; the Base Height of the South Reference Line shall be 946 feet above sea level; and the Base Height of the West Reference Line shall be 953 feet above sea level.

In order to determine the Allowed Maximum Height of any portion of any building, improvement, construction, built-up ground, trees or other vegetation on the Shenandoah Land or the Authority Land, first determine the horizontal distance in feet (herein called the "Set Back Distance" or "SBD") from that portion of the Improvement whose height is being determined to the Appropriate Reference Line, as measured along a line perpendicular to the Appropriate Reference Line from that portion of the Improvement whose height is being determined. Then:

A. If the SBD is 100 feet or less, the Allowed Maximum Height shall be the Base Height of the Appropriate Reference Line plus thirty percent (30%) of the SBD.

B. If the SBD is greater than 100 feet, but less than 300 feet, the Allowed Maximum Height shall be the Base Height of the Appropriate Reference Line plus thirty (30) feet plus fifteen percent (15%) of the SBD that is greater than 100 feet.

C. If the SBD is greater than 300 feet, the Allowed Maximum Height shall be the Base Height of the Appropriate Reference Line plus sixty (60) feet plus ten percent (10%) of the SBD that is greater than 300 feet.

6. NON-EXCLUSIVE EASEMENT

The Solar Easements herein granted are non-exclusive easements in that all parties hereto and their successors and assigns can also use and enjoy the sunlight and sun rays in the Easement Air Space above their respective lands, but such right to use this sunlight and sun rays does not permit Shenandoah, Authority, Hudgens-Russell No. 1, Bleyle, Hudgens-Russell No. 4 or Scott Builders Co. their successors or assigns to shade, deflect or prevent Georgia Power's access to sunlight and sun rays over, across and through the Easement Air Space for the purposes set forth herein.

7. TERM

The term of this Solar Easement Agreement shall commence on the date hereof and shall terminate on the date on which title to the Georgia Power Land reverts to Shenandoah, its successors and assigns.

8. EXCEPTIONS TO SOLAR EASEMENTS

Anything provided herein to the contrary notwithstanding, any improvement or improvements constructed or growing on Encumbered Land which exceed the Allowed Maximum Height shall not be deemed to be a violation of this Agreement or the Solar Easements granted herein, provided that such improvement or improvements, individually or in the aggregate, meet the following criteria (such improvement or improvements are referred to herein individually and collectively as "Improvement in Question", or Improvements in Question", respectively):

Within any circular areas of space (measured horizontally) in the Easement Air Space, which circular area has a radius of 50 feet, there may exist one or more Improvements in Question which exceed the Allowed Maximum Height, provided that (a) the area of such Improvement in Question or the aggregate area of such Improvements in Question does not exceed 50 square feet in total area, measured in a vertical plane parallel to the Appropriate Reference Line; and (b) the cross-sectional diameter or width of such Improvement in Question, measured perpendicular to the longest axis, does not exceed 12 inches as to a single Improvement in Question, or 12 inches in the aggregate if there is more than one Improvement in Question within a given 50 foot radius circular area.

9. AMENDMENTS

The Solar Easements granted hereunder and all rights, and interests, set forth in this Agreement may be altered, amended, modified, cancelled or terminated only by means of an instrument executed solely by all parties hereto or their respective successors and assigns, except for automatic termination as set forth in Paragraph 7 hereof.

10. WARRANTIES

Shenandoah does hereby warrant its fee simple title to the Shenandoah Land, and Shenandoah, Hudgens-Russell No. 4, and Scott Builders do hereby warrant their right, power and capacity to create and convey the Solar Easements granted hereunder and to execute this Agreement.

Authority does hereby warrant its fee simple title to the Authority Land and Hudgens-Russell No. 1 and Bleyle do hereby warrant their leasehold except to the extent of such individual general partner's or such limited partner's interest in such partnership.

IN WITNESS WHEREOF, the parties have caused this Agreement to be executed and sealed the day and year first above written.

Signed, sealed and delivered in the presence of:

Witness

Notary Public

Witness

Notary Public

Witness

Notary Public

Witness

Notary Public

Witness

Notary Public

Signed, sealed and delivered in the presence of:

Witness

Notary Public

SHENANDOAH, LTD., acting by and through its Sole Corporate General Partner, Shenandoah Development, Inc.

By: _____
Dieter Franz, Chief Executive Officer/General Manager

DEVELOPMENT AUTHORITY OF COWETA COUNTY

By: _____

BLEYLE OF AMERICA, INC.

By: _____
Title: _____

D. SCOTT HUDGENS, JR. and HERMAN J. RUSSELL
d/b/a HUDGENS-RUSSELL JOINT VENTURE NO. 1
and d/b/a HUDGENS-RUSSELL JOINT VENTURE NO. 4.

By: _____
D. Scott Hudgens, Jr.

By: _____
Herman J. Russell

SCOTT BUILDERS CO.

By: _____
President

GEORGIA POWER COMPANY

By: _____

Its: _____
(Corporate Seal)

APPROVED, JOINED IN AND CONSENTED TO by THE FIRST NATIONAL BANK OF ATLANTA, as Trustee under that certain Indenture and Deed of Trust dated as of March 15, 1974, recorded in Deed Book 244, page 333, Coweta County, Georgia Records.

Signed, sealed and delivered in the presence of:

THE FIRST NATIONAL BANK OF ATLANTA,
as Trustee

Witness

By: _____
Trust Officer

Notary Public

(Attach Seal)

APPROVED, JOINED IN AND CONSENTED TO by DECATUR FEDERAL SAVINGS AND LOAN ASSOCIATION, as Grantee under that certain Deed to Secure Debt from Development Authority of Coweta County (for the Authority Land) recorded in Deed Book 282, Page 813, aforesaid records (affecting the Authority Land).

Signed, sealed and delivered in the presence of:

DECATUR FEDERAL SAVINGS AND LOAN
ASSOCIATION

Witness

By: _____

Notary Public

(Attach Seal)

APPENDIX F
ENVIRONMENTAL IMPACT ASSESSMENT - SHENANDOAH STE-LSE

DRAFT
ENVIRONMENTAL IMPACT ASSESSMENT
OF THE
SOLAR TOTAL ENERGY - LARGE SCALE EXPERIMENT
AT THE
BLEYLE KNITWEAR PLANT,
SHENANDOAH, GEORGIA

MAY 1978

DIVISION OF SOLAR TECHNOLOGY
DEPARTMENT OF ENERGY

APPENDIX F
ENVIRONMENTAL IMPACT ASSESSMENT
SHENANDOAH STE-LSE

F.1 DESCRIPTION OF THE PROPOSED ACTION

The Federal action addressed by this Environmental Impact Assessment (EIA) is support by the Department of Energy (DOE) of a Solar Total Energy - Large Scale Experiment (STE-LSE) at the Bleyle knitwear plant in Shenandoah, Georgia. This EIA was prepared for fulfilling DOE's objectives under the guidelines for environmental review contained in Title 10, Code of Federal Regulations, Part 711 to evaluate the environmental impacts of proposed DOE actions at the earliest meaningful point in the decision-making process.

The objective of the project is to demonstrate that a Solar Total Energy system can effectively augment the energy needs of a typical industrial plant. In support of this objective and to fulfill its own prime responsibility to encourage and demonstrate feasibility of advanced energy systems, DOE proposes to fund assembly and testing of a Solar Total Energy-Large Scale Experiment on the Shenandoah site. The following sections will describe the project in terms of location, project objectives, specific project activities and requirements, restoration of site environs, projected plant operations, and known environmental issues.

F.1.1 SITE LOCATION AND SURFACE FEATURES

F.1.1.1 Existing Structures and Property Ownership

The proposed Solar Total Energy - Large Scale Experiment will be located in Shenandoah, Georgia. Shenandoah is a new town near Newnan, about 40 kilometers (25 miles) southwest of Atlanta as shown in Figure F-1. This new community is being developed by Shenandoah Development Incorporated (SDI) which was established in 1969 by Unioamerica - Incorporated. Approximately 30 square kilometers (7,400 acres) are currently being improved by SDC.

The site that was made available by SDI for the proposed total energy facility is defined in Figure F-2 (Plat I). It consists of approximately 23,000 square meters (5.72 acres) of gently sloping land. As depicted in Figure F-3, the site is near the intersections of Interstate 85 and Georgia Highway 34. The site is connected to Newnan by Georgia Highway 34 and to Atlanta by Interstate 85. The Bleyle knitwear mill is located along the west property line of the development. Bleyle, a German knitwear manufacturing company, has initiated the first phase of their development program which consists of constructing a 2,300 square meters (25,000 ft²) manufacturing plant. Prior to 1981, as part of a second phase development, Bleyle plans to expand the mill's capacity by increasing the floor area to 3,900 square meters (42,000 ft²). A third phase may be instituted in the future expanding their production facilities to 8,550 square meters (92,000 ft²). Conceptual design of the STE-LSE has been based on the 42,000 square feet expansion.

Access to the Bleyle facilities will be via Amlajack Boulevard. The property adjacent to the north boundaries of the Bleyle facility/STES site is neither owned nor controlled by SDI. Located near the northeast corner of the collector tract is a parcel of land measuring 15 meters by 44 meters (50 x 143 ft). This property is owned by the Housing and Urban Development Administration (HUD) and is designated as a green area. Green areas are intended to be land which will never be developed. However, the HUD property can be modified to control erosion at the STES site. This will be discussed in a later section.

Positioned directly south of the site on a parcel of land with a peak elevation of 296 meters (970 ft) is a 3785 cubic meters (1,000,000 gallon) water tower. The height of the water tower is approximately 51 meters (166 ft). SDI owns and operates the water facility.

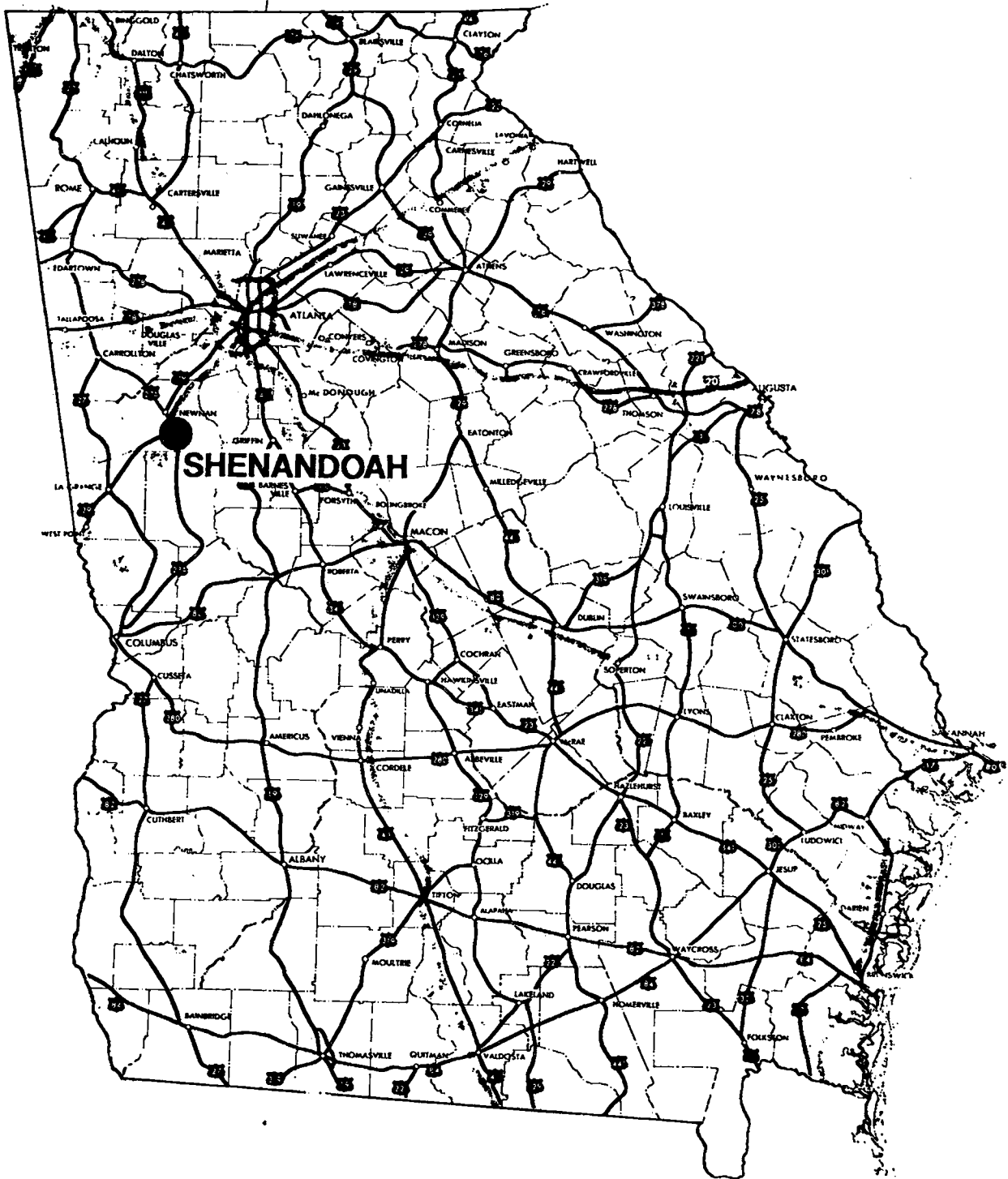


Figure F-1. Location Map

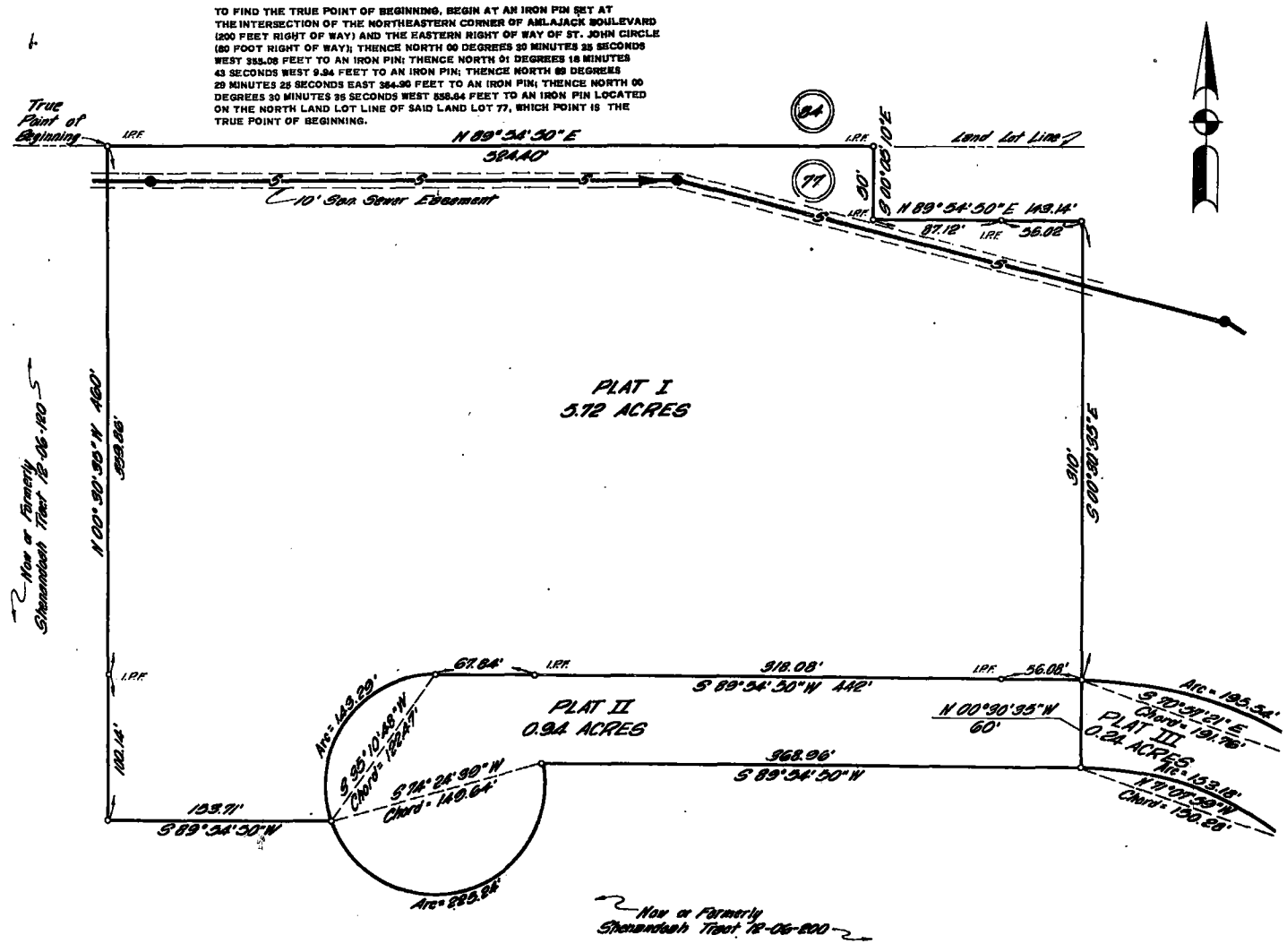




Figure F-3. Aerial Photograph - Looking South

Located on the STE-SITE itself are two man made structures. The first is a meteorological station on a 6 meter by 6 meter (20 ft by 20 ft) concrete pad. This station will eventually be dismantled and repositioned on top of the STE-LSE mechanical building to record data in conjunction with STE-LSE operations. The second structure is a twenty centimeter (8 in) concrete sanitary sewer line. The concrete pipe is located approximately 2.7 meters (9 ft) below the existing grade evaluation. Service to the sewer is via two manholes located on Figure F-2. It should be noted that the sanitary sewer has a three meter (10 ft) easement and that manhole elevations will need to be adjusted to any changes in surrounding ground elevations.

All other lands that adjoin the collector boundary line are owned by SDI. SDI has plans to install a road southeast of the site to provide access to Amlajack Boulevard. Since the region between the collector field and Amlajack Boulevard has not been assigned to a third party by SDC, the exact position of the road is not final. The land in this area will be graded in conjunction with STE-LSE site preparation. This will reduce the potential for shadowing the solar collector field and thus enhance system performance.

F.1.2 PROJECT DESCRIPTION

This project consists of the design, construction, operation, and technical evaluation of a solar total energy system providing power to a knitwear factory operated by Bleyle of America, Inc. The project is currently underway, and significant milestones are indicated on the accompanying chart. The factory, initially equipped with its own independent (conventional) energy source, will derive greater than 60 percent of its annual energy needs from the sun when the solar system becomes operational in 1981. Backup energy for the factory will be available from fossil fuel (oil) supplies to provide energy on cloudy days.

The site for this experiment was selected from competitive proposals as the application most nearly meeting the project requirements. The location is in the industrial park of Shenandoah, Georgia, about 25 miles south of the Atlanta airport. The land has been provided at no cost by the Shenandoah Development Corp. Exclusive use of the land will remain with the U.S. Government for the term of the agreement.

Under terms of the Cooperative Agreement, the Georgia Power Company and DOE share site costs on a 50-50 basis for those activities of common interest. Additional services are provided to DOE by the Georgia Power and their participants on a reimbursable basis. The schedule for the STE-LSE project is shown on Figure F-4.

Member organizations of the Georgia Power team and their activities include:

- Shenandoah Development, Inc.
Developer and factory building owner
- Georgia Institute of Technology
Solar consultation to Georgia Power
- Heery and Heery, Inc.
Site architectural and engineering liaison services
- Owens-Corning Fiberglas
Energy conservation services
- Westinghouse Electric Corp.
Site liaison

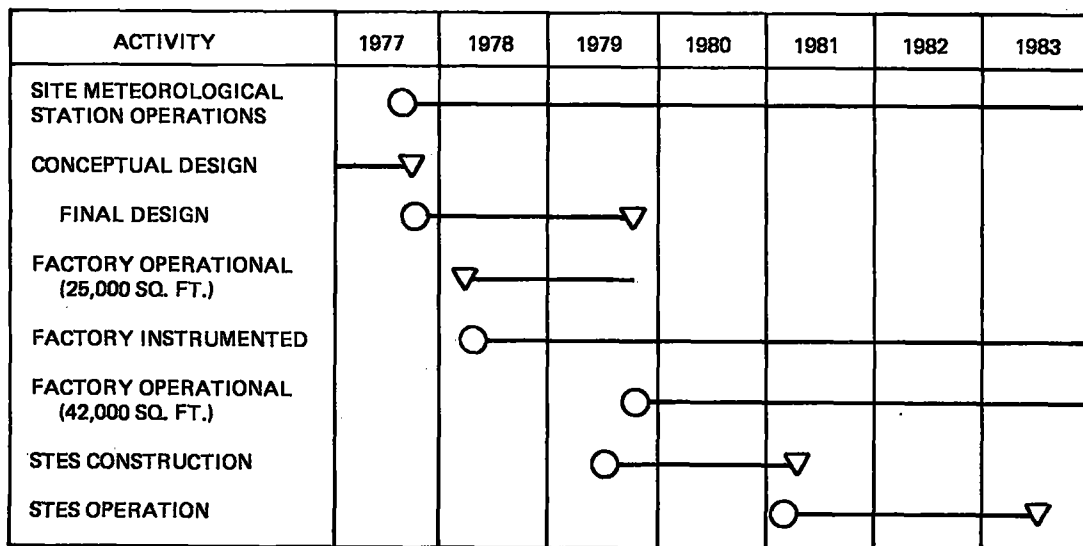


Figure F-4. Project Schedule

General Electric Company, Space Division (GE/SD) has been selected following a competitive conceptual design phase as the designer of the DOE funded and owned solar total energy system. Sandia Laboratories is DOE's technical manager for the Solar Total Energy - Large Scale Experiment. Members of the GE team and their activities are:

Scientific-Atlanta, Inc.
Parabolic Dish reflector for the solar collectors

Lockwood-Greene, Engineers
Engineering and Architectural Designs

The factory is extensively instrumented by Georgia Power to provide data for determining the factory energy use profiles for solar total energy system design and project performance. Sandia Laboratories has installed a meteorology station on the STES site to determine the solar energy available and to measure the weather. Heery and Heery has constructed the meteorology station site and Georgia Institute of Technology is operating the station for Sandia. Owens-Corning Fiberglas has contributed energy consultation services to Georgia Power and insulating materials for the Shenandoah Building.

The solar total energy system is initially sized to supply approximately 3.5 megawatts thermal power and 300 kilowatts electrical power. The system will supply 442^oK (337^oF) process steam in addition to a major portion of the knitwear factory's electrical, heating, air conditioning and hot water requirements. The 2323 m² (25,000 square-foot) knitwear manufacturing plant will employ 90 people, later expanding to 3902 m² (42,000 ft) and 300 employees. The accompanying line drawing (Figure F-5) depicts an artist's concept of the physical layout of the Solar Total Energy - Large Scale Experiment.

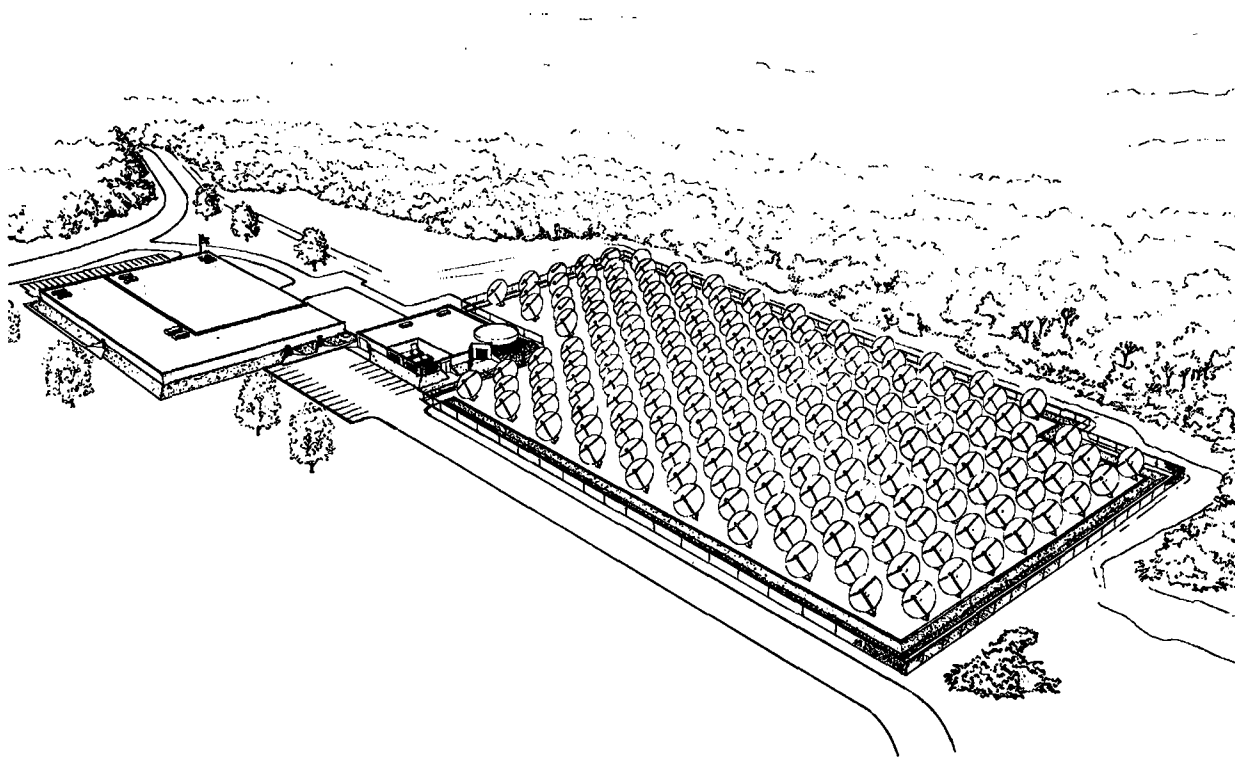


Figure F-5. Artist's Concept - STE-LSE Shenandoah

F. 1.3 OPERATION

The accompanying schematic (Figure F-6) shows the operation of the Shenandoah Solar Total Energy Large-Scale Experiment. Operation of the solar total energy system begins with circulation of a heat transfer fluid through the receiver tubes of a parabolic dish solar collector field. Solar radiation is focused on the receivers by the collectors and heats the transfer fluid to temperatures of 589°K (600°F) or more. The heat transfer fluid is then pumped to a heat exchanger or to thermal storage for later use.

In the heat exchanger, the heat transfer fluid boils and super-heats the steam working fluid, and the heat transfer fluid is returned to the collectors to repeat its cycle. The super-heated working fluid drives a multi-stage steam turbine which in turn drives an electrical generator that produces electricity for the system electrical requirements. Steam is extracted for knitwear manufacturing processes. The working fluid exhausted from the prime mover is cooled as it passes through a water-cooled condenser. Condenser cooling water is then used for heating, air conditioning, or hot water.

F. 2 ENVIRONMENTAL ASSESSMENT

A detailed environmental assessment study has been conducted for the proposed STE-LSE site by a team of technical specialists from the Georgia Department of Natural Resources. Pertinent information has been extracted and is presented here to provide a complete environmental overview. There are no known pre-existing environmental issues. The adverse environmental effects due to the STES are discussed in Section F. 2.13.

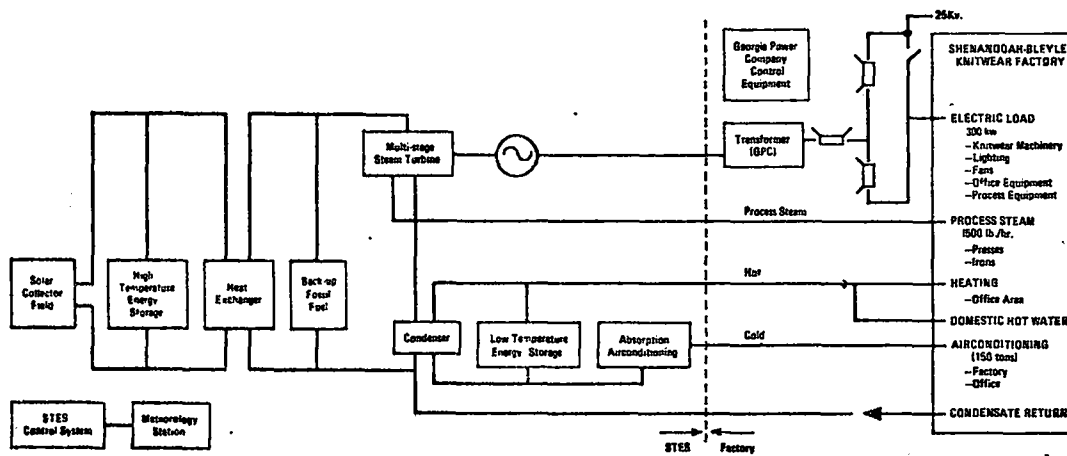


Figure F-6. Simplified System Schematic

F.2.1 GEOLOGY

The proposed site is situated in the Greenville Slope District of the Midland Georgia subsection of the Piedmont Physiographic Province. The topography is gently rolling with 2-10 percent slopes. The depth of weathered material is variable and ranges from 3-21 meters (10-70 feet). The site is located in a low seismic risk zone. The only significant impact on the geology of the site will occur during the clearing of vegetation from the area which will expose the soil to the forces of erosion. The rate and degree of erosion both during and after construction will be controlled by following accepted engineering procedures.

F.2.2 SOILS

There are four different series of soils on the site. In general, sandy and sandy-clay loams are characteristic. The soils have low to moderate shrinkswell potentials implying relatively stable soil conditions for foundations.

F.2.3 CLIMATE

It is not expected that there will be any impact on the climate outside of the property lines. With respect to the site itself, microclimatological effects will take place with the clearing of vegetation and the construction of the facility. These effects, which will occur on a small scale, are as follows: decrease in relative humidity, decrease in surface roughness, increase in average windspeed, increase in turbulence, increase in albedo, and increase in the sensible heat at the expense of latent heat.

F.2.4 SURFACE WATER HYDROLOGY

The STES-LSE site lies within the headwaters of the White Oak Creek Watershed of the Flint River Basin. The average annual runoff in the watershed is about 0.013 cubic meters per second per square kilometer (1.2 cubic feet per second per square mile). During the most severe drought on record, which occurred in 1954, the minimum one-day stream-flow in the vicinity of the project site was less than 0.0057 cubic meters (0.2 ft³) per second. The creeks in and around the STES-LSE site are small streams of limited capacity mainly because they are headwaters of the drainage basin. Some accumulated runoff will occur as a result of the devegetation and development. Any possible stream bank overflow will not be detrimental to the proposed development which will be well outside any flood hazard area.

F.2.5 GROUND WATER HYDROLOGY

The availability and quality of ground water in the Piedmont Province is complex. In general, the yield of water wells constructed to obtain their maximum yield will average about 0.114 cubic meters (30 gallons) per minute. Extreme yields range from 0 to 0.032 cubic meters per second (500 gallons per minute). There are several producing wells on or near the Shenandoah new town; however, many attempts at drilling wells in certain areas, such as for single-family residential use, have not produced water in sufficient quality and quantity. Depending on the location in the aquifer from which water is taken, iron may be present and, thus, require treatment for removal. The STE-LSE is not expected to cause any significant impact on the ground water resources of the area. However, there will be a slight decrease in the amount of recharge due to decreased vegetation and the impervious condition of the soil in some areas of the site.

F.2.6 FLORA

About 35 percent of the site is cleared land: abandoned pastures, fields and farm land. In the past, it has been maintained in stands of fescue and bahia grasses. The rest of the proposed site is covered with varying densities of second-growth mixed pine-hardwood canopy with pines predominating. Scattered individual trees represent ages beyond 30 years. The site does not contain any rare or endangered species.

A large part of the canopy vegetation will be removed, and this will result in a permanent impact to the trees and also to the understory plant species, which have limiting factors such as nutrients, pH and quantity of light.

F.2.7 FAUNA

A faunal inventory was prepared from field observations made at the proposed STE-LSE site for each representative habitat and from a literature research for the habitats common to the Georgia Piedmont. Among the mammals found, the most numerous were white-tailed deer, rabbits, squirrels, and cotton rats. Most birds on the site are songbirds, but there is also a dense population of quail. Several snakes, lizards, frogs, and turtles were observed on the site. There are no known endangered species present, nor is the acreage at this site likely to be designated critical habitat for any endangered species.

Habitat alteration in any area may prove to be harmful or beneficial to fauna depending upon the extent, character, and permanence of alteration. It is possible that alteration will be beneficial to some species while detrimental to others. If one considers that 23,000 square meters (5.72 acres) of land will be cleared for the STES and that little consideration will be given to wildlife, then the net impact of the project will be negative upon existing wildlife population.

F.2.8 ARCHAEOLOGY AND HISTORY

A preliminary survey of the site was conducted in order to determine if any archaeological or historical resources were evident on the project site, and no unique historical evidence was found. The general area shows some remnants of land-use practices as exhibited by road networks, town sites, and farming. There are no structures on the site at present other than the meteorological station and sewer line previously mentioned. The preliminary survey of the site did not reveal any archaeological resources. If any such resources exist, they are probably well below the surface since most of the area has undergone extensive farming in the past. Since Georgia has been occupied for about 10,000 years, there is a possibility of archaeological resources occurring all over the state.

In regard to impacts of the proposed STE-LSE project on the archaeology and history of the area, the construction of the facility will alter the physical record of land-use practices and patterns undertaken since the land cession of 1825. However, land-use patterns can be preserved via photographs and study reports. If anything of archaeological significance is below the surface, it will be studied and reported in accordance with federal procedures.

F.2.9 AIR QUALITY

F.2.9.1 General

Since the STES-LSE site is located in Coweta County, which is part of the metropolitan Atlanta intrastate air quality control region, the climatic data for this region will also apply to the STE-LSE site.

F.2.9.2 State and Federal Ambient Air Quality Standards

The State and Federal ambient air quality standards are presented in Table F-1.

F.2.9.3 Site Conditions

F.2.9.3.1 Winds

The wind direction which predominates during all seasons is from the northwest. Light winds (less than 3.6 meters per second or (8 miles per hour) predominate during all seasons and steady winds of more than 9.4 meters per second (21 miles per hour) rarely occur.

Table F-1. Ambient Air Standards Summary

Compound	Units*	Georgia	Federal Regs.		Time Interval	Reference Measurement Method
			Primary	Secondary		
Sulfur Dioxide	ug/m ³ ppm	715 (1hr) 0.28	-	1300 (3hr) 0.5		West-Cacke
	ug/m ³ ppm	330 0.09	365 0.14	-	24 hour	West-Cacke
	ug/m ³ ppm	43 0.015	80 0.03	-	annual mean	West-Cacke
Particulates	ug/m ³	150	260	150	24 hour	Hi-Vol
	ug/m ³	60	75	60	annual geom. mean	Hi-Vol
Carbon Monoxide	mg/m ³ ppm	40 35	40 35	40 35	1 hour	NDIR
	mg/m ³ ppm	10 9	10 9	10 9	8 hour	NDIR
Total Oxidants (Ozone)	ug/m ³ ppm	98 0.05	160 0.08	160 0.08	1 hour	Chemiluminescence
Total Non-Methane Hydrocarbons	ug/m ³	98	160	160	3-hr. Morning avg.	FID
Nitrogen Dioxide,	ug/m ³ ppm	100 0.05	100 0.05	100 0.05	annual mean	Cond. Method-Arse Chemiluminescence
NO ₂	ug/m ³ ppm	300 0.15	-	-	24 hour	

*Standard Conditions: SO₂ - 0°C, 1 atm.; CO, Ox, HC - 25°C, 1 ntr

ug/m³ - micrograms per cubic meter

mg/m³ - milligrams per cubic meter

This area is relatively unaffected by major cyclonic activity during these seasons. Winds containing an easterly component are at a minimum for all seasons except the fall months when the easterly winds make up a secondary maximum frequency. The minimum frequencies for all seasons are from the southerly and northerly quadrants.

F. 2. 9. 3. 2 Nearby Air Pollution Sources

Air pollution sources located in the vicinity of the proposed STE-LSE site do exist. The largest air pollution source is Georgia Power Company's Plant Yates, which is located some 16 kilometers (10 miles) northwest of the STE-LSE site. Plant Yates is a fossil-fuel fired, steam-electric generating plant (1, 250 MW) which emits particulate matter, sulfur dioxide, oxides of nitrogen, and hydrocarbons. These emissions are controlled by electrostatic precipitators; however, some 5.5×10^{-4} Kilogram per second (19.03 tons/year) of particulate matter and 0.017 Kilogram per second (598.5 tons/year) of sulfur dioxide are emitted to the ambient air. Nevertheless, Plant Yates is in compliance with the rules of the Georgia Department of Natural Resources, Environmental Protection Division, Chapter 391-3-1 Amended, Air Quality Control.

The Coweta General Hospital is located some 6.4 kilometers (4 miles) west of the STE-LSE site. This hospital operates a Joseph Goder Model 1510 incinerator to incinerate pathological waste. A Combustall Model 400 incinerator incinerates rubbish, mixture of paper, cardboard cartons, wood scraps, rags, plastic bags, and biological and pathological wastes at the Newnan Hospital, which is some 4.8 kilometers (3 miles) west of the proposed STE-LSE site. The particulate emissions from both of these incinerators are insignificant and in compliance.

Within 6.4 kilometers (4 miles) of the STE-LSE site, the William L. Bonnell Company, Inc., operates an aluminum extrusion operation (mechanical finishing). The buffing operation polishes finished extruded metal to a fine finish. The dust produced by this process is picked up by a vacuum system, and the fine particulates are removed from the gas stream by means of a wet scrubber (Rotoclone). The particulate emissions from the scrubber's stack are estimated to be 2.9×10^{-5} Kilogram per second (one ton/year) which is relatively insignificant and in compliance.

The C.W. Matthews Contracting Company's hot mix asphalt plant is located 8 kilometers (5 miles) northeast of the proposed STE-LSE site. This facility emits approximately 8.6×10^{-5} kilogram per second (3 tons/year) of particulate matter and 1.7×10^{-4} kilogram per second (6 tons/year) of sulfur dioxide from a dry collector and a baghouse. These emissions are insignificant and in compliance.

The only nearby air pollution sources of concern is Vulcan Material Company's Madras Quarry. At this quarry, granite particulates are given off by primary crushing, secondary crushing and screening, and washing-plant operations. These particulates are controlled, for the most part, by water sprays and a washing screen; however, approximately 8.0×10^{-4} kilogram per second (27.81 tons/year) of granite particulates are emitted to the surrounding atmosphere. Since there is a great deal of vegetation surrounding the Madras Quarry, it is doubtful that the granite particulates would travel any more than 1.6 kilometer (1 mile) downwind. As stated previously, the wind direction which predominates during all seasons is from the northwest. The STE-LSE site is located approximately 5 kilometers (3 miles) southwest of the Madras Quarry.

F. 2. 9. 3. 3 Mobile Sources

Carbon monoxide ambient air data is not available from the Newnan Hospital Road sampling site. The Environmental Protection Division has determined that the carbon monoxide levels are well below the State carbon monoxide ambient air standards (Rules of Georgia Department of Natural Resources, Environmental Protection Division, Chapter 391-3-1 Amended, Air Quality Control).

F. 2. 9. 3. 4 Ambient Air Data

The following ambient air data for Coweta County is taken from the high volume sampler and the SO₂ continuous sampler readings made at the Newnan Hospital Road sampling site, which has been in operation since April 1974. The suspended particulate data from the high volume sampler is expressed as the annual geometric mean. The SO₂ data from the SO₂ continuous sampler is expressed as the annual arithmetic mean. These annual means are compared with their respective state ambient air quality standard (Rules of Georgia Department of Natural Resources, Environmental Protection Division, Chapter 391-3-1 Amended, Air Quality Control). All ambient air data has units of micrograms/cubic meter.

	<u>State Standard</u>	<u>1974</u>	<u>1975</u>
Suspended particulates	60 ug/m ³	47 ug/m ³	39.78 ug/m ³
SO ₂	43 ug/m ³	31 ug/m ³	19.56 ug/m ³

It should be noted that the above ambient air data for both pollutants is well below the state ambient air quality standards. Since the prevailing wind direction is from the northwest, the above data also indicates that the stack emissions from Plant Yates are not producing any State ambient air quality standard violations. No ambient air data exists from the Newnan-Coweta County Hospital Road sampling site on carbon monoxide, nitrogen dioxide, photochemical oxidants, and non-methane hydrocarbons.

The STE-LSE site is located approximately 6 to 8 kilometers (4 to 5 miles) northeast of the Newnan Hospital Road sampling site. Since it is outside the city of Newnan and in a rural area, the ambient air quality at the STE-LSE site itself should be much better than the ambient air quality at the Newnan Hospital Road sampling site.

F. 2. 9. 4 Air Quality Summary

1. The air quality in the vicinity of the STE-LSE site is in compliance with the State ambient air quality standards.
2. It is not expected that the STE-LSE facility will contribute enough particulate, sulfur dioxide, nitrogen oxides, oxidants, or total hydrocarbons to make a significant change in the existing air quality.
3. The impact of any support or spin-off industries that occur in the vicinity of the site should be negligible because of the State of Georgia's Environmental Protection Division's authority to influence the location of industries through various regulations. In particular, the State of Georgia has been delegated the authority to conduct the required program to prevent significant deterioration of air quality.
4. With respect to mobile sources, considering the location of the proposed STE-LSE site and the existing conditions, it can be assumed that the impact of the carbon monoxide from the residents' and/or employees' vehicles will not produce a violation of the State carbon monoxide air quality standard.

F. 2. 10 WATER SUPPLY

Since the city of Newnan, Georgia serves Shenandoah through a 0.51 meter (20 in.) water main, there is abundant water supply for the STE-LSE site. Shenandoah has a 3785 cubic meter (one-million-gallon) storage tank and a contract with Newnan to supply the water. Shenandoah plans to build a 0.13 cubic meter per second (three-million-gallons per day) water treatment plant by 1981 which will be supplied by Lake Shenandoah and a 0.61 meter (24-inc.) main line from Line Creek.

F.2.11 WATER QUALITY

F.2.11.1 State Regulatory Programs

The policy of the Georgia Water Quality Control Act of 1964, as amended, is to provide prudent use of water resources to the maximum benefit of the people in order to restore and maintain a reasonable degree of purity in waters of the State and to require, where necessary, reasonable treatment of sewage, industrial wastes, and other wastes prior to their discharge into the waters of the State. The Environmental Protection Division of the Georgia Department of Natural Resources, which has responsibility for the quality of these water resources, establishes and maintains a water quality control program adequate for present and future needs of the State.

The standards promulgated under the water quality rules and regulations are to provide enhancement of water quality and prevention of pollution and to protect the public health and welfare in accordance with the public interest for drinking-water supplies, conservation of fish and game, and other beneficial uses. Surface waters are classified by category, each with a specific definition of usage. Those waters in the State whose existing quality is better than established standards on the date standards became effective are to be maintained at high quality; the State of Georgia has the power to authorize new developments when it has been affirmatively demonstrated to the State that a change is justifiable to provide necessary economic or social development.

F.2.11.2 Water Quality Standards

For water quality management and planning purposes, the fifteen major river basins of Georgia are subdivided into smaller watersheds, or Water Quality Management Units (WQMU). The town of Shenandoah lies in the White Oak Creek WQMU of the Flint River Basin. All streams in this WQMU are classified as fishing waters. The criteria in Georgia's rules and regulations for water quality control for fishing waters are the following:

1. Dissolved Oxygen. There must be a daily average of 0.006 kg/m^3 (6.0 mg/l) and no less than 0.005 kg/m^3 (5.0 mg/l) at all times for waters designated as trout streams by the Georgia Game and Fish Division. A daily average of 0.005 kg/m^3 (5.0 mg/l) and no less than 0.004 kg/m^3 (4.0 mg/l) at all times is required for waters supporting warm-water species of fish.
2. pH. The pH must be within the range of 6.0-8.5.
3. Bacteria. Fecal coliform must not exceed a geometric mean of 1,000 per 100 ml, based on at least four samples taken over a 30-day period and must not exceed a maximum of 4,000 per 100 ml.
4. Temperature. Temperature must not exceed 305°K (90°F). At no time is the temperature of the receiving waters to be increased more than 2.5°K (4.5°F) above intake temperatures, except that in estuarine waters the increase will not be more than 1°K (1.8°F). In streams designated as trout or small-mouth bass waters by the Georgia Game and Fish Division, there shall be no elevation or depression of natural stream temperatures.
5. Toxic Wastes, Other Deleterious Materials. There must be none in concentrations that would harm man, fish and game, or other beneficial aquatic life.

No water quality studies have been conducted on White Oak Creek in the vicinity of the STE-LSE site. However, the City of Newnan currently uses the stream as its sole supply of potable water and maintains a raw-water pumping station less than 5.3 kilometers (3.3 miles) downstream from the site. Since the quality of the raw-water supply is good and meets state drinking water standards (which are the same as fishing standards for pH, dissolved oxygen, temperature and bacteria), it is obvious that the quality of water at the proposed site is good and meets the fishing standards.

F. 2.11.3 Point Wastewater Sources

Four wastewater sources in the southeastern outskirts of Newnan discharge into Turkey Creek, which flows into White Oak Creek 1.6 kilometers (1 mile) downstream from the Newnan water intake. The two major sources are industries: Gold Kist Park and West Point Pepperell, Inc. These industries discharge processed wastewater after treatment, and both are required by permits to achieve higher levels of treatment by July 1, 1977. The unincorporated village of East Newnan has an untreated discharge of sewage, but treatment alternatives are being studied in the facilities planning process currently being conducted by the city of Newnan. Federal grant funds under P. O. 92-500 will be available for proper handling of this discharge. The fourth source of wastewater in Turkey Creek is the Quail Hollow Mobile Home Park, which has adequate wastewater treatment facilities.

Studies by the Georgia Environmental Protection Division in 1968 and 1971 showed that Turkey Creek does not meet water quality standards because of these four waste sources. However, this problem will be largely resolved shortly with the completion of upgrading at the two industrial treatment facilities.

F. 2.11.4 Wastewater Collection and Treatment for Shenandoah

The developers of Shenandoah have recently constructed, with the appropriate approvals by the Georgia Environmental Protection Division, a 0.013 cubic meter per second (300,000 gallons per day) wastewater treatment facility and initial portions of the sewage collection system for the new town. The facility is located north of the Central of Georgia Railway at the confluence of Turkey and White Oak Creeks. The treatment facility is designed to provide a very high degree of treatment for oxygen-demanding materials, and neither the present system nor future expansions thereof will cause violations of water quality standards in White Oak Creek. There is some minor potential for detrimental impact to water quality from erosion during any development. Coweta County has adopted and implemented a soil erosion and sediment control resolution applicable to such a development as the STE-LSE. The ordinance conforms to the requirements of the Georgia Erosion and Sedimentation Control Act of 1975. The guidelines will be implemented at the site during construction, and thus the water quality impact will be negligible.

F. 2.12 SOLID WASTE MANAGEMENT

F. 2.12.1 General

As defined by the Rules and Regulations for Solid Waste Management, Chapter 391-3-4 of the Georgia Environmental Protection Division, solid waste means putrescible and non-putrescible wastes, except water-caused body waste, and shall include garbage, rubbish (paper, cartons, boxes, wood, tree branches, yard trimmings, furniture and appliances, metal, tin cans, glass, crockery or dunnage), industrial wastes (waste materials generated in industrial operations), residue from incineration, food processing wastes, demolition wastes, abandoned automobiles, dredging wastes, construction wastes, and any other waste material in a solid or semi-solid state.

F. 2.12.2 Shenandoah and Coweta County

Coweta County generates all categories of solid waste in varying amounts. A solid waste management plan for Coweta County meeting the requirements of Section 6, Act 1486, Georgia Laws 1972, as amended, and Section 391-3-4-.05, Plans Required, amended, of the rules and regulations for solid waste management was approved November 20, 1974. This plan forecasts types and amounts of solid waste to be generated through the year 1985 including provisions for the residential development of Shenandoah. This plan does not include a forecast of increase in the amount of industrial wastes. Shenandoah and Coweta Counties are served by one solid waste disposal site (sanitary landfill) which is owned and operated by the county. The disposal site is located approximately 13 kilometers (8 miles) west of Shenandoah on Ishman Ballard Road. The site comprises 8×10^4 square meters (20 acres) with future expansion onto adjacent county property as required. All waste materials, except abandoned vehicles and hazardous wastes, are accepted for disposal. Coweta County has agreed to handle all solid waste disposal needs of Shenandoah which has no

plans for on-site disposal of solid wastes. All solid waste produced by the STE-LSE can be handled off-site, most probably at the Ishman Ballard Road Disposal site which is currently operated in accordance with a Georgia-approved Solid Waste Management Plan. There are also several private disposal sites within a radius of 56 kilometers (35 miles) that are readily accessible by I-85 or Georgia State Routes 34 and 54. In addition, several companies in Atlanta are in the waste reprocessing and recycling business. Coweta Co. has assumed responsibility for providing solid waste collection services within the county. Although the county operates no county-wide collection service of its own, it has contracted with a private company, Countrywide Sanitary Service, to provide service to all unincorporated areas of the county. The city of Newnan operates a collection system and uses the Ishman Ballard Road site for disposal.

Countywide Sanitary Service, Coweta Sanitary Service, and Georgia Waste Systems have solid waste handling permits for collection. Two other local private collection firms have not yet obtained permits. Collection for the STE-LSE is expected to be handled by private contract with one of the local collection companies since they generally handle commercial and industrial areas of the county.

There will be a small increase in solid waste production in the area due to the construction of the STE-LSE on the site. However, adequate facilities are available to handle it.

F. 2. 13 ADVERSE ENVIRONMENTAL EFFECTS

Siltation and sedimentation appear in many of the environmental investigations as adverse impacts. Soils, geology, water quality, surface hydrology, and fauna investigators have all identified this problem which will result from earth-moving operations. Increased runoff and decreased infiltration of rain-water resulting from paving and building construction are related problems that contribute to the sedimentation. Both can be mitigated.

It is anticipated that site and regional aesthetics will be degraded by the facility itself, by the traffic moving to and from the site, and by disposal sites in the area that will handle STE-LSE solid waste. Careful attention to aesthetic design of the STE-LSE will minimize these problems.

Site preparation and construction could destroy any unknown sub-surface archaeological sites, if present. However, by following federal guidelines for federal projects, losses will be prevented.

The loss of plant and animal life on the site is an impact that, over the short term, cannot be avoided or mitigated. However, no rare or endangered species are involved, and no species will be jeopardized by the project. Furthermore, a long-term solution where areas that cannot be developed are allowed through natural succession to revert to low-land hardwood forest can result in a more productive and diverse plant animal community without interference with research activities. The net result would be a long-term positive impact requiring little, if any, investment.

F. 2. 13. 1 STES Related

The following discussion addresses the major potential adverse environmental effects specifically related to operation of the STE-LSE. It should be recognized that this discussion merely identifies these effects and that they will be dealt with during definitive system design through the development of pollution control procedures and/or the design of pollution abatement systems.

F. 3. 13. 2 Collector Cleaning

During testing and operation of the Solar Total Energy System, the collector surfaces will have to be cleaned at one to two week intervals. Current procedures call for the use of a biodegradable detergent spray wash followed by a deionized water rinse. This water can enter the environment through drainage systems and, depending upon the specific detergent used, can provide nutrients for increased algae growth in the receiving waters. Discussions with personnel responsible for operation of the recently

constructed Shenandoah Sewage Treatment Plant indicated that there is the possibility of routing collector cleaning water to this plant. A final agreement will depend upon detergent concentration, total water volume per cleaning, and frequency of cleaning.

F.2.13.3 Fossil-Fired Backup

The fossil-fired backup heater of the STE-LSE will use natural gas provided from existing gas mains of the Atlanta Gas Light Company. Violation of the Federal or State of Georgia Air Quality Standards could possibly occur through improper operation or maintenance of the system, although this is far less likely with natural gas than with oil. No problems are anticipated.

F.2.13.4 Environmentally Hazardous Materials

The only materials used in the STE-LSE which could potentially fall into this category are the collector and storage heat transfer fluid—Dow Corning Syltherm 800—and the water treatment chemicals used to condition boiler feed water. The effects of a Syltherm spill on the environment are relatively minor compared to many liquids. It will turn grass brown and will not allow water to permeate the spill area. Syltherm 800 has a life expectancy in soil of approximately 1.2 years before turning to sand. It is not harmful to fish or animals although large amounts taken internally by humans will cause diarrhea. A chemically similar liquid is a major component of the antacid product Digel. The relatively benign nature of Syltherm 800 does not, however, preclude extensive leakage and spillage protection. The collector field will be paved and sloped toward the northeast corner, at which point an oil separation system will insure that only rain water is allowed to drain off the STE-LSE property. Within the mechanical building, all Syltherm containing components are located within a curbed area which diverts any spillage or leakage to a common sump area for removal. Water treatment chemicals will be stored and used in such a manner that inadvertent spills or leaks cannot reach the environment through floor drains, personnel contamination, etc.

F.2.13.5 Cooling Tower and Boiler Blowdown

In order to reduce the buildup of solids in circulating cooling water and in the steam boiler and boiler water, discharge (blowdowns) are frequently performed at the cooling tower and the boiler. These blowdowns are generally high in pH and always high in total solids containing sodium, phosphate, and corrosion products. Small quantities of hydrazine may also be present in boiler blowdown. None of these blowdowns can be discharged directly to the environment. The water will have to be treated and then may be discharged or perhaps recycled.

As part of the discussions with personnel responsible for operating the Shenandoah Sewage Treatment Plant, the feasibility of directing cooling tower and boiler blowdowns to the sewage plant was examined. Depending upon the nature, quantity, and frequency of the blowdown, it may be possible to pump these discharges to the sewage treatment plant either directly or with pretreatment.

F.2.13.6 Solid Waste

In order to provide acceptable quality boiler feed water and to provide for any necessary waste water treatment, various types of water purification media such as ion exchange resin, activated carbon, and cartridge-type filters will be utilized. When these media are expended, they must be replaced and the spent media directed to a licensed sanitary landfill without spillage or other incident during handling or transportation. Operation and administrative procedures will be developed to address these situations. Based upon a more refined definition of the STES design, pollution control procedures and systems will be designed to prevent illegal discharges to the environment either through routine operations or inadvertently.

F.2.14 IRREVERSIBLE AND IRRETRIEVABLE COMMITMENTS OF RESOURCES

Most irreversible and irretrievable commitments of resources resulting from the implementation of the project will involve natural resources occurring in other areas of the State, Nation, or world which will be expended on the site. Human and financial resources will also be involved. Off-site resources include building materials (whether mineral or timber) needed to construct buildings, roads, utility lines, and pipes; employee residences and offices or research equipment; fossil fuels for energy; human labor to construct the facility, to provide labor for the research project and to provide police protection and community services; and money to pay for construction, maintenance, operations, and salaries. Water used by the site will not be available to other users; it will be treated and returned to the streams. Chemicals involved in treatment will be lost. Solid waste generated on the site will be placed on landfills and may or may not be irretrievably lost.

The only irreversible commitment of on-site resources will be the loss of animal and plant life when the site is cleared for development. Lives of individual plants and animals will be lost, but no species will be threatened and no rare or endangered species are involved.

F.3 POTENTIAL ENVIRONMENTAL IMPACTS

Site preparation will require removal of existing vegetation which consists of fescue and bahia grasses and second-growth pine trees. No rare or endangered species are involved. Grading of the area under the collector field is not likely to cause significant erosion, especially in light of the anti-erosion measures designed into the grading and paving plan. During erection of the collector field and construction of the mechanical building, there will be minor construction noise. No blasting and minimal use of heavy equipment is anticipated. Construction activity will be confined to property under control of Shenandoah Development Incorporated and in the industrial area of Shenandoah. Little or no disturbance of local residents through noise, dust, or construction activity is expected.

Construction activities will have little effect on wildlife species. None breed in the area and there is little dependence on the area for food.

Operation of the Solar Total Energy System will produce some exhaust gas pollution from the back-up fossil heater, but net exhaust gas will be decreased due to the high displacement of the Bleyle plant energy needs by solar energy and the resultant greatly lowered utilization of the Bleyle natural gas process steam and heating boilers. The STE-LSE will have some low level thermal energy (366°K or 200°F) dissipated through two roof-top cooling towers. This should have a negligible environmental effect.

The solar collectors will reflect light and thus will require fencing to maintain observers at a safe distance estimated at present to be a minimum of about six meters (20 feet). The solar collectors will be designed to withstand a 40-m/sec. (90 mph) wind. Such winds are extremely rare. If, however, an extremely high wind were to tear loose some collectors, the potential destruction they might cause would be trivial compared to other effects of such a hurricane.

Only a very few (1-3) personnel will be needed to operate the facility. In addition, fluctuating numbers of researchers will visit the site. No impacts will result from the small work force.

F.4 ALTERNATIVES TO THE PROPOSED ACTION

The reasonably available alternatives to the proposed action are to delay or not to construct the project. The purpose of the proposed project is to demonstrate the feasibility of solar total energy in a typical industrial application. In this context, a delay or abandonment of the project would result in a commensurate delay in the demonstration of solar total energy in the 300 kW range. The project will serve the dual roles of conservation of fossil energy and demonstration of an alternate energy concept with high potential for future energy savings.

APPENDIX G
SOLAR COLLECTOR SUBSYSTEM FAILURE MODES EFFECTS
CRITICALITY AND SAFETY ANALYSIS

Table G-1. Shenandoah STES, Failure Mode Effects Criticality and Safety Analysis (Page 1 of 4)

SUBSYSTEM SOLAR ENERGY COLLECTION
 COMPONENT SOLAR COLLECTION

SHENANDOAH STES

FAILURE MODE EFFECTS CRITICALITY AND SAFETY ANALYSIS

PAGE 1 OF 4

DATE 7/27/78

BY J.F. KENT

G-1

UNIT OR ASSEMBLY	FUNCTION	FAILURE MODES	PROBABLE CAUSE	FAILURE EFFECT ON		CRITICALITY CATEGORY		REMARKS
				NEXT HIGHER ASSEMBLY	STES OPERATION	SAFETY	MISSION	
1.3 JACK & MOTOR ASSY - ELEVATION AXIS	ORIENT DISH FOR SEASON ELEVATION OF SUN; VERTICAL MOTION - 47° RANGE	FAILURE TO PROVIDE PROPER ELEVATION DUE TO MOTOR OR JACK FAILURE	BRUSHES, WIRING OR BEARING FAILURE. FATIGUING/AGING EFFECTS. CONTROL CIRCUIT FAILURE.	DISH ORIENTATION IN VERTICAL AXIS INHIBITED. SPECIFIC COLLECTOR DEACTIVATED UNTIL FAULT IS CORRECTED	COLLECTOR FIELD OPERATION NOT AFFECTED UNTIL MORE THAN 5% OF COLLECTORS ARE "DOWN" STES OPERATION - NORMAL.	D	3	GEARBOX, BEARINGS & MOTOR LUBED AND CHECKED PER REGULAR MAINTENANCE. CYCLED DAILY.
2.0 DISH ASSY (PARABOLOIDAL)	COLLECT, REFLECT AND FOCUS SUNS RAYS ON RECEIVER TO HEAT SILICONE B FLUID TO 750°F.							
2.1 DISH ASSY-LEAFS OR STRIPS (N = 20) (ALUMINUM BASE AND B/U STRUCTURAL STIFFENER)	MAINTAIN DIMENSIONAL INTEGRITY TO PROVIDE FOCUSED SUN ENERGY (MIN 50 BTU/HR - FT ²) TO THE SILICONE B FLUID IN THE RECEIVER (--20 INDIVIDUAL LEAFS)	LEAF(S) FAIL TO ADEQUATELY FOCUS (REFLECT) SUNS RAYS ON RECEIVER	BACKUP STRUCTURE OR LEAF STRUCTURAL DAMAGE DUE TO HIGH WINDS (90 MPH) OR LIGHTNING; SURFACE DAMAGE DUE TO HAIL-STONES OR OTHER WIND DRIVEN PARTICLES SUCH AS SAND/SMALL STONE, GRAVEL, ETC.	COLLECTOR ASSEMBLY IN-ACTIVATED UNTIL FAULT CORRECTED.	COLLECTOR FIELD OPERATION NOT SIGNIFICANTLY AFFECTED UNTIL MORE THAN 5% OF COLLECTORS ARE "DOWN" STES OPERATION UNAFFECTED.	D	3	REFLECTOR PETALS INDIVIDUALLY REPLACED.
2.2 REFLECTIVE SURFACE POLISHED ALUMINUM AND TRANSPARENT PROTECTIVE SURFACE	REFLECT SUNS RAYS TO RECEIVER WITH HIGH EFFICIENCY (50 BTU/HR-FT ² AS ABOVE)	DEGRADED/DAMAGED SURFACE-HENCE POOR COLLECTION EFFICIENCY (DEGRADATION OVER 20 YR LIFE)	STORM DAMAGE - SURFACE DAMAGE (PEENING) DUE TO HAILSTONES OR WIND DRIVEN PARTICLES SAND, GRAVEL SMALL STONES. POSSIBLE AGING EFFECTS.	SAME AS ABOVE	SAME AS ABOVE	D	3	ALUMINUM IS COVERED BY TRANSPARENT PROTECTIVE COATING WHICH WILL BE A SILICON RTV.

Table G-1. Shenandoah STES, Failure Mode Effects Criticality and Safety Analysis (Page 2 of 4)

SUBSYSTEM SOLAR ENERGY COLLECTION
 COMPONENT SOLAR COLLECTOR

SHENANDOAH STES
 FAILURE MODE EFFECTS CRITICALITY AND SAFETY ANALYSIS

PAGE 2 OF 4
 DATE 7/27/78
 BY J.F. KERT

UNIT OR ASSEMBLY	FUNCTION	FAILURE MODES	PROBABLE CAUSE	FAILURE EFFECT ON		CRITICALITY CATEGORY		REMARKS	
				NEXT HIGHER ASSEMBLY	STES OPERATION	SAFETY	MISSION		
1	MOUNT & DRIVE ASSY.	PROVIDE SUPPORT AND MECHANISMS FOR TWO AXIS MOTION OF THE DISH (REFLECTOR) ASSY. RANGE OF AXIS MOTION: 47° - ELEVATION 180° - POLAR AXIS							
1.1	SUPPORT STRUCTURE	PROVIDE SUPPORT FOR DISH AND PIPING; MAINTAIN DIMENSIONAL INTEGRITY OVER WIDE RANGE OF WEATHER CONDITIONS	DEFLECTION/DISTORTION IN EXCESS OF DESIGN LIMITS LEADING TO PIPING LEAKS OR CONSTRAINED AXES MOTION	STORMS-HIGH WIND LOADS OR LIGHTNING; FATIGUE FAILURES AND UNDETECTED FABRICATION FLAWS (E.G. WEAK WELDS)	SPECIFIC COLLECTOR INACTIVATED UNTIL FAULT CORRECTED.	COLLECTOR FIELD OPERATION NOT AFFECTED UNTIL MORE THAN 5% OF COLLECTORS ARE "DOWN" STES OPERATION-NORMAL.	C	3	DESIGNED FOR WIND LOADS UP TO 90 MPH. PLANNED TESTING TO PROOF DESIGN.
1.2	JACK & MOTOR ASSY - POLAR AXIS	ORIENT DISH ASSY TO TRACK SUN FROM EAST TO WEST (180° TRAVEL-1/2° INCREMENTS)	FAILURE TO TRAVERSE DUE TO MOTOR OR JACK FAILURE	BRUSHES, WIRING OR BEARING FAILURE; CONTROL CIRCUIT FAILURE; FATIGUING OR AGING EFFECTS.	DISH TRACKING EAST-WEST IS INHIBITED. SPECIFIC COLLECTOR OR INACTIVATED UNTIL FAULT CORRECTED.	SAME AS ABOVE	D	3	"JACKUATOR" GEAR BOX WITH SQUARE ACME THREAD AND BEARING (BOOT PROTECTED) ARE LUBED PER REGULAR MAINTENANCE. ASSEMBLY IS CYCLED DAILY.
1.2.1	HIGH SPEED MOTOR FOR DEFOCUS MOTION	HIGH SPEED MOTOR TO TRAVERSE RAPIDLY AND DEFOCUS DISH ON RECEIPT OF OVER TEMP SIGNAL FROM RECEIVER	FAILURE TO DEFOCUS DISH IN RESPONSE TO O.T. SIGNAL.	FAILURE LIKELY IN CONTROL CIRCUIT (RELAY) SINCE MOTOR IS ACTIVE FOR NORMAL TRAVERSE MOTION.	OVERTEMP PROTECTION (1ST LEVEL) LOST, DAMAGE TO RECEIVER/PIPING IS POSSIBLE. COLLECTOR SHUTDOWN IS REQUIRED.	SAME AS ABOVE	C	3	SUN MOVEMENT MAY ALLEVIATE O.T. CONDITION IF TRACKING IS ABSENT. IMMEDIATE SECONDARY ACTION MAY BE REQUIRED.

G-2

Table G-1. Shenandoah STES, Failure Mode Effects Criticality and Safety Analysis (Page 3 of 4)

SUBSYSTEM SOLAR ENERGY COLLECTION
 COMPONENT SOLAR COLLECTOR

SHENANDOAH STES

FAILURE MODE EFFECTS CRITICALITY AND SAFETY ANALYSIS

PAGE 3 OF 4
 DATE 7/27/78
 BY J.F. KENT

G 1 3

UNIT OR ASSEMBLY	FUNCTION	FAILURE MODES	PROBABLE CAUSE	FAILURE EFFECT ON		CRITICALITY CATEGORY		REMARKS
				NEXT HIGHER ASSEMBLY	STES OPERATION	SAFETY	MISSION	
3.0 RECEIVER & PIPING ASSY	PROVIDE VEHICLE WHERE SILICONE B FLUID IS HEATED TO 750°F BY FOCUSED SUN RAYS AND FLEXIBLE TUBING TO CONVEY FLUID TO AND FROM THE HEATING COILS.							
3.1 RECEIVER-COATED STEEL CAN WITH CAVITY. CONTAINS COILED STACKED TUBES.	HEATER-VEHICLE WHERE SILICONE B FLUID IS HEATED TO 750 F.	COILED TUBE JOINT LEAKAGE	OVER TEMPERATURE CONDITION, UNDETECTED BUT INCIPIENT WEAK COIL JOINT/WELD. FATIGUING/AGING EFFECTS.	COLLECTOR DEACTIVATION AND ISOLATION REQUIRED UNTIL FAULT CORRECTED.	COLLECTOR FIELD OPERATION NOT SIGNIFICANTLY AFFECTED UNTIL MORE THAN 5% OF COLLECTORS ARE "DOWN" STES OPERATION-NORMAL.	C	3	"GENEROUS" DESIGN MARGIN AND TEST PROGRAM INCORPORATED TO PROVIDE A FAULT FREE DESIGN.
3.2 PIPING - ROTARY JOINTS, BELLOW PIPING AND NESTED LAYER, REINFORCED INSULATION.	CONDUCT SILICONE "B" FLUID TO AND FROM RECEIVER AND THE COLLECTOR FIELD MANIFOLD.	JOINT LEAKAGE	FATIGUING/AGING EFFECTS UNDETECTED INCIPIENT WEAK WELD.	COLLECTOR DEACTIVATION AND ISOLATION REQUIRED UNTIL FAULT CORRECTED.	POSSIBLE IMPACT ON ADJACENT COLLECTORS. DEGRADED COLLECTOR FIELD/STES OPERATION POSSIBLE.	C	2	20 YEAR LIFE DESIGN GOAL INCORPORATED INTO DESIGN SELECTION AND TEST PROGRAM.
		INSULATION DEGRADATION-CRACKING/SHIFTING	FATIGUING/AGING EFFECTS.	NO EFFECT - CORRECT DURING SCHEDULED PREVENTIVE MAINTENANCE. IF WIDESPREAD OVER TOTAL COLLECTOR - PIPING, COLLECTOR MAY BE DE-ACTIVATED.	SAME AS ABOVE.	D	3	HEAT LOSS DUE TO DEGRADED INSULATION ON A COLLECTOR WILL SERVE TO SHIFT ENERGY LOAD TO OTHER ACTIVE COLLECTORS IN THE FIELD.
4.0 CONTROL ASSY. INCLUDES LOCAL CIRCUITRY COMPRISED OF CONTROL BOX WITH RELAYS. POSITION POT (1/2") AND SUN SENSOR (48/CENTRAL CONTROL MICRO PROCESSOR)	PROVIDE ELECTRICAL SIGNALS TO COLLECTOR JACKUATOR MOTORS SO THAT COLLECTOR ADEQUATELY "TRACKS" SUN-TWO AXIS TRACKING IS PROVIDED.							

Table G-1. Shenandoah STES, Failure Mode Effects Criticality and Safety Analysis (Page 4 of 4)

SUBSYSTEM SOLAR ENERGY COLLECTION
 COMPONENT SOLAR COLLECTOR

SHENANDOAH STES
 FAILURE MODE EFFECTS CRITICALITY AND SAFETY ANALYSIS

PAGE 4 OF 4
 DATE 7/27/78
 BY J.F. KENT

UNIT OR ASSEMBLY	FUNCTION	FAILURE MODES	PROBABLE CAUSE	FAILURE EFFECT ON		CRITICALITY CATEGORY		REMARKS
				NEXT HIGHER ASSEMBLY	STES OPERATION	SAFETY	MISSION	
4.1 SUN SENSOR	PROVIDES SUN CENTERING INFORMATION TO THE CENTRAL CONTROL MICROPROCESSOR. THIS INFORMATION IS PROCESSED AND RESULTS IN CONTROL SIGNALS WHICH ACTUATE JACKUATOR MOTORS TO MOVE DISH TO OPTIMUM TRACKING POSITION.	ERROR SIGNAL OR NO SIGNAL TO MICROPROCESSOR (µP) IN CENTRAL CONTROL FROM EITHER DETECTOR SET. ONE 2 DETECTOR SET FOR DECLINATION AND ONE FOR POLAR POSITIONING.	DETECTOR OR NULL CIRCUITRY FAILURE.	DEGRADED DISH ORIENTATION, OR POSSIBLE "HOT SPOT" DEVELOPMENT IF TRACKING IS NOT OPTIMUM. DEFOCUS MEASURES AND/OR COLLECTOR DEACTIVATION MAY BE REQUIRED UNTIL FAILURE/FAULT IS CORRECTED.	STES OPERATION NORMAL COLLECTOR FIELD NOT SIGNIFICANTLY AFFECTED UNTIL MORE THAN 5% OF COLLECTORS ARE "DOWN"	C	3	SUN SENSOR SIGNALS TO THE CENTRAL CONTROL ARE UTILIZED FOR COMPARISON AND POSITIONING FIRST BY THE PRE-PROGRAMMED COARSE CONTROL AND SECONDLY BY THE OPTICAL FINE CONTROL CIRCUITRY. COARSE CONTROL IN ~1° TO 2° FINE CONTROL ~1/8 DEGREE.
4.2 POSITION "POT" (S)	POSITION POTENTIOMETER(S) PROVIDES DISH POLAR AND DECLINATION AXIS POSITION SIGNAL TO THE CENTRAL CONTROLLER UP.	ERROR SIGNAL OR "NO SIGNAL" TO UP IN CENTRAL CONTROL.	ELECTRICAL CIRCUIT FAILURE.	SAME AS ABOVE	SAME AS ABOVE	C	3	48 POSITION POT. SIGNAL TO EACH CENTRAL CTL UP (POSITION TO 1/2" INCREMENTS) LOW FAILURE PROBABILITY.
4.3 CONTROL BOX-RELAYS	RELAYS CONTACTS GATE CONTROL POSITIONING PULSES TO THE JACKUATOR MOTORS FOR DECLINATION POLAR AND TRAVERSE DEFOCUS.	CONTRACTS FAIL TO CLOSE ON COMMAND OR REMAIN CLOSED (WELDED) AFTER COMMAND	RELAY CONTAMINATION, INTERNAL RELAY STRUCTURAL FAILURE WELD CLOSED, STRUCTURAL FAILURE OR SPRING FAILURE.	DEGRADED/LOSS DISH MOTION, POSSIBLE "HOT SPOT" IN RECEIVER. DISH ORIENTATION NOT CONTROLLED, COLLECTOR DEACTIVATION REQUIRED.	SAME AS ABOVE	C	3	APPROX. 8 RELAYS PER COLLECTOR CONTROL BOX 48 BOXES PER EACH CENTRAL CONTROL UP.
4.4 OVER TEMPERATURE (OT) SENSOR	OVER TEMPERATURE SENSOR DETECTS "HOT SPOT" OR SILICONE B FLUID HIGH TEMPERATURE AND SENDS SIGNAL TO CENTRAL CONTROL UP.	FAILS TO SENSE OR SEND OT SIGNAL TO CENTRAL CONTROL UP.	SENSOR FAILURE OR ELECTRICAL CIRCUIT FAILURE.	DEFOCUS INHIBITED, RECEIVER/ COLLECTOR DAMAGE PROBABLE. COLLECTOR DEACTIVATION REQUIRED.	POSSIBLE IMPACT ON ADJACENT COLLECTORS. DEGRADED COLLECTOR FIELD/ STES OPERATION POSSIBLE.	C	2	OT SENSOR CHECK ALSO PROMINENT IN REGULAR PM PROCEDURES. LC FAILURE PROBABILITY.

G-4

APPENDIX H
ABSORPTION AIR CONDITIONER FAILURE MODES EFFECTS
CRITICALITY AND SAFETY ANALYSIS

Table H-1. Shenandoah STES, Failure Mode Effects Criticality and Safety Analysis (Page 1 of 7)

TABLE 1
 SUBSYSTEM COOLING SUBSYSTEM
 COMPONENT ABSORPTION AIR CONDITIONER (AAC)
 AND TUS COMPONENTS

SHENANDOAH STES
 FAILURE MODE EFFECTS CRITICALITY AND SAFETY ANALYSIS

PAGE 1 OF 7
 DATE 6/9/78
 BY J.F. KENT

UNIT OR ASSEMBLY	FUNCTION	FAILURE MODES	PROBABLE CAUSE	FAILURE EFFECT ON		CRITICALITY CATEGORY		REMARKS
				NEXT HIGHER ASSEMBLY	STES OPERATION	SAFETY	MISSION	
1. SINGLE STAGE ABSORPTION COLLECTOR GENERATOR-TRANE MODEL ABC-03F, 354 TONS.	PROVIDE CHILLED SYSTEM WATER TO BLEYLE FAN COIL (AIR CONDITIONING) UNIT	FAILURE TO PROVIDE CHILLED 45° WATER TO BLEYLE.	VARIOUS CAUSES IDENTIFIED BELOW.	THERMAL UTILIZATION SYSTEM (TUS) NOT EMPLOYED EFFECTIVELY.	STES COOLING NOT PROVIDED TEMPORARILY, BUT STES OPERATION NORMAL FOR ELECTRICAL POWER & PROCESS STEAM. BLEYLE COOLING SYSTEM IS A BACK-UP.	D	3	COOLING SUBSYSTEM, ESPECIALLY THE AAC UNIT, IS CONSIDERED OVERALL TO BE BENIGN WITH RESPECT TO SAFETY.
1. SHELL (STRUCTURE) -- ALL MAJOR SECTIONS WITHIN ONE SHELL (CONCENTRATOR, CONDENSER, EVAPORATOR & ABSORBER)	MAINTAIN HERMETIC INTEGRITY FOR INTERNAL VACUUM CONDITIONS (.01 TO .1 ATM) OF THE LITHIUM BROMIDE WATER ABSORPTION REFRIGERATION CYCLE	LOSS OF HERMETIC INTEGRITY (LEAKTIGHTNESS) - AIR LEAKAGE INTO SHELL INTERIOR.	UNDETECTED BUT INCIPIENT WEAR SURFACE OR SEAM WELD, JOINT, FATIGUING OR AGING EFFECTS.	LEAKAGE CUTS CAPACITY, PROMOTES CORROSION AND CAN CAUSE CRYSTALLIZATION WITHIN AAC UNIT. IT CAN FORCE UNSCHEDULED SHUTDOWNS. TUS NOT EMPLOYED EFFECTIVELY.	STES COOLING NOT PROVIDED TEMPORARILY, BUT STES OPERATION NORMAL FOR ELECTRICAL POWER & PROCESS STEAM. BLEYLE COOLING SYSTEM IS A BACK-UP.	D	3	HERMETIC INTEGRITY IS FIRST IN DESIGN PRIORITIES. AAC TOTALLY FACTORY ASSEMBLED AND VACUUM TESTED BY MASS SPECTROMETRY BEFORE SHIPMENT. FIELD ASSEMBLY NOT REQUIRED. SINGLE SHELL CONTRIBUTES TO H RELIABILITY (AVAILABILITY).
2. HEADERS & TUBE BUNDLES/SUPPORTS A. CONCENTRATOR	HEADERS ARE THE SEALED CAPPED ACCESS PORTS FOR MAINTENANCE ACTIONS ON TUBES. HEAT IS ADDED VIA CUPRO-NICKEL TUBES WHICH INTERNALLY PORT TUS 210°F WATER. LI BR DISTILLED WATER SOLUTION IS EXTERNAL. PRESSURE ABOUT 70 MM Hg. FIXED & FLOATING SUPPORTS CONTROL TUBE EXPANSION SUCH THAT TUBES EXPAND TOGETHER IN TIME SAME DIRECTION AND DO NOT TOUCH.	2.A.1) WATER LEAKAGE AT TUBE ENDS (IN ANNULAR GROOVE OF TUBE SHEETS) OR ALONG TUBE LENGTH. 2.A.2) PITTING REDUCTION IN HEAT TRANSFER EFFICIENCY	UNDETECTED WEAK JOINT, FATIGUING/AGING EFFECTS OR EROSION EFFECTS CORROSION EFFECTS	HOT TUS WATER ENTERS & DILUTES LI Br SOLUTION BELOW WORKABLE CONCENTRATION, AAC SHUTDOWN & MAINTENANCE ACTION REQUIRED. REDUCTION IN AAC EFFICIENCY, HENCE CAPACITY. EVENTUAL NEED FOR SHUT DOWN AND MAINTENANCE ACTION.	STES COOLING NOT PROVIDED TEMPORARILY, BUT STES OPERATION NORMAL FOR ELECTRICAL POWER & PROCESS STEAM. BLEYLE COOLING SYSTEM IS A BACK-UP. STES COOLING NOT PROVIDED TEMPORARILY, BUT STES OPERATION NORMAL FOR ELECTRICAL POWER & PROCESS STEAM. BLEYLE COOLING SYSTEM IS A BACK-UP.	D	3	AT EITHER END, HEADERS REMOVED FOR ACCESS TO ANY TUBE BUNDLE ALL TUBES INDIVIDUALLY REPLACED FLOW INTERIOR TO Cu-Ni TUBES LIMITED TO 12 FPS. TUBES TESTED TO 150% OF 400 P DESIGN PRESSURE. COPPER-NICKEL (Cu-Ni) TUBES USED. THEY ARE HIGHLY RESISTANT TO CORROSION. (PLAIN COPPER IS TO FORMATION OF CUPROUS-OXIDE WHICH IS SOLUBLE IN LI Br). PURE COPPER IS VULNERABLE WHEN EVER AIR LEAKAGE OCCURS.

I-H

Table H-1. Shenandoah STES, Failure Mode Effects Criticality and Safety Analysis (Page 2 of 7)

TABLE 1.

SUBSYSTEM COOLING SUBSYSTEM

SHENANDOAH STES

PAGE 2 OF 7

COMPONENT ABSORPTION AIR CONDITIONER (AAC)
AND TUS COMPONENTS

FAILURE MODE EFFECTS CRITICALITY AND SAFETY ANALYSIS

DATE 6/9/78

BY J.F. KENT

UNIT OR ASSEMBLY	FUNCTION	FAILURE MODES	PROBABLE CAUSE	FAILURE EFFECT ON		CRITICALITY CATEGORY		REMARKS
				NEXT HIGHER ASSEMBLY	STES OPERATION	SAFETY	MISSION	
II CONT'D								
B. CONDENSER (OPERATING PRESS = 70 MM Hg) HIGH PRESSURE REFRIGERANT (WATER) VAPOR IS CONDENSED & FALLS AS LIQUID TO BOTTOM OF CONDENSER. IT RELEASES HEAT OF VAPORIZATION TO COOLING WATER FLOWING THROUGH TUBE BUNDLE.	HEADERS ARE SEALED/ CAPPED ACCESS PORTS FOR TUBE MAINTENANCE. HEAT OF VAPORIZATION TRANSFERRED TO COOLING TOWER WATER FLOWING INSIDE OF Cu NI TUBES.	1) LEAKAGE AT TUBE ENDS OR ALONG TUBE LENGTH	UNDETECTED WEAK JOINT, FATIGUING/AGING EFFECTS	WORKING SOLUTION DILUTED BELOW WORKABLE CONCENTRATION. AAC SHUTDOWN & MAINTENANCE ACTION REQUIRED.	STES COOLING TEMPORARILY LOST BUT STES OPERATION NORMAL FOR ELECTRICAL POWER & PROCESS STEAM. BLEYLE COOLING IS A BACK-UP.	D	3	SAME AS I 2. A.1 ABOVE BUT COPPER TUBES ARE PRESSURE TESTED TO 150% OF 150 PSI DESIGN PRESSURE.
		2) PITTING OR FOULING -- REDUCED HEAT TRANSFER EFFICIENCY	CORROSION	SAME AS I 2. A.2 ABOVE	SAME AS ABOVE	D	3	COPPER TUBES USED SINCE WATER FLOWS INSIDE TUBES AND WATER VAPOR & LIQUID ARE OUTSIDE. THIS IS HIGH PRESSURE ZONE (70 MM Hg) NOT AFFECTED BY AIR LEAKAGE AND FORMATION OF CUPROUS OXIDE.
C. EVAPORATOR (OPER. PRESS = 7 MM Hg). LIQUID REFRIGERANT WATER FLASHES TO VAPOR IN PASSING THROUGH ORIFICE TO LOW PRESSURE REGION - THE EVAPORATOR. THE REFRIGERATION CYCLE STARTS HERE. ADDITIONAL LIQUID FLASHES TO VAPOR AFTER BEING SPRAYED OVER TUBE BUNDLE WHICH HAS SYSTEM WATER FLOWING INSIDE.	LIQUID REFRIGERANT (H ₂ O) IN FLASHING TO VAPOR CAUSES TEMP. OF REMAINING LIQUID TO DROP. FLASHING/ COOLING CONTINUES UNTIL TEMP. FALLS TO SATURATION TEMP. AT LOW PRESSURE (7MM Hg) COOLED (40°F) LIQUID IS PUMPED FROM A STORAGE AREA TO SPRAY "TREES" OVER TUBE BUNDLES WHERE EVAPORATION TAKES PLACE. HEAT OF VAPORIZATION COMES FROM THE SYSTEM WATER LOWERING THIS CHILLED WATER ABOUT 10°F.	1) LEAKAGE AT TUBE ENDS (IN ANNULAR GROOVES OR TUBE SHEETS) OR ALONG TUBE LENGTH.	WEAK JOINT, FATIGUING/AGING EFFECTS.	SYSTEM (CHILLED) WATER DILUTES WORKING SOLUTION BELOW WORKABLE CONCENTRATION. AAC SHUTDOWN & MAINTENANCE ACTION REQUIRED.	STES COOLING TEMPORARILY LOST BUT STES OPERATION NORMAL FOR ELECTRICAL POWER & PROCESS STEAM. BLEYLE COOLING IS A BACK-UP.	D	3	SAME AS I 2. B.1 ABOVE
		2) PITTING- REDUCED HEAT TRANSFER EFFICIENCY	CORROSION	REDUCTION IN AAC COOLING CAPACITY. EVENTUAL NEED FOR SHUTDOWN AND MAINTENANCE ACTION.	STES COOLING TEMPORARILY LOST BUT STES OPERATION NORMAL FOR ELECTRICAL POWER & PROCESS STEAM. BLEYLE COOLING IS A BACK-UP.	D	3	SAME AS I 2. A.2 ABOVE.

H-2

Table H-1. Shenandoah STES, Failure Mode Effects Criticality and Safety Analysis (Page 3 of 7)

TABLE 1.

SUBSYSTEM COOLING SUBSYSTEM

SHENANDOAH STES

PAGE 3 OF 7

COMPONENT Absorption Air Conditioner (AAC)
AND TUS COMPONENTS.

FAILURE MODE EFFECTS CRITICALITY AND SAFETY ANALYSIS

DATE 6/23/78

BY J.F. KENT

UNIT OR ASSEMBLY	FUNCTION	FAILURE MODES	PROBABLE CAUSE	FAILURE EFFECT ON		CRITICALITY CATEGORY		REMARKS
				NEXT HIGHER ASSEMBLY	STES OPERATION	SAFETY	MISSION	
D. ABSORBER (OPER. PRESS = 6MM Hg) LOW PRESSURE REFRIGERANT VAPOR IS ABSORBED INTO CONCENTRATED SALT SOLUTION, DILUTING IT.	COOLING TOWER WATER INSIDE CU-NI TUBES TAKES AWAY HEAT RELEASED WHEN VAPOR RETURNS TO LIQUID STATE. AFFINITY OF THE ABSORBENT FOR REFRIGERANT VAPOR IS A FUNCTION OF ABSORBENT CONCENTRATION & TEMPERATURE. THE MORE CONCENTRATED AND COOLER THE GREATER THE AFFINITY FOR WATER VAPOR.	1) LEAKAGE AT TUBE ENDS (IN ANNULAR GROOVES OF TUBE SHEETS) OR ALONG TUBE LENGTH.	WEAK JOINT, FATIGUING/AGING EFFECTS.	SAME AS 2. B.1 ABOVE	STES COOLING TEMPORARILY LOST BUT STES OPERATION NORMAL FOR ELECTRICAL POWER & PROCESS STEAM. BLEYLE COOLING IS A BACK-UP.	D	3	SAME AS 1.2. B.1 ABOVE
		2) PITTING OR FOULING -- REDUCED HEAT TRANSFER EFFICIENCY.	CORROSION	REDUCTION IN AAC COOLING CAPACITY - EVENTUAL NEED FOR SHUTDOWN AND MAINTENANCE ACTION.	SAME AS ABOVE	D	3	SAME AS 1.2 A.2
3. EXTERNAL PIPING A. BETWEEN MAJOR AAC SECTIONS, E.G. ABSORBER & CONCENTRATOR	CONDUCT L.P. PUMPED SOLUTION BETWEEN ABSORBER & CONCENTRATOR VIA THE HEAT EXCHANGER; FROM EVAPORATOR & ABSORBER WELLS TO SPRAY TUBES.	AIR INTAKE LEAKAGE AT FLANGED JOINTS, COUPLINGS	UNDETECTED WEAK JOINTS, FATIGUING/AGING EFFECTS.	PURGE PUMP MUST BE EXERCISED MORE THAN NORMAL (ONCE A WEEK - AVG.) AAC CAPACITY REDUCTION AND/OR CRYSTALLIZATION MAY DEVELOP. UNSCHEDULED SHUTDOWN FOR MAINTENANCE ACTION.	STES COOLING TEMPORARILY NOT PROVIDED, BUT STES OPERATION OTHERWISE NORMAL FOR PROCESS STEAM AND ELECTRICAL OUTPUT. BLEYLE COOLING IS A BACK-UP.	D	3	ENTIRE UNIT FACTORY ASSEMBLED AND LEAK TESTED. VERY LOW PROBABILITY OF OCCURRENCE.
B. COOLING/HEATING WATER SYSTEMS & (CHILLED) WATER TO AND FROM AAC MAJOR SECTIONS.	CONDUCT EXTERNAL WATER INTO & OUT OF MAJOR SECTIONS OF AAC.	LEAKAGE AT JOINTS SEAMS.	UNDETECTED WEAK JOINT, FATIGUING/AGING EFFECTS.	IF LEAKAGE IS EXCESSIVE, UNSCHEDULED SHUTDOWN OF AAC FOR MAINTENANCE ACTION.	SAME AS ABOVE.	D	3	SAME AS ABOVE FOR ADDITIONAL DATA REFER TO: UNIT II-COOLING WATER, PAGE 6. UNIT III-HOT WATER SPLY PAGE UNIT IV -CHILLED WATER SPLY. PAGE 7.

8-H

Table H-1. Shenandoah STES, Failure Mode Effects Criticality and Safety Analysis (Page 4 of 7)

TABLE 1.

SUBSYSTEM COOLING SUBSYSTEM

COMPONENT ABSORPTION AIR CONDITIONER (AAC)
& TUS COMPONENTS

SHENANDOAH STES

FAILURE MODE EFFECTS CRITICALITY AND SAFETY ANALYSIS

PAGE 4 OF 7

DATE 6/23/78

BY J.F. KENT

UNIT OR ASSEMBLY	FUNCTION	FAILURE MODES	PROBABLE CAUSE	FAILURE EFFECT ON		CRITICALITY CATEGORY		REMARKS
				NEXT HIGHER ASSEMBLY	STES OPERATION	SAFETY	MISSION	
HERMETIC PUMP — MOTOR (UNIT PUMP) HAS 3 PUMP IMPELLERS ON COMMON SHAFT.	MOTOR DRIVES THREE (3) PUMPS JOINTLY. PUMP(S) PUSH SOLUTION INTERNALLY BETWEEN ABSORBER & CONCENTRATOR VIA THE HEAT EXCHANGER, FROM EVAPORATOR AND ABSORBER LIQUID WELLS TO SPRAY TUBES.	MOTOR FAILURE (ELECTRICAL OR MECHANICAL FAILURE).	BRUSHES, WIRING OR BEARING FAILURE, OVERTEMP. CUTOUT FAILURE.	SOLUTION NOT CIRCULATED, COOLING CAPABILITY LOST. AAC MACHINE SHUTDOWN FOR MAINTENANCE ACTION.	STES COOLING TEMPORARILY NOT PROVIDED, BUT STES OPERATION OTHERWISE NORMAL FOR PROCESS STEAM AND ELECTRICAL OUTPUT BLEYLE COOLING IS A BACK-UP.	D	3	PUMP AND MOTOR BEARING COOLED BY REFRIGERANT WATER FROM EVAPORATOR WELL. WATER PASSES THRU MECH/MAGNETIC STRAINER. MOTOR IS REMOVABLE WITHOUT BREAKING MACHINE VACUUM OR REMOVING SOLUTION.
		PUMP FAILURE (ANY ONE OF THREE) eg. BEARING/ IMPELLER FAILURE	IMPROPER LUBRICATION WEAROUT OR AGING DEGRADATION	SAME AS ABOVE	SAME AS ABOVE			PUMP BEARING(S) ALSO REPLACEABLE WITHOUT REMOVING SOLUTION OR ALLOWING AIR TO ENTER UNIT.
HEAT EXCHANGER (AND BYPASS) IMPROVES ECONOMY OF SYSTEM OPERATION. REDUCES AMOUNT OF HEAT THAT MUST BE ADDED TO BRING DILUTE SOLUTION TO A "BOIL" IN CONCENTRATOR. IT ALSO REDUCES TEMP OF CONCENTRATED SOLUTION, THEREBY REDUCING AMOUNT OF HEAT TO BE REMOVED FROM THE ABSORBER SECTION.	EXCHANGE HEAT BETWEEN "COOL" DILUTE SOLUTION (BEING TRANSFERRED FROM ABSORBER TO CONCENTRATOR) AND THE HOT, CONCENTRATED SOLUTION BEING TRANSFERRED FROM THE CONCENTRATOR TO THE ABSORBER. BYPASS FACILITATES DECRYSTALLIZATION.	CRYSTALLIZATION WITH POSSIBLE BLOCKED FLOW PASSAGE IN CONCENTRATED FLOW PASSAGE.	LARGER THAN NORMAL TEMP. DROP IN CONCENTRATED SOLUTION FLOW PASSAGE OR POWER FAILURE WITH IMPROPER DILUTION ACTION AT SHUTDOWN WHICH INHIBITS NORMAL START-UP/ OPERATION.	HIGHER TEMP. & PRESSURE OF SYSTEM OPERATION, REDUCED CAPACITY, EVENTUAL SYSTEM SHUTDOWN & MAINTENANCE ACTION.	SAME AS ABOVE	D	3	H/X BYPASS CONNECTING CONCENTRATOR DIRECTLY TO ABSORBER SERVES TO LIMIT THE SOLUTION CONCENTRATION LEVEL IN CONCENTRATOR, ESPECIALLY DURING START-UP, FOR BLOCKED FLOW, DIRECT PASSAGE TO ABSORBER OF HOT CONCENTRATED SOLUTION SERVES TO RAISE TEMP. OF DILUTE SOLUTION IN H/X. THIS EXTRA TEMP. SERVES TO DISOLVE (BREAK-UP) CRYSTALS, FREEING BLOCKED PASSAGES. BY-PASS TUBES HAVE LIQUID TRAP TO MAINTAIN SEAL BETWEEN CONCENTRATOR AND ABSORBER.

H-4

Table H-1. Shenandoah STES, Failure Mode Effects Criticality and Safety Analysis (Page 5 of 7)

TABLE 1.

SUBSYSTEM COOLING SUBSYSTEM
 COMPONENT Absorption Air Conditioner (AAC)
 AND TUS COMPONENTS.

SHENANDOAH STES

FAILURE MODE EFFECTS CRITICALITY AND SAFETY ANALYSIS

PAGE 5 OF 7

DATE 6/26/78

BY J.F. KENT

UNIT OR ASSEMBLY	FUNCTION	FAILURE MODES	PROBABLE CAUSE	FAILURE EFFECT ON		CRITICALITY CATEGORY		REMARKS
				NEXT HIGHER ASSEMBLY	STES OPERATION	SAFETY	MISSION	
PURGE SYSTEM IT CONSISTS OF PICK-UP TUBES & A PURGE CHAMBER WHICH ARE LOCATED IN THE ABSORBER. THIS CHAMBER IS VENTED TO A VACUUM PUMP. THIS IS A MECHANICAL POTARY OIL SEALED VANE PUMP, A LOW VOLUME TWO STAGE UNIT WHICH OPERATES AT VERY LOW SUCTION PRESSURE.	THE PURGE SYSTEM COLLECTS & VENTS NON-CONDENSABLE GASES (SUCH AS AIR) TO THE SUCTION SIDE OF THE PURGE VACUUM PUMP WHICH COMPRESSES THESE GASES TO A PRESSURE HIGH ENOUGH FOR DISCHARGE TO THE ATMOSPHERE.	PUMP FAILURE OR DAMAGED PARTS LEADING TO INEFFICIENT OPERATION. MOTOR FAILURE ELECTRICAL OR MECHANICAL.	WATER OR OTHER CONDENSABLE VAPOR MAY CONTAMINATE OIL. IF CORROSIVE THIS CAN LEAD TO DAMAGED PUMP PARTS. BRUSHES, WIRING, CONTROL CIRCUIT OR BEARING FAILURE.	INEFFICIENT OPERATION - REDUCED CAPACITY, EVENTUALLY UNIT SHUTDOWN FOR MAINTENANCE ACTION. INABILITY TO OPERATE PURGE SYSTEM, EVENTUAL UNIT SHUTDOWN FOR MAINTENANCE ACTION.	STES COOLING TEMPORARILY NOT PROVIDED, BUT STES OPERATION OTHERWISE NORMAL FOR PROCESS STEAM AND ELECTRICAL OUTPUT. BLEYLE COOLING IS A BACK-UP. SAME AS ABOVE.	D	3	PURGE SYSTEM IS USUALLY ACTIVATED FOR TWO HOURS ONCE A WEEK. NON CONDENSABLE GASES MIGRATE TO THE ABSORBER, THE LOWEST PRESSURE ZONE OF THE AAC UNIT, AND FINALLY TO THE PURGE CHAMBER WHICH IS MAINTAINED AT AN EVEN LOWER PRESSURE AND TEMPERATURE BECAUSE ITS TUBES ARE EXPOSED TO THE LOWEST HEAT TRANSFER LOADING OF ALL TUBES IN THE ABSORBER.
CONTROL SYSTEM WITH ELECTRICAL POWER "ON" AAC UNIT AUTOMATICALLY OPERATES AFTER THE CHILLED WATER PUMP IS ACTIVATED ALL SYSTEM MOTOR STARTERS, CAPACITY MODULATION CONTROLS & SAFETY DEVICES ARE CONSOLIDATED INTO A SINGLE INTER-LOCKED SYSTEM. IT ASSURES PROPER SEQUENCE & PROTECTION AGAINST MECHANICAL FAILURE & IMPROPER PROCEDURES.	SENSING CHILLED WATER TEMP. THE PNEUMATIC TEMP. CONTROL AUTOMATICALLY THROTTLES QUANTITY OF HOT WATER SUPPLIED TO THE CONCENTRATOR, THUS MODULATING CAPACITY BETWEEN 10% & 100%. WHEN COOLING IS NOT REQUIRED, UNIT AUTOMATICALLY DILUTES ABSORBENT SOLUTION TO PREVENT CRYSTALLIZATION AS SOLUTION COOLS TO AMBIENT TEMPERATURE SAFETY CONTROLS STOP SYSTEM OPERATION OR PREVENT UNIT DAMAGE OR INJURY TO PERSONNEL.	SYSTEM PROVIDES EXCESSIVE COOLING OR INSUFFICIENT COOLING. INADVERTENT SYSTEM SHUTDOWN START-UP INHIBITED	CAPACITY CONTROLS-TEMP. SENSING AND/OR CONTROL ELEMENT FAILURES. SAFETY CONTROLS OPERATE TO CORRECT MALFUNCTION OR SAFETY CONTROL DEVICE MALFUNCTION. SAFETY CONTROLS PREVENTED START-UP DUE TO AN ACTUAL FAULT OR DUE TO FAILURE OF A ONE OR MORE SAFETY DEVICES WHICH INCLUDE: a) MOTOR TEMP. CTL-HTR b) LIQUID LEVEL SWITCH-PUMP MOTOR COOLANT. c) LOW TEMP. CTL-EVAPORATOR. d) HIGH TEMP CTL-HOT WATER LINE e) HIGH TEMP CTL-COOLING WATER LINE	SYSTEM THROTTLING NOT EFFECTIVE, EVENTUAL UNIT SHUTDOWN FOR MAINTENANCE ACTION. UNIT SHUTDOWN UNTIL FAULT CORRECTED. SAME AS ABOVE	SAME AS ABOVE SAME AS ABOVE SAME AS ABOVE	D	3	FOR A GIVEN REFRIGERATING EFFECT THE TEMP. & CONCENTRATION OF THE LIQUID SOLUTION IN THE ABSORBER IS CONTROLLED. CONCENTRATION IS REGULATED BY FLOW OF HOT WATER IN THE CONCENTRATOR. ON A RISE IN "CHILLED" WATER TEMP. HEAT IS INCREASED TO THE CONCENTRATOR (MORE FLOW). PRIOR TO SHUTDOWN UNIT PUMPS RUN ABOUT FOUR MINUTES UNDER A TIME DELAY CONTROLLER RELAY TO PROVIDE PROPER MIXING OF DILUTE AND CONCENTRATED SOLUTIONS - CRYSTALLIZATION, WHICH WAS THE MOST COMMON FAILURE MODE IN EARLIER DESIGNS, IS PREVENTED/ALLEVIATED BY THE ABOVE CONTROL PROCEDURE.

H-5

Table H-1. Shenandoah STES, Failure Mode Effects Criticality and Safety Analysis (Page 6 of 7)

PAGE 6 OF 7
 DATE 6/30/78
 BY J.F. KENT

TABLE 1
 SUBSYSTEM COOLING SUBSYSTEM
 COMPONENT ABSORPTION AIR CONDITIONER (AAC)
 AND TUS COMPONENTS.

SHENANDOAH STES
 FAILURE MODE EFFECTS CRITICALITY AND SAFETY ANALYSIS

UNIT OR ASSEMBLY	FUNCTION	FAILURE MODES	PROBABLE CAUSE	FAILURE EFFECT ON		CRITICALITY CATEGORY		REMARKS
				NEXT HIGHER ASSEMBLY	STES OPERATION	SAFETY	MISSION	
II. COOLING WATER (COOLING TOWER) SUPPLY TO AAC. IT INCLUDES : a) AAC COOLING WATER & TUBE BUNDLES THROUGH ABSORBER & CONDENSER b) COOLING TOWER & FAN c) PUMPS/MOTORS d) PLUMBING-VALVES (FLOW CTL, CHECK, GATE).	COOLING WATER IN CIRCULATING FROM COOLING TOWER THROUGH AAC AND BACK TO TOWER PICKS UP HEAT OF ABSORPTION IN ABSORBER AND HEAT OF LIQUIFICATION IN CONDENSER.	LOSS OF FLOW	FAILURE OF PUMPS/MOTORS.	COOLING WATER SUPPLY LOST AAC UNIT DOWN, MAINTAINANCE ACTION REQUIRED.	STES OPERATION NORMAL FOR ELECT. OUTPUT & PROCESS STEAM. BLEYLE COOLING AVAILABLE AS BACK-UP.	D	3	LOW FAILURE PROBABILITY. CHECKOUT AND REPAIR/REPLACE PART OF SCHEDULED DOWNTIME PERIOD PREVENTIVE MAINTENANCE
		INEFFICIENT HEAT TRANSFER BY TUBE BUNDLES IN AAC ABSORBER OR CONDENSER.	AAC CONTROL FAILURE OR TUS FAILURE TO PROVIDE 210°F WATER.	AAC CAPACITY DEGRADED ULTIMATELY LEADING TO AAC SHUTDOWN FOR MAINTENANCE ACTION.	STES OPERATION NORMAL EXCEPT WHEN AAC IS SHUTDOWN FOR REPAIRS - BLEYLE COOLING IS USED AS BACK-UP.	D	3	DUST, FOREIGN PARTICLES AND WATER HARDNESS CAUSE FORMATION OF SLUDGE AND SCALE. MECHANICAL AND CHEMICAL METHODS (PART OF PREVENTATIVE MAINT.) EMPLOYED TO RESTORE HEAT TRANSFER CAPABILITY.
III. HOT WATER SUPPLY (FROM TUS) TO AAC (AND PLANT HTG. UNIT) CONCENTRATOR TUS INCLUDES : - CONDENSOR TEMP. CTL & AAC SUPPLY-LO TEMP STORAGE TANK. • H/X • COOLING TOWER • PLUMBING & VALVES - MOTORS & PUMPS - PLANT HEATING • H/X • PLUMBING & VALVES	HOT WATER THROUGH CONCENTRATOR BOILS DILUTE SOLUTION OF LI B+ SOLUTION. HOT WATER PROVIDES HEAT ENERGY TO DRIVE THE ABSORPTION CYCLE.	LOSS OF HOT WATER SUPPLY	TUS FAILURE-GENERALLY PUMP/MOTOR OR PLUMBING	NO HEAT ENERGY AAC UNIT, AND AAC SHUTDOWN. MAINT. ACTION REQUIRED.	STES OPERATION NORMAL FOR ELECT. & PROCESS STEAM. BLEYLE COOLING AVAILABLE AS BACK-UP.	D	3	LOW FAILURE PROBABILITY. EQUIPMENTS EMPLOYED IN TUS HAVE HIGH AVAILABILITY INDEX DUE TO REGULARITY OF PREVENTIVE MAINTENANCE SCHEDULE.
		INSUFFICIENT FLOW (NOT ENOUGH HEAT ENERGY) FOR HIGH CAPACITY.	AAC CONTROL FAILURE OR TUS FAILURE TO PROVIDE 210°F WATER.	AAC EFFICIENCY & CAPACITY DEGRADED. EVENTUAL SHUTDOWN & MAINTENANCE ACTION REQUIRED.	STES OPERATION NORMAL EXCEPT WHEN AAC SHUTDOWN. BLEYLE COOLING AVAILABLE AS BACK-UP.	D	3	SAME AS ABOVE
		HOT WATER "FLASHING" TO STEAM-DAMAGE TO CONCENTRATOR TUBE BUNDLE.	AAC HIGH TEMP CONTROL FAILURE OR 2-WAY FLOW VALVE (HOT WATER FLOW LIMITER) FAILURE (EXIT LINE)	AAC SHUTDOWN, MAINTENANCE ACTION REQUIRED.	STES OPERATION NORMAL FOR ELECT. & PROCESS STEAM. BLEYLE COOLING AVAILABLE AS BACK-UP.	D	3	NOT A HOT WATER SUPPLY FAILURE BUT RATHER AN AAC FLOW CONTROL FAILURE. LOW FAILURE PROBABILITY- CHECKED REGULARLY AS PART OF PREVENTIVE MAINTENANCE

H-6

Table H-1. Shenandoah STES, Failure Mode Effects Criticality and Safety Analysis (Page 7 of 7)

TABLE 1.

SUBSYSTEM: COOLING SUBSYSTEM
 COMPONENT: AAC & TUS COMPONENTS

SHENANDOAH STES
 FAILURE MODE EFFECTS CRITICALITY AND SAFETY ANALYSIS

PAGE 7 OF 7
 DATE 6/30/78
 BY J.F. KENT

UNIT OR ASSEMBLY	FUNCTION	FAILURE MODES	PROBABLE CAUSE	FAILURE EFFECT ON		CRITICALITY CATEGORY		REMARKS
				NEXT HIGHER ASSEMBLY	STES OPERATION	SAFETY	MISSION	
IV. "SYSTEM" (CHILLED) WATER SUPPLY TO PLANT. IT INCLUDES: - AAC EVAPORATOR TUBE BUNDLE & CIRCULATING WATER. - MOTOR & PUMP - PLUMBING & VALVES	"CHILLED" WATER PROVIDES HEAT OF EVAPORATION TO AAC EVAPORATOR. THIS "SYSTEM" WATER (INSIDE TUBES) BECOMES CHILLED. ($\Delta T = 10^\circ$, EXIT TEMP. 45°F) AND IS CIRCULATED THROUGH THE PLANT FAN COIL UNIT TO PROVIDE "COOLING"	LOSS OF FLOW	FAILURE OF PUMP/MOTOR OR CONTROL CIRCUIT.	COOLING LOST, AAC SHUTDOWN MAINTENANCE ACTION REQUIRED.	STES OPERATION NORMAL FOR ELECT. & PROCESS STEAM. BLEYLE COOLING AVAILABLE AS BACK-UP.	0	3	LOW FAILURE PROBABILITY. CHECKED REGULARLY AS PART OF PREVENTIVE MAINTENANCE.
		REDUCED FLOW	PLUMBING LEAK OR BLOCKED STRAINER INTERNAL (IN EVAPORATOR HEADER BUNDLE) OR IN EXTERNAL "CHILLED" SUPPLY LINES.	COOLING CAPACITY OF AAC REDUCED. EVENTUAL AAC SHUTDOWN FOR REPAIRS-INTERNAL OR EXTERNAL TO AAC.	STES OPERATION NORMAL EXCEPT WHEN AAC SHUTDOWN FOR REPAIRS. BLEYLE COOLING IS A BACK-UP.	0	3	LOW FAILURE PROBABILITY. CHECKED REGULARLY AS PART OF PREVENTIVE MAINTENANCE.

H-7/H-8

APPENDIX I
HIGH TEMPERATURE THERMAL ENERGY STORAGE FAILURE MODES
EFFECTS CRITICALITY AND SAFETY ANALYSIS

Table I-1. Shenandoah STES, Failure Mode Effects Criticality and Safety Analysis (Page 1 of 4)

PAGE 1 OF 4

SUBSYSTEM HIGH TEMP. THERMAL ENERGY STORAGE (TES)

SHENANDOAH STES

DATE 7/27/78

COMPONENT TES COMPONENTS

FAILURE MODE EFFECTS CRITICALITY AND SAFETY ANALYSIS

BY J.F. KENT

TABLE 1

UNIT OR ASSEMBLY	FUNCTION	FAILURE MODES	PROBABLE CAUSE	FAILURE EFFECT ON		CRITICALITY CATEGORY		REMARKS
				NEXT HIGHER ASSEMBLY	STES OPERATION	SAFETY	MISSION	
TES TANK SYSTEM (4 TANKS -- 1 1HR TANK 9M BTU 3 LGE TANKS, 30.4M BTU, EACH)	STORE AND MAINTAIN SOLAR COLLECTED ENERGY IN HIGH TEMP RANGE, 500° TO 750°F WITH MINIMUM ENERGY LOSS AND MINIMUM LOSS/DEGRADATION OF OIL (SYLTERM), THE ENERGY TRANSPORT FLUID (FROM COLLECTOR FILLED TO TES).	VARIED AS DESCRIBED BELOW FOR IDENTIFIED ASSEMBLIES, BUT FAILURES WHICH REDUCE STORAGE CAPACITY.	VARIED, SEE BELOW	FAILURES TO ANY ONE TANK FORCING ITS SHUTDOWN IMPOSE A NEED FOR AN ADJUSTMENT IN OPERATING SEQUENCE WHICH IS EASILY ACCOMMODATED BY A FOUR TANK SYSTEM.	MINOR IMPACT IN STES OPERATION. POSSIBLE DELAY IN SWITCH OVER TO SOLAR ENERGY DURING A "STORAGE DEPLETED START-UP, IF THE ONE HOUR TANK IS DOWN". MINOR CAPACITY CONSTRAINT.	D	3 TO 2	FOUR TANK SYSTEM PROVIDES VERSATILE SOLAR ENERGY STORAGE FUNCTION. ALMOST NORMAL OPERATION POSSIBLE WITH ONE TANK DOWN FOR REPAIRS. STORAGE CAPACITY, 4 TANKS 100 X 10 ⁶ BTU
<u>A. TANK DESIGN</u>								
1. STRUCTURE -- WALLS, FLOOR, BASE, DOME WITH ACCESS HATCH	PROVIDE SEALED ENCLOSURE AND STORAGE CAPACITY FOR COLLECTED SOLAR ENERGY. ENERGY STORED VIA HOT TRICKLE "OIL" PASSAGE OVER TACONITE "SPHERES". THE STORAGE MEDIA. SEAL MAINTAINS ATMOSPHERE (N ₂) CONTROL TO PREVENT ADVERSE EFFECTS OF OXIDATION OF SYLTERM.	LEAKS IN STRUCTURAL ELEMENTS AFFECTING LOSS OF NITROGEN AND POSSIBLY SYLTERM.	UNDETECTED WEAK JOINT. FATIGUING/AGING EFFECTS.	EXCESSIVE RATE OF DEPLETION OF NITROGEN FROM SUPPLY TANKS AND CORRESPONDING NEED FOR MAKE-UP "OIL". AFFECTED TANK SHUT DOWN FOR REPAIRS.	SAME AS ABOVE	D	3 TO 2	LOW FAILURE PROBABILITY. STANDARD TANK DESIGN METHODS EMPLOYED. HIGH STRENGTH BOILER PLATE USED (A 285 MEDIUM GRADE B/C) AND LOW WALL STRESSES OVER OPERATING TEMP RANGE. ALSO THERE IS A DIFFERENTIAL EXPANSION COMPATIBILITY BETWEEN TANK WALLS AND TACONITE "SPHERES". MAX. WALL STRESS (AT t = .375") IS APPROXIMATELY 9 KSI.

I-1

Table I-1. Shenandoah STES, Failure Mode Effects Criticality and Safety Analysis (Page 2 of 4)

SUBSYSTEM HIGH TEMP. THERMAL ENERGY STORAGE (STES)

COMPONENT TES COMPONENTS

SHENANDOAH STES

FAILURE MODE EFFECTS CRITICALITY AND SAFETY ANALYSIS

TABLE 1

PAGE 2 OF 4

DATE 7/27/78

BY J.F. KENT

UNIT OR ASSEMBLY	FUNCTION	FAILURE MODES	PROBABLE CAUSE	FAILURE EFFECT ON		CRITICALITY CATEGORY		REMARKS
				NEXT HIGHER ASSEMBLY	STES OPERATION	SAFETY	MISSION	
2. INSULATION- EXTERNAL SURFACES COVERED. TYPICAL THICKNESS 14" (INSULATION ALSO APPLIED TO THE INTER TANK MANIFOLD - PIPING & VALVES)	MAINTAIN HIGH INTERNAL TANK TEMP., MINIMIZE HEAT (ENERGY) LOSS IN STORAGE AND MAINTAIN EXTERNAL FACE INSULATION TEMP. AT 120°F FOR PURPOSES OF ENERGY CONSERVATION AND SAFETY.	INSULATION STRUCTURAL INTEGRITY IMPAIRED - HENCE AN INCREASE IN HEAT LOSS.	DAMAGE DUE TO ACCIDENT CARELESSNESS DURING MAINTENANCE. POSSIBLE FAULTY INSTALLATION NOT DETECTED AT INITIAL INSPECTION.	REDUCTION IN AFFECTED TANK AND POSSIBLY TOTAL TES STORAGE EFFICIENCY. DEPENDING ON DEGREE OF INSULATION "LOSS" AND DISCLOSURE BY PHYSICAL INSPECTION, AFFECTED TANK MAY BE SHUT DOWN FOR REPAIRS.	MINOR IMPACT ON STES OPERATION. POSSIBLE DELAY IN SWITCH OVER TO SOLAR ENERGY DURING A "STORAGE DEPLETED START-UP IF THE ONE HOUR TANK IS DOWN". MINOR CAPACITY CONSTRAINT.	D TO C	3 TO 2	LOW FAILURE PROBABILITY. PERFORMANCE MONITORING AND PHYSICAL INSPECTIONS READILY DISCLOSE INSULATION PROBLEMS. OPERATING PERSONNEL INSTRUCTED TO FOLLOW STANDARD SAFETY PRACTICES FOR HIGH TEMPERATURE ZONES.
3. TANK RELIEF AND VENT VALVES	RELIEVE/VENT GASES (N ₂ VAPOR, ETC) PRODUCED DURING NORMAL OPERATION.	FAILURE TO RELIEVE GAS PRESSURE AT SET PRESSURE LEVEL.	AGING EFFECTS.	HIGHER THAN NORMAL TANK INTERNAL PRESSURE BUT NOT HIGH ENOUGH TO CAUSE HIGH WALL STRESSES. MAINTENANCE ACTION REQUIRED TO RELIEVE/VENT TANKS, POSSIBLY REPLACE VALVES. SOME OIL DEGRADATION POSSIBLE.	MINOR IMPACT ON STES OPERATION. POSSIBLE CAPACITY CONSTRAINT.	D	3 TO 2	OIL DEGRADATION, HENCE A NEED TO ADD MORE THAN NORMAL MAKE-UP OIL AND A NEED TO DRAIN MORE FREQUENTLY FROM TANK CLEAN-OUT PORTS, SUMPS, AND SLUDGE DRAINS.
4. SLUDGE DRAIN (SLUDGE FORMED PRIMARILY FROM FACONITE DUST COMBINING WITH SWL THERM DURING TEMP. CYCLING)	PROVIDE COLLECTION POINT AND MEANS TO DRAIN OFF ACCUMULATED SLUDGE.	BLOCKAGE OF VALVE OR DRAINAGE PORT.	IMPROPER MAINTENANCE PRACTICES, INFREQUENT DRAINAGE OPERATIONS.	SLUDGE BUILDUP IN AFFECTED TANK, REDUCED TANK EFFICIENCY, HENCE OVERALL TES EFFICIENCY. AFFECTED TANKS DOWN FOR REPAIRS.	MINOR IMPACT ON STES OPERATION. POSSIBLE CAPACITY CONSTRAINT.	D	3 TO 2	SLUDGE FORMATION AND DRAINAGE HAS DIRECT IMPACT ON QUANTITY MAKE-UP OIL REQUIRED. SLUDGE DRAINAGE IS A REGULARLY SCHEDULED PREVENTIVE MAINTENANCE PROCEDURE. SLUDGE DRAIN & CLEAN-OUT PORTS PROVIDE MAINTAINABILITY CONVENIENCE.

I-2

Table I-1. Shenandoah STES, Failure Mode Effects Criticality and Safety Analysis (Page 3 of 4)

SUBSYSTEM HIGH TEMP. THERMAL ENERGY STORAGE (TES)

SHENANDOAH STES

PAGE 3 OF 4

COMPONENT TES COMPONENTS

FAILURE MODE EFFECTS CRITICALITY AND SAFETY ANALYSIS

DATE 7/27/78

TABLE 1

BY J. P. KENT

UNIT OR ASSEMBLY	FUNCTION	FAILURE MODES	PROBABLE CAUSE	FAILURE EFFECT ON		CRITICALITY CATEGORY		REMARKS
				NEXT HIGHER ASSEMBLY	STES OPERATION	SAFETY	MISSION	
5. TRICKLE MANIFOLD (TOP & BOTTOM MANIFOLDS ARE OF SAME DESIGN. THIS FEATURE PROVIDES VERSATILITY TO USE THE BASELINE DESIGN, TRICKLE OIL, OR TO CHANGE TO DUAL MEDIA MODE.	DISTRIBUTE OIL EVENLY OVER THE CROSS SECTION OF THE STORAGE MEDIA TO ACHIEVE UNIFORM TEMPERATURE DISTRIBUTION.	BLOCKAGE OF DRILLED HOLES IN MANIFOLD PIPING OR UNEVEN DISTRIBUTION OF TRICKLE FLOW THROUGH PIPING.	BUILD-UP OF SLUDGE-LIKE COATINGS AROUND FLOW OPENINGS, CIRCULATED SLUDGE. MOST LIKELY AGING AFFECTS.	REDUCED OPERATING EFFICIENCY, HENCE DEGRADATION OF THERMAL STORAGE CAPACITY AFFECTED. TANK SHUT DOWN FOR MAINTENANCE ACTIONS.	MINOR IMPACT ON STES OPERATION. POSSIBLE CAPACITY CONSTRAINT.	D	3 TO 2	DUAL MEDIA IS A DEMONSTRATED BACK-UP MODE OF OPERATION.
6. TANK INSTRUMENTATION FLUID LEVEL TEMP. AND PRESSURE INDICATORS.	PROVIDE OPERATIONAL DATA ON STATUS OF TANK INTERIOR PRIMARILY, FLUID LEVEL, TEMPERATURE AND PRESSURE FOR OPERATION AND CONTROL DECISIONS.	FAIL TO PROVIDE SIGNALS OR GIVE ERRONEOUS INDICATIONS.	AGING EFFECTS, DRIFT.	NEGLECTIBLE IMPACT ON TES OPERATION - POSSIBLE SHUT DOWN OF TANK FOR INSTRUMENTATION REFURBISHMENT.	NEGLECTIBLE IMPACT IN STES OPERATION.	D	3	STRAIN GAUGE INSTRUMENTATION USED ON 1 HOUR AND "FIRST" LARGE TANK TO PROVIDE DATA ON TANK STRESS LEVELS OVER TEMPERATURE RANGE (500°-750° AND TO CHECK COMPATIBILITY/ DIFFERENTIAL EXPANSION EFFECT BETWEEN TACONITE "SPHERES" AND TANK WALLS.
7. STORAGE MEDIA TACONITE SPHERES (TRANSFER FLUID IS SYLTHERM 800 AND INERT GAS IS N ₂ AT PRESSURES JUST ABOVE AMBIENT).	PROVIDE MEDIA OR MATERIAL WHICH STORES ENERGY AT ELEVATED TEMPERATURES (500-750°F) WITH MINIMAL DEGRADATION OVER 0-20 PSIG RANGE.	SPALLING - DUST FORMATION BY REPEATED CYCLING LEADING TO SLUDGE FORMATION, DEPLETION OF TACONITE MASS, HENCE LOWER CAPACITY.	AGING CYCLING EFFECTS.	REDUCED STORAGE CAPACITY SLUDGE FORMATION WHICH MAY INFLUENCE NEED FOR MORE THAN NORMAL MAKE-UP OIL AND MORE FREQUENT PREVENTIVE MAINT. ACTIONS.	SAME AS ABOVE	D	3	TACONITE/SYLTHERM 800 TEST D INDICATES ACCEPTABLE COMPATIBILITY UNDER SYSTEM TEMPERATURE AND N ₂ ATMOSPHERE CONDITIONS. ADDITIONAL TEST IS PLANNED TO VERIFY IF COMPATIBILITY REMAINS SATISFACTORY OVER A LONG PERIOD OF OPERATION.

I-3

Table I-1. Shenandoah STES, Failure Mode Effects Criticality and Safety Analysis (Page 4 of 4)

SUBSYSTEM HIGH TEMP. THERMAL ENERGY STORAGE (TES)
 COMPONENT TES COMPONENTS

SHENANDOAH STES

FAILURE MODE EFFECTS CRITICALITY AND SAFETY ANALYSIS

TABLE 1

PAGE 4 OF 4
 DATE 1/27/78
 BY J.F. KENT

UNIT OR ASSEMBLY	FUNCTION	FAILURE MODES	PROBABLE CAUSE	FAILURE EFFECT ON		CRITICALITY CATEGORY		REMARKS
				NEXT HIGHER ASSEMBLY	STES OPERATION	SAFETY	MISSION	
8. <u>FLOW CONTROL & DISTRIBUTION</u>								
1. MANIFOLD - PIPING & VALVES VALVES INCLUDE: SAFETY RELIEF VALVES, LEAK VALVES, CHECK VALVES. FLOW SELECTION VALVES. FLOW CONTROL VALVES. SHUTOFF, GATE VALVES.	CONDUCT AND TRANSFER "HOT" SYLTHEM OIL TO BETWEEN AND FROM TES TANKS FOR PURPOSE OF CHARGING OR DISCHARGING STORAGE THERMAL ENERGY.	LEAKAGE - (AT FLANGES OR VALVE BONNETS) OR PIPE LEAKS OR VALVE SEALS	AGING, THERMAL CYCLING EFFECTS	REDUCED THERMAL STORAGE CAPACITY. AFFECTED TES PLUMBING SECTION(S) SHUT DOWN FOR REPAIR.	MINOR IMPACT IN STES OPERATION.	0	3 10 2	MATERIAL SELECTION BASED ON COMPATIBILITY WITH OIL (SYLTHEM) OVER TEMP. RANGE. PLUMBING INCLUDED PROMINENTLY AS PART OF PREVENTIVE MAINTENANCE SCHEDULE.
2. TRANSFER PUMP - PUMPS OUTLET OIL FROM ONE HOUR TANK TO LARGE TANKS.	TRANSFER HOT OIL FLOW TO THE THREE LARGE TANKS IN SUCCESSION (ONE AT A TIME); DURING EXCESS SOLAR ENERGY STORAGE PERIODS.	MOTOR/MOTOR FAILURE	ELECTRICAL/ MECHANICAL FAILURES - MOST LIKELY AGING EFFECTS.	TES OPERATION INHIBITED. TES "DOWN" FOR MAINTENANCE ACTION. FOSSIL HEATER IS A BACK-UP. IF THERMAL GRADIENT PROBLEM OCCURS DUE TO PUMP OUTAGE.	STES OPERATION ADJUSTED FROM SOLAR TO FOSSIL ENERGY.	0	2	ALTHOUGH ONE PUMP/MOTOR SET IS EMPLOYED, A SPARE SET IS PLANNED. REPLACEMENT WILL BE ACCOMPLISHED WITH MINIMAL SYSTEM DEPENDENCE ON FOSSIL BACK-UP. LOW FAILURE PROBABILITY.
3. CONTROL AIR SUPPLY	PNEUMATIC CONTROL AIR IS SUPPLIED TO FLOW AND TRANSFER SELECTION CONTROL VALVES IN THE TES PLUMBING.	LOSS OF CONTROL AIR.	LINE LEAK/RUPTURE OR MOTOR COMPRESSOR FAILURE (ELECTRICAL OR MECHANICAL FAILURE)	VALVES MOVE TO FAIL-SAFE POSITION AS REQUIRED TO ACCOUNT FOR EXCESS ENERGY UNTIL COLLECTOR FIELD-STEAM GENERATOR DEMANDS ARE BALANCED. TES OPERATION ABNORMAL UNTIL CONTROL AIR RESTORED.	STES OPERATION MAY REQUIRE COLLECTOR FIELD PARTIAL OPERATION/DEFOCUS, POSSIBLE USE OF FOSSIL BACK-UP.	0	2	CONTROL AIR SUPPLY SERVICED REGULARLY DURING STES NORMAL DOWN-TIME PERIODS. VERY LOW PROBABILITY OF FAILURE.

I-4

APPENDIX J
SYSTEM AND CONTROLS FAILURE MODE EFFECTS CRITICALITY
AND SAFETY ANALYSIS

Table J-1. Shenandoah STES, Failure Mode Effects Criticality and Safety Analysis (Page 1 of 5)

SHENANDOAH STES

FAILURE MODE EFFECTS CRITICALITY AND SAFETY ANALYSIS

PAGE 1 OF 5

DATE 6/26/78

BY J.F. KENT

SUBSYSTEM SYSTEM FMEA

COMPONENT _____

REF. RELIAB. BLOCK DIAGRAMS, FIGURES 1 TO 3

I-F

UNIT OR ASSEMBLY	FUNCTION	FAILURE MODES	PROBABLE CAUSE	FAILURE EFFECT ON		CRITICALITY CATEGORY		REMARKS
				NEXT HIGHER ASSEMBLY	STES OPERATION	SAFETY	MISSION	
1. CENTRAL CONTROL - A DISTRIBUTED CONTROL SYSTEM COMPRISED OF <ul style="list-style-type: none"> • A MINICOMPUTER PLUS • PERIPHERALS (SUCH AS TAPE, DISK, PRINTER, KEYBOARD & DISPLAY) AND • 7 REMOTE PROCESSORS (MICRO COMPUTER) • STATUS PANEL - KEY PARAMETERS MONITORED CONTINUOUSLY 	CONTROL OF SUBSYSTEMS, SOLAR COLLECTION, THERMAL ENERGY STORAGE PCS AND THERMAL UTILIZATION. PROVIDE SUPERVISORY CONTROL FOR NORMAL, EMERGENCY & MAINTENANCE OPERATIONAL MODES. IT HAS CAPABILITY TO MONITOR, RECORD AND PROVIDE ALARMS VIA THE 7 REMOTE MICROCOMPUTERS.	FAILURE TO CONTROL STES SUBSYSTEMS.	VARIOUS CAUSES IDENTIFIED BELOW	BACK-UP(S) REQUIRED TO PROVIDE ENERGY FOR AFFECTED SUBSYSTEM OR TO THE SYSTEM DEPENDENT UPON WHAT FAILED, ONE OF 7 REMOTE PROCESSORS OR THE MINICOMPUTER. MAINTENANCE ACTION REQUIRED.	STES OPERATION INHIBITED, BACK-UP(S) AVAILABLE FOR PLANT OPERATION.	D	2 TO 1	SUBSYSTEMS OPERATE HIGHLY INDEPENDENTLY. SUBSYSTEM INTERFACES EXIST BUT THERE LITTLE NEED FOR INTERACTION, COMMUNICATION WITH EACH OTHER. DISTRIBUTED CONTROL (7 REMOTE MICROPROCESSORS) PROVIDES BENEFITS OF HARDWARE AND SOFTWARE MODULARITY RELATIVE TO FLEXIBILITY FOR DESIGN CHANGES AND FAULT TOLERANCE. WIRING COMPLEXITY IS REDUCED SINCE REMOTE PROCESSORS ARE LOCATED NEAR SENSORS FOR SHORT RUNS. THE WIRING FROM EACH REMOTE PROCESSOR IS A SINGLE SERIAL LINE (NOT HUNDREDS OF SENSOR LEADS).
1.1 CENTRAL PROCESSOR-MINI-COMPUTER(DEC-1134A) PERIPHERAL INCLUDING TAPE, DISK, KEYBOARD AND DISPLAYS	PROVIDE SUPERVISORY CONTROL OF SUBSYSTEMS FOR NORMAL, EMERGENCY & MAINTENANCE OPERATIONS. MONITOR, RECORD AND PROVIDE ALARMS.	FAILURE TO PROVIDE CONTROL SIGNALS OR DISPLAY, RECORD INFORMATION	ELECTRICAL FAILURE INTERNAL TO MINI-COMPUTER OR IN PERIPHERALS.	SYSTEM OPERATION MAY CONTINUE UNDER CONTROL BY REMOTE PROCESSORS. MAINTENANCE ACTION REQUIRED ALARMS/ARCHIVING LOST	STES OPERATION UNINTERRUPTED.	D	3 TO 2	CONTROLS DESIGNED SO THAT REMOTE PROCESSORS MAY BE PROGRAMMED TO CONTROL RESPECTIVE SUBSYSTEMS INDEPENDENTLY UNTIL CENTRAL PROCESSOR IS BROUGHT BACK ON-LINE. LOW FAILURE PROBABILITY.

Table J-1. Shenandoah STES, Failure Mode Effects Criticality and Safety Analysis (Page 2 of 5)

SHENANDOAH STES
FAILURE MODE EFFECTS CRITICALITY AND SAFETY ANALYSIS

SUBSYSTEM SYSTEM FMEA

PAGE 2 OF 5

COMPONENT ---

DATE 6/28/78

REF. RELIAB. BLOCK DIAGRAMS, FIGURES 1 TO 3

BY J.F. KENT

J-2

UNIT OR ASSEMBLY	FUNCTION	FAILURE MODES	PROBABLE CAUSE	FAILURE EFFECT ON		CRITICALITY CATEGORY		REMARKS
				NEXT HIGHER ASSEMBLY	STES OPERATION	SAFETY	MISSION	
1.2 REMOTE PROCESSORS (SEC 11/03-LC), MDEMS, ETC. a) SOLAR COLLECTION S/S 4 UNITS (ONE PER ZONE)	FOR ANY ONE ZONE --- PROVIDE COLLECTOR ZONE CONTROLS FOR COLLECTOR TRACKING (POINT, DEFOCUS, STOW) AND FIELD TEMPERATURE CONTROL (FLUID TEMP, SECTOR CONTROL, MAX TEMP. - THRESHOLD.	FAILURE TO PROVIDE TRACKING OR TEMP. CONTROL	ELECTRICAL FAILURE	ONE ZONE (SECTOR) OF COLLECTOR FIELD SHUT DOWN FOR MAINTENANCE ACTION - REMAINING 3 ZONES REMAIN OPERATIONAL.	STES OPERATION CONTINUES NORMALLY, UTILIZING HIGH TEMP. STORAGE OR (DEPENDENT ON TIME OF FAILURE) A BACK-UP ENERGY SOURCE SUCH AS FOSSIL HEATER.	D	3 TO 2	VERY LOW FAILURE PROBABILITY LOGISTICS POLICY FOR SPARE REMOTE MICROPROCESSOR(S) CAN REDUCE DOWNTIME SIGNIFICANTLY.
b) REMOTE PROCESSOR-HIGH TEMP. TES. ONE MICROPROCESSOR FOR 4 TANKS, A ONE-HOUR TANK AND 3 LARGE TANKS.	PROVIDE CONTROLS/ DATA FOR TANK STATUS (TEMP. & LEVEL) AND LOGIC CONTROL FOR TANK TRANSFER	FAILURE TO PROVIDE OR PROCESS SIGNALS FOR CONTROL OR DATA ACQUISITION OR PROVIDE SPURIOUS SIGNALS TO CENTRAL PROCESSOR	INTERNAL ELECTRICAL FAILURE	HIGH TEMP. THERMAL ENERGY STORAGE OPERATION SHUT DOWN AND MAINTENANCE ACTION REQUIRED. CENTRAL CONTROL MAY SELECT COLLECTOR FIELD TOTAL SHUTDOWN & OPERATION VIA BACK-UP FOSSIL HEATER DURING INTERIM PERIOD.	STES OPERATION ON SOLAR ENERGY/STORED ENERGY INHIBITED BUT B/U OPERATION/FOSSIL HEATER) AVAILABLE.	D	2	EMERGENCY KEYBOARD OVERRIDE COMMAND ON CENTRAL CONTROL CONSOLE CAN CALL FOR FAIL-SAFE POSITION ON ALL PNEUMATIC VALVES IN THE PIPING FOR HI-TEMP. TES. VERY LOW FAILURE PROBABILITY
c) REMOTE PROCESSOR-POWER CONVERSION SYSTEM (PCS), ELECTRICAL SYSTEM	PROVIDE CONTROLS/ DATA ON STEAM PRODUCTION (TEMP, PRESS, FLOW) FEED-WATER, DAERATION, DEMINERALIZATION, TURBINE SPEED & LOAD PLUS INSTRUMENTATION, FOSSIL BACK BACK-UP, AND ON ELECTRICAL POWER GENERATION AND SWITCHING.	FAILURE TO PROVIDE OR PROCESS SIGNALS FOR STEAM PRODUCTION OR ELECTRICAL POWER GENERATION OR SWITCHING	INTERNAL ELECTRICAL FAILURE	TURBINE/ALT SET HAS SELF-CONTAINED CONTROLS AND PCS CAN CONTINUE TO FUNCTION. IN WORST CASE, PCS SHUT DOWN MAY BE REQUIRED FOR ELECTRICAL POWER & PROCESS STEAM. TUS COOLING/HEATING MAY STILL BE AVAILABLE.	STES OPERATION NORMAL. IN WORST CASE, GPC ELECTRICAL POWER AND BLEYLE STEAM AVAILABLE AS B/U.	D	3-2	EMERGENCY SHUTDOWN OF POWER CONVERSION SYSTEM MAY IMPOSE TIME/OPERATING CONSTRAINTS (SOLAR COLLECTION & HIGH TEMP TES OPERATION. VERY LOW FAILURE PROBABILITY

Table J-1. Shenandoah STES, Failure Mode Effects Criticality and Safety Analysis (Page 3 of 5)

SHENANDOAH STES
FAILURE MODE EFFECTS CRITICALITY AND SAFETY ANALYSIS

SUBSYSTEM SYSTEM FMEA
COMPONENT --

PAGE 3 OF 5

DATE 6/28/78

BY J.F. KENT

REF. RELIAB. BLOCK DIAGRAMS, FIGURES 1 TO 3

UNIT OR ASSEMBLY	FUNCTION	FAILURE MODES	PROBABLE CAUSE	FAILURE EFFECT ON		CRITICALITY CATEGORY		REMARKS
				NEXT HIGHER ASSEMBLY	STES OPERATION	SAFETY	MISSION	
1.2 d) REMOTE PROCESSOR- LOW TEMP STORAGE TUS BLEYLE PLANT FACTORY/PROCESS DATA	PROVIDE CONTROLS/ DATA ON AAC/HEATING SYSTEMS, COOLING TOWERS, CONDENSER, BLEYLE FACTORY & PROCESS DATA AND INSTRUMENTATION	FAILURE TO PROVIDE OR PROCESS SIGNALS FOR LOW TEMP STORAGE TUS OPERATION OR BLEYLE PLANT PROCESS DATA.	INTERNAL ELECTRICAL FAILURE	SHUTDOWN TUS AND MAINTENANCE ACTION REQUIRED. SWITCH TO B/U BLEYLE COOLING/HEATING AND MANUAL CONTROL FOR CONDENSOR/COOLING TOWER PORTION OF TUS.	STES OPERATION CONTINUES TO PROVIDE ELECTRICAL POWER & PROCESS STEAM: ONLY STES COOLING/HEATING AFFECTED.	D	3 TO 2	MANUAL OVERRIDE OF TUS CONTROLS SIMPLIFY FAILURE ACCOMMODATION. VERY LOW FAILURE PROBABILITY
2. SOLAR COLLECTION (COLLECTOR FIELD) SUBSYSTEM INCLUDES ACQUISITION & TRACKING, EMERG- ENCY DEFOCUS AND STORAGE PROVISIONS FOR 192 COLLECTORS	COLLECT SOLAR ENERGY RAISING TEMP OF CIRCULATING SYLTHEM 600 TO 750°F (Δt = 250°F ABOVE 500°F). INSULATION LEVELS FOR EACH COLLECTOR: -50 TO 300 BTU/FT ² HR. -AVG 200 BTU/FT ² -HR	FAILURE TO PROVIDE ADEQUATE INSOLAT- ATION ENERGY TO ACHIEVE DISCHARGE TEMP.	ELECTRICAL OR MECHANICAL FAILURES	COLLECTOR FIELD, POSSIBLY AFFECTED ZONE ONLY, SHUT DOWN UNTIL FAULT CORRECTED.	STES OPERATION CONTINUES BUT WITH CONSTRAINTS TO COLLECTOR FIELD OUTPUT. COLLECTOR FIELD NOT SIGNIFICANTLY AFFECTED UNTIL MORE THAN 5% OF COLLECTORS ARE DOWN.	D	3 TO 2	FOSSIL BACK-UP IS AVAILABLE, DEPENDING ON TIME OF FAILURE, HI TEMP TES MAY ALSO BE FIRST UTILIZED.
		FAILURE TO DEFOCUS IN EMERGENCY	SAME AS ABOVE	STORM/PARTICLE DAMAGE POSSIBLE LEADING TO DEGRADED OUTPUT. AFFECTED COLLECTOR(S) AND SECTOR INACTIVATED UNTIL FAULT CORRECTED (ASSUMES FAILURE OCCURS TO ISOLATED COLLECTORS).	STES OPERATION CONTINUES BUT WITH CONSTRAINTS TO COLLECTOR FIELD OUTPUT. COLLECTOR FIELD NOT SIGNIFICANTLY AFFECTED UNTIL MORE THAN 5% OF COLLECTORS ARE DOWN	D	3 TO 2	FOSSIL BACK-UP IS AVAILABLE, DEPENDING ON TIME OF FAILURE HI TEMP TES MAY ALSO BE FIRST UTILIZED.
	ACQUISITION OF ENERGY VIA FOCUSING SUN'S RAYS ON RECEIVER.	EYE INJURY TO PERSONNEL, OPERAT- ING AND/OR VISITORS.	POSSIBLE EYE HAZARD BEYOND TWO OR MORE FOCAL LENGTHS FROM DISH.	NO EFFECT ON FUNCTIONAL EQUIPMENT.	NO EFFECT ON STES OPERATION.	A	3	PROBLEM OF POSSIBLE EYE HAZARD PRESENTLY IDENTIFIED AND UNDER INVESTIGATION. CONSIDER USE OF AN OPACQUE FENCE AND OTHER PROVISIONS INSIDE THE FENCE FOR THE PROTECTION OF EQUIPMENT AND PERSONNEL, AND VISITORS.

1-8

Table J-1. Shenandoah STES, Failure Mode Effects Criticality and Safety Analysis (Page 4 of 5)

SHENANDOAH STES

FAILURE MODE EFFECTS CRITICALITY AND SAFETY ANALYSIS

PAGE 4 OF 5

DATE 6/28/78

BY J.F. KENT

SUBSYSTEM SYSTEM FMEA

COMPONENT ---

REF. RELIABILITY BLOCK DIAGRAMS, FIGURES 1 TO 3

UNIT OR ASSEMBLY	FUNCTION	FAILURE MODES	PROBABLE CAUSE	FAILURE EFFECT ON		CRITICALITY CATEGORY		REMARKS
				NEXT HIGHER ASSEMBLY	STES OPERATION	SAFETY	MISSION	
3. HI TEMPERATURE-THERMAL ENERGY STORAGE (TES) SUB-SYSTEM INCLUDES: 1 SMALL (1 HR) TANK 3 LARGER TANKS CONTROLS - PNEUMATIC & ELECTRICAL, PIPING & VALVES	STORE ENERGY BY TRICKLE-OIL CIRCULATION OVER ROCKS (TACONITE) WITHIN 4 INSULATED TANKS. TEMPERATURE RANGE 500-750°F; STORAGE CAPACITY, 100 x 10 ⁶ BTU. MAINTAIN HIGH TEMP LEVEL AND NITROGEN (N ₂) ATMOSPHERE TO MINIMIZE OIL DEGRADATION (SYLTHERM 800 IS DEGRADED BY O ₂)	N ₂ DEPLETION AND EXPOSURE TO AIR-OIL DEGRADATION INSULATION DAMAGE	LEAKAGE AT JOINT(S) OR SEAL(S) DUE TO AGING EFFECTS.	REDUCED STORAGE CAPACITY REQUIRING REPLACEMENT OF OIL & SHUT DOWN TO CORRECT LEAK(S) POSSIBLE LIMIT TO OVERALL DAILY (SHIFT) COVERAGE FOR SOLAR ENERGY SUPPLIED.	STES OPERATION CONTINUES BUT DEPENDENCE UPON FOSSIL BACK-UP MAY INCREASE.	D	3 TO 2	STES DESIGNED TO PROVIDE A MINIMUM OF 60% OF ANNUAL LOAD TO BLEYLE PLANT.
			IMPROPER (BUT) UNDETECTED INST'L'N DEFECT PLUS AGING EFFECTS; ACCIDENTAL DAMAGE DURING MAINTENANCE ACTIONS.	NO APPARENT EFFECT ON YES OR SYSTEM BUT TOTAL SYSTEM EFFICIENCY NOT REALIZED OR DEMONSTRATED.	NO EFFECT ON STES OPERATION.	D	3	INSULATION DAMAGE NORMALLY DISCLOSED VIA VISUAL EXAMINATION
4. POWER CONVERSION SUBSYSTEM (PCS) INCLUDES: - (H/X) STEAM GENERATOR - TURBINE/ALTERNATOR - CONDENSER - DEMINERALIZER - DEAERATOR - FEEDWATER CTL - B/U FOSSIL HTR. - ELECT. SWITCHGEAR - CONTROLS-TURB & ALTERNATOR.	PCS CONVERTS SOLAR (OR FOSSIL B/U) ENERGY TO "STEAM" ENERGY VIA STEAM GENERATOR (H/X) - FOR USE IN THE TURBINE/ALTERNATOR TO PRODUCE ELECTRICAL ENERGY. - FOR PRODUCTION OF PROCESS STEAM - FOR COOLING/HEATING VIA TUS	FAILS TO PROVIDE ELECTRICAL ENERGY (480V, 60HZ, 200-400KW)	TURBINE/ALTERNATOR SET & SUPPORT EQPMT. FAILURE	ELECTRICAL GENERATORS/DISTRIBUTING EQPMT. OUTPUT LOST. SWITCH TO GPC POWER AS B/U. TURBINE/ALT. SET DOWN FOR REPAIRS.	STES OPERATION FRACTIONAL. PROCESS STEAM & TUS FOR COOLING/HEATING STILL AVAILABLE.	D-A	2 TO 1	FAILURES IN EQUIPMENT USING HIGH PRESS/TAMP STEAM MAY CAUSE OR LEAD TO HAZARDOUS CONDITIONS TO PERSONNEL. SAFETY RULES AND TRAINING ASSUMED "IN-FORCE". EQPMT. HAS HIGH AVAILABILITY
		FAILS TO PROVIDE PROCESS STEAM.	EXTRACTION (PROCESS) STEAM EQUIPMENT OR CONTROLS FAILURE.	PROCESS (EXTRACTION) STEAM SUPPLY TO BLEYLE LOST. BLEYLE B/U STEAM AVAIL. MAINT. ACTION REQUIRED.	STES OPERATION NORMAL WITH RESPECT TO ELECTRICAL AND COOLING/HEATING OUTPUT.	D-A	3 - 2	
		FAILS TO PROVIDE ENERGY IN CONDENSER COOLANT LOOP TO TUS	CONDENSOR/CONDENSER COOLANT LOOP EQPMT. (PART OF TUS) FAILURE.	LOW TEMP STORAGE (TUS) ENERGY FOR COOLING/HEATING OF BLEYLE PLANT INHIBITED. BLEYLE COOLING/HEATING B/U AVAILABLE MAINT. ACTION REQUIRED.	STES OPERATION NORMAL FOR ELECTRICAL POWER & PROCESS STEAM OUTPUT.	D	3 - 2	SAFETY (HAZARDS) CONSIDERED TO BE LESS SEVERE FOR TUS FLUIDS. LOW PROBABILITY OF OCCURRENCE.

J-4

Table J-1. Shenandoah STES, Failure Mode Effects Criticality and Safety Analysis (Page 5 of 5)

SHENANDOAH STES
FAILURE MODE EFFECTS CRITICALITY AND SAFETY ANALYSIS

SUBSYSTEM SYSTEM FMEA

COMPONENT _____

REF. RELIABILITY BLOCK DIAGRAMS, FIGURES 1 TO 3

PAGE 5 OF 5

DATE 6/28/78

BY J.F. KENT

UNIT OR ASSEMBLY	FUNCTION	FAILURE MODES	PROBABLE CAUSE	FAILURE EFFECT ON		CRITICALITY CATEGORY		REMARKS
				NEXT HIGHER ASSEMBLY	STES OPERATION	SAFETY	MISSION	
CONT'D 4. POWER CONVERSION SUBSYSTEM (PCS) OUTPUTS: ELEC. -200-400 KW H/X STEAM -700PSIG/ 720°F PROC. 0-1380 LBS/HX STEAM 115 PSIG COND. PRESS. - 5 PSIG COND. COOLANT OUTLET TEMP. -210°F		FAILS TO PROVIDE "WORKING" STEAM AT STEAM GENERATOR (H/X OUTPUT)	SOLAR ENERGY SUPPLY OR FOSSIL B/U FAILURE, H/X FAILURE	"WORKING" STEAM LOST. B/U SERVICES REQUIRED -- GPC ELECTRICAL, BLEYLE STEAM AND COOLING/HEATING, MAINT. ACTION REQUIRED.	STES DOWN	D-A	1 TO 15	HAZARDOUS CONDITIONS TO PERSONNEL/EQPMY POSSIBLE. ADDITIONAL PROBLEMS COULD BE IMPOSED IN COLLECTOR FIELD OR TES WITH RESPECT TO ACTION FOR EXCESS ENERGY. RESPONSE CHARACTERISTICS OF CONTROLS ALLEVIATE CONDITION. LOW PROBABILITY OF OCCURRENCE.
5. THERMAL UTILIZATION SUBSYSTEM (TUS) REQUIREMENTS: - CONDENSER COOLANT LOOP & CTLS INCLUDING COOLING TOWER LOW TEMP. STORAGE TANK PUMPS VALVES, H/X - AAC UNIT COOLING TOWER PUMPS, VALVES - CHILLED WATER LOOP PUMP, VALVES - HEATING LOOP H/X, PUMP	TUS IS A LOW TEMP. ENERGY STORAGE SUBSYSTEM WHICH STORES CONDENSER PROVIDED HEAT ENERGY. BY THIS FUNCTION IT CONTROLS CONDENSOR TEMPERATURE AND PROVIDES HEAT ENERGY FOR THE COOLING (AAC) OR HEATING LOADS OF THE BLEYLE PLANT.	FAILS TO CONTROL CONDENSOR TEMP. FAILS TO PROVIDE "HOT"(210°F) WATER) TO AAC SYSTEM (OR HEATING LOOP)	COOLING TOWER/PUMP/CONTROL FAILURE. CONTROLS, VALVES OR PUMP/MOTOR FAILURE.	EFFICIENCY OF TURB/ALT SET MAY BE AFFECTED - REDUCED OUTPUT POSSIBLE. MAINT. ACTION REQUIRED, BUT ONLY IF OPERATING LIMITS EXCEEDED. STES COOLING (HEATING) SUPPLY INHIBITED - MAINT. ACTION REQUIRED - BLEYLE COOLING HEATING B/U AVAILABLE.	STES OPERATION CONTINUES AS "NORMAL". WORST CASE SWITCH FROM STES TO GPC GRID FOR ELECTRICAL POWER. STES OPERATION CONTINUES "NORMAL" WITH ELECTRICAL POWER & PROCESS STEAM OUTPUT.	D D	3 - 2 3 - 2	PREVENTIVE MAINT. ACTIONS DURING DOWNTIME PERIODS. LOW PROBABILITY OF OCCURRENCE. PREVENTIVE MAINT. ACTIONS DURING DOWNTIME PERIODS.. LOW PROBABILITY OF OCCURRENCE.

9-P/I-6

APPENDIX K
DERIVATION OF GARVER'S EQUATION

APPENDIX K

DERIVATION OF GARVER'S EQUATIONS

From Figure 7.6-5 shown in Section 7.6, Reliability Assessment,

$$r = b e^{x/m}$$

where r = forced outage rate
 b = constant
 x = characteristic slope
 m = characteristic slope

In terms of availability, A :

$$A = 1 - r = 1 - b e^{x/m}$$

Assume a system designed to a specified availability

A_{L_1} at a peak load L_1

$$A_{L_1} = 1 - b e^{L_1/m}$$

Now add a generation unit of capacity C and availability

a. The availability for load L_1 is increased:

$$A_{L_1} = A_{L_1} + a(A_{L_1 - c} - A_{L_1})$$

Thus a larger peak load L_2 can be handled at the specified reliability.

$$\begin{aligned} A_{L_2} &= (1 - b e^{L_2/m}) + a \left(\left(1 - b e^{\frac{L_2 - C}{m}} \right) - (1 - b e^{\frac{L_2}{m}}) \right) \\ &= (1 - b e^{L_2/m}) + a (b e^{L_2/m} - b e^{L_2 - C/m}) \\ &= 1 - b e^{L_2/m} (1 - a + a e^{-C/m}) \end{aligned}$$

Equating A_{L_1} to A_{L_2} and solving for $L_2 - L_1$ will yield additional load carrying capability C^* .

$$A_{L_1} = A_{L_2}$$

$$1 - b e^{L_1/m} = 1 - b e^{L_2/m} (1 - a + a e^{-c/m})$$

$$\text{or } e^{L_1/m} = e^{L_2/m} (1 - a + a e^{-c/m})$$

Taking natural logs of both sides:

$$L_1/m = L_2/m + \ln (1 - a + a e^{-c/m})$$

$$C^* = L_2 - L_1 = -m \ln (1 - a + a e^{-c/m})$$

$$= -m \ln \left[\frac{(1-a)e^{cm} + a}{e^{c/m}} \right]$$

$$= -m \left[\ln (1-a e^{c/m} + a) - c/m \right]$$

$$= c - m \ln \left[a + (1-a) e^{c/m} \right]$$

Substituting $r = 1 - a$ yields Garver's equation:

$$C^* = c - m \ln \left((1-r) + r e^{c/m} \right)$$

APPENDIX L
REFLECTIVE SURFACE TESTS

APPENDIX L

REFLECTIVE SURFACE TESTS

L.1 OPTICAL PROPERTIES

The optical property characterization of reflecting materials consisted of two tests: (1) total hemispherical reflectance, and (2) specular reflectance. The qualitative comparison test for diffuse reflectance was also used for screening and comparing samples before and after environmental testing.

L.1.1 TOTAL HEMISPHERICAL MEASUREMENTS

This measurement was obtained with a Beckman DK-IL spectroreflectometer. The measurement consisted of determining the reflectance characteristics of each reflector material based on a Ba_2SO_4 reference standard as a function of wavelength from 350 to 1750 nM weighted against the solar spectrum and summed.

L.1.2 SPECULAR REFLECTANCE

Two types of reflectance measurements are typically used to characterize a reflecting surface: total hemispherical and specular. It is relatively easy to rank a mirror performance on the basis of its solar average hemispherical reflectance value alone, but it is not obvious whether a mirror with a high specular reflectance for a given receiving aperture is better than one with a lower value of specularity but with a higher hemispherical reflectance. Therefore, to ascertain the effect of measured specular reflectance on overall collector performance, a mathematical data analysis procedure is used. The procedure is based on the approximation that a reflected beam profile from a reflector sample can be characterized by the sum of two or three normal distributions. The data analysis derives three standard deviations, σ_1 , σ_2 , and σ_3 , and two weighting factors, A and B, which are directly related to $N_{(r)}$, the fraction of the total light reflected off of the reflecting surface which passes through a collecting aperture with radius r (Reference L-1).

$$N_{(r)} = 1 - A \exp(-r^2/2\sigma_1^2) - (B) \exp(-r^2/2\sigma_2^2) - (1-A-B) \exp(-r^2/2\sigma_3^2).$$

The three standard deviations with the weighting factors can then be used to calculate the performance of the collector.

A procedure has been developed for making specularity measurements with a He-Ne laser ($\lambda = .6324\mu m$). The laser beam, initially 1 mm in diameter, is widened to about 6 mm with a beam expander. At this point the beam appears as a bright central spot superimposed on a faint background of light. To remove the background, the beam is passed through a 7 mm (0.277 inch) circular aperture. A profile of the beam taken with the detecting apparatus in position 1 (see Figure L-1) shows that the laser intensity can be described as a normal distribution with a standard deviation of 0.93 mm (0.0365 inch). The profile is taken by aiming the beam at circular collecting apertures of different diameters set in front of the integrating chamber. If the intensity is characterized by a normal distribution,

$$I = I_0 e^{\left(\frac{-r^2}{2\sigma^2}\right)}$$
$$\text{Power} = \int I \, d\text{Area} = \int I 2\pi r \, dr \text{ (for a circular aperture)}$$
$$= 2\pi I_0 \sigma^2 \left(1 - e^{\left(\frac{-r^2}{2\sigma^2}\right)}\right)$$

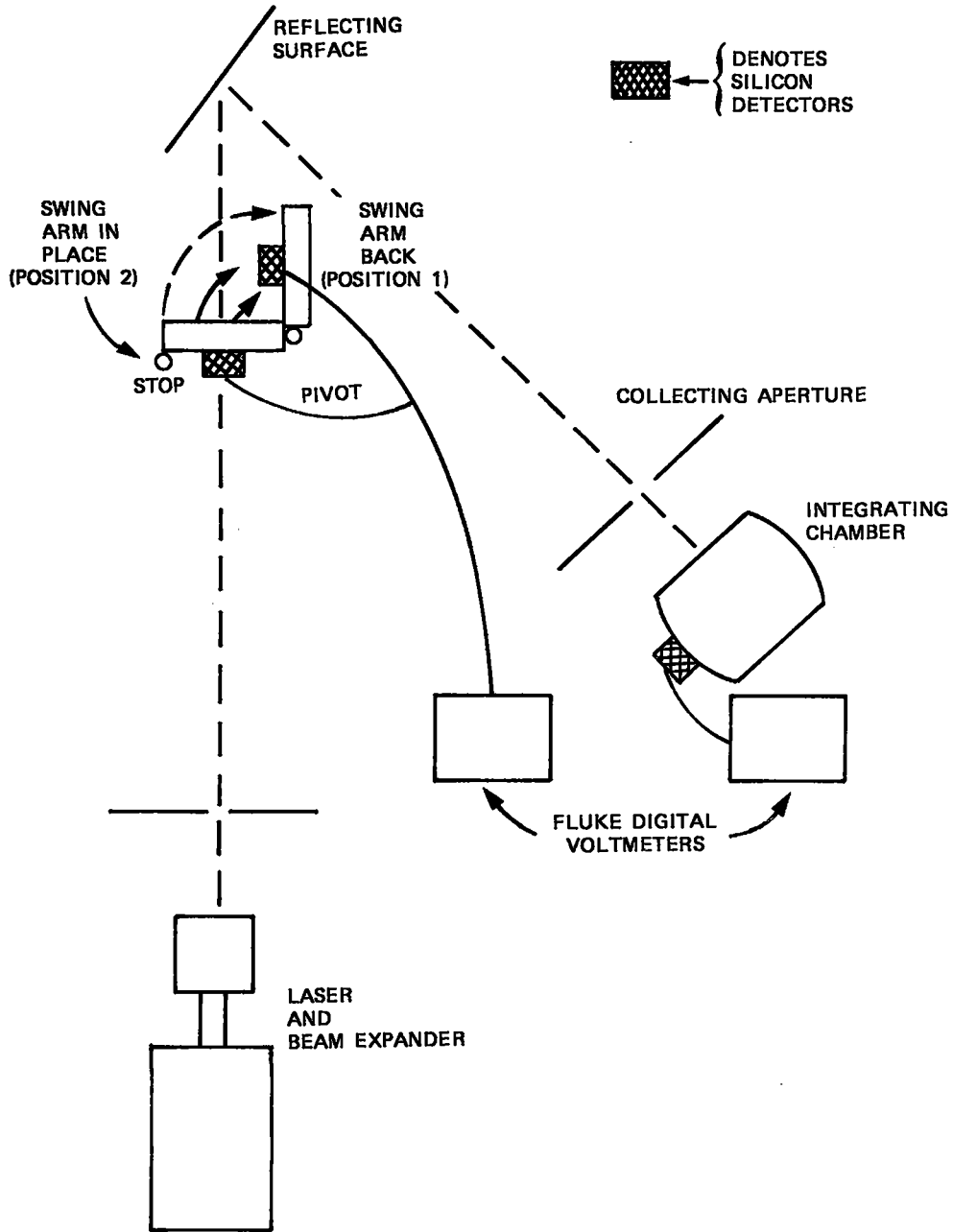


Figure L-1. Specularity Profile Measurement Apparatus

The fraction of total power passing through an aperture of radius r is $\frac{P(r)}{P_{\text{total}}}$, which is defined as $N(r)$.

$$N(r) = \frac{2\pi I_0 \sigma^2 \left(1 - e^{-\frac{r^2}{2\sigma^2}}\right)}{2\pi I_0 \sigma^2} = 1 - e^{-\frac{r^2}{2\sigma^2}}$$

When measuring the specularity of a sample surface, the test apparatus is arranged as in position 2 of Figure L-1. It is assumed that the reflecting surface scatters light so that the intensity of the scattered light can be described as a sum of three normal distributions;

$$I(r) = I_{01} e^{-\frac{r^2}{2\sigma_1^2}} + I_{02} e^{-\frac{r^2}{2\sigma_2^2}} + I_{03} e^{-\frac{r^2}{2\sigma_3^2}}$$

Then;

$$P(r) = 2\pi I_{01} \sigma_1^2 \left(1 - e^{-\frac{r^2}{2\sigma_1^2}}\right) + 2\pi I_{02} \sigma_2^2 \left(1 - e^{-\frac{r^2}{2\sigma_2^2}}\right) + 2\pi I_{03} \sigma_3^2 \left(1 - e^{-\frac{r^2}{2\sigma_3^2}}\right)$$

$$\text{and } \frac{P(r)}{P_{\text{total}}} = N(r) = \frac{2\pi I_{01} \sigma_1^2 \left(1 - e^{-\frac{r^2}{2\sigma_1^2}}\right) + 2\pi I_{02} \sigma_2^2 \left(1 - e^{-\frac{r^2}{2\sigma_2^2}}\right) + 2\pi I_{03} \sigma_3^2 \left(1 - e^{-\frac{r^2}{2\sigma_3^2}}\right)}{2\pi I_{01} \sigma_1^2 + 2\pi I_{02} \sigma_2^2 + 2\pi I_{03} \sigma_3^2}$$

which is of the form

$$N(r) = A \left(1 - e^{-\frac{r^2}{2\sigma_1^2}}\right) + B \left(1 - e^{-\frac{r^2}{2\sigma_2^2}}\right) + (1 - A - B) \left(1 - e^{-\frac{r^2}{2\sigma_3^2}}\right)$$

$$= 1 - A e^{-\frac{r^2}{2\sigma_1^2}} - B e^{-\frac{r^2}{2\sigma_2^2}} - (1 - A - B) e^{-\frac{r^2}{2\sigma_3^2}}$$

If the laser were a point source, σ_1 , σ_2 , and σ_3 would be the standard deviations associated with the specularity of the surface. Since the laser is not a point source, σ_1^2 and σ_2^2 are combinations of the laser and the reflecting surface.

$$\sigma_1^2 = \sigma_{\text{laser}}^2 + \sigma_{\text{reflector}}^2$$

The previous relations follow from the fact that the convolution of the normal laser distribution with the three normal distributions associated with the reflecting surface results in three new normal distributions whose variances have the relations shown above.

To determine variances for the reflecting surface, the following procedure is used. With the use of a number of circular collecting apertures with different diameters, the reflected power passing through each aperture is measured. After each measurement, the laser beam is referenced with a silicon solar cell mounted on a pivot in front of the laser. Dividing the power reading at the integrating chamber by the power output of the laser normalizes the results and compensates for thermal fluctuations in the laser. A final reflectance measurement is then made with the collecting apparatus moved in close to the reflector sample so that essentially all of the reflected beam passes into the integrating chamber. The value measured here corresponds to P_{total} reflected and is used as a divisor for all of the previous variable aperture power measurements. Since $P(r)/P_{\text{total}} = N(r)$, this yields a set of observed $N(r)$ values which can then be fit to the mathematical equation described earlier.

Once weighting factors and variances have been found to describe the observed $N(r)$ values, the last step is to factor out the contribution of the laser to determine the actual scattering characteristics of the reflector itself. Weighting factors are left unchanged since these are not affected by the laser. The variances, however, are modified. As shown earlier $\sigma_{\text{reflector}}^2 = \sigma_{\text{laser}}^2 - \sigma_{\text{laser}}^2$. This yields a standard deviation with units of distance. To get a standard deviation in milliradians $\sqrt{\sigma_{\text{reflector}}^2}$ (mils) is divided by R (inches) where R is the distance from the reflecting surface to the collecting apertures. ($R = 20$ inches for the apparatus.) This leaves the weighting factors from before and yields variances in the corrected form.

L. 1.3 DIFFUSE REFLECTANCE

This measurement was made using a Beckman DK-1L spectroreflectometer. The flat reflecting samples were mounted such that the light beam passing through the entrance aperture of the integrating chamber struck the test sample and the specular component of the reflected beam was reflected back out the entrance aperture. Only the diffuse component was detected.

This measurement should not be compared to the specular reflectance measurement. The diffuse measurement is useful in comparing before results for a given sample to after results for the same sample to determine if degradation has occurred. The measurement is also used to distinguish gross differences in the reflecting behavior of two different samples.

L.2 ENVIRONMENTAL TESTS

The tests described below were used to simulate a 20 year exposure to environmental conditions at the Shenandoah site including periodic cleaning.

L.2.1 PRECONDITIONING

All test samples were conditioned for 24 hours at 45 ± 5 percent relative humidity and $294 \pm 1^\circ\text{K}$ ($21 \pm 1^\circ\text{C}$) immediately prior to and after environmental tests for the purpose of measuring physical or optical performance.

L.2.2 ADHESION

The purpose of this test was to determine the adherence of the reflector and protective film coatings to the substrate. Adhesion was determined by applying a strip of adhesive tape to a parallel scribed area of the

coated sample using a constant pressure on a standard roller. The tape was then snapped-pulled at 90° to the substrate (FED-STD-141A, Method 6302 Equivalent). No coating should have been removed.

L.2.3 SALT SPRAY (FOG) TEST

This test was used to determine the relative corrosion resistance of coated reflector samples. The test was conducted in a standard salt spray chamber in accordance with FED-STD-141A, Method 6061, for a period of 15 days.

L.2.4 TEMPERATURE CYCLE STABILITY

The purpose of this test was to determine reflector sample thermal stability to freeze-thaw-dry cycles. Samples were exposed to 25 cycles of the following:

- 20 min at 294°K or 70°F
- 2 hrs at 219°K or -65°F
- 20 min at 294°K or 70°F
- 2 hrs at 339°K or 150°F

L.2.5 ABRASION

This test was designed to determine the relative resistance of film and coating systems to abrasion by falling sand and dirt. Natural silica sand and dirt (sand-natural silica of grade which passed through a No. 100 sieve; dirt-local variety of a grade which also passed through a No. 100 sieve) were allowed to fall on a 3 cm² area of a sample at a rate of 15-20 gms/min. at a velocity of about 10 m/sec. A total of 30 gms of material was used (FED-STD-141A, Method 6191 Equivalent). This was a comparative test in which the optical results of the samples were compared to those of glass exposed to identical abrasion tests.

L.2.6 ACCELERATED WEATHERING

The purpose of this test was to determine the effects of a given set of heat, moisture, and ultraviolet exposure cycles on the reflector samples. Based on ASTM-G53-77, the test consisted of exposing the samples to 16 and 20 hours of condensation produced by exposing the test surface to a heated (316°K or 110°F), saturated mixture of air and water vapor (93 ± 3 percent relative humidity) while the sample's reverse side was exposed to cool room air. The samples were then exposed to simulated solar ultraviolet (20 sun equivalent) at a temperature of 339°K (150°F) for four hours. The test was run for 15 cycles. A Hanovia mercury-xenon solar simulator was used to provide ultraviolet radiation at approximately 20 suns intensity in the wavelength region below 400 μm based on the AM2 spectrum.

L.2.7 CLEANABILITY

The purpose of this test was to determine the washability of soiled reflector samples when exposed to a standard cleaning technique. The reflector samples had a standard soiling medium applied (FED-STD-141A, Method 6141) and were then subjected to a cleaning technique. The cleaning technique consisted of the following:

1. Placing five-micron dust particles on the surface to be tested.
2. Rinsing the dust with water

3. Wiping the surface using a weak detergent/water solution (Joy, Liquinox, etc.) 10 times in the x direction of the sample and 10 times in the y direction, with this cycle repeated 25 times for each wiping material, for a total of 2000 rubs.

Cotton swab	500 rubs	
Cotton gauze	500 rubs	
Cotton cloth	500 rubs	
Soft bristle brush	500 rubs	Total = 2000 rubs

4. Rinsing with water

L.2.8 COMBINED EFFECTS TEST

L.2.8.1 Abrasion/Salt

First the samples were subjected to sand abrasion and then subjected to salt spray. The purpose of this test was to evaluate degradation based on an interaction of one environment with another.

L.2.8.2 Abrasion/Weathering

Samples were first subjected to sand abrasion and then to weathering.

L.2.8.3 Salt/Abrasion/Weathering

Samples were first subjected to salt spray, then to sand, and finally to weathering.

L.3 REFERENCES

- L-1 R. B. Pettit, "Characterization of the Reflected Beam Profile of Solar Mirror Materials," Sandia Laboratories, Albuquerque.